

Advances in Experimental Medicine and Biology 1077

Heung Jae Chun · Kwideok Park  
Chun-Ho Kim · Gilson Khang *Editors*

# Novel Biomaterials for Regenerative Medicine

 Springer

---

# Advances in Experimental Medicine and Biology

Volume 1077

Editorial Board:

IRUN R. COHEN, *The Weizmann Institute of Science, Rehovot, Israel*

ABEL LAJTHA, *N.S. Kline Institute for Psychiatric Research,  
Orangeburg, NY, USA*

JOHN D. LAMBRIS, *University of Pennsylvania, Philadelphia, PA, USA*

RODOLFO PAOLETTI, *University of Milan, Milan, Italy*

NIMA REZAEI, *Tehran University of Medical Sciences Children's Medical  
Center, Children's Medical Center Hospital, Tehran, Iran*

More information about this series at <http://www.springer.com/series/5584>

---

Heung Jae Chun • Kwideok Park  
Chun-Ho Kim • Gilson Khang  
Editors

# Novel Biomaterials for Regenerative Medicine

 Springer

*Editors*

Heung Jae Chun  
The Catholic University of Korea  
Seoul, South Korea

Kwideok Park  
Korea Institute of Science  
and Technology  
Seoul, South Korea

Chun-Ho Kim  
Korea Institute of Radiological  
and Medical Sciences  
Seoul, South Korea

Gilson Khang  
Chonbuk National University  
Jeonju, South Korea

ISSN 0065-2598                      ISSN 2214-8019 (electronic)  
Advances in Experimental Medicine and Biology  
ISBN 978-981-13-0946-5              ISBN 978-981-13-0947-2 (eBook)  
<https://doi.org/10.1007/978-981-13-0947-2>

Library of Congress Control Number: 2018952634

© Springer Nature Singapore Pte Ltd. 2018

This work is subject to copyright. All rights are reserved by the Publisher, whether the whole or part of the material is concerned, specifically the rights of translation, reprinting, reuse of illustrations, recitation, broadcasting, reproduction on microfilms or in any other physical way, and transmission or information storage and retrieval, electronic adaptation, computer software, or by similar or dissimilar methodology now known or hereafter developed.

The use of general descriptive names, registered names, trademarks, service marks, etc. in this publication does not imply, even in the absence of a specific statement, that such names are exempt from the relevant protective laws and regulations and therefore free for general use.

The publisher, the authors and the editors are safe to assume that the advice and information in this book are believed to be true and accurate at the date of publication. Neither the publisher nor the authors or the editors give a warranty, express or implied, with respect to the material contained herein or for any errors or omissions that may have been made. The publisher remains neutral with regard to jurisdictional claims in published maps and institutional affiliations.

This Springer imprint is published by the registered company Springer Nature Singapore Pte Ltd. The registered company address is: 152 Beach Road, #21-01/04 Gateway East, Singapore 189721, Singapore

---

## Preface

Regenerative medicine is a branch of multidisciplinary research in tissue engineering and molecular biology, which deals with the process of replacing, engineering, or regeneration of human cells, tissues, or organs to restore or establish normal function. Regenerative medicine is leading the innovation of life sciences and medicine with various expansion toward stem cells, cell therapy, and tissue engineering, and hence it is now becoming a pillar of the advanced medical industry. In regeneration medicine fields, biomaterials are essential tools for replacing part of a living system or to function in intimate contact with the living tissue. Therefore, this book introduces the recent trends of biomaterials derived either from nature or synthesized in the laboratory using a variety of chemical approaches utilizing metallic components, polymers, ceramics, or composite materials. The book consists of 5 main parts and 28 chapters containing recent topics reported by a number of prominent researches in these fields.

### **Part I reviews the fate of stem cells regulated by biomaterials.**

Chapter 1 is an introduction to the human placenta laminin-111 as a multifunctional protein for tissue engineering and regenerative medicine. In Chap. 2, a novel strategy for simple and robust expansion of human pluripotent stem cells using botulinum hemagglutinin is introduced. Polycaprolactone scaffolds used for the growth and differentiation of dental stem cells of apical papilla are summarized in Chap. 3. The impact of three-dimensional culture systems on hepatic differentiation of pluripotent stem cells and beyond is introduced in Chap. 4.

### **Controlling of signal pathway of stem cell by biomaterials is discussed in Part II.**

In Chap. 5, modulation of the osteoimmune environment in the development of biomaterials for osteogenesis is reviewed. For tissue regeneration and disease modeling, novel biomimetic microphysiological systems are summarized in Chap. 6. Chapter 7 contains the feasibility of silk fibroin in wound healing process. In Chap. 8, the role of natural-based biomaterials in advanced therapies for autoimmune diseases is described.

**Part III describes functional biomaterials for regenerative medicine.**

Content of Chap. 9 includes recent advancements in decellularized matrix-based biomaterials for musculoskeletal tissue regeneration. In Chap. 10, clinical applications of injectable biomaterials are introduced. Advanced injectable alternatives for osteoarthritis are discussed in Chap. 11. Chapters 12, 13 and 14 introduce fabrication of hydrogel materials, injectable nanocomposite hydrogels and electrosprayed nano(micro)particles, and advances in waterborne polyurethane-based biomaterials for biomedical applications, respectively. Content reviewed in Chap. 15 is medical applications of collagen and hyaluronan in regenerative medicine.

**Part IV shows the review on inorganic biomaterials for regenerative medicine.**

Calcium phosphate biomaterials for clinical application in dentistry are described in Chap. 16. In Chap. 17, stem cell and advanced nano bioceramic interactions are discussed. Chap. 18 introduces recent trend in hydroxyapatite (HAp) synthesis and the synthesis report of nanostructure HAp by hydrothermal reaction. Use of  $\text{TiO}_2$  in the bone regeneration is discussed in Chap. 19.

**Finally, Part V introduces the recent trends of smart natural biomaterials for regenerative medicine.**

Chapter 20 reviews the feasibility of silk fibroin-based scaffold for bone tissue engineering. Chapter 21 explains characteristics of collagen Type I as a versatile biomaterial. Techniques of tissue-inspired interfacial coatings for regenerative medicine are described in Chap. 22. Chapters 23, 24 and 25 introduce naturally derived biomaterials, mussel-inspired biomaterials, and chitosan for tissue engineering applications, respectively. Chapter 26 reviews demineralized dentin matrix (DDM) as a carrier for recombinant human bone morphogenetic proteins (rhBMP-2). Prospects of natural polymeric scaffolds in peripheral nerve tissue regeneration are introduced in Chap. 27. In Chap. 28, chitosan-based dressing materials for problematic wound management are reviewed.

We offer a special thanks to all participants who have generously devoted their time, energy, experience, and intelligence for successful completion of this book. Their efforts will contribute to next generation who studies regenerative medicine based on biomaterials. Finally, we really appreciate the effort of Dr. Sue Lee, the publishing editor of biomedical sciences of Springer Nature, who made a great effort to publish this book. Also we would like to appreciate Mrs. Ok Kyun Choi and Yong Woon Jeong at Gilson's Lab for e-mailing all authors, editing, pressing, and so on as boring

and tedious works. Without their support, this huge work would not have been possible.

**Acknowledgement** This research was supported by the Basic Science Research Program through the National Research Foundation of Korea (NRF), funded by the Ministry of Science, ICT and Future Planning (NRF-2017R1A2B3010270), and the Korea Health Technology R&D Project through the Korea Health Industry Development Institute (KHIDI), funded by the Ministry of Health and Welfare.

Seoul, South Korea

Heung Jae Chun

Kwideok Park

Chun-Ho Kim

Jeonju, South Korea

Gilson Khang



---

# Contents

## Part I The Fate of Stem Cell by Biomaterials

- 1 Human Placenta Laminin-111 as a Multifunctional Protein for Tissue Engineering and Regenerative Medicine ..... 3**  
Johannes Hackethal, Christina M. A. P. Schuh,  
Alexandra Hofer, Barbara Meixner, Simone Hennerbichler,  
Heinz Redl, and Andreas H. Teuschl
- 2 A Novel Strategy for Simple and Robust Expansion of Human Pluripotent Stem Cells Using Botulinum Hemagglutinin ..... 19**  
Mee-Hae Kim and Masahiro Kino-oka
- 3 Growth and Differentiation of Dental Stem Cells of Apical Papilla on Polycaprolactone Scaffolds ..... 31**  
Mohamed Jamal, Yaser Greish, Sami Chogle,  
Harold Goodis, and Sherif M. Karam
- 4 Impact of Three-Dimensional Culture Systems on Hepatic Differentiation of Puripotent Stem Cells and Beyond ..... 41**  
Thamil Selvee Ramasamy, Agnes Lee Chen Ong, and Wei Cui

## Part II Controlling of Signal Pathway of Stem Cell by Biomaterials

- 5 Modulation of the Osteoimmune Environment in the Development of Biomaterials for Osteogenesis..... 69**  
Fei Wei and Yin Xiao
- 6 Novel Biomimetic Microphysiological Systems for Tissue Regeneration and Disease Modeling ..... 87**  
Karim I. Budhwani, Patsy G. Oliver, Donald J. Buchsbaum,  
and Vinoy Thomas
- 7 Silk Fibroin in Wound Healing Process ..... 115**  
Md. Tipu Sultan, Ok Joo Lee, Soon Hee Kim, Hyung Woo Ju,  
and Chan Hum Park
- 8 The Role of Natural-Based Biomaterials in Advanced Therapies for Autoimmune Diseases..... 127**  
Helena Ferreira, Joana F. Fangueiro, and Nuno M. Neves

### Part III Functional Biomaterials for Regenerative Medicine

- 9 Recent Advancements in Decellularized Matrix-Based Biomaterials for Musculoskeletal Tissue Regeneration**..... 149  
Hyunbum Kim, Yunhye Kim, Mona Fendereski, Nathaniel S. Hwang, and Yongsung Hwang
- 10 Clinical Applications of Injectable Biomaterials**..... 163  
Hatice Ercan, Serap Durkut, Aysel Koc-Demir, Ayşe Eser Elçin, and Yaşar Murat Elçin
- 11 Advanced Injectable Alternatives for Osteoarthritis**..... 183  
Şebnem Şahin, Süleyman Ali Tuncel, Kouroush Salimi, Elif Bilgiç, Petek Korkusuz, and Feza Korkusuz
- 12 Fabrication of Hydrogel Materials for Biomedical Applications** ..... 197  
Jen Ming Yang, Olajire Samson Olanrele, Xing Zhang, and Chih Chin Hsu
- 13 Injectable Nanocomposite Hydrogels and Electrospayed Nano(Micro)Particles for Biomedical Applications** ..... 225  
Nguyen Vu Viet Linh, Nguyen Tien Thinh, Pham Trung Kien, Tran Ngoc Quyen, and Huynh Dai Phu
- 14 Advances in Waterborne Polyurethane-Based Biomaterials for Biomedical Applications** ..... 251  
Eun Joo Shin and Soon Mo Choi
- 15 Medical Applications of Collagen and Hyaluronan in Regenerative Medicine** ..... 285  
Lynn L. H. Huang, Ying-Hui Amy Chen, Zheng-Ying Zhuo, Ya-Ting Hsieh, Chia-Ling Yang, Wei-Ting Chen, Jhih-Ying Lin, You-Xin Lin, Jian-Ting Jiang, Chao-Hsung Zhuang, Yi-Ching Wang, Hanhhieu Nguyendac, Kai-Wei Lin, and Wen-Lung Liu

### Part IV Inorganic Biomaterials for Regenerative Medicine

- 16 Bioceramics for Clinical Application in Regenerative Dentistry**..... 309  
Ika Dewi Ana, Gumilang Almas Pratama Satria, Anne Handrini Dewi, and Retno Ardhani
- 17 Stem Cell and Advanced Nano Bioceramic Interactions** ..... 317  
Sevil Köse, Berna Kankilic, Merve Gizer, Eda Ciftci Dede, Erdal Bayramli, Petek Korkusuz, and Feza Korkusuz
- 18 Recent Trends in Hydroxyapatite (HA) Synthesis and the Synthesis Report of Nanostructure HA by Hydrothermal Reaction**..... 343  
Pham Trung Kien, Huynh Dai Phu, Nguyen Vu Viet Linh, Tran Ngoc Quyen, and Nguyen Thai Hoa

<b>19</b>	<b>Modification of Titanium Implant and Titanium Dioxide for Bone Tissue Engineering</b> .....	355
	Tae-Keun Ahn, Dong Hyeon Lee, Tae-sup Kim, Gyu chol Jang, SeongJu Choi, Jong Beum Oh, Geunhee Ye, and Soonchul Lee	
 <b>Part V Smart Natural Biomaterials for Regenerative Medicine</b>		
<b>20</b>	<b>Silk Fibroin-Based Scaffold for Bone Tissue Engineering</b> .....	371
	Joo Hee Choi, Do Kyung Kim, Jeong Eun Song, Joaquim Miguel Oliveira, Rui Luis Reis, and Gilson Khang	
<b>21</b>	<b>Collagen Type I: A Versatile Biomaterial</b> .....	389
	Shiplu Roy Chowdhury, Mohd Fauzi Mh Busra, Yogeswaran Lokanathan, Min Hwei Ng, Jia Xian Law, Ude Chinedu Cletus, and Ruszymah Binti Haji Idrus	
<b>22</b>	<b>Tissue-Inspired Interfacial Coatings for Regenerative Medicine</b> .....	415
	Mahmoud A. Elnaggar and Yoon Ki Joung	
<b>23</b>	<b>Naturally-Derived Biomaterials for Tissue Engineering Applications</b> .....	421
	Matthew Brovold, Joana I. Almeida, Iris Pla-Palacín, Pilar Sainz-Arnal, Natalia Sánchez-Romero, Jesus J. Rivas, Helen Almeida, Pablo Royo Dachary, Trinidad Serrano-Aulló, Shay Soker, and Pedro M. Baptista	
<b>24</b>	<b>Mussel-Inspired Biomaterials for Cell and Tissue Engineering</b> .....	451
	Min Lu and Jiashing Yu	
<b>25</b>	<b>Chitosan for Tissue Engineering</b> .....	475
	Chun-Ho Kim, Sang Jun Park, Dae Hyeok Yang, and Heung Jae Chun	
<b>26</b>	<b>Demineralized Dentin Matrix (DDM) As a Carrier for Recombinant Human Bone Morphogenetic Proteins (rhBMP-2)</b> .....	487
	In Woong Um	
<b>27</b>	<b>Prospects of Natural Polymeric Scaffolds in Peripheral Nerve Tissue-Regeneration</b> .....	501
	Roqia Ashraf, Hasham S. Sofi, Mushtaq A. Beigh, Shafquat Majeed, Shabana Arjamand, and Faheem A. Sheikh	
<b>28</b>	<b>Chitosan-Based Dressing Materials for Problematic Wound Management</b> .....	527
	Ji-Ung Park, Eun-Ho Song, Seol-Ha Jeong, Juha Song, Hyoun-Ee Kim, and Sukwha Kim	

---

**Part I**

**The Fate of Stem Cell by Biomaterials**



# Human Placenta Laminin-111 as a Multifunctional Protein for Tissue Engineering and Regenerative Medicine

Johannes Hackethal, Christina M. A. P. Schuh, Alexandra Hofer, Barbara Meixner, Simone Hennerbichler, Heinz Redl, and Andreas H. Teuschl

## Abstract

Laminins are major components of all basement membranes surrounding nerve or vascular tissues. In particular laminin-111, the prototype of the family, facilitates a large spectrum of fundamental cellular responses in all eukaryotic cells. Laminin-111 is a biomaterial frequently used in research, however it is primarily isolated from non-human origin or

produced with time-intensive recombinant techniques at low yield.

Here, we describe an effective method for isolating laminin-111 from human placenta, a clinical waste material, for various tissue engineering applications. By extraction with Tris-NaCl buffer combined with non-protein-denaturation ammonium sulfate precipitation and rapid tangential flow filtration steps, we could effectively isolate native laminin-111 within only 4 days. The resulting material was biochemically characterized using a combination of dot blot, SDS-PAGE, Western blot and HPLC-based amino acid

The work was performed at the Ludwig Boltzmann Institute for Experimental and Clinical Traumatology; Austrian Cluster for Tissue Regeneration, Donaueschingenstraße 13, 1200 Vienna, Austria.

J. Hackethal (✉) · B. Meixner · H. Redl  
Ludwig Boltzmann Institute for Experimental and Clinical Traumatology in AUVA Trauma Research Center, Vienna, Austria

Austrian Cluster for Tissue Regeneration,  
Vienna, Austria  
e-mail: [Johannes.Hackethal@trauma.lbg.ac.at](mailto:Johannes.Hackethal@trauma.lbg.ac.at)

C. M. A. P. Schuh  
Ludwig Boltzmann Institute for Experimental and Clinical Traumatology in AUVA Trauma Research Center, Vienna, Austria

Austrian Cluster for Tissue Regeneration,  
Vienna, Austria

Laboratory of Nano-Regenerative Medicine, Faculty of Medicine, Cells for Cells, Universidad de Los Andes, Santiago, Chile

A. Hofer  
Research Area Biochemical Engineering, Institute of Chemical Engineering, Vienna University of Technology, Vienna, Austria

S. Hennerbichler  
Austrian Cluster for Tissue Regeneration,  
Vienna, Austria

Red Cross Blood Transfusion Service of Upper Austria, Linz, Austria

A. H. Teuschl  
Austrian Cluster for Tissue Regeneration,  
Vienna, Austria

Department of Biochemical Engineering, University of Applied Sciences Technikum Wien,  
Vienna, Austria

analysis. Cytocompatibility studies demonstrated that the isolated laminin-111 promotes rapid and efficient adhesion of primary Schwann cells. In addition, the bioactivity of the isolated laminin-111 was demonstrated by (a) using the material as a substrate for outgrowth of NG 108-15 neuronal cell lines and (b) promoting the formation of interconnected vascular networks by GFP-expressing human umbilical vein endothelial cells.

In summary, the isolation procedure of laminin-111 as described here from human placenta tissue, fulfills many demands for various tissue engineering and regenerative medicine approaches and therefore may represent a human alternative to various classically used xenogenic standard materials.

---

**Keywords**

Laminin-111 · Placenta · Schwann cells · NG 108-15 · Vasculogenesis

---

## 1.1 Introduction

Basement membranes (BMs) are specialized extracellular sheet-like matrices underlying epithelia in all mammals [1]. They are key elements during embryogenesis and are mainly composed of laminins, collagen-4 and heparin sulfate proteoglycans [2], joined together by nidogens, perlecan and other proteins [3].

In this regard, the primary function of laminins, a family of large heterotrimeric ( $\alpha$ ,  $\beta$ ,  $\gamma$ ) glycoproteins present in BMs, is to interact with receptors anchored in the plasma membrane of cells, such as endothelial or neuronal cells [1]. Laminin-111, a 800-kDa protein, is the prototype of the family and the best characterized laminin isoform [1, 3]. It is adhesive for most cell types, promotes cell survival *in vitro* and has various biological key activities [3–5], including cell

adhesion, proliferation, differentiation and migration [1, 6]. Laminins are frequently used for *in vitro* and *in vivo* neuronal cell cultivation [7–11], angiogenesis [5, 12], wound healing [6, 13–15], or stem cell studies [16, 17].

Laminin-111 was the first laminin type isolated by Ruppert Timpl from Engelbreth-Holmes Sarcoma (EHS) mouse material during the 1970s [18]. For several years this has been the only known laminin isoform [19]. Since its discovery, many attempts have been made to isolate laminin-111 from a human source such as placenta [20–24] or produce it recombinantly [25, 26]. However, no human equivalent to the mouse tumor derived EHS laminin-111 is available for large-scale production and therefore, more than 30 years after its discovery, laminin-111 extracted from xenogenic EHS tumor tissue is still the frequently used gold standard for various *in vitro* and *in vivo* research protocols [27].

The aim of this study was to establish an effective method for isolation of human placental laminin-111 (pLm-111). The method was based on an extraction step via Tris-NaCl buffer to yield a laminin-rich protein fraction, followed by a protein precipitation step using 30% ammonium chloride combined with a series of diafiltration and salt precipitation steps to remove non-laminin contaminants and therefore purify the laminin-111 isolates. The resulting purified laminin-111 was biochemically characterized using a combination of dot blot, sodium dodecyl sulfate polyacrylamide gel electrophoresis (SDS-PAGE), Western blot and HPLC-based amino acid analysis. The *in vitro* biocompatibility and bioactivity of laminin-111 was demonstrated using NG 108-15 neuronal cell lines, Schwann cells and GFP-expressing human umbilical vein endothelial cells (gfpHUVEC).

---

## 1.2 Materials and Methods

If not stated otherwise all chemicals were purchased from Sigma Aldrich and of analytical grade.

### 1.2.1 Collection of Human Placenta Tissue

Placenta material was collected after caesarian section from the Landes-Kinderklinik Hospital Linz, Austria (with the permission of the local ethical board and informed consent from all donors), delivered to LBI Trauma laboratories on dry ice, and stored at  $-20^{\circ}\text{C}$  until the isolation procedure was performed.

### 1.2.2 Isolation Procedure of Placenta Laminin-111 (pLm-111)

All isolation steps were performed in a cold-room at  $4^{\circ}\text{C}$ . For all diafiltration steps in this protocol the tangential flow filtration (TFF) Ultralab™ system PALL (VWR, Vienna, Austria) has been used, equipped with a 100 kDa cut-off Ultrasette™ tangential flow filter.

After thawing, the placenta was dissected free of the outer membranes, amnion and chorion as well as of the umbilical cord. The residual basal tissue was used for the isolation process. Blood components were removed by repetitive homogenization steps of 100 g basal placenta tissue in 200 mL phosphate buffered saline (PBS) without  $\text{Ca}^{2+}/\text{Mg}^{2+}$  using a blender (Braun Type 4184, Kronberg, Germany) and subsequent centrifugation at  $3.000 \times g$  for 5 min using a Heraeus Multifuge™ (Beckman Instruments GmbH Type 1 S-R, Vienna, Austria). The supernatant fluid containing blood components was discarded, pellets were resuspended in fresh PBS and centrifuged again (three times). Thereafter, the procedure was repeated three times with aqua dest.

Subsequently, 100 g wet weight of blood-free basal tissue were homogenized for 60 s in 100 mL Tris-NaCl buffer (50 mM Tris, 0.5 M NaCl, 4 mM EDTA, 2 mM N-Ethylmaleimide (NEM), pH 7.4) using the blender. Suspension was stirred overnight on a magnetic stirrer at 200 rpm and subsequently centrifuged at  $7.000 \times g$  for 15 min. Supernatants were collected and crystalline ammonium sulfate ( $[\text{NH}_4]_2\text{SO}_4$ ) was added to

adjust for 30% final concentration. After 2 h of stirring, the extract was centrifuged at  $7.000 \times g$  for 15 min. Pellets were collected in 150 mL Tris-buffered saline (TBS) buffer and diafiltrated against  $10\times$  volumes of TBS. To precipitate collagen-4 contaminants, NaCl concentration was adjusted to 1.7 M by adding 150 mL of 3.4 M NaCl at a constant flow rate of 2 mL/min using a Minipuls Evolution® roller pump (Gilson Inc., Vienna, Austria) and stirred overnight at 200 rpm. Subsequently, the suspension was centrifuged at  $7.000 \times g$  for another 15 min. Supernatant containing native pLm-111 was either (a) diafiltrated against at least 3 volumes of TBS and stored at  $-80^{\circ}\text{C}$  (native pLm-111), or (b) diafiltrated against aqua dest. to remove residual salts, and concentrated to approximately 200 mL using TFF, and lyophilized (Christ Alpha 1-4 lyophilizer, Heraeus Schauer GmbH, Vienna, Austria). The resulting lyophilized pLm-111 was stored at  $-20^{\circ}\text{C}$  for up to 12 months before further use.

### 1.2.3 Biochemical Identification of pLm-111

#### 1.2.3.1 Dot Blots

For native pLm-111 detection, dot blots were performed.  $2 \mu\text{L}$  of either 1 mg/mL EHS laminin-111, pLm-111 (native or lyophilized), collagen-1 or recombinant laminin-111 from fibroblast cell culture (Sigma Aldrich, Vienna, Austria) were pipetted in duplicates on nitrocellulose membranes (Peglab, Erlangen, Germany) and air-dried for 60 min. Thereafter, membranes were blocked with 5% skim milk powder in TBS buffer for 60 min and incubated with 1:2000 diluted monoclonal primary laminin-111 antibodies in TBS for another 60 min. After washing with TBS, membranes were incubated with peroxidase conjugated secondary antibodies (Abcam, CA, USA) for 60 min and signals were detected using a Multiimage Light Cabinet (BioZym, NY, USA).

#### 1.2.3.2 SDS PAGE/Western Blot

SDS PAGE and western blot analysis were performed as previously described using the XCell

SureLock™ Mini-Cell Electrophoresis System (Invitrogen, Vienna, Austria) [28, 29]. Briefly, 20 µg per lane of EHS laminin-111 (control), or lyophilized pLm-111 reconstituted in TBS buffer were resolved on 3–8% SDS-polyacrylamide gels (NuSep®, VWR, Austria), stained with 0.25% (w/v) Coomassie Brilliant Blue, or transferred onto nitrocellulose membranes (Peqlab) using the XCell II Blot Module (Invitrogen, Vienna, Austria). Membranes were blocked with 5% milk powder in TBS buffer containing 0.1% Tween (TBS/T) and incubated with anti-laminin-111 (polyclonal 1:2000, AB11575, Abcam, USA) in 5% BSA-TBS/T at 4 °C overnight. Subsequently, membranes were incubated with peroxidase conjugated secondary antibodies (R1364HRP, Arctis GmbH, Germany) in 5% milk-TBS/T, and signals were detected using a Multiimage Light Cabinet (BioZym).

### 1.2.3.3 Amino Acid Analysis

Amino acid quantification was performed as previously described [30]. Briefly, pLm-111 was digested following a two-step protocol (enzymatical followed by chemical). 75 mg of lyophilized sample were incubated with 1 mL of 0.0125% protease from *Streptomyces griseus* in 1.2% TRIS/ 0.5% SDS pH 7.5 (adjusted with 0.1% HCl) solution for 72 h at 37 °C. Then 1 mL of 4% formic acid in ddH<sub>2</sub>O was added for chemical pre-digestion and the suspension was incubated for 2 h at 108 °C followed by lyophilization. The dried samples were reconstituted in 5 mL 0.6% TRIS and 7 M guanidine hydrochloride pH 8 for 2 h. After centrifugating (Sigma centrifuge, 3–18 K) the sample at 4800 rpm for 15 min at 4 °C, 1 mL of the supernatant was combined with 0.5 mL 4 M methansulfonic acid solution containing 0.2% tryptamine and incubated for 1 h at 160 °C. Subsequently, the solution was quantitatively transferred into a 5 mL volumetric flask, 225 µL 8 M NaOH and 0.25 mL internal standard were added and the flask was filled up with 2.2 M sodium acetate solution. The samples were then directly used for HPLC analysis.

A multi-amino acid standard mix was prepared by mixing the amino acid standard, a solu-

tion containing 2.5 mM each of asparagine, glutamine and tryptophan in MQ, a solution containing 2.5 mM each of taurine and hydroxyproline in 0.1 M HCl and a solution of the internal standards, i.e. 25 mM each of norvaline and sarcosine in 0.1 M HCl. Ten different concentrations of this standard mixture, ranging between 45 mg/L and 0.5 mg/L, were used for calibration.

The HPLC system Ultimate 3000 (Thermo Fisher Scientific, USA) was equipped with a pump (LPG-3400SD), a split-loop auto-sampler (WPS-3000 SplitLoop), a column oven (Col. Comp. TCC-3000SD) and a fluorescence detector (FLD-3400RS). Chromeleon 7.2 software was used for the control of the device as well as for the quantification of the peak areas. Chromatographic separation was achieved with a reversed phase column (Agilent Eclipse AAA, 3x 150 mM, 3.5 µm) a guard column (Agilent Eclipse AAA, 4.6 × 12.5 mM, 5 µm) and a gradient using eluent (A) 40 mM NaH<sub>2</sub>PO<sub>4</sub> monohydrate pH 7.8 and eluent (B) MeOH/ACN/MQ (45/45/10, v/v/v). The protocol was run at a flow-rate of 1.2 mL min<sup>-1</sup>, the column oven temperature was set to 40 °C and the injection volume was 10 µL. As most amino acids have no fluorophore in their structure, an in-needle derivatization step was performed using 0.4 M borate buffer, 5 mg/mL ortho-phthalaldehyde (OPA) in 0.4 M borate buffer containing 1% of 3-MPA, 2.5 mg/mL Fmoc and 1 M acetic acid for pH adjustment. In order to guarantee sample quantification despite the derivatization step, every sample was spiked with 25 mM sarcosine in 0.1 M HCl and 25 mM norvaline in 0.1 M HCl as internal standards. Primary amines and norvaline were detected at Ex 340 nm/Em 450 nm and secondary amines and sarcosine were detected at Ex 266 nm/Em 305 nm.

### 1.2.4 In Vitro Biocompatibility Testing of Isolated pLm-111

All *in vitro* experiments were performed with lyophilized pLm-111.



## 1.2.5 Adhesion

### 1.2.5.1 Primary Schwann Cell Isolation

All animals were euthanized according to established protocols, which were approved by the City Government of Vienna in accordance with the Austrian Law and the Guide for the Care and Use of Laboratory Animals as defined by the National Institute of Health.

Prior to Schwann cell isolation, sciatic nerves of adult male Sprague Dawley rats were dissected and kept in PBS on ice. Schwann cell isolation was performed as previously described [31], adapted from Kaekhaw et al. [32]. Cells were cultured in DMEM-D-valine (PAA, Austria), supplemented with 10% FCS, 2 mM L-Glutamine (PAA, Austria), 1% antibiotics (PAA, Austria), N<sub>2</sub> supplement (Invitrogen, Germany), 10 µg/mL bovine pituitary extract and 5 µM forskolin.

### 1.2.5.2 Primary Schwann Cell Adhesion

For the Schwann cell culture, tissue culture plastic (TCP) was coated with poly-L-lysine and/or EHS laminin-111 or pLm-111. Briefly, 96-well plates were incubated with 0.01% (w/v) poly-L-lysine for 15 min at room temperature in a laminar flow-hood. Poly-L-lysine was removed and plates were left to dry for at least 2 h. Subsequently, wells were incubated with EHS laminin-111 or pLm-111 reconstituted in PBS (100 µg/mL) and incubated at 37 °C for 30 min. Laminin-111 solution was removed and plates were washed twice with PBS followed by UV sterilization.

Cell viability of Schwann cells on TCP, poly-L-lysine, EHS laminin-111, pLm-111 or on combinations of poly-L-Lysin with either EHS laminin-111 or pLm-111 was determined using MTT assay. Schwann cells, seeded at a density of  $4 \times 10^3$  cells/cm<sup>2</sup> (n = 18), were incubated with culture medium containing 650 µg/mL MTT [3-(4,5-dimethylthiazol-2-yl)-2,5-diphenyltetrazolium] bromide for 1 h in a cell culture incubator (37 °C, 5% CO<sub>2</sub> and 80% humidity). MTT reagent was discarded and MTT formazan precipitate was dissolved in 100 µL DMSO per well of a 96 well plate by shaking in dark for 20 min. Light absorbance at 550 nm was measured immediately and optical density (OD)

values were corrected for an unspecific background on a microplate reader (Tecan Sunrise; Tecan Switzerland).

Proliferation of Schwann cells on TCP, poly-L-lysine (Lysin), EHS laminin-111, pLm-111 or on combinations of poly-L-Lysin with either EHS laminin-111 or pLm-111 was evaluated using a 5-bromo-2-deoxyuridine uptake assay (BrdU; Cell Proliferation ELISA assay Kit; Roche Diagnostics, Switzerland), according to manufacturer's instructions. Briefly, 96-well plates of all groups were seeded with Schwann cells at a density of  $4 \times 10^3$  cells/cm<sup>2</sup> (n = 18). Medium was changed to Schwann cell medium containing 100 µM BrdU and cells were incubated for 24 h at standard cell culture conditions (37 °C and 5% CO<sub>2</sub>). The culture plates were fixed with FixDenat<sup>®</sup> solution and incubated with anti-BrdU POD antibody solution for 45 min at room temperature. After washing the plate with PBS twice, substrate solution containing tetramethyl benzidine was added for 20 min. The reaction was stopped using 1 M H<sub>2</sub>SO<sub>4</sub> and absorption was measured at 450 nm with 690 nm as reference wavelength on an automatic microplate reader (Tecan Sunrise; Tecan Switzerland).

## 1.2.6 NG 108-15 Outgrowth

NG 108–15 cell lines were purchased from ECACC (#88112302, Salisbury, U.K.) and cultured in DMEM high glucose supplemented with 10% FCS, 1% glutamine and 1% Pen/Strep.

24 well plates were incubated with 250 µL of EHS laminin-111 or pLm-111 at 100 µg/mL and UV sterilized for 30 min. Laminin solutions were removed and 12,000 cells were seeded (6000 cells/cm<sup>2</sup>, n = 12) on TCP, EHS laminin-111, or pLm-111 in medium supplemented with 20 ng/mL human beta neurotrophic growth factor β-NGF (Peprotech, Vienna, Austria) and incubated at 37 °C. Photographs were taken after 24, 48 and 72 h using an epifluorescence microscope (DMI6000B, Leica GmbH, Vienna, Austria). The neurite outgrowth was analyzed as previously described [33]. Briefly, microscopy pictures were processed in a blinded manner with Adobe

Photoshop software by adjusting contrast/brightness. Then the neurite outgrowth was analyzed using AngioSys software (TCS Cellworks, London, UK). The obtained values were further statistically analyzed using Prism 5 (Graphpad, CA, USA).

### 1.2.6.1 Immunostaining

For actin/DAPI staining, the medium was aspirated and cells were washed with PBS before fixation in 4% formaldehyde for 10 min. The cells were washed three times with PBS, stained with Alexa Fluor 488 phalloidin (1:40) (Invitrogen) in the dark for 20 min, and washed two additional times with PBS. Then, DAPI staining (1:1000) for 5 min and two additional washing steps were performed before imaging on an epifluorescence microscope (DMI6000B, Leica GmbH, Vienna, Austria).

## 1.2.7 gfpHUVEC Network Formation

### 1.2.7.1 Human Umbilical Vein Endothelial Cells (HUVEC) Isolation

HUVEC were isolated from umbilical cords of healthy donors with the authorization of the local ethics committee of Upper Austria with written informed consent of the donors and according to established protocols as previously described [34, 35]. Cells (p6-p9) were cultured in EGM-2 medium (Lonza, Basel, Switzerland) supplemented with 5% FCS. Isolated HUVEC were retrovirally infected with expression vectors for fluorescent proteins using the Phoenix Amphi system as described elsewhere [36].

Network formation was investigated using a previously described vasculogenesis assay [37–39]. Briefly, 50  $\mu\text{L}$  of pLm-111, EHS laminin-111, EHS collagen-4 or calf skin collagen-1 were pipetted per well in 96 well plates at two different concentrations of 500  $\mu\text{g}/\text{mL}$  or 1  $\text{mg}/\text{mL}$ , UV sterilized for 30 min and incubated at 37  $^{\circ}\text{C}$  for 2 h. Coating solutions were removed and 15.000 GFP-HUVECs were seeded (40.000 cells/ $\text{cm}^2$ ,  $n = 12$ ) in 100  $\mu\text{L}$  of EGM-2 medium. After 48 h

of cultivation the networks were imaged and analyzed as previously described [33]. Fluorescence microscopic pictures of two independent experiments (different pLm-111 donors) were taken from two different fields per well and processed in a blinded way using Adobe Photoshop software (Adobe Systems, San Jose, USA) by adjusting contrast/brightness. Then, tube formation was analyzed using AngioSys software (TCS Cellworks, London, UK) and the AngioSys values were analyzed using Prism 5 (Graphpad).

## 1.3 Data Analysis

All experimental data is presented as mean  $\pm$  standard deviation (SD) if not stated otherwise. Normal distribution of data was tested with the Kolmogorov–Smirnov test. One-way analysis of variance (ANOVA) with Tukey’s post hoc test was used to calculate statistical significance. For the NG108-15 outgrowth assay, a Two-Way ANOVA with Bonferroni post-test was used. P-values  $<0.05$  were considered statistically significant. All calculations were performed using GraphPad software (GraphPad software, Inc., San Diego, CA, USA).

## 1.4 Results

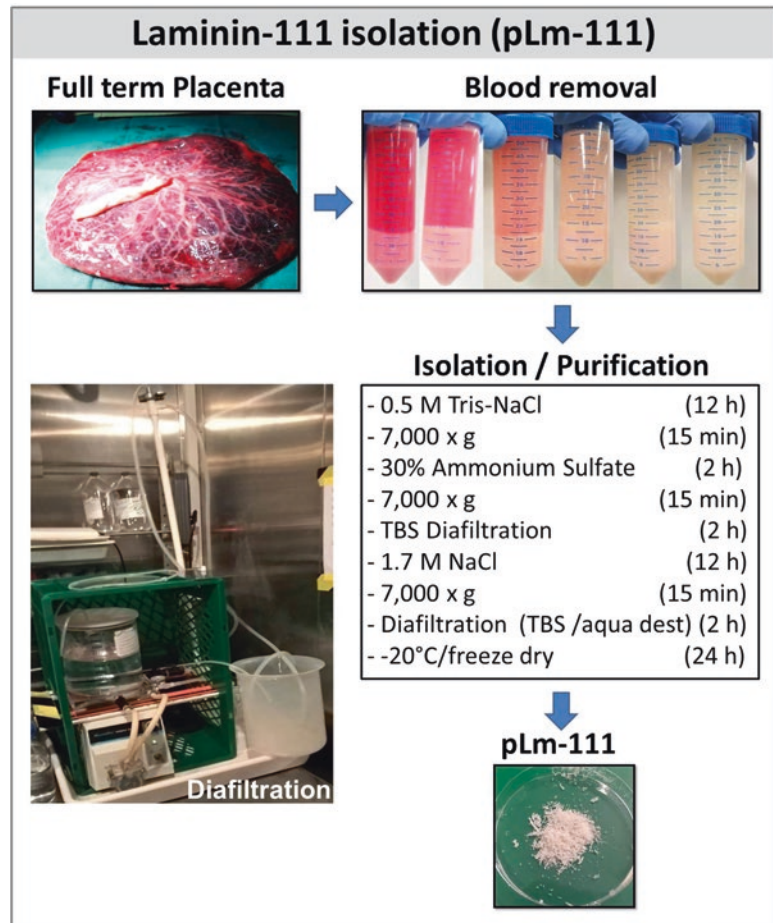
### 1.4.1 Extraction of pLm-111 from Placenta

#### 1.4.1.1 Yield and Purity

We have developed an effective method for isolating pLm-111 by extraction with a Tris-NaCl buffer combined with non-protein-denaturing ammonium sulfate precipitation and rapid tangential flow filtration steps.

A detailed flow chart of the method is shown in Fig. 1.1. After defrosting, the chorionic membrane was removed and basal villous tissue was isolated. Major blood components were removed using PBS buffer/aqua dest. Thereafter, collagen remnants were removed and the residual laminin-111 diafiltrated against physiologic TBS buffer. The mean amount of *pLm-111* after isolation was

**Fig. 1.1** Graphical overview of steps required for the introduced rapid and efficient isolation of laminin-111 from human placenta (pLm-111). *Full term placenta* is dissected free of amnion/chorion followed by centrifugation to *remove blood components*, and further *isolation/purification* steps (salt-precipitation and diafiltration) to separate laminin-111. Final freeze-drying leads to powdery laminin-111 isolates



175 ± 35 mg/100 g wet weight basal tissue (n = 7).

By the use of Dot blot and monoclonal antibodies we assessed the presence of native laminin-111 in TBS buffer (Fig. 1.2a). After diafiltration and freeze-drying, laminin-111 is denatured and is therefore not detectable by the used monoclonal antibody (Fig. 1.2b). By using SDS-PAGE gels stained with Coomassie blue we assessed major protein bands in lyophilized pLm-111 (Fig. 1.2c) between 200 and 300 kDa. In western blot analysis using polyclonal antibodies, laminin-111 bands were clearly detected and matching with the major bands from the SDS-PAGE (Fig. 1.2d).

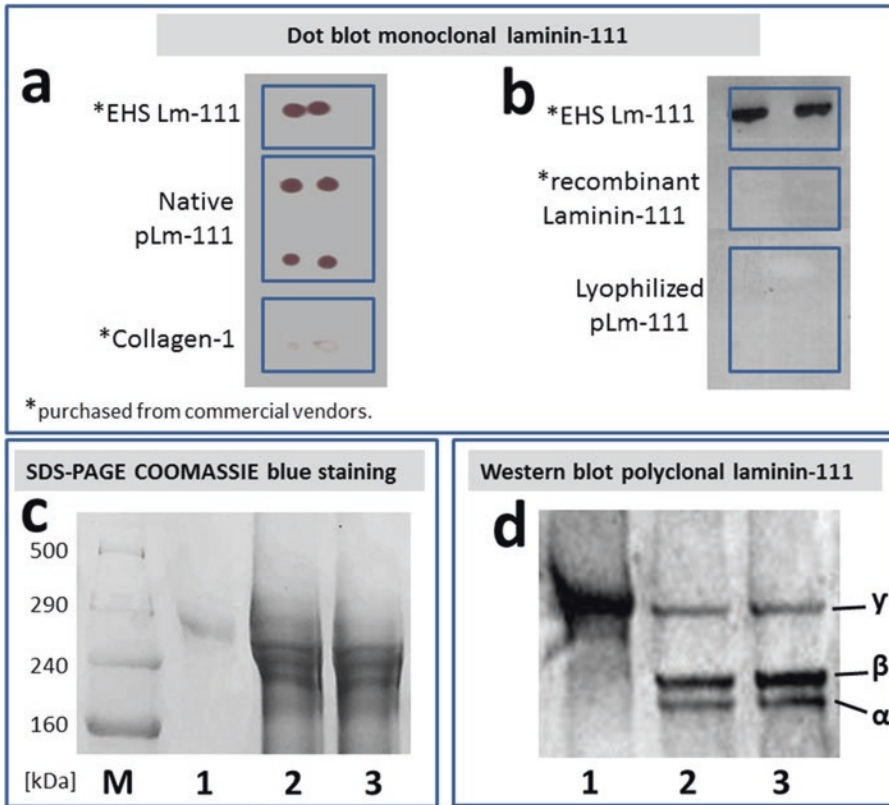
Table 1.1 lists the amino acid composition of human laminin-111  $\alpha$ ,  $\beta$  and  $\gamma$ -chains ([www.uni-prot.org](http://www.uni-prot.org)), pLm-111 from three different donors

and the amino-acid composition of EHS collagen-4 and human collagen-4 from placenta.

## 1.4.2 Biocompatibility of pLm-111

### 1.4.2.1 Schwann Cell Viability

The MTT assay was used to analyze Schwann cell viability on pLm-111 compared to EHS laminin-111. Cell viability on all three single coatings was significantly increased compared to the TCP control group (OD values: lysin 1536 ± 220, EHS laminin-111 1776 ± 195, pLm-111 1763 ± 216, TCP 503 ± 42, n = 18, Fig. 1.3a) but no significant difference among the three coating groups could be detected (p = 0.78). Schwann cells cultured on both combined coatings of lysin and EHS laminin-111 or lysine and pLm-111



**Fig. 1.2** Isolated laminin-111 characterized by (a) Representative immunoblot of duplicates of 2  $\mu$ g of purchased Engelbreth-Holmes Sarcoma (EHS) laminin-111, isolated native pLm-111 from two independent donors, purchased collagen-1 from rat tail against a monoclonal laminin-111 antibody. (b) Representative immunoblot showing duplicates of 2  $\mu$ g of cell culture laminin-111, EHS laminin-111 or lyophilized pLm-111 from two independent donors against a polyclonal laminin-111 anti-

body. (c) Coomassie blue stained 3–8% SDS-polyacrylamide gel showing marker (M) (HiMark, Life Technologies), (1) EHS laminin-111 and (2, 3) two independent lyophilized pLm-111 isolates from two different donors. (d) Corresponding immunoblot showing 20  $\mu$ g of (1) EHS laminin-111 and (2, 3) two independent lyophilized pLm-111 isolates from two independent donors loaded per lane and a primary antibody against polyclonal laminin-111

showed increased viability (between 33% and 46%) compared to the single coatings or the TCP control. There were no significant differences between lysin/EHS laminin-111 and lysin/pLm-111 (OD values: lysin/EHS laminin-111  $2285 \pm 230$ , lysin/pLm-111  $2362 \pm 216$ ,  $p = 0.75$ ).

The results of the proliferation analysis were similar to the viability assays. Schwann cells show higher proliferation on all three single coatings, compared to TCP (OD values: Lysin  $3681 \pm 512$ , EHS Laminin-111  $3722 \pm 470$ , pLm-1,113,822  $\pm 474$ , TCP  $1871 \pm 122$ ,  $n = 18$ , Fig. 1.3b). No significant difference could be observed between the single coating groups

( $p = 0.87$ ). Proliferation on combined coating of lysine and EHS laminin-111 or lysine and pLm-111 resulted in increased proliferation (between 23% and 33%) compared to the single coatings or the TCP but no differences between EHS laminin-111 and pLm-111 were detectable (OD values: EHS Laminin-111  $4938 \pm 297$ , pLm-111  $5034 \pm 381$ ,  $p = 0.79$ ).

#### 1.4.2.2 NG 108-15 Outgrowth

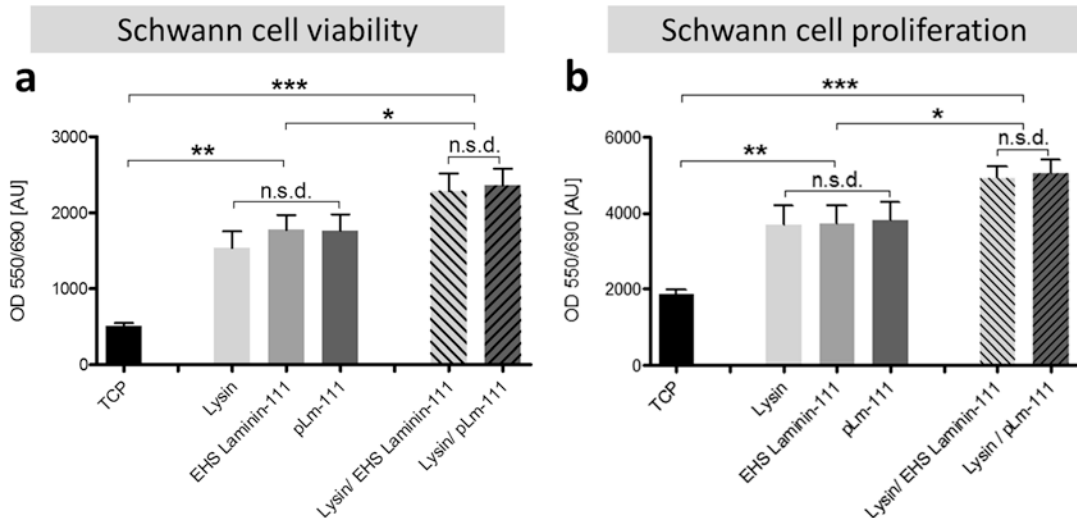
An outgrowth assay was used to analyze NG 108–15 cells on pLm-111 compared with EHS laminin-111 (Fig. 1.4). After 24 h, the total neurite outgrowth (TCP  $86 \pm 3 \mu\text{m}$ , EHS

**Table 1.1** Amino acid composition of pLM-111 (mean  $\pm$  SD) from human placenta (Residues per 1,000 total amino acids residues)

Amino acids	Human laminin-111 <sup>a</sup>				pLM-111 (mean $\pm$ SD, n = 3)	EHS tumor collagen-4 [57]	Human collagen-4 [58]
	$\alpha$ laminin-111	$\beta$ laminin-111	$\gamma$ laminin-111				
Alanine	61.4	66.6	86.4	73.1 $\pm$ 1.4	45	33.5	
Arginine	50.1	49.3	59.7	48.1 $\pm$ 2.8	30	30.5	
Aspartic acid	102.7	110.9	128	76.1 $\pm$ 5	52	53.5	
Cysteine	52.3	71.1	62.2	51.6 $\pm$ 5.2	7	–	
Glutamic acid	131.7	136.1	129.9	94.1 $\pm$ 5.1	103	100.5	
Glycine	80.3	70.5	70.2	105.4 $\pm$ 10.9	280	339	
Histidine	28.7	21.8	16.8	16.0 $\pm$ 0.8	11	7.6	
Hydroxyproline	–	–	–	16.1 $\pm$ 2.4	102	97	
Isoleucine	38.7	39.2	30.5	39.6 $\pm$ 1.6	25	30.5	
Leucine	91	76.7	73.3	72.5 $\pm$ 3.5	54	52.5	
Lysine	44.7	47.6	50.3	46.2 $\pm$ 4.6	49	58.6	
Methionine	12.6	17.9	13.7	51.1 $\pm$ 8.7	12	12	
Phenylalanine	27.1	30.8	30.5	28.5 $\pm$ 1.3	31	30	
Proline	46	48.7	44.1	57.8 $\pm$ 0.7	66	87.5	
Serine	76.9	67.2	61.5	59.6 $\pm$ 2.4	60	12.5	
Threonine	53.9	52.1	60.3	49.1 $\pm$ 2.1	34	17	
Tryptophane	7.6	7.3	6.8	4.4 $\pm$ 1.3	–	–	
Tyrosine	30.9	31.4	28	26 $\pm$ 1.6	9	9.8	
Valine	63.6	54.9	47.9	84.6 $\pm$ 2.9	30	28	
Total	1,000	1,000	1,000	1,000	1,000	1,000	

Table contains amino acid analysis of pLM-111 isolates (n = 3) and reference values for human laminin-111, EHS tumor collagen 4 and human collagen 4 as control

<sup>a</sup>amino acid quantification according to [www.uniprot.org](http://www.uniprot.org)



**Fig. 1.3** Schwann cell viability (MTT assay) and proliferation (BrdU assay) 24 h after seeding on tissue culture plastic (TCP) compared to EHS laminin-111 and pLm-111 coated wells (100  $\mu\text{g}/\text{mL}$ ), as well as poly-L-lysine/EHS laminin-111 and poly-L-lysine/pLm-111. Data is

presented as mean + SD; significance tested with 1-way ANOVA followed by Tukey's post test; \*, \*\* and \*\*\* indicates significant difference of  $p < 0.05$ ,  $0.01$  and  $0.005$ , respectively;  $n = 18$

laminin-111,  $268 \pm 13 \mu\text{m}$ , pLm-111,  $519 \pm 16 \mu\text{m}$ ,  $n = 12$ ) and the number of tubules (TCP  $5 \pm 1$ , EHS laminin-111  $11 \pm 3$ , pLm-111  $20 \pm 2$ ,  $n = 12$ ) on pLm-111 were significantly increased compared to the TCP control and EHS laminin-111, but no significant difference between EHS laminin-111 and TCP could be detected. After 48 h, the total neurite outgrowth (TCP  $71 \pm 6 \mu\text{m}$ , EHS laminin-111,  $590 \pm 110 \mu\text{m}$ , pLm-111,  $848 \pm 240 \mu\text{m}$ ,  $n = 12$ ) and the number of tubules (TCP  $3 \pm 1$ , EHS laminin-111  $21 \pm 5$ , pLm-111  $33 \pm 9$ ,  $n = 12$ ) on both coatings were significantly increased compared to the TCP control, but no significant difference between EHS laminin-111 and pLm-111 could be detected. After 72 h, the total neurite outgrowth (TCP  $96.9 \pm 1 \mu\text{m}$ , EHS laminin-111,  $382 \pm 4 \mu\text{m}$ , pLm-111  $1024 \pm 6 \mu\text{m}$ ,  $n = 12$ ) and the number of tubules (TCP  $6 \pm 1$ , EHS laminin-111  $20 \pm 4$ , pLm-111  $47 \pm 5$ ,  $n = 12$ ) on pLm-111 were significantly increased compared to EHS laminin-111.

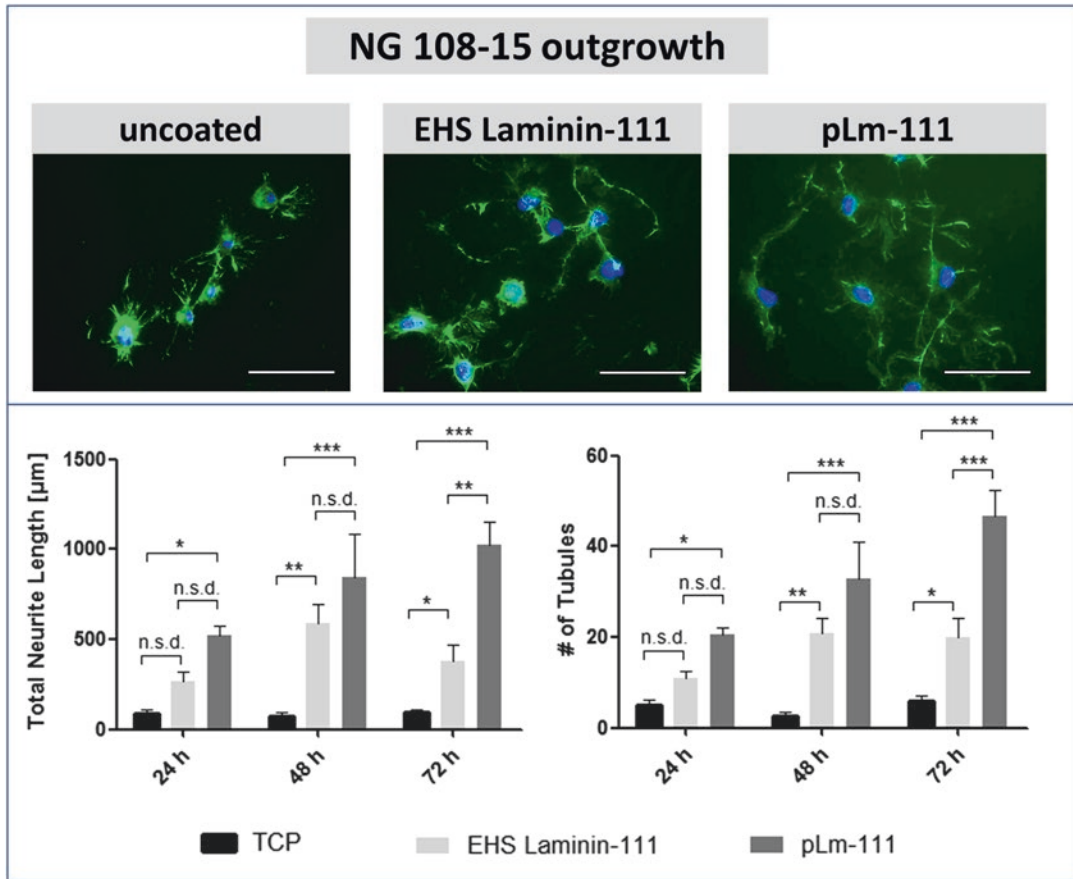
#### 1.4.2.3 HUVEC Network Formation

A well-established vasculogenesis assay was used to analyze gfpHUVEC with fully supplemented EGM-2 medium on pLm-111 from two

independent isolations (donors D1; D2) and compared with EHS laminin-111 (Fig. 1.5). After 24 h, a cell network was formed on EHS laminin-111 and pLm-111 at 1 mg/mL but neither on EHS collagen-4 nor on lower pLm-111 coating concentrations or TCP. After 48 h, the networks were analyzed. There was no significant difference between the number of tubules (EHS laminin-111,  $134 \pm 17$ , pLm-111 D1  $124 \pm 13$ ; D2  $157 \pm 18$ ,  $n = 12$ ) or the total tubule length (EHS laminin-111  $35 \pm 6 \text{ mM}$ , pLm-111 D1  $37 \pm 2$ ; D2  $42 \pm 5 \text{ mM}$ ,  $p < 0.5$ ,  $n = 12$ ) between both laminin-111 coatings. The mean tubule length (EHS laminin-111,  $240 \pm 7 \mu\text{m}$ , pLm-111 D1  $315 \pm 17$ ; D2  $300 \pm 13 \mu\text{m}$ ,  $n = 12$ ) and the number of junctions (EHS laminin-111,  $284 \pm 28$ , pLm-111 D1  $410 \pm 42$ ; D2  $463 \pm 47$ ,  $n = 12$ ) were significantly increased on pLm-111 compared to EHS laminin-111.

## 1.5 Discussion

Although laminin-111 from EHS tissue was already described more than 30 years ago, about 20,000 laminin publications in 2016 proved the ongoing interest in this key protein [2].



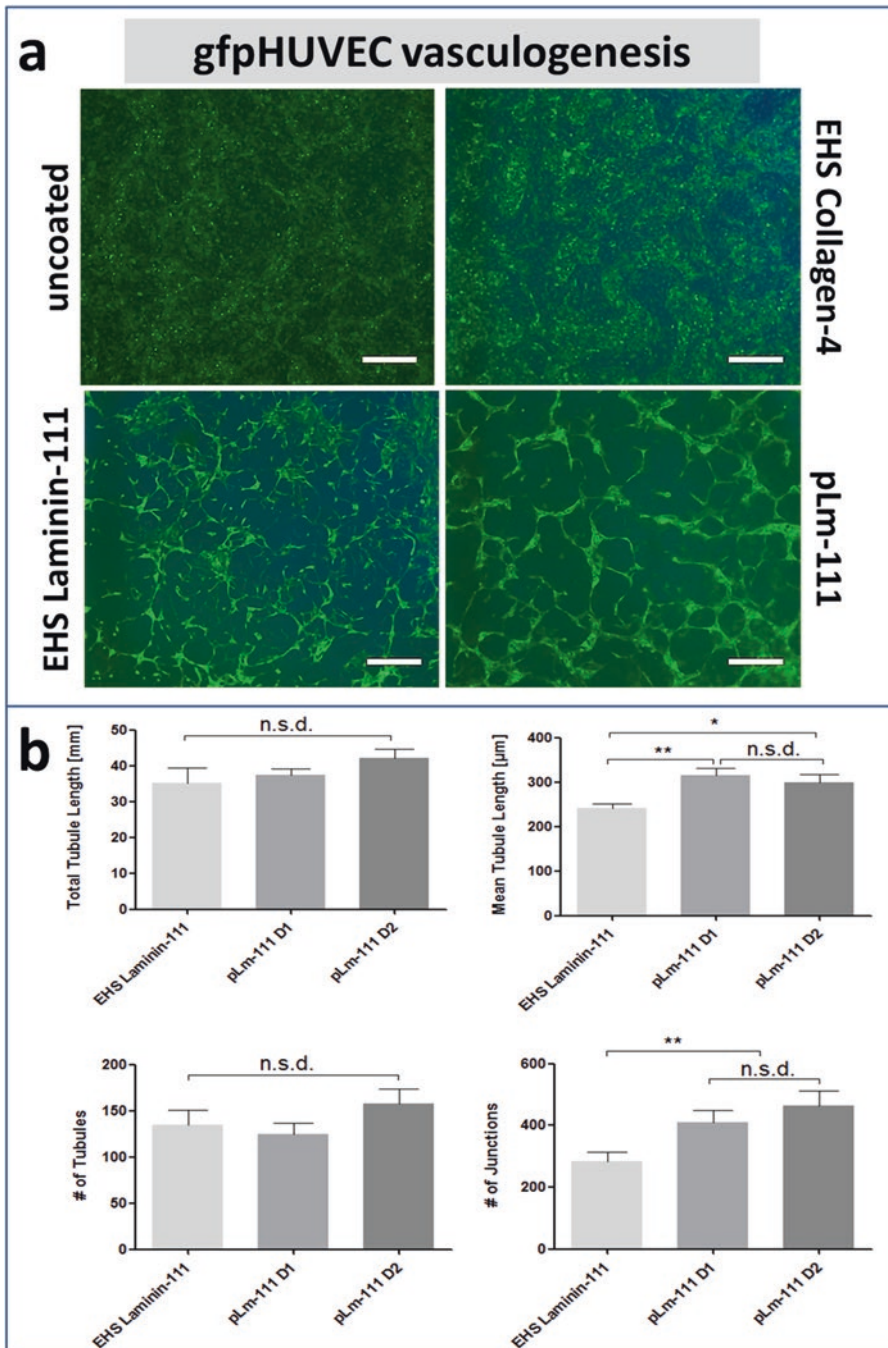
**Fig. 1.4** Upper panel: fluorescence micrographs of phalloidin (green) and DAPI (blue) stained NG 108-15 cells cultivated on tissue culture plastic (TCP), EHS laminin-111 or pLm-111 at concentrations of 100  $\mu\text{g}/\text{mL}$ ; Scale bars = 100  $\mu\text{m}$ ; Lower panel: analysis of the neurite outgrowth: total neural length and number of tubules per

field of view of NG108 cells after 24, 48 and 72 h of cultivation. Data is presented as mean + SD; significance tested with 2-way ANOVA followed by Bonferroni post test; \* and \*\* indicate significant difference of  $p < 0.05$ , 0.01 and 0.005, respectively;  $n = 12$

Laminin-111 is naturally present during embryonic development and has been shown to be a useful biomaterial for the cultivation of stem cells [7, 26, 40, 41]. Beside, it has been used for various applications in tissue engineering and regenerative medicine, eg. cultivation of neuronal cells [7, 11], angiogenesis studies [5, 13], or wound healing studies [6, 15]. A robust method for culturing human pluripotent stem cells under xeno-free conditions is an important tool for stem cell research and for the development of regenerative medicine [42]. Especially in the research of muscle tissue biology, laminin-111 has been shown to improve skeletal muscle stem cell quality and function [43]. In this regard, *Goudenne*

*et al.* could demonstrate that intramuscular injection of laminin-111 increased muscle strength and resistance in mice and could potentially be used to treat Duchenne muscular dystrophy [44].

Regarding clinical applicability, caution must be taken regarding the tissue origin of the extracted biomaterials. Proteins extracted from xenogenic tumor tissues are not suitable for clinical applications. Non-human proteins are reported to provoke immune responses in patients [45], and carry the risk of xenogenic disease transmission [46, 47]. Therefore, human sources are regarded as the best option for the generation of medicinal products [30]. In this regard, human placenta is a highly vascularized organ [48], and



**Fig. 1.5** pLm-111 at higher concentrations promotes vasculogenesis using gfpHUVeC (a) Fluorescence micrographs of gfpHUVeC 48 h after seeding on EHS laminin-111, pLm-111, or EHS collagen-4 at concentrations of 1 mg/mL. Scale bar = 400 µm. (b) Network characteristics (total/mean tube length, number of junctions/tubules) of

gfpHUVeC, seeded on EHS laminin-111 or pLm-111 from two independent donors (pLm-111 D1; D2). Data is presented as mean + SD; significance tested with 1-way ANOVA followed by Tukey's post test; \*, \*\* and \*\*\* indicates significant difference of  $p < 0.05$ ,  $0.01$  and  $0.005$ , respectively;  $n = 12$



it therefore harbors high amounts of basal membrane proteins [49]. Human placenta tissue is available in sufficient amounts and consistent quality for large industrial scale processes. Moreover, it has been shown to exhibit excellent anti-inflammatory and antibacterial properties, [50] which has been favoring its use to treat non-healing wounds for decades [51–53].

Commercial success of a medicinal product is dependent on the balance of efficacy and cost-effectiveness [54]. Several studies have been performed to isolate laminin isoforms from placenta using salt precipitation or pepsin digestion and chromatography [20–24]. However, the protocols to isolate laminin-111 described in the literature to date are time consuming, work intensive and show low extraction efficiency. By modifying the protocols described in literature, we were able to (1) significantly increase the extraction efficiency of laminin-111 yield from placenta tissue compared to reported isolation protocols and (2) to shorten the isolation time from almost 2 weeks to a total of only 4 processing days (Fig. 1.1) [20–22]. In our protocols, tangential flow filtration instead of dialysis was used since it was less time-consuming and further allows easy and rapid concentration of laminin isolates. Collagen-4 remnants were removed by precipitation with 1.7 M NaCl [18].

Native laminin-111 from human placenta was assessed using Dot Blots. Residual salts from TBS buffer were removed by tangential flow filtration against aqua dest and the proteins were freeze-dried to make process ability and storage easier. On the average,  $175 \pm 35$  mg of laminin-111 was isolated from 100 g of placenta tissue using the isolation protocol described here. In western blot analysis for laminin-111 and SDS-PAGE analysis, two bands around 200 kDa were clearly visible, which represent the  $\alpha 1$  and  $\beta 1$  chains, as described in literature [1, 19, 55]. Interestingly, a third protein band was visible with a molecular weight of approximately 300 kDa in both the pLm-111 isolates and in EHS laminin used as control. This high molecular weight band most likely represents the reduced  $\gamma$ -chain, which usually appears around 400 kDa [2, 19]. The HPLC- based amino acid

quantification analysis is consistent with the data from [www.uniprot.com](http://www.uniprot.com), however low amounts of hydroxyproline were still detectable. Most probably, these could be attributed to impurities of the isolate with collagen-4, another major component of BMs beside laminin [55].

Freeze-dried pLm-111 was used as a coating substrate and compared to xenogenic standard proteins using Schwann cells. These experiments indicated that the pLm-111 isolates show bioactivity comparable to commercially available xenogenic proteins. Furthermore, pLm-111 promoted rapid attachment of various cells including Schwann cells, HUVEC or NIH3T3 fibroblasts (data not shown). NG 108-15 cells rapidly developed a complex neurite outgrowth on pLm-111 with at least similar effectiveness compared to xenogenic proteins.

In addition, laminin-111 is the principal factor for endothelial cells to differentiate into interconnected tubules on Matrigel, a laminin-111-rich (around 70%) gel, extracted from basement membrane tumor materials from mice [56]. However, beside its tumorigenic origin, Matrigel is a heterogenic mixture of various extracellular matrix proteins and pro-angiogenic growth factors. For potential clinical applications, a single protein would be an advantageous material. EHS laminin-111 at concentrations of 1 mg/mL promotes the differentiation of gfpHUVEC into interconnected networks, but so does pLm-111 from human origin with at least similar performance (total/mean tube length, number of tubules/junctions).

The 2D cell culture experiments described above have been performed with freeze-dried laminin-111 stored at  $-20$  °C for at least 6 months. Moreover, in other *in vitro* experiments we have used the isolated lyophilized pLm-111 materials after storing them for up to 18 months without noticing alterations in stability or activity (data not shown).

To conclude, we could establish a simple, rapid and effective method to isolate laminin-111 from human placenta. This pLm-111 clearly demonstrates its applicability as a biomaterial of human origin with strong bioactive potential for a broad spectrum of *in vitro* and potentially *in vivo* tissue engineering approaches.

## 1.6 Conclusion

Summarizing, we established an effective method for isolating laminin-111 from human placenta, a clinical waste material. Laminins are routinely used in cell culture to on the one hand improve attachment of cells (eg Schwann cells), and on the other hand induce specific functions (eg HUVEC). The availability of this potent and versatile protein offers new, fully human, approaches for neuronal and endothelial *in vitro* tissue engineering and may provide a new platform technology for clinical use with an increased overall safety profile for patients.

**Acknowledgement** The authors acknowledge Red Cross Blood Transfusion Service, Linz, Upper Austria for providing the placenta tissue, Dr. Wolfgang Holthöner, Severin Mühleder, MSc, for providing the HUVEC and Mag. med. vet. James Ferguson for reviewing the manuscript. This work was partially funded by the City of Vienna Competence Team Tissue Engineering Signaltissue (MA23 Project-#18-08).

**Disclosure Statement** None.

## References

- Aumailley M (2013) The laminin family. *Cell Adhes Migr* 7:48–55
- Simon-Assmann (2013) The laminin family. *Cell Adhes Migr* 7:44–47
- Eklblom P, Lonai P, Talts JF (2003) Expression and biological role of laminin-1. *Matrix Biol* 22:35–47
- Hozumi K et al (2012) Reconstitution of laminin-111 biological activity using multiple peptide coupled to chitosan scaffolds. *Biomaterials* 33:4241–4250
- Ponce ML, Kleinman HK (2003) Identification of redundant angiogenic sites in laminin  $\alpha$ 1 and  $\gamma$ 1 chains. *Exp Cell Res* 285:189–195
- Iorio V, Troughton LD, Hamill KJ (2015) Laminins: roles and utility in wound repair. *Adv Wound Care* 4:250–263
- Flanagan L a, Rebaza LM, Derzic S, Schwartz PH, Monuki ES (2006) Regulation of human neural precursor cells by laminin and integrins. *J Neurosci Res* 83:845–856
- Madison R, da Silva CF, Dikkes P, Chiu TH, Sidman RL (1985) Increased rate of peripheral nerve regeneration using bioresorbable nerve guides and a laminin-containing gel. *Exp Neurol* 88:767–772
- Bilozur ME, Hay ED (1988) Neural crest migration in 3D extracellular matrix utilizes laminin, fibronectin, or collagen. *Dev Biol* 125:19–33
- Rangappa N, Romero A, Nelson KD, Eberhart RC, Smith GM (2000) Laminin-coated poly(L-lactide) filaments induce robust neurite growth while providing directional orientation. *J Biomed Mater Res* 51:625–634
- Biernaskie J et al (2007) Skin-derived precursors generate myelinating Schwann cells that promote remyelination and functional recovery after contusion spinal cord injury. *J Neurosci* 27:9545–9559
- Kidd KR, Williams SK (2004) Laminin-5-enriched extracellular matrix accelerates angiogenesis and neovascularization in association with ePTFE. *J Biomed Mater Res A* 69:294–304
- Malinda KM, Wysocki AB, Koblinski JE, Kleinman HK, Ponce ML (2008) Angiogenic laminin-derived peptides stimulate wound healing. *Int J Biochem Cell Biol* 40:2771–2780
- Min SK et al (2010) The effect of a laminin-5-derived peptide coated onto chitin microfibers on re-epithelialization in early-stage wound healing. *Biomaterials* 31:4725–4730
- Hashimoto T, Suzuki Y, Tanihara M, Kakimaru Y, Suzuki K (2004) Development of alginate wound dressings linked with hybrid peptides derived from laminin and elastin. *Biomaterials* 25:1407–1414
- Gjorevski N et al (2016) Designer matrices for intestinal stem cell and organoid culture. *Nat Publ Gr* 539:560–564
- Horejs C-M et al (2014) Biologically-active laminin-111 fragment that modulates the epithelial-to-mesenchymal transition in embryonic stem cells. *Proc Natl Acad Sci USA* 111:5908–5913
- Timpl R, Rohde H, Robey PG, Rennard SI, Foidart JM, Martin GR (1979) Laminin-A glycoprotein from basement membranes. *Biochemistry* 21:6188–6193
- Aumailley M, Smyth N (1998) The role of laminins in basement membrane function. *J Anat* 193(Pt 1):1–21
- Brown JC, Spragg JH, Wheeler GN, Taylor PW (1990) Identification of the B1 and B2 subunits of human placental laminin and rat parietal-yolk-sac laminin using antisera specific for murine laminin-beta-galactosidase fusion proteins. *Biochem J* 270:463–468
- Brown JC, Wiedemann H, Timpl R (1994) Protein binding and cell adhesion properties of two laminin isoforms (AmB1eB2e, AmB1sB2e) from human placenta. *J Cell Sci* 107(Pt 1):329–338
- Wewer U et al (1983) Human laminin isolated in a nearly intact, biologically active form from placenta by limited proteolysis. *J Biol Chem* 258(20):12654–12660
- Engvall E, Earwicker D, Haaparanta T, Ruoslahti E, Sanes JR (1990) Distribution and isolation of four laminin variants; tissue restricted distribution of heterotrimers assembled from five different subunits. *Cell Regul* 1:731–740
- Champlaud MF et al (2000) Posttranslational modifications and beta/gamma chain associations of human laminin alpha1 and laminin alpha5 chains: purification of laminin-3 from placenta. *Exp Cell Res* 259:326–335

25. Cameron K et al (2015) Recombinant laminins drive the differentiation and self-organization of hESC-derived hepatocytes. *Stem Cell Rep* 5:1250–1262
26. Miyazaki T et al (2008) Recombinant human laminin isoforms can support the undifferentiated growth of human embryonic stem cells. *Biochem Biophys Res Commun* 375:27–32
27. Wondimu Z et al (2006) Characterization of commercial laminin preparations from human placenta in comparison to recombinant laminins 2 ( $\alpha 2\beta 1\gamma 1$ ), 8 ( $\alpha 4\beta 1\gamma 1$ ), 10 ( $\alpha 5\beta 1\gamma 1$ ). *Matrix Biol* 25:89–93
28. Weihs AM et al (2014) Shock wave treatment enhances cell proliferation and improves wound healing by ATP release-coupled extracellular signal-regulated kinase (ERK) activation. *J Biol Chem* 289:27090–27104
29. Duhamel RC (1983) Differential staining of collagens and non-collagens with Coomassie brilliant blue G and R. *Coll Relat Res* 3:195–204
30. Hackethal J et al (2017) An effective method of *Atelocollagen* type 1/3 isolation from human placenta and its *in vitro* characterization in two-dimensional and three-dimensional cell culture applications. *Tissue Eng Part C Methods* 23:274–285
31. Schuh CMAP et al (2016) Extracorporeal shockwave treatment: a novel tool to improve Schwann cell isolation and culture. *Cytotherapy* 18:760–770
32. Kaewkhaw R, Scutt AM, Haycock JW (2012) Integrated culture and purification of rat Schwann cells from freshly isolated adult tissue. *Nat Protoc* 7:1996–2004
33. Holthoner W et al (2012) Adipose-derived stem cells induce vascular tube formation of outgrowth endothelial cells in a fibrin matrix. *J Tissue Eng Regen Med* 4:524–531
34. Rohringer S et al (2017) The impact of wavelengths of LED light-therapy on endothelial cells. *Sci Rep* 7:1–11
35. Holthoner W et al (2017) Endothelial cell-derived extracellular vesicles size-dependently exert pro-coagulant activity detected by thromboelastometry. *Sci Rep* 7:1–9
36. Knezevic L et al (2017) Engineering blood and lymphatic microvascular networks in fibrin matrices. *Front Bioeng Biotechnol* 5:1–12
37. Arnaoutova I, Kleinman HK (2010) In vitro angiogenesis: endothelial cell tube formation on gelled basement membrane extract. *Nat Protoc* 5:628–635
38. Uriel S et al (2009) Extraction and assembly of tissue-derived gels for cell culture and tissue engineering. *Tissue Eng Part C Methods* 15:309–321
39. Goodwin AM (2007) In vitro assays of angiogenesis for assessment of angiogenic and anti-angiogenic agents. *Microvasc Res* 74:172–183
40. Sorkio A et al (2014) Structure and barrier properties of human embryonic stem cell-derived retinal pigment epithelial cells are affected by extracellular matrix protein coating. *Tissue Eng Part A* 20:622–634
41. Takayama K et al (2013) Long-term self-renewal of human ES/iPS-derived hepatoblast-like cells on human laminin 111-coated dishes. *Stem Cell Rep* 1:332–335
42. Rodin S, Antonsson L, Hovatta O, Tryggvason K (2014) Monolayer culturing and cloning of human pluripotent stem cells on laminin-521–based matrices under xeno-free and chemically defined conditions. *Nat Protoc* 9:2354–2368
43. Zou K, DeLisio M (2014) Laminin-111 improves skeletal muscle stem cell quantity and function following eccentric exercise. *Stem Cells Transl Med* 3:1013–1022
44. Goudenege S et al (2010) Laminin-111: a potential therapeutic agent for Duchenne muscular dystrophy. *Mol Ther* 18:2155–2163
45. Flynn L, Hrabchak C, Woodhouse KA (2006) Biological skin substitutes for wound cover and closure. *Expert Rev Med Devices* 3(3):1–20
46. Pacak C a, MacKay A, Cowan DB (2014) An improved method for the preparation of Type I collagen from skin. *J Vis Exp* 83:e51011
47. Browne S, Zeugolis DI, Pandit A (2013) Collagen: finding a solution for the source. *Tissue Eng Part A* 19:1491–1494
48. Schneider KH et al (2016) Decellularized human placenta chorion matrix as a favorable source of small-diameter vascular grafts. *Acta Biomater* 29:125–134
49. Wang Y, Zhao S (2010) *Vascular biology of the placenta*, vol 2. Morgan & Claypool LIFE Sciences, San Rafael, p 1
50. Lobo SE et al (2016) The placenta as an organ and a source of stem cells and extracellular matrix: a review. *Cells Tiss Org* 270:239–252
51. Burgos H, Herd A, Bennett JP (1989) Placental angiogenic and growth factors in the treatment of chronic varicose ulcers: preliminary communication. *J R Soc Med* 82:598–599
52. Shukla VK, Rasheed M a, Kumar M, Gupta SK, Pandey SS (2004) A trial to determine the role of placental extract in the treatment of chronic non-healing wounds. *J Wound Care* 13:177–179
53. Navadiya SK, Vaghani YL, Patel MP (2012) Study of topical placental extract versus povodine iodine and saline dressing in various diabetic wounds. *Nat J Med Res* 2:411–413
54. Place ES, Evans ND, Stevens MM (2009) Complexity in biomaterials for tissue engineering. *Nat Mater* 8:457–470
55. Kleinman HK et al (1982) Isolation and characterization of type IV procollagen, laminin, and heparan sulfate proteoglycan from the EHS sarcoma. *Biochemistry* 21:6188–6193
56. Kubota Y, Kleinman HK, Martin GR, Lawley TJ (1988) Role of laminin and basement membrane in the morphological differentiation of human endothelial cells into capillary-like structures. *J Cell Biol* 107:1589–1598
57. Timpl R, Martin GR, Bruckner P, Wick G, Wiedemann H (1978) Nature of the collagenous protein in a tumor basement membrane. *Eur J Biochem* 84:43–52
58. MacWright RS, Benson V a, Lovello KT, van der Rest M, Fietzek PP (1983) Isolation and characterization of pepsin-solubilized human basement membrane (type IV) collagen peptides. *Biochemistry* 22:4940–4948



# A Novel Strategy for Simple and Robust Expansion of Human Pluripotent Stem Cells Using Botulinum Hemagglutinin

Mee-Hae Kim and Masahiro Kino-oka

## Abstract

Clinical and industrial application of human pluripotent stem cells (hPSCs) has been hindered by the lack of robust strategies to sustain cultures in an undifferentiated state. Here, we describe a simple and robust method to culture and propagate hPSCs, which we anticipate will remove major roadblocks in investigating the basic properties of undifferentiated hPSCs and accelerate cell-based manufacturing. We also provide an overview of the use of botulinum hemagglutinin, an inhibitor of E-cadherin, to maintain and expand various hPSC lines in an undifferentiated state in different culture conditions. Hemagglutinin selectively removes cells that have lost the undifferentiated state, dissociates aggregates *in situ*, and is easy to use, scalable, and reproducible.

## Keywords

Human pluripotent stem cells · Botulinum hemagglutinin · E-cadherin disruption · Removal of differentiated cells · Undifferentiated state · High-density culture · Suspension culture

## 2.1 Introduction

Human pluripotent stem cells (hPSCs), including human embryonic stem cells (hESCs) and human induced pluripotent stem cells (hiPSCs), hold great clinical and industrial potential, because of unlimited self-renewal in culture and capacity to differentiate into any cell type [18, 44, 45]. Although methods to optimize hPSC expansion and differentiation have advanced considerably, efficiency, reproducibility, and product quality are ongoing challenges [14].

In two-dimensional monolayer culture, hiPSCs spontaneously lose the undifferentiated state, *i.e.*, deviate from the undifferentiated state, dramatically transforming into large, flat cells [15–17] that gradually take over the colony with passage, and eventually the entire culture vessel. The nature of these cells remains unclear; for example, it is not known whether expression of lineage markers in these cells is only sporadic or a coherent departure from pluripotency. Although spontaneous loss of the undifferentiated state is expected and signifies pluripotency, it may interfere with culture maintenance and intended use if left uncontrolled. Thus, several strategies have been proposed to eliminate these cells based on morphological features [35, 48]. However, as morphological analysis is subjective, industrial-scale cell production would probably require methods independent of individual experts.

In conventional three-dimensional suspension culture, hiPSCs form aggregates that grow in size

M.-H. Kim · M. Kino-oka (✉)  
Department of Biotechnology, Graduate School  
of Engineering, Osaka University, Suita, Osaka, Japan  
e-mail: [mh-kim@bio.eng.osaka-u.ac.jp](mailto:mh-kim@bio.eng.osaka-u.ac.jp);  
[kino-oka@bio.eng.osaka-u.ac.jp](mailto:kino-oka@bio.eng.osaka-u.ac.jp)

over time [1, 4, 27, 34]. However, these aggregates also deposit a collagen-rich shell that, along with mass transport limitations, impedes the delivery of oxygen and essential nutrients, especially in larger aggregates of highly metabolically active cells, and results in necrosis and differentiation [46, 50]. To address this issue, alternative methods were recently described [1, 2, 4], and stirred culture systems such as spinner flasks and stirred-tank bioreactors are also widely used [2, 11, 29, 32, 33, 52]. In addition, several factors such as inoculation density, medium composition, and culture conditions can be manipulated as needed. Nevertheless, lack of understanding of the nature of hPSC aggregates in suspension culture, and of a scalable method for long-term propagation, limits usefulness.

Considering the biological differences between undifferentiated cells and deviated cells in monolayers, as well as physiological changes during aggregate growth in suspension, we hypothesized that disruption of the epithelial barrier may facilitate the maintenance and expansion of undifferentiated cells. To this end, *Clostridium botulinum* hemagglutinin, a component of the large botulinum neurotoxin complex that directly binds E-cadherin and disrupts cell–cell adhesion at adherens junctions [23, 40–42], may be useful.

In this chapter, we first introduce fundamental mechanisms related to the maintenance and expansion of undifferentiated hiPSCs, as inferred from morphological and biological features. We then review recent advances in hPSC culture strategies, as well as in experimental approaches to investigate hPSC physiology, with an emphasis on the application and the industrial and clinical potential of hemagglutinin-based processing of cells and tissues.

---

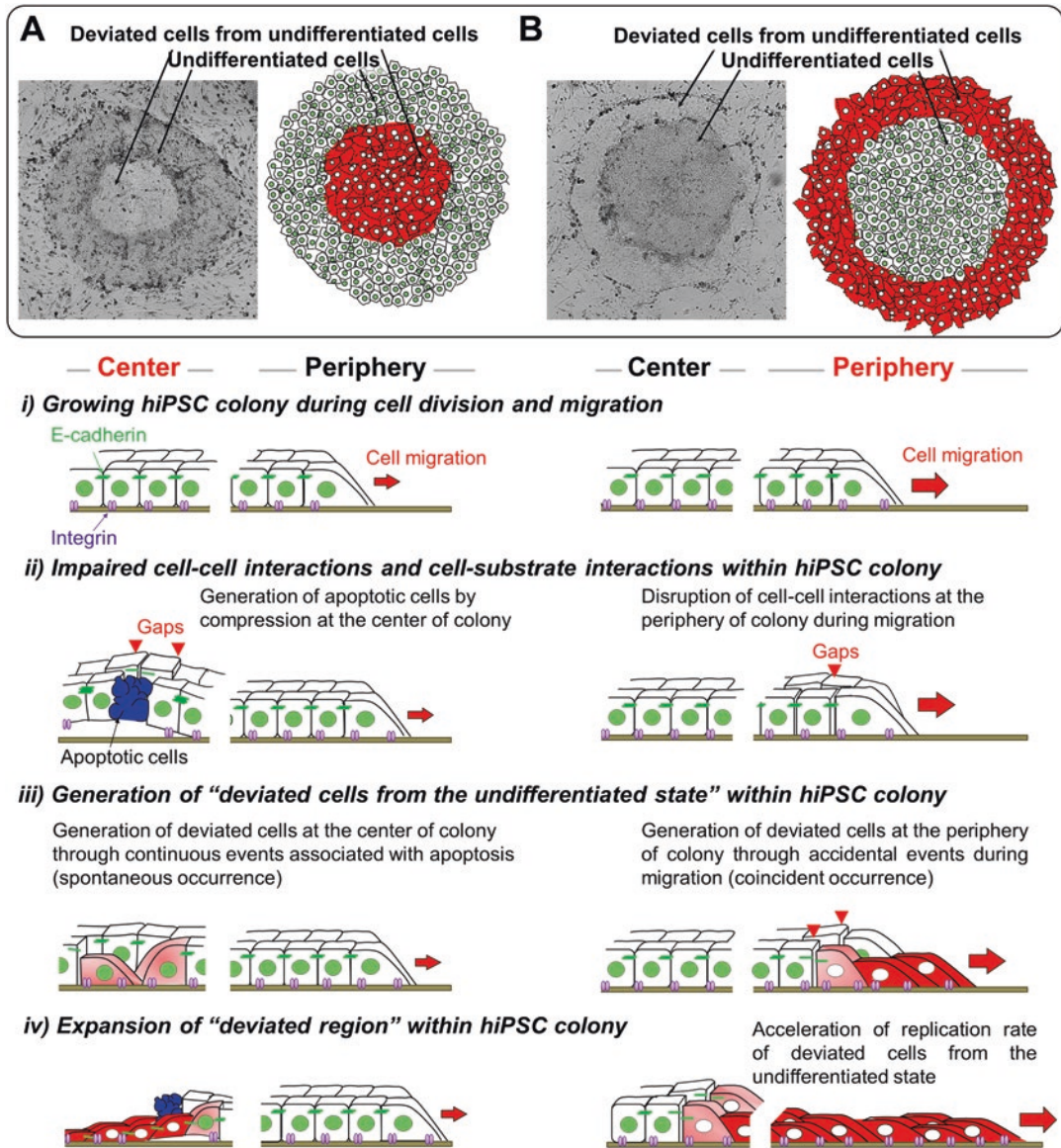
## 2.2 Principles Underlying the Maintenance and Expansion of Undifferentiated hPSCs

Based on a growing body of research, cell-cell and cell-substrate interactions are now known to influence commitment and differentiation in hPSCs. Indeed, hESC and hiPSC colonies exhibit

structural characteristics of polarized epithelial cells, and form cell-cell adhesions via E-cadherin and integrin [22, 38]. This dynamic structure physically connects neighboring cells, couples intercellular adhesive contacts to the cytoskeleton, and helps define the apical-basal axis in each cell [3, 6, 26]. Cell-cell and cell-substrate adhesions are also spatially regulated and coordinated [20], such as by interactions between actin and Rho GTPases, membrane turnover and trafficking, and interplay between cell-cell and cell-substrate adhesion [9, 21]. In addition, the Ras GTPase Rap1 regulates endocytic membrane recycling to control cell junctions and stabilize apical-basal polarity, both of which are essential for colony formation and self-renewal [19, 24, 25, 36]. Indeed, Rap1 coordinates E-cadherin, integrin, and cytoskeleton reorganization, and restores hiPSC structure and function after loss of E-cadherin. Collectively, these studies provide not only critical insights into the behavior of undifferentiated hiPSCs, but also unique and powerful opportunities to culture and maintain stem cells.

### 2.2.1 Mechanism of Loss of Undifferentiated State in Monolayer Culture

Proposed mechanisms for the spontaneous and dramatic loss of the undifferentiated state in monolayer culture are illustrated in Fig. 2.1 [12, 13, 16] for hiPSC colonies cultured on SNL and MEF feeder cells. On SNL feeder cells, hiPSCs grow outward, with cells simultaneously dividing and migrating, gradually becoming larger and more tightly packed (Fig. 2.1a). Consequently, cell motility steadily decreases while the cell density at the center increases. Notably, central cells then partially detach from the substrate, exhibit morphological changes consistent with apoptosis, enlarge, and flatten. It appears that the contraction of a blebbing apoptotic cell drags neighboring cells into the space it vacates, thereby inducing loss of undifferentiated state. Ultimately, a large number of cells dissociate from colonies and disperse as single cells.



**Fig. 2.1** Deviation of the undifferentiated state in hiPSC colonies growing on SNL (a) and MEF feeder cells (b). (Modified from [12, 16])

Conversely, loss of the undifferentiated state in colonies cultured on MEF feeder cells is associated with rapidly proliferating and outwardly migrating cells at the periphery of the colony (Fig. 2.1b). It is likely that the enhanced migration of peripheral cells is due to reduced cell-cell interactions, resulting in accelerated replication of deviated cells and highlighting cell migration, cell-substrate interactions, and E-cadherin-

mediated cell-cell adhesions as essential parameters in maintaining undifferentiated hiPSCs. Indeed, loss of E-cadherin maybe useful as a marker of deviated cells. The differences in migration are likely due to differences in the microenvironments provided by feeder cells. Remarkably, exposure to Rac1 inhibitor or activator to inhibit or activate cell migration, respectively, switches the deviation from the central to

the peripheral region, and vice versa, consistent with a switch in cell migration [12]. Taken together, the data indicate that cell migration is a crucial inducer of loss of the undifferentiated state, and should thus be controlled.

### 2.2.2 Mechanism of hPSC Aggregate Growth in Suspension Culture

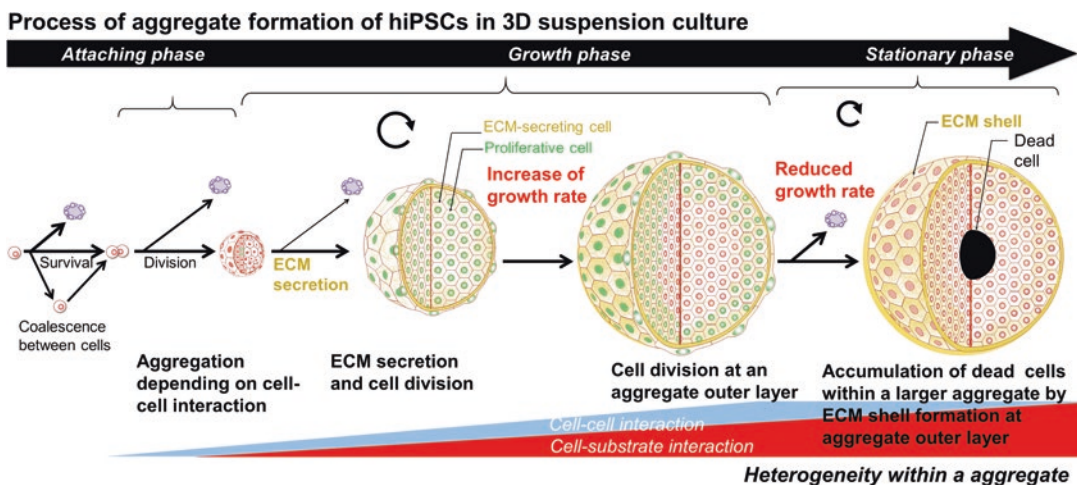
Suspension cultures are an attractive, scalable platform for large-scale cell production. In such cultures, aggregates form via the proposed mechanism illustrated in Fig. 2.2, in which single seed cells encounter other cells and establish cell-cell adhesions via E-cadherin. These aggregates then grow in size over time, and coalesce into even larger aggregates, ultimately resulting in reduced proliferation and necrosis [1, 4, 27, 34] due to impeded diffusion of oxygen and nutrients from the surface into densely agglomerated cells ([37,50]). Finally, accumulation of collagen type I around aggregates [27, 28] limits not only growth, but also microenvironmental stimulation, cell-cell adhesion, and cell-cell signaling. Therefore, an optimal aggregate size and suitable passaging methods are important to maximize proliferation rate and cell numbers. In addition, suspension cultures generally require

prior harvest of seed cells using proteolytic enzymes [10, 32], which, however, may cause cell damage and elicit apoptosis [31, 49]. Hence, it may be necessary to also optimize steps prior to suspension culture.

### 2.3 Simple and Robust Expansion of hiPSCs Using Botulinum Hemagglutinin

State-of-the-art methods for monolayer or suspension hPSC cultures are cumbersome, and may elicit unintentional spontaneous differentiation with each passage or manipulation. Accordingly, the development of simple, effective, and robust methods has attracted significant attention [14, 47], to accommodate not only the cellular response to manipulation and culture conditions, but also potential operator errors.

Integrin- and cadherin-mediated cell-cell adhesions are now well-known to be critical in many aspects of cell state or differentiation [24, 25]. In particular, cadherin subtypes tend to be abundantly expressed in distinct cell types during spontaneous differentiation [8]. For example, deviating cells in hiPSC colonies express less E-cadherin than undifferentiated cells [16]. Of note, neutralizing antibodies to E-cadherin degrades cell-cell contacts in human ESCs with-



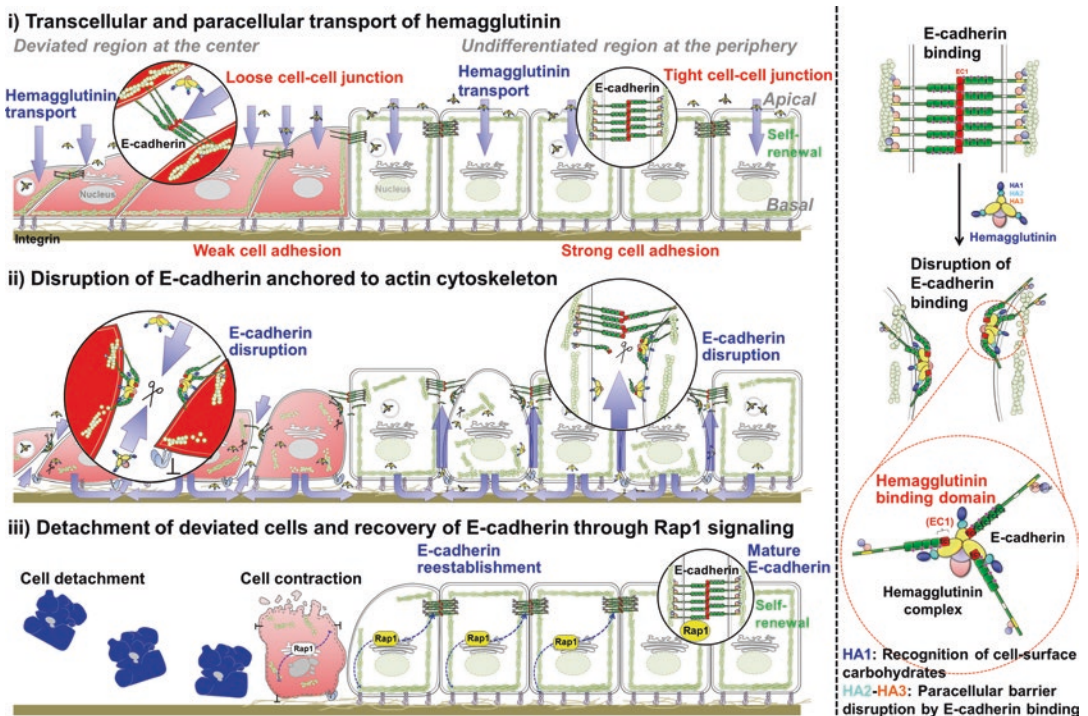
**Fig. 2.2** Cell survival, growth, and necrosis in aggregates formed by hiPSCs in suspension culture

out affecting cellular viability or inducing differentiation. Similarly, a peptide that inhibits E-cadherin transhomodimerization sustains proliferation of undifferentiated ESCs [24]. Taken together, these studies imply that differences in expression of total cadherin and cadherin subtypes may provide the most robust basis of selection between deviated and undifferentiated hiPSCs [15, 17].

### 2.3.1 Selective Removal of Deviated Cells Using Botulinum Hemagglutinin

Based on its ability to block E-cadherin and disrupt the epithelial barrier, we have attempted to use hemagglutinin to selectively eliminate deviated cells according to Fig. 2.3, which also highlights the distinct modes of action of hemagglutinin against E cadherin [17].

(a) *Temporal disruption of E-cadherin-mediated cell-cell adhesions in hiPSC colonies.* Hemagglutinin is functionally and structurally separable into HA1, which binds cell-surface carbohydrates, and HA2-HA3, which binds E-cadherin and disrupts paracellular barriers [23, 40–42]. The latter recognizes the first extracellular cadherin domain (EC1) in E-cadherin with high specificity, forming extensive intermolecular interactions [23], and altering the structural and functional integrity of cell-cell junctions. Importantly, hemagglutinin distinguishes between deviated and undifferentiated cells, since highly organized E-cadherin molecules in the latter are anchored to the actin cytoskeleton and are resistant to hemagglutinin disruption, and thus preserve apical-basal polarity. In contrast, weaker E-cadherin junctions in the former are rapidly and effectively disrupted by hemagglutinin binding.



**Fig. 2.3** Proposed mechanisms by which hemagglutinin removes deviated cells from hiPSC colonies. (Modified from [17])



- (b) *Detachment of deviated cells through disruption of E-cadherin anchored to the actin cytoskeleton.* Shortly after exposure to hemagglutinin, E-cadherin ring-like structures disappear, adhesion belts formed by E-cadherin lose the circular F-actin geometry, and basal stress fibers and focal adhesions diminish. Since each intercellular adhesive junction is subject to opposing actomyosin contractile stresses independently generated by the interacting cells, and since the actin cytoskeleton in hiPSCs connects cell-cell junctions to focal adhesions, it is likely that changes in cytoskeletal tension directly affect barrier structure and function. In addition, loss of cell-cell adhesion elicits cytoskeleton-mediated cell contraction, which is cytotoxic. Indeed, cell-cell adhesion promotes survival by inhibiting such contraction, and deviated cells appear rounded presumably as a result of contraction prior to detachment. Accordingly, cell viability and attachment may depend on the residual strength of cadherin- and integrin-mediated adhesions following exposure to hemagglutinin. Collectively, these observations suggest that integrin-dependent actin-cytoskeleton contraction and degradation of integrin may facilitate detachment of deviated cells following exposure to hemagglutinin.
- (c) *Rescue of E-cadherin and actin cytoskeleton in undifferentiated cells through Rap1.* Loss of E-cadherin-mediated cell-cell adhesion also alters cytoskeletal organization and focal adhesion via Rap1 [19, 24, 30, 36], the activation of which restores the structure and function of E-cadherin and integrin in undifferentiated cells. Subsequent to Rap1 activation, actin fibers form radial structures that are capped with E-cadherin, and are morphologically reminiscent of zipper-like junctions observed at nascent cell-cell adhesions. In deviated cells, however, E-cadherin disruption by hemagglutinin appears irreversible, and promotes further dispersion of hemagglutinin to other E-cadherin molecules, finally resulting in detachment and removal of these cells. These findings indicate that

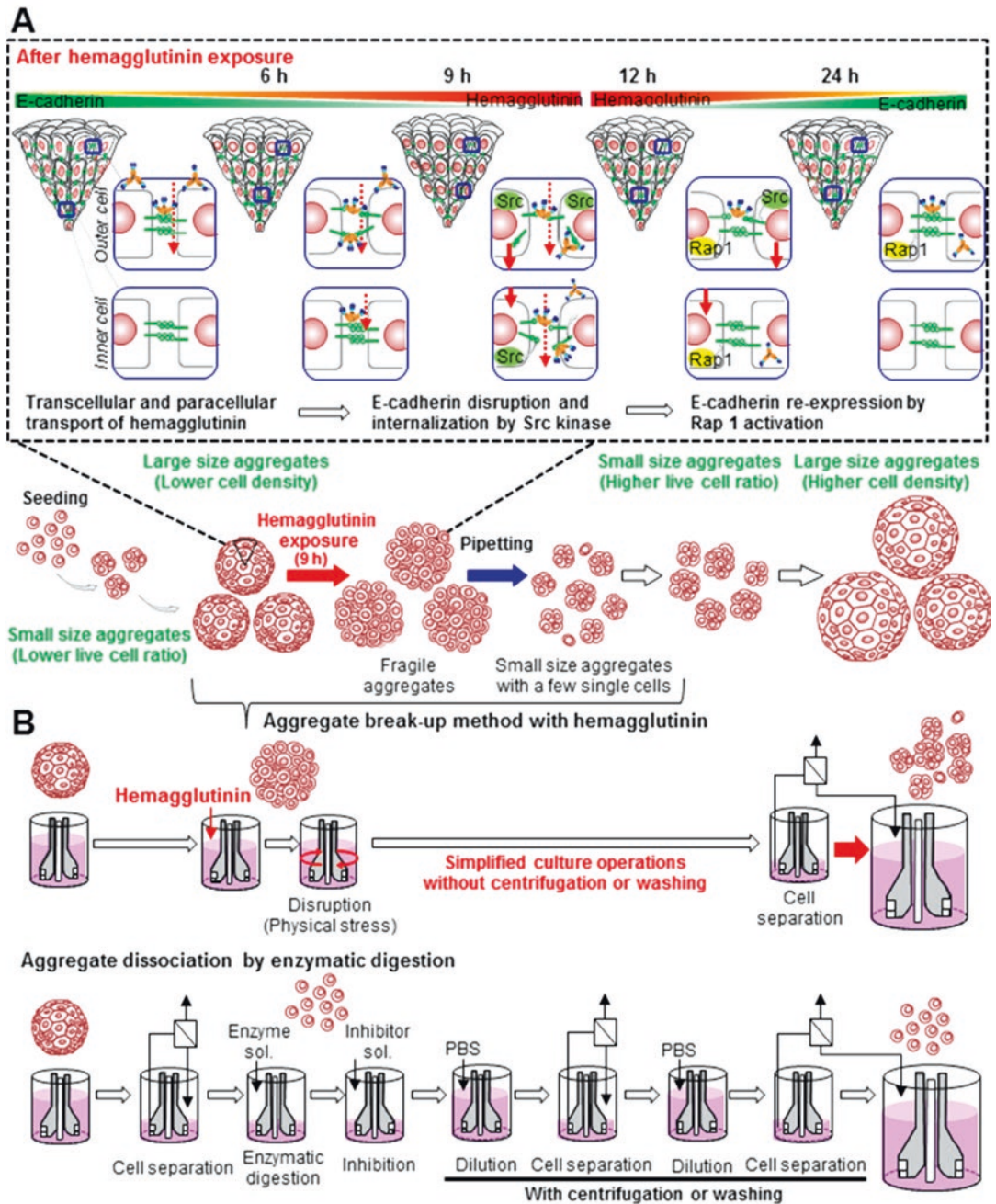
E-cadherin expression is fully reversible, and that the effects of hemagglutinin depend on the restoration of E-cadherin structure and function through cytoskeletal factors.

In any case, the effects of hemagglutinin are dose- and time-dependent, and its application should be optimized to achieve a balance between selective removal of deviating cells and recovery of undifferentiated cells. Indeed, high concentrations of hemagglutinin completely disrupts E-cadherin junctions, resulting in failure to recover, while a drop in hemagglutinin concentration only disrupts E-cadherin without removing deviated cells. Hence, an optimal combination of hemagglutinin dose, time between doses, and duration between passages may have to be established. There have been several recent reports demonstrating some success with this approach for various hiPSC cell lines, regardless of the presence or absence of feeder cells. Importantly, pluripotency was sustained in these experiments, demonstrating the robustness of the method and the stability of the resulting hiPSC cultures.

### 2.3.1.1 Hemagglutinin-Mediated *in situ* Dissociation of hPSC Aggregates to Establish High-Density Suspension Cultures

To achieve high-density suspension cultures, a simple method was developed to disaggregate hiPSCs cells *in situ* using hemagglutinin [28]. The proposed molecular basis of this approach is illustrated in Fig. 2.4.

- (a) *Temporal disruption of E-cadherin-mediated cell-cell adhesions in hiPSC aggregates.* In the presence of hemagglutinin, aggregates became easy to manipulate and dissociate by pipetting, although not immediately (0–6 h) or long after (12–24 h) exposure. At 6 h, hemagglutinin has probably disrupted E-cadherin-mediated cell-cell adhesions at peripheral cells, and has likely penetrated into central cells as a result via extracellular dispersion, the primary mode of transport. Importantly, hemagglutinin is observed at this point only in intercellular barriers of



**Fig. 2.4** Mechanisms of colony disaggregation by hemagglutinin, resulting in high-density hiPSCs suspension cultures (a), and simplified protocols (b). (Modified from [28])

central cells, indicating specific binding to E-cadherin. Most E-cadherin junctions at these barriers are disrupted at 9 h, and aggregates become dissociable by pipetting.

Disruption of cell-cell adhesions then appears to stimulate Src signaling, which in turn activates endocytosis [5] and significantly depletes E-cadherin from the surface. At 12

h, however, aggregates again become resistant to disaggregation, since internalized E-cadherin has been recycled in central cells via Rap1 [5, 15, 17], and has formed new cell-cell adhesions. However, hemagglutinin activity seems to persist in peripheral cells after 12 h, since these cells continue to express E-cadherin less abundantly. Detection of hemagglutinin in the cytoplasm at 12 h indicates a secondary, transcellular mode of transport. After 24 h, hemagglutinin diminishes significantly, likely by cellular uptake, and E-cadherin is re-expressed throughout the aggregate [23]. These results suggest that hiPSCs can be disaggregation *in situ* in suspension culture.

- (b) *Simplified protocols following disaggregation with hemagglutinin.* Hemagglutinin-treated hiPSC aggregates are more viable and reach higher densities than enzymatically dissociated aggregates. Indeed, enzymatic digestion in conventional suspension culture causes cell damage and apoptosis [31, 39, 51]. In particular, degradation of the extracellular matrix may trigger apoptosis because integrin signaling supports growth and proliferation [7, 43]. In addition, the enzyme used for digestion would have to be removed along with the degraded extracellular matrix. In contrast, hemagglutinin treatment preserves most cell-cell adhesions and extracellular matrix, resulting in higher viability. Although the apparent specific growth rates was found to be similar, higher fold-expansion was achieved with hemagglutinin ( $13.2 \pm 2.3$ -fold) than with enzymatic digestion ( $5.5 \pm 1.3$ -fold) [52]. Finally, hemagglutinin does not need to be removed, since it does not compromise hiPSC proliferation or pluripotency, and is spontaneously inactivated. Thus, the method enables high-density cultures without enzymatic treatment or subsequent clean up.
- (c) *High-density culture of hiPSCs from hemagglutinin-treated aggregates.* This method can overcome the aggregate size limitation through the break-up of hiPSC aggregates into small sizes by hemagglutinin to

obtain a high cell density and maintaining pluripotency in suspension culture. Higher cell densities ( $4.5 \pm 0.2 \times 10^6$  cells mL<sup>-1</sup>) were achieved with hemagglutinin-treated aggregates than with untreated aggregates. In addition, the apparent specific growth rate of untreated hiPSCs decreased significantly in 96–192 h because of increasing aggregate size. Moreover, higher glucose consumption and lactic acid production were observed in cultures of hemagglutinin-treated aggregates. Densities of  $2.0 \times 10^6$  cells mL<sup>-1</sup> have also been reported for conventional aggregate suspension cultures [1, 2, 33], although these are still significantly lower than for hemagglutinin-treated aggregates. Collectively, the studies highlight hemagglutinin treatment as a promising technique to prevent cell loss during seeding, to simplify protocols, and to obtain high cell densities and high growth rates in suspension culture.

---

## 2.4 Development of hPSC Culture Methods as a Way to Enhance Bioprocessing

To improve productivity and efficiency in office environments [14, 15, 17], some tools may have to be developed. Of these, stationery items used on a daily basis are among the most important, including paper and pencil, which accommodate different writing styles and skill levels, and can be adapted to meet the needs of a user. Similarly, it is necessary to develop robust culture tools to maintain undifferentiated hiPSCs. In the same way that good writing implements provide “paper and pencil to write beautiful letters” and “an eraser to correct mistakes”, hiPSC cultures require suitable substrate and nutrient media to prevent loss of the undifferentiated state, and these have been extensively investigated. However, something equivalent to an eraser, in this context to remove cells that have lost the undifferentiated state, does not yet exist, but will be indispensable. We have now demonstrated that hemagglutinin helps establish and maintain undifferentiated hiPSCs by selectively removing

deviated cells or by dissociating hiPSC aggregates in high-density cultures. These techniques may enable maintenance of undifferentiated hiPSCs in any media, by operators of all skill levels or by an automated bioreactor. Accordingly, these techniques may overcome the limitations of conventional cell cultures, and thereby enable large-scale production of hiPSCs for industrial and clinical purposes.

## 2.5 Conclusions

Many approaches have been attempted to develop a simple and robust method to culture undifferentiated hiPSCs. These methods typically exploit variations in adhesion strength and E-cadherin turnover to selectively remove deviated cells and dissociate hiPSC aggregates *in situ*. Positive feedback from Rap1 can then restore E-cadherin to intercellular junctions, and thereby rebuild cell-cell contacts and colony structure. Indeed, selective removal of deviated cells using hemagglutinin has been demonstrated in various culture conditions, in various hiPSC lines, in the presence or absence of feeder cells, and without loss of pluripotency. The method is simple and scalable, enables high-density hiPSC cultures without enzymatic treatment and subsequent cleanup, and minimizes cell loss during seeding. Therefore, hemagglutinin may enable the establishment of simple, robust, and stable closed systems for large-scale monolayer and suspension cultures of hiPSCs, a critical step towards controlled bioprocessing and manufacturing of stem cells for clinical and industrial applications.

**Acknowledgments** This work was supported by “Development of cell manufacturing and processing system for industrialization of regenerative medicine” (No. P14006), a project commissioned by Japan Agency for Medical Research and Development.

## References

1. Abbasalizadeh S, Larijani MR, Samadian A, Baharvand H (2012) Bioprocess development for mass production of size-controlled human pluripotent stem cell aggregates in stirred suspension bioreactor. *Tiss Eng Part C Methods* 18(11):831–851. <https://doi.org/10.1089/ten.TEC.2012.0161>
2. Amit M, Chebath J, Margulets V, Laevsky I, Miropolsky Y, Shariki K, Peri M, Blais I, Slutsky G, Revel M, Itskovitz-Eldor J (2010) Suspension culture of undifferentiated human embryonic and induced pluripotent stem cells. *Stem Cell Rev* 6(2):248–259. <https://doi.org/10.1007/s12015-010-9149-y>
3. Baum B, Georgiou M (2011) Dynamics of adherens junctions in epithelial establishment, maintenance, and remodeling. *J Cell Biol* 192(6):907–917. <https://doi.org/10.1083/jcb.201009141>
4. Bauwens CL, Peerani R, Niebruegge S, Woodhouse KA, Kumacheva E, Husain M, Zandstra PW (2008) Control of human embryonic stem cell colony and aggregate size heterogeneity influences differentiation trajectories. *Stem Cells* 26(9):2300–2310. <https://doi.org/10.1634/stemcells.2008-0183>
5. Balzac F, Avolio M, Degani S, Kaverina I, Torti M, Silengo L, Small JV, Retta SF (2005) E-cadherin endocytosis regulates the activity of Rap1: a traffic light GTPase at the crossroads between cadherin and integrin function. *J Cell Sci* 118(20):4765–4783. <https://doi.org/10.1242/jcs.02584>
6. Cavey M, Lecuit T (2009) Molecular bases of cell–cell junctions stability and dynamics. *Cold Spring Harb Perspect Biol* 1(5):a002998. <https://doi.org/10.1101/cshperspect.a002998>
7. Chang BS, Choi YJ, Kim JH (2015) Collagen complexes increase the efficiency of iPSC cells generated using fibroblasts from adult mice. *J Reprod Dev* 61(2):145–153. <https://doi.org/10.1262/jrd.2014-081>
8. Draper JS, Pigott C, Thomson JA, Andrews PW (2002) Surface antigens of human embryonic stem cells: changes upon differentiation in culture. *J Anat* 200(3):249–258. <https://doi.org/10.1046/j.1469-7580.2002.00030.x>
9. Hogan C, Serpente N, Cogram P, Hosking CR, Bialucha CU, Feller SM, Braga VM, Birchmeier W, Fujita Y (2004) Rap1 regulates the formation of E-cadherin-based cell–cell contacts. *Mol Cell Biol* 24(15):6690–6700. <https://doi.org/10.1128/MCB.24.15.6690-6700.2004>
10. Haraguchi Y, Matsuura K, Shimizu T, Yamato M, Okano T (2015) Simple suspension culture system of human iPSC cells maintaining their pluripotency for cardiac cell sheet engineering. *J Tiss Eng Regen Med* 9(12):1363–1375. <https://doi.org/10.1002/term.1761>
11. Hunt MM, Meng G, Rancourt DE, Gates ID, Kallos MS (2014) Factorial experimental design for the culture of human embryonic stem cells as aggregates in stirred suspension bioreactors reveals the potential for interaction effects between bioprocess parameters. *Tissue Eng Part C Methods* 20(1):76–89. <https://doi.org/10.1089/ten.TEC.2013.0040>
12. Kim M-H, Kino-oka M (2015) Maintenance of an undifferentiated state of human induced pluripotent stem cells through migration-dependent regulation of the balance between cell-cell and cell-substrate inter-

- actions. *J Biosci Bioeng* 119(6):617–622. <https://doi.org/10.1016/j.jbiosc.2014.10.024>
13. Kim M-H, Kino-oka M (2014) Switching between self-renewal and lineage commitment of human induced pluripotent stem cells via cell-substrate and cell-cell interactions on a dendrimer-immobilized surface. *Biomaterials* 35(22):5670–5678. <https://doi.org/10.1016/j.biomaterials.2014.03.085>
  14. Kim M-H, Kino-oka M (2018) Bioprocessing strategies for pluripotent stem cells based on Waddington's epigenetic landscape. *Trends Biotechnol* 36(1):89–104. <https://doi.org/10.1016/j.tibtech.2017.10.006>
  15. Kim M-H, Matsubara Y, Fujinaga Y, Kino-oka M (2017a) A simple and robust method for culturing human-induced pluripotent stem cells in an undifferentiated state using botulinum hemagglutinin. *Biotechnol J* 13(2). <https://doi.org/10.1002/biot.201700384>
  16. Kim M-H, Masuda E, Kino-oka M (2014) Kinetic analysis of deviation from the undifferentiated state in colonies of human induced pluripotent stem cells on feeder layers. *Biotechnol Bioeng* 111(6):1128–1138. <https://doi.org/10.1002/bit.25188>
  17. Kim M-H, Sugawara Y, Fujinaga Y, Kino-oka M (2017b) Botulinum hemagglutinin-mediated selective removal of cells deviating from the undifferentiated state in hiPSC colonies. *Sci Rep* 7(1):93. <https://doi.org/10.1038/s41598-017-00083-1>
  18. Kimbrel EA, Lanza R (2015) Current status of pluripotent stem cells: moving the first therapies to the clinic. *Nat Rev Drug Discov* 14(10):681–692. <https://doi.org/10.1038/nrd4738>
  19. Knox AL, Brown NH (2002) Rap1 GTPase regulation of adherens junction positioning and cell adhesion. *Science* 295(5558):1285–1288. <https://doi.org/10.1126/science.1067549>
  20. Kopecki Z, O'Neill GM, Arkell RM, Cowin AJ (2011) Regulation of focal adhesions by Flightless I involves inhibition of paxillin phosphorylation via a Rac1-dependent pathway. *J Invest Dermatol* 131(7):1450–1459. <https://doi.org/10.1038/jid.2011.69>
  21. Kovacs EM, Ali RG, McCormack AJ, Yap AS (2002) E-cadherin homophilic ligation directly signals through Rac and phosphatidylinositol 3-kinase to regulate adhesive contacts. *J Biol Chem* 277(8):6708–6718. <https://doi.org/10.1074/jbc.M109640200>
  22. Krtolica A, Genbacev O, Escobedo C, Zdravkovic T, Nordstrom A, Vabuena D, Nath A, Simon C, Mostov K, Fisher SJ (2007) Disruption of apical-basal polarity of human embryonic stem cells enhances hematopoietic differentiation. *Stem Cells* 25(9):2215–2223. <https://doi.org/10.1634/stemcells.2007-0230>
  23. Lee K, Zhong X, Gu S, Kruegel AM, Dorner MB, Perry K, Rummel A, Dong M, Jin R (2014) Molecular basis for disruption of E-cadherin adhesion by botulinum neurotoxin A complex. *Science* 344(6190):1405–1410. <https://doi.org/10.1126/science.1253823>
  24. Li L, Wang S, Jezierski A, Moalim-Nour L, Mohib K, Parks RJ, Retta SF, Wang L (2010) A unique interplay between Rap1 and E-cadherin in the endocytic pathway regulates self-renewal of human embryonic stem cells. *Stem Cells* 28(2):247–257. <https://doi.org/10.1002/stem.289>
  25. Li L, Bennett SA, Wang L (2012) Role of E-cadherin and other cell adhesion molecules in survival and differentiation of human pluripotent stem cells. *Cell Adh Migr* 6(1):59–70. <https://doi.org/10.4161/cam.19583>
  26. Mellman I, Nelson WJ (2008) Coordinated protein sorting, targeting and distribution in polarized cells. *Nat Rev Mol Cell Biol* 9(11):833–845. <https://doi.org/10.1038/nrm2525>
  27. Nath SC, Horie M, Nagamori E, Kino-oka M (2017a) Size- and time-dependent growth properties of human induced pluripotent stem cells in the culture of single aggregate. *J Biosci Bioeng* 124(4):469–475. <https://doi.org/10.1016/j.jbiosc.2017.05.006>
  28. Nath SC, Tokura T, Kim MH, Kino-oka M (2017b) Botulinum hemagglutinin-mediated in situ break-up of human induced pluripotent stem cell aggregates for high-density suspension culture. *Biotechnol Bioeng* 115(4):910–920. <https://doi.org/10.1002/bit.26526>
  29. Nie Y, Walsh P, Clarke DL, Rowley JA, Fellner T (2014) Scalable passaging of adherent human pluripotent stem cells. *PLoS One* 9(1):e88012. <https://doi.org/10.1371/journal.pone.0088012>
  30. Retta SF, Balzac F, Avolio M (2006) Rap1: a turn-about for the crosstalk between cadherins and integrins. *Eur J Cell Biol* 85(3-4):283–293. <https://doi.org/10.1016/j.ejcb.2005.09.007>
  31. Ohgushi M, Matsumura M, Eiraku M, Murakami K, Aramaki T, Nishiyama A, Muguruma K, Nakano T, Suga H, Ueno M, Ishizaki T, Suemori H, Narumiya S, Niwa H, Sasai Y (2010) Molecular pathway and cell state responsible for dissociation-induced apoptosis in human pluripotent stem cells. *Cell Stem Cell* 7(2):225–239. <https://doi.org/10.1016/j.stem.2010.06.018>
  32. Olmer R, Haase A, Merkert S, Cui W, Palecek J, Ran C, Kirschning A, Scheper T, Glage S, Miller K, Curnow EC, Hayes ES, Martin U (2010) Long term expansion of undifferentiated human iPS and ES cells in suspension culture using a defined medium. *Stem Cell Res* 5(1):51–64. <https://doi.org/10.1016/j.scr.2010.03.005>
  33. Olmer R, Lange A, Selzer S, Kasper C, Haverich A, Martin U, Zweigerdt R (2012) Suspension culture of human pluripotent stem cells in controlled, stirred bioreactors. *Tiss Eng Part C Methods* 18(10):772–784. <https://doi.org/10.1089/ten.TEC.2011.0717>
  34. Otsuji TG, Bin J, Yoshimura A, Tomura M, Tateyama D, Minami I, Yoshikawa Y, Aiba K, Heuser JE, Nishino T, Hasegawa K, Nakatsuji N (2014) A 3D sphere culture system containing functional polymers for large-scale human pluripotent stem cell production. *Stem Cell Reports* 2(5):734–745. <https://doi.org/10.1016/j.stemcr.2014.03.012>
  35. Paull D, Sevilla A, Zhou H, Hahn AK, Kim H, Napolitano C, Tsankov A, Shang L, Krumholz K, Jagadeesan P, Woodard CM, Sun B, Vilboux T, Zimmer M, Forero E, Moroziewicz DN, Martinez H,

- Malicdan MC, Weiss KA, Vensand LB, Dusenberry CR, Polus H, Sy KT, Kahler DJ, Gahl WA, Solomon SL, Chang S, Meissner A, Eggan K, Noggle SA (2015) Automated, high-throughput derivation, characterization and differentiation of induced pluripotent stem cells. *Nat Methods* 12(9):885–892. <https://doi.org/10.1038/nmeth.3507>
36. Price LS, Hajdo-Milasinovic A, Zhao J, Zwartkruis FJ, Collard JG, Bos JL (2004) Rap1 regulates E-cadherin-mediated cell–cell adhesion. *J Biol Chem* 279(34):35127–35132. <https://doi.org/10.1074/jbc.M404917200>
37. Sachlos E, Auguste DT (2008) Embryoid body morphology influences diffusive transport of inductive biochemicals: a strategy for stem cell differentiation. *Biomaterials* 29(34):4471–4480. <https://doi.org/10.1016/j.biomaterials.2008.08.012>
38. Sathananthan H, Pera M, Trounson A (2002) The fine structure of human embryonic stem cells. *Reprod Biomed Online* 4(1):56–61
39. Singh H, Mok P, Balakrishnan T, Rahmat SN, Zweigerdt R (2010) Upscaling single cell-inoculated suspension culture. *Stem Cell Res* 4(3):165–179. <https://doi.org/10.1016/j.scr.2010.03.001>
40. Sugawara Y, Matsumura T, Takegahara Y, Jin Y, Tsukasaki Y, Takeichi M, Fujinaga Y (2010) Botulinum hemagglutinin disrupts the intercellular epithelial barrier by directly binding E-cadherin. *J Cell Biol* 189(4):691–700. <https://doi.org/10.1083/jcb.200910119>
41. Sugawara Y, Fujinaga Y (2011) The botulinum toxin complex meets E-cadherin on the way to its destination. *Cell Adh Migr* 5(1):34–36. <https://doi.org/10.4161/cam.5.1.13574>
42. Sugawara Y, Yutani M, Amatsu S, Matsumura T, Fujinaga Y (2014) Functional dissection of the *Clostridium botulinum* type B hemagglutinin complex: identification of the carbohydrate and E-cadherin binding sites. *PLoS One* 9(10):e111170. <https://doi.org/10.1371/journal.pone.0111170>
43. Suh HN, Han HJ (2011) Collagen I regulates the self-renewal of mouse embryonic stem cells through  $\alpha 2\beta 1$  integrin- and DDR1-dependent Bmi-1. *J Cell Physiol* 226(12):3422–3432
44. Takahashi K, Yamanaka S (2006) Induction of pluripotent stem cells from mouse embryonic and adult fibroblast cultures by defined factors. *Cell* 126(4):663–676. <https://doi.org/10.1016/j.cell.2006.07.024>
45. Trounson A (2006) The production and directed differentiation of human embryonic stem cells. *Endocr Rev* 27(2):208–219. <https://doi.org/10.1210/er.2005-0016>
46. Van Winkle AP, Gates ID, Kallos MS (2012) Mass transfer limitations in embryoid bodies during human embryonic stem cell differentiation. *Cells Tissues Organs* 196(1):34–47. <https://doi.org/10.1159/000330691>
47. Villa-Diaz LG, Ross AM, Lahaan J, Krebsbach PH (2013) Concise review: the evolution of human pluripotent stem cell culture: from feeder cells to synthetic coatings. *Stem Cells* 31(1):1–7. <https://doi.org/10.1002/stem.1260>
48. Wakao S, Kitada M, Kuroda Y, Ogura F, Murakami T, Niwa A, Dezawa M (2012) Morphologic and gene expression criteria for identifying human induced pluripotent stem cells. *PLoS One* 7(12):e48677. <https://doi.org/10.1371/journal.pone.0048677>
49. Watanabe K, Ueno M, Kamiya D, Nishiyama A, Matsumura M, Wataya T, Takahashi JB, Nishikawa S, Muguruma K, Sasai Y (2007) A ROCK inhibitor permits survival of dissociated human embryonic stem cells. *Nat Biotechnol* 25(6):681–686. <https://doi.org/10.1038/nbt1310>
50. Wu J, Rostami MR, Olaya DPC, Tzanakakis ES (2014) Oxygen transport and stem cell aggregation in stirred-suspension bioreactor cultures. *PLoS One* 9(7):e102486. <https://doi.org/10.1371/journal.pone.0102486>
51. Xu Y, Zhu X, Hahm HS, Wei W, Hao E, Hayek A, Ding S (2010) Revealing a core signaling regulatory mechanism for pluripotent stem cell survival and self-renewal by small molecules. *Proc Natl Acad Sci USA* 107(18):8129–8134. <https://doi.org/10.1073/pnas.1002024107>
52. Zweigerdt R, Olmer R, Singh H, Haverich A, Martin U (2011) Scalable expansion of human pluripotent stem cells in suspension culture. *Nat Protoc* 6(5):689–700. <https://doi.org/10.1038/nprot.2011.318>



# Growth and Differentiation of Dental Stem Cells of Apical Papilla on Polycaprolactone Scaffolds

Mohamed Jamal, Yaser Greish, Sami Chogle, Harold Goodis, and Sherif M. Karam

## Abstract

Biodegradable scaffolds are useful tools in the field of tissue engineering and regenerative medicine. The aim of this study was to

test the potential of the human stem cells of apical papilla (SCAP) to attach, proliferate and differentiate on a polycaprolactone (PCL)-based scaffolds. SCAP were extracted from the root apical papillae of freshly extracted immature premolar teeth by using enzymatic digestion. Porous PCL scaffolds were fabricated using particle leaching method and NaCl or mannitol as porogens. SCAP of passage 3 were seeded on non-porous and porous PCL scaffolds for up to 14 days. For control, cells were cultured on glass coverslips. Picogreen DNA quantification was used to assay for cell proliferation. Cell differentiation and development of calcification nodules were examined using scanning electron microscopy and alizarin red staining. SCAP showed a comparable attachment, growth and proliferation patterns on PCL scaffolds and coverslips. Cell proliferation was enhanced on mannitol scaffolds at all time points. Calcification nodules were detected in all PCL scaffolds while it was not present on glass coverslips. These nodules were detected on NaCl-scaffolds by day 7 and on mannitol and non-porous scaffolds by day 14. In conclusion, SCAP were able to attach, proliferate and differentiate on PCL scaffolds without using any inductive media, indicating their potential application for dental tissue regeneration.

M. Jamal

Department of Anatomy, College of Medicine and Health Sciences, UAE University, Al-Ain, United Arab Emirates

Department of Endodontics, Hamdan Bin Mohamed College of Dental Medicine, Mohamed Bin Rashid University of Medicine and Health Sciences, Dubai, United Arab Emirates  
e-mail: [mohamed.jamal@mbru.ac.ae](mailto:mohamed.jamal@mbru.ac.ae)

Y. Greish

Department of Chemistry, College of Science, UAE University, Al-Ain, United Arab Emirates  
e-mail: [y.afifi@uaeu.ac.ae](mailto:y.afifi@uaeu.ac.ae)

S. Chogle

Department of Endodontics, Henry M. Goldman School of Dental Medicine, Boston University, Boston, MA, USA  
e-mail: [schogle@bu.edu](mailto:schogle@bu.edu)

H. Goodis

Department of Preventive & Restorative Dental Sciences, School of Dentistry, University of California, San Francisco, CA, USA  
e-mail: [Harold.Goodis@ucsf.edu](mailto:Harold.Goodis@ucsf.edu)

S. M. Karam (✉)

Department of Anatomy, College of Medicine and Health Sciences, UAE University, Al-Ain, United Arab Emirates  
e-mail: [skaram@uaeu.ac.ae](mailto:skaram@uaeu.ac.ae)

**Keywords**

Polycaprolactone · Stem cells of apical papilla · Dental stem cells · Calcification nodules · Porous scaffolds · Regenerative endodontics

**3.1 Introduction**

Several case reports in the literature have shown that immature teeth with necrotic pulp and periapical lesions can be treated to overcome the infection and rescue root development and apical closure [1–4]. These reports demonstrate the ability of the pulp or pulp-like tissue to regenerate and maintain root development. The details of this remarkable process of immature pulp regenerative potential are not completely understood [5, 6]. In addition, it is unknown which stem cells and/or growth factors are involved in this regeneration process [7, 8].

The discovery and isolation of the stem cells of apical papilla or SCAP could partially explain the regenerative potential of immature pulp [9]. Accordingly, a treatment protocol was proposed in some cases of necrotic pulp, by initiating bleeding from the periapical tissue [3]. Consequently, blood would fill the root canal system and transport some stem cells from the periapical tissues. Stem cells would then populate the blood clot formed in the root canal. From an anatomical point of view, the most probable cell type to fill the root canal space is the SCAP [9–11]. This theory of SCAP involvement in pulp regeneration is further supported by the findings that SCAP were able to regenerate pulp-dentin like tissue both *in vivo* and *in vitro* [9, 12]. Therefore, the SCAP have become an attractive stem cell type to study their biological features in details and to explore the possibility of their use in the regenerative therapy of dental pulp necrosis.

To develop a therapeutic regenerative model, there is a need to identify not only the cell source, but also a scaffold that would provide a three-dimensional microenvironment to allow the cells

to grow and differentiate. Ideally, the scaffold should then gradually degrade to allow the new regenerated tissue to grow and fill up the pulp space. Therefore, the scaffold should be made from a biocompatible and biodegradable material [13, 14]. Polycaprolactone (PCL) is a biocompatible, slow degrading synthetic polymer, which has been used as a scaffold material in several tissue regeneration models and also has different other applications in medicine and dentistry [15–20]. The main aim of this study was to investigate the ability of SCAP to attach, proliferate and differentiate on different forms of PCL-based scaffolds. Results obtained from this study could provide a basis to design a model for regenerative endodontics.

**3.2 Material and Methods****3.2.1 SCAP Isolation and Cultures**

Intact caries-free premolars were extracted from 10–14 years old patients (n = 3). The teeth had incompletely formed root apices. The patients were healthy and required teeth extraction as part of their orthodontic treatment. Informed consent forms were signed by the parents before teeth extractions. The apical papillae were microdissected and SCAP were isolated and cultured as described by Sonoyama et al. [9]. Briefly, the papillae were minced and digested in a physiological solution containing 3 mg/ml collagenase type I (GIBCO/Invitrogen) and 4 mg/ml dispase (GIBCO/Invitrogen) for 45 min at 37 °C. Isolated cells were then plated in culture dishes containing alpha-modification of Eagle's medium (GIBCO/Invitrogen) supplemented with 15% fetal bovine serum (GIBCO/Invitrogen), 2 mM L-glutamine (GIBCO/Invitrogen), 100 U/ml penicillin and 100 mg/ml streptomycin (GIBCO/Invitrogen) and allowed to grow in a humidified incubator (Thermo Scientific) adjusted at 37 °C and 5% CO<sub>2</sub>. Once the cells reached 80% confluence, several passages were carried out. All experiments were done on passage 3.



### 3.2.2 Scaffold Fabrication

Polycaprolactone (PCL) porous scaffolds were prepared using a particle leaching technique [21], where two types of porogens; namely sodium chloride (NaCl; Aldrich, USA) and mannitol (Aldrich, USA), were used. Briefly, a 25% w/v PCL solution was prepared by dissolving PCL particles (Aldrich, USA) in chloroform and stirring until a homogenous solution was achieved. Porogen particles, 10 g of NaCl or mannitol, were added to the solution and stirred until the porogen particles were completely dispersed in the PCL solution. The solution was poured into glass Petri dishes and left under the hood for 24 h to allow evaporation of chloroform. After drying, a uniform sheet of PCL scaffold was formed. Scaffolds were subjected to a leaching procedure by soaking in distilled water for 24 h. After complete leach out of the porogen particles, porous PCL scaffolds were obtained. In addition to the two types of porous scaffolds, pure PCL nonporous scaffolds were prepared using the same method. Scaffold sheets were cut into small round pieces with a 6.5 mm radius. For control, glass coverslips of the same surface area were used. All scaffolds were examined with stereomicroscope, inverted microscope and scanning electron microscope (SEM) to evaluate their surface topography and microstructural characteristics.

### 3.2.3 SCAP Culture

Before cell seeding, all scaffolds were sterilized by soaking in 70% ethanol for 1 h under a laminar flow hood and then subjected to an ultraviolet light for another 1 h before allowed to dry. Sterile scaffolds were incubated in modified Eagle's culture media and left overnight in a humidified incubator at 37 °C and 5% CO<sub>2</sub>. Approximately 30,000 cells from passage 3 suspended in 100 µl of culture media, were seeded onto scaffolds and coverslips placed into 12-well plates and allowed

to grow in the CO<sub>2</sub> incubator at 37 °C. After 12 h, 1 ml of culture media was added to each well. The media was changed every 2–3 days.

### 3.2.4 Assessment of Attachment, Proliferation and Differentiation of SCAP

#### 3.2.4.1 Toluidine Blue Staining

On days 2, 7 and 14, cell-seeded scaffolds were removed from the culture plates and fixed with 4% paraformaldehyde. Cells were permeabilized with 0.1% Triton X-100 and toluidine blue (0.1%, Agar Scientific Limited) was added to the surface of scaffolds for 1 min. Stained cells grown on the scaffolds were examined with a stereomicroscope (LEICA, MZI6A, Danaher, Germany) and an inverted microscope (Olympus IX71, Tokyo, Japan) to assess cell attachment and proliferation on the different types of scaffolds. Three scaffolds from each type and the control coverslips were examined for each of the different periods of culture.

#### 3.2.4.2 Alizarin Red-Toluidine Blue Double Staining

To detect mineralization, cells on different scaffolds and coverslips from days 2, 7 and 14 were initially stained with toluidine blue, washed with PBS, and then stained with alizarin red solution (pH = 4.2) for 15 min and finally 1% toluidine blue stain was added for 1 min. All scaffolds were examined with stereo and inverted microscopes. Three scaffolds from each type and coverslips were stained and examined.

#### 3.2.4.3 DNA Quantification

The total DNA content was measured by using Quant-iT™ PicoGreen® dsDNA quantification kit (Molecular Probes, Invetrogen, USA). Each scaffold from days 2, 7 and 14 was transferred to a 50 ml tube with 5 ml of deionized water added to lyse the cells. The cell-seeded scaffolds together with the water were frozen at -80 °C

overnight. The lysed cells were thawed and then ultrasonicated using Sonic Ruptor 250 Ultrasonic Homogenizer (Omni International, Kennesaw, GA, USA) for 10 min. Equal volumes of the sample and the Picogreen reagent were mixed and added to 96 microwell plates and incubated for 2–5 min. DNA was measured on a fluorescence microplate reader with excitation of 265 nm and emission of 450 nm and the DNA amounts were calculated from a standard curve. Three scaffolds from each type and coverslips were subjected for total DNA quantification. The analysis was repeated at three different times.

#### 3.2.4.4 SEM

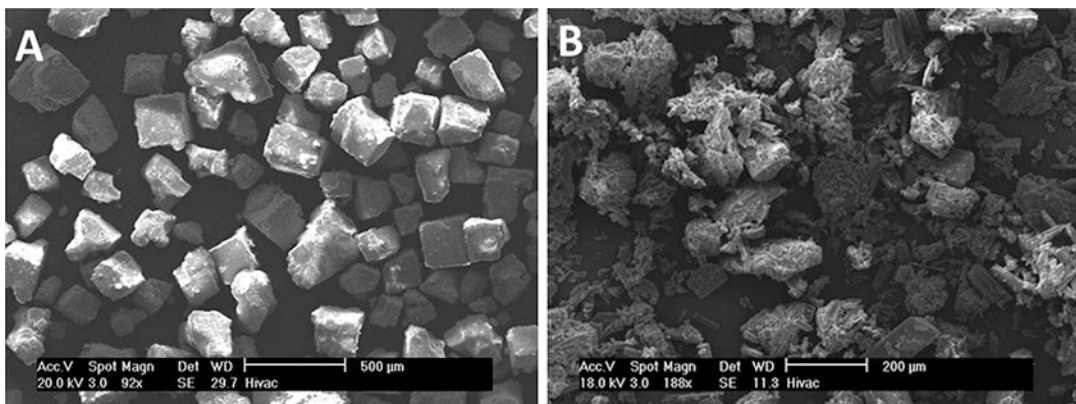
To examine the cellular morphology, distribution, and the elemental composition, scaffolds from experimental and control groups were processed for SEM and energy dispersive X-ray spectroscopy (EDXS) (XL-30 Phillips, Amsterdam, Netherlands). Scaffolds with cells cultured for 2, 7 and 14 days were fixed with 4% paraformaldehyde for 1 h and post-fixed in 1% osmium tetroxide for 10 min. Cells on all scaffolds were dehydrated using a series of increasing concentrations of ethanol. Finally, scaffolds were mounted on aluminum stubs, coated with gold using a sputter coater, and finally examined using SEM. Three scaffolds from each type and coverslips were examined at 3 different times.

### 3.3 Results

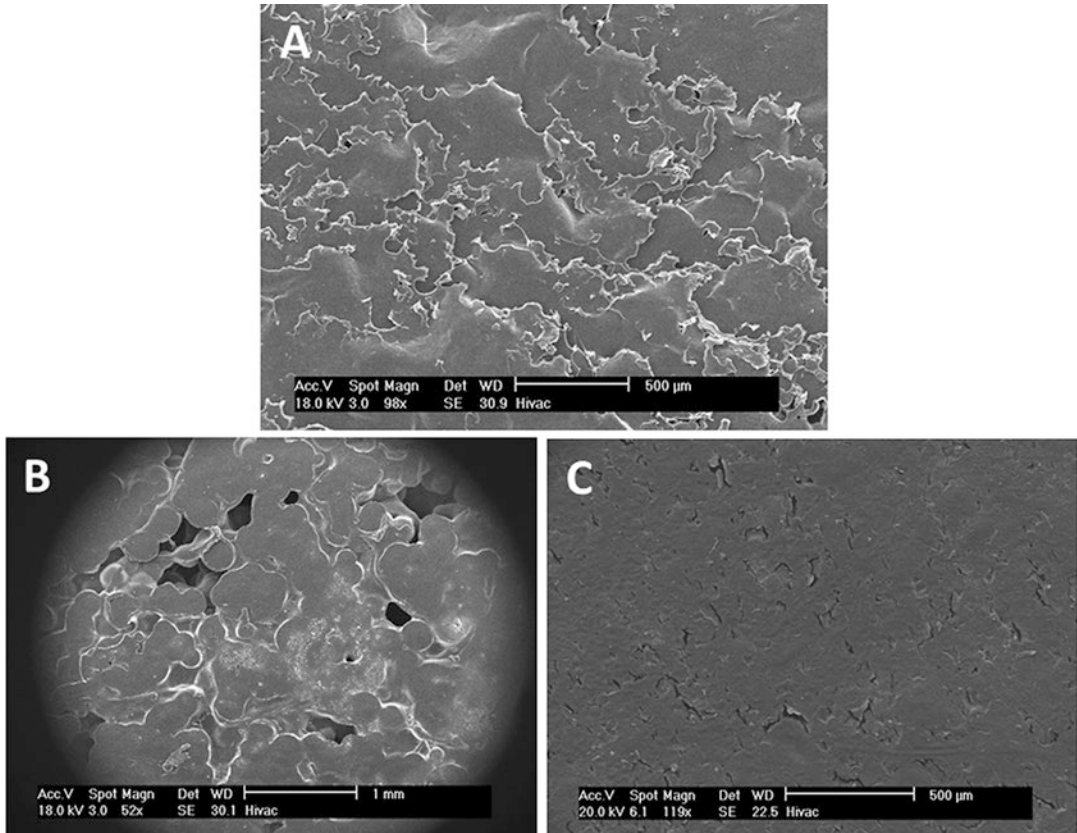
#### 3.3.1 Scaffolds' Surface Topography and Pores Characteristics

SEM observations demonstrated that the NaCl particles used as porogens were mostly cuboidal in shape with an average particle diameter of 150–250  $\mu\text{m}$  (Fig. 3.1a). On the other hand, mannitol appeared as short, needle-like microfibers with average dimensions of 65  $\mu\text{m}$  in length and 10  $\mu\text{m}$  in diameter (Fig. 3.1b). The fibers appeared as aggregates possibly due to their physical and chemical interactions.

Figure 3.2a shows SEM micrograph of a non-porous PCL scaffold, showing the presence of a rough surface with irregular topography and a layer architecture. On the other hand, SEM observations of the scaffolds with NaCl-created pores showed their homogeneous distribution within the polymeric matrix. The pores varied in size and morphology due to overlap between the NaCl particles during mixing and casting. Due to the characteristic morphology of the NaCl particles, the created porosity was more of an isolated than interconnected. However, in places where NaCl particles were close to each other, interconnected pores were created (Fig. 3.2b). Scaffolds with mannitol-created pores had a homogeneous distribution of pores with fiber-like morphology rep-



**Fig. 3.1** Scanning electron micrographs of pure NaCl (a) and mannitol (b) porogens used in the preparation of porous PCL scaffolds



**Fig. 3.2** Scanning electron micrographs of non-porous (a) and porous PCL scaffolds using 10% NaCl (b) and 10% mannitol (c)

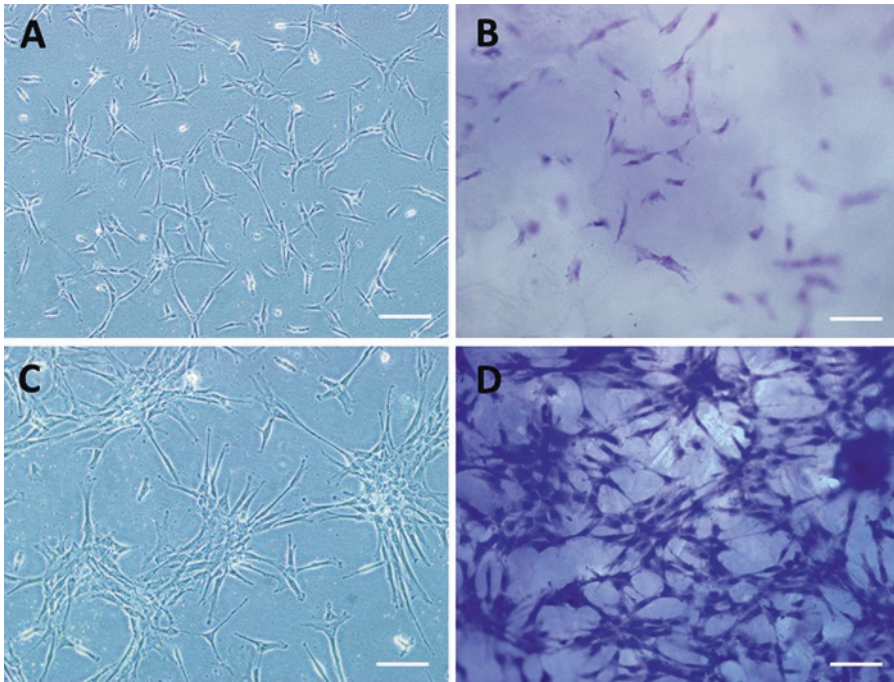
resenting the mannitol fibers. There were more pores per scaffold in this group in comparison to the scaffolds with NaCl-created pores. In addition, the pores were smaller, but with more inter-connectivity than those of NaCl-created pores (Fig. 3.2c).

### 3.3.2 Assessment of Proliferation and Differentiation of SCAP on PCL Scaffolds

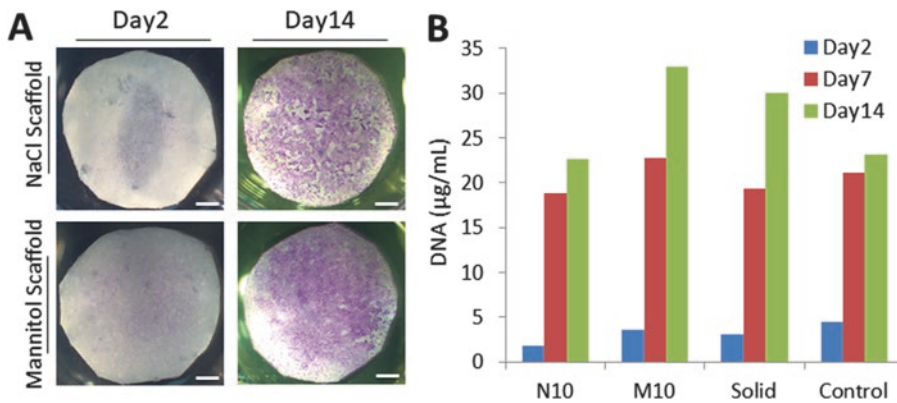
TB staining showed a similar growth pattern of SCAP on different types of scaffolds, in culture dish and on glass coverslips (Fig. 3.3). On day 1 post-seeding, cells appeared to be attached in isolated pattern (Fig. 3.3a, b), while on day 7, the cells began to form colonies with a star shape

(Fig. 3.3c, d). TB staining and stereomicroscopic analysis showed that the amount of SCAP and the area they cover consistently increase from day 2 to day 14 (Fig. 3.4a).

To obtain some information on the number of cells growing on the scaffolds, the amount of DNA was quantified on the 3 time points (days 2, 7 and 14). The results revealed that on day 2, the amounts of DNA reflecting the numbers of cells were almost similar in the porous scaffolds and the control glass coverslips (Fig. 3.4b). On day 7, there was an increase in the number of SCAP, indicating their proliferation, in comparison to day 2 in all groups, with highest DNA value for mannitol-scaffolds while NaCl-scaffolds were associated with the highest percentage of increase in cell number. By day 14, DNA value continued to increase, with mannitol-scaffolds maintained



**Fig. 3.3** Growth pattern of SCAP on culture flasks (**a** and **c**) and on PCL scaffolds (**b** and **d**), after 2 days (**a** and **b**) and 7 days (**c** and **d**) of incubation. Scale bar = 50  $\mu\text{m}$



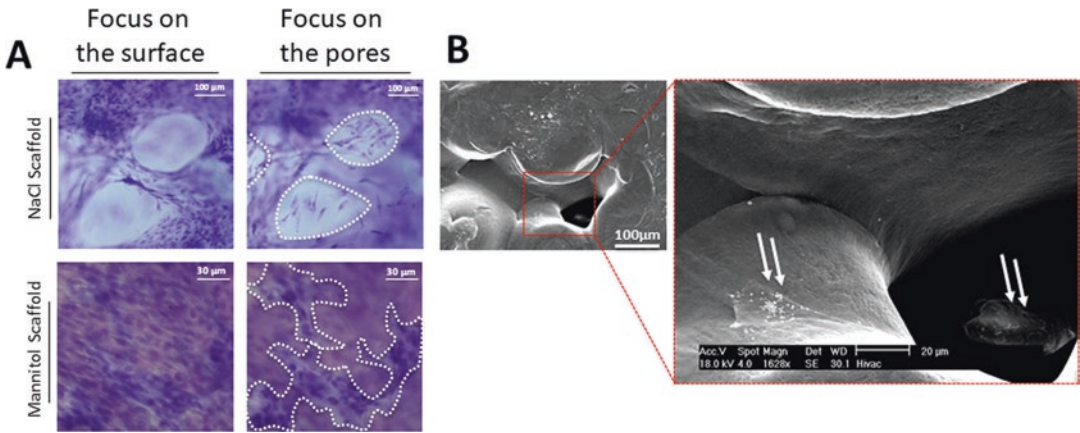
**Fig. 3.4** (a) Stereomicroscopic images of SCAP growing on NaCl- and mannitol-porous scaffolds for 2 and 14 days after TB staining. Scale bar = 2 mm. (b) Bar chart representing total DNA values of SCAP growing on porous

PCL scaffolds using 10% NaCl (N10) and 10% mannitol (M10), non-porous (solid) PCL scaffolds and on glass coverslips (control) for 2, 7 and 14 days in culture

the highest DNA value which indicated the highest number of cells (Fig. 3.4b). Figure 3.5 shows stereoscopic and SEM micrographs of mannitol and NaCl porous scaffolds after TB staining demonstrating extension of cell growth within the pores.

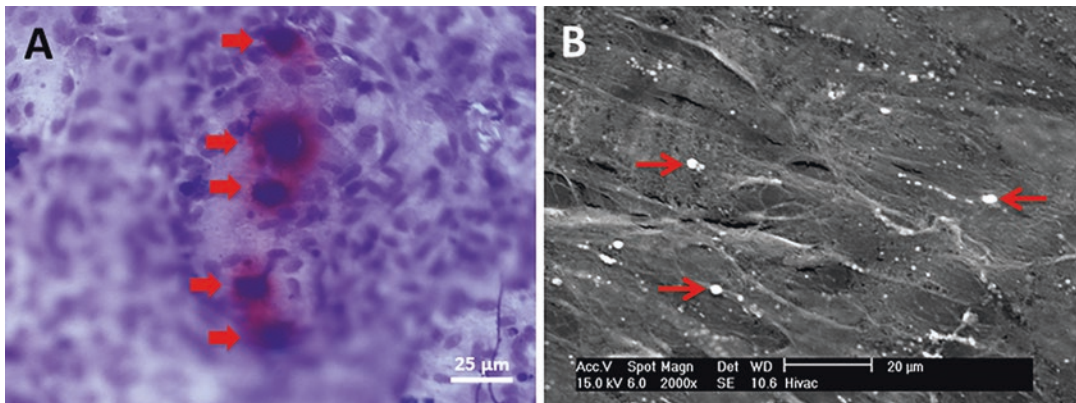
### 3.3.3 SCAP's Differentiation

Double staining with alizarin red and toluidine blue was used to test whether calcification nodules (sign differentiation) were developed by the cultured cells. If present, the nodules would



**Fig. 3.5** Stereomicroscopic and SEM images of SCAP cultured on PCL scaffolds extending into their pores. (a) SCAP growing on NaCl- and mannitol-porous scaffolds for 14 days and stained with TB. Note that images are taken with different focal plans to demonstrate cell growth on the external surface and also extending within the

pores (indicated by white dotted borders) of the scaffolds. (b) SEM micrographs obtained at low and high magnifications showing SCAP growing on NaCl-porous scaffold (left double arrows) and extending within the pore (right double arrows)



**Fig. 3.6** Light (a) and SEM (b) micrographs of SCAP cultured on NaCl-porous scaffold for 14 days. (a) TB-AR double staining showing an evidence of calcification

nodules (arrows). (b) SEM shows the beginning of forming small calcification nodules (arrows)

acquire red-orange stain with blackish center. After examining all the samples, we found no staining in the control group in all time points examined. The same result was found in all experimental groups examined on day 2. SCAP cultured on NaCl-scaffolds started to show signs of calcification on day 7, while on day 14 the number and size of calcification nodules increased (Fig. 3.6a). SCAP cultured on mannitol-scaffolds and non-porous scaffolds started to

show calcification nodules only on day 14. Moreover, SEM micrograph of day 14 NaCl-scaffold indicate the presence of extracellular matrix and nodule like clusters (Fig. 3.6b). The mineral nature of the calcification nodules was analyzed by energy dispersive X-ray spectroscopy (EDXS) and it revealed the components of the calcification nodules and the presence of calcium and phosphorous deposit at a Ca:P ratio of 1.5–1.6.

### 3.4 Discussion

The apical papilla is a soft tissue with a smooth surface found at the apex of the dental pulp. Histologically, the apical papilla is made of loose connective tissue including a few blood vessels and many mesenchymal cells [10, 11]. From this papilla, SCAP have been isolated and characterized for the first time by Sonoyama et al. [9]. These cells attracted the interest of many researchers as they could be the stem cells responsible for the process of regenerative endodontics. Several *in vivo* and *in vitro* models were developed to investigate the potential of these cells to regenerate different tissues [9–12]. In the present study, we have isolated and cultured SCAP to test their potential to attach, proliferate and differentiate on synthetic porous and non-porous PCL scaffolds.

To achieve our aims, first, SCAP were isolated by enzymatic digestion of apical papilla of extracted human permanent immature premolars. Second, non-porous PCL-based scaffolds were fabricated, seeded with the isolated SCAP and examined at 3 time points: 2, 7, and 14 days post-seeding. Growth, proliferation and differentiation pattern of SCAP were compared with those growing in culture flasks at the same time points. Glass cover slips of the same size and surface area of scaffolds were used as control for the comparison. Using glass cover slips provides a better ability of matching the number of cells and amount of culture media to those on scaffolds and the possibility of processing the cells on cover slips for immunohistochemistry. The findings showed a comparable attachment, growth and proliferation pattern of SCAP growing in culture flasks, on coverslips and on scaffolds. These results confirm the suitability of the PCL-based scaffold for the growth of SCAP. This finding is in agreement with other studies which showed the biocompatibility of PCL but with different types of stem cells, including dental pulp stem cells [22]. By day 7, signs of differentiation of SCAP were noticed in both non-porous PCL and control samples. The signs of differentiation were manifested by (a) change in the morphology of the cells from stellate to longitudinal, and

(b) calcification and mineralization evidences from Alizarin red stain or SEM and EDXS.

It is generally believed that when some cells become in close contact with each other, they can be triggered to differentiate, and once they form multilayers they start mineralization [23]. In this study, it was observed that, by day 7, the cells became close to each other and acquired large longitudinal morphology with oval nucleus. By day 14, the number of differentiated cells increased and covered almost all the surface area in both glass and PCL scaffolds. Interestingly, calcification nodules were noticed by day 14, only in PCL scaffolds and this was manifested by Alizarin stain and SEM. These results could be attributed to the well-known biocompatibility of PCL in addition to its rough surface caused by the gradual evaporation of the solvent during scaffolds preparation. In contrast, the glass coverslip has a smooth surface, which may not allow stratification of SCAP cells.

One of the requirements of a scaffold to be used in tissue regeneration, is to have interconnected pores. This porosity and interconnectivity is essential to ensure sufficient transport of oxygen and nutrients towards the cells and allow removal of metabolic products [24]. Porosity may also have a positive effect on cell attachment [22, 24]. Variations in the size, shape and number of pores within the scaffold might have an effect on cell attachment, proliferation and differentiation. One of the aims of this study was to investigate this effect. Therefore, porous scaffolds were prepared using particle leaching technique. It is easy, economic and has been successfully and commonly used before to create porous scaffolds for engineering bone, heart valve and other tissues [25–27]. To create pores with this technique, water soluble porogens were used. The percentage, size and shape of pores depend on the type and morphology of the porogen particulates. NaCl is one of the most commonly used porogens, and it has been used before in many studies including those involved in dental pulp regeneration. Another less commonly used porogen is the mannitol, which is also water-soluble. In the present study, the proliferation and differentiation of SCAP seeded on non-porous and porous PCL

scaffolds were compared at different time points after seeding. The porous scaffolds were created using 10% of either NaCl or mannitol. Two days post-seeding, the light microscopic examination revealed that mannitol-porous and non-porous scaffolds showed better growth of SCAP than NaCl-porous scaffolds. This was also reflected in the DNA analysis, although the cells were proliferating in a similar rate in all groups. This can be explained by the fact that mannitol-porous scaffolds have more surface area than NaCl-porous scaffolds. The SEM and stereomicroscopic examination of the latter revealed that it has larger pores than mannitol ones and thus limiting the area for cells to attach. Another supporting finding, is the fact that there were more cells on the glass-coverslip (which has the maximum surface area) and that cells were growing all over the available surface, and this is supported by the DNA analysis as well. On day 2, there were no signs of differentiation and cells on all scaffolds or coverslips didn't form monolayer.

On day 7, there was a significant increase in the number of cells growing on all scaffolds or glass coverslips. In addition, cells started to differentiate as they became elongated in areas where they were in close contact with each other. This change in cell shape was apparent in all PCL scaffolds. Interestingly, there were also signs of calcification and formation of mineralization nodules in NaCl-scaffolds only. This was manifested by the Alizarin red stain, SEM and EDXS analysis. By day 14, cells continued to proliferate in mannitol and non-porous scaffolds, with increased calcification and mineralization nodules on NaCl-scaffolds. In contrast, cells on mannitol and non-porous scaffolds started to show calcification nodules. This finding was also supported by the DNA analysis (Fig. 3.4), and this can be explained by the fact that many cells in NaCl scaffolds have already differentiated by day 7 and reduced their proliferation rate by day 14. This could be explained by the characteristic feature of the surface area of different scaffolds. So, it seems that cells on NaCl-scaffolds contact each other and form multilayers in a shorter time than those on mannitol- and non-porous scaffold, and therefore, differentiate and form mineralization

nodules earlier than other cells growing on other scaffolds. These findings indicate the osteogenic/odontogenic potential of the SCAP *in vitro*.

---

### 3.5 Conclusion

The results of this study indicate that SCAP attach, proliferate and differentiate on PCL-based scaffolds. According to literature search, this is the first time to culture SCAP on such synthetic material. The differentiation of SCAP on PCL scaffolds occurred without using any inductive media or growth factors. These findings indicate that PCL does not only support but also induces SCAP to differentiate. Therefore, PCL is a promising material to use for future regenerative endodontics protocols.

---

### References

1. Windley W, Teixeira F, Levin L, Sigurdsson A, Trope M (2005) Disinfection of immature teeth with a triple antibiotic paste. *J Endod* 31(6):439–443
2. Iwaya SI, Ikawa M, Kubota M (2001) Revascularization of an immature permanent tooth with apical periodontitis and sinus tract. *Dent Traumatol* 17(4):185–187
3. Banchs F, Trope M (2004) Revascularization of immature permanent teeth with apical periodontitis: new treatment protocol? *J Endod* 30(4):196–200
4. Chueh L, Huang G (2006) Immature teeth with Periradicular periodontitis or abscess undergoing Apexogenesis: a paradigm shift. *J Endod* 32(12):1205–1213
5. Diogenes A, Henry MA, Teixeira FB, Hargreaves KM (2013) An update on clinical regenerative endodontics. *Endod Top* 28(1):2–23
6. Hargreaves KM, Diogenes A, Teixeira FB (2014) Paradigm lost: a perspective on the design and interpretation of regenerative endodontic research. *J Endod* 40(4 Suppl):S65–S69
7. Huang GTJ, Al-Habib M, Gauthier P (2013) Challenges of stem cell-based pulp and dentin regeneration: a clinical perspective. *Endod Top* 28(1):51–60
8. Yu J, Jamal M, Garcia-Godoy F, Huang GTJ (2015) Dental pulp stem cell niche. In: *Tissue-specific stem cell niche*. Cham, Springer, pp 163–189 (*Stem Cell Biology and Regenerative Medicine*; vol. 97)
9. Sonoyama W, Liu Y, Fang D, Yamaza T, Seo B-M, Zhang C et al (2006) Mesenchymal stem cell-mediated functional tooth regeneration in swine. *PLoS One* 1:e79

10. Sonoyama W, Liu Y, Yamaza T, Tuan RS, Wang S, Shi S et al (2008) Characterization of the apical papilla and its residing stem cells from human immature permanent teeth: a pilot study. *J Endod* 34(2):166–171
11. Huang GTJ, Sonoyama W, Liu Y, Liu H, Wang S, Shi S (2008) The hidden treasure in apical papilla: the potential role in pulp/dentin regeneration and bioroot engineering. *J Endod* 34(6):645–651
12. Huang GTJ, Yamaza T, Shea LD, Djouad F, Kuhn NZ, Tuan RS et al (2010) Stem/progenitor cell-mediated de novo regeneration of dental pulp with newly deposited continuous layer of dentin in an in vivo model. *Tissue Eng Part A* 16(2):605–615
13. Hayashi T (1994) Biodegradable polymers for biomedical uses. *Prog Polym Sci* [Internet] 19(4):663–702 Available from: <http://cat.inist.fr/?aModele=afficheN&cpsidt=4191425>
14. Gunatillake P, Mayadunne R, Adhikari R (2006) Recent developments in biodegradable synthetic polymers. *Biotechnol Ann Rev* [Internet] 12:301–347 Available from: <http://eutils.ncbi.nlm.nih.gov/entrez/eutils/eflink.fcgi?dbfrom=pubmed&id=17045198&retmode=ref&cmd=prlinks>
15. Bezwada RS, Jamiolkowski DD, Lee IY, Agarwal V, Persivale J, Trenka-Benthin S et al (1995) Monocryl suture, a new ultra-pliable absorbable monofilament suture. *Biomaterials* [Internet] 16(15):1141–1148 Available from: <http://eutils.ncbi.nlm.nih.gov/entrez/eutils/eflink.fcgi?dbfrom=pubmed&id=8562789&retmode=ref&cmd=prlinks>
16. Sun H, Mei L, Song C, Cui X, Wang P (2006) The in vivo degradation, absorption and excretion of PCL-based implant. *Biomaterials* [Internet]. 27(9):1735–1740 Available from: <http://eutils.ncbi.nlm.nih.gov/entrez/eutils/eflink.fcgi?dbfrom=pubmed&id=16198413&retmode=ref&cmd=prlinks>
17. Ma G, Song C, Sun H, Yang J, Leng X (2006) A biodegradable levonorgestrel-releasing implant made of PCL/F68 compound as tested in rats and dogs. *Contraception* [Internet]. Available from: <http://www.sciencedirect.com/science/article/pii/S0010782406000886>
18. Miner MR, Berzins DW, Bahcall JK (2006) A comparison of thermal properties between gutta-percha and a synthetic polymer based root canal filling material (Resilon). *JOEN* [Internet] 32(7):683–686 Available from: <http://eutils.ncbi.nlm.nih.gov/entrez/eutils/eflink.fcgi?dbfrom=pubmed&id=16793481&retmode=ref&cmd=prlinks>
19. Zalfen AM, Nizet D, Jérôme R, Franckenne F, Foidart JM et al (2008) Controlled release of drugs from multi-component biomaterials. *Acta Biomater* [Internet] 4(6):1788–1796 Available from: <http://eutils.ncbi.nlm.nih.gov/entrez/eutils/eflink.fcgi?dbfrom=pubmed&id=18583206&retmode=ref&cmd=prlinks>
20. Alani A, Knowles JC, Chrzanowski W, Ng Y-L, Gulabivala K (2009) Ion release characteristics, precipitate formation and sealing ability of a phosphate glass–polycaprolactone-based composite for use as a root canal obturation material. *Dent Mater* [Internet] 25(3):400–410 Available from: <http://linkinghub.elsevier.com/retrieve/pii/S010956410800273X>
21. Liao C-J, Chen C-F, Chen J-H, Chiang S-F, Lin Y-J, Chang K-Y (2001) Fabrication of porous biodegradable polymer scaffolds using a solvent merging/particulate leaching method. *J Biomed Mater Res* [Internet] 59(4):676–81. Available from: <https://doi.org/10.1002/jbm.10030>
22. Yang X, Yang F, Walboomers XF, Bian Z, Fan M, Jansen JA (2010) The performance of dental pulp stem cells on nanofibrous PCL/gelatin/nHA scaffolds. *J Biomed Mater Res A* 93(1):247–257
23. Bellows CG, Aubin JE, Heersche JN, Antosz ME (1986) Mineralized bone nodules formed in vitro from enzymatically released rat calvaria cell populations. *Calcif Tissue Int* 38(3):143–154
24. Agrawal CM, Ray RB (2001) Biodegradable polymeric scaffolds for musculoskeletal tissue engineering. *J Biomed Mater Res* 55(2):141–150
25. Sodian R, Sperling JS, Martin DP, Egozy A, Stock U, Mayer JE et al (2000) Fabrication of a trileaflet heart valve scaffold from a polyhydroxyalkanoate biopolyester for use in tissue engineering. *Tissue Eng* 6(2):183–188
26. Annabi N, Nichol JW, Zhong X, Ji C, Koshy S, Khademhosseini A et al (2010) Controlling the porosity and microarchitecture of hydrogels for tissue engineering. *Tissue Eng Part B Rev* 16(4):371–383
27. Thadavirul N, Pavasant P, Supaphol P (2014) Development of polycaprolactone porous scaffolds by combining solvent casting, particulate leaching, and polymer leaching techniques for bone tissue engineering. *J Biomed Mater Res A* 102(10):3379–3392





# Impact of Three-Dimensional Culture Systems on Hepatic Differentiation of Pluripotent Stem Cells and Beyond

Thamil Selvee Ramasamy, Agnes Lee Chen Ong, and Wei Cui

## Abstract

Generation of functional hepatocytes from human pluripotent stem cells (hPSCs) is a vital tool to produce large amounts of human hepatocytes, which hold a great promise for biomedical and regenerative medicine applications. Despite a tremendous progress in developing the differentiation protocols recapitulating the developmental signalling and stages, these resulting hepatocytes from hPSCs yet achieve maturation and functionality comparable to those primary hepatocytes. The absence of 3D milieu in the culture and differ-

entiation of these hepatocytes may account for this, at least partly, thus developing an optimal 3D culture could be a step forward to achieve this aim. Hence, review focuses on current development of 3D culture systems for hepatic differentiation and maturation and the future perspectives of its application.

## Keywords

Tissue engineering · Regenerative medicine · 3D culture · Hepatocytes · Pluripotent stem cells

T. S. Ramasamy (✉)  
Stem Cell Biology Laboratory, Department of  
Molecular Medicine, Faculty of Medicine, University  
of Malaya, Kuala Lumpur, Malaysia

Cell & Molecular Biology Laboratory, The Dean's  
Office, Faculty of Medicine, University of Malaya,  
Kuala Lumpur, Malaysia

Department of Surgery and Cancer, Institute of  
Reproductive and Developmental Biology, Imperial  
College London, London, UK  
e-mail: [selvee@ummc.edu.my](mailto:selvee@ummc.edu.my)

A. L. C. Ong  
Stem Cell Biology Laboratory, Department of  
Molecular Medicine, Faculty of Medicine, University  
of Malaya, Kuala Lumpur, Malaysia

W. Cui  
Department of Surgery and Cancer, Institute of  
Reproductive and Developmental Biology, Imperial  
College London, London, UK

## 4.1 Pluripotent Stem Cells Provide a Valuable Resource for Hepatocytes: Strength and Challenges

### 4.1.1 Human Hepatocellular Resource Is in Demand

The liver plays an essential role in detoxification, maintenance of homeostasis and metabolism in the body. This highly complex functionally complex organ consists of various cell types including hepatocytes, Kupffer cells, sinusoids and bile duct cells. Hepatocytes performs most of the specialised liver functions including aid digestion by producing bile acids, express detoxification cascade related enzymes, secrete serum proteins and

control the bulk of intermediary metabolism. Despite a low level of cell turnover normally, the liver has a unique feature which can regenerate cells upon destruction by certain short-term injuries, toxins, aging or diseases, subsequently to restore its functional state. The regeneration of the liver occurs without any external cellular resources through activation of organ residing stem cells. The presence of facultative hepatic stem cells within the intra-hepatic biliary tree are activated for rapid re-entry into the cell cycle from G<sub>0</sub> phase, and then differentiate into parenchymal cells; hepatocytes and bile ducts cells. However, the liver slowly loses its regenerative ability completely upon persistent liver injury, which causes chronic liver failure. On another note, acute liver failure is characterised by damage in a relatively short duration, in which part of the liver relatively has the ability to regenerate to support the liver function that was impaired. Although it may be possible for the trace residue liver cells to regenerate for restoration of liver function ultimately, this needs time. In these conditions, external support or cellular resources to support the impaired liver function necessitate to treat patients with liver failure.

Hepatocytes are in demand to bridge the gap of waiting for a liver donor due to the indispensable requirement to recover the partially or completely failed liver. This could be achieved by functional hepatocyte-embedded bioartificial liver device or by hepatocyte transplantation to restore the impaired function of failed liver or to correct metabolic liver diseases [40]. Despite these remarkably effective treatment strategies, the demand for transplantable human hepatocellular resources is ever-escalating. However, the shortage of available suitable donors is another crucial issue affecting transplantation, apart from the lack of well-established methodology and standard to grow and expand hepatocytes to a scalable format in culture while maintaining their functionality. Not only human hepatocytes are valuable for cell therapy application, but also instrumental for screening and development of pharmaceutical drugs. They serve as a cellular platform to assess the metabolism of xenobiotics and drugs in which the current practise heavily

relies on the animal models that may not effectively reflect metabolic processes and pathways in human. The demand for ideal hepatocellular resources for various fundamental and translational medical applications is discussed in the following section.

#### **4.1.1.1 Treatments for Liver Failure**

The patients with acute liver failure and end stage liver diseases are relying on donor organ transplantation as treatment. However, due to the limited availability of organ donors, it is essential to explore alternative hepatocyte approaches and resources to support human liver function during liver failure.

#### **Cell-Based Therapy for Liver Diseases**

Human embryonic stem cells (hESCs)-derived hepatocytes have emerged as a potential source for cell-based therapy. Due to the shortage of donor livers, cell-based therapy would be an alternative treatment for patients with liver failure to either allow the recovery of liver regeneration capacity or to bridge the gap prior to organ transplantation. hESC-derived hepatocytes would be the ideal choice for both tissue transplantation and BAL devices. A number of animal studies have demonstrated that it may possible to restore the lost function of the organ by transplantation of stem cell-derived hepatocytes [2, 9, 31, 171, 172, 181].

#### **Bioartificial Liver Devices**

A remarkable advancement in treatment of liver diseases is the development of bioartificial liver (BAL) devices which are known as extracorporeal devices embedded with functional hepatocytes to deliver therapeutic support for acute liver failure patients. The BAL-type devices are not a permanent solution to replace liver function, but only as a supportive device. Its function is by either bridging individual's liver functions or allowing natural liver regeneration following acute liver failure until an organ transplant is possible [140]. A hollow fiber-type BAL has been developed by Mizumoto et al. [116], with mouse ESCs (mESCs) immobilized inside it. The rats with liver failure were able to recover after treated

with BAL module under perfusion conditions containing hepatic differentiated mESCs, exhibiting liver-specific functions.

Researchers have been exploring on the innovative technologies in tissue engineering and stem cell research in the effort to provide solution for regenerative medicine. In the development of stem cell-derived liver technology, there are three key criteria to consider; (1) an efficient directed differentiation, (2) an expandable cellular resource and (3) high fidelity function. While use of stem cell-derived hepatocytes seems to be very favourable for cell-based therapy and BAL devices, characterisation of properties and function of the stem cell derived hepatocytes, the safety and post transplantation complications and unlimited cell sourcing need to be taken into consideration for successful therapeutic outcomes.

#### 4.1.1.2 Drug Screening and Toxicological Studies

##### Toxicity Screening for Drug Discovery

An efficient *in vitro* hepatic differentiation that generates functional cells could greatly improve the competence of drug development process. The process of drug development is costly with thousands of compounds unsuccessful at the pre-clinical stage, and the costs of introducing a drug to the market are estimated to range between \$800 million and \$2 billion [129]. The liver toxicity test is a measure for the safety of new drug, since the liver plays vital role in xenobiotic metabolism.

In the development of new drug, pharmaceutical R&D pipeline utilizes either primary hepatocyte culture or animal models for the prediction of potential drug hepatotoxicology, but both systems lack of a few critical safety aspects of drug development. Despite animal models are useful for *in vivo* drug testing, there is still a huge demand for human hepatocytes to overcome the differences in liver function among species, including induction of cytochrome P450 (CYP) [84]. Furthermore, the emphasis on the 3Rs principles; development of humane experimental framework that reduce, refine and replace the use of animals in research, has led to the need for an alternative methodology

or technology to reduce the use of animals in drug testing procedure. On the other hand, due to the scarcity of human hepatocytes, deriving human hepatocytes from hESCs is promising strategy to overcome the issues associated with toxicity screening for screening and discovery of drug. Efficient hepatic differentiation from hESCs could produce unlimited functional hepatocyte source and useful for toxicity screening in the pharmaceutical industry.

Remarkably, iPSC-derived hepatocytes from different patient is the latest development in the field that the technology improve drug toxicity assessment and development of effective personalised drug [4, 193]. Studies have showed that these cells derived from patients with metabolic deficiency can be used for specific disease modelling which could be useful for drug evaluation [16, 134]. On a specific note, Sirenko et al. [154] developed high-content imaging-based screening assays using iPSC-derived neuronal culture to study the efficacy and safety for drug development that this can be extended to develop liver toxicological workflow.

#### 4.1.1.3 Understanding Hepatocellular Related Disease Progression

Human pluripotent stem cells (hPSCs), both ESCs and induced pluripotent stem cells (iPSCs), showed evident potential in modelling liver pathology including infectious, genetic, metabolic diseases, thereby offering an innovative and cost-effective *in vitro* strategy to unravel the mechanisms pathophysiology of hepatic disorders. While liver transplantation models are widely available for key liver disorders, relevant hiPSC-based models are only available for few disorders including cirrhosis, metabolic diseases and polycystic disease [141]. Nevertheless, there is a great need for modelling cancer, cholestatic diseases and acute hepatic failure using human pluripotent stem cells.

The development of therapeutics has been hampered by greater lack of understanding of molecular mechanisms of injury, degeneration and infection, partly due to availability of *in vitro* and *in vivo* models that recapitulate molecular and cellular features of disease phenotypes. It is note-

worthy that great initiative has been taken in this aspect and that hiPSC-derived hepatocyte-like cells are employed as model to study virus infection including dengue, hepatitis C to unravel key phases of virus-host interactions [13, 86, 147].

#### **4.1.2 Pluripotent Stem Cells Provide Excellent Cellular Resources for Hepatocyte Generation**

##### **4.1.2.1 Alternative Models to Primary Hepatocytes**

Although the most ideal cell sources that could be used for treatment of liver diseases are the primary human hepatocytes, their restricted accessibility and phenotypic instability mean that alternative unlimited source of cells with least invasive procedure are needed together, for hepatocyte regeneration and replacement.

Human hepatoma carcinoma cell lines, including HepG2 and its clonal derivative C3A, have been embedded in extracorporeal liver-assist devices in patients from clinical trials [35]. However, the therapeutic outcomes is not significant which could be due to the poor function of HepG2 cells concerning their activities of mixed oxidase and ammonia detoxification [127]. Furthermore, patients' safety concerns have been raised with regards to the transmigration of tumour nodules outgrowth through a cut-off membrane of BAL system. Before being recognised suitable for BAL support, HepG2 cells require major improvement in safety and liver-specific functions aspects despite their scalable properties. Some hepatoma cells (HepaRG and HuH7) showed increased CYP3A4 activity compared to HepG2 cells [71, 155], but the basal activity is still lower than human hepatocytes, suggesting the limitation in hepatoma or hepatocellular carcinoma cells for hepatotoxicity and drug metabolism studies.

Alternatively, several studies have shown that hepatic stem cells are responsible for liver regeneration. These multipotent cells share similar characteristics to hepatoblasts, which reside in the Canals of Hering of mature adult liver, and the

ductal plates of foetal liver. Due to their expansion, differentiation potential and their role in liver regeneration, these cells considered to be beneficial in the development of cell-based therapy or BAL applications. The population of cells can be identified and isolatable using cell surface markers such as E-cadherin, EpCAM, CD29 and CD133 from foetal and postnatal donors and have been shown to engraft into liver tissue, following the cell transplantation in an animal model [144]. Although this may be a promising approach for applications in hepatocellular transplantation and BAL devices, the quantity of these cells is minute in the liver, thus sourcing and scaling up for therapeutic applications is a great challenge.

Trans-differentiation of bone marrow (BM)-derived stem cells, also known as mesenchymal stem cells (MSCs) is another way to generate hepatocyte-like cells. Differentiation of mouse, rat and human BM-derived multipotent adult progenitor cells with a cocktail of growth factors such as HGF, FGF2, EGF, DEX, OSM and nicotinamide, were able to express several liver-specific markers [3, 27, 47, 91, 146, 157]. These cells had showed several characteristics of functional hepatocytes including production of urea and albumin, expression of transcription factors and CYP activity. Liver of intoxicated rodents were engrafted with human BM-MSCs and differentiated into human hepatocytes, which demonstrated functional engraftment [7], express liver-specific markers [142] and improved liver fibrosis [197] and liver functions [83]. However, a few researchers postulate this as the fusion of recipient hepatocytes and BM-derived stem cells, rather than trans-differentiation event [185]. Besides, these adult stem cells also showed inconsistencies in their hepatic differentiation capacity [137, 186], while some claims that trans-differentiation of MSCs towards hepatocytes can happen without cell fusion [7, 142]. Hence, further studies are required to justify this and to ensure these MSCs of a greater benefit for liver disease treatment.

##### **4.1.2.2 Pluripotent Stem Cell-Derived Hepatocytes**

The progress made in differentiation of pluripotent stem cell into hepatocytes holds a great

promise for the liver failure treatment and differentiation from these cells have been shown to generate many different cell types. The successful isolation and culture of mouse and human ESCs many years ago has initiated a new prospectus of potential cell sources for cell therapy, developmental biology studies and other biomedical applications.

Both mESCs and hESCs owned two unique properties: (i) an unlimited capacity to generate themselves, named self-renewal and (ii) developmental potential to differentiate into all three derivatives of the primary germ layers: ectoderm, mesoderm and endoderm, termed pluripotency [177]. Owing to their unique properties, hESCs are excellent cell model for the study of developmental biology, since the restrained accessibility of early embryos and the limited tissue and stage-specific cells limit further research work into developmental changes. Moreover, hESCs supply a cell resource to generate wide varieties of cell types that could be utilised in regenerative medicine and many other biomedical and cell therapy applications such as (1) development of cell-based therapies for treatment of liver diseases; and (2) to study the development of particular lineage and (3) drug discovery and toxicology.

hESCs hold a promising unlimited source for the generation of hepatocytes to be utilised in toxicity screening and cell-based therapy. The idea of the hESCs differentiation process in recapitulating *in vivo* liver development has been extensively studied and replicated in many research [12, 51, 52, 130, 133, 181]. However, a more rigorous and accurate understanding of the instructive signals that govern the hESCs into the hepatocyte lineage and ultimately obtaining functional matured hepatocytes is in demand. Thus, there is a need for better understanding on the culture system underlying hepatic maturation and functionality *in vitro*, thus ensuring an improved technology for the liver-associated field.

Generation of induced Pluripotent Stem Cells (iPSCs) is a major breakthrough in the field of stem cell and regenerative medicine, holds immense potential in understanding disease

mechanism and development of personalised medicine. Promisingly, a latest study showed that transplantation of human iPSC-derived hepatocyte sheet have shown to successfully rescue mice from acute hepatic failure that this effect was mediated predominately by hepatocyte growth factor secreted from the human iPS-HLC sheet [120]. Considering iPSC technology pave a path for a personalised therapy, it provides an opportunity for genetic correction through gene editing technology for the diseases developed due to mutations, hence transplantation of the corrected iPSCs that further differentiated into specialised cell types will then evade tissue rejection and the need for immunosuppression. However, the exogenous genes used for reprogramming of somatic cells into iPSC state have the potential to cause adverse clinical effects including teratoma formation. If these obstacles can be resolved, iPSCs mostly likely be employed in treating many degenerative and genetic diseases including liver diseases. Not only for transplantation for regenerative purpose, iPSC technology provides relevant model or tool for disease modelling and development of personalised therapeutics or drugs.

#### **4.1.3 *In Vitro* Step-Wise Differentiation Milieu Produces Immature/Foetal-Like Hepatocytes**

The applications of hPSCS in biomedical field such as drug screening, require differentiation into functional hepatocytes comparable those *in vivo*. Meanwhile, for cell-based therapy application, it has been shown that progenitor or foetal-like hepatocytes were able to perform as these cells will be able to continue to be matured in the *in vivo* microniche to support the impaired function of the liver. Nevertheless, the efficiency of hESCs *in vitro* differentiation has been the ultimate focus of deriving hepatocytes for both applications. In the past decades, tremendous effort have been channelled in developing protocols to generate hepatocyte-like cells that the protocols generally be classified into two

differentiation or culture strategies; (1) spontaneous differentiation (via embryoid body formation) and, (2) directed and step-wise differentiation.

#### 4.1.3.1 Spontaneous Differentiation by Embryoid Bodies

The very early protocols in development of hepatic cells used formation of sphere-like aggregates called embryoid bodies (EBs), which, to a certain extent, mimics the early development of embryo. This protocol yields hepatocytes along with varieties of cell types, which often requires isolation or purification of hepatocytes from the differentiated EBs. Early hepatocyte specific markers, including ALB, AFP, transferrin, HNF4- $\alpha$  [69], GST, FoxA2 [115] and TDO2 were expressed in these derived cell population, to carry out certain hepatocyte functions, such as ICG uptake [190]. As they have neither been tested nor able to show terminal hepatic differentiation and functionality, such as steroid metabolism or CYP enzyme activity, they are still classified as early endodermal-hepatic cells. It could be due to some factors that are absent from other cell types, thereby affecting efficiency of hepatocyte differentiation. This EB-based spontaneous differentiation method rather limits the derivation of hepatocytes on scalable manner, since the hepatocyte population from a mixed population of many cell lineages is relatively low in number. With the aim to tackle this limitation, studies have described that cytokine-mediated differentiation following isolation or sorting of EB-derived hepatic cells, results in higher percentages of mature hepatic cells. Gouon-Evans et al. [48] reported that FACS-sorted mouse EB cells have yielded hepatocytes with better functional index. These mature hepatocyte-like cells from a highly enriched population (45-75%) were developed and characterised by the expression of CYP, major enzymes associated with bio-activation and drug metabolism, such as CYP3A11 and CYP7A1, glycogen storage and production of ALB upon addition of FGF2, Activin A and BMP-4. This finding indeed recapitulate the roles of growth factors and cytokines in governing and directing stem cells into a par-

ticular lineage with better differentiation efficiency.

The advantages that can be offered by the EB system include mimicking *in vivo* embryo organogenesis and development, providing a three-dimensional (3D) structure and providing some worthwhile information for lineage-specific differentiation in the presence of other cell types. Baharvand et al. [8] has cultured EBs with collagen scaffold 3D culture system supplemented with differentiation inducing growth factors. They suggested that this method is more efficient than 2D cultures in inducing hepatocyte differentiation as the latter system does not recapitulate the developmental microniche which is an essential coordination for cellular differentiation and maturation. Hence, the complex nature of EBs and specifically the presence of cells from other lineages have limit this tool to be developed as an ideal *in vitro* hepatic differentiation strategy, considering that a multiple-phased sequential differentiation is essential to augment derivation of desired population.

#### 4.1.3.2 Directed Hepatic Differentiation

Differentiation strategies to achieve more controlled and efficient derivation of therapeutically relevant cell types from stem cells are mainly by; (i) supplementation of stage specific differentiation inducing growth factors and cytokines, (ii) constitutive expression of hepatic-specific transcription factors, (iii) co-culture with other cell types and (iv) application of ECM or biomaterials and (v) biodegradable scaffolds based 3D culture, or (vi) a combination of any of these strategies [12, 62, 63, 70, 92, 160]. The differentiated cells yielded from these strategies have exhibited typical hepatocyte morphology, performed hepatocyte function to a certain degree and expressed nearly all commonly assessed hepatocyte markers. Table 4.1 summarises studies on hepatic differentiation of human embryonic stem cells (hESCs) or human induced pluripotent stem cells (hiPSCs) in different 3D culture system, which will be discussed in the following sections. Fundamentally, these strategies are developed by translating lessons from

**Table 4.1** Studies on hepatic differentiation of human embryonic stem cells (hESCs) or human induced pluripotent stem cells (hiPSCs) in different 3D culture systems

3D methods	Cell types	Materials	Growth factors/other factors	Expression/functionality	References
Collagen scaffold/collagen-coated dishes	hESCs	–	EB, HGF, aFGF, OSM, Dex, ITS	TAT, CK18, CK19, TDO, ATT, G6P, CYP7A1, secretion of AFP and ALB, production of urea.	[8]
Nanopillar plate	hESCs/ iPSCs	–	Genetic modification, FOXA2 & HNF4a overexpression, activin A, BMP4, FGF4, HGF, OSM, Dex, ITS	ALB, A1AT, CYP1A2, CYP2C19, CYP2C9, CYP2D6, CYP3A4, CYP7A1, ASGR1, c-Met	[169]
Co-culture using type I collagen/Swiss 3T3 cell sheets	hESCs/ iPSCs	Gelatin gel, cell sheet, matrigel	FOXA2 & HNF4a overexpression, activin A, bFGF, BMP4, FGF4, HGF, FGF1, FGF10, OSM, Dex	ALB, HNF4a, CYP2C9, CYP7A1, CYP1A2, CYP3A5, GSTA1, GSTA2, UGT1A1	[119]
Biochips	iPSCs	polydimethylsiloxane	Activin A, B27, HGF, bFGF, BMP4, OSM	HNF4a, CYP3A4, CYP1A2, ALB, AFP, CK19, CD144, glucose consumption, secretion of ALB, production of lactate	[89]
Micropatterned platform	hESCs	Microstencils, thin gelatin methacrylate hydrogels	B27, Wnt3a, activin A, bFGF, BMP4, FGF4, FGF8b, HGF, OSM, Dex	ALB, AFP, HNF4a, TAT, PXR, PPAR $\alpha$ , UGT1A1, UGT1A3, GSTA1, CYP1A2, CYP3A4, CYP3A7, CYP7A1, MDRI, MRP2, SLC01B3, OCT1, ABCC6, ABCC3, secretion of ALB, production of urea	[191]
Microcarriers in static culture/ stirred bioreactors	hESCs	crosslinked dextran microbead, macroporous gelatin, purified collagen beads	Activin A, BMP4, aFGF, HGF, ITS, Dex	ASGPR-1, ALB, AFP, G6P, MGST1, FV, HNF4a, NTCP, ORM1, CYP3A4, MRP2, GST $\alpha$ , PEPCCK1, secretion of ALB, production of urea	[131]
Scaffold-free microspheroid/3D hollow-fiber perfusion bioreactor	iPSCs	–	HGF, OSM	HNF4a, AFP, ALB, CYP1A2, CYP3A4, CK18, glucose consumption, lactate production, production of urea, secretion of AFP, ALB and A1AT	[109]
Hollow fiber-based perfusion bioreactors	hESCs	–	Activin A, FGF4, BMP2, HGF, OSM	HNF4a, ALB, A1AT, G6P, CYP3A4, CYP3A7, ARG1, ASL, ASS1, CPS1, OTC, CK8, CK18, glucose consumption, lactate production, secretion of ALB, production of urea	[112]
Hollow fiber membrane bioreactor	iPSCs	–	Activin A, B27, Wnt3a, HGF, OSM	CYP1A2, CYP2B6, CYP3A4, CYP2C9, CK18, CK19, HNF4a, glucose consumption, lactate production, secretion of AFP and ALB, production of urea	[41]

(continued)

Table 4.1 (continued)

3D methods	Cell types	Materials	Growth factors/other factors	Expression/functionality	References
Sealable stirred-suspension bioreactor	ESCs/ iPSCs	-	Activin A, B27, HGF, FGF4, OSM, Dex	HNF4a, AFP, ALB, TAT, CDH1, ASGPR1, CK18, glucose consumption, secretion of ALB, production of urea, ICG and LGL uptake, collagen synthesis	[187]
Spheroid	ESCs/ iPSCs	Galactosylated cellulosic sponges	Activin A, Wnt3a, bFGF, BMP4, FGF1, FGF4, FGF8b, HGF, Follistatin-288, OSM, ITS, Dex	AFP, CYP1A1, ALB, CYP3A4, CYP1A2, CYP2B6, ASGPR, MRP2, AAT, HNF4a, secretion of ALB, production of urea	[175]
Spheroid	hESCs	-	Activin A, Wnt3a, bFGF, BMP4, FGF8b, aFGF, FGF4, ITS, Dex, HGF, Follistatin	UGT1A1, ALB, ARG1, HNF4a, FVII, ASGPR-1, PEPCCK, AFP, CK8, CK18, CYP1A1/2, CYP2B6/7, CX32, secretion of ALB	[163]
Multicellular spheroid	iPSCs	-	EB, activin A, bFGF, TGFβ, FGF4, BMP4, WIF1, DKK1, OSM, HGF, ITS	CYP1B1, CYP3A4, CYP3A7, CYP2B6, CYP2C9, CK18, AFP, ALB, HNF4a, secretion of ALB, AFP and fibrinogen, ammonia metabolism, production of urea	[132]
Alginate scaffold	hESCs	-	B27, activin A, NaB HGF, OSM,	ALB, ApoF, TO, CYP3A4, CYP7A1, secretion of urea	[134]
Collagen hydrogel	iPSCs	-	Activin A, bFGF, BMP4, LY-294002, insulin, transferrin, HGF, OSM	MAOB, UGT1A1, NNMT, ABCC2, CYP3A4, secretion of ALB, A1AT and AFP	[44]
Hydrogel (agarose microwells, nanofibrillar cellulose, animal extracellular matrix-based)	iPSCs	-	B27, activin A, bFGF, BMP4, HGF, EGF, OSM	AFP, ALB, HNF4a, CYP1A2, CYP2C9, CYP3A4, CYP2B6, UGT1A1, SLCO1B1, SLOC10A1, ABCB11, ABCC2, ABCB1, secretion of ALB	[179]
Nanofiber hydrogel scaffold	iPSCs	-	EBs, activin A, bFGF, HGF, Dex	ALB, ASGPR, CYP1A2, CYP2D6, CYP7A1, CYP3A7, CYP3A4, CYP2C9, secretion of ALB, production of urea	[99]



developmental biology of endodermal and hepatic lineages into *in vitro* systems, which are discussed further in the following sections.

### Directed Hepatocyte Differentiation by Growth Factors and Small Chemicals

One of the major research areas of stem cell biology is the efficient differentiation of PSCs towards a specific lineage in a controlled and robust manner. Due to the multi-stage development process in liver (as discussed in Sect. 4.1.2), many procedures have been developed for hESCs differentiation into hepatocytes by sequential supplementation of various cocktails of cytokines/growth factors based on the animal developmental biology. ESCs differentiation to hepatocytes in this method mimics the liver development *in vivo*, which includes the following stages: (i) formation of definitive endoderm, (ii) hepatoblast specification, (iii) hepatocyte maturation.

Definitive endoderm (DE) differentiation is crucial for the formation of endoderm derivatives such as hepatocytes, intestine cells and pancreas [2, 20, 51, 59, 93] and the Nodal signalling pathway has an important role in this specific differentiation. Hence, Activin, which is a surrogate of Nodal and the most well-established factor, is used in the protocol for DE induction. After a high dose Activin A treatment, a significant upregulation of the expression of DE specific transcription factors, such as Mix, Sox17, GATA4 and GATA6 factors, is shown in hESCs. Multiple studies have shown that the dose of Activin A affects the production of DE from hESCs; only higher concentrations of Activin A leads to DE differentiation, whereas low levels favour the mesoderm lineage [2, 12, 20, 51, 173]. DE differentiation from hESCs is can be initiated through mesoendoderm, a transient bipotent progenitor stage, which has close resemblance to the primitive streak *in vivo*. After treatment for a day, cells co-express both endoderm markers (Sox17 and FoxA2) and mesoderm markers (brachyury, Mixl1 and gooseoid). By day 3–5 of differentiation, only the expression of endoderm markers is shown in most cells, while mesoderm markers

diminished. Moreover, CXCR4, the cell surface marker is highly expressed in DE cells.

Apart from Activin, other small molecules or signalling pathways such as the Wnt/ $\beta$ -catenin signalling activation factors, LiCl, Wnt3a and BIO are reported to stimulate Activin-induced DE differentiation, [52, 165]. Along with Activin, ESCs treated with a combination of these factors can lead to enhance DE differentiation efficiency [52, 165]. Another molecule, sodium butyrate, is a histone deacetylase inhibitor described to improve the homogeneity of Activin A-induced definitive endoderm differentiation from hESCs [67], by selectively ablating the undifferentiated hESCs [52]. Additionally, PI3K suppression with LY-294002 inhibitor has been reported in several studies to enhance Activin-induced DE differentiation [108, 181, 194]. To date, strategies to direct DE differentiation from ESCs using these methods can produce up to 80% DE cells [20, 51, 52, 181].

Subsequent to formation of DE, is the hepatic specification, which mainly achieved by supplement of medium with addition of growth factors, BMP-2 and FGF4 [2, 12, 112, 181]. Both growth factors provide signals to direct definitive endoderm into a hepatic fate and become hepatic progenitors [26] via regulation of hepatic endodermal genes, FoxA and Gata factors [17]. Furthermore, the chemical treatment of DE such as sodium butyrate or dimethylsulfoxide has also been shown to promote hepatocyte formation [19, 52, 136], most likely by affecting chromatin mediated transcription. Small molecule-based approach in hepatic differentiation of hESCs has been shown to generate morphological and functional hepatocyte-like cells that were similar or better compared to using growth factors [174]. The hepatic specification is assessed by the gene expression of hepatocyte-associated markers, such as ALB, AFP, HNF4 $\alpha$  and CK19.

The next step to generate functional hepatocytes is A set of defined combination of cytokines, HGF and OSM, have been used in hepatocyte maturation of ESC-derived hepatoblasts [2, 12, 52, 133, 151, 181]. HGF facilitates hepatoblast maturation selectively into hepatocytes via the hepatic regulator, CCAAT/enhancer

binding protein (C/EBP $\alpha$ ) [167]. Moreover, it also controls proliferation of hepatocyte in the fetal liver [184]. Dexamethasone, a steroid hormone, is used in some studies too [2, 9, 131, 163], for upregulation of CYP2A6 expression through increasing of HNF4 $\alpha$  binding to the proximal promoter [128].

The sequential differentiation mimicking developmental stages induce differentiation of hESCs to hepatocytes within a duration period of 15–28 days, depending on the type of hESC lines, and can generate up to 70% of hepatocytes in the final cell population. These hepatocytes not only useful for application, but also contribute as a potential *in vitro* model system to elucidate the molecular mechanisms underlying DE and hepatocyte differentiation. On the other hand, the functional capacity of these hepatocytes is not complete when compared to primary hepatocytes. Further development is required to produce scalable and functional hepatocytes for potential applications.

### Over-Expression of Hepatic Enriched Transcription Factor

The hepatic differentiation from pluripotent stem cells induced by growth factors/cytokines, which could be necessary to activate the downstream transcription factors. Interestingly, investigation on effect of ectopic expression of these downstream transcription factors has been carried out by several studies and the results revealed that the effects are similar in ESCs differentiation towards the hepatic lineage. For example, FoxA2 expression, which is a hepatic-specific transcription factor, has improved hepatic differentiation in both mESCs and hESCs [70, 88, 169]. Furthermore, a constant expandable endodermal phenotype is induced, following sufficient constitutive Sox17 expression in hESCs [148]. There was a dramatic increment of the expression of liver-specific markers without exogenous Activin A in Sox17-transgenic cells. In addition to *in vitro* differentiation, cell therapy and transplantation of hepatic progenitor cells with over-expressed HNF4A was a success in mice model of liver fibrosis [164]. The *in vitro* differentiation of hepatic progenitor cells to hepatic parenchymal cells was achieved

via the adenovirus-mediated HNF4 transduction, and this results in increased cholesterol, albumin and glucose levels in post cell transplant mice. Several groups also have generated human induced hepatocytes by direct hepatic reprogramming from fibroblasts through overexpression of a set of liver-enriched transcription factors such FOXA2, FOXA3, GATA4 HNF4A and HNF1A [56, 121, 153, 159], and therefore, facilitates the differentiation and proliferation of hepatocytes.

### Co-culture System with Other Cell Types

It has been suggested that the homotypic and heterotypic interactions in liver may have roles in hepatocyte functionality, as the micro-architecture of liver exhibits both interaction between cells. Indeed, compelling evidence shows that several non-hepatocyte cell types in the liver can improve hepatocyte maturation and functionality in co-culture systems. For instant, a group has showed an increase in gene expression in mature hepatocytes after co-culture of Thy-1 positive mesenchymal cells isolated from mouse foetal liver with AFP-producing ESC-derived hepatocytes [62]. Similarly, the regenerative liver has been shown to stimulate hepatic differentiation from ESCs [60]. These studies propose that ESCs could potentially be driven towards a hepatic fate via liver-specific cues from co-cultured cells. Cho et al. [15] have shown that a double sequential co-culture of hepatocytes with ESCs and fibroblast cells, results in cells exhibiting good hepatic morphology, functionality and gene expression. The liver comprises of many cells types, predominately hepatocytes (approximately 70–80%). In another study, non-parenchymal cells are required by hepatoblasts purified from mouse foetal liver for expression of hepatocyte markers and proliferation [125]. Interestingly, the combination of co-culture and 3D culture system can mimic human liver micro-structure and generate functional hepatocyte-like cells [119, 171].

The process of liver regeneration first involves the proliferation of parenchymal and non-parenchymal cells through highly orchestrated signalling events and cell-cell and cell-matrix

communications [39]. In addition, several studies have shown that Kupffer, stellate and sinusoidal endothelial cells release mitogenic factors that facilitate proliferation of hepatocytes both *in vivo* and *in vitro* models [103]. Interestingly, studies by Michalopoulos et al. [111] and Mitaka et al. [113] showed that co-culture with non-parenchymal cells yield higher number of hepatocytes, supporting the role of microniche in generation of therapeutically relevant cell types via secretomes and cell-to cell communications.. Not only the number, Soto-Gutiérrez et al. [160] demonstrated that when mESC-derived endoderm cells (EB, then further differentiated into DE) were co-cultured with non-parenchymal cells, they generated better functional hepatocytes assessed by their capacity to produce albumin, metabolize ammonia, lidocaine and diazepam in comparison to primary mouse hepatocytes.. The development of micropatterning technique which enable culturing of cells for controlled interactions provide further insight role of heterotypic interaction in governing the cellular fates. Micropatterned culture of hepatocyte-Kupffer cells affect the hepatocyte functionality through both cell-cell contacts and soluble factors secreted by co-cultured fibroblasts and human umbilical vein endothelial cells [198]. Similarly, hepatocyte function was shown to be improved by co-culture of iPSC-derived hepatocyte with endothelial cells in multicomponent hydrogel fibers that, vascularization was evident after implantation of this heterotypic cell system into a mouse model [30]. This effect is mediated efficiently by having an optimal ratio of various cell types and the right combination of cell types. While the effect can be mediated through 2 different modes; cell-cell contact or/and secretomes, a more recent study by Freyer et al. [42] showed that culture medium composition plays a significant role hepatic differentiation of hiPSCs co-cultured with human umbilical vein endothelial cells (HUVEC) that produced a superior differentiation index than those co-cultured with HUVEC. Taken all these together, current research direction is focusing on dissecting the complex microenvironment that govern cellular fates.

Several studies on 3D culture methods with scaffolds, bioreactors, spheroids, biochips, co-culturing, micropatterning have been carried out to facilitate hepatic differentiation of hESCs and iPSCs to hepatocyte-like cells. Stepwise differentiation protocol is commonly used by sequential addition of growth factors and other factors such as activin A and BMP4 followed by FGF4, HGF, ITS, OSM and Dex in culture media. Most differentiated cells in these 3D culture systems displayed several phenotypes of hepatocytes, including upregulation of hepatic gene expression (AFP, ALB, TAT, A1AT and HNF4a), increase in CYP isoenzyme activity, secretion of ALB and urea, as well as glucose consumption and lactate production. Some studies also reported that the 3D culture system was able to maintain the cell viability and hepatic differentiation efficiency.

#### 4.1.4 Achieving Efficient Differentiation and Functional Maturation: Challenge to Be Overcome

It has become a critical concern to have a functional and scalable source of hepatocytes in order to have successful drug toxicity screening. It becomes challenging to maintain both stem cell-derived and primary hepatocytes in their differentiated characteristics, since they tend to rapidly lose their differentiated function in culture [49, 161], which is often associated with loss of cell polarity and polygonal morphology. Studies have shown that lack of sufficient cell contacts between neighbouring hepatocytes may lead to loss of hepatocyte function and decrease in the hepatic gene expression [10, 195]. Previously, the conventional two-dimensional (2D) culture formats that are often applied to culture hepatocytes, do not mimic the similar response of cells in the 3D milieu of tissues *in vivo* [1, 166]. Hence, these cells showed a significant decrease in their functionality, such as loss of both canalicular structures and membrane transport activities [68, 97, 106] and a reduction in CYP activity [55, 135]. This phenomenon involves fundamental

changes in gene expression concomitant with a declined transcription of associated liver-specific genes, which is termed as dedifferentiation. The key factor facilitating the dedifferentiation event is the insufficient cellular niche which is a specialised tissue microenvironment providing for tissue survival, generation and function. This niche contains three major aspects, namely; (i) cell-cell contacts (ii) extracellular matrix components and (iii) soluble factors [28, 143].

Therefore, the most drastic improvement of both cell function and survival may be achieved by recreating av3D *in vitro* cell culture configuration to recapitulate the niche in liver [49], which is important to obtain and maintain the functionality of hepatocytes. Moreover, it is a crucial prerequisite to an improved culture system by having better understanding of the cell-cell contacts that modulate the behaviour of hepatocytes *in vitro*.

## 4.2 Three-Dimensional Culture: A System to Improve Hepatocyte Quality and Function

### 4.2.1 3D Culture System Provides a Milieu for Better Cellular Differentiation and Function

Generally, the function of differentiated human hepatocyte in 2D monolayer culture is short-lived and the suboptimal culture conditions that unable to recapitulate the environment in the liver is thought to be the cause. Thus, the culture hepatocyte function from both the liver and stem cells could be enhanced with the stimulation of *in vivo* environment from development of culture conditions. development. In order to achieve this, a 3D culture system could enhance both the functional and differentiation efficiency. On the other hand, some parameters such as seeding procedure, optimal scaffolding and cells' behaviour characterisation requires optimisation to establish a successful 3D cell culture in this scaffold.

Thus far, alginate has been discovered to be an excellent choice among several other biomaterials and scaffolds that have been tested. Alginate,

a biocompatible polymer widely employed for 3D scaffold in many cells types including liver is a polysaccharide derived from brown seaweed. Aside from the application of scaffold in tissue engineering, it has also been applied in basic biological studies as extracellular matrix (ECM) and in drug delivery system [5, 6, 87]. In the field of tissue engineering, alginate-based capsulation has been extensively used and applied to various type of cells such as ESCs [37, 43, 101, 133], primary hepatocytes [36, 45], human hepatocarcinoma cell lines [18, 77, 149] and hepatoblast [14]. The alginate-based approach facilitates the formation of spheroid [45], which has more advantage compared to other scaffolds particularly in promoting production of ECM via cell-cell contact and are formed partially by specific ECM. These hepatic spheres also exhibited better liver-specific functions and an extended viability in culture [45, 46, 80, 82].

#### 4.2.1.1 hESCs Based

As the protocols for hepatic differentiation of ESCs mostly focus on sequential differentiation using cocktail of growth factors, it has a benefit over other strategies (as discussed in Sect. 4.1.3) in generation of the most efficient differentiation. The cells are important in artificial liver devices and drug discovery but there are some drawbacks in these methods in the maintenance and maturation of the differentiated cells. Therefore, the current differentiation protocols need further improvement.

Research has described various strategies to maintain *in vitro* functionality of hepatocytes in 3D culture with either co-cultures of hepatocytes with endothelial cells [79, 90] and non-parenchymal cells [120, 171, 189] or enriched hepatocyte populations [57, 58]. While 3D culture plays a role in maintaining the adult primary hepatocyte functionality for a prolonged period, the system has also been shown to stimulate foetal hepatocytes to differentiation to a mature phenotype and maintain the functions [66, 150]. This indicates the use of 3D culture to support differentiation, maturation and maintenance of the hepatocytes. Hence, the combination of 3D culture and hESCs differentiation is predicted to

hold a great potential for higher quality of hepatocytes. Therefore, the soluble factors and cell-cell contacts could improve maturation through the well-adjusted culture conditions that recapitulate *in vivo* environment.

In order to produce hepatocytes from ESCs, a few studies have attempted to create 3D systems [8, 60]. All these studies were conducted, either after the *in vitro* EBs formation in suspension culture and transfer of EBs to the scaffold or by ESCs seeding into the 3D scaffold for differentiation into EBs, the differentiation of hepatocytes continues from the EBs in the scaffold. The attempts to obtain fully functional mature hepatocytes are unsuccessful, despite all these efforts, which could be explained by the inefficient DE differentiation from EB formation method. Therefore, the incorporation an enriched hESC-derived DE into the 3D scaffold may enhance the maturation of hESCs and the yield of hepatocytes.

It is essential to understand the control of highly sophisticated cell biology processes in all 2D and 3D differentiation methods. Additional challenges involving cell organisation, survival, attachment and differentiation in 3D culture systems, remain largely unknown, thus warrant further research to understand the cell behaviour for better hepatocyte function and differentiation.

## 4.2.2 Development of 3D Culture System

Various methods have been established to develop physiologically significant models in a reproducible and controllable approach, knowing that 3D microniche is crucial for maintenance of cell function. The two strategies mainly used by these methods are; suspension cultures and biomaterial-based scaffolds/hydrogels.

### 4.2.2.1 Formation of Spheroids and Aggregates in Suspension Cultures

Moscona first observed the spontaneous formation of aggregates *in vitro* by using a rotational technique in 1961 [117] and many years later,

another 3D aggregates were formed by plating cells in an ultra-low or non-adherent culture dish containing serum-free medium. The resulting aggregates were named 'spheroids' [85] and exhibited deposition of ECM consists of fibronectin, laminin and collagen, histotypic (one cell type) reorganisation, as well as extended survival and improved metabolic and production of plasma protein, such as secretion of ALB and transferrin induction [139, 180]. This method is simple and inexpensive to carry out using non-adhesive to produce spheroids, even though the spheroids exhibited differences in shape, cell number and size [196].

Several groups have successfully produced hanging drop technique, a fast, homogenous and inexpensive spheroid formation method [74, 75, 95]. Initially, this method was developed to facilitate the formation and cultivate EBs, through microgravity at the liquid-air interface. Although this method limits the scalability of 3D sphere formation, the culture model has been useful for studying molecular and cellular events during the interaction of two different cell types as well as angiogenesis in tumoursphere culture [23, 178]. A number of rotary culture systems has been developed to overcome the disadvantages of stationary culture method and it becomes feasible to have massive cell production, while providing an enrichment in 3D-induced functionality [78].

### 4.2.2.2 Biomaterials Scaffold/Hydrogel Based 3D Formation

Another 3D modelling system that has been widely used is the biodegradable scaffolds/hydrogels. This particular system supports the Biomaterial-based scaffolds/hydrogels support the formation of organoids or tissue like structures eventually recapitulates the *in vivo* micro-environment. 3D scaffold-based culture systems made from various type of materials have been shown to enhance various differentiation protocols including osteogenesis [29], haematopoiesis [96], neural differentiation [124, 168], and provide greater support for hepatocyte proliferation and functionality than routine 2D cell culture system [36, 45].

Both natural and synthetic biodegradable biomaterials have close resemblance to the native tissue, thus making them a promising scaffold materials for soft tissue engineering. Since the nature of cell interaction depends on the scaffold's features, both the internal morphology (pore size and porosity) and chemistry of the scaffolds impose great impact on the nature of tissue regeneration and functionality improvement. Fundamentally, biomaterial scaffolds provide one of these two cues for cellular behaviours; (i) acting as the extracellular matrix (exogenous) and/or (ii) promoting lineage-specific ECM expression (endogenous) [183] through enhanced cell-cell contact. Therefore, it is of utmost important that the biomaterial influence and suitability on cell functions are clearly understood before the creation of optimal cell niche. Several 3D cellular model systems using scaffolds/hydrogels made from biomaterials, such as alginate [6, 34, 38, 45, 133], collagen [8, 44, 60], matrigel [63, 145], hyaluronic acid [183] and chitosan [33] have been widely used. Among various biomaterials, alginate is of special interest for hepatic tissue engineering. Interestingly, iPSC-derived hepatocyte-like cells via 3D co-aggregation with stromal cells and encapsulation with alginate capsules, have been successfully engrafted in immunocompetent mice [158]. The secretion of albumin and A1AT and gene expression of hepatic markers in iPSC-hepatocyte-like cells/stromal cells aggregates were comparable to human hepatocytes/stromal cells aggregates.

Over the years, researchers have been improving the various available scaffolds for better outcomes in tissue engineering applications. Recently, a study has showed that hPSC-derived DE cells attached better to acellular matrix derived from HepaRG, expressing hepatocyte-specific markers, compared to other matrices [72], shedding light on the important role of specific matrices in promoting hepatic differentiation and maturation. Besides, comparing with randomly oriented polyethersulfone (PES) nanofibers, aligned PES nanofibrous scaffolds could improve the iPSCs differentiation into hepatocyte-like cells and functions [102]. Culturing of ESCs on substrate stiffness that is similar to human

liver has advantage on maturation of ESCs-derived hepatocytes [114], which could further improve the function of hepatocyte-like cells.

While a preference for stem cell-derived hepatocytes is expressed for liver-based technology, it remains a challenge to provide an absolutely functional hepatocyte resource. The research focusing on the development and application of 3D culture is progressively developed latest, innovative and advance sophisticated strategies/technologies, which are discussed in the following sections.

#### 4.2.2.3 Static vs. Dynamic Culture

Static culture involves culturing of cells in stagnant media. The most common method uses to achieve static culture is through the formation of spheroids or multicellular aggregates. The adherent cells aggregate through low suspension culture in low-adhesion culture plate, rotating culture and hanging drop techniques [107]. Generally, EBs are utilised to induce differentiation in pluripotent stem cells as they are able to differentiate into three germ layers and provide the environment that mimics embryonic development [64]. Studies have shown that 3D spheroid culture improved the functionality of ESCs-differentiated hepatocyte [132, 163, 170]. However, this method is not suitable for large scale cell expansion and long-term suspension culture. Some of the cells agglomerate, become apoptotic and non-proliferative due to limited perfusion of oxygen and nutrients to the centre of the spheroids with accumulation of waste [32]. On the other hand, bioreactors such as spinner flasks, fed-batch, rotating wall vessel and mechanical force bioreactors can be incorporated into culture system to create dynamic culture conditions. The bioreactors are useful for higher cell densities culture and overcome the limitation of static culture by introducing continuous agitation, resulting in increasing oxygen and nutrients flow to the cells and removing cellular waste metabolites. Besides, both culture methods can be modified by integration of either natural or synthetic biomaterials including microcarriers, microcapsules and microfluids. These biomaterials are able to mimic the properties of stem cell niche for maintenance and differentiation of cells [107].

#### 4.2.2.4 Micropatterned Cultures

Micropatterning has been widely used for cellular analyses, cell-based sensing and tissue engineering applications. Cells are highly sensitive to the microenvironment in *in vitro* culture and micropatterning enable manipulation of those important properties of the microenvironment (structures, volume and biochemical composition) that influence cell growth, differentiation, migration and cell fate [110, 123]. It involves fabrication of plastic or glass culture surface and enable control over cell and tissue architectures with differential cell adhesion patterns [176]. The first step in micropattern culture is the generation of an adhesiveness-controlled pattern onto culture substrate. The cells are seeded and adhered on target region of culture substrate and washed to remove non-adherent cells. For co-culture, the non-adhesive surface is reactivated and the second cell type is seeded and adhered to the area without the first cell population, producing patterned co-culture [21]. Examples of materials that are used to facilitate and prevent cell adhesion includes extracellular matrix proteins (collagen, laminin and fibronectin), BSA, agarose, PEG and poly-lactide [123]. A study has showed that agarose micropatterning on glass culture surface enabled analysis of differentiated HepaRG cells and high throughput genotoxicity testing [110] while micropatterned co-cultures of mESCs and stellate cells with combination of growth factor arrays can further enhance hepatic differentiation of mESCs [182]. As most hepatic differentiation involved interruptive protocols, study by Yao et al. [191] has achieved a more homogenous and uninterrupted hepatic differentiation of hESCs using 3D multi-layered colonies with microstencil array.

#### 4.2.2.5 3D-Bioprinting Technology

In recent years, researchers have made a major breakthrough by developing 3D bioprinters which enable the fabrication of large 3D vascularised tissue for transplantation purpose. These bio constructs enhance the cell survival, proliferation and differentiation by having better vascularisation mimicking the *in vivo* microenvironment [11].

Bioprinting employs controlled and precise delivery and placement of living cells, biomaterials and biochemicals to fabricate functional 3D constructs. Design approaches including tissue self-assembly, biomimicry and mini-tissue blocks can be used in combination for printing of multifunctional components or structures. It is crucial to determine the suitable biomaterials, differentiation and growth factors and types of cells prior to construction of tissues and organs [118]. The most widely use bioprinting system for cell deposition are extrusion bioprinting, laser bioprinting and ink jet bioprinting. Extrusion bioprinting has the capacity to deliver bioink/cells from syringe at relatively high viscosity or cell concentration but it produces pressure along the nozzle, leading to possible apoptosis and deformation of bioink encapsulated cells. Ink jet bioprinting has a cartridge loaded with bioink/cells and printed in droplets. It has problem with printing with high cell concentration or viscous materials. Laser bioprinting uses laser stimulation to allow vaporization of sacrificial materials and delivers bioink/cells droplet on collection substrates. This method is able to overcome limitations of extrusion and ink jet bioprinting by reducing shear stress, nozzle clogging and allows printing with viscous bioink and high cell densities [61]. It is noteworthy that both mechanical and shear stresses can trigger differentiation of stem cells to different cell types in [152, 162], suggesting the importance of selecting suitable strategy for specific type of cells.

Interestingly, Ma et al. [100] has developed a 3D bioprinted hydrogel-based triculture model (hiPSC-hepatic progenitor cells embedded with adipose-derived stem cells and human umbilical vein endothelial cells) that showed functional and phenotypic enhancements in the hiPSCs such as high expression levels of liver-specific genes, enhanced secretion of metabolic products and improved morphological characteristics. Besides, a small portion of human liver model has been constructed by another group with bioprinting technology. The model has the ability to maintain liver metabolic functions and bile acid secretion [81]. Printing complex hollow organ and large tissue construct with embedded vascular features and

incorporation of multiple materials can be challenging with the current bioprinting approaches. Despite that, 3D bioprinting technology remains a promising tool for drug screening, tissue transplantation and regenerative therapies [105].

Thus, organ printing is a new emerging enabling technology paradigm which enables us to produce a large scale living human organ constructs which offer a better alternative to classic biodegradable scaffold-based approach in tissue engineering.

### 4.2.3 Challenges and Prospects of 3D Culture in Achieving Hepatic Maturation

The differentiation of hESCs along the hepatic cell lineage has undergone remarkable changes over the decades, ranging from generation of EB to growth factor directed differentiation. The progress of hepatocyte generation has been substantial, with greatest improvement up to 70–80% efficiency. Although advancement towards the development of improved protocols is profound, further functional improvement and a good efficient reproducibility are still hindered by existing problems. Identification of these problems, from all relevant studies, holds great initiative for future research before being fully employed for toxicology studies, cell therapy or for BAL device incorporation.

#### 4.2.3.1 Inherent of Cellular Sources

Often heterogeneous characteristics of hESCs is attributed by variation between derivation of the different lines, culture media and methods, passage numbers and fluctuating plasticity during *in vitro* passaging. In particular, their differentiation kinetics and factors required for efficient differentiation were different between the hESCs lines we have tested so far, namely H1, H7 and H9 lines [24, 50, 156]. Thus, this represents a major barrier in development of robust differentiation protocols and often requires a customised differentiation procedure.

Another major hurdle in yielding sufficient number of high quality hepatocytes in culture as

most culture systems are not efficient in deriving phenotypically same quality of cells. FACS sorting cells based on their cell surface markers or genetically engineered markers can enrich for certain cell types, which then can be expanded and differentiated [20, 48, 53, 54, 104, 192]. Incorporation of this technique would be, therefore, very promising in order to obtain relatively pure cell population.

#### 4.2.3.2 Sourcing Therapeutically and Pharmaceutically Valuable Hepatocytes at Large Scale

Meanwhile stepwise differentiation using differentiation factors and 3D culture have been shown to yield higher number of functional hepatocytes, they do not proliferate when they are switched into efficient differentiation mode in 3D culture system [122, 188]. This leads to the question of how to develop sufficient number of mature hepatocyte-like cells derived from hESC which will be made available for downstream applications such as cell therapy, BAL technology and toxicology studies. To overcome this hurdle, it may provide a better strategy to expand cells at early progenitor stage or hepatoblasts with high proliferative capacity to sufficient number before transferring into 3D culture system to achieve better differentiation and maturation.

#### 4.2.3.3 Development of Defined and Xenogeneic-Free Culture Components

Another challenge relating to sourcing hPSC-derived hepatocytes for clinical application is that most protocols are developed to be undefined culture conditions, either by co-culture or the use of serum. Hence, it produces variable outcomes due to its undefined conditions, mainly caused by varying factors produced by cells in the co-culture system. This could be overcome by the development and use of small molecules and synthetic biocompatible ECMs which can substitute for xeno-derived ECMs. The use of serum may contribute to stochastic differentiation into hepatocytes that development of serum-free conditions or the use of serum-replacement factors may be favoured.



### 4.3 Current State-Of Art in Development of Engineered Tissue and Organs

#### 4.3.1 3D Printer for Bioengineered Tissue

##### 4.3.1.1 Bioreactors

A very constructive technology development that aid better culture technology is the development of bioreactors. The increasing recent interest in *in vitro* culture of hepatocytes and many other tissue/cell types in 3D format has resulted in the introduction of bioreactors in an attempt to more closely stimulate *in vivo* liver architecture. This would further extend the survival and functional lifetime of hepatocytes past those of the static culture of 3D hepatocytes. Progressively, such systems have been shown to incorporate into BAL support systems and resulted in a promising outcome both *in vitro* and in experimental animal models of acute liver failure [22, 65, 94]. Following successful testing in animal models, phase I clinical studies were carried out on patients with acute liver failure and showed beneficial effects on the patients [25, 76]. Besides, studies on 3D culture of hESCs and iPSCs with hollow fiber perfusion and stirred-suspension bioreactors have reported cells differentiation into hepatocyte-like cells along with upregulation of hepatic gene expression, hepatic metabolism and secretory functions [41, 109, 112, 187].

##### 4.3.2 Vascularization

Despite many research works have dedicated towards generation of functional hepatocyte culture system, developing a three-dimensional vascularised liver or hepatocellular system remains as great challenge. Intriguingly, Takebe et al. [172] has developed a culture system to generate a vascularised and functional human liver from iPSCs which achieved by the three-dimensional self-organisation of hepatic precursor cells (endodermal cells) with endothelial and mesen-

chymal cells recapitulating organogenesis interactions. These *in vitro* generated liver buds were able to connect to the host vessels with short period of time upon transplantation into a mice model.

It is essential to have functional vascularization system during development of the tissue construct. Growth/pro-angiogenic factors such as bFGF, VEGF, PDGF and angiopoietin-1 are loaded on biomaterial scaffolds enhance vascular development. A study has showed that VEGF enhanced vascularization of scaffolds transplanted on rat liver lobules and the hepatocyte engraftment [73]. In addition, the construct's engineering and design are relative important too to ensure cell viability with sufficient oxygen and nutrients perfusion. The combinations of channelled scaffolds and micropatterning techniques with varying concentrations of growth factors could also promote migration of vascular cells. Other current approaches such as angiogenic factors-transfected cells and co-culture-based techniques, bioreactors systems, microfluidics, modular assembly and *in vivo* systems have shown to promote cell viability, stimulate angiogenesis and formation of capillary-like structure [98, 126, 138]. However, there is a need to fully understand the nutrients and oxygen requirements of the tissue for efficient *in vivo* transplantation.

---

#### 4.4 Implication of 3D Culture in Liver Disease and Future Perspective

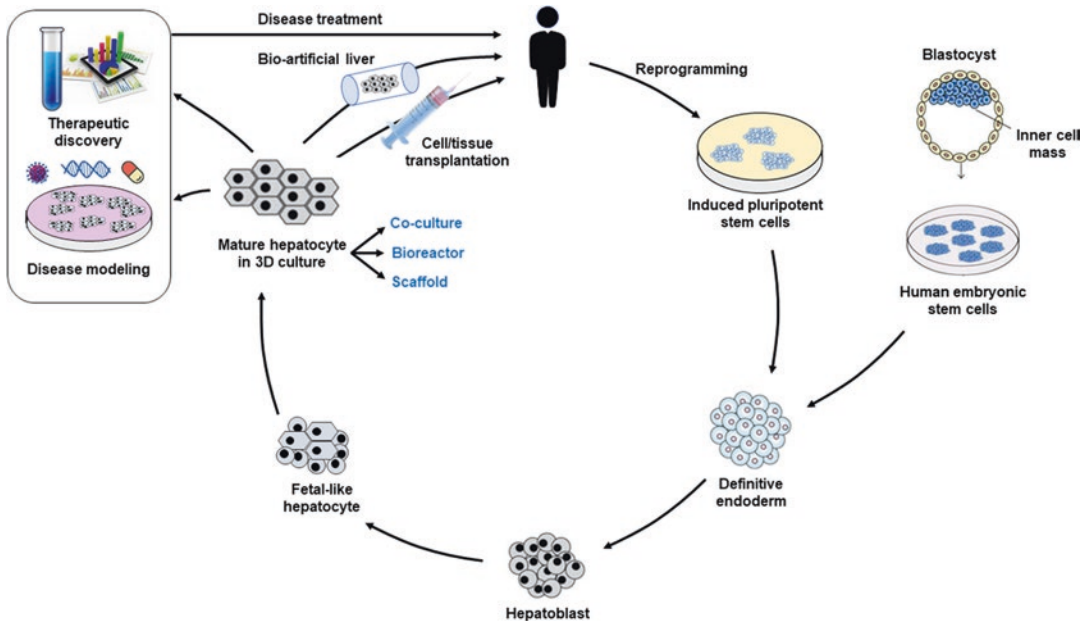
In conclusion, hPSCs hold a great potential as an unlimited resource in hepatocytes production for development of bioartificial devices, cell therapy, disease modelling and screening for therapeutics. The concept of hPSCs differentiation process mimicking the *in vivo* liver development has been recapitulated in several studies [12, 51, 52, 133, 181, 194]. The hepatocytes generated from 3D culture approaches, including co-culture with other cell types, bioreactor systems and generation of scaffolds, are critical for the applications in cell/tissue transplantation, generation of bio-

artificial liver, therapeutic discovery and disease modelling. For a better culture system, further insights into which instructive cues and how do these signals direct hPSCs into the hepatocyte lineage would pave a path to achieve the ultimate goal (Fig. 4.1).

Achieving functional maturation of hepatocytes remains one of the key challenges for hESC-derived hepatocytes, and even in primary hepatocytes, as they lose their *in vivo* niche when growing in monolayer. Thus, recreating the niche *in vitro* is the key step needed to improve the maturation of hESC-derived hepatocytes. Technological advancement using various strategies in deriving hepatocytes from embryonic and induced pluripotent stem cells has promoted further investigation into better strategies to yield the mature hepatocytes which are in greatest demand. Hepatocyte functionality improvement shown in 3D culture in complement with many other culture conditions indicates that the final maturation steps require an *in vivo* environment. This includes homotypic and heterotypic cell interactions to provide a micro-niche suitable for functionality modulation. This seems to be a very complex net-

work of cellular interactions, and is still largely not understood both *in vivo* and *in vitro*.

As for the future, despite continual improvement in *in vitro* differentiation of hESCs into the hepatic lineage, we need to take the state-of-art such as bioprinting, organ on chip, vascularization and many other complement systems into consideration. It is vital to be very strategised in employing these new technological improvements and approaches that may be inter-related and could be the success of applications of hESCs/hiPSCs-derived hepatocytes. Indeed, this holds immense potential in sourcing for hepatocytes (universal source and patient specific), and therefore clinically useful. The increasing recent interest in *in vitro* culture of hepatocytes in 3D format has resulted in the introduction of innovative bioreactors in an attempt to more closely stimulate *in vivo* liver architecture. This would further extend the survival and functional lifetime of hepatocytes past those of the static culture of 3D hepatocytes. Such systems have been shown to incorporate into BAL support systems and resulted in a promising outcome both *in vitro* and in experimental animal models of acute liver failure.



**Fig. 4.1** Schematic presentation of the specific stages during *in vitro* hepatocyte differentiation of embryonic stem cells and induced pluripotent stem cells in 3D culture system

**Acknowledgements** This work was supported by the University of Malaya Research Grant (UMRG RG465-12HTM) and Ministry of Education Malaysia, Fundamental Research Grant Scheme (FRGS FP044-2014B).

## References

- Abbott A (2003) Cell culture: biology's new dimension. Nature Publishing Group, Reino Unido
- Agarwal S, Holton KL, Lanza R (2008) Efficient differentiation of functional hepatocytes from human embryonic stem cells. *Stem Cells* 26(5):1117–1127
- Al Ghrbawy NM, Afify RAAM, Dyaa N, El Sayed AA (2016) Differentiation of bone marrow: derived mesenchymal stem cells into hepatocyte-like cells. *Indian J Hematol Blood Transfus* 32(3):276–283
- Anson BD, Kolaja K, Kamp TJ (2011) Opportunities for human iPS cells in predictive toxicology. *Clin Pharmacol Ther* 89(5):754–758
- Atala A, Cima LG, Kim W, Paige KT, Vacanti JP, Retik AB, Vacanti CA (1993) Injectable alginate seeded with chondrocytes as a potential treatment for vesicoureteral reflux. *J Urol* 150(2):745–747
- Augst AD, Kong HJ, Mooney DJ (2006) Alginate hydrogels as biomaterials. *Macromol Biosci* 6(8):623–633
- Aurich I, Mueller LP, Aurich H, Luetzkendorf J, Tisljar K, Dollinger MM, Schormann W, Walldorf J, Hengstler JG, Fleig WE, Christ B (2007) Functional integration of hepatocytes derived from human mesenchymal stem cells into mouse livers. *Gut* 56(3):405–415
- Baharvand H, Hashemi SM, Kazemi Ashtiani S, Farrokhi A (2006) Differentiation of human embryonic stem cells into hepatocytes in 2D and 3D culture systems in vitro. *Int J Dev Biol* 50(7):645–652
- Basma H, Soto-Gutiérrez A, Yannam GR, Liu L, Ito R, Yamamoto T, Ellis E, Carson SD, Sato S, Chen Y (2009) Differentiation and transplantation of human embryonic stem cell-derived hepatocytes. *Gastroenterology* 136(3):990–999 e994
- Ben-Ze'ev A, Robinson GS, Bucher N, Farmer SR (1988) Cell-cell and cell-matrix interactions differentially regulate the expression of hepatic and cytoskeletal genes in primary cultures of rat hepatocytes. *Proc Natl Acad Sci* 85(7):2161–2165
- Bertassoni LE, Cecconi M, Manoharan V, Nikkhah M, Hjortnaes J, Cristino AL, Barabaschi G, Demarchi D, Dokmeci MR, Yang Y (2014) Hydrogel bioprinted microchannel networks for vascularization of tissue engineering constructs. *Lab Chip* 14(13):2202–2211
- Cai J, Zhao Y, Liu Y, Ye F, Song Z, Qin H, Meng S, Chen Y, Zhou R, Song X (2007) Directed differentiation of human embryonic stem cells into functional hepatic cells. *Hepatology* 45(5):1229–1239
- Carpentier A, Tesfaye A, Chu V, Nimgaonkar I, Zhang F, Lee SB, Thorgeirsson SS, Feinstone SM, Liang TJ (2014) Engrafted human stem cell-derived hepatocytes establish an infectious HCV murine model. *J Clin Invest* 124(11):4953–4964
- Cheng N, Wauthier E, Reid L (2008) Mature human hepatocytes from ex vivo differentiation of alginate-encapsulated hepatoblasts. *Tissue Eng A* 14(1):1–7
- Cho CH, Parashurama N, Park EY, Suganuma K, Nahmias Y, Park J, Tilles AW, Berthiaume F, Yarmush ML (2008) Homogeneous differentiation of hepatocyte-like cells from embryonic stem cells: applications for the treatment of liver failure. *FASEB J* 22(3):898–909
- Choi SM, Kim Y, Shim JS, Park JT, Wang RH, Leach SD, Liu JO, Deng C, Ye Z, Jang YY (2013) Efficient drug screening and gene correction for treating liver disease using patient-specific stem cells. *Hepatology* 57(6):2458–2468
- Cirillo LA, Lin FR, Cuesta I, Friedman D, Jarnik M, Zaret KS (2002) Opening of compacted chromatin by early developmental transcription factors HNF3 (FoxA) and GATA-4. *Mol Cell* 9(2):279–289
- Coward SM, Legallais C, David B, Thomas M, Foo Y, Mavri-Damelin D, Hodgson HJ, Selden C (2009) Alginate-encapsulated HepG2 cells in a fluidized bed bioreactor maintain function in human liver failure plasma. *Artif Organs* 33(12):1117–1126
- Czysk K, Minger S, Thomas N (2015) DMSO efficiently down regulates pluripotency genes in human embryonic stem cells during definitive endoderm derivation and increases the proficiency of hepatic differentiation. *PLoS One* 10(2):e0117689
- D'Amour KA, Agulnick AD, Eliazar S, Kelly OG, Kroon E, Baetge EE (2005) Efficient differentiation of human embryonic stem cells to definitive endoderm. *Nat Biotechnol* 23(12):1534
- D'Arcangelo E, McGuigan AP (2015) Micropatterning steps. *BioTechniques* 58(1):13–23
- Damania A, Hassan M, Shirakigawa N, Mizumoto H, Kumar A, Sarin SK, Ijima H, Kamihira M, Kumar A (2017) Alleviating liver failure conditions using an integrated hybrid cryogel based cellular bioreactor as a bioartificial liver support. *Sci Rep* 7:40323
- De Ridder L, Cornelissen M, De Ridder D (2000) Autologous spheroid culture: a screening tool for human brain tumour invasion. *Crit Rev Oncol Hematol* 36(2):107–122
- Deb KD, Sarda K (2008) Human embryonic stem cells: preclinical perspectives. *J Transl Med* 6(1):7
- Demetriou AA, Brown RS, Busuttill RW, Fair J, McGuire BM, Rosenthal P, Am Esch JS, Lerut J, Nyberg SL, Salizzoni M, Fagan EA, de Hemptinne B, Broelsch CE, Muraca M, Salmeron JM, Rabkin JM, Metselaer HJ, Pratt D, De La Mata M, McChesney LP, Everson GT, Lavin PT, Stevens AC, Pitkin Z, Solomon BA (2004) Prospective, randomized, multicenter, controlled trial of a bioarti-

- ficial liver in treating acute liver failure. *Ann Surg* 239(5):660–670
26. Deutsch G, Jung J, Zheng M, Lórá J, Zaret KS (2001) A bipotential precursor population for pancreas and liver within the embryonic endoderm. *Development* 128(6):871–881
  27. di Bonzo LV, Ferrero I, Cravanzola C, Mareschi K, Rustichell D, Novo E, Sanavio F, Cannito S, Zamara E, Bertero M, Davit A, Francica S, Novelli F, Colombatto S, Fagioli F, Parola M (2008) Human mesenchymal stem cells as a two-edged sword in hepatic regenerative medicine: engraftment and hepatocyte differentiation versus profibrogenic potential. *Gut* 57(2):223–231
  28. Discher DE, Mooney DJ, Zandstra PW (2009) Growth factors, matrices, and forces combine and control stem cells. *Science* 324(5935):1673–1677
  29. Du D, Furukawa KS, Ushida T (2009) 3D culture of osteoblast-like cells by unidirectional or oscillatory flow for bone tissue engineering. *Biotechnol Bioeng* 102(6):1670–1678
  30. Du C, Narayanan K, Leong MF, Wan AC (2014) Induced pluripotent stem cell-derived hepatocytes and endothelial cells in multi-component hydrogel fibers for liver tissue engineering. *Biomaterials* 35(23):6006–6014
  31. Duan Y, Catana A, Meng Y, Yamamoto N, He S, Gupta S, Gambhir SS, Zern MA (2007) Differentiation and enrichment of hepatocyte-like cells from human embryonic stem cells in vitro and in vivo. *Stem Cells* 25(12):3058–3068
  32. Edmondson R, Broglie JJ, Adcock AF, Yang L (2014) Three-dimensional cell culture systems and their applications in drug discovery and cell-based biosensors. *Assay Drug Dev Technol* 12(4):207–218
  33. Elçin E, Elçin M, Pappas G (1998) Neural tissue engineering: adrenal chromaffin cell attachment and viability on chitosan scaffolds. *Neurol Res* 20(7):648–654
  34. Elkayam T, Amitay-Shaprut S, Dvir-Ginzberg M, Harel T, Cohen S (2006) Enhancing the drug metabolism activities of C3A—a human hepatocyte cell line—by tissue engineering within alginate scaffolds. *Tissue Eng* 12(5):1357–1368
  35. Ellis AJ, Hughes RD, Wendon JA, Dunne J, Langley PG, Kelly JH, Gislason GT, Sussman NL, Williams R (1996) Pilot-controlled trial of the extracorporeal liver assist device in acute liver failure. *Hepatology* 24(6):1446–1451
  36. Falasca L, Miccheli A, Sartori E, Tomassini A, Devirgiliis LC (2001) Hepatocytes entrapped in alginate gel beads and cultured in bioreactor: rapid repolarization and reconstitution of adhesion areas. *Cells Tissues Organs* 168(3):126–136
  37. Fang S, Qiu YD, Mao L, Shi XL, Yu DC, Ding YT (2007a) Differentiation of embryoid-body cells derived from embryonic stem cells into hepatocytes in alginate microbeads in vitro. *Acta Pharmacol Sin* 28(12):1924–1930
  38. Fang Y, Al-Assaf S, Phillips GO, Nishinari K, Funami T, Williams PA, Li L (2007b) Multiple steps and critical behaviors of the binding of calcium to alginate. *J Phys Chem B* 111(10):2456–2462
  39. Fausto N (2001) Liver regeneration: from laboratory to clinic. *Liver Transpl* 7(10):835–844
  40. Fox IJ, Chowdhury JR (2004) Hepatocyte transplantation. *Am J Transp* 4(Suppl 6):7–13
  41. Freyer N, Knöspel F, Strahl N, Amini L, Schrade P, Bachmann S, Damm G, Seehofer D, Jacobs F, Monshouwer M (2016) Hepatic differentiation of human induced pluripotent stem cells in a perfused three-dimensional multicompartment bioreactor. *BioRes Open Access* 5(1):235–248
  42. Freyer N, Greuel S, Knöspel F, Strahl N, Amini L, Jacobs F, Monshouwer M, Zeilinger K (2017) Effects of co-culture media on hepatic differentiation of hiPSC with or without HUVEC co-culture. *Int J Mol Sci* 18(8):1724
  43. Gerecht-Nir S, Cohen S, Ziskind A, Itskovitz-Eldor J (2004) Three-dimensional porous alginate scaffolds provide a conducive environment for generation of well-vascularized embryoid bodies from human embryonic stem cells. *Biotechnol Bioeng* 88(3):313–320
  44. Gieseck RL III, Hannan NR, Bort R, Hanley NA, Drake RA, Cameron GW, Wynn TA, Vallier L (2014) Maturation of induced pluripotent stem cell derived hepatocytes by 3D-culture. *PLoS One* 9(1):e86372
  45. Glicklis R, Shapiro L, Agbaria R, Merchuk JC, Cohen S (2000) Hepatocyte behavior within three-dimensional porous alginate scaffolds. *Biotechnol Bioeng* 67(3):344–353
  46. Glicklis R, Merchuk JC, Cohen S (2004) Modeling mass transfer in hepatocyte spheroids via cell viability, spheroid size, and hepatocellular functions. *Biotechnol Bioeng* 86(6):672–680
  47. Gómez-Lechón MJ, Tolosa L (2013) Hepatogenic differentiation: comparison between adipose tissue-derived stem cells and bone marrow mesenchymal stem cells. In: *Stem cells and cancer stem cells*, vol 10. Springer, Dordrecht, pp 45–57
  48. Gouon-Evans V, Boussemart L, Gadue P, Nierhoff D, Koehler CI, Kubo A, Shafritz DA, Keller G (2006) BMP-4 is required for hepatic specification of mouse embryonic stem cell-derived definitive endoderm. *Nat Biotechnol* 24(11):1402
  49. Guguen-Guillouzo C (1986) Role of homotypic and heterotypic cell interactions in expression of specific functions by cultured hepatocytes. *Isol Cult Hepatocyte* 1:270–278
  50. Guhr A, Kurtz A, Friedgen K, Löser P (2006) Current state of human embryonic stem cell research: an overview of cell lines and their use in experimental work. *Stem Cells* 24(10):2187–2191
  51. Hay DC, Fletcher J, Payne C, Terrace JD, Gallagher RC, Snoeys J, Black JR, Wojtacha D, Samuel K, Hannoun Z (2008a) Highly efficient differentiation of hESCs to functional hepatic endoderm requires

- ActivinA and Wnt3a signaling. *Proc Natl Acad Sci* 105(34):12301–12306
52. Hay DC, Zhao D, Fletcher J, Hewitt ZA, McLean D, Urruticoechea-Uriguen A, Black JR, Elcombe C, Ross JA, Wolf R (2008b) Efficient differentiation of hepatocytes from human embryonic stem cells exhibiting markers recapitulating liver development in vivo. *Stem Cells* 26(4):894–902
53. Heo J, Factor VM, Uren T, Takahama Y, Lee JS, Major M, Feinstone SM, Thorgeirsson SS (2006) Hepatic precursors derived from murine embryonic stem cells contribute to regeneration of injured liver. *Hepatology* 44(6):1478–1486
54. Holtzinger A, Streeter PR, Sarangi F, Hillborn S, Niapour M, Ogawa S, Keller G (2015) New markers for tracking endoderm induction and hepatocyte differentiation from human pluripotent stem cells. *Development (Cambridge, England)* 142(24):4253–4265
55. Hu Y, Oscarson M, Johansson I, Yue Q-Y, Dahl M-L, Tabone M, Arincò S, Albano E, Ingelman-Sundberg M (1997) Genetic polymorphism of human CYP2E1: characterization of two variant alleles. *Mol Pharmacol* 51(3):370–376
56. Huang P, Zhang L, Gao Y, He Z, Yao D, Wu Z, Cen J, Chen X, Liu C, Hu Y, Lai D, Hu Z, Chen L, Zhang Y, Cheng X, Ma X, Pan G, Wang X, Hui L (2014) Direct reprogramming of human fibroblasts to functional and expandable hepatocytes. *Cell Stem Cell* 14(3):370–384
57. Ijima H, Kakeya Y, Yokonuma T, Hou Y-T, Takei T (2009a) Composition of culture medium is more important than co-culture with hepatic non-parenchymal cells in albumin production activity of primary rat hepatocytes, and the effect was enhanced by hepatocytes spheroid culture in collagen gel. *Biochem Eng J* 45(3):226–231
58. Ijima H, Kubo T, Hou Y-T (2009b) Primary rat hepatocytes form spheroids on hepatocyte growth factor/heparin-immobilized collagen film and maintain high albumin production. *Biochem Eng J* 46(2):227–233
59. Ikonomou L, Kotton DN (2015) Derivation of endodermal progenitors from pluripotent stem cells. *J Cell Physiol* 230(2):246–258
60. Imamura T, Cui L, Teng R, Johkura K, Okouchi Y, Asanuma K, Ogiwara N, Sasaki K (2004) Embryonic stem cell-derived embryoid bodies in three-dimensional culture system form hepatocyte-like cells in vitro and in vivo. *Tissue Eng* 10(11–12):1716–1724
61. Irvine SA, Venkatraman SS (2016) Bioprinting and differentiation of stem cells. *Molecules* 21(9):1188
62. Ishii T, Yasuchika K, Fujii H, Hoppo T, Baba S, Naito M, Machimoto T, Kamo N, Suemori H, Nakatsuji N (2005) In vitro differentiation and maturation of mouse embryonic stem cells into hepatocytes. *Exp Cell Res* 309(1):68–77
63. Ishii T, Fukumitsu K, Yasuchika K, Adachi K, Kawase E, Suemori H, Nakatsuji N, Ikai I, Uemoto S (2008) Effects of extracellular matrixes and growth factors on the hepatic differentiation of human embryonic stem cells. *Am J Physiol Gastrointest Liver Physiol* 295(2):G313–G321
64. Itskovitz-Eldor J, Schuldiner M, Karsenti D, Eden A, Yanuka O, Amit M, Soreq H, Benvenisty N (2000) Differentiation of human embryonic stem cells into embryoid bodies compromising the three embryonic germ layers. *Mol Med* 6(2):88
65. Jauregui HO, Mullan CJP, Trenkler D, Naik S, Santangini H, Press P, Muller TE, Solomon BA (1995) In vivo evaluation of a hollow fiber liver assist device. *Hepatology* 21(2):460–469
66. Jiang J, Kojima N, Kinoshita T, Miyajima A, Yan W, Sakai Y (2002) Cultivation of fetal liver cells in a three-dimensional Poly-L-lactic acid scaffold in the presence of oncostatin M. *Cell Transplant* 11(5):403–406
67. Jiang W, Shi Y, Zhao D, Chen S, Yong J, Zhang J, Qing T, Sun X, Zhang P, Ding M (2007) In vitro derivation of functional insulin-producing cells from human embryonic stem cells. *Cell Res* 17(4):333
68. Jigorel E, Le Vee M, Boursier-Neyret C, Bertrand M, Fardel O (2005) Functional expression of sinusoidal drug transporters in primary human and rat hepatocytes. *Drug Metab Dispos* 33(10):1418–1422
69. Jones EA, Tosh D, Wilson DI, Lindsay S, Forrester LM (2002) Hepatic differentiation of murine embryonic stem cells. *Exp Cell Res* 272(1):15–22
70. Kanda S, Shiroy A, Ouji Y, Birumachi J, Ueda S, Fukui H, Tatsumi K, Ishizaka S, Takahashi Y, Yoshikawa M (2003) In vitro differentiation of hepatocyte-like cells from embryonic stem cells promoted by gene transfer of hepatocyte nuclear factor 3  $\beta$ . *Hepato Res* 26(3):225–231
71. Kanebratt KP, Andersson TB (2008) Evaluation of HepaRG cells as an in vitro model for human drug metabolism studies. *Drug Metab Dispos* 36(7):1444–1452
72. Kanninen LK, Porola P, Niklander J, Malinen MM, Corlu A, Guguen-Guillouzo C, Urtti A, Yliperttula ML, Lou Y-R (2016) Hepatic differentiation of human pluripotent stem cells on human liver progenitor HepaRG-derived acellular matrix. *Exp Cell Res* 341(2):207–217
73. Kedem A, Perets A, Gamlieli-Bonshtein I, Dvir-Ginzberg M, Mizrahi S, Cohen S (2005) Vascular endothelial growth factor-releasing scaffolds enhance vascularization and engraftment of hepatocytes transplanted on liver lobes. *Tissue Eng* 11(5–6):715–722
74. Kelm JM, Fussenegger M (2004) Microscale tissue engineering using gravity-enforced cell assembly. *Trends Biotechnol* 22(4):195–202
75. Kelm JM, Djonov V, Ittner LM, Fluri D, Born W, Hoerstrup SP, Fussenegger M (2006) Design of custom-shaped vascularized tissues using microtissue

- spheroids as minimal building units. *Tissue Eng* 12(8):2151–2160
76. Kerkhove M-PVD, Florio ED, Scuderi V, Mancini A, Belli A, Bracco A, Dauri M, Tisone G, Nicuolo GD, Amoroso P, Spadari A, Lombardi G, Hoekstra R, Calise F, Chamuleau RAFM (2002) Phase I clinical trial with the AMC-bioartificial liver. *Int J Artif Organ* 25(10):950–959
  77. Khalil M, Shariat-Panahi A, Tootle R, Ryder T, McCloskey P, Roberts E, Hodgson H, Selden C (2001) Human hepatocyte cell lines proliferating as cohesive spheroid colonies in alginate markedly upregulate both synthetic and detoxificatory liver function. *J Hepatol* 34(1):68–77
  78. Khaoustov VI, Darlington GJ, Soriano HE, Krishnan B, Risin D, Pellis NR, Yoffe B (1999) Induction of three-dimensional assembly of human liver cells by simulated microgravity. *In Vitro Cell Dev Biol Anim* 35(9):501–509
  79. Kim K, Ohashi K, Utoh R, Kano K, Okano T (2012) Preserved liver-specific functions of hepatocytes in 3D co-culture with endothelial cell sheets. *Biomaterials* 33(5):1406–1413
  80. Kim Y, Kang K, Jeong J, Paik SS, Kim JS, Park SA, Kim WD, Park J, Choi D (2017) Three-dimensional (3D) printing of mouse primary hepatocytes to generate 3D hepatic structure. *Ann Surg Treat Res* 92(2):67–72
  81. Kizawa H, Nagao E, Shimamura M, Zhang G, Torii H (2017) Scaffold-free 3D bio-printed human liver tissue stably maintains metabolic functions useful for drug discovery. *Biochem Biophys Rep* 10:186–191
  82. Kneser U, Kaufmann PM, Fiegel HC, Pollok JM, Kluth D, Herbst H, Rogiers X (1999) Long-term differentiated function of heterotopically transplanted hepatocytes on three-dimensional polymer matrices. *J Biomed Mater Res A* 47(4):494–503
  83. Kuo TK, Hung SP, Chuang CH, Chen CT, Shih YRV, Fang SCY, Yang VW, Lee OK (2008) Stem cell therapy for liver disease: parameters governing the success of using bone marrow mesenchymal stem cells. *Gastroenterology* 134(7):2111–2121 e2113
  84. Lake B (2009) Species differences in the hepatic effects of inducers of CYP2B and CYP4A subfamily forms: relationship to rodent liver tumour formation. *Xenobiotica* 39(8):582–596
  85. Landry J, Bernier D, Ouellet C, Goyette RA, Marceau N (1985) Spheroidal aggregate culture of rat liver cells: histotypic reorganization, biomatrix deposition, and maintenance of functional activities. *J Cell Biol* 101(3):914–923
  86. Lang J, Vera D, Cheng Y, Tang H (2016) Modeling dengue virus-hepatic cell interactions using human pluripotent stem cell-derived hepatocyte-like cells. *Stem Cell Rep* 7(3):341–354
  87. Lanza RP, Ecker DM, Kührtreiber WM, Marsh JP, Ringeling J, Chick WL (1999) Transplantation of islets using microencapsulation: studies in diabetic rodents and dogs. *J Mol Med* 77(1):206–210
  88. Lavon N, Benvenisty N (2005) Study of hepatocyte differentiation using embryonic stem cells. *J Cell Biochem* 96(6):1193–1202
  89. Leclerc E, Kimura K, Shinohara M, Danoy M, Le Gall M, Kido T, Miyajima A, Fujii T, Sakai Y (2017) Comparison of the transcriptomic profile of hepatic human induced pluripotent stem like cells cultured in plates and in a 3D microscale dynamic environment. *Genomics* 109(1):16–26
  90. Lee D-H, Yoon H-H, Lee J-H, Lee K-W, Lee S-K, Kim S-K, Choi J-E, Kim Y-J, Park J-K (2004a) Enhanced liver-specific functions of endothelial cell-covered hepatocyte hetero-spheroids. *Biochem Eng J* 20(2–3):181–187
  91. Lee KD, Kuo TK, Whang-Peng J, Chung YF, Lin CT, Chou SH, Chen JR, Chen YP, Lee OKS (2004b) In vitro hepatic differentiation of human mesenchymal stem cells. *Hepatology* 40(6):1275–1284
  92. Levenberg S, Huang NF, Lavik E, Rogers AB, Itskovitz-Eldor J, Langer R (2003) Differentiation of human embryonic stem cells on three-dimensional polymer scaffolds. *Proc Natl Acad Sci* 100(22):12741–12746
  93. Lewis SL, Tam PP (2006) Definitive endoderm of the mouse embryo: formation, cell fates, and morphogenetic function. *Dev Dyn* 235(9):2315–2329
  94. Li AP, Barker G, Beck D, Colburn S, Monsell R, Pellegrin C (1993) Culturing of primary hepatocytes as entrapped aggregates in a packed bed bioreactor: a potential bioartificial liver. *In Vitro Cell Dev Biol Anim* 29(3):249–254
  95. Lin RZ, Ho CT, Liu CH, Chang HY (2006) Dielectrophoresis based-cell patterning for tissue engineering. *Biotechnol J* 1(9):949–957
  96. Liu H, Roy K (2005) Biomimetic three-dimensional cultures significantly increase hematopoietic differentiation efficacy of embryonic stem cells. *Tissue Eng* 11(1–2):319–330
  97. Liu X, Chism JP, LeCluyse EL, Brouwer KR, Brouwer KL (1999) Correlation of biliary excretion in sandwich-cultured rat hepatocytes and in vivo in rats. *Drug Metab Dispos* 27(6):637–644
  98. Lovett M, Lee K, Edwards A, Kaplan DL (2009) Vascularization strategies for tissue engineering. *Tissue Eng B Rev* 15(3):353–370
  99. Luo Y, Lou C, Zhang S, Zhu Z, Xing Q, Wang P, Liu T, Liu H, Li C, Shi W (2018) Three-dimensional hydrogel culture conditions promote the differentiation of human induced pluripotent stem cells into hepatocytes. *Cytotherapy* 20(1):95–107
  100. Ma X, Qu X, Zhu W, Li Y-S, Yuan S, Zhang H, Liu J, Wang P, Lai CSE, Zanella F (2016) Deterministically patterned biomimetic human iPSC-derived hepatic model via rapid 3D bioprinting. *Proc Natl Acad Sci* 113(8):2206–2211
  101. Maguire T, Novik E, Schloss R, Yarmush M (2006) Alginate-PLL microencapsulation: effect on the differentiation of embryonic stem cells into hepatocytes. *Biotechnol Bioeng* 93(3):581–591

102. Mahmoodinia Maymand M, Soleimanpour-lichaei HR, Ardeshiryajimi A, Soleimani M, Enderami SE, Nojehdehi S, Behjati F, Kabir Salmani M (2017) Improvement of hepatogenic differentiation of iPSC cells on an aligned polyethersulfone compared to random nanofibers. *Artif Cell Nanomed Biotechnol* 46:853–860
103. Malik R, Selden C, Hodgson H (2002) The role of non-parenchymal cells in liver growth. Paper presented at the Seminars in cell & developmental biology
104. Mallanna SK, Cayo MA, Twaroski K, Gundry RL, Duncan SA (2016) Mapping the cell-surface N-glycoproteome of human hepatocytes reveals markers for selecting a homogeneous population of iPSC-derived hepatocytes. *Stem Cell Rep* 7(3):543–556
105. Mandrycky C, Wang Z, Kim K, Kim D-H (2016) 3D bioprinting for engineering complex tissues. *Biotechnol Adv* 34(4):422–434
106. Maurice M, Schell MJ, Lardeux B, Hubbard AL (1994) Biosynthesis and intracellular transport of a bile canalicular plasma membrane protein: studies in vivo and in the perfused rat liver. *Hepatology* 19(3):648–655
107. McKee C, Chaudhry GR (2017) Advances and challenges in stem cell culture. *Colloids Surf B Biointerfaces* 159:62–77
108. McLean AB, D'Amour KA, Jones KL, Krishnamoorthy M, Kulik MJ, Reynolds DM, Sheppard AM, Liu H, Xu Y, Baetge EE (2007) Activin efficiently specifies definitive endoderm from human embryonic stem cells only when phosphatidylinositol 3-kinase signaling is suppressed. *Stem Cells* 25(1):29–38
109. Meier F, Freyer N, Brzeszczynska J, Knöspel F, Armstrong L, Lako M, Greuel S, Damm G, Ludwig-Schwelling E, Deschl U (2017) Hepatic differentiation of human iPSCs in different 3D models: a comparative study. *Int J Mol Med* 40(6):1759–1771
110. Mercey E, Obeïd P, Glaise D, Calvo-Muñoz M-L, Guguen-Guillouzo C, Fouqué B (2010) The application of 3D micropatterning of agarose substrate for cell culture and in situ comet assays. *Biomaterials* 31(12):3156–3165
111. Michalopoulos GK, Barua L, Bowen WC (2005) Transdifferentiation of rat hepatocytes into biliary cells after bile duct ligation and toxic biliary injury. *Hepatology* 41(3):535–544
112. Miki T, Ring A, Gerlach J (2011) Hepatic differentiation of human embryonic stem cells is promoted by three-dimensional dynamic perfusion culture conditions. *Tissue Eng Part C Method* 17(5):557–568
113. Mitaka T, Sato F, Mizuguchi T, Yokono T, Mochizuki Y (1999) Reconstruction of hepatic organoid by rat small hepatocytes and hepatic nonparenchymal cells. *Hepatology* 29(1):111–125
114. Mittal N, Tasnim F, Yue C, Qu Y, Phan D, Choudhury Y, Tan M-H, Yu H (2016) Substrate stiffness modulates the maturation of human pluripotent stem-cell-derived hepatocytes. *ACS Biomater Sci Eng* 2(9):1649–1657
115. Miyashita H, Suzuki A, Fukao K, Nakauchi H, Taniguchi H (2002) Evidence for hepatocyte differentiation from embryonic stem cells in vitro. *Cell Transplant* 11(5):429–434
116. Mizumoto H, Amimoto N, Miyazawa T, Tani H, Ikeda K, Kajiwara T (2018) In vitro and ex vivo functional evaluation of a hollow fiber-type bioartificial liver module containing ES cell-derived hepatocyte-like cells. *Adv Biomed Eng* 7:18–27
117. Moscona A (1961) Rotation-mediated histogenetic aggregation of dissociated cells: a quantifiable approach to cell interactions in vitro. *Exp Cell Res* 22:455–475
118. Murphy SV, Atala A (2014) 3D bioprinting of tissues and organs. *Nat Biotechnol* 32(8):773
119. Nagamoto Y, Tashiro K, Takayama K, Ohashi K, Kawabata K, Sakurai F, Tachibana M, Hayakawa T, Furue MK, Mizuguchi H (2012) The promotion of hepatic maturation of human pluripotent stem cells in 3D co-culture using type I collagen and Swiss 3T3 cell sheets. *Biomaterials* 33(18):4526–4534
120. Nagamoto Y, Takayama K, Ohashi K, Okamoto R, Sakurai F, Tachibana M, Kawabata K, Mizuguchi H (2016) Transplantation of a human iPSC-derived hepatocyte sheet increases survival in mice with acute liver failure. *J Hepatol* 64(5):1068–1075
121. Nakamori D, Akamine H, Takayama K, Sakurai F, Mizuguchi H (2017) Direct conversion of human fibroblasts into hepatocyte-like cells by ATF5, PROX1, FOXA2, FOXA3, and HNF4A transduction. *Sci Rep* 7(1):16675
122. Nakamura T, Nakayama Y, Ichihara A (1984) Reciprocal modulation of growth and liver functions of mature rat hepatocytes in primary culture by an extract of hepatic plasma membranes. *J Biol Chem* 259(13):8056–8058
123. Nakanishi J, Takarada T, Yamaguchi K, Maeda M (2008) Recent advances in cell micropatterning techniques for bioanalytical and biomedical sciences. *Anal Sci* 24(1):67–72
124. Nisbet D, Moses D, Gengenbach T, Forsythe JS, Finkelstein D, Horne MK (2009) Enhancing neurite outgrowth from primary neurones and neural stem cells using thermoresponsive hydrogel scaffolds for the repair of spinal cord injury. *J Biomed Mater Res A* 89(1):24–35
125. Nitou M, Sugiyama Y, Ishikawa K, Shiojiri N (2002) Purification of fetal mouse hepatoblasts by magnetic beads coated with monoclonal anti-e-cadherin antibodies and their in vitro culture. *Exp Cell Res* 279(2):330–343
126. Novosel EC, Kleinhans C, Kluger PJ (2011) Vascularization is the key challenge in tissue engineering. *Adv Drug Deliv Rev* 63(4):300–311
127. Nyberg SL, Rimmel RP, Mann HJ, Peshwa MV, Hu W-S, Cerra FB (1994) Primary hepatocytes outperform Hep G2 cells as the source of biotransformation functions in a bioartificial liver. *Ann Surg* 220(1):59

128. Onica T, Nichols K, Larin M, Ng L, Maslen A, Dvorak Z, Pascucci J-M, Vilarem M-J, Maurel P, Kirby GM (2008) Dexamethasone-mediated up-regulation of human CYP2A6 involves the glucocorticoid receptor and increased binding of hepatic nuclear factor 4 $\alpha$  to the proximal promoter. *Mol Pharmacol* 73(2):451–460
129. Orloff MJ, Isenberg JI, Wheeler HO, Haynes KS, Jinich-Brook H, Rapier R, Vaida F, Hye RJ (2009) Randomized trial of emergency endoscopic sclerotherapy versus emergency portacaval shunt for acutely bleeding esophageal varices in cirrhosis. *J Am Coll Surg* 209(1):25–40
130. Palakkan AA, Drummond R, Anderson RA, Greenhough S, Tv K, Hay DC, Ross JA (2015) Polarisation and functional characterisation of hepatocytes derived from human embryonic and mesenchymal stem cells. *Biomed Rep* 3(5):626–636
131. Park Y, Chen Y, Ordovas L, Verfaillie CM (2014) Hepatic differentiation of human embryonic stem cells on microcarriers. *J Biotechnol* 174:39–48
132. Pettinato G, Ramanathan R, Fisher RA, Mangino MJ, Zhang N, Wen X (2016) Scalable differentiation of human iPSCs in a multicellular spheroid-based 3D culture into hepatocyte-like cells through direct Wnt/ $\beta$ -catenin pathway inhibition. *Sci Rep* 6:32888
133. Ramasamy TS, Yu JS, Selden C, Hodgson H, Cui W (2013) Application of three-dimensional culture conditions to human embryonic stem cell-derived definitive endoderm cells enhances hepatocyte differentiation and functionality. *Tissue Eng Part A* 19(3–4):360–367
134. Rashid ST, Corbineau S, Hannan N, Marciniak SJ, Miranda E, Alexander G, Huang-Doran I, Griffin J, Ahrlund-Richter L, Skepper J (2010) Modeling inherited metabolic disorders of the liver using human induced pluripotent stem cells. *J Clin Invest* 120(9):3127–3136
135. Rodriguez-Antona C, Donato M, Boobis A, Edwards R, Watts P, Castell JV, Gómez-Lechón M-J (2002) Cytochrome P450 expression in human hepatocytes and hepatoma cell lines: molecular mechanisms that determine lower expression in cultured cells. *Xenobiotica* 32(6):505–520
136. Rogler LE (1997) Selective bipotential differentiation of mouse embryonic hepatoblasts in vitro. *Am J Pathol* 150(2):591
137. Rountree CB, Barsky L, Ge S, Zhu J, Senadheera S, Crooks GM (2007) A CD133-expressing murine liver oval cell population with bilineage potential. *Stem Cells* 25(10):2419–2429
138. Rouwkema J, Khademhosseini A (2016) Vascularization and angiogenesis in tissue engineering: beyond creating static networks. *Trends Biotechnol* 34(9):733–745
139. Sakai Y, Naruse K, Nagashima I, Muto T, Suzuki M (1996) Short-term hypothermic preservation of porcine hepatocyte spheroids using UW solution. *Cell Transplant* 5(4):505–511
140. Sakiyama R, Blau BJ, Miki T (2017) Clinical translation of bioartificial liver support systems with human pluripotent stem cell-derived hepatic cells. *World J Gastroenterol* 23(11):1974–1979
141. Sampaziotis F, Segeritz CP, Vallier L (2015) Potential of human induced pluripotent stem cells in studies of liver disease. *Hepatology* 62(1):303–311
142. Sato Y, Araki H, Kato J, Nakamura K, Kawano Y, Kobune M, Sato T, Miyanishi K, Takayama T, Takahashi M (2005) Human mesenchymal stem cells xenografted directly to rat liver are differentiated into human hepatocytes without fusion. *Blood* 106(2):756–763
143. Scadden DT (2006) The stem-cell niche as an entity of action. *Nature* 441(7097):1075
144. Schmelzer E, Zhang L, Bruce A, Wauthier E, Ludlow J, Yao H, Moss N, Melhem A, McClelland R, Turner W (2007) Human hepatic stem cells from fetal and postnatal donors. *J Exp Med* 204(8):1973–1987
145. Schug M, Heise T, Bauer A, Storm D, Blaszkewicz M, Bedawy E, Brulport M, Geppert B, Hermes M, Föllmann W (2008) Primary rat hepatocytes as in vitro system for gene expression studies: comparison of sandwich, Matrigel and 2D cultures. *Arch Toxicol* 82(12):923–931
146. Schwartz RE, Reyes M, Koodie L, Jiang Y, Blackstad M, Lund T, Lenvik T, Johnson S, Hu W-S, Verfaillie CM (2002) Multipotent adult progenitor cells from bone marrow differentiate into functional hepatocyte-like cells. *J Clin Invest* 109(10):1291–1302
147. Schwartz RE, Trehan K, Andrus L, Sheahan TP, Ploss A, Duncan SA, Rice CM, Bhatia SN (2012) Modeling hepatitis C virus infection using human induced pluripotent stem cells. *Proc Natl Acad Sci* 109(7):2544–2548
148. Séguin CA, Draper JS, Nagy A, Rossant J (2008) Establishment of endoderm progenitors by SOX transcription factor expression in human embryonic stem cells. *Cell Stem Cell* 3(2):182–195
149. Selden C, Shariat A, McCloskey P, Ryder T, Roberts E, Hodgson H (1999) Three-dimensional in vitro cell culture leads to a marked upregulation of cell function in human hepatocyte cell lines—an important tool for the development of a bioartificial liver machine. *Ann N Y Acad Sci* 875(1):353–363
150. Semino CE, Merok JR, Crane GG, Panagiotakos G, Zhang S (2003) Functional differentiation of hepatocyte-like spheroid structures from putative liver progenitor cells in three-dimensional peptide scaffolds. *Differentiation* 71(4–5):262–270
151. Shan J, Schwartz RE, Ross NT, Logan DJ, Thomas D, Duncan SA, North TE, Goessling W, Carpenter AE, Bhatia SN (2013) Identification of small molecules for human hepatocyte expansion and iPSC differentiation. *Nat Chem Biol* 9(8):514–520



152. Shav D, Einav S (2010) The effect of mechanical loads in the differentiation of precursor cells into mature cells. *Ann NY Acad Sci* 1188(1):25–31
153. Simeonov KP, Uppal H (2014) Direct reprogramming of human fibroblasts to hepatocyte-like cells by synthetic modified mRNAs. *PLoS One* 9(6):e100134
154. Sirenko O, Hesley J, Rusyn I, Cromwell EF (2014) High-content assays for hepatotoxicity using induced pluripotent stem cell-derived cells. *Assay Drug Dev Technol* 12(1):43–54
155. Sivertsson L, Ek M, Darnell M, Edebert I, Ingelman-Sundberg M, Neve EP (2010) CYP3A4 catalytic activity is induced in confluent Huh7 hepatoma cells. *Drug Metab Dispos* 38(6):995–1002
156. Skottman H, Narkilahti S, Hovatta O (2007) Challenges and approaches to the culture of pluripotent human embryonic stem cells. *Regen Med* 2:265–263
157. Snykers S, Vanhaecke T, Papeleu P, Luttun A, Jiang Y, Vander Heyden Y, Verfaillie C, Rogiers V (2006) Sequential exposure to cytokines reflecting embryogenesis: the key for in vitro differentiation of adult bone marrow stem cells into functional hepatocyte-like cells. *Toxicol Sci* 94(2):330–341
158. Song W, Lu Y-C, Frankel AS, An D, Schwartz RE, Ma M (2015) Engraftment of human induced pluripotent stem cell-derived hepatocytes in immunocompetent mice via 3D co-aggregation and encapsulation. *Sci Rep* 5:16884
159. Song G, Pacher M, Balakrishnan A, Yuan Q, Tsay H-C, Yang D, Reetz J, Brandes S, Dai Z, Pützer BM, Araúzo-Bravo MJ, Steinemann D, Luedde T, Schwabe RF, Manns MP, Schöler HR, Schambach A, Cantz T, Ott M, Sharma AD (2016) Direct reprogramming of hepatic myofibroblasts into hepatocytes in vivo attenuates liver fibrosis. *Cell Stem Cell* 18(6):797–808
160. Soto-Gutiérrez A, Navarro-Alvarez N, Zhao D, Rivas-Carrillo JD, Lebkowski J, Tanaka N, Fox IJ, Kobayashi N (2007) Differentiation of mouse embryonic stem cells to hepatocyte-like cells by co-culture with human liver nonparenchymal cell lines. *Nat Protoc* 2(2):347
161. Steward AR, Dannan GA, Guzelian PS, Guengerich FP (1985) Changes in the concentration of seven forms of cytochrome P-450 in primary cultures of adult rat hepatocytes. *Mol Pharmacol* 27(1):125–132
162. Stolberg S, McCloskey KE (2009) Can shear stress direct stem cell fate? *Biotechnol Prog* 25(1):10–19
163. Subramanian K, Owens DJ, Raju R, Firpo M, O'Brien TD, Verfaillie CM, Hu W-S (2013) Spheroid culture for enhanced differentiation of human embryonic stem cells to hepatocyte-like cells. *Stem Cells Dev* 23(2):124–131
164. Suetsugu A, Nagaki M, Aoki H, Motohashi T, Kunisada T, Moriwaki H (2008) Differentiation of mouse hepatic progenitor cells induced by hepatocyte nuclear factor-4 and cell transplantation in mice with liver fibrosis. *Transplantation* 86(9):1178–1186
165. Sumi T, Tsuneyoshi N, Nakatsuji N, Suemori H (2008) Defining early lineage specification of human embryonic stem cells by the orchestrated balance of canonical Wnt/ $\beta$ -catenin, Activin/Nodal and BMP signaling. *Development* 135(17):2969–2979
166. Sun T, Jackson S, Haycock JW, MacNeil S (2006) Culture of skin cells in 3D rather than 2D improves their ability to survive exposure to cytotoxic agents. *J Biotechnol* 122(3):372–381
167. Suzuki A, Iwama A, Miyashita H, Nakauchi H, Taniguchi H (2003) Role for growth factors and extracellular matrix in controlling differentiation of prospectively isolated hepatic stem cells. *Development* 130(11):2513–2524
168. Syková E, Jendelová P, Urdzíkova L, Lesný P, Hejčl A (2006) Bone marrow stem cells and polymer hydrogels—two strategies for spinal cord injury repair. *Cell Mol Neurobiol* 26(7–8):1111–1127
169. Takayama K, Inamura M, Kawabata K, Katayama K, Higuchi M, Tashiro K, Nonaka A, Sakurai F, Hayakawa T, Furue MK (2012) Efficient generation of functional hepatocytes from human embryonic stem cells and induced pluripotent stem cells by HNF4 $\alpha$  transduction. *Mol Ther* 20(1):127–137
170. Takayama K, Kawabata K, Nagamoto Y, Kishimoto K, Tashiro K, Sakurai F, Tachibana M, Kanda K, Hayakawa T, Furue MK, Mizuguchi H (2013) 3D spheroid culture of hESC/hiPSC-derived hepatocyte-like cells for drug toxicity testing. *Biomaterials* 34(7):1781–1789
171. Takebe T, Sekine K, Enomura M, Koike H, Kimura M, Ogaeri T, Zhang R-R, Ueno Y, Zheng Y-W, Koike N (2013) Vascularized and functional human liver from an iPSC-derived organ bud transplant. *Nature* 499(7459):481
172. Takebe T, Zhang R-R, Koike H, Kimura M, Yoshizawa E, Enomura M, Koike N, Sekine K, Taniguchi H (2014) Generation of a vascularized and functional human liver from an iPSC-derived organ bud transplant. *Nat Protoc* 9(2):396
173. Takenaga M, Fukumoto M, Hori Y (2007) Regulated Nodal signaling promotes differentiation of the definitive endoderm and mesoderm from ES cells. *J Cell Sci* 120(12):2078–2090
174. Tasnim F, Phan D, Toh Y-C, Yu H (2015) Cost-effective differentiation of hepatocyte-like cells from human pluripotent stem cells using small molecules. *Biomaterials* 70:115–125
175. Tasnim F, Toh Y-C, Qu Y, Li H, Phan D, Narmada BC, Ananthanarayanan A, Mittal N, Meng RQ, Yu H (2016) Functionally enhanced human stem cell derived hepatocytes in galactosylated cellulosic sponges for hepatotoxicity testing. *Mol Pharm* 13(6):1947–1957
176. Théry M (2010) Micropatterning as a tool to decipher cell morphogenesis and functions. *J Cell Sci* 123(24):4201–4213
177. Thomson JA, Itskovitz-Eldor J, Shapiro SS, Waknitz MA, Swiergiel JJ, Marshall VS, Jones JM (1998)

- Embryonic stem cell lines derived from human blastocysts. *Science* 282(5391):1145–1147
178. Timmins N, Dietmair S, Nielsen L (2004) Hanging-drop multicellular spheroids as a model of tumour angiogenesis. *Angiogenesis* 7(2):97–103
  179. Toivonen S, Malinen MM, Küblbeck J, Petsalo A, Urtti A, Honkakoski P, Otonkoski T (2016) Regulation of human pluripotent stem cell-derived hepatic cell phenotype by three-dimensional hydrogel models. *Tissue Eng A* 22(13–14):971–984
  180. Tong JZ, De Lagausie P, Furlan V, Cresteil T, Bernard O, Alvarez F (1992) Long-term culture of adult rat hepatocyte spheroids. *Exp Cell Res* 200(2):326–332
  181. Touboul T, Hannan NR, Corbinau S, Martinez A, Martinet C, Branchereau S, Mainot S, Strick-Marchand H, Pedersen R, Di Santo J (2010) Generation of functional hepatocytes from human embryonic stem cells under chemically defined conditions that recapitulate liver development. *Hepatology* 51(5):1754–1765
  182. Tuleuova N, Lee JY, Lee J, Ramanculov E, Zern MA, Revzin A (2010) Using growth factor arrays and micropatterned co-cultures to induce hepatic differentiation of embryonic stem cells. *Biomaterials* 31(35):9221–9231
  183. Turner WS, Schmelzer E, McClelland R, Wauthier E, Chen W, Reid LM (2007) Human hepatoblast phenotype maintained by hyaluronan hydrogels. *J Biomed Mater Res B Appl Biomater* 82(1):156–168
  184. Uehara Y, Minowa O, Mori C, Shiota K, Kuno J, Noda T, Kitamura N (1995) Placental defect and embryonic lethality in mice lacking hepatocyte growth factor/scatter factor. *Nature* 373(6516):702–705
  185. Vassilopoulos G, Russell DW (2003) Cell fusion: an alternative to stem cell plasticity and its therapeutic implications. *Curr Opin Genet Dev* 13(5):480–485
  186. Vig P, Russo FP, Edwards RJ, Tadrous PJ, Wright NA, Thomas HC, Alison MR, Forbes SJ (2006) The sources of parenchymal regeneration after chronic hepatocellular liver injury in mice. *Hepatology* 43(2):316–324
  187. Vosough M, Omidinia E, Kadivar M, Shokrgozar M-A, Pournasr B, Aghdami N, Baharvand H (2013) Generation of functional hepatocyte-like cells from human pluripotent stem cells in a scalable suspension culture. *Stem Cells Dev* 22(20):2693–2705
  188. Xia K, Xue H, Dong D, Zhu S, Wang J, Zhang Q, Hou L, Chen H, Tao R, Huang Z (2006) Identification of the proliferation/differentiation switch in the cellular network of multicellular organisms. *PLoS Comput Biol* 2(11):e145
  189. Yamada K, Kamihira M, Iijima S (2001) Self-organization of liver constitutive cells mediated by artificial matrix and improvement of liver functions in long-term culture. *Biochem Eng J* 8(2):135–143
  190. Yamada T, Yoshikawa M, Kanda S, Kato Y, Nakajima Y, Ishizaka S, Tsunoda Y (2002) In vitro differentiation of embryonic stem cells into hepatocyte-like cells identified by cellular uptake of indocyanine green. *Stem Cells* 20(2):146–154
  191. Yao R, Wang J, Li X, Jung Jung D, Qi H, Kee KK, Du Y (2014) Hepatic differentiation of human embryonic stem cells as microscaled multilayered colonies leading to enhanced homogeneity and maturation. *Small* 10(21):4311–4323
  192. Yin Y, Lim YK, Salto-Tellez M, Ng SC, Lin CS, Lim SK (2002) AFP+, ESC-derived cells engraft and differentiate into hepatocytes in vivo. *Stem Cells* 20(4):338–346
  193. Yu Y, Wang X, Nyberg SL (2014) Potential and challenges of induced pluripotent stem cells in liver diseases treatment. *J Clin Med* 3(3):997–1017
  194. Yu JS, Ramasamy TS, Murphy N, Holt MK, Czapiewski R, Wei SK, Cui W (2015) PI3K/mTORC2 regulates TGF-beta/Activin signalling by modulating Smad2/3 activity via linker phosphorylation. *Nat Commun* 6:7212
  195. Yuasa C, Tomita Y, Shono M, Ishimura K, Ichihara A (1993) Importance of cell aggregation for expression of liver functions and regeneration demonstrated with primary cultured hepatocytes. *J Cell Physiol* 156(3):522–530
  196. Yuhas JM, Li AP, Martinez AO, Ladman AJ (1977) A simplified method for production and growth of multicellular tumor spheroids. *Cancer Res* 37(10):3639–3643
  197. Zhao D-C, Lei J-X, Chen R, Yu W-H, Zhang X-M, Li S-N, Xiang P (2005) Bone marrow-derived mesenchymal stem cells protect against experimental liver fibrosis in rats. *World J Gastroenterol: WJG* 11(22):3431
  198. Zinchenko YS, Schrum LW, Clemens M, Coger RN (2006) Hepatocyte and kupffer cells co-cultured on micropatterned surfaces to optimize hepatocyte function. *Tissue Eng* 12(4):751–761

---

**Part II**

**Controlling of Signal Pathway of Stem Cell  
by Biomaterials**



# Modulation of the Osteoimmune Environment in the Development of Biomaterials for Osteogenesis

# 5

Fei Wei and Yin Xiao

## Abstract

In spite of inherent regenerative ability of bone, large amounts of fracture patients still display delayed or compromised bone healing due to patients' age status, trauma severity or the developmental anomalies or infections, which requires therapeutic intervention. Bone regeneration involves different cells (immune cells, progenitors and mesenchymal stem cells, etc) and subsequent signaling molecules (chemokines, cytokines and growth factors, etc). The quantity and quality of immune cells influx into the site of injury and the subsequent cytokine production form a unique osteoimmune environment. Current strategies on repairing bone defects have largely focused on the development of suitable bone substitute materials, which may have potential osteoinductive, and/or osteoconductive properties. Various studies have been reported to develop the immuno-active or immunomodulatory biomaterials, which could fully explore the early osteoimmune environment in order to achieve better bone regeneration.

## Keywords

Osteoimmune environment · Immunomodulation · Biomaterial · Bone regeneration · Osteogenesis

## 5.1 Early Osteoimmune Environment in Bone Healing

Bone healing involves four different stages (inflammatory, soft callus phase, hard callus phase, and bone remodelling stage), among which the initial inflammatory phase represent the most important stage throughout the entire bone regeneration process [120]. In general, the instant rupture of blood vessels and the formation of fracture haematoma governing the healing process commences. It has long been suggested that the generation of blood clot is indispensable for the bone healing, in which the absence can severely impede the bone repair process [115]. Grundnes and Reikeras demonstrated that removal of fracture haematoma at indicated times in rats resulted in impaired fracture healing [43]. However, the cellular composition of the haematoma remains poorly understood because of the complexity of early osteoimmune environment. Only a few reports on bone haematoma composition have been reported so far. It has been demonstrated the formed blood clot acts as temporary scaffold for the infiltration of immune cells, including neutrophils, macrophages and lymphocytes.

F. Wei · Y. Xiao (✉)  
Institute of Health and Biomedical Innovation,  
Queensland University of Technology, Kelvin Grove,  
QLD, Australia  
e-mail: [f2.wei@hdr.qut.edu.au](mailto:f2.wei@hdr.qut.edu.au); [yin.xiao@qut.edu.au](mailto:yin.xiao@qut.edu.au)

### 5.1.1 Neutrophils Act as First Immunomodulator for Bone Regeneration

Neutrophils represents the first and one of the most important immune cells which influx into blood clot [42, 49]. As the most abundant leukocyte in humans and mice, neutrophils function by clearing cell debris and decreasing the occurrence of wound infection. Previous studies indicated that patients would suffer from retarded wound healing due to insufficient neutrophils populations or dysfunction to adhere to the endothelium or extracellular matrix [74, 116]. It seems that the role of neutrophils in bone healing process is far more important than previously appreciated. Increased neutrophils recruitment induced by low dose recombinant human tumour necrosis factor (rhTNF) administration at the fracture site led to the accelerated fracture healing in normal and osteoporotic bone in murine tibial fracture model [12]. In addition, depletion of neutrophils in the fracture site by using specific neutrophils-blocking antibodies led to impaired neutrophil mobilization and recruitment, which in turn, resulted in delayed bone regeneration and remodelling compared to the isotope treatment group. Another study showed similar result which indicated that leukocytes may contribute to fracture healing by rapidly synthesizing fibronectin within 48 h after injury [4]. The formation of this major extracellular matrix may further stabilize cell-to-cell adhesion and support the recruitment and infiltration of stromal into the haematoma in the relatively late stage. These studies support the concept that the early inflammatory phase where neutrophil infiltration and the secreted factors occur, represent a key rate-controlling step in fracture healing. However, negative effect of neutrophils on bone repair has been recorded by other researchers in rats [12, 22]. A study was performed by systemic administration of neutrophil-neutralizing antiserum in rats with growth plate injury models showed increased mesenchymal cell osteoblastic differentiation

potential compared to the control group, further indicating that neutrophil-mediated early inflammatory response may be involved in the downstream regulation of chondrogenic and osteogenic cascades [21].

### 5.1.2 Monocytes/Macrophages

Macrophages, derived from haemopoietic progenitors or via circulating monocyte precursors, are essential components of innate immunity and play a central role in inflammation, host defence, homeostasis and regeneration [6, 78, 79, 81]. Among all the immune cells, macrophages are one of the most important cells in the bone regenerative process due to their remarkable diversity and plasticity. It is noteworthy that macrophages have been reported to be actively involved throughout all the healing phases [10]. In general, reducing macrophages numbers or compromising macrophages functions led to the impaired or delayed bone healing in various animal models [118]. This further indicated their significant role in bone healing process due to their modulatory role to angiogenic and osteogenic effect.

### 5.1.3 Lymphocyte

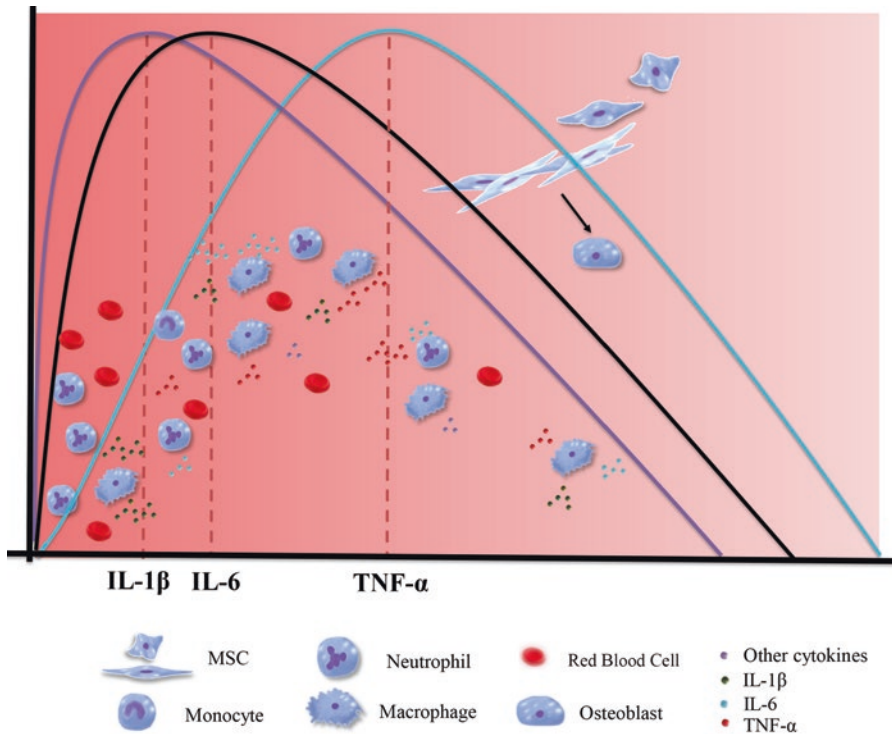
Although the immune cells infiltrate the fracture site immediately upon damage, the role of T cells and B cells on bone regeneration are more or less ambiguous. Little is still known about the functional role of lymphocytes in the immediate and later stage of bone healing. Previous studies using femoral fracture model in mice indicated a dynamic changing patterns of T and B lymphocytes. At later stages where adaptive immunity dominates, T and B cells entered the callus through inner blood vessels. In addition, it has been suggested the direct interaction of lymphocytes with osteoclast precursors and osteoblast, indicating the immunoregulatory role of T and B cells in later stage of bone healing [67].

### 5.1.4 Cytokines Secretory Profiles in Early Osteoimmune Environment

The rapid infiltration of large amount of immune cells into the bone healing site makes the proposition that proinflammatory and anti-inflammatory cytokines secreted by immune cells play an important role in the bone healing process. The first 24 h after fracture induces a pronounced expression of proinflammatory cytokines, which is characterized by consecutive and overlapping expression of interleukin-1 $\beta$  (IL-1 $\beta$ ), interleukin-6 (IL-6) and TNF- $\alpha$  [66]. The expression levels of pro-inflammatory cytokines decline rapidly within a few days. Interestingly, the expression levels of TNF- $\alpha$  and IL-1 $\beta$  in the bone healing process exhibit a biphasic pattern, where the initial peak occurs within the first 24 h, followed by a second peak at terminal bone remodelling phase [87]. These proinflammatory cytokines, mainly secreted by the proinflammatory macrophages, are extremely important in maintaining the early osteoimmune environment, in further recruitment of mesenchymal cells to the fracture site, and in stimulation of mesenchymal stems cell proliferation and differentiation. Previous studies indicated that abolishing or inhibiting initial proinflammatory stages by local administration of nonsteroidal anti-inflammatory drugs resulted compromised bone healing compared to normal bone healing models [1, 28, 94, 101, 107]. The effect of each proinflammatory cytokine on osteogenesis and bone healing process has been extensively studied *in vitro* and *in vivo*. However, the complex nature of early osteoimmune environment and multi-functional roles of proinflammatory cytokines at fracture site require further extensive study to understand the role of osteoimmune environment in early bone healing. Figure 5.1 summarizes the some of the key regulators of early inflammatory environment during bone regeneration.

The IL-1 $\beta$  secretion pattern during natural bone healing and its role in bone regeneration has been inconsistent in previous *in vitro* and *in vivo*

studies. The effect of IL-1 $\beta$  and TNF- $\alpha$  on osteogenic differentiation of mesenchymal stem cells were tested *in vitro* previously. The results indicated that both cytokines could inhibit the osteogenic-differentiation of murine-derived mesenchymal stem cells *in vitro* [69]. However, another studies using low dose IL-1 $\beta$  and TNF- $\alpha$  stimulation on human mesenchymal stem cells indicated increased alkaline phosphatase activity and mineralization *in vitro* [26]. This is further supported by experiments using human periodontal ligament stem cells stimulated with different dosage of IL-1 $\beta$  *in vitro*. It seems that the effect of IL-1 $\beta$  on mesenchymal stem cells are dose dependent, in which low concentration of IL-1 $\beta$  could enhance the osteogenesis of human periodontal ligament stem cells, while high concentration could inhibit the osteogenesis via activating of nuclear factor- $\kappa$ B (NF- $\kappa$ B) and mitogenactivated protein kinase (MAPK) signaling pathway [80]. Another *in vitro* study demonstrated similar stimulatory effect of IL-1 $\beta$  on osteoblast proliferation and increased mineralization. However, total opposite results were noted in murine bone marrow derived mesenchymal stem cells. This discrepancy can be explained, at least partially, by the vast differences in IL-1 $\beta$  concentration and stromal cells involved in different studies [37, 96]. Further *in vivo* studies using Interleukin 1 Receptor 1-deficient mice exhibited no significant differences in callus, cartilage, and bone matrix production at days 7, 10, 14, and 28 post-fracture compared to wild-type counterparts [71]. In addition, only subtle effect of IL-1 $\beta$  on bone regeneration rate can be observed when local administration of IL-1 $\beta$  at the fracture site in murine tibial fracture model [71]. The effect of IL-1 on bone remodelling were further tested by using IL-1 $\alpha$ -deficient, IL-1 $\beta$ -deficient and IL-1 $\alpha/\beta$  double-deficient mice. It seems that the IL-1-deficient mice exhibited increased femur mineral density, trabecular bone mass and cortical thickness compared to wild-type counterparts [73]. IL-1 $\beta$  may have a dual role in physiological and inflammatory conditions. Therefore, the role of IL-1 $\beta$  on bone regen-



**Fig. 5.1** Cytokine secretion profiles and cells involvement in initial inflammatory process. Peak expression of major pro-inflammatory cytokines are depicted schematically. The changing pattern of immune cells and cytokine secretory profiles in early inflammatory stage are also

shown schematically. The cross-interaction of diverse cytokines could sustain the early osteoimmune microenvironment and act as important mediator for early mesenchymal stem cell recruitment, osteogenesis and vascularisation

eration is more complicated than previously appreciated.

Events in bone healing are also considerably influenced by other pro-inflammatory cytokines in the prevailing microenvironment. With a focus on the clinical translation of pro-inflammatory cytokines treatment during bone fracture, many groups have extensively examined the effect of TNF- $\alpha$  on osteogenesis and bone forming ability. It seems that TNF- $\alpha$  may also have dual role in physiological and inflammatory environment. The role of TNF- $\alpha$  on mesenchymal cell migration and fracture healing outcomes can also be concentration- and time-dependent. *In vitro* study using human mesenchymal stem cells stimulated with TNF- $\alpha$  demonstrated enhanced expression of osteogenic-related proteins, mineralization and activation of NF- $\kappa$ B signalling pathway [47]. TNF- $\alpha$  also increase the recruitment of mesen-

chymal stem cells to the injured site by enhancing the expression of migratory related proteins, such as intercellular adhesion molecule-1 (ICAM-1) and vascular cell adhesion protein-1 (VCAM-1) [31]. Positive role of TNF- $\alpha$  on bone healing has also been studied in animal fracture models. *In vivo* study using TNF- $\alpha$  receptor (p55(-)/p75(-)))-deficient mice fracture model indicated the important modulatory role of TNF- $\alpha$  in postnatal endochondral bone formation [36]. Addition of 1 ng/mL TNF- $\alpha$  at the fracture site could accelerate the fracture healing in murine slow-healing fractures model, while high dose TNF- $\alpha$  has inhibitory effect [38]. However, persistent pro-inflammatory environment with high TNF- $\alpha$  concentration can lead to bone destruction. Previous study indicate that long-term elevated TNF- $\alpha$  levels in murine fracture model can result higher non-union fracture rate and delayed fracture heal-

ing [45]. Similar results also indicated that sustained supplementation of TNF- $\alpha$  for seven consecutive days resulted impaired bone growth and bone destruction, which can be reversed by administration of TNF- $\alpha$  inhibitor [30]. This is consistent in inflammatory-related diseases, like rheumatoid arthritis, where sustained and elevated levels of TNF are noted [7, 50, 125]. These studies are clear indications that precise modulation of TNF- $\alpha$  level holds significant clinical translational promises for accelerated bone regeneration.

The third key factor with a significant role during the initial inflammatory stage appears to be IL-6. Similar to TNF- $\alpha$ , IL-6 also exhibits a biphasic expression pattern, in which the mRNA expression level of IL-6 peaks shortly after fracture and again during endochondral ossification stage [64]. The role of IL-6 on human mesenchymal stem cells has been previously investigated *in vitro*. One of the study indicated that IL-6 plays an important role in maintaining stemness of mesenchymal stem cells via ERK1/2 signalling pathway [95]. Blockade of IL-6 signalling by administration of IL-6 neutralizing antibody in mice femur osteotomy models demonstrated compromised fracture healing compared to isotope control group. These results indicated that IL-6 signalling pathway might play crucial role in early fracture repair. Similar results can be noted in tibial fractures models using IL-6 knock-outs mice. One of the study indicated the absence of IL-6 signalling pathway significantly reduced the osteoclastogenesis and impaired callus strength [113]. Another knockout study also indicated the delayed callus maturity and mineralization compared with the not-knockout mice, especially in early stages of bone regeneration [125]. These results may support the concept that pro-inflammatory cytokines may be able to modulate the bone healing process via directly regulating the early osteoimmune environment. Therefore, this osteoimmune environment, where the interaction of different cytokines, immune cells, and mesenchymal stem cells interacted, is more dynamic than previously appreciated.

## 5.2 Modulation of Early Osteoimmune Environment via Biomaterials Offers Huge Potential for Better Bone Regeneration

To date, in a proportion of patients who suffered from severe soft-tissue injury, open fractures or the presence of multiple injuries, persistent local and systemic inflammation predispose to compromised bone healing [40, 68, 85, 108]. It seems that the existence of significant discrepancy in the early osteoimmune environment between normal and delayed bone healing regarding blood clot formation, cytokine profiles, and cell populations, etc. Previous investigations on cytokine secretory profiles in normal and delayed bone healing models demonstrated that both pro-inflammatory and anti-inflammatory cytokines have increased significantly in the delay fracture healing models compared to the normal healing samples [98], indicating the potential therapeutic strategies by altering the initial cytokine response for better bone regeneration. The successful bone healing requires the incorporation of a number of cells and various molecular factors. Different osteoimmune environment may in turn, lead to different outcomes that favour or hinder bone regeneration under certain circumstances. Therefore, it is reasonable to speculate that positive or negative outcome of bone regeneration can be achieved via modulating the early osteoimmune environment under the influence of biomaterial implantation. The ideal therapy for bone healing would entail local regulation of osteoimmune environment by using immunomodulatory biomaterials incorporated with/without pro-osteogenic factor(s) at the time of surgical treatment, among which the cytokines/chemokines secreted around the osteoimmune environment play an indispensable role in this process. Therefore, how to modulate the temporal and spatial pattern of the pro-inflammatory and anti-inflammatory cytokines, how to coordinate the different stages of bone regeneration, and how to smart-driven the unfavourable osteoimmune environment via immunomodulatory biomaterials toward better outcome need to be fully investigated.



### 5.2.1 Traditional Titanium Scaffold

Titanium and titanium alloys are one of the most important scaffolds for dental and orthopaedic implantation due to their good biocompatibility and mechanical properties [59]. However, severe injuries caused by surgical procedure together with particles released from titanium implants into the micro-environment may trigger marked pro-inflammatory response, which are detrimental to normal bone regeneration [27, 93]. Macrophages, as key immune cells in engulfing titanium particles, can produce massive pro-inflammatory cytokines into the surrounding micro-environment [89]. Such acute or long-term inflammation can cause fibrous capsule development, and foreign body giant cells formation, which may finally impair implant integration and tissue regeneration [2, 65]. As a result, researchers tried to develop titanium implants with inflammation modulation properties, thereby prolonging the life-span of titanium implants [39, 106]. Attempts have been made to modify the titanium substrates with rough sandblasted acid etched (SLA), or hydrophilic SLA (modSLA) treatment, which demonstrated decreased pro-inflammatory interleukins expression and increased anti-inflammatory IL-10 level of cells cultured on SLA and modSLA surfaces [55, 123]. It seems that modulation of titanium surface roughness can significantly influence immune cells inflammatory response, which in turn, increase osseointegration rate [23, 52]. The effect of rough titanium surface on early stage blood clot formation and its subsequent effect on MSC recruitment and osteogenesis have also been investigated previously. The results indicated that rough titanium-blood interaction could induce significant increase of rat bone marrow mesenchymal stromal cells proliferation and recruitment, thus potentiating its wound healing ability [124]. Therefore, the influences of rough titanium surfaces on bone regeneration are more complicated than previously appreciated. Other surface coating technique, such as plasma-based coating, plasma sprayed hydroxyapatite (HA)

coating, biomimetic calcium phosphate (CaP) coating, and alumina coating, ect [57] have also been widely used for titanium surface modification. For example, plasma-based  $\text{Sr}_2\text{ZnSi}_2\text{O}_7$  (SZS) ceramic was used to modify the titanium surface in our previous study. The SZS coatings exhibited slow ions releasing properties compared to the hydroxyapatite (HA) coatings. Such SZS-coated titanium surface demonstrated significant immune-regulatory properties with significant reduction of pro-inflammatory cytokines and increase of osteogenic-related factors [17].

In recent years, polydopamine-based one-step coating method gains more and more attention due to the simplicity and cost-effectiveness. Polymerized dopamine (polydopamine) coating is a mussel-inspired biomimetic surface modification technique widely used for tissue engineering [76]. It exhibits high affiliation towards biomolecules containing amine and thiol functional groups, which can be broadly used to immobilize a vast range of macromolecule on different material surfaces. Therefore, modification of metallic implants with polydopamine coating have been investigated in the past several years and showed great promises in bone regeneration [24, 48, 54, 58, 72, 90]. Polydopamine-assisted collagen coating on titanium surfaces has demonstrated better uniformity and distribution compared to passive adsorption coating, which can significantly enhance the pre-osteoblast adhesion and differentiation *in vitro* [127]. Polydopamine-assisted antibiotic coating on titanium surfaces has also been investigated previously, since biofilm formation onto implant interfaces have been regarded as one of the main reasons for implant failure. Antibiotic-decorated titanium implant showed long-lasting adhesion and antibacterial activity to various bacteria strains [46]. Such non-toxic and effective antibiotic coating method offers researchers and orthopaedics effective approach to prevent infections on the implant interface. Additionally, polydopamine-based modification can be widely applied on a wide range of surfaces. Such modification can significantly increase the initial cell

attachment without significant alteration of the sub-structure of biomaterials. For example, porous SiO<sub>2</sub> scaffolds with polydopamine coating demonstrated improved bone marrow mesenchymal stromal cells attachment, proliferation, and mineralization compared to the uncoated surfaces [119].

### 5.2.2 Scaffolds with Sequential Cytokines Release Functions

It is not clear the exact roles of various macrophage subsets and cytokine secretory profiles in disease progression, especially in bone healing process. It seems that the cytokines secretory profiles are one of the most influential factors in these physiological and pathological conditions. Therefore, instead of considering different cytokines as isolating molecules, they should be viewed as an overall environment, especially in the early inflammatory stage during bone healing where platelets, neutrophils, monocytes/macrophages and lymphocytes are trapped within the cross-linked haematoma matrix, in which they have long been neglected before. To test this hypothesis, several recent studies have analysed the pro-angiogenic potential of conditioned media derived from macrophages under different polarization status. Among all the macrophage phenotypes generated *in vitro*, M1 polarised cells secreted the highest angiogenic factors like VEGF, while M2a and M2c polarised macrophages secreted the highest levels of PDGF-BB and MMP-9, respectively. Additional analysis of subcutaneous-implanted biomaterial further reveals that biomaterials elicited both M1 and M2 phenotypes. This represents the most successful revascularization and neo-angiogenic group compared to the extreme M1 and M2 polarising states [102]. Therefore, it seems that the presence of both M1 and M2 phenotypes and balanced cytokine secretory profiles is one of the key factors for successful angiogenesis and scaffold vascularization. This conclusion is somehow; further supported by their successive studies

using sequentially M1 and M2 cytokines released scaffold and murine subcutaneous implantation models. It has been shown that M1 secreted cytokines are mainly responsible for the initiation of angiogenesis, while M2 generated cytokines mediate vessel maturation [102]. Therefore, specific scaffolds were designed with the initial release of M1 phenotypic inducing cytokines followed by M2 macrophages inducing cytokines. However, the result here is more intricate than their previous study. It seems that both scaffold with M1 inducing cytokines or combo polarization cytokines can lead to increased vascularization after 2 weeks of subcutaneous implantation compared to the negative control. In addition, more CD31<sup>+</sup> blood vessels could be observed in M1 inducing scaffold compared to the combo samples [103]. However, the effect of different macrophage phenotypes and the influence of cytokine secretory profiles on bone healing process have not been examined. The overlapping of pro-inflammatory and anti-inflammatory cytokines secretory profiles, together with their dynamic changes within the bone healing micro-environment, has resulted in considerable confusion in the published literature regarding the role of different phenotypes macrophages and cytokines secretory profiles during bone healing process.

Bone morphogenetic protein-2 (BMP2), which belongs to the transforming growth factor- $\beta$  (TGF- $\beta$ ), is one of the most important osteoinductive molecules for bone formation and remodelling [105]. Numerous studies have demonstrated that BMP2 can initiate the osteoblastic differentiation and accelerate the regeneration of mineralized tissue *in vivo* in different bone-defect models [8, 53]. Recombinant human BMP2 and BMP7 have been approved (eg: INFUSE<sup>®</sup> Bone Graft, Medtronic) by the United States Food and Drug Association (FDA) as osteoinductive adjuvants for use in human surgery [82]. Several implantable carriers, such as absorbable collagen sponges, gelatin,  $\beta$ -tricalcium phosphate ( $\beta$ -TCP), polylactic-co-glycolic acid (PLGA) microspheres, and hyaluronic acid (HA), etc.

have been used as delivery system for BMP2 [35, 61, 91]. However, poor retention of BMP2 by some of the carriers can be noted from the implantation sites, thus requiring high dosage of BMP2 for effective bone formation [9, 109]. Numerous complications have also been recorded, thus comprising the safety utilization of BMP2. Apart from osteogenesis, angiogenesis also plays an important role for bone regeneration. The formation of new vascular network and branching of the pre-existing ones are crucial for efficient nutrient supply, transportation of biomolecules, and maintenance of essential environment for bone regeneration [44, 60]. Vascular endothelial growth factor (VEGF) is one of the most important angiogenic molecules during bone regeneration. Previous studies have indicated the stimulatory role of VEGF on bone formation in various animal models. Coupling of osteogenesis and angiogenesis have long been suggested in bone regeneration therapeutic strategies as cellular communication between VEGF and BMP families may lead to the potential synergies among effective cells network [99, 114]. During normal bone regeneration, VEGF demonstrated high secretary profiles during early stages of bone healing while BMP peaked at later time point [19, 41]. Therefore, biomaterials manipulating sequential cytokines release profiles offers huge therapeutic promises. Previous studies using double layered-scaffold with BMP-2 in the inner microspheres and VEGF in the outer layer suggested markedly increased ectopic bone formation in rat subcutaneous model [62]. Such composite with sequential release strategies offers orthopaedics and researchers new insight into beneficial strategies for enhancement of bone regeneration.

### 5.2.3 Micro-patterned Scaffold

In recent years, surface modification technologies using microfabrication on scaffolds have gained increasing trends due to the versatility, compatibility and precise modulation capability of this technology on cell behaviour on nanoscale level. Such microarchitecture (porosity, intercon-

nectivity, and pore geometry) and micro-textures (micro-patterns) changes on scaffold surface, which are smaller than normal cell shape, offers unique stimulatory structure and cues to the functional development and behaviour changes of cells and tissues [126]. This microarchitecture and cells interaction may, in turn, regulate the early osteoimmune environment of bone regeneration via cytokines and chemokines secretion of immune cells and mesenchymal stem cells recruitment. Cell morphological differences have been recorded under different stages of cellular polarization/proliferation states [104]. The most typical examples for cell shape changes would be macrophages, which M1 polarization induced bone marrow-derived macrophages (BMDMs) into a pancake-like morphology, while M2 polarization cytokine caused cellular elongation [84]. M1 and M2 macrophage phenotypes demonstrate different cytokine profiles, which represent different immune environments. The plasticity of macrophages implies the potential strategies to modulate macrophage response in bone regenerative medicine. Studies performed using micropatterned cell culture substrates showed that 20- $\mu\text{m}$  wide lines-induced cellular elongation led to M2 phenotypes changes of macrophages [84]. This phenomenon indicated the remarkable immunomodulatory role of micropatterned scaffold in regulating osteoimmune environment in favour of pro-healing outcome. Optimized pore size also plays an important role in macrophage polarization as 30–40  $\mu\text{m}$  pore size biomaterials appear to promote M2 polarization, while non-porous or random-porous-size materials may enhance M1 subpopulation [34]. Such conclusion was further supported by our previous study in which different pore sizes (0 nm, 15 nm, 50 nm, 100 nm, and 200 nm) on anodic alumina scaffold affected macrophage spreading and cell morphology, which in turn, offered different osteoimmune environment for the osteogenesis of bone marrow stromal cells [16]. Additionally, controlled nanotopography with different sized gold nanoparticles and tailored surface chemistry in our previous study also demonstrated marked difference in osteoimmune environment in terms of macrophage inflammatory cytokines, osteoclastic

activities, and osteogenic, angiogenic, and fibrogenic factors expression [14]. These results are clear indications that nano-engineered surface offers huge potential to manipulate the osteoimmune environment in favour of osteogenesis. Persistent local and systemic inflammation can be frequently noted in patients who suffered from severe soft-tissue injury, open fractures or the presence of multiple injuries, which are detrimental to bone regeneration [36]. Via modulating macrophage polarization through microfabrication of scaffold, which could precisely modulate the immune microenvironment of cells and cytokine secretion profiles, different bone healing immune environmental cues could be obtained.

In addition, a number of studies have been published presenting results of the modulating osteoblast/mesenchymal stem cells behaviour and osteogenesis via a three-dimensional (3D) structure-based microfabrication technology. Scaffold with micro-pillar and micro-ridge textures offers favourable attachment surface for pre-osteoblast cells compared to the un patterning control, which in turn, stimulate the osteogenic differentiation of pre-osteoblast cells [11]. Micropatterned poly ( $\epsilon$ -caprolactone) (PCL) consisting of grooved pillars demonstrated significant increase of cell and tissue alignment compared to the random-porous PCL scaffold in murine subcutaneous implantation model [92]. Blood vessel formation and angiogenic factors also play an important role in large tissue and bone repair. The role of micropatterned scaffold on angiogenesis have also been investigated previously. Collagen scaffolds incorporated with micropatterned VEGF showed more blood vessels formation in nude mice subcutaneous implantation models compared to control collagen sponge [88]. Another study using micropatterned scaffolds with different inter-channel spacing revealed increased blood vessels numbers compared to the random-pore scaffold [111]. Therefore, the potential modulatory role of micropatterned scaffold on cellular behaviours offers fundamental theoretical basis for regulating the early osteoimmune environment for favourable osteogenesis and accelerated bone regeneration.

#### 5.2.4 Plasma Ion Immersion Implantation (PIII) Modified Scaffold

Surface modification using Plasma Ion Immersion Implantation (PIII) technique have been shown to have huge biomedical applications promises due to high biocompatibility, efficiency, and versatility [130]. Through PIII modification, surface characterizations of the scaffold can be enhanced, while the original bulk property and topography are still maintained at the same time. Such changing offers superior adhesion capacity for many cells, including immune cells and mesenchymal stem cells. The osteo-modulation effects of plasma-modified surface on mesenchymal stem cells (MSCs) or osteoblasts have been clearly demonstrated *in vitro* and *in vivo* [128–130]. For instance, nitrogen and carbon PIII-modified titanium implants showed improved osteoblastic differentiation *in vitro* and increased bone regeneration in rat bone defect model [130]. In addition, human MSCs seeded onto the oxygen PIII-modified titanium implants demonstrated increased differentiation and mineralization abilities [122]. More recently, magnesium-doped titanium surface via PIII-based strategy demonstrated significant immunomodulatory role on macrophages phenotypic shifts, further indicating important modulatory role of PIII-modification on cellular behavior [75]. In addition, previous studies have also shown that PIII-treated surface can change the chemical composition of materials by generating a hydrophilic surface, which are capable of forming covalent bonds to immobilize proteins through radicals embedded in a sub-surface layer [18]. The covalently bonded proteins on the surface can markedly regulate the attachment, proliferation, and differentiation of various cells *in vitro*, such as human coronary endothelial cells, human dermal fibroblast (HDF) and human umbilical vein endothelial cell (HUVEC), etc. [5, 18]. These studies are clear indications that manipulation of the osteo-modulation effect generated by PIII treatment and further utilization of such microenvironment offer huge potential to provide an effective approach for future bone regeneration.

### 5.2.5 Bio-membrane Guided Scaffold for Bone Regeneration

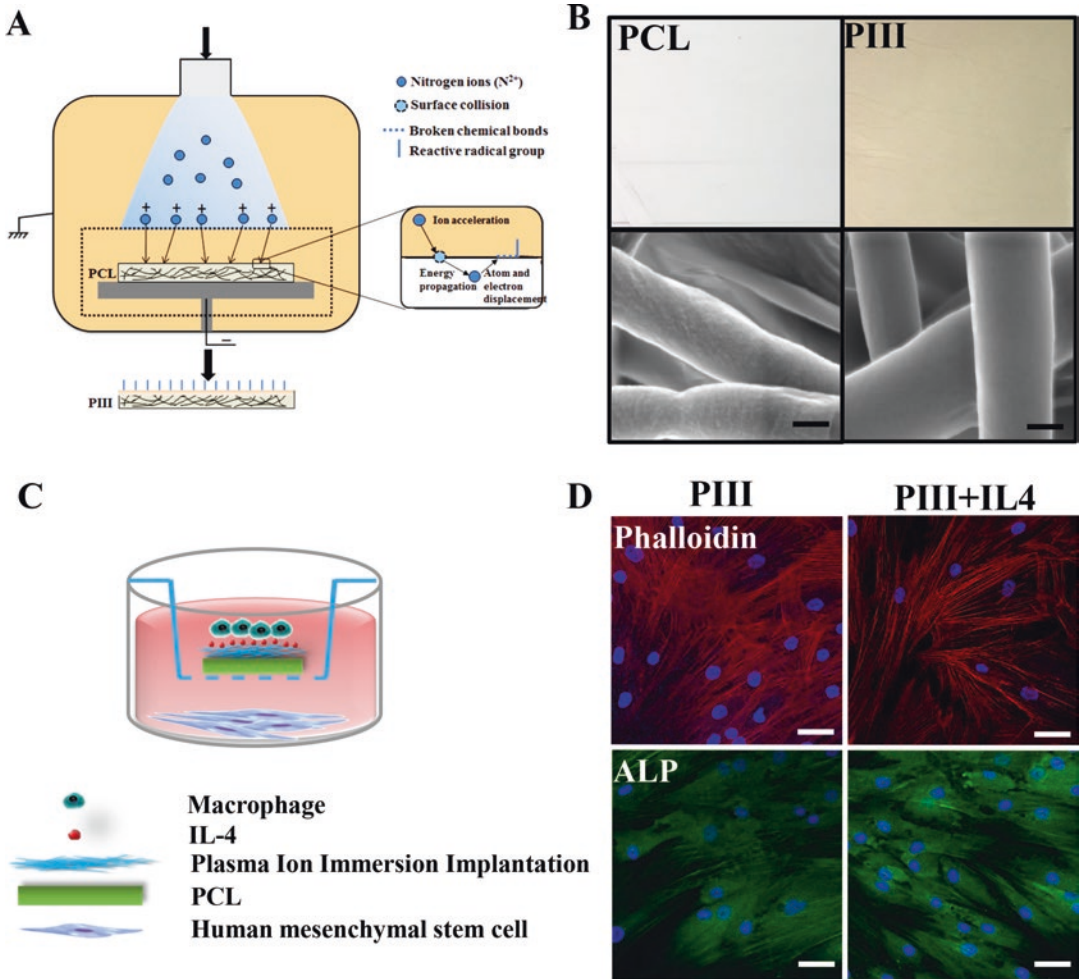
Bio-membrane guided scaffolds have been successfully designed and have demonstrated significantly immunomodulatory role on osteogenesis and bone healing. Such guided bone regeneration technique offers researchers and orthopaedics useful surgical method to increase the proliferation of osteogenic cells at bone defect site with precise immunoregulatory properties [25]. Non-resorbable expanded-polytetrafluoroethylene (e-PTFE, Teflon) have been firstly introduced and widely used since 1982 [77]. Such biocompatible materials can cover the defect area and maintain their structural integrity during implantation. However, the need of removal the non-resorbable biomaterial and other limitations restrain their application [83]. Currently, several barrier membranes have already been used in clinical areas, such as most commonly used bioresorbable collagen membranes. Several novel membranes with increased biocompatibility, and tissue integration properties have already been developed, such as polymer-based membrane, nanofibrous membranes, and alginate membranes, etc. [97]. Polycaprolactone (PCL) is a US Food and Drug Administration (FDA)-approved biocompatible and bioresorbable material for tissue regeneration [56]. Although PCL scaffolds have been shown to support bone regeneration *in vivo* in previous studies, lack of bioactivity limits their application in future bone tissue engineering [33]. Osteoinductive molecules or growth factors play an important role in bone healing process. The concept of adding osteoinductive molecules into the membrane have long been investigated by numerous researchers in the past decades. Platelet-derived growth factor (PDGF-BB), fibroblast growth factor (FGF2), and recombinant human bone morphogenetic protein-2 have been used as loading agents in various *in vivo* and *in vitro* studies to test their effect on osteogenesis, in which improved bone formation has been achieved by modifying bio-membrane guided scaffolds [20, 121]. Previous studies have shown

that PIII treated surfaces are able to covalently immobilize cytokines without the need for additional linker chemistry, thus offering huge application potential in medical prostheses and diagnostic devices industries [70]. In our previous study, PIII treated PCL surface with IL4 immobilization indicated altered inflammatory response of macrophages, which in turn, led to the differed angiogenic cytokines secretory levels and elicit enhanced osteogenesis of human mesenchymal stem cells (hBMSCs) in *in vitro* co-culture models (Fig. 5.2).

However, challenges remain in maintaining effective therapeutic concentrations of osteoinductive molecules as well as maintaining slow release properties of scaffold at target site in order to achieve therapeutic efficacy. Therefore, researchers are still trying to develop novel bio-membrane based scaffold with improved osteoinductive molecules releasing systems. Other release strategies, such as sequential cytokines release-based bio-membrane, can also be designed for their effect in critically-sized segmental bone defects models. Such controlled spatiotemporal release patterns may optimize the regeneration results by minimizing the concomitant adverse effects. In addition, combined cytokine release strategies, in which the osteoinductive molecules and other growth factors synergies can be established in order to amplify the optimal combination results of different cytokines. However, long-term observations regarding the safety and biocompatibility of bio-membrane barrier in both animal models and human trials are still needed, especially for those scaffolds with cytokine releasing properties.

### 5.2.6 Ion Doping

The role of different ions on bone regeneration has been extensively reported due to their regulatory role in bone cells and immune cells. Metallic ion doping on scaffold materials have been widely used as modification techniques for the improvement of the mechanical and osteoinductive properties of biomaterials [15]. Cooper, strontium, zinc, magnesium, silver and silicon,



**Fig. 5.2** (a) Plasma immersion ion implantation protocol on PCL surface. (b) Representative SEM images of PCL and PIII surface. Scale bars: 400 nm. (c) Experimental protocol of the indirect co-culture study. IL-4 (200 ng/ml in sterile PBS) was added to each scaffold for 1 h at room temperature. RAW264.7 cells seeded on PIII and PIII+IL4 surfaces were placed on 0.4  $\mu$ m hanging cell insert, while

hBMSCs were cultured in to lower chamber. (d) IL-4-immobilized PIII surface enhanced *in vitro* osteogenesis via modulation of macrophages phenotype. Representative confocal microscopy images of hBMSCs co-cultured with RAW264.7 cells on PIII and PIII+IL4 surfaces. Cells were stained by Alexa Fluor 594-conjugated phalloidin, ALP (green), and DAPI. All scale bars: 50  $\mu$ m

etc. have been tested *in vitro* and *in vivo* previously [3, 51, 112]. *In vitro* study using copper-doped mesoporous silica nanospheres on macrophages indicated significant immunomodulatory role of such scaffold on macrophages, which in turn, induced the robust osteogenic differentiation for bone mesenchymal stem cells [100].  $\beta$ -tricalcium phosphate is a calcium phosphate ceramic that is widely used as a bone substitute materials. Attraction of macrophages to  $\beta$ -TCP particles was previously demonstrated *in*

*vitro*, whereby macrophages migrated towards the biomaterial by emitting cytoplasmic extensions [32]. Additionally, magnesium doped  $\beta$ -TCP (Mg- $\beta$ -TCP) demonstrated M2 macrophage polarization ability *in vitro*, which the osteogenic differentiation of bone marrow stromal cells was significantly enhanced by stimulating with Mg- $\beta$ -TCP-derived conditioned medium [13]. The effect of magnesium doping on osteogenesis can be further corroborated by the new bone formation on magnesium doped

polycaprolactone (PCL) scaffolds[117]. Dual or multiple ions incorporation strategies have also been introduced in various cell culture and *in vivo* models. For example, strontium and lithium ion doped bioactive glass demonstrated increased tissue integration, vascularity, and bone regeneration compared to the single lithium-doped samples [63]. Therefore, modification of biomaterials with controlled release of metal ions may create unique immunomodulatory environment that can, alone or in combination with other modification strategies, control inflammatory response and accelerate bone regeneration.

### 5.2.7 Biomimetic-Inspired Scaffold

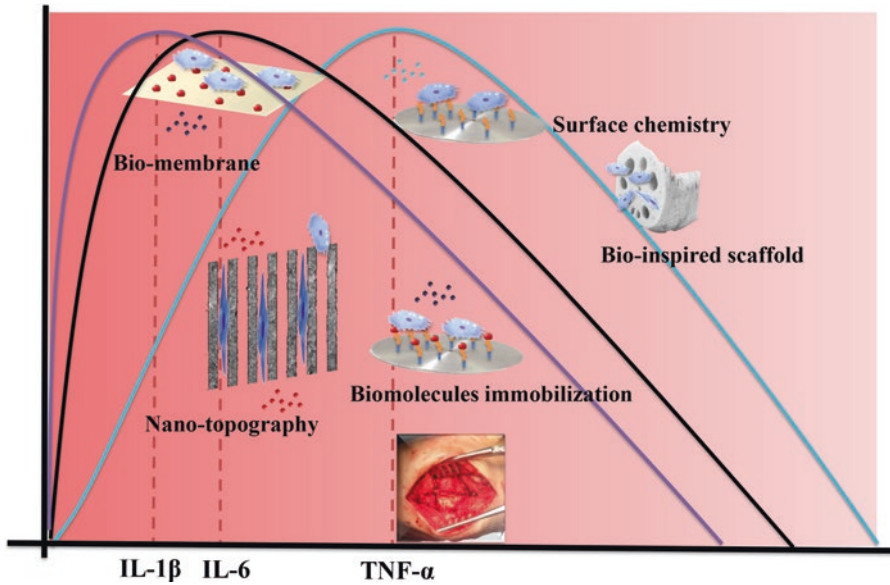
Over the past decades, researchers in various filed have tried to learn from the pre-existing hierarchical structures in nature, which converged into the banner of biomimetic. Therefore, scientists in biomaterial field have tried to developed biomimetic-inspired scaffold for better bone regeneration. Bone is a highly hierarchical organized composite with sophisticated structures, ranging from macroscale to nanolevel. Therefore, the idea of biomimetic-inspired scaffold should partially or fully mimic the biological structure of nanofibrous collagen, satisfy certain moderate of porosity for efficient nutrient supply, and could resist to various mechanical pressures at the same time. So far, several attempts on biomimetic-related biomaterial development has been explored by several researchers under different perspectives. For example, lotus root-inspired multi-channel scaffold showed improved mesenchymal stem cells attachment and proliferation *in vitro*. Further *in vivo* studies using rat muscle model and rabbit calvarial defects model indicated increased neo-vascularisation and new bone formation, respectively [29]. Another study using magnesium-doped hydroxyapatite/type I collagen scaffold, which mimic the human osteogenic niche, demonstrated enhanced osteogenesis *in vitro* and large volume of new bone

formation in rabbit [86]. Interestingly, it seems that the potential of nature-inspired scaffolds are beyond imagination. Researchers inspired by the host escape mechanism of influenza virus have designed polymer carrier to precisely control the release profile of small interfering RNA for the therapeutic application in many diseases[110]. Therefore, biomaterial inspired by mimicry of natural structures may provide researchers new insight into biomaterial design and development, thus paving the way for future clinical applications for such novel and functional biomaterials.

---

### 5.3 Biomaterial and Osteoimmune Environment Interaction-Future Direction?

The successful bone repair requires the incorporation of a number of cells and various molecular factors, among which the osteoimmune environment plays a key role in determining this process. Therefore, it is critical to understand the importance of this osteoimmune environment, how this microenvironment coordinates bone repair, and mechanisms governing the osteoimmune environment. In addition, the effect of different biomaterials on such osteoimmune environment should be fully considered, as biomaterials are no longer considered as inert object with no modulatory properties. Therefore, it is critical to understand the equilibrium and interaction between implants and osteoimmune environment since neither of these two elements is solely independent. Generating favourable osteoimmune environment through biomaterials-based strategy at initial stage may have the function to precisely influence the final outcome of bone regeneration. As many exciting studies are currently underway, it is possible to speculate that novel functional scaffold with precise osteoimmune environment modulation properties will be discovered in the near future (Fig. 5.3).



**Fig. 5.3** Future directions for ‘smart’ biomaterial design. Generating the favourable osteoimmune environments through biomaterials-based strategies at initial stage may potentially influence the final outcome of bone regenera-

tion. Therefore, fully exploration and modulation of early osteoimmune environment of bone regeneration holds significant clinical translational promises

## References

- Altman RD, Latta LL, Keer R, Renfree K, Hornicek FJ, Banovac K (1995) Effect of nonsteroidal antiinflammatory drugs on fracture healing: a laboratory study in rats. *J Orthop Trauma* 9:392–400
- Anderson JM, Rodriguez A, Chang DT (2008) Foreign body reaction to biomaterials. *Semin Immunol* 20:86–100
- Bari A, Bloise N, Fiorilli S, Novajra G, Vallet-Regi M, Bruni G, Torres-Pardo A, Gonzalez-Calbet JM, Visai L, Vitale-Brovarone C (2017) Copper-containing mesoporous bioactive glass nanoparticles as multifunctional agent for bone regeneration. *Acta Biomater* 55:493–504
- Bastian OW, Koenderman L, Alblas J, Leenen LP, Blokhuis TJ (2016) Neutrophils contribute to fracture healing by synthesizing fibronectin(+) extracellular matrix rapidly after injury. *Clin Immunol* 164:78–84
- Bax DV, Kondyurin A, Waterhouse A, McKenzie DR, Weiss AS, Bilek MMM (2014) Surface plasma modification and tropoelastin coating of a polyurethane co-polymer for enhanced cell attachment and reduced thrombogenicity. *Biomaterials* 35:6797–6809
- Benoit M, Desnues B, Mege JL (2008) Macrophage polarization in bacterial infections. *J Immunol* 181:3733–3739
- Binder NB, Puchner A, Niederreiter B, Hayer S, Leiss H, Bluml S, Kreindl R, Smolen JS, Redlich K (2013) Tumor necrosis factor-inhibiting therapy preferentially targets bone destruction but not synovial inflammation in a tumor necrosis factor-driven model of rheumatoid arthritis. *Arthritis Rheum* 65:608–617
- Bougioukli S, Jain A, Sugiyama O, Tinsley BA, Tang AH, Tan MH, Adams DJ, Kostenuik PJ, Lieberman JR (2016) Combination therapy with BMP-2 and a systemic RANKL inhibitor enhances bone healing in a mouse critical-sized femoral defect. *Bone* 84:93–103
- Bouyer M, Guillot R, Lavaud J, Plettinx C, Olivier C, Curry V, Boutonnat J, Coll JL, Peyrin F, Jossereand V et al (2016) Surface delivery of tunable doses of BMP-2 from an adaptable polymeric scaffold induces volumetric bone regeneration. *Biomaterials* 104:168–181
- Brancato SK, Albina JE (2011) Wound macrophages as key regulators of repair origin, phenotype, and function. *Am J Pathol* 178:19–25
- Cha HD, Hong JM, Kang TY, Jung JW, Ha DH, Cho DW (2012) Effects of micro-patterns in three-dimensional scaffolds for tissue engineering applications. *J Micromech Microeng* 22:125002
- Chan JK, Glass GE, Ersek A, Freidin A, Williams GA, Gowers K, Espirito Santo AI, Jeffery R, Otto WR, Poulosom R et al (2015) Low-dose TNF augments fracture healing in normal and osteoporotic



- bone by up-regulating the innate immune response. *EMBO Mol Med* 7:547–561
13. Chen Z, Mao X, Tan L, Friis T, Wu C, Crawford R, Xiao Y (2014a) Osteoimmunomodulatory properties of magnesium scaffolds coated with beta-tricalcium phosphate. *Biomaterials* 35:8553–8565
  14. Chen ZT, Bachhuka A, Han SW, Wei F, Lu S, Visalakshan RM, Vasilev K, Xiao Y (2017a) Tuning chemistry and topography of nanoengineered surfaces to manipulate immune response for bone regeneration applications. *ACS Nano* 11:4494–4506
  15. Chen ZT, Klein T, Murray RZ, Crawford R, Chang J, Wu CT, Xiao Y (2016) Osteoimmunomodulation for the development of advanced bone biomaterials. *Mater Today* 19:304–321
  16. Chen ZT, Ni SY, Han SW, Crawford R, Lu S, Wei F, Chang J, Wu CT, Xiao Y (2017b) Nanoporous microstructures mediate osteogenesis by modulating the osteo-immune response of macrophages. *Nanoscale* 9:706–718
  17. Chen ZT, Yi DL, Zheng XB, Chang J, Wu CT, Xiao Y (2014b) Nutrient element-based bioceramic coatings on titanium alloy stimulating osteogenesis by inducing beneficial osteoimmunomodulation. *J Mater Chem B* 2:6030–6043
  18. Cheng XY, Kondyurin A, Bao S, Bilek MMM, Ye L (2017) Plasma immersion ion implantation of polyurethane shape memory polymer: surface properties and protein immobilization. *Appl Surf Sci* 416:686–695
  19. Cho TJ, Gerstenfeld LC, Einhorn TA (2002) Differential temporal expression of members of the transforming growth factor beta superfamily during murine fracture healing. *J Bone Miner Res* 17:513–520
  20. Chung EJ, Chien KB, Aguado BA, Shah RN (2013) Osteogenic potential of BMP-2-releasing self-assembled membranes. *Tissue Eng Part A* 19:2664–2673
  21. Chung R, Cool JC, Scherer MA, Foster BK, Xian CJ (2006) Roles of neutrophil-mediated inflammatory response in the bony repair of injured growth plate cartilage in young rats. *J Leukoc Biol* 80:1272–1280
  22. Claes L, Recknagel S, Ignatius A (2012) Fracture healing under healthy and inflammatory conditions. *Nat Rev Rheumatol* 8:133–143
  23. Dai XH, Wei Y, Zhang XH, Meng S, Mo XJ, Liu X, Deng XL, Zhang L, Deng XM (2015) Attenuating immune response of macrophage by enhancing hydrophilicity of Ti surface. *J Nanomater* 2015:1
  24. Deng Y, Sun Y, Bai Y, Gao X, Zhang H, Xu A, Huang E, Deng F, Wei S (2016) In vitro biocompatibility/osteogenesis and in vivo bone formation evaluation of peptide-decorated apatite nanocomposites assisted via polydopamine. *J Biomed Nanotechnol* 12:602–618
  25. Dimitriou R, Mataliotakis GI, Calori GM, Giannoudis PV (2012) The role of barrier membranes for guided bone regeneration and restoration of large bone defects: current experimental and clinical evidence. *BMC Med* 10:81
  26. Ding J, Ghali O, Lencel P, Broux O, Chauveau C, Devedjian JC, Hardouin P, Magne D (2009) TNF-alpha and IL-1beta inhibit RUNX2 and collagen expression but increase alkaline phosphatase activity and mineralization in human mesenchymal stem cells. *Life Sci* 84:499–504
  27. Eger M, Sterer N, Liron T, Kohavi D, Gabet Y (2017) Scaling of titanium implants entrains inflammation-induced osteolysis. *Sci Rep Uk* 7:39612
  28. Engesaeter LB, Sudmann B, Sudmann E (1992) Fracture healing in rats inhibited by locally administered indomethacin. *Acta Orthop Scand* 63:330–333
  29. Feng C, Zhang W, Deng C, Li G, Chang J, Zhang Z, Jiang X, Wu C (2017) 3D printing of lotus root-like biomimetic materials for cell delivery and tissue regeneration. *Adv Sci (Weinh)* 4:1700401
  30. Fernandez-Vojvodich P, Karimian E, Savendahl L (2011) The biologics anakinra and etanercept prevent cytokine-induced growth retardation in cultured fetal rat metatarsal bones. *Horm Res Paediatr* 76:278–285
  31. Fu XB, Han B, Cai S, Lei YH, Sun TZ, Sheng ZY (2009) Migration of bone marrow-derived mesenchymal stem cells induced by tumor necrosis factor-alpha and its possible role in wound healing. *Wound Repair Regen* 17:185–191
  32. Gamblin AL, Brennan MA, Renaud A, Yagita H, Lezot F, Heymann D, Trichet V, Layrolle P (2014) Bone tissue formation with human mesenchymal stem cells and biphasic calcium phosphate ceramics: the local implication of osteoclasts and macrophages. *Biomaterials* 35:9660–9667
  33. Gao X, Song J, Ji P, Zhang X, Li X, Xu X, Wang M, Zhang S, Deng Y, Deng F et al (2016) Polydopamine-templated hydroxyapatite reinforced Polycaprolactone composite nanofibers with enhanced Cytocompatibility and osteogenesis for bone tissue engineering. *ACS Appl Mater Interfaces* 8:3499–3515
  34. Garg K, Pullen NA, Oskeritzian CA, Ryan JJ, Bowlin GL (2013) Macrophage functional polarization (M1/M2) in response to varying fiber and pore dimensions of electrospun scaffolds. *Biomaterials* 34:4439–4451
  35. Geiger M, Li RH, Friess W (2003) Collagen sponges for bone regeneration with rhBMP-2. *Adv Drug Deliv Rev* 55:1613–1629
  36. Gerstenfeld LC, Cho TJ, Kon T, Aizawa T, Tsay A, Fitch J, Barnes GL, Graves DT, Einhorn TA (2003) Impaired fracture healing in the absence of TNF-alpha signaling: the role of TNF-alpha in endochondral cartilage resorption. *J Bone Miner Res Off J Am Soc Bone Miner Res* 18:1584–1592
  37. Gilbert LC, Rubin J, Nanes MS (2005) The p55 TNF receptor mediates TNF inhibition of osteoblast differentiation independently of apoptosis. *Am J Phys Endocrinol Metab* 288:E1011–E1018

38. Glass GE, Chan JK, Freidin A, Feldmann M, Horwood NJ, Nanchahal J (2011) TNF- $\alpha$  promotes fracture repair by augmenting the recruitment and differentiation of muscle-derived stromal cells. *Proc Natl Acad Sci USA* 108:1585–1590
39. Goodman SB, Yao Z, Keeney M, Yang F (2013) The future of biologic coatings for orthopaedic implants. *Biomaterials* 34:3174–3183
40. Greenblatt MB, Shim JH (2013) Osteoimmunology: a brief introduction. *Immun Netw* 13:111–115
41. Groeneveld EH, Burger EH (2000) Bone morphogenetic proteins in human bone regeneration. *Eur J Endocrinol* 142:9–21
42. Groggaard B, Gerdin B, Reikeras O (1990) The polymorphonuclear leukocyte: has it a role in fracture healing? *Arch Orthop Trauma Surg* 109:268–271
43. Grundnes O, Reikeras O (1993) The importance of the hematoma for fracture healing in rats. *Acta Orthop Scand* 64:340–342
44. Hao SS, Meng J, Zhang Y, Liu J, Nie X, Wu FX, Yang YL, Wang C, Gu N, Xu HY (2017) Macrophage phenotypic mechanomodulation of enhancing bone regeneration by superparamagnetic scaffold upon magnetization. *Biomaterials* 140:16–25
45. Hashimoto J, Yoshikawa H, Takaoka K, Shimizu N, Masuhara K, Tsuda T, Miyamoto S, Ono K (1989) Inhibitory effects of tumor necrosis factor alpha on fracture healing in rats. *Bone* 10:453–457
46. He S, Zhou P, Wang LX, Xiong XL, Zhang YF, Deng Y, Wei SC (2014) Antibiotic-decorated titanium with enhanced antibacterial activity through adhesive polydopamine for dental/bone implant. *J R Soc Interface* 11:20140169
47. Hess K, Ushmorov A, Fiedler J, Brenner RE, Wirth T (2009) TNF  $\alpha$  promotes osteogenic differentiation of human mesenchymal stem cells by triggering the NF- $\kappa$ B signaling pathway. *Bone* 45:367–376
48. Ho C, Wang K, Shie M, Chen Y, Wang B (2017) The osteogenesis and degradation of 3D printed calcium silicate/polydopamine/polycaprolactone scaffolds for bone regeneration. *Tiss Eng Pt A* 23:S105–S105
49. Hofer HP, Kukovetz E, Egger G, Wildburger R, Quehenberger F, Schaur RJ (1994) Polymorphonuclear leucocyte migration response in uneventful wound healing following trauma surgery. A contribution to the search for objectifiable criteria in wound healing monitoring. *Arch Orthop Trauma Surg* 113:170–173
50. Hoff P, Maschmeyer P, Gaber T, Schutze T, Raue T, Schmidt-Bleek K, Dziurla R, Schellmann S, Lohanatha FL, Rohner E et al (2013) Human immune cells' behavior and survival under bioenergetically restricted conditions in an in vitro fracture hematoma model. *Cell Mol Immunol* 10:151–158
51. Hoppe A, Mourino V, Boccaccini AR (2013) Therapeutic inorganic ions in bioactive glasses to enhance bone formation and beyond. *Biomater Sci Uk* 1:254–256
52. Hotchkiss KM, Reddy GB, Hyzy SL, Schwartz Z, Boyan BD, Olivares-Navarrete R (2016) Titanium surface characteristics, including topography and wettability, alter macrophage activation. *Acta Biomater* 31:425–434
53. Hsu WK, Sugiyama O, Park SH, Conduah A, Feeley BT, Liu NQ, Krenke L, Virk MS, An DS, Chen IS et al (2007) Lentiviral-mediated BMP-2 gene transfer enhances healing of segmental femoral defects in rats. *Bone* 40:931–938
54. Huang S, Liang N, Hu Y, Zhou X, Abidi N (2016) Polydopamine-assisted surface modification for bone biosubstitutes. *Biomed Res Int* 2016:2389895
55. Hyzy SL, Olivares-Navarrete R, Hutton DL, Tan C, Boyan BD, Schwartz Z (2013) Microstructured titanium regulates interleukin production by osteoblasts, an effect modulated by exogenous BMP-2. *Acta Biomater* 9:5821–5829
56. Iqbal S, Rashid MH, Arbab AS, Khan M (2017) Encapsulation of anticancer drugs (5-fluorouracil and paclitaxel) into polycaprolactone (PCL) nanofibers and in vitro testing for sustained and targeted therapy. *J Biomed Nanotechnol* 13:355–366
57. Jemat A, Ghazali MJ, Razali M, Otsuka Y (2015) Surface modifications and their effects on titanium dental implants. *Biomed Res Int* 2015:1
58. Jiang Y, Wang B, Jia Z, Lu X, Fang L, Wang K, Ren F (2017) Polydopamine mediated assembly of hydroxyapatite nanoparticles and bone morphogenetic protein-2 on magnesium alloys for enhanced corrosion resistance and bone regeneration. *J Biomed Mater Res A* 105:2750–2761
59. John AA, Jaganathan SK, Supriyanto E, Manikandan A (2016) Surface modification of titanium and its alloys for the enhancement of osseointegration in orthopaedics. *Curr Sci India* 111:1003–1015
60. Kaner D, Zhao H, Arnold W, Terheyden H, Friedmann A (2017) Pre-augmentation soft tissue expansion improves scaffold-based vertical bone regeneration – a randomized study in dogs. *Clin Oral Implants Res* 28:640–647
61. Kempen DH, Lu L, Hefferan TE, Creemers LB, Maran A, Classic KL, Dhert WJ, Yaszemski MJ (2008) Retention of in vitro and in vivo BMP-2 bioactivities in sustained delivery vehicles for bone tissue engineering. *Biomaterials* 29:3245–3252
62. Kempen DHR, Lu LC, Heijink A, Hefferan TE, Creemers LB, Maran A, Yaszemski MJ, Dhert WJA (2009) Effect of local sequential VEGF and BMP-2 delivery on ectopic and orthotopic bone regeneration. *Biomaterials* 30:2816–2825
63. Khan PK, Mahato A, Kundu B, Nandi SK, Mukherjee P, Datta S, Sarkar S, Mukherjee J, Nath S, Balla VK et al (2016) Influence of single and binary doping of strontium and lithium on in vivo biological properties of bioactive glass scaffolds. *Sci Rep Uk* 6:32964
64. Kidd LJ, Stephens AS, Kuliwaba JS, Fazzalari NL, Wu AC, Forwood MR (2010) Temporal pattern of gene expression and histology of stress fracture healing. *Bone* 46:369–378

65. Klopffleisch R, Jung F (2017) The pathology of the foreign body reaction against biomaterials. *J Biomed Mater Res A* 105:927–940
66. Kon T, Cho TJ, Aizawa T, Yamazaki M, Nooh N, Graves D, Gerstenfeld LC, Einhorn TA (2001) Expression of osteoprotegerin, receptor activator of NF-kappaB ligand (osteoprotegerin ligand) and related proinflammatory cytokines during fracture healing. *J Bone Miner Res Off J Am Soc Bone Miner Res* 16:1004–1014
67. Konnecke I, Serra A, El Khassawna T, Schlundt C, Schell H, Hauser A, Ellinghaus A, Volk HD, Radbruch A, Duda GN et al (2014) T and B cells participate in bone repair by infiltrating the fracture callus in a two-wave fashion. *Bone* 64:155–165
68. Konstantinidis I, Papageorgiou SN, Kyrgidis A, Tzellos TG, Kouvelas D (2013) Effect of non-steroidal anti-inflammatory drugs on bone turnover: an evidence-based review. *Rev Recent Clin Trials* 8:48–60
69. Lacey DC, Simmons PJ, Graves SE, Hamilton JA (2009) Proinflammatory cytokines inhibit osteogenic differentiation from stem cells: implications for bone repair during inflammation. *Osteoarthr Cartil* 17:735–742
70. Landau S, Szklanny AA, Yeo GC, Shandalov Y, Kosobrodova E, Weiss AS, Levenberg S (2017) Tropoelastin coated PLLA-PLGA scaffolds promote vascular network formation. *Biomaterials* 122:72–82
71. Lange J, Sapozhnikova A, Lu CY, Hu D, Li X, Miclau T, Marcucio RS (2010) Action of IL-1 beta during fracture healing. *J Orthop Res* 28:778–784
72. Lee GH, Makkar P, Paul K, Lee BT (2018) Comparative bone regeneration potential studies of collagen, heparin, and polydopamine-coated multi-channelled BCP granules. *ASAIO J* 64:115–121
73. Lee YM, Fujikado N, Manaka H, Yasuda H, Iwakura Y (2010) IL-1 plays an important role in the bone metabolism under physiological conditions. *Int Immunol* 22:805–816
74. Lekstrom-Himes JA, Gallin JI (2000) Immunodeficiency diseases caused by defects in phagocytes. *New Engl J Med* 343:1703–1714
75. Li B, Cao H, Zhao Y, Cheng M, Qin H, Cheng T, Hu Y, Zhang X, Liu X (2017) In vitro and in vivo responses of macrophages to magnesium-doped titanium. *Sci Rep* 7:42707
76. Liebscher J, Mrowczynski R, Scheidt HA, Filip C, Hadade ND, Turcu R, Bende A, Beck S (2013) Structure of polydopamine: a never-ending story? *Langmuir* 29:10539–10548
77. Maas CS, Gnepp DR, Bumpous J (1993) Expanded polytetrafluoroethylene (Gore-Tex soft-tissue patch) in facial augmentation. *Arch Otolaryngol Head Neck Surg* 119:1008–1014
78. Mantovani A, Locati M (2009) Orchestration of macrophage polarization. *Blood* 114:3135–3136
79. Mantovani A, Sica A, Locati M (2005) Macrophage polarization comes of age. *Immunity* 23:344–346
80. Mao CY, Wang YG, Zhang X, Zheng XY, Tang TT, Lu EY (2016) Double-edged-sword effect of IL-1 beta on the osteogenesis of periodontal ligament stem cells via crosstalk between the NF-kappa B, MAPK and BMP/Smad signaling pathways. *Cell Death Dis* 7:e2296
81. Martinez FO, Sica A, Mantovani A, Locati M (2008) Macrophage activation and polarization. *Front Biosci: J Virtual Libr* 13:453–461
82. McKay WF, Peckham SM, Badura JM (2007) A comprehensive clinical review of recombinant human bone morphogenetic protein-2 (INFUSE (R) bone graft). *Int Orthop* 31:729–734
83. McKeown A, Beattie RF, Murrell GA, Lam PH (2016) Biomechanical comparison of expanded polytetrafluoroethylene (ePTFE) and PTFE interpositional patches and direct tendon-to-bone repair for massive rotator cuff tears in an ovine model. *Should Elb* 8:22–31
84. McWhorter FY, Wang TT, Nguyen P, Chung T, Liu WF (2013) Modulation of macrophage phenotype by cell shape. *P Natl Acad Sci USA* 110:17253–17258
85. Mensah KA, Li J, Schwarz EM (2009) The emerging field of osteoimmunology. *Immunol Res* 45:100–113
86. Minardi S, Corradetti B, Taraballi F, Sandri M, Van Eps J, Cabrera FJ, Weiner BK, Tampieri A, Tasciotti E (2015) Evaluation of the osteoinductive potential of a bio-inspired scaffold mimicking the osteogenic niche for bone augmentation. *Biomaterials* 62:128–137
87. Mountziaris PM, Mikos AG (2008) Modulation of the inflammatory response for enhanced bone tissue regeneration. *Tissue Eng Part B Rev* 14:179–186
88. Oh HH, Lu H, Kawazoe N, Chen G (2012) Spatially guided angiogenesis by three-dimensional collagen scaffolds micropatterned with vascular endothelial growth factor. *J Biomater Sci Polym Ed* 23:2185–2195
89. Pajarinen J, Kouri VP, Jansen E, Li TF, Mandelin J, Kontinen YT (2013) The response of macrophages to titanium particles is determined by macrophage polarization. *Acta Biomater* 9:9229–9240
90. Pan H, Zheng Q, Guo X, Wu Y, Wu B (2016) Polydopamine-assisted BMP-2-derived peptides immobilization on biomimetic copolymer scaffold for enhanced bone induction in vitro and in vivo. *Colloids Surf B: Biointerfaces* 142:1–9
91. Patterson J, Siew R, Herring SW, Lin AS, Guldberg R, Stayton PS (2010) Hyaluronic acid hydrogels with controlled degradation properties for oriented bone regeneration. *Biomaterials* 31:6772–6781
92. Pilipchuk SP, Monje A, Jiao Y, Hao J, Kruger L, Flanagan CL, Hollister SJ, Giannobile WV (2016) Integration of 3D printed and micropatterned polycaprolactone scaffolds for guidance of oriented collagenous tissue formation in vivo. *Adv Health Mater* 5:676–687
93. Ping ZC, Wang ZR, Shi JW, Wang LL, Guo XB, Zhou W, Hu XY, Wu XX, Liu Y, Zhang W et al (2017) Inhibitory effects of melatonin on titanium

- particle-induced inflammatory bone resorption and osteoclastogenesis via suppression of NF-kappa B signaling. *Acta Biomater* 62:362–371
94. Pountos I, Georgouli T, Blokhuis TJ, Pape HC, Giannoudis PV (2008) Pharmacological agents and impairment of fracture healing: what is the evidence? *Injury* 39:384–394
  95. Pricola KL, Kuhn NZ, Haleem-Smith H, Song YJ, Tuan RS (2009) Interleukin-6 maintains bone marrow-derived mesenchymal stem cell Stemness by an ERK1/2-dependent mechanism. *J Cell Biochem* 108:577–588
  96. Rifas L (2006) T-cell cytokine induction of BMP-2 regulates human mesenchymal stromal cell differentiation and mineralization. *J Cell Biochem* 98:706–714
  97. Sam G, Pillai BR (2014) Evolution of barrier membranes in periodontal regeneration—“are the third generation membranes really here?”. *J Clin Diagn Res* 8:ZE14–ZE17
  98. Schmidt-Bleek K, Schell H, Lienau J, Schulz N, Hoff P, Pfaff M, Schmidt G, Martin C, Perka C, Buttgerit F et al (2014) Initial immune reaction and angiogenesis in bone healing. *J Tissue Eng Regen Med* 8:120–130
  99. Sharmin F, McDermott C, Lieberman J, Sanjay A, Khan Y (2017) Dual growth factor delivery from biofunctionalized allografts: sequential VEGF and BMP-2 release to stimulate allograft remodeling. *J Orthop Res* 35:1086–1095
  100. Shi MC, Chen ZT, Farnaghi S, Friis T, Mao XL, Xiao Y, Wu CT (2016) Copper-doped mesoporous silica nanospheres, a promising immunomodulatory agent for inducing osteogenesis. *Acta Biomater* 30:334–344
  101. Simon AM, O'Connor JP (2007) Dose and time-dependent effects of cyclooxygenase-2 inhibition on fracture-healing. *J Bone Joint Surg Am* 89:500–511
  102. Spiller KL, Anfang RR, Spiller KJ, Ng J, Nakazawa KR, Daulton JW, Vunjak-Novakovic G (2014) The role of macrophage phenotype in vascularization of tissue engineering scaffolds. *Biomaterials* 35:4477–4488
  103. Spiller KL, Nassiri S, Witherel CE, Anfang RR, Ng J, Nakazawa KR, Yu T, Vunjak-Novakovic G (2015) Sequential delivery of immunomodulatory cytokines to facilitate the M1-to-M2 transition of macrophages and enhance vascularization of bone scaffolds. *Biomaterials* 37:194–207
  104. Sridharan R, Cameron AR, Kelly DJ, Kearney CJ, O'Brien FJ (2015) Biomaterial based modulation of macrophage polarization: a review and suggested design principles. *Mater Today* 18:313–325
  105. Stahli A, Miron RJ, Bosshardt DD, Sculean A, Gruber R (2016) Collagen membranes adsorb the transforming growth factor-beta receptor I kinase-dependent activity of enamel matrix derivative. *J Periodontol* 87:583–590
  106. Stanford CM (2010) Surface modification of biomedical and dental implants and the processes of inflammation, wound healing and bone formation. *Int J Mol Sci* 11:354–369
  107. Sudmann E, Dregelid E, Bessesen A, Morland J (1979) Inhibition of fracture healing by indomethacin in rats. *Eur J Clin Invest* 9:333–339
  108. Takayanagi H (2005) Inflammatory bone destruction and osteoimmunology. *J Periodontol Res* 40:287–293
  109. Tannoury CA, An HS (2014) Complications with the use of bone morphogenetic protein 2 (BMP-2) in spine surgery. *Spine J* 14:552–559
  110. Truong NP, Gu WY, Prasad I, Jia ZF, Crawford R, Xiao Y, Monteiro MJ (2013) An influenza virus-inspired polymer system for the timed release of siRNA. *Nat Commun* 4:1902
  111. Varoni EM, Altomare L, Cochis A, GhalayaniEsfahani A, Cigada A, Rimondini L, De Nardo L (2016) Hierarchic micro-patterned porous scaffolds via electrochemical replica-deposition enhance neo-vascularization. *Biomed Mater* 11:025018
  112. Vasconcelos DM, Santos SG, Lamghari M, Barbosa MA (2016) The two faces of metal ions: from implants rejection to tissue repair/regeneration. *Biomaterials* 84:262–275
  113. Wallace A, Cooney TE, Englund R, Lubahn JD (2011) Effects of interleukin-6 ablation on fracture healing in mice. *J Orthop Res* 29:1437–1442
  114. Wang Q, Zhang YX, Li B, Chen L (2017) Controlled dual delivery of low doses of BMP-2 and VEGF in a silk fibroin-nanohydroxyapatite scaffold for vascularized bone regeneration. *J Mater Chem B* 5:6963–6972
  115. Wang X, Friis TE, Masci PP, Crawford RW, Liao WB, Xiao Y (2016) Alteration of blood clot structures by interleukin-1 beta in association with bone defects healing. *Sci Rep Uk* 6:35645
  116. Wilgus TA, Roy S, McDaniel JC (2013) Neutrophils and wound repair: positive actions and negative reactions. *Adv Wound Care* 2:379–388
  117. Wong HM, Chu PK, Leung FKL, Cheung KMC, Luk KDK, Yeung KWK (2014) Engineered polycaprolactone-magnesium hybrid biodegradable porous scaffold for bone tissue engineering. *Prog Nat Sci Mater* 24:561–567
  118. Wu AC, Raggatt LJ, Alexander KA, Pettit AR (2013) Unraveling macrophage contributions to bone repair. *BoneKey Rep* 2:373
  119. Wu CT, Fan W, Chang J, Xiao Y (2011) Mussel-inspired porous SiO<sub>2</sub> scaffolds with improved mineralization and cytocompatibility for drug delivery and bone tissue engineering. *J Mater Chem* 21:18300–18307
  120. Xing Z, Lu C, Hu D, Yu YY, Wang X, Colnot C, Nakamura M, Wu Y, Miclau T, Marcucio RS (2010) Multiple roles for CCR2 during fracture healing. *Dis Model Mech* 3:451–458
  121. Yamano S, Haku K, Yamanaka T, Dai J, Takayama T, Shohara R, Tachi K, Ishioka M, Hanatani S, Karunakaran S et al (2014) The effect of a bioactive

- collagen membrane releasing PDGF or GDF-5 on bone regeneration. *Biomaterials* 35:2446–2453
122. Yang CH, Li YC, Tsai WF, Ai CF, Huang HH (2015) Oxygen plasma immersion ion implantation treatment enhances the human bone marrow mesenchymal stem cells responses to titanium surface for dental implant application. *Clin Oral Implants Res* 26:166–175
  123. Yang HW, Tang XS, Tian ZW, Wang Y, Yang WY, Hu JZ (2017) Effects of nano-hydroxyapatite/polyetheretherketone-coated, sandblasted, large-grit, and acid-etched implants on inflammatory cytokines and osseointegration in a peri-implantitis model in beagle dogs. *Med Sci Monit* 23:4601–4611
  124. Yang J, Zhou Y, Wei F, Xiao Y (2016) Blood clot formed on rough titanium surface induces early cell recruitment. *Clin Oral Implants Res* 27:1031–1038
  125. Yang X, Ricciardi BF, Hernandez-Soria A, Shi Y, Pleshko Camacho N, Bostrom MP (2007) Callus mineralization and maturation are delayed during fracture healing in interleukin-6 knockout mice. *Bone* 41:928–936
  126. Yi H, Ur Rehman F, Zhao C, Liu B, He N (2016) Recent advances in nano scaffolds for bone repair. *Bone Res* 4:16050
  127. Yu XH, Walsh J, Wei M (2014) Covalent immobilization of collagen on titanium through polydopamine coating to improve cellular performances of MC3T3-E1 cells. *RSC Adv* 4:7185–7192
  128. Zhang W, Liu J, Shi HG, Liu N, Yang K, Shi LX, Gu B, Wang HY, Ji JH, Chu PK (2015a) Effects of plasma-generated nitrogen functionalities on the upregulation of osteogenesis of bone marrow-derived mesenchymal stem cells. *J Mater Chem B* 3:1856–1863
  129. Zhang W, Liu N, Shi H, Liu J, Shi L, Zhang B, Wang H, Ji J, Chu PK (2015b) Upregulation of BMSCs osteogenesis by positively-charged tertiary amines on polymeric implants via charge/iNOS signaling pathway. *Sci Rep* 5:9369
  130. Zhao Y, Wong SM, Wong HM, Wu S, Hu T, Yeung KW, Chu PK (2013) Effects of carbon and nitrogen plasma immersion ion implantation on in vitro and in vivo biocompatibility of titanium alloy. *ACS Appl Mater Interfaces* 5:1510–1516



# Novel Biomimetic Microphysiological Systems for Tissue Regeneration and Disease Modeling

Karim I. Budhwani, Patsy G. Oliver,  
Donald J. Buchsbaum, and Vinoy Thomas

## Abstract

Biomaterials engineered to closely mimic morphology, architecture, and nanofeatures of naturally occurring *in vivo* extracellular matrices (ECM) have gained much interest in regenerative medicine and *in vitro* biomimetic platforms. Similarly, microphysiological systems (MPS), such as lab-chip, have drummed up momentum for recapitulating precise biomechanical conditions to model the *in vivo* microtissue environment. However, porosity of *in vivo* scaffolds regulating barrier and interface functions is generally absent in lab-chip systems, or otherwise introduces considerable cost, complexity, and an unrealistic uniformity in pore geometry. We address this by integrating electrospun nanofibrous porous scaffolds in MPS to develop the lab-on-a-brane (LOB) MPS for more effectively modeling transport, air-liquid interface, and tumor

progression and for personalized medicine applications.

## Keywords

Nanomedicine · nanotechnology · electrohydrodynamic · atomization · electrospinning · tissue engineering · microphysiological systems · disease model

## 6.1 Background

*Descriptive anatomy is to physiology what geography is to history, and just as it is not enough to know the typography of a country to understand its history, so also it is not enough to know the anatomy of organs to understand their functions.*  
(Claude Bernard. Paris, 1878)

Microphysiological systems (MPS) find applications in a broad array of domains including tissue engineering for regenerative medicine, *in vitro* platforms that closely mimic specific *in vivo* parameters to gain a deeper understanding of physiology and pathophysiology, and therapeutic evaluation of treatment options from testing new formulations and genes to optimal delivery mechanisms. Essentially, MPS combine architectural and environmental aspects, including the interplay of one with the other, of the target tissue to simulate both structural mechanics – such as stiffness, stretch, porosity, morphology, and so

K. I. Budhwani  
Departments of Radiation Oncology and Materials  
Science & Engineering, The University of Alabama at  
Birmingham, Birmingham, AL, USA

P. G. Oliver · D. J. Buchsbaum  
Department of Radiation Oncology, The University  
of Alabama at Birmingham, Birmingham, AL, USA

V. Thomas (✉)  
Department of Materials Science & Engineering, The  
University of Alabama at Birmingham,  
Birmingham, AL, USA  
e-mail: [vthomas@uab.edu](mailto:vthomas@uab.edu)

on – and biodynamic elements including fluid flow, pressure, and shear. In this chapter we will first review *in vivo* characteristics of tissue, with a focus on interfaces supporting barrier and transport functions, followed by engineering tissue scaffolds for MPS and, finally, integrating these engineered scaffolds in MPS to model *in vivo* physiological and pathophysiological conditions.

At its core, tissue engineering is about selecting suitable biomaterials for fabricating scaffolds designed to support cell fates leading to functional target tissue and then combining the engineering scaffold in a physiologically relevant environment with cells and additional biological and chemical formulations. Despite successes and Food and Drug Administration (FDA) approvals for human applications, engineered tissue constructs have not as yet gained widespread use in human patients.

### 6.1.1 Disease Models and Drug Development

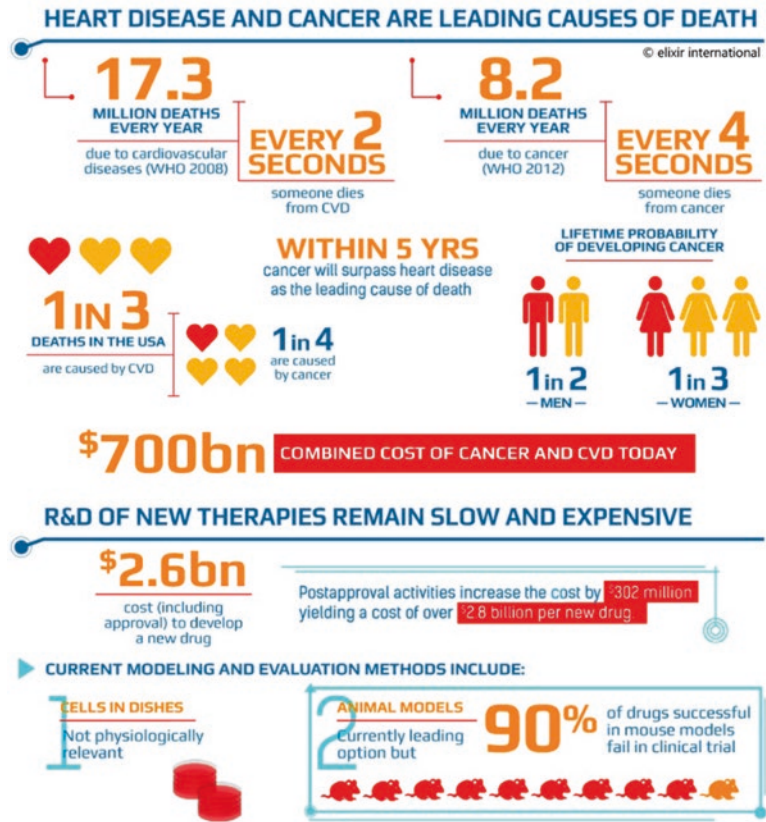
However, that is not to say that bench-to-bedside prospects for tissue engineering are bleak. On the contrary, the rise in the number of patients diagnosed with genetic disorders, such as cancers, is pushing the demand for developing next generation disease models and personalized medicine treatment efficacy evaluation assays. Already today, cardiovascular diseases (CVD) and cancer claim over 25 million lives in the USA exacting a tremendous toll on patients, caregivers, and society. In 2010 alone, \$290 billion (American Association for Cancer Research estimates) was incurred globally in direct cost of treatment alone. About \$125 billion was incurred in United States in 2010 which exceeded the National Institutes of Health (NIH) 2015 budget by more than 400%. And these are showing no signs of abating, instead, as shown in Fig. 6.1, estimated lifetime probability of developing cancer will increase, over the next five years, to 1-in-2 for men and 1-in-3 for women [39, 105]; resulting in cancer surpassing cardiovascular diseases (CVD) to become the leading cause of death worldwide.

### 6.1.2 Drug Discovery

Despite the significant toll exerted by these disorders and advances made in pre-discovery and discovery phases of drug development – including high-throughput screening and other miniaturized assays [12, 61, 77, 87, 90, 137], combinatorial chemistry, and computational models and databanks [11, 26, 36, 60, 69, 125, 128] – discovery of new drugs and other treatment options, including delivery mechanisms, remains quite slow and expensive. One reason for this dissonance is that assays and methods for evaluating efficacy of new treatments (Fig. 6.1) during pre-clinical evaluation are simply inadequate. Static culture dishes fail to recapitulate the *in vivo* microenvironment, making cells far from physiologically relevant, and animal models, though physiologically relevant, are limited indicators of success in subsequent human trials [51, 52, 68, 94, 107].

Cell culture models in dishes, while offering various advantages including relative ease (seeding, imaging, containment, and so on), scale, cost, precision (reproducibility at least with same cell lines), fall short in 3 key areas: (a) **Morphology**: the uniform, smooth, flat, non-porous surface of petri dishes is in stark contrast with the non-woven, random, network of nanofibers comprising porous *in vivo* substrates. (b) **Material**: Most dishes and plates are made of polystyrene or glass while water-rich *in vivo* extracellular matrix (ECM) is composed of various fibrous proteins such as collagens, elastins, laminins, and fibronectins and proteoglycans such as hyaluronic acid, decorin, aggrecan, and perlecan [32, 81]. (c) **Mechanics**: Young's modulus, a measure of stiffness (elastic response), for collagen [13] (500 KPa) is five orders of magnitude lower than that for glass and polystyrene ( $65 \times 10^6$  and  $3.5 \times 10^6$  KPa respectively), which when compounded with *in vivo* fluid dynamics (absent in static cell culture dishes) can lead to significant differences in cell fates due to biomechanical cues and matrix remodeling. Animal models overcome these shortcomings but at the expense of relative **ease**, **scale**, **reproducibility** (precision), and **cost** [106]. Moreover, neither

**Fig. 6.1** Potential for improving disease modeling and therapeutic R&D with biomimetic MPS. © elixir international. (Reproduced with permission. All rights reserved)



static culture models nor animal models are suitable for **personalized medicine** (patient specific) applications.

### 6.1.3 Tissue Microenvironment

Impeding advancement in understanding diseases and the subsequent development and testing of effective treatment options is often the parallel, multivariate nature of tissue and organ systems resulting from dynamic interplay of biological, chemical, and physical forces at the molecular, micro, and macro scale [23, 35, 37, 48, 53, 71, 76, 98, 115, 119, 126, 129]. Developing models that isolate variables or sub-systems, aid in the deeper understating of the specific mechanisms under examination but at the expense of muting any cross-talk along isolated boundaries. High-throughput screening (HTS) systems [12, 61, 77, 90, 137] investigating efficacy on small

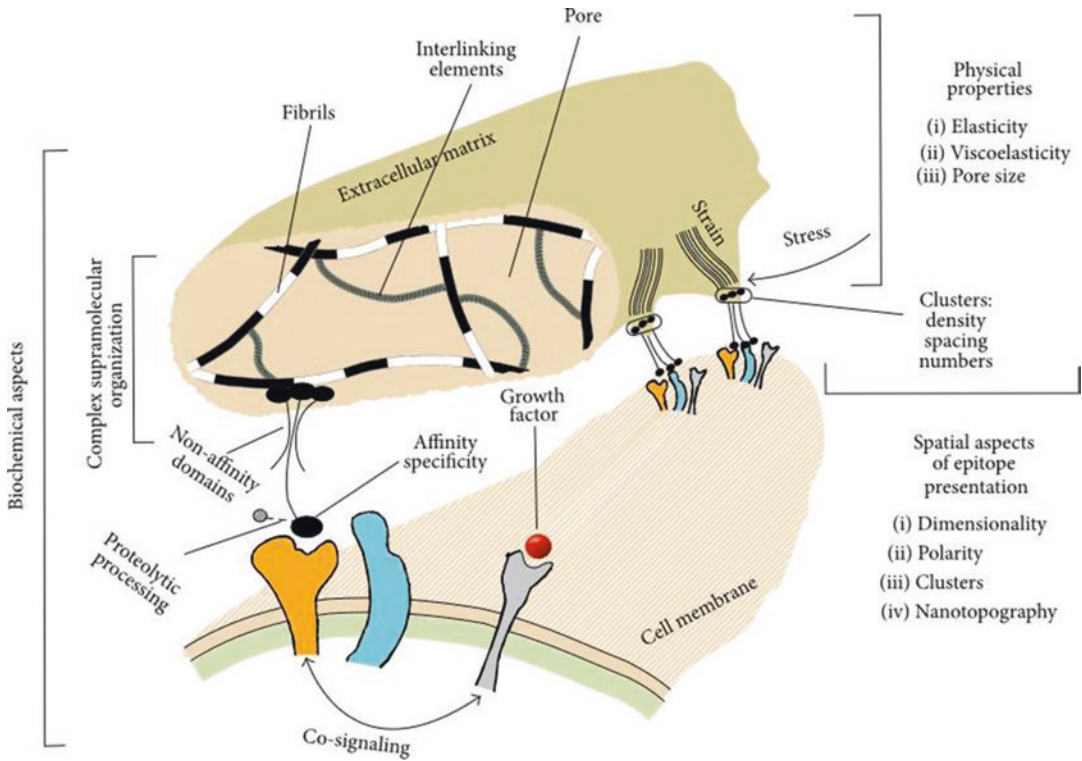
sets of biomolecules, for instance, offer a significant upstream performance advantage at the expense of escalating downstream costs from failed clinical trials. That said, optimal design with deliberate and established isolation boundaries can provide rich abstractions to assist both in disease modeling and development and evaluation of new treatment options.

## 6.2 Tissue Structure and Environment

*The whole organism subsists only by means of the reciprocal action of the single elementary parts.* (Theodor Schwann. Theory of the Cells, 1847)

The extracellular matrix, or ECM, is the non-cellular component of tissue that provides structural rigidity and support to organs and tissues as the de facto scaffolding. This water-rich and fibrous scaffolding is composed of various fibrous





**Fig. 6.2** Structure and composition of *in vivo* extracellular matrix (ECM). Key features include (a) Complex fibrous network with various other biochemical components, (b) Stiffness/elasticity of the network provide structural support and biomechanical cues driving cell fates, (c) Pores regulating cellular and molecular transport, (d) Viscoelasticity, which allows polymeric constituents to

behave both as elastic solid and viscous fluid as a function of time or temperature, is key to matrix deformation and subsequent remodeling of ECM, (e) Undergird morphology varies richly with respect to fiber diameter distribution, substrate thickness, adhesion profiles, surface area topography, and so on. (Reproduced here from Stem Cells International [3] under Creative Commons Attribution License)

proteins such as collagens, elastins, fibronectins, laminins, and proteoglycans such as hyaluronic acid, aggrecan, decorin, and perlecan [32, 81]. As illustrated in Fig. 6.2, supramolecular components, such as fibrils, fiber bundles, or fiber networks, assembled from collagen proteins provide mechanical support and biological signaling for cellular adhesion, cellular proliferation, and tissue morphogenesis [3, 99]. Further, the ability of the ECM to withstand high compressive forces without loss of properties comes from a covalently cross-linked gel of glycosaminoglycan chains (proteoglycans) which remains unsolubilized and gets very elongated due to the hydrophilic network of saccharide chains. Although this network is unsolubilized, soluble growth factors that influence morphology and physiological function of the tissue can be integrated.

Despite these common base constituents, there is considerable variance in the specific composition and morphology of the undergirding ECM not only between tissue structures from different systems but also at different sites within a tissue. This heterogeneity stems from a variety of factors including type of tissue, ECM site within a specific tissue structure, and the physiological state of the tissue [32]. In fabricating scaffolds and substrates for engineered tissue, whether for patient or MPS applications, it is therefore important to recapitulate these variations in ECM composition and morphology to accurately mimic the resulting biomechanical and biochemical cues which, in turn, direct cell fates including proliferation and, in the case of stem cells, differentiation to a directed lineage. In providing structure, support, and through appropriate bio-

mechanical and biochemical cues, the ECM plays a key role in driving cell fates and function.

### 6.2.1 ECM Scaffolding and Cell Fates

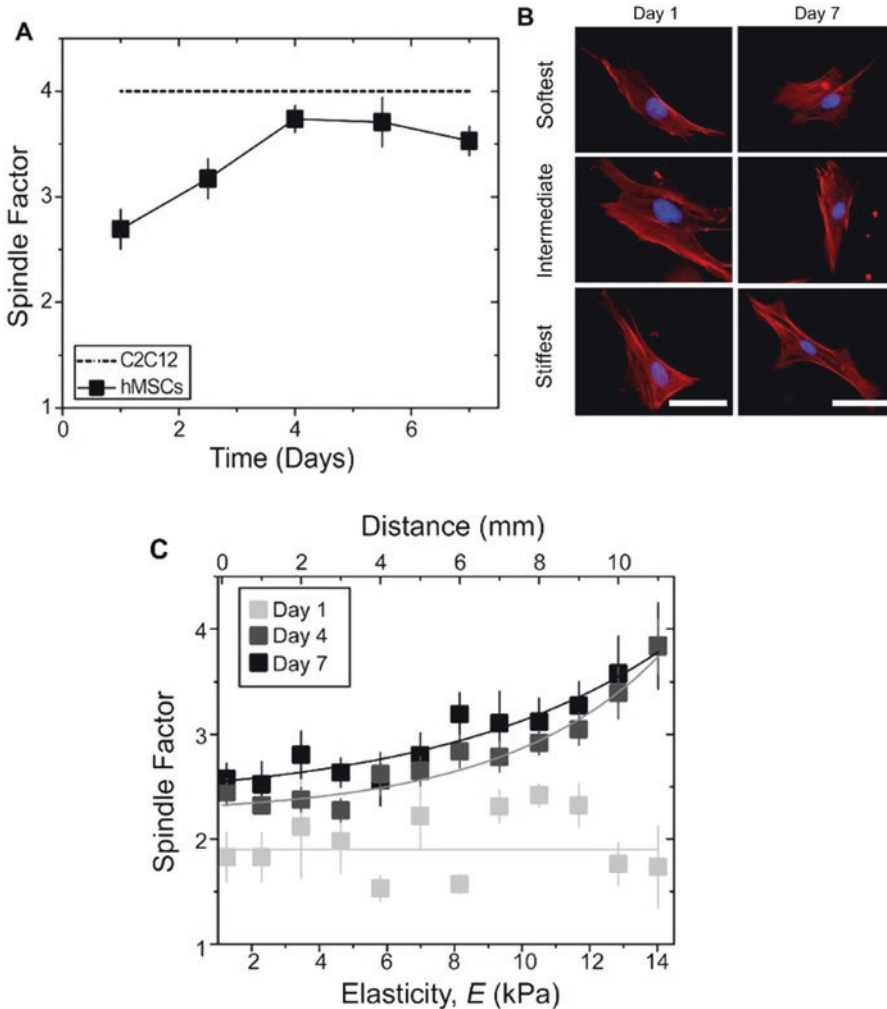
While ECM provide tissue with structural support, biomechanical and biochemical cues, cells are the building blocks and builders of tissue. This building also includes remodeling the underlying ECM itself. Cells respond to signals and cues they receive from their local environment. This response can initiate a chain of responses that not only modulate cell fates but also the secretion of proteins that ultimately result in matrix remodeling, thereby changing the local environment and downstream signaling. A better understanding of cellular response to biomechanical signals such as stiffness and morphology – specifically in resulting cell fates, local environment interaction and subsequent organization into tissue systems and organs – has provided researchers and biomedical engineers with the ability to identify and tune scaffolding properties to mend damaged tissue or even create new ones.

### 6.2.2 Stiffness of Scaffolds and Fibers

Cellular responses to elastic properties of tissue engineering substrates have been shown to impact differentiation of stem cells. This is particularly pronounced for anchorage dependent cells [14, 17, 28, 29, 46, 62, 63, 78, 85, 89, 130–132, 136] as proliferating cells respond to the initial pull against the ECM and mechano-transducer signals proportional to the required matrix deformation force [29]. Figure 6.3 highlights the impact of matrix stiffness on mesenchymal stem cell (MSC) morphology [116] where the spindle-factor is a measure of cellular morphology derived simply by dividing the major by the minor axes. As shown in the image, morphological changes in cells can be observed as a function

of culture time and ECM stiffness. On methacrylamide/chitosan hydrogels (with laminin to promote cellular adhesion), of varying moduli, proliferation of neural stem/progenitor cells (NSPC) peaked on substrates with 3.5 kPa stiffness, neuronal differentiation was optimal when stiffness was under 1 kPa, and oligodendrocyte differentiation was favored when stiffness was above 7 kPa [63]. Cellular growth and migration was observed only for the softest scaffolds in this study. Human MSC (HMSC) from adipogenic and osteogenic cells in thiol-hyaluronic acid hydrogels were found to differentiate into adipogenic cells with a larger spreading area and thin elongated processes on stiffer substrates in the 4 kPa range, while spindle-shaped osteogenic differentiation was observed on 0.15 kPa stiffness substrates [136]. Another study, of iPSC-derived embryoid bodies on substrates with varying stiffness (0.6 kPa, 14 kPa, 50 kPa, and 1 GPa), found [78] that differentiation toward cardiac and neural tissue lineages was favorable in polyacrylamide (pAA) 0.6 kPa substrates compared to the control 1 GPa polystyrene tissue culture plates.

In terms of stiffness, electrospun fibers offer higher Young's modulus (or stiffness) than hydrogels. In our studies [109, 110, 112] of nanomechanical properties of electrospun fibers, moduli ranged from 0.2 GPa (collagen type I) to 0.6–0.8 GPa (collagen/nanohydroxyapatite (nHA) composite), depending on chemistry and diameter of fibers, and stiffness increased further with chemical-crosslinking [109]. Alignment of fibers also contributed to stiffness with increased modulus of fibers from scaffolds with aligned fibers (depending on rotation speeds for fiber alignment) [110]. Improved HMSC adhesion and survival was observed on higher stiffness PCL/nHA electrospun substrates compared to PCL and collagen substrates [91]. Additionally, MSCs on PCL/collagen/nHA scaffolds showed higher levels of phosphorylated FAK, an integrin activation marker and signaling molecule implicated in cell survival and osteoblastic differentiation [91]. These studies highlight that composition and stiffness of scaffolds are key parameters in directing cell growth and function.



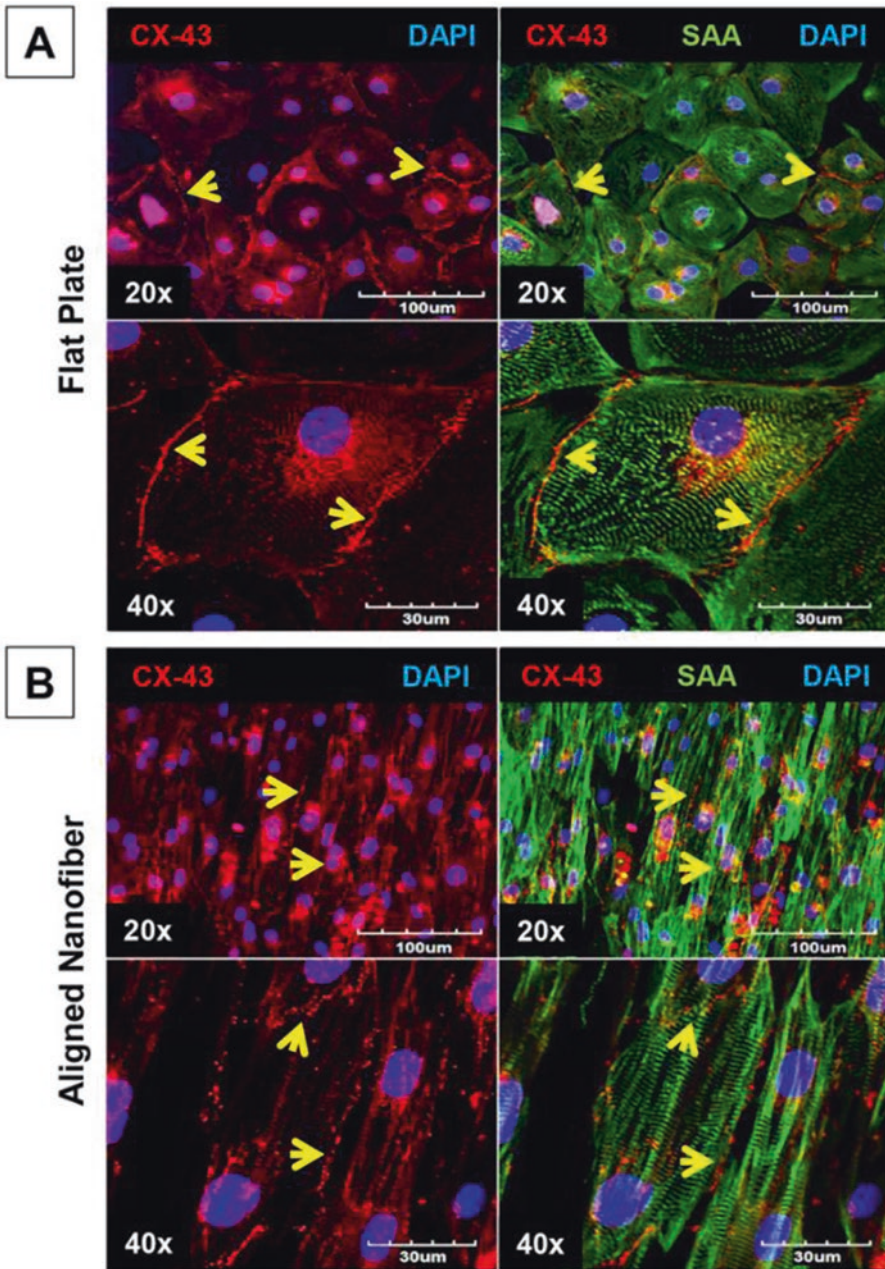
**Fig. 6.3** Impact of matrix stiffness. (a) MSC spindle factor increases on 11 kPa while C2C12 myoblasts remain steady. (b) MSC stiffness induced morphological changes,

scale bar: 12.5  $\mu\text{m}$ . (c) Spindle-factor of MSC over time. (Reproduced here with permission from PLoS ONE [116] under Creative Commons Attribution License)

### 6.2.3 Morphology of Fibers

In addition to composition and stiffness, morphological attributes of the substrate such as fiber diameter, orientation, and porosity influence cell fates [1, 6, 16, 19, 45, 67, 70, 75, 79, 100, 121, 124]. It has been shown that fiber orientation has a dramatic impact on cell fates, particularly in cardiac and neural tissue. Neural precursors from mouse embryonic stem cells (ESC), for instance, more readily differentiated into mature motor neurons and interneurons on aligned poly( $\epsilon$ -caprolactone) (PCL) scaffolds [1]. Similarly,

aligned fiber scaffolds provide better contact guidance for nerve and cardiomyocyte elongation compared to randomly oriented substrates as shown in Fig. 6.4; human iPSC derived cardiomyocytes (hiPSC-CM) show improved cell alignment and elongation on electrospun aligned nanofibrous poly(lactide-co-glycolide) (PLGA) substrates compared to evenly distributed generally round-shaped morphology on flat plates [54]. Beyond alignment and elongation, better physiological outcomes, including increased electrical coupling and cell-cell communication, were also observed by immunostain-



**Fig. 6.4** Fiber orientation. Cellular alignment and gap junctions of iPSC derived cardiomyocytes on (a) flat plate vs. (b) aligned electrospun polylactide-co-glycolide (PLGA) nanofibrous substrate. Cells characterized with

CX-43 (Red), SAA (Green) and DAPI (Blue). (Adapted and reproduced here with permission from PLoS ONE [54] under Creative Commons Attribution License)

ing for cell-cell electrical coupling gap junctional protein Connexin 43 (CX-43). In addition to structural support and guidance, the scaffolding must also facilitate cellular and nutrient transport for which, adequate porosity, in terms of pore sizes and density, is vital.

Electrospinning is an optimal method for fabricating nanofibrous scaffolds with tunable porosity to target specific tissue systems and sites. Processing parameters can be further adjusted to tailor the nanofibrous substrate for larger bulk surface area, to increase cellular adhesion, by decreasing fiber diameters. This also results in greater porosity. However, in reducing fiber diameters, individual pore sizes also shrink, which could impede transport of some cells into the interior of the scaffold [6]. Chondrogenic differentiation, for instance, was found to be greater for MSC on PCL microfibers than on nanofibrous substrates likely due to smaller pore sizes of nanofibrous substrates, precluding MSC from penetrating deeper into the scaffold, whereas larger pores characteristic of microfibrous substrates allowed for completely colonizing the scaffold [6]. One way to overcome this is by modulating fiber density across the substrate resulting in larger average pore sizes. On the other end of the pore size spectrum, smaller pore sizes are better suited in applications such as our *lab-on-a-brane* [13] (LOB) capillary mimicking *in vivo* regulation of transendothelial molecular transport.

#### 6.2.4 Microarchitecture and Materials

As described earlier, during tissue regeneration and indeed for tissue engineering applications, cells rely greatly on the extracellular environment for structural support, adhesion capabilities, proliferation capacity, alignment guidance, elongation and more, until they can remodel and build their natural ECM for homeostasis. The microarchitecture and materials must therefore closely mimic the *in vivo* ECM while allowing for tuning biomechanical properties and mechanisms for providing biochemical cues based on target sys-

tem, tissue type and site. Further, since *in vivo* ECM are generally networks of nanofibers, nanofibrous substrates are an optimal structural choice for regenerative therapy applications.

Optimal materials for engineered tissue scaffolding are determined by the target application. For instance, for engineering scaffolding for hard tissue such as bone, metals and ceramics [18, 111] offer optimal biomechanical properties [58], whereas polymers are more suitable for soft tissue systems. Engineers further narrow polymer selection from among biopolymers, synthetic biodegradable polymers, or their blends and copolymers [4, 58]. Synthetic polymers commonly used for fabricating tissue scaffolding include PCL, poly(lactic acid), and poly(glycolic acid). In addition to collagen, commonly used biopolymers include silk and chitosan, and natural carbohydrates such as alginate and agarose. Several tradeoffs must be considered when deciding between natural and synthetic materials.

Being innately bioresponsive and biodegradable is an advantage for natural protein fibers in biomedical applications, but it is not without constraints. Consider biodegradability for instance, while advantageous overall, absence of control over the rate of hydrolytic or proteolytic degradation makes natural fibers unsuitable for applications with tighter requirements over synchronized degradation of engineered scaffold with tissue regeneration. Processing difficulty and greater variances in mechanical properties among batches of natural polymers are other weaknesses of such materials. On the flip side, synthetic polymers offer advantages in parameters such as tunable degradation rates, higher precision polymer structure, enhanced mechanical properties, and lower cost due to ease of bulk production, but are inferior to natural materials in offering binding sites for anchorage-dependent cells, for instance, or may produce potentially acidic or cytotoxic degradation by-products among other drawbacks. Hybrid polymers, that effectively combine natural and synthetic polymers to optimize aspects from both for achieving application-driven properties, are increasingly used in engineered tissue scaffolding for regenerative medicine and next generation MPS. Nanofibrous PLGA/collagen

scaffolds were shown to outperform similarly electrospun PLGA nanofibers for ESC proliferation and target differentiation into cardiomyocytes [93].

---

### 6.3 Engineered Biomimetic ECM Scaffolds

*There's Plenty of Room at the Bottom.* (Richard P. Feynman. American Physical Society, Caltech, 1959)

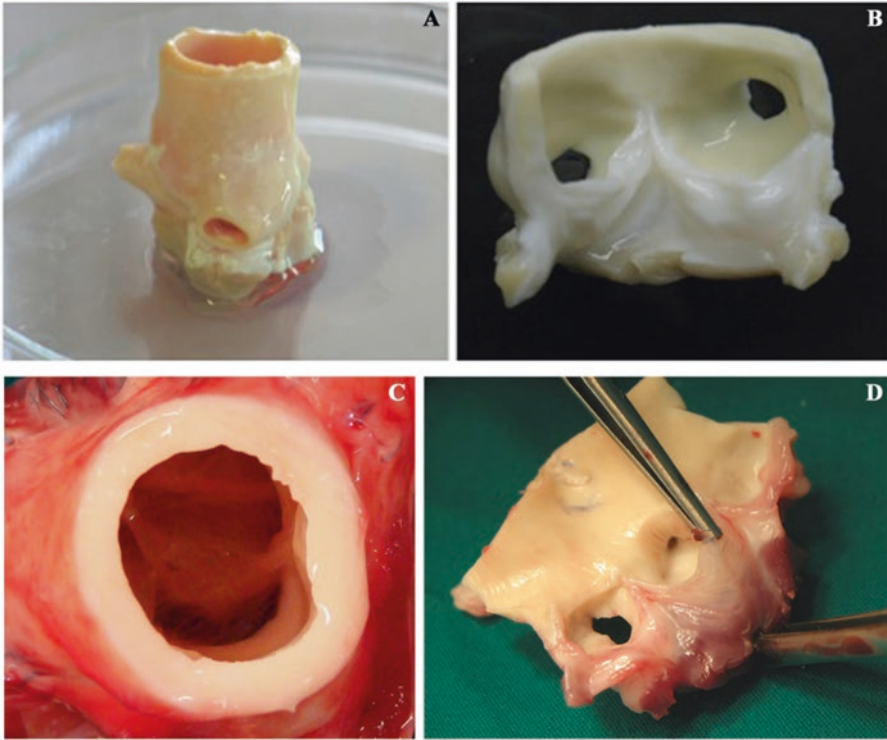
While they may not have been referred to as such, nanotechnology and nanofabrication methods have long pervaded various spheres of human endeavor; including the fine arts, with some accounts tracing creative applications of colloidal gold and silver in enhancing the visual intrigue of works of art as far back as the fourth century [84]. Between then and now, the course of human history and knowledge has been greatly influenced by innovative applications of nanotechnology, but it was only in 1959, with the canonical lecture by Feynman at Caltech, that a vision for the deliberate exploration of the atomic scale was distinctly articulated [31]. Since then, nanotech has rapidly ballooned and branched out into many subdomains. Nanomedicine is one such domain. The NIH define nanomedicine as a branch of nanotechnology that focuses on “highly specific medical intervention at the molecular scale for curing disease or repairing damaged tissues, such as bone, muscle, or nerve,” [83] restricting the size scale to under 100 nm, which is in the intracellular or sub-cellular domain. However, in the context of this chapter, we expand the definition of nanomedicine to include the immediate nanofibrous extracellular local environment and its interaction, interplay, and interventions at the sub-micron level (sub-700 nm). Nanostructured biopolymers exhibiting nanofibrous morphology have gained much interest in regenerative medicine and *in vitro* biomimetic systems due, primarily, to the close approximation of this nanofibrous morphology to nanofeatures found in natural ECM.

Of particular interest within this subdomain are advances in controlling material properties

and optimizing morphology of nanofibrous engineered tissue scaffolds and substrates for biomimetic MPS and regenerative medicine applications. Despite the growing momentum in regenerative medicine toward repairing or replacing diseased or damaged tissue using synthetic or natural constructs, complexities in cellular response compounded by variables, such as substrate morphology, composition, topography, geometry, adhesion profiles, cell-cell and cell-ECM crosstalk, and a myriad of other factors impede rapid translation from research to clinical applications. A host of biomimetic MPS, including our recent LOB platform [13], therefore have been investigated for enabling rapid development of *in vitro* evaluation models to bridge the chasm from bench research to clinical applications. Much attention has also been focused on characterizing the interplay between various aspects of the substrate and resulting cellular response. Optimally, scaffold materials chemistry and physical morphology would not only mimic the natural environment but also foster cellular growth, proliferation, and – for stem cells – differentiation into the target lineage. In many applications, it may also be desired for the biomimetic scaffold to ultimately give way to the natural process of cellular remodeling of the ECM. In this section we examine three distinct methods for producing tissue scaffolds and substrates used in tissue regeneration and MPS applications.

#### 6.3.1 Decellularized ECM

Before detailing methods that use materials to fabricate new scaffolds for engineered tissue, it is noteworthy to discuss decellularized ECMs whereby new tissue is engineered by repurposing existing tissue scaffold. In this approach, cells of a donor organ are stripped using various [5, 44, 133] protocols, leaving behind only the decellularized natural scaffold (Fig. 6.5) which is subsequently used to grow new tissue. In theory, since the regenerated tissue would be cultured using the patient's own cells, the risk or magnitude of any immunogenic rejections would be mitigated. This approach, which has been used to engineer



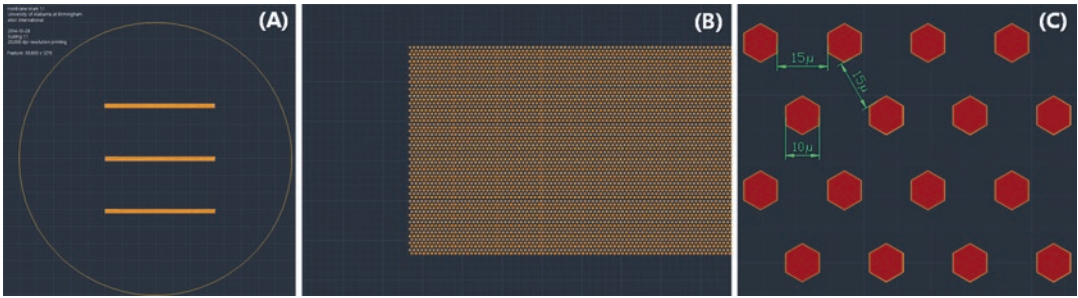
**Fig. 6.5** Macroscopic allogeneic aortic valve substitutes after decellularization (a, b) and explant at 15 months (c, d). (Adapted and reproduced here with permission from PLoS ONE [44] under Creative Commons Attribution License)

heart, liver, lung, and kidney tissue, offers the additional prospect for repurposing otherwise discarded human tissue scaffolding from routine surgical procedures.

Clinically applied examples range from decellularized dermis for burn injuries to decellularized vessels for restoring vascular function [5, 44]. Although such repurposed tissue scaffolds have shown promising results in tissue repair, they are not without drawbacks, particularly in terms of mechanical properties, immunogenicity, degradation, and cross-contamination. Moreover, decellularized ECM from animal tissues pose other challenges such as dimensional or scaling mismatch between donor and target tissues, variances and mismatches in compositional profile and rates of enzymatic degradation, and risks associated with xenogeneic pathogens.

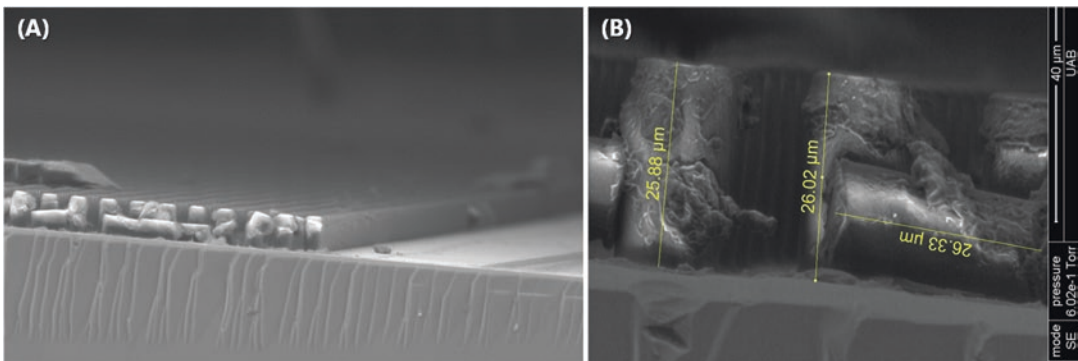
### 6.3.2 Photolithography

Photolithography is a common fabrication technique used for creating high-fidelity uniform microporous and non-porous membrane substrates for *in vitro* microtissue models. In this method, virtually nanoscale features are “imprinted” on a thin, typically, polydimethyl siloxane (PDMS) membrane by a process similar to computer microchip manufacturing. The models created using this method often include the moniker “chip” – as in *lab-on-a-chip* [9] – due to this adaption of computer chip fabrication processes. This method essentially involves three steps: (a) designing an appropriate mask, (b) creating a stamp, or master, by patterning SU-8 on silicon wafers, and finally (c) spin-coating PDMS on the master to manufacture the final microporous thin membrane. Let’s look at each of these closely.



**Fig. 6.6** A negative resist mask design with 10  $\mu\text{m}$  features spaced 15  $\mu\text{m}$  apart in 3 channels. (a) The complete mask. (b) A section of a porous channel patterned on the

mask. (c) Detailed view of individual  $\mu\text{scale}$  features comprising the porous channel pattern. © elixir international. (Reproduced with permission. All rights reserved)



**Fig. 6.7** Photolithography Master with 192,000 hexagonal posts  $\sim 10\ \mu\text{m}$  in diameter spaced  $\sim 15\ \mu\text{m}$  apart on silicon wafer. (a) 300  $\mu\text{m}$  resolution of rows of posts. (b) 40  $\mu\text{m}$  resolution of posts. Note, images of cracked silicon

wafer taken after membrane was fabricated, hence, some residual PDMS deposits and broken posts can also be seen. © elixir international. (Reproduced with permission. All rights reserved)

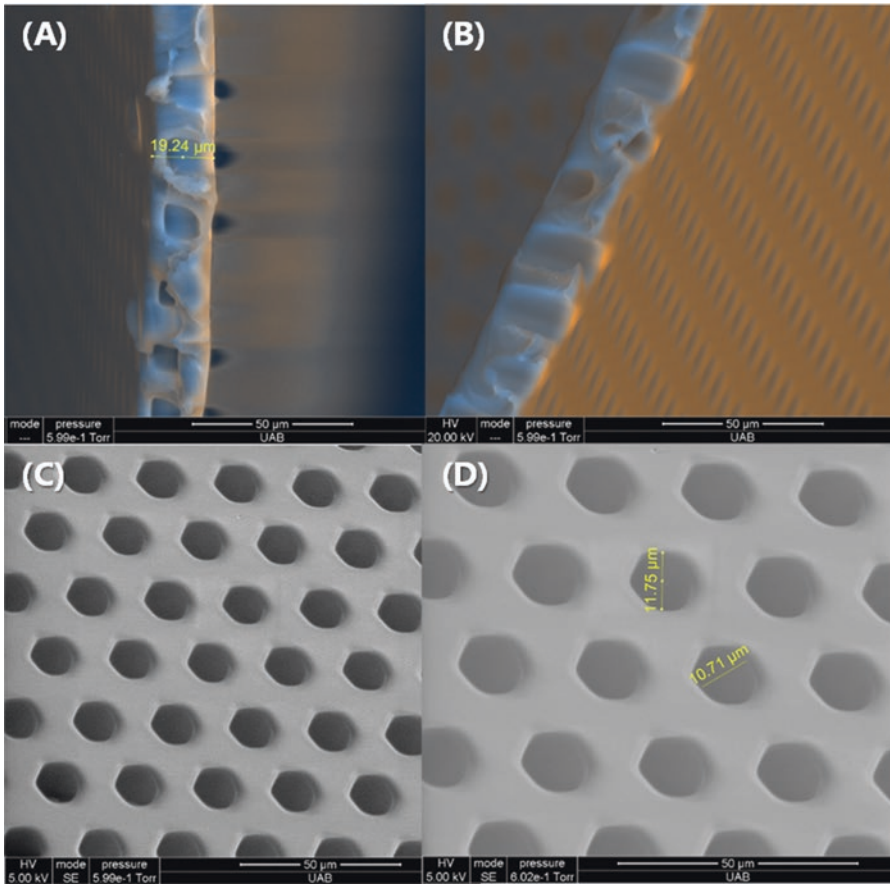
Low cost photolithography masks are typically made using polyester film, however, these may not faithfully reproduce very fine features, in which case, soda lime glass or quartz masks are preferred. The primary role of the mask is to allow (or block) high intensity ultraviolet (UV) light to selectively cure photoresist coated on a silicon wafer, thereby optically transferring the pattern from the mask onto the photolithography master. With negative photoresist, only the exposed regions on the wafer are cross-linked and retained, the remaining uncured photoresist is washed away during development. An example of a negative resist mask design, with channels of 10  $\mu\text{m}$  diameter hexagonal pores, is shown in Fig. 6.6.

Based on required features, photolithography parameters, including the amount of photoresist and spin and cure protocols, must be carefully

selected for creating a suitable master (or stamp) from which the final scaffold would be created. The master shown in Fig. 6.7, for instance, was created by spinning 10g of photoresist using a two-speed spin protocol and cured using a glass mask in conformal contact to produce the desired set of 192,000 posts, each post being  $\sim 25\ \mu\text{m}$  tall.

Finally, the master is used to stamp micropatterned or microporous substrate membranes which would subsequently be used in microtissue models. Material and fabrication parameters for this part of the process must also be carefully selected to produce substrates with properties that accurately reflect the target microtissue environment. While producing micropatterned substrates using this method is common, fabricating and detaching microporous thin membranes can be challenging including pores occluded with





**Fig. 6.8** PDMS membranes 20 μm thick with 10 μm pores. SEM showing (a) Membrane cross-section. (b) Rows of through pores. (c, d) Hexagonal unoccluded

micropores. © elixir international. (Reproduced with permission. All rights reserved)

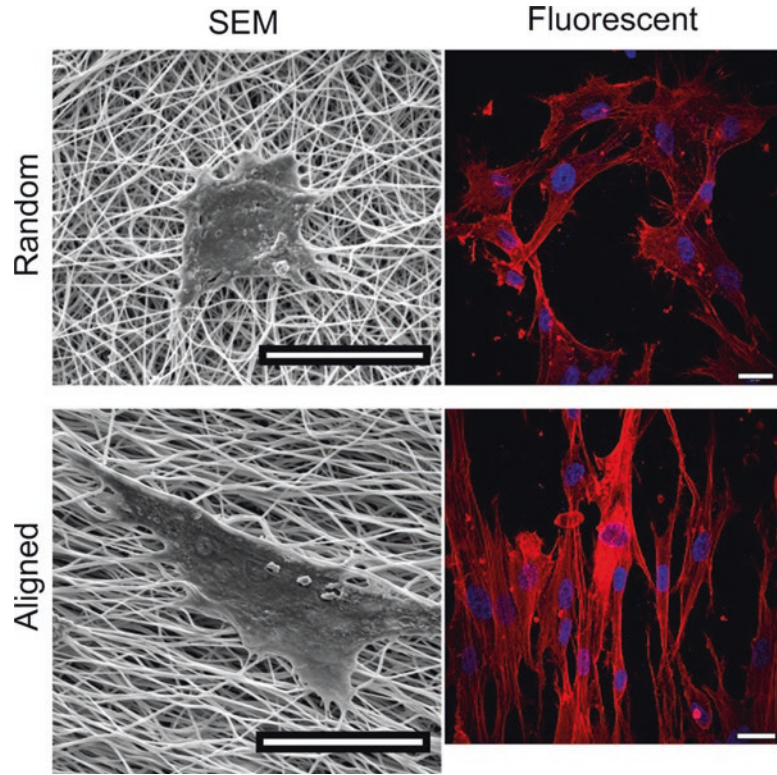
photoresist residue, uneven membrane thickness, and tears along porous channels during membrane detachment from substrate.

One approach to overcoming some of those challenges is described thoroughly by Huh et al [41]. Alternatively, thin microporous membranes (Fig. 6.8) can also be fabricated without PDMS backings during stamping. In our approach, we spun PDMS directly onto the silanized photolithography master, placed a rectangular piece of ordinary transparency film (polyethylene terephthalate or PET) over the micropatterned area, and a glass slide over the PET film, while carefully applying gentle pressure to ensure photoresist posts from the master make contact with the PET film to produce completely through pores in the membrane.

This class of substrates, which offers many benefits including ease of seeding and imaging, has been shown to successfully mimic *in vivo* biomechanical properties, particularly in terms of the Young's modulus, which is an important factor in driving cell fates. It has also been shown to successfully model transport and barrier interface functions in various *in vitro* models, including the alveolar-capillary interface of the human lung with pulmonary epithelial and endothelial cell (EC) layers on either side of a vacuum stretched microporous PDMS scaffold fabricated using soft photolithography.

However, there are also considerable limitations. While this class of scaffolds successfully mimics biomechanical stiffness, the non-uniform

**Fig. 6.9** Random (top) vs. aligned (bottom) electrospun PCL+Gel fibers. SEM (left) and fluorescent images (right) show cellular interactions with the substrate morphology. Scale bars are 20 $\mu$ m. (Adapted and reproduced here with permission from PLoS ONE [30] under Creative Commons Attribution License)



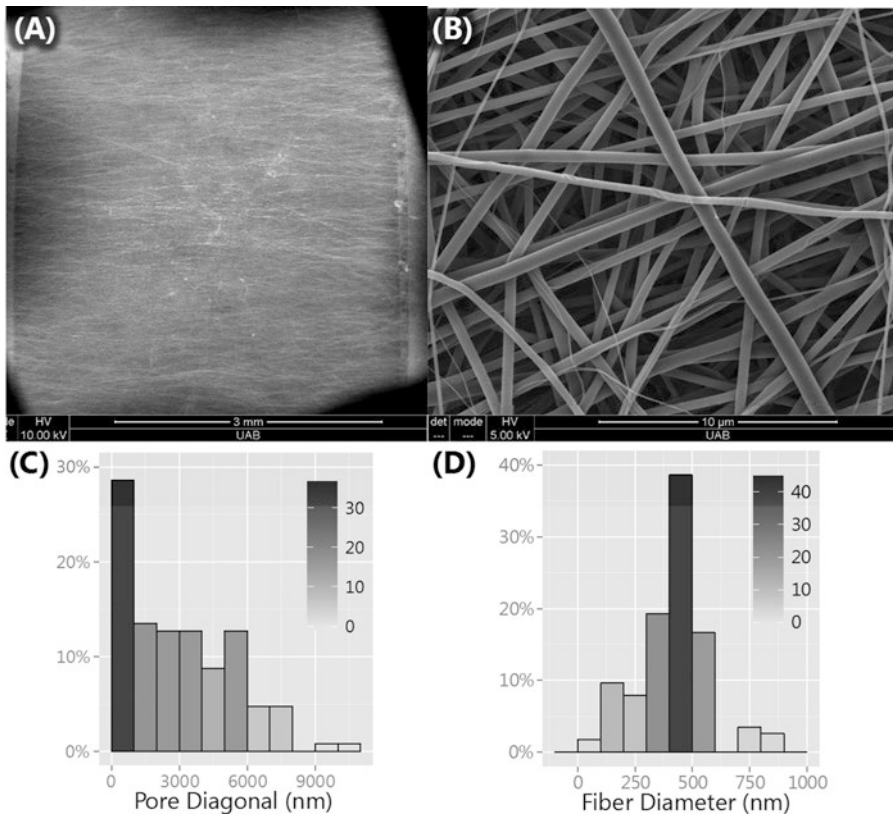
nanofibrous bundle architecture of *in vivo* ECM is entirely absent resulting in characteristically distinct adhesion profiles and morphology of cells. Furthermore, recapitulating three-dimensional tissue architectures, although it has been done, is non-trivial at best. And, since these scaffolds are typically not made of materials naturally occurring *in vivo*, applications other than lab-chip, bioreactors, and similar *in vitro* models, particularly in regenerative medicine, are limited.

### 6.3.3 Electrohydrodynamic Atomization (EHDA)

Electrospinning is an electrohydrodynamic atomization fabrication method which has been widely published since the early 1900s [135] and continues to remain attractive for fabricating a diverse range of nanofibrous scaffolds and substrates, primarily due to its simple and repeatable process that allows for reproducible results and the ease with which the process can be modulated to achieve tunable fiber sizes, fiber orientation,

and porosity, among other characteristics [82, 117]. This versatility enables electrospun nanofibrous membranes to closely mimic *in vivo* ECM for a range of disparate tissue system configurations for tissue engineering [10, 49, 59, 101, 112] applications. Parameters and resulting impact on fibers have been discussed in various research manuscripts [6, 97, 138].

Essentially, electrospinning is the drawing and whipping of a polymer solution into nanofibers by the interplay of gravity, surface tension, electrostatic, and mechanical forces; mechanical forces, applied typically by way of syringe pumps, push polymer solution out of a nozzle while electrostatic forces, in concert with or normal to gravity, counteract surface tension to draw a charged polymer jet toward the grounded collecting plate (or mandrel) positioned across from the syringe needle. Diameter, orientation, density, porosity, and other properties of the resulting fibrous scaffold can be adjusted [13, 20, 47, 103] by varying several parameters. For instance, as shown in Fig. 6.9, collecting electrospun fibers onto a spinning mandrel or disk yields uniaxially



**Fig 6.10** Electrospun nanofibrous scaffold sandwiched between PDMS chambers. (a) SEM of scaffold across full width of channel. (b) SEM showing nanofibrous morphology and interconnected network of pores. (c, d)

Distribution of fiber diameters (median: 425 nm) and poresize (280 nm to 10.7 μm) among larger pores. © IOP Publishing. (Adapted and reproduced with permission. All rights reserved [13])

aligned fibers [30]; while using a stationary grounded plate results in non-woven, randomly oriented fibrous scaffolds (Fig. 6.10).

This is but one example of the ease with which electrospinning parameters and process can be adapted to produce scaffolds with a diverse range of feature sets to target appropriate tissue systems and sites. Electrospinning process parameters and the effects of modulating those on the resulting fibrous scaffolds [21, 56, 57, 92, 95, 109] have been reviewed extensively. By simply adjusting the applied voltage, for instance, diameters of electrospun fibers can be tuned from hundreds of nanometers to a few microns. Similarly, bulk surface area, fiber density, and porosity of scaffolds can be tuned for target adhesion profiles, transport, and microtissue architecture including modulating mechanical properties such

as stiffness. Scaffolds can also be treated with attachment factors by protein adsorption, immobilization, or other surface functionalization treatments. And despite seemingly harsh solvents and processing conditions, living cells have been integrated in the electrospinning process resulting in homogenous distribution of viable cells [134]. Thus, while phase separation and self-assembly have also been used to produce nanofibrous structures, electrospinning is among the fastest growing techniques for fabricating these scaffolds in research due to its relative simplicity, low cost, ease of modification, and applicability with natural fibers, synthetic fibers, and ceramics [2, 8, 108].

Electrospinning also allows for easily tuning chemical composition, fiber-geometry, fiber-orientation and density, and introducing soluble

growth factors or basement membrane proteins making resulting scaffolds particularly suitable for biomimetic applications including regenerative therapy [13, 102, 113, 118]. Various fiber properties, tuned simply by modulating electrospinning process parameters, have been shown to influence cell fates. Aligned nanofibers, for instance, induce cell migration along fiber axis and improve differentiation compared to random nanofibers [34, 65, 100, 127] in MSC and adult stem cells (ASC). Finer fiber diameters, modulated by solution concentration, conductivity, or applied voltage, improve multi-directional proliferation and differentiation, while large diameters lead to cell extension along single fibers [19, 123] in ESC and neural stem cells (NSC). Compositional changes, including protein coatings, induce biochemical cues that affect cell proliferation and promote differentiation [7, 50, 80, 96, 121]. Tuning fiber conductivity, by adding electrically stimulatory nanoparticles, has been used to induce differentiation into a specific lineage [22, 104]. And finally, rough fibers have been shown to be better suited for MSC proliferation [15, 72].

## 6.4 Case Study: Biomimetic Tissue and Disease Modeling MPS

*We are fashioned creatures, but half made up.*  
(Mary Wollstonecraft Shelley. Frankenstein, 1818)

In this section we briefly walk through a case study in engineering biomimetic microtissue and MPS as effective and efficient *in vitro* platforms to facilitate investigation of specific aspects of physiological and pathophysiological conditions and evaluate efficacy of new formulations. As previously alluded, investigators have explored several configurations for MPS including 3D, layered, or multi-well co-cultures [42, 43, 55, 86, 88], bioreactors [64], and microfluidics *organs-on-a-chip* [74, 120, 122]. While organs-on-a-chip are typically single culture systems, these have been connected via fluid flow circuits to simulate interfaces between organs or full-body-lab-on-chip [40] to successfully recapitulate elements of

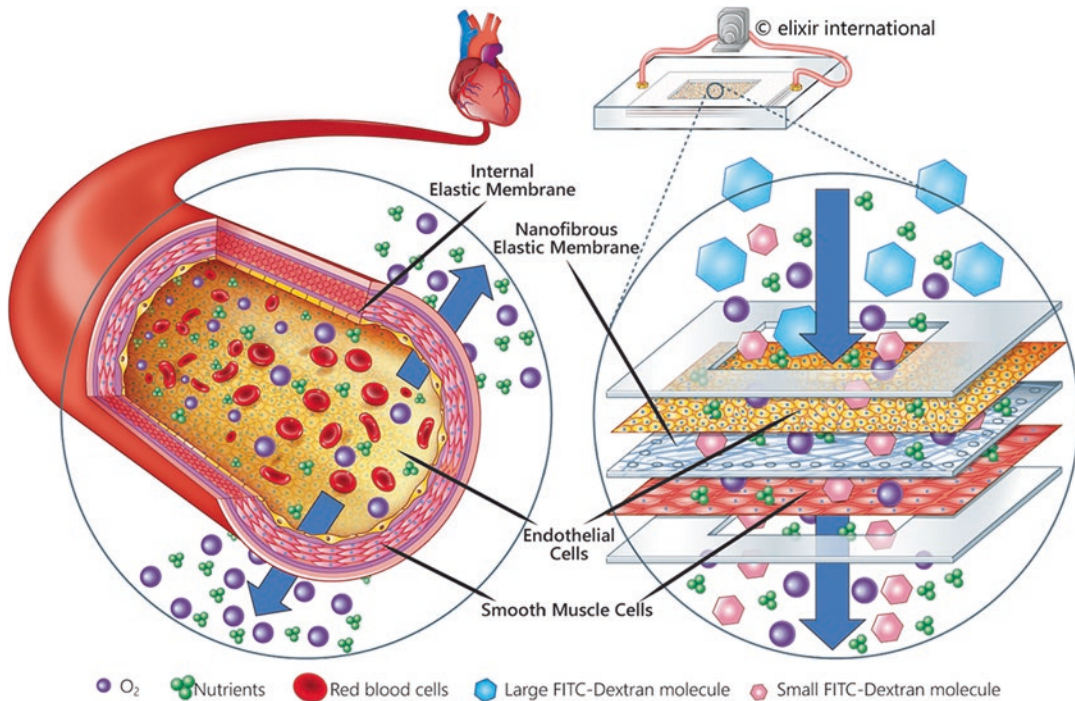
the *in vivo* microenvironment, however, conspicuously absent in most of these are the fundamental pathways for molecular transport: pores.

One way around this limitation is by using photolithography fabricated microporous membranes, which has been shown to form an effective interface between pulmonary epithelial and EC layers in mimicking the alveolar-capillary interface of the human lung [42]. However, while barrier and transport functions were successfully recapitulated, the architecture of the scaffold – highly organized arrangement of uniform size pores – was not representative of *in vivo* ECM. In this case study, we combine electrospun nanofibrous membranes, which better mimic *in vivo* ECM, with lab-on-a-chip microfluidics, which simulate *in vivo* pressure, flow and stretch conditions, to recapitulate the organ-capillary interface in the LOB MPS that regulates transendothelial molecular transport optimized for effective pharmacokinetic evaluation as show in Fig. 6.11.

### 6.4.1 LOB Microtissue Culture Chamber

**PDMS Housings** PDMS cell chamber housings, each comprised of two 1mm thick 60 × 20 mm<sup>2</sup> rectangular pieces for the upper and lower chambers of the housing, were fabricated from 10 g of thoroughly mixed and degassed 15:1 (wt/wt) PDMS (Sylgard 184 Silicone Elastomer Kit. Dow Corning, USA). The mix was poured slowly onto a clean flat glass plate affixed to the base of a petri dish and allowed to cure overnight at 60 °C. Using a stencil, rectangular chambers with a central channel (25×4 mm<sup>2</sup>) were cut out from the cured PDMS. Corners of the resulting chambers were also cut out to improve bonding [41]. Finally, these were sterilized using 70% ethanol, dried, and exposed to UV radiation for further sterilization.

**Nanofibrous Porous Scaffolds** Three sets of materials were used to fabricate the nanofibrous porous thin membranes to form the channel scaffolds in LOB microtissue culture chambers. 10%



**Fig. 6.11** Illustration highlighting anatomical and physiological characteristics of blood vessels and transport regulation vis-à-vis the LOB. Nanofibrous electrospun membrane, mimicking *in vivo* structural and mechanical

properties, integrated with lab-chip platform, simulating *in vivo* flow, pressure, stretch, and shear. © elixir international. (Reproduced with permission. All rights reserved)

(wt%) solutions of Nylon 6 (RTP Company, USA), collagen (freeze-dried soluble calf-skin collagen sponge. Sigma-Aldrich, USA), and collagen+PLLA (PLLA source: Absorbable Polymers, Birmingham, AL, USA) in 1,1,1,3,3,3-hexafluoro-2-propanol (HFP) (Sigma-Aldrich, USA) were prepared and spun directly onto prefabricated PDMS device chambers using a high-voltage power supply (Gamma High Voltage Research, M826, USA), a syringe pump (KD Scientific Apparatus, USA) fitted with a syringe lure locked to a 21½ gauge stainless-steel needle, and an aluminum collector. Edges of the collector were covered with insulation so that only rectangular areas corresponding to the channels in the PDMS chambers were exposed. Collector was rotated every 15 minutes to evenly distribute fibers. Upon completion of electrospinning, PDMS chambers with freshly electrospun nanofibrous scaffolds were moved to a vacuum desiccator to dry overnight. Electrospinning

**Table 6.1** Electrospinning parameters

Parameter	Value
Applied voltage	15 kV
Solution feeding rate	1 mL/h
Total volume	1.5 mL
Collector distance*	20 cm
Collector area	10×20 cm <sup>2</sup>

\*distance measured from needle tip

parameters [66, 114] were used as tuning gauges to obtain desired fiber diameter and poresize. Final values of these parameters, listed in Table 6.1, resulted in  $70 \pm 20 \mu\text{m}$  thick nanofibrous scaffolds with non-beaded  $425 \pm 157 \text{ nm}$  diameter fibers and up to 82% porosity. While fibers aligned along shortest conduction distance over long ranges, short-range fiber alignment was generally random, with a well interconnected network of pores over short and long ranges. Mechanical properties, listed in Table 6.2, showed stiffness for all nanofibrous scaffolds

**Table 6.2** Mechanical properties of electrospun nanofibrous scaffolds

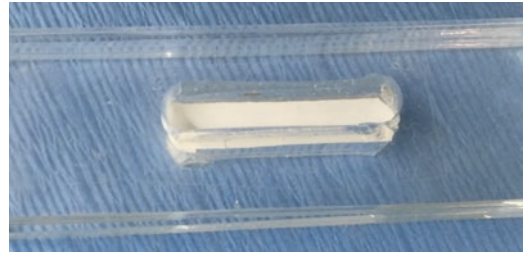
Scaffold Material	Young's Modulus (kPa)				Strength (GPa)			
	Low	High	Mean	sd <sup>a</sup>	Low	High	Mean	sd <sup>a</sup>
Nylon-6	323	471	405.49	56.54	8.58	11.25	9.96	1.22
Collagen+PLLA	427	608	515.36	80.98	2.03	2.29	2.18	0.10

<sup>a</sup>sd standard deviation

consistent with previously reported values for collagen fibers. Nylon-6 membranes offered higher strength and durability. Both the composition and stiffness were found to be compatible with *in vivo* vascular collagen matrix.

**Self-Rivet** Next each PDMS chamber with nanofibrous scaffolding was bonded with an open (no scaffolding) chamber to complete the microtissue co-culture housing so that the nanofibrous electrospun scaffold, mimicking *in vivo* vascular ECM, formed the microporous interface between top and bottom PDMS chambers. Before bonding, all chambers were sterilized with 70% ethanol mist, fully dried, and placed under UV radiation for 120 min. On chambers with electrospun membranes, approximately 500  $\mu\text{m}$  diameter holes were bored along edges and on the corners of the membrane, to expose underlying PDMS for *self-riveting*. Next, the *self-rivet* ready chambers (with membrane side facing up) and counterpart membrane-less chambers, were treated for 45s with 500-700 mTorr O<sub>2</sub> plasma pressure, brought in conformal contact so that channels on both chambers aligned, clamped and cured at 70 °C for 90 minutes to form securely bonded LOB co-culture microtissue housings. Completed housings are shown in Fig. 6.12 and SEM images of sandwiched membranes from these housings are shown in Fig. 6.10.

**Microfluidics** The co-culture microtissue was subsequently clamped in reusable polycarbonate cassettes – with fittings for fluid inlets and outlets for both top and bottom cell chambers – and connected to the LOB microfluidics circuit assembly to simulate *in vivo* biomechanical loading. Note that given the *invertible sandwich* architecture of

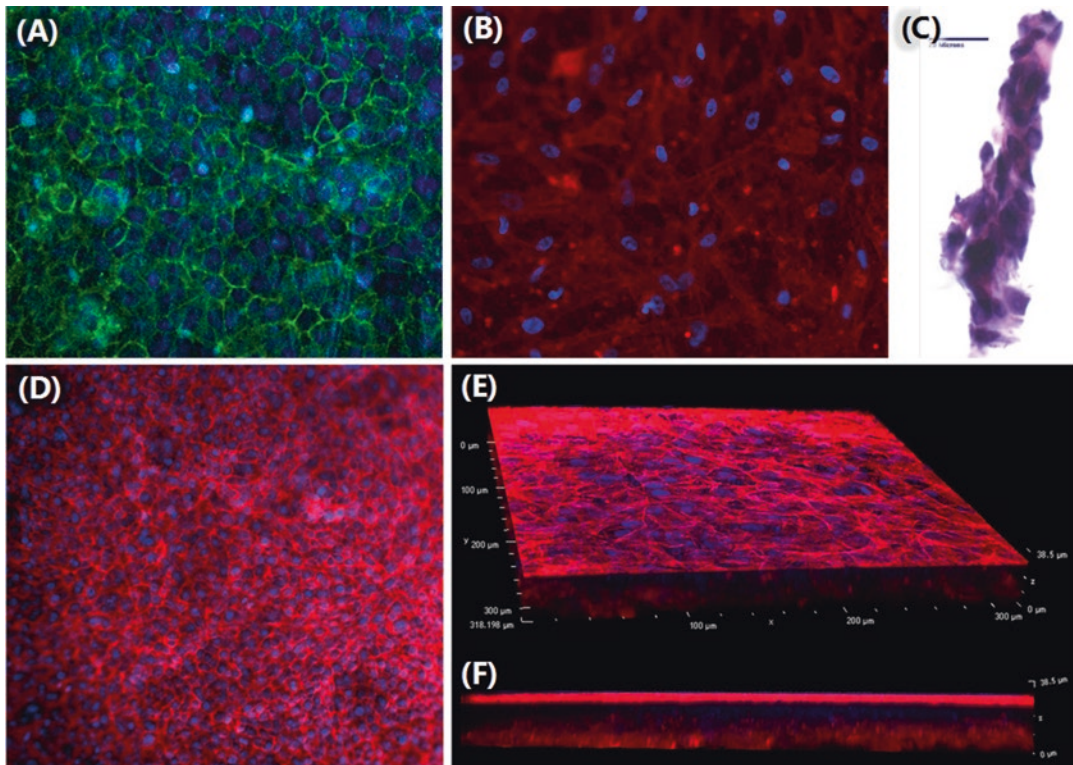


**Fig. 6.12** LOB co-culture microtissue housings with nanofibrous electrospun scaffolding securely bonded between 2 PDMS chambers. © elixir international. (Reproduced with permission. All rights reserved)

housings and cassettes, in which the central electrospun nanofibrous membrane always remains suspended, care must be exercised to ensure that adequate media is available to both top and bottom chambers during static culture and under flow conditions. Fig. 6.13 shows fluorescent, histology, and 3D confocal images obtained from LOB microtissue of SMC and EC blood vessel interface and lung microvasculature interface where alveolar epithelial cells were in an air-liquid interface while the endothelium was maintained under hemodynamic conditions.

#### 6.4.2 Modeling In Vivo Organ-Capillary Interface in the LOB

In order to model transendothelial molecular transport, the LOB was setup as shown in Fig. 6.14a, with the endothelial monolayer side of the membrane in the tissue culture chamber facing up. Other components in the circuit included a pump (Ismatec CP-78017-10), tunable resistance to modulate pressure in the loop, and a one-way valve to prevent reverse flow. The circuit was also fitted with flow (Transonic ME2PXN) and pressure (Validyne Engineering



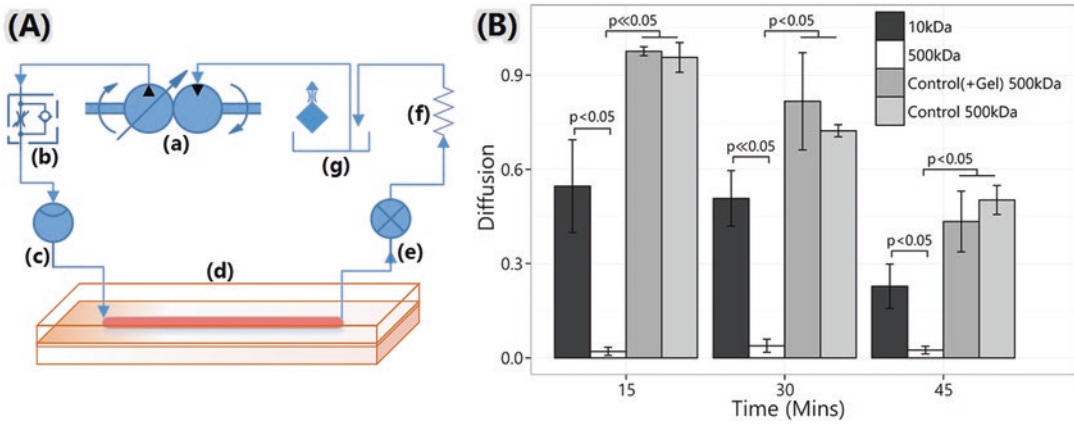
**Fig. 6.13** Recapitulating *in vivo* blood vessel microenvironment. (a) Endothelial monolayer on nanofibrous electrospun scaffold with adherens junction formation seen with staining for  $\beta$ -catenin. (b) Smooth muscle cells oriented along fiber direction with consistent cell-cell contact in x-y plane and across layers similar to *in vivo* vessel architecture. (c) H&E of 3D smooth muscle tissue around nanofiber bundles. © IOP Publishing. (Adapted and reproduced with permission. All rights reserved [13]).

(d) Endothelial monolayer with preferred orientation in direction of fluid flow and actin filaments predominantly oriented towards cell periphery. (e, f) 3D confocal images of lung microvasculature across nanofibrous electrospun scaffold where alveolar epithelial cells (top) were in an air-liquid interface while the endothelium, on the other side of the scaffold, was under hemodynamic conditions. © elixir international. (Reproduced with permission. All rights reserved)

P55D) sensors wired into a computer running a LabVIEW® monitoring program to record pressure and flow waveforms. The tissue was conditioned for flow and pressure for 60 minutes, after which, it was subjected to target *in vivo* hemodynamic loading conditions with flow rate and pressure maintained at  $3 \pm 1$  mL/min and  $80 \pm 5$  mm Hg, respectively. Microtissue was kept under hemodynamic conditions for between 24 and 48 hours based on experimental objectives.

The barrier function of the interface was assessed and monitored under hemodynamic load conditions using an independent flow sensor connected to the bottom chamber, or collector, to ensure no flow was recorded in that chamber. In addition, a FITC-Dextran permeability assay was

used to assess both the barrier and interface functions. Dextran is a polysaccharide with molecular mass ranging from 3 to 2000 kDa [27, 38, 73]. Transport and barrier functions were tested using 10 kDa (LifeTechnologies, USA. D1821) and 500 kDa (LifeTechnologies, USA. D7136) respectively. As shown in Fig. 6.14B, smaller molecules, representing nutrients and drug formulations, diffused across the interface while larger molecules were prevented from breaching the barrier. Thus, the morphology and phenotype of cells (Fig. 6.13) and the transport and barrier function of the resulting organ-capillary interface (Fig. 6.14), were successfully recapitulated in the LOB using electrospun nanofibrous scaffolds integrated in a microfluidics circuit.



**Fig. 6.14** LOB organ-capillary interface transendothelial molecular transport assay. (a) Setup integrating tissue co-culture chamber [d], with electrospun nanofibrous porous membrane sandwiched between two PDMS housings, in microfluidic circuit with a pump [a], one-way valve [b], flow [c] and pressure [e] sensors, resistance [f] to tune pressure, and perfusion media [g]. (b) Results from FITC-

Dextran permeability tests confirming transport and barrier functions with small FITC-dextran molecules (10 kDa) diffusing across the interface while larger molecules (500 kDa) prevented from flowing across. © IOP Publishing. (Adapted and reproduced with permission. All rights reserved [13])

### 6.4.3 Tumor-Train: Modeling Tumor Progression in the LOB

The modular LOB platform can be easily tailored and scaled from the simplest – single microtissue chamber – to several chambers connected in series, parallel, or any combination thereof for mimicking a range of physiological or pathophysiological conditions. As shown in Fig. 6.15a, a multiunit LOB with two co-culture microtissue chambers (c1 and c2) connected in series, dubbed *tumor-train*, was used to model pancreatic tumor microenvironment and progression.

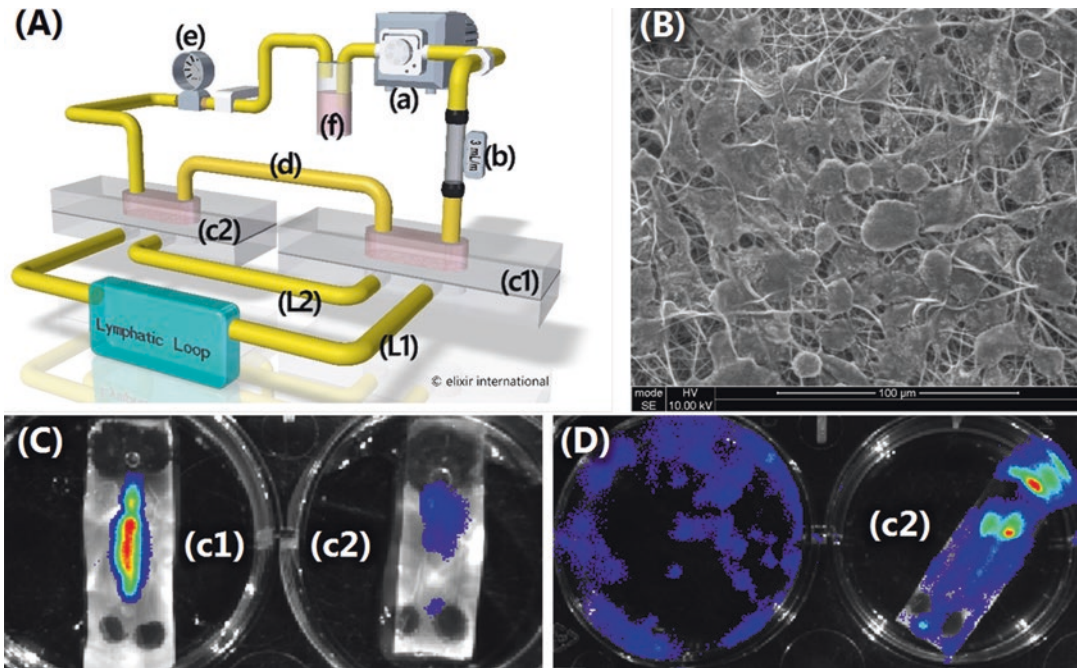
The flexibility to model and connect multiple tissue/organ systems in highly modular Lego®-like configurations is particularly useful for modeling diseases involving multiple organ systems – such as cancers – and for predicting toxicity and therapeutic efficacy of candidate drugs. This level of modular configurational control is simply not possible in static cell culture or animal models. In addition, *tumor-train* offers the distinct advantage of being a humanized system, i.e. containing human cellular components; making it, not merely configurable but, configurable in a human tissue context to specific diseases, pathways, and other variables under

investigation. Figure 6.15 highlights this feature where after 72-hours of conditioning, luciferase-tagged tumor cells were observed to invade non-tumorous “healthy” microtissue (c2) from “tumorous” microtissue (c1). Moreover, invasive cells from the *tumor-train* also showed a more aggressive proliferation profile compared to that of the non-invasive cancer cells that remained at the “primary tumor” site (c1).

## 6.5 Future Perspectives

A Tufts/Duke University study [24, 25] assigns more than 30% of the cost of approved drugs to pre-human costs; about \$1.5 billion of \$3.9 billion. While firms categorize costs differently, a Boston University [33] study estimates that pharmaceutical companies spend \$34.4 billion annually on preclinical research. Compound this with the finding that 90% of drugs effective in pre-human studies fail in human trials [68, 94]. While the LOB may not altogether replace animals, it could substantially reduce the number used in preclinical evaluation. Further, its ability to isolate, control, and recapitulate specific physiological and pathophysiological conditions within a





**Fig. 6.15** *Tumor-Train* tumor microenvironment and disease progression model. (a) Setup integrating two tissue co-culture chambers, with S2VP10-Luc “tumorous” tissue in [c1] and “healthy” tissue downstream in [c2] connected in series [d]. A semi-independent lymphatic loop [L1, L2] was also integrated in the microfluidic circuit while the remaining components, including the pump [a], one-way valve [not shown], flow [b] and pressure [e] sensors, resistance [not shown], and perfusion media [f], mirrored those from Figure 6.14. (b) Environmental SEM of

tumorous  $\mu$ Tissue with cancer cells growing many layers deep into nanofibrous matrix. (c) Luciferase tagged cancer cells migrated ~18cm from primary tumorous  $\mu$ tissue [c1] downstream and attached to healthy  $\mu$ tissue [c2] downstream and attached to healthy  $\mu$ tissue of untagged fibroblasts [c2]. (d) Microtissue from [c2] was placed in static culture for 48 hours and then moved to a fresh well for imaging. Relatively aggressive proliferation profile was observed in cells that invaded healthy microtissue. © elixir international. (Reproduced with permission. All rights reserved)

humanized tissue microenvironment coupled with the capacity to connect multiple LOB micro-tissue units in series and/or parallel to model various organ systems such as kidney, lung (including liquid/air interface), and liver, allows for pharmacokinetic and pharmacodynamic analysis under highly configurable parameters which is simply not possible in animal models. A nominal decrease in preclinical costs of merely 2%, from LOB adoption, translates into estimated savings of **\$688 million annually** to the pharmaceutical industry. Such savings would increase capacity to investigate more compounds thereby expediting the pace at which new treatments are discovered and delivered to patients. Similarly, from a regenerative medicine perspective, advances in nanotechnology particularly within

the context of nanomedicine will help address the already large and steadily widening toll imposed by conditions such as cardiovascular diseases and cancer. We see the potential from advances in stem cell and nanotechnology domains being realized both at the intracellular – sub 100 nm – and extracellular size scales – sub 750 nm – over the next five to fifteen years. Further, it is our opinion that this exploration will continue to transcend traditionally isolated disciplines in developing better substrates and tissue systems, designing and scaling more effective models for identifying, evaluating and delivering therapeutic agents, and deriving and administering patient specific – personalized or precision medicine – treatments; thereby enhancing both the quantity and quality of lives of people around the world.

**Acknowledgements** In addition to elixir international® and the National Science Foundation (NSF EPS 1158862, DMR 1460392 REU), for their generous support, we thank P. Sethu, M.N. Saleh, S. Pillay, C.A. Monroe, U.K. Vaidya, M.L. Weaver, HW. Jun, G. Walcott, H. Budhwani, J.R. Richter, K.F. Goliwas, A. Gangrade, A.T. Wood, H. Zhang, and J. Rogers for their insight and expertise. We would also like to acknowledge UAB Comprehensive Cancer Center (CCC), UAB Scanning Electron Microscope Lab, and Research Machine Shop for use of facilities and equipment.

## Abbreviations

ASC	Adult stem cells
AACR	American Association for Cancer Research
CVD	Cardiovascular diseases
EC	Endothelial cells
ECM	Extracellular matrix (or matrices)
EHDA	Electrohydrodynamic atomization
ESC	Embryonic stem cells
FDA	Food and Drug Administration
FITC	Fluorescein isothiocyanate
HTS	High-throughput screening
HMSC	Human mesenchymal stem cells
iPSC	Induced pluripotent stem cells
LOB	Lab-on-a-brane
MSC	Mesenchymal stem cells
nHA	Nanohydroxyapatite
NIH	National Institutes of Health
NSC	Neural stem cells
NSF	National Science Foundation
NSPC	Neural stem/progenitor cells
pAA	Polyacrylamide
PCL	Poly( $\epsilon$ -caprolactone)
PDMS	Polydimethyl siloxane
PET	Polyethylene terephthalate
PG	Proteoglycans
PLGA	Poly(lactide-co-glycolide)
SC	Stem cells
SEM	Scanning electron microscopy
SMC	Smooth muscle cells
UV	Ultraviolet

## References

- Abbasi N, Hashemi SM, Salehi M, Jahani H, Mowla SJ, Soleimani M, Hosseinkhani H (2015) Influence of oriented nanofibrous PCL scaffolds on quantitative gene expression during neural differentiation of mouse embryonic stem cells. *J Biomed Mater Res A* 104(1):155–164. <https://doi.org/10.1002/jbm.a.35551>

- Agarwal S, Greiner A, Wendorff JH (2013) Functional materials by electrospinning of polymers. *Prog Polym Sci* 38(6):963–991. <https://doi.org/10.1016/j.progpolymsci.2013.02.001>
- Akhmanova M, Osidak E, Domogatsky S, Rodin S, Domogatskaya A (2015) Physical, spatial, and molecular aspects of extracellular matrix of in vivo niches and artificial scaffolds relevant to stem cells research. *Stem Cells Int*. <https://doi.org/10.1155/2015/167025>
- Ashammakhi N, Ndreu A, Piras A, Nikkola L, Sindelar T, Ylikauppila H et al (2006) Biodegradable nanomats produced by electrospinning: expanding multifunctionality and potential for tissue engineering. *J Nanosci Nanotechnol* 6(9):2693–2711. <https://doi.org/10.1166/jnn.2006.485>
- Badylak SF, Freytes DO, Gilbert TW (2015) Extracellular matrix as a biological scaffold material: structure and function. *Acta Biomater* 23(S):S17–S26. <https://doi.org/10.1016/j.actbio.2015.07.016>
- Bean AC, Tuan RS (2015) Fiber diameter and seeding density influence chondrogenic differentiation of mesenchymal stem cells seeded on electrospun poly( $\epsilon$ -caprolactone) scaffolds. *Biomed Mater* 10(1):15018. <https://doi.org/10.1088/1748-6041/10/1/015018>
- Bhaaerathy V, Venugopal J, Gandhimathi C, Ponpandian N, Mangalaraj D, Ramakrishna S (2014) Biologically improved nanofibrous scaffolds for cardiac tissue engineering. *Mater Sci Eng C Mater Biol Appl* 44:268–277. <https://doi.org/10.1016/j.msec.2014.08.018>
- Bhardwaj N, Kundu SC (2010) Electrospinning: a fascinating fiber fabrication technique. *Biotechnol Adv* 28:325–347. <https://doi.org/10.1016/j.biotechadv.2010.01.004>
- Bhatia SN, Ingber DE (2014) Microfluidic organs-on-chips. *Nat Biotechnol* 32(8):760–772. <https://doi.org/10.1038/nbt.2989>
- Biazar E, Keshel SH, Sahebzamani A, Hamidi M, Ebrahimi M (2014) The healing effect of unrestricted somatic stem cells loaded in nanofibrous poly hydroxybutyrate-co-hydroxyvalerate scaffold on full-thickness skin defects. *J Biomater Tissue Eng* 4(1):20–27. <https://doi.org/10.1166/jbt.2014.1137>
- Bild AH, Yao G, Chang JT, Wang Q, Potti A, Chasse D et al (2006) Oncogenic pathway signatures in human cancers as a guide to targeted therapies. *Nature* 439(7074):353–357. <https://doi.org/10.1038/nature04296>
- Bleicher KH, Böhm H, Müller K, Alanine AI (2003) A guide to drug discovery: Hit and lead generation: beyond high-throughput screening. *Nat Rev Drug Discov* 2(5):369. <https://doi.org/10.1038/nrd1086>
- Budhwani KI, Thomas V, Sethu P (2016) Lab-on-a-brane: nanofibrous polymer membranes to recreate organ–capillary interfaces.

- J Micromech Microeng 26(3):35013. <https://doi.org/10.1088/0960-1317/26/3/035013>
14. Cardwell RD, Kluge JA, Thayer PS, Guelcher SA, Dahlgren LA, Kaplan DL, Goldstein AS (2015) Static and cyclic mechanical loading of mesenchymal stem cells on elastomeric, electrospun polyurethane meshes. *J Biomech Eng* 137(7). <https://doi.org/10.1115/1.4030404>
  15. Chan CW, Hussain I, Waugh DG, Lawrence J, Man HC (2014) Effect of laser treatment on the attachment and viability of mesenchymal stem cell responses on shape memory NiTi alloy. *Mater Sci Eng C Mater Biol Appl* 42:254–263. <https://doi.org/10.1016/j.msec.2014.05.022>
  16. Chang JC, Fujita S, Tonami H, Kato K, Iwata H, Hsu SH (2013) Cell orientation and regulation of cell-cell communication in human mesenchymal stem cells on different patterns of electrospun fibers. *Biomed Mater* 8(5):55002. <https://doi.org/10.1088/1748-6041/8/5/055002>
  17. Chen G, Dong C, Yang L, Lv Y (2015) 3D Scaffolds with Different Stiffness but the Same Microstructure for Bone Tissue Engineering. *ACS Appl Mater Interfaces* 7(29):15790–15802. <https://doi.org/10.1021/acsami.5b02662>
  18. Chowdhury S, Thomas V, Dean D, Catledge SA, Vohra YK (2005) Nanoindentation on porous bio-ceramic scaffolds for bone tissue engineering. *J Nanosci Nanotechnol* 5(11):1816–1820
  19. Christopherson GT, Song H, Mao HQ (2009) The influence of fiber diameter of electrospun substrates on neural stem cell differentiation and proliferation. *Biomaterials* 30(4):556–564. <https://doi.org/10.1016/j.biomaterials.2008.10.004>
  20. Chuangchote S, Supaphol P (2006) Fabrication of aligned poly(vinyl alcohol) nanofibers by electrospinning. *J Nanosci Nanotechnol* 6(1):125–129(5). <https://doi.org/10.1166/jnm.2006.043>
  21. Cramariuc B, Cramariuc R, Scarlet R, Manea LR, Lupu IG, Cramariuc O (2013) Fiber diameter in electrospinning process. *J Electrostat* 71(3):189–198. <https://doi.org/10.1016/j.elstat.2012.12.018>
  22. Crowder SW, Liang Y, Rath R, Park AM, Maltais S, Pintauro PN et al (2013) Poly(epsilon-caprolactone)-carbon nanotube composite scaffolds for enhanced cardiac differentiation of human mesenchymal stem cells. *Nanomedicine (London)* 8(11):1763–1776. <https://doi.org/10.2217/nmm.12.204>
  23. Danhier F, Feron O, Préat V (2010) To exploit the tumor microenvironment: Passive and active tumor targeting of nanocarriers for anti-cancer drug delivery. *J Control Release* 148(2):135–146. <https://doi.org/10.1016/j.jconrel.2010.08.027>
  24. DiMasi JA, Hansen RW, Grabowski HG (2003) The price of innovation: new estimates of drug development costs. *J Health Econ* 22(2):151–185. [https://doi.org/10.1016/S0167-6296\(02\)00126-1](https://doi.org/10.1016/S0167-6296(02)00126-1)
  25. DiMasi JA, Hansen RW, Grabowski HG, Lasagna L (1991) Cost of innovation in the pharmaceutical industry. *J Health Econ* 10(2):107–142. [https://doi.org/10.1016/0167-6296\(91\)90001-4](https://doi.org/10.1016/0167-6296(91)90001-4)
  26. Drews J (2000) Drug discovery: a historical perspective. *Science* 287(5460):1960–1964. <https://doi.org/10.1126/science.287.5460.1960>
  27. Egawa G, Nakamizo S, Natsuaki Y, Doi H, Miyachi Y, Kabashima K (2013) Intravital analysis of vascular permeability in mice using two-photon microscopy. *Sci Rep* 3:1932. <https://doi.org/10.1038/srep01932>
  28. Engler AJ, Griffin MA, Sen S, Bonnemann CG, Sweeney HL, Discher DE (2004) Myotubes differentiate optimally on substrates with tissue-like stiffness: pathological implications for soft or stiff microenvironments. *J Cell Biol* 166(6):877–887. <https://doi.org/10.1083/jcb.200405004>
  29. Engler AJ, Sen S, Sweeney HL, Discher DE (2006) Matrix elasticity directs stem cell lineage specification. *Cell* 126(4):677–689. <https://doi.org/10.1016/j.cell.2006.06.044>
  30. Fee T, Surianarayanan S, Downs C, Zhou Y, Berry J (2016) Nanofiber alignment regulates NIH3T3 cell orientation and cytoskeletal gene expression on electrospun PCL+gelatin nanofibers. *PLoS ONE* 11(5):1–12. <https://doi.org/10.1371/journal.pone.0154806>
  31. Feynman RP (1960) There's plenty of room at the bottom. *Eng Sci* 23(5):22–36. Retrieved from <http://www.zyvex.com/nanotech/feynman.html>
  32. Frantz C, Stewart KM, Weaver VM (2010) The extracellular matrix at a glance. *J Cell Sci* 123:4195–4200. <https://doi.org/10.1242/jcs>
  33. Freedman LP, Cockburn IM, Simcoe TS (2015) The economics of reproducibility in preclinical research. *PLoS Biol* 13(6):1–9. <https://doi.org/10.1371/journal.pbio.1002165>
  34. Fujita S, Shimizu H, Suye S (2012) Control of differentiation of human mesenchymal stem cells by altering the geometry of nanofibers. *J Nanotechnol* 2012:1–9. <https://doi.org/10.1155/2012/429890>
  35. Fukumura D, Jain RK (2007) Tumor microenvironment abnormalities: causes, consequences, and strategies to normalize. *J Cell Biochem* 101(4):937–949. <https://doi.org/10.1002/jcb.21187>
  36. Gaulton A, Bellis LJ, Bento AP, Chambers J, Davies M, Hersey A et al (2012) ChEMBL: a large-scale bioactivity database for drug discovery. *Nucleic Acids Res* 40(D1):1100–1107. <https://doi.org/10.1093/nar/gkr777>
  37. Hanahan D, Coussens LM (2012) Accessories to the crime: functions of cells recruited to the tumor microenvironment. *Cancer Cell* 21(3):309–322. <https://doi.org/10.1016/j.ccr.2012.02.022>
  38. Hoffmann A, Bredno J, Wendland M, Derugin N, Ohara P, Wintermark M (2011) High and low molecular weight fluorescein isothiocyanate (fitc)-dextrans to assess blood-brain barrier disruption: technical considerations. *Transl Stroke Res* 2(1):106–111. <https://doi.org/10.1007/s12975-010-0049-x>

39. Hoyert DL (2012) 75 years of mortality in the United States, 1935–2010. NCHS Data Brief 88(88):1–8. Retrieved from <http://www.ncbi.nlm.nih.gov/pubmed/22617094>
40. Huh D, Hamilton GA, Ingber DE (2011) From 3D cell culture to organs-on-chips. *Trends Cell Biol* 21(12):745–754. <https://doi.org/10.1016/j.tcb.2011.09.005>
41. Huh D, Kim HJ, Fraser JP, Shea DE, Khan M, Bahinski A et al (2013) Microfabrication of human organs-on-chips. *Nat Protoc* 8(11):2135–2157. <https://doi.org/10.1038/nprot.2013.137>
42. Huh D, Leslie DC, Matthews BD, Fraser JP, Jurek S, Hamilton GA et al (2012a) A human disease model of drug toxicity-induced pulmonary edema in a lung-on-a-chip microdevice. *Sci Transl Med* 4(159):159ra147. <https://doi.org/10.1126/scitranslmed.3004249>
43. Huh D, Torisawa YS, Hamilton GA, Kim HJ, Ingber DE (2012b) Microengineered physiological biomimicry: organs-on-chips. *Lab Chip* 12(12):2156–2164. <https://doi.org/10.1039/c2lc40089h>
44. Iop L, Bonetti A, Naso F, Rizzo S, Cagnin S, Bianco R et al (2014) Decellularized allogeneic heart valves demonstrate self-regeneration potential after a long-term preclinical evaluation. *PLoS ONE* 9(6). <https://doi.org/10.1371/journal.pone.0099593>
45. Jahani J, Kaviani S, Hassannpour-Ezatti M, Soleimani M, Kaviani Z, Zonoubi Z (2011) The effect of aligned and random electrospun fibrous scaffolds on rat mesenchymal stem cell proliferation. *Cell J* 14(1):31–38
46. Jeffords ME, Wu J, Shah M, Hong Y, Zhang G (2015) Tailoring material properties of cardiac matrix hydrogels to induce endothelial differentiation of human mesenchymal stem cells. *ACS Appl Mater Interfaces* 7(20):11053–11061. <https://doi.org/10.1021/acsami.5b03195>
47. Jose MV, Steinert BW, Thomas V, Dean DR, Abdalla M a, Price G, Janowski GM (2007) Morphology and mechanical properties of Nylon 6/MWNT nanofibers. *Polymer* 48(4):1096–1104. <https://doi.org/10.1016/j.polymer.2006.12.023>
48. Joyce JA (2005) Therapeutic targeting of the tumor microenvironment. *Cancer Cell* 7(6):513–520. <https://doi.org/10.1016/j.ccr.2005.05.024>
49. Junka R, Valmikinathan CM, Kalyon DM, Yu X (2013) Laminin functionalized biomimetic nanofibers for nerve tissue engineering. *J Biomater Tissue Eng* 3(4):494–502. <https://doi.org/10.1166/jbt.2013.1110>
50. Kai D, Prabhakaran MP, Stahl B, Eblenkamp M, Wintermantel E, Ramakrishna S (2012) Mechanical properties and in vitro behavior of nanofiber-hydrogel composites for tissue engineering applications. *Nanotechnology* 23(9):95705. <https://doi.org/10.1088/0957-4484/23/9/095705>
51. Kamb A (2005) What's wrong with our cancer models? *Nat Rev Drug Des Discov* 4(2):161–165. <https://doi.org/10.1038/nrd1635>
52. Kelland LR (2004) “Of mice and men”: values and liabilities of the athymic nude mouse model in anti-cancer drug development. *Eur J Cancer* 40(6):827–836. <https://doi.org/10.1016/j.ejca.2003.11.028>
53. Kessenbrock K, Plaks V, Werb Z (2010) Matrix metalloproteinases: regulators of the tumor microenvironment. *Cell* 141(1):52–67. <https://doi.org/10.1016/j.cell.2010.03.015>
54. Khan M, Xu Y, Hua S, Johnson J, Belevych A, Janssen PML et al (2015) Evaluation of changes in morphology and function of human induced pluripotent stem cell derived cardiomyocytes (hiPSC-CMs) cultured on an aligned-nanofiber cardiac patch. *PLoS ONE* 10(5):e0126338. <https://doi.org/10.1371/journal.pone.0126338>
55. Khetani SR, Bhatia SN (2008) Microscale culture of human liver cells for drug development. *Nat Biotechnol* 26(1):120–126. <https://doi.org/10.1038/nbt1361>
56. Khorshidi S, Solouk A, Mirzadeh H, Mazinani S, Lagaron JM, Sharifi S, Ramakrishna S (2015) A review of key challenges of electrospun scaffolds for tissue-engineering applications. *J Tissue Eng Regen Med*. <https://doi.org/10.1002/term.1978>
57. Kim CH, Jung YH, Kim HY, Lee DR (2006) Effect of collector temperature on the porous structure of electrospun fibers. *Macromol Res* 14(1):59–65
58. Ko Y-M, Choi D-Y, Jung S-C, Kim B-H (2015) Characteristics of plasma treated electrospun polycaprolactone (PCL) nanofiber scaffold for bone tissue engineering. *J Nanosci Nanotechnol* 15(1):192–195. <https://doi.org/10.1166/jnn.2015.8372>
59. Kocbek P, Pelipenko JAN, Kristl J, Rošić R, Kocbek P, Pelipenko JAN et al (2013) Nanofibers and their biomedical use. *Acta Pharmaceutica (Zagreb, Croatia)* 63(3):295–304. <https://doi.org/10.2478/acph-2013-0024>
60. Kolb HC, Sharpless KB (2003) The growing impact of click chemistry on drug discovery. *Drug Discov Today* 8(24):1128–1137. [https://doi.org/10.1016/S1359-6446\(03\)02933-7](https://doi.org/10.1016/S1359-6446(03)02933-7)
61. Kubinyi H (2003) Drug research: myths, hype and reality. *Nat Rev Drug Discov* 2(8):665–668. <https://doi.org/10.1038/nrd1156>
62. Lee J, Abdeen AA, Huang TH, Kilian KA (2014) Controlling cell geometry on substrates of variable stiffness can tune the degree of osteogenesis in human mesenchymal stem cells. *J Mech Behav Biomed Mater* 38:209–218. <https://doi.org/10.1016/j.jmbbm.2014.01.009>
63. Leipzig ND, Shoichet MS (2009) The effect of substrate stiffness on adult neural stem cell behavior. *Biomaterials* 30(36):6867–6878. <https://doi.org/10.1016/j.biomaterials.2009.09.002>
64. Leite SB, Teixeira AP, Miranda JP, Tostões RM, Clemente JJ, Sousa MF et al (2011) Merging bio-reactor technology with 3D hepatocyte-fibroblast culturing approaches: Improved in vitro models for toxicological applications. *Toxicol In*

- Vitro 25(4):825–832. <https://doi.org/10.1016/j.tiv.2011.02.002>
65. Leung M, Cooper A, Jana S, Tsao CT, Petrie TA, Zhang M (2013) Nanofiber-based in vitro system for high myogenic differentiation of human embryonic stem cells. *Biomacromolecules* 14(12):4207–4216. <https://doi.org/10.1021/bm4009843>
  66. Li W, Laurencin CT, Caterson EJ, Tuan RS, Ko FK (2001) Electrospun nanofibrous structure: a novel scaffold for tissue engineering. *J Biomed Mater Res* 60(4):614–621. Retrieved from [http://so.med.wanfangdata.com.cn/ViewHTML/PeriodicalPaper\\_JJ0210742604.aspx](http://so.med.wanfangdata.com.cn/ViewHTML/PeriodicalPaper_JJ0210742604.aspx)
  67. Lim SH, Mao HQ (2009) Electrospun scaffolds for stem cell engineering. *Adv Drug Deliv Rev* 61(12):1084–1096. <https://doi.org/10.1016/j.addr.2009.07.011>
  68. Lindsley CW (2014) New statistics on the cost of new drug development and the trouble with CNS drugs. *ACS Chem Neurosci* 5(12):1142
  69. Lipinski CA, Lombardo F, Dominy BW, Feeney PJ (2012) Experimental and computational approaches to estimate solubility and permeability in drug discovery and development settings. *Adv Drug Deliv Rev* 64(SUPPL):4–17. <https://doi.org/10.1016/j.addr.2012.09.019>
  70. Liu C, Zhu C, Li J, Zhou P, Chen M, Yang H, Li B (2015) The effect of the fibre orientation of electrospun scaffolds on the matrix production of rabbit annulus fibrosus-derived stem cells. *Bone Res* 3:15012. <https://doi.org/10.1038/boneres.2015.12>
  71. Lorusso G, Rüegg C (2008) The tumor microenvironment and its contribution to tumor evolution toward metastasis. *Histochem Cell Biol* 130(6):1091–1103. <https://doi.org/10.1007/s00418-008-0530-8>
  72. Lotkov AI, Psakh'e SG, Meisner LL, Matveeva VA, Artem'eva LV, Meisner SN, Matveev AL (2012) The effect of chemical composition and roughness of titanium nickelide surface on proliferative properties of mesenchymal stem cells. *Inorg Mater Appl Res* 3(2):135–144. <https://doi.org/10.1134/S2075113312020116>
  73. Ma C, Wang X-F (2008). In vitro assays for the extracellular matrix protein-regulated extravasation process. *CSH Protocols*, 2008, pdb.prot5034. <https://doi.org/10.1101/pdb.prot5034>
  74. Ma H, Liu T, Qin J, Lin B (2010) Characterization of the interaction between fibroblasts and tumor cells on a microfluidic co-culture device. *Electrophoresis* 31(10):1599–1605. <https://doi.org/10.1002/elps.200900776>
  75. Ma J, He X, Jabbari E (2011) Osteogenic differentiation of marrow stromal cells on random and aligned electrospun poly(L-lactide) nanofibers. *Ann Biomed Eng* 39(1):14–25. <https://doi.org/10.1007/s10439-010-0106-3>
  76. Ma X-J, Dahiya S, Richardson E, Erlander M, Sgroi DC (2009) Gene expression profiling of the tumor microenvironment during breast cancer progression. *Breast Cancer Res: BCR* 11(1):R7. <https://doi.org/10.1186/bcr2222>
  77. Macarron R, Banks MN, Bojanic D, Burns DJ, Cirovic DA, Garyantes T et al (2011) Impact of high-throughput screening in biomedical research. *Nat Rev Drug Discov* 10(3):188–195. <https://doi.org/10.1038/nrd3368>
  78. Macrí-Pellizzeri L, Pelacho B, Sancho A, Iglesias-García O, Simón-Yarza AM, Soriano-Navarro M et al (2015) Substrate stiffness and composition specifically direct differentiation of induced pluripotent stem cells. *Tissue Eng A* 21(9–10):1633–1641. <https://doi.org/10.1089/ten.TEA.2014.0251>
  79. Mahairaki V, Lim SH, Christopherson GT, Xu L, Nasonkin I, Yu C et al (2011) Nanofiber matrices promote the neuronal differentiation of human embryonic stem cell-derived neural precursors in vitro. *Tissue Eng Part A* 17(5–6):855–863. <https://doi.org/10.1089/ten.TEA.2010.0377>
  80. Maldonado M, Wong LY, Echeverria C, Ico G, Low K, Fujimoto T et al (2015) The effects of electrospun substrate-mediated cell colony morphology on the self-renewal of human induced pluripotent stem cells. *Biomaterials* 50:10–19. <https://doi.org/10.1016/j.biomaterials.2015.01.037>
  81. Mecham RP (ed) (2011) *The extracellular matrix – an overview*. Springer, St. Louis
  82. Miao J, Miyauchi M, Simmons TJ, Dordick JS, Linhardt RJ (2010) Electrospinning of nanomaterials and applications in electronic components and devices. *J Nanosci Nanotechnol* 10(9):5507–5519. <https://doi.org/10.1166/jnn.2010.3073>
  83. National Institutes of Health (n.d.) Nanomedicine. Retrieved January 1, 2015, from <https://commonfund.nih.gov/nanomedicine/overview>
  84. National Nanotechnology Initiative (n.d.) Nanotechnology timeline. Retrieved January 1, 2015, from <http://www.nano.gov/timeline>
  85. Nezarati RM, Eifert MB, Dempsey DK, Cosgriff-Hernandez E (2015) Electrospun vascular grafts with improved compliance matching to native vessels. *J Biomed Mater Res B Appl Biomater* 103(2):313–323. <https://doi.org/10.1002/jbm.b.33201>
  86. Nishikawa M, Kojima N, Yamamoto T, Fujii T, Sakai Y (2008) An advanced in vitro liver tissue model by combination of on-site oxygenation and double-layer coculture with fibroblasts. *AATEX* 14(Special Issue):659–663
  87. Pantoliano MW, Petrella EC, Kwasnoski JD, Lobanov VS, Myslik J, Graf E et al (2001) High-density miniaturized thermal shift assays as a general strategy for drug discovery. *J Biomol Screen Off J Soc Biomol Screen* 6(6):429–440. <https://doi.org/10.1177/108705710100600609>
  88. Park JH, Chung BG, Lee WG, Kim J, Brigham MD, Shim J et al (2010) Microporous cell-laden hydrogels for engineered tissue constructs. *Biotechnol Bioeng* 106(1):138–148
  89. Park JS, Chu JS, Tsou AD, Diop R, Tang Z, Wang A, Li S (2011) The effect of matrix stiffness on the

- differentiation of mesenchymal stem cells in response to TGF- $\beta$ . *Biomaterials* 32(16):3921–3930. <https://doi.org/10.1016/j.biomaterials.2011.02.019>
90. Persidis A (1998) High-throughput screening. Advances in robotics and miniaturization continue to accelerate drug lead identification. *Nat Biotechnol* 16(5):488–489. <https://doi.org/10.1038/nbt0598-488>
  91. Phipps MC, Clem WC, Catledge S a, Xu Y, Hennessy KM, Thomas V et al (2011) Mesenchymal stem cell responses to bone-mimetic electrospun matrices composed of polycaprolactone, collagen I and nanoparticulate hydroxyapatite. *PLoS ONE* 6(2):1–8. <https://doi.org/10.1371/journal.pone.0016813>
  92. Pillay V, Dott C, Choonara YE, Tyagi C, Tomar L, Kumar P et al (2013) A review of the effect of processing variables on the fabrication of electrospun nanofibers for drug delivery applications. *J Nanomater* 2013:1–22. <https://doi.org/10.1155/2013/789289>
  93. Prabhakaran MP, Mobarakeh LG, Kai D, Karbalaie K, Nasr-Esfahani MH, Ramakrishna S (2014) Differentiation of embryonic stem cells to cardiomyocytes on electrospun nanofibrous substrates. *Jf Biomed Mater Res Part B Appl Biomat* 102(3):447–454. <https://doi.org/10.1002/jbm.b.33022>
  94. Press Association (2014). Why tests on mice may be of little use. *The Telegraph*, pp 3–5. Retrieved from <http://www.telegraph.co.uk/science/science-news/11241310/Why-tests-on-mice-be-of-little-use.html>
  95. Ramesh Kumar P, Khan N, Vivekanandhan S, Satyanarayana N, Mohanty AK, Misra M (2012) Nanofibers: effective generation by electrospinning and their applications. *J Nanosci Nanotechnol* 12(1):1–25. <https://doi.org/10.1166/jnn.2012.5111>
  96. Ravichandran R, Venugopal JR, Sundarajan S, Mukherjee S, Ramakrishna S (2013) Cardiogenic differentiation of mesenchymal stem cells on elastomeric poly (glycerol sebacate)/collagen core/shell fibers. *World J Cardiol* 5(3):28–41. <https://doi.org/10.4330/wjc.v5.i3.28>
  97. Rederstorff E, Rethore G, Weiss P, Sourice S, Beck-Cormier S, Mathieu E et al (2015) Enriching a cellulose hydrogel with a biologically active marine exopolysaccharide for cell-based cartilage engineering. *J Tissue Eng Regen Med*. <https://doi.org/10.1002/term.2018>
  98. Reynolds TY, Rockwell S, Glazer PM (1996) Genetic instability induced by the tumor microenvironment. *Cancer Res* 56(24):5754–5757. Retrieved from <http://www.ncbi.nlm.nih.gov/pubmed/8971187%5Cn>, <http://cancerres.aacrjournals.org/content/56/24/5754.full.pdf>
  99. Rozario T, DeSimone DW (2010) The extracellular matrix in development and morphogenesis: a dynamic view. *Dev Biol* 341(1):126–140. <https://doi.org/10.1016/j.ydbio.2009.10.026>
  100. Safaeijavan R, Soleimani M, Divsalar A, Eidi A, Ardeshtyrlajimi A (2014) Comparison of random and aligned PCL nanofibrous electrospun scaffolds on cardiomyocyte differentiation of human adipose-derived stem cells. *Iran J Basic Med Sci* 17(11):903–911
  101. Salaam AD, Mishra M, Nyairo E, Dean D (2014) Electrospun polyvinyl alcohol/nanodiamond composite scaffolds: morphological, structural, and biological analysis. *J Biomater Tissue Eng* 4(3):173–180. <https://doi.org/10.1166/jbt.2014.1152>
  102. Schindler C, Williams BL, Patel HN, Thomas V, Dean DR (2013) Electrospun polycaprolactone/polyglyconate blends: miscibility, mechanical behavior, and degradation. *Polymer (United Kingdom)* 54(25):6824–6833. <https://doi.org/10.1016/j.polymer.2013.10.025>
  103. Sheets K, Wang J, Meehan S, Sharma P, Ng C, Khan M et al (2013) Cell-fiber interactions on aligned and suspended nanofiber scaffolds. *J Biomater Tissue Eng* 3(4):355–368. <https://doi.org/10.1166/jbt.2013.1105>
  104. Sridhar S, Venugopal JR, Sridhar R, Ramakrishna S (2015) Cardiogenic differentiation of mesenchymal stem cells with gold nanoparticle loaded functionalized nanofibers. *Colloids Surf B: Biointerfaces* 134:346–354. <https://doi.org/10.1016/j.colsurfb.2015.07.019>
  105. Sweeney SM (2014) AACR cancer progress report 2015. *Am Assoc Cancer Res* 126. <https://doi.org/10.1158/1078-0432.CCR-12-2891>
  106. Taetle R, Honeysett JM, Rosen F, Shoemaker R (1986) Use of nude mouse xenografts as preclinical drug screens: Further studies on in vitro growth of xenograft tumor colony-forming cells. *Cancer* 58(9):1969–1978. [https://doi.org/10.1002/1097-0142\(19861101\)58:9<1969::AID-CNCR2820580903>3.0.CO;2-4](https://doi.org/10.1002/1097-0142(19861101)58:9<1969::AID-CNCR2820580903>3.0.CO;2-4)
  107. Takimoto CH (2001) Why drugs fail: of mice and men revisited. *Clin Cancer Res* 7(2):229–230
  108. Tamayol A, Akbari M, Annabi N, Paul A, Khademhosseini A, Juncker D (2013) Fiber-based tissue engineering: progress, challenges, and opportunities. *Biotechnol Adv* 31(5):669–687. <https://doi.org/10.1016/j.biotechadv.2012.11.007>
  109. Thomas V, Dean DR, Jose MV, Mathew B, Chowdhury S, Vohra YK (2007a) Nanostructured biocomposite scaffolds based on collagen coelectrospun with nanohydroxyapatite. *Biomacromolecules* 8(2):631–637. <https://doi.org/10.1021/bm060879w>
  110. Thomas V, Dean DR, Vohra YK (2006a) Nanostructured biomaterials for regenerative medicine. *Curr Nanosci* 2(3):155–177. <https://doi.org/10.1007/978-1-4614-1080-5>
  111. Thomas V, Jagani S, Johnson K, Jose MV, Dean DR, Vohra YK, Nyairo E (2006b) Electrospun bioactive nanocomposite scaffolds of polycaprolactone and nanohydroxyapatite for bone tissue engineering. *J Nanosci Nanotechnol* 6(2):487–493
  112. Thomas V, Jose MV, Chowdhury S, Sullivan JF, Dean DR, Vohra YK (2006c) Mechano-morphological studies of aligned nanofibrous scaffolds of polycaprolactone fabricated by electrospinning. *J Biomater*

- Scie Polym Edn 17(9):969–984. <https://doi.org/10.1163/156856206778366022>
113. Thomas V, Zhang X, Catledge SA, Vohra YK (2007b) Functionally graded electrospun scaffolds with tunable mechanical properties for vascular tissue regeneration. *Biomed Mater (Bristol, England)* 2(4):224–232. <https://doi.org/10.1088/1748-6041/2/4/004>
  114. Thompson CJ, Chase GG, Yarin AL, Reneker DH (2007) Effects of parameters on nanofiber diameter determined from electrospinning model. *Polymer* 48(23):6913–6922. <https://doi.org/10.1016/j.polymer.2007.09.017>
  115. Trédan O, Galmarini CM, Patel K, Tannock IF (2007) Drug resistance and the solid tumor micro-environment. *J Natl Cancer Inst* 99(19):1441–1454. <https://doi.org/10.1093/jnci/djm135>
  116. Tse JR, Engler AJ (2011) Stiffness gradients mimicking in vivo tissue variation regulate mesenchymal stem cell fate. *PLoS ONE* 6(1). <https://doi.org/10.1371/journal.pone.0015978>
  117. Tucker N, Stanger JJ, Staiger MP, Razzaw H, Hofman K (2012) The history of the science and technology of electrospinning from 1600 to 1995. *J Eng Fibers Fabrics* 7:63–73
  118. Tyagi P, Catledge SA, Stanishevsky A, Thomas V, Vohra YK (2009) Nanomechanical properties of electrospun composite scaffolds based on polycaprolactone and hydroxyapatite. *J Nanosci Nanotechnol* 9(8):4839–4845
  119. Vakoc BJ, Lanning RM, Tyrrell JA, Padera TP, Bartlett LA, Stylianopoulos T et al (2009) Three-dimensional microscopy of the tumor microenvironment in vivo using optical frequency domain imaging. *Nat Med* 15(10):1219–1223. <https://doi.org/10.1038/nm.1971>
  120. van der Meer AD, van den Berg A (2012) Organ-on-chips: breaking the in vitro impasse. *Integr Biol (Camb)* 4(5):461–470. <https://doi.org/10.1039/c2ib00176d>
  121. van Manen EH, Zhang W, Walboomers XF, Vazquez B, Yang F, Ji W et al (2014) The influence of electrospun fibre scaffold orientation and nano-hydroxyapatite content on the development of tooth bud stem cells in vitro. *Odontology* 102(1):14–21. <https://doi.org/10.1007/s10266-012-0087-9>
  122. Wagner I, Materne E-M, Brincker S, Süßbier U, Frädlich C, Busek M et al (2013) A dynamic multi-organ-chip for long-term cultivation and substance testing proven by 3D human liver and skin tissue coculture. *Lab Chip* 13(18):3538–3547. Retrieved from <http://www.ncbi.nlm.nih.gov/pubmed/23648632>
  123. Wang J, Ye R, Wei Y, Wang H, Xu X, Zhang F et al (2012) The effects of electrospun TSF nanofiber diameter and alignment on neuronal differentiation of human embryonic stem cells. *J Biomed Mater Res A* 100(3):632–645. <https://doi.org/10.1002/jbm.a.33291>
  124. Wang Z, Cui Y, Wang J, Yang X, Wu Y, Wang K et al (2014) The effect of thick fibers and large pores of electrospun poly(epsilon-caprolactone) vascular grafts on macrophage polarization and arterial regeneration. *Biomaterials* 35(22):5700–5710. <https://doi.org/10.1016/j.biomaterials.2014.03.078>
  125. Wells JA, McClendon CL (2007) Reaching for high-hanging fruit in drug discovery at protein-protein interfaces. *Nature* 450(7172):1001–1009. <https://doi.org/10.1038/nature06526>
  126. Whiteside TL (2008) The tumor microenvironment and its role in promoting tumor growth. *Oncogene* 27(45):5904–5912. <https://doi.org/10.1038/onc.2008.271>
  127. Wise JK, Yarin AL, Megaridis CM, Cho M (2009) Chondrogenic differentiation of human mesenchymal stem cells on oriented nanofibrous scaffolds - engineering the superficial zone of articular cartilage. *Tissue Eng Part A* 15(4):10
  128. Wishart DS, Knox C, Guo AC, Shrivastava S, Hassanali M, Stothard P et al (2006) DrugBank: a comprehensive resource for in silico drug discovery and exploration. *Nucleic Acids Res* 34(Database issue):D668–D672. <https://doi.org/10.1093/nar/gkj067>
  129. Yang L, Pang Y, Moses HL (2010) TGF- $\beta$  and immune cells: an important regulatory axis in the tumor microenvironment and progression. *Trends Immunol* 31(6):220–227. <https://doi.org/10.1016/j.it.2010.04.002>
  130. Ye K, Wang X, Cao L, Li S, Li Z, Yu L, Ding J (2015) Matrix stiffness and nanoscale spatial organization of cell-adhesive ligands direct stem cell fate. *Nano Lett* 15(7):4720–4729. <https://doi.org/10.1021/acs.nanolett.5b01619>
  131. Yeung T, Georges PC, Flanagan LA, Marg B, Ortiz M, Funaki M et al (2005) Effects of substrate stiffness on cell morphology, cytoskeletal structure, and adhesion. *Cell Motil Cytoskeleton* 60(1):24–34. <https://doi.org/10.1002/cm.20041>
  132. Young DA, Choi YS, Engler AJ, Christman KL (2013) Stimulation of adipogenesis of adult adipose-derived stem cells using substrates that mimic the stiffness of adipose tissue. *Biomaterials* 34(34):8581–8588. <https://doi.org/10.1016/j.biomaterials.2013.07.103>
  133. Youngstrom DW, Barrett JG, Jose RR, Kaplan DL (2013) Functional characterization of detergent-decellularized equine tendon extracellular matrix for tissue engineering applications. *PLoS ONE* 8(5). <https://doi.org/10.1371/journal.pone.0064151>
  134. Zanatta G, Steffens D, Braghioroli DI, Fernandes RA, Netto CA, Pranke P (2012) Viability of mesenchymal stem cells during electrospinning. *Braz J Med Biol Res* 45(2):125–130. <https://doi.org/10.1590/s0100-879x2011007500163>
  135. Zeleny J (1917) Instability of electrified liquid surfaces. *Phys Rev* 10(1):1–6. <https://doi.org/10.1103/PhysRev.10.1>
  136. Zhao W, Li X, Liu X, Zhang N, Wen X (2014) Effects of substrate stiffness on adipogenic and osteogenic differentiation of human mesenchymal stem cells.

- Mater Sci Eng C Mater Biol Appl 40:316–323. <https://doi.org/10.1016/j.msec.2014.03.048>
137. Zheng W, Spencer RH, Kiss L (2004) High throughput assay technologies for ion channel drug discovery. *Assay Drug Dev Technol* 2(5):543–552. <https://doi.org/10.1089/adt.2004.2.543>
138. Zhu B, Li W, Lewis RV, Segre CU, Wang R (2015) E-spun composite fibers of collagen and dragline silk protein: fiber mechanics, biocompatibility, and application in stem cell differentiation. *Biomacromolecules* 16(1):202–213. <https://doi.org/10.1021/bm501403f>





# Silk Fibroin in Wound Healing Process

# 7

Md. Tipu Sultan, Ok Joo Lee, Soon Hee Kim,  
Hyung Woo Ju, and Chan Hum Park

## Abstract

Silk fibroin (SF), a natural bioproduct, has been extensively used in biological and biomedical fields including wound healing due to its robust biocompatibility, less immunogenic, non-toxic, non-carcinogenic, and biodegradable properties. SF in different morphologic forms, such as hydrogels, sponges, films, electrospun nanofiber mats, and hydrocolloid dressings, have been successfully used for therapeutic use as wound dressings to induce the healing process. SF has also been known to promote wound healing by increasing the cell growth, proliferation, and migration of different cells types involved in the different phase of wound healing process. In this review, we summarize the different morphologic forms of SF that have been used in the treatment of various wound healing process.

We also discuss the effect of SF on various cells types during the SF-induced healing process. Furthermore, we highlight molecular signaling aspects of the SF-induced healing process.

## Keywords

Silk fibroin · Shape · Wound healing · Wound dressings · Signaling pathways

## 7.1 Introduction

Wound healing is a complicated process that involves interactions with different cells and matrices, among various overlapping phases of events including inflammation, new tissue formation, and remodeling of tissue taking place [18, 57, 83]. Inflammation is the first phase of wound healing, which occurs immediately after injury and can last for up to 2 days. Activation of the inflammatory pathways, coagulation cascade, and immune system are needed to prevent continuing blood and fluid losses, to remove dead and dying tissues and to stop infection. Inflammatory cells such as neutrophils and macrophages play numerous critical roles to support the repair process by removing pathogens or injured cells through phagocytosis, and via the production of several cytokines and growth factors [24, 85]. The new tissue formation is the

M. T. Sultan · O. J. Lee · S. H. Kim · H. W. Ju  
Nano-Bio Regenerative Medical Institute,  
College of Medicine, Hallym University,  
Chuncheon, South Korea

C. H. Park (✉)  
Nano-Bio Regenerative Medical Institute,  
College of Medicine, Hallym University,  
Chuncheon, South Korea

Department of Otorhinolaryngology-Head  
and Neck Surgery, Chuncheon Sacred Heart Hospital,  
Hallym University College of Medicine,  
Chuncheon, South Korea  
e-mail: [hlpch@paran.com](mailto:hlpch@paran.com)

second phase of wound healing, which is associated with angiogenesis, re-epithelialization, granulation tissue configuration, matrix/collagen deposition, and wound contraction [24, 53, 85]. The wound healing process is accomplished by the maturation or remodeling phase, which can stay for a year or more depending on the extent of the injury, and is coupled with the remodeling of the epidermis and extracellular matrix (ECM) [27, 53].

There are several wound dressing biomaterials on the market in the present day, such as those composed of hydrocolloids [98], alginates [93], polyurethane [44], collagen [70, 87], chitosan [63], and hyaluronic acid [92]. To display enhanced wound healing, dressing's materials should exhibit biocompatibility, an ability to provide a favorable moist environment for wound, confer protection against dust and pathogen, control of structure for gaseous permeation, the biodegradability of the material to escape disrupting the wound site, waterproofness and easy application and removal [78].

SF, a fibrous protein derived from *Bombyx mori*, has been extensively applied as a promising biomaterial for tissue engineering and regeneration applications [33, 38, 39, 55]. Compared with other biomaterials, such as polylactic acid and collagen, SF has exceptional mechanical strength, toughness, and thermal stability. Also, SF is proved to contain the tripeptide Arg-Gly-Asp (RGD) sequences that can support cell adhesion, proliferation, and migration [3, 7, 10, 30] of various cell types, including epithelial, endothelial, fibroblast, keratinocyte, glial, and osteoblasts [52, 100, 102]. The application of SF as a suture for wound treatment [3, 62] started centuries ago. Several studies have reported that SF in different forms, such as hydrogels [20], sponges [75], films [20, 43], electrospun nanofiber mats [76], and hydrocolloid dressings [48], have been successfully used for therapeutic use as wound dressings to promote the healing process [67, 79, 91, 97]. In this chapter, we focus on several morphologic forms of SF used in wound healing, cellular response to SF during the healing process, and mechanisms underlying the SF-induced wound healing process.

## 7.2 SF in Different Forms for Wound Healing Applications

SF can be tailored to hold a wide range of forms such as powder, solution, fibers, hydrogels, films, and sponges via different treatment approaches. Due to the ease of processing in diverse forms and control ability of molecular structure and morphology, SF-based biomaterials has been extensively used in several morphologic forms in different wound healing applications (Table 7.1).

### 7.2.1 SF Solution

SF solution can be obtained by degumming the silk cocoons in an aqueous solution of 0.02 M Na<sub>2</sub>CO<sub>3</sub> by boiling for 40 min at 95 °C, flowed by washing with distilled water to eliminate the glue-like sericin proteins [14, 47, 52, 66, 67]. Subsequently, degummed SF was solubilized with CaCl<sub>2</sub>, ethanol, and H<sub>2</sub>O (at a molar ratio of 1:2:8) for 50 min at 98 °C. This solution was then filtered through the dialysis membrane for

**Table 7.1** Different morphologic forms of SF for various wound treatments

Morphological form	Types of wounds	References
Solution	Partial-thickness skin wound	[1, 4, 52, 68]
	Scratch wound	
	Corneal epithelial wound	
	Burn injury	
Hydrogel	Burn wound	[34, 89]
	Scratch wound	
Film	Full-thickness skin wounds	[65, 86]
	Acute dermal wound	
Sponge	Full-thickness skin wounds	[75, 87]
Electrospun silk fibroin mat	Burn wound	[2, 33, 76]
	Full-thickness dermal wound	
	Chronic non-healing wound	
Hydrocolloid dressing	Burn wound	[48]



**Fig. 7.1** Schematic of SF extraction procedure. Silk cocoon was degummed with an aqueous solution of 0.02 M Na<sub>2</sub>CO<sub>3</sub> by boiling for 40 min at 95 °C, and then washed with distilled water to eliminate the glue-like sericin pro-

teins. Degummed SF was solubilized with CaCl<sub>2</sub>, ethanol, and H<sub>2</sub>O (at a molar ratio of 1:2:8) for 50 min at 98 °C. This solution was then filtered through the dialysis membrane for 3 days to obtain SF solutions [14, 47, 52, 66, 67]

3 days to obtain SF solutions (Fig. 7.1). It has been demonstrated that SF in solution state induced wound healing in a scratch wound model *in vitro* [52]. Recently Park et al. exhibited that silk solution significantly induced healing effect both *in vitro* and *in vivo* [68]. They used a scratch wound model with NIH3T3 cells and a partial excision skin wound model with rat for *in vitro* and *in vivo* for the evaluation of silk solution wound healing ability, respectively. Solubilized silk-derived protein (SDP) as an eye drop has also been applied to enhance rabbit corneal epithelial wound healing process [1]. The regenerated SF solution can be applied to formulate different types of ointment and creams for various wound healing purposes.

## 7.2.2 SF Hydrogels

Hydrogels are three-dimensional polymeric networks with high swelling ratio which are in aqueous solution. Due to the relatively good biocompatibility, hydrogels generally fabricates with naturally derived polymers, such as collagen [59], hyaluronic acid [9], chitosan [56], SF [34, 45], alginate [8], and gelatin [94]. Gelation of the SF solution can be maintained by temperature, calcium ion concentration, pH, and polymer blending with materials like polyethylene oxide (PEO) to produce a hydrogel [23, 42, 72]. Hydrogels have been extensively applied in a wide range of biomedical applications including wound treatment [16, 35]. The silk-based hydro-

gel has been shown to have potential effects on wound healing. The favorable effects of SF not only for the induction of cell attachment, growth, proliferation, migration, and production of extracellular matrix (ECM) but also for the enhancement of the hydrogel mechanical strength that is fabricated from other natural polymers [36]. SF-based hydrogel have been reported for burn-induced wound healing applications in a rat model [34]. Biomimetic hydrogel loaded with silk and L-proline demonstrated significantly improved wound healing effect *in vitro* [89]. It has also been reported that silk hydrogel contain *Centella asiatica* extract and hydrocortisone acetate used for healing of pressure sores *in vivo* [46]. Although SF hydrogels have been successfully applied in many studies for wound treatment, SF hydrogels should essentially be designed by mimicking the structure and function of the native extracellular matrix (ECM) proteins, which offer mechanical support and regulate cellular activities during the healing process.

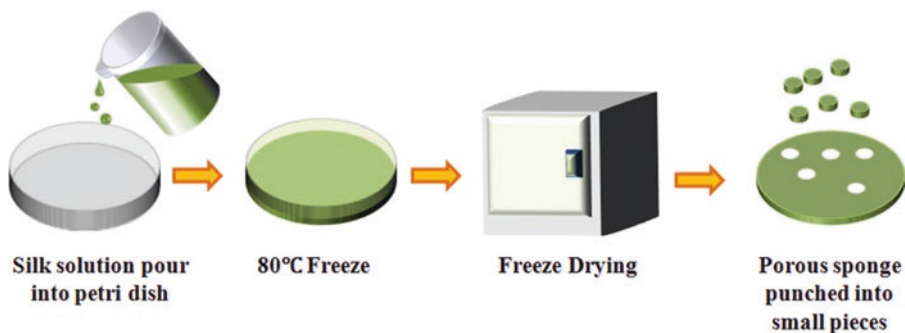
### 7.2.3 SF Films

SF membranes offer a well-designed and straightforward biomaterial of choice medical applications. Due to the intrinsically less complicated character of membranes, these materials offer quick characterization and design with regards to scaffold development. Silk films have been employed for the healing of full-thickness skin wounds in rats, and it showed faster healing with a lower inflammatory response than traditional

porcine-based wound dressings [86]. Recently, Zhang et al. evaluated the clinical application capability of the SF film to treat donor site wounds in a randomized single-blind parallel controlled clinical trial. They observed treatment with the SF film significantly promoted the wound healing speed and reduced the occurrence of adverse events as compared to the commercial dressing. From their observation, they demonstrated that the SF film is an effective and safe biomaterial for skin repair and regeneration, which can be easily translated to the future clinical treatment of skin wounds [105]. Padol et al. discovered that SF film, as a novel wound healing material, is very efficient with epidermal growth factor for the acute wound [65]. Since silk film offers numerous advantages over other dressing materials such as transparent, easily obtainable, sterilizable, allowing easy observation of tissue regeneration during the healing process, it could be clinically useful for wound treatment.

### 7.2.4 SF Sponges

Porous sponges are significant tissue engineering materials and regenerated SF solutions also have been utilized in the fabrication of porous sponges [5, 37, 49, 60, 75, 81]. Sponge scaffolds provide a framework of interconnected pores with a high amount of surface area within a defined three-dimensional volume, which allows for cell attachment and tissue ingrowths. SF porous sponges can be obtained using gas forming, porogens, freeze-drying (Fig. 7.2), freeze-drying/



**Fig. 7.2** Schematic process for the preparation of the porous SF sponge using the freeze-drying method [87]

foaming, and electrospun fibers [51, 58, 103, 104, 106]. Due to the fragile nature of SF sponge, SF as a hybrid sponge with others polymers has been successfully applied in several studies for wound healing applications [41, 87]. Roh et al. have been tested silk protein alginate sponge for dressing of full-thickness skin defect on rat-model [74]. Lee et al. suggested that the silk/duck's feet collagen hybrid sponge could be used as a dermal replacement for full-thickness skin defects [47].

### 7.2.5 Electrospun SF Mats

Recently, scientists have extensively focused on developing micro to nanofiber-based dressings for wound healing that can mimic the native dermal ECM with large surface area and high porosity. Nowadays electrospinning SF solution is a favored processing methods for obtaining nano to micro-scale fibers that result in a high degree of available surface area for use in developing scaffolds for tissue engineering and regenerative medicine purposes [19, 32, 40, 54]. Electrospun SF nanofibrous materials have been widely studied with functional properties such as high porosity, biocompatibility, and less inflammation for wound healing treatment. In numerous studies, electrospun silk materials have been reported as an ideal wound dressing material [84, 97]. Chutipakdeevong et al. developed an electrospun SF fiber mat which exhibited good support for cellular adhesion with accelerated wound healing [15]. To promote wound healing, Akturk et al. have been developed an electrospun SF/gold nanoparticle 3D matrices which accelerated the wound healing process without toxic effect both *in vitro* and *in vivo* [2]. It has also been revealed that the incorporation of growth factors into electrospun silk mats induced chronic wound healing process [76]. However conventional electrospun SF nanosheet has limitations for a wound healing application due to the problem associated with electric resistance to increase electrospun mat thickness (<1 mm) of SF nanosheet and the inability to provide large pore structure. These structural constraints result in lesser water

absorbability and fast drying of wound bed. Therefore, SF nanosheet obtained with a conventional electrospinning method has limitations for application in wound treatment in comparison to foam type dressings including alginate sponge, and polyurethane foam used in clinical treatments. To overcome these limitations, recently our group has been developed an electrospun SF nanomatrix with bulk volume and large pores using a modified electrospinning method combined with porogens (sodium chloride crystal) dispensing apparatus [33]. We revealed that our nanomatrix effectively promoted healing process by suppressing inflammation, and inducing re-epithelialization with less scar formation and short healing period in a second-degree burn wound rat model. Furthermore, Lee et al. have addressed an efficient design to fabricate SF nanofibers. They poured different size of NaCl crystals during electrospinning, which enhances large pores within the electrospun fibers. Their improvisation to the conventional electrospinning method resulted in thick nanofiber mats with highly porous structures within the nanofibers, which favorably lead to improvements in cell proliferation and infiltration. Also, they investigated the wound healing effect of their 3D SF nanofiber matrix produced by this method, and they found a significant healing effect with less contracture in compare to Matriderm® (a commercial wound dressing) in a full-thickness skin defect rat model.

---

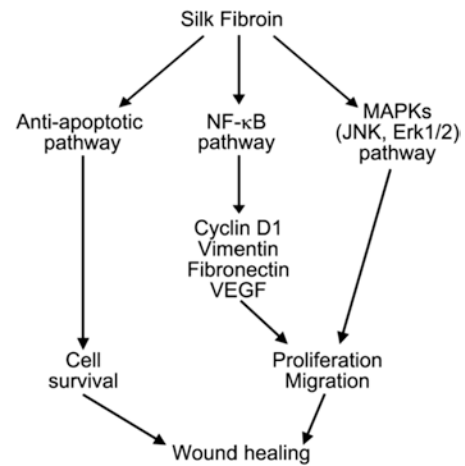
### 7.3 Cellular Response to SF During Wound Healing Process

Several types of cells such as neutrophils, lymphocytes, monocytes, macrophages, fibroblasts, keratinocytes, mesenchymal, and endothelial cells are implicated in the wound healing process [26]. Inflammatory cells have several functions in both early and late phases of inflammation [24]. Neutrophils are the first inflammatory cells appear at the spot of injury, followed by macrophages, monocytes, and lymphocytes. They engage in the phagocytosis of microorganisms

and cell debris and are an essential source of cytokines and growth factors [71, 96]. Mediators produced by macrophages and nearby cells start the proliferative phase of the healing process. The proliferative phase of the wound healing starts with the proliferation and migration of keratinocytes and fibroblasts into the wound edge. These cells are implicated in the deposition of collagen and wound construction. Macrophages, endothelial, fibroblasts, and epithelial cells are accountable for matrix remodeling in the maturation or remodeling phase. Most likely interactions between mesenchymal and epithelial cells continuously control homeostasis and skin integrity [88]. In wound healing, several cell types proliferate and migrate [17], with fibroblasts as critical components of the normal wound healing from the late inflammatory phase until achievement of complete epithelialization [21]. Early studies revealed that SF increased cell growth and cell proliferation [20, 38, 39, 52, 100, 102]. SF solution, when coated on polyurethane and poly (carbonate) urethane films and scaffolds, enhanced the adhesion and proliferation of human fibroblasts [13, 69]. It has also been reported that SF solution induced the cell proliferation and migration of primary human dermal fibroblasts (HDF) cells and NIH3T3 cells with significant healing response in a wound scratch healing model [68]. A similar result has been demonstrated in a previous study where SF accelerated human skin fibroblast proliferation [102]. Another study revealed that SF nanofibers mat enhanced fibroblast cells proliferation up to 7 days culture [80]. Thus SF in different forms induced healing process of different wound healing by increasing the cells proliferation and migration of various cells type involves in different stages of healing process.

#### 7.4 SF and Wound Healing Mechanism

Successful wound healing is a complicated process requires the interaction of several cell types, cytokines, growth factors, and extracellular cellular matrix (ECM) components. During wound healing process, several complex cellular signal-



**Fig. 7.3** Silk fibroin induces wound healing by activating different cellular pathways and via increasing cell survival, proliferation, and migration [4, 52, 68]

ing including AKT/mTOR signaling [101], Wnt and Notch signaling [82], mitogen-activated protein kinase (MAPK) signaling [11, 90], and transforming growth factor beta (TGF- $\beta$ ) signaling [12] take place in a closely coordinated cascade to heal the injury. SF has been known as a potential dressing for wound treatment for more than one hundred years. So far, few studies have demonstrated the mechanistic aspects of the SF-induced wound healing process *in vitro* [52] or *in vivo* [4, 68] (Fig. 7.3).

Cellular pathways such as AKT/mTOR signaling [101] and MAPK signaling [11, 90] had a significant role in wound healing processes. A recent study explored that SF stimulated cell migration in a scratch wound assay via the activation of c-Jun N-terminal kinases 1/2 (JNK1/2) and extracellular signal-regulated kinases 1/2 (ERK 1/2) [52]. More recently Aykac et al. have been reported that SF exerted a protective effect in burn injury in a rat model via inactivation of apoptotic pathway [4]. Although NF- $\kappa$ B has been known as a modulator of the inflammatory responses and immune cell functions, it is evident that the stimulation of NF- $\kappa$ B in wound healing is a common matter [28, 82, 95]. NF- $\kappa$ B signals have been involved in scratch injury [27], corneal epithelial wound healing [95], and cutaneous wound healing [11, 29]. Recently our group has been explored that SF induced skin

wound healing effects in a rat model via activating the canonical pathway of NF- $\kappa$ B signaling [68]. Numerous cytokines and growth factors have been known to play a critical role in wound healing process. These comprise tumor necrosis factor- $\alpha$  (TNF- $\alpha$ ), interleukin-1 $\beta$  (IL-1 $\beta$ ), interleukin-6 (IL-6), interleukin-8 (IL-8), interleukin-10, transforming growth factor (TGF  $\alpha$  and TGF  $\beta$ ), vascular endothelial growth factor (VEGF), epidermal growth factor (EGF), and as well as platelet-derived growth factor family [27, 88, 96]. Several studies revealed that SF suppressed the increased proinflammatory cytokines during inflammation phase of wound that results in protective effect in cells and tissues during wound healing [4, 33].

Different types of wound healing such as burn, bruise, ulceration, which may lead to different healing progress of the wound. Previous evidences revealed that cyclin D1, vimentin, fibronectin, and VEGF has a significant role in several types of wound healing process including burn, bruise and ulceration. Fibronectin is known to involved in the healing process of burn [61], ulcer [25, 99], and bruise [50]. It has been demonstrated that VEGF regulated the healing process of ulcer [6, 73], bruise [64], and burn [22]. Early evidence revealed that cyclin D1 played a profound role in ulcer [77] and burn [31] wound healing process. In our previous study, we revealed that NF- $\kappa$ B signaling pathway regulated SF-accelerated healing process via modulating its regulated proteins such as vimentin, fibronectin, VEGF, and cyclin D1 [68]. From these evidence it can be speculated that SF could be a useful material for all of the wound healing process. Thus, more studies needed to be conducted to explore the mechanistic insight in SF-induced wound healing processes.

## 7.5 Conclusions and Future Perspective

SF, as one of the most ancient natural polymers, has attracted intense interest in recent decades for various astonishing biomedical applications including wound healing due to their competent biocompatibility, least inflammatory response to

host tissue, comparatively slow biodegradation rates compared to other materials, ease of use, and easy availability. It has been revealed to be a promising biomaterial in several forms, such as solution, hydrogels, sponges, films, hydrocolloid dressings and electrospun SF nanofiber mats in various wound healing applications. However, silk fibroin has some disadvantages including easy fragmentation, brittleness, and difficulty in creating a uniform thickness. Although numerous literature are available on SF and modified SF (composites/blends/derivatives) for wound healing, there are many challenges remain to be explored in the process of wound healing. Further studies are needed to improve the potential effect of SF for different types of wound healing applications.

Furthermore, SF has been used efficiently in therapeutic practice to enhance tissue regeneration and promote wound healing via cell proliferation, migration and differentiation, little effort into the molecular signaling (cellular/biochemical) mechanisms underlying these phenomena have been reported. Therefore intense research is needed to be carried out to explore mechanistic basis for SF on the wound to fabricate a new array of SF-based biomaterials for treatment of different types of wound healing.

**Acknowledgements** This work was supported by the National Research Foundation of Korea (NRF) grant funded by the Korea government (MSIP; grant No.: NRF-2016R1E1A1A01942120), by the Korea Health Technology R&D Project through the Korea Health Industry Development Institute (KHIDI), funded by the Ministry of Health & Welfare, South Korea (grant No.: HI17C1229), and Hallym University research fund.

## References

1. Abdel-Naby W et al (2017) Treatment with solubilized Silk-Derived Protein (SDP) enhances rabbit corneal epithelial wound healing. *PLoS One* 12:e0188154. <https://doi.org/10.1371/journal.pone.0188154>
2. Akturk O et al (2016) Wet electrospun silk fibroin/gold nanoparticle 3D matrices for wound healing applications. *RSC Adv* 6:13234–13250. <https://doi.org/10.1039/c5ra24225h>
3. Altman GH et al (2003) Silk-based biomaterials. *Biomaterials* 24:401–416

4. Aykac A, Karanlik B, Sehirli AO (2018) Protective effect of silk fibroin in burn injury in rat model. *Gene* 641:287–291. <https://doi.org/10.1016/j.gene.2017.10.036>
5. Aytemiz D et al (2013) Small-diameter silk vascular grafts (3 mm diameter) with a double-raschel knitted silk tube coated with silk fibroin sponge. *Adv Healthcare Mater* 2:361–368. <https://doi.org/10.1002/adhm.201200227>
6. Bao P, Kodra A, Tomic-Canic M, Golinko MS, Ehrlich HP, Brem H (2009) The role of vascular endothelial growth factor in wound healing. *J Surg Res* 153:347–358. <https://doi.org/10.1016/j.jss.2008.04.023>
7. Bini E, Foo CW, Huang J, Karageorgiou V, Kitchel B, Kaplan DL (2006) RGD-functionalized bio-engineered spider dragline silk biomaterial. *Biomacromolecules* 7:3139–3145. <https://doi.org/10.1021/bm0607877>
8. Bouhadir KH, Lee KY, Alsberg E, Damm KL, Anderson KW, Mooney DJ (2001) Degradation of partially oxidized alginate and its potential application for tissue engineering. *Biotechnol Prog* 17:945–950. <https://doi.org/10.1021/bp010070p>
9. Burdick JA, Prestwich GD (2011) Hyaluronic acid hydrogels for biomedical applications. *Adv Mater* 23:H41–H56. <https://doi.org/10.1002/adma.201003963>
10. Chen J et al (2003) Human bone marrow stromal cell and ligament fibroblast responses on RGD-modified silk fibers. *J Biomed Mater Res A* 67:559–570. <https://doi.org/10.1002/jbm.a.10120>
11. Chen J, Chen Y, Yang Z, You B, Ruan YC, Peng Y (2016) Epidermal CFTR suppresses MAPK/NF-kappaB to promote cutaneous. *Wound Healing Cell Physiol Biochem* 39:2262–2274. <https://doi.org/10.1159/000447919>
12. Cheng F, Shen Y, Mohanasundaram P, Lindstrom M, Ivaska J, Ny T, Eriksson JE (2016) Vimentin coordinates fibroblast proliferation and keratinocyte differentiation in wound healing via TGF-beta-Slug signaling. *Proc Natl Acad Sci U S A* 113:E4320–E4327. <https://doi.org/10.1073/pnas.1519197113>
13. Chiarini A, Petrini P, Bozzini S, Dal Pra I, Armato U (2003) Silk fibroin/poly(carbonate)-urethane as a substrate for cell growth: in vitro interactions with human cells. *Biomaterials* 24:789–799
14. Chung EJ, Ju HW, Park HJ, Park CH (2015) Three-layered scaffolds for artificial esophagus using poly(varepsilon-caprolactone) nanofibers and silk fibroin: an experimental study in a rat model. *J Biomed Mater Res A* 103:2057–2065. <https://doi.org/10.1002/jbm.a.35347>
15. Chutipakdeevong J, Ruktanonchai UR, Supaphol P (2013) Process optimization of electrospun silk fibroin fiber mat for accelerated wound healing. *J Appl Polym Sci* 130:3634–3644. <https://doi.org/10.1002/app.39611>
16. Drury JL, Mooney DJ (2003) Hydrogels for tissue engineering: scaffold design variables and applications. *Biomaterials* 24:4337–4351
17. Eming SA, Martin P, Tomic-Canic M (2014) Wound repair and regeneration: mechanisms, signaling, and translation. *Sci Transl Med* 6:265sr266. <https://doi.org/10.1126/scitranslmed.3009337>
18. Falanga V (2005) Wound healing and its impairment in the diabetic foot. *Lancet* 366:1736–1743. [https://doi.org/10.1016/S0140-6736\(05\)67700-8](https://doi.org/10.1016/S0140-6736(05)67700-8)
19. Fan S, Zhang Y, Shao H, Hu X (2013) Electrospun regenerated silk fibroin mats with enhanced mechanical properties. *Int J Biol Macromol* 56:83–88. <https://doi.org/10.1016/j.ijbiomac.2013.01.033>
20. Fini M et al (2005) The healing of confined critical size cancellous defects in the presence of silk fibroin hydrogel. *Biomaterials* 26:3527–3536 doi:S0142-9612(04)00869-5 [pii]. <https://doi.org/10.1016/j.biomaterials.2004.09.040>
21. Forrest L (1983) Current concepts in soft connective tissue wound healing. *Br J Surg* 70:133–140
22. Fu SC, Chau YP, Lu KS, Kung HN (2011) beta-lapachone accelerates the recovery of burn-wound skin. *Histol Histopathol* 26:905-914 doi:10.14670/HH-26.905
23. Gil ES, Hudson SM (2007) Effect of silk fibroin interpenetrating networks on swelling/deswelling kinetics and rheological properties of poly(N-isopropylacrylamide) hydrogels. *Biomacromolecules* 8:258–264. <https://doi.org/10.1021/bm060543m>
24. Gonzalez AC, Costa TF, Andrade ZA, Medrado AR (2016) Wound healing – a literature review. *An Bras Dermatol* 91:614–620 doi:S0365-05962016000500614 [pii]. <https://doi.org/10.1590/abd1806-4841.20164741>
25. Grinnell F, Ho CH, Wysocki A (1992) Degradation of fibronectin and vitronectin in chronic wound fluid: analysis by cell blotting, immunoblotting, and cell adhesion assays. *J Invest Dermatol* 98:410–416 doi:S0022-202X(92)91008-W [pii]
26. Guo S, Dipietro LA (2010) Factors affecting wound healing. *J Dent Res* 89:219–229 doi:0022034509359125 [pii]. <https://doi.org/10.1177/0022034509359125>
27. Gurtner GC, Werner S, Barrandon Y, Longaker MT (2008) Wound repair and regeneration. *Nature* 453:314–321 doi:nature07039 [pii]. <https://doi.org/10.1038/nature07039>
28. Haas AF, Wong JW, Iwahashi CK, Halliwell B, Cross CE, Davis PA (1998) Redox regulation of wound healing? NF-kappaB activation in cultured human keratinocytes upon wounding and the effect of low energy HeNe irradiation. *Free Radic Biol Med* 25:998–1005 doi:S0891-5849(98)00135-X [pii]
29. Heo SC, Jeon ES, Lee IH, Kim HS, Kim MB, Kim JH (2011) Tumor necrosis factor-alpha-activated human adipose tissue-derived mesenchymal stem cells accelerate cutaneous wound healing through paracrine mechanisms. *J Invest Dermatol* 131:1559–1567 doi:S0022-202X(15)35324-0 [pii]. <https://doi.org/10.1038/jid.2011.64>



30. Hersel U, Dahmen C, Kessler H (2003) RGD modified polymers: biomaterials for stimulated cell adhesion and beyond. *Biomaterials* 24:4385–4415
31. Irrera N et al (2015) Epoetin alpha and epoetin zeta: a comparative study on stimulation of angiogenesis and wound repair in an experimental model of burn. *Injury Biomed Res Int* 2015:968927. <https://doi.org/10.1155/2015/968927>
32. Jin HJ, Fridrikh SV, Rutledge GC, Kaplan DL (2002) Electrospinning Bombyx mori silk with poly(ethylene oxide). *Biomacromolecules* 3:1233–1239
33. Ju HW et al (2016) Wound healing effect of electrospun silk fibroin nanomatrix in burn-model. *Int J Biol Macromol* 85:29–39 doi:S0141-8130(15)30243-9 [pii]. <https://doi.org/10.1016/j.ijbiomac.2015.12.055>
34. Ju HW et al (2014) Silk fibroin based hydrogel for regeneration of burn induced wounds. *Tissue Eng Regen Med* 11:203–210. <https://doi.org/10.1007/s13770-014-0010-2>
35. Kamoun EA, Kenawy ES, Chen X (2017) A review on polymeric hydrogel membranes for wound dressing applications: PVA-based hydrogel dressings. *J Adv Res* 8:217–233. [https://doi.org/10.1016/j.jare.2017.01.005S2090-1232\(17\)30024-3](https://doi.org/10.1016/j.jare.2017.01.005S2090-1232(17)30024-3) [pii]
36. Kapoor S, Kundu SC (2016) Silk protein-based hydrogels: promising advanced materials for biomedical applications. *Acta Biomater* 31:17–32 doi:S1742-7061(15)30210-5 [pii]. <https://doi.org/10.1016/j.actbio.2015.11.034>
37. Kawakami M, Tomita N, Shimada Y, Yamamoto K, Tamada Y, Kachi N, Suguro T (2011) Chondrocyte distribution and cartilage regeneration in silk fibroin sponge. *Biomed Mater Eng* 21:53–61. <https://doi.org/10.3233/BME-2011-0656>
38. Kim HJ, Kim UJ, Vunjak-Novakovic G, Min BH, Kaplan DL (2005a) Influence of macroporous protein scaffolds on bone tissue engineering from bone marrow stem cells. *Biomaterials* 26:4442–4452 doi:S0142-9612(04)00993-7 [pii]. <https://doi.org/10.1016/j.biomaterials.2004.11.013>
39. Kim JH et al (2016a) Osteoinductive silk fibroin/titanium dioxide/hydroxyapatite hybrid scaffold for bone tissue engineering. *Int J Biol Macromol* 82:160–167 doi:S0141-8130(15)00535-8 [pii]. <https://doi.org/10.1016/j.ijbiomac.2015.08.001>
40. Kim KH et al (2005b) Biological efficacy of silk fibroin nanofiber membranes for guided bone regeneration. *J Biotechnol* 120:327–339. <https://doi.org/10.1016/j.jbiotec.2005.06.033>
41. Kim SH et al (2016b) Fabrication of duck's feet collagen-silk hybrid biomaterial for tissue engineering. *Int J Biol Macromol* 85:442–450 doi:S0141-8130(15)30273-7 [pii]. <https://doi.org/10.1016/j.ijbiomac.2015.12.086>
42. Kim UJ, Park J, Li C, Jin HJ, Valluzzi R, Kaplan DL (2004) Structure and properties of silk hydrogels. *Biomacromolecules* 5:786–792. <https://doi.org/10.1021/bm0345460>
43. Kimura T, Yamada H, Tsubouchi K, Doi K (2007) Accelerating effects of silk fibroin on wound healing in hairless descendants of mexican hairless dogs. *J Appl Sci Res* 3:1306–1314
44. Konrad D, Tsunoda M, Weber K, Corney SJ, Ullmann L (2002) Effects of a topical silver sulfadiazine polyurethane dressing (Mikacure) on wound healing in experimentally infected wounds in the pig. A pilot study. *J Exp Animal Sci* 42:31–43. [https://doi.org/10.1016/S0939-8600\(02\)80004-9](https://doi.org/10.1016/S0939-8600(02)80004-9)
45. Lee JM, Sultan MT, Kim SH, Kumar V, Yeon YK, Lee OJ, Park CH (2017) Artificial auricular cartilage using silk fibroin and polyvinyl alcohol hydrogel. *Int J Mol Sci* 18 doi:ijms18081707 [pii]. <https://doi.org/10.3390/ijms18081707>
46. Lee MS, Seo SR, Kim JC (2012) A beta-cyclodextrin, polyethyleneimine and silk fibroin hydrogel containing Centella asiatica extract and hydrocortisone acetate: releasing properties and in vivo efficacy for healing of pressure sores. *Clin Exp Dermatol* 37:762–771. <https://doi.org/10.1111/j.1365-2230.2011.04331.x>
47. Lee OJ et al (2014) Development of artificial dermis using 3D electrospun silk fibroin nanofiber matrix. *J Biomed Nanotechnol* 10:1294–1303
48. Lee OJ et al (2016) Fabrication and characterization of hydrocolloid dressing with silk fibroin nanoparticles for wound healing. *Tissue Engineering and Regenerative Medicine* 13:218–226. <https://doi.org/10.1007/s13770-016-9058-5>
49. Liu H, Fan H, Wang Y, Toh SL, Goh JC (2008) The interaction between a combined knitted silk scaffold and microporous silk sponge with human mesenchymal stem cells for ligament tissue engineering. *Biomaterials* 29:662–674. <https://doi.org/10.1016/j.biomaterials.2007.10.035>
50. Liu NG, Chen YJ, Huang XH (2002) Expression of EIIIA-fibronectin in injured rat skin used in estimation of wound interval. *Fa Yi Xue Za Zhi* 18:129–131
51. Makaya K, Terada S, Ohgo K, Asakura T (2009) Comparative study of silk fibroin porous scaffolds derived from salt/water and sucrose/hexafluoroisopropanol in cartilage formation. *J Biosci Bioeng* 108:68–75 doi:S1389-1723(09)00134-0 [pii]. <https://doi.org/10.1016/j.jbiosc.2009.02.015>
52. Martinez-Mora C, Mrowiec A, Garcia-Vizcaino EM, Alcaraz A, Cenis JL, Nicolas FJ (2012) Fibroin and sericin from Bombyx mori silk stimulate cell migration through upregulation and phosphorylation of c-Jun. *PLoS One* 7:e42271. <https://doi.org/10.1371/journal.pone.0042271> PONE-D-12-08826 [pii]
53. Midwood KS, Williams LV, Schwarzbauer JE (2004) Tissue repair and the dynamics of the extracellular matrix. *Int J Biochem Cell Biol* 36:1031–1037. <https://doi.org/10.1016/j.biocel.2003.12.003> S1357272503004291 [pii]
54. Min BM, Lee G, Kim SH, Nam YS, Lee TS, Park WH (2004) Electrospinning of silk fibroin nanofibers and its effect on the adhesion and spreading of

- normal human keratinocytes and fibroblasts in vitro. *Biomaterials* 25:1289–1297
55. Moon BM et al (2017) Novel fabrication method of the peritoneal dialysis filter using silk fibroin with urease fixation system. *J Biomed Mater Res B Appl Biomater* 105:2136–2144. <https://doi.org/10.1002/jbm.b.33751>
  56. Murakami K et al (2010) Hydrogel blends of chitin/chitosan, fucoidan and alginate as healing-impaired wound dressings. *Biomaterials* 31:83–90 doi:S0142-9612(09)00961-2 [pii]. <https://doi.org/10.1016/j.biomaterials.2009.09.031>
  57. Mutsaers SE, Bishop JE, McGrouther G, Laurent GJ (1997) Mechanisms of tissue repair: from wound healing to fibrosis. *Int J Biochem Cell Biol* 29:5–17 doi:S135727259600115X [pii]
  58. Nam YS, Yoon JJ, Park TG (2000) A novel fabrication method of macroporous biodegradable polymer scaffolds using gas foaming salt as a porogen additive. *J Biomed Mater Res* 53:1–7. [https://doi.org/10.1002/\(SICI\)1097-4636\(2000\)53:1<1::AID-JBMT>3.0.CO;2-R](https://doi.org/10.1002/(SICI)1097-4636(2000)53:1<1::AID-JBMT>3.0.CO;2-R) [pii]
  59. Niiyama H, Kuroyanagi Y (2014) Development of novel wound dressing composed of hyaluronic acid and collagen sponge containing epidermal growth factor and vitamin C derivative. *J Artif Organs* 17:81–87. <https://doi.org/10.1007/s10047-013-0737-x>
  60. Nishida A, Yamada M, Kanazawa T, Takashima Y, Ouchi K, Okada H (2010) Use of silk protein, sericin, as a sustained-release material in the form of a gel, sponge and film. *Chem Pharm Bull* 58:1480–1486
  61. Olczyk P, Komosinska-Vashev K, Wisowski G, Mencner L, Stojko J, Kozma EM (2014) Propolis modulates fibronectin expression in the matrix of thermal injury. *Biomed Res Int* 2014:748101. <https://doi.org/10.1155/2014/748101>
  62. Omenetto FG, Kaplan DL (2010) New opportunities for an ancient material. *Science* 329:528–531. doi:329/5991/528 [pii] 10.1126/science.1188936
  63. Ong SY, Wu J, Moochhala SM, Tan MH, Lu J (2008) Development of a chitosan-based wound dressing with improved hemostatic and antimicrobial properties. *Biomaterials* 29:4323–4332 doi:S0142-9612(08)00512-7 [pii]. <https://doi.org/10.1016/j.biomaterials.2008.07.034>
  64. Ota S et al (2011) Intramuscular transplantation of muscle-derived stem cells accelerates skeletal muscle healing after contusion injury via enhancement of angiogenesis. *Am J Sports Med* 39:1912–1922 doi:0363546511415239 [pii]. <https://doi.org/10.1177/0363546511415239>
  65. Padol AR, Jayakumar K, Shridhar NB, Narayana Swamy HD, Narayana Swamy M, Mohan K (2011) Safety evaluation of silk protein film (a novel wound healing agent) in terms of acute dermal toxicity, acute dermal irritation and skin sensitization. *Toxicol Int* 18:17–21. <https://doi.org/10.4103/0971-6580.75847>
  66. Park HJ et al (2015) Fabrication of 3D porous silk scaffolds by particulate (salt/sucrose) leaching for bone tissue reconstruction. *Int J Biol Macromol* 78:215–223 doi:S0141-8130(15)00216-0 [pii]. <https://doi.org/10.1016/j.ijbiomac.2015.03.064>
  67. Park YR et al (2016) Three-dimensional electrospun silk-fibroin nanofiber for skin tissue engineering. *Int J Biol Macromol* 93:1567–1574 doi:S0141-8130(16)30867-4 [pii]. <https://doi.org/10.1016/j.ijbiomac.2016.07.047>
  68. Park YR et al (2017) NF-kappaB signaling is key in the wound healing processes of silk fibroin. *Acta Biomater* doi:S1742-7061(17)30762-6 [pii]. <https://doi.org/10.1016/j.actbio.2017.12.006>
  69. Petrini P, Parolari C, Tanzi MC (2001) Silk fibroin-polyurethane scaffolds for tissue engineering. *J Mater Sci Mater Med* 12:849–853 doi:381126 [pii]
  70. Powell HM, Supp DM, Boyce ST (2008) Influence of electrospun collagen on wound contraction of engineered skin substitutes. *Biomaterials* 29:834–843 doi:S0142-9612(07)00858-7 [pii]. <https://doi.org/10.1016/j.biomaterials.2007.10.036>
  71. Rajan V, Murray RZ (2008) The duplicitous nature of inflammation in wound repair. *Wound Practice Res* 16:122–129
  72. Ribeiro M, de Moraes MA, Beppu MM, Monteiro FJ, Ferraz MP (2014) The role of dialysis and freezing on structural conformation, thermal properties and morphology of silk fibroin hydrogels. *Biomater* 4:e28536. <https://doi.org/10.4161/biom.28536>
  73. Rivard A et al (1999) Rescue of diabetes-related impairment of angiogenesis by intramuscular gene therapy with adeno-VEGF. *Am J Pathol* 154:355–363 doi:S0002-9440(10)65282-0 [pii]. [https://doi.org/10.1016/S0002-9440\(10\)65282-0](https://doi.org/10.1016/S0002-9440(10)65282-0)
  74. Roh D-H et al (2006a) Wound healing effect of silk fibroin/alginate-blended sponge in full thickness skin defect of rat. *J Mater Sci Mater Med* 17:547–552. <https://doi.org/10.1007/s10856-006-8938-y>
  75. Roh DH et al (2006b) Wound healing effect of silk fibroin/alginate-blended sponge in full thickness skin defect of rat. *J Mater Sci Mater Med* 17:547–552. <https://doi.org/10.1007/s10856-006-8938-y>
  76. Schneider A, Wang XY, Kaplan DL, Garlick JA, Egles C (2009) Biofunctionalized electrospun silk mats as a topical bioactive dressing for accelerated wound healing. *Acta Biomater* 5:2570–2578 doi:S1742-7061(08)00405-4 [pii]. <https://doi.org/10.1016/j.actbio.2008.12.013>
  77. Seah CC, Phillips TJ, Howard CE, Panova IP, Hayes CM, Asandra AS, Park HY (2005) Chronic wound fluid suppresses proliferation of dermal fibroblasts through a Ras-mediated signaling pathway. *J Invest Dermatol* 124:466–474 doi:S0022-202X(15)32153-9 [pii]. <https://doi.org/10.1111/j.0022-202X.2004.23557.x>
  78. Seaman S (2002) Dressing selection in chronic wound management. *J Am Podiatr Med Assoc* 92:24–33
  79. Sheikh FA et al (2015) 3D electrospun silk fibroin nanofibers for fabrication of artificial

- skin. *Nanomedicine* 11:681–691 doi:S1549-9634(14)00571-1 [pii]. <https://doi.org/10.1016/j.nano.2014.11.007>
80. Sheikh FA et al (2014) A comparative mechanical and biocompatibility study of poly( $\epsilon$ -caprolactone), hybrid poly( $\epsilon$ -caprolactone)–silk, and silk nanofibers by colloidal electrospinning technique for tissue engineering. *J Bioact Compat Polym* 29:500–514. <https://doi.org/10.1177/0883911514549717>
81. Shen W, Chen X, Chen J, Yin Z, Heng BC, Chen W, Ouyang HW (2010) The effect of incorporation of exogenous stromal cell-derived factor-1 alpha within a knitted silk-collagen sponge scaffold on tendon regeneration. *Biomaterials* 31:7239–7249. <https://doi.org/10.1016/j.biomaterials.2010.05.040>
82. Shi Y et al (2015) Wnt and Notch signaling pathway involved in wound healing by targeting c-Myc and Hes1 separately. *Stem Cell Res Ther* 6:120 doi:10.1186/s13287-015-0103-4 10.1186/s13287-015-0103-4 [pii]
83. Singer AJ, Clark RA (1999) Cutaneous wound healing. *N Engl J Med* 341:738–746. <https://doi.org/10.1056/NEJM199909023411006>
84. Srivastava CM, Purwar R, Kannaujia R, Sharma D (2015) Flexible silk fibroin films for wound dressing. *Fibers Polym* 16:1020–1030. <https://doi.org/10.1007/s12221-015-1020-y>
85. Stadelmann WK, Digenis AG, Tobin GR (1998) Physiology and healing dynamics of chronic cutaneous wounds. *Am J Surg* 176:26S–38S
86. Sugihara A et al (2000) Promotive effects of a silk film on epidermal recovery from full-thickness skin wounds. *Proc Soc Exp Biol Med* 225:58–64 doi:pse22507 [pii]
87. Sultan MT et al (2017) Fabrication and characterization of the porous duck's feet collagen sponge for wound healing applications. *J Biomater Sci Polym Ed*:1–12. <https://doi.org/10.1080/09205063.2017.1367636>
88. Szabowski A, Maas-Szabowski N, Andrecht S, Kolbus A, Schorpp-Kistner M, Fusenig NE, Angel P (2000) c-Jun and JunB antagonistically control cytokine-regulated mesenchymal-epidermal interaction in skin. *Cell* 103:745–755 doi:S0092-8674(00)00178-1 [pii]
89. Thangavel P, Ramachandran B, Kannan R, Muthuvijayan V (2017) Biomimetic hydrogel loaded with silk and l-proline for tissue engineering and wound healing applications. *J Biomed Mater Res B Appl Biomater* 105:1401–1408. <https://doi.org/10.1002/jbm.b.33675>
90. Thiraisingam T et al (2010) MAPKAPK-2 signaling is critical for cutaneous wound healing. *J Invest Dermatol* 130:278–286 doi:S0022-202X(15)34516-4 [pii]. <https://doi.org/10.1038/jid.2009.209>
91. Unger RE, Peters K, Wolf M, Motta A, Migliaresi C, Kirkpatrick CJ (2004) Endothelialization of a non-woven silk fibroin net for use in tissue engineering: growth and gene regulation of human endothelial cells. *Biomaterials* 25:5137–5146. <https://doi.org/10.1016/j.biomaterials.2003.12.040> S0142961203011670 [pii]
92. Uppal R, Ramaswamy GN, Arnold C, Goodband R, Wang Y (2011) Hyaluronic acid nanofiber wound dressing—production, characterization, and in vivo behavior. *J Biomed Mater Res B Appl Biomater* 97:20–29. <https://doi.org/10.1002/jbm.b.31776>
93. Vassallo IM, Formosa C (2015) Comparing calcium alginate dressings to vacuum-assisted closure: a clinical trial. *Wounds* 27:180–190
94. Verma V, Verma P, Kar S, Ray P, Ray AR (2007) Fabrication of agar-gelatin hybrid scaffolds using a novel entrapment method for in vitro tissue engineering applications. *Biotechnol Bioeng* 96:392–400. <https://doi.org/10.1002/bit.21111>
95. Wang L, Wu X, Shi T, Lu L (2013) Epidermal growth factor (EGF)-induced corneal epithelial wound healing through nuclear factor kappaB subtype-regulated CCCTC binding factor (CTCF) activation. *J Biol Chem* 288:24363–24371 doi:M113.458141 [pii]. <https://doi.org/10.1074/jbc.M113.458141>
96. Werner S, Grose R (2003) Regulation of wound healing by growth factors and cytokines. *Physiol Rev* 83:835–870. <https://doi.org/10.1152/physrev.00031.200283/3/835> [pii]
97. Wharram SE, Zhang X, Kaplan DL, McCarthy SP (2010) Electrospun silk material systems for wound healing. *Macromol Biosci* 10:246–257. <https://doi.org/10.1002/mabi.200900274>
98. Wyatt D, McGowan DN, Najarian MP (1990) Comparison of a hydrocolloid dressing and silver sulfadiazine cream in the outpatient management of second-degree burns. *J Trauma* 30:857–865
99. Wysocki AB, Grinnell F (1990) Fibronectin profiles in normal and chronic wound fluid. *Lab Invest* 63:825–831
100. Xia Q et al (2004) A draft sequence for the genome of the domesticated silkworm (*Bombyx mori*). *Science* 306:1937–1940 doi:306/5703/1937 [pii] 10.1126/science.1102210
101. Xing W et al (2015) Acemannan accelerates cell proliferation and skin wound healing through AKT/mTOR signaling pathway. *J Dermatol Sci* 79:101–109 doi:S0923-1811(15)00116-4 [pii] 10.1016/j.jdermsci.2015.03.016
102. Yamada H, Igarashi Y, Takasu Y, Saito H, Tsubouchi K (2004) Identification of fibroin-derived peptides enhancing the proliferation of cultured human skin fibroblasts. *Biomaterials* 25:467–472 doi:S0142961203005404 [pii]
103. Yan LP, Oliveira JM, Oliveira AL, Caridade SG, Mano JF, Reis RL (2012) Macro/microporous silk fibroin scaffolds with potential for articular cartilage and meniscus tissue engineering applications. *Acta Biomater* 8:289–301 doi:S1742-7061(11)00430-2 [pii] 10.1016/j.actbio.2011.09.037

104. Yoon JJ, Park TG (2001) Degradation behaviors of biodegradable macroporous scaffolds prepared by gas foaming of effervescent salts. *J Biomed Mater Res* 55:401–408 doi:10.1002/1097-4636(20010605)55:3<401::AID-JBM1029>3.0.CO;2-H [pii]
105. Zhang W et al (2017) Silk fibroin biomaterial shows safe and effective wound healing in animal models and a randomized controlled clinical Trial. *Adv Healthc Mater*:6. <https://doi.org/10.1002/adhm.201700121>
106. Zhang X, Cao C, Ma X, Li Y (2012) Optimization of macroporous 3-D silk fibroin scaffolds by salt-leaching procedure in organic solvent-free conditions. *J Mater Sci Mater Med* 23:315–324. <https://doi.org/10.1007/s10856-011-4476-3>



# The Role of Natural-Based Biomaterials in Advanced Therapies for Autoimmune Diseases

Helena Ferreira, Joana F. Figueiro,  
and Nuno M. Neves

## Abstract

Autoimmune diseases (ADs) constitute a heterogeneous group of more than 100 pathophysiological conditions in which an immune response against the self is observed. The incidence and prevalence of these chronic diseases are increasing with inherently high social and economic impacts. The currently available therapies generally focus on reducing the activity of the immune system and, therefore, can present severe side effects such as enhanced patient susceptibility to opportunistic infections. Advanced therapies emerged as promising treatments and with real curative potential for ADs. Additionally, the use of natural polymers to engineer gene therapies, cell therapies and/or tissue-engineered medicinal products presents specific advantages. Natural polymers present higher affinity with biological systems than synthetic polymers, and frequently have a chemical structure and

motifs similar to those existing in the extracellular matrix of the tissues. They also have good biological performance, making them very strong candidates for advanced therapy medicinal products. This review discusses the therapeutic advances and provides demonstrative examples of the role of natural-based biomaterials for the development of advanced therapies for ADs.

## Keywords

Advanced therapies · Autoimmune diseases · Cell therapy · Gene therapy · Natural-based biomaterials · Stem cells

\*Author contributed equally with all other contributors.  
Helena Ferreira and Joana F. Figueiro.

H. Ferreira (✉) · J. F. Figueiro  
3B's Research Group, I3Bs – Research Institute on Biomaterials, Biodegradables and Biomimetics, University of Minho, Headquarters of the European Institute of Excellence on Tissue Engineering and Regenerative Medicine, Guimarães, Portugal

ICVS/3B's – PT Government Associate Laboratory, Braga, Portugal  
e-mail: [helenaferreira@i3bs.uminho.pt](mailto:helenaferreira@i3bs.uminho.pt);  
[joana.figueiro@i3bs.uminho.pt](mailto:joana.figueiro@i3bs.uminho.pt)

N. M. Neves  
3B's Research Group, I3Bs – Research Institute on Biomaterials, Biodegradables and Biomimetics, University of Minho, Headquarters of the European Institute of Excellence on Tissue Engineering and Regenerative Medicine, Guimarães, Portugal

ICVS/3B's – PT Government Associate Laboratory, Braga, Portugal

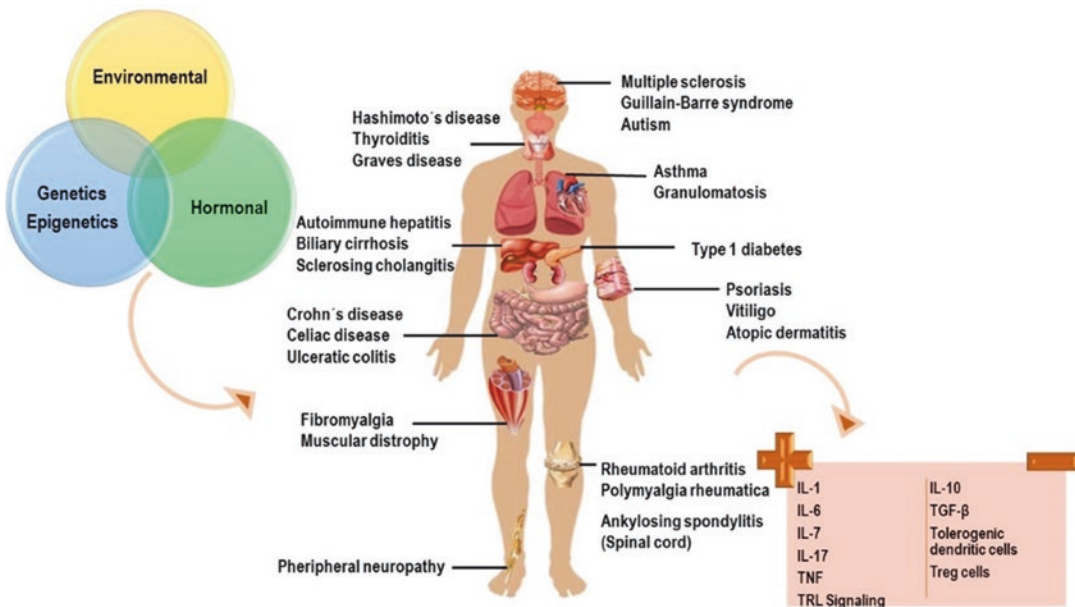
The Discoveries Centre for Regenerative and Precision Medicine, Headquarters at University of Minho, Avepark 4805-017 Barco, Guimarães, Portugal  
e-mail: [nuno@i3bs.uminho.pt](mailto:nuno@i3bs.uminho.pt)

### 8.1 Fundamentals of Advanced Therapies for ADs

According to the American Autoimmune Related Disease Association (AARDA), autoimmune diseases (ADs) consist of a group of more than one hundred pathophysiological conditions. The incidence and prevalence of ADs are both increasing over the last decades [62], affecting 5–10% of the world population, and being women more frequently affected than men [79, 88].

Traditionally, these immune-mediated diseases are divided in two groups, namely into organ-specific and non-organ-specific or systemic ADs [41, 96]. Despite the clinical heterogeneity of ADs even within a single disease variant [21], they are characterized by an inappropriate and harmful immune response against the patient own organs, tissues or cells (Fig. 8.1). The physiological and primary function of the immune system is to protect the organism against diseases. Therefore, this complex system must be able to distinguish self (e.g. cell receptors, hormones and growth factors) from non-self (e.g. viruses, bacteria and toxins) and self-presenting

modifications (e.g. tumor cells and virus infected cells) in order to destroy and debug them [24]. Two major and cooperative pillars are responsible for immunity, namely the innate (inborn) and adaptive (acquired) immune system. Innate immune responses are the first line of defense against pathogens, initiating the host response with posterior activation of the adaptive immune system [90]. The innate system comprises physical barriers (e.g. skin and saliva), several immune cells (e.g. monocytes, macrophages and neutrophils) and soluble factors (e.g. cytokines and chemokines). Unlike the innate defense, the adaptive immune response is highly specific, destroying the invading pathogens and any toxins produced by them. Additionally, it can provide long lasting protection that will allow for a fast defense response in the event of a new contact with that specific pathogen [90]. The adaptive immune system involves T lymphocytes, responsible for cell-mediated immune responses and B lymphocytes, responsible for humoral immune responses [20, 42]. In the last years, it has been described that all individuals present a “healthy level” of autoimmunity, which is essential for the protec-



**Fig. 8.1** Schematic illustration of some ADs in the human body as well as of the factors that can be responsible for their development. ADs can affect a single organ

(organ-specific diseases) or several organs (non-organ-specific or systemic diseases), leading to positive and negative regulation of several signalling biomolecules

tion against the development of degenerative diseases [12]. Moreover, the human body developed specific mechanisms to replace or purge autoreactive B lymphocytes that are produced [113]. Indeed, self-reactivity is by no means rare [118]. Therefore, a disturbance in the homeostasis of those biological processes triggers an abnormal immune response and consequently a debilitating and chronic condition –AD-, by the loss of immunological tolerance to specific self-antigens.

ADs present an enormous disease burden regarding human suffering and economic costs [93]. Common ADs include rheumatoid arthritis, multiple sclerosis, Graves' disease, systemic lupus erythematosus, type 1 diabetes, psoriasis, celiac disease and inflammatory bowel disease. Although the exact etiology of ADs is still unknown, it is well recognized that genetic, epigenetic, hormonal and environmental factors have an important role in the disease susceptibility and progression [24, 70, 73] (Fig. 8.1).

In the last years, a better understanding of ADs immunopathogenesis and increasing knowledge of the immune system led to a dramatic change in the available treatments modalities, aiming generally to control the overactive immune response and inflammation. Unfortunately, a treatment that restores health is still to be developed [79]. However, biological therapies (e.g. monoclonal antibodies), which can target defined pathways of the adaptive immune response have been used in the clinic with satisfactory outcomes [15]. Nevertheless, these therapies are quite expensive and can present severe side effects, such as enhanced patient susceptibility to opportunistic infections or cancer [15]. Therefore, new therapeutic strategies with more efficacy and specificity and avoiding the collateral effects are needed to significantly improve the currently available treatments of ADs.

The design of strategic and effective therapeutic plans should take into account several factors, namely (i) the AD in question and its specific biomarkers; (ii) the clinical stage of the disease; and (iii) the clinical background of the patient comprising the diagnostic tests, the environmental and immunological information, and the treat-

ments previous performed. Therefore, a personalized health care is fundamental to (i) know what, how and when signalling pathways need to be targeted, (ii) improve the therapeutic outcomes, (iii) mitigate toxicity and (iv) prevent succeeding diseases/comorbidities. Additionally, an early diagnosis and onset of treatment is extremely important to minimize, e.g., the damage of organs, the loss of physical mobility and the increased likelihood of death.

Advanced therapy medicinal products (ATMPs) have emerged as promising therapies for ADs, due to their potential to cure severe chronic conditions [45]. Indeed, gene therapy, cell therapy, tissue-engineered medicines or their combination [33] have been considered the health's future and a great opportunity for therapeutic innovation [83]. However, despite the nomenclature of ATMPs was only introduced in 2007 by the European Commission Regulation No 1394/2007, the clinical use of medicinal products based on cells or genes, for example, initiated previously. Indeed, since 1950s that hematopoietic stem cell transplantation has become an established treatment for patients with advanced or refractory diseases [49], becoming in the mid-1990s an accepted therapeutic procedure for patients with severe ADs [51]. Besides hematopoietic stem cells, there are several types of stem cells, such as neural, embryonic and mesenchymal stem cells that provide an unprecedented hope in the treatment of ADs. Table 8.1 presents examples of ATMPs recommended by the European Medicines Agency (EMA) to treat some ADs.

The association of cells with a supporting matrix -scaffold- can be an advantageous solution to maximize their efficacy. Indeed, excluding blood circulating cells, most cells are anchorage-dependent and in the tissues they attach to the extracellular matrix (ECM) [19]. The scaffold provides both the surface and the structural support for the cells to attach, proliferate and differentiate leading to the restoration or regeneration of the defective tissues [18, 19]. Additionally, the scaffolds can be enriched with drugs or growth factors enabling achieving the desired therapeutic effect.

**Table 8.1** ATMPs recommended by the European Medicines Agency for the treatment of ADs [31]

Product description	Disease	Medicinal product classification	Date/status
Allogeneic human glial-restricted precursors (EMA/664954/2017)	Amyotrophic lateral sclerosis	Tissue engineered	14/09/2017
Human umbilical cord blood-derived mesenchymal stem cells (EMA/534881/2017)	Atopic dermatitis	Somatic cell therapy	30/06/2017
Freshly isolated autologous adipose-derived mesenchymal stem cells (EMA/417057/2017)	Autoimmune drug resistant epilepsy	Somatic cell therapy	06/06/2017
Allogenic Wharton's jelly-derived mesenchymal stem cells (EMA/417124/2017)	Amyotrophic lateral sclerosis	Somatic cell therapy	06/06/2017
Bone marrow-derived lineage negative heterogenic stem and progenitor cells (EMA/54559/2017)	Amyotrophic lateral sclerosis in adults	Tissue engineered	19/12/2016
Bone marrow-derived autologous non-haematopoietic stem cells (EMA/758163/2016)	Multiple sclerosis	Tissue engineered	04/11/2016
Bone marrow-derived autologous non-hematopoietic stem cells (EMA/264406/2016)	Type I diabetes	Somatic cell therapy	21/12/2015
Adipose-derived mesenchymal stem cells (EMA/555245/2015)	Rheumatoid arthritis and systemic lupus erythematosus	Somatic cell therapy	26/01/2015
Bone marrow-derived autologous non-hematopoietic stem cells (EMA/264542/2016)	Rheumatoid arthritis	Somatic cell therapy	21/12/2015
Human mesenchymal stem cells-derived from Wharton's jelly tissue of umbilical cord (EMA/240980/2016)	Amyotrophic lateral sclerosis	Somatic cell therapy	27/10/2015
Human mesenchymal stem cells-derived from adipose tissue (EMA/240982/2016)	Amyotrophic lateral sclerosis	Somatic cell therapy	27/10/2015
Human mesenchymal stem cells derived from bone marrow (EMA/240985/2016)	Amyotrophic lateral sclerosis	Somatic cell therapy	27/10/2015

Scaffolds are typically engineered using ceramics and/or polymers. The choice of the material used to produce the scaffold is critical to mediate the biological activity of the cells [18]. Ceramics, such as hydroxyapatite and tri-calcium phosphate, are mainly used for bone tissue engineering and in combination with polymers, to improve their mechanical and biological properties [18]. Regarding their origin, polymers may be classified as natural or synthetic. Both natural and synthetic polymers present advantages and disadvantages in the biomedical field [10, 77], being the concrete application that usually determines which one to use. Natural polymers present chemistry and structure with an inherent affinity with biological systems and with the ECM of many tissues [76]. Moreover, the well-designed molecular structure and unique properties of many natural polymers cannot be reproduced in the lab [110]. Natural polymers can also be modified to improve their characteris-

tics, modulating their chemical, mechanical and bioactive properties [100].

Naturally occurring polymers are produced by living organisms (animals, plants and microorganisms) and can be divided into three major classes according to their chemical structure, namely polysaccharides (e.g. alginate, hyaluronic acid, agarose and cellulose), proteins (e.g. collagen, gelatin, elastin and silk fibroin) and polyesters (e.g. polyhydroxyalkanoates) [3, 116]. Polysaccharides are widely used for cell encapsulation, mainly due to their ability to form hydrogels under mild conditions [30]. Indeed, hydrogels present several interesting properties: (i) enable the mild immobilization of cells and other therapeutic agents, such as drugs and growth factors; (ii) have a predictable swelling and degradation; (iii) enable designing self-assembly systems or devices that can be regulated by environmental parameters, such as pH or temperature; (iv) have a controlled porosity; (v)



enable obtaining homogenous cell distribution; (vi) can be infiltrated by cells after implantation; and (vii) can be administered by injection [6, 19, 103]. Besides cell encapsulation, natural polymers can also be used to develop effective delivery systems for different therapeutic agents [28, 86, 92, 117]. Polymers can also be associated to other natural materials, namely to lipids. Lipids, as natural polymers, are responsible for multiple and essential biological roles in living organisms. These biologically essential organic molecules are, for example, the main components of biomembranes, a storage of energy and important signaling molecules [34]. According to LIPID MAPS Lipid Classification System, lipids can be divided in eight categories – fatty acyls, glycerolipids, glycerophospholipids, sphingolipids, sterol lipids, prenol lipids, saccharolipids and polyketides – that can be further subclassified. Polymer-lipid hybrid systems present unique advantages, for instance as delivery devices allow: (i) the co-encapsulation of therapeutic agents or imaging agents presenting radically different properties, (ii) enhancing the loading capacity of medicines, (iii) a higher control of the release of therapeutic agents, (iv) an increased uptake and intracellular transport of the encapsulated material and (v) circumventing the membrane efflux transporter-mediated multidrug resistance of cancer cells [43, 122]. Lipids can also enable developing valuable delivery systems, such as liposomes, which are successfully used in the clinic. Indeed, liposomes were one of the first delivery carriers approved by the Food and Drug Administration (FDA). The major component of any liposome is phospholipids, but others lipids can be included, like cholesterol as stabilizer [14]. Additionally, as its lipid bilayer resemble the cell membrane, liposomes are also widely used as membrane models [36, 37].

Delivery devices are extremely important, for example, in gene therapy. Indeed, the association of therapeutic agents with appropriate delivery devices that allow their carry, protection and release in a controlled and sustained way, until they reach their target, has led to the “golden era” of medicine. Indeed, several therapeutic agents, such as nucleic acids, peptides and proteins,

should be administered using an appropriate carrier that allows enhancing their therapeutic efficacy by increasing their half-life (e.g. by avoiding their physical denaturation or proteolytic degradation) and ensuring the preservation of their active form. Indeed, the development of a delivery system that increases the therapeutic index of bioactive agents will dramatically improve the patients’ quality of life.

---

## 8.2 Advanced Therapies

The therapeutic target of the ADs is the dysregulated immune system. The long-term administration of conventional treatments can lead to high toxicity and susceptibility of the patients to develop other opportunistic infections. The reduced capacity of the immune system drastically affects the patient’s quality of life. Therefore, there is an urgent need of advanced, innovative and more effective treatments to give a new hope to millions of patients’ worldwide suffering with ADs. In the last years, intense research efforts were directed to new therapies able to (i) specifically target the autoreactive cells, without compromising the normal function of the immune system; (ii) restore the immune tolerance over time, avoiding the necessity of long-term immunosuppressant therapies; (iii) have reduced or no toxicity and side effects and (iv) be more cost-effective than the current therapeutic approaches [94]. We will review the literature reporting the latest advanced therapies with biomaterials for ADs.

### 8.2.1 Gene-Based Therapies

Gene therapy is based on the therapeutic delivery of genetic material (e.g. plasmid DNA –pDNA, complementary DNA –cDNA, small interfering RNA –siRNA, short hairpin RNA –shRNA, and microRNA –miRNA), being a promising strategy for several pathologies, including ADs. The general mechanism of action of these functional genes comprises the inactivation or replacement of the defective gene in the target cells [99]. The

first successful transfer of a functioning gene into a living mouse was performed in 1980 by Martin Cline, however only about 10 years later was successfully performed the first gene transfer in humans. In the last decade, gene therapy research has been greatly expanded due to the promising results in ameliorating disease progression and symptoms in several animal models [87, 115]. However, despite its potential, only in 2017, the first gene therapy was approved by FDA. This strategy, which aims to treat blood cancers, such as leukemia, is based on the genetically reprogramming of patients' immune cells, namely T-cells, with a gene that contains a protein called a chimeric antigen receptor (CAR). This protein will allow the binding of T-cells with leukemia cells presenting at their surface the antigen CD19, leading to their killing. This treatment is also awaiting approval for lymphoma. Indeed, it is anxiously expected that new approaches follow the same trend for other serious and life-threatening diseases. However, gene therapy does not necessarily have to serve as an alternative to conventional therapies but instead may complement and improve them.

Clinical trials comprehending gene therapy have been recently completed or are ongoing to find new solutions for ADs, such as NCT00185848 and NCT02727764 for rheumatoid arthritis, NCT00617032 and NCT00126724 for psoriatic arthritis or ankylosing spondylitis, NCT02404298 for Clarkson Syndrome and muscular ADs and NCT02769767 for multiple sclerosis. In ADs, gene therapy aims to regulate the proinflammatory cytokines or molecule levels and the local infiltration of lymphocytes through the delivery and expression of therapeutic genes in the target cells [99].

The efficient and specific intracellular delivery of the genetic material in the target cell is a key point to obtain the desired therapeutic effect. Since genetic material cannot freely cross cell membranes, appropriate delivery systems are required to facilitate its access to the desired intracellular site of action. Additionally, the use of delivery systems is very important to protect genes from chemical and enzymatic degradation by nucleases, to increase their half-life in blood

circulation, to provide their specific delivery into the cytoplasm and nucleus of the target cells and also to provide an escape from endosomal and/or lysosomal degradation [40, 125].

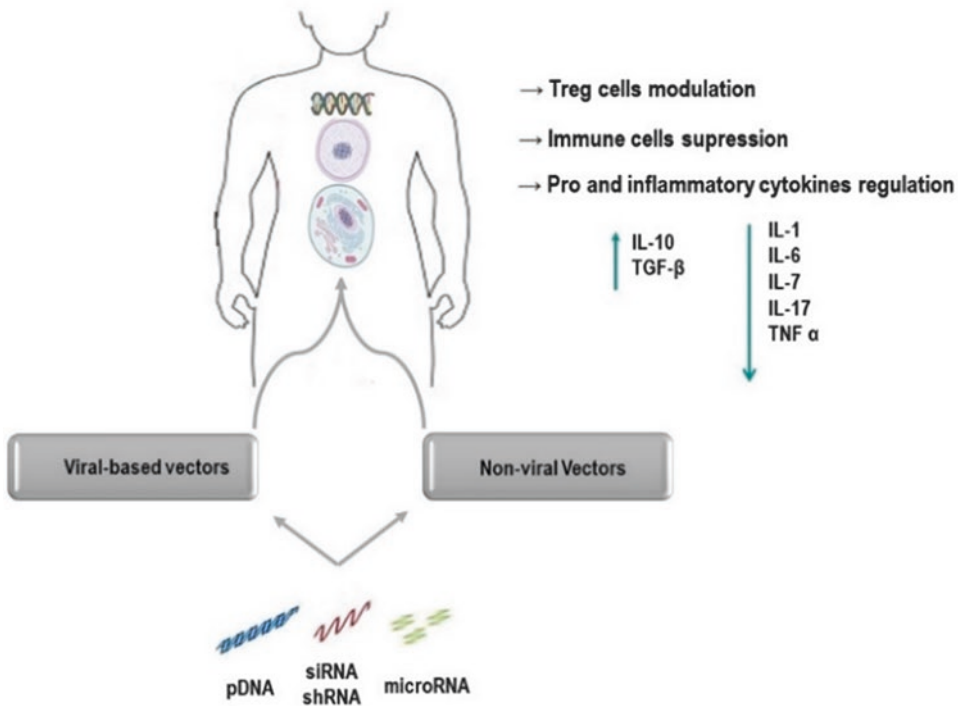
To cross the cell membrane and ultimately to reach the cell nucleus, genetic material can be incorporated in (i) viral-based vectors to deliver exogenous transgenes and introduce those genes in the host cell, allowing their replication along with the host DNA during the S phase of mitosis, usually in actively dividing cells and (ii) non-viral vectors to deliver exogenous transgene by nonintegrating vectors predominantly in postmitotic cells (e.g., neurons, muscle fibers, and hepatocytes) [59] (Fig. 8.2). To produce non-viral vectors, natural biomaterials with low toxicity and immunogenicity are highly recommended [28]. The biomaterials used for gene delivery are essentially cationic polymers or lipids, which are consequently positively charged, and easily conjugated with the negatively charged nucleic acids due to electrostatic interactions [27, 111].

The gene-based therapies for the management and possible treatments of ADs comprise a range of different and innovative approaches that will be further discussed.

### 8.2.1.1 Viral-Based Vectors

The use of viral-based vectors to deliver genetic material for ADs is mainly focused in adenovirus and retrovirus, such as lentivirus. Viral vectors are based on modified or inactivated virus, where areas of its genome suffered a modification or depletion leading to a modified replication and a safer virus. This strategy is one of the most used tools to effectively deliver transgenes. Relatively to non-viral vectors, viral vectors present the advantage of having a relatively higher transfection capacity only with a single administration. In this sense, virus particles act as "natural" adjuvants to efficiently deliver genetic materials to cells [59].

Apart from their advantages, the use of viral vectors in patients can be accompanied with some potential risks. Indeed, the immunogenicity of viral vectors can induce inflammatory responses leading to degeneration and toxin production, and ultimately to death [67]. Additionally,



**Fig. 8.2** Schematic illustration of the gene therapy approaches used in the management of ADs

the risk of integration of the virus DNA into the host genome is a theoretical concern. Consequences of this integration are the occurrence of mutations, which can lead to tumorigenesis [101] and the transactivation of neighboring genome sequences. Other limitation of these vectors includes the concentration of them that is necessary to obtain a transgenic capacity. Indeed, virus concentrations many orders of magnitude higher than those encountered in natural infections are needed to achieve the desired transfection [1, 38, 124]. Despite these concerns, these vectors are widely used due to their undoubtedly high transfection capacity. However, their use should take into account patients' condition, such as severity and progression of disease.

The use of viral vectors for ADs will be further discussed providing the latest research advances.

### Lentiviral Vectors

Lentiviruses belong to the family of retrovirus and are reported as alternative therapeutic strate-

gies for ADs. An example of them is the human immunodeficiency virus (HIV). Lentiviruses are virus with long incubation times, with a suitable stability and with a unique ability to translocate across the nuclear membrane and infect nondividing cells [13, 97]. This ability is, therefore, particularly useful for gene transfer to nondividing cells, such as monocytes, neurons and antigen presenting cells (APCs) [85, 120].

The use of lentivirus to suppress or activate genes for the regulation of immune responses in ADs is the main strategy adopted. A study performed by Liu and co-workers [69] demonstrated that regulating calcium entry through CRACM1 (the pore-forming subunit of calcium release-activated calcium (CRAC) channels; also known as ORAI1) may be beneficial for the management of rheumatoid arthritis. For that purpose, it was used a shRNA-based lentivirus in order to *in vivo* suppress the CRACM1 gene expression and activation. This gene is associated with the growth and proliferation of T cells, B cells and osteoclasts, being important cellular targets in

rheumatoid arthritis treatment. The results suggested that the silencing of CRACM1 reduced local inflammation through the reduction of inflammatory cytokines (IL), such as IL-6, IL-17, and interferon- $\gamma$  (IFN- $\gamma$ ). Lentivirus also revealed potential for the *in vivo* carry of miRNA-873 as a new approach to treat systemic lupus erythematosus [68]. Indeed, in those patients, the expression of miRNA-873 that can facilitate the differentiation of CD4<sup>+</sup> T cells into Th17 lineage (responsible for the expression of inflammatory ILs) is up-regulated. It is known that the gene Forkhead boxO1 (Foxo1), that is a Th17 suppressor, regulates that differentiation. Thus, this study demonstrated that Foxo1 is a target of miR-873 in regulating inflammatory responses in systemic lupus erythematosus. After *in vivo* gene transfection, it was observed an attenuation of the disease severity. Other example includes the use of lentivirus to silence a gene, namely B7-2, in a pristine-induced mouse model of lupus nephritis. This gene is present in APCs and is involved in the regulation of the regulatory T (Treg) cells. The silencing of B7-2 gene resulted in the attenuation of the over-activity of splenic immune cells, including macrophages, dendritic cells, granulocytes and B-cells. Overall, the progression of the disease reflected in the secretion of ILs, immune complexes accumulation/deposition in kidneys, and the renal inflammatory damage were relieved compared to the control group. Thus, the lentivirus was efficient in the transfection and these results suggest an opportunity for delaying the progression of lupus-like diseases [57].

### Adenoviral Vectors

Adenoviruses are being studied as effective gene delivery vectors for ADs. This virus presents a protein capsid with a DNA genome, encoding ~20 proteins, without the lipid envelope [105]. These proteins are expressed in viral DNA replication and present regulatory functions promoting the virus control of the cell. The use of adenoviral vectors is mainly correlated with its genetic stability, well-defined biology, the suitable transfection of cells and the possibility to be produced in large scale [26]. Adenovirus presents a higher transfection capacity and consequently

higher transgene expression than other virus vectors (e.g. retrovirus) since that most human cells express the primary adenovirus receptor and the secondary integrin receptors.

The generality of adenovirus vectors are genetically modified versions of the human Adenovirus 5. Despite their use in treatment, these vectors are also being currently used for induction of ADs in animal models, such as autoimmune hepatic fibrogenesis [46], autoimmune myocarditis [2] and Grave's diseases [47]. These vectors have been revealed a relatively safe and effective profile. For example, these vectors were used in an *in vivo* model of experimental autoimmune encephalomyelitis (EAE). Specifically, the delivery of IL-23 receptor cDNA was performed by the adenovirus 5 in order to block its interaction with IL-23, which is a key molecule in maintaining the response mediated by Th17 cells. The results showed that the adenovirus was able to promote *in vitro* and *in vivo* transfection. *In vivo* results also confirmed the transgene expression [81].

In type 1 diabetes, an *in vivo* model of non-obese diabetic (NOD) mice was treated with anti-CD20 and an adenoviral vector-mediated interleukin-10 therapy [109]. This combination seems to benefit the expression of Treg cells and several ILs involved in the pathogenesis of diabetes (e.g. IL-4, INF- $\gamma$ ). Additionally, this approach was able to protect pancreatic islet cells, since that the treated mice group presented higher C-peptide. This molecule is a precursor of insulin that directly reflects the function of pancreatic  $\beta$ -cells. Furthermore, the Th1/Th2 imbalance was reversed, being this cell ratio often associated with ADs. Thus, this approach revealed to be a promisor treatment for type 1 diabetes.

In autoimmune myocarditis, an adenovirus vector was used to deliver antisense CIITA. CIITA is a transcriptional coactivator that acts as a key regulatory factor of the major histocompatibility complex (MHC)-II expression, which is related with the induction of immune responses. The results shown that 21 days after immunization, both groups of mice (preventive and treatment) presented a suitable transfection and a higher

expression of MHC-II in mice heart tissues than in other tissues (e.g. spleen) [16].

### 8.2.1.2 Non-viral-Based Vectors

Non-viral-based vectors can overcome the limitations of the above mentioned viral-based vectors, namely the risks associated with the use of virus in therapies. During the past 20 years, the focus of research and development has been driven toward the development of vectors that could combine low genotoxicity and immunogenicity with high efficient delivery. Although viral vectors continued to be developed for multiple indications, there is an effort to develop non-viral vectors to overcome the risks of viral-vectors, as already mentioned, that can greatly limit their acceptance in clinical trials. Additionally, non-viral vectors are more cost-effective than viral vectors. The main drawback associated with the non-viral-based vectors is their lower transfection efficiency into the cell nucleus and lower loading capacity of genes than the viral vectors. Thus, a balance of these advantages and limitations should be taken into account in order to select the ideal vector. Non-viral vectors can be developed from a range of biocompatible and biodegradable materials, including natural polymers and lipids (cationic liposomes).

### Natural Polymer-Based Vectors

Chitosan is the most common naturally derived cationic polymer used for gene therapy. This natural cationic polymer is described as safe due to its reported *in vitro* and *in vivo* biocompatibility. Additionally, it can be combined with other natural polymers (e.g. dextran, collagen, gelatin, cellulose, and cyclodextrin) to modulate its properties. A study using thiolate glycol chitosan nanoparticles to deliver a Notch1 targeting siRNA (siRNA-NPs) [54] reported their anti-inflammatory effect in a collagen-induced arthritis model [61]. This signaling receptor is associated with the regulation of inflammatory responses in rheumatoid arthritis. The *in vivo* results showed an accumulation of the particles in the synovial joints. It was also highlighted that the use of the siRNA-NPs can avoid side effects associated with the  $\gamma$ -secretase inhibitor and the

non-specific Notch1 inhibition in undesired tissue sites. The same combination of polymers was used to carry siRNA for *in vivo* targeting of tumor necrosis factor  $\alpha$  (TNF- $\alpha$ ), using the previously referred collagen-induced arthritis model [61]. The suppression or neutralization of TNF- $\alpha$  will down-regulate the systemic inflammation observed in ADs. The siRNA/thiolated glycol chitosan particles after systemic injection into mice were rapidly and selectively accumulated in the arthritic joints. The developed particles were able to suppress paw swelling and progressive joint destruction. Another study revealed the ability of chitosan-based particles to transfect astrocytes isolated from healthy and EAE-induced B6 mice [56]. This study demonstrated a different cell permeability and transfection efficiency of large-sized particles in astrocytes. These differences were attributed to the polymer/DNA ratio, suggesting that higher ratio means that DNA was more compactly wrapped by chitosan, forming a particle presenting a smaller diameter and a high positive charge.

Another target for ADs treatment is the transcription factor nuclear factor-kappa B (NF- $\kappa$ B), which is associated with the production of inflammatory mediators. To deliver this transcription factor, Wardwell and co-workers [119] designed N-trimethyl chitosan-polysialic acid nanoparticles coated with decoy oligodeoxynucleotides. The results showed that these particles provide suitable stability for nucleic acid and facilitate cellular penetration in human synovial sarcoma cells, an *in vitro* model of rheumatoid arthritis. In another study, chitosan nanomicelles modified with oleic acid and linoleic acid (nanomicelle-based polyplexes) were used to prevent autoimmune diabetes [75]. For that, the nanomicelle-based polyplexes carried a plasmid DNA for encoding IL-4 and IL-10 in a streptozotocin induced diabetic mouse model. The results revealed the transfection capacity of this system in pancreatic islets of the animals. Additionally, the animals treated with plasmid DNA in chitosan nanomicelles, showed significantly lower blood glucose levels and higher ILs expression compared to the control group. Therefore, this study revealed the ability of chito-

san nanomicelle-based polyplexes to protect the pancreatic islets from insulinitis.

### Cationic Liposomes

Cationic liposomes are one of the most promising non-viral vectors for the delivery of therapeutic genes. They are usually produced using cationic lipids mixed or not with neutral phospholipids. The incorporation of neutral lipids in the cationic liposome formulations promote a higher rate of transfection, which can be modulated by the ratio of cationic/neutral lipid used [29]. The positive charge of cationic liposomes will allow for their complexation with nucleic acids (negatively charged) forming the lipoplexes (cationic liposome–gene complexes). The development of negatively charged liposomes has also been considered, being in this case the nucleic acid complexed with a positively charged polymer [60].

Despite the synthetic cationic lipids being more frequently used, efforts have been made in the last decades to develop gene carriers derived from natural resources. For that, natural lipids (e.g. phospholipids and steroids) are linked to amine-containing cationic groups (e.g. amino acids and polyamine) to develop new biocompatible cationic lipids [11].

There are several studies reporting cationic liposomes-mediated transfection both *in vitro* and *in vivo* [25, 35], but no clinical product has yet emerged. Rheumatoid arthritis is an example of an AD where cationic liposomes were used to reduce the cytosolic phospholipase A2 $\alpha$  (cPLA2 $\alpha$ ) expression [25]. The siRNA-mediated cPLA2 $\alpha$  gene silencing in mice with collagen-induced arthritis resulted in a reduction of the disease severity, demonstrating the therapeutic potential of the developed delivery system. A similar liposome composition was used to demonstrate the silencing specificity of three pro-inflammatory cytokines (IL-1, IL-6, and IL-18) in the same animal model previously referred of rheumatoid arthritis [53]. This siRNA-based immunotherapy preferentially targeted monocyte/macrophage cells and led to a reduction of the disease severity, including inflammation and joint destruction. In a general approach to prevent

the inflammatory component of many diseases, such as in atherosclerosis (recent data reports its autoimmune nature [58]), Leuschner and co-workers [63] developed a lipid nanoparticle to carry siRNA for silencing the expression of the chemokine receptor CCR2 responsible for the migration of the inflammatory monocyte subset. Regarding atherosclerosis, after administration of the developed formulation in the diseased mice, the number of atherosclerotic plaques and the infarct size after coronary artery occlusion were reduced.

Considering the previous examples, it is possible to conclude that gene therapy through the use of viral and non-viral vectors is a valid and promising strategy to deliver specific genes into the target cells. The main aim of gene therapy, as previously referred, is to control the immune responses, by silencing or by attenuating the expression of genes involved in the pathophysiology of the disease (Fig. 8.2). These genes are therefore, mainly related with the regulation of immune cells and ILs, which modulate the immunological responses observed in ADs.

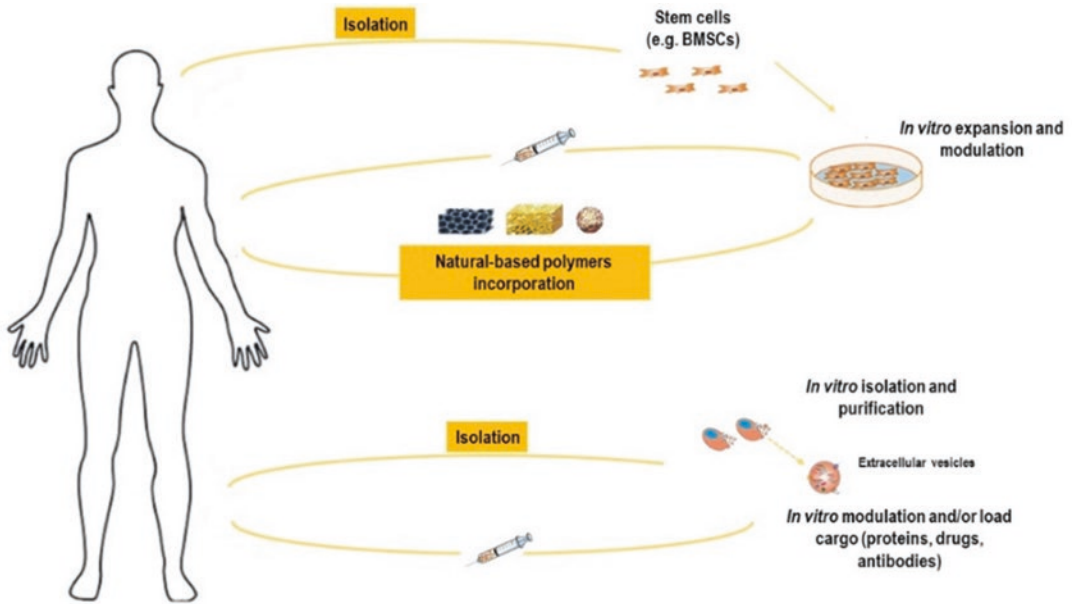
---

## 8.3 Cell-Based Therapies

Cell therapies for ADs are gaining increased interest. Frequently, the transplantation of autologous cells is preferred to avoid non-desirable immune responses. For that, the cells are isolated from the patients and further manipulated for posterior injection (Fig. 8.3). The administration of the cells can be advantageously performed through scaffolds or delivery systems. We will summarize some of the current strategies that are being investigated regarding cell or cell-derived vesicles (extracellular vesicles) therapies for the treatment of ADs.

### 8.3.1 Stem Cells

Stem cells are widely studied to treat, regenerate and restore biological functions of tissues and cells [76, 89]. Its clinical impact has already been demonstrated in bone marrow transplants and



**Fig. 8.3** Schematic illustration of the cell therapies that can be used for the treatment of ADs. Those strategies comprehend the use of autologous stem cells and EVs which are manipulated and further injected into the patients

blood transfusion procedures routinely performed for many decades [4]. Stem cells present the inherent ability of self-renewal and capacity to differentiate into several cell lineages. This feature is important for the natural replacement of aged or apoptotic cells as well as for the regeneration of damaged tissues. Additionally, stem cell differentiation can be induced with several growth factors or interleukins that are expressed by the desired cells. The potential of stem cells for the treatment of ADs is based on their ability to reduce the inflammation, to modulate the immune response and tolerability and to stimulate the regeneration of the damaged tissues [108]. Table 8.2 presents ongoing and completed clinical trials using stem cells for ADs.

Mesenchymal stem cells (MSCs) are one of the most promising adult stem cell types for developing new therapies. MSCs can be isolated from adipose tissue (ADMSCs) or bone marrow (BMSCs). Even though BMSCs have been providing promising results in several studies (Table 8.2), ADMSCs are also an attractive source for autologous stem cell therapies given its abundance. Adipose tissue contains a higher number of MSCs than bone marrow, which can

be easily obtained using minimally invasive procedures [91]. The differentiation and immunomodulatory potencies of ADMSCs are reported to be equivalent to those of BMSCs [64]. Indeed, allogeneic ADMSCs were able to ameliorate autoimmune diabetes in diabetic NOD mice by attenuating the Th1 immune response concomitant with the expansion/proliferation of Tregs [8]. This result highlights the ability of those cells to maintain the function of  $\beta$ -cells and also to be immune regulatory. In a study involving co-transplantation of islets with ADMSCs obtained from the adipose tissue of chronic pancreatitis patients, it was obtained an improvement of islet survival and function [102]. Autologous ADMSCs were also used in the clinical treatment of patients with multiple sclerosis, where it was revealed their safety and ability to reduce the progression of the disease during 1 year [104]. ADMSCs also showed beneficial therapeutic effects on the peripheral blood mononuclear cells of rheumatoid arthritis patients [5]. Indeed, they were able to reduce inflammation by inhibition of IL-17 and IL-21 effects.

As already mentioned, the use of stem cells alone is beneficial, however it is advantageous

**Table 8.2** Clinical trials involving cell therapies for the treatment of ADs and performed in the last 3 years [23]

Disease	ID	Study designation	Phase	Country	Latest update
Multiple sclerosis	NCT174583	Autologous BMSC administered intravenously in patients diagnosed with multiple sclerosis	I/II	Spain	2018
Autoimmune neurologic diseases	NCT00716066	Carmustine, etoposide, cytarabine, melphalan, and antithymocyte globulin followed by peripheral blood stem cell transplant in treating patients with autoimmune neurologic disease that did not respond to previous therapy	II	USA	2017
Type 1 diabetes mellitus	NCT02644759	Transplantation of autologous stem cells for the treatment of type 1 diabetes mellitus	I/II	Arabia	2017
Multiple sclerosis	NCT00273364	Stem cell therapy for patients with multiple sclerosis failing alternate approved therapy- a randomized study	III	USA	2017
Systemic lupus erythematosus/rheumatoid arthritis/sharp's syndrome	NCT02741362	Safety and efficacy of adipose derived stem cells in refractory rheumatoid arthritis, systemic lupus erythematosus or sharp's syndrome	I	USA	2017
Type 1 diabetes mellitus	NCT00315133	Safety and efficacy study of autologous stem cell transplantation for early onset type 1 diabetes mellitus	I/II	Brazil	2017
Systemic lupus erythematosus	NCT03171194	Phase I MSC for systemic lupus erythematosus	I	USA	2017
Autoimmune skin diseases	NCT02824393	Experimental autologous MSC therapy in the treatment of chronic autoimmune urticaria	I	Turkey	2016
Systemic lupus/ erythematosus systemic sclerosis	NCT00849745	Nonmyeloablative allogenic stem cell transplant for severe ADs	I	USA	2016
Multiple sclerosis	NCT01099930	Autologous stem cell transplant for multiple sclerosis	II	Canada	2016
Systemic sclerosis/systemic lupus erythematosus/dermatomyositis/juvenile rheumatoid arthritis	NCT00010335	Pilot study of total body irradiation in combination with cyclophosphamide, anti-thymocyte globulin, and autologous CD34-selected peripheral blood stem cell transplantation in children with refractory autoimmune disorders	I	USA	2015
Autoimmune diseases of the nervous system/multiple sclerosis	NCT01056471	Autologous ADMSC in patients with secondary progressive multiple sclerosis	I/II	Spain	2015



their association with biomaterials. After the isolation of the cells and their *in vitro* expansion, the cells can be attached or incorporated in different substrates. The local delivery of cells in an adequate time frame will determine their efficient engraftment [82]. The biomaterials should be biodegradable, biocompatible and provide excellent stability. For that, natural polymers are usually chosen since they present excellent characteristics.

A strategy involving the co-encapsulation of BMSCs and mouse pancreatic  $\beta$  cells in alginate-chitosan-alginate microcapsules was developed to treat diabetic mice [71]. The results revealed an increased insulin secretion approximately 28 days after transplantation and a reduction of the blood glucose levels. Alginate was also used to deliver human embryonic stem cell (hESC)-derived beta cells for treating type 1 diabetes with promising results. Alginate was able to protect against foreign body reactivity in immune-competent mice at least for 6 months [84]. Various cell-based replacement therapies for type 1 diabetes are based in the generation of insulin-producing cells from MSCs. To promote their differentiation, scaffolds based in polyvinyl alcohol (PVA) and platelet-rich plasma (PRP) [32], or collagen/hyaluronic acid [52] were used. The use of these biomaterials as substrate for stem cells as well as of the described differentiation methodologies, revealed to be able to promote stem cells differentiation into insulin-producing cells.

Although the combination of stem cells with natural polymers is being useful for ADs treatment, there are very few examples of successful application of this strategy. The main applications are based on the treatment of the symptoms and not of the causes of those diseases. Additionally, the ADs chronicity character requires innovative interventions to avoid the progression of the associated injuries. Therefore, the use of stem cells combined with natural polymers for modulating the immune system is still a growing strategy that can provide new alternatives in the future for the treatment of ADs.

### 8.3.2 Extracellular Vesicles

Extracellular vesicles (EVs) promote the intercellular communication and are able to transfer their cargo, including proteins, lipids and RNAs, between cells [50]. EVs are small vesicles (50–1000 nm) released by various cells by exocytosis and present a lipid bilayer structure, formed by the fusion of multivesicular bodies with the plasma membrane [80]. In recent years, it was recognized the involvement of those vesicles, such as microvesicles and exosomes, in immune signaling and inflammation. Indeed, it was already described the ability of EVs to suppress inflammation and to control the Treg cells through genetically modification of bone marrow-derived dendritic cells (BMDC) [17, 55]. These achievements demonstrate the promising use of these vesicles as immunotherapeutics, but more research is needed to understand their role in modulating immune responses.

EVs represent an important tool for both diagnostic and therapeutic purposes due to the singular ability to interact with the recipient cells. These vesicles present the faculty to attach to target cells by a range of surface adhesion proteins and vector ligands (e.g. integrins, tetraspanins, CD11b and CD18 receptors), and deliver their cargo to target cells [9, 112]. Likewise, according to their characteristics and origin, the EVs demonstrate a specific cell tropism, i.e. a natural ability to target a specific cell [121]. Since MSCs have shown suppressive effects on many types of immune cells both *in vitro* and *in vivo*, MSC-derived EVs are been investigated for ADs. For example, MSC-derived EVs had shown ability to inhibit the activation of antigen-presenting cells (APCs) and to suppress the development of T helper 1 (Th1) and Th17 cells, attenuating the immune response in diabetes and uveoretinitis animal models [98]. The capacity of MSC-derived EVs to inhibit the migration of inflammatory cells in a uveitis model was also demonstrated [7]. Other studies also revealed that hBMSC-derived EVs have the potential for driving the osteogenic differentiation, without any chemical or genetic osteoinductor [78], illustrating their

potential for regenerative medicine. EVs can also be loaded with specific cargo that can be directly introduced on them [48] or obtained by modulation of their producer cells. As already mentioned, EVs can exhibit strong potential to regulate immune responses and therefore the encapsulation of therapeutic agents on them can promote synergistic therapeutic effects [106]. For instance, EVs encapsulating curcumin were used as a strategy to treat brain inflammatory diseases [126]. In this study, their ability to target and to be internalized by microglial cells, inducing subsequently their apoptosis was demonstrated.

Despite EVs being mainly proposed as promising candidate biomarkers, more research regarding their potential therapeutic use for ADs is being developed. Because of their heterogeneity, the analysis and isolation of a pure population of EVs is complex. However, their potential in future therapies for ADs relies in the capacity to use them as reliable sources of self-antigens enabling inducing specific tolerance to those self-antigens by the immune system. Thus, EVs clearly need to be further investigated to develop their full potential in innovative ADs therapies.

In summary, the use of cell therapies (or cell-derived vesicles) for ADs is a promising approach mainly due to their ability to restore the normal immune system as well as to regenerate the damaged tissues. Indeed, their therapeutic potential has been demonstrated in several clinical trials. Thus, in the upcoming years, it is believed that clinical cell-based therapies will become a reality for ADs patients.

### 8.3.3 Stem Cell-Based Gene Therapy

Stem cell-based gene therapy meets the advantages of the stem cell and gene therapies and can provide synergistic effects in the treatment of ADs [95]. Indeed, stem cell therapy is a promising strategy to overcome the limitations of the current treatment methods, but to attain its full therapeutic potential may be necessary to adjust or modify the cell properties. For that, genetic engineering is very appealing. In this sense, stem

cells can be transfected *in vitro* using similar methods to those used in direct gene transfer, such as genetically-engineered viruses (e.g. lentivirus and adenovirus) and nano- or microparticles (e.g. cationic liposomes). These methods should not compromise the immunological properties of the engineered cells neither elicit a strong immune response after their transplantation [22, 44, 114]. Therefore, instead of a direct gene transfer, as referred before, in this therapeutic approach the genes of interest will be delivered using living cells. The major advantage of the *in vitro* genetic manipulation of cells is to have a higher control of the process than *in vivo*. Additionally, the use of stem cells as vectors for genes will allow an efficient and stable endogenous gene expression and will circumvent the *in vivo* short half-life of exogenously expressed genes [72].

There are several and promising examples in the literature using stem cell-based gene delivery in ADs treatment. For instance, in a general approach for ADs treatment, Hajizadeh-Sikaroodi and co-workers [44] genetically engineered ADMSCs for IL-17 suppression through expression of IL-27. Therefore, after *in vitro* transduction of the ADMSCs with two subunits of IL-27 included in a lentiviral vector, the cells were able to express high levels of functional IL-27.

To treat multiple sclerosis, Makar and co-workers [74], for example, explored the therapeutic potential of brain-derived neurotrophic factor (BDNF) gene transfected BMSCs in EAE mice, an animal model of multiple sclerosis. In mice that received the genetically engineered BMSCs, the EAE onset was significantly delayed and the clinical severity was greatly reduced in comparison with control receiving BMSC transfected with an empty vector lacking the BDNF gene. In the same animal model, the effect of the human ciliary neurotrophic factor (CNTF)-overexpressed MSC therapy was also explored [39]. As observed in the previous study, the intravenous injection of MSCs transfected with the CNTF gene led to a remarkable neuronal functional recovery in the EAE mice.

Genetically engineered stem cells led to promising outcomes in type 1 diabetes. BMSCs expressing human insulin gene were transplanted in a mice model of type 1 diabetes to reduce the clinical manifestations of this AD [123]. The human insulin gene transfected BMSC therapy was able to increase the body weight and to significantly reduce the blood glucose levels. The same animal model was used to evaluate the effect of betatrophin (hormone that increases the expansion of insulin-secreting  $\beta$ -cells and production of insulin) overexpression by human ADMSCs [107]. The transplantation of these genetically modified stem cells was also able to ameliorate the hyperglycemia and weight loss as well as to increase the ratio of  $\beta$ -cells per islet. Human and rat ADMSCs were also transduced with pancreatic duodenal homeobox 1 (PDX-1) gene to obtain insulin-producing cells [66]. Indeed, the transplantation of ADMSC-expressing PDX-1 in diabetic rats enables increasing the levels of insulin in response to increasing concentrations of glucose. The same gene was introduced in human BMSCs by Li and co-workers [65]. As observed for ADMSCs, the genetically modified BMSCs were able to differentiate into insulin-secreting cells, constituting, therefore, another possible cell source for the treatment of type I diabetes.

## 8.4 Concluding Remarks

The current therapeutic approaches for ADs are mostly directed to control the immune response. This can be accomplished by the suppression or induction of tolerance by the immune cells involved in the autoimmunity and by the positive or negative regulation of ILs and related biomolecules. However, there is still no effective cure for the ADs. The major challenges in the development of effective therapies for ADs are to increase the target specificity and to reduce the immunological adverse events associated to the treatment. Advanced therapies are gaining an enormous interest mainly due to the potential to generate specific and highly effective therapeutic strategies overcoming the limitations of currently

available therapies. Additionally, the association of genes and/or cells with natural-based biomaterials can boost their therapeutic efficiency. The discussed strategies revealed being promising for the regulation of the deregulated immune response using different mechanisms and targets. Some advanced therapies are already in clinical trials and can induce long-term remissions. It is expected that these advanced and innovative approaches will become alternatives to conventional therapies for the management and eventually for the cure of ADs.

**Acknowledgements** The authors wish to acknowledge the *Programa Operacional Norte 2020* under the research project FRONThERA (NORTE-01-0145-FEDER-000023) and the Fundação para a Ciência e Tecnologia do Ministério da Ciência e Tecnologia (FCT, Portugal) under the research project SPARTAN (PTDC/CTM-BIO/4388/2014).

## References

1. Aiuti A, Cossu G, de Felipe P, Galli MC, Narayanan G, Renner M, Voltz-Girolt C (2013) The committee for advanced therapies' of the European Medicines Agency reflection paper on management of clinical risks deriving from insertional mutagenesis. *Hum Gene Ther Clin Dev* 24(2):47–54. <https://doi.org/10.1089/humc.2013.119>
2. Anna-Maria M, Andrea F, Hugo AK, Ziya K (2015) Mouse models of autoimmune diseases -autoimmune myocarditis. *Curr Pharm Des* 21(18):2498–2512. <https://doi.org/10.2174/1381612821666150316123711>
3. Aravamudhan A, Ramos DM, Nada AA, Kumbar SG (2014) Chapter 4: Natural polymers: polysaccharides and their derivatives for biomedical applications natural and synthetic biomedical polymers. Elsevier, Oxford, pp 67–89. <https://doi.org/10.1016/B978-0-12-396983-5.00004-1>
4. Atkins HL, Bowman M, Allan D, Anstee G, Arnold DL, Bar-Or A, Freedman MS (2016) Immunoablation and autologous haemopoietic stem-cell transplantation for aggressive multiple sclerosis: a multicentre single-group phase 2 trial. *Lancet* 388(10044):576–585. [https://doi.org/10.1016/S0140-6736\(16\)30169-6](https://doi.org/10.1016/S0140-6736(16)30169-6)
5. Baharlou R, Ahmadi-Vasmehjani A, Faraji F, Atashzar MR, Khoubyari M, Ahi S, Navabi SS (2017) Human adipose tissue-derived mesenchymal stem cells in rheumatoid arthritis: regulatory effects on peripheral blood mononuclear cells activation. *Int Immunopharmacol* 47:59–69. <https://doi.org/10.1016/j.intimp.2017.03.016>

6. Bahram M, Mohseni N, Moghtader M (2016) An introduction to hydrogels and some recent applications. In: Majee SB (ed) Emerging concepts in analysis and applications of hydrogels. InTech, Rijeka, p Ch. 02. <https://doi.org/10.5772/64301>
7. Bai L, Shao H, Wang H, Zhang Z, Su C, Dong L, Zhang X (2017) Effects of mesenchymal stem cell-derived exosomes on experimental autoimmune uveitis. *Sci Rep* 7(1):4323. <https://doi.org/10.1038/s41598-017-04559-y>
8. Bassi ÊJ, Moraes-Vieira PMM, Moreira-Sá CSR, Almeida DC, Vieira LM, Cunha CS, Câmara NOS (2012) Immune regulatory properties of allogeneic adipose-derived mesenchymal stem cells in the treatment of experimental autoimmune diabetes. *Diabetes* 61(10):2534–2545. <https://doi.org/10.2337/db11-0844>
9. Batrakova EV, Kim MS (2015) Using exosomes, naturally-equipped nanocarriers, for drug delivery. *J Control Release* 219:396–405. <https://doi.org/10.1016/j.jconrel.2015.07.030>
10. Bhatia S (2016) Natural polymers vs synthetic polymer. In: Springer C (ed) Natural polymer drug delivery systems. Springer, Cham. <https://doi.org/10.1007/978-3-319-41129-3>
11. Bhattacharya S, Biswas J (2010) Understanding membranes through the molecular design of lipids. *Langmuir* 26(7):4642–4654. <https://doi.org/10.1021/la9011718>
12. Blach-Olszewska Z, Leszek J (2007) Mechanisms of over-activated innate immune system regulation in autoimmune and neurodegenerative disorders. *Neuropsychiatr Dis Treat* 3(3):365–372 ISSN: 1176-6328
13. Blessing D, Déglon N (2016) Adeno-associated virus and lentivirus vectors: a refined toolkit for the central nervous system. *Curr Opin Virol* 21:61–66. <https://doi.org/10.1016/j.coviro.2016.08.004>
14. Briuglia M-L, Rotella C, McFarlane A, Lamprou DA (2015) Influence of cholesterol on liposome stability and on in vitro drug release. *Drug Deliv Transl Res* 5(3):231–242. <https://doi.org/10.1007/s13346-015-0220-8>
15. Bruno V, Battaglia G, Nicoletti F (2011) The advent of monoclonal antibodies in the treatment of chronic autoimmune diseases. *Neurol Sci* 31(3):283–288. <https://doi.org/10.1007/s10072-010-0382-6>
16. Cai G, Zhang J, Liu L, Shen Q (2005) Successful treatment of experimental autoimmune myocarditis by adenovirus-mediated gene transfer of antisense CIITA. *J Mol Cell Cardiol* 38(4):593–605. <https://doi.org/10.1016/j.yjmcc.2005.01.009>
17. Cai Z, Zhang W, Yang F, Yu L, Yu Z, Pan J, Wang J (2012) Immunosuppressive exosomes from TGF- $\beta$ 1 gene-modified dendritic cells attenuate Th17-mediated inflammatory autoimmune disease by inducing regulatory T cells. *Cell Res* 22(3):607–610. <https://doi.org/10.1038/cr.2011.196>
18. Carletti E, Motta A, Migliaresi C (2011) Scaffolds for tissue engineering and 3D cell culture. *Methods Mol Biol* 695:17–39. [https://doi.org/10.1007/978-1-60761-984-0\\_2](https://doi.org/10.1007/978-1-60761-984-0_2)
19. Chan BP, Leong KW (2008) Scaffolding in tissue engineering: general approaches and tissue-specific considerations. *Eur Spine J* 17(Suppl 4):467–479. <https://doi.org/10.1007/s00586-008-0745-3>
20. Charles A, Janeway J, Medzhitov R (2002) Innate immune recognition. *Annu Rev Immunol* 20(1):197–216. <https://doi.org/10.1146/annurev.immunol.20.083001.084359>
21. Cho JH, Feldman M (2015) Heterogeneity of autoimmune diseases: pathophysiologic insights from genetics and implications for new therapies. *Nat Med* 21:730. <https://doi.org/10.1038/nm.3897>
22. Claudius C, Rashmi G, Hema M, Hanno N, Christiane JB, Reinhard K, Peter JN (2007) Genetically engineered stem cells for therapeutic gene delivery. *Curr Gene Ther* 7(4):249–260. <https://doi.org/10.2174/156652307781369119>
23. Clinical Trials Gov (2017) <https://clinicaltrials.gov/>. Accessed in 23/01/2018.
24. Coronel-Restrepo N, Posso-Osorio I, Naranjo-Escobar J, Tobón GJ (2017) Autoimmune diseases and their relation with immunological, neurological and endocrinological axes. *Autoimm Rev* 16(7):684–692. <https://doi.org/10.1016/j.autrev.2017.05.002>
25. Courties G, Baron M, Presumey J, Escriou V, van Lent P, Scherman D, Davignon JL (2011) Cytosolic phospholipase A2alpha gene silencing in the myeloid lineage alters development of Th1 responses and reduces disease severity in collagen-induced arthritis. *Arthritis Rheum* 63(3):681–690. <https://doi.org/10.1002/art.30174>
26. Crystal RG (2014) Adenovirus: the first effective in vivo gene delivery vector. *Hum Gene Ther* 25(1):3–11. <https://doi.org/10.1089/hum.2013.2527>
27. Cupino TL, Watson BA, Cupino AC, Oda K, Ghamsary MG, Soriano S, Kirsch WM (2018) Stability and bioactivity of chitosan as a transfection agent in primary human cell cultures: a case for chitosan-only controls. *Carbohydr Polym* 180:376–384. <https://doi.org/10.1016/j.carbpol.2017.10.021>
28. Dang JM, Leong KW (2006) Natural polymers for gene delivery and tissue engineering. *Adv Drug Deliv Rev* 58(4):487–499. <https://doi.org/10.1016/j.addr.2006.03.001>
29. Dass CR, Choong PF (2006) Selective gene delivery for cancer therapy using cationic liposomes: in vivo proof of applicability. *J Control Release* 113(2):155–163. <https://doi.org/10.1016/j.jconrel.2006.04.009>
30. de Vos P, Lazarjani HA, Poncelet D, Faas MM (2014) Polymers in cell encapsulation from an enveloped cell perspective. *Adv Drug Deliv Rev* 67-68:15–34. <https://doi.org/10.1016/j.addr.2013.11.005>
31. EMA, European Medicinal Agency (2017) Summaries of scientific recommendations on classification of advanced therapy medicinal products
32. Enderami SE, Soleimani M, Mortazavi Y, Nadri S, Salimi A (2017) Generation of insulin-producing cells from human adipose-derived mesenchymal

- stem cells on PVA scaffold by optimized differentiation protocol. *J Cell Physiol.* <https://doi.org/10.1002/jcp.26266>
33. European Commission (2009) Commission Directive 2009/120/EC of 14 September 2009 amending Directive 2001/83/EC of the European Parliament and of the Council on the Community code relating to medicinal products for human use as regards advanced therapy medicinal products. Off J Eur Union
  34. Fahy E, Cotter D, Sud M, Subramaniam S (2011) Lipid classification, structures and tools. *Biochim Biophys Acta* 1811(11):637–647. <https://doi.org/10.1016/j.bbailip.2011.06.009>
  35. Felgner PL, Gadek TR, Holm M, Roman R, Chan HW, Wenz M, Danielsen M (1987) Lipofection: a highly efficient, lipid-mediated DNA-transfection procedure. *Proc Natl Acad Sci USA* 84(21):7413–7417 ISSN: 0027-8424
  36. Ferreira H, Lucio M, Lima JL, Matos C, Reis S (2005a) Effects of diclofenac on EPC liposome membrane properties. *Anal Bioanal Chem* 382(5):1256–1264. <https://doi.org/10.1007/s00216-005-3251-z>
  37. Ferreira H, Lucio M, Lima JL, Matos C, Reis S (2005b) Interaction of clonixin with EPC liposomes used as membrane models. *J Pharm Sci* 94(6):1277–1287. <https://doi.org/10.1002/jps.20351>
  38. Finn JD, Nichols TC, Svoronos N, Merricks EP, Bellenger DA, Zhou S, Arruda VR (2012) The efficacy and the risk of immunogenicity of FIX Padua (R338L) in hemophilia B dogs treated by AAV muscle gene therapy. *Blood* 120(23):4521–4523. <https://doi.org/10.1182/blood-2012-06-440123>
  39. Ganesh BB, Cheatem DM, Sheng JR, Vasu C, Prabhakar BS (2009) GM-CSF-induced CD11c+CD8a—dendritic cells facilitate Foxp3+ and IL-10+ regulatory T cell expansion resulting in suppression of autoimmune thyroiditis. *Int Immun* 21(3):269–282. <https://doi.org/10.1093/intimm/dxn147>
  40. Ganju A, Khan S, Hafeez BB, Behrman SW, Yallapu MM, Chauhan SC, Jaggi M (2017) miRNA nanotherapeutics for cancer. *Drug Discov Today* 22(2):424–432. <https://doi.org/10.1016/j.drudis.2016.10.014>
  41. Gershwin ME, Shoenfeld Y (2011) Cutting-edge issues in organ-specific autoimmunity. *Clin Rev Allergy Immunol* 41(2):123–125. <https://doi.org/10.1007/s12016-011-8283-x>
  42. Giancchetti E, Delfino DV, Fierabracci A (2017) NK cells in autoimmune diseases: linking innate and adaptive immune responses. *Autoimmu Rev.* <https://doi.org/10.1016/j.autrev.2017.11.018>
  43. Grigoras AG (2017) Polymer-lipid hybrid systems used as carriers for insulin delivery. *Nanomedicine* 13(8):2425–2437. <https://doi.org/10.1016/j.nano.2017.08.005>
  44. Hajizadeh-Sikaroodi S, Hosseini A, Fallah A, Estiri H, Noormohammadi Z, Salehi M, Kazemi B (2014) Lentiviral mediating genetic engineered mesenchymal stem cells for releasing IL-27 as a gene therapy approach for autoimmune diseases. *Cell J (Yakhteh)* 16(3):255–262 ISSN: 2228-5806
  45. Hanna E, Rémuzat C, Auquier P, Toumi M (2016) Advanced therapy medicinal products: current and future perspectives. *J Mark Access Health Pol* 4. <https://doi.org/10.3402/jmahp.v4.31036>
  46. Hintermann E, Ehser J, Bayer M, Pfeilschifter JM, Christen U (2013) Mechanism of autoimmune hepatic fibrogenesis induced by an adenovirus encoding the human liver autoantigen cytochrome P450 2D6. *J Autoimm* 44:49–60. <https://doi.org/10.1016/j.jaut.2013.05.001>
  47. Hou X, Zhou J, Yang R, Liu SS, Bi M, Liu T, Li YS (2017) Effect of halofuginone on the pathogenesis of autoimmune thyroid disease in different mice models. *Endocr Metab Immune Disord Targets* 17(2):141–148. <https://doi.org/10.2174/1871530317666170424101256>
  48. Hung ME, Leonard JN (2016) A platform for actively loading cargo RNA to elucidate limiting steps in EV-mediated delivery. *J Extracell Vesicles* 5:1–13. <https://doi.org/10.3402/jev.v5.31027>
  49. Juric MK, Ghimire S, Ogonek J, Weissinger EM, Holler E, van Rood JJ, Greinix HT (2016) Milestones of hematopoietic stem cell transplantation – from first human studies to current developments. *Front Immunol* 7:470. <https://doi.org/10.3389/fimmu.2016.00470>
  50. Katsiogiannis S (2015) Extracellular vesicles: evolving contributors in autoimmunity. *Immunopathol Dis Therap* 6(3–4):163–170. <https://doi.org/10.1615/ForumImmunDisTher.2016016491>
  51. Kelsey PJ, Oliveira MC, Badoglio M, Sharrack B, Farge D, Snowden JA (2016) Haematopoietic stem cell transplantation in autoimmune diseases: from basic science to clinical practice. *Curr Res Transl Med* 64(2):71–82. <https://doi.org/10.1016/j.retram.2016.03.003>
  52. Khorsandi L, Khodadadi A, Nejad-Dehbashi F, Saremy S (2015) Three-dimensional differentiation of adipose-derived mesenchymal stem cells into insulin-producing cells. *Cell Tissue Res* 361(3):745–753. <https://doi.org/10.1007/s00441-015-2140-9>
  53. Khoury M, Escriou V, Courties G, Galy A, Yao R, Largeau C, Apparailly F (2008) Efficient suppression of murine arthritis by combined anticytokine small interfering RNA lipoplexes. *Arthritis Rheum* 58(8):2356–2367. <https://doi.org/10.1002/art.23660>
  54. Kim MJ, Park J-S, Lee SJ, Jang J, Park JS, Back SH, Kim K (2015) Notch1 targeting siRNA delivery nanoparticles for rheumatoid arthritis therapy. *J Control Release* 216:140–148. <https://doi.org/10.1016/j.jconrel.2015.08.025>
  55. Kim SH, Bianco NR, Shufesky WJ, Morelli AE, Robbins PD (2007) Effective treatment of inflammatory disease models with exosomes derived from dendritic cells genetically modified to express IL-4. *J Immunol* 179(4):2242–2249. <https://doi.org/10.4049/jimmunol.179.4.2242>

56. Kong F, Liu G, Zhou S, Guo J, Chen S, Wang Z (2017a) Superior transfection efficiency of phagocytic astrocytes by large chitosan/DNA nanoparticles. *Int J Biol Macromol* 105:1473–1481. <https://doi.org/10.1016/j.ijbiomac.2017.06.061>
57. Kong Y, Wang J, Shen LJ, Zhu YQ, Shen H, Shi Q, Huang L (2017b) B7-2 gene silencing by lentivirus-mediated delivery of shRNA reduces progression of experimental lupus nephritis. *Int J Clin Exp Pathol* 10(6):6198–6209 ISSN:1936–2625
58. Kotsiafti A, Eleutheriou D, Stabouli S (2017) Atherosclerosis as an autoimmune disease. *Hell J Atheroscler* 8(3):76–85
59. Kotterman MA, Chalberg TW, Schaffer DV (2015) Viral vectors for gene therapy: translational and clinical outlook. *Annu Rev Biomed Eng* 17:63–89. <https://doi.org/10.1146/annurev-bioeng-071813-104938>
60. Lee RJ, Huang L (1996) Folate-targeted, anionic liposome-entrapped polylysine-condensed DNA for tumor cell-specific gene transfer. *J Biol Chem* 271(14):8481–8487. <https://doi.org/10.1074/jbc.271.14.8481>
61. Lee SJ, Lee A, Hwang SR, Park J-S, Jang J, Huh MS, Kim K (2014) TNF- $\alpha$  gene silencing using polymerized siRNA/Thiolated glycol chitosan nanoparticles for rheumatoid arthritis. *Mol Ther* 22(2):397–408. <https://doi.org/10.1038/mt.2013.245>
62. Lerner A, Jeremias P, Matthias T (2015) The world incidence and prevalence of autoimmune diseases is increasing. *Int J Celiac Dis* 3(4):151–155. <https://doi.org/10.12691/ijcd-3-4-8>
63. Leuschner F, Dutta P, Gorbатов R, Novobrantseva TI, Donahoe JS, Courties G, Nahrendorf M (2011) Therapeutic siRNA silencing in inflammatory monocytes in mice. *Nat Biotechnol* 29:1005. <https://doi.org/10.1038/nbt.1989>
64. Li C-y, Wu X-y, Tong J-b, Yang X-x, Zhao J-l, Zheng Q-f, Ma Z-j (2015) Comparative analysis of human mesenchymal stem cells from bone marrow and adipose tissue under xeno-free conditions for cell therapy. *Stem Cell Res Ther* 6(1):55. <https://doi.org/10.1186/s13287-015-0066-5>
65. Li Y, Zhang R, Qiao H, Zhang H, Wang Y, Yuan H, Pei X (2007) Generation of insulin-producing cells from PDX-1 gene-modified human mesenchymal stem cells. *J Cell Physiol* 211(1):36–44. <https://doi.org/10.1002/jcp.20897>
66. Lin G, Wang G, Liu G, Yang L-J, Chang L-J, Lue TF, Lin C-S (2009) Treatment of type 1 diabetes with adipose tissue-derived stem cells expressing pancreatic duodenal Homeobox 1. *Stem Cells Dev* 18(10):1399–1406. <https://doi.org/10.1089/scd.2009.0010>
67. Lin J, Zhi Y, Mays L, Wilson JM (2007) Vaccines based on novel adeno-associated virus vectors elicit aberrant CD8+ T-cell responses in mice. *J Virol* 81(21):11840–11849. <https://doi.org/10.1128/jvi.01253-07>
68. Liu L, Liu Y, Yuan M, Xu L, Sun H (2017a) Elevated expression of microRNA-873 facilitates Th17 differentiation by targeting forkhead box O1 (Foxo1) in the pathogenesis of systemic lupus erythematosus. *Biochem Biophys Res Commun* 492(3):453–460. <https://doi.org/10.1016/j.bbrc.2017.08.075>
69. Liu S, Kiyoi T, Takemasa E, Maeyama K (2017b) Intra-articular lentivirus-mediated gene therapy targeting CRACM1 for the treatment of collagen-induced arthritis. *J Pharmacol Sci* 133(3):130–138. <https://doi.org/10.1016/j.jphs.2017.02.001>
70. Lleo A, Invernizzi P, Gao B, Podda M, Gershwin ME (2010) Definition of human autoimmunity – autoantibodies versus autoimmune disease. *Autoimmunol Rev* 9(5):A259–A266. <https://doi.org/10.1016/j.autrev.2009.12.002>
71. Long R, Liu Y, Wang S, Ye L, He P (2017) Co-microencapsulation of BMSCs and mouse pancreatic  $\beta$  cells for improving the efficacy of type I diabetes therapy. *Int J Artif Organs* 40(4):169–175. <https://doi.org/10.5301/ijao.5000555>
72. Lu X, Wang X, Nian H, Yang D, Wei R (2017) Mesenchymal stem cells for treating autoimmune dacryoadenitis. *Stem Cell Res Ther* 8:126. <https://doi.org/10.1186/s13287-017-0593-3>
73. Lucas CL, Lenardo MJ (2015) Identifying genetic determinants of autoimmunity and immune dysregulation. *Curr Opin Immunol* 37:28–33. <https://doi.org/10.1016/j.coi.2015.09.001>
74. Makar TK, Bever CT, Singh IS, Royal W, Sahu SN, Sura TP, Trisler D (2009) Brain-derived neurotrophic factor gene delivery in an animal model of multiple sclerosis using bone marrow stem cells as a vehicle. *J Neuroimmunol* 210(1):40–51. <https://doi.org/10.1016/j.jneuroim.2009.02.017>
75. Mandke R, Singh J (2012) Cationic nanomicelles for delivery of plasmids encoding Interleukin-4 and Interleukin-10 for prevention of autoimmune diabetes in mice. *Pharm Res* 29(3):883–897. <https://doi.org/10.1007/s11095-011-0616-1>
76. Mano JF, Silva GA, Azevedo HS MPB, Sousa RA, Silva S, Reis RL (2007) Natural origin biodegradable systems in tissue engineering and regenerative medicine: present status and some moving trends. *J R Soc Interface* 4(17):999–1030. <https://doi.org/10.1098/rsif.2007.0220>
77. Martins A, Ferreira H, Reis RL, Neves NM (2016a) Delivery systems made of natural-origin polymers for tissue engineering and regenerative medicine applications. In: *Biomaterials from nature for advanced devices and therapies*. Wiley, Hoboken, pp 581–611. <https://doi.org/10.1002/9781119126218.ch31>
78. Martins M, Ribeiro D, Martins A, Reis RL, Neves NM (2016b) Extracellular vesicles derived from osteogenically induced human bone marrow mesenchymal stem cells can modulate lineage commitment. *Stem Cell Rep* 6(3):284–291. <https://doi.org/10.1016/j.stemcr.2016.01.001>
79. Mascolo M, McNeill A, Fernandes M (2017) Autoimmune diseases – modern diseases. Available at <http://www.europarl.europa.eu/supporting-analyses>. Accessed Jan 2018

80. Mincheva-Nilsson L, Baranov V (2010) The role of placental exosomes in reproduction. *Am J Reprod Immunol* 63(6):520–533. <https://doi.org/10.1111/j.1600-0897.2010.00822.x>
81. Miralles M, Eixarch H, Tejero M, Costa C, Hirota K, Castano AR, Chillón M (2017) Clinical and histopathological amelioration of experimental autoimmune encephalomyelitis by AAV vectors expressing a soluble interleukin-23 receptor. *Neurotherapeutics* 14(4):1095–1106. <https://doi.org/10.1007/s13311-017-0545-8>
82. Mooney DJ, Vandenburgh H (2008) Cell delivery mechanisms for tissue repair. *Cell Stem Cell* 2(3):205–213. <https://doi.org/10.1016/j.stem.2008.02.005>
83. Morrow D, Ussi A, Migliaccio G (2017) Addressing pressing needs in the development of advanced therapies. *Front Bioeng Biotechnol* 5:55. <https://doi.org/10.3389/fbioe.2017.00055>
84. Motte E, Szepessy E, Suenens K, Stange G, Bomans M, Jacobs-Tulleneers-Thevissen D, Pipeleers D (2014) Composition and function of macroencapsulated human embryonic stem cell-derived implants: comparison with clinical human islet cell grafts. *Am J Physiol Endocrinol Metab* 307(9):E838–E846. <https://doi.org/10.1152/ajpendo.00219.2014>
85. Naldini L, Blömer U, Gage FH, Trono D, Verma IM (1996) Efficient transfer, integration, and sustained long-term expression of the transgene in adult rat brains injected with a lentiviral vector. *Proc Natl Acad Sci USA* 93(21):11382–11388 ISSN: 0027–8424
86. Nndi CN, Nelson AO, Okezie IA (2014) Naturapolyceutics: the science of utilizing natural polymers for drug delivery. *Polymers* 6(5):1312–1332. <https://doi.org/10.3390/polym6051312>
87. Negre O, Bartholomae C, Beuzard Y, Cavazzana M, Christiansen L, Courne C, Veres G (2015) Preclinical evaluation of efficacy and safety of an improved lentiviral vector for the treatment of beta-thalassemia and sickle cell disease. *Curr Gene Ther* 15(1):64–81 ISSN: 1566-5232
88. Ngo ST, Steyn FJ, McCombe PA (2014) Gender differences in autoimmune disease. *Front Neuroendocrinol* 35(3):347–369. <https://doi.org/10.1016/j.yfrne.2014.04.004>
89. O'Brien FJ (2011) Biomaterials & scaffolds for tissue engineering. *Mater Today* 14(3):88–95. [https://doi.org/10.1016/S1369-7021\(11\)70058-X](https://doi.org/10.1016/S1369-7021(11)70058-X)
90. Patel P, Chatterjee S (2018) Chapter 1: Innate and adaptive immunity: barriers and receptor-based recognition immunity and inflammation in health and disease. Academic Press, pp 3–13. <https://doi.org/10.1016/B978-0-12-805417-8.00001-9>
91. Ra JC, Kang SK, Shin IS, Park HG, Joo SA, Kim JG, Kurtz A (2011) Stem cell treatment for patients with autoimmune disease by systemic infusion of culture-expanded autologous adipose tissue derived mesenchymal stem cells. *J Transl Med* 9:181. <https://doi.org/10.1186/1479-5876-9-181>
92. Raveendran S, Rochani AK, Maekawa T, Kumar DS (2017) Smart carriers and nanohealers: a nanomedical insight on natural polymers. *Materials* (Basel) 10(8). <https://doi.org/10.3390/ma10080929>
93. Rose NR (2004) Autoimmune disease 2002: an overview. *J Investig Dermatol Symp Proc* 9(1):1–4. <https://doi.org/10.1111/j.1087-0024.2004.00837.x>
94. Rosenblum MD, Gratz IK, Paw JS, Abbas AK (2012) Treating human autoimmunity: current practice and future prospects. *Sci Transl Med* 4(125):125sr121. <https://doi.org/10.1126/scitranslmed.3003504>
95. Satija NK, Singh VK, Verma YK, Gupta P, Sharma S, Afrin F, Gurudutta GU (2009) Mesenchymal stem cell-based therapy: a new paradigm in regenerative medicine. *J Cell Mol Med* 13(11–12):4385–4402. <https://doi.org/10.1111/j.1582-4934.2009.00857.x>
96. Scully C (2014) 18 – Autoimmune disease Scully's medical problems in dentistry, 7th edn. Churchill Livingstone, Oxford, pp 466–480 ISBN: 978-0-7020-5401-3
97. Sharon D, Kamen A (2018) Advancements in the design and scalable production of viral gene transfer vectors. *Biotechnol Bioeng* 115(1):25–40. <https://doi.org/10.1002/bit.26461>
98. Shigemoto-Kuroda T, Oh JY, D-k K, Jeong HJ, Park SY, Lee HJ, Lee RH (2017) MSC-derived extracellular vesicles attenuate immune responses in two autoimmune murine models: type 1 diabetes and uveoretinitis. *Stem Cell Rep* 8(5):1214–1225. <https://doi.org/10.1016/j.stemcr.2017.04.008>
99. Shu S-A, Wang J, Tao M-H, Leung PSC (2015) Gene therapy for autoimmune disease. *Clin Rev Allergy Immunol* 49(2):163–176. <https://doi.org/10.1007/s12016-014-8451-x>
100. Sionkowska A (2011) Current research on the blends of natural and synthetic polymers as new biomaterials: review. *Prog Polym Sci* 36(9):1254–1276. <https://doi.org/10.1016/j.progpolymsci.2011.05.003>
101. Sokol M, Wabl M, Ruiz IR, Pedersen FS (2014) Novel principles of gamma-retroviral insertional transcription activation in murine leukemia virus-induced end-stage tumors. *Retrovirology* 11:36. <https://doi.org/10.1186/1742-4690-11-36>
102. Song L, Sun Z, Kim DS, Gou W, Strange C, Dong H, Wang H (2017) Adipose stem cells from chronic pancreatitis patients improve mouse and human islet survival and function. *Stem Cell Res Ther* 8(1):192. <https://doi.org/10.1186/s13287-017-0627-x>
103. Stancu IC, Lungu A, Iovu H (2014) 3 – Hydrogels for bone regeneration biomaterials for bone regeneration (pp 62–86). Woodhead Publishing. <https://doi.org/10.1533/9780857098104.1.62>
104. Stepien A, Dabrowska NL, Maciagowska M, Macoch RP, Zolocinska A, Mazur S, Pojda Z (2016) Clinical application of autologous adipose stem cells in patients with multiple sclerosis: preliminary results. *Mediat Inflamm* 6:5302120. <https://doi.org/10.1155/2016/5302120>
105. Stewart PL, Burnett RM (1995) Adenovirus structure by X-ray crystallography and electron

- microscopy. In: Doerfler W, Böhm P (eds) *The molecular repertoire of adenoviruses I*, Current topics in microbiology and immunology, vol 199/1. Springer, Berlin/Heidelberg. [https://doi.org/10.1007/978-3-642-79496-4\\_2](https://doi.org/10.1007/978-3-642-79496-4_2)
106. Sun D, Zhuang X, Xiang X, Liu Y, Zhang S, Liu C, Zhang H-G (2010) A novel nanoparticle drug delivery system: the anti-inflammatory activity of curcumin is enhanced when encapsulated in exosomes. *Mol Ther* 18(9):1606–1614. <https://doi.org/10.1038/mt.2010.105>.
  107. Sun L-L, Liu T-J, Li L, Tang W, Zou J-J, Chen X-F, Shi Y-Q (2017) Transplantation of betatrophin-expressing adipose-derived mesenchymal stem cells induces  $\beta$ -cell proliferation in diabetic mice. *Int J Mol Med* 39(4):936–948. <https://doi.org/10.3892/ijmm.2017.2914>
  108. Tanaka Y (2015) Human mesenchymal stem cells as a tool for joint repair in rheumatoid arthritis. *Clin Exp Rheumatol* 33(4 Suppl 92):S58–S62 ISSN: 0392-856X
  109. Tang AP, Li C, Chen ZH, Li T (2017) Anti-CD20 monoclonal antibody combined with adenovirus vector-mediated IL-10 regulates spleen CD4+/CD8+ T cells and T-bet/GATA-(3) expression in NOD mice. *Mol Med Rep* 16(4):3974–3982. <https://doi.org/10.3892/mmr.2017.7111>
  110. Tarcha PJ (1990) *Polymers for controlled drug delivery*. Taylor & Francis, London ISBN 9780849356520
  111. Tekie FS, Kiani M, Zakerian A, Pilevarian F, Assali A, Soleimani M, Atyabi F (2017) Nano polyelectrolyte complexes of carboxymethyl dextran and chitosan to improve chitosan-mediated delivery of miR-145. *Carbohydr Polym* 159:66–75. <https://doi.org/10.1016/j.carbpol.2016.11.067>.
  112. Thery C, Amigorena S, Raposo G, Clayton A (2006) Isolation and characterization of exosomes from cell culture supernatants and biological fluids. *Curr Protoc Cell Biol*, Chapter 3. Unit 3.22. <https://doi.org/10.1002/0471143030.cb0322s30>
  113. Tiegs SL, Russell DM, Nemazee D (2011) Receptor editing in self-reactive bone marrow B cells. *J Immunol* 186(3):1313–1324 ISSN: 0022-1767
  114. Treacy O, Ryan AE, Heinzl T, O'Flynn L, Cregg M, Wilk M, Ritter T (2012) Adenoviral transduction of mesenchymal stem cells: in vitro responses and in vivo immune responses after cell transplantation. *PLoS One* 7(8):e42662. <https://doi.org/10.1371/journal.pone.0042662>
  115. Urbanati F, Wherley J, Geiger S, Fernandez BC, Kaufman ML, Cooper A, Kohn DB (2017) Preclinical studies for a phase 1 clinical trial of autologous hematopoietic stem cell gene therapy for sickle cell disease. *Cytherapy* 19(9):1096–1112. <https://doi.org/10.1016/j.jcjt.2017.06.002>
  116. Velema J, Kaplan D (2006) *Biopolymer-Based Biomaterials as Scaffolds for Tissue Engineering*. In: Lee K, Kaplan D (eds) *Tissue engineering I*. Springer, Berlin/Heidelberg, pp 187–238. *Adv Biochem Engin/Biotechnol* 102: 187–238. [https://doi.org/10.1007/10\\_013](https://doi.org/10.1007/10_013)
  117. Vo TN, Kasper FK, Mikos AG (2012) Strategies for controlled delivery of growth factors and cells for bone regeneration. *Adv Drug Deliv Rev* 64(12):1292–1309. <https://doi.org/10.1016/j.addr.2012.01.016>
  118. Wardemann H, Nussenzweig MC (2007) B-cell self-tolerance in humans advances in immunology, vol 95. Academic Press, San Diego, pp 83–110. [https://doi.org/10.1016/S0065-2776\(07\)95003-8](https://doi.org/10.1016/S0065-2776(07)95003-8)
  119. Wardwell PR, Forstner MB, Bader RA (2015) Investigation of the cytokine response to NF-kappa B decoy oligonucleotide coated polysaccharide based nanoparticles in rheumatoid arthritis in vitro models. *Arthritis Res Ther* 17:10. <https://doi.org/10.1186/s13075-015-0824-x>
  120. Weinberg JB, Matthews TJ, Cullen BR, Malim MH (1991) Productive human immunodeficiency virus type 1 (HIV-1) infection of nonproliferating human monocytes. *J Exp Med* 174(6):1477–1482. <https://doi.org/10.1084/jem.174.6.1477>
  121. Wiklander OP, Nordin JZ, O'Loughlin A, Gustafsson Y, Corso G, Mager I, Andaloussi SE (2015) Extracellular vesicle in vivo biodistribution is determined by cell source, route of administration and targeting. *J Extracell Vesicles* 4:26316. <https://doi.org/10.3402/jev.v4.26316>
  122. Wu XY (2016) Strategies for optimizing polymer-lipid hybrid nanoparticle-mediated drug delivery. *Expert Opin Drug Deliv* 13(5):609–612. <https://doi.org/10.1517/17425247.2016.1165662>
  123. Xu J, Zhu MY, Lu YH, Lu Y, Wang ZW (2007) Treatment of type 1 diabetes by transplantation of bone-derived mesenchymal stem cells expressing human insulin gene: experiment with mice. *Zhonghua Yi Xue Za Zhi* 87(36):2557–2560 ISSN: 0376-2491
  124. Yuasa K, Yoshimura M, Urasawa N, Ohshima S, Howell JM, Nakamura A, Takeda S (2007) Injection of a recombinant AAV serotype 2 into canine skeletal muscles evokes strong immune responses against transgene products. *Gene Ther* 14(17):1249–1260. <https://doi.org/10.1038/sj.gt.3302984>
  125. Zhang Y, Wang Z, Gemeinhart RA (2013) Progress in microRNA delivery. *J Control Release* 172(3):962–974. <https://doi.org/10.1016/j.jconrel.2013.09.015>
  126. Zhuang X, Xiang X, Grizzl W, Sun D, Zhang S, Axtell RC, Zhang H-G (2011) Treatment of brain inflammatory diseases by delivering exosome encapsulated anti-inflammatory drugs from the nasal region to the brain. *Mol Ther* 19(10):1769–1779. <https://doi.org/10.1038/mt.2011.164>



---

**Part III**

**Functional Biomaterials for Regenerative  
Medicine**



# Recent Advancements in Decellularized Matrix-Based Biomaterials for Musculoskeletal Tissue Regeneration

Hyunbum Kim, Yunhye Kim, Mona Fendereski,  
Nathaniel S. Hwang, and Yongsung Hwang

## Abstract

The native extracellular matrix (ECM) within different origins of tissues provides a dynamic microenvironment for regulating various cellular functions. Thus, recent regenerative medicine and tissue engineering approaches for modulating various stem cell functions and their contributions to tissue repair include the utilization of tissue-specific decellularized matrix-based biomaterials. Because of their unique capabilities to mimic native extracellular microenvironments based on their three-dimensional structures, biochemical compositions, and biological cues, decellularized matrix-based biomaterials have been recognized as an ideal platform for engineering an artificial stem cell niche. Herein, we describe the most commonly used decellularization methods and their potential applications in musculoskeletal tissue engineering.

## Keywords

Decellularization · Extracellular matrix (ECM) · Biomaterials · Scaffold · Microenvironment · Musculoskeletal tissue regeneration

## 9.1 Decellularized Matrix as a Source of Novel Biomimetic Material

Regenerative medicine and tissue engineering approaches to repair damaged or degenerated tissues include the combinatorial use of stem cells, biomaterials, and various cell signaling molecules [1]. Particularly, based on the sources of scaffolding materials, biomaterials can be categorized as either natural or synthetic materials [2, 3]. Biomaterials derived from natural sources consisting of native extracellular matrix (ECM),

Authors Hyunbum Kim and Yunhye Kim have been equally contributed to this chapter.

H. Kim  
School of Chemical and Biological Engineering,  
Institute of Chemical Processes, Seoul National  
University, Seoul, South Korea

Soonchunhyang Institute of Medi-bio Science  
(SIMS), Soonchunhyang University,  
Cheonan-si, Chungcheongnam-do, South Korea  
e-mail: [tiggerhy@snu.ac.kr](mailto:tiggerhy@snu.ac.kr)

Y. Kim · M. Fendereski · Y. Hwang (✉)  
Soonchunhyang Institute of Medi-bio Science  
(SIMS), Soonchunhyang University,  
Cheonan-si, Chungcheongnam-do, South Korea  
e-mail: [yshwang0428@sch.ac.kr](mailto:yshwang0428@sch.ac.kr)

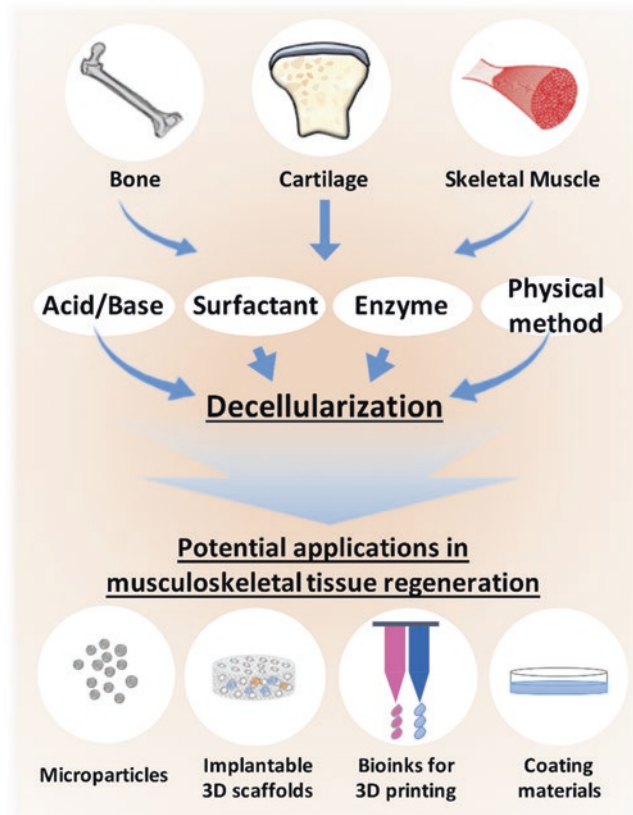
N. S. Hwang  
School of Chemical and Biological Engineering,  
Institute of Chemical Processes, Seoul National  
University, Seoul, South Korea  
e-mail: [nshwang@snu.ac.kr](mailto:nshwang@snu.ac.kr)

such as collagens, chondroitin sulfate, and hyaluronic acid have been shown to create a favorable microenvironment for supporting *in vitro* cell adhesion, proliferation, and differentiation [4–6]. Similarly, synthetic polymer-based biomaterials have been utilized to provide artificial extracellular microenvironments to embedded or encapsulated stem cells, allowing these cells to undergo *in vitro* proliferation and promoting their directed differentiation into target tissue-specific cells [3, 7]. However, although these natural and synthetic biomaterials are considered to be biocompatible, the host immune system identifies them as foreign materials because of their synthesis processes and sources, and the presence of xenogeneic and allogenic cellular antigens, resulting in pro-inflammatory responses and immune-mediated rejection of the transplanted biomaterials [8, 9].

Recent studies demonstrated that to achieve the most effective contribution to functional *in*

*vivo* tissue regeneration, scaffolding biomaterials, which fully mimic the physicochemical properties of target tissue and have an immunomodulatory capability, are highly demanded [10, 11]. Thus, decellularized matrices from native tissues or organs as biomimetic scaffolding materials have been recognized as a novel platform in the field of regenerative medicine and tissue engineering. For example, these approaches include the utilization of decellularized matrices for understanding the specific physicochemical properties of the native ECM and providing a tissue-specific biological scaffold for engineering functional tissues by harnessing cell-cell/cell-matrix interactions [12, 13]. This can be achieved through a process known as decellularization, which involves multiple steps for removing the total cellular and nuclear materials within native tissues while preserving the complex three-dimensional microstructures, mechanical integrity, and unique biochemical

**Fig. 9.1** Schematic for the generation of musculoskeletal tissue-specific extracellular matrix-based biomaterials through decellularization



compositions of native ECMs and their intrinsic biological cues with minimum immune-associated detrimental effects [14–16]. These biological scaffolds derived from decellularized tissues have been extensively used in both *in vitro* studies and pre-clinical *in vivo* applications, and therefore we highlight the currently available methods for decellularization and recent applications of decellularized matrix-based biomaterials for musculoskeletal tissue regeneration (Fig. 9.1).

---

## 9.2 Common Methods for Decellularization

### 9.2.1 Acid-/Base-Based Decellularization

Acids, such as peracetic acid, acetic acid, and hydrochloric acid, and bases, such as sodium hydroxide and calcium hydroxide, have been widely used to solubilize cell membrane and cytoplasmic components of cells and remove biomolecules within native tissues or organs by catalyzing hydrolytic degradation [17, 18]. Although peracetic acid and acetic acid treatments for decellularizing tissues effectively remove nucleic acids and other cellular components while preserving multiple growth factors within tissues, these acid treatments undesirably lead to increased stiffness of the decellularized matrix with significantly decreased elasticity and the failure strain value, resulting in inferior mechanical properties compared to their non-treated counterparts [19]. Similarly, although alkaline solutions including either sodium hydroxide or calcium hydroxide were shown to destroy cellular and nuclear components, they also eliminate growth factors from the tissues and decrease ECM stiffness by degrading collagen fibrils and disrupting collagen crosslinks [20, 21].

### 9.2.2 Surfactant-Based Decellularization

Surfactant-based decellularization agents utilize ionic, non-ionic, and zwitterionic detergents,

which are known to efficiently lyse the cell membrane and remove cellular components from tissues by disrupting the phospholipid membrane [22]. Numerous studies have demonstrated the potential use of sodium dodecyl sulfate (SDS), an ionic detergent, as a decellularization agent, as it can readily eliminate cellular and nuclear materials even from thick and dense tissues [23, 24]. However, despite its strong decellularization ability for multiple tissues and organs including the cartilage, heart, blood vessels, kidney, lung, and small intestine, SDS can cause a high degree of disruption of ECM microstructures and damage signaling proteins and growth factors within tissues [18]. In addition, because of the ionic and cytotoxic nature of SDS, complete removal of SDS from the decellularized tissues is difficult and SDS causes cytotoxicity to cells within the decellularized matrix-based scaffolds [19]. Triton X-100, a non-ionic detergent, is a mild decellularization agent compared to SDS and has been commonly used in combination with ammonium hydroxide to efficiently remove remnant DNA within the tissues by breaking up lipid-lipid and lipid-protein associations [25, 26]. Another zwitterionic detergent, 3-[(3-cholamidopropyl) dimethylammonio]-1-propanesulfonate (CHAPS), has been extensively used as a non-denaturing decellularization agent for thin tissues of organs, such as lung, nerve, and blood vessels, because of its ability to have both non-ionic and ionic properties [27].

### 9.2.3 Enzyme-Based Decellularization

Various enzyme-based decellularization methods involve the use of a nuclease, protease, and collagenase in combination with chelating agents. Among the various enzymes, trypsin is the most extensively used proteolytic decellularization agent, generally employed with ethylenediaminetetraacetic acid (EDTA), to selectively break cell adherent proteins on the carbon side of arginine and lysine [28]. However, extended treatment with trypsin/EDTA has shown to disrupt elastin, collagens, and glycos-

aminoglycans (GAGs), resulting in the loss of mechanical stability of decellularized tissues [29]. Nucleases, including DNases and RNases, have also been utilized in decellularization methods to cleave nucleic acids and therefore can remove cellular and nuclear materials after cell lysis [30, 31].

### 9.2.4 Physical Method-Based Decellularization

Recent advances in developing an efficient decellularization method with a higher yield and minimum toxicity utilize physical treatments, including multiple freeze-thaw cycles, high hydrostatic pressure (HHP), and supercritical carbon dioxide without introducing any chemical agents [15]. Multiple freeze-thaw treatments of tissues disrupt cellular membrane and lyse cells by forming intercellular ice crystals when the tissues to be decellularized are exposed to freeze-thaw cycles between subzero ( $-80\text{ }^{\circ}\text{C}$ ) and physiological ( $37\text{ }^{\circ}\text{C}$ ) temperatures [32]. Although freeze-thaw treatment can maintain the biochemical composition and microstructure of the ECM during decellularization processes, complete elimination of cellular debris and genetic materials released during cell lysis are problematic and lead to immune-associated rejection of the transplanted decellularized matrix within *in vivo* host environments [33]. To bypass the use of toxic detergents or other chemical agents, another physical method for decellularizing tissues by using a high hydrostatic pressure greater than 600–980 MPa has been applied to soft tissues with loosely organized ECMs, such as liver, lung, cornea, and blood vessels [34–36]. Recently, supercritical carbon dioxide was reported as a detergent-free decellularization agent because of its unique physical properties [37, 38]. For example, at the supercritical phase, with a pressure above 7.38 MPa and temperature above  $32\text{ }^{\circ}\text{C}$ , supercritical carbon dioxide shows high diffusivity and low viscosity with non-toxic and relatively inert characteristics, allowing it to remove cellular and nuclear materials, whereas the mechanical

stability and biochemical contents of the ECM are well-preserved.

---

## 9.3 Potential Applications of Decellularized Matrix-Based Biomaterials in Musculoskeletal Tissue Engineering

Numerous studies examining a variety of tissue engineering and regenerative medicine applications have been conducted to examine the potential of decellularized ECM as scaffolding biomimetic materials to facilitate the repair and reconstruction of damaged tissues by providing native extracellular microenvironmental cues to regulate cell-matrix/cell-cell interactions of either transplanted donor stem cells or host endogenous stem cell populations. Some of the most important approaches that have employed aforementioned decellularization methods for musculoskeletal tissue regeneration are described.

### 9.3.1 Bone Tissue

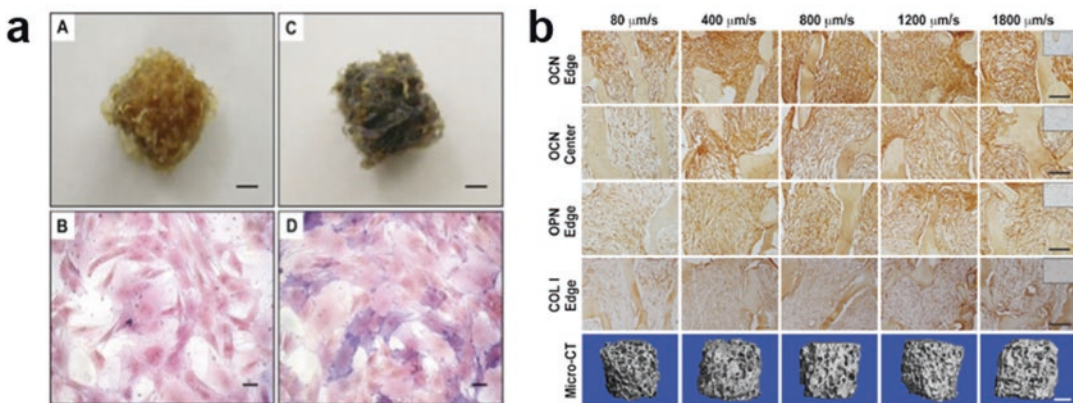
The most effective treatment for large bone defects mainly relies on the transplantation of either natural bone grafts such as allografts and autografts or synthetic bone grafts, which are composed of synthetic polymers, bioinert metals, or bioceramics [39, 40]. Despite the most promising approach for bone healing involving transplantation of autologous bone grafts, several concerns such as pain, donor-site morbidity, infection, hematoma, and other complications may occur [41, 42]. In addition, although emerging evidence has demonstrated that synthetic polymer-based artificial bone grafts provide natural bone-matching mechanical properties, these bone grafts cannot fully mimic the native bone extracellular microenvironment with osteoconductive, osteoinductive, and osteogenic capabilities to orchestrate spatiotemporal bone remodeling and bone homeostasis [43–45]. In fact, these dynamic extracellular components of bone tissues are composed primarily of collagen

type I with small fractions of other collagens (types V and XII), glycoproteins, bone matrix proteins including osteonectin, osteopontin, bone sialoprotein, and osteocalcin, and several growth factors such as bone morphogenetic proteins (BMPs) and transforming growth factor- $\beta$  (TGF- $\beta$ ) (Cheng and Solorio 2014; [46]).

Recently, decellularized bone matrix (DecBM) which retains the biological cues described above has been shown to overcome the current limitations of synthetic material-based bone grafts [10, 47]. For example, Hashimoto et al. used a high hydrostatic pressure treatment ( $\sim 980$  MPa) to successfully decellularize porcine bone tissues and investigated whether these DecBMs could induce osteogenic differentiation of rat mesenchymal stem cells (rMSCs) [48]. In their study, cells seeded onto the DecBM promoted initial cell adhesion, proliferation, and further osteogenic differentiation of rMSCs into mature osteoblasts, even in the absence of dexamethasone, compared to cells on tissue culture polystyrene (TCPS) (Fig. 9.2a). In addition to DecBM-mediated robust *in vitro* osteogenesis, the authors demonstrated that *in vivo* transplanted cell-laden DecBM could support the infiltration of host cells into the DecBM with newly formed vasculatures without causing immune responses. Similarly, Gothard et al. introduced DecBM into

alginate hydrogels containing growth factor-loaded poly(lactic-co-glycolic acid) (PLGA) microparticles, and they evaluated the *in vivo* osteogenic potential of DecBM/alginate hydrogels [49]. The authors demonstrated that DecBM/alginate hydrogels could support the infiltration of host cells and promote ectopic bone formation not only by the DecBM/alginate scaffolds alone, but also by osteogenic/angiogenic growth factor-encapsulated microparticles.

Another interesting approach for engineering fully viable and critical-sized ( $\sim 0.5$  cm) compact bone-like scaffolds using human embryonic stem cells (hESCs) and human mesenchymal stem cells (hMSCs) was reported by Vunjak-Novakovic et al. [50, 51]. The authors utilized DecBM as three-dimensional scaffolds and additionally incorporated a perfusion-based bioreactor culture system to support maximum cell viability and osteogenic differentiation of hESCs for a longer period of *in vitro* culture (Fig. 9.2b). After 5 weeks *in vivo*, osteogenically pre-committed hESC-laden DecBMs within host tissues showed robust ectopic bone formation with no signs of teratomas, whereas teratoma formation occurred when undifferentiated hESCs were seeded within the DecBM or when no bioreactor culture system was used to induce *in vitro* osteogenic differentiation of hESCs. Taken together, these results sug-



**Fig. 9.2** Decellularized bone matrix-based biomaterials for bone tissue engineering. (a) Alkaline phosphatase staining of rat mesenchymal stem cells cultured on decellularized bone/bone marrow (A: day 0, C: day 21) compared to cells cultured on TCPS (B: day 0, D: day 21).

(Reproduced with permission from Ref. [48], Copyright© 2011, Elsevier) (b) hMSC-laden decellularized bone constructs engineered by perfusion bioreactor culture system to repair large bone defects. (Reproduced with permission from Ref. [51], Copyright© 2010, Elsevier)

gest that decellularized bone tissues possess osteoconductive, osteoinductive, and osteogenic potential equivalent to that of native bone tissues.

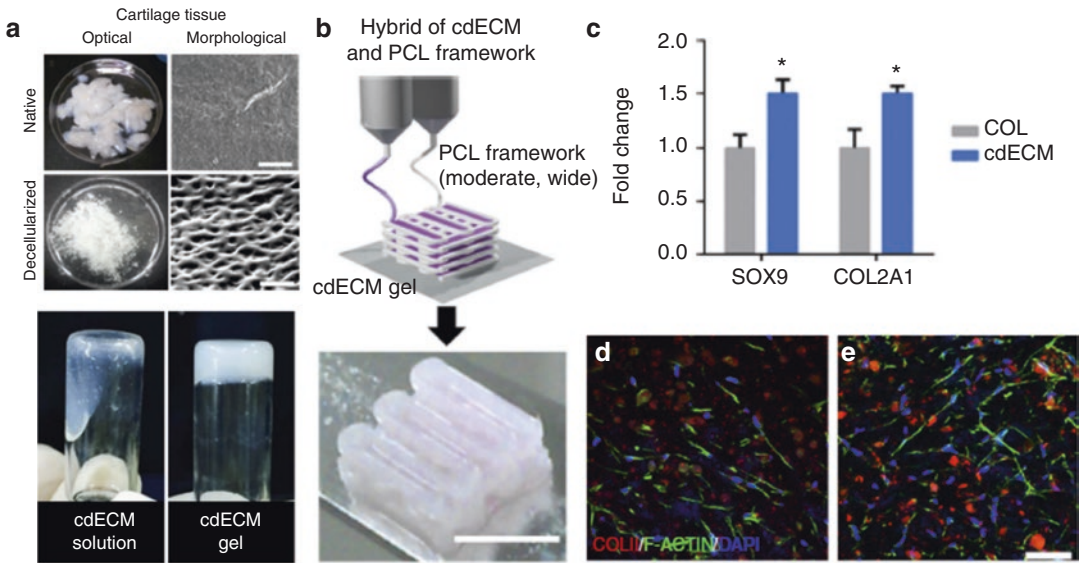
### 9.3.2 Cartilage Tissue

Articular cartilage provides mechanical stability against load-bearing and has a low-friction surface; however, its regenerative capability is limited because of the avascular nature of articular cartilage [52]. The cartilage ECM is composed mainly of collagen type II and glycosaminoglycans [53]. Defects in articular cartilage can be caused by traumatic injury, congenital defects, or degenerative arthritis, resulting in failure of cartilage ECM remodeling [54]. Clinically available treatments for cartilage defects involve autologous chondrocyte implantation, bone marrow stimulation, mosaicplasty, and subchondral abrasion. However, these treatments frequently require multiple stages of surgical procedures and have shown limited success in full regeneration of functional hyaline cartilage [55]. As alternative approaches, synthetic biomaterials have been used to repair cartilage defects because of their biomimetic properties such as water content, mechanical strength, and the three-dimensional microenvironment; however, these biomaterials still require either additional growth factors or sophisticatedly designed microporous structures to induce chondrogenic differentiation of both transplanted and endogenous stem cells [6, 56].

To address these issues, decellularized cartilage ECM-based materials have been gaining attention as potential therapeutic candidates as implantable biomaterials because of their intrinsic biochemical and biomechanical properties, which is equivalent to the native cartilage tissue, and their immunomodulatory capability [57–60]. Guo and coworkers successfully synthesized decellularized human cartilage tissue-derived porous 3D scaffolds and demonstrated their chondrogenic potential using canine mesenchymal stem cells [61]. The authors reported that the

pore size of 3D scaffolds was approximately 230  $\mu\text{m}$ , allowing seeded cells to easily penetrate and proliferate within the scaffolds. The seeded cells showed successful ectopic *in vivo* cartilage tissue formation in nude mice. In addition, they further investigated the *in vivo* chondrogenic potential to repair cartilage defects by transplanting autologous human adipose-derived stem cells-laden scaffolds into full-thickness cartilage defects in rabbits for 6 months [62]. The authors evaluated the degree of cartilage repair over the short-term (3 months) and long-term (6 months) by biochemical, biomechanical, and histological evaluations, and concluded that neo-cartilage tissue formation and integration with host tissues through cartilage ECM remodeling were fully achieved at 6 months after surgery.

Numerous other studies have attempted to utilize decellularized cartilage tissue in the form of microparticles rather than whole tissues to promote chondrogenesis for cartilage tissue repair. For example, Sutherland et al. investigated the chondroinductive properties of decellularized cartilage tissues using a pellet culture of rMSCs, and the results showed that decellularized and freeze-milled cartilage microparticles alone induced chondrogenic differentiation of rMSCs in the absence of any chondrogenic supplements. These results were comparable to those of cells cultured with chondrogenic supplements in the absence of decellularized cartilage tissues [63]. Similarly, Yin et al. utilized decellularized cartilage microparticles with an average diameter of 263  $\mu\text{m}$  to evaluate their *in vitro* and *in vivo* chondrogenic potential using bone marrow stromal cells [64]. In their study, in the absence of chondrogenic growth factors, the cells were able to adhere to the cartilage microparticles and formed cartilage-like micro-tissue aggregates, evident by the abundant production of cartilage-specific ECMs. Moreover, when these cell-laden aggregates were transplanted into cartilage defects in a rat model, the defects were nearly filled with hyaline-like cartilage tissues, demonstrating the *in vivo* chondrogenic potential of the decellularized cartilage matrix.



**Fig. 9.3** Decellularized cartilage matrix-based bioinks for 3D printing of cell-laden engineered cartilage tissues. (a) Optical images of decellularized cartilage tissue and gelation of decellularized cartilage ECM (cdECM). (b)

3D printed cell-laden engineered cartilage tissue. (c–e) Improved chondrogenic differentiation of hMSCs compared to that of cells encapsulated within collagen. (Reproduced with permission from Ref. [65], Copyright© 2014, Springer Nature)

Another important approach utilizing decellularized cartilage tissue involving 3D printable bioinks has been pioneered by Cho and his coworkers [65]. In their study, they developed a novel 3D bioprinting method for solubilizing cartilage tissue as pH-sensitive pre-gel bioinks and transform cell-laden bioinks to 3D gelled cell-printed structures (Fig. 9.3a–b). To achieve tissue-specific mechanical strength, they also incorporated a polycaprolactone (PCL) framework into the cell-laden 3D structures. These novel cell-laden 3D constructs were shown to promote successful *in vitro* chondrogenic differentiation of human mesenchymal stem cells compared to collagen-based scaffolds, which was validated by upregulated chondrogenic gene markers and cartilage-specific ECM deposition (Fig. 9.3c–e). Thus, the decellularized cartilage ECM shows better performance over either synthetic polymer-based biomaterials or single ECM-based biomaterials and provides crucial cues for *in vitro* proliferation and differentiation of stem cells, as well as *in vivo* functional engraftment within host microenvironments.

### 9.3.3 Skeletal Muscle Tissue

Skeletal muscle is composed of hierarchically organized and three-dimensional bundles of myofibers surrounded by skeletal muscle-specific ECM [66, 67]. The biochemical, biomechanical, and topographical properties of the skeletal muscle ECM, including collagens, proteoglycans, glycoproteins, and other matrix remodeling enzymes, have been shown to play a significant role in skeletal muscle homeostasis and regeneration by modulating cellular adhesion, migration, and differentiation of muscle-specific stem cells, known as satellite cells, into multinucleated muscle fibers [68–71].

Numerous studies have been conducted to develop methods for decellularizing skeletal muscles using physical methods such as multiple freeze–thawing processes, enzymatic treatment with trypsin, or various detergent solutions including SDS, sodium deoxycholate, and Triton X-100 [72–75]. For example, the research groups of Dyke and Christman established a method for obtaining solubilized ECM from the decellular-

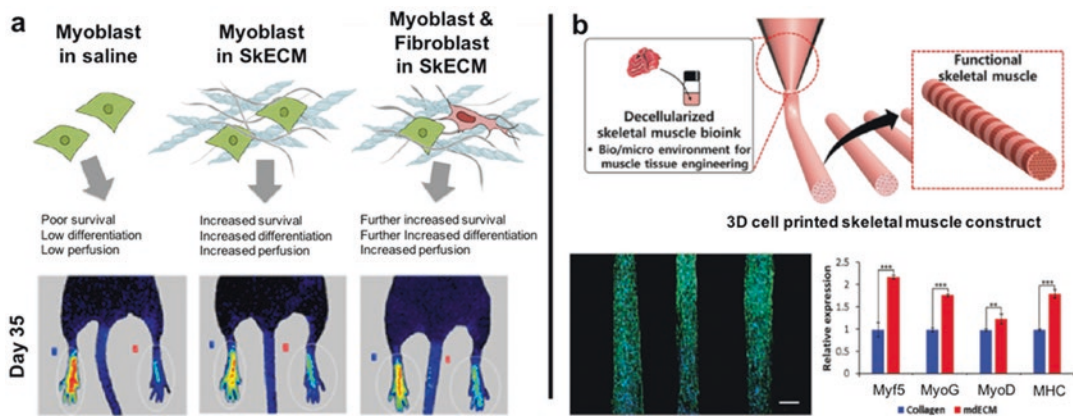


ized skeletal muscle tissues and investigated its potential as a novel coating material for inducing myogenic differentiation of myoblasts [76, 77]. Their results confirmed that decellularized ECM retained a complex mixture of muscle-specific proteins, peptides, and growth factors after decellularization processes, as characterized by mass spectroscopy. Moreover, cells cultured on the skeletal muscle ECM-coated substrate underwent faster proliferation and significantly enhanced myogenic differentiation compared to non-coated or collagen-coated substrates.

Similarly, Chaturvedi et al. developed a decellularization method using phospholipase A2 and compared it to conventional decellularization methods [78]. The results indicated that the skeletal muscle-specific ECM was mostly retained without the loss of numerous glycoproteins and that solubilized ECM coating promoted myogenic differentiation of murine myoblasts in serum-free medium. Furthermore, when the authors seeded cells into decellularized 3D skeletal muscle rather than the ECM-coated substrate, they found that the seeded cells sensed the topographical features of skeletal muscles and that the topography guided myotube formation and oriented myofiber bundles.

In another study, by structuring the microenvironment of skeletal muscle progenitor cells with decellularized skeletal muscle ECM similar to native tissue, Farrar and coworkers investigated the regenerative potential of a decellularized 3D skeletal muscle ECM scaffold using a lateral gastrocnemius (LGAS) muscle defect model [79]. After removing a part of the LGAS muscle from Sprague-Dawley rats, the authors initially transplanted a 3D decellularized skeletal muscle ECM scaffold into the defect to promote skeletal muscle regeneration. Although the transplanted skeletal muscle ECM scaffold promoted new vessel formation and myofiber growth at the defect, there was no functional recovery at 42 days after transplantation. In contrast, when the authors transplanted the same skeletal muscle ECM scaffold with rat MSCs, the cell-laden scaffolds promoted robust blood vessel formation and partially improved functional recovery. These results suggest that cell-secreted trophic factors are also required for the functional recovery of damaged skeletal muscles.

To enhance the survival and functional engraftment of transplanted cells into ischemic muscle, recapitulation of the skeletal muscle microenvironments has been reported. Rao et al. used injectable skeletal muscle ECM-based bio-



**Fig. 9.4** Decellularized matrix-based biomaterials for skeletal muscle tissue engineering. **(a)** *In vivo* transplantation of skeletal muscle progenitors with fibroblast using decellularized skeletal muscle ECM (SkECM) to improve cell survival, engraftment, and vascularization. (Reproduced with permission from Ref. [80], Copyright©

2017, American Chemical Society) **(b)** 3D printing-based engineered 3D functional skeletal muscle-like bundles composed of major skeletal muscle ECM. (Reproduced with permission from Ref. [81], Copyright© 2016, John Wiley and Sons)

materials that could form nanofibrous hydrogels when heated to physiological temperature [80]. In their study, the authors showed that co-transplanting myoblasts with fibroblasts using injectable biomaterials into ischemic muscle significantly improved the viability, vascularization, and function engraftment of transplanted cells (Fig. 9.4a). Recently, another innovative approach for mimicking the structural and functional properties of skeletal muscle using 3D bioprinting techniques has been demonstrated by Choi et al. [81]. The authors developed decellularized skeletal muscle ECM-based bioinks to achieve prepare skeletal muscle-like cell-laden scaffolds (Fig. 9.4b). By controlling the architectures of cell-laden ECM constructs, alignment of embedded myoblasts was controlled, resulting in enhanced myogenic differentiation through fusion of mononucleated myoblasts into multinucleated myotubes. Moreover, these cell-laden ECM constructs exhibited visible contrac-

tion upon electrical stimuli, suggesting that decellularized skeletal muscle ECM provided a biomimetic microenvironment equivalent to that of native skeletal muscle tissues. Thus, combining decellularization methods with 3D cell-printing technologies shows great potential for treating muscle wasting. The various decellularization methods for native musculoskeletal tissues are summarized in Table 9.1.

## 9.4 Conclusion

In summary, recent technological breakthroughs in the field of regenerative medicine and tissue engineering have been achieved by incorporating dynamic biological cues into a biomaterial for functional tissue regeneration. Decellularized tissue-based matrix is among the most attractive biomimetic materials and shows great beneficial effects in a variety of biomedical applications.

**Table 9.1** Summary of various decellularization methods for bone, cartilage and skeletal muscle tissues described in this chapter

Sources of tissue	Decellularization methods	Reagents	References
Bone	Physical method/ Enzyme	1. Hydrostatic pressurization at 980 MPa at 30 °C for 10 min	Hashimoto et al. [48]
		2. 0.2 mg/mL of DNase I at 37 °C for 3 weeks	
		3. 80%v/v ethanol washing at 37 °C for 3 days	
	Enzyme/Physical method	1. 0.05% Trypsin/0.02% EDTA at 37 °C for 24 h	Gothard et al. [49]
	Surfactant/Enzyme	2. Repeated snap freezing and lyophilization	Grayson et al. [51] and Marolt et al. [50]
		1. 0.1% EDTA at room temp. for overnight at 4 °C	
2. 0.5% SDS in 10 mM Tris for 24 h at room temp			
Cartilage	Physical method/ Enzyme/Surfactant	3. 50 U/mL DNase, 1 U/mL RNase in 10 mM Tris for 3–5 h at 37 °C	Yang et al. [61] and Kang et al. [62]
		1. Physical pulverization	
		2. 3.5% phenylmethyl sulfonyl fluoride (PMSF) and 0.1% EDTA for 60 mins	
		3. 1% TritonX-100 in hypotonic Tris-HCl for 12 h at 4 °C	
	Enzyme/Surfactant/ Osmotic shock	4. 50 U/mL DNase and 1 U/mL RNase in 10 mM Tris-HCl at 37 °C	Sutherland et al. [63]
		1. hypertonic salt solution (HSS) treatment at 21 °C for overnight	
		2. 2 cycles of 0.05% TritonX-100	
		3. 0.0625 KU/mL benzonase at 37 °C for overnight	
		4. 1% sodium-lauroyl sarcosine at 21 °C for overnight	
		5. 40% ethanol washing	

(continued)

**Table 9.1** (continued)

Sources of tissue	Decellularization methods	Reagents	References
	Physical method/ Surfactant/Enzyme	1. Physical pulverization	Yin et al. [64]
		2. 0.5–2% SDS with 1–3% TritonX-100 at 4 °C for 8 h	
3. 50 U/mL DNase and 1 U/mL RNase at 37 °C for 4 h			
	Physical method/ Surfactant/Enzyme/ Osmotic shock	1. Physical pulverization	Pati et al. [65]
		2. Hypotonic 10 mM Tris-HCl buffer (pH 8.0) treatment	
		3. 6 cycles of freeze-thaw	
		4. 0.25% trypsin at 37 °C for 24 h	
		5. Hypertonic 1.5 M NaCl in 50 mM Tris-HCl buffer (pH 8.0) treatment at 37 °C for 4 h	
		6. 50 U/mL DNase and 1 U/mL RNase in 10 mM Tris-HCl (pH 7.5) at 37 °C for 4 h	
		7. Hypotonic 10 mM Tris-HCl buffer (pH 8.0) treatment for 20 h	
		8. 1% TritonX-100 for 24 h	
Skeletal muscle	Physical method/ Surfactant/Enzyme	1. Physical pulverization by slicing tissues (<500 μm)	Stern et al. [76]
		2. 0.05% trypsin with EDTA for 1 h	
		3. 1% TritonX-100 for 5 days	
	Physical method/ Surfactant	1. Physical pulverization by mincing tissues (<1 mm <sup>3</sup> )	DeQuach et al. [77]
		2. 1% SDS for 4–5 days	
	Physical method/ Surfactant/Enzyme	1. Physical pulverization by slicing tissues (<10 μm)	Chaturvedi et al. [78]
		2. 170 U/mL phospholipase for 30 min	
		3. 0.5% SDS in 20 mM Tris buffer (pH 8.0) for 30 mins	
		4. 0.15 M NaCl with 1x cOmplete protease inhibitor for 30 mins	
		5. 3.4 M NaCl in 20 mM Tris for 2 h	
		6. 75 U/mL DNaseI in 40 mM Tris-HCl (pH 8.0), 10 mM MgSO <sub>4</sub> and 1 mM CaCl <sub>2</sub>	
	Solvent/Surfactant	1. Chloroform for 4–5 days	Merritt et al. [79]
2. 2% SDS for 1 week			
3. 0.1 M Tris buffer (pH 9.0) for 4 h			
Physical method/ Surfactant/Enzyme	1. Physical pulverization by mincing tissues (<1 mm <sup>3</sup> )	Rao et al. [80]	
	2. 1% SDS for 5 days		
	3. isopropyl alcohol for 24 h		
Physical method/ Surfactant/Enzyme/ Solvent	1. Physical pulverization by mincing tissues (<1 mm <sup>3</sup> )	Choi et al. [81]	
	2. 1% SDS for 5 days		
	3. 0.5% TritonX-100 for 24 h		
	4. 50 U/mL DNase in PBS for 12 h		
	5. Isopropyl alcohol for 12 h		

Presently, complete decellularization of target tissue by combinations of physical, enzymatic, and chemical treatments is considered to be very important; however, preservation of the structural and functional components of the native ECM is equally important.

Despite the promising results of both *in vitro* and *in vivo* studies, some challenges remain regarding their pre-clinical/clinical applications. First, although various decellularization processes based on single or combinatorial methods provide a certain degree of removal of cellular and nuclear components of each tissue, the most efficient protocol for target tissues must be further optimized. Second, despite the previously reported immunomodulatory ability, to accelerate the use of decellularization-based technologies from the bench to the bedside, potential safety issues and risk factors of decellularized materials must be carefully evaluated. Third, identifying the specific molecular mechanism of decellularized material-mediated assembly of host stem cell populations or consequent donor cell contribution to tissue regeneration is necessary. If these issues can be overcome in further research and development studies, decellularization technology has an excellent potential to provide a great impact on cell-based translational research.

**Acknowledgement** This research was supported by the Basic Science Research Program through the National Research Foundation of Korea (NRF) funded by the Ministry of Education (2016K1A4A3914725) and partially supported by the Soonchunhyang University Research Fund.

## References

- Langer R (2000) Biomaterials in drug delivery and tissue engineering: one laboratory's experience. *Acc Chem Res* 33(2):94–101
- Shin H, Jo S, Mikos AG (2003) Biomimetic materials for tissue engineering. *Biomaterials* 24(24):4353–4364
- Lutolf MP, Hubbell JA (2005) Synthetic biomaterials as instructive extracellular microenvironments for morphogenesis in tissue engineering. *Nat Biotechnol* 23(1):47–55. <https://doi.org/10.1038/nbt1055>
- Tibbitt MW, Anseth KS (2009) Hydrogels as extracellular matrix mimics for 3D cell culture. *Biotechnol Bioeng* 103(4):655–663. <https://doi.org/10.1002/bit.22361>
- Hwang NS, Varghese S, Zhang Z, Elisseeff J (2006) Chondrogenic differentiation of human embryonic stem cell-derived cells in arginine-glycine-aspartate-modified hydrogels. *Tissue Eng* 12(9):2695–2706. <https://doi.org/10.1089/ten.2006.12.2695>
- Kim H, Lee Y, Kim Y, Hwang Y, Hwang N (2017) Biomimetically reinforced polyvinyl alcohol-based hybrid scaffolds for cartilage tissue engineering. *Polymers* 9(12):655
- Hwang Y, Phadke A, Varghese S (2011) Engineered microenvironments for self-renewal and musculoskeletal differentiation of stem cells. *Regen Med* 6(4):505–524. <https://doi.org/10.2217/rme.11.38>
- Badylak SF, Freytes DO, Gilbert TW (2009) Extracellular matrix as a biological scaffold material: structure and function. *Acta Biomater* 5(1):1–13. <https://doi.org/10.1016/j.actbio.2008.09.013>
- Brown BN, Valentin JE, Stewart-Akers AM, McCabe GP, Badylak SF (2009) Macrophage phenotype and remodeling outcomes in response to biologic scaffolds with and without a cellular component. *Biomaterials* 30(8):1482–1491. <https://doi.org/10.1016/j.biomaterials.2008.11.040>
- Saldin LT, Cramer MC, Velankar SS, White LJ, Badylak SF (2017) Extracellular matrix hydrogels from decellularized tissues: structure and function. *Acta Biomater* 49:1–15. <https://doi.org/10.1016/j.actbio.2016.11.068>
- Dziki JL, Huleihel L, Scarritt ME, Badylak SF (2017) Extracellular matrix bioscaffolds as immunomodulatory biomaterials. *Tissue Eng Part A* 23(19–20):1152–1159. <https://doi.org/10.1089/ten.TEA.2016.0538>
- Badylak SF, Taylor D, Uygun K (2011) Whole-organ tissue engineering: decellularization and recellularization of three-dimensional matrix scaffolds. *Annu Rev Biomed Eng* 13:27–53. <https://doi.org/10.1146/annurev-bioeng-071910-124743>
- Ott HC, Matthiesen TS, Goh SK, Black LD, Kren SM, Netoff TI, Taylor DA (2008) Perfusion-decellularized matrix: using nature's platform to engineer a bioartificial heart. *Nat Med* 14(2):213–221. <https://doi.org/10.1038/nm1684>
- Zhang W, Zhu Y, Li J, Guo Q, Peng J, Liu S, Yang J, Wang Y (2016) Cell-derived extracellular matrix: basic characteristics and current applications in orthopedic tissue engineering. *Tissue Eng Part B Rev* 22(3):193–207. <https://doi.org/10.1089/ten.TEB.2015.0290>
- Cheng CW, Solorio LD, Alsberg E (2014) Decellularized tissue and cell-derived extracellular matrices as scaffolds for orthopaedic tissue engineering. *Biotechnol Adv* 32(2):462–484. <https://doi.org/10.1016/j.biotechadv.2013.12.012>
- Spang MT, Christman KL (2018) Extracellular matrix hydrogel therapies: *in vivo* applications and development. *Acta Biomater* 68:1–14. <https://doi.org/10.1016/j.actbio.2017.12.019>

17. Crapo PM, Gilbert TW, Badylak SF (2011) An overview of tissue and whole organ decellularization processes. *Biomaterials* 32(12):3233–3243. <https://doi.org/10.1016/j.biomaterials.2011.01.057>
18. Gilpin A, Yang Y (2017) Decellularization strategies for regenerative medicine: from processing techniques to applications. *Biomed Res Int* 2017:9831534. <https://doi.org/10.1155/2017/9831534>
19. Syed O, Walters NJ, Day RM, Kim HW, Knowles JC (2014) Evaluation of decellularization protocols for production of tubular small intestine submucosa scaffolds for use in oesophageal tissue engineering. *Acta Biomater* 10(12):5043–5054. <https://doi.org/10.1016/j.actbio.2014.08.024>
20. Gorschewsky O, Puetz A, Riechert K, Klakow A, Becker R (2005) Quantitative analysis of biochemical characteristics of bone-patellar tendon-bone allografts. *Biomed Mater Eng* 15(6):403–411
21. Reing JE, Brown BN, Daly KA, Freund JM, Gilbert TW, Hsiong SX, Huber A, Kullas KE, Tottey S, Wolf MT, Badylak SF (2010) The effects of processing methods upon mechanical and biologic properties of porcine dermal extracellular matrix scaffolds. *Biomaterials* 31(33):8626–8633. <https://doi.org/10.1016/j.biomaterials.2010.07.083>
22. Heerklotz H (2008) Interactions of surfactants with lipid membranes. *Q Rev Biophys* 41(3–4):205–264. <https://doi.org/10.1017/S0033583508004721>
23. Lumpkins SB, Pierre N, McFetridge PS (2008) A mechanical evaluation of three decellularization methods in the design of a xenogeneic scaffold for tissue engineering the temporomandibular joint disc. *Acta Biomater* 4(4):808–816. <https://doi.org/10.1016/j.actbio.2008.01.016>
24. Nakayama KH, Batchelder CA, Lee CI, Tarantal AF (2010) Decellularized rhesus monkey kidney as a three-dimensional scaffold for renal tissue engineering. *Tissue Eng Part A* 16(7):2207–2216. <https://doi.org/10.1089/ten.TEA.2009.0602>
25. Uygun BE, Soto-Gutierrez A, Yagi H, Izamis ML, Guzzardi MA, Shulman C, Milwid J, Kobayashi N, Tilles A, Berthiaume F, Hertl M, Nahmias Y, Yarmush ML, Uygun K (2010) Organ reengineering through development of a transplantable recellularized liver graft using decellularized liver matrix. *Nat Med* 16(7):814–820. <https://doi.org/10.1038/nm.2170>
26. Gilpin SE, Ren X, Okamoto T, Guyette JP, Mou H, Rajagopal J, Mathisen DJ, Vacanti JP, Ott HC (2014) Enhanced lung epithelial specification of human induced pluripotent stem cells on decellularized lung matrix. *Ann Thorac Surg* 98(5):1721–1729.; discussion 9. <https://doi.org/10.1016/j.athoracsur.2014.05.080>
27. Petersen TH, Calle EA, Colehour MB, Niklason LE (2012) Matrix composition and mechanics of decellularized lung scaffolds. *Cells Tissues Organs* 195(3):222–231. <https://doi.org/10.1159/000324896>
28. Keane TJ, Swinehart IT, Badylak SF (2015) Methods of tissue decellularization used for preparation of biologic scaffolds and in vivo relevance. *Methods* 84:25–34. <https://doi.org/10.1016/j.jymeth.2015.03.005>
29. Fu Y, Fan X, Tian C, Luo J, Zhang Y, Deng L, Qin T, Lv Q (2016) Decellularization of porcine skeletal muscle extracellular matrix for the formulation of a matrix hydrogel: a preliminary study. *J Cell Mol Med* 20(4):740–749. <https://doi.org/10.1111/jcmm.12776>
30. Elder BD, Kim DH, Athanasiou KA (2010) Developing an articular cartilage decellularization process toward facet joint cartilage replacement. *Neurosurgery* 66(4):722–727.; discussion 7. <https://doi.org/10.1227/01.NEU.0000367616.49291.9F>
31. Petersen TH, Calle EA, Zhao L, Lee EJ, Gui L, Raredon MB, Gavrilov K, Yi T, Zhuang ZW, Breuer C, Herzog E, Niklason LE (2010) Tissue-engineered lungs for in vivo implantation. *Science* 329(5991):538–541. <https://doi.org/10.1126/science.1189345>
32. Flynn LE (2010) The use of decellularized adipose tissue to provide an inductive microenvironment for the adipogenic differentiation of human adipose-derived stem cells. *Biomaterials* 31(17):4715–4724. <https://doi.org/10.1016/j.biomaterials.2010.02.046>
33. Xing Q, Yates K, Tahtinen M, Shearier E, Qian Z, Zhao F (2015) Decellularization of fibroblast cell sheets for natural extracellular matrix scaffold preparation. *Tissue Eng Part C Methods* 21(1):77–87. <https://doi.org/10.1089/ten.TEC.2013.0666>
34. Lin P, Chan WC, Badylak SF, Bhatia SN (2004) Assessing porcine liver-derived biomatrix for hepatic tissue engineering. *Tissue Eng* 10(7–8):1046–1053. <https://doi.org/10.1089/ten.2004.10.1046>
35. Funamoto S, Nam K, Kimura T, Murakoshi A, Hashimoto Y, Niwaya K, Kitamura S, Fujisato T, Kishida A (2010) The use of high-hydrostatic pressure treatment to decellularize blood vessels. *Biomaterials* 31(13):3590–3595. <https://doi.org/10.1016/j.biomaterials.2010.01.073>
36. Sasaki S, Funamoto S, Hashimoto Y, Kimura T, Honda T, Hattori S, Kobayashi H, Kishida A, Mochizuki M (2009) In vivo evaluation of a novel scaffold for artificial corneas prepared by using ultrahigh hydrostatic pressure to decellularize porcine corneas. *Mol Vis* 15:2022–2028
37. Seo Y, Jung Y, Kim SH (2018) Decellularized heart ECM hydrogel using supercritical carbon dioxide for improved angiogenesis. *Acta Biomater* 67:270–281. <https://doi.org/10.1016/j.actbio.2017.11.046>
38. Halfwerk FR, Rouwkema J, Gossen JA, Grandjean JG (2018) Supercritical carbon dioxide decellularised pericardium: mechanical and structural characterisation for applications in cardio-thoracic surgery. *J Mech Behav Biomed Mater* 77:400–407. <https://doi.org/10.1016/j.jmbbm.2017.10.002>
39. Calori GM, Mazza E, Colombo M, Ripamonti C (2011) The use of bone-graft substitutes in large bone defects: any specific needs? *Injury* 42(Suppl 2):S56–S63. <https://doi.org/10.1016/j.injury.2011.06.011>
40. Lutolf MP, Weber FE, Schmoekel HG, Schense JC, Kohler T, Muller R, Hubbell JA (2003) Repair of bone defects using synthetic mimetics of collagenous

- extracellular matrices. *Nat Biotechnol* 21(5):513–518. <https://doi.org/10.1038/nbt818>
41. Banwart JC, Asher MA, Hassanein RS (1995) Iliac crest bone graft harvest donor site morbidity. A statistical evaluation. *Spine* 20(9):1055–1060
  42. Phadke A, Hwang Y, Kim SH, Kim SH, Yamaguchi T, Masuda K, Varghese S (2013) Effect of scaffold microarchitecture on osteogenic differentiation of human mesenchymal stem cells. *Eur Cell Mater* 25:114–129
  43. Datta N, Holtorf HL, Sikavitsas VI, Jansen JA, Mikos AG (2005) Effect of bone extracellular matrix synthesized in vitro on the osteoblastic differentiation of marrow stromal cells. *Biomaterials* 26(9):971–977. <https://doi.org/10.1016/j.biomaterials.2004.04.001>
  44. Papadimitropoulos A, Scotti C, Bourguine P, Scherberich A, Martin I (2015) Engineered decellularized matrices to instruct bone regeneration processes. *Bone* 70:66–72. <https://doi.org/10.1016/j.bone.2014.09.007>
  45. Nyberg E, Rindone A, Dorafshar A, Grayson WL (2017) Comparison of 3D-printed poly-varepsilon-caprolactone scaffolds functionalized with tricalcium phosphate, hydroxyapatite, Bio-Oss, or decellularized bone matrix. *Tissue Eng Part A* 23(11–12):503–514. <https://doi.org/10.1089/ten.TEA.2016.0418>
  46. Gruskin E, Doll BA, Futrell FW, Schmitz JP, Hollinger JO (2012) Demineralized bone matrix in bone repair: history and use. *Adv Drug Deliv Rev* 64(12):1063–1077. <https://doi.org/10.1016/j.addr.2012.06.008>
  47. Lee DJ, Diachina S, Lee YT, Zhao L, Zou R, Tang N, Han H, Chen X, Ko CC (2016) Decellularized bone matrix grafts for calvaria regeneration. *J Tissue Eng* 7:2041731416680306. <https://doi.org/10.1177/2041731416680306>
  48. Hashimoto Y, Funamoto S, Kimura T, Nam K, Fujisato T, Kishida A (2011) The effect of decellularized bone/bone marrow produced by high-hydrostatic pressurization on the osteogenic differentiation of mesenchymal stem cells. *Biomaterials* 32(29):7060–7067. <https://doi.org/10.1016/j.biomaterials.2011.06.008>
  49. Gothard D, Smith EL, Kanczler JM, Black CR, Wells JA, Roberts CA, White LJ, Qutachi O, Peto H, Rashidi H, Rojo L, Stevens MM, El Haj AJ, Rose FR, Shakesheff KM, Oreffo RO (2015) In vivo assessment of bone regeneration in alginate/bone ECM hydrogels with incorporated skeletal stem cells and single growth factors. *PLoS One* 10(12):e0145080. <https://doi.org/10.1371/journal.pone.0145080>
  50. Marolt D, Campos IM, Bhumiratana S, Koren A, Petridis P, Zhang G, Spitalnik PF, Grayson WL, Vunjak-Novakovic G (2012) Engineering bone tissue from human embryonic stem cells. *Proc Natl Acad Sci U S A* 109(22):8705–8709. <https://doi.org/10.1073/pnas.1201830109>
  51. Grayson WL, Marolt D, Bhumiratana S, Frohlich M, Guo XE, Vunjak-Novakovic G (2011) Optimizing the medium perfusion rate in bone tissue engineering bioreactors. *Biotechnol Bioeng* 108(5):1159–1170. <https://doi.org/10.1002/bit.23024>
  52. Temenoff JS, Mikos AG (2000) Review: tissue engineering for regeneration of articular cartilage. *Biomaterials* 21(5):431–440
  53. Kock L, van Donkelaar CC, Ito K (2012) Tissue engineering of functional articular cartilage: the current status. *Cell Tissue Res* 347(3):613–627. <https://doi.org/10.1007/s00441-011-1243-1>
  54. Sophia Fox AJ, Bedi A, Rodeo SA (2009) The basic science of articular cartilage: structure, composition, and function. *Sports Health* 1(6):461–468. <https://doi.org/10.1177/1941738109350438>
  55. Makris EA, Gomoll AH, Malizos KN, Hu JC, Athanasiou KA (2015) Repair and tissue engineering techniques for articular cartilage. *Nat Rev Rheumatol* 11(1):21–34. <https://doi.org/10.1038/nrrheum.2014.157>
  56. Ahn CB, Kim Y, Park SJ, Hwang Y, Lee JW (2017) Development of arginine-glycine-aspartate-immobilized 3D printed poly(propylene fumarate) scaffolds for cartilage tissue engineering. *J Biomater Sci Polym Ed* 1–15. <https://doi.org/10.1080/09205063.2017.1383020>
  57. Benders KE, van Weeren PR, Badylak SF, Saris DB, Dhert WJ, Malda J (2013) Extracellular matrix scaffolds for cartilage and bone regeneration. *Trends Biotechnol* 31(3):169–176. <https://doi.org/10.1016/j.tibtech.2012.12.004>
  58. Burdick JA, Mauck RL, Gorman JH 3rd, Gorman RC (2013) Acellular biomaterials: an evolving alternative to cell-based therapies. *Sci Transl Med* 5(176):176ps4. <https://doi.org/10.1126/scitranslmed.3003997>
  59. Gong YY, Xue JX, Zhang WJ, Zhou GD, Liu W, Cao Y (2011) A sandwich model for engineering cartilage with acellular cartilage sheets and chondrocytes. *Biomaterials* 32(9):2265–2273. <https://doi.org/10.1016/j.biomaterials.2010.11.078>
  60. Rowland CR, Colucci LA, Guilak F (2016) Fabrication of anatomically-shaped cartilage constructs using decellularized cartilage-derived matrix scaffolds. *Biomaterials* 91:57–72. <https://doi.org/10.1016/j.biomaterials.2016.03.012>
  61. Yang Q, Peng J, Guo Q, Huang J, Zhang L, Yao J, Yang F, Wang S, Xu W, Wang A, Lu S (2008) A cartilage ECM-derived 3-D porous acellular matrix scaffold for in vivo cartilage tissue engineering with PKH26-labeled chondrogenic bone marrow-derived mesenchymal stem cells. *Biomaterials* 29(15):2378–2387. <https://doi.org/10.1016/j.biomaterials.2008.01.037>
  62. Kang H, Peng J, Lu S, Liu S, Zhang L, Huang J, Sui X, Zhao B, Wang A, Xu W, Luo Z, Guo Q (2014) In vivo cartilage repair using adipose-derived stem cell-loaded decellularized cartilage ECM scaffolds. *J Tissue Eng Regen Med* 8(6):442–453. <https://doi.org/10.1002/term.1538>
  63. Sutherland AJ, Beck EC, Dennis SC, Converse GL, Hopkins RA, Berkland CJ, Detamore MS (2015) Decellularized cartilage may be a chondroinductive

- material for osteochondral tissue engineering. *PLoS One* 10(5):e0121966. <https://doi.org/10.1371/journal.pone.0121966>
64. Yin H, Wang Y, Sun Z, Sun X, Xu Y, Li P, Meng H, Yu X, Xiao B, Fan T, Wang Y, Xu W, Wang A, Guo Q, Peng J, Lu S (2016) Induction of mesenchymal stem cell chondrogenic differentiation and functional cartilage microtissue formation for in vivo cartilage regeneration by cartilage extracellular matrix-derived particles. *Acta Biomater* 33:96–109. <https://doi.org/10.1016/j.actbio.2016.01.024>
  65. Pati F, Jang J, Ha DH, Won Kim S, Rhie JW, Shim JH, Kim DH, Cho DW (2014) Printing three-dimensional tissue analogues with decellularized extracellular matrix bioink. *Nat Commun* 5:3935. <https://doi.org/10.1038/ncomms4935>
  66. Teodori L, Costa A, Marzio R, Perniconi B, Coletti D, Adamo S, Gupta B, Tarnok A (2014) Native extracellular matrix: a new scaffolding platform for repair of damaged muscle. *Front Physiol* 5:218. <https://doi.org/10.3389/fphys.2014.00218>
  67. Qazi TH, Mooney DJ, Pumberger M, Geissler S, Duda GN (2015) Biomaterials based strategies for skeletal muscle tissue engineering: existing technologies and future trends. *Biomaterials* 53:502–521. <https://doi.org/10.1016/j.biomaterials.2015.02.110>
  68. Crawley S, Farrell EM, Wang W, Gu M, Huang HY, Huynh V, Hodges BL, Cooper DN, Kaufman SJ (1997) The alpha7beta1 integrin mediates adhesion and migration of skeletal myoblasts on laminin. *Exp Cell Res* 235(1):274–286. <https://doi.org/10.1006/excr.1997.3671>
  69. Gillies AR, Lieber RL (2011) Structure and function of the skeletal muscle extracellular matrix. *Muscle Nerve* 44(3):318–331. <https://doi.org/10.1002/mus.22094>
  70. Wang YX, Rudnicki MA (2011) Satellite cells, the engines of muscle repair. *Nat Rev Mol Cell Biol* 13(2):127–133. <https://doi.org/10.1038/nrm3265>
  71. Hwang Y, Seo T, Hariri S, Choi C, Varghese S (2017) Matrix topographical cue-mediated myogenic differentiation of human embryonic stem cell derivatives. *Polymers* 9(11):580
  72. Conconi MT, De Coppi P, Bellini S, Zara G, Sabatti M, Marzaro M, Zanon GF, Gamba PG, Parnigotto PP, Nussdorfer GG (2005) Homologous muscle acellular matrix seeded with autologous myoblasts as a tissue-engineering approach to abdominal wall-defect repair. *Biomaterials* 26(15):2567–2574. <https://doi.org/10.1016/j.biomaterials.2004.07.035>
  73. Merritt EK, Hammers DW, Tierney M, Suggs LJ, Walters TJ, Farrar RP (2010) Functional assessment of skeletal muscle regeneration utilizing homologous extracellular matrix as scaffolding. *Tissue Eng Part A* 16(4):1395–1405. <https://doi.org/10.1089/ten.TEA.2009.0226>
  74. DeQuach JA, Lin JE, Cam C, Hu D, Salvatore MA, Sheikh F, Christman KL (2012) Injectable skeletal muscle matrix hydrogel promotes neovascularization and muscle cell infiltration in a hindlimb ischemia model. *Eur Cell Mater* 23:400–412 discussion 12
  75. Ungerleider JL, Johnson TD, Rao N, Christman KL (2015) Fabrication and characterization of injectable hydrogels derived from decellularized skeletal and cardiac muscle. *Methods* 84:53–59. <https://doi.org/10.1016/j.ymeth.2015.03.024>
  76. Stern MM, Myers RL, Hammam N, Stern KA, Eberli D, Kritchevsky SB, Soker S, Van Dyke M (2009) The influence of extracellular matrix derived from skeletal muscle tissue on the proliferation and differentiation of myogenic progenitor cells ex vivo. *Biomaterials* 30(12):2393–2399. <https://doi.org/10.1016/j.biomaterials.2008.12.069>
  77. DeQuach JA, Mezzano V, Miglani A, Lange S, Keller GM, Sheikh F, Christman KL (2010) Simple and high yielding method for preparing tissue specific extracellular matrix coatings for cell culture. *PLoS One* 5(9):e13039. <https://doi.org/10.1371/journal.pone.0013039>
  78. Chaturvedi V, Dye DE, Kinnear BF, van Kuppevelt TH, Grounds MD, Coombe DR (2015) Interactions between skeletal muscle myoblasts and their extracellular matrix revealed by a serum free culture system. *PLoS One* 10(6):e0127675. <https://doi.org/10.1371/journal.pone.0127675>
  79. Merritt EK, Cannon MV, Hammers DW, Le LN, Gokhale R, Sarathy A, Song TJ, Tierney MT, Suggs LJ, Walters TJ, Farrar RP (2010) Repair of traumatic skeletal muscle injury with bone-marrow-derived mesenchymal stem cells seeded on extracellular matrix. *Tissue Eng Part A* 16(9):2871–2881. <https://doi.org/10.1089/ten.TEA.2009.0826>
  80. Rao N, Agmon G, Tierney MT, Ungerleider JL, Braden RL, Sacco A, Christman KL (2017) Engineering an injectable muscle-specific microenvironment for improved cell delivery using a nanofibrous extracellular matrix hydrogel. *ACS Nano* 11(4):3851–3859. <https://doi.org/10.1021/acs.nano.7b00093>
  81. Choi YJ, Kim TG, Jeong J, Yi HG, Park JW, Hwang W, Cho DW (2016) 3D cell printing of functional skeletal muscle constructs using skeletal muscle-derived bioink. *Adv Healthc Mater* 5(20):2636–2645. <https://doi.org/10.1002/adhm.201600483>



# Clinical Applications of Injectable Biomaterials

# 10

Hatice Ercan, Serap Durkut, Aysel Koc-Demir,  
Ayşe Eser Elçin, and Yaşar Murat Elçin

## Abstract

Regenerative medicine is an interdisciplinary field that aims to regenerate the lost or diseased tissues through the combinational use of cells, biomolecules and/or biomaterials. Injectable biomaterials have been comprehensively evaluated for use in this field for their prominent properties, such as ease of handling, providing a better integration of the native tissue by filling irregular defects and having controllable chemical and physical properties. This class of biomaterials can be developed from natural or synthetic origin materials, decellularized matrices or from combinations of materials to form composites. Injectable biomaterials enable minimally invasive approach when compared with traditional open surgeries, which can reduce the

cost, and speed up the recovery time for the patients. Cells, growth factors and/or bioactive molecules can be effectively delivered to the target tissue using injectable biomaterials, making them desirable for a number of clinical applications. This chapter gives an overview on injectable biomaterials and their clinical applications in soft, hard, and cardiovascular tissue regeneration.

## Keywords

Injectable biomaterials · Stimuli-responsive hydrogels · In-situ gelling · Clinical applications · Tissue engineering · Regenerative medicine · Scaffolds · Biopolymers

H. Ercan · S. Durkut · A. Koc-Demir · A. E. Elçin  
Tissue Engineering, Biomaterials and  
Nanobiotechnology Laboratory, Faculty of Science,  
Stem Cell Institute, Ankara University, Ankara,  
Turkey

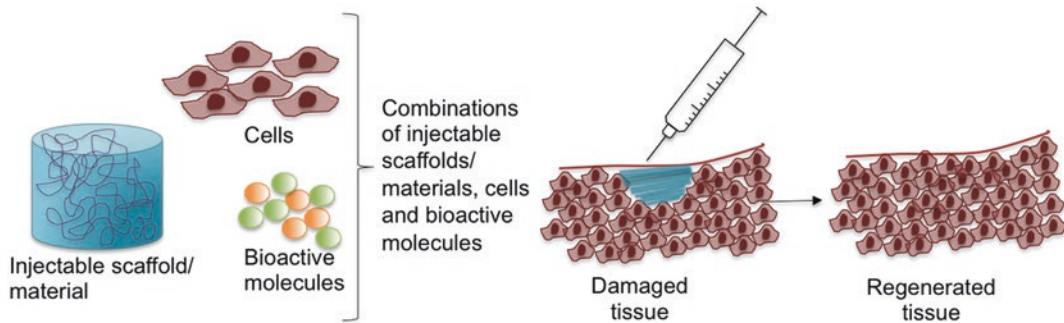
Y. M. Elçin (✉)  
Tissue Engineering, Biomaterials and  
Nanobiotechnology Laboratory, Faculty of Science,  
Stem Cell Institute, Ankara University, Ankara,  
Turkey

Biovalda Health Technologies, Inc., Ankara, Turkey

## 10.1 Introduction

Tissue engineering is a field that intends to restore or replace the damaged tissues with the combination of cells, biochemical factors and scaffolds [1]. Tissue engineering scaffolds ensure a structural support as an artificial extracellular matrix (ECM) for cell attachment, growth, proliferation, differentiation and organization into a three-dimensional (3-D) structure. In addition, the scaffold should facilitate transport of nutrients, oxygen, growth factors and waste removal. An ideal biomaterial scaffold assists new tissue formation and remodeling by allowing cells to





**Fig. 10.1** Injectable biomaterials in tissue engineering applications

maintain their microenvironment [2]. The scaffold material can vary based on the application and tissue type. A wide range of biomaterials from natural or synthetic sources can be developed with the aim to regenerate tissues [3, 4].

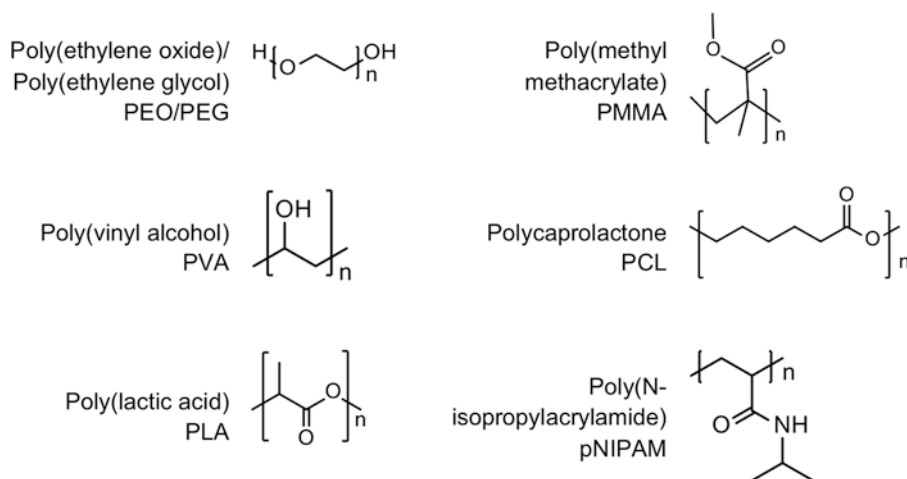
Injectable biomaterials have remarkable advantages over other preformed scaffold types and are prevalently used in tissue engineering [5–8] (Fig. 10.1). They also have potential cell-free uses, e.g. in the orthopedic surgery [9], and in the reconstructive surgery field [6]. Injectable biomaterials also find application in drug delivery [10]. An invasive surgery will be required for scaffold implantation, however injectable scaffolds can be delivered in-situ by minimally invasive technique through needle-cannula injection avoiding complications associated with open surgery. This property could be imperative in circumstances where tissues cannot be reached by a large incision, such as stroke treatment in the brain, etc. [11]. Also applying injectable biomaterials will reduce the infection risks of the open surgery. Lacking of any sutures will provide freedom of action to the patient and will shorten the patient's remission time. Injectable biomaterials should have an appropriate viscosity to fill the defect site and its hardening time should be controllable in order to integrate with the defect. Besides, injectable biomaterials should not cause any host response, and should provide a mechanical support for tissue regeneration as a template [10]. In this chapter, an overview of injectable biomaterials, and their clinical use in soft, hard, and cardiovascular tissue regeneration is given.

## 10.2 Sources of Injectable Biomaterials

Injectable biomaterials enable complex treatments through a minimally invasive surgical procedure. This property is required especially in cases where the lesion cannot be reached or in cases where a large incision is counter indicated, such as treatment of stroke in the brain [11]. Second important feature of injectable biomaterials is that they can easily integrate with the native tissue by filling the irregular defects, thus allowing customization for the patient [8]. To fulfill a variety of treatment needs, injectable biomaterials should display properties such as, mechanical resistance, biocompatibility, biodegradability and tissue-specific interactions. Injectable biomaterials and their properties can vary depending on the tissue of interest [12–16]. They can be categorized into three main classes on the basis of source; i.e. synthetic polymers, natural polymers, and decellularized matrices.

### 10.2.1 Synthetic Polymers

Synthetic polymers are used as injectable biomaterials to benefit from their controllable chemical and physical properties. In addition to being combined with growth factors, they have tunable matrix structure and chemical composition. The crosslinking density, gel formation dynamics, mechanical properties and degradation rate of synthetic polymers can be adjusted to the needs.



**Fig. 10.2** Chemical structures of common synthetic polymers

The most frequently used synthetic-origin injectable biomaterials are; poly(ethylene oxide) (PEO), poly(ethylene glycol) (PEG), poly(vinyl alcohol) (PVA), poly(lactic acid) (PLA), poly(propylene fumarate) (PPF) and poly(propylene fumarate-co-ethylene glycol) (P(PF-co-EG)) [14, 17] (Fig. 10.2).

Poly(ethylene oxide) is FDA approved for a number of medical applications. It is a photo-crosslinked polymer with hydrophilic properties. PEO can be modified with the suitable photoinitiator for crosslinking by UV exposure [14]. Sims et al. have developed an injectable cartilage biomaterial by combining bovine chondrocytes with PEO and have injected into the nude mouse model. Histological analyses at 6 and 12 weeks confirmed the formation of neo-cartilage without any adverse inflammatory response [18].

In a study by Aho and co-workers, an injectable composite of poly( $\epsilon$ -caprolactone-co-D,L-lactic acid) (PCLA) and bioactive glass S53P4 (BAG) was used as synthetic bone filler in a rabbit cancellous and cartilaginous subchondral defect model. Thus, the composite structure provided an interface with the host tissue. The high rate of bone bioactivity index and increased bone coverage index indicated good osteoconductivity. These values correlated with the amount of glass in the composite [19].

Poly(methyl methacrylate) (PMMA) has widely been used in dental and bone repair applications [20–22]. PMMA is used as combination of a monomer liquid and polymer powder. PMMA-based injectable biomaterials are especially useful for vertebral augmentation in the clinics due to their ease of handling, structural integrity, and radiopacity [23].

Poly(lactic acid) is an aliphatic polyester which has been recognized as biocompatible and biodegradable, as its degradation products can be naturally metabolized in-vivo [24]. Homopolymers of lactic acid can be stereoregular with D- or L- configurations, or racemic mixtures of D- and L-lactic acid units [25, 26]. Stereoregular D- and L-PLA have been used as crosslinking moieties by forming stereocomplexes, which also provide propulsive forces to make in-situ forming hydrogels [27, 28]. PLA has been utilized in many biomedical applications, including drug delivery and as structural component of internal fixation devices [29].

Stimuli responsive hydrogels are a class of biopolymers which respond to changes in their environment [30]. Many hydrogels can undergo reversible changes in phase transition, from a solution-to-gel or gel-to-solution, connected with their chemical properties and the type of stimulus. This group of materials can be stimulated by pH, temperature, ionic strength, specific ions or mol-

ecules, electric field, magnetic field, and light. Among them, the most studied ones are the pH- and temperature-responsive (thermo-sensitive) hydrogels. The networks of pH-sensitive polymers change from neutral to charged state, with the changes in the environmental pH. In the biomedical field pH-sensitive hydrogels are commonly applied in the body parts having different pH levels, such as the stomach, intestine, blood vessels, vagina or tumor sites [31].

Thermo-responsive hydrogels undergo gelation upon change (increase or decrease) in the temperature [32]. They show two types of characteristic behavior in aqueous solution, known as the lower critical solution temperature (LCST) and the upper critical solution temperature (UCST). Below the LCST, the polymer is hydrophilic and soluble and above the LCST, the polymer becomes more hydrophobic and insoluble, thus causing a collapse into a gel form [33]. In-situ gelled hydrogels can be used for the sustained release of therapeutics at a targeted site. These biomaterials undergo sol-gel transition after introduction into the body; thus gelation occurs in-situ at physiological temperature based on the thermo-sensitive character. The biomaterial degrades gradually over time, allowing localized release of the therapeutic at the desired site of the body.

Lei et al. [34] have used PLA as an injectable, and have designed a radiopaque thermogel based on PLA-PEG hydrogel system. They used mPEG-PLA diblock and PLA-PEG-PLA triblock copolymers end-capped with triiodo benzoic acid derivatives. The obtained TIB-capped mPEG-PLA thermogel showed good injectability and high level of in-vivo radiopacity at different administration sites [34]. Thermo-responsive hydrogels also find use in cell encapsulation and tissue engineering applications [35].

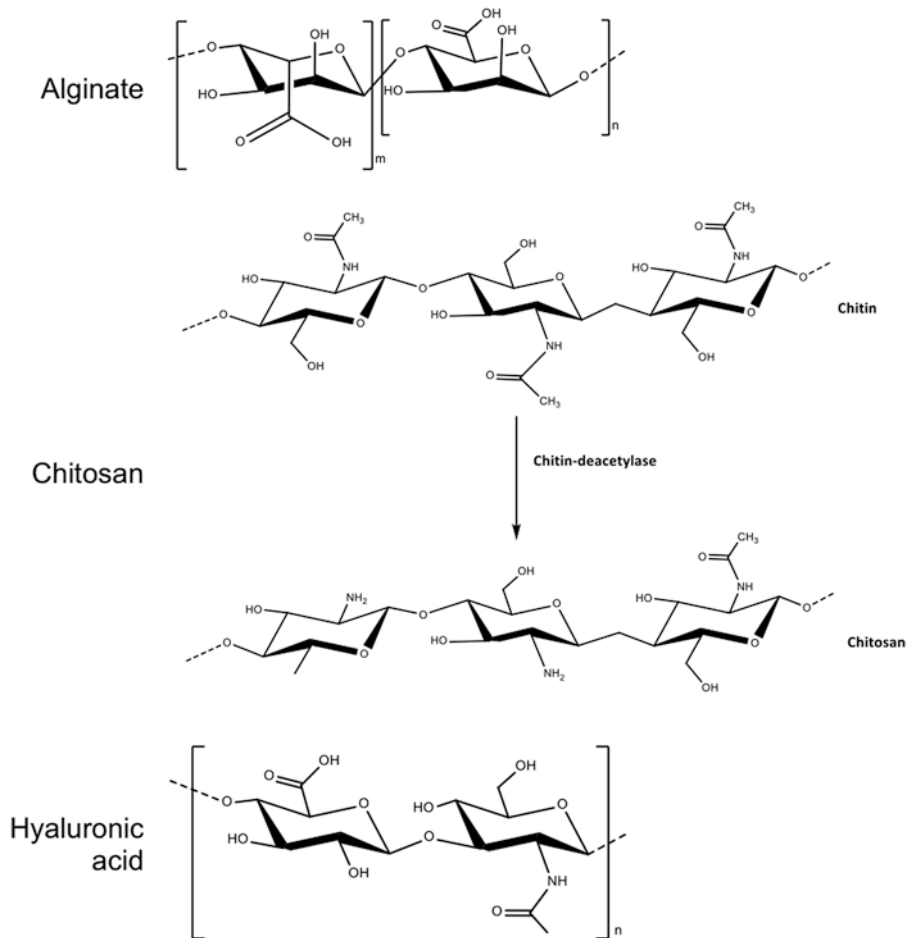
Injectable biomaterials can fill the irregular bone defects. Also therapeutic agents can be incorporated into an aqueous solution without the need for organic solvents. Kim et al. have developed an injectable pH and thermo-sensitive multi-block copolymer, PCLA-PEG-PCLA for bone tissue engineering [36]. The copolymer encapsulates human multipotent stromal cells (hMSCs)

and recombinant human bone morphogenetic protein-2 (rhBMP-2) with high efficiency. When subcutaneously injected into the mice, at the seventh week researchers observed human mesenchymal stem cells (hMSC) differentiation, and the formation of mineralized ectopic tissue with high levels of alkaline phosphatase (ALP) activity [36].

For cardiac repair, biodegradable and temperature-sensitive gels are a valid option due to the gelation property in physiological conditions, maintaining molecular bioactivity and cell viability. Wu et al. described the production of a temperature-sensitive polyester, poly(D-valerolactone) (PVL)-PEG-PVL in conjugation with vascular endothelial growth factor (VEGF) and investigated its reparative capacity on a myocardial infarction (MI) model. PVL-PEG-PVL in liquid form (at room temperature) transformed into solid form when injected. As the result, improvement in ventricular function with a decrease in negative cardiac remodeling was observed. Also, polymer conjugated with VEGF promoted localized angiogenesis [37].

## 10.2.2 Natural Polymers

Collagen, chitosan, alginate and hyaluronic acid (HA) offer properties resembling the natural ECM, so that biological environment accepts and degrades scaffolds made from these natural polymers (Fig. 10.3). Owing to the biomimetic properties, natural polymers are compatible with the cells and cellular interactions [38]. Main disadvantages of these biomaterials are their low mechanical strength and fast degradation rate. Injectable hydrogels contain hydrophilic chains that make them soluble in water. After crosslinking, insoluble networks are formed which leads to the swelling of the material in water. Water molecules surrounding the polymer chains act as plasticizers, thus decreasing their mechanical properties. To enhance the mechanical properties, chemically crosslinkable groups are introduced into the chains. Mechanical properties of physically crosslinked injectable hydrogels are generally weaker when compared to covalently crosslinked hydrogels. Crosslinking density,



**Fig. 10.3** Common natural polymers and their structures

types of bonds and the structure of the polymer can affect the mechanical properties of crosslinked hydrogels [16]. However, with refined techniques and/or new recombinant approaches it is possible to overcome the mechanical limitations of natural origin biomaterials. The degradation rate and mechanical properties of natural biopolymers can be improved by combining them with synthetic materials [12].

Collagen is a highly utilized natural polymer as a biomaterial. It is abundant in mammalian tissues as the ECM component, and comprised of three polypeptide chains forming a three-stranded structure. Collagen can form fibers by self-aggregation and cross-linking. Collagen degradation is governed by metalloprotease activity, specifically serine proteases and collagenases. In

comparison to some other natural polymers, collagen exhibits good biodegradability, weak antigenicity and superior biocompatibility, making it a preferred biomaterial for medical applications [39].

Alginate is a naturally occurring linear hydrophilic polysaccharide, composed of (1-4)-linked  $\alpha$ -L-guluronic acid (G) and  $\beta$ -D-mannuronic acid (M) monomers. Gelation of alginate occurs through cooperative binding between G units caused by divalent cations (such as  $Mg^{2+}$ ,  $Ba^{2+}$ , or  $Ca^{2+}$ ) [40]. The mechanical properties and the crosslinking density of alginate gels are altered by changing the M/G ratio, and the molecular weight [14]. The characteristic gelation property of alginate enables its use in drug delivery, cell encapsulation, and tissue engineering [41]. Cells

encapsulated in alginate could allow minimally invasive operations for the treatment of orthopaedic deformities. For example, Dobratz et al. reported that in-situ molded cell-encapsulated alginate scaffold maintained its stability for more than 38 weeks upon implantation [42].

Injectable composite biomaterials have also been used as cell delivery vehicles in tissue engineering of the bone. Beta-tricalcium phosphate ( $\beta$ -TCP) is a synthetic calcium phosphate bioceramic displaying optimal osteoconductivity and biodegradability. It can be combined with collagen, fibrin and/or alginate gels as scaffold for bone tissue engineering. In a study by [43], it was found that MSC-laden alginate- $\beta$ -TCP composite subcutaneously injected into nude mice supported new bone formation and osteogenic differentiation of MSCs.

Chitosan is a semi-crystalline, linear polysaccharide consisting of  $\beta$ - (1-4) 2-amino-2-deoxy-D-glucose unit repeats. It is formed by the N-deacetylation of chitin [44], where the crystallinity is determined by the amount of deacetylation. Chitosan becomes soluble in dilute acids below pH 5, as the free amino groups become protonated. pH-dependent solubility of chitosan enables processing under mild conditions. Chitosan is degraded through hydrolysis (by lysozyme and other proteolytic enzymes). Degradation kinetics is directly related to the degree of crystallinity [45]. Its biocompatibility, biodegradability and low immunogenicity properties enable the use of chitosan as an injectable biomaterial [46]. For example, Mwale et al. investigated the feasibility of cell-laden genipin cross-linked chitosan glutamate for the treatment of nucleus pulposus (NP) as a supplementation of the degenerate intervertebral disk (IVD) on an in-vitro cadaveric intervertebral disk model [47]. Chitosan and its degradation products can be utilized as nutrients for the cartilage [46]. Lu and co-workers evaluated the use of intra-articular chitosan injection in a rat defect model, and found that chitosan significantly decreased epiphyseal cartilage thickness and increased chondrocyte density of the articular cartilage [48]. This finding suggests that injectable chito-

san could be a sound alternative for cartilage regeneration.

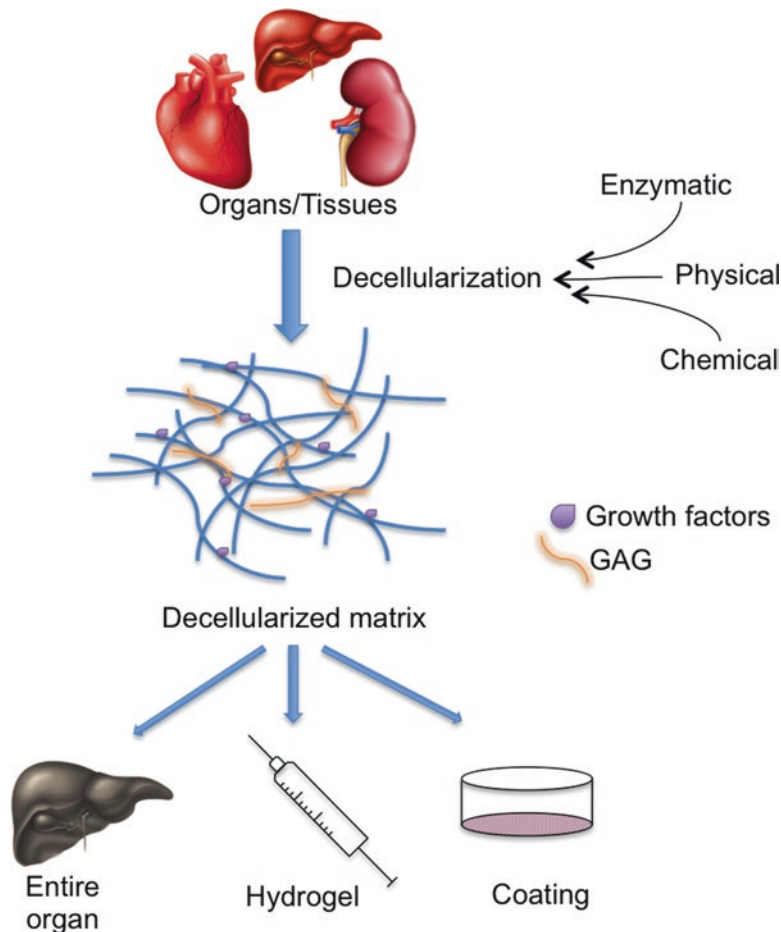
Hyaluronic acid is present in nearly all tissues of vertebrate organisms. It comprises of D-glucuronic acid and N-acetyl-D-glucosamine repeating disaccharide units [49]. HA hydrogels are formed through covalent crosslinking by utilizing hydrazide derivatives, annealing and esterification [50]. HA is important for many biological processes, *i.e.* cell differentiation, proteoglycan organization, nutrient diffusion and tissue hydration. HA is fully biodegradable, non-thrombogenic and non-immunogenic. HA finds use as biological absorber, lubricant and an injectable biomaterial for regenerative applications [51].

Fibrin is widely used as sealant in clinical applications. It contributes to natural wound healing [52]. Fibrin gels are formed through enzymatic polymerization of fibrinogen in the presence of thrombin and its degradation rate can be controlled by a proteinase inhibitor, apronitin. Evidence suggests that fibrin gels induce cell proliferation, matrix synthesis and cell migration [53]. Fibrin glue is useful in a number of tissue engineering applications; one of them is the bone tissue engineering. Zhu et al. evaluated the ectopic (subcutaneous) bone tissue formation potential of a platelet-rich fibrin gel containing BMP-2 and bone marrow MSCs in a nude mice model [54]. Bone tissue formation was observed after 12 weeks, indicating the regenerative osteogenic potential, and that platelet-enriched fibrin glue was better than platelet-rich plasma (PRP) [54]. In a different application, Christman et al. evaluated fibrin glue as wall support and its use as injectable scaffold (with and without myoblasts) in a rat post-MI heart model [55]. Researchers noted improvement in cellular retention and survival with significant positive changes in cardiac function.

### 10.2.3 Decellularized Matrices

Scaffolds derived from the decellularization of tissues and organs have come into prominence in the last decade [56]. They are currently gaining

**Fig. 10.4** Concept of decellularization process



use for regenerative applications for tissue and organ replacement [57]. Upon decellularization of fresh tissues/organs, a complex combination of functional and structural proteins that constitute the extracellular matrix (ECM) remains (Fig. 10.4). As known, ECM is formed by the biological activity of resident cells. ECM components are organized in a 3-D pattern specific to tissue type. It provides cues to cells for migration, proliferation and differentiation [58, 59].

Cardiac tissue does not have significant regenerative capacity, so it cannot completely repair itself after an ischemic injury which may lead to negative left ventricular remodeling [60]. Success of cell-based cardiac repair or cardiac patch treatments is limited by poor cell survival and retention. Current cardiac regenerative approaches are mostly focused on injectable biomaterials alone

or in combination with cells [61–63]. Seif-Naraghi et al. evaluated the use of decellularized porcine pericardium as an injectable biomaterial on rat myocardium and observed infiltration of vascular cells. Moreover, the team reported c-kit cell existence at the injection site, indicating recruitment of resident progenitors [64].

Cellular transplantation combined with biomaterial support may influence cardiac repair. An example is the study by [65], in which acellular porcine small intestine submucosa (SIS)-derived ECM was found to promote angiogenesis. Porcine SIS is a source for glycosaminoglycans and glycoproteins which facilitates successful cell function and attachment [65]. In another study, Zhao et al. reported an increase in stem cell factor expression, recruitment of bone marrow-derived c-kit positive cells, and an

increase in VEGF expression, following injection of SIS-ECM into the MI model, suggesting that decellularized biomaterial has favorable effects on cardiac remodeling [66].

Singelyn et al. proposed a decellularized myocardium-based injectable biomaterial for vascularization [63]. The myocardial matrix promoted vascular cell infiltration, and new arteriole formation was observed after 11 days. Later, the group evaluated the self-assembling gel derived from decellularized ventricular ECM in a MI model, and found that the injectable biomaterial increased the number of endogenous cardiomyocytes and preserved cardiac function post-MI [67].

DeQuach et al. [68] investigated the potential of decellularized skeletal muscle ECM-based hydrogel injectable for treating peripheral artery disease (PAD) in an hind limb ischemia model. Upon injection, a porous scaffold was formed which promoted cell infiltration to the damaged zone. ECM injectable increased capillary and arteriole density 1 week after injection, and recruited higher number of MyoD-positive and desmin-positive cells compared to positive control. The results show that injectable ECM hydrogels can be further developed as a stand-alone therapy for the treatment of ischemia caused by PAD [68].

---

### 10.3 Clinical Applications of Injectable Biomaterials

The use of injectable biomaterials is becoming an attractive alternative to surgical implantation, when factors such as patient comfort, post-op recovery, costs and other complications are considered. Implantation of pre-formed scaffolds with limited information about the size or shape of the defect is usually inefficient. However, injectable biomaterials can be tuned to assume a pre-formed shape after delivery [5, 69]. Injectable

biomaterial approach also offers a more homogeneous distribution of bioactive molecules, and cells within the prospective graft. For these reasons, they are becoming prevalent in many clinical treatments, including cardiovascular, orthopaedic, and plastic/reconstructive surgery applications [70].

#### 10.3.1 Cardiovascular Applications

Upon MI, left ventricle (LV) remodeling is characterized by the degradation of the ECM. Direct injection of biomaterials into the infarcted zone can potentially limit this process. Frey et al. investigated the effectiveness of an injectable bioabsorbable scaffold (IK-5001), composed of calcium gluconate and sodium alginate, in preventing and possibly counteracting adverse LV remodeling in MI cases. Twenty seven patients (age  $54 \pm 9$  years) received IK-5001 through the coronary artery 7 days after MI. It was found that the procedure and the material was safe, did not disrupt coronary blood flow and myocardial perfusion, and no additional myocardial injury was observed [71].

Reduction of LV wall stress is an important aspect of heart failure (HF). Algisyl-LVR™, which basically consists of calcium alginate is intended to prevent deterioration of HF patients who suffer from dilated LV. Lee et al. evaluated the efficiency of Algisyl-LVR™ hydrogel injections for reducing LV wall stress of 11 HF patients with an ejection fraction (EF) <40% [72]. Three months after treatment, wall thickness increased by ~20%. Results showed that after treatment end-systolic volume (ESV) decreased further by ~30%, while the end-diastolic volume (EDV) did not decrease significantly. The overall results show that Algisyl-LVR™ treatment may be a promising approach in treating dilated LV.

Another study (AUGMENT-HF trial) investigated direct injection of alginate-hydrogel into

**Table 10.1** Examples of injectable biomaterials used in orthopedic surgery

Product/company	Composition	Related references
Norian SRS/Synthes®, West Chester, PA	$\alpha$ -TCP, CaCO <sub>3</sub> , MCPM	Zimmermann et al. [74], Gómez et al. [75], Sanchez-Sotelo et al. [76] and Lobenhoffer et al. [77]
Sinovial® (Yaral®, Intragel®), Lugano, Switzerland	Sodium hyaluronidate/Hyaluronan/Hyaluronic acid	Theiler and Bruhlmann [78] and Roux et al. [79]
BoneSource™/Stryker-Howmedica-Osteonics, Rutherford, NJ	DCP, TTCP	Dickson et al. [80]
Mimix™/Biomet, Jacksonville, FL	TTCP, $\alpha$ -TCP, trisodium citrate	
ChronOS™ inject/Depuy Synthes, Leeds, UK	$\beta$ -TCP, MCMP, MgHPO <sub>4</sub> ·3H <sub>2</sub> O, MgSO <sub>4</sub> , Na <sub>2</sub> H <sub>2</sub> P <sub>2</sub> O <sub>7</sub>	Joeris et al. [81], Arora et al. [82] and Oh et al. [83]
Calcibon®/Biomet, Berlin, Germany	$\alpha$ -TCP, DCP, CaCO <sub>3</sub> , PHA	Friesenbichler et al. [84]
Cerament™/BoneSupport AB, Lund, Sweden	CaSO <sub>4</sub> · <sup>1/2</sup> H <sub>2</sub> O, HA	Kaczmarczyk et al. [85]
BonePlast®/Zimmer Biomet, Warsaw, IN	CaSO <sub>4</sub> · <sup>1/2</sup> H <sub>2</sub> O	Johnson and Clayer [86] and Clayer [87]
Cortoss®/Orthovita Inc., Malvern, PA	Bis-GMA, Bis-EMA, TEGMA, glass and ceramic fillers, barium boroaluminosilicate, silica	Boyd et al. [88], Bae et al. [89], Bae et al. [90] and Jacobson et al. [91]
HydroSet™/Stryker, Kalamazoo, MI	TetCP, DCPD, trisodium citrate	
Cementek® LV/Teknimed, Vic-en-Bigorre, France	$\alpha$ -TCP, TTCP, Na glycerophosphate, DMS	

Abbreviations: *Bis-EMA* bisphenol-a-ethoxy dimethacrylate, *Bis-GMA* bisphenol-a-glycidyl dimethacrylate, *DCP* dicalcium phosphate, *DMS* dimethylsiloxane, *MCPM* monobasic calcium phosphate monohydrate, *TCP* tricalcium phosphate, *TEGMA* triethylene glycol dimethacrylate, *TTCP* tetracalcium phosphate

the myocardium to alter the size and shape of dilated ventricles of 113 patients (age 18–79 years). Researchers administered alginate-hydrogel through left thoracotomy with multiple intra-myocardial injections. The treatment was shown to increase exercise capacity and improvements in chronic HF patients [73].

### 10.3.2 Orthopaedic Applications

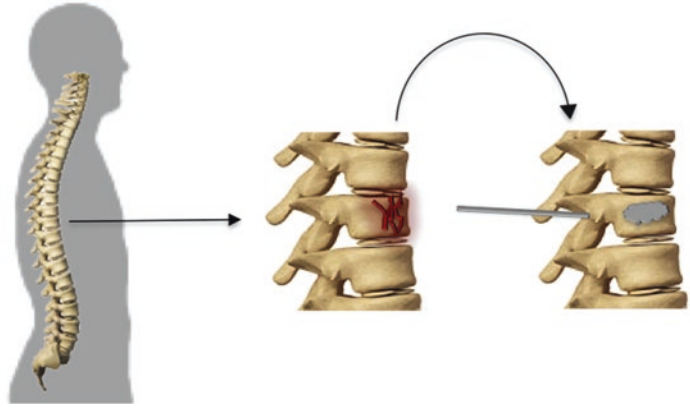
Injectable biomaterials applications are widespread in the orthopedic surgery field. Some examples are given in Table 10.1. Vertebral fractures mostly cause persistent acute pain, which negatively affects patient mobility and life

quality. Jensen et al. tested the efficacy of PMMA injections in 29 patients (19 women and 10 men) with back pain refractory to analgesic therapy. All patients had acute pain which inhibited their physical activity. Vertebroplasty technique (Fig. 10.5) was applied with fluoroscopic injection of PMMA. Twenty four hours after the application, 90% of the subjects displayed improved mobility and pain relief [92].

Allegretti et al. [93] used PMMA injections for the treatment of symptomatic haemangiomas, metastatic fractures and osteoporotic fractures. Twelve patients (5 female, 7 male) participated in the study (age 29–69 years; mean age 57.6). Intra-operative vertebroplasty (IVP) was performed during a single session under fluoroscopic



**Fig. 10.5** Vertebroplasty technique



control. Compared to the pre-surgical state, all cases displayed a significant reduction of their symptoms (33.8 months follow-up). The visual analogue scale (VAS) score showed that the pain intensity was reduced after the treatment [93].

Calcium phosphate-based hydraulic cements, termed as cancellous bone cement present potential for filling irregular bony voids. They harden at physiological pH and body temperature. Compared to PMMA cements, they have much better non-cytotoxic property. Jupiter et al. investigated the clinical utility of Norian SRS injection for extra-articular fractures of the distal radius. Five women patients (age 49–57 years) with fractures or limb injury participated in the study [94]. The treatment was performed under local or general anesthesia using fluoroscopic control. The outcomes were assessed by radiographic and functional evaluations (1-year follow-up). No intra-articular extrusion and no clinically detectable problems were observed. Norian SRS was bioabsorbable through osteoclastic activity, and in three patients the material was completely resorbed at 6 months [94]. Similarly, Wolff et al. used Norian SRS as a bone mineral substitute for the treatment of viscerocranium or calvaria in 27 patients (age 37–76 years). They reported no signs of infection, or inflammation in any of the patients [95].

Hyaluronic acid is normally found in the healthy cartilage matrix. However, HA content is altered in osteoarthritis (OA), characterized by the reduction of viscosity and elasticity of the synovial fluid. Derivatives of HA products may hold promise in OA cases. In a study by Evanich et al., 84 patients (100 knees) with symptomatic OA were treated with intra-articular injections of Synvisc® (hylan G-F 20), for three sequential weeks (10-months follow-up) [96]. Synvisc® is a chemically-crosslinked elastoviscous high molecular weight fluid containing hylan A and hylan B polymers. Clinical efficacy was evaluated by the increase in activity level, degree of pain relief and reported satisfaction. As the result, HA injection was advised for patients with significant surgical risk factors. However, this treatment was not advised in cases with collapsed joint space or significant bone loss [96, 97].

In a study by Roux et al., the efficiency of sodium hyaluronidate injection on the osteoarthritic carpometacarpal joint of the thumb (CMCJ) was evaluated in 42 patients (mean 64.8 years). However, there were no significant differences for pain relief and function between groups [79]. In another study, the efficiency of intra-articular HA injection or its combination with corticosteroid (CS) on the duration between diagnosis of knee OA to knee arthroplasty (KA)

was investigated. 267,345 OA patients participated in the study between 2005 and 2012. It was found that, HA injections in medicare knee OA patients are associated with longer time to KA [98].

Marcia et al. evaluated the effect of absorbable and injectable calcium bone cement (Cerament™, Bone Support, Sweden) in comparison to PMMA in patients with vertebral fractures. Thirty three patients (age 29–84 years) participated in the study, and the clinical outcome was evaluated by using ODI questionnaire and VAS score. Also the team utilized X-ray, CT, and MRI assessments post-procedure at 1, 6 and 12 months. ODI and VAS scores demonstrated a significant pain relief. The results showed that the injectable bone cement was an effective substitute in treatment of vertebral fractures [99].

PRP is an autologous source of growth factors approved for various medical applications and has a potential to enhance tissue regeneration. For example, [100] aimed to explore the efficiency of PRP injections for degenerative lesions of articular cartilage. Clinical evaluation on 91 patients with OA showed improved activity in younger subjects, and notable improvement in patients older than 65 years. These findings confirm that intra-articular PRP injection treatment is safe, and useful for early degenerative articular pathology of the knee [100].

### 10.3.3 Plastic and Reconstructive Surgery Applications

Facial fillers have become a primary option for facial rejuvenation due to nonsurgical delivery procedure. Dermal fillers, including HA, collagen, PLLA, and liquid silicone aim long-lasting soft-tissue augmentation without side effects [101].

Since temporary treatment options are limited, there is requirement for more persistent and

effective treatment options for facial lipoatrophy. At this point, liquid silicone became an option for treatment. In 1972, Rees et al. treated 73 subjects with liquid injectable silicone. Approximately 90% of the cases had displayed improvement in facial contour [102]. In another study, Jones et al. investigated 1000-cSt silicone oil injection treatment of HIV-associated lipoatrophy. Seventy seven patients with HIV-related facial lipoatrophy participated in this study in which they received Silikon 1000 (Alcon Labs., Ft. Worth, TX) or VitreSil 1000 (Richard James, Inc., Peabody, MA). This study suggests that injectable silicone is a feasible option for HIV-related facial lipoatrophy [103]. Similarly Chen et al. investigated the safety and efficacy of a 1000-cSt highly purified silicone fluid injection to 20 HIV-related facial lipoatrophy patients. Adverse events including edema and erythema were observed in 3 patients. After the treatment, study reported self-rated severity of lipoatrophy through the CLSS and presented a complete decrease in CLSS score in 75% of the patients [104].

PLLA is widely preferred in cosmetic procedures owing to the increase in fibroblast proliferation and collagen production upon deep dermal injections. Clinical studies on HIV-related facial lipoatrophy have shown that injectable PLLA is well-tolerated and effective [105]. In a study by Moyle et al., the tolerability and efficacy of PLLA (New-Fills; Medifill, London, UK) injection in 30 patients with HIV-related facial lipoatrophy was demonstrated [106]. In 2006, the same group evaluated the efficacy and long-term safety of PLLA injections, and found no serious side effects after 2 years [107]. In another study, PLLA was used in >7000 treatments in >2500 patients. Correction with injectable PLLA (Sculptra) lasted for 18 to 24 months in most patients. The reports showed that injectable PLLA provided an effective treatment for patients seeking facial volumetric correction [108].

Lowe et al. used injectable PLLA to correct facial volume deficits caused by ageing or disease in the nasolabial fold region of 221 patients. Reported adverse events, including bruising, swelling and discomfort, were resolved within 2–7 days. This study demonstrated that injectable PLLA could be a valid option for corrective interventions of facial areas with volume loss [109].

Poly(alkylimide) gel is a non-toxic, non-biodegradable and non-allergenic polymer. In a study by Loutfy et al., PAIG (Bio-Alcamid™, Milan, Italy) injection was applied to treat HIV-associated facial lipoatrophy in 31 patients, and found to be a valid method [110]. Similarly, Karim et al. evaluated the long-term effects of PAIG injections on facial lipoatrophy in 17 HIV-positive patients. As a single-stage procedure, PAIG was found to be effective to significantly decrease the facial lipoatrophy of the patients [111].

Calcium hydroxyapatite is used in different forms in cosmetic and reconstructive surgery. For example, CaHA gel (Radiesse, BioForm Medical, San Mateo, CA) comprises of synthetic CaHA microspheres (30%) suspended in an aqueous carrier gel (70%). The safety and effectiveness of CaHA gel in HIV-associated lipoatrophy patients was confirmed by [112]. Similarly, Berlin et al. evaluated efficacy of the CaHA filler for soft tissue augmentation by evaluating levels of collagen expression. Findings showed CaHA filler safely stimulates new collagen deposition and contributes to the clinical improvement in subjects with rhytids [113].

In a particular study, 138 patients with prominent nasolabial folds were randomized to receive either bovine collagen (Zyplast) or hyaluronic acid gel (Restylane; Q-Med, Uppsala, Sweden). Findings indicated similar effectiveness for Zyplast and Restylane in corrective ability of the nasolabial folds. On the other hand, hyaluronic acid gel caused a significantly longer-lasting correction in comparison to bovine collagen, along with permanent success in some patients [114].

Hyaluronic acid shows rapid degradation, making it unsuitable for soft tissue filler in cosmetic surgery. Chemical cross-linked of hyaluronic acid becomes an insoluble viscoelastic polymer and shows resistance to enzymatic degradation. Carruthers et al. [115] compared the safety and the efficacy of two cross-linked HA gel product, Restylane Perlane (Q-Med, Uppsala, Sweden) and Hylaform (Genzyme Corp., Cambridge, MA). 150 patients were treated with Restylane and Hylaform on the contralateral nasolabial folds of their faces. Findings indicated that both products were effective, while Restylane Perlane provided a more durable esthetic improvement than Hylaform [115]. In another study, Levy et al. compared two HA products, Restylane Perlane and Juvéderm ULTRA 3 in a single blind clinical trial setting. 126 patients (mean age of 53 years) were treated with both products at contralateral nasolabial folds. There was no significant difference between products related to the patient assessment of post-treatment smoothness and appearance [116]. Some examples of injectable biomaterials used in plastic and reconstructive surgery are given in Table 10.2.

---

## 10.4 Conclusions

In this chapter, we attempted to give an overview of some of the types and clinical applications of injectable biomaterials. As a matter of fact, the success of an injectable biomaterial depends on its design, which includes physical, chemical and biological properties tailored for the specific tissue type and related use. Injectable biomaterials have shown promising results in many tissue engineering applications; thus, common concerns are possible toxicity of initiators, monomers or macromers contacting the tissue, the rate of polymerization and potential harm caused by the remnants of toxic solvents and/or degradation products. Since there is no single injectable that meets all the requirements, it is important to balance the advantages and disadvantages of a biomaterial for each application.

**Table 10.2** Clinical use of some injectable biomaterials in plastic and reconstructive surgery

Main component	Product/company	Related references
Poly(L-lactic acid)	Sculptra®/Sanofi-Aventis – Dermik Labs., Bridgewater, NJ; Sinclair Pharma Paris, France (in Europe)	Valantin et al. [105], Vlegaar [108], Moyle et al. [107], Lam et al. [117], Burgess and Quiroga [118], Duracinsky et al. [119] and Lowe et al. [109]
	New Fill®/Valeant, Laval, Quebec, Canada	
Poly(alkylimide)	Bio-Alcamid™/Polymekon Biotech Industry, Milan, Italy	Lahiri and Waters [120], George et al. [121], Gómez-de la Fuente et al. [122] and Protopapa et al. [123]
Poly(methyl methacrylate)	Artecoll/Rofil Medical Int., Breda, The Netherlands	Solomon et al. [124], Karnik et al. [125], Cohen et al. [126] and Chen et al. [127]
	Artefill/Artes Medical, San Diego, CA	
Liquid silicone	Silikon 1000/Alcon Labs., Ft. Worth, TX	Jones et al. [103], Chen et al. [104], Orentreich and Leone [128] and Jacinto [129]
	VitreSil 1000/Richard James, Inc., Peabody, MA	
	Silskin/Richard-James, Inc., Peabody, MA	
	Adatosil 5000/Bausch & Lomb, Rochester, NY	
Calcium hydroxylapatite	Radiesse®/Bioform Medical Inc., San Mateo, CA	Kasbekar and Sherman [130], Carruthers and Carruthers [112], Berlin et al. [113], Alam et al. [131], Daley et al. [132] and Smith et al. [133]
Collagen	Zyplast® – Zyderm®/McGhan Medical Inc., Santa Barbara, CA	Narins et al. [114], Downie et al. [134], Sclafani et al. [135] and Lupo et al. [136]
	Cosmoderm – Cosmoplast/Allergan-Inamed Corp., Santa Barbara, CA	
	Cymetra/LifeCell Corp., Branchburgh, NJ, USA	Sclafani et al. [135]
	Dermalogen/Collagenesis Corp., Beverly, MA	
	Autologen/Collagenesis Inc., Beverly, MA	
	Resoplast/Rofil Medical Int., Breda, The Netherlands	
	Fascian®/Fascia Biosystems, Beverly Hills, CA	
Hyaluronic acid	Restylane®/Q-Med, Uppsala, Sweden	Narins et al. [114], Downie et al. [134], Arsiwala [138], Wu et al. [139], Kinney [140], Moers-Carpi et al. [141] and Chen et al. [127]
	Perlane®/Medicis Pharm. Corp., Scottsdale, AZ	
	Hylaform/Biomatrix Inc., Ridgefield, NJ	Grimes et al. [142]
	Hyaluderm/LCA Pharmaceutical, Chartres, France	
	Captique/Inamed, Santa Barbara, CA	Onesti et al. [143] and Grimes et al. [142]
	Matridur/BioPolymerGmbH & Co. KG, Montabaur, Germany	
	Puragen Plus/Mentor Corp., Santa Barbara, CA	Kinney [140] and Onesti et al. [143]
	Juvederm/Allergan Inc., Irvine, CA	Baumann et al. [144], Grimes et al. [142], Lupo et al. [136] and Moers-Carpi et al. [141]

**Competing Interests** Y.M.E. is the founder and director of Biovalda, Inc. (Ankara, Turkey). The authors declare no competing interests in relation to this article.

## References

- Langer R, Vacanti JP (1993) Tissue engineering. *Science* 260(5110):920–926. <https://doi.org/10.1126/science.8493529>
- Elcin YM (2004) Stem cells and tissue engineering. *Adv Exp Med Biol* 553:301–316. [https://doi.org/10.1007/978-0-306-48584-8\\_23](https://doi.org/10.1007/978-0-306-48584-8_23)
- Emin N, Elcin AE, Elcin YM (2012) Creation of a tissue development model in an artificial biomimetic niche microenvironment. Abstracts of the 3rd TERMIS world congress 2012. *J Tissue Eng Regen Med* 6(Suppl 1):198. <https://doi.org/10.1002/term.1586>
- Shin H, Jo S, Mikos AG (2003) Biomimetic materials for tissue engineering. *Biomaterials* 24(24):4353–4364. [https://doi.org/10.1016/S0142-9612\(03\)00339-9](https://doi.org/10.1016/S0142-9612(03)00339-9)
- Hou Q, Bank PAD, Shakesheff KM (2004) Injectable scaffolds for tissue regeneration. *J Mater Chem* 14:1915–1923. <https://doi.org/10.1039/b401791a>
- Kretlow JD, Young S, Klouda L, Wong M, Mikos AG (2009) Injectable biomaterials for regenerating complex craniofacial tissues. *Adv Mater* 21(32–33):3368–3393. <https://doi.org/10.1002/adma.200802009>
- Wang H, Zhou J, Liu Z, Wang C (2010) Injectable cardiac tissue engineering for the treatment of myocardial infarction. *J Cell Mol Med* 14(5):1044–1055. <https://doi.org/10.1111/j.1582-4934.2010.01046.x>
- Young DA, Christman KL (2012) Injectable biomaterials for adipose tissue engineering. *Biomed Mater* 7(2):024104. <https://doi.org/10.1088/1748-6041/7/2/024104>
- Lewis G (2006) Injectable bone cements for use in vertebroplasty and kyphoplasty: state-of-the-art review. *J Biomed Mater Res Part B: Appl Biomater* 76B(2):456–468. <https://doi.org/10.1002/jbm.b.30398>
- Kretlow JD, Klouda L, Mikos AG (2007) Injectable matrices and scaffolds for drug delivery in tissue engineering. *Adv Drug Deliv Rev* 59(4–5):263–273. <https://doi.org/10.1016/j.addr.2007.03.013>
- Rahman CV, Saeed A, White LJ, Gould TWA, Kirby GTS, Sawkins MJ, Alexander C, Rose FRAJ, Shakesheff KM (2012) Chemistry of polymer and ceramic-based injectable scaffolds and their applications in regenerative medicine. *Chem Mater* 24(5):781–795. <https://doi.org/10.1021/cm202708n>
- Kona S, Wadajkar AS, Nguyen KT (2011) Chapter 6 – Tissue engineering applications of injectable biomaterials. In: *Injectable biomaterials: science and applications*. Woodhead Publishing, pp 142–182. <https://doi.org/10.1533/9780857091376.2.142>
- Naahidi S, Jafari M, Logan M, Wang Y, Yuan Y, Bae H, Dixon B, Chen P (2017) Biocompatibility of hydrogel-based scaffolds for tissue engineering applications. *Biotechnol Adv* 35(5):530–544. <https://doi.org/10.1016/j.biotechadv.2017.05.006>
- Drury JL, Mooney DJ (2003) Hydrogels for tissue engineering: scaffold design variables and applications. *Biomaterials* 24(24):4337–4351. [https://doi.org/10.1016/S0142-9612\(03\)00340-5](https://doi.org/10.1016/S0142-9612(03)00340-5)
- Hong LTA, Kim YM, Park HH et al (2017) An injectable hydrogel enhances tissue repair after spinal cord injury by promoting extracellular matrix remodeling. *Nat Commun* 8(1):533. <https://doi.org/10.1038/s41467-017-00583-8>
- Qiu Y, Hamilton SK, Temenof J (2011) Chapter 4 – Improving mechanical properties of injectable polymers and composites. In: *Injectable biomaterials: science and applications*. Woodhead Publishing, pp 61–91. <https://doi.org/10.1533/9780857091376.1.61>
- Spector M, Lim TC (2016) Injectable biomaterials: a perspective on the next wave of injectable therapeutics. *Biomed Mater* 11(1):014110. <https://doi.org/10.1088/1748-6041/11/1/014110>
- Sims CD, Butler PE, Casanova R, Lee BT, Randolph MA, Lee WP, Vacanti CA, Yaremchuk MJ (1996) Injectable cartilage using polyethylene oxide polymer substrates. *Plast Reconstr Surg* 98(5):843–850. <https://doi.org/10.1097/00006534-199610000-00015>
- Aho AJ, Tirri T, Kukkonen J, Strandberg N, Rich J, Seppälä J, Yli-Urpo A (2004) Injectable bioactive glass/biodegradable polymer composite for bone and cartilage reconstruction: concept and experimental outcome with thermoplastic composites of poly(epsilon-caprolactone-co-D,L-lactide) and bioactive glass S53P4. *J Mater Sci Mater Med* 15(10):1165–1173. <https://doi.org/10.1023/B:JMSM.0000046401.50406.9b>
- Arenas-Arrocena MC, Argueta-Figueroa L, García-Contreras R, Martínez-Arenas O, Camacho-Flores B, Rodríguez-Torres MP, Fuente-Hernández J, Acosta-Torres LS (2017) Chapter 3: New trends for the processing of poly(methyl methacrylate) biomaterial for dental prosthodontics. In: Reddy BSR (ed) *Materials science – acrylic polymers in health-care*, CC BY 3.0 license. <https://doi.org/10.5772/intechopen.69066>
- Kenny SM, Buggy M (2003) Bone cements and fillers: a review. *J Mater Sci Mater Med* 14(11):923–938. <https://doi.org/10.1023/A:1026394530192>
- Vaishya R, Chauhan M, Vaish A (2013) Bone cement. *J Clin Orthop Trauma* 4(4):157–163. <https://doi.org/10.1016/j.jcot.2013.11.005>
- Jaeblohn T (2010) Polymethylmethacrylate: properties and contemporary uses in orthopaedics. *J Am Acad Orthop Surg* 18(5):297–305. <https://doi.org/10.5435/00124635-201005000-00006>
- Narayanan G, Vernekar VN, Kuyinu EL, Laurencin CT (2016) Poly (lactic acid)-based biomaterials for

- orthopaedic regenerative engineering. *Adv Drug Deliv Rev* 107:247–276. <https://doi.org/10.1016/j.addr.2016.04.015>
25. Basu A, Kunduru KR, Doppalapudi S, Domb AJ, Khan W (2016) Poly(lactic acid) based hydrogels. *Adv Drug Deliv Rev* 107:192–205. <https://doi.org/10.1016/j.addr.2016.07.004>
  26. Ramot Y, Haim-Zada M, Domb AJ, Nyska A (2016) Biocompatibility and safety of PLA and its copolymers. *Adv Drug Deliv Rev* 107:153–162. <https://doi.org/10.1016/j.addr.2016.03.012>
  27. Jing Y, Quan C, Liu B, Jiang Q, Zhang C (2016) A mini review on the functional biomaterials based on poly(lactic acid) stereocomplex. *Polym Rev* 56(2):262–286. <https://doi.org/10.1080/15583724.2015.1111380>
  28. Li S, Vert M (2003) Synthesis, characterization, and stereocomplex-induced gelation of block copolymers prepared by ring-opening polymerization of L (D)-lactide in the presence of poly (ethylene glycol). *Macromolecules* 36:8008–8014. <https://doi.org/10.1021/ma034734i>
  29. Shasteen C, Choy YB (2011) Controlling degradation rate of poly(lactic acid) for its biomedical applications. *Biomed Eng Lett* 1:163–167. <https://doi.org/10.1007/s13534-011-0025-8>
  30. Seker S, Arslan YE, Durkut S, Elçin AE, Elçin YM (2014) Chapter: 14 Nanotechnology for tissue engineering and regenerative medicine. In: *Nanopatterning and nanoscale devices for biological applications*, pp 339–366
  31. Kocak G, Tuncer C, Büttin V (2017) pH-responsive polymers. *Polym Chem* 8:144–176. <https://doi.org/10.1039/c6py01872f>
  32. Durkut S, Elçin YM (2017) Synthesis and characterization of thermosensitive poly(N-vinylcaprolactam)-g-collagen. *Artif Cell Nanomed B* 45(8):1665–1674. <https://doi.org/10.1080/21691401.2016.1276925>
  33. Bearat HH, Vernon BL (2011) Chapter 11 Environmentally responsive injectable materials. In: *Injectable biomaterials: science and applications*. Woodhead Publishing, pp 263–297. <https://doi.org/10.1533/9780857091376.3.263>
  34. Lei K, Shen W, Cao L, Yu L, Ding J (2015) An injectable thermogel with high radiopacity. *Chem Commun* 51:6080–6083. <https://doi.org/10.1039/c5cc00049a>
  35. Liow SS, Dou Q, Kai D, Karim AA, Zhang K, Xu F, Loh XJ (2016) Thermogels: in situ gelling biomaterial. *ACS Biomater Sci Eng* 2:295–316. <https://doi.org/10.1021/acsbomaterials.5b00515>
  36. Kim HK, Shim WS, Kim SE, Lee KH, Kang E, Kim JH, Kim K, Kwon IC, Lee DS (2009) Injectable in situ-forming pH/thermo-sensitive hydrogel for bone tissue engineering. *Tissue Eng Part A* 15(4):923–933. <https://doi.org/10.1089/ten.tea.2007.0407>
  37. Wu J, Zeng F, Huang XP, Chung JC, Konecny F, Weisel RD, Li RK (2011) Infarct stabilization and cardiac repair with a VEGF-conjugated, injectable hydrogel. *Biomaterials* 32(2):579–586. <https://doi.org/10.1016/j.biomaterials.2010.08.098>
  38. Mano JF, Silva GA, Azevedo HS, Malafaya PB, Sousa RA, Silva SS, Boesel LF, Oliveira JM, Santos TC, Marques AP, Neves NM, Reis RL (2007) Natural origin biodegradable systems in tissue engineering and regenerative medicine: present status and some moving trends. *J R Soc Interface* 4(17):999–1030. <https://doi.org/10.1098/rsif.2007.0220>
  39. Lee CH, Singla A, Lee Y (2001) Biomedical applications of collagen. *Int J Pharm* 221(1–2):1–22. [https://doi.org/10.1016/S0378-5173\(01\)00691-3](https://doi.org/10.1016/S0378-5173(01)00691-3)
  40. Rowley JA, Madlambayan G, Mooney DJ (1999) Alginate hydrogels as synthetic extracellular matrix materials. *Biomaterials* 20(1):45–53. [https://doi.org/10.1016/S0142-9612\(98\)00107-0](https://doi.org/10.1016/S0142-9612(98)00107-0)
  41. Kuo CK, Ma PX (2001) Ionically-crosslinked alginate hydrogels as scaffolds for tissue engineering: part 1. Structure, gelation rate and mechanical properties. *Biomaterials* 22(6):511–521. [https://doi.org/10.1016/S0142-9612\(00\)00201-5](https://doi.org/10.1016/S0142-9612(00)00201-5)
  42. Dobratz E, Kim S, Voglewede A, Park SS (2009) Injectable cartilage: using alginate and human chondrocytes. *Arch Facial Plast Surg* 11(1):40–47. <https://doi.org/10.1001/archfacial.2008.509>
  43. Matsuno T, Hashimoto Y, Adachi S, Omata K, Yoshitaka Y, Ozeki Y, Umezū Y, Tabata Y, Nakamura M, Satoh T (2008) Preparation of injectable 3D-formed beta-tricalcium phosphate bead/alginate composite for bone tissue engineering. *Dent Mater J* 27(6):827–834. <https://doi.org/10.4012/dmj.27.827>
  44. Nettles DL, Elder SH, Gilbert JA (2002) Potential use of chitosan as a cell scaffold material for cartilage tissue engineering. *Tissue Eng* 8(6):1009–1016. <https://doi.org/10.1089/107632702320934100>
  45. Suh JKF, Matthew HWT (2000) Application of chitosan-based polysaccharide biomaterials in cartilage tissue engineering: a review. *Biomaterials* 21(24):2589–2598. [https://doi.org/10.1016/S0142-9612\(00\)00126-5](https://doi.org/10.1016/S0142-9612(00)00126-5)
  46. Berger J, Reist M, Mayer JM, Felt O, Peppas NA, Gurny R (2004) Structure and interactions in covalently and ionically crosslinked chitosan hydrogels for biomedical applications. *Eur J Pharm Biopharm* 57(1):19–34. [https://doi.org/10.1016/S0939-6411\(03\)00161-9](https://doi.org/10.1016/S0939-6411(03)00161-9)
  47. Mwale F, Iordanova M, Demers CN, Steffen T, Roughley P, Antoniou J (2005) Biological evaluation of chitosan salts cross-linked to genipin as a cell scaffold for disk tissue engineering. *Tissue Eng* 11(1–2):130–140. <https://doi.org/10.1089/ten.2005.11.130>
  48. Lu JX, Prudhommeaux F, Meunier A, Sedel L, Guillemain G (1999) Effects of chitosan on rat knee cartilages. *Biomaterials* 20(20):1937–1944. [https://doi.org/10.1016/S0142-9612\(99\)00097-6](https://doi.org/10.1016/S0142-9612(99)00097-6)
  49. Fraser JR, Laurent TC, Laurent UB (1997) Hyaluronan: its nature, distribution, functions and

- turnover. *J Intern Med* 242(1):27–33. <https://doi.org/10.1046/j.1365-2796.1997.00170>
50. Campoccia D, Doherty P, Radice M, Brun P, Abatangelo G, Williams DF (1998) Semisynthetic resorbable materials from hyaluronan esterification. *Biomaterials* 19(23):2101–2127. [https://doi.org/10.1016/S0142-9612\(98\)00042-8](https://doi.org/10.1016/S0142-9612(98)00042-8)
  51. Xu X, Jha AK, Harrington DA, Farach-Carson MC, Jia X (2012) Hyaluronic acid-based hydrogels: from a natural polysaccharide to complex networks. *Soft Matter* 8(12):3280–3294. <https://doi.org/10.1039/C2SM06463D>
  52. Seker S, Lalegül O, Elcin AE, Gurman G, Elcin YM (2012) Regenerative and angiogenic capacity of rat bone marrow MSCs encapsulated in fibrin microbeads in a rat muscle injury model: preliminary study. Abstracts of the 3rd TERMIS world congress 2012. *J Tissue Eng Regen Med* 6(Suppl 1):158. <https://doi.org/10.1002/term.1586>
  53. Lee KY, Mooney DJ (2001) Hydrogels for tissue engineering. *Chem Rev* 101(7):1869–1879. <https://doi.org/10.1021/cr000108x>
  54. Zhu SJ, Choi BH, Jung JH, Lee SH, Huh JY, You TM, Lee HJ, Li J (2006) A comparative histologic analysis of tissue-engineered bone using platelet-rich plasma and platelet-enriched fibrin glue. *Oral Surg Oral Med Oral Pathol Oral Radiol Endod* 102(2):175–179. <https://doi.org/10.1016/j.tripleo.2005.08.034>
  55. Christman KL, Fok HH, Sievers RE, Fang Q, Lee RJ (2004) Fibrin glue alone and skeletal myoblasts in a fibrin scaffold preserve cardiac function after myocardial infarction. *Tissue Eng* 10(3–4):403–409. <https://doi.org/10.1089/107632704323061762>
  56. Parmaksiz M, Dogan A, Odabas S, Elçin AE, Elçin YM (2016) Clinical applications of decellularized extracellular matrices for tissue engineering and regenerative medicine. Topical review *Biomed Mater* 11(2):022003. <https://doi.org/10.1088/1748-6041/11/2/022003>
  57. Parmaksiz M, Elçin AE, Elçin YM (2017) Decellularization of bovine small intestinal submucosa and its use for the healing of a critical-sized full-thickness skin defect, alone and in combination with stem cells, in a small rodent model. *J Tissue Eng Regen M* 11(6):1754–1765. <https://doi.org/10.1002/term.2071>
  58. Badylak SF, Freytes DO, Gilbert TW (2009) Extracellular matrix as a biological scaffold material: structure and function. *Acta Biomater* 5(1):1–13. <https://doi.org/10.1016/j.actbio.2008.09.013>
  59. Crapo PM, Gilbert TW, Badylak SF (2011) An overview of tissue and whole organ decellularization processes. *Biomaterials* 32(12):3233–3243. <https://doi.org/10.1016/j.biomaterials.2011.01.057>
  60. Dogan A, Parmaksiz M, Elcin AE, Elcin YM (2016) Extracellular matrix and regenerative therapies from the cardiac perspective. *Stem Cell Rev* 12(2):202–213. <https://doi.org/10.1007/s12015-015-9641-5>
  61. Christman KL, Lee RJ (2006) Biomaterials for the treatment of myocardial infarction. *J Am Coll Cardiol* 48(5):907–913. <https://doi.org/10.1016/j.jacc.2006.06.005>
  62. Dogan A, Elcin AE, Elcin YM (2017) Translational applications of tissue engineering in cardiovascular medicine. *Curr Pharm Des* 23(6):903–914. <https://doi.org/10.2174/138161282366616111141954>
  63. Singelyn JM, DeQuach JA, Seif-Naraghi SB, Littlefield RB, Schup-Magoffin PJ, Christman KL (2009) Naturally derived myocardial matrix as an injectable scaffold for cardiac tissue engineering. *Biomaterials* 30(29):5409–5416. <https://doi.org/10.1016/j.biomaterials.2009.06.045>
  64. Seif-Naraghi SB, Salvatore MA, Schup-Magoffin PJ, Hu DP, Christman KL (2010) Design and characterization of an injectable pericardial matrix gel: a potentially autologous scaffold for cardiac tissue engineering. *Tissue Eng Pt A* 16(6):2017–2027. <https://doi.org/10.1089/ten.TEA.2009.0768>
  65. Badylak S, Obermiller J, Geddes L, Matheny R (2003) Extracellular matrix for myocardial repair. *Heart Surg Forum* 6(2):E20–E26. <https://doi.org/10.1532/hsf.917>
  66. Zhao ZQ, Puskas JD, Xu D, Wang NP, Mosunjac M, Guyton RA, Vinten-Johansen J, Matheny R (2010) Improvement in cardiac function with small intestine extracellular matrix is associated with recruitment of C-kit cells, myofibroblasts, and macrophages after myocardial infarction. *J Am Coll Cardiol* 55(12):1250–1261. <https://doi.org/10.1016/j.jacc.2009.10.049>
  67. Singelyn JM, Sundaramurthy P, Johnson TD, Schup-Magoffin PJ, Hu DP, Faulk DM, Wang J, Mayle KM, Bartels K, Salvatore M, Kinsey AM, Demaria AN, Dib N, Christman KL (2012) Catheter-deliverable hydrogel derived from decellularized ventricular extracellular matrix increases endogenous cardiomyocytes and preserves cardiac function post-myocardial infarction. *J Am Coll Cardiol* 59(8):751–763. <https://doi.org/10.1016/j.jacc.2011.10.888>
  68. DeQuach JA, Lin JE, Cam C, Hu D, Salvatore MA, Sheikh F, Christman KL (2012) Injectable skeletal muscle matrix hydrogel promotes neovascularization and muscle cell infiltration in a hindlimb ischemia model. *Eur Cell Mater* 23:400–412. <https://doi.org/10.22203/eCM.v023a31>
  69. Bencherif SA, Sands RW, Bhatta D, Arany P, Verbeke CS, Edwards DA, Mooney DJ (2012) Injectable preformed scaffolds with shape-memory properties. *Proc Natl Acad Sci U S A* 109(48):19590–19595. <https://doi.org/10.1073/pnas.1211516109>
  70. Zhang Z (2017) Injectable biomaterials for stem cell delivery and tissue regeneration. *Expert Opin Biol Ther* 17(1):49–62. <https://doi.org/10.1080/14712598.2017.1256389>
  71. Frey N, Linke A, Süselbeck T, Müller-Ehmsen J, Vermeersch P, Schoors D, Rosenberg M, Bea F, Tuvia S, Leor J (2014) Intracoronary delivery of

- injectable bioabsorbable scaffold (IK-5001) to treat left ventricular remodeling after ST-elevation myocardial infarction: a first-in-man study. *Circ Cardiovasc Interv* 7(6):806–812. <https://doi.org/10.1161/CIRCINTERVENTIONS.114.001478>
72. Lee LC, Wall ST, Klepach D, Ge L, Zhang Z, Lee RJ, Hinson A, Gorman JH, Gorman RC, Guccione JM (2013) Algisyl-LVR™ with coronary artery bypass grafting reduces left ventricular wall stress and improves function in the failing human heart. *Int J Cardiol* 168(3):2022–2028. <https://doi.org/10.1016/j.ijcard.2013.01.003>
  73. Anker SD, Coats AJ, Cristian G, Dragomir D, Pusineri E, Piredda M, Bettari L, Dowling R, Volterrani M, Kirwan BA, Filippatos G, Mas JL, Danchin N, Solomon SD, Lee RJ, Ahmann F, Hinson A, Sabbah HN, Mann DL (2015) A prospective comparison of alginate-hydrogel with standard medical therapy to determine impact on functional capacity and clinical outcomes in patients with advanced heart failure (AUGMENT-HF trial). *Eur Heart J* 36(34):2297–2309. <https://doi.org/10.1093/eurheartj/ehv259>
  74. Zimmermann R, Gabl M, Lutz M, Angermann P, Gschwentner M, Pechlaner S (2003) Injectable calcium phosphate bone cement Norian SRS for the treatment of intra-articular compression fractures of the distal radius in osteoporotic women. *Arch Orthop Trauma Surg* 123(1):22–27. <https://doi.org/10.1007/s00402-002-0458-8>
  75. Gómez E, Martín M, Arias J, Carceller F (2005) Clinical applications of Norian SRS (calcium phosphate cement) in craniofacial reconstruction in children: our experience at hospital La Paz since 2001. *J Oral Maxillofac Surg* 63(1):8–14. <https://doi.org/10.1016/j.joms.2004.09.008>
  76. Sanchez-Sotelo J, Munuera L, Madero R (2000) Treatment of fractures of the distal radius with a remodellable bone cement: a prospective, randomised study using Norian SRS. *J Bone Joint Surg Br* 82(6):856–863. <https://doi.org/10.1302/0301-620X.82B6.10317>
  77. Lobenhoffer P, Gerich T, Witte F, Tschern H (2002) Use of an injectable calcium phosphate bone cement in the treatment of tibial plateau fractures: a prospective study of twenty-six cases with twenty-month mean follow-up. *J Orthop Trauma* 16(3):143–149. <https://doi.org/10.1097/00005131-200203000-00001>
  78. Theiler R, Bruhlmann P (2005) Overall tolerability and analgesic activity of intra-articular sodium hyaluronate in the treatment of knee osteoarthritis. *Curr Med Res Opin* 21(11):1727–1733. <https://doi.org/10.1185/030079905X65547>
  79. Roux C, Fontas E, Breuil V, Brocq O, Albert C, Euller-Ziegler L (2007) Injection of intra-articular sodium hyaluronidate (Sinovial) into the carpometacarpal joint of the thumb (CMC1) in osteoarthritis. A prospective evaluation of efficacy. *Joint Bone Spine* 74(4):368–372. <https://doi.org/10.1016/j.jbspin.2006.08.008>
  80. Dickson KF, Friedman J, Buchholz JG, Flandry FD (2002) The use of bone-source hydroxyapatite cement for traumatic metaphyseal bone void filling. *J Trauma* 53(6):1103–1108. <https://doi.org/10.1097/01.TA.0000033760.65011.52>
  81. Joeris A, Ondrus S, Planka L, Gal P, Slongo T (2010) ChronOS inject in children with benign bone lesions--does it increase the healing rate? *Eur J Pediatr Surg* 20(1):24–28. <https://doi.org/10.1055/s-0029-1241866>
  82. Arora R, Milz S, Sprecher C, Sitte I, Blauth M, Lutz M (2012) Behaviour of ChronOS™ inject in metaphyseal bone defects of distal radius fractures: tissue reaction after 6–15 months. *Injury* 43(10):1683–1688. <https://doi.org/10.1016/j.injury.2012.06.006>
  83. Oh CW, Park KC, Jo YH (2017) Evaluating augmentation with calcium phosphate cement (ChronOS inject) for bone defects after internal fixation of proximal tibial fractures: a prospective, multicenter, observational study. *Orthop Traumatol Surg Res* 103(1):105–109. <https://doi.org/10.1016/j.otsr.2016.10.006>
  84. Friesenbichler J, Maurer-Ertl W, Bergovec M, Holzer LA, Ogris K, Leitner L, Leithner A (2017) Clinical experience with the artificial bone graft substitute calcibon used following curettage of benign and low-grade malignant bone tumors. *Sci Rep* 7(1):1736. <https://doi.org/10.1038/s41598-017-02048-w>
  85. Kaczmarczyk J, Sowinski P, Goch M, Katulka K (2015) Complete twelve month bone remodeling with a bi-phasic injectable bone substitute in benign bone tumors: a prospective pilot study. *BMC Musculoskelet Disord* 16:369. <https://doi.org/10.1186/s12891-015-0828-3>
  86. Johnson LJ, Clayer M (2013) Aqueous calcium sulphate as bone graft for voids following open curettage of bone tumours. *ANZ J Surg* 83(7–8):564–570. <https://doi.org/10.1111/j.1445-2197.2012.06175.x>
  87. Clayer M (2008) Injectable form of calcium sulphate as treatment of aneurysmal bone cysts. *ANZ J Surg* 78(5):366–370. <https://doi.org/10.1111/j.1445-2197.2008.04479.x>
  88. Boyd D, Towler MR, Wren A, Clarkin OM (2008) Comparison of an experimental bone cement with surgical simplex P, Spineplex and Cortoss. *J Mater Sci Mater Med* 19(4):1745–1752. <https://doi.org/10.1007/s10856-007-3363-4>
  89. Bae H, Hatten HP Jr, Linovitz R, Tahernia AD, Schaufele MK, McCollom V, Gilula L, Maurer P, Benyamin R, Mathis JM, Persenaire M (2012) A prospective randomized FDA-IDE trial comparing cortoss with PMMA for vertebroplasty: a comparative effectiveness research study with 24-month follow-up. *Spine (Phila Pa 1976)* 37(7):544–550. <https://doi.org/10.1097/BRS.0b013e31822ba50b>
  90. Bae H, Shen M, Maurer P, Peppelman W, Beutler W, Linovitz R, Westerlund E, Peppers T, Lieberman I, Kim C, Girardi F (2010) Clinical experience



- using cortoss for treating vertebral compression fractures with vertebroplasty and kyphoplasty: twenty four-month follow-up. *Spine (Phila Pa 1976)* 35(20):E1030–E1036. <https://doi.org/10.1097/BRS.0b013e3181dcd475>
91. Jacobson RE, Granville M, Hatgis J, Berti A (2017) Low volume vertebral augmentation with Cortoss® cement for treatment of high degree vertebral compression fractures and vertebra plana. *Cureus* 9(2):e1058. <https://doi.org/10.7759/cureus.1058>
  92. Jensen ME, Evans AJ, Mathis JM, Kallmes DF, Cloft HJ, Dion JE (1997) Percutaneous polymethylmethacrylate vertebroplasty in the treatment of osteoporotic vertebral body compression fractures: technical aspects. *AJNR Am J Neuroradiol* 18(10):1897–1904 9403451
  93. Allegretti L, Mavilio N, Fiaschi P, Bragazzi R, Pacetti M, Castelletti L, Saitta L, Castellan L (2014) Intra-operative vertebroplasty combined with posterior cord decompression-a report of twelve cases. *Interv Neuroradiol* 20(5):583–590. <https://doi.org/10.15274/INR-2014-10019>
  94. Jupiter JB, Winters S, Sigman S, Lowe C, Pappas C, Ladd AL, Van Wagoner M, Smith ST (1997) Repair of five distal radius fractures with an investigational cancellous bone cement: a preliminary report. *J Orthop Trauma* 11(2):110–116. <https://doi.org/10.1097/00005131-199702000-00008>
  95. Wolff KD, Swaid S, Nolte D, Böckmann RA, Hölzle F, Müller-Mai C (2004) Degradable injectable bone cement in maxillofacial surgery: indications and clinical experience in 27 patients. *J Craniomaxillofac Surg* 32(2):71–79. <https://doi.org/10.1016/j.jcms.2003.12.002>
  96. Evanich JD, Evanich CJ, Wright MB, Rydlewicz JA (2001) Efficacy of intraarticular hyaluronic acid injections in knee osteoarthritis. *Clin Orthop Relat Res* 390:173–181 PMID: 11550864
  97. Cheng OT, Souzdalnitski D, Vrooman B, Cheng J (2012) Evidence-based knee injections for the management of arthritis. *Pain Med* 13(6):740–753. <https://doi.org/10.1111/j.1526-4637.2012.01394.x>
  98. Ong KL, Anderson AF, Niazi F, Fierlinger AL, Kurtz SM, Altman RD (2016) Hyaluronic acid injections in medicare knee osteoarthritis patients are associated with longer time to knee arthroplasty. *J Arthroplast* 31(8):1667–1673. <https://doi.org/10.1016/j.arth.2016.01.038>
  99. Marcia S, Boi C, Dragani M, Marini S, Marras M, Piras E, Anselmetti GC, Masala S (2012) Effectiveness of a bone substitute (CERAMENT™) as an alternative to PMMA in percutaneous vertebroplasty: 1-year follow-up on clinical outcome. *Eur Spine J* 21(Suppl 1):S112–S118. <https://doi.org/10.1007/s00586-012-2228-9>
  100. Kon E, Buda R, Filardo G, Di Martino A, Timoncini A, Cenacchi A, Fornasari PM, Giannini S, Marcacci M (2010) Platelet-rich plasma: intra-articular knee injections produced favorable results on degenerative cartilage lesions. *Knee Surg Sports Traumatol Arthrosc* 18(4):472–479. <https://doi.org/10.1007/s00167-009-0940-8>
  101. Johl SS, Burgett RA (2006) Dermal filler agents: a practical review. *Curr Opin Ophthalmol* 17(5):471–479. <https://doi.org/10.1097/OI.icu.0000243021.20499.4b>
  102. Rees TD, Ashley FL, Delgado JP (1973) Silicone fluid injections for facial atrophy: a ten-year study. *Plast Reconstr Surg* 52(2):118–127 4578999
  103. Jones DH, Carruthers A, Orentreich D, Brody HJ, Lai MY, Azen S, Van Dyke GS (2004) Highly purified 1000-cSt silicone oil for treatment of human immunodeficiency virus-associated facial lipoatrophy: an open pilot trial. *Dermatol Surg* 30(10):1279–1286. <https://doi.org/10.1111/j.1524-4725.2004.30406.x>
  104. Chen F, Carruthers A, Humphrey S, Carruthers J (2013) HIV-associated facial lipoatrophy treated with injectable silicone oil: a pilot study. *J Am Acad Dermatol* 69(3):431–437. <https://doi.org/10.1016/j.jaad.2013.03.025>
  105. Valantin MA, Aubron-Olivier C, Ghosn J, Laglenne E, Pauchard N, Schoen H, Bousquet R, Katz P, Costagliola D, Katlama C (2003) Polylactic acids implants (new-fill) to correct facial lipoatrophy in HIV- infected patients: results of the open-label study VEGA. *AIDS* 17(17):2471–2477. <https://doi.org/10.1097/01.aids.0000088226.55968.46>
  106. Moyle GJ, Lysakova L, Brown S, Sibtain N, Healy J, Priest C, Mandalia S, Barton SE (2004) A randomized open-label study of immediate versus delayed polylactic acid injections for the cosmetic management of facial lipoatrophy in persons with HIV infection. *HIV Med* 5(2):82–87. <https://doi.org/10.1111/j.1468-1293.2004.00190.x>
  107. Moyle GJ, Brown S, Lysakova L, Barton SE (2006) Long-term safety and efficacy of poly-L-lactic acid in the treatment of HIV-related facial lipoatrophy. *HIV Med* 7(3):181–185. <https://doi.org/10.1111/j.1468-1293.2006.00342.x>
  108. Vleggaar D (2005) Facial volumetric correction with injectable poly-L-lactic acid. *Dermatol Surg* 31(11 Pt 2):1511–1517. <https://doi.org/10.2310/6350.2005.31236>
  109. Lowe NJ, Maxwell CA, Lowe P, Shah A, Patnaik R (2009) Injectable poly-l-lactic acid: 3 years of aesthetic experience. *Dermatol Surg* 35(Suppl 1):344–349. <https://doi.org/10.1111/j.1524-4725.2008.01061.x>
  110. Loutfy MR, Raboud JM, Antoniou T, Kovacs C, Shen S, Hal-penny R, Ellenor D, Ezekiel D, Zhao A, Beninger F (2007) Immediate versus delayed polyalkylimide gel injections to correct facial lipoatrophy in HIV-positive patients. *AIDS* 21(9):1147–1155. <https://doi.org/10.1097/QAD.0b013e3281c6148d>
  111. Karim RB, de Lint CA, van Galen SR, van Rozelaar L, Nieuwkerk PT, Askarizadeh E, Hage JJ (2008) Long-term effect of polyalkylimide gel injections on severity of facial lipoatrophy and quality of life of HIV-positive patients. *Aesthet Plast Surg* 32(6):873–878. <https://doi.org/10.1007/s00266-008-9189-8>

112. Carruthers A, Carruthers J (2008) Evaluation of injectable calcium hydroxylapatite for the treatment of facial lipoatrophy associated with human immunodeficiency virus. *Dermatol Surg* 34(11):1486–1499. <https://doi.org/10.1111/j.1524-4725.2008.34323.x>
113. Berlin AL, Hussain M, Goldberg DJ (2008) Calcium hydroxylapatite filler for facial rejuvenation: a histologic and immunohistochemical analysis. *Dermatol Surg* 34(Suppl 1):S64–S67. <https://doi.org/10.1111/j.1524-4725.2008.34245.x>
114. Narins RS, Brandt F, Leyden J, Lorenc ZP, Rubin M, Smith S (2003) A randomized, double-blind, multicenter comparison of the efficacy and tolerability of restylane versus zyplast for the correction of nasolabial folds. *Dermatol Surg* 29(6):588–595. <https://doi.org/10.1046/j.1524-4725.2003.29150.x>
115. Carruthers A, Carey W, De Lorenzi C, Remington K, Schachter D, Sapra S (2005) Randomized, double-blind comparison of the efficacy of two hyaluronic acid derivatives, restylane perlane and hylaform, in the treatment of nasolabial folds. *Dermatol Surg* 31(11 Pt 2):1591–1598. <https://doi.org/10.2310/6350.2005.31246>
116. Levy PM, De Boule K, Raspaldo H (2009) A split-face comparison of a new hyaluronic acid facial filler containing pre-incorporated lidocaine versus a standard hyaluronic acid facial filler in the treatment of naso-labial folds. *J Cosmet Laser Ther* 11(3):169–173. <https://doi.org/10.1080/14764170902833142>
117. Lam SM, Azizzadeh B, Graivier M (2006) Injectable poly-L-lactic acid (Sculptra): technical considerations in soft-tissue contouring. *Plast Reconstr Surg* 118(3 Suppl):55S–63S. <https://doi.org/10.1097/01.prs.0000234612.20611.5a>
118. Burgess CM, Quiroga RM (2005) Assessment of the safety and efficacy of poly-L-lactic acid for the treatment of HIV-associated facial lipoatrophy. *J Am Acad Dermatol* 52(2):233–239. <https://doi.org/10.1016/j.jaad.2004.08.056>
119. Duracinsky M, Leclercq P, Herrmann S, Christen MO, Dolivo M, Goujard C, Chassany O (2014) Safety of poly-L-lactic acid (new-fill®) in the treatment of facial lipoatrophy: a large observational study among HIV-positive patients. *BMC Infect Dis* 1(14):474. <https://doi.org/10.1186/1471-2334-14-474>
120. Lahiri A, Waters R (2007) Experience with bio-alcamid, a new soft tissue endoprosthesis. *J Plast Reconstr Aesthet Surg* 60(6):663–667. <https://doi.org/10.1016/j.bjps.2006.07.010>
121. George DA, Erel E, Waters R (2012) Patient satisfaction following bio-alcamid injection for facial contour defects. *J Plast Reconstr Aesthet Surg* 65(12):1622–1626. <https://doi.org/10.1016/j.bjps.2012.06.017>
122. Gómez-de la Fuente E, Alvarez-Fernández JG, Pinedo F, Naz E, Gamo R, Vicente-Martín FJ, López-Estebanar JL (2007) Cutaneous adverse reaction to bio-alcamid® implant. *Actas Dermosifiliogr* 98(4):271–275. [https://doi.org/10.1016/S1578-2190\(07\)70442-0](https://doi.org/10.1016/S1578-2190(07)70442-0)
123. Protopapa C, Giuseppe S, Caporale D, Cammarota N (2003) Bio-Alcamid™ in drug-induced lipodystrophy. *J Cosmet Laser Ther* 5:226–230. <https://doi.org/10.1080/14764170310021922>
124. Solomon P, Sklar M, Zener R (2012) Facial soft tissue augmentation with Artecoll®: a review of eight years of clinical experience in 153 patients. *Can J Plast Surg* 20(1):28–32 PMID 23598763
125. Karnik J, Baumann L, Bruce S, Callender V, Cohen S, Grimes P, Joseph J, Shamban A, Spencer J, Tedaldi R, Werschler WP, Smith SR (2014) A double-blind, randomized, multicenter, controlled trial of suspended polymethylmethacrylate microspheres for the correction of atrophic facial acne scars. *Am Acad Derm* 71(1):77–83. <https://doi.org/10.1016/j.jaad.2014.02.034>
126. Cohen SR, Berner CF, Busso M, Gleason MC, Hamilton D, Holmes RE, Romano JJ, Rullan PP, Thaler MP, Ubogy Z, Vecchione TR (2006) ArteFill: a long-lasting injectable wrinkle filler material—summary of the U.S. food and drug administration trials and a progress report on 4- to 5-year outcomes. *Plast Reconstr Surg* 118(3 Suppl):64S–76S. <https://doi.org/10.1097/01.prs.0000234873.00905.a4>
127. Chen L, Li SR, Yu P, Wang ZX (2014) Comparison of artecoll, restylane and silicone for augmentation rhinoplasty in 378 Chinese patients. *Clin Invest Med* 37(4):E203–E210. <https://doi.org/10.25011/cim.v37i4.21725>
128. Orentreich D, Leone AS (2004) A case of HIV-associated facial lipoatrophy treated with 1000-cs liquid injectable silicone. *Dermatol Surg* 30(4 Pt 1):548–551. <https://doi.org/10.1111/j.1524-4725.2004.30175.x>
129. Jacinto SS (2005) Ten-year experience using injectable silicone oil for soft tissue augmentation in the Philippines. *Dermatol Surg* 31:1550–1554. <https://doi.org/10.2310/6350.2005.31240>
130. Kasbekar AV, Sherman IW (2013) Closure of minor tracheoesophageal fistulae with calcium hydroxylapatite. *Auris Nasus Larynx* 40(5):491–492. <https://doi.org/10.1016/j.anl.2013.01.008>
131. Alam M, Havey J, Pace N, Pongpruthiphan M, Yoo S (2011) Large-particle calcium hydroxylapatite injection for correction of facial wrinkles and depressions. *J Am Acad Dermatol* 65(1):92–96. <https://doi.org/10.1016/j.jaad.2010.12.018>
132. Daley T, Damm DD, Haden JA, Kolodychak MT (2012) Oral lesions associated with injected hydroxyapatite cosmetic filler. *Oral Surg Oral Med Oral Pathol Oral Radiol* 114(1):107–111. <https://doi.org/10.1016/j.oooo.2012.03.012>
133. Smith S, Busso M, McClaren M, Bass LS (2007) A randomized, bilateral, prospective comparison of calcium hydroxylapatite microspheres versus human-based collagen for the correction of nasolabial folds. *Dermatol Surg* 33(Suppl 2):S112–S121. <https://doi.org/10.1111/j.1524-4725.2007.33350.x>
134. Downie J, Mao Z, Rachel Lo TW, Barry S, Bock M, Siebert JP, Bowman A, Ayoub A (2009) A

- double-blind, clinical evaluation of facial augmentation treatments: a comparison of PRI 1, PRI 2, Zyplast® and Perlane®. *J Plast Reconstr Aesthet Surg* 62(12):1636–1643. <https://doi.org/10.1016/j.bjps.2008.06.056>
135. Sclafani AP, Romo T, Jacono AA (2002) Rejuvenation of the aging lip with an injectable acellular dermal graft (Cymetra). *Arch Facial Plast Surg* 4(4):252–257. <https://doi.org/10.1001/archfaci.4.4.252>
  136. Lupo MP, Smith SR, Thomas JA, Murphy DK, Beddingfield FC (2008) Effectiveness of Juvéderm ultra plus dermal filler in the treatment of severe nasolabial folds. *Plast Reconstr Surg* 121(1):289–297. <https://doi.org/10.1097/01.prs.0000294968.76862.83>
  137. Bauman L (2004) CosmoDerm/CosmoPlast (human bioengineered collagen) for the aging face. *Facial Plast Surg* 20(2):125–128. <https://doi.org/10.1055/s-2004-861752>
  138. Arsiwala SZ (2010) Safety and persistence of non-animal stabilized hyaluronic acid fillers for nasolabial folds correction in 30 Indian patients. *J Cutan Aesthet Surg* 3(3):156–161. <https://doi.org/10.4103/0974-2077.74492>
  139. Wu Y, Sun N, Xu Y, Liu H, Zhong S, Chen L, Li D (2016) Clinical comparison between two hyaluronic acid-derived fillers in the treatment of nasolabial folds in Chinese subjects: BioHyalux versus Restylane. *Arch Dermatol Res* 308(3):145–151. <https://doi.org/10.1007/s00403-016-1630-2>
  140. Kinney BM (2006) Injecting puragen plus into the nasolabial folds: preliminary observations of FDA trial. *Aesthet Surg J* 26(6):741–748. <https://doi.org/10.1016/j.asj.2006.10.008>
  141. Moers-Carpi M, Vogt S, Santos BM, Planas J, Vallve SR, Howell DJ (2007) A multicenter, randomized trial comparing calcium hydroxylapatite to two hyaluronic acids for treatment of nasolabial folds. *Dermatol Surg* 33(Suppl 2):S144–S151. <https://doi.org/10.1111/j.1524-4725.2007.33354.x>
  142. Grimes PE, Thomas JA, Murphy DK (2009) Safety and effectiveness of hyaluronic acid fillers in skin of color. *J Cosmet Dermatol* 8(3):162–168. <https://doi.org/10.1111/j.1473-2165.2009.00457.x>
  143. Onesti M, Toscani M, Curinga G, Chiummariello S, Scuderi N (2009) Assessment of a new hyaluronic acid filler. Double-blind, randomized, comparative study between Puragen and Captique in the treatment of nasolabial folds. *In Vivo* 23(3):479–486 19454518
  144. Baumann LS, Shamban AT, Lupo MP, Monheit GD, Thomas JA, Murphy DK, Walker PS, JUVEDERM vs. ZYPLAST Nasolabial Fold Study Group (2007) Comparison of smooth-gel hyaluronic acid dermal fillers with cross-linked bovine collagen: a multicenter, double-masked, randomized within-subject study. *Dermatol Surg* 33(Suppl 2):S128–S135. <https://doi.org/10.1111/j.1524-4725.2007.33352.x>



# Advanced Injectable Alternatives for Osteoarthritis

# 11

Şebnem Şahin, Süleyman Ali Tuncel,  
Kouroush Salimi, Elif Bilgiç, Petek Korkusuz,  
and Feza Korkusuz

## Abstract

Osteoarthritis (OA) is a common form of arthritis, which is characterized by progressive degradation of joint cartilage resulting in pain, joint stiffness, deformity and disability that is also recently related to an increased incidence of mortality. Inhibition of the extracellular matrix (ECM) production by chondrocytes and accumulation of catabolic mediators associated with matrix degradation are the cause of OA. Nonsurgical treatments for OA can be characterised as symptom-modifying or disease-modifying approaches. It's estimated that 10% of the world population

older than 60 years demonstrated symptoms of OA (Messier SP, Callahan LF, Beavers DP et al., *BMC Musculoskelet Disord* 18(1):91, 2017). A virtue of chondrocytes has a limited proliferation capability; nonsurgical OA therapies mostly include native cartilage extracellular component injections like hyaluronic acid, anti-inflammatory effected autologous cell implantations, platelet rich plasma injections and medicals like corticosteroids. Stem cells are searched to cure OA recently. Also nowadays we can develop injectable release systems, biocompatible hydrogels and micro/nano sized carriers to make these medicals more effective. In this review we cover injectable alternatives to modify the natural course of OA that gives a window for patients between conventional treatment methods and joint replacement surgery.

Ş. Şahin  
Department of Nanotechnology and Nanomedicine,  
Graduate School of Science and Engineering,  
Hacettepe University, Ankara, Turkey

S. A. Tuncel  
Department of Chemical Engineering, Faculty of  
Engineering, Hacettepe University, Ankara, Turkey  
e-mail: [atuncel@hacettepe.edu.tr](mailto:atuncel@hacettepe.edu.tr)

K. Salimi  
Department of Chemical Engineering, Faculty of  
Engineering and Natural Sciences, Ankara Yildirim  
Beyazit University, Ankara, Turkey

E. Bilgiç · P. Korkusuz  
Department of Histology and Embryology, Faculty of  
Medicine, Hacettepe University, Ankara, Turkey  
e-mail: [petek@hacettepe.edu.tr](mailto:petek@hacettepe.edu.tr)

F. Korkusuz (✉)  
Department of Sports Medicine, Faculty of Medicine,  
Hacettepe University, Ankara, Turkey

## Keywords

Osteoarthritis · Cartilage · Chondrocytes ·  
Hyaluronan · Glycosaminoglycan ·  
Chondroitin sulfate

## 11.1 Introduction

Osteoarthritis (OA) affects the whole joint structure including menisci, ligaments and subchondral bone and causes progressive changes in cartilage

and inflammation of synovial fluid. [11]. It's estimated prevalence is 35% people whose aged between 50 and 59 years, and 55% for people over 70 years [37]. The lifetime risk for knee OA is 45% [62] and hip OA is 25%, respectively [63]. OA is mostly related to overweight, cartilage injuries, aging and heredity [41]. In early OA, chondrocytes expose a proliferative response, increased synthesis of cartilage extracellular matrix components like type II collagen and aggrecan as an early attempt at repair and increased synthesis of catabolic cytokines and matrix degrading enzymes [31]. Major problem in clinical OA treatment is damaged articular cartilage has poor healing potency by virtue of its hypovascularity and hypocellularity [33].

Oral glucosamine (GA) and chondroitin sulfate (CS), which are native components of joint cartilage matrix, intake is preferred by patients for more than 30 years to decrease pain and improve function in OA treatment (Table 11.1). CS in the joint space provides a structural support, slowing cartilage destruction, helping in maintaining the structural integrity and homeostasis of the tissue and reducing OA symptoms [12, 45]. Also, GA has potential chondroprotective effects on cartilage with OA [82]. Information on serum and joint cartilage accumulation of these molecules however is lacking.

To deliver the therapeutic agent directly into the articular cavity, intra-articular (IA) injections represent a therapy that is often used in the control of OA [76]. OA therapies with IA injections have a good safety profile and several products can be used including hyaluronic acid (HA) injections, platelet rich plasma (PRP) injections, expanded stem cell injections, non-steroidal anti-inflammatory drug (NSAID) injections and biomaterials (eg, nano-micro carriers, hydrogels and drug delivery/release systems).

## 11.2 Hyaluronic Acid (HA) Injections

Intra-articular (IA) hyaluronic acid (HA) injections is the most common used non-surgical therapy for OA. HA is responsible for the viscoelastic properties of the synovial fluid and cartilage

extracellular matrix (Fig. 11.1). HA is a long, non-sulfated glycosaminoglycan that contains the repeating disaccharide unit of N-acetyl glucosamine and glucuronic acid [60].

Exogenous HA injection improves chondrocyte HA and proteoglycan synthesis, increases the production and activity of pro-inflammatory mediators and matrix metalloproteinases. Hyaluronan also suppresses cartilage degeneration and prevent cartilage for damage [61].

FDA approved IA HA injections are, Hylan G-F 20 (Synvisc®), Hylan G-F 20 (Synvisc-One™), Sodium hyaluronate (Hyalgan®, Supartz®, Euflexxa™, Monovisc™, Gel-Syn™, GenVisc® 850). High molecular weight Hyaluronan (Orthovisc®), Hyaluronic acid (Gel-One®), High molecular weight viscoelastic hyaluronan (Hymovis®), ([bcbswyn.com](http://bcbswyn.com)).

Chondrocytes cultured in culture media with HA have significantly greater rates of DNA proliferation and extracellular matrix production, compared with chondrocytes cultured without HA [1]. Studies have also shown that IA HA injection decreases arthritic lesions in experimental animal models of articular cartilage injury [7, 50, 67, 61, 21, 23, 56, 66, 75]. HA injections reduce synovial fluid levels of intercellular adhesion molecule-1 (ICAM-1) and vascular cell adhesion molecule-1 (VCAM-1) and improved WOMAC pain and stiffness score of patients with knee OA [47].

Due to a wide variety of IA-HA products, which molecular weight of IA-HA product should be used or how many injections should be applied for OA therapies is a contention. Ultra-high molecular weight viscosupplement (UHMW-HA) is a safe and effective treatment for hip osteoarthritis. A single dose of UHMW-HA was as effective as two doses of medium molecular weight hyaluronan (MMW-HA) resulting in similar reductions of pain and disability [16]. If we compared multiple and single injection of HA, 2–4 and  $\geq 5$  injection of HA decreased pain, while single injection did not. And multiple IA injections of HA treatment in knee OA has better results compared with IA-saline injections. [17]

Conrozier et al. [18], The goal of their study is to obtain pilot data from daily practice conditions

**Table 11.1** Oral GA and CS intake for OA treatment

Study	Dose	Method	Results	References
After oral glucosamine therapy synovial and plasma <b>glucosamine</b> concentrations in osteoarthritic patients	<b>Oral</b> 1500 mg crystalline glucosamine sulphate	Liquid chromatography-tandem mass spectrometry	After treatment, <b>plasma</b> median value increased 52.0–1282 ng/ml, <b>synovial</b> glucosamine concentration increased 36.5–777 ng/ml.	[72]
Evaluation of the effect of <b>glucosamine</b> on an experimental rat osteoarthritis model	<b>Oral</b> Glucosamine hydrochloride (GlcN; 1000 mg/kg/day)	Mankin score, toluidine blue staining of proteoglycans, serum biomarkers such as CTX-II (type II collagen degradation) and CPII (type II collagen synthesis) with ELISA.	GlcN has a potential to exhibit a chondroprotective action on OA by inhibiting type II collagen degradation and enhancing type II collagen synthesis.	[64]
The human pharmacokinetics of oral ingestion of <b>glucosamine and chondroitin sulphate</b> taken separately or in combination	<b>Oral</b> 1500 mg of glucosamine, 1200 mg of CS	Fluorophore-assisted carbohydrate electrophoresis (FACE)	CS amount in human plasma are about 20 µg/ml. The endogenous concentration and CS disaccharide composition were not detectably altered by ingestion of CS, when the CS was taken alone or in combination with GlcN.	[40]
Effect of the administering of an green tea supplement with <b>N-acetyl glucosamine</b> on biomarkers for cartilage metabolism	1000 mg GlcNAc-containing diet	<b>Serum</b> C2C and PIICP were measured with ELISA	C2C/PIICP ratio was decrease on GlcNAc group. (reduction of type II collagen degradation and increase of type II collagen synthesis) but <b>there was no significant difference between the two groups.</b>	[81]
Effect of <b>N-acetyl glucosamine</b> administration on cartilage metabolism	500 or 1000 mg/day	<b>Serum</b> C2C and PIICP were measured with ELISA	<b>No significant change</b> in the biomarkers for type II collagen degeneration and synthesis during and after the intervention with the placebo and two.	[53]
Effect of the <b>N-acetyl glucosamine</b> and proteoglycan containing supplement on locomotor functions of subjects with knee pain	526.5 mg of N-acetyl glucosamine (GlcNAc) and 33.6 mg of proteoglycan tablets (NGPS)	VAS, JKOM, JOA	The study reveals that intake of NGPS is <b>significantly</b> effective for relieving knee pain and improving knee function when walking or climbing stairs, swelling and bending or stretching.	[65]

C2C Collagen Type II Cleavage, PIICP Procollagen II C-Terminal Propeptide, VAS Visual Analog Scale, JKOM Japanese Knee Osteoarthritis Score, JOA Japanese Orthopedic Association Score

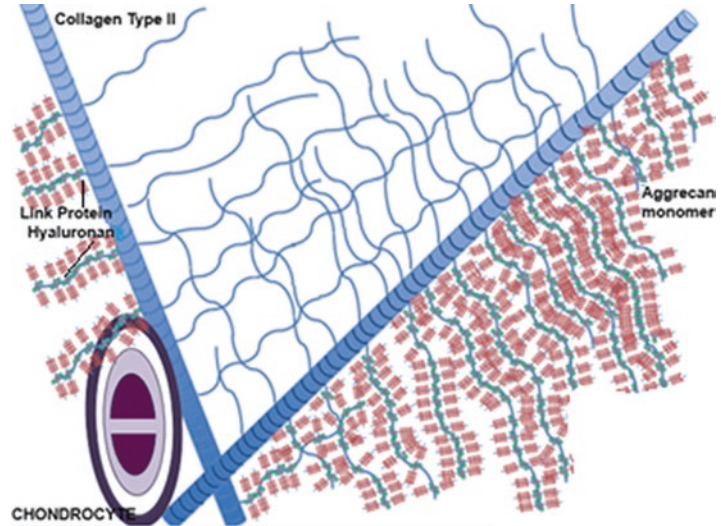
of a IA injection made of a cross-linked high-molecular weight HA combined with mannitol in patients with knee OA. They reported no treatment-related severe adverse event and efficacy was rated as good or very good in 77% of the cases.

Doria et al. [22], studied to compare the clinical efficacy of ultrasound-guided intra-articular

injections of autologous platelet rich plasma (PRP) versus hyaluronic acid (HA) for symptomatic early osteoarthritis (OA) of the hip and they found that both groups showed a significant improvement.

Ishijima et al. [39], compared intra articular HA injections versus oral NSAIDs for the treatment of knee OA. Their study was multi-center,

**Fig. 11.1** Extracellular matrix structure of cartilage. (Originally drawn by Korkusuz F)



randomized, open-label and non-inferiority. They resulted early efficacy of IA-HA is similar to NSAIDs yet IA-HA injections is more safe than NSAIDs injections. Also, Elsway et al. [25], did a similar comparative study to IA corticosteroids versus IA-HA treatment of knee OA. After 6 months of the treatment, both HA and corticosteroid groups showed improvement in pain and knee function, but the IA-HA was superior to corticosteroid on long-term follow-up. This result supports that IA HA injection is an effective long-term therapeutic option for patients with OA of the knee.

### 11.3 Platelet-Rich Plasma (PRP) Injections

Platelet-rich plasma (PRP) is a concentrated extract of platelets from autologous blood and is an another injectable treatment alternative in osteoarthritis [74]. PRP is categorized into four groups, depending on leukocyte and fibrin ingredient: pure platelet-rich plasma (P-PRP); leukocyte- and platelet-rich plasma (L-PRP); pure platelet-rich fibrin (P-PRF); and leukocyte- and platelet-rich fibrin (L-PRF) [24].

PRP contains platelet growth factors like transforming growth factor beta (TGF- $\beta$ ), platelet-derived growth factor (PDGF), insulin like growth factor (IGF), fibroblast growth

factor-2 (FGF), connective tissue growth factor (CTGF) which promotes chondrocyte differentiation, proliferation and stimulates HA production by synovial cells [69] (Table 11.2).

PRP injections for OA treatment are safe and more effective than placebo. Single injection of PRP improves in all Western Ontario and McMaster Universities Arthritis Index (WOMAC) parameters (pain, stiffness, physical function, and total score) [71, 77]. PRP injections to osteoarthritic knee are more effective than corticosteroids. Provides pain relief, higher quality of life and activities of daily living. However it didn't improve sporting ability. PRP was significantly more helpful for relieving patients' pain (VAS) compared to corticosteroids [29]. PRP injections provide decrease synovial fluid (SF) volume, SF total protein concentrations, inflammatory proteins and serum biomarker of cartilage degeneration (S.Coll2-1) on the knee OA patients [14, 27].

Smolina and Khimion [79], investigated safety and efficacy of the PRP use in early stages of the knee OA, and they observed no adverse events. They concluded that 3 IA injections of PRP added to the standard treatment of knee OA improves functional activity, reduces pain and probably can maintain relief in patients with the early stages of disease. Gobbi et al. [30], studied a similar study and they concluded too IA PRP injections into the knee for symptomatic early

**Table 11.2** Results of PRP injections of OA therapies

Study	Number of patients	Disease	Parameters	Result	References
PRP vs HA injection	180	1 and 2 stage of OA	KSS and VAS score	PRP is more efficient than HA	[49]
PRP injection	24	OA combined with supra-patellar bursitis	SF volume, total proteins, Lequesne index values	Significant decreases in SF total protein concentrations, volumes, and Lequesne index values	[14]
PRP injection	127	Early stage of OA	VRS, WOMAC, ROM, knee and IKDC score	Significant reduction in pain and improvement in knee function	[36]
PRP injection	40	OA	VAS score	Decrease of VAS score	[44]
PRP injection	78	OA	WOMAC score	WOMAC scores showing significant improvement	[71]

SF Synovial fluid, KSS Knee Society's Knee Scoring System, VAS Visual Analog Scale, VRS Visual Rating Scale, ROM Range of motion, IKDC International Knee Documentation Committee, WOMAC Western Ontario and McMaster Universities Arthritis Index

stages of OA are a valid treatment option. They found a significant reduction in pain and improvement in function on early OA patients.

Gormeli et al. [32], compared PRP and HA injections with osteoarthritic knee and they observed the knee scores of patients treated with multiple PRP injections were significantly improved than patients whose of the other groups. But they found no significant difference in the scores of patients injected with one dose of PRP or HA. Also, Raeissadat et al. [73], did a similar study, they compared PRP and HA injections and they found WOMAC pain score and bodily pain significantly improved in both groups; however, better results were determined in the PRP group compared to the HA group.

## 11.4 Medical Treatment

Immunosuppressive drug therapies are widely used for OA in order to inhibit catabolic activity of chondrocytes. Corticosteroids have both anti-inflammatory and immunosuppressive effects [5]. They decrease vascular permeability and inhibit aggregation of inflammatory cells, phagocytosis, production of neutrophil superoxide, metalloprotease, prostaglandin and leukotrienes [19, 70]. Corticosteroids mostly used for OA therapies due to their anti-inflammatory effects. FDA labeled corticosteroids are methyl-

prednisone acetate, triamcinolone acetate, betamethasone acetate, betamethasone sodium phosphate, triamcinolone hexacetonide and dexamethasone.

McAlindon et al. [59], studied 2-year randomized placebo controlled double-blind trial of IA triamcinolone vs. saline injections with OA. They injected intra-articularly 40 mg triamcinolone acetate every 3 months and followed progression of cartilage loss and pain. IA triamcinolone injections resulted in significantly greater cartilage volume loss than did saline for a mean change in index compartment cartilage thickness of -0.21 mm vs -0.10 mm. However they observed no significant difference in pain. Saline group had 3 treatment-related adverse events compared with 5 in the triamcinolone group.

Cheng et al. [15], used IA injection of Torin-1 in articular cartilage in a rabbit OA model. The mammalian target of rapamycin (mTOR) protein kinase plays a key role in the regulation of cell proliferation, motility, metabolism, survival and autophagy. Torin-1 is a specific inhibitor of mTOR and major immunosuppressant. IA injection of Torin-1 reduces degeneration of articular cartilage in collagenase-induced OA by autophagy activation. Collagenase type II was injected rabbits combined two IA injections of Torin-1. Significantly reduced degeneration of the articular cartilage after induction of OA. Autophagosomes, Beclin-1



and LC3 expressions were increased in the chondrocytes from Torin-1 treated rabbits. Also MMP-13 and VEGF expressions are reduced at 8 weeks after collagenase injection.

Bannuru et al. [8], they assess the relative efficacy of IA HA injections in comparison with NSAIDs for knee OA, and both groups showed improvement pain from baseline. Also they couldn't find statistically significant difference between the groups in function or stiffness.

Also Tammachote et al. [80], studied to compare the efficacy of single IA injection of hyaluronic acid (hylan G-F 20) with triamcinolone acetonide for knee OA patients. They reported that following at the 6 months triamcinolone acetonide provided similar improvement in knee pain, function, and range of motion compared with HA injections, with better pain control in the first week and better knee functional improvement in the second week.

Low-dose (1µM) Ral has the potential to cease or reduce the matrix degradation in OA. Kavas et al. [48], investigate the effects of Raloxifene (Ral) on degeneration-related changes in osteoarthritis (OA)-like chondrocytes using two- and three-dimensional models. They studied in two-dimensional and three-dimensional OA model and evaluated caspase-3 activity, gene expressions of collagen II, aggrecan, alkaline phosphatase (ALP), matrix metalloproteinases (MMP-13, 3 and 2) expressions and extra cellular matrix deposition. They resulted 1 µM Ral enhanced activities involved with matrix, but when they increase the dose these effects reversed except ALP gene expression and sGAG deposition.

Ohtori et al. [68], they investigated efficacy of direct injection of etanercept (TNFα inhibitor)

into knee joints for pain in moderate and severe knee OA. They were divided patients into two groups; hyaluronic acid (HA) and etanercept injection. No adverse events were observed in either group but significant pain relief was found in the etanercept group at 1 and 2 weeks by VAS, and at 4 weeks by WOMAC score, compared with the HA group

## 11.5 Stem Cell Therapies

Cell-based regenerative therapy have also been focused as an emerging regime for cartilage regeneration. Unlike chondrocytes implantation, the use of stem cells for regeneration of human articular cartilage is still investigational [54, 84]. Bone marrow mesenchymal stem cells (BM-MSCs) and adipose derived stromal cells (ADSCs) using in OA therapies for several years. Both type of cells are inhibits progression of OA and provide cartilage repair [20, 78] (Table 11.3). BM-MSCs has several advantages like multipotency, immunomodulatory activity, demonstrating featured safety and efficacy for cartilage regeneration [13, 43]. However, clinical applications of BM-MSCs have limitations by the painful surgical procedure, an excessively low cell yield and physiological circumstance of donors [3, 28, 35].

In a recent *in vitro* study, extracellular vesicles (EVs) secreted by bone marrow mesenchymal stem cells (BM-MSC-EVs) inhibit the adverse effects of inflammatory agents on cartilage homeostasis. When co-cultured with OA chondrocytes, BMMSC-EVs cancelled the TNF-α-mediated upregulation of cyclooxygenase 2 and pro-inflammatory interleukins and inhibited

**Table 11.3** The cells applied for OA therapies and WOMAC score improvement at the end of the study

Cells	Time	Total WOMAC Score improvement	Number of patients	References
ADSCs (SVF)	2 years	23 points	10	[9]
BM-MSCs	12 months	16.5 points	30	[55]
AD-MSCs	6 months	21.4 points	18	[42]
ADSCs (SVF)	6 months	15.8 points	13	[87]
BM-MSCs	30 months	29.3 points	18	[26]

ADSC Adipose derived stromal cells, BM-MSC bone marrow mesenchymal stem cell, AD-MSC Adipose derived mesenchymal stem cells, SVF Stromal vascular fraction, WOMAC Western Ontario and McMaster Universities Osteoarthritis Index, PRP Platelet rich plasma, HA Hyaluronic acid

TNF- $\alpha$ -induced collagenase activity. BM-MSC-EVs also supported cartilage regeneration *in vitro* [83].

Al-Najar et al. [2], did a phase I/II study with intra-articular injection of expanded autologous bone marrow mesenchymal cells in moderate and severe knee osteoarthritis, and they found normalized The Knee Injury and Osteoarthritis Outcome Score (KOOS) improved significantly, also mean knee cartilage thickness measured by MRI improved significantly.

Lamo-Espinoza et al. [55], compared IA injections of two different doses of autologous bone marrow mesenchymal stem cells (BM-MSC) vs. HA with 30 patients diagnosed with knee OA. After 12 month followed up, no adverse effects were reported and BM-MSC implement patients improved according to VAS during all follow-up evaluations and median value (IQR) for control and were also superior according to WOMAC. Motion ranges remained unaltered in the control group but improved with BM-MSCs. MRI results showed that joint damage decreased only in the BM-MSC group, albeit slightly.

Jo et al. [42], studied IA injection of MSC for the treatment of OA of the knee. They used 3 doses of autologous adipose tissue derived MSCs (AD-MSCs) for IA injection. In the high dose group, size of cartilage defect decreased while the volume of cartilage increased, WOMAC score improved and thick hyalin-like cartilage regeneration was observed.

Yokota et al. [87], used adipose derived stromal vascular fraction (SVF) cells for IA injections in patients with knee OA. They harvested 200 mL or more subcutaneous adipose tissue using tumescent liposuction technique. These cells injected into articular cavity of both knees directly. They reported no serious adverse events and 1 month after SVF injection all the scores of JKOM, WOMAC and VAS were significantly improved over baseline.

Applications of MSCs and PRP together for OA therapies have presented promising results [9], studied intra-articular injection in the knee of adipose derived stromal cells (SVF) and platelet rich plasma (PRP) for osteoarthritis, and the patients reported a reduction in pain levels,

especially after 3 months. They reported no severe adverse events or complications which means SVF+PRP injection is a safe therapy for knee OA. Also Bastos et al. [10], did a similar study, their purpose is to compare the effectiveness and safety of intra-articular injections of autologous expanded mesenchymal stromal stem cells alone (MSCs), or in combination with platelet-rich plasma (MSCs + PRP), in patients with knee OA. They studied with eighteen radiographic symptomatic knee OA patients. They resulted KOOS improved significantly throughout the 12 months for both groups ( $p < 0.05$ ). No statistically significant differences between groups were found in KOOS subscales and global score improvements at 12-month end-point. The MSCs and MSCs+PRP groups both exhibited significant improvements in the pain, function and daily living activities ( $p < 0.05$ ). They concluded that adding PRP to the MSCs injections did not provide additional benefit [34], investigated effects of intra-articular injection of MSCs associated with PRP in a rabbit model of OA. They studied with undifferentiated MSCs and MSCs differentiated to chondrocytes. MSC-treated group showed improved macroscopic changes on the articular surface. However they reported there are no difference in between groups that were treated with MSC differentiated chondrocytes and those that were not.

However, there are studies about stem cell injections in the literature that have negative results. In a recent clinical study, following direct injection of ADSCs, 76% of 37 patients showed abnormality in cartilage regeneration, especially with large cartilage lesions ( $\geq 5.4 \text{ cm}^2$ ) [52]. However, when the same group studied fibrin glue as a scaffold for ADSC injection, the results showed a significant difference between the scaffold and non-scaffold group in International Cartilage Repair Society (ICRS) grades ( $P = 0,028$ ). 12 of the 17 lesions (58%) in scaffold group and 9 of the 39 lesions (23%) in non-scaffold group achieved a grade of I or II [51].

It was recommended that a convenient scaffold should be developed for treating patients with big cartilage defects, since ADSCs seeded in scaffolds may have better viability, containment

and accumulation [52]. Also, directly injected cells usually have limited cell retention and survival capacity at the target site. The applicability of IA injected ADSCs for knee joint repair was questioned, because 1 month after IA injection of ADSCs, only 15% of cells was detectable in the joint of experimental animal model, and this number further decreased to 1.5% in 6 months [58].

In conclusion, IA injections of autologous expanded MSCs are safe and have a beneficial effect on symptoms in patients with symptomatic knee osteoarthritis. It reduces pain, improve the function, WOMAC, VAS and JKOM scores, KOOS, decrease the cartilage degradation and improve the cartilage regeneration. The safety of stem cell-seeded scaffolds already demonstrated in multiple *in vivo* animal models and small-scale humans trials [51], the next step is to confirm their safety and efficacy in large-scale human trials. And the stem cell-seeded scaffolds should be compared with the delivery of stem cells alone.

## 11.6 Biomaterials

Biomaterials are commonly using on OA therapies. Hydrogels, nano and micro sized particles, spheres, drug encapsulation and controlled drug delivery systems are the most used technologies for OA therapy (Fig. 11.2). Especially, hyaluronic acid, chondroitin sulfate and other GAGs using for carriers due to they are natural components of articular cartilage. Also biocompatible materials like polyethylene glycol (PEG), poly D,L-lactide (PDL) and poly- $\epsilon$ -caprolactone (PCL) are the most encountered carriers.

Due to clinical limitations, most of these studies are *in vitro* or *in vivo* with experimental animals. There are a few examples below.

Yao et al. [85], their objective was induce the differentiation of BMMSCs to chondrocytes in three-dimensional culture. They prepared PEG hydrogel with glucosamine (GA) and encapsulated the human BMMSCs. 5 and 10 mM concentrations of the GA-modified PEG hydrogels promoted the chondrogenesis of hBMSCs. In 8 weeks, the subcutaneous

transplantation of 10 mM GA-modified hydrogels with hBMSCs formed cartilage-like blocks *in vivo* and when glucosamine increase, the modified hydrogels downregulated the fibrosis and hypertrophic cartilage markers in protein level.

Hurtig et al. [38], studied poly D,L-lactide and polyethylene glycol (PDL-PEG) combined with celecoxib for OA therapy and they observed targeted delivery of NSAID to the synovial membrane can significantly reduce intra articular inflammation while minimizing systemic exposure.

Aydin et al. [4], studied *in vitro* and *in vivo* evaluation of doxycycline-chondroitin sulfate/PCL microspheres for intraarticular treatment of osteoarthritis. They prepared doxycycline (D) and doxycycline-chondroitin sulfate loaded poly- $\epsilon$ -caprolactone microspheres (D-CSMS) as IA delivery systems. They found D-CSMS had a positive contribution on all *in vivo* treatment outcomes and showed potential as a new strategy for treatment when applied to OA knee joints.

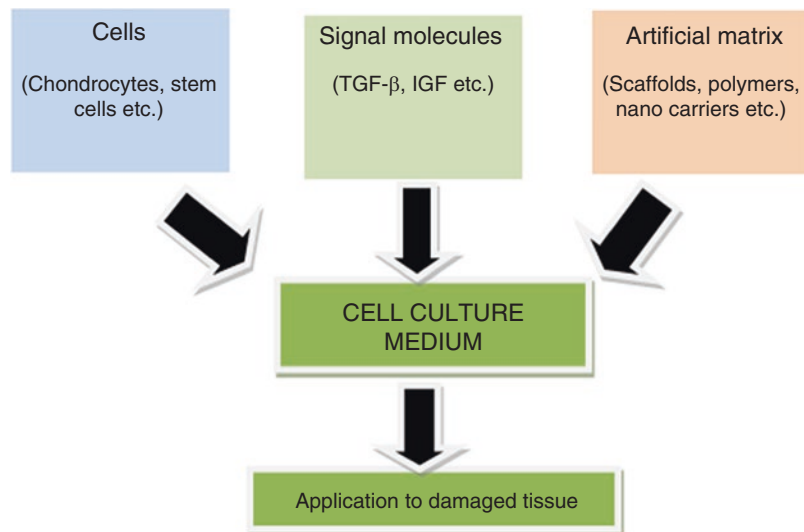
Yin et al. [86], made a novel chondroitin sulfate decorated nano platinum for the treatment of osteoarthritis and *in-vitro* cytotoxicity of PtNPs against the osteoarthritis chondrocytes showed their biocompatibility, hence the obtained nanoparticles may have future scope in the treatment of osteoarthritis.

Bajpayee et al. [6], they developed Avidin nano-carriers for dexamethasone delivering into the cartilage and studied for catabolic effects on cytokine challenged cartilage *in vitro*. And they observed single dose Avidin-DEX suppressed cytokine-induced sGAG loss over, rescued IL-1 $\alpha$  induced cell death and restored sGAG synthesis levels without causing cytotoxicity.

Liu et al. [57], studied articular cartilage regeneration on the rabbits with cartilage defects. They used human acellular amniotic membrane loaded with bone marrow mesenchymal stem cells They showed that treated cartilage showed improved results as compared to the control group, suggesting that MSCs play important roles in cartilage defect repair.

Kandel et al. [46], studied with MM-II, is a novel intra-articular bio-lubricant made of lipo-

**Fig. 11.2** Schematic tissue engineering applications for joint cartilage. (Drawn by Sahin S)



somes suspended aqueous solution. They compared MM-II with IA-HA injections. They found that IA MM-II injections are safe and effective. The pain reduction action was more rapid and sustained up to 3 months compared with HA.

In conclusion, OA is a chronic joint disease that is characterized by pain, loss of function and deformity where disease-modifying approaches are currently used. The recent approach by modifying the natural progress of OA using GAG, CS and HA by injecting them intra-articularly is open to research. The molecular mechanism how these molecules are incorporated into the joint cartilage matrix needs further research. Their effect on decreasing pain and inflammation is also open for discussion. Intracellular pathways of chondrocyte for maintaining joint cartilage homeostasis need further evaluation. Nano biomaterials to deliver GAG, CS and HA into the joint space are searched these days. We could produce controlled release systems, smaller molecules of high-weight molecules, so cells are easily intake and integrate their metabolic pathways. Also mimicking ECM of cartilage is improve of treatment of OA.

Oral treatments of OA may not be as effective as injectable treatments. Due to cartilage tissue lack the blood vessels and diffuse from synovial fluid, it is really difficult to reach the tissue from gastro-intestinal system. So we focused on the injectable therapies.

HA injections are good for pain reduction and synthesis ECM from chondrocytes but it shows no anti-inflammatory effect. PRPs and medical treatments (corticosteroids or other experimental drugs) decrease inflammatory molecules of cartilage, reducing pain and stiffness. However they are didn't stimulate to chondrocytes produce ECM. Also stem cells excrete anti-inflammatory molecules and they too reduce pain and offer a better life quality to OA patients. However in the cell therapies there are many difficulties like painful surgical procedures and low cell yield. Also, directly injection of MSCs may causes abnormal cartilage repair and increase the thickness of cartilage tissue. There are many positive resulted stem cell therapy studies exist in literature, but directly injected cells have restricted retention and survival capacity at the target site. Using biocompatible scaffolds to stem cell injections may improve the conservation of the cells.

## References

1. Akmal M, Singh A, Anand A, Kesani A, Aslam N, Goodship A, Bentley G (2005) The effects of hyaluronic acid on articular chondrocytes. *J Bone Joint Surg (Br)* 8:1143–1149. <https://doi.org/10.1302/0301-620X.87B8.15083>
2. Al-Najar M, Khalil H, Al-Ajlouni J, Al-Antary E, Hamdan M, Rahmeh R, Alhattab D, Samara O, Yasin

- M, Abdullah AA, Al-Jabbari E, Hmaid D, Jafar H, Awidi A (2017) Intra-articular injection of expanded autologous bone marrow mesenchymal cells in moderate and severe knee osteoarthritis is safe: a phase I/II study. *J Orthop Surg Res* 12(1):190. <https://doi.org/10.1186/s13018-017-0689-6>
3. Alt EU, Senst C, Murthy SN, Slakey DP, Dupin CL, Chaffin AE, Kadowitz PJ, Izadpanah R (2012) Aging alters tissue resident mesenchymal stem cell properties. *Stem Cell Res* 8:215–225. <https://doi.org/10.1016/j.scr.2011.11.002>
  4. Aydin O, Korkusuz F, Korkusuz P, Tezcaner A, Bilgic E, Yaprakci V, Keskin D (2014) In vitro and in vivo evaluation of doxycycline-chondroitin sulfate/PCL microspheres for intraarticular treatment of osteoarthritis. *J Biomed Mater Res B Appl Biomater* Aug 103(6):1238–1248. <https://doi.org/10.1002/jbm.b.33303>
  5. Ayhan E, Kesmezacar H, Akgun I (2014) Intraarticular injections (corticosteroid, hyaluronic acid, platelet rich plasma) for the knee osteoarthritis. *World J Orthod* 5(3):351–361. <https://doi.org/10.5312/wjo.v5.i3.351>
  6. Bajpayee AG, Quadir MA, Hammond PT, Grodzinsky AJ (2016) Charge based intra-cartilage delivery of single dose dexamethasone using Avidin nano-carriers suppresses cytokine-induced catabolism long term. *Osteoarthr Cartil* 24(1):71–81. <https://doi.org/10.1016/j.joca.2015.07.010>
  7. Balazs EA, Denlinger JL (1989) Clinical uses of hyaluronan. *Ciba Found Symp* 143:265–275
  8. Bannuru RR, Vaysbrot EE, Sullivan MC, McAlindon TE (2014) Relative efficacy of hyaluronic acid in comparison with NSAIDs for knee osteoarthritis: a systematic review and meta-analysis. *Semin Arthritis Rheum* 43(2014):593–599. <https://doi.org/10.1016/j.semarthrit.2013.10.002>
  9. Bansal H, Comella K, Leon J, Verma P, Agrawal D, Koka P, Ichim T (2017) Intra-articular injection in the knee of adipose derived stromal cells (stromal vascular fraction) and platelet rich plasma for osteoarthritis. *J Transl Med* 15:141. <https://doi.org/10.1186/s12967-017-1242-4>
  10. Bastos R, Mathias M, Andrade R, Bastos R, Balduino A, Schott V, Rodeo S, Espregueira-Mendes J (2018) Intra-articular injections of expanded mesenchymal stem cells with and without addition of platelet-rich plasma are safe and effective for knee osteoarthritis. *Knee Surg Sports Traumatol Arthrosc*. <https://doi.org/10.1007/s00167-018-4883-9>
  11. Bijlsma JW, Berenbaum F, Lefeber FP (2011) Osteoarthritis: an update with relevance for clinical practice. *Lancet* 377:2115–2126. [https://doi.org/10.1016/S0140-6736\(11\)60243-2](https://doi.org/10.1016/S0140-6736(11)60243-2)
  12. Bruyere O, Altman RD, Reginster JY (2016) Efficacy and safety of glucosamine sulfate in the management of osteoarthritis: evidence from real-life setting trials and surveys. *Semin Arthritis Rheum* 45(4 Suppl):S12–S17. <https://doi.org/10.1016/j.semarthrit.2015.11.011>
  13. Centeno CJ, Schultz JR, Cheever M, Freeman M, Faulkner S, Robinson B, Hanson R (2011) Safety and complications reporting update on the re-implantation of culture-expanded mesenchymal stem cells using autologous platelet lysate technique. *Curr Stem Cell Res Ther* 6:368–378 PMID: 22023622
  14. Chen CPC, Cheng CH, Hsu CC, Lin HC, Tsai YR, Chen JL (2017) The influence of platelet rich plasma on synovial fluid volumes, protein concentrations, and severity of pain in patients with knee osteoarthritis. *Exp Gerontol* 93:68–72. <https://doi.org/10.1016/j.exger.2017>
  15. Cheng NT, Guo A, Yp C (2016) Intra-articular injection of Torin 1 reduces degeneration of articular cartilage in a rabbit osteoarthritis model. *Bone Joint Res* 5:218–224. <https://doi.org/10.1302/2046-3758.56.BJR2015-0001>
  16. Clementi D, D'Ambrosi R, Bertocco P, Bucci MS, Cardiles C, Ragni P, Giuffreda G, Ragone V (2017) Efficacy of a single intra-articular injection of ultra-high molecular weight hyaluronic acid for hip osteoarthritis: a randomized controlled study. *Eur J Orthop Surg Traumatol*. <https://doi.org/10.1007/s00590-017-2083-9>
  17. Concoff A, Sancheti P, Niazi F, Shaw P, Rosen J (2017) The efficacy of multiple versus single hyaluronic acid injections: a systematic review and meta-analysis. *BMC Musculoskelet Disord* 18(1):542. <https://doi.org/10.1186/s12891-017-1897-2>
  18. Conrozier T, Bozgan AM, Bossert M, Sondag M, Lohse-Walliser A, Balblanc JC (2016) Standardized follow-up of patients with symptomatic knee osteoarthritis treated with a single intra-articular injection of a combination of cross-linked hyaluronic acid and mannitol. *Clin Med Insights Arthritis Musculoskelet Disord* 2016(9):175–179. <https://doi.org/10.4137/CMAMD.S39432>
  19. Creamer P (1999) Intra-articular corticosteroid treatment in osteoarthritis. *Curr Opin Rheumatol* 11: 417–421. PMID: 10503664
  20. Desando G, Cavallo C, Sartoni F, Martini L, Parrilli A, Veronesi F, Fini M, Giardino R, Facchini A, Grigolo B (2013) Intra-articular delivery of adipose derived stromal cells attenuates osteoarthritis progression in an experimental rabbit model. *Arthritis Res Ther* 15(1):R22. <https://doi.org/10.1186/ar4156>
  21. Ding M, Danielsen CC, Hvid I (2005) Effects of hyaluronan on three-dimensional microarchitecture of subchondral bone tissues in Guinea pig primary osteoarthritis. *Bone* 36:489–501. <https://doi.org/10.1016/j.bone.2004.12.010>
  22. Doria C, Mosele GR, Caggiari G, Puddu L, Ciurlia E (2017) Treatment of early hip osteoarthritis: ultrasound-guided platelet rich plasma versus hyaluronic acid injections in a randomized clinical

- trial. *Joints* 5(3):152–155. <https://doi.org/10.1055/s-0037-1605584>
23. Echigo R, Mochizuki M, Nishimura R, Sasaki N (2006) Suppressive effect of hyaluronan on chondrocyte apoptosis in experiment induced acute osteoarthritis in dog. *J Vet Med Sci* 68(8):899–902
  24. Ehrenfest D, Rasmusson L, Albrektsson T (2009) Classification of platelet concentrates: from pure platelet-rich plasma (P-PRP) to leucocyte- and platelet-rich fibrin (L-PRF). *Trend Biotechnol* 27(3):158–167. PMID: 19187989
  25. Elsayy SA, Hamdy M, Ahmed MS (2017) Intra-articular injection of hyaluronic acid for treatment of osteoarthritis knee: comparative study to intra-articular corticosteroids. *Egypt Rheumatol Rehabil* 44:143–146. [https://doi.org/10.4103/err.err\\_55\\_16](https://doi.org/10.4103/err.err_55_16)
  26. Emadedin M, Ghorbani Liastani M, Fazeli R, Mohseni F, Moghadasali R, Mardpour S, Hosseini SE, Niknejadi M, Moeininia F, Aghahosseini Fanni A, Baghban Eslamnejhad R, Vosough Dizaji A, Labibzadeh N, Mirazimi Bafghi A, Baharvand H, Aghdami N (2015) Long-term follow-up of intra-articular injection of autologous mesenchymal stem cells in patients with knee, ankle, or hip osteoarthritis. *Arch Iran Med* 18(6):336–344 015186/AIM.003
  27. Fawzy RM, Hashaad NI, Mansour AI (2017) Decrease of serum biomarker of type II collagen degradation (Coll2-1) by intra-articular injection of an autologous plasma-rich-platelet in patients with unilateral primary knee osteoarthritis. *Eur J Rheumatol* 4:93–97. <https://doi.org/10.5152/eurjrheum.2017.160076>
  28. Fenema EM, Renard AJ, Leusink A, van Blitterswijk CA, de Boer J (2009) The effect of bone marrow aspiration strategy on the yield and quality of human mesenchymal stem cells. *Acta Orthop* 80:618–621. <https://doi.org/10.3109/17453670903278241>
  29. Forogh B, Mianehsaz E, Shoae S, Ahadi T, Raissi GR, Sajadi S (2015) Effect of single injection of platelet-rich plasma in comparison with corticosteroid on knee osteoarthritis: a double-blind randomized clinical trial. *J Sports Med Phys Fitness* 56(7–8):901–908
  30. Gobbi A, Lad D, Karnatzikos G (2015) The effects of repeated intra-articular PRP injections on clinical outcomes of early osteoarthritis of the knee. *Knee Surg Sports Traumatol Arthrosc* 23(8):2170–2177. <https://doi.org/10.1007/s00167-014-2987-4>
  31. Goldring MB (2000) The role of the chondrocyte in osteoarthritis. *Arthritis Rheum* 43(9):1916–1926. [https://doi.org/10.1002/1529-0131\(200009\)43:9<1916::AID-ANR2>3.0.CO;2-I](https://doi.org/10.1002/1529-0131(200009)43:9<1916::AID-ANR2>3.0.CO;2-I)
  32. Gormeli G, Gormeli CA, Ataoglu B, Colak C, Aslanturk O, Ertem K (2017) Multiple PRP injections are more effective than single injections and hyaluronic acid in knees with early osteoarthritis: a randomized, double-blind, placebocontrolled trial. *Knee Surg Sports Traumatol Arthrosc* 25(3):958–965. <https://doi.org/10.1007/s00167-015-3705-6>
  33. Gu X, Li C, Yin F, Yang G (2017) Adipose-derived stem cells in articular cartilage regeneration: current concepts and optimization strategies. *Histol Histopathol* 15:11955. <https://doi.org/10.14670/HH-11-955>
  34. Hermeto LC, DeRossi R, Oliveira RJ, Pesarini JR, Antonioli-Silva AC, Jardim PH, Santana AE, Deffune E, Rinaldi JC, Justulin LA (2016) Effects of intra-articular injection of mesenchymal stem cells associated with platelet-rich plasma in a rabbit model of osteoarthritis. *Genet Mol Res* 2(3):15. <https://doi.org/10.4238/gmr.15038569>
  35. Hernigou P, Desroches A, Queinnee S, Flouzat Lachaniette CH, Poignard A, Allain J, Chevallier N, Rouard H (2014) Morbidity of graft harvesting versus bone marrow aspiration in cell regenerative therapy. *Int Orthop* 38:1855–1860. <https://doi.org/10.1007/s00264-014-2318-x>
  36. Huang PH, Wang CJ, Chou WY, Wang JW, Ko JY (2017) Short-term clinical results of intra-articular PRP injections for early osteoarthritis of the knee. *Int J Surg* 42:117–122. <https://doi.org/10.1016/j.ijssu.2017.04.067>
  37. Hunter DJ, Neogi T, Hochberg MC (2011) Quality of osteoarthritis management and the need for reform in the US. *Arthritis Care Res (Hoboken)* 63(1):31–38. <https://doi.org/10.1002/acr.20278>
  38. Hurtig MB, Shive MS, Kapoor M, Grizot S, Mohamed NN, Foster Roberts G, Marshall W (2016) Intra-articular injection of a polymer/celecoxib formulation for long-term control of postoperative inflammation. *Osteoarthr Cartil* 24(1):S526–S527. <https://doi.org/10.1016/j.joca.2016.01.962>
  39. Ishijima M, Nakamura T, Shimizu K, Hayashi K, Kikuchi H, Soen S, Omori G, Yamashita T, Uchio Y, Chiba J, Ideno Y, Kubota M, Kurosawa H, Kaneko K (2014) Intra-articular hyaluronic acid injection versus oral non-steroidal anti-inflammatory drug for the treatment of knee osteoarthritis: a multi-center, randomized, open-label, non-inferiority trial. *Arthritis Res Ther* 16(1):1. <https://doi.org/10.1186/ar4446>
  40. Jackson CG, Plaasza AH, Sandyz JD, Huax C, Kim-Rolandsx S, Barnhillk JG, Harrisk CL, Cleggy DO (2010) The human pharmacokinetics of oral ingestion of glucosamine and chondroitin sulfate taken separately or in combination. *Osteoarthr Cartil* 18(3):297–302. <https://doi.org/10.1016/j.joca.2009.10.013>
  41. Jerosch J (2011) Effects of glucosamine and chondroitin sulfate on cartilage metabolism in OA: outlook on other nutrient partners especially omega-3 fatty acids. *Int J Rheumatol* 2011:969012. <https://doi.org/10.1155/2011/969012>
  42. Jo CH, Lee YG, Shin WH, Kim H, Chai JW, Jeong EC, Kim JE, Shim H, Shin JS, Shin IS, Ra JC, Oh S, Yoon KS (2014) Intra-articular injection of mesenchymal stem cells for the treatment of osteoarthritis of

- the knee: a proof-of-concept clinical trial. *Stem Cells* 32:1254–1266. <https://doi.org/10.1002/stem.1634>
43. Johnstone B, Yoo JU (1999) Autologous mesenchymal progenitor cells in articular cartilage repair. *Clin Orthop Relat Res* 367:S156–S162
  44. Kadam R, Agrawal A, Chhallani A, Pandhre S, Gupta A, Sawant R (2017) To assess the effects of platelet rich plasma application on pain in osteoarthritis knee. *Int J Res Orthop* 3(3):436–439. <https://doi.org/10.18203/issn.2455-4510.IntJResOrthop20171005>
  45. Kahan A, Uebelhart D, De Vathaire F, Delmas PD, Reginster JY (2009) Long-term effects of chondroitins 4 and 6 sulfate on knee osteoarthritis: the study on osteoarthritis progression prevention, a two-year, randomized, double-blind, placebo-controlled trial. *Arthritis Rheum* 60(2):524–533. <https://doi.org/10.1002/art.24255>
  46. Kandel L, Dolev Y, Rivkind G, Liebergall M, Mattan Y, Barenholz Y, Shimonov R, Chevalier X (2014) Safety and efficacy of MM-II, an intra-articular injection of liposomes, in moderate knee osteoarthritis. Prospective randomized double-blinded study. *Osteoarthr Cartil* 22:S193. <https://doi.org/10.1016/j.joca.2014.02.367>
  47. Karatay S, Kiziltunc A, Yildirim K, Karanfil RC, Senel K (2004) Effects of different hyaluronic acid products on synovial fluid levels of intercellular adhesion molecule-1 and vascular cell adhesion molecule-1 in knee osteoarthritis. *Ann Clin Lab Sci* 34(3):330–335 PMID: 15487709
  48. Kavas A, Cagatay ST, Banerjee S, Keskin D, Tezcaner A (2013) Potential of Raloxifene in reversing osteoarthritis-like alterations in rat chondrocytes: an in vitro model study. *J Biosci* 38:135–147. <https://doi.org/10.1007/s12038-012-9282-7>
  49. Kilincoglu V, Yeter A, Servet E, Kangal M, Yildirim M (2015) Short term results comparison of intra-articular platelet-rich plasma (prp) and hyaluronic acid (ha) applications in early stage of knee osteoarthritis. *Int J Clin Exp Med* 8(10):18807–18812. ISSN:1940–5901/IJCEM0009103
  50. Kim CH, Lee BJ, Yoon J, Seo KM, Lee JW, Choi ES, Hong JJ, Lee YS, Park JH (2001) Therapeutic effect of hyaluronic acid on experimental osteoarthritis of ovine temporomandibular joint. *J Vet Med Sci*;63(10):1083–9. PMID: 11714023
  51. Kim YS, Choi YJ, Suh DS, Heo DB, Kim YI, Ryu JS, Koh YG (2015) Mesenchymal stem cell implantation in osteoarthritic knees: is fibrin glue effective as a scaffold? *Am J Sports Med* 43(1):176–185. <https://doi.org/10.1177/0363546514554190>
  52. Koh YG, Choi YJ, Kwon OR, Kim YS (2014) Second-look arthroscopic evaluation of cartilage lesions after mesenchymal stem cell implantation in osteoarthritic knees. *Am J Sports Med* 42:1628–1637. <https://doi.org/10.1177/0363546514529641>
  53. Kubomura D, Ueno T, Yamada M, Tomonaga A, Nagaoka I (2017) Effect of N-acetylglucosamine administration on cartilage metabolism and safety in healthy subjects without symptoms of arthritis: a case report. *Exp Ther Med* 13(4):1614–1621. <https://doi.org/10.3892/etm.2017.4140>
  54. Kuroda R, Ishida K, Matsumoto T (2007) Treatment of a full-thickness articular cartilage defect in the femoral condyle of an athlete with autologous bone-marrow stromal cells. *Osteoarthritis Cartil* Feb 15(2):226–231. <https://doi.org/10.1016/j.joca.2006.08.008>
  55. Lamo-Espinoza JM, Mora G, Blanco JF, Granero-Molto F, Nunez-Cordoba JM, Sanchez-Echenique C, Bondia JM, Aquerreta JD, Andreu EJ, Ornilla E, Villaron EM, Valenti-Azcarate A, Sanchez-Guijo F, del Canizo MC, Valenti-Nin JR, Prosper F (2016) Intra-articular injection of two different doses of autologous bone marrow mesenchymal stem cells versus hyaluronic acid in the treatment of knee osteoarthritis: multicenter randomized controlled clinical trial (phase I/II). *J Transl Med* 14(1):246. <https://doi.org/10.1186/s12967-016-0998-2>
  56. Leach JB, Schmidt CE (2004) Hyaluronan. *Encyclopedia of biomaterials and biomedical engineering*. Marcel Dekker, New York, pp 779–789
  57. Liu PF, Guo L, Zhao DW, Zhang ZJ, Kang K, Zhu RP, Yuan XL (2014) Study of human acellular amniotic membrane loading bone marrow mesenchymal stem cells in repair of articular cartilage defect in rabbits. *Genet Mol Res* 13(3):7992–8001. <https://doi.org/10.4238/2014>
  58. Maumus M, Manferdini C, Toupet K, Peyrafitte JA, Ferreira R, Facchini A, Gabusi E, Bourin P, Jorgensen C, Lisignoli G, Noël D (2013) Adipose mesenchymal stem cells protect chondrocytes from degeneration associated with osteoarthritis. *Stem Cell Res* 11:834–844. <https://doi.org/10.1016/j.scr.2013.05.008>
  59. McAlindon TE, LaValley HFW, Price LL, Driban JB, Zhang M, Ward RJ (2017) Effect of intra-articular triamcinolone vs saline on knee cartilage volume and pain in patients with knee osteoarthritis: a randomized clinical trial. *JAMA* 317(19):1967–1975. <https://doi.org/10.1001/jama.2017.5283>
  60. Messier SP, Callahan LF, Beavers DP et al (2017) Weight-loss and exercise for communities with arthritis in North Carolina (we-can): design and rationale of a pragmatic, assessor-blinded, randomized controlled trial. *BMC Musculoskelet Disord* 18(1):91 <https://doi.org/10.1186/s12891-017-1441-4>
  61. Moreland LW (2003) Intra-articular hyaluronan (hyaluronic acid) and hylans for the treatment of osteoarthritis: mechanisms of action. *Arthritis Res Ther* 5:54–67. <https://doi.org/10.1186/ar623>
  62. Murphy L, Schwartz TA, Helmick CG, Renner JB, Tudor G, Koch G, Dragomir A, Kalsbeek WD, Luta G, Jordan JM (2008) Lifetime risk of symptomatic knee osteoarthritis. *Arthritis Rheum* 59(9):1207–1213. <https://doi.org/10.1002/art.24021>
  63. Murphy LB, Helmick CG, Schwartz TA, Renner JB, Tudor G, Koch GG, Dragomir AD, Kalsbeek WD, Luta G, Jordan JM (2010) One in four people may

- develop symptomatic hip osteoarthritis in his or her lifetime. *Osteoarthr Cartil* 18(11):1372–1379. <https://doi.org/10.1016/j.joca.2010.08.005>
64. Naito K, Watari T, Furuhashi A, Yomogida S, Sakamoto K, Kurosawa H, Kaneko K, Nagaoka I (2010) Evaluation of the effect of glucosamine on an experimental rat osteoarthritis model. *Life Sci* 86(13–14):538–543. <https://doi.org/10.1016/j.lfs.2010.02.015>
  65. Naraoka Y, Harada H, Katagiri M, Yamamura H, Shirasawa T (2017) N-acetyl glucosamine and proteoglycan containing supplement improves the locomotor functions of subjects with knee pain. *Drug Discov Ther* 11(3):140–145. <https://doi.org/10.5582/ddt.2017.01019>
  66. Necas J, Bartosikova L, Brauner P, Kolar J (2008) Hyaluronic acid (hyaluronan): a review. *Vet Med* 53(8):397–411
  67. Neo H, Ishimaru JI, Kurita K, Goss AN (1997) The effect of hyaluronic acid on experimental temporomandibular joint osteoarthritis in the sheep. *J Oral Maxillofac Surg* 55:1114–1119. [https://doi.org/10.1016/S0278-2391\(97\)90293-7](https://doi.org/10.1016/S0278-2391(97)90293-7)
  68. Ohtori S, Orita S, Yamauchi K, Eguchi Y, Ochiai N, Kishida S, Kuniyoshi K, Aoki Y, Nakamura J, Ishikawa T, Miyagi M, Kamoda H, Suzuki M, Kubota G, Sakuma Y, Oikawa Y, Inage K, Sainoh T, Sato J, Shiga Y, Abe K, Fujimoto K, Kanamoto H, Toyone T, Inoue G, Takahashi K (2015) Efficacy of direct injection of etanercept into knee joints for pain in moderate and severe knee osteoarthritis. *Yonsei Med J* 56(5):1379–1383. <https://doi.org/10.3349/ymj.2015.56.5.1379>
  69. Ornetti P, Nourissat G, Berenbaum F, Sellam J, Richette P, Chevalier X (2016) Does platelet-rich plasma have a role in the treatment of osteoarthritis? *Joint Bone Spine* 83(1):31–36. <https://doi.org/10.1016/j.jbspin.2015.05.002>
  70. Ostergaard M, Halberg P (1998) Intra-articular corticosteroids in arthritic disease: a guide to treatment. *BioDrugs* 9:95–103. PMID: 18020548
  71. Patel S, Dhillon MS, Aggarwal S, Marhawa N, Jain A (2013) Treatment with platelet-rich plasma is more effective than placebo for knee osteoarthritis: a prospective, double-blind, randomized trial. *Am J Sports Med* 41(2):356–364. <https://doi.org/10.1177/0363546512471299>
  72. Persiani S, Rotini R, Trisolino G, Rovati LC, Locatelli M, Paganini D, Antonioli D, Roda A (2007) Synovial and plasma glucosamine concentrations in osteoarthritic patients following oral crystalline glucosamine sulphate at therapeutic dose. *Osteoarthr Cartil* 15:764–772. <https://doi.org/10.1016/j.joca.2007.01.019>
  73. Raeissadat SA, Babae M, Rayegani SM, Hashemi Z, Hamidieh AA, Mojangi P, Vanda HF (2017) An overview of platelet products (PRP, PRGF, PRF, etc.) in the Iranian studies. *Future Sci OA* 3(4):FSO231. <https://doi.org/10.4155/fsoa-2017-0045>
  74. Rodriguez-Merchan EC (2013) Intraarticular injections of Platelet-Rich Plasma (PRP) in the Management of Knee Osteoarthritis. *Arch Bone Joint Surg* 1(1):5–8 <http://abjs.mums.ac.ir>
  75. Roth A, Mollenhauer J, Wagner A, Fuhrmann R, Straub A, Venbrocks RA, Petrow P, Brauer R, Schubert H, Ozegowski J, Peschel G, Muller PJ (2005) Intra-articular injections of high-molecular-weight hyaluronic acid have biphasic effects on joint inflammation and destruction in rat antigen-induced arthritis. *Arthritis Res Ther* 7:677–686. <https://doi.org/10.1186/ar1725>
  76. Santilli V, Paoloni M, Mangone M, Alvitte F, Bernetti A (2016) Hyaluronic acid in the management of osteoarthritis: injection therapies innovations. *Clin Cases Miner Bone Metab* 13(2):131–134. <https://doi.org/10.11138/ccmbm/2016.13.2.131>
  77. Shen L, Yuan T, Chen S, Xie X, Zhang C (2017) The temporal effect of platelet-rich plasma on pain and physical function in the treatment of knee osteoarthritis: systematic review and meta-analysis of randomized controlled trials. *J Orthop Surg Res* 12:16. <https://doi.org/10.1186/s13018-017-0521-3>
  78. Singh A, Goel SC, Gupta KK, Kumar M, Arun GR, Patil H, Kumaraswamy V, Jha S (2014) The role of stem cells in osteoarthritis. *Bone Joint Res* 3:32–37. <https://doi.org/10.1302/2046-3758.32.2000187>
  79. Smolina L, Khimion L (2016) Autologous Platelet-Rich Plasma (PRP) in osteoarthritis treatment. *Ann Rheum Dis* 75:838. <https://doi.org/10.1136/annrheumdis-2016-eular.1630>
  80. Tammachote N, Kanitnate S, Yakumpor T, Panichkul P (2016) Intra-articular, single-shot Hylan G-F 20 hyaluronic acid injection compared with corticosteroid in knee osteoarthritis. *J Bone Joint Surg Am* 98:885–892. <https://doi.org/10.2106/JBJS.15.00544>
  81. Tomonaga A, Fukagawa M, Ikeda H, Hori T, Ohkawara M, Nagaoka I (2016) Evaluation of the effect of the administering of an N-acetylglucosamine-containing green tea supplement on biomarkers for cartilage metabolism in healthy individuals without symptoms of arthritis: a randomized double-blind placebo-controlled clinical study. *Funct Foods Health Dis* 6(12):788–808. <https://doi.org/10.3892/etm.2016.3480>
  82. Vasiliadis HS, Tsikopoulos K (2017) Glucosamine and chondroitin for the treatment of osteoarthritis. *World J Orthop* 8:1–11. <https://doi.org/10.5312/wjo.v8.i1.1>
  83. Vonk LA, van Dooremalen SFJ, Liv N, Klumperman J, Coffey PJ, Saris DBF, Lorenwicz MJ (2018) Mesenchymal stromal/stem cell-derived extracellular vesicles promote human cartilage regeneration in vitro. *Theranostics* 8(4):906–920. <https://doi.org/10.7150/thno.20746>
  84. Wakitani S, Imoto K, Yamamoto T (2002) Human autologous culture expanded bone marrow mesenchymal cell transplantation for repair of cartilage defects in osteoarthritic knees. *Osteoarthr Cartil* 2002;10:199–206. <https://doi.org/10.1053/joca.2001.0504>



85. Yao H, Xue J, Wang Q, Xie R, Li W, Liu S, Cai J, Qin D, Wang DA, Ren L (2017) Glucosamine-modified polyethylene glycol hydrogel-mediated chondrogenic differentiation of human mesenchymal stem cells. *Mater Sci Eng C Mater Biol Appl* 1(79):661–670. <https://doi.org/10.1016/j.msec.2017.05.043>
86. Yin XF, Wang LL, Chu XC (2017) A novel chondroitin sulfate decorated nano platinum for the treatment of osteoarthritis. *Mater Sci Eng C Mater Biol Appl* 78:452–456. <https://doi.org/10.1016/j.msec.2017.04.028>
87. Yokota N, Yamakawa M, Shirata T, Kimura T, Kaneshima H (2017) Clinical results following intra-articular injection of adipose-derived stromal vascular fraction cells in patients with osteoarthritis of the knee. *Regen Ther* 6:108–112. <https://doi.org/10.1016/j.reth.2017.04.002>



# Fabrication of Hydrogel Materials for Biomedical Applications

# 12

Jen Ming Yang, Olajire Samson Olanrele,  
Xing Zhang, and Chih Chin Hsu

## Abstract

Hydrogels are three-dimensional hydrophilic polymeric networks that can be made from a wide range of natural and synthetic polymers. This review discusses recent advanced engineering methods to fabricate hydrogels for biomedical applications with emphasis in cardiac constructs and wound healing. Layer-by-Layer (LbL) assembly offers a tissue-engineered construct with robust and highly ordered structures for cell proliferation and differentiation. Three-dimensional printings, including inkjet printing, fused deposition modeling, and stereolithographic apparatus, have been widely employed to fab-

ricate complex structures (e.g., heart valves). Moreover, the state-of-the-art design of intelligent/stimulus-responsive hydrogels can be used for a wide range of biomedical applications, including drug delivery, glucose delivery, shape memory, wound dressings, and so on. In the future, an increasing number of hydrogels with tunable mechanical properties and versatile functions will be developed for biomedical applications by employing advanced engineering techniques with novel material design.

## Keywords

Hydrogels · 3D printing · Layer-by-layer · Tissue engineering · Heart valve · Wound dressing

Authors Jen Ming Yang and Olajire Samson Olanrele have been equally contributed to this chapter.

J. M. Yang (✉)

Department of Chemical and Materials Engineering,  
Chang Gung University,  
Tao Yuan, Taiwan, Republic of China

Department of General Dentistry, Chang Gung  
Memorial Hospital,  
Tao Yuan, Taiwan, Republic of China

Division of Pediatric Infectious Diseases, Department  
of Pediatrics, Chang Gung Memorial Hospital,  
Taoyuan, Taiwan, Republic of China  
e-mail: [jmyang@mail.cgu.edu.tw](mailto:jmyang@mail.cgu.edu.tw)

O. S. Olanrele · X. Zhang (✉)

Institute of Metal Research, Chinese Academy of  
Sciences, Shenyang, Liaoning, People's Republic of  
China

School of Materials Science and Engineering,  
University of Science and Technology of China,  
Hefei, Anhui, People's Republic of China  
e-mail: [xingzhang@imr.ac.cn](mailto:xingzhang@imr.ac.cn)

C. C. Hsu

Department of Physical Medicine and Rehabilitation,  
Chang Gung Memorial Hospital at Keelung,  
Keelung, Taiwan, Republic of China

School of Traditional Chinese Medicine, Chang Gung  
University, Taoyuan, Taiwan, Republic of China

## 12.1 Introduction

Hydrogels are three-dimensional (3D) networks of polymer chains that have high water absorbing capacity [14, 82, 111]. From the historical point of view, the first hydrogel (poly(2-hydroxyethyl methacrylate)) used in ophthalmometry was proposed by Wichterle and Lim in 1960s [152]. Since then, hydrogels have emerged as potential candidates for various biomedical applications, including tissue engineering and drug delivery.

Hydrogels can be made from a wide range of polymers [27, 29, 50, 93, 127, 137], including synthetic polymers (e.g., polyethylene glycol [PEG], poly(acrylamide) [PAAM], and poly(vinyl alcohol) [PVA]) and natural polymers (e.g., fibrin, collagen, hyaluronic acid [HA], and alginate). Hydrogel materials have many desirable features, such as biocompatibility, nontoxicity, predictable degradation rates, tunable mechanical properties, and good elasticity [130, 138, 151, 172, 173].

Hydrogels are basically constructed from cross-linking networks and can be classified as physically cross-linked or chemically cross-linked hydrogels [24, 138]. Controlling the structure of hydrogel networks allows the proper design and characterization of hydrogel scaffold degradation, bioactive molecule diffusion, and cell migration through the network [60, 179]. Hydrogel networks at the molecular level can be elucidated using combined theories of equilibrium swelling, rubber elasticity, and other predictive models [3, 15, 26, 39, 86, 88, 109, 110]. Peppas et al. summarized three key parameters for defining the structures of hydrogels:

- Equilibrium polymer volume fraction in the swollen state ( $v_{2,s}$ )
- Average molecular weight between cross-links ( $M_c$ )
- Network mesh (or pore) size ( $\xi$ )
- These parameters can be further defined by the following constitutive equations:

$$v_{2,s} = V_p / V_{gel} = Q^{-1} \quad (12.1)$$

$$M_c = M_o / 2X \quad (12.2)$$

$$\xi = v_{2,s}^{-\frac{1}{3}} (\gamma_o^2)^{\frac{1}{2}} = Q^{\frac{1}{3}} (\gamma_o^2)^{1/2} \quad (12.3)$$

$V_p$  is the volume of the polymer.  $V_{gel}$  is the volume of the swollen gel.  $Q$  is the equilibrium volumetric swelling ratio.  $M_o$  is the molecular weight of the polymer repeating unit.  $X$  is the degree of cross-linking.  $(\gamma_o^2)^{1/2}$  is the root-mean-square end-to-end distance of network chains between two adjacent cross-links in the equilibrium state. The network mesh (or pore) size, ( $\xi$ ), is descriptive of the distance between consecutive junctions, cross-links, or tie points.

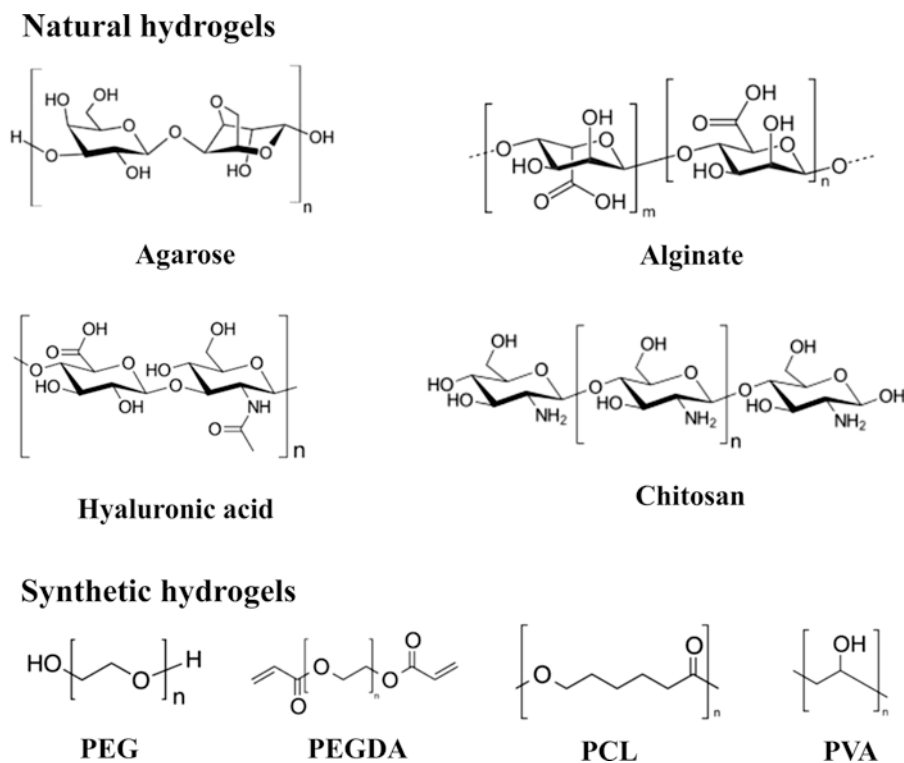
This review highlights recent advanced engineering methods, including 3D printing, Layer-by-Layer (LbL) assembly, and the microfluidic technique for fabricating hydrogels and their potential biomedical applications (especially for cardiac constructs and wound healing). We also discuss the state-of-the-art fabrication of smart/intelligent/stimulus-responsive hydrogels and their wide range of biomedical applications, including drug delivery, glucose delivery, shape memory, and diagnosis.

## 12.2 Classification of Hydrogels

Hydrogels are generally classified based on their chemical compositions, cross-linking methods, microstructures, ionic charges, and degradation rates, among others [115, 148].

### 12.2.1 Hydrogel Origin/Source

Hydrogels consist of two categories that are based on chemical composition: (i) synthetic materials and (ii) naturally derived materials. Hydrogels of natural polymers are able to mimic natural tissue constructs. However, these hydrogels are usually prone to permanent breakage because of their limited mechanical strength. Hydrogels that are made of synthetic polymers have high mechanical strength and tunable physicochemical properties [43]. Figure 12.1 shows the chemical structures of various natural and



**Fig. 12.1** The chemical structures of various natural and synthetic hydrogels that have been used for biomedical applications

synthetic hydrogels that have been used for biomedical applications.

### 12.2.1.1 Natural Polymer-Based Hydrogels

Natural polymer-based hydrogels, including collagen, HA, gelatin, fibrin, alginate, chitosan, agarose, keratin, cellulose and decellularized extracellular matrix (dECM), have been used for biomedical applications [55]. Natural polymers, such as alginate, gelatin, and collagen can be used as bioink due to their excellent biocompatibility, cell encapsulating prowess and intrinsic ability akin to the complex tissue microenvironments thereby providing dynamics clue for cellular activities [106].

### 12.2.1.2 Synthetic Polymer-Based Hydrogels

Biocompatible synthetic polymers have been widely used as scaffold materials for various biomedical applications owing to their excellent

mechanical strength and tailorable physicochemical properties which enhance the output of the printed constructs. The materials of the synthetic polymers are cost effective, with no risk of pathogenic invasion in engineered constructs [106]. Synthetic polymers namely polycaprolactone (PCL), poly (ethylene glycol) diacrylate (PEGDA), poly(lactic-co-glycolide) (PLGA), polyvinyl alcohol (PVA) have been reportedly used for bioprinting of tissue engineered constructs. The combination of synthetic and natural polymer blends (i.e., hybrid polymers or modified polysaccharides; e.g., HA and dextran methacrylate) has been employed to control hydrogel matrix architecture, which in turn improves the cellular response [8, 108].

### 12.2.2 Cross-Linking Methods

Hydrogels can be classified into physically and chemically cross-linked hydrogels based on their

cross-linking mechanisms [138]. Physical cross-linking is normally achieved via physical processes, such as crystallite formation, polymer chain complexion, hydrophobic interaction, and hydrogen bonding. Chemical or covalent cross-linking forms as a result of covalent bond junctions. Physically cross-linked hydrogels are reversible because of conformational changes that prevent them from dissolving in aqueous media, whereas, chemically cross-linked hydrogels are permanent and irreversible because of configurational changes. The hydrogel matrix of the chemically cross-linked hydrogels is well stabilized during gelation process which consequently improves the hydrogel flexibility and spatiotemporal precision [170]. Radical polymerization (polymerization of end-functionalized macromers in the presence of a cross-linking agent) is one of the most widely used methods to prepare chemically cross-linked gels [103]. The type and degree of cross-linking influence macroscopic properties of hydrogels, including the degree of swelling, mechanical property and molecule transportation through the hydrogel meshes [13].

### 12.2.3 Interpenetrating Network

Based on different compositions and network structures, hydrogels can be classified as (i) homo-polymers, (ii) copolymers, (iii) semi-interpenetrating networks (IPNs), and (iv) interpenetrating networks [1]. Homo-polymer hydrogels are usually cross-linked by one monomer species in hydrophilic environment [148], whereas copolymer hydrogels comprise of networks of two or more types of hydrophilic monomer units [159]. The hybrid of one cross-linked and another non cross-linked polymer forms semi-interpenetrating network hydrogels [53, 169]. Interpenetrating polymeric hydrogels form through reaction of monomers in polymeric network [148].

## 12.3 Advanced Engineering Methods for Hydrogel Fabrication

Over the years, hydrogels that have been used as tissue engineering scaffolds usually possess low mechanical integrity and lack of structural complexity. Recently, the broadened applications of hydrogels require advanced engineering techniques to spatially manipulate the physical and chemical properties of hydrogels and hence control their architectural precision [170].

Key parameters (e.g., vascularization for the adequate transport of oxygen and metabolites, control over matrix architecture by regulating porosity and mechanical properties, the presentation of biological signaling motifs, and the microenvironmental control of cell-cell and cell-matrix interactions) have been considered when fabricating tissue-engineered constructs [81, 113, 118, 121]. Different fabrication techniques, such as 3D printing, LbL fabrication, microfluidic-based fabrication, electrospinning, and self-assembly, have been explored to modulate key parameters of hydrogels and thus spatially confer cellular architecture or hydrogel functionality.

### 12.3.1 Three-Dimensional Printing

Three-dimensional (3D) printing, often referred to as additive manufacturing (AM), has been employed to fabricate structures of precise geometries by depositing materials onto a moving platform according to a computer-controlled process [45, 62, 77]. Three-dimensional printing is a rapid prototyping (RP)-based approach that has excellent 3D microfabrication capacity for tissue engineering constructs [90, 91]. The technology employs computer-aided design (CAD) to model the construct and convert it into a compatible format, followed by fabrication of the construct using a printer [181].

The history of 3D printing can be traced back to the early 1990s when Sachs and colleagues made available the first rapid prototyping method to fabricate models at the Massachusetts Institute of Technology [22, 23]. Many advanced approaches have been implemented in 3D printing techniques, including inkjet printing, fused deposition modeling (FDM), and laser-based stereolithography [38, 74, 76, 133, 137].

Inkjet printing is an inexpensive process that relies on the deposition of a rheologically tailored ink filament that is made of nanoparticle colloids or organic materials to build 3D structures [38]. Inkjet printers can be classified as drop-on-demand or continuous-flow type printers based on the flow rate of bioinks [76]. The inkjet printing has been mainly used with low viscosity bioink materials, which is not able to print 3D volumetric constructs with low shape fidelity due to insufficient mechanical strength of printed objects [132].

Fused deposition modeling employs thermoplastic-based materials that pass through a heated extrusion nozzle, which are melted and deposited on a building platform in an LbL manner [51]. One of the captivating advantages of FDM is the creation of complex scaffolds with good mechanical strength and outstanding geometric accuracy [21]. However, the challenges for FDM include temperature sensitivity and limited choice of materials.

Stereolithographic apparatus is currently the most widely used AM technology to build 3D scaffolds for tissue engineering applications. The technology builds 3D structures by curing or solidifying a photosensitive resin through the use of an irradiated ultraviolet laser beam. The instrument setup consists of a vessel that contains a photosensitive resin, a moveable platform on which the model is built, and a computer-controlled laser beam that is operated in a defined CAD pattern [6, 31]. Compared with other AM techniques, SL has the potential to fabricate complex 3D structures with very high resolution and accuracy [90]. However, material constraints, such as the need for low viscosity and transparent

materials, the high printer cost, and the long duration of printing, are the main drawbacks of SL techniques [38].

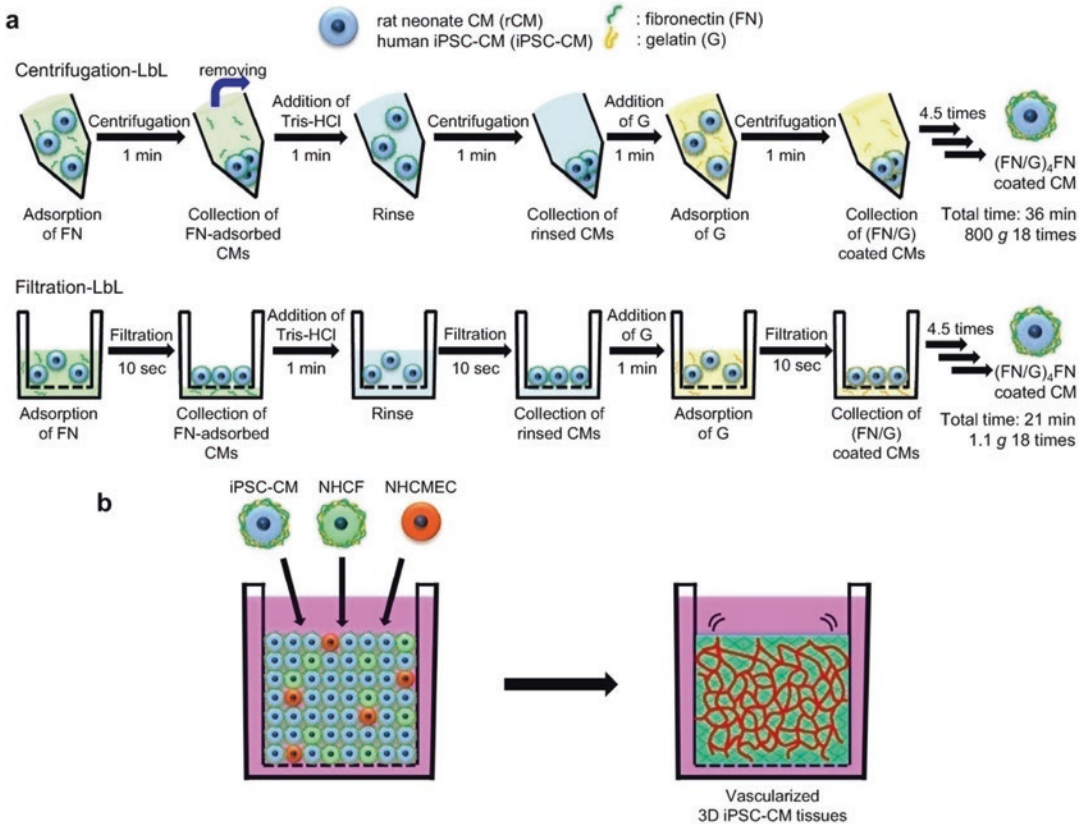
The significance of bioprinting technology is the ability to create 3D tissue structures that can encapsulate cells and also mimic physiological environments. Numerous factors, including material cytotoxicity, printability, and mechanical property are needed to be considered when used for 3D printing. The most widely used biomaterials for bioprinting are hydrogels, also called bioinks; a liquid precursor which solidifies into a cross-linked polymeric structure after the printing process [77].

Presently, various 3D printing techniques have been used to fabricate 3D scaffolds and eliminate the limitations peculiar to traditional printing process [64, 102, 106]. Compared with traditional manufacturing processes, 3D printing techniques are more flexible and rapid, especially when creating parts with complex architectures and compositional variations [64]. The use of medical imaging data, such as magnetic resonance imaging (MRI) and computed tomography (CT), for 3D printing provides a platform for creating patient-specific implants that have anatomical geometries of the defective part [90, 131, 166].

Recently, technical advances in 3D printing suggest the possibility of fabricating human cell-based tissue models by depositing live cells and growth factors along with biomaterial scaffolds during printing [5, 77]. For example, cardiac tissue valves, blood vessels, and whole heart for tissue engineering have been successfully developed using different 3D printing-based tissue engineering approaches [46, 133]. However, there is limited availability or choice of raw materials for 3D printing nowadays.

### 12.3.2 Layer-by-Layer (LbL) Fabrication

LbL fabrication technology has tremendous potential to create intricate cardiac constructs



**Fig. 12.2** Schematic diagrams of (a) nanofilm fibronectin and gelatin coated cell using LbL filtration techniques and (b) constructed of vascularized 3D iPSC-CM tissues [2]. (Reprinted with permission from Elsevier)

that feature biomimetic structural complexities with better cell organization, maturation, and cell-cell electrical coupling. For example, multi-layer tissue that was composed of cell-adhered poly-L-lysine-graphene oxide (PLL-GO) thin films on a graphene-methacrylated gelatin (GO-GelMA) hybrid hydrogel was constructed in LbL manner. The effects of PLL-GO concentration on the architectural network of the multilayer cell construct, cell adhesion affinity, the viability of cardiomyocytes, endothelial cells (ECs), and human mesenchymal stem cells (hMSCs), and construct electrical propagation were also investigated. Live/dead assays that were performed with the constructs showed excellent cell viability, and PLL-GO effectively provided an adhesive surface necessary to maintain interactions between the cells and the stacked

layers with no cytotoxic effects. Furthermore, incorporation of cardiomyocytes in PLL-GO resulted in synchronous beating pattern under a low external electric field [134].

An LbL filtration technique was employed to fabricate nanometer-sized fibronectin and gelatin ECM films onto an iPSC-CM (human cardiomyocyte (CM) tissues derived from human induced pluripotent stem cells (iPSCs)) surface as shown in Fig. 12.2. The findings revealed that at high cell viability (95%) of the 3D tissue, the micro vessels of the blood capillary served as an exchange media for vital nutrients and oxygen for the cells encapsulated within 3D tissues. The introduction of human cardiac fibroblasts (HCFs) into 3D-iPSC-CM tissues enhanced tissue organization and induced blood capillary networks [2].

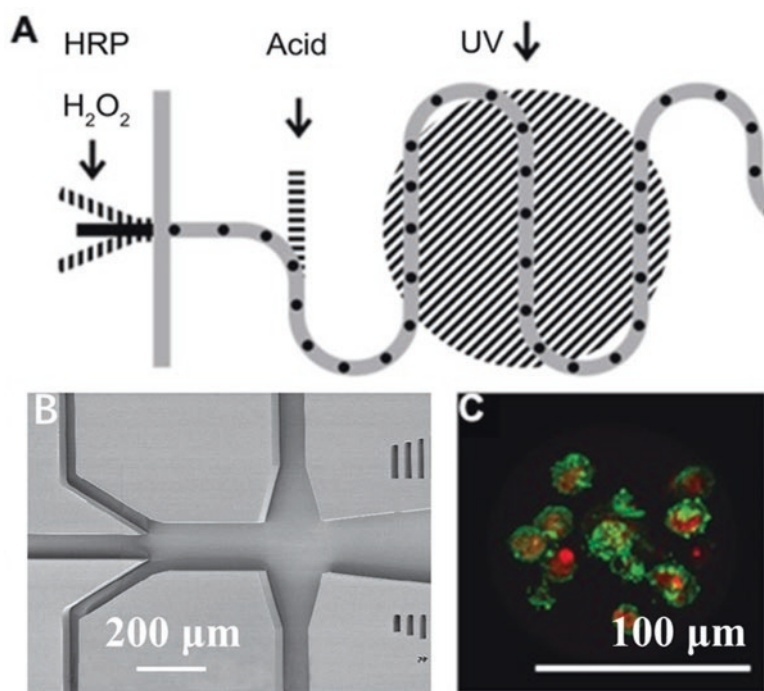
### 12.3.3 Microfluidic-Based Fabrication

Microfluidic technology exploits such characteristics as a small size and the laminar flow of liquid for engineering geometry, composition, and functionality in hydrogel constructs [17]. The density and pore size that are associated with nutrients and waste transportation play a crucial role in delivering soluble biochemical factors and oxygen through the scaffolds.

Microfluidic systems have been widely exploited for the microfabrication of hydrogel structures that can be used for tissue engineered vessels, lung and cartilage. For example, microfluidic devices with bifurcated motifs have been used to generate highly functionalized polystyrene-based vascular structures.

The microfluidic systems have the potential to confer functionality on structures with endothelialized cells. To this end, primary human umbilical vein endothelial cells (HUVECs) cultured inside semicircular microfluidic device adhere to the bifurcated networks of the device to form lumen-like structure. Microfluidic techniques allow precise control and manipulation of fluids which inherently influence the physiological conditions of 3D culture models.

Microfluidic systems have provided a platform to generate bioactive, stem cell-laden microgels with well-defined physical and chemical microenvironments that enhance cell proliferation, function, and differentiation (Fig. 12.3; [57]). Siltanen et al. fabricated heparin-based hydrogels for encapsulating mouse embryonic stem cells for the formation of spheroids with enhanced endodermic differentiation [136].



**Fig. 12.3** (a) Schematic diagram of the universal microfluidic chip used for production of photo cross-linked PEGDA, ionic cross-linked alginate, and enzymatically cross-linked Dex-TA microgels. Dashed areas depict the initiation point for photo, ionic, and enzymatic cross-linking. (b) Scanning electron image of the droplet form-

ing nozzle with inlets for HRP and  $H_2O_2$  to crosslink Dex-TA. (c) The confocal image of hMSCs encapsulated in a Dex-TA microgel after 14 days of culture. Red colour indicates the nucleus while green colour depicts the cytoskeleton of the encapsulated cells [57]. (Reprinted with permission from John Wiley & Sons, Inc)



## 12.4 Advanced Engineering of Hydrogels for Cardiac Constructs and Repair

Cardiac tissue engineering (CTE) is an evolving field that offers the possibility of restoring contractile function and retaining the pumping features of the human heart. The aim of tissue engineering is to develop autologous and functional biomaterials that can be implanted into injured tissues. Based on this concept, CTE has been introduced as a promising technique to benefit patients with cardiovascular disease [79]. The strategic protocols involve designing suitable scaffolds for cardiac tissue engineering by possessing three key features (*i*) anisotropic mechanical properties that provides physiological relevance similar to those of native cardiac tissue, (*ii*) an anisotropic structure that reproduces the fibre suitable for the cardiac tissue alignment, and (*iii*) conductive properties for electrical signalling interaction that provides synchronous beating behaviour for cells in cardiac microenvironment [9, 11, 34, 72]. Recent advances in the engineering of hydrogels for cardiac constructs and repair by 3D printing will be further discussed.

### 12.4.1 Three-Dimensional Printing-Based Approaches for Cardiac Tissue Constructs and Regeneration

Three-dimensional printing is a powerful tool that is pertinent to repairing and regenerating damaged cardiac tissue after myocardial ischemia. Among microfabrication strategies, 3D printing has shown tremendous potential to create intricate cardiac constructs that feature biomimetic structural complexities [66] that have been employed to generate 3D architecture of cardiac tissue patches, valves, blood vessels, and whole heart models.

#### 12.4.1.1 Three-Dimensional Printing for Myocardial Tissue

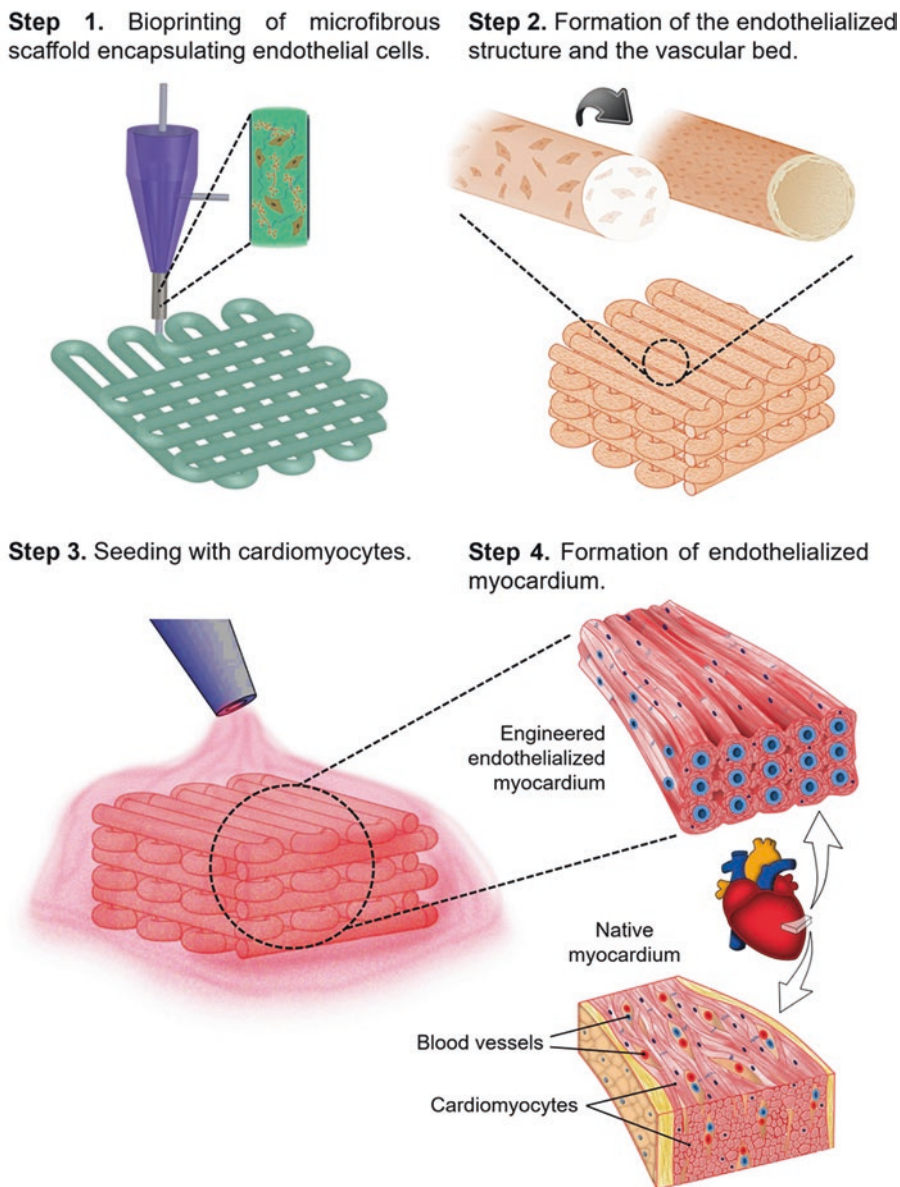
Upon myocardial infarction, cardiac muscles (primarily cardiomyocytes) lose their contractil-

ity because of insufficient blood pumping by the heart to injured cardiac tissue. As a result, the elaborate architecture of the myocardium is transformed into non-functional scar tissue through fibroblast activation, which consequently inhibits cardiac cellular communication [37, 69] and results in ischemia or eventually death when the diseased condition is not well managed.

Cell therapy is a treatment option for damaged cardiac tissue, in which cells are implanted in the affected site. However, the ability of the cells to survive and properly integrate into heart tissue during implantation determines the effectiveness of therapy with regard to cardiac tissue regeneration. Thus, cell therapy may not achieve desirable cardiac tissue repair because of the limited supply of oxygen to the implanted cells in the heart [40, 116]. To overcome these limitations, 3D printing has been employed to fabricate 3D complex structures with homogeneously dispersed cells.

Highly controlled oriented 3D tissue models that were composed of hydroxybutyl chitosan (HBC) and HCFs were fabricated using an LbL technique and a 3D printing system [146]. A thermo-responsive polymer, HBC, was laminated to a height of  $1124 \pm 14 \mu\text{m}$  using a robotic dispensing 3D printer, followed by an LbL coating of HCFs with ECM nano films that were later seeded and cultured on the HBC gel of different frames (square, triangular, rectangular, and circular). The cell orientation in the  $2 \text{ mm} \times 15 \text{ mm}$  rectangular gel frame was extended in one direction compared with the  $3 \text{ mm} \times 15 \text{ mm}$  rectangular gel frame. The observed alignment of F-actin fibers on the  $2 \text{ mm}$  short-side rectangular HBC gel frame as a result of HCF and human dermal microvascular endothelial (HMVEC) co-culture confirmed vascularization of the orientation-controlled 3D tissues.

Zhang and colleagues developed an *in vitro* model to mimic the efficacy of endothelium cells inside the cardiac tissue microenvironment (Fig. 12.4). HUVECs were printed with a GelMA-alginate bioink using an Organovo NovoGen MMX commercial extrusion printer and coaxial nozzle. Cell-laden bioink was extruded from the inner nozzle, and the outer



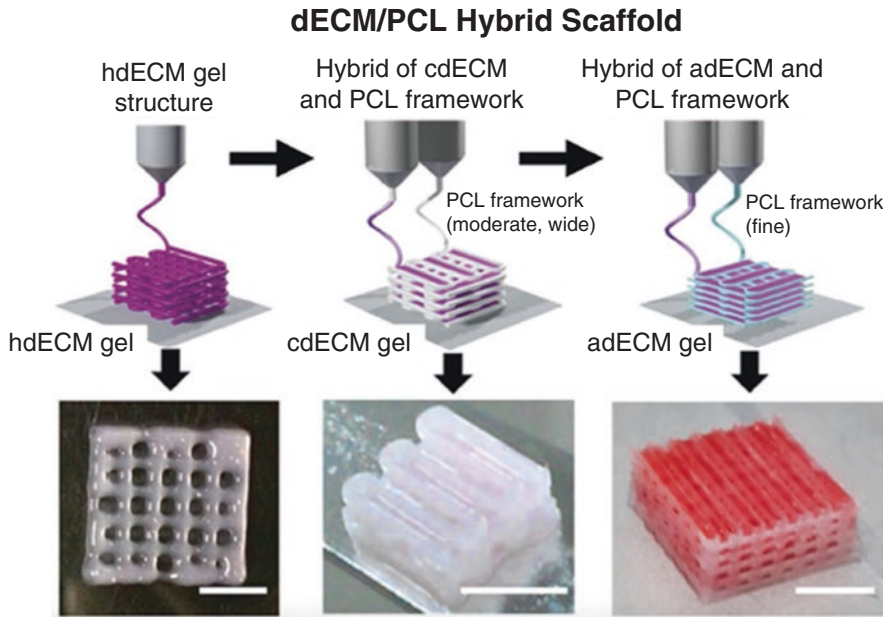
**Fig. 12.4** Fabrication processes for an endothelialized myocardium construct using 3D bioprinting technique. Step 1: bioprinting of an endothelialized cells embedded fibrous structure. Step 2: vascularisation of the endothelialized structure for cellular interactions. Step 3: seeding

of endothelialized scaffold with cardiomyocytes. Step 4: formation of endothelialized myocardium with physiological relevance that structurally resembled the native myocardium [172, 173]. (Reprinted with permission from Elsevier)

nozzle continuously dispensed calcium chloride until the extruded strut was fully polymerized. After endothelialization of the tissue construct by the self-assembly of endothelial cells, viability of the cardiomyocyte-seeded construct was evaluated and reported to exhibit cardiac maturation

and sarcomeric bandings that are necessary for proper cardiac contractility [172, 173].

Decellularized extracellular matrices of whole organs have been shown to have great potential to provide instructional cues to cells to achieve a proper phenotype. Myocardial-

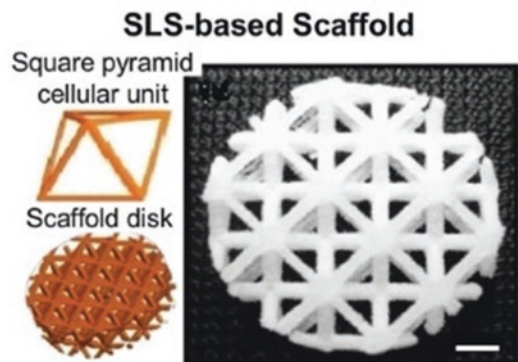


**Fig. 12.5** Three-dimensional multi-bioprinting of patient-specific decellularized bioink within a PCL polymeric framework [107]. Abbreviations: decellularized extracellular matrix (dECM), adipose decellularized

extracellular matrix (adECM), cartilage decellularized extracellular matrix (cdECM), heart decellularized extracellular matrix (hdECM). (Reprinted with permission from Springer Nature)

based bioinks that were derived from decellularized ECMs of heart tissue have been developed, which were simultaneously printed with a PCL polymeric framework using a multi-head bioprinting system (Fig. 12.5). The platform enabled the 3D bioprinting of patient-specific tissue constructs using a mixture of dECMs and myoblasts. The cardiogenic differentiation of myoblasts and long-term survival and function of the constructs were achieved after 14 days of cell culture. This study provided promising advances in cell-personalized treatment via the use of patient-specific dECMs [107].

A selective laser sintering (SLS) technique was also used to create a porous PCL scaffold with square pyramid-shaped cellular sub units (Fig. 12.6). The PCL samples yielded ~89% of a strain-sintered structure with tensile stiffness of ~0.43 MPa, surface roughness of ~34  $\mu\text{m}$ , and porosity of ~48%. The functional controlled porosity and efficient mass transport of the pyramid units were attributed to the mechanical properties of the 3D scaffolds during the fabrication process. The findings revealed the high



**Fig. 12.6** Three-dimensional scaffold with square pyramid cellular shape subunits fabricated using selective laser sintering [167]. (Reprinted with permission from Elsevier)

cell viability of seeded myoblasts after 21 days of culture [167].

### 12.4.1.2 Three-Dimensional Printing of Heart Valves

Valvular heart diseases, also called cardiovascular aortic heart disease (CAVD), are among the major causes of death worldwide. To date, the

only treatment option for severe CAVD is surgical valve replacement. Because of a dearth of donors, mechanical valves and bioprosthetic heart valves are mainly used for heart valve replacement surgery [55, 171]. These strategies have advantages and disadvantages. For example, mechanical valves are mechanically strong with high durability than biological valves. However, the application of mechanical valves is limited by reported cases of hemorrhage and thromboembolism; thus, they require life time treatment with anticoagulants [16]. Biological valves that are made from either an allogenic or xenogenic tissue source requires no life time administration of anticoagulants by patient, but they have shorter durability because of degeneration, calcification, and fibrosis, which may cause immunogenic complications [18, 135].

To overcome these limitations, tissue engineering-based heart valves have emerged as promising candidates for mitigating the need for long-term medication and ameliorate the hemodynamic properties of the replacement valve. Notably, the predominant function of heart valves is to maintain unidirectional blood flow through cyclic opening and closing during cardiac systole and diastole. The following desirable characteristics must be manifest for artificial heart valves: (i) minimal regurgitation of blood upstream, (ii) low transvalvular pressure gradient, (iii) minimal thrombogenic response, and (iv) high capacity to repair damaged tissue [59, 101].

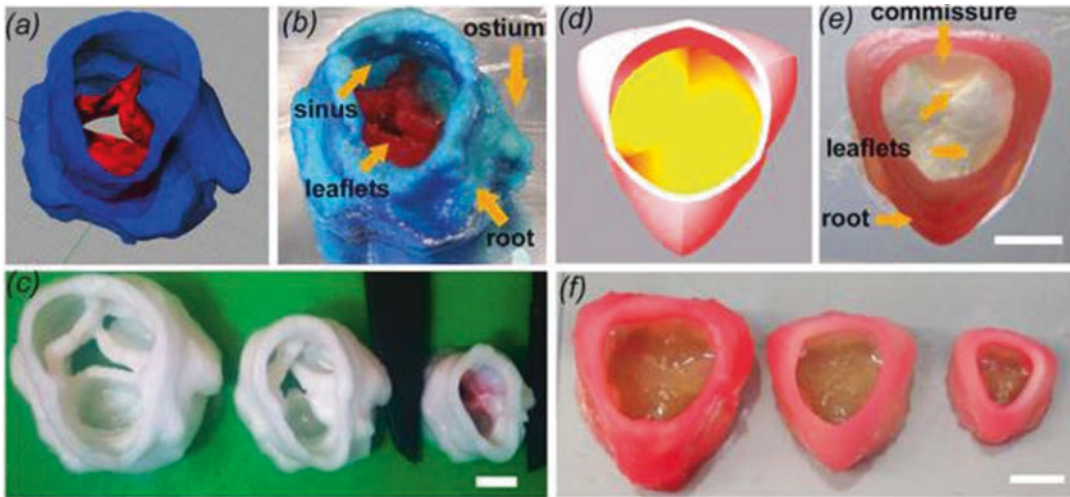
Three-dimensional printing-based tissue engineering technology has been used to improve the outcome of tissue-engineered heart valves because of its potential to fabricate patient-specific heart valves with anatomical geometry and microstructural complexity that can allow intrinsic biomechanical and hemodynamic functions [101]. Schaefermeier et al. employed an STL silicone-based model to physiologically design a 3D heart valve scaffold that resembled the complex natural anatomical structure of a human aortic homograft using thermoplastic poly-4-hydroxybutyrate (P4HB) polymer [125]. The trileaflet heart valve, which contained the sinus of Valsalva, was fabricated without any suture or stent. The valve scaffold had shape

fidelity of  $3 \pm 4\%$  compared with the homograft. Although mild stenosis and regurgitation were observed in the valve scaffold without suture, the avoidance of the leaflet suture improved the hemodynamic function of the heart valve constructs [128, 141].

The Butcher group at Cornell University worked extensively on the 3D printing of tissue-engineered heart valves [35, 36, 59]. An extrusion-based printer (Fab@Home Model 1) was used to print a heterogeneous aortic valve structure using composite hydrogels of PEGDA and alginate (Fig. 12.7). Two aortic valve geometries (i.e., an axisymmetric aortic valve that was generated in SolidWorks and micro-CT-scanned porcine aortic valve translated into printable STL geometries) were created for printing. The suitable extrusion viscosity for the PEGDA hydrogel during printing was achieved by adding 10–15% w/v alginate to PEGDA while NaCl salt was used to maintain the pH of the hydrogel. The mechanical properties of the PEGDA hydrogels were tuned from 20 to 300 kPa by varying the weight ratios of different molecular weight PEGDA blends.

Based on the PEGDA blend formulation, heterogeneous valves with different internal diameters (12–18 mm) were printed with rigid hydrogels with mechanical stiffness of  $\sim 75$  kPa for the root and soft hydrogels with mechanical stiffness of  $\sim 5$  kPa for leaflets. Shape fidelity was evaluated by micro-CT, and the larger printed valve was found to have greater shape fidelity. Porcine aortic valve interstitial cells (PAVICs) exhibited spread morphology and good viability ( $\sim 100\%$ ) over 21 days of culture on 3D-printed heart valve scaffolds. The study reported that 3D hydrogel printing has the potential to fabricate anatomical heterogeneous valve conduits that support cell engraftment [59].

The printability of methacrylated hydrogels from a mixture of gelatin and HA with a human aortic valvular interstitial cells (HAVICs) suspension was also investigated [36]. The remodeling process of the printed hydrogels was achieved by the deposition of ECMs (collagens and glycosaminoglycans) that were derived from the HAVICs. The cell phenotype was influenced by the stiffness of these printed hydrogels, in which softer hydrogels induced fibroblastic behavior in the HAVICs.



**Fig. 12.7** Printing heterogeneous valve and scaled valve constructs. (a) Porcine aortic valve model was (b) printed, where root was formed with 700 MW PEG-DA hydrogel while the leaflets were formed with 700/8000 MW PEG-DA hydrogels. Key features such as the coronary ostium and sinuses were present (c) Scaffolds were

printed with 700 MW PEG-DA at different scale for fidelity analysis, where the inner diameters (ID) were 22, 17, and 12 mm. (d) Axisymmetric valve model was (e) printed with two blends of hydrogels (f) and at 22, 17, and 12 mm ID [59]. Scale bar = 1 cm. (Reprinted with permission from IOP Publishing)

Similarly, Butcher's group demonstrated the potential of 3D printing technology to fabricate mechanically robust living trileaflet heart valves using valvular cells [35]. The 3D extrusion-based Fab@Home Model 1 printer was employed to print an aortic heart valve using alginate/gelatin hydrogel mixtures. A micro-CT image of a porcine aortic valve was translated into an STL file geometry, which was used to print a hydrogel valve. To print the hydrogel valve, two different cells (smooth muscle cells [SMCs] and PAVICs) were separately mixed with the alginate/gelatin gel at a density of  $1 \times 10^7$  cells/ml. The SMCs were encapsulated into the aortic root sinus region while PAVICs were encapsulated in the aortic valve leaflet. These two types of cells had high viability ( $\sim 81\%$  for SMCs and  $\sim 83\%$  for PAVICs). Additionally, the cell-laden hydrogel valves exhibited better mechanical integrity than the acellular heart valves after printing.

Researchers at Kosair Children's Hospital in Louisville, Kentucky, printed a 3D whole-heart model using biocompatible synthetic material. The printed heart was reportedly had anisotropic mechanical features similar to the paediatric heart and serve as a replacement for the defective heart

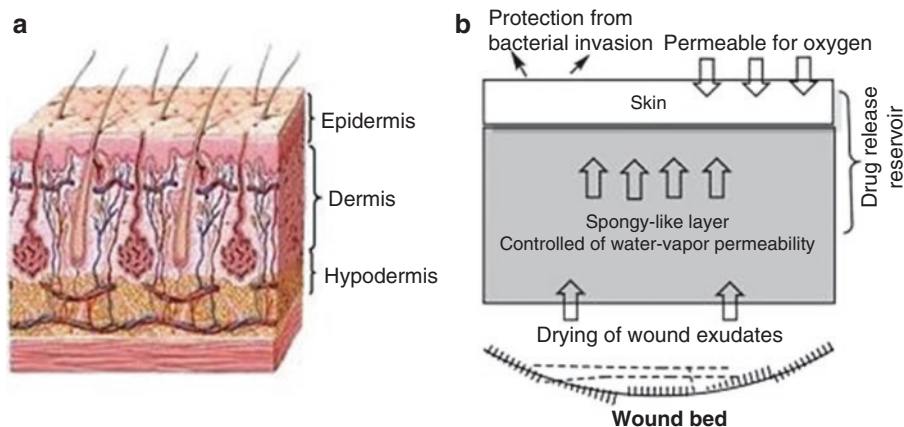
in the infant. However, the heart did not exhibit the tenacity to remodel as the child grew [65].

Although 3D printing has been exploited to develop a complex geometry of a heart valve with good mechanical integrity and excellent cell growth, the challenges of vascularizing the structure of engineered heart valve tissue constructs for proper oxygen/nutrient delivery have not yet been addressed.

## 12.5 Advanced Engineering of Hydrogels for Wound Dressing and Healing

### 12.5.1 Skin

Skin is the principle exterior defense system, which protects inner body systems from microorganism attack, contamination, infection, and the external environment. Skin plays a vital role in regulating the temperature of the body and transmitting external environment information, such as pain and heat [67]. **Skin** is composed of three main layers: epidermis, dermis, and hypodermis (subcutaneous tissue). The diagnostic structural



**Fig. 12.8** Schematic representation of (a) normal skin structure and (b) design of an ideal wound dressing membrane [67]. (Reprinted with permission from Elsevier)

details of normal human skin are shown in Fig. 12.8. The epidermis is a vascular, and cells are shed and renewed every 4–6 weeks. The epidermis forms an external barrier that provides the function of protection and waterproofing. **The dermis**, the living layer of skin, is supportive connective tissue, which is rich in fibers and makes the skin elastic and strong. The epidermis and dermis are clearly separated but firmly anchored together by conical papillae. **Subcutaneous tissue** is a fat cell sliding layer that performs transition and storage functions of water and fat.

### 12.5.2 Wounds and Wound Healing

Wounds are a disruption of the continuity of the epithelial lining of the skin or mucosa that results from physical or thermal damage. When wounds occur, a set of complex biochemical events occur in a closely orchestrated cascade to repair the damage. Wound healing or wound repair is the body's natural process of regenerating dermal and epidermal tissue. According to the duration and nature of the healing process, the wound is categorized as acute or chronic [120, 143]. Traumatic wounds, surgical wounds, and dermabrasion are considered acute wounds. They heal within a predictable and expected time frame, usually 8–12 weeks, depending on the size, depth, and extent of damage to the epidermis and

dermis [117, 129]. Venous ulcers, arterial ulcers, pressure ulcers, and perforating diabetic foot ulcers result in chronic wounds. Chronic wounds require a longer healing time (up to months) and leave serious scars. Some factors delay the healing of chronic wounds, such as diabetes, dryness of the wound, and infections [10].

The wound healing process can be divided into three or four distinct phases. The three-phase concept includes inflammatory, fibroblastic, and maturation [49], also described as inflammation, proliferation, and remodeling [89]. The four-phase concept includes the hemostasis phase (immediately after injury), inflammatory phase (shortly after injury to tissue during which swelling occurs), proliferation phase (when new tissues and blood vessels are formed), and remodeling phase (when the remodeling of new tissue occurs; [25, 28, 33, 63, 144, 150]). In the three-phase concept, the hemostasis phase is contained within the inflammatory phase. These healing phases are affected by specific and individual factors (e.g., nutrition, patient age, disease, and size, depth, and causation of the wound; [114]).

### 12.5.3 Wound Dressing

A dressing can be a sterile pad or compress that is applied to the wound to promote healing and protect it from further damage. Rapid and proper

healing is important for the treatment of wounds. In cases of severe and large amounts of skin loss, immediate coverage of the wound surface with a dressing is needed. The selection of dressing should be based on its ability. One or more of the following characteristics of the wound dressing should be ensured [30, 158]. (1) The dressing material should be able to absorb the liquid that exudes from the wounded area. (2) The dressing material should permit water evaporation at a certain rate and allow no microbial transport. (3) The material should enhance epidermal migration and promote angiogenesis and connective tissue synthesis. (4) The material should maintain a moist environment at the wound/dressing interface. (5) The material should provide thermal insulation and mechanical protection for the body. (6) The material should allow gas exchange between wounded tissue and the environment. (7) The material should be non-adherent to the wound and easily removed without trauma. (8) The material should provide some debridement action to enhance leucocyte migration and remove dead tissue and/or foreign particles.

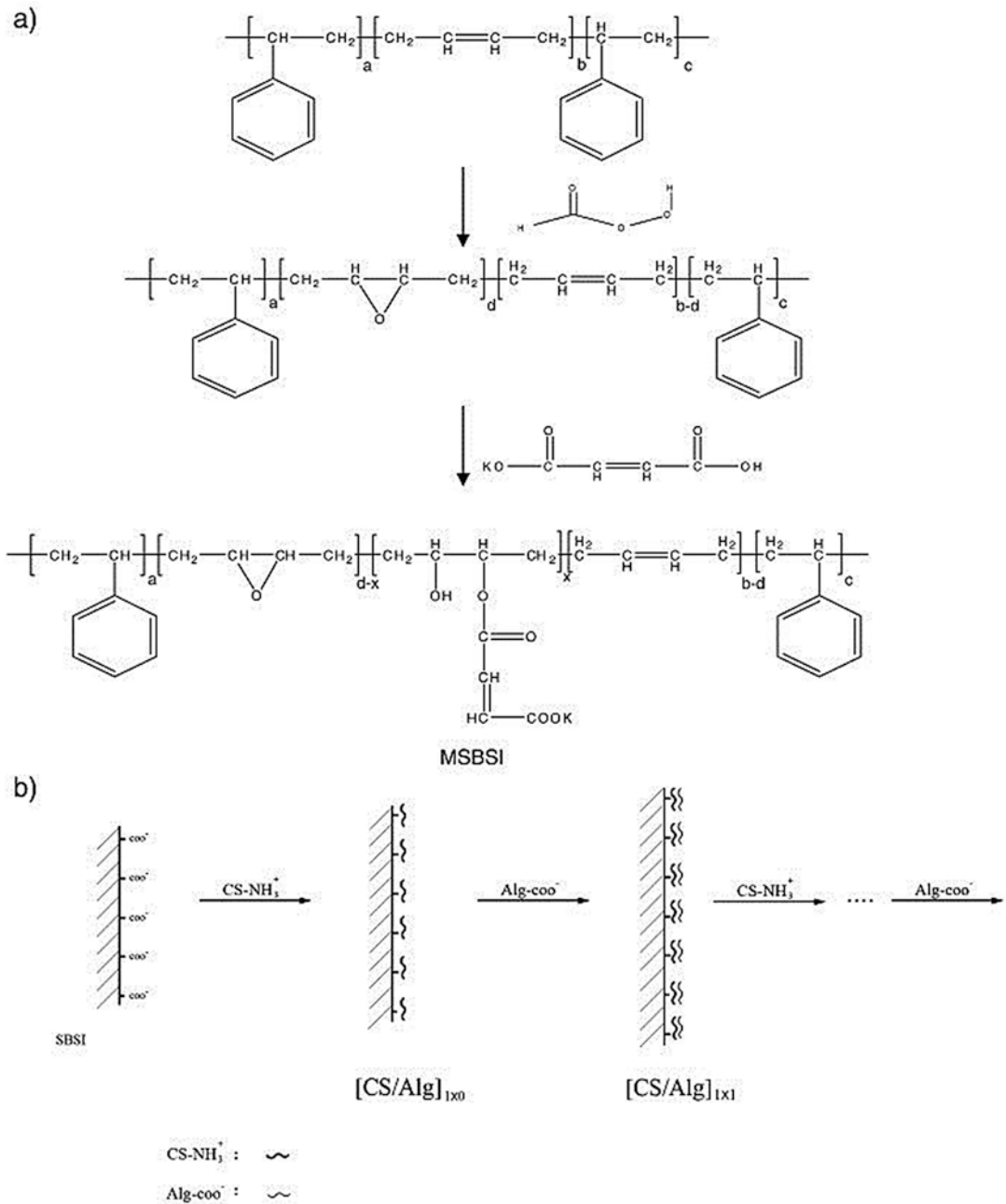
The dressing materials that are used for wounds and burns can be classified into traditional, biological, and artificial dressings [140]. Traditional wound dressing products, including gauze, lint, plaster, bandages (natural or synthetic), and cotton wool, are dry and used as primary or secondary dressings to protect the wound from contamination [10]. Since traditional dressings fail to provide a moist environment for the wound, they have been replaced by modern dressings that have more advanced formulations [10]. Modern wound dressings have been developed to facilitate the function of the wound rather than just cover it. Modern wound dressings are usually based on synthetic polymers and are classified as passive, interactive, and bioactive products [28, 63, 119, 142].

Biological “auto-grafting” dressings consist of normal and fresh skin that is donated from foreign bodies (e.g., humans, animals, or cadavers). These materials consist of collagen-type struc-

tures, including elastin and lipids. They are the most suitable materials for the complete healing of deep, chronic wounds and burns, but one drawback of these materials is insufficient donor tissue for deep or large wounds [71].

Artificial dressings are fabricated from synthetic materials, such as non biological materials and polymers, that are not found in the constituents of skin [149]. In the mid 1980s, polyurethane (PU) foams, hydrocolloids, and iodine-containing gels were introduced as wound dressings that have important characteristics that provide moisture and absorbing fluids. During the mid-1990s, synthetic wound dressings expanded into various groups of products, including hydrogels, hydrocolloids, alginates, synthetic foam dressings, silicone meshes, tissue adhesives, vapor-permeable adhesive films, and silver/collagen-containing dressings [30].

Some commercial products of PU are available for the application of wound dressings. For example, the commercial products OpSite<sup>®</sup> and Tegaderm<sup>®</sup> are a sterile, semipermeable film of PU that is coated with acrylic adhesive. They are transparent to allow wound checks and suitable for shallow wounds with low exudates. The commercial products Allevyn<sup>®</sup> and Lyofoam<sup>®</sup> are PU or silicone foams. They are designed to absorb large amounts of exudates [155]. Polyurethane and styrene-butadiene-styrene block copolymers (SBS) are well-known thermoplastic elastomers that have gained considerable attention and applications in recent years. To enhance the performance and application of SBS for wound dressings, the SBS membrane has been modified with epoxidation, followed by a ring opening reaction with potassium hydrogen maleate to prepare the maleate SBS ionomer membrane that contains a COO<sup>-</sup> group. The maleate SBS ionomer membrane was further modified with an LbL self-assembly deposition technique. The different chitosan/alginate multilayer films were deposited on the maleate SBS ionomer membrane surface to achieve the tri-steps modified SBS membrane (Fig. 12.9; [155, 158]). The tri-steps modified



**Fig. 12.9** Three-step modification of SBS: (a) Preparation of MSBSI, (b) Preparation with LbL technique [155]. (Reprinted with permission from Elsevier)



SBS membranes are sterile and semipermeable, have bactericidal activity, and are transparent to allow wound checks; they can be considered appropriate for shallow wounds with low exudates [155].

#### 12.5.4 Hydrogels for Wound Dressings

Various synthetic and naturally derived materials may be used as hydrogels [157]. Poly(ethylene oxide), poly(vinyl alcohol), poly(hydroxyethyl methacrylate), poly(ethylene glycol dimethacrylate), poly(acrylic acid), and their derivatives are synthetic hydrogels. Agarose, alginate, chitosan, collagen, gelatin, and HA are naturally derived hydrogels [157]. Hydrogels are similar to those of human tissues, possess excellent tissue compatibility, and have become attractive to the field of biomaterials [139]. Hydrogels have the following basic properties. (1) Hydrogels have a high water content that may absorb from 10–20% (an arbitrary lower limit) up to thousands of times their dry weight in water, helping granulated tissues and epithelia in a moist environment. (2) With soft elastic properties, hydrogels provide easy application and removal after wounds are healed, without any damage. (3) Because of the soothing and cooling effect, the temperature of cutaneous wounds can be decreased by hydrogels. Hydrogels are often used for dry chronic wounds, necrotic wounds, pressure ulcers, and burn wounds [30]. Some commercial hydrogel dressing materials have appeared on the market under brand names. For example, *Intrasite™ Gel* is a clear amorphous hydrogel that contains a modified carboxymethyl cellulose polymer, propylene glycol, and water. *NU-gel™* is a transparent hydroactive amorphous gel that contains sodium alginate that gently and effectively debrides necrotic tissue and fibrinous slough. *Aquaform™* contains calcium alginate that rehydrates dry or necrotic tissue to help facilitate autolytic debridement and prevent low exuding wounds from drying out. *Tegagel®* is classified as a calcium alginate dressing and made from the calcium salt of alginic acid.

*Tegagel* may be used for the management of a variety of exuding wounds, including leg ulcers, pressure sores, and ischemic and diabetic wounds. *Geliper™* hydrogel composed of two interlaced networks, one of polyacrylamide and one of agar, provides optimal physiological conditions for wound healing [52, 73].

Hydrogels with a single component have low mechanical strength, and recent trends involve the generation of composite or hybrid hydrogel membranes to meet typical wound dressing requirements. For example, an hydroxyl-terminated polybutadiene (HTPB)-based PU solution was prepared, and then the PU solution was modified with *N*-isopropyl acrylamide by ultraviolet radiation without degassing to achieve a thermo-sensitive membrane (PUNIPAAm). Chitosan was then impregnated onto the PUNIPAAm surface and treated by freeze-drying to create chitosan-containing PUNIPAAm (PUNIPAAm-chi). The results showed that these thermo-sensitive PUNIPAAm membranes had low cytotoxicity and could support cell adhesion and growth. Based on antibacterial ability and water vapor transmission rates, the permeance and permeability of the various PUNIPAAm-chi membranes are comparable to commercial products, and PUNIPAAm-chi may be considered for wound dressings [161, 162]. A tri-layer membrane as artificial skin for extensive burn injury was developed by Lin [84]. The tri-layer wound dressing was successfully prepared by subsequent high-energy plasma treatment,  $\gamma$ -ray irradiation, ultraviolet light exposure, and lyophilization. The first layer was a 3D tri-copolymer sponge of gelatin/hyaluronan/chondroitin-6-sulfate with 70% porosity and a 20–100  $\mu\text{m}$  pore size. The second layer was a so-called auto-stripped layer that was composed of poly-*N*-isopropylacrylamide (PNIPAAm). The third layer was composed of a polypropylene (PP) nonwoven fabric, which provided an open structure for exudate drainage that reduced the risk of secondary infection. The modification of PP for wound dressings was also studied by Yang [156, 160]. Based on thermo-sensitivity and antibacterial ability, the modified nonwoven fabric could be considered for wound dressings. As

shown in the review by Kamoun [67], natural polymers and their derivatives, such as sodium alginate, chitosan, dextran, *N*-*O*-carboxymethyl chitosan, hydroxyethyl starch, glucan, HA, poly-*N*-acetylglucosamine, silk, and gelatin, have been used as hydrogel membranes for wound dressings or skin substitutes.

---

## 12.6 Advanced Engineering of Stimulus-Responsive Hydrogels for Biomedical Applications

### 12.6.1 Stimulus-Responsive Hydrogels

Stimulus-responsive hydrogels are generally referred to as “environmentally sensitive”, “smart,” or “intelligent” hydrogels because of their ability to receive, transmit, or process a stimulus and respond by producing a useful effect [54]. These hydrogels can undergo dramatic phase transitions or rapid physicochemical changes under the influence of minimal and specific external stimuli [42, 61, 83].

Physical stimuli can include light, pressure, temperature, electric or magnetic fields, mechanical stress, and radiation energy from various sources, which affect energy level transitions and change molecular interactions at critical onset points. Chemical stimuli, such as pH, ionic factors, and chemical agents, can influence interactions between polymer chains and solvents and between polymer chains at the molecular level.

The combinatory effect of two or more stimulus-responsive mechanisms into one hydrogel system gives rise to a special class of hydrogels, called dual-responsive hydrogels [87]. Dual-responsive hydrogels can respond simultaneously and independently to more than one external stimulus. For example, poly(*N*-isopropylacrylamide-co-propylacrylic acid) and copolymers of poly(*N*-isopropylacrylamide-co-propylacrylic acid) were reported to exhibit a sharp response to minimal signals of both pH and temperature [41, 122, 168]. Biochemical stimuli

involve responses to enzymes, antigens, ligands, and other biochemical agents [47].

Stimulus-responsive hydrogels have been proposed for numerous biomedical applications, ranging from drug delivery to tissue engineering because of their quick responsiveness and active targeting properties [70, 75, 80, 104].

#### 12.6.1.1 Temperature-Responsive Hydrogels

Temperature-responsive hydrogels are prepared from polymers that exhibit a temperature-induced transition from a state of preferential polymer-water interaction to a state of preferential polymer-polymer interaction [48]. At a critical solution temperature, temperature-responsive polymers exhibit a phase transition between polymer and solution, depending on the polymer chain composition [153].

For example, poly(*N*-isopropylacrylamide) (PNIPAM), poly(vinyl methylether) (PVME), and poly(*N*-vinylcaprolactam) (PNVC) have shown to possess lower critical solution temperature (LCST) which invariably make them to undergo phase separation in water [153]. The side chains of the aforementioned polymers contain both superhydrophilic and superhydrophobic groups. Therefore, these polymers have an inherent ability to simultaneously switch between contracted and expanded states (superhydrophobic or superhydrophilic; [80]). At a temperature below the LCST, water molecules interact with the polymer super hydrophilic groups via hydrogen bonds, thereby causing expansion in the hydrogel. However, at the temperature above LCST, hydrophobicity of the polymer interacting chains depletes the hydrogen bond formations, which consequently expel water and caused polymer network contractions [126, 153].

Shape memory gels have been used for surgical procedures that require automatic healing for mechanical deformations and rapid closures for sutures. The potential of thermal-responsive gels to recall their initial structure upon a change in temperature after being deformed make them suitable for this application. Shape memory gels were prepared from acrylic acid and stearyl acrylate [105]. The polymer experienced change in

shape as the temperature changes. Such polymer assumed a deformed and a stable state in alcohol upon cooling. At high temperature, there is a switch in polymer configuration from temporary deformed state to original geometry.

### 12.6.1.2 pH-Responsive Hydrogels

Another stimulus-responsive hydrogel that has been widely studied is pH-responsive polymer. Upon their response to environmental changes in pH, the ionizable pendant of the polymer chain can accept or donate protons. The ionization level of the pendant group dramatically changes around the  $pK_a$  and  $pK_b$ , causing alterations of the water-holding capacity of polymer chains [87]. There are two types of pH-responsive hydrogels: weak polyacids and weak polybases. The typical example of weak polyacids is poly(acrylic acid), which accept protons at low pH via carboxylic groups and later release protons above its  $pK_a$ , thereby leading to a sudden increase in the hydrodynamic volume and swelling capability of the hydrogel [19]. By contrast, in weak polybases, such as poly(*N,N'*-diethylaminoethyl methacrylate), ionization of the amine pendant group occurs at critical pH below  $pK_b$ , resulting in hydrophilic swelling of the hydrogel through more electrostatic repulsive forces [19, 87].

A pH-responsive hydrogel was developed for drug delivery to treat colon inflammation. The hydrogel contained azoaromatic moieties as the cross-linker species, which improved the functionality of the entire hydrogel chain and also moderated the release profile of the target drug. The hydrogels resisted swelling in both the stomach and intestine because of the presence of cross-linker species. Only in the colon, cross-linker species triggered the formation of azoreductase enzymes by micro-flora that resided in the colon, which degraded the cross-linkers species, thereby allowing fast release of the entrapped drugs [44].

Polysaccharide-based pH-responsive hydrogels have gained considerable attention as potential candidates for various biomedical applications ranging from wound dressing to drug delivery system. To this end, chitosan have been proposed

as nanofilm to encapsulate a prefabricated poly(lactic acid) scaffold and as well hydrophilic analogues for the uptake of ketoprofen. Such hybrid materials can permit the delivery of relevant bioactive agents and facilitate cellular interactions and differentiation that are necessary to therapeutically induce the formation of new tissue [112].

### 12.6.1.3 Glucose-Responsive Hydrogels

The treatment of diabetes involves periodical checking of blood sugar level and administration to compensate for any shortage observed [178]. However, multiple subcutaneous insulin injections reduce patient compliance. Recently, smart insulin delivery systems have been developed to shorten the injection time, which can homeostatically regulate the level of blood glucose [124, 175–177]. Therefore, glucose-sensitive hydrogels have gained considerable attention in the development of self-regulated insulin systems for the controlled regulation of blood glucose levels [92]. Glucose-responsive polymeric systems are typically based on the enzymatic oxidation of glucose by glucose oxidase (GOD), the binding of glucose with concanavalin A (ConA), or reversible covalent bond formation between glucose and boronic acids.

Glucose oxidase is the most widely used enzyme in the glucose-sensitive drug delivery system (DDS) because it oxidizes glucose into gluconic acid. The enzymatic action of GOD on glucose is highly specific, especially when GOD is incorporated with a pH-responsive polymer, generating gluconic acid and  $H_2O_2$ , which change the pH in the polymer microenvironment [32, 174]. Thus, the pH change that is triggered by GOD induces a swelling-shrinkage process in hydrogel matrices that contain insulin. Therefore, pH-sensitive hydrogels that contain glucose oxidase can be a therapeutic strategy for diabetic patients to regulate insulin release in response to glucose concentrations [85]. Peppas and colleagues synthesized poly(methacrylic acid) (PMAA)-graft-ethylene glycol-based glucose-responsive hydrogels in the presence of GOD. The polymer was reported to be swollen at

neutral and high temperature due to repulsive force acting within the negatively charged methacrylate units of the polymer. Furthermore, the reduction of pH triggers GOD to oxidize glucose, which consequently led to collapse of the gel. Similarly, the gel responsiveness was attributed to  $\pi - \pi$  interactions between the carboxyl and ether groups of the ethylene glycol units via hydrogen bond [56].

Lectins are multivalent proteins that tend to bind carbohydrates and interact with glycopolymers on the cell surface, thus causing the aggregation of cells. However, the introduction of competitively binding glucose prevents cell aggregation. The tenacity of lectin to bind glucose provides a platform for fabricating glucose-sensitive systems that are subjected to glucose regulation [92]. Tetradentate ConA-based lectin has been suitably employed for this purpose. It is noteworthy that conA-glycogen gel preferential bind ConA with free glucose which further cause gel-sol transitions [20].

Complexation behavior between phenylboronic acid and a polyol compound has provided useful insights into construction of a special glucose-responsive material. Hisamitsu et al. have synthesized a glucose-responsive hydrogel composed of terpolymers of 3-acrylamidophenylboronic acid (APBA), (*N,N*-

dimethylamino) propylacrylamide (DMA), and DMA. At physiological pH, there was complex formation between boronic acid groups that are present in the terpolymer and poly(vinyl alcohol) (PVA; [58]). The competitive displacement of PVA at high glucose concentrations led to a decrease in cross-link density and caused swelling of the hydrogel and the release of insulin (Fig. 12.10).

#### 12.6.1.4 Enzyme-Responsive Hydrogels

Enzyme-responsive materials are typically composed of an enzyme-sensitive substrate and another component that directs or controls interactions that lead to macroscopic transitions. Physiological changes that may occur as a result of catalytic actions of the enzyme on the substrate include the swelling/deswelling of gels, the transformation of surface properties, or changes in supramolecular architecture [147]. These properties allow enzyme-sensitive hydrogels to be used as enzyme sensors and enzyme-sensitive DDSs. For example, the microflora that reside in the colon produce microbial enzymes. Azoreductases are predominately used for colon-specific drug delivery. Azo-aromatic bonds have been used as cross-linker species to produce azoreductase; an enzyme-sensitive hydrogel

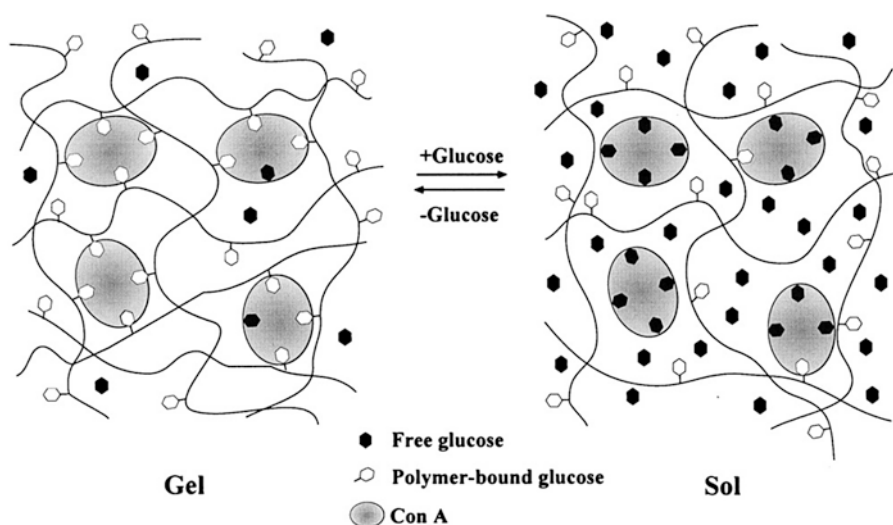


Fig. 12.10 Sol-gel transition of a glucose-sensitive hydrogel [115]. (Reprinted with permission from Elsevier)

which can serve as colon target drug delivery sensors.

The hydrogels that were based on biocompatible copolymers of *N,N*-dimethylacrylamide (DMAAm) and *tert*-butylacrylamide (BAAm) exhibited improvements in mechanical properties and cross-linking agents that contained azoaromatic bonds. The susceptibility of the hydrogel to low swelling in the stomach (at low pH) conferred a protective shield for protein drugs against digestion by proteolytic enzymes. However, changes in pH triggered the ionization of carboxylic acid groups, which caused hydrogel swelling. The enzymatic activity of azoreductases toward the cross-linker spices in the hydrogel matrix degraded to release the protein drugs [44, 165].

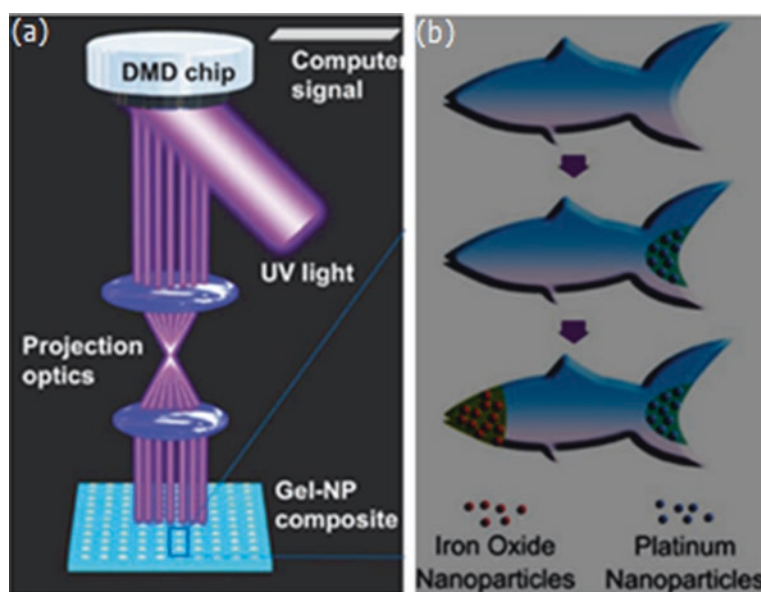
### 12.6.2 Engineered Smart/Intelligent/Stimulus-Responsive Hydrogels: Case Reports

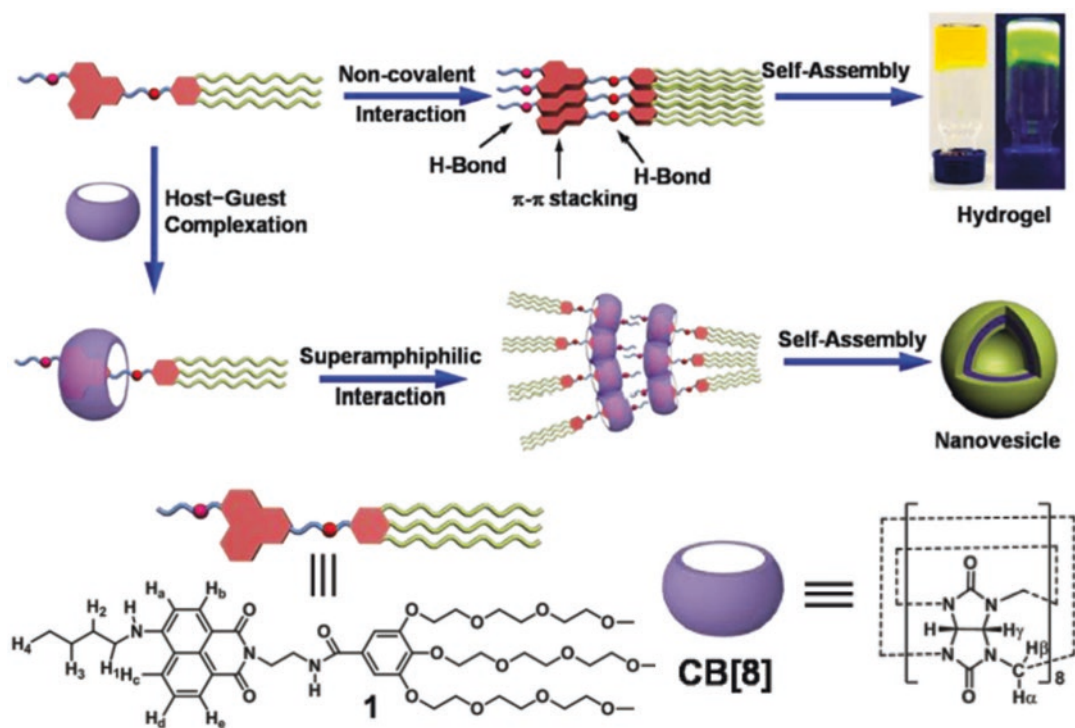
A functionalized smart artificial microfish with diverse biomimetic structures and locomotive capabilities was fabricated using advanced 3D printing technology, called microscale continuous optical printing ( $\mu$ COP; Fig. 12.11). With the

$\mu$ COP system, a uniform arrays ( $\sim 30\mu\text{m}$  thickness,  $\sim 120\mu\text{m}$  length) of complex 3D microfish were fabricated using PEGDA (MW = 700 Da) at a concentration (40 wt%) in water with functionalized nanoparticles in the presence of 1 wt% lithium phenyl-2,4,6-trimethylbenzoylphosphinate as the photoinitiator [180]. Pt nanoparticles were encapsulated in PEGDA for the tail of microfish, which facilitated self-propulsion of the microswimmer's tail through the catalytic decomposition of the peroxide fuel. PEGDA-containing magnetic  $\text{Fe}_3\text{O}_4$  nanoparticles were encapsulated and polymerized at the head portion of the fish, which guided the motion of the microfish. Energy-dispersive X-ray (EDX) spectroscopy data supported localization of the functional nanoparticles with high accuracy at specific positions in the microfish. Functional polydiacetylene (PDA) toxin-neutralizing nanoparticles were also integrated into the hydrogel matrix of the fish body and showed good detoxification potential.

A new class of stimulus-responsive drugs was fabricated using the self-assembly method (Fig. 12.12). The self-assembly of a naphthalimide derivative formed a functionalized hydrogel with a low critical gelation concentration driven by  $\pi - \pi$  and multiple hydrogen

**Fig. 12.11** (a) Schematic illustration of the  $\mu$ COP method to fabricate microfish. (b) Schematic illustration of taxis-induced microfish by functionalized Pt nanoparticle (at the tail portion of the fish and  $\text{Fe}_3\text{O}_4$  nanoparticle (at the fish head) for catalytic propulsion and magnetic control respectively [180]. (Reprinted with permission from John Wiley & Sons, Inc)





**Fig. 12.12** Diagrammatic representations of hydrogel and nanovesicles formation achieved by  $\pi-\pi$  hydrogen

bonding interactions with functionalized CB and derivative of naphthalimide [154]. (Reprinted with permission from John Wiley & Sons, Inc)

bonding (i.e., noncovalent) interactions in aqueous solution. The super amphiphilic interaction of a host-guest naphthalimide derivative and cucurbit[n]uril(CB[n]) led to the self-assembly formation of nanovesicles with diameters of 80–200 nm. Various spectroscopic techniques and molecular dynamics (MD) simulations confirmed self-assembly of the hydrogel and nanovesicles. The drug nanocarriers presented cellular –inducing efficacy and drug-loading tenacity as confirmed by confocal laser scanning microscope (CLSM) and MTT experiments. The cytotoxicity assay showed that DOX-loaded nanocarriers possessed high anticancer effects [154].

Novel photo responsive capsules that were composed of polyelectrolyte/carbon nanotube composites were prepared. Water-solubilized single-walled carbon nano tube (SWCNT) microcapsules were fabricated using LbL and template-assisted methods and used as polyanion and

near-infrared (NIR) absorbers [123]. The anticancer drug was loaded into the SWCNT-embedded hollow capsules, and the latter was irradiated with a NIR laser beam. Similarly, therapeutic disulfide cross-linked poly(methacrylic acid) (PMAA) were also developed by LbL assembly of complexes formed by poly(vinyl pyrrolidone) and thiol based-PMAA on the silica particle templates, which in turn control the rate of degradation in the polymer capsule [7].

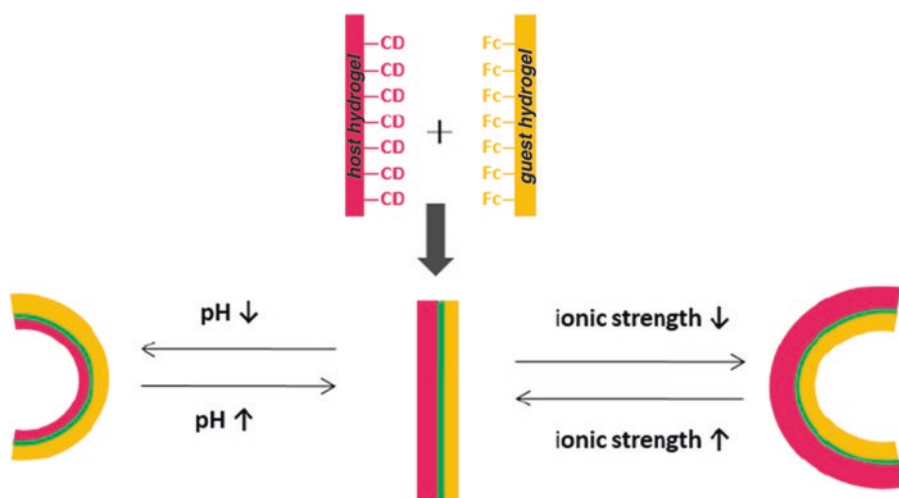
Controlled drug delivery systems (DDS) have drawn considerable attention because of its safety and enhanced therapeutic efficiency of drugs actively target at a delivery sites. A controlled DDS was prepared by integrating 1,6-hexanediol diacrylate (HDDA) microcapsule with copolymer poly(N-isopropylacrylamide-co-methacrylic acid) (poly(NIPAAm-co-MAA)). The nanoporous HDDA core-shell capsule were fabricated based on inkjet printing combined with an ultraviolet polymerization process. The HDDA

particles were printed at optimal concentration of 2.5 wt% in the presence of Photocure-1173 as the initiator [164]. The thermo-responsive poly(NIPAAm-co-MAA) copolymer was grafted onto the surface of HDDA microcapsules by free radical-initiated polymerization. The copolymerization of an appropriate molar ratio of MAA (methacrylic acid) adjusted the LCST of the thermos-responsive copolymer to a physiological temperature. With temperature changes around the LCST ( $38^{\circ}\text{C}$ ), the particles underwent reversible change swell-collapsed conformations. Because of this, the copolymer-modified nanopore served as a “retractable gate” for the controlled release of encapsulated drug molecules [164].

Micro-sized bovine serum albumin (BSA) protogel with pH responsive features were fabricated by polymerization of BSA monomers in LbL version using two-photon lithography. For the polymerization reaction, rose bengal serve as the photoinitiator [78]. Precise control of the swelling extent of BSA protogels and its programmable directionality that was tailored by two-photon lithography resulted in an inducible chiral structure (i.e., from achiral to chiral) and free-standing trap-like structures. The chiral center of the structures could be switched on or off upon changes in pH. Likewise, the programma-

ble changes in directional shape of the trap-like structures depended on changes in pH, which can act as microbotic arms to capture microobjects. The dynamic, shape-shifting, pH-responsive, free-standing BSA hydrogel can be used as a smart material for creating biomimetic, stimulus-responsive, chemo-mechanical micro actuators [78].

The combination of two or more hydrogel strips results in supramolecular interactions of hydrogel strips at interfaces. Smart pH-responsive hydrogel strips were fabricated through the macroscopic self-assembly of highly functionalized two different hydrogel strips (Fig. 12.13). The host-guest interactions between the strips provide strong adhesion required to form a laminate. Changes in pH caused swelling/deswelling of the hydrogel strip (Fig. 12.13). At low pH, the hydrogel strip de-swelled, causing the laminates to bend to the left side. At the initial pH, the bending action was recovered, and the laminate returned to the resting state. At lower ionic strength, the host hydrogel experienced a large extent of swelling, and the laminate bent toward the right side. The computational analysis showed that the designed 3D-responsive structures of smart hydrogels exhibited specific actuating behavior as a one-way flexible and torsional actuator after simulation [163].



**Fig. 12.13** Actuating behavior of the bi-hydrogel strip functionalized by  $\beta$ -cyclodextrin rings and adamantyl moieties [163]. (Reprinted with permission from SPIE Publications)

## 12.7 Conclusions and Future Perspectives

Novel hydrogel design and fabrication are of great interest because of their wide range of applications in various domains, such as biomedicine, tissue engineering, drug delivery, and wound dressings, among others. The aims are to construct hydrogel scaffolds with well-defined architectures, tunable porosity and pore sizes, excellent mechanical strength, and dynamic cues that are required to mimic the properties of native tissues and organ structures. Advanced engineering strategies have been used to gain spatiotemporal control over hydrogels through sophisticated chemistries and fabrication techniques [68].

Numerous advanced techniques have been used to design and fabricate highly functionalized hydrogel scaffolds for biomedical applications. For example, LbL assembly provides a tissue engineering construct with highly ordered structures for cell proliferation and differentiation [12]. Three-dimensional bioprinting offers superior resolution, enables the precise spatial distribution of cells and biomaterials within complex 3D structures, and accommodates large material versatility. Three-dimensionally printed constructs have shown tremendous potential to repair and regenerate damaged cardiac tissue and heart valves after myocardial ischemia. However, the vasculature of 3D-printed heart valve tissue constructs should be addressed in the future to achieve proper oxygen/nutrient delivery [4].

Various smart hydrogels that are responsive to external stimuli within a physiological range have been proposed for widespread biomedical applications [80]. The design parameters that are crucial for smart and biomimetic material fabrication and their potential application in biomedical fields were also discussed in this review. Smart hydrogels are often designed at the molecular level before considering the desired applications. Tailorable biodegradable moiety incorporated in the microstructure of smart polymers controllably minimized biodegradability of the polymer for short and long time applications [47]. Furthermore, the controlled polymerization process of smart and biomimetic hydrogels has led to the fabrication of smart materials with

well-defined macromolecular blocks and stimulus-responsive characteristics for drug delivery, diagnosis, and tissue engineering applications.

Overall, significant advances have been made in the fabrication of hydrogels for biomedical applications. However, there is limited availability or choice of hydrogel materials for clinical trials or applications. In the future, an increasing number of hydrogels with tunable mechanical properties and versatile functions will be developed for biomedical applications by employing advanced engineering techniques with novel material design.

---

## References

1. Ahmed EM (2015) Hydrogel: Preparation, characterization, and applications: A review. *J Adv Res* 6:105–121
2. Amano Y, Nishiguchi A, Matsusaki M, Iseoka H, Miyagawa S, Sawa Y, Seo M, Yamaguchi T, Akashi M (2016) Development of vascularized iPSC derived 3D-cardiomyocyte tissues by filtration layer-by-layer technique and their application for pharmaceutical assays. *Acta Biomater* 33:110–121
3. Amsden B (1998) Solute diffusion within hydrogels. Mechanisms and models. *Macromolecules* 31:8382–8395
4. Annabi N, Tsang K, Mithieux SM, Nikkhah M, Ameri A, Khademhosseini A, Weiss AS (2013) Highly elastic micropatterned hydrogel for engineering functional cardiac tissue. *Adv Funct Mater* 23:4950–4959
5. Bajaj P, Schweller RM, Khademhosseini A, West JL, Bashir R (2014) 3D biofabrication strategies for tissue engineering and regenerative medicine. *Annu Rev Biomed Eng* 16:247–276
6. Bártolo PJ (2011) Stereolithography: materials, processes and applications. Springer, New York/Dordrecht/Heidelberg/London, pp 1–340
7. Becker AL, Zelikin AN, Johnston AP, Caruso F (2009) Tuning the formation and degradation of layer-by-layer assembled polymer hydrogel microcapsules. *Langmuir* 25:14079–14085
8. Bertassoni LE, Cecconi M, Manoharan V, Nikkhah M, Hjortnaes J, Cristino AL, Barabaschi G, Demarchi D, Dokmeci MR, Yang Y, Khademhosseini A (2014) Hydrogel bioprinted microchannel networks for vascularization of tissue engineering constructs. *Lab Chip* 14(13):2202–2211
9. Best C, Onwuka E, Pepper V, Sams M, Breuer J, Breuer C (2016) Cardiovascular tissue engineering: preclinical validation to bedside application. *Physiology* 31(1):7–15



10. Boateng JS, Matthews KH, Stevens HN, Eccleston GM (2008) Wound healing dressings and drug delivery systems: a review. *Indian J Pharm Sci* 97:2892–2923
11. Boffito M, Sartoria S, Ciardella G (2014) Polymeric scaffolds for cardiac tissue engineering: requirements and fabrication technologies. *Polym Int* 63:2–11
12. Borges J, Rodrigues LC, Reis RL, Mano JF (2014) Layer-by-layer assembly of light-responsive polymeric multilayer systems. *Adv Funct Mater* 24:5624–5648
13. Bryant SJ, Vernerey FJ (2016) Programmable hydrogels for cell encapsulation and neo-tissue growth to enable personalized tissue engineering. *Adv Health Mater* 7:1–13
14. Caló E, Khutoryanskiy VV (2015) Biomedical applications of hydrogels: a review of patents and commercial products. *Eur Polym J* 65:252–267
15. Canal T, Peppas NA (1989) Correlation between mesh size and equilibrium degree of swelling of polymeric networks. *J Biomed Mater Res* 23:1183–1193
16. Cannegieter SC, Rosendaal FR, Briët E (1994) Thromboembolic and bleeding complications in patients with mechanical heart valve prostheses. *Circulation* 89(2):635–641
17. Cha C, Oh J, Kim K, Qiu Y, Joh M, Shin SR, Wang X, Unal GC, Wan KT, Liao R, Khademhosseini A (2014) Microfluidics-assisted fabrication of gelatin-silica core-shell microgels for injectable tissue constructs. *Biomacromolecules* 15:283–290
18. Chambers J (2014) Prosthetic heart valves. *Int J Clin Pract* 68:1227–1230
19. Chen JP, Cheng TH (2006) Thermo-responsive chitosan-graft-poly(N-isopropylacrylamide) injectable hydrogel for cultivation of chondrocytes and meniscus cells. *Macromol Biosci* 6(12):1026–1039
20. Cheng SY, Gross J, Sambanis A (2004) Hybrid pancreatic tissue substitute consisting of recombinant insulin-secreting cells and glucoseresponsive material. *Biotechnol Bioeng* 87:863–873
21. Chia HN, Wu BM (2015) Recent advances in 3D printing of biomaterials. *J Biol Eng* 9(4):1–14
22. Chu C, Graf G, Posen DW (2008) Design for additive manufacturing of cellular structures. *Comput Aided Des Appl* 5:680–696
23. Chua LK, Leong KF, Lim CS (2004) Rapid prototyping: principles and applications. World Scientific Publishing, Singapore
24. Chung HJ, Park TG (2009) Self-assembled and nanostructured hydrogels for drug delivery and tissue engineering. *Nano Today* 4:429–437
25. Clark RA (1996) Wound repair overview and general considerations. The molecular and cellular biology of wound repair, 2nd edn. Plenum, New York, pp 3–5
26. Cruise GM, Scharp DS, Hubbell JA (1998) Characterization of permeability and network structure of interfacially photopolymerized poly(ethylene glycol) diacrylate hydrogels. *Biomaterials* 19:1287–1294
27. Daamen WF, Veerkamp JH, van Hest JC, van Kuppevelt TH (2007) Elastin as a biomaterial for tissue engineering. *Biomaterials* 28(30):4378–4398
28. Degreef HJ (1998) How to heal a wound fast. *Dermatol Clin* 16:365–375
29. Deshmukh M, Singh Y, Gunaseelan S, Gao D, Stein S, Sinko PJ (2010) Biodegradable poly(ethylene glycol) hydrogels based on a self-elimination degradation mechanism. *Biomaterials* 31(26):6675–6684
30. Dhivya S, Padma VV, Santhini E (2015) Wound dressings – a review. *Biomedicine* 5(4):24–28
31. Díaz Lantada A, Valle-Fernández RD, Morgado PL, Muñoz-García J, Muñoz-Sanz JL, Muñoz-Guijosa JM, Otero JE (2010) Development of personalized annuloplasty rings: combination of CT images and CAD-CAM tools. *Ann Biomed Eng* 38:280–290
32. Díez P, Sánchez A, Gamella M, Martínez-Ruiz P, Aznar E, de la Torre C, Murguía JR, Martínez-Mañez R, Villalonga R, Pingarrón JM (2014) Toward the design of smart delivery systems controlled by integrated enzyme-based biocomputing ensembles. *J Am Chem Soc* 136:9116–9123
33. Dowsett C, Newton H (2005) Wound bed preparation: time in practice. *Wounds UK* 1:58–70
34. Drury JL, Mooney DJ (2003) Hydrogels for tissue engineering: scaffold design variables and applications. *Biomaterials* 24(24):4337–4351
35. Duan B, Hockaday LA, Kang KH, Butcher JT (2013) 3D bioprinting of heterogeneous aortic valve conduits with alginate/gelatin hydrogels. *J Biomed Mater Res A* 101A:1255–1264
36. Duan B, Kapetanovic E, Hockaday LA, Butcher JT (2014) Three-dimensional printed trileaflet valve conduits using biological hydrogels and human valve interstitial cells. *Acta Biomater* 10:1836–1846
37. Eschenhagen T, Zimmermann WH (2005) Engineering myocardial tissue. *Circ Res* 97(12):1220–1231
38. Farahani RD, Dube M, Therriault D (2016) Threedimensional printing of multifunctional nanocomposites: manufacturing techniques and applications. *Adv Mater* 28:5794–5821
39. Flory PJ (1953) Principles of polymer chemistry. Cornell University Press, Ithaca, p 672
40. Gaetani R, Doevendans PA, Metz CH, Alblas J, Messina E, Giacomello A, Sluijter JP (2012) Cardiac tissue engineering using tissue printing technology and human cardiac progenitor cells. *Biomaterials* 33(6):1782–1790
41. Gan LH, Gan YY, Deen GR (2000) Poly(N-acryloyl-N'-propylpiperazine): a new stimuli-responsive polymer. *Macromolecules* 33:7893–7897
42. Gao Y, Li X, Serpe MJ (2015) Stimuli-responsive microgel-based etalons for optical sensing. *RSC Adv* 5:44074–44087
43. Garnica-Palafox IM, Sánchez-Arévalo FM (2016) Influence of natural and synthetic crosslinking reagents on the structural and mechanical properties of chitosan-based hybrid hydrogels. *Carbohydr Polym* 151:1073–1081

44. Ghandehari H, Kopeckova P, Kopecek J (1997) In vitro degradation of pH-sensitive hydrogels containing aromatic azo bonds. *Biomaterials* 18(12):861–872
45. Giannopoulos AA, Chepelev L, Sheikh A, Wang A, Dang W, Akyuz E, Hong C, Wake N, Pietila T, Dydynski PB, Mitsouras D, Rybicki, FJ (2015) 3D printed ventricular septal defect patch: a primer for the 2015 Radiological Society of North America (RSNA) hands-on course in 3D printing. *3D Print Medi* 1(3):1–20
46. Giannopoulos AA, Mitsouras D, Yoo SJ, Liu PP, Chatzizisis YS, Rybicki FJ (2016) Applications of 3D printing in cardiovascular diseases. *Nat Rev Cardiol* 13:701–718
47. Gil ES, Hudson SM (2004) Stimuli-responsive polymers and their bioconjugates. *Prog Polym Sci* 29:1173–1222
48. Gil ES, Hudson SM (2007) Effect of silk fibroin interpenetrating networks on swelling/deswelling kinetics and rheological properties of poly (N-isopropylacrylamide) hydrogels. *Biomacromolecules* 8:258–264
49. Gilmore MA (1991) Phases of wound healing. *Dimens Oncol Nurs* 5(3):32–34
50. Glowacki J, Mizuno S (2007) Collagen scaffolds for tissue engineering. *Biopolymers* 89(5):338–344
51. Goyanes A, Det-Amornrat U, Basit JA, Gaisford S (2016) 3D scanning and 3D printing as innovative technologies for fabricating personalized topical drug delivery systems. *J Control Release* 234:41–46
52. Gupta B, Agarwal R, Alam MS (2010) Textile-based smart wound dressings. *Ind J Fibre Textile Res* 35:174–187
53. Hacker MC, Mikos AG (2011) Synthetic polymers. In: *Principles of regenerative medicine*, 2nd edn. Academic Press, San Diego, pp 587–622
54. Harvey JA (1995) Smart materials. In: Kroschwitz JI, Howe-Grant M (eds) *Encyclopedia of chemical technology*. Wiley, New York, pp 502–514
55. Hasan A, Khattab A, Islam MA, Hweij KA, Zeitouny J, Waters R, Sayegh M, Hossain MM, Paul A (2015) Injectable hydrogels for cardiac tissue repair after myocardial infarction. *Adv Sci* 1500122:1–18
56. Hassan CM, Doyle FJ, Peppas NA (1997) Dynamic behavior of glucoseresponsive poly(methacrylic acid-g-ethylene glycol) hydrogels. *Macromolecules* 30:6166–6173
57. Henke S, Leijten J, Kemna E, Neubauer M, Fery A, van den Berg A, van Apeldoorn A, Karperien M (2016) Enzymatic crosslinking of polymer conjugates is superior over ionic or UV crosslinking for the on-chip production of cell-laden microgels. *Macromol Biosci* 16:1524–1532
58. Hisamitsu I, Kataoka K, Okano T, Sakurai Y (1997) Glucose-responsive gel from phenylborate polymer and poly(vinyl alcohol): prompt response at physiological pH through the interaction of borate with amino group in the gel. *Pharm Res* 14:289–293
59. Hockaday LA, Kang KH, Colangelo NW, Cheung PY, Duan B, Malone E, Wu J, Girardi LN, Bonassar LJ, Lipson H, Chu CC, Butcher JT (2012) Rapid 3D printing of anatomically accurate and mechanically heterogeneous aortic valve hydrogel scaffolds. *Biofabrication* 4(3):1–12
60. Hoffman AS (2002) Hydrogels for biomedical applications. *Adv drug deliver Rev* 43(1):3–12
61. Hoffman AS (2013) Stimuli-responsive polymers: biomedical applications and challenges for clinical translation. *Adv Drug Deliver Rev* 65:10–16
62. Hollister SJ (2005) Porous scaffold design for tissue engineering. *Nat Mater* 4:518–524
63. Hunt TK, Hopf H, Hussain Z (2000) Physiology of wound healing. *Adv Skin Wound Care* 13:6–11
64. Hutmacher DW, Sittinger M, Risbud MV (2004) Scaffold-based tissue engineering: rationale for computer aided design and solid free-form fabrication systems. *Trends Biotechnol* 22:354–362
65. Jana S, Lerman A (2015) Bioprinting a cardiac valve. *Biotech Adv* 33:1503–1521
66. Jia W, Gungor-Ozkerim PS, Zhang YS, Yue K, Zhu K, Liu W, Pi Q, Byambaa B, Dokmeci MR, Shin SR, Khademhosseini A (2016) Direct 3D bioprinting of perfusable vascular constructs using a blend bioink. *Biomaterials* 106:58–68
67. Kamoun EA, Kenawy ES, Chen X (2017) A review on polymeric hydrogel membranes for wound dressing applications: PVA-based hydrogel dressings. *J Adv Res* 8:217–233
68. Kamperman T, Henke S, van den Berg A, Shin SR, Tamayol A, Khademhosseini A, Karperien M, Leijten J (2017) Single cell microgel based modular bioinks for uncoupled cellular micro- and macroenvironments. *Adv Healthc Mater* 6:1600913
69. Karikkineth BC, Zimmermann WH (2013) Myocardial tissue engineering and heart muscle repair. *Curr Pharm Biotechnol* 14(1):4–11
70. Kashyap N, Kumar N, Kumar MR (2005) Hydrogels for pharmaceutical and biomedical applications. *Crit Rev Ther Drug Carrier Syst* 22:107–150
71. Kearney JN (2001) Clinical evaluation of skin substitutes. *Burns* 27:545–551
72. Kehl D, Weber B, Hoerstrup SP (2016) Bioengineered living cardiac and venous valve replacements: current status and future prospects. *Cardiovasc Pathol* 25:300–305
73. Kickhöfen B, Wokalek H, Scheel D, Ruh H (1986) Chemical and physical properties of a hydrogel wound dressing. *Biomaterials* 7(1):67–72
74. Kim MS, Hansgen AR, Wink O, Quaipe RA, Carroll JD (2008) Rapid prototyping: a new tool in understanding and treating structural heart disease. *Circulation* 117:2388–2394
75. Kost J, Langer R (2001) Responsive polymeric delivery systems. *Adv Drug Deliv Rev* 46(1–3):125–148
76. Le HP (1998) Progress and trends in ink-jet printing technology. *J Imaging Sci Technol* 42:49–62

77. Lee VK, Dai G (2016) Printing of three-dimensional tissue analogs for regenerative medicine. *Biomed Eng Soc* 45(1):115–131
78. Lee MR, Phang IY, Cui Y, Lee YH, Ling XY (2015) Shape-shifting 3D protein microstructures with programmable directionality via quantitative nanoscale stiffness modulation. *Small* 11(6):740–748
79. Li Y, Zhang D (2017) Artificial cardiac muscle with or without the use of scaffolds. *Biomed Res Int* 8473465:1–15
80. Li Y, Huang G, Zhang X, Li B, Chen Y, Lu T, Lu TJ, Xu F (2013) Magnetic hydrogels and their potential biomedical applications. *Adv Funct Mater* 23:660–672
81. Li S, Zhang HG, Li DD, Wu JP, Sun CY, Hu QX (2017) Characterization of engineered scaffolds with spatial prevascularized networks for bulk tissue regeneration. *ACS Biomater Sci Eng* 3:2493–2501
82. Lia Q, Liua C, Wena J, Wua Y, Shana Y, Liaoa J (2017) The design, mechanism and biomedical application of self-healing hydrogels. *Chinese Chem Lett* 28:1857–1874
83. Lim HL, Hwang Y, Kar M, Varghese S (2014) Smart hydrogels as functional biomimetic systems. *Biomater Sci* 2:603–618
84. Lin FH, Tsai JC, Chen TM, Chen KS, Yang JM, Kang PL, Wu TH (2007) Fabrication and evaluation of auto-stripped tri-layer wound dressing for extensive burn injury. *Mater Chem Phys* 102:152–158
85. Luo J, Cao S, Chen X, Liu S, Tan H, Wu W, Li J (2012) Super long-term glycemic control in diabetic rats by glucose-sensitive lbl films constructed of supramolecular insulin assembly. *Biomaterials* 33:8733–8742
86. Lustig SR, Peppas NA (1988) Solute diffusion in swollen membranes. 9. Scaling laws for solute diffusion in gels. *J Appl Polym Sci* 36:735–747
87. Mano JF (2008) Stimuli-responsive polymeric systems for biomedical applications. *Adv Eng Mater* 2008 10(6):515–527
88. Mason MN, Metters AT, Bowman CN, Anseth KS (2001) Predicting controlled-release behavior of degradable PLA-b-PEG-b-PLA hydrogels. *Macromolecules* 34:4630–4635
89. Maxson S, Lopez EA, Yoo D, Danilkovitch-Miagkova A, Leroux MA (2012) Concise review: role of mesenchymal stem cells in wound repair. *Stem Cells Transl Med* 1(2):142–149
90. Melchels FP, Feijen J, Grijpma DW (2010a) Review on stereolithography and its applications in biomedical engineering. *Biomaterials* 31:6121–6130
91. Melchels FP, Bertoldi K, Gabbriellini R, Velders AH, Feijen J, Grijpma DW (2010b) Mathematically defined tissue engineering scaffold architectures prepared by stereolithography. *Biomaterials* 31(27):6909–6916
92. Miyata T, Uragama T, Nakamaeb K (2002) Biomolecule-sensitive hydrogels. *Adv Drug Deliver Rev* 54:79–98
93. Mol A, van Lieshout MI, Dam-deVeen CG, Neuenchwander S, Hoerstrup SP, Baaijens FP, Bouten CV (2005) Fibrin as a cell carrier in cardiovascular tissue engineering applications. *Biomaterials* 26(16):3113–3121
94. Mosadegh B, Xiong G, Dunham S, Min KJ (2015) Current progress in 3D printing for cardiovascular tissue engineering. *Biomed Mater* 10(3):1–12
95. Murphy SV, Atala A (2014) 3D bioprinting of tissues and organs. *Nat Biotechnol* 32:773–785
96. Nguyen TK, West JL (2002) Photopolymerizable hydrogels for tissue engineering applications. *Biomaterials* 23(22):4307–4314
97. Nicodemus GD, Bryant SJ (2008) Cell encapsulation in biodegradable hydrogels for tissue engineering applications. *Tissue Eng Part B* 14(2):149
98. Osada Y, Matsuda A (1995) Shape memory in hydrogels. *Nature* 376(6537):219
99. Park JH, Jang J, Lee SJ, Cho DW (2017) Three-dimensional printing of tissue/organ analogues containing living cells. *Ann Biomed Eng* 45(1):180–194
100. Pati F, Jang J, Ha DH, Kim SW, Rhie JW, Shim JH, Kim DH, Cho DW (2014) Printing three-dimensional tissue analogues with decellularized extracellular matrix bioink. *Nat Commun* 5:1–11
101. Pati F, Song TH, Rijal G, Jang J, Kim SW, Cho DW (2015) Ornamenting 3D printed scaffolds with cell-laid extracellular matrix for bone tissue regeneration. *Biomaterials* 37:230–241
102. Peppas NA, Keys KB, Torres-Lugo M, Lowman AM (1999) Poly(ethylene glycol)-containing hydrogels in drug delivery. *J Control Release* 62:81–87
103. Peppas NA, Huang Y, Torres-Lugo M, Ward JH, Zhang J (2000) Physicochemical foundations and structural design of hydrogels in medicine and biology. *Annu Rev Biomed Eng* 2:9–29
104. Peppas NA, Hilt JZ, Khademhosseini A, Langer R (2006) Hydrogels in biology and medicine: from molecular principles to bionanotechnology. *Adv Mater* 18:1345–1360
105. Prabakaran M, Rodrigues-Perez MA, de Saja JA, Mano JF (2007) Preparation and characterization of poly(L-lactic acid)-chitosan hybrid scaffolds with drug release capability. *J Biomed Mater Res B* 81:427–434
106. Pradhan KA, Keller JL, Sperduto L, Slater JH (2017) Fundamentals of laser-based hydrogel degradation and applications in cell and tissue engineering. *Adv Health Mater* 1700681:1–28
107. Purna SK, Babu M (2000) Collagen based dressing—a review. *Burns* 26(1):54–62
108. Qiu Y, Park K (2001) Environment-sensitive hydrogels for drug delivery. *Adv Drug Deliv Rev* 53:321–339
109. Radisic M, Malda J, Epping E, Geng WL, Langer R, Vunjak-Novakovic G (2006) Oxygen gradients correlate with cell density and cell viability in engineered cardiac tissue. *Biotechnol Bioeng* 93:332–343

110. Rajendran S, Anand SC (2011) Hi-tech textiles for interactive wound therapies. In: Handbook of medical textiles. Woodhead Publishing, Oxford
111. Richards D, Jia J, Yost M, Markwald R, Mei Y (2017) 3D Bioprinting for vascularized tissue fabrication. *Ann Biomed Eng* 45(1):132–147
112. Rivera AE, Spencer JM (2007) Clinical aspects of full-thickness wound healing. *Clin Dermatol* 25:39–48
113. Robson MC, Steed DL, Franz MG (2001) Wound healing: biological features and approaches to maximize healing trajectories. *Curr Prob Surg* 38:77–89
114. Rouwkema J, Khademhosseini A (2016) Vascularization and angiogenesis in tissue engineering: beyond creating static networks. *Trends Biotechnol* 34(9):733–745
115. Rzaev ZM, Dincer S, Piskin E (2007) Functional copolymers of N-isopropylacrylamide for bioengineering applications. *Prog Polym Sci* 32:534–595
116. Saito H, Kato N (2016) Polyelectrolyte/carbon nanotube composite microcapsules and drug release triggered by laser irradiation. *Jpn J Appl Phys Pt* 155:03DF06
117. Sato K, Yoshida K, Takahashi S, Anzai J (2011) pH- and sugar-sensitive layer-by-layer films and microcapsules for drug delivery. *Adv Drug Deliv Rev* 63:809–821
118. Schaefermeier PK, Szymanski D, Weiss F, Fu P, Lueth T, Schmitz C, Meiser BM, Reichart B, Sodian R (2008) Design and fabrication of three-dimensional scaffolds for tissue engineering of human heart valves. *Eur Surg Res* 42:49–53
119. Schild HG (1992) Poly(N-isopropylacrylamide): experiment, theory and application. *Prog Polym Sci* 17:163–249
120. Schmedlen RH, Masters KS, West JL (2002) Photocrosslinked polyvinyl alcohol hydrogels that can be modified with cell adhesion peptides for use in tissue engineering. *Biomaterials* 23(22):4325–4332
121. Schoen FJ, Levy RJ (1999) Tissue heart valves: current challenges and future research perspectives. *J Biomed Mater Res* 47:439–465
122. Schreml S, Szeimies RM, Prantl L, Karrer S, Landthaler M, Babilas P (2010) Oxygen in acute and chronic wound healing. *Br J Dermatol* 163:257–268
123. Seliktar D (2012) Designing cell-compatible hydrogels for biomedical applications. *Science* 336:1124–1128
124. Seol YJ, Kang TY, Cho DW (2012) Solid freeform fabrication technology applied to tissue engineering with various biomaterials. *Soft Matter* 8:1730–1735
125. Seol YJ, Kang HY, Lee SJ, Atala A, Yoo JJ (2014) Bioprinting technology and its applications. *Eur J Cardiothorac Surg* 46(3):342–348
126. Shafiee A, Atala A (2016) Printing technologies for medical applications. *Trends Mol Med* 22:254–265
127. Shin SR, Bolagh BA, Gao X, Nikkhah M, Jung SM, Pirouz AD, Kim SB, Kim SM, Dokmeci MR, Tang XS, Khademhosseini A (2014) Layer-by-layer assembly of 3D tissue constructs with functionalized graphene. *Adv Funct Mater* 24:6136–6144
128. Siddiqui RF, Abraham JR, Butany J (2009) Bioprosthetic heart valves: modes of failure. *Histopathology* 55(2):135–144
129. Siltanen C, Yaghoobi M, Haque A, You J, Lowen J, Soleimani M, Revzin A (2016) Microfluidic fabrication of bioactive microgels for rapid formation and enhanced differentiation of stem cell spheroids. *Acta Biomater* 34:125–132
130. Skardal A, Atala A (2015) Biomaterials for integration with 3D bioprinting. *Ann Biomed Eng* 43:730–746
131. Slaughter BV, Khurshid SS, Fisher OZ, Khademhosseini K, Peppas NA (2009) Hydrogels in regenerative medicine. *Adv Mater* 21:3307–3329
132. Sood A, Granick MS, Tomaselli NL (2014) Wound dressings and comparative effectiveness data. *Adv Wound Care* 3(8):511–529
133. Stashak TS, Farstvedt E, Othic A (2004) Update on wound dressings: indications and best use. *Clin Tech Equine Pract* 3:148–163
134. Stock UA, Nagashima M, Khalil PN, Nollert GD, Herden T, Sperling JS, Moran A, Lien J, Martin DP, Schoen FJ, Vacanti JP, Mayer JE (2000) Tissue-engineered valved conduits in the pulmonary circulation. *J Thorac Cardiovasc Surg* 119:732–740
135. Streckler-Mcgraw MK, Jones TR, Baer DG (2007) Soft tissue wounds and principles of healing. *Emerg Med Clin North Am* 25:1–22
136. Szycher M, Lee SJ (1992) Modern wound dressings: a systemic approach to wound healing. *J Biomater Appl* 7:142–213
137. Tarnuzzer RW, Schultz GS (1996) Biochemical analysis of acute and chronic wound environments. *Wound Repair Regen* 4:321–325
138. Tsukamoto Y, Akagi T, Shima F, Akashi M (2017) Fabrication of orientation-controlled 3D tissues using a layer-by-layer technique and 3D printed a thermoresponsive gel frame. *Tissue Eng Part C* 23(6):357–365
139. Ulijin RV (2006) Enzyme-responsive materials: a new class of smart biomaterials. *J Mater Chem* 16:2217–2225
140. Ullah F, Othman MB, Javed F, Ahmada Z, Akil HM (2015) Classification, processing and application of hydrogels: a review. *Mater Sci Eng C* 57:414–433
141. Van der Veen VC, Van der Wal M, van Leeuwen MC, Magda MW (2010) Biological background of dermal substitutes. *Burns* 36(3):305–321
142. Vanwijck R (2000) Surgical biology of wound healing. *Bulletin et memoires de l'Academieroyale de medecine de Belgique* 156:175–184
143. Vermonden T, Censi R, Hennink WE (2012) Hydrogels for protein delivery. *Chem Rev* 112:2853–2888
144. Wichterle O, Lim D (1960) Hydrophilic gels for biological use. *Nature* 185:117–118

145. Xiao CH, Tian HY, Zhuang XL, Chen XS, Jing XB (2009) Recent developments in intelligent biomedical polymers. *Sci China Ser B Chem* 52(2):117–130
146. Xu XD, Li X, Chen H, Qu Q, Zhao L, Agren H, Zhao Y (2015) Host–guest interaction-mediated construction of hydrogels and nanovesicles for drug delivery. *Small* 11(44):5901–5906
147. Yang JM, Huang HT (2012) Evaluation of tri-steps modified styrene-butadiene-styrene block copolymer membrane for wound dressing. *Mater Sci Eng C* 32:1578–1587
148. Yang JM, Lin HT (2004) Properties of chitosan containing PP-g-AA-g-NIPAAmbigraft nonwoven fabric for wound dressing. *J Membrane Sci* 243:1–7
149. Yang JM, Su WY (2011) Preparation and characterization of chitosan hydrogel membrane for the permeation of 5-fluorouracil. *Mater Sci Eng C* 31:1002–1009
150. Yang JM, Tsai SC (2010) Biocompatibility of epoxidized styrene–butadiene–styrene block copolymer membrane. *Mater Sci Eng C* 30(8):1151–1156
151. Yang L, Chu JS, Fix JA (2002) Colon-specific drug delivery: new approaches and in vitro/in vivo evaluation. *Int J Pharm* 235:1–15
152. Yang JM, Lin W, Wu TH, Chen CC (2003) Wettability and antibacterial assessment of chitosan containing radiation induced graft nonwoven fabric of polypropylene-g-acrylic acid. *J Appl Polym Sci* 90:1331–1336
153. Yang JM, Yang SJ, Lin HT, Chen JK (2007) Modification of HTPB-based polyurethane with temperature-sensitive poly(N-isopropyl acrylamide) for biomaterial usage. *J Biomed Mater Res Part B Appl Biomater* 80(1):43–51
154. Yang JM, Yang SJ, Lin HT, Wu TH, Chen HJ (2008) Chitosan containing PU/poly(NIPAAm) thermosensitive membrane for wound dressing. *Mater Sci Eng C* 28:150–156
155. Yang X, Ma C, Li C, Xie Y, Huang X, Jin Y, Zhu Z, Liu J, Li T (2015) Three dimensional responsive structure of tough hydrogels. *Electroactive Polym Actuators Devices* 9430:1–6
156. Yang J, Katagiri D, Mao S, Zeng H, Nakajima H, Kato S, Uchiyama K (2016) Inkjet printing based assembly of thermoresponsive core–shell polymer microcapsules for controlled drug release. *J Mater Chem B* 4:4156–4163
157. Yeh PY, Kopeckova P, Kopecek P (1995) Degradability of hydrogels containing azoaromatic crosslinks. *Macromol Chem Phys* 196:2183–2202
158. Yeong WY, Chua CK, Leong KF, Chandrasekaran M (2004) Rapid prototyping in tissue engineering: challenges and potential. *Trends Biotechnol* 22:354–362
159. Yeong WY, Sudarmadji N, Yu HN, Chua CK, Leong KF, Venkatraman SS, Boey YC, Tan LP (2010) Porous polycaprolactone scaffold for cardiac tissue engineering fabricated by selective laser sintering. *Acta Biomater* 6:2028–2034
160. Yin X, Hoffman AS, Stayton PS (2016) Poly(N-isopropylacrylamide-co-propylacrylic acid) copolymers that respond sharply to temperature and pH. *Biomacromolecules* 7(5):1381–1385
161. Zhai M, Li J, Yi M, Ha H (2000) The swelling behaviour of radiation prepared semi-interpenetrating polymer networks composed of polyNIPAAm and hydrophilic polymers. *Radiat Phys Chem* 58:397–400
162. Zhang YS, Khademhosseini A (2017) Advances in engineering hydrogels. *Science* 356(3627):1–10
163. Zhang X, Xu B, Puperi DS, Wu Y, Westc JL, Grande-Allena KJ (2015) Application of hydrogels in heart valve TissueEngineering. *J Long-Term Eff Med Implants* 25(1–2):105–134
164. Zhang YS, Arneri A, Bersini S, Shin SR, Zhu K, Goli-Malekabadi Z, Aleman J, Colosi C, Busignani F, Dell'Erba V, Bishop C, Demarchi D, Moretti M, Rasponi M, Dokmeci MR (2016a) Bioprinting 3D microfibrillar scaffolds for engineering endothelialized myocardium and heart-on-a-chip. *Biomaterials* 110:45–59
165. Zhang YS, Yue K, Aleman J, Mollazadeh-Moghaddam K, Bakht SM, Yang J, Jia W, Dell'Erba V, Assawes P, Shin SR, Dokmeci M, Oklu R, Khademhosseini A (2016b) 3D Bioprinting for tissue and organ fabrication. *Ann Biomed Eng* 45(1):148–163
166. Zhao W, Zhang H, He Q, Li Y, Gu J, Li L, Li H, Shi J (2011) A glucose-responsive controlled release of insulin system based on enzyme multilayers-coated mesoporous silica particles. *Chem Commun* 47:9459–9461
167. Zhao L, Xiao C, Ding J, He P, Tang Z, Pang X, Zhuang X, Chen X (2013) Facile one-pot synthesis of glucose-sensitive nanogel via thiol-ene click chemistry for self-regulated drug delivery. *Acta Biomater* 9:6535–6543
168. Zhao L, Xiao C, Ding J, Zhuang X, Gai G, Wang L, Chen X (2015) Competitive binding-accelerated insulin release from a polypeptide nanogel for potential therapy of diabetes. *Polym Chem* 6:3807–3815
169. Zhao L, Xiao C, Wang L, Gai G, Ding J (2016) Glucose-sensitive polymer nanoparticles for self-regulated drug delivery. *Chem Commun* 52:7633–7652
170. Zhao L, Wang L, Zhang Y, Xiao S, Bi F, Zhao J, Gai G, Ding J (2017) Glucose oxidase-based glucose-sensitive drug delivery for diabetes treatment. *Polymers* 9(255):1–21
171. Zhu J, Marchant RE (2011) Design properties of hydrogel tissue-engineering scaffolds. *Expert Rev Med Devices* 8(5):607–626
172. Zhu W, Li J, Leong YJ, Rozen I, Qu X, Dong R, Wu Z, Gao W, Chung PH, Wang J, Chen S (2015) 3D-Printed artificial microfish. *Adv Mater* 27:4411–4417
173. Zorlutuna P, Annabi N, Camci-Unal G, Nikkha M, Cha JM, Nichol JW, Manbachi A, Bae H, Chen S, Khademhosseini A (2012) Microfabricated biomaterials for engineering 3D tissues. *Adv Mater* 24:1782–1804



# Injectable Nanocomposite Hydrogels and Electrospayed Nano(Micro)Particles for Biomedical Applications

Nguyen Vu Viet Linh, Nguyen Tien Thinh,  
Pham Trung Kien, Tran Ngoc Quyen,  
and Huynh Dai Phu

## Abstract

Polymeric scaffolds have played important roles in biomedical applications due to their potentially practical performance such as delivery of bioactive components and/or regenerative cells. These materials were well-

designed to encapsulate bioactive molecules or/and nanoparticles for enhancing their performance in tissue regeneration and drug delivery systems. In the study, several multi-functional nanocomposite hydrogel and polymeric nano(micro)particles-electrospayed platforms were described from their fabrication methods and structural characterizations to potential applications in the mentioned fields. Regarding to their described performance, these multifunctional nanocomposite biomaterials could pay many ways for further studies that enables them apply in clinical applications.

N. V. V. Linh · H. D. Phu (✉)  
Faculty of Materials Technology, Ho Chi Minh City  
University of Technology (HCMUT), Vietnam  
National University, Ho Chi Minh City, Vietnam

National Key Lab for Polymer and Composite  
Materials, HCMUT, Ho Chi Minh City, Vietnam  
e-mail: [nguyenvuvietlinh@hcmut.edu.vn](mailto:nguyenvuvietlinh@hcmut.edu.vn);  
[hdphu@hcmut.edu.vn](mailto:hdphu@hcmut.edu.vn)

N. T. Thinh  
Graduate School of Science and Technology, Vietnam  
Academy of Science and Technology,  
Ho Chi Minh City, Vietnam

Department of Pharmacy and Medicine, Tra Vinh  
University, Tra Vinh City, Vietnam

P. T. Kien  
Faculty of Materials Technology, Ho Chi Minh City  
University of Technology (HCMUT), Vietnam  
National University, Ho Chi Minh City, Vietnam

T. N. Quyen (✉)  
Graduate School of Science and Technology, Department  
of Pharmacy and Medicine, Vietnam Academy of  
Science and Technology, Ho Chi Minh City, Vietnam  
e-mail: [tnquyen@iams.vast.vn](mailto:tnquyen@iams.vast.vn)

## Keywords

Injectable hydrogel · Nanocomposite ·  
Polysaccharide · Electro spray · Biomedical  
applications

## 13.1 Introduction

There has been a high demand of biomaterials in therapeutic treatment, replacement or regeneration of damaged tissues/organs, diagnostic procedure and etc. leading to many studies on various advanced biocompatible and biodegradable materials recently [1]. Among of them, injectable and biocompatible polysaccharide-based hydrogels have paid much attention [2, 3]. The hydrogels

fabricate from hydrophilic polymers, which can retain significant amount of water or bio-fluid allowing transportation of substances such as nutrients and by-products from cell metabolism. Moreover, these materials were well-designed to implant in a minimally invasive surgical operation, improve patient compliance, degrade along with regeneration process of typical tissues and deliver drug/bioactive compounds/cells on the treated sites [4–6]. Up to now, various injectable hydrogel scaffolds have been fabricated via physical interactions of polymers or chemical reactions of functional polymers such as hydrophobic interaction, stereocomplex affect, electrostatic interaction, photochemical reaction, Michael-type reaction, Schiff-base reaction and enzyme-mediated crosslinking reactions [7–9]. Preparation of the injectable horseradish peroxidase enzyme-mediated hydrogels is emerging as an effective method because it is a highly specific reaction, which avoids side reactions or production of toxic by-products leading to harm with cells and living body [5, 9]. Every obtained scaffold has exhibited some particular points on physical property, speech of matrix dissolution, compatibility and etc. Recently, incorporation of nanoparticles and the hydrogels produced multifunctional injectable nanocomposite biomaterials for extending their applications in tissue engineering, drug delivery, antimicrobial materials, and bio-sensing systems.

Besides performance of the mentioned nanocomposite hydrogels, polymeric nano(micro)particles (NMPs) recently have exhibited a great potential in biomedical applications. The nanoparticles could be fabricated via two physical and chemical methods. In the physical methods, polymeric NMPs are fabricated via various techniques such as freeze drying, spray drying, nano(micro) precipitation, self-assembly of amphiphilic copolymers or phospholipids, electrospinning, solvent evaporation and so on in which polymers are dissolved in solutions. For the chemical methods, most of NMPs obtains from polymerization of monomer solutions that could be listed as micro emulsion, conventional emulsion, controlled radical, surfactant-free emulsion and etc. [10]. These polymeric NMPs have received great interest due to their structural

versatility in fabricating process that could efficiently load and release bioactive compounds, chemotherapeutics, contrast agents, proteins and nucleic acids to the desired sites. Moreover, the drug release behavior of the particles is also adjustable by their structural materials and fabricating methods that satisfy with treatment and harmony with physiologically internal conditions such as pH, enzyme and biochemical reactions. An incorporation of the particles with external stimuli such as temperature, near-IR irradiation, UV-Vis light, magnetic fields, ultrasound energy and etc., have also paved other ways for these materials in biomedical applications [11].

In this study, we introduce some injectable nanocomposite hydrogel systems and electro-sprayed NMPs that have been recently developed and performed a great potential for applying various biomedical fields. In the chapter, besides some advanced biomaterials were published from developed countries, many our studies are also included to indicate an extensive development of these advanced biomedical materials in over the world.

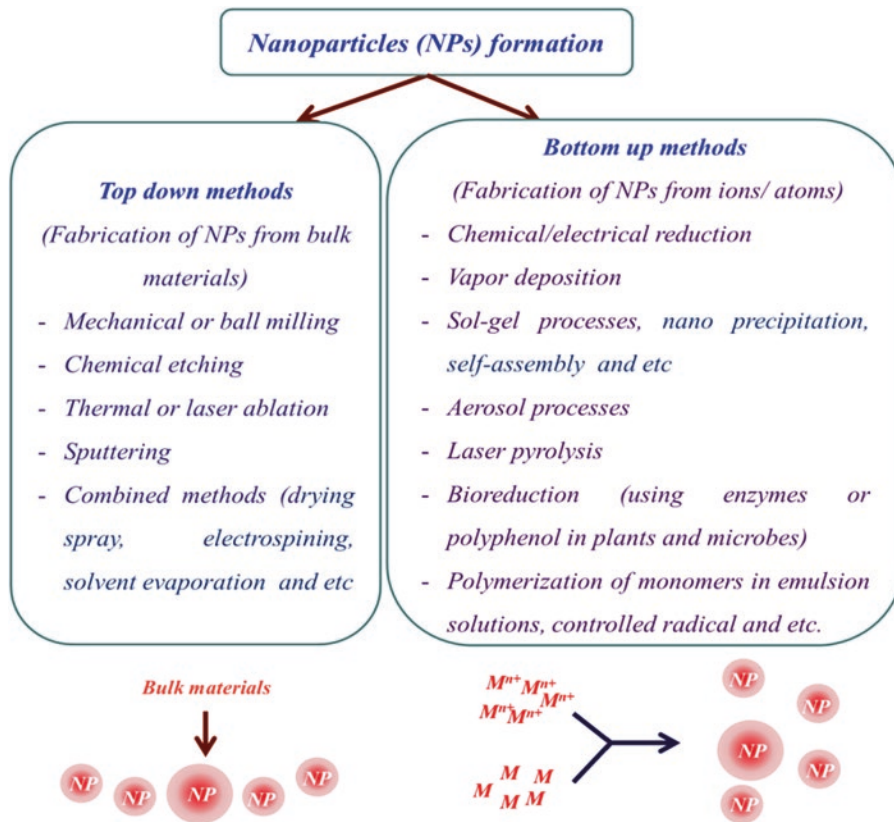
---

## 13.2 Injectable Nanocomposite Hydrogel for Biomedical Applications

### 13.2.1 Nanoparticles

In recent years, several metallic nanoparticles (NPs) have been emerging as the alternative candidates in many conventional materials due to their novel well-known properties such as antibacterial, antiplasmodial, anti-inflammatory, anticancer, antiviral, and antifungal activities [12–22]. Some kinds of inorganic and organic nanoparticles also exhibited osteoinductive and osteoconductive activities or high efficiency in drug delivery that have offered much potential in biomedical applications [23–28].

Approaches to produce nanoparticles are classified as “top down” and “bottom up” methods (Fig. 13.1). The top-down method used various physical and chemical processes to achieve the small-sized nanoparticles from its bulk form. Of bottom up approach, the nanoparticles can be



**Fig. 13.1** Methods for fabrication of nano(micro)particles

synthesized from ions, joining atoms, molecules or small particles. The bottom up approach mostly relies on chemical and biological methods of production [29, 30]. Among different types of nanoparticle production, chemical synthesis is known as the most popular method using in commercial scale due to the high efficiency compared to other methods. The obtained nanoparticles targeted for various biomedical applications. Until now hundreds of nanoparticles-based products approved in clinical applications or successes in clinical trial phases [31–35].

### 13.2.2 Nanocomposites and Biological Nanocomposites

Nanocomposites is well-known as a biphasic material in which has one nano-sized solid phase

dispersed in the bulk matrix. The material has early applied in paint engineering and cosmetic from middle 1950s. Thereafter, there had been widely studied and developed on the nanoparticles or nanofibers-based reinforcing materials for industrial applications. The nanomaterial phase exhibiting large surface area contributes to significantly enhance interaction between the dispersing phase and the bulk matrix resulting in a mechanical improvement as compared to bulk materials. According to their bulk matrices, they could be classified into three main categories: Ceramic matrix nanocomposites (CMNCs), metal matrix nanocomposites (MMNCs) and polymer matrix nanocomposites (PMNCs) [24, 25, 36]. PMNCs have been frequently used in fabrication of scaffolds for tissue engineering or drug delivery, antimicrobial materials, and biosensors systems.

In tissue regeneration and drug delivery fields, many calcium phosphate-based PMNCs possess

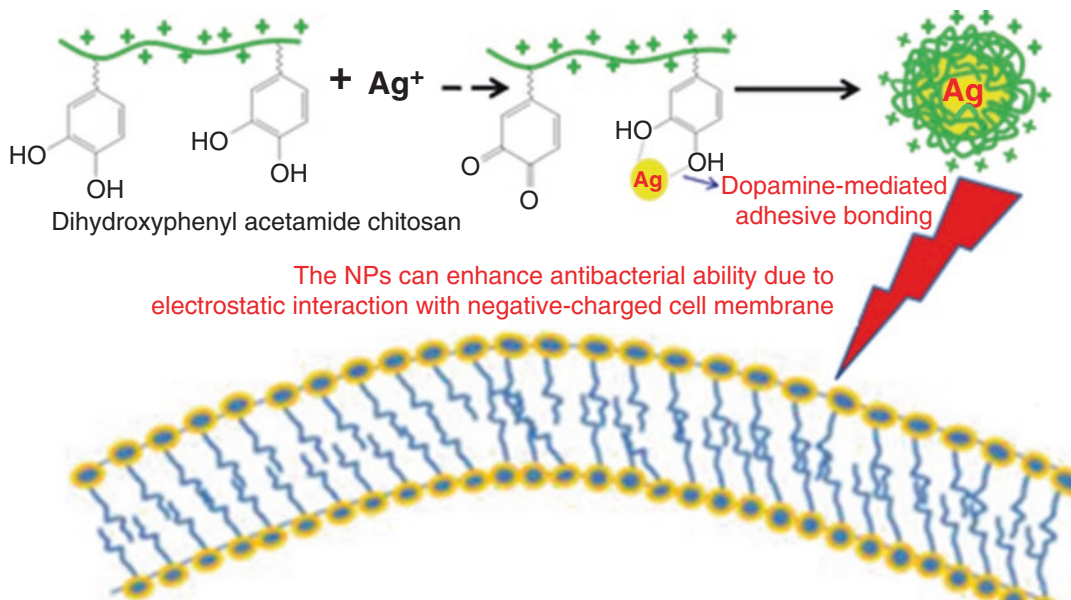


a similar structure with biological nanocomposites such as exoskeleton of arthropods and animal bone as well as biocompatibility and biodegradation. Several kinds of mineral nanoparticles like hydroxyapatite, biphasic calcium phosphate, bio-glass etc. have been dispersed in the polymers producing bioactive nanocomposite materials for tissue regeneration. Hydroxyapatite (HA), a calcium phosphate, possesses chemical composition and structure similar to mineral phase in human bones with osteoinductive and osteoconductive properties that has been utilized to fabricate artificial bionanocomposites for bone implantation [23–27]. Abundance of nano-sized HA and polymers exhibit a high biocompatibility and good mechanical properties that match with requirements for bone implant engineering [23–27]. Biphasic calcium phosphate and bio-glass are also some similar properties of HA. However, these materials exhibit a high bio-mineralization rate via an enhanced formation of crystalline hydroxyapatite that contributes to new bone formation. Some studies also indicated that calcium phosphate nanoparticles dispersed in polymer matrices can partially protect some loaded biomolecules and polymer from biodegradation [32, 37]. The calcium phosphate nanoparticles-based materials have recently used as a platform for delivery of bioactive molecules, drugs and genes. Calcium phosphate-alginate nanocomposite performs a high drug loading efficiency (caffeic, chlorogenic and cisplatin), control release of the drugs and improvement in anticancer activity on human osteosarcoma [38, 39]. Several kinds of calcium phosphate nanoparticles and biopolymers-based nanocomposites delivered effectively growth factors and/or osteogenic drugs (BMP-2, FGF-2, bisphosphonate, dexamethasone etc.) that are considering as a novel generation of the osteogenic stimulating scaffolds for bone regeneration [38–43].

Regarding outstanding properties of metal nanoparticles on antimicrobial activity, there has an emerging approach in which utilized them in fabrication of antimicrobial nanocomposite for

practical applications such as agriculture, health-care, and the industry. As prepared at nanoscale, the nanoparticles exhibit a highly active facet that is more biologically reactive as compared to the bulk counterpart [40, 43]. It is well-known that various biological polymers are elastic and flexible to fabricate equipments, biomedical devices and household items. The incorporation of the antimicrobial nanoparticles and polymers produced several kinds of active nanocomposites as well as improvement in nanoparticles' stability [40, 43]. In some cases, the formulation could increase a higher antimicrobial activity as compared to their own nanoparticles due to synergic effects of the constituents such as antimicrobial or/and structural properties of polymeric phase and the active nanoparticles as sampled in Fig. 13.2 [24, 25, 44, 45].

An emerging approach of the biological nanocomposites in fabrication of biosensors and flexible electronics should be herein discussed. Regarding to the elastic property of polymers and the specific interactions of nanoparticles, various biological nanocomposites have developed for several biomedical applications such as pathogen detection, cancer tracking, detection of small biomolecules etc. [46]. In fact, S.K. Shukla et al. developed an indium-tin oxide glass substrate-based bio-electrode that coated glucose oxidase-immobilized ZnO/chitosan-graft-poly(vinyl alcohol). The bio-electrode potentially responded to the glucose down to 1.2 mM. In the electrode, ZnO play an important role in the enzyme immobilization and its excellent stability. Wang also reported a gold nanoparticles-bacterial cellulose nanocomposite that effectively immobilized glucose oxidase and horseradish peroxidase for coating the glassy carbon electrode. Gold nanorod particles-doped polyaniline and gold-graphene/chitosan nanocomposites performed a high efficiency in immobilizing glucose oxidase and cholesterol oxidase, respectively, and others that have exhibited a great potential of nanocomposite-based biosensors [47–52].



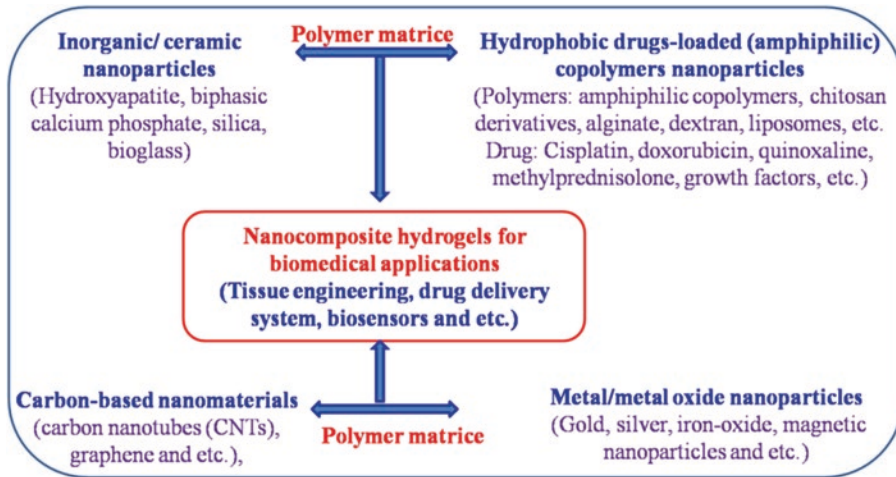
**Fig. 13.2** Illustration of the formation of silver nanoparticles and cationic chitosan composite for enhancing antibacterial activity

### 13.2.3 Hydrogels and Nanocomposite Hydrogels in Biomedical Applications

It is well-known that hydrogel scaffolds are playing an important role in biomedical applications due to their practical performances such as delivery of bioactive components, platforms for tissue engineering [53–55]. The hydrogels consist of hydrophilic polymers network are prepared via various physical, chemical and enzyme-mediated methods in which can encapsulate or immobilize bioactive molecules, drugs, enzyme and nanoparticles for tissue engineering or controlled drug delivery, antimicrobial materials, biosensors systems etc. [53–57]. With swellable and porous properties in aqueous solution, the hydrogel systems facilitate the transportation of substances from cell metabolism, control delivery of drugs, provision of signals from various biologically specific interactions [58].

Nanocomposite hydrogels (NC gels) have recently emerged as approaches to extend appli-

cable fields of these mentioned platforms that based on an incorporation of the hydrogels with nanoparticles. By incorporating the interactions between nanoparticles and hydrogel network as well as physical, chemical, electrical, biological as well as swelling/de-swelling properties of either material alone, NC gels could lead to an innovative means for producing multi-compartment and multifunctional materials. For example, Meisam Omidi reported a thermo- and/or pH sensitive, electro-responsive, magnetically responsive or light-responsive NC gel based on chitosan and carbon dots (CDs) exhibiting potentially dual applications as antibacterial and pH-sensitive nano-agents for enhancing wound healing and monitoring the pH at the same time. The NC gel had a strong antibacterial activity [59]. Moreover, under daylight at various pH values, the color of the CDs changes from bright yellow towards dark yellow when increasing the pH values indicating the pH sensitivity of the CDs even under daylight, whereas under UV light, the fluorescence intensity of the CDs is obviously affected from acidic milieu towards



**Fig. 13.3** Approaches in fabrication of nanocomposite hydrogel for biomedical applications

basic. This NC gels can be utilized as an outstanding pH-sensitive probe for biomedical applications, especially for monitoring the pH values during the wound healing process [59]. Various carbon, polymeric, ceramic and/or metallic nanomaterials-incorporated hydrogels exhibited biological, optical and ambient stimulus properties, which can be potential to apply in clinical fields like tissue engineering, drug delivery system and biosensors as demonstrated in Fig. 13.3 [58, 60, 61].

#### 13.2.4 Injectable Nanocomposite Hydrogels in Biomedical Applications

For some implanted biomaterials and bio-microfluid devices, *in situ* fabrication of various hydrogel platforms has paid much attention because it allows monomers (macromolecules) to form a 3-D network that enables the hydrogels conform to the shape of the defect sites or substrate of the devices resulting in its better bio-interaction, increment in interconnectivity, site-specific drugs delivery, enhancing bioavailability and minimizing side effects and/or match with the structural device [62–66]. Moreover, these *in situ* implanted materials could improve

patient compliance due to its minimally invasive surgical operation. Up to now, various injectable nanocomposite hydrogels have been reported at which were prepared via physical or chemical methods. These materials could be formed by hydrophobic interaction, stereocomplex effect, electrostatic interaction, photochemical reaction, Michael-type reaction, Schiff-base reaction and enzyme-mediated crosslinking reactions [66–68]. Every obtained scaffold has exhibited some different behaviors on physical property, speech of matrix dissolution, drug delivery rate, compatibility and etc.

In tissue regeneration, various NC gels have been *in situ* fabricated from the combination of biodegradable polymers and bioactive inorganic materials, which proved an improvement in mechanical properties and mineralization of the nanocomposite materials for bone tissue engineering [8, 69]. Fu reported an injectable biodegradable thermo-sensitive nano-hydroxyapatite and poly(ethylene glycol)-poly( $\epsilon$ -caprolactone)-poly(ethylene glycol)-based nanocomposite hydrogel exhibiting a potential for orthopedic tissue engineering. The group also found that the injectable nano-hydroxyapatite dispersed PEG-PCL-PEG copolymer/collagen hydrogel performed a high cytocompatibility and better calvarial bone regeneration as compared the self-



**Fig. 13.4** Horseradish peroxidase-mediated fabrication of chitosan/gelatin and BCP nanoparticles-based nanocomposite hydrogel for born tissue regeneration

healing defects [70]. Dang also introduced the injectable NC gel using biphasic calcium phosphate (BCP), gelatin, and oxidized alginate [71]. The alginate-gelatin-BCP hydrogels provided a favorable environment for bone in growth and possibly biodegradation as compared with pure hydrogel (alginate-gelatin hydrogel). The NC gel implanted to femoral bone defects exhibited a regenerated bone surface/volume ratio and bone surface density higher than that of the hydrogel-filled incisions. Other injectable NC gel were fabricated from fibrin nanoparticles and bioglass-loaded chitin/poly(butylene succinate) enhanced the osteoinductive properties [72]. We have also developed an enzyme-mediated and biodegradation-controllable BCP -loaded chitosan/gelatin hydrogel as demonstrated in Fig. 13.4 that stimulated bio-mineralization as well as proliferation of bone marrow mesenchymal stem cells (MSCs) [73]. Our obtained results indicated that these injectable nanocomposite hydrogels could be promising in bone regeneration.

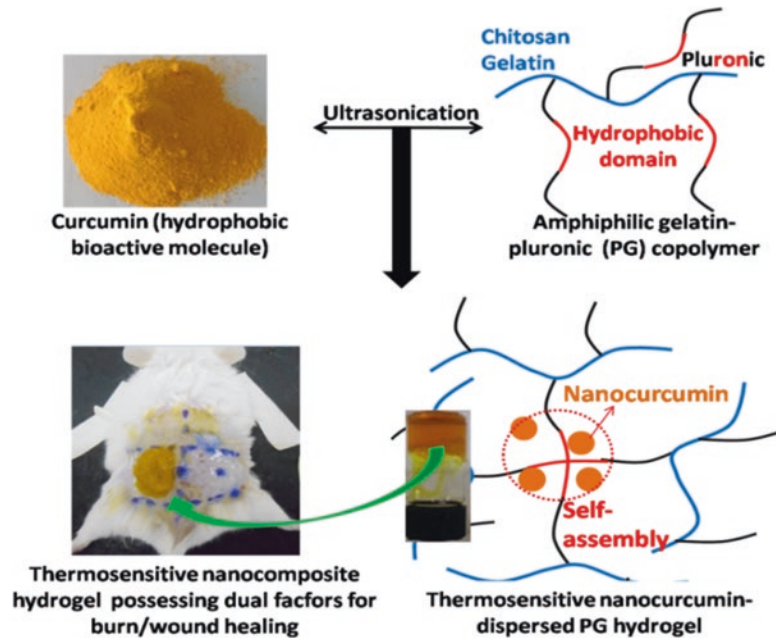
Various nanocomposite hydrogels have also been well-performed in burn or wound healing. Our group in situ prepared curcumin nanoparticle in an amphiphilic pluronic F127-g-chitosan copolymer solution resulting fabrication of a temperature responsive NC gel. The synergic incorporation has also produced a multifunctional nanocomposite hydrogels by the combination of dual bioactive chitosan and nanocurcumin components that has also led to NP-gels against

growth of both gram bacteria. Moreover, the injectable NC gel enhanced 3rd burn healing rate as compared to Silvirin (a commercial drugs for burn treatment). Preparation and application of the hydrogels are demonstrated in Fig. 13.5 [74].

Li also reported an injectable curcumin nanoparticles-loaded N,O-carboxymethyl chitosan/oxidized alginate hydrogel exhibiting a high wound healing efficiency [75]. The system may also be applied for internal wounds due to its ability in minimally invasive implantation. Moreover, some injectable NC-gels have also developed from incorporation of antibacterial metallic nanoparticles in biocompatible and bioactive hydrogels for inhibiting microbe growth at wound sites [76, 77].

Utilization of some inorganic and carbon-based nanomaterials for enhancing efficiency of various injectable delivery systems has recently become an approach. Renae developed an injectable silicate nanoplatelets and gelatin-based hydrogel to effectively deliver the hMSC growth factor and enhance proliferation of human endothelial cells resulting in produced significantly myocardial angiogenesis at the injected site [78]. An injectable NC gel for effective vasculogenesis and cardiac repair was developed based DNA-VEGF-complexed polyethylenimine – graphene oxide nano-sheets and methacrylated gelatin (GelMA) hydrogels [79]. Gold nano-rods doped into a thermally responsive hydrogels were able to induce the contraction of the thermo-responsive

**Fig. 13.5** Thermosensitive biocompatible chitosan/gelatin and curcumin-based nanocomposite hydrogel for burn healing



hydrogels and trigger the release of loaded doxorubicin to inhibit breast cancer under NIR irradiation [80]. Other NIR-responsive nanoparticles such as carbon nanotubes and graphene oxide nanoparticles were also incorporated into thermosensitive polymers to harness NIR for remotely controlled drug delivery [81, 82]. The stimuli responsive NC gel has also developed from dopamine nanoparticle-loaded pNIPAAm-co-pAAM hydrogel, in which was loaded bortezomib and doxorubicin to apply in photo/thermal therapy and multidrug chemotherapy. NIR laser and dopamine nanoparticles controlled release behaviors of doxorubicin and bortezomib, respectively [83]. Gold nanorods were dispersed into the injectable *N*-isopropylacrylamide and methacrylated poly- $\beta$ -cyclodextrin copolymers-based hydrogels loaded doxorubicin that showed as an effectively long-term drug delivery platform in chemophotothermal synergistic cancer therapy. In addition, abundance of amphiphilic nature-driven copolymers performed a great biological properties could be utilized for fabricating several kinds of injectable materials [84, 85]. Such injectable multifunctional nanocomposite hydrogels would be well performed clinically in near future.

### 13.3 Electrospayed Microparticles for Biomedical Applications

In recent years, several nano (micro)particles (NMPs) have been emerging as the potential candidates in various drugs delivery systems due to their structural versatility in fabricating process that could efficiently load and deliver bioactive compounds, chemotherapeutics, proteins and nucleic acids to the desired site. Drug release behavior of the particles is moreover adjustable by their structural materials. We therefore focus on efficiency of electrospaying method in controlling drug delivery.

#### 13.3.1 Introduction of Electrospaying Method for Drug Delivery

Electrospaying is a significant technique for fabricating polymeric solid microparticles in drug carrier application. There are a lot of prospective advantages of this method such as simple one-step process, no or limited denaturation of biomacromolecules (drugs and proteins), high

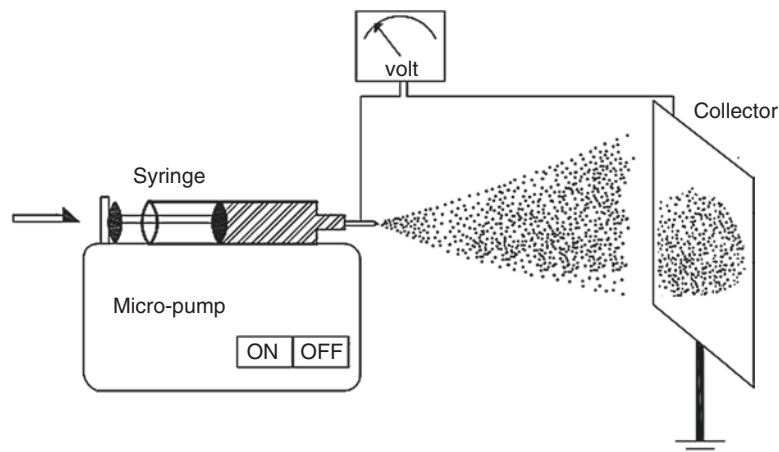
hydrophobic/hydrophilic drug encapsulation efficiency (EE) and loading capacity (LC), controlling the morphology and size of solid particles and high permeability to small molecules [86–88]. Similar to some well-known drug delivery systems, electrospaying technique fabricated particles have been studying to reduce or overcome these drawbacks of conventional therapeutic treatment by their prolong drug release and release onsite with a safe dose. Therefore, the particles have been one of the most efficient platforms for drug delivery system and tissue engineering. The mechanism release of drug from the particulate microparticles consists of 2 steps: The initial step is burst release since the drugs in and on their surface diffuse to the environment. The second step is release at slow and more constant by releasing the drug inside the particles due to the erosion of microparticles, consequences of degradation polymer matrix [89, 90]. The release profile was influenced by the morphology, size and size distribution of the microparticles [91–93]. In more details, the wrinkle and hollow particles have pores and larger surface area than that of the dense spheres, in consequence, the fluids penetrate inner the particles faster and the drugs are able to diffuse easily and rapidly. Whereas, the dense particles can reduce the fluid penetration and diffusion of drug in the polymer matrix because the drugs can move out of the particles through the pores so that it can maintain the constant release kinetics. In addition, the polymer concentration as well as the molecular weight of polymers (Mw), can tailor the morphology of particles and their release profile [94–97]. The low molecule weight of polymers causes intermolecular interaction weaken, thus it cannot encapsulate drug effectively and allow the diffusion of drug from the polymer more easily [93]. Besides, burst release can happen from smaller particles size. Microparticles with smaller size make the drug release faster due to the penetration of fluid and diffusion of drugs to the environment. They have a larger surface area to volume ratio than bigger particles so that they are eroded quickly as a consequence of degradation polymer matrix [98, 99]. Furthermore, the size distribution of polymeric particles causes uncontrollable

release rate of drug since the different size have different the drug release rate.

According to the of the essential literature of drug release and some factors which influence on release rate, the release of drug can be tailored by controlling the morphology and size of the microparticles. For electrospaying technique, how the morphology and size can be controlled? The fundamental principle of electrospaying method is that the high voltage was applied between the tip of the needle and the collector. Thanks to the electrical field force, the charged droplet issued from the tip will fly to the collector and form solid particles. During electrospaying, there was the competition between the coulomb fission and the polymer diffusion in the droplets. When the solvent evaporated, the charge density was increased inner the droplet and so that the coulomb fission divided a primary droplet into smaller droplets [98–100]. Finally, the solid particles were collected on the collector, as a consequence of the absolute evaporation of solvent as demonstrated in Fig. 13.6.

According to a basic theory of this method, adjusting the solvent, polymer concentration and flow rate seriously influenced the morphology of the electrospayed particles. Each solvent has specific properties such as electrical conductivity, evaporation rate, and viscosity so that it causes the changing morphologies. For faster-evaporating solvent as dichloromethane (DCM) has a low boiling point (40 °C) or chloroform (boiling point is 56 °C), the solvent in the droplet is evaporated quickly while the polymer chains don't have enough time to diffuse to inside the droplet. In addition, the surface of particles change solid although the solvent still is inner the particles, and during the time solvent diffuse and emit to the environment. Therefore, the final particles on the collector are wrinkles or even hollows and porous. From the opposite side, the low evaporating solvent as dimethyl formamide (DMF) and tetrahydrofuran (THF) have boiling points at 152 °C and 65 °C, respectively. The polymer chains have more time to diffuse from the surfaces of microparticles to inner when the solvent move out and evaporate completely. These result reported

**Fig. 13.6** Demonstration of an electro spraying technique for fabrication of particles was fabricated in our group



that electro sprayed particles are smaller and smooth surface as well as dense [94, 96, 98, 101]. Beside different evaporation rate, each solvent has different conductivity (or dielectric constant), it causes dissimilar to Coulomb fission in the droplet and leads to different particles size. Xie *et al.* reported that the size of PCL particles reduced when the conductivity of polymer solution increase, as a consequence of using different solvent as DCM ( $0.000275 \mu\text{S}/\text{cm}$ ) and Acetonitrile ( $0.071 \mu\text{S}/\text{cm}$ ) [94].

The second factor influences the morphology of microparticles is the chain entanglements in electro sprayed solution. The number of chain entanglements depends on the polymer concentration and molecular weight (Mw) [98, 102–104]. There are a few entanglements when the polymer concentration or Mw of polymer is low, thus electro sprayed particles is a film, disk, or semi-sphere in shape. Whereas, high polymer concentration or high molecular weight, the polymer solution occurs with higher density of chain entanglements, in consequence, tapered particles, beaded fibers, and event fibers will be created. The electro sprayed microspheres were achieved when the chain entanglements were generated effectively. And the electro sprayed droplet cannot be separated and deformed by Coulomb fission [105, 106]. The low Mw polymer can create the microspheres at high polymer concentration instead of hollow and porous par-

ticles, whereas high Mw polymer can generate the microspheres at low concentration. Because the polymer chains of high Mw polymer are longer, they overlap together easier and enhances the formation of the entanglements in the droplets [93, 102, 107].

Flow rate factor also effects on the morphology of the electro sprayed particles. A high flow rate causes particles deformed, aggregated and inconsistent morphology as a result of incompletely solvent evaporation. At the same polymer solution, the high flow rate produces a lower amount of chain entanglements and higher amount of solvent in the droplet, so that the polymer matrix cannot conserve the droplet integrity under the Coulomb fission and solvent evaporation. As a result, when the particles impact on the collector, they are collapsed and deformed. For example, the PLGA particles were deformed and stick together at the flow rate of 2 mL/h while at 1 mL/h, they formed the separated microparticles [93, 108]. Moreover, the size of particles created by a high flow rate is bigger than that of low flow rate [94, 95].

Apart from solvent, polymer concentration and flow rate, applied voltage is one of factors influences on morphology of the particles. When the applied voltage increased, the droplets were highly charged. Therefore, the microspheres were stretched and changed to elongated particles, tapered particles or beaded fibers [106,

109]. In addition, the high voltage strengthens the electric field force so that it makes the electrospaying mode change and it impacts on the size and size distribution or even the morphology. For instances, the multi-jet mode causes the irregular shape of particles and broaden the size distribution while the Taylor cone-jet mode generates the homogeneous particles and monodispersity. The morphology of particles is stable and homogeneous with the mono cone-jet mode however, the size of particles is increased slightly if the applied voltage increased, as a consequence of increasing Coulomb fission [93, 101].

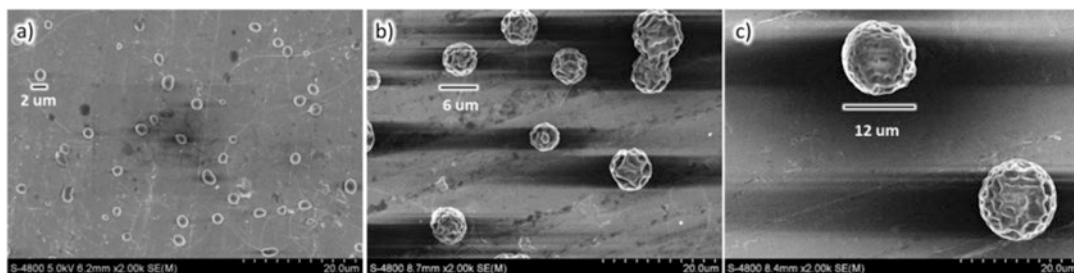
In case of collecting distance, it should be enough far to avoid deformed and aggregated particles because the solvent cannot evaporate completely and stay inside particles. In Arya's reported, chitosan particles were deformed and stick together at collecting distance of 6 cm, in consequence, it created a film while microspheres were formed separately at 7 cm [103]. Increasing the distances not only help polymer chain have time to diffuse and rearrange within the particles but also solvent was evaporated completely, so that more microspheres were obtained [93]. When the collecting distance is expanded enough far to create separate particles, the size of the particles is decreased when the collecting distance increase, as a result of the droplet had been still divided to smaller particles thanks to coulomb fission. However, at the constant voltage, if the collecting distance is too far and it overcomes the limitation, which maximizes of electric field force, the particles size will reduce [93, 108].

Besides all factors were regarded above, a diameter of the needle (Gauge) also influenced on particles size and size distribution. The microparticles which were produced by a bigger gauge have smaller size because the size of the droplet (or the volume of the droplet) at the tip of the needle reduces, in consequences, the final particles on the collector have smaller sizes [93]. However, the big gauge (small size of inner diameter's needle) can create the multi-jet mode, it leads to polydispersity and unrepeatable particles.

### 13.3.2 Fabricating Mono-Distribution and Homogeneous Morphology of PCL NMPs by Studying Electrospaying Modes and Tailoring the Parameters Processing

In this research, some kinds of solvent and solvent mixture were used to investigate the influence of solvent on microparticles morphology. With the main purpose of fabrication the homogeneous particles with smooth surfaces, the DMF solvent was chosen [94, 96, 97, 101]. Therefore, it has been used a mixture of two solvent. When the mixture solvent of DMF and chloroform (DMF/CHCl<sub>3</sub> = 3/1) was created, the morphology of particles was heterogeneous such as beaded fibers, elongated particles, and fibers (Fig. 13.7a). Because the physical properties of the solvent mixture such as solubility, evaporation rate and dielectric constant depended on both chloroform (56 °C, 4.8) and DMF (154 °C, 36.7) [110–112], so that the mixture caused an unstable spraying mode and formed collapsed, unstable and unrepeatable microparticles. Especially, the different conductivity (or dielectric constant) caused dissimilar to Coulomb fission in the droplet and leads to different particles size [110]. Therefore, the solvent mixture made undesirable morphology of PCL particles and should not be used for electrospaying. According to Fig. 13.7b and c, the electrospayed particles were microspheres although they were wrinkled. This phenomenon was explained that DCM and chloroform had high evaporation rate (their low boiling points, DCM (40 °C) and chloroform (56 °C) [113]), It made the external surface of particles are solidified quickly and became wrinkled. Furthermore, the dielectric constant of chloroform (4.8) was lower than DCM (9.1) so that the Coulomb fission formed from the electrostatic force is smaller in consequence; the size of PCL/DCM particles was smaller than the size of PCL/chloroform particles.





**Fig. 13.7** Microparticles SEM micrographs of 4% PCL solutions in different solvents (a) Mixture of Chloroform with DMF = 1:3 (v/v), (b) Chloroform, (c) DCM. (Applied

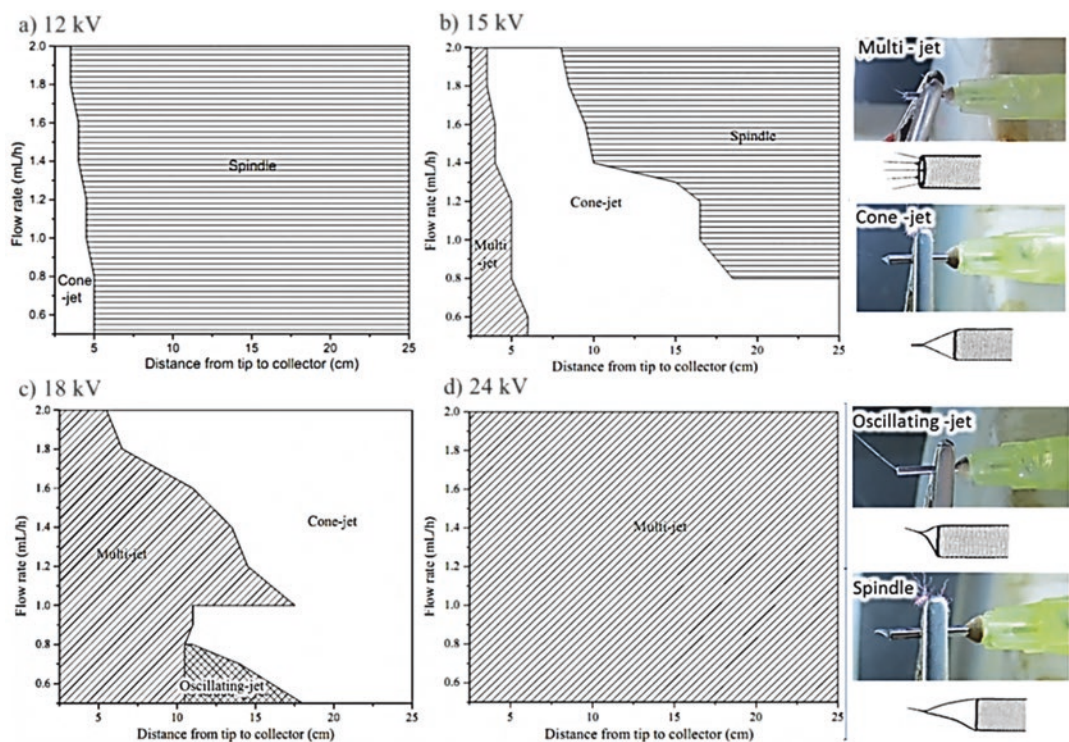
voltage: 18 kV, collecting distance: 18 cm, flow rate: 1 mL/h, gauge 20G)

According to some previous studies, the electro-spraying mode appreciably influenced both morphology and the size of the microparticles since the shape of the primary droplet issued from the tip of the needle can be formed some unstable spraying modes such as dripping, multi-jet, spindle and oscillating [109, 114]. These spraying modes are the undesirable because of their instability and unpredictability. In more details, multi-jet mode and oscillating-jet generate the satellite and secondary droplets, resulting in a broader size distribution and unrepeatable particles shapes. In case of dripping and spindle mode, the particles are bigger and deformed because the solvent still exists inside the particles. Whereas, the cone-jet mode generated almost uniform morphology and size of particles, especially the Taylor cone-jet was the most stable mode can maintain the spraying mode permanently as well as obtain homogeneous morphology and the mono-dispersity [98, 100, 109, 114, 115].

Our results indicated that when the flow rate was lower 2 mL/h and the collecting distance was from 5 cm to 25 cm, the surface tension of PCL solution was higher than the coulomb fission as a consequence of weak electrostatic force (Fig. 13.8a). It led to the polymer drop which ejected on the tip of the needle had irregular shapes as a spindle. In spindle mode, the droplets, as well as electro-sprayed particles, contained solvent so that the particles were deformed and aggregated. When the collecting distance was shorter (2.5–5 cm), the cone-jet mode was formed because the electric field force was strengthened

but this area was narrow. Increasing voltage to 15 kV, the spindle mode area decreased (flow rate of 0.8 mL/h to 2 mL/h, distance from 10 cm to 25 cm) while the cone-jet mode area increased (flow rate of 0.4 mL/h to 0.8 mL/h, distance from 6 cm to 25 cm and another area as seen in Fig. 13.8b).

Moreover, the multi-jet mode was appeared at the short distance in spite of small areas, as a consequence of high electric field force. The cone-jet mode area is biggest when the applied voltage is 18 kV, it spread from 0.5 mL/h to 2 mL/h of flow rate and from 15 cm to 25 cm of collecting distance. Besides, at 18 kV, the oscillating-jet mode (the vacant cone was formed at the tip of the needle and it changed position irregularly appeared when the flow rate is low (0.5–0.8 mL/h) and the collecting distance increased from 10 cm to 17 cm whereas the spindle mode vanished (Fig. 13.8c) [114]. It was a result of strengthening electrostatic force thanks to increasing applied voltage and the presence of a small solution volume ejected from tip of needle as a result of low flow rate. Especially, at the short collecting distance from 2.5 to 10 cm, the electric field force was strengthened by a high potential and a short collecting distance so that it overcame the surface tension of polymer solution, as a result of the larger multi-jet area. In addition, increasing flow rate generated a greater volume of solution so that the cone-jet mode was obtained more easily, however, it also depended on the electrical field force, if it is strong, the multi-jet mode was created. Therefore, when the applied voltage was increased to 24 kV, the multi-jet mode was



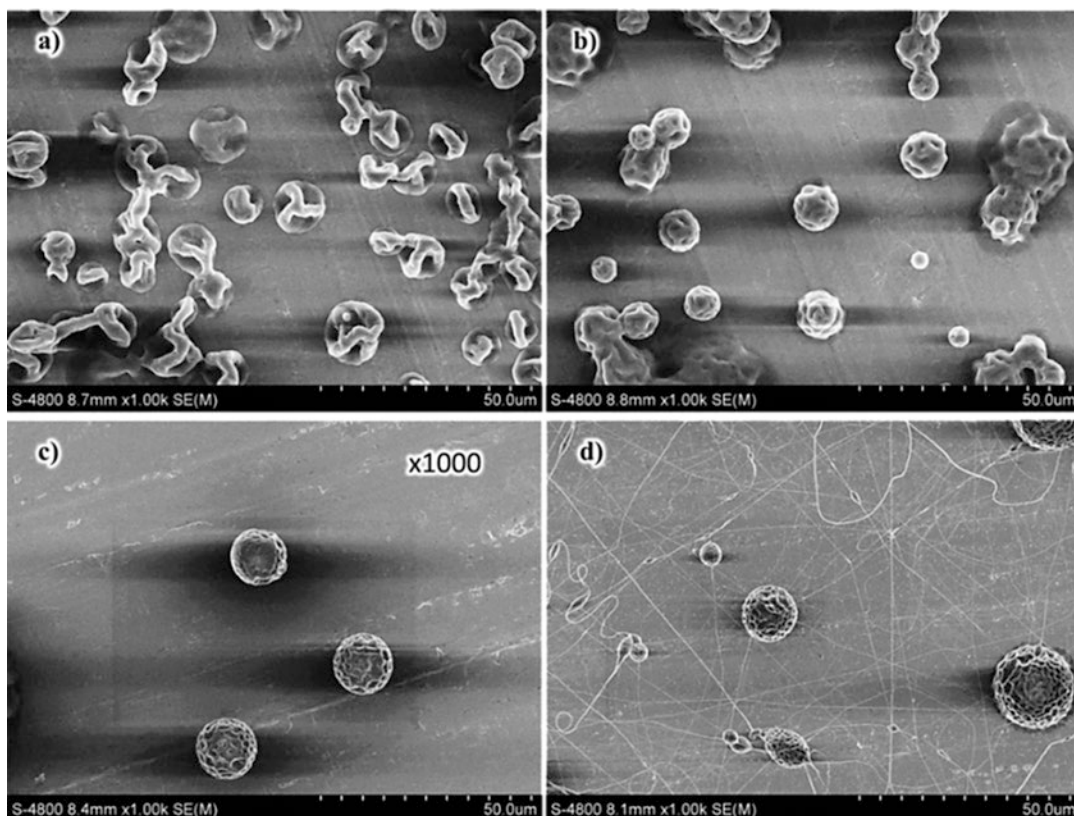
**Fig. 13.8** Mode selection maps to generate electrospaying modes (a) 12 kV, (b) 15 kV, (c) 18 kV, (d) 24 kV (4.5% PCL in DCM, 20G)

spread to all the flow rate of 0.5–2.0 mL/h and the collecting distance of 2.5–25.0 cm. The voltage applied to the needle and the collector was so high that it overcame the surface tension of the polymer droplets. Multi-jet generates the separation of a primary droplet into many small jets, so that, secondary and satellite particles appeared, in consequence, the solid particles were heterogeneous and had high distribution [114].

Another significant factor influenced on the morphology of PCL particles is polymer concentration. Although using different solvents as chloroform and DCM, the polymer concentration had the similar effects on the morphology of the electrospayed particles. At very low concentration, 1% PCL in chloroform, the morphology of the particles was hollow and semi-spherical as a consequence of lack chain entanglements in solution (Fig. 13.9a). Increasing Polymer concentration to 3% PCL in chloroform or 3.5% and 4% PCL in DCM, the entanglements weren't still enough to create microspheres; they generated corrugated

or distorted particles (Fig. 13.9c and Fig. 13.10a, b). Whereas, high polymer concentration caused the tapered particles, beaded fibers and event fibers, as a result of a huge amount of chain entanglements in the droplet (Figs. 13.9d and 13.10d). The microspheres were obtained at 4% PCL in chloroform and 4.5% PCL in DCM (Figs. 13.9c and 13.10d), as a result of the significant chain entanglements in droplets. This phenomenon is explained that the intermolecular interaction of polymer is different in the dissimilar solvent; it is stronger in chloroform than in DCM so that the chain entanglements were created more in chloroform.

Furthermore, microspheres had a tendency to agglomerate together if the surface of microspheres had been wetting, consequences of solvent still inside microspheres. The solvent still remained inside had evaporated during it flew from the tip of the needle to the collector. At the same processing parameters, the surface wetting property of particles had increased belong to the



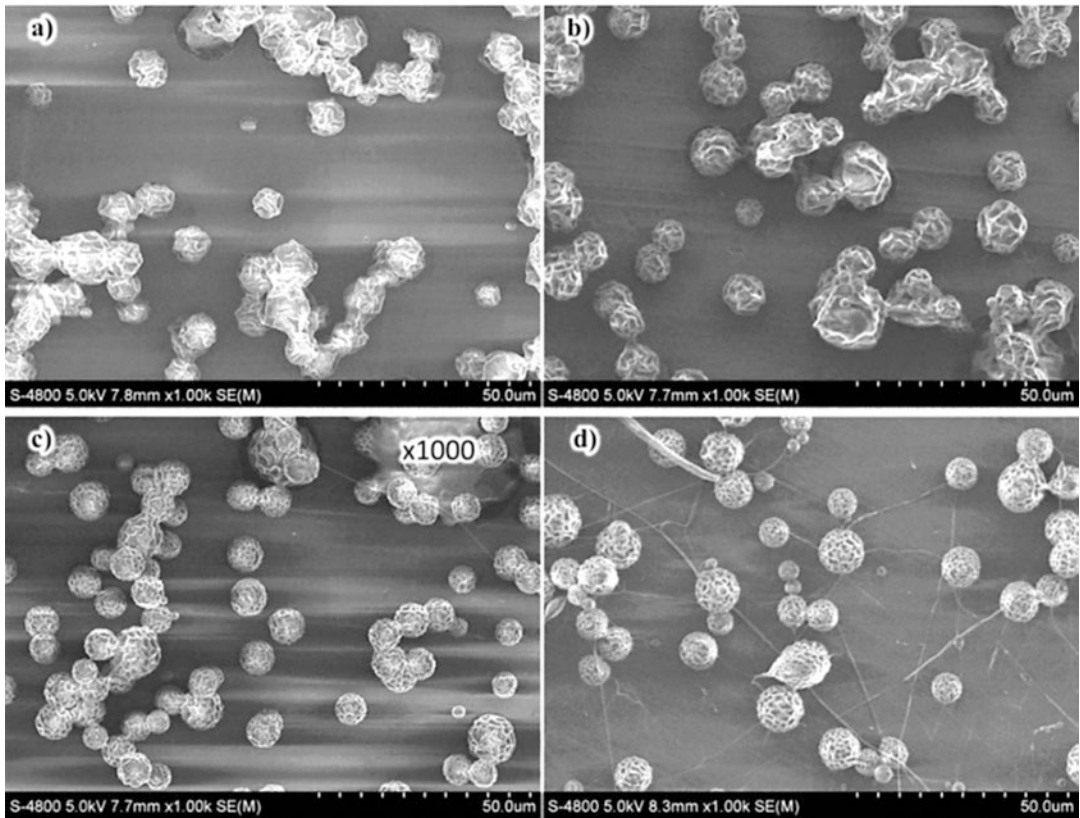
**Fig. 13.9** SEM micrographs of PCL microparticles in chloroform with different polymer concentration (a) 1%, (b) 3%, (c) 4%, and (d) 5% (voltage: 15 kV, collecting distance: 15 cm, flow rate: 1 mL/h, gauge 20G)

increased amount of solvent in PCL solutions. Therefore, the microspheres reduced agglomeration together when the PCL concentration was increased from 3.5% to 5% (Fig. 13.10).

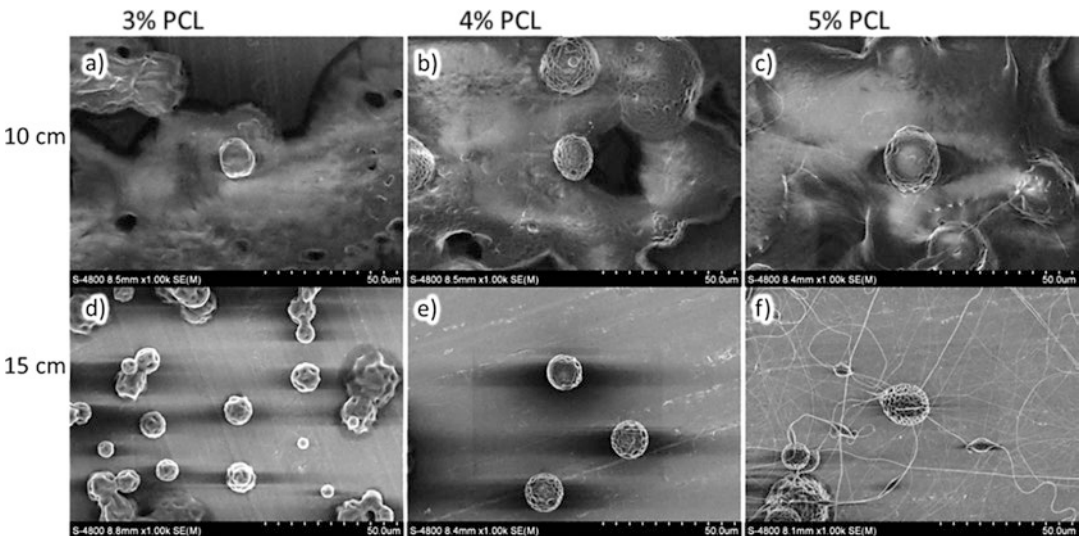
As showed in Fig. 13.11, near distances (10 cm) caused the particles deformed and collapsed since a lot of solvents were still inside the particles. When the final droplets (or the particles), which contained solvent impacted on the collector, they were plashed and covered on the collector [93, 103]. When other particles flew from the tip to collector and hit on it, they stick with the first particles, as a result, it created a film although the polymer concentration increased to 5%. Increasing collecting distance to 15 cm, the separate particles were generated, especially at high polymer concentration (4% and 5% PCL) (Fig. 13.11e and f). The reason is that chloroform had more time to evaporate and polymer can diffuse significantly in the droplet. However,

solution 3% PCL generated the deformed aggregated particles (Fig. 13.11d) while 4% and 5% PCL solution did not have the aggregation of particles. It was a result of the higher amount of solvent in 3% PCL solution than others. Therefore, the collecting distance should be over 15 cm for solvent evaporation completely.

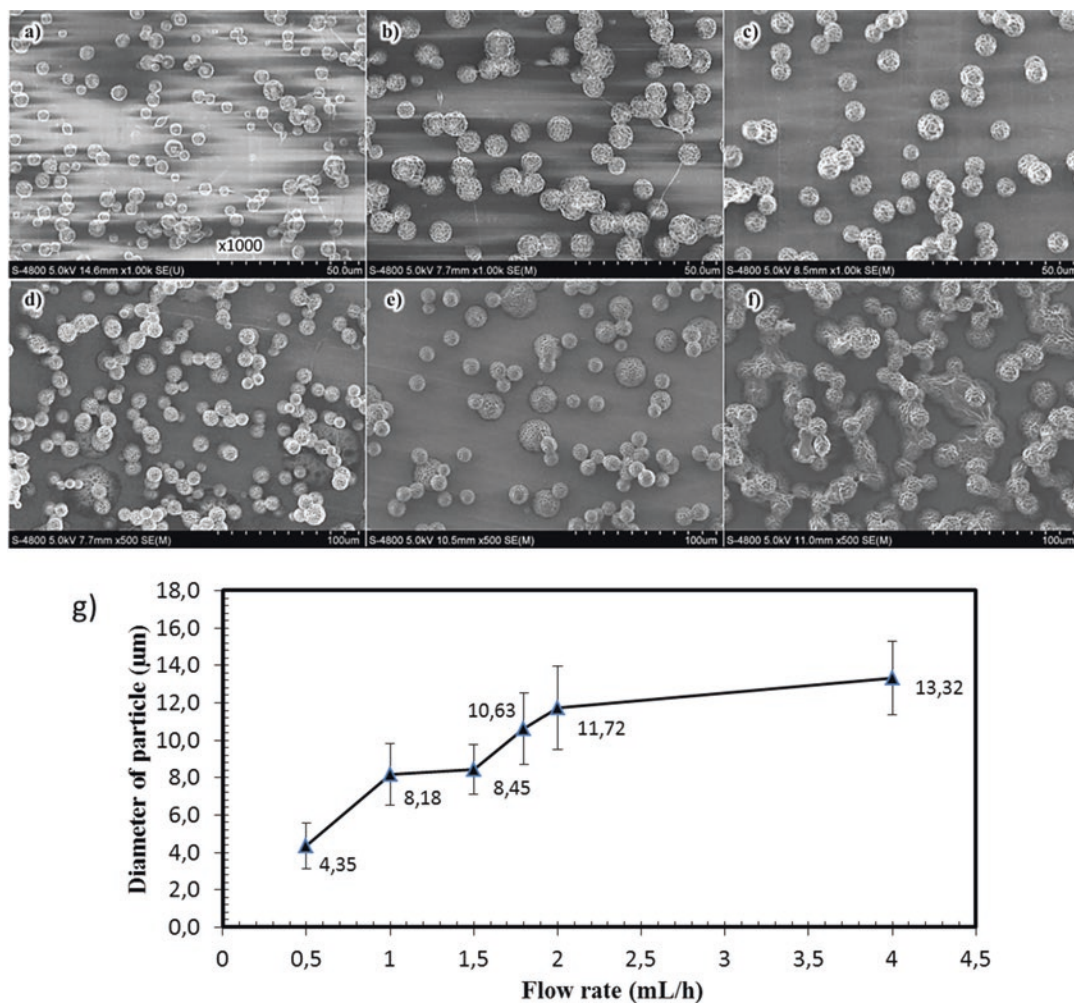
Changing faster-evaporated solvent like DCM, the microspheres were obtained at 4.5% PCL. The electrospayed particles were obtained homogeneous and separated microspheres at collecting distance of 20 cm while at 15 cm a heterogeneous morphology such as spheres, tapered particles, microbeads, and fibers was created. Because the chain entanglements had more time to diffuse and rearranged structure inside the droplet and solvent can evaporate completely when the collecting distance increased to 20 cm. When the distance was increased to 25 cm, the particles turned to corrugated spheres and the size distribution of particles



**Fig. 13.10** SEM micrographs of PCL microparticles in DCM with different polymer concentration (a) 3.5%, (b) 4%, (c) 4.5%, and (d) 5%(voltage: 18 kV, collecting distance: 20 cm, flow rate: 1 mL/h, gauge 20G)



**Fig. 13.11** SEM micrographs of PCL microparticles in chloroform with different polymer concentration (a) 3% PCL-10 cm, (b) 4% PCL-10 cm, (c) 5%PCL -10 cm (d) 3% PCL – 15 cm, (e) 4% PCL-15 cm, (f) 5% PCL -15 cm (flow rate 1 mL/h, voltage: 15 kV, gauge 20G)



**Fig. 13.12** SEM micrographs of particles with different flow rate (a) 0.5 mL/h, (b) 1 mL/h, (c) 1.5 mL/h, (d) 1.8 mL/h, (e) 2 mL/h (f) 4 mL/h and (g) the diagram of

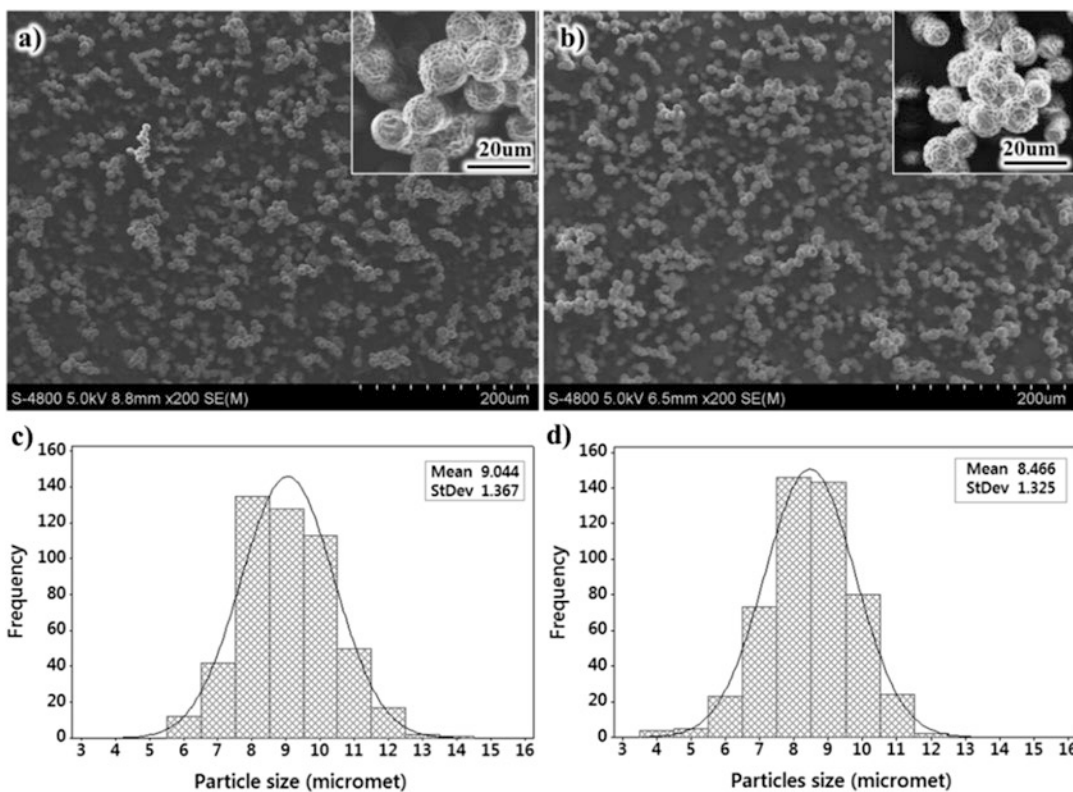
effect of the flow rate on the diameter of PCL particles (4.5% PCL in DCM, collecting distance: 20 cm, voltage: 18 KV, gauge 20G)

became broader than using 20 cm consequences of reducing electric field force [116]. The long collecting distances can overcome the limitation, which maximizes of electric field force, the particles size will reduce [93, 108]. The average diameter of particles reduced from 11.73  $\mu\text{m}$  to 7.93  $\mu\text{m}$  when the collecting distance increased gradually from 15 to 20 cm, as a result of increasing the time for separating droplets by the Coulomb fission into smaller particles. These results showed that with 20 cm distances, the homogeneous microspheres and narrow size distribution were obtained so that it was an optimal

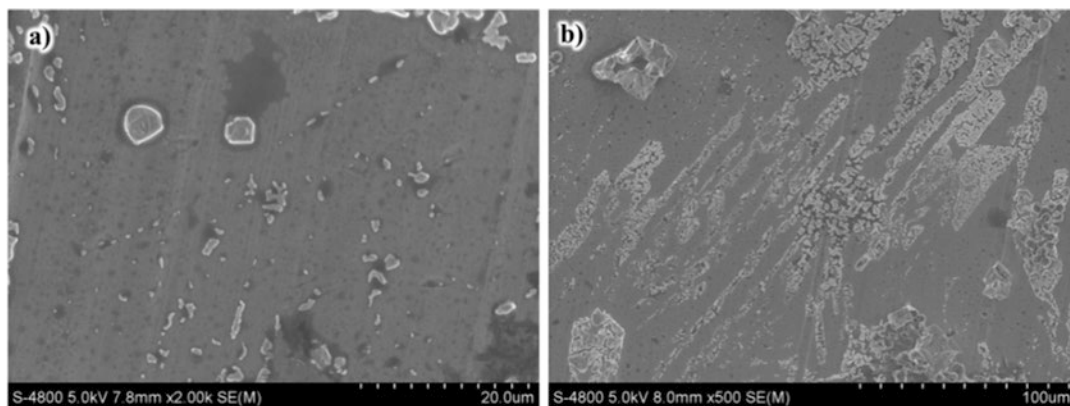
value [114]. At the same polymer solution of 4.5% PCL in DCM, low flow rate (0.5 mL/h and 1 mL/h) created a small primary droplet and high charge density, so that the Coulomb fission were strengthened and tend to separate to secondary and satellite particles. Besides, the volume of the cone issued from the tip of the needle was small, thanks to the solvent evaporation, the density of chain entanglements in the droplet were increased. Therefore, the electrospayed particles were heterogeneous and irregular in shapes such as spheres, tapered particles, beaded fibers and fibers (Fig. 13.12a and b).

According to Fig. 13.12c, d, e, microspheres were generated at flow rate from 1.5 mL/h to 2 mL/h, however, they were deformed and stick together or on collector when flow rate was higher (1.8 mL/h and 2 mL/h), as a consequence of the presence of solvent inside particles. The separate and homogeneous microspheres were obtained at flow rate 1.5 mL/h and the average of their diameter was 8.45  $\mu\text{m}$  with the smallest standard deviation (SD) of 1.33  $\mu\text{m}$  so that it was the optimize value in this experiments (Fig. 13.12c and g). The average diameter of particles was increased from 4.35  $\mu\text{m}$  to 13.32  $\mu\text{m}$  when the flow rate increased gradually from 0.5 mL/h to 4 mL/h (Fig. 13.12g). The reason is that at a high flow rate, the solution volume ejected from the needle increased so the size of particles was bigger, besides, some microparticles were collapsed and spread on the collector and this causes the bigger size.

Next factor effect on the size and size distribution of PCL microspheres is applied voltage so that it was investigated with different value 15 kV and 18 kV (because the cone-jet mode area was created at this value) (Fig. 13.8b and c). The optimal values for fabricating homogeneous microspheres such as the flow rate of 1.5 mL/h, polymer concentration of 4.5% PCL in DCM and the collecting distance of 20 cm were fixed. The microspheres were obtained at both 15 kV and 18 kV, however, the aggregation was generated at smaller applied voltage (15 kV) and the size of microspheres is bigger (9.044  $\mu\text{m}$ ) than the particles size using 18 kV (8.466  $\mu\text{m}$ ). The lower applied voltage caused the lower electric field force; in consequence, the coulomb fission was weaker to separate to smaller particles. In addition, due to the bigger size, the solvent was still inside the particles and microparticles were aggregated (Fig. 13.13).



**Fig. 13.13** SEM images and the size distribution histograms of PCL microparticles with different applied voltage. (a,c) 15 kV, (b,d) 18 kV, (collecting distance: 20 cm, flow rate: 1.5 mL/h, 4.5% PCL in DCM, 20G)



**Fig. 13.14** SEM images of electrospayed PCL particles after 40 days in in-vitro testing

Our studies indicated that the solvent in the PCL particles was evaporated completely after drying 48 h and it was determined by GC-MS testing. It determined that the electrospayed microparticles are non-toxic and can be used in pharmacy. Furthermore, after 40 days, the particles were degraded and formed fragment (Fig. 13.14). It showed that the particles were eroded quickly, as a consequence of degradation polymer matrix. The electrospayed PCL particles are suitable to apply for the permanent treatment some diseases in pharmacy and medicine application.

### 13.3.3 Fabrication Insulin or Paclitaxel Loaded Microparticles by Electrospaying

In drug carrier application, polymer types were chosen to depend on their desirable degradation and the release of drug from the polymer matrix. Both PLGA and PLA microparticles were suitable for short-term drug delivery due to a lot of ester groups in the structure. In the other hand, the PCL backbones have lack of ester groups and contain high crystalline so that their degradation is slow, as a result, PCL particles are suitable for long-term release system [87, 104, 117, 118]. According to some previous studies, PLGA encapsulated some kind of hydrophilic and hydrophobic drugs such as Rhodamine B [86],

Rifampicin [101], Celecoxib [92], oestradiol [98] and Taxol [119]. Although their encapsulation efficiency (EE) was high, the initial burst release happened in few hours. Increasing the number of drugs in electrospayed particles, the drug release becomes faster because of the porosity inside the particles and corrugated surfaces [92, 101, 119]. Besides PLGA particles, PLA particles can encapsulate BSA with high EE (81%) and LC (91%) [92] or the hydrophobic drug – Beclomethasone dipropionate (BDP) with EE 54% and the hydrophilic drug – Salbutamol sulfate (SS) EE = 56% [120]. In a report of Jing Wei Xie and Chi-Hwa Wang, Bovine Serum Albumin (BSA) – loaded PLGA particles fabricated by electrospaying had 20–21  $\mu\text{m}$  diameter with wrinkle surfaces (without emulsion) or smooth surface (with emulsion and 5–10% PluronicF127). The EE was 40–77%. An initial burst release was happened due to the BSA located on or in the wrinkle particles surface. The protein was diffused from the particles to the medium easily in few hours so that the BSA release gained 40–55% after 24 h. In case using emulsion with PluronicF127, the electrospayed BSA-loaded microparticles could maintain the sustained release, however, it was complicated to create the water-oil emulsion [119, 121]. Another research of their group is fabricating Paclitaxel (PTX) or Taxol-loaded PCL microparticles for treating the glioma C6 brain tumor. The particles size was 6–12  $\mu\text{m}$  with high EE (93–97%) [99]. The initial burst still was generated in 1–2 days. After that,

the drug release was maintained 10–27% amount of total drugs encapsulated in the particles within 22 days.

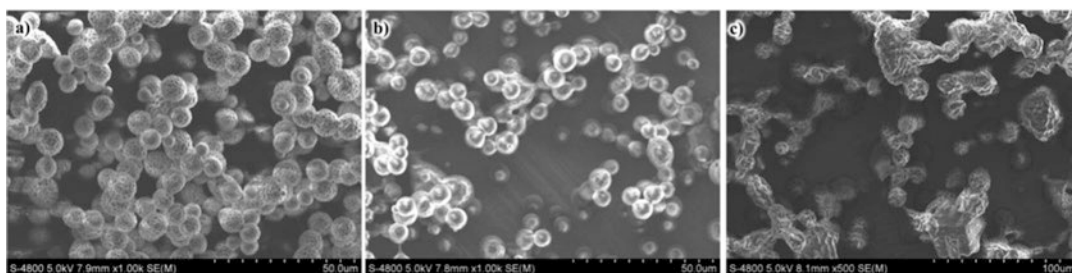
In some studies, the effects of polymer concentration and electrospayed processing parameters on the morphology and size of PCL drug/protein-loaded microparticles such as Taxol, Paclitaxel [94, 99],  $\beta$ -Oestradiol [98], Bovine serum albumin (BSA) [121] were investigated. However, the insulin-loaded PCL microparticles producing by electrospaying method have been new carrier system and need to develop in the pharmaceutical application.

Firstly, the mixture including PCL, Insulin, and DCM was prepared by dissolving mechanically PCL in DCM at room temperature. Then the insulin/PCL solution was prepared in a 10 ml glass syringe with stainless steel needle 20G (inner diameter 1.19) and placed in a Syringe pump (Top-5300, Japan). The high voltage (18 kV) was applied to the needle and the collector plate, which was covered with aluminum foil. During electrospaying, the droplets were separated into small particles and thanks to the solvent evaporation; the solid insulin-loaded PCL particles were formed. Then, they were dried for 2 days at room temperature to remove solvent completely.

Following all investigating of the effects of solvent, PCL concentration and parameters processing on the morphology, size and size distribution of the electrospayed of microparticles, these experiments were conducted with the flow rate of 1.2 mL/h, the applied voltage of 18 kV, needle gauge of 20G, and 4.5% PCL in DCM solvent. We used PTX which is hydrophobic drug

and insulin which is hydrophilic drug to fabricate the drug-loaded microparticles by electrospaying. The method fabricated PTX-loaded PCL particles was similar to insulin-loaded PCL. The results indicated that the nature of drug impact on the distribution of drug inside the polymer matrix, and morphology's particles.

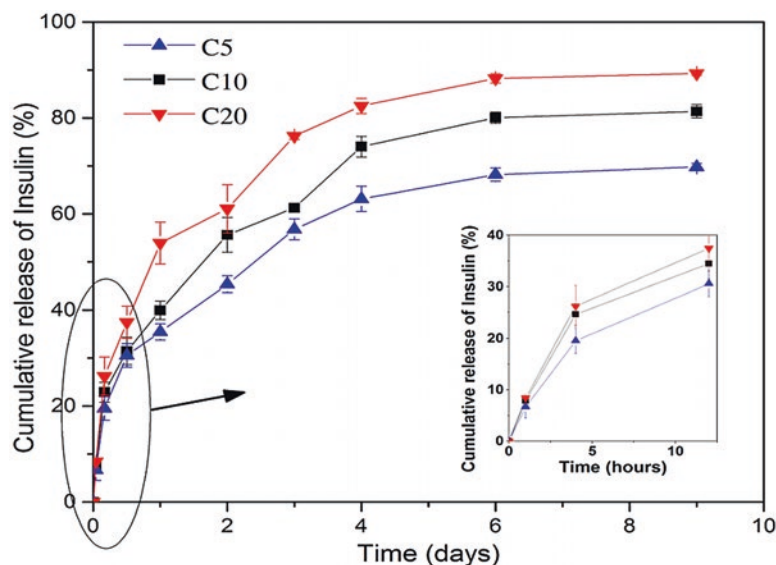
The morphology of PTX-loaded particles (15% PTX/PCL, wt/wt) is microspheres with smooth surfaces (Fig. 13.15b) as compared unloaded PCL particles (Fig. 13.15a). Hydrophobic macromolecules can be compatible with PCL, so that small molecule of PTX could fill the hollow, pore and wrinkle on the structure of particles, leading to the smooth and dense particles [99]. Besides, the size of the PTX-loaded particles is smaller (6.98  $\mu\text{m}$ ) than the PCL microspheres (8.47  $\mu\text{m}$ ). This phenomenon can be explained like that, the PTX/PCL solution had bigger surface tension than the PCL solution, so that the Taylor cone-jet mode was formed, as a result of their size distribution was monodispersity. In contrary, the size distribution of PCL particles was bidispersity due to the secondary and satellites droplet, as a consequence of non-Taylor cone-jet mode formation. In case of insulin, a hydrophilic drug, it was unincorporated in PCL solution, which is hydrophobic so that the mixture of insulin and PCL solution was a suspension. Lack of solubility of the insulin in polymer solution caused not only the sedimentation during spraying but also the migration of drug on and near the surface particles [122]. As showed in Fig. 13.15c, the morphologies of the insulin-loaded particles were collapsed and irregular particles. This is a result of unincorporated insulin/



**Fig. 13.15** SEM images of PCL microparticles (a) blank (no drug) (b) 15% PTX/PCL (wt/wt) and (c) 20% insulin/PCL (wt/wt) (collecting distance: 20 cm, flow rate: 1.2 mL/h, 4.5% PCL in DCM, 20G)



**Fig. 13.16** The release of insulin from chitosan NMPs in different amount of insulin (C5, C10 and C20: 5%, 10%, 20% insulin in chitosan particles)



PCL suspension and lack of diffusion of the drug as well as polymer in solution. This system can be created by combining both hydrophobic (PTX) and hydrophilic drug (insulin) with PCL.

Chitosan, another natural polymer was used in fabricating electrosprayed NMPs in our study. The polysaccharide can load the Ampicillin, BSA, and Doxorubicin [103, 123, 124] with high EE. Our research focuses on fabricating the insulin-loaded chitosan by electrospraying method. The effect of insulin concentration on the release of drug was investigated. Thanks to controllable morphology and size of the particles, the degradation and the release of drug sustained over the investigated time as seen in Fig. 13.16. The drug carrier system should be studied further for extending its practical applications. Such electrosprayed drug-loaded particles could be emerging delivery systems in future [87, 88, 104, 125–127].

### 13.4 Future Perspective

Regarding to the above demonstration, preparation of polymeric nanoparticles or/and incorporation of several kinds of nanoparticles into injectable hydrogel systems produced multifunctional nanocomposite biomaterials that have paid many ways to apply in tissue engineering, drug

delivery, antimicrobial materials, and etc. these systems effectively delivery from various chemotherapeutic drugs/proteins/gene to bioactive compounds as well as phytochemicals. The structure of these materials has been gradually well-designed to satisfy with treatment and harmony with physiologically internal conditions such as pH, enzyme and biochemical reactions. They also incorporated with external stimuli (temperature, near-IR irradiation, UV-Vis light, magnetic fields, ultrasound energy and etc.) to enhance effectiveness in biomedical applications. Such injectable multifunctional nanocomposite hydrogels would be well-performed clinically in near future. Other corporations of metallic or carbon-based nanoparticles could also improve the efficiency of conventional drugs via an additionally synergistic effect of the photo/thermal therapy.

For electrosprayed NMPs, the technique could also be studied further for applications due to their high drug loading efficiency and prolong drug release onsite with a safety dose. It is also potential practically because the electrosprayed NMPs could be produced in large scale in which loading various drugs and bioactive compound without denaturation.

**Acknowledgement** This research is funded by Vietnam National University Ho Chi Minh City (VNU-HCM)

under grant number B2015-20a-01. Some of the material characterization facilities are supported by National key lab for Polymer and Composite Materials-HCMUT, VAST and HUIFI. This work was also financially supported by Vietnam Academy of Science and Technology (VAST) under Grant Number VAST03.08/17-18 and Vietnam National Foundation for Science & Technology Development (NAFOSTED) [grant number 106-YS.99-2014.33].

## References

1. Yuan Y, Lin D, Chen F, Liu C (2014) Clinical translation of biomedical materials and the key factors towards product registration. *J Orthop Transl* 2(2):49–55
2. Li Y, Rodrigues J, Tomás H (2012) Injectable and biodegradable hydrogels: gelation, biodegradation and biomedical applications. *Chem Soc Rev* 41(6):2193–2221
3. Scaffaro R, Lopresti F, Maio A, Suter F, Botta L (2017) Development of polymeric functionally graded scaffolds: a brief review. *J Appl Biomater Funct Mater* 15(2):107–121
4. Schmaljohann D (2006) Thermo- and pH-responsive polymers in drug delivery. *Adv Drug Deliv Rev* 58(15):1655–1670
5. Kurisawa M, Chung JE, Yang YY, Gao SJ, Uyama H (2005) Injectable biodegradable hydrogels composed of hyaluronic acid-tyramine conjugates for drug delivery and tissue engineering. *Chem Commun* 34:4312–4314
6. Wu YL, Wang H, Qiu YK, Liow SS, Li Z, Loh XJ (2016) PHB-based gels as delivery agents of chemotherapeutics for the effective shrinkage of tumors. *Adv Healthc Mater* 5(20):2679–2685
7. Shu XZ, Liu Y, Palumbo FS, Luo Y, Prestwich GD (2004) In situ crosslinkable hyaluronan hydrogels for tissue engineering. *Biomaterials* 25:1339–1348
8. Ito T, Yeo Y, Highley CB, Bellas E, Benitez CA, Kohane DS (2007) The prevention of peritoneal adhesions by in-situ cross-linking hydrogels of hyaluronic acid and cellulose derivatives. *Biomaterials* 28(6):3418–3426
9. Milczek EM Commercial applications for enzyme-mediated protein conjugation: new developments in enzymatic processes to deliver functionalized proteins on the commercial scale. *Chem Rev* 118:119–141. <https://doi.org/10.1021/acs.chemrev.6b00832>
10. Nasir A, Kausar A, Younus A (2015) A review on preparation, properties and applications of polymeric nanoparticle-based materials. *Polym-Plast Technol Eng* 54(4):325–341
11. Elsbahya M, Wooley KL (2012) Design of polymeric nanoparticles for biomedical delivery applications. *Chem Soc Rev* 41(7):2545–2561
12. Rastogi L, Arunachalam J (2013) Synthesis and characterization of bovine serum albumin–copolymer nanocomposites for antibacterial applications. *Colloids Surf B Biointerfaces* 108:134–141
13. Adavallan K, Krishnakumar N (2014) Mulberry leaf extract mediated synthesis of gold nanoparticles and its anti-bacterial activity against human pathogens. *Adv Nat Sci Nanosci Nano Technol* 5(2):25018
14. Cao VD, Nguyen PP, Vo QK, Nguyen CK, Nguyen XC, Dang CH, Tran NQ (2014) Ultrafine copper nanoparticles exhibiting a powerful antifungal/killing activity against *Corticium salmonicolor*. *Bull Kor Chem Soc* 35(9):2645–2648
15. Nguyen TH, Huynh CK, Niem VVT, Vo VT, Tran NQ, Nguyen DH, Anh MNT (2016) Microwave-assisted synthesis of chitosan/polyvinyl alcohol silver nanoparticles gel for wound dressing applications. *Int J Polym Sci* 2016:1584046
16. Tra TN, Huynh CK, Hoai NTT, Bao BC, Tran NQ, Vo VT, Nguyen TH (2016) Fabrication of electrospun polycaprolactone coated with chitosan-silver nanoparticles membranes for wound dressing applications. *J Mater Sci Mater Med* 27(10):156
17. Suriyakalaa U, Antony JJ, Suganya S, Siva D, Sukirtha R, Kamalakkannan S, Pichiah PBT, Achiraman S (2013) Hepatocurative activity of biosynthesized silver nanoparticles fabricated using *Andrographis paniculata*. *Colloids Surf B Biointerfaces* 102:189–194
18. Mody VV, Siwale R, Singh A, Mody HR (2010) Introduction to metallic nanoparticles. *J Pharm Bioallied Sci* 2(4):282–289
19. Cao VD, Tran NQ, Nguyen TPP (2015) Synergistic effect of citrate dispersant and capping polymers on controlling size growth of ultrafine copper nanoparticles. *J Exp Nanosci* 10(8):576–587
20. Ngo HM, Nguyen PP, Tran NQ (2014) Preparation of nanoclusters encapsulating ultrafine platinum nanoparticles. *Asian J Chem* 26(23):8079–8083
21. Cu TS, Cao VD, Nguyen CK, Tran NQ (2014) Preparation of silver core-chitosan shell nanoparticles using catechol-functionalized chitosan and antibacterial studies. *Macromol Res* 22(4):418–423
22. Ho VA, Le PT, Nguyen TP, Nguyen CK, Nguyen VT, Tran NQ (2015) Silver core-shell nanoclusters exhibiting strong growth inhibition of plant-pathogenic fungi. *J Nanomater* 16(1):13
23. Nandi SK, Roy S, Mukherjee P, Kundu B, De DK, Basu D (2010) Orthopaedic applications of bone graft & graft substitutes: a review. *Indian J Med Res* 132:15–30
24. Kalita SJ, Bhardwaj A, Bhatt HA (2017) Nanocrystalline calcium phosphate ceramics in biomedical engineering. *Mater Sci Eng C* 27(3):441–449
25. Choi BS, Kim SH, Yun SJ, Ha HJ, Kim MS, Yang YI, Son Y, Khang G, Rhee JM, Lee HB (2008) Demineralized bone particle (DBP) suppressed the inflammatory reaction of poly (lactide-co-glycolide) scaffold. *Tissue Eng Regen Med* 3:295
26. Kaito T, Mukai Y, Nishikawa M, Ando W, Yoshikawa H, Myoui A (2006) Dual hydroxyapatite composite

- with porous and solid parts : experimental study using canine lumbar inter body fusion model. *J Biomed Mater Res B Appl Biomater* 78:378–384
27. Santos MH, Valerio P, Goes AM, Leite MF, Heneine LG, Mansur HS (2007) Biocompatibility evaluation of hydroxyapatite/ collagen nanocomposites doped with Zn<sup>2+</sup>. *Biomed Mater* 2:135–141
  28. Nguyen TTT, Tran TV, Tran NQ, Nguyen CK, Nguyen DH (2017) Hierarchical self-assembly of heparin-PEG end-capped porous silica as a redox sensitive nanocarrier for doxorubicin delivery. *Mater Sci Eng C: Mater Biol Appl* 70(2):947–954
  29. Liua Y, Maib S, Li N, Yiud CKY, Maoa J, Pashleye DH, Tay FR (2011) Differences between top-down and bottom-up approaches in mineralizing thick, partially-demineralized collagen scaffolds. *Acta Biomater* 7(4):1742–1751
  30. Mittal AK, Chisti Y, Banerjee UC (2013) Synthesis of metallic nanoparticles using plant extracts. *Biotechnol Adv* 31:346–356
  31. Ma P, Mumper RJ (2013) Paclitaxel, nano-delivery systems: a comprehensive review. *J Nanomed Nanotechnol* 4(2):1000164
  32. Anselmo AC, Mitragotri S (2016) Nanoparticles in the clinic. *Bioeng Transl Med* 1(1):10–29
  33. Choi JH, Bae JW, Choi JW, Joung YK, Tran NQ, Park KD (2011) Self-assembled nanogel of pluronic-conjugated heparin as a versatile drug nanocarrier. *Macromol Res* 19(2):180–188
  34. Nguyen H, Nguyen NH, Tran NQ, Nguyen CK (2015) Improved method for cisplatin-loading dendrimer and behavior of the complex nanoparticles in vitro release and cytotoxicity. *J Nanosci Nanotechnol* 15(6):4106–4110
  35. Tong NNA, Nguyen TP, Nguyen CK, Tran NQ (2016) Aquated cisplatin and heparin-pluronic nanocomplexes exhibiting sustainable release of active platinum compound and nci-h460 lung cancer cell anti-proliferation. *J Biomater Sci Polym Ed* 27(8):709–720
  36. Van TD, Tran NQ, Nguyen DH, Nguyen CK, Tran DL, Nguyen TP (2016) Injectable hydrogel composite based gelatin-PEG and biphasic calcium phosphate nanoparticles for bone regeneration. *J Electron Mater* 45(5):2415–2422
  37. Tang R, Cai Y (2008) Calcium phosphate nanoparticles in biomineralization and biomaterials. *J Mater Chem* 18:3775–3787
  38. Son KD, Kim YJ (2017) Anticancer activity of drug-loaded calcium phosphate nanocomposites against human osteosarcoma. *Biomater Res* 21:13
  39. AEI F, Kim JH, Kim HW (2015) Osteoinductive fibrous scaffolds of biopolymer/mesoporous bioactive glass nanocarriers with excellent bioactivity and long-term delivery of osteogenic drug. *ACS Appl Mater Interfaces* 7(2):1140–1152
  40. Vichery C, Nedelec JM (2016) Bioactive glass nanoparticles: from synthesis to materials design for biomedical applications. *Materials* 9(4):288
  41. Yoon SJ, Park KS, Kim MS, Rhee JM, Khang G, Lee HB (2007) Repair of diaphyseal bone defects with calcitriol-loaded PLGA scaffolds and marrow stromal cells. *Tissue Eng* 13(5):1125–1133
  42. Sheikh FA, Ju HW, Moon BM, Lee OJ, Kim JH, Park HJ, Kim DW, Kim DK, Jang JE, Khang G PCH (2015) Hybrid scaffolds based on PLGA and silk for bone tissue engineering. *J Tissue Eng Regen Med* 10(3):209–221
  43. Kamalaldin N, Jaafar M, Zubairi S, Yahaya B (2017) Physico-mechanical properties of HA/TCP pellets and their three-dimensional biological evaluation in vitro. *Adv Exp Med Biol*. Springer, Boston, MA. [https://doi.org/10.1007/5584\\_2017\\_130](https://doi.org/10.1007/5584_2017_130)
  44. Domènech B, Muñoz M, Muraviev DN, Macanás J (2013) Polymer-silver nanocomposites as antibacterial materials. *Formatex Res Cent* 1:630–640
  45. Benn T, Cavanagh B, Hristovski K, Posner JD, Westerhoff P (2010) The release of nanosilver from consumer products used in the home. *J Environ Qual* 39(6):1875–1882
  46. Boomi P, Prabu HG, Mathiyarasu J (2013) Synthesis and characterization of polyaniline/Ag-Ptnanocomposite for improved antibacterial activity. *Colloids Surf B Biointerfaces* 103:9–14
  47. Huang L, Yang H, Zhang Y, Xiao W (2016) Study on synthesis and antibacterial properties of Ag NPs/GO nanocomposites. *J Nanomater* 2016:1–9
  48. Tavakoli J, Tang Y (2017) Hydrogel based sensors for biomedical applications: an updated review. *Polymers* 9(8):364
  49. Shukla SK, Deshpande SR, Shukla SK, Tiwari A (2012) Fabrication of a tunable glucose biosensor based on zinc oxide/chitosan-graft-poly(vinyl alcohol) core-shell nanocomposite. *Talanta* 99:283–287
  50. Wang W, Li HY, Zhang DW, Jiang J, Cui YR, Qiu S, Zhou YL, Zhang XX Fabrication of bienzymatic glucose biosensor based on novel gold nanoparticles-bacteria cellulose nanofibers nanocomposite. *Electroanalysis* 22(21):2543–2550
  51. Tamer U, Seçkin Aİ, Temur E, Torul H (2011) Fabrication of biosensor based on polyaniline/gold nanorod composite. *Int J Electrochem* 2011:869742
  52. Zhang H, Li P, Wu M (2015) One-step electrode position of gold-graphene nanocomposite for construction of cholesterol biosensor. *Biosens J* 4(2):1000128
  53. Tran NQ, Joung YK, Choi JH, Park KM, Park KD (2012) In situ-forming quercetin-conjugated heparin hydrogels for blood compatible and antiproliferative metal coating. *J Bioact Compat Polym* 27(4):313–326
  54. Nguyen TP, Ho VA, Nguyen DH, Nguyen CK, Tran NQ, Lee YK, Park KD (2015) Enzyme-mediated fabrication of the oxidized chitosan hydrogel for tissue sealant. *J Bioact compat polym* 30(4):412–423
  55. Tong NNA, Nguyen TH, Nguyen DH, Nguyen CK, Tran NQ (2015) In situ preparation and characterizations of cationic dendrimer-based hydrogels

- for controlled heparin release. *J Macromol Sci A* 52(10):830–837
56. Nguyen CK, Tran NQ, Nguyen TP, Nguyen DH (2016) Biocompatible nanomaterials based on dendrimers, hydrogels and hydrogel nanocomposites for use in biomedicine. *Adv Nat Sci Nanosci Nanotechnol* 8(1):015001
57. Nguyen TBT, Dang TLH, Nguyen TTT, Tran DL, Nguyen DH, Nguyen VT, Nguyen CK, Nguyen TH, Le VT, Tran NQ (2016) Green processing of thermo-sensitive nanocurcumin-encapsulated chitosan hydrogel towards biomedical application. *Green Process synth* 5(6):511–520
58. Culver HR, Clegg JR, Peppas NA (2017) Analyte-responsive hydrogels: intelligent materials for biosensing and drug delivery. *Acc Chem Res* 50(2):170–178
59. Omid M, Yadegari A, Tayebi L (2017) Wound dressing application of pH-sensitive carbon dots/chitosan hydrogel. *Acc Chem Res* 7:10638–10649
60. Merino S, Martín C, Kostarelou K, Prato M, Vázquez E (2015) Nanocomposite hydrogels: 3D polymer-nanoparticle synergies for on-demand drug delivery. *ACS Nano* 9(5):4686–4697
61. Gao W, Zhang Y, Zhang Q, Zhang L (2016) Nanoparticle-hydrogel: a hybrid biomaterial system for localized drug delivery. *Ann Biomed Eng* 44(6):2049–2061
62. Nguyen CK, Nguyen DH, Tran NQ (2013) Tetric-grafted chitosan hydrogel as an injectable and biocompatible scaffold for biomedical applications. *J Biomater Sci* 24(14):1636–1648
63. Tran NQ, Joung YK, Lih E, Park KM, Park KD (2011) RGD-conjugated in situ forming hydrogels as cell-adhesive injectable scaffolds. *Macromol Res* 19:300–306
64. Tiwari A, Grailler JJ, Pilla S, Steeber DA, Gong S (2001) Biodegradable hydrogels based on novel photopolymerizable guar gum–methacrylate macromonomers for in situ fabrication of tissue engineering scaffolds. *Acta Biomater* 5(9):3441–3452
65. Lee KY, Mooney DJ (2001) Hydrogels for tissue engineering. *Chem Rev* 101(7):1869–1880
66. Tran NQ, Joung YK, Lih E, Park KM, Park KD (2010) Supramolecular hydrogels exhibiting fast in situ gel forming and adjustable degradation properties. *Biomacromol* 11(3):617–625
67. Shu XZ, Liu Y, Palumbo FS, Luo Y, Prestwich GD (2004) In situ crosslinkable hyaluronan hydrogels for tissue engineering. *Biomaterials* 25(7–8):1339–1348
68. Nguyen TP, Van TD, Nguyen CK, Nguyen DH, Tran DL, Tran NQ (2014) Injectable hydrogel composites based chitosan and BCP nanoparticles for bone regeneration. *Adv Nat Sci: NanoSci Nanotechnol* 45(5):2415–2422
69. Fu SZ, Guo G, Gong CY, Zeng S, Liang H, Luo F, Zhang XN, Zhao X, Wei YQ, Qian ZY (2009) Injectable biodegradable thermosensitive hydrogel composite for orthopedic tissue engineering. *J Phys Chem B* 113(52):16518–16525
70. Fu S, Ni P, Wang B, Chu B, Zheng L, Luo F, Luo J, Qian Z (2012) Injectable and thermo-sensitive PEG-PCL-PEG copolymer/collagen/n-HA hydrogel composite for guided bone regeneration. *Biomaterials* 33(19):4801–4809
71. Dang TLH, Van TD, Truong MD, Tran NQ, Tran LBH, Nguyen KH, Nguyen CK, Nguyen TP (2016) Mineralization of oxidized alginate gelatin biphasic calcium phosphate hydrogel composite for bone regeneration. *J Mater Sci Eng Adv Technol* 14(1):19–38
72. Priya MV, Sivshanmugam A, Boccaccini AR, Goudouri OM, Sun W, Hwang N, Deepthi S, Nair SV, Jayakumar R (2016) Injectable osteogenic and angiogenic nanocomposite hydrogels for irregular bone defects. *Biomed Mater* 11(3):035017
73. Nguyen TT, Nguyen TP, Bui TT, Nguyen TT, Nguyen HBSL, Tran QS, Nguyen TP, Nguyen CK, Nguyen DH, Tran NQ (2017) Enzymatic preparation of modulated-biodegradable hydrogel nanocomposites based chitosan/gelatin and biphasic calcium phosphate nanoparticles. *J Sci Technol* 55(1B):185–192
74. Nguyen TP, Doan BHP, Dang DV, Nguyen CK and Tran NQ (2014) Enzyme-mediated in situ preparation of biocompatible hydrogel composites from chitosan derivative and biphasic calcium phosphate nanoparticles for bone regeneration. *Adv Nat Sci Nanosci Nanotechnol* 5:015012
75. Li X, Chen S, Zhang B, Li M, Diao K, Zhang Z, Li J, Xu Y, Wang X, Chen H (2012) In situ injectable nano-composite hydrogel composed of curcumin, N,O-carboxymethyl chitosan and oxidized, alginate for wound healing application. *Int J Pharm* 437(1–2):110–119
76. González-Sánchez MI, Perni S, Tommasi G, Morris NG, Hawkins K, López-Cabarcos E, Prokopovich P (2015) Silver nanoparticle based antibacterial methacrylate hydrogels potential for bone graft applications. *Mater Sci Eng C Mater Biol Appl* 50:332–340
77. Jiang H, Zhang G, Xu B, Feng X, Bai Q, Yang G, Li H (2016) Thermosensitive antibacterial Ag nanocomposite hydrogels made by a one-step green synthesis strategy. *New J Chem* 40(8):6650–6657
78. Waters R, Pacelli S, Maloney R, Paul A (2016) Local delivery of stem cell growth factors with injectable hydrogels for myocardial therapy. *Front Bioeng Biotechnol Conference Abstract: 10th World Biomaterials Congress*. <https://doi.org/10.3389/conf.FBIOE.2016.01.00063>
79. Paul A, Hasan A, Kindi HA, Gaharwar AK, Rao VTS, Nikkiah M, Shin SR, Krafft D, Dokmeci MR, Shum-Tim D, Khademhosseini A, Shum-Tim D, Khademhosseini A (2014) Injectable graphene oxide/hydrogel-based angiogenic gene delivery system for vasculogenesis and cardiac repair. *ACS Nano* 8(8):8050–8062
80. Zhao X, Ding X, Deng Z, Zheng Z, Peng Y, Tian C, Long X (2006) A kind of smart gold nanoparticle-hydrogel composite with tunable thermo-switchable electrical properties. *New J Chem* 30(6):915–920

81. Zhu CH, Lu Y, Peng J, Chen JF, Yu SH (2012) Photothermally sensitive poly(n-isopropylacrylamide)/graphene oxide nanocomposite hydrogels as remote light-controlled liquid microvalves. *Adv Funct Mater* 22(19):4017–4022
82. Yan B, Boyer JC, Habault D, Branda NR, Zhao Y (2012) Near infrared light triggered release of biomacromolecules from hydrogels loaded with upconversion nanoparticles. *J Am Chem Soc* 134(40):16558–16561
83. Ghavami Nejad A, SamariKhalaj M, Aguilar LE, Park CH, Kim CS (2016) pH/NIR light-controlled multidrug release via a mussel-inspired nanocomposite hydrogel for chemo-photothermal cancer therapy. *Scientific Reports* 6. Article number: 33594
84. Nguyen TNA, Cao VD, Nguyen CK, Nguyen TP, Nguyen XTDT, Tran NQ (2017) Thermosensitive heparin-pluronic copolymer as effective dual anti-cancer drugs delivery system for combination cancer therapy. *Int J Nanotechnol* 15(1/2/3):174–187
85. Le PN, Huynh CK, Tran NQ (2018) Advances in thermosensitive polymer-grafted platforms for biomedical applications. *Mater Sci Eng C*. <https://www.sciencedirect.com/science/article/pii/S0928493117340742>. <https://doi.org/10.1016/j.msec.2018.02.006>
86. Almería B, Deng W, Fahmy TM, Gomez A (2010) Controlling the morphology of electrospray-generated PLGA microparticles for drug delivery. *J Colloid Interface Sci* 343(1):125–133
87. Bock N, Dargaville TR, Woodruff MA (2012) Electrospraying of polymers with therapeutic molecules: state of the art. *Prog Polym Sci* 37(11):1510–1551
88. Nguyen DN, Clasen C, Van den Mooter G (2016) Pharmaceutical applications of electrospraying. *J Pharm Sci* 105(9):2601–2620
89. Freiberg S, Zhu XX (2004) Polymer microspheres for controlled drug release. *Int J Pharm* 282(1–2):1–18
90. Dinarvand R, Sepehri N, Manoochehri S, Rouhani H, Atyabi F (2011) Polylactide-co-glycolide nanoparticles for controlled delivery of anticancer agents. *Int J Nanomedicine* 6:877–895
91. Bock N, Woodruff MA, Huttmache DW, Dargaville TR (2011) Electrospraying, a reproducible method for production of polymeric microspheres for biomedical applications. *Polymers* 3:131–149
92. Xu Y, Hanna MA (2006) Electrospray encapsulation of water-soluble protein with polylactide: effects of formulations on morphology encapsulation efficiency and release profile of particles. *Int J Pharm* 320:30–36
93. Bohr A, Kristensen J, Stride E, Dyas M, Edirisinghe M (2011) Preparation of microspheres containing low solubility drug compound by electrohydrodynamic spraying. *Int J Pharm* 412:59–67
94. Xie J, Marijnissen JC, Wang CH (2006) Microparticles developed by electrohydrodynamic atomization for the local delivery of anticancer drug to treat C6 glioma in vitro. *Biomaterials* 27:3321–3332
95. Jafari-Nodoushan M, Barzin J, Mobedi H (2015) Size and morphology controlling of PLGA microparticles produced by electrohydrodynamic atomization. *Polym Adv Technol* 26:502–513
96. Wu Y, Clark RL (2007) Controllable porous polymer particles generated by electrospraying. *J Colloid Interface Sci* 310:529–535
97. Park CH, Lee J (2009) Electrosprayed polymer particles: effect of the solvent properties. *J Appl Polym Sci* 114:430–437
98. Enayati M, Ahmad Z, Stride E, Edirisinghe M (2010) Size mapping of electric field-assisted production of polycaprolactone particles. *J R Soc Interface* 7(4):S393–S402
99. Ding L, Lee T, Wang CH (2005) Fabrication of monodispersed Taxol-loaded particles using electrohydrodynamic atomization. *J Control Release* 102:395–413
100. Nguyen VVL, Tran NH, Huynh DP (2017) Taylor cone-jet mode in the fabrication of electrosprayed microspheres. *J Sci Technol* 55(1B):209–214
101. Hong Y, Li Y, Yin Y, Li D, Zou G (2008) Electrohydrodynamic atomization of quasi-monodisperse drug-loaded spherical/wrinkled microparticles. *J Aerosol Sci* 39(6):525–536
102. Meng F, Jiang Y, Sun Z, Yin Y, Li Y (2009) Electrohydrodynamic liquid atomization of biodegradable polymer microparticles: effect of electrohydrodynamic liquid atomization variables on microparticles. *J Appl Polym Sci* 113(1):526–534
103. Arya N, Chakraborty S, Dube N, Katti DS (2009) Electrospraying: a facile technique for synthesis of chitosan-based micro/nanospheres for drug delivery applications. *J Biomed Mater Res B Appl Biomater* 88(1):17–31
104. Xie J, Jiang J, Davoodi P, Srinivasan MP, Wang C-H (2015) Electrohydrodynamic atomization: a two-decade effort to produce and process micro-/nanoparticulate materials. *Chem Eng Sci* 125:32–57
105. Gupta P, Elkins C, Long TE, Wilkes GL (2005) Electrospinning of linear homopolymers of poly(methyl methacrylate): exploring relationships between fiber formation, viscosity, molecular weight and concentration in a good solvent. *Polymer* 46(13):4799–4810
106. Shenoy SL, Bates WD, Frisch HL, Wnek GE (2005) Role of chain entanglements on fiber formation during electrospinning of polymer solutions: good solvent, non-specific polymer–polymer interaction limit. *Polymer* 46(10):3372–3384
107. Zhou FL, Hubbard Cristinacce PL, Eichhorn SJ, Parker GJ (2016) Preparation and characterization of polycaprolactone microspheres by electrospraying. *Aerosol Sci Technol* 50(11):1201–1215
108. Yao J, Lim LK, Xie J, Hua J, Wang CH (2008) Characterization of electrospraying process for polymeric particle fabrication. *J Aerosol Sci* 39:987–1002

109. Enayati M, Ahmad Z, Stride E, Edirisinghe M (2009) Preparation of polymeric carriers for drug delivery with different shape and size using an electric jet. *Curr Pharm Biotechnol* 10(6):600–608
110. Luo CJ, Stride E, Edirisinghe M (2012) Mapping the influence of solubility and dielectric constant on electrospinning polycaprolactone solutions. *Macromolecules* 45(11):4669–4680
111. Smallwood M (1996) Chloroform. In: *Handbook of organic solvent properties*. Butterworth-Heinemann, Oxford, pp 141–143
112. Smallwood M (1996) Dimethylformamide. In: *Handbook of organic solvent properties*. Butterworth-Heinemann, Oxford, pp 245–247
113. Smallwood M (1996) *Handbook of organic solvent properties*. Butterworth-Heinemann, Oxford, pp 137–151
114. Jaworek A, Krupa A (1999) Classification of the modes of EHD spraying. *J Aerosol Sci* 30(7):873–893
115. Jaworek A (2008) Electrostatic micro- and nanocapsulation and electroemulsification: a brief review. *J Microencapsul* 25(7):443–468
116. Nguyen VVL, Tran NH, Huynh DP (2017) Electro spray method: processing parameters influence on morphology and size of PCL particles. *J Sci Technol* 55:215–221
117. Lu J, Hou R, Yang Z, Tang Z (2015) Development and characterization of drug-loaded biodegradable PLA microcarriers prepared by the electro spraying technique. *Int J Mol Med* 36(1):249–254
118. Woodruff MA, Hutmacher DW (2010) The return of a forgotten polymer—Polycaprolactone in the 21st century. *Prog Polym Sci* 35(10):1217–1256
119. Xie J, Lim L K, Phua Y, Hua J, Wang CH (2006) Electrohydrodynamic atomization for biodegradable polymeric particle production. *J Colloid Interface Sci* 302(1):103–112
120. Valo H, Peltonen L, Vehviläinen S, Karjalainen M, Kostiaainen R, Laaksonen T, Hirvonen J (2009) Electro spray encapsulation of hydrophilic and hydrophobic drugs in poly (L-lactic acid) nanoparticles. *Small* 5(15):1791–1798
121. Xie J, Wang CH (2007) Encapsulation of proteins in biodegradable polymeric microparticles using electro spray in the Taylor cone-jet mode. *Biotechnol Bioeng* 97(5):1278–1290
122. Zeng J, Yang L, Liang Q, Zhang X, Guan H, Xu X, Chen X, Jing X (2005) Influence of the drug compatibility with polymer solution on the release kinetics of electrospun fiber formulation. *J Control Release* 105(1–2):43–51
123. Xu Y, Hanna MA (2007) Electrospayed bovine serum albumin-loaded tripolyphosphate cross-linked chitosan capsules: synthesis and characterization. *J Microencapsul* 24(2):143–151
124. Songsurang K, Praphairaksit N, Siraleartmukul K, Muangsin N (2011) Electro spray fabrication of doxorubicin-chitosantripolyphosphate nanoparticles for delivery of doxorubicin. *Arch Pharm Res* 34(4):583–592
125. Mo R, Jiang T, Di J, Tai W, Gu Z (2014) Emerging micro-and nanotechnology based synthetic approaches for insulin delivery. *Chem Soc Rev* 43(10):3595–3629
126. Pohlmann AR, Fonseca FN, Paese K, Detoni CB, Coradini K, Beck RCR, Guterres SS (2013) Poly( $\epsilon$ -caprolactone) microcapsules and nanocapsules in drug delivery. *Expert Opin Drug Deliv* 10(5):623–638
127. Zamani M, Prabhakaran MP, Ramakrishna S (2013) Advances in drug delivery via electrospun and electrospayed nanomaterials. *Int J Nanomedicine* 8:2997–3017



# Advances in Waterborne Polyurethane-Based Biomaterials for Biomedical Applications

# 14

Eun Joo Shin and Soon Mo Choi

## Abstract

Polyurethane (PU) is one of the most popular synthetic elastomers and widely employed in biomedical fields owing to the excellent biocompatibility and hemocompatibility known today. In addition, PU is simply prepared and its mechanical properties such as durability, elasticity, elastomer-like character, fatigue resistance, compliance or tolerance in the body during the healing, can be mediated by modifying the chemical structure. Furthermore, modification of bulk and surface by incorporating biomolecules such as anticoagulants or biorecognizable groups, or hydrophilic/hydrophobic balance is possible through altering chemical groups for PU structure. Such modifications have been designed to improve the acceptance of implant. For these reason, conventional solventborne (solvent-based) PUs have established the standard for high performance systems, and extensively used in medical devices such as dressings, tubing, antibacterial membrane, catheters to total artificial heart and blood con-

tacting materials, etc. However, waterborne polyurethane (WPU) has been developed to improve the process of dissolving PU materials using toxic organic solvents, in which water is used as a dispersing solvent. The prepared WPU materials have many advantages, briefly (1) zero or very low levels of organic solvents, namely environmental-friendly (2) non-toxic, due to absence of isocyanate residues, and (3) good applicability caused by extensive structure/property diversity as well as an environment-friendly fabrication method resulting in increasing applicability. Therefore, WPUs are being in the spotlight as biomaterials used for biomedical applications. The purpose of this review is to introduce an environmental-friendly synthesis of WPU and consider the manufacturing process and application of WPU and/or WPU based nanocomposites as the viewpoint of biomaterials.

## Keywords

Polyurethane · Waterborne · Biomaterials · Regenerative medicine · Scaffold · Tissue engineering

E. J. Shin  
Department of Organic Materials and Polymer  
Engineering, Dong-A University, Busan, South Korea

S. M. Choi (✉)  
Regional Research Institute for Fiber & Fashion  
Materials, Yeungnam University,  
Gyeongsan, South Korea  
e-mail: [smchoi@ynu.ac.kr](mailto:smchoi@ynu.ac.kr)

## 14.1 Introduction

Solvent-borne polyurethanes (PUs) has long been used as high-performance materials, and the standard of their manufacturing systems has been widely used. The processing and application of solvent-borne PUs involve evaporation of organic solvents, which adds to volatile organic compounds (VOCs) content in the atmosphere. Thus, different environment protection agencies have taken serious steps to reduce VOC emission from the industrial sector and issued guidelines to combat the same [63]. Under such circumstances, a paradigm shift in research has been observed in the development ecofriendly polymeric materials. As a result of such efforts, waterborne polyurethane (WPU) has emerged out as one of the greener alternatives [37, 96].

The WPU is formed when a polyurethane prepolymer containing isocyanate functional group is subjected to disperse into water either directly or by means of the phase-inversion emulsification process. Further, after dispersion these polyurethanes are chain extended with a diamine in the water phase.

The WPU is of great importance due to their extraordinary characteristics of containing lower levels of volatile organic content (VOC). Further, water-based PUs are versatile and environmentally friendly coating materials that are available in a wide range of film hardness and solid content. They contain no free isocyanate residuals and possess high blocking resistance, weather resistance, long-term flexibility, UV resistance, and high abrasion resistance. Owing to all the required characteristics of coating materials, water-based PUs are rapidly growing segment of the polyurethane coatings industry [64, 65, 72, 77, 113]. Waterborne PU technology used water as the primary dispersion solvent. The resultant waterborne PU materials gave many advantages: (1) zero or very low levels of VOCs (environmentally friendly), (2) absence of isocyanate residues (nontoxic) and (3) good applicability, versatility, and a wide range of superior properties, such as abrasion resistance, impact strength, and low

temperature flexibility. Waterborne PUs are used in various industries, majorly in paints and coatings. In addition, they are used as binders in hygiene coatings, insulating coatings, concrete sealers, industrial coatings, architectural coatings, paper coatings, leather & textile finishing, printing ink, and various other applications [17, 32, 81, 103]. Particularly, urethane used for medical use should be required to have biodegradability, good affinity for human body, and no environmental hazard. WPU have increasingly focused owing to possibility of tailoring properties caused by altering the chemical structure and composition, nontoxicity by absence of isocyanate residues, the excellent biocompatibility [112], as well as zero levels of organic solvents, namely environmental-friendly fabrication method, thereby being difficult to integrate cells. Consequently, water-dispersed polyurethane (WPU) is inevitably required as biomaterials for biomedical applications. Nowadays, several studies are underway to manufacture biodegradable and environmentally friendly polyurethanes.

With the growing environmental awareness and regulations formulated by the governments in developed and emerging economies to keep the VOCs below 350 g/l are expected to drive the water-based PUs market in near future. Major players, namely, Covestro AG (Germany), The DOW Chemical Company (U.S.), BASF SE (Germany), and various other global players are focusing on expanding and developing water-based PUs.

However, most WPUs are linear thermoplastic polymers and have a relatively low average molecular weight. Therefore, some properties of WPUs, such as water resistance, solvent resistance and mechanical property, are inferior to that of solvent-based polyurethanes [11]. In order to overcome this, many studies have been carried out, such as crosslinking modification [10, 96, 124], chain extender [72] and composites of nanoparticles [37]. The main purpose of this article is to introduce the general features and applications of WPU, and to list the types of diol, isocyanate, and chain extender that are mainly



used in biomaterials. The research on WPU field based on new oligomer polyols provides potential application possibilities in the field of medicine. In particular, it has great research value and tremendous potential for access to eco-friendly materials, such as polyol, which is obtained from vegetable oil, which is a renewable resource.

Based on its specific mechanical properties such as elasticity, flexibility, tensile strength, biocompatibility, and durability, PUs, especially WPUs have been greatly employed in the development of biomedical applications, involving engineered artificial tissues, wound dressings, antibacterial membranes, etc. A great number of research have been conducted on optimizing its properties required for specific applications, and lots of result have been published over time. However, scarcely reviews and books on the biomedical application of only WPUs have been published, which provide researches an information on the advances of WPUs in medical devices as yet. In this chapter, the following topics will be merged: synthesis of WPUs, properties, WPU as biomaterials, and applications in biomedical area.

### 14.1.1 Biomedical Polymers for Biomaterials

A biomaterial is any substitutes, which has been engineered to interact with biological systems for a medical purpose, for example, a therapeutic, and a diagnostic one. The biomaterials have been often used to replace or improve an injured tissue, or to accomplish a complex function. Biomaterials for biomedical applications involve metals, ceramics, pyrolytic carbon materials, composites and polymers. In order to use in biomedical area, biomaterials need to possess key properties for this; proper mechanical strength matched with desired tissue, a capacity to perform its functions, and biocompatibility, also mentioned as bioaffinity. Mechanical strength is desired to maintain a proper performance. Lastly biocompatibility is discussed in details in next part.

### 14.1.2 Biocompatibility

It is essential to understand the interactions between biomaterials and the surrounding biological environment for design of biomedical devices. The term is associated with the behavior of biomaterials in diverse biological phase. The definition of biocompatibility has advanced over the years from one of biological inactivity to some degree of interaction between the biomaterials and surrounding tissue implanted. In other words, it is the ability of a biomaterial to accomplish some biological process with a proper host response. In addition, it can be discussed in terms of hemocompatibility and histocompatibility. The former is rarely defined comparing in biocompatibility. It is usually related to thrombosis what should not occur. The latter includes less or no toxicity, and acceleration of neo tissue formation around an implant.

Chemical modification of urethanes has evolved to provide convenient and effective tools for deformation of biomaterials, which providing desirable properties for biomedical applications. Efforts with the biomaterials and medical materials described above have resulted in a multifunctional urethane-based biocompatible material that meets the specific requirements of each application. The diversity of chemical modification of urethanes in modern biomaterial designs, which have been further upgraded, also affects a wide range of applications, particularly in the field of medical engineering. To render WPU biodegradable, researchers have attempted to incorporate biodegradable polymeric materials into the backbone of WPU. The biodegradable polymeric materials can be long-chain polyols, chain extenders, or diisocyanates.

---

## 14.2 Waterborne Polyurethane Synthesis

Generally, PUs are incompatible with water because of the presence of hydrophobic isocyanates that cannot be dispersed in water and react with water. The hydrophilic modification of the

poly (diisocyanate) shows water dispersibility by the introduction of a hydrophilic group distributed along the chain of the polyurethane prepolymer. The water-dispersible polyurethane (WBPU) coating solution was developed by introducing ionic groups into the PU backbone [80], which can be synthesized or dispersed in water as an ionomer with little solvent used by introducing a carboxylic acid or tertiary amine to the structure. Therefore, water-based processes have reduced environmental concerns about hazardous air pollutants (HAPs), toxic hazards from volatile organic compounds (VOCs), and residual solvents [48, 57]. Depending on these ionic groups, WPU can be classified as cationic, anionic and nonionic. Nonionic types include hydrophilic soft segment pendant groups such as polyethylene oxide. Cationic dispersion contains N-methyl diethanol amine and poly(tetramethylene adipate diol) and poly(tetramethylene glycol) (PTMG), poly(propylene glycol) (PPG), poly(ethylene glycol) (PEG) and dimethylpropanoic acid (DMPA) are categorized as anionic dispersions. The ionomer is neutralized to form salts. These groups are built into the chain structure during polymer preparation [127]. B. K. Kim et al. reported the connection relationships of anionic and nonionic monomers or the position of those hydrophilic groups in polyurethane should also have an influence on the dispersion and stability properties of WPU [64, 65]. That is, a combination of ionic and nonionic monomers, typically containing oxyethyl segments, has a synergistic effect on WPU and induces stable dispersion in fine particle size and low hydrophilic groups.

The most important processes used to manufacture WPU are the acetone process, the prepolymer mixing process, the melt dispersion process and the ketamine process. Generally, the molecular weight is controlled by the molar ratio of NCO/OH and chain extender. The synthesis process varies depending on how the diamines ( $-\text{NH}_2$ ) and diols ( $-\text{OH}$ ) are used to change the chain extension step that is generally performed. Various changes can be made depending on the application of the final product [57].

Polyurethane is a segmented polymer composed of a soft segment and a hard segment,

which constitute a unique microphase separated. The PU ionomer contains an ionic group which is introduced into a hard or soft segment having a predetermined property. The dispersion of the polymer in water and the properties of final products are influenced by the type and content of the ionic centers and macrolides as soft segments. In addition, reaction conditions such as reaction temperature, stirring speed, rate of addition of components and order of addition have a significant effect on the properties of the aqueous dispersion [42, 92].

### 14.2.1 Classification of Waterborne Polyurethane

The water-dispersed polyurethane is classified into an aqueous solution type, a colloid type and an emulsion depending on the particle size and the degree of water absorption, and is divided into anionic, nonionic and cationic depending on the type of the hydrophilic group (Table 14.1). It is divided into dry type, reactive curing type and UV curing type. These hydrophilic groups include  $-\text{COOH}$ ,  $-\text{SO}_3\text{H}$ ,  $-\text{CH}_2\text{CH}_2\text{O}-$ , tertiary amine, and the like. However, these water-dispersible polyurethanes are environmentally friendly, but they are generally less competitive in terms of economy, physical properties, water resistance, and processability than solvent types.


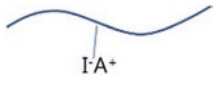
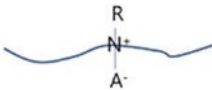
The effective method for making PU dispersible in water is to introduce ionic and/or nonionic hydrophilic moieties into its backbone structure (Table 14.2). When the polyurethane water dispersion exhibits ionic properties, it is necessary to consider how the bonding that may occur when mixing with an ionic additive in a post-process is affected. However, the nonionic water dispersion is ionically stable and is preferred in some fields, but it has a disadvantage with weak dispersibility in water and lower physical properties than anionic polyurethane.

The cationic polyurethane can be synthesized by the following four steps. Step 1, polyol and isocyanate are reacted at  $70 \sim 75^\circ\text{C}$  for  $3 \sim 4$  h to prepare an isocyanate terminated prepolymer. Step 2, ionomer is added and reacted at 60 to

**Table 14.1** Classification of water dispersed PU according to dispersion state

Items	Type		
	Aqueous solution	Colloid	Emulsion
Dispersion state	Solution-micelle	Dispersion	Dispersion
Appearance	Transparent	Translucent	Opaque
Particle size ( $\mu\text{m}$ )	0.001	0.01~0.1	0.1

**Table 14.2** Classification of water-dispersible PU according to ionic type

Items	Type		
	Non ionic	Anionic	Cationic
Structure			
Side group	$-(\text{CH}_2\text{CH}_2\text{O})-$	$-\text{COO}-\text{Na}^+$ $-\text{SO}_3\text{Na}^+$	$\begin{matrix} \text{R} \\   \\ \text{N}^+ \\   \\ \text{A}^- \end{matrix}$ Mainly quaternary ammonium groups
Isocyanate	hydrogenated methylene diphenylene diisocyanate (HMDI)	Isophorone diisocyanate (IPDI)	Isophorone diisocyanate (IPDI) toluene-2,4- diisocyanate (TDI)
Polyol	monomethoxypolyethylene glycol (MPEG), polybutylene succinate diol (PBSD), polybutylene adipate diol (PBAD), polyethylene glycol (PEG), Polyethylene glycol (PEG), polypropylene glycol (PPG)	Polyethylene glycol (PEG), Polycarbonate diol(PCDL), Polycaprolactone diol(PCL)	Poly(neopentylglycol adipate) (PNGA), PPG, PTMG, Polycaprolactone diol(PCDL) PEG, Polyester polyol
Ionomer	–	Dimethylol propionic acid (DMPA), triethylamine (TEA)	N-methyl diethanolamine (MDEA), 3-dimethyl amino 1,2-propane diol (DMPA) dibutyltindilaurate (DBTL)
Chain extender	1,4-butabediol (BD)	1,4-butabediol (BD), Ethylene diamine (ED)	Acetic acid
References	Li et al. [76] and Yang et al. [143]	Na Liu et al. [83], Lei et al. [74] and Kumar Gaddam [31]	Li et al. [80], Wu [134] and Sukhawipat et al. [118]

65 °C for 1–2 h to extend the chain. Step 3, the tertiary amines of the chain-extended prepolymer are reacted with acetic acid, DMS, HCl at 50 °C for 1–2 h to quaternary ammonium salt. Step 4, the neutralized prepolymer is dispersed in water with vigorous stirring at 40–45 °C. At this time, phase transition occurs, and viscosity change should be considered. As a water dispersion method, it is common to add a prepolymer to

water, but in some cases, a dispersion method in which water is added to the prepolymer is also adopted. Solid contents are generally around 35%.

Recently, the anionic type of waterborne PU have been emerging as practical type. This type of waterborne PU possesses pendant ionized carboxylic acid groups. Anionic waterborne PUs with carboxylic acid groups can be synthesized

by a four-step process. In the first step, macromonomer diisocyanate is prepared by reacting excess diisocyanate with a long-chain polyol and/or low molecular weight glycol. Then carboxylic acid-containing macromonomer diisocyanate is prepared through the hydrophilization of macromonomer diisocyanate in the second step, where bis-hydroxycarboxylic acid, such as dimethylolpropionic acid (DMPA), is incorporated into the backbone of macromonomer diisocyanate. The next step involves the neutralization of carboxylic acid with tertiary amine. Finally, the anionic PU prepolymer is vigorously sheared and stirred in water diamine. Chain extension in water causes the residual isocyanate group to transform into urea linkage resulting in an anionic PU that is stably dispersed in water.

Depending on the type of polyol used here, they are classified as polycarbonate-based, polyether-based and polyester-based WPU. García-Pacios et al. showed polycarbonate-based WPUs displayed a lower degree of phase separation between the soft and the hard segment and higher adhesive strength than the regular polyether-based and polyester-based WPUs [35]. In some studies, polycarbonate-based WPUs were also proved possessing excellent hydrolysis resistance and weatherability. In addition, organic solvent resistance is found to be great property for the polycarbonate-based WPUs [34, 119].

The degradation can be tailored through an appropriate choice of the soft segment. Polyether-based polyurethanes are resistant to biodegradation. If the polyol is a polyester, then polyurethanes are readily biodegradable [95]. Biodegradable polyesters used are PCL, PLA and PGA [39, 45]. It is assumed that the degradation rate is governed by soft segments, where esters bounds are located. The urethane bounds, which are located in hard segment, are not easily hydrolysed.

In synthesizing WPU, water plays the role of chain extender to react with terminal isocyanate groups. For this reason, WPU synthesized without addition of a chain extender may be used in eco-friendly or biodegradable applications [156]. The influence of the nature of the chain extender on biodegradability was studied only recently [121]. Introducing a chain extender with hydro-

lysable ester linkage allowed to the polyurethane hard segment to be degradable. Most common isocyanates, however, are toxic, so aliphatic biocompatible diisocyanates have been used. Poly(ester urethane)s were prepared by reaction of lysine diisocyanate with polyester diols based on lactide or  $\epsilon$ -caprolactone [117, 148]. 1,4-diisocyanatobutane is another biocompatible diisocyanate.

### 14.2.2 Dispersion, Particle Stabilization of Waterborne Polyurethane

Here, the role of water used as a dispersant is described as follows. In polar solvents such as acetone, the PU ionomer solution spontaneously disperses when the water is added. The transformation of an organic solution to an aqueous dispersion takes place in several steps. According to Dieterich, the addition of water at an early stage leads to a sharp drop in viscosity due to a decrease in ionic bonding [20]. The ionic bond formed by the neutralization of the ion center is a reversible process, and water reduces ionic bonds between molecular chains. As more water is added, the hydrophobic chain segment decreases due to the decrease in acetone concentration and the hydrophobic chain-induced hydrophobic interaction increases the viscosity of the hydrophobic chain. Further addition of water leads to turbidity and the formation of a dispersed phase, followed by turbidity and rearrangement to microspheres where ions are formed on the surface of the particles of the aggregate, resulting in reduced the viscosity. Some studies have suggested that water molecules are first adsorbed on the surface of the hard segment microionic lattices and then continuously introduced into disordered and ordered hard domains [9]. The water dispersion interferes with the ordering of the hard domain, resulting in a phase separation between the soft segment and the hard segment.

The stabilization mechanisms of ionomer dispersion and non-ionomer dispersion are different [20, 105]. The ionomer dispersion is stabilized by forming an electric double layer between the

ionic components. One layer binds to PU chemically, and the counterion migrates into the water phase around the particle. Interference of electric double layers of different particles causes particle repulsion and contributes to stabilization of dispersion. Adding an inert electrolyte to the ionomer dispersion reduces the range of bilayer repulsion and induces coagulation by providing additional ions at the water phase. In nonionomer dispersion, the hydrophilic PEO segments are fixed to the particle surface and stretched into the water phase. The stabilization mechanism for this type of particle structure can be explained in terms of entropy repulsion. As the particles approach closely, the freedom of movement of the PEO chain in the water phase is limited and entropy is reduced. Therefore, the repulsion between particles is naturally induced [61].

---

### 14.3 Design of Waterborne Polyurethane Biomaterials

The most common way to obtain biorenewable and biodegradable water-dispersible polyurethanes is to include biodegradable and bio-based components in the water-dispersible PU main chain during polymer synthesis.

WPU is used in a wide range of applications from chemical engineering to medical part, which contains cosmetic and chemical applications. WPU dispersions have been gaining increasing importance in a wide range of applications because of their excellent properties, such as adhesion to various substrates, resistance to chemicals, solvents, and water, abrasion resistance, high tensile strength and elongation, flexibility, toughness, and water vapor permeability. Recently, polyurethane films with high water vapor permeability have been used in medical applications, breathable coating fabrics, and special adhesives [64, 65]. In addition to film, WPU is also used for coating medical devices and equipment. Continued research and development on WPU's other application development in the medical field is expected to improve this market in the future.

#### 14.3.1 Introduction of Bio-based Polyol Materials

Vegetable oils are widely used bio-based renewable resources due to their low toxicity, inherent biodegradability, ready availability, and relatively low price. As such, a great deal of effort has been made to develop waterborne PUs from vegetable oils [91].

A challenge in the synthesis of vegetable oil-based, environmentally friendly waterborne PU is the high crosslinking of the PU prepolymers caused by high hydroxyl functionality of the vegetable oil based polyols. Vegetable oils are also susceptible to hydrolytic breakdown due to the three ester bonds in their structure. Vegetable oil-based waterborne PU bonds may degrade when exposed to excessive humidity, releasing amines and carbon dioxide and they are also susceptible to microorganism attack [72].

Since plant-derived fats and oils can be extracted directly for monomers, fine chemicals and polymers, there is a great possibility of replacing currently used petrochemicals. The synthesis of monomers as well as polymers from vegetable fats and oils offers promising new opportunities because they are used in many ways in industry. These oils make highly pure fatty acids available that may be used for chemical conversions and for the synthesis of chemically pure compounds such as oleic acid from "new sunflower," linoleic acid from soybean, linolenic acid from linseed, erucic acid from rapeseed, and ricinoleic acid from castor oil. The most important parameters affecting the physical and chemical properties of oils are stereochemistry, the degree of unsaturation and the length of the carbon chain of fatty acids.

In castor oil, the most abundant fatty acid is ricinoleic acid ((9Z,12R)-12-hydroxy-9-octadecenoic acid), providing additional natural chemical functionality for modifications, crosslinking or polymerization [41]. Castrol oil, which has inherent hydroxyl groups in its structure, was the first vegetable oil directly used in the synthesis of waterborne PUs. Other vegetable oils, such as sunflower, corn, palm, rapeseed, soybean, and linseed oils, much be modified into polyols for syn-

thesizing waterborne PUs [129, 138]. Vegetable oil-based polyols are long-chain polyols that offer promise in producing biorenewable waterborne PUs. The various types of vegetable oil-based polyols can be used to synthesize bio-based PUD and PU materials with a wide range of colloidal and physical properties. Castor oil's unique structure, with ~90% of the fatty acid chains in the oil bearing a hydroxyl group, eliminates the need for chemical modification of the triglyceride to produce polyols for PU synthesis [90]. Madbouly et al. successfully synthesized via homogeneous solution polymerization in methyl ethyl ketone followed by solvent exchange with water. Thermally induced gelation was observed for PUDs with a solid content  $\geq 27$  wt%. The kinetics of thermally induced gelation behavior of PUDs was investigated analyzing the real-time evolution of  $G'$ ,  $G''$ ,  $\eta^*$ , and  $\tan\delta$  at constant temperatures (55, 60, 65, and 70 °C) and angular frequencies for different solid contents. These biorenewable PUDs exhibited rich and complex viscoelastic behavior and can serve as excellent model systems for more detailed explorations of rheology and macromolecular structure under flow and deformation conditions for other PUDs. Castor oil-based waterborne PUs show good mechanical properties in terms of both tensile strength ( $9.3 \pm 1.5$  MPa) and elongation at break ( $520 \pm 20\%$ ). Thus they have been used to modify plasticized starch to prepare novel biodegradable materials with high performance [129]. Siva Sankar Panda et al. synthesized successfully from castor oil-based polyol, isophorone diisocyanate and dimethylol propionic acid with NCO/OH ratio of 1.5. And then, different weight percentages of cloisite 30B (1, 2, and 3 wt%) were loaded with WPUDs to prepare nanocomposite films [99] (Scheme 14.1).

A soybean oil-based waterborne PU dispersion has also been successfully prepared from toluene-2,4-diisocyanate, DMPA, and a chlorinated soybean-oil-based polyol [88].

After that they synthesized WPUs containing 50~60 wt% of bionewable components, which have been prepared using methoxylated soybean oil polyols (MSOLs) with hydroxyl functionality ranging from 2.4 to 4.0. The particle sizes of the

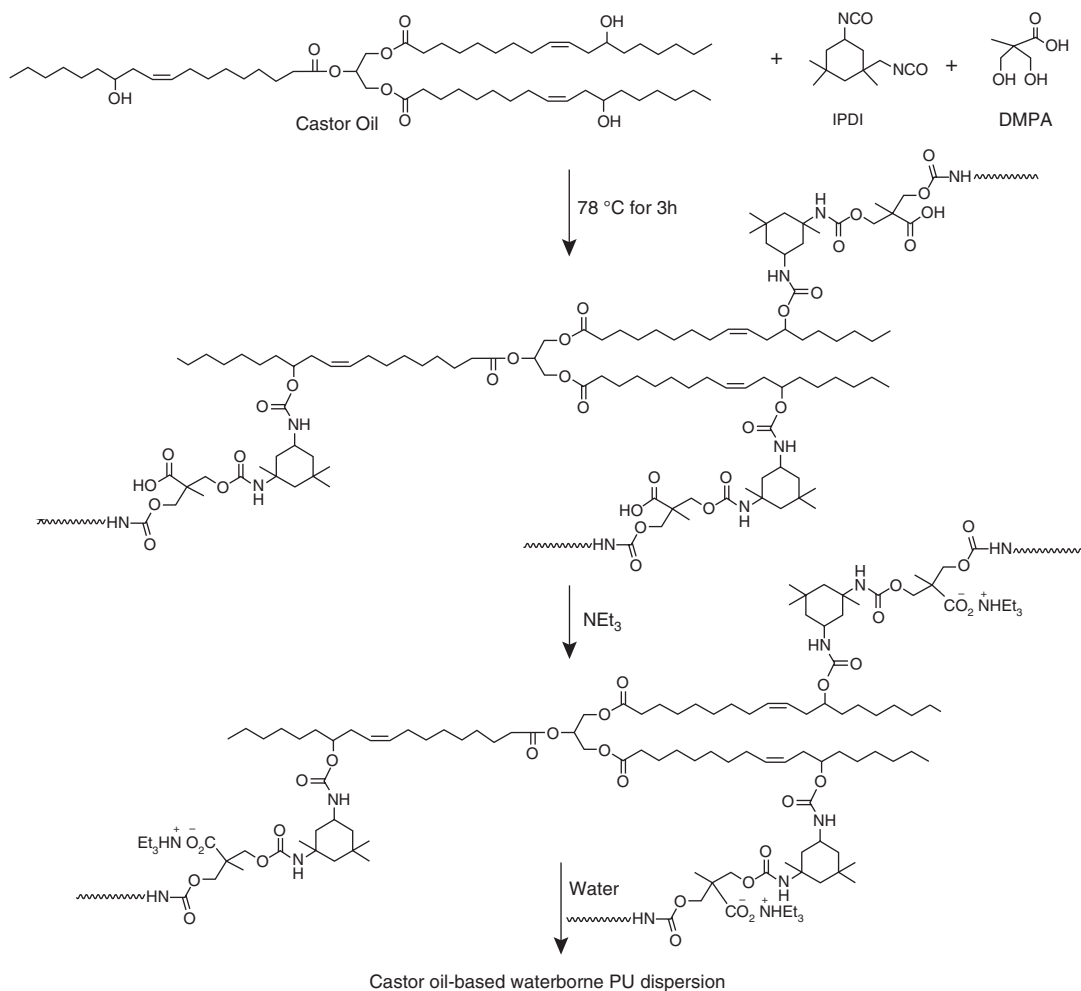
resultant waterborne PUs range from 12 to 130 nm. An increase in the hydroxyl functionality of the MSOLs significantly improved the cross-link density of the waterborne PUs. These novel films exhibit tensile stress-strain behavior ranging from elastomeric polymers to rigid plastics and possess Young's moduli ranging from 8 to 720 MPa, ultimate tensile strengths ranging from 4.2 to 21.5 MPa, and percent elongation at break values ranging from 16 to 280%, and resulted in biorenewable PUs ranging from elastomeric polymers to ductile plastics [86] (Scheme 14.2).

Sariah Saalah et al. synthesized a series of waterborne polyurethane dispersions derived from jatropha oil-based polyol (JOL) with different OH numbers ranging from 138 to 217 mgKOH/g. The results reveal that with increasing OH number, the DMPA content and hard segment content significantly decrease the particle size from 1.1  $\mu\text{m}$  to 53 nm, indicating increasing stability of the dispersions. JPU films exhibit the stress-strain behavior of an elastomeric polymer with a Young's modulus ranging from 1 to 28 MPa, a tensile strength of 1.8 to 4.0 MPa and elongation at break ranging from 85 to 325% [109].

Ismail Omrani et al. synthesized the WPU from bio-based polyol, which was derived from sunflower oil. The polyol containing carboxylic acid groups from sunflower oil was prepared and used in the production of biodegradable WPU. The synthesized WPU was loaded by the drug and its loading ability was studied. Drug release studies have shown controlled release of raloxifene from anionic nanoparticles predominantly driven by diffusion-based mechanisms [97, 98] (Schemes 14.3 and 14.4).

### 14.3.2 Introduction of Bio-based Chain Extender Materials

Chain extenders can also be substituted with bio-based components in the synthesis of waterborne PUs. The chain extender can be replaced with a bio-based component in WPU synthesis. For example, Hong Chen et al. used L-lysine (PU-L),



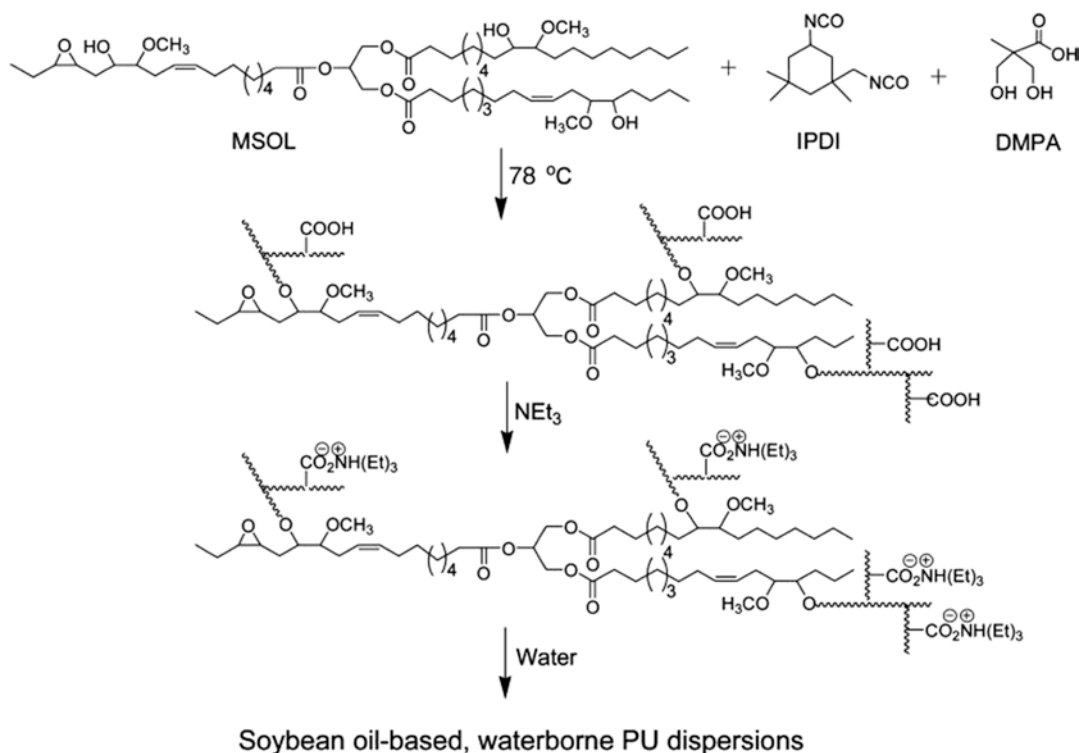
**Scheme 14.1** Elementary steps for the synthesis of Castor oil-based waterborne PU dispersion. (Adapted with permission from Madbouly et al. [90]. Copyright (2013) American Chemical Society)

ethylenediamine (PU-E), and their mixture (PU-L-E) as chain extenders of WPU. The produced emulsion exhibited satisfactory freeze/thaw stability. Films cast from emulsions exhibited excellent mechanical properties and good antiblood coagulation character [12].

Chitosan, a derivative of an abundant naturally occurring polysaccharide, has active amino groups, exhibits much higher reactivity and water solubility. So, chitosan can be used to chain waterborne PU in water. Chitosan has unique biological properties such as toxicity, biocompatibility, anticoagulant and biodegradability. Dan Xu et al. prepared a novel blood-compatible WPU film, which

can be synthesized with chitosan as a chain extender. Its properties showed antibacterial and antifungal activity as well as excellent mechanical and anticoagulant properties. Though these films had hydrophilic groups, they were not soluble in water due to crosslinking. Based on mechanical properties and blood compatibility of the materials, these films can be a candidate for bio-applications [139] (Scheme 14.5).

Gelatin from cold fish skin also can be introduced into waterborne PUs by covalent bonding, to reinforce and render biodegradability. Lee et al. chemically modified gelatin with vinyltrimethoxysilane and incorporated the modified



**Scheme 14.2** Synthesis of soybean-oil-based waterborne polyurethane dispersions. (Adapted with permission from Lu and Larock [86]. Copyright (2008) American Chemical Society)

gelatin into waterborne PU with terminal hydroxyl ethyl acrylate groups by UV polymerization. The waterborne PU showed excellent mechanical properties and water resistant properties along with significantly enhanced biodegradability both in trypsin solution and in soil [73].

## 14.4 Waterborne Polyurethane for Biomedical Applications

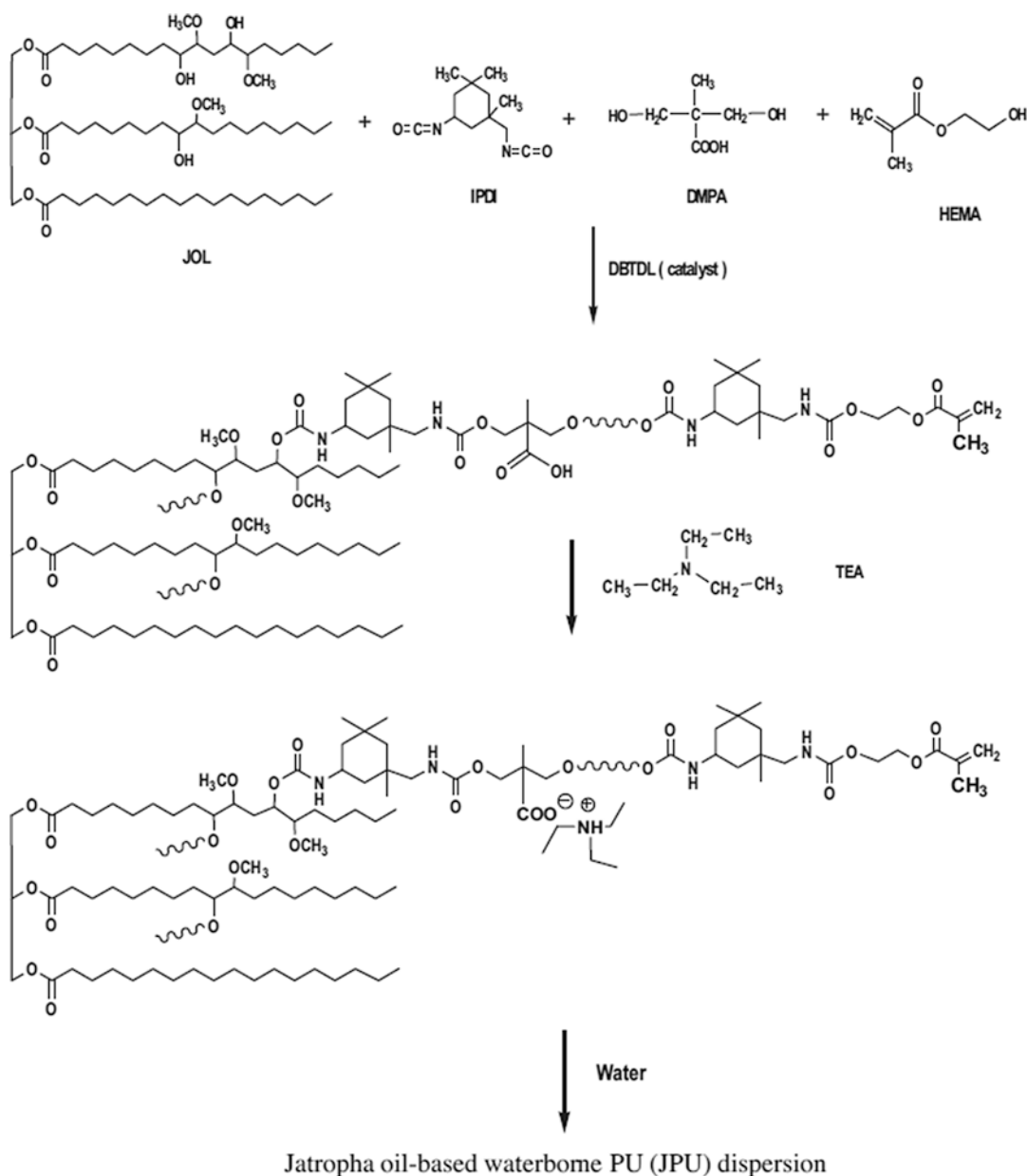
Waterborne polyurethane (WPU) has been enormously employed as an environment friendly material in various biomedical applications such as tissue regeneration, antibacterial, wound dressings, water purification due to abrasion resistance, wide substrate suitability, better mechanical properties in terms of elasticity, flexibility, tensile strength as well as biocompatibility. For using in various applications, the materials can be prepared by either alone or with other polymers including natural or synthetic polymer

for altering chemical composition resulting in modulating mechanical, physicochemical, and biological properties. Furthermore, many researches have conducted on modification of WPU, the addition of inorganic nanomaterials is also common approaches among them mentioned above, including SiO<sub>2</sub> [149], Carbon [71], graphene [62], nanoclays [30], etc.

### 14.4.1 Tissue Engineering

The final goal of tissue engineering is to replace, maintain, and enhance injured tissues. The key strategy for tissue regeneration is to engineer bioconstructs providing biomechanical, cellular, physicochemical, and molecular cue in order to repair damaged tissue. The engineered constructs should ideally mimic properties, architecture, morphology of natural tissues to replace injured site. Although autograft and allografts are a gold standard for tissue replacement, they have major



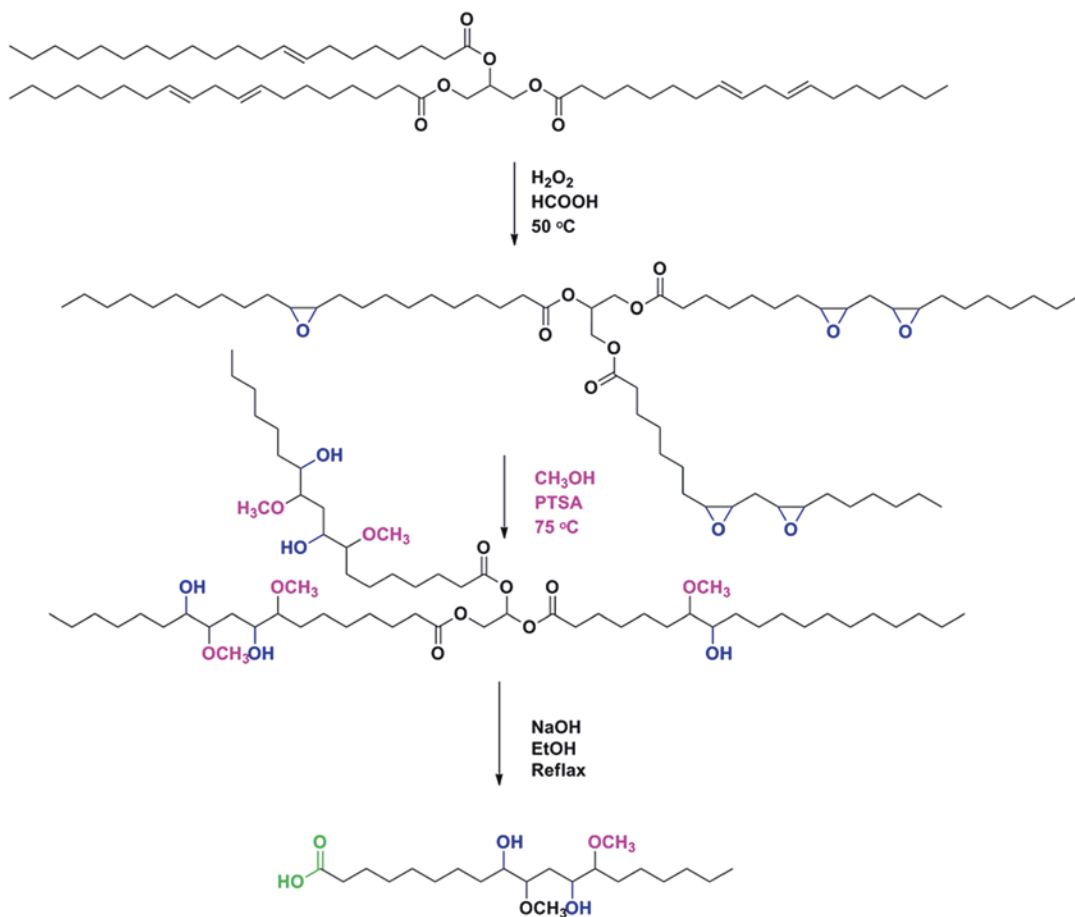


**Scheme 14.3** Reaction scheme for synthesis of waterborne polyurethane dispersions. (Adapted with permission from Saalah et al. [109]. Copyright (2015) Elsevier)

limitation such as complications, causing pain and infection, donor shortage. Therefore, the employment of biomaterials is currently a promising approach for an alternative treatment.

Waterborne polyurethanes (WPU) have mainly focused due to possibility of controlling properties altering the chemical structure and

composition, nontoxicity, no flammability, the excellent biocompatibility [112] and an eco-friendly fabrication method comparing with solvent-borne polyurethanes involving toxic organic solvents causing in residue of the solvent in the resultant product, thereby being difficult to integrate cells [50, 51, 130]. Xu et al. investi-

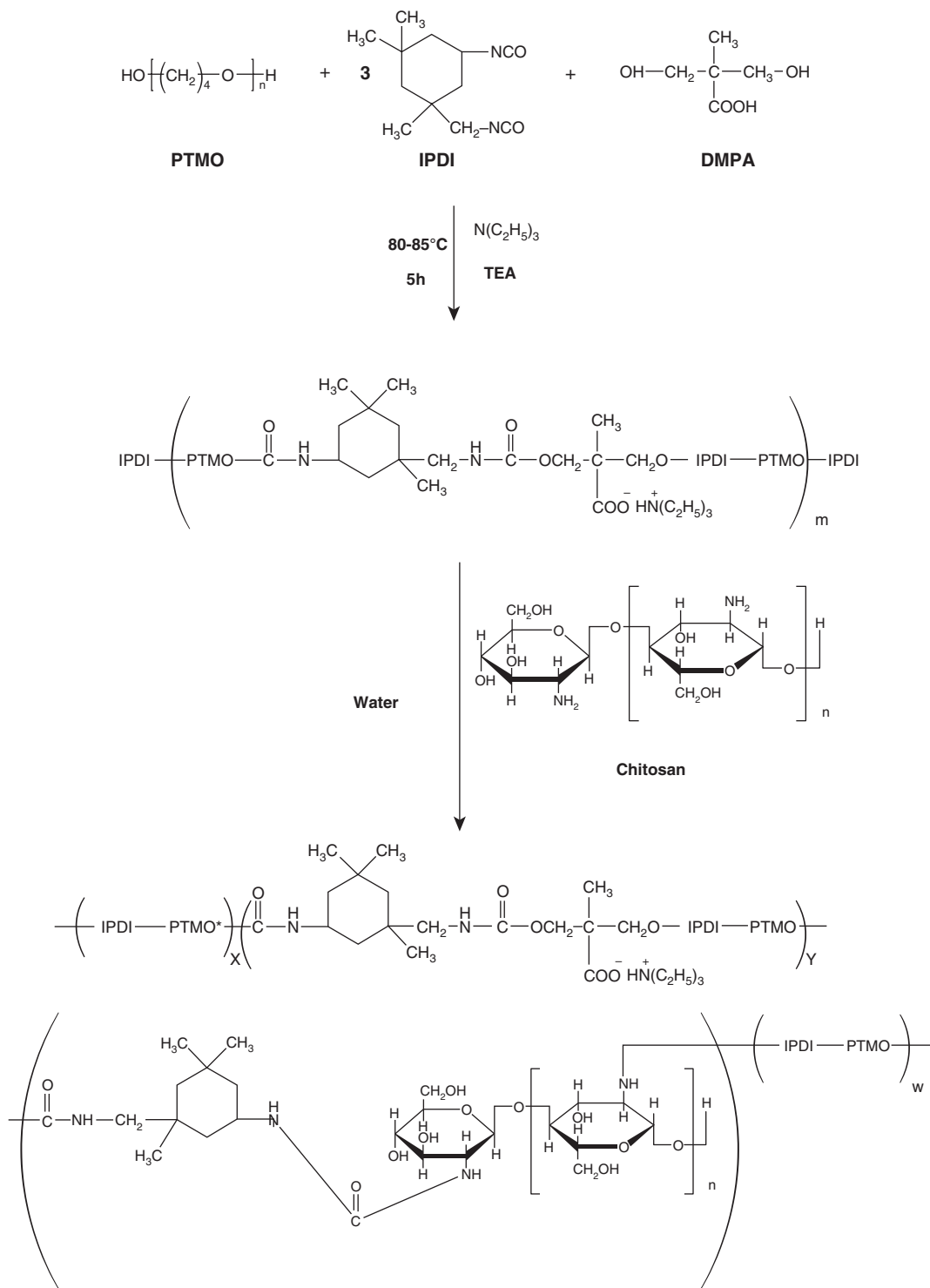


**Scheme 14.4** The synthesis route of DHA from sun flower oil. (Adapted with permission from Omrani et al. [97, 98]. Copyright (2017) John Wiley and Sons)

gated to evaluate BSMC growth and morphology on waterborne polyurethane membranes in comparison with PLGA, a generally used biomaterial for repairing injured bladder and proved that it was greater than PLGA membranes. Hsu et al. fabricated peripheral nerve conduits from biodegradable PU which was synthesized by a waterborne process. The conduits with asymmetric microporous structure were prepared from 15% PU dispersion by the freeze-drying method. The porous structure was interconnective with pore size of  $23\text{ }\mu\text{m}$ . The interconnected porous structure allows high permeability resulting in helping cell proliferation. The histology of regenerated nerve after 6 weeks post implantation at the mid-section of the conduit was showed in Fig. 14.1. The areas of regenerated axons were

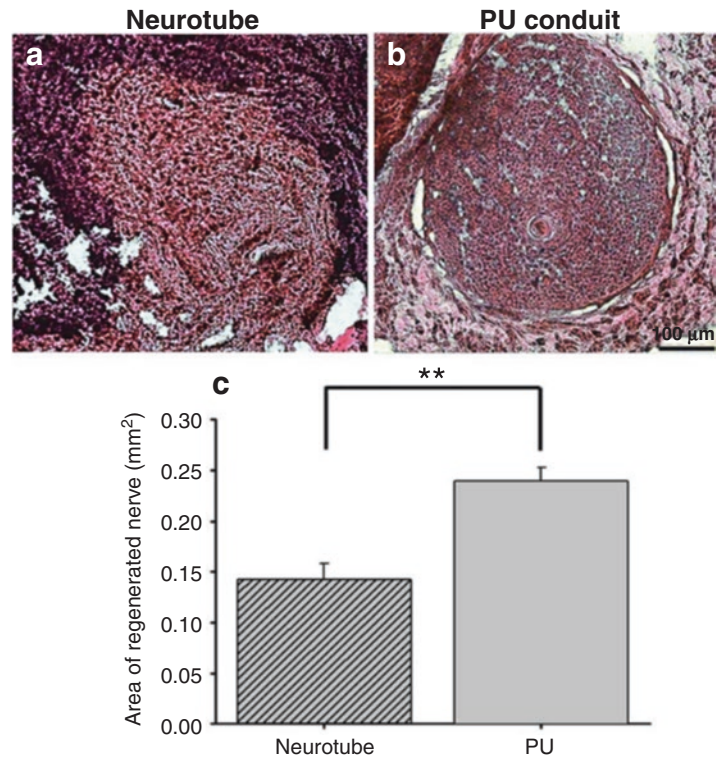
about  $0.24\text{ mm}^2$  and  $0.14\text{ mm}^2$  for WPU and Neurotube, respectively. In addition, the morphology of nerve fibers of WPU conduits was more organized comparing with Neurotube. As a result, the fabricated WPU conduits proved potential applications in peripheral nerve tissue engineering [49].

Nanofibrous scaffolds without any organic solvents were fabricated through electrospinning biodegradable WPU emulsion blending with aqueous poly(vinyl alcohol) (PVA) by Wu et al. The nontoxic WPU prepared by using poly(ethylene glycol) (PEG) and poly( $\epsilon$ -caprolactone) (PCL) as soft segment, L-lysine diisocyanate (LDI) as hard segment, 1,3-propanediol(PDO) and L-lysine as chain extender are fabricated.



**Scheme 14.5** Synthesis of WPU urea emulsion with chitosan as the chain extender. (Adapted with permission from Xu et al. [139]. Copyright (2008) John Wiley and Sons)

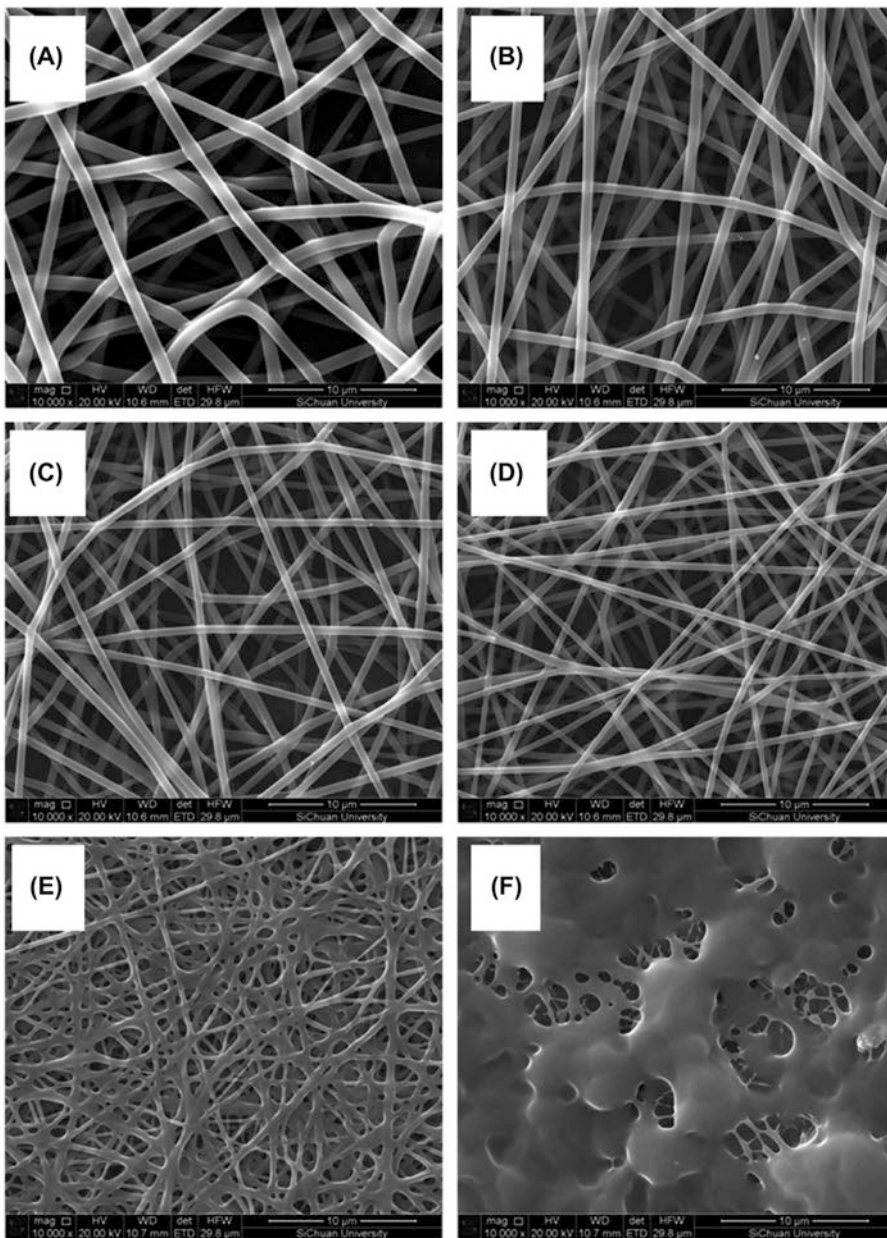
**Fig. 14.1** Histology of the regenerated nerve at 6 weeks in (a) Neurotube and (b) the PU nerve conduits. (c) The quantitative data of the area of regenerated nerve inside the conduit obtained from the image analysis of histology at the middle portion of the explant. (Adapted with permission from Hsu et al. [49]. Copyright (2017) John Wiley and Sons)



As shown in Fig. 14.2, altering the mass ratio of PVA to WPU changes the diameter and morphology of fiber effectively. The fabricated scaffolds with high porosity and interconnected pore could be obtained by consisting of homogeneous fibers excepting in the 1/9 ratio. The surfaces of electrospun nanofibers are smooth and the diameters decrease from 964 to 370 nm with increasing the ratio of WPU, because of crystallization of PVA. Also, the nanofiber mats showed outstanding biocompatibility, accordingly they have lots of potential for excellent biomaterials for tissue regeneration [137].

3D printing has been a potential approach to fabricate customized scaffolds providing surrounding environments to attach, migrate, and proliferate cells resulting in guiding to grow tissue. Biocompatible and biodegradable materials applicable for 3D printing are rare [50, 51, 145]. Although synthetic polymers with biodegradability such as polylactic acid (PLA), polyglycolic acid (PGA), and polylactic-co-glycolic acid (PLGA) could degrade at high temperature

or require to dissolve in organic solvent for printing [144] they do not possess a proper elasticity similar to that of natural tissue. Among materials for 3D printing, it is possible that waterborne polyurethane mimics biomechanics of natural tissue. Hung et al. developed 3D printing system employing water dispersion of biodegradable polyurethane elastomer with a viscosity enhancer [53]. Water based printing have been advantageous for integrating biomolecules such as growth factors into materials in order to enhance the functionality of the fabricated scaffolds. Also, they developed customized waterborne polyurethane scaffolds with cell aggregation capacity via 3D printing and controlled release function. The 3D printed waterborne polyurethane scaffolds integrated self-clustering MSCs could guide to regenerate tissue and release the incorporated bioactive compound without any exogenous induction medium. Finally, the group confirmed the effectiveness of the developed scaffolds for regenerating cartilage defect [54].



**Fig. 14.2** SEM images of PVA/WPU nanofiber mats that electrospun with various mass ratios of PVA/WPU (A)10/0, (B)9/1, (C)7/3, (D)5/5, (E)3/7, and (F)1/9 (total

polymer concentration 15 wt%, TCD 15 cm, and applied voltage 20 kV). (Adapted with permission from Wu et al. [137]. Copyright (2017) Taylor & Francis)

#### 14.4.2 Drug Delivery

Currently polyurethanes (PUs) have gotten attention as a polymers that can be employed in lots of areas such as biomaterials due to adhesion to various substrates, resistance to chemicals, sol-

vents, and water, abrasion resistance, high tensile strength and elongation, flexibility, toughness, and water vapor permeability [116, 147]. Therefore, many medical devices including blood pumps, prosthetic heart, valves and insulation, have prepared from PUs [21, 93]. Degradable

PUs are generally synthesized by polyaddition reaction of degradable polyester or polycarbonate diols with diisocyanate [125, 128]. The PUs with degradable ester bonds degrade slowly, and accordingly are not matchable with sustained release applications [52, 97, 98, 155]. To date, micro or nanocarriers with disulfide bonds have drawn lots of research efforts, due to the presence of redox-potential gradient between the extracellular and intracellular milieu [55]. L-cysteine and glutathione (GSH), which are reducing agents, can split disulfide bond via thiol-disulfide exchange reaction [141]. Lili et al. developed successfully novel redox-responsive micelles self-assembled with disulfide containing cross-linked structure in hydrophobic segment. It is found that doxorubicin (DOX) as anticancer is efficiently released from the fabricated micelles to cytosol, and the release rate could be accelerated by the presence of comparatively high concentrations of glutathione (GSH). The carrier fabricated using disulfide linkage enable intracellular delivery by allowing an accelerated release of incorporated drugs. However, almost carriers prepared from a disulfide bond between hydrophobic and hydrophilic blocks generally lack control of sensibility and micellization [16]. Biodegradable polyurethane-based micelles with redox responsive properties is emerging materials in drug delivery system [5]. The presence of disulfide bones in PUs can lead to the break of polymer chain resulting in collapsing nanocarriers. Although introducing carboxylic acid or tertiary amine into their structure, PUs is able to be synthesize and dispersed in water either alone or with little solvent used [135]. The waterborne process decreased the environmental issue regarding toxic organic solvents. Waterborne polyurethane (WPU) possesses the ionic groups enabling PU particles to be dispersed in water. The WPU have drawn attention in biomedical area owing to their versatility and environment-friendly process. It is reported that WPU is possible for carrying hydrophobic compounds including an anticancer drug due to no toxicity as well as low cost.

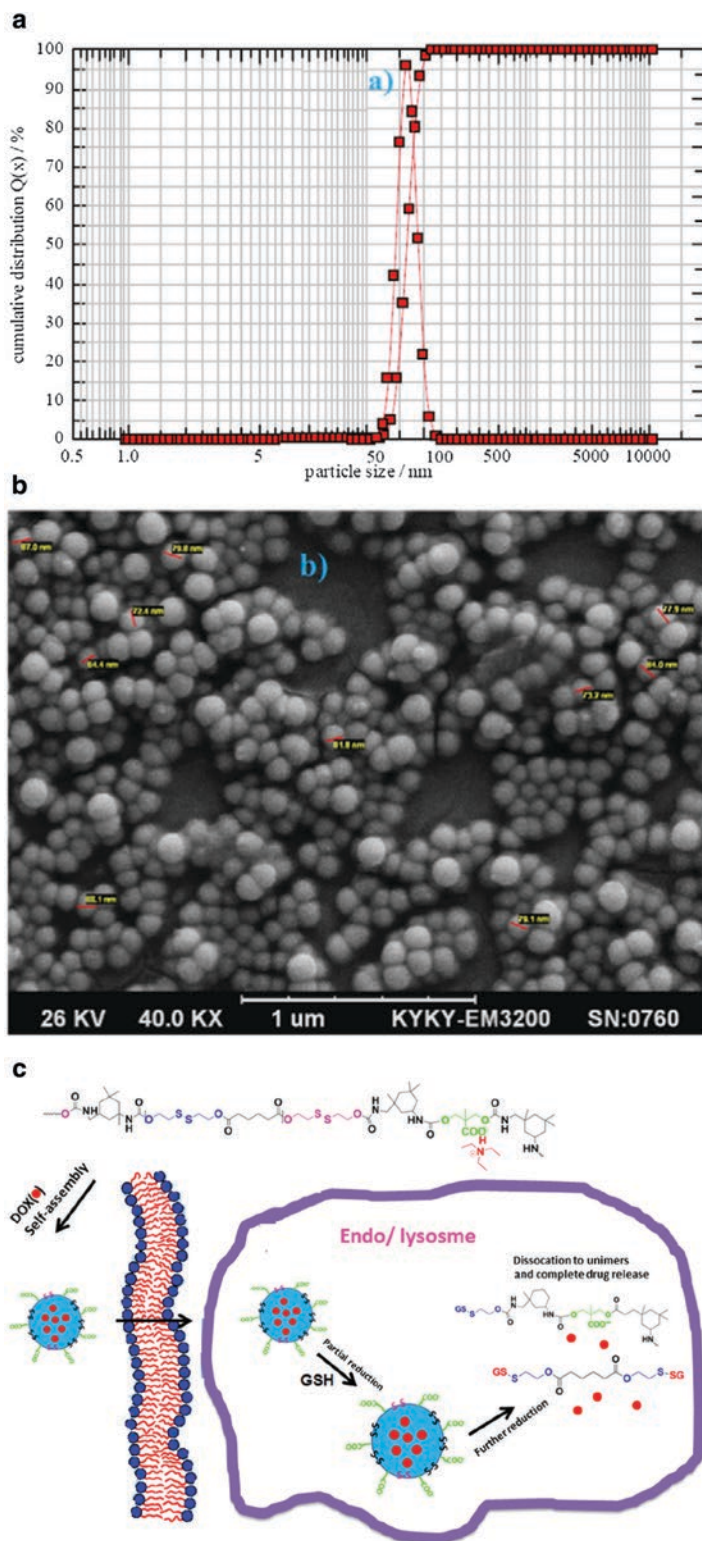
Recently, Omrani et al. reported that WPU nanocarriers with disulfide bonds in both hard

and soft segment were prepared for redox-triggered intracellular delivery of DOX. As shown in Fig. 14.3, the polyester diol bearing disulfide bonds was prepared using disulfide-labeled polyester diol, bis (2-hydroxyethyl) disulfide, DMPA and isophorone diisocyanate. In Fig. 14.3, DLS displayed that the fabricated nanocarriers had a size of 92 nm, in addition SEM micrograph exhibits that the WPU nanocarriers had a homogeneous distribution with good stability. In analysis of release DOX, it was demonstrated that the enhanced DOX release at 10 mM reducing agent concentration was caused by the disassembly of WPU nanocarriers owing to the DTT-induced disulfide bond cleavage. It was proved that the developed WPU nanocarriers possess merits including ease process, nontoxicity, good stability at physiological condition, fast degradation at reductive environment, and trigger drug release by GSH concentration [97, 98].

Moreover, Ajorlou et al. reported that the fabricated WPU nanomicelles loaded paclitaxel showed inhibitory effects on growth of cancerous cells and the size and weight of the mice tumors decreased during treatment with folate decorated nanomicelles. In addition, the performance of the fabricated nanomicelles was a lot better than commercializing drug, Taxol® [1].

Gene therapy is a promising treatment for genetic diseases. Cationic polymers including polyurethane, which form complexes with DNA for gene transfection, are generally employed as non-viral carriers [115, 126]. Biodegradable polymers have been attracted attention as transfection reagents, because of lower risk resulted from polymer accumulation [100]. Although the cationic polymer has high transfection efficiency, they have still considerable toxicity. Yang et al. developed *N,N*-diethylethylenediamine-polyurethane (DEDA-PU), bearing tertiary amines in the backbone and side chains for gene delivery [142]. Jian et al. synthesized lysine-based poly(urethane-co-ester) PMMD bearing ester linkages in the backbone and tertiary amines in the side chain, to improve the self-assembly efficiency of nanoparticles with DNA [58]. However, these PU as transfection reagents has drawbacks such as difficult synthesizing as

**Fig. 14.3** The distribution of size determined by DLS (a) and SEM micrograph (b) of reduction-sensitive WPU, the scheme of glutathione-degradable WPU nanocarriers for redox-triggered intracellular DOS delivery (c). (Adapted with permission from Omrani et al. [97, 98]. Copyright (2017) Elsevier)



carriers as well as use of toxic organic solvent. Wu et al. synthesized biodegradable cationic polyurethane nanoparticles (NPs) with tertiary ammonium group through an environment-friendly waterborne process. It was demonstrated that the new cationic elastomer waterborne polyurethane with excellent antibacterial activity (100%) was formed into NPs and films. Moreover, it showed the ability to form complexes with plasmid DNA and little cytotoxicity [135].

Consequently, these waterborne polyurethane nanocarriers above mentioned, can be preferable candidates as biodegradable vehicles for drug/gene delivery system.

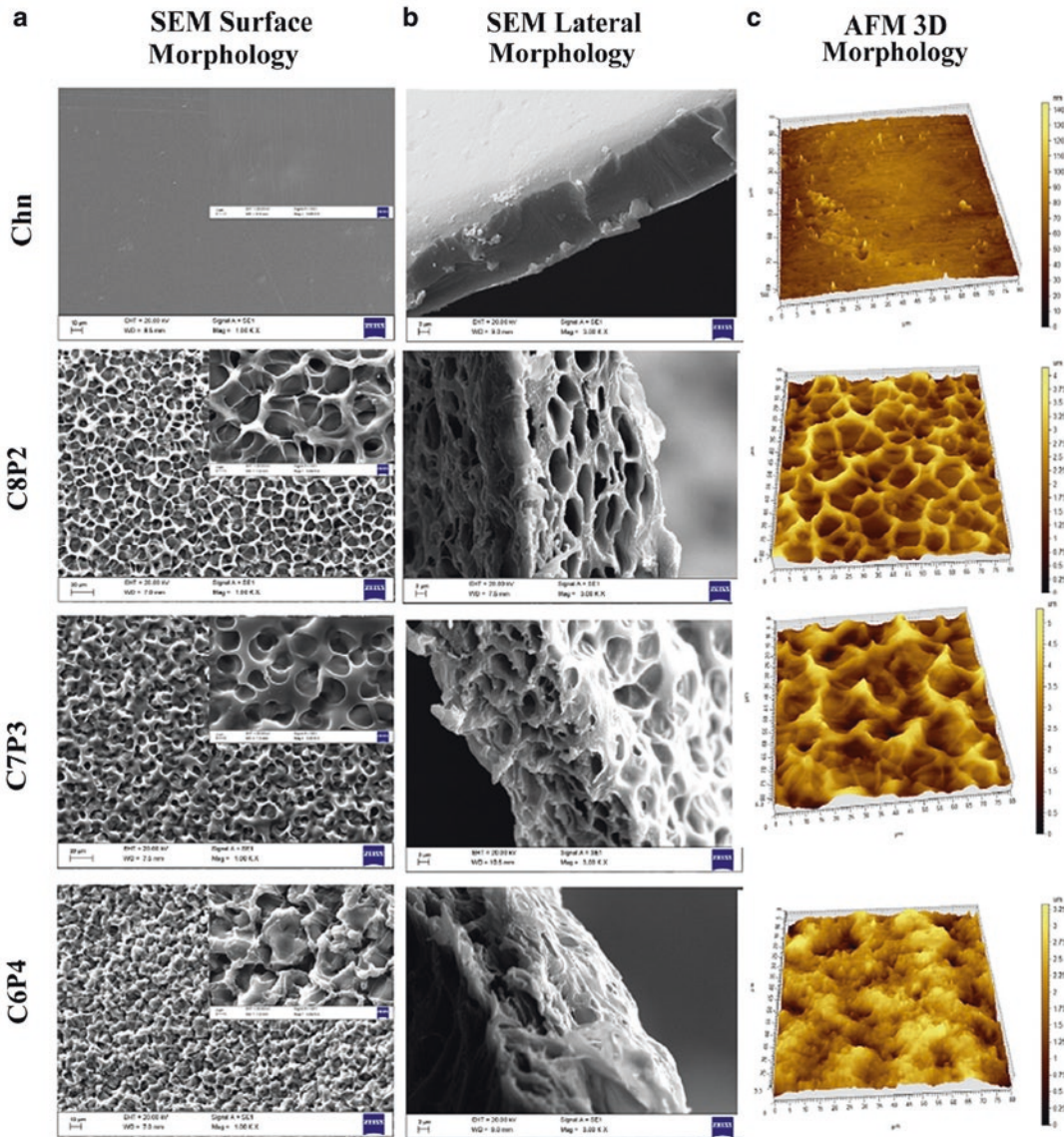
### 14.4.3 Wound Healing

Wound healing is complex, dynamic, and physiological responses of a living tissue caused by physical, chemical, mechanical or thermal injury. It accompanies a process to substitute lost cells and matrix components, and skin layer, which results in facilitating wound regeneration and restoring tissue integrity [14]. The process for wound healing is categorized into 3 or 4 dynamic and overlapping phases-inflammatory (homeostasis and inflammation), proliferative (granulation, contraction, and epithelialization) and remodeling (maturation), which has also been denoted as hemostasis, inflammatory, proliferation, and remodeling phase. The inflammatory phase is distinguished by accumulating lots of neutrophils and macrophages involved in by the by the secretion of inflammatory mediators like reactive oxygen species (ROS), reactive nitrogen species (RNS), cytokines, etc. [6]. In case of medical treatment to full-thickness (FT) wound complications caused by chemical injury, burns, secondary infections, and diabetes, non-toxic surface engineered matrices of biomaterials can be used as wound dressing materials with the function to protect from external mechanical stress as well as microbial infections. These wound dressing biomaterials should possess the following properties; it has to be swollen by absorbing an exudation in its polymer network from wound without dissolving by the

surrounding liquid. Therefore, the materials enable to provide proper conditions for healing process by mimicking native tissue environment; for example, glycosaminoglycans (GAGs), alginate, poly (vinyl pyrrolidone), gelatin poly (ethylene glycol), hyaluronic acid, etc. [2, 19, 28, 60, 70, 78, 106, 131]. Almost these cases, it is necessary to use covalent crosslinker for maintaining their structure during desired period. However, the chemicals as crosslinker are often toxic, thereby requiring an additional confirmation about bioaffinity.

Polyurethane as a wound dressing material have been commercially in the spotlight because of main characters such as biocompatibility, mechanical properties, elasticity in particular, flexibility, good oxygen/carbon dioxide permeability [6]. Accordingly, polyurethane-based dressings have been commercialized, mainly OpSite<sup>®</sup>, 3 M<sup>®</sup> Tegaderm<sup>®</sup>, and Bioclusive<sup>®</sup> [26, 94], though they have restricted absorbent property with only a barrier from microbial infection for chronic wound. Currently, comparing with conventional solvent-borne polyurethane, waterborne polyurethane have greatly attention and been employed either alone or with other nature or synthetic polymers for wound restoration. It is associated with a binary colloidal system consisting polyurethane particles dispersed in water [94]. The polyurethane dispersion scaffolds prepared with poly(ethylene glycol) were informed to imbibe, followed by being swollen in aqueous condition without dissolving, primarily owing to strong hydrogen bond between dispersed hard segment, namely urethane and urea, and poly(ethylene glycol) soft segment causing phase separated morphology. Yoo and Kim proved that the resultant waterborne polyurethane hydrogel fabricated in their study has a great potential for novel wound dressing materials, which support and retain the sufficient moist condition required to prevent scab formation and dehydration in the wound bed, resulting in retarding in tissue regeneration and scar formation [147]. In addition, they prepared waterborne polyurethane/poly(N-vinylpyrrolidone) (PVP) composite films with various PVP by in situ polymerization in an aqueous medium. With





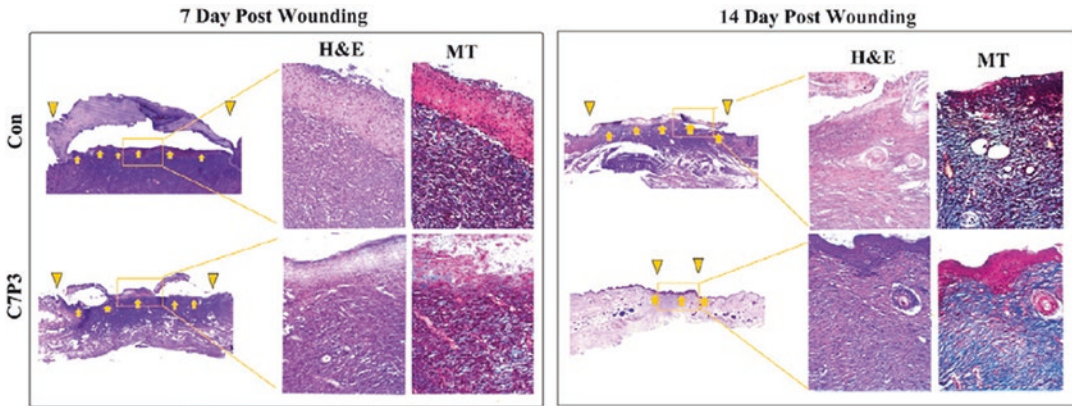
**Fig. 14.4** Morphological characterization of the Chitosan and Chitosan/WPU scaffolds (a) surface (b) lateral morphologies observed by SEM and (c) AFM micrographs of the four different compositions (according to composition

by ratio of blending Chn:WPU, Chn 10:0/C8P2 8:2, C7P3 7:3, C6P4 6:4). (Adapted with permission from Bankoti et al. [6]. Copyright (2017) Elsevier)

increasing the content of PVP in composite films, the tensile strength declined, while its elongation at break increased, as well as water absorption [146].

Bankoti et al. fabricated waterborne polyurethane/anti-bacterial chitosan scaffolds with different ratios which self-organized to form macroporous hydrogels at room temperature on

drying. The morphological analysis of chitosan and chitosan/WPU was performed by SEM and AFM microscopy as shown in Fig. 14.4. The fabricated chitosan scaffold did not exhibit any porosity, while the C8P2 with composition (chitosan:WPU, 8:2) C7P3 (chitosan:WPU, 7:3) possessed highly interconnected porous network. It was found that the porosity and pore size



**Fig. 14.5** Images of Masson's Trichrome and H&E stained histological sections of day 7 and day 14 after initial wounding; yellow arrow represents wound area and

yellow inverted triangles represent healing wound edges. (Adapted with permission from Bankoti et al. [6]. Copyright (2017) Elsevier)

increased with increasing WPU dispersion content in compositions. The interconnected porous structure would allow an exudation evaporation and gas exchange which is essential for wound care.

In Fig. 14.5, H&E staining reveals that both control and C7P3 showing higher cellular infiltration and neovascularization was more occurred in wounds covered with C7P3 comparing to control. This result in C9P3 was caused by its structure with interconnected pore. Also, this staining at 14 day after wounding proved that re-epithelialization was more taken place in wounds covered by C7P3. The histological study showed faster wound healing using C7P3 as compared with control in terms of increased closure rate, more collagen synthesis, and higher re-epithelialization. Therefore, it was concluded the prepared chitosan/WPU hydrogel scaffolds was promising dressings for full-thick ness wound regeneration [6].

As above, these many positive results support the potential of WPU-based scaffolds to be used for an artificial skin graft.

#### 14.4.4 Antibacterial Materials

Microbial contamination on the surface of materials results in not only the formation of multi resistant bacterial strains, pathogenic infections

but also materials damage. The hazards mentioned above have posed a health threat [114, 153], packaging industry of food [3, 150, 151], biosensors, water purification system [150, 151], etc. Common strategies are used for embedding antibiotics [108], triclosan [123]. Antimicrobial products have drawn a great attention from industrial area. Many researchers have been performed for developing of alternative antibacterial therapeutics such as quaternary ammonium salts (QAS) [75], Ag [107], antimicrobial peptides [33], and guanidine polymers [102] destroying bacteria membrane or escaping intracellular components from bacterial cells. However, it has a critical issue with masking by biomolecules film or residues of cells resulting in interrupting further bacterial interactions as well as causing side effects [13]. Therefore the development of waterborne antibacterial materials embedding antibiotics via simple fabrication methods is a crucial strategy to combat microbial contamination of materials [82]. Nowadays, antibacterial and antifouling materials have focused on surface modification in regard to waterborne polyurethane as an immobilizing surface of materials owing to mechanical and physical properties as well as low cost since 2009 [22–25]. In addition, waterborne polyurethanes (WPU) have attracted attention because of possibility of tailoring their properties altering the composition, a widespread applications, non-toxicity, non-flammability, and

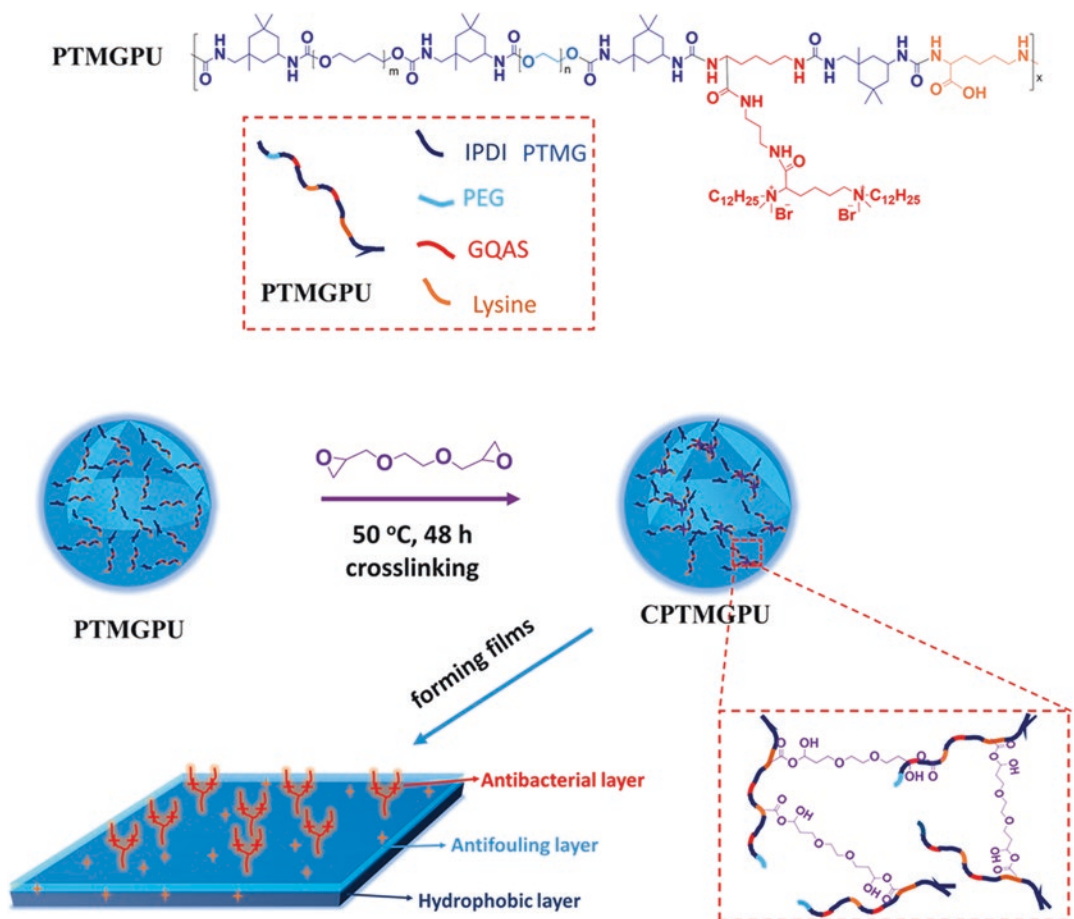
environment-friendly approaches in comparison with solvent-borne polyurethane. [18, 27] Zhang et al. also developed WPU materials with good antibacterial activity using IPDI, PTMG, PEG, L-lysine and a novel GQAS diamine EG12 by a facile polymerization strategy without any organic agent [153]. Hendessi et al. developed WPU nanocomposite films incorporating carvacrol loaded HNTs as antibacterial nanofillers resulting in sustained releasing of natural antibacterial agents. The nanocomposites demonstrated growth inhibition and killing bacterial activity and also, they offered surfaces with strong potential for preventing bacterial colonization [46]. Anionic WPU/Ag nanocomposites prepared by Wattanodorn [132] displayed sustained silver ion release over 21 days, causing in excellent antibacterial activities as well as enhancement of tensile strength and Young's modulus.

Even if the WPU composites above mentioned exhibited a dramatically enhancement of antibacterial activities, the use of biocides may introduce adverse effects including cytotoxicity, inflammatory responses, and hypersensitivity. A use of lysozyme, proteases, and glucosidases has been proposed as an alternative to bond covalently enzymes on polymer material surfaces [84, 85, 122], however the process of covalent bonding, unfortunately occurred in organic conditions, leads to denature a part of enzymes. WPU have been considered as green materials with highly tunable properties. Moreover, it has good compatibility to embed enzyme [84, 85]. Wu et al. reported that waterborne cationic polyurethane (WPU) nanoparticles (NPs) exhibit excellent antibacterial activity against *Escherichia coli* (*E. coli*) and *Staphylococcus aureus* (*S. aureus*). The number of colonies formed in all other groups reduced comparing with initial values. The antibacterial ratio of WPU NPs has reached 100% during a contact time of 3 h. For also the fabricated WPU films, it reached 100% against both *E. coli* and *S. aureus* after a contact time of 24 h. Zhang et al. successfully fabricated crosslinked WPUs containing quaternary ammonium salts with long-term stability, excellent antibacterial activity and biocompatibility by the crosslinking

of poly(ethylene glycol) (PEG), polyoxytetramethylene glycol (PTMG), isophorone diisocyanate (IPDI), L-lysine, and its derivative diamine consisting of gemini QAS (GQAS) with ethylene glycol diglycidyl ether (EGDE) through simple method as shown in Fig. 14.6. The fabricated WPU films are consisted of a gemini quaternary ammonium salt (GQAS) antibacterial upper layer and an antifouling PEG sublayer, with largely improved stability by crosslinking. The films display recyclable contact-active bactericidal activity. Also, the crosslinked WPUs are potentially biocompatible both in vitro and in vivo without toxicity on surrounding tissues. Accordingly, the crosslinked waterborne polyurethane systems have potential of implants and medical devices to combat microbial infections [154].

Chinese government has established more stringent drinking water criterion based on the standard of drinking water quality (GB5749-2006) involving the concentration of ammonia nitrogen below less than 0.5 mg/L. [23]. In water treatment area, an efficient plan for dealing with removal of ammonia nitrogen from micro-polluted water has become a matter of grave concern. In comparison to the conventional approach of growing nitrifying bacteria for biological ammonia nitrogen removal processes, immobilization of nitrifying bacteria can be more effective in retaining biomasses for nitrification process even in very short hydraulic retention times (HRT) and low ammonia concentration environment in an up-flow inner circulation reactor with 10% pellets stuffing ratio in volume.

Wijffels and Tramper showed that nitrifying bacteria show various nitrification characteristics depending on different ammonia concentrations. [133] Studies related to the effect of nitrification on environmental factors at low ammonia concentrations have been hardly ever reported, especially in cells immobilized. Recently, WPU was employed as a novel supporting material with specific mechanical and chemical properties for the entrapment and immobilization of single nitrifying or denitrifying bacteria strains for wastewater treatment [24]. Dong et al. reported that WPU immobilized nitrifying bacteria displayed efficient removal of ammonia nitrogen



**Fig. 14.6** Schematic structure of PTMGPU and the preparation of CPTMGPU films. (Adapted with permission from Zhang et al. [154]. Copyright (2017) American Chemical Society)

from wastewater with stability for long-term period, thereby being a promising water treatment approach in long duration. These WPU materials have great potential for antibacterial applications.

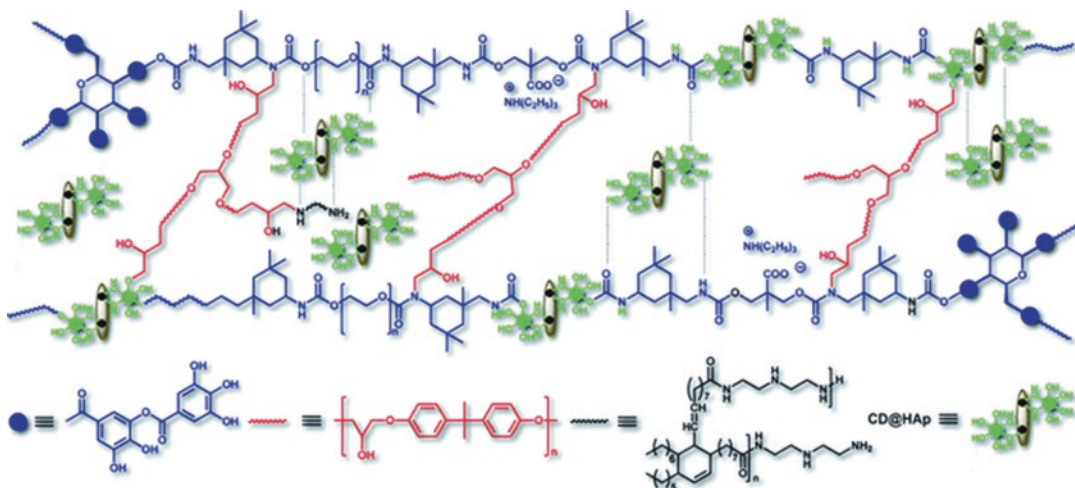
## 14.5 WPU Nanocomposites and Curing

Since the physical properties of WPU are lower than that of general PU, nanocomposites or curing processes are used for industrial applications. Most preferred coating material are biobased WPU and its nanocomposites as high performing environmentally benign systems with good abrasion resistance, impact resistance, flexibility

hardness, gloss, reduced flammability, chemical resistance, durability, high adhesive strength, low viscosity, easy cleaning and weather-ability, in addition to zero or low emission of VOCs. Further an in situ fabricated waterborne nanocomposites exhibited better performance than the pristine WPU due to the strong interactions between the PU matrix and the interactional functional groups of the nanoparticles [152].

### 14.5.1 Nanocomposites

WPU/Ag nanocomposites films were prepared through mixing aqueous solution of  $\text{AgNO}_3$  and WPU reduced by  $\text{NaBH}_4$ . The particle size of Ag is dependent on the concentration of  $\text{AgNO}_3$ .



**Scheme 14.6** Thermosetting in situ carbon dot/hydroxy apatite/WPU nanocomposite. (Adapted with permission from Gogoi et al. [38]. Copyright (2016) Royal Society of Chemistry)

Higher  $\text{AgNO}_3$  concentration results in larger particle [136]. Chou et al. produced WPU/Ag nanocomposites by mixing the waterborne PU with the nanoparticle suspension, casting and drying at  $60^\circ\text{C}$  [15]. All these nanocomposites exhibited good antibacterial properties (Scheme 14.6).

Satyabrat Gogoi et al. synthesized a carbon dot/hydroxy apatite nano hybrid. This nano hybrid was successfully fabricated as a bio-based waterborne multi-branched polyurethane system using in-situ technology. The evaluation of mechanical and biological properties showed excellent benefits over the properties of the hydroxyapatite/polyurethane system. The results can be used as bone substitutes [38].

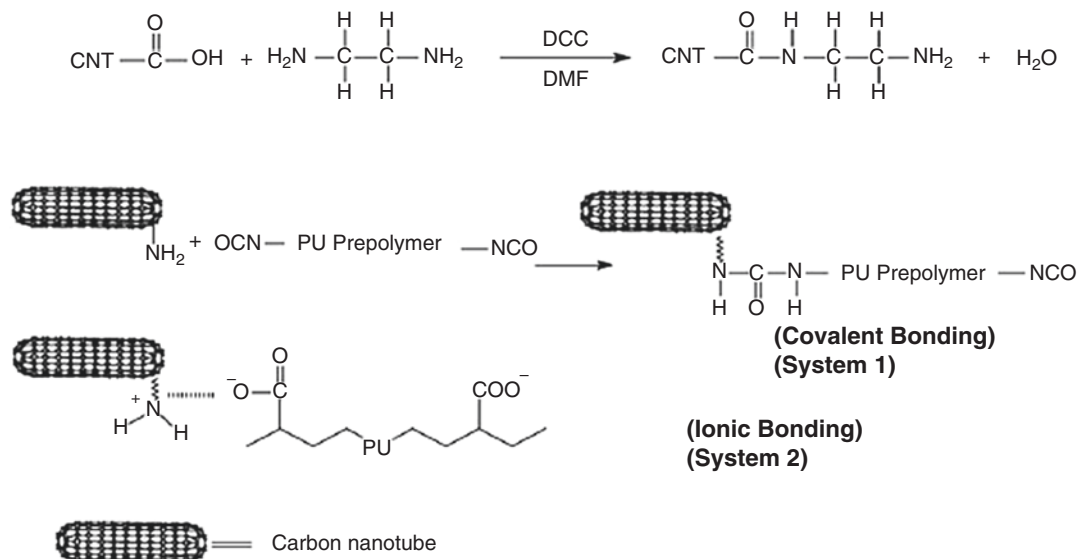
WPU nanocomposites with  $\text{ZnO}$ ,  $\text{TiO}_2$ ,  $\text{Fe}_2\text{O}_3$ ,  $\text{SiO}_2$ , clay, cellulose nanocrystals (CNC), silk, polyhedral oligomeric silsesquioxane (POSS) [89], functionalized carbon nanotube (CNT) etc. Hsu-Chiang Kuan et al. successfully prepared nanocomposite consists of multiwall carbon nanotube (CNT)/waterborne polyurethane (WPU) nanocomposite for increasing the physical properties of nanocomposite due to covalent bonding system between modified CNT and WPU [71].

Many researchers also have been reported in the literature about cellulose nanocrystal/WPU

nanocomposite, which exhibits typical behavior of composites reinforced by agents with a high ratio and good adhesion. Although the ductility of the final nanocomposites was slightly reduced, the Young's modulus and strength were significantly improved [8, 101]. Arantzazu Santamari et al. observed, the polyurethane microstructure was altered by varying the NCO/OH ratio. At low NCO/OH ratio, soft ordered domains were observed, whereas at higher NCO/OH ratio, hard ordered domains were obtained. These PU microstructures act as crystal growth inhibitors or nucleating agents to induce other behaviors of the CNC reinforcement to control the properties of the final material [111] (Scheme 14.7).

Silk fibroin (SF) is an attractive material well known for its structural, biological and hemodynamic properties. WPU/SF is a promising scaffold material for tissue engineering applications. Significant strengthening and toughening can be achieved by introducing SF powder into the WPU formulations [120].

Nanocomposites with  $\text{ZnO}$  and  $\text{TiO}_2$  could be used protecting coating materials. Coatings containing  $\text{ZnO}$  and  $\text{TiO}_2$  microparticles have the low surface tension, which improve coating penetration into matrix and reduce photodegradation. Therefore, they intended to be used coating materials [104, 110]. Such nanocomposites with



**Scheme 14.7** Covalent bonding and ionic bonding between the carbon nanotube and waterborne polyurethane. (Adapted with permission from Kuan et al. [71]. Copyright (2005) Elsevier)

metal oxide such as  $\text{TiO}_2$ ,  $\text{ZnO}$ ,  $\text{Al}_2\text{O}_3$ ,  $\text{SiO}_2$ , etc.) afford antibacterial hygienic coating and thus find applications in marine coatings. A PUD/silica nanocomposite obtained by in situ formation of  $\text{SiO}_2$  nanoparticles through hydrolysis and condensation reactions of tetraethoxysilane (TEOS) with or without methyltriethoxysilane (MTES) in PUD exhibited good abrasion resistance and could be used as coatings for fabric, leather, and paper [40] (Scheme 14.8).

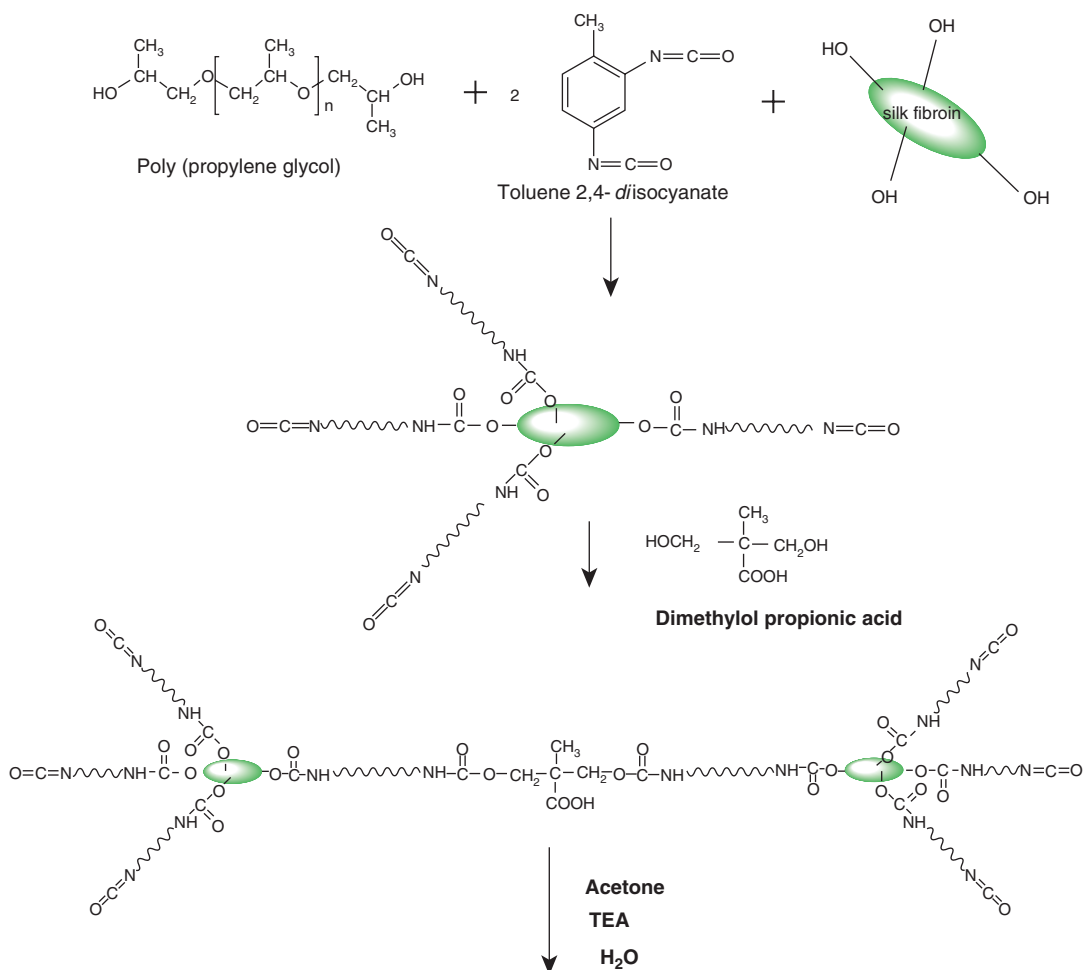
PEDOT/PSS particles also are used as composites with WPU solution. Highly conductive and stretchable polymer films were prepared by blending a conductive polymer, poly(3,4-ethylenedioxythiophene), polystyrenesulfonate (PEDOT:PSS), with highly stretchable waterborne polyurethane (WPU). The two polymers have good miscibility at a wide range of blending ratios. This method provides a facile method to develop highly stretchable conductive polymer films [79]. Rui Zhou et al. suggested Stretchable or wearable electric heaters developed by using composites of intrinsically conductive poly(3,4-ethylenedioxythiophene):poly(styrene sulfonic acid) (PEDOT:PSS), elastomeric waterborne polyurethane (WPU) and reduced graphene oxide (rGO) for arthritis, stiff

muscles, joint injuries, and injuries to the deep tissue of skin [157]. The mechanical properties of WPU/nanocomposites tested by several authors are shown in Table 14.3.

### 14.5.2 Curing

In recent days, the importance application on bio-material of WPU is coating process due to zero or low VOC content, water resistance, low temperature flexibility, pH stability, excellent weathering resistance, superior solvent resistance, and desirable chemical and mechanical properties. Among many processing methods to curing, UV-cured WPU coating is preferable due to their environmentally friendly nature, fast curing, and low energy requirements [4, 140].

Ultraviolet (UV) curable WPU coating was obtained from HEMA-capped oligomer, butyl acrylate (BA) and multifunctional acrylates (TPGDA) as reactive diluents, and Darocur 1173 as photoinitiator by Jicheng Xu et al. Ultraviolet (UV) cured WPUA films prepared from HEMA-capped oligomer, butyl acrylate (BA), and multifunctional acrylates (TPGDA) as reactive diluents and with Darocur 1173 as photoinitiator, showed



**Scheme 14.8** Schematic representation of the preparation of the WPU-SF dispersions in Water/Acetone. (Adapted from Tao et al. [120])

good mechanical and thermal properties with good microstructures, which was used to protect iron materials of iron cultural relics.

Waterborne UV-curable polyurethane dispersion was also obtained by a phase-inversion emulsification technique using water-soluble poly(ethylene glycol) monomethyl ether methacrylate surface-modified silica. DMA analysis revealed the formation of strong covalent interactions between the WUPU chain and modified aqueous colloidal silica. The mechanical properties of the WUPU/silica hybrid films displayed higher storage modulus as modified aqueous colloidal silica content increased to 10 wt%. The

resulting high-transparency nanocomposite films are promising materials for high-performance water-based UV-curable coatings [150, 151].

## 14.6 Conclusions and Future Perspectives

Waterborne polyurethanes (WPU) are a widely utilized in versatile areas of materials, including coatings, adhesives, sealants, elastomers [29, 36, 59, 69] and in addition, as scaffold materials for tissue regeneration as well as delivering vehicles in drug delivery system [56]. Although

**Table 14.3** Classification of mechanical properties of WPU nanocomposites

Nanocomposites material	Young's modulus (MPa)	Tensile strength (MPa)	Strain at break (%)	References
PEDOT:PSS	18.3 ± 0.7	5.3	860	[157] [79]
PEDOT:PSS/graphene oxide(1 wt%)	18.2 ± 0.2	12.5	530	[157]
Silk fibroin	0.3–3.91	0.56–8.94	1067–2480	[120]
Multiwall carbon nanotube(2.5 phr)	110 ± 10	12 ± 1	–	[71]
Clay	1.7–6.9	15.0–33.6	517–794	[64], [65]
Cellulose nanocrystals	80–160	18–27	450–780	[111] [8]
Hydroxyapatite	30.87	17.47 ± 0.67	205 ± 3	[38]
Carbon dot decorated hydroxyapatite	38.26	20.43 ± 0.35	221 ± 2	[38]
Silver	40–130	15–33	400	[132]

polyurethane can be divided into 2 types according to the dispersions, solvent-borne and water-borne, the waterborne polyurethane, namely dispersed in water condition, has been concerned with their applications owing to environment-friendly fabrication approach, higher durability, and preferable tailoring capability. It is mightily important to understand behaviors in rheological [7, 43, 44] and mechanical properties [66–68] of WPU for modulating its flow during employments in not only coating to fibers, sealants, sizing of glass fiber, but also tailoring mechanical properties of WPU products [47]. WPU composites have been rigorously conducted in both academia and industry, because of its simplicity and efficiency in developing novel materials with a goal of reinforcement using microscale or nanoscale fillers.

In this chapter we have introduced to waterborne polyurethane mechanical, chemical, and biological properties and reviewed their applications in biomedical areas. Recently, WPU elastomers have been widely regarded as one of popular biomaterials, owing to their excellent mechanical properties, especially tensile strength and elasticity, higher durability, capacity of tailoring capability, and blood and tissue compatibility. As reviewed in this chapter, the properties mentioned above are partially determined by the reagents selected for synthesis from the large range of possible precursors.

These properties can be adjusted using appropriate selection of components (macroglycol, diisocyanate, and chain extender), in particular structure and composition, optimization of polymerization conditions, post-synthesis modification.

The mechanical properties of WPU are influenced by the fabrication methods. Almost these factors attribute to the performance of PUs in biomedical applications. Also, additives, conditions of processing can alter the functions of biomaterials and understanding about this correlation can help to comprehend the conversion from a biomaterial to a biomedical device. This correlation is useful to design materials for medical devices, especially to overcome the obstacles of thrombosis on the surface, infection, and calcification of engineered WPU materials.

Eventually, a biomaterial in biomedical applications is the key in the function of medical devices, and is a significant constituent of regenerative medicine and surgery. Therefore, the advance of developed biomaterials can be depended on progress in the biological science, engineering, and medical science. In spite of the limitations of using synthetic materials for biomedical applications, researches for using PUs and WPUs in particular have persistently investigated. Courtesy of its various chemistries finally causing tailored mechanical properties engineered by researchers, continued in the line



of considering as biomaterials. Since the biomaterial is a rising answer for regenerative medicine, WPU with an eco-friendly fabrication method will be employed in new ways as part of the therapeutic strategy.

Besides, the WPU advanced applications can be extended to special attributes like shape memory, self-healing, self-cleaning composites with biodegradability and biocompatibility, etc. Especially, applications of WPU nanocomposites are unlimited due to the extraordinary performance of nanomaterials. However the changes in the properties of such nanocomposites by various nanomaterials at different dose levels are not consistent and particularly the mechanism behind these phenomena are still unclear.

**Acknowledgements** This research was supported by the Basic Science Research Program of the National Research Foundation of Korea (NRF) funded by the Ministry of Education (NRF-2015R1C1A2A01056027 and NRF-2016R1A6A3A11930280).

## References

- Ajorlou E, Khosroushahi AY, Yeganeh H (2016) Novel water-borne polyurethane nanomicelles for cancer chemotherapy: higher efficiency of folate receptors than TRAIL receptors in a cancerous Balb/C mouse model. *Pharm Res* 33(6):1426–1439. <https://doi.org/10.1007/s11095-016-1884-6>
- Alizadeh M, Abbasi F, Khoshfetrat AB, Ghaleh H (2013) Microstructure and characteristic properties of gelatin/chitosan scaffold prepared by a combined freeze-drying/leaching method. *Mater Sci Eng C* 33(7):3958–3967. <https://doi.org/10.1016/j.msec.2013.05.039>
- Alvarez Gonza'lez A, Igarzabal CI (2013) Soy protein–poly (lactic acid) bilayer films as biodegradable material for active food packaging. *Food Hydrocoll* 33(2):289–296. <https://doi.org/10.1016/j.foodhyd.2013.03.010>
- Athawale VD, Kulkarni MA (2010) Polyester polyols for waterborne polyurethanes and hybrid dispersions. *Prog Polym Coat* 67(1):44–54. <https://doi.org/10.1016/j.porgcoat.2009.09.015>
- Babanejad N, Nikjeh MA, Amini M, Dorkoosh FA (2014) A nanoparticulate raloxifene delivery system based on biodegradable carboxylated polyurethane: design, optimization, characterization, and in vitro evaluation. *J Appl Polym Sci* 131(1):39668–39678. <https://doi.org/10.1002/app.39668>
- Bankoti K, Rameshbabu AP, Datta S, Maity PP, Goswami P, Datta P, Ghosh SK, Mitra A, Dhara S (2017) Accelerated healing of full thickness dermal wounds by macroporous waterborne polyurethane-chitosan hydrogel scaffolds. *Mater Sci Eng C* 81:133–143. <https://doi.org/10.1016/j.msec.2017.07.018>
- Bazyleva AB, Hasan MA, Fulem M, Becerra M, Shaw JM (2009) Bitumen and heavy oil rheological properties: reconciliation with viscosity measurements. *J Chem Eng Data* 55(3):1389–1397. <https://doi.org/10.1021/je900562u>
- Cao X, Habibi Y, Lucia LA (2009) One-pot polymerization, surface grafting, and processing of waterborne polyurethane-cellulose nanocrystal nanocomposites. *J Mater Chem* 19:7137–7145. <https://doi.org/10.1039/B910517D>
- Chan WC, Chen SA (1988) Polyurethane ionomers: effects of emulsification on properties of hexamethylene diisocyanate-based polyether polyurethane cationomers. *Polymer* 29(11):1995–2001. [https://doi.org/10.1016/0032-3861\(88\)90173-5](https://doi.org/10.1016/0032-3861(88)90173-5)
- Chen GN, Chen KN (1997) Self-curing behaviors of single pack aqueous-based polyurethane system. *J Appl Polym Sci* 63(12):1609–1623. [https://doi.org/10.1002/\(SICI\)1097-4628\(19970321\)63:12<1609::AID-APP12>3.0.CO;2-V](https://doi.org/10.1002/(SICI)1097-4628(19970321)63:12<1609::AID-APP12>3.0.CO;2-V)
- Chen GN, Chen KN (1999) Hybridization of aqueous-based polyurethane with glycidyl methacrylate copolymer. *J Appl Polym Sci* 71(6):903–913. [https://doi.org/10.1002/\(SICI\)1097-4628\(19990207\)71:6<903::AID-APP6>3.0.CO;2-O](https://doi.org/10.1002/(SICI)1097-4628(19990207)71:6<903::AID-APP6>3.0.CO;2-O)
- Chen H, Jiang X, He L, Zhang T, Xu M, Yu X (2002) Novel biocompatible waterborne polyurethane using L-lysine as an extender. *J Appl Polym Sci* 84(13):2474–2480. <https://doi.org/10.1002/app.10568>
- Cheng G, Xue H, Zhang Z et al (2008) A switchable biocompatible polymer surface with self-sterilizing and nonfouling capabilities. *Angew Chem Int Ed* 120(46):8963–8966. <https://doi.org/10.1002/ange.200803570>
- Choi SM, Singh D, Han SS (2016) Wound care: skin tissue regeneration, encyclopedia of biomedical polymers and polymeric. *Biomaterials*:8258–8276. <https://doi.org/10.1081/E-EBPP-120050587>
- Chou CW, Hsu SH, Chang H, Tseng SM, Lin HR (2006) Enhanced thermal and mechanical properties and biostability of polyurethane containing silver nanoparticles. *Polym Degrad Stab* 91:1017–1024. <https://doi.org/10.1016/j.polymdegradstab.2005.08.001>
- Chu Y, Yu H, Ma Y, Zhang Y, Chen W, Zhang G, Wei H, Zhang X, Zhuo R, Jiang X (2014) Synthesis and characterization of biodegradable pH and reduction dual-sensitive polymeric micelles for doxorubicin delivery. *J Polym Sci Part A* 52(13):1771–1780. <https://doi.org/10.1002/pola.27192>

17. Coutinho FMB, Delpech MC (2000) Waterborne anionic polyurethanes and poly(urethane-urea) s-influence of the chain extender on mechanical and adhesive properties. *Polym Test* 19(8):939–952. [https://doi.org/10.1016/S0142-9418\(99\)00066-5](https://doi.org/10.1016/S0142-9418(99)00066-5)
18. Dai L, Long Z, Hong R, Deng X, He H, Liu W (2014) Electrospun polyvinyl alcohol/waterborne polyurethane composite nanofibers involving cellulose nanofibers. *J Appl Polym Sci* 131(22):41051/1–41051/6. <https://doi.org/10.1002/app.41051>
19. Dash M, Chiellini F, Ottenbrite RM, Chiellini E (2011) Chitosan—a versatile semi-synthetic polymer in biomedical applications. *Prog Polym Sci* 36(8):981–1014. <https://doi.org/10.1016/j.progpolymsci.2011.02.001>
20. Dieterich D (1981) Aqueous emulsions, dispersions and solutions of polyurethanes; synthesis and properties. *Prog Org Coat* 9:281–340. [https://doi.org/10.1016/0033-0655\(81\)80002-7](https://doi.org/10.1016/0033-0655(81)80002-7)
21. Ding M, Song N, He X, Li J, Zhou L, Tan H, Fu Q, Gu Q (2013) Toward the next-generation nanomedicines: design of multifunctional multiblock polyurethanes for effective cancer treatment. *ACS Nano* 7(3):1918–1928. <https://doi.org/10.1021/nm4002769>
22. Dong Y, Zhang Z, Deng YY, Wang Y (2009) Immobilization of nitrifying bacteria in waterborne polyurethane hydrogel for removal of ammonium nitrogen from wastewater. In: 3rd International conference on bioinformatics and biomedical engineering, IEEE Xplore. <https://doi.org/10.1109/ICBBE.2009.5162924>
23. Dong Y, Zhang Z, Jin Y, Li Z, Lu J (2011) Nitrification performance of nitrifying bacteria immobilized in waterborne polyurethane at low ammonia nitrogen concentrations. *J Environ Sci* 23(3):366–371. [https://doi.org/10.1016/S1001-0742\(10\)60418-4](https://doi.org/10.1016/S1001-0742(10)60418-4)
24. Dong Y, Zhang Z, Jin Y, Lu J, Cheng X, Li J, Deng YY, Feng YN, Chen D (2012) Nitrification characteristics of nitrobacteria immobilized in waterborne polyurethane in wastewater of corn-based ethanol fuel production. *J Environ Sci* 24(6):999–1005. [https://doi.org/10.1016/S1001-0742\(11\)60893-0](https://doi.org/10.1016/S1001-0742(11)60893-0)
25. Dong HH, Wang W, Song ZZ, Dong H, Wang JF, Sun SS, Zhang ZZ, Ke M, Zhang Z, Wu WM, Zhang G, Ma J (2017) A high-efficiency denitrification bioreactor for the treatment of acrylonitrile wastewater using waterborne polyurethane immobilized activated sludge. *Bioresour Technol* 239:472–481. <https://doi.org/10.1016/j.biortech.2017.05.015>
26. Eaglstein WH (1985) Experiences with biosynthetic dressings. *J Am Acad Dermatol* 12:434–440. [https://doi.org/10.1016/S0190-9622\(85\)80006-2](https://doi.org/10.1016/S0190-9622(85)80006-2)
27. Fang C, Zhou X, Yu Q, Liu S, Guo D, Yu R (2014) Synthesis and characterization of low crystalline waterborne polyurethane for potential application in water-based ink binder. *Prog Org Coat* 77(1):61–71. <https://doi.org/10.1016/j.porgcoat.2013.08.004>
28. Florczyk SJ, Wang K, Jana S, Wood DL, Sytsma SK, Sham J, Kievit FM, Zhang M (2013) Porous chitosan-hyaluronic acid scaffolds as a mimic of glioblastoma microenvironment ECM. *Biomaterials* 34(38):10143–10150. <https://doi.org/10.1016/j.biomaterials.2013.09.034>
29. Florian P, Jena KK, Allauddin S, Narayan R, Raju KVS (2010) Preparation and characterization of waterborne hyperbranched polyurethane-urea and their hybrid coatings. *Ind Eng Chem Res* 49(10):4517–4527. <https://doi.org/10.1021/ie900840g>
30. Fu H, Yan C, Zhou W, Huang H (2013) Preparation and characterization of a novel organic montmorillonite/fluorinated waterborne polyurethane nanocomposites: effect of OMMT and HFBMA. *Compos Sci Technol* 85:65–72. <https://doi.org/10.1016/j.compscitech.2013.05.018>
31. Gaddam SK (2016) Anionic waterborne polyurethane dispersions from maleated cotton seed oil polyol carrying ionisable groups. *Colloid Polym Sci* 294(2):347–355. <https://doi.org/10.1007/s00396-015-3787-1>
32. Gao C, Xu X, Ni J, Lin W, Zheng Q (2009) Effects of castor oil, glycol semi-ester, and polymer concentration on the properties of waterborne polyurethane dispersions. *Polym Eng Sci* 49(1):162–167. <https://doi.org/10.1002/pen.21235>
33. Gao G, Lange D, Hilpert K et al (2011) The biocompatibility and biofilm resistance of implant coatings based on hydrophilic polymer brushes conjugated with antimicrobial peptides. *Biomaterials* 32(16):3899–3909. <https://doi.org/10.1016/j.biomaterials.2011.02.013>
34. García-Pacios V, Iwata Y, Colera M, Martín-Martínez JM (2011) Influence of the solids content on the properties of waterborne polyurethane dispersions obtained with polycarbonate of hexanediol. *Int J Adhes Adhes* 31(8):787–794. <https://doi.org/10.1016/j.ijadhadh.2011.05.010>
35. Garcia-Pacios V, Colera M, Iwata Y, Martín-Martínez JM (2013) Incidence of the polyol nature in waterborne polyurethane dispersions on their performance as coatings on stainless steel. *Prog Org Coat* 76(12):1726–1729. <https://doi.org/10.1016/j.porgcoat.2013.05.007>
36. Ghosh B, Urban MW (2009) Self-repairing oxetane-substituted chitosan polyurethane networks. *Science* 323(5920):1458–1460. <https://doi.org/10.1126/science.1167391>
37. Gogoi S, Karak N (2014) Biobased biodegradable waterborne hyperbranched polyurethane as an eco-friendly sustainable material. *ACS Sustain Chem Eng* 2(12):2730–2738. <https://doi.org/10.1021/sc5006022>
38. Gogoi S, Kumar M, Mandal BB, Karak N (2016) A renewable resource based carbon dot decorated hydroxyapatite nanohybrid and its fabrication with waterborne hyperbranched polyurethane for bone tissue engineering. *RSC Adv* 6:26066–26076. <https://doi.org/10.1039/c6ra02341j>
39. Guelcher SA, Gallagher KM, Didier JE, Klindedt DB, Doctor JS, Goldstein AS (2005) Synthesis of

- biocompatible segmented polyurethanes from aliphatic diisocyanates and diurea diol chain extenders. *Acta Biomater* 1(4):471–484. <https://doi.org/10.1016/j.actbio.2005.02.007>
40. Guo YH, Guo JJ, Miao H, Teng LJ, Huang Z (2014) Properties and paper sizing application of waterborne polyurethane emulsions synthesized with isophorone diisocyanate. *Prog Org Coat* 77(5):988–996. <https://doi.org/10.1016/j.porgcoat.2014.02.003>
  41. Gurunathan T, Mohanty S, Nayak SK (2015) Effect of reactive organoclay on physicochemical properties of vegetable oil-based waterborne polyurethane nanocomposites. *RSC Adv* 5(15):11524–11533. <https://doi.org/10.1039/C4RA14601H>
  42. Harjunalanen T, Lahtinen M (2003) The effects of altered reaction conditions on the properties of anionic poly(urethane-urea) dispersions and films cast from the dispersions. *Eur Polym J* 39:817–824. [https://doi.org/10.1016/S0014-3057\(02\)00279-3](https://doi.org/10.1016/S0014-3057(02)00279-3)
  43. Hasan MA, Shaw JM (2010) Rheology of reconstituted crude oils: artifacts and asphaltenes. *Energy Fuel* 24:6417–6427. <https://doi.org/10.1021/ef101185x>
  44. Hasan MA, Fulem M, Bazyleva A, Shaw JM (2009) Rheological properties of nanofiltered athabasca bitumen and maya crude oil. *Energy Fuel* 23:5012–5021. <https://doi.org/10.1021/ef900313r>
  45. Hassan MK, Mauritz KA, Storey RF, Wiggins JS (2006) Biodegradable aliphatic thermoplastic polyurethane based on poly( $\epsilon$ -caprolactone) and L-lysine diisocyanate. *J Polym Sci A-Polym Chem* 44(9):2990–3000. <https://doi.org/10.1002/pola.21373>
  46. Hendessi S, Sevinis EB, Unal S, Unal H (2016) Antibacterial sustained-release coating from halloysite nanotubes/waterborne polyurethanes. *Prog Org Coat* 101:253–261. <https://doi.org/10.1016/j.porgcoat.2016.09.005>
  47. Hsu SH, Tang CM, Tseng HJ (2006) Biocompatibility of poly(ether)urethane-gold nanocomposites. *J Biomed Mater Res Part A* 79A:759–770. <https://doi.org/10.1002/jbm.a.30879>
  48. Hsu SH, Hung KC, Lin YY, Su CH, Yeh HY, Jeng US, Lu CY, Dai SA, Fu WE, Lin JC (2014) Water-based synthesis and processing of novel biodegradable elastomers for medical applications. *J Mater Chem B* 2:5083–5092. <https://doi.org/10.1039/C4TB00572D>
  49. Hsu SH, Chang WC, Yen CT (2017) Novel flexible nerve conduits made of water-based biodegradable polyurethane for peripheral nerve regeneration. *J Biomed Mater Res A* 105(5):1383–1392. <https://doi.org/10.1002/jbm.a.36022>
  50. Huang GS, Tseng CS, Yen BL, Dai LG, Hsieh PS, Hsu HS (2013a) Solid freeform-fabricated scaffolds designed to carry multicellular mesenchymal stem cell spheroids for cartilage regeneration. *Eur Cell Mater* 26(13):179–194. <https://doi.org/10.22203/eCM.v026a13>
  51. Huang Y, He K, Wang X (2013b) Rapid prototyping of a hybrid hierarchical polyurethane-cell/hydrogel construct for regenerative medicine. *Mater Sci Eng C* 33(6):3220–3229. <https://doi.org/10.1016/j.msec.2013.03.048>
  52. Huang F, Cheng R, Meng F, Deng C, Zhong Z (2015) Micelles based on acid degradable poly(acetal urethane): preparation, pH-sensitivity, and triggered intracellular drug release. *Biomacromolecules* 16(7):2228–2236. <https://doi.org/10.1021/acs.biomac.5600625>
  53. Hung KC, Tseng CS, Hsu SH (2014) Synthesis and 3D printing of biodegradable polyurethane elastomer by a water-based process for cartilage tissue engineering applications. *Adv Healthc Mater* 3(10):1578–1587. <https://doi.org/10.1002/adhm.201400018>
  54. Hung KC, Tseng CS, Dai LG, Hsu SH (2016) Water-based polyurethane 3D printed scaffold with controlled release function for customized cartilage tissue engineering. *Biomaterials* 83:156–168. <https://doi.org/10.1016/j.biomaterials.2016.01.019>
  55. Huo M, Yuan J, Tao L, Wei Y (2014) Redox-responsive polymers for drug delivery: from molecular design to applications. *Polym Chem* 5:1519–1528. <https://doi.org/10.1039/C3PY01192E>
  56. Jabbari E, Khakpour M (2000) Morphology of and release behavior from porous polyurethane microspheres. *Biomaterials* 21(2):2073–2079. [https://doi.org/10.1016/S0142-9612\(00\)00135-6](https://doi.org/10.1016/S0142-9612(00)00135-6)
  57. Jang JY, Jhon YK, Cheong IW, Kim JH (2002) Effect of process variables on molecular weight and mechanical properties of water-based polyurethane dispersion. *Colloids Surf A Physicochem Eng Asp* 196(2–3):135–143. [https://doi.org/10.1016/S0927-7757\(01\)00857-3](https://doi.org/10.1016/S0927-7757(01)00857-3)
  58. Jian JY, Chang JK, Shau MD (2009) Synthesis and characterizations of new lysine-based biodegradable cationic poly(urethane-co-ester) and study on self-assembled nanoparticles with DNA. *Bioconjug Chem* 20(4):774–779. <https://doi.org/10.1021/bc800499w>
  59. Jung YC, Kim HH, Kim YA, Kim JH, Cho JW, Endo M, Dresselhaus MS (2010) Optically active multi-walled carbon nanotubes for transparent, conductive memory-shape polyurethane film. *Macromolecules* 43(14):6106–6112. <https://doi.org/10.1021/ma101039y>
  60. Khong TT, Aarstad OA, Skjåk-Bræk G, Draget KI, Vårum KM (2013) Gelling concept combining chitosan and alginate proof of principle. *Biomacromolecules* 14(8):2765–2771. <https://doi.org/10.1021/bm400610b>
  61. Kim BK (1996) Aqueous polyurethane dispersions. *Colloid Polym Sci* 274:599–611. <https://doi.org/10.1007/BF00653056>
  62. Kim YJ, Kim BK (2014) Synthesis and properties of silanized waterborne polyurethane/graphene nanocomposites. *Colloid Polym Sci* 292(1):51–58. <https://doi.org/10.1007/s00396-013-3054-2>

63. Kim BK, Kim TK, Jeong HM (1994) Aqueous dispersion of polyurethane anionomers from H<sub>12</sub>MDI/IPDI, PCL, BD, and DMPA. *J Appl Polym Sci* 53:371–378. <https://doi.org/10.1002/app.1994.070530315>
64. Kim BK, Yang JS, Yoo SM, Lee JS (2003a) Waterborne polyurethanes containing ionic groups in soft segments. *Colloid Polym Sci* 281:461–468. <https://doi.org/10.1007/s00396-002-0799-4>
65. Kim BK, Seo JW, Jeong HM (2003b) Morphology and properties of waterborne polyurethane/clay nanocomposites. *Eur Polym J* 39(1):85–91. [https://doi.org/10.1016/S0014-3057\(02\)00173-8](https://doi.org/10.1016/S0014-3057(02)00173-8)
66. Kim AK, Hasan MA, Nahm S, Cho S (2005a) Evaluation of compressive mechanical properties of Al-foams using electrical conductivity. *Compos Struct* 71:191–198. <https://doi.org/10.1016/j.compstruct.2004.10.016>
67. Kim AK, Hasan MA, Choen SS, Lee HJ (2005b) The constitutive behavior of metallic foams using nanoindentation technique and Fe modeling. *Key Eng Mater* 297/300:1050. <https://doi.org/10.4028/www.scientific.net/KEM.297-300.1050>
68. Kim AK, Hasan MA, Lee HJ, Cho SS (2005c) Characterization of submicron mechanical properties of Al-alloy foam using nanoindentation technique. *Mater Sci Forum* 475–479:4199–4202. <https://doi.org/10.4028/www.scientific.net/MSF.475-479.4199>
69. Kim H, Miura Y, Macosko CW (2010) Graphene/polyurethane nanocomposites for improved gas barrier and electrical conductivity. *Chem Mater* 22(11):3441–3450. <https://doi.org/10.1021/cm100477v>
70. Kim HL, Jung GY, Yoon JH, Han JS, Park YJ, Kim DG, Zhang M, Kim DJ (2015) Preparation and characterization of nano-sized hydroxyapatite/alginate/chitosan composite scaffolds for bone tissue engineering. *Mater Sci Eng C* 54:20–25. <https://doi.org/10.1016/j.msec.2015.04.033>
71. Kuan HC, Ma CCM, Chang WP, Yuen SM, Wu HH, Lee TM (2005) Synthesis, thermal, mechanical and rheological properties of multiwall carbon nanotube/waterborne polyurethane nanocomposite. *Compos Sci Technol* 65(11–12):1703–1710. <https://doi.org/10.1016/j.compscitech.2005.02.017>
72. Lamba NMK, Woodhouse KA, Cooper SL (2007) Polyurethans in biomedical applications, vol 1998. CRC Press, New York, pp 205–241
73. Lee TJ, Kwon SH, Kim BK (2014) Biodegradable sol–gel coatings of waterborne polyurethane/gelatin chemical hybrids. *Prog Org Coat* 77(6):1111–1116. <https://doi.org/10.1016/j.porgcoat.2014.03.011>
74. Lei L, Zhong L, Lin X, Li Y, Xia Z (2014) Synthesis and characterization of waterborne polyurethane dispersions with different chain extenders for potential application in waterborne ink. *Chem Eng J* 253:518–525. <https://doi.org/10.1016/j.cej.2014.05.044>
75. Li P, Poon YF, Li W et al (2010) A polycationic antimicrobial and biocompatible hydrogel with microbe membrane suctioning ability. *Nat Mater* 10:149–156. <https://doi.org/10.1038/nmat2915>
76. Li B, Peng D, Zhao N, Mu Q, Li J (2013) The physical properties of nonionic waterborne polyurethane with a polyether as side chain. *J Appl Polym Sci* 127(3):1848–1852. <https://doi.org/10.1002/app.37915>
77. Li Y, Noordover BA, van Benthem RA, Koning CE (2014) Reactivity and regio-selectivity of renewable building blocks for the synthesis of water-dispersible polyurethane prepolymers. *ACS Sustain Chem Eng* 2(4):788–797. <https://doi.org/10.1021/sc400459q>
78. Li Q, Ma L, Gao C (2015b) Biomaterials for in situ tissue regeneration: development and perspectives. *J Mater Chem B* 3(46):8921–8938. <https://doi.org/10.1039/C5TB01863C>
79. Li P, Du D, Guo L, Guob Y, Ouyang J (2016) Stretchable and conductive polymer films for high-performance electromagnetic interference shielding. *J Mater Chem C* 4:6525–6532. <https://doi.org/10.1039/C6TC01619G>
80. Li M, Liu F, Li Y, Qiang X (2017) Synthesis of stable cationic waterborne polyurethane with a high solid content: insight from simulation to experiment. *RSC Adv* 7(22):13312–13324. <https://doi.org/10.1039/c7ra00647k>
81. Liu HL, Dai SA, Fu KY, Hsu SH (2010) Antibacterial properties of silver nanoparticles in three different sizes and their nanocomposites with a new waterborne polyurethane. *Int J Nanomedicine* 19(5):1017–1028. <https://doi.org/10.2147/IJN.S14572>
82. Liu SQ, Yang C, Huang Y et al (2012) Antimicrobial and antifouling hydrogels formed in situ from polycarbonate and poly(ethylene glycol) via Michael addition. *Adv Mater* 24(48):6484–6489. <https://doi.org/10.1002/adma.201202225>
83. Liu N, Zhao Y, Kang M, Wang J, Wang X, Feng Y, Yin N, Li Q (2014) The effects of the molecular weight and structure of polycarbonatediols on the properties of waterborne polyurethanes. *Prog Org Coat* 82:46–56. <https://doi.org/10.1016/j.porgcoat.2015.01.015>
84. Liu K, Su Z, Miao S, Ma G, Zhang S (2016a) Enzymatic waterborne polyurethanetowards robust and environmentally friendly anti-biofouling coating. *RSC Adv* 6:31698–31704. <https://doi.org/10.1039/C6RA04583A>
85. Liu K, Su Z, Miao S, Ma G, Zhang S (2016b) Production of carotenoids by the isolated yeast of *Rhodotorula glutinis*. *Biochem Eng J* 113:107–113. <https://doi.org/10.1016/j.bej.2007.01.004>
86. Lu Y, Larock RC (2008) Soybean-oil-based waterborne polyurethane dispersion: effects of polyol functionality and hard segment content on properties. *Biomacromolecules* 9(11):3332–3340. <https://doi.org/10.1021/bm801030g>
87. Lu Y, Larock RC (2010) Soybean oilbased, aqueous cationic polyurethane dispersions: synthesis and properties. *Prog Org Coat* 69:31–37. <https://doi.org/10.1016/j.porgcoat.2010.04.024>
88. Lu Y, Larock RC (2011) Synthesis and properties of grafted latices from a soybean oil-based waterborne polyurethane and acrylics. *J Appl Polym Sci* 119(6):3305–3314. <https://doi.org/10.1002/app.29029>

89. Madbouly SA, Otaigbe JU (2009) Recent advances in synthesis, characterization and rheological properties of polyurethanes and POSS/polyurethane nanocomposites dispersions and films. *Prog Polym Sci* 34(12):1283–1332. <https://doi.org/10.1016/j.progpolymsci.2009.08.002>
90. Madbouly SA, Xia Y, Kessler MR (2013) Rheological behavior of environmentally friendly castor oil-based waterborne polyurethane dispersions. *Macromolecules* 46(11):4606–4616. <https://doi.org/10.1021/ma400200y>
91. Meier MRA, Metzger JO, Schubert US (2007) Plant oil renewable resources as green alternatives in polymer science. *Chem Soc Rev* 36(11):1788–1802. <https://doi.org/10.1039/B703294C>
92. Mohaghegh SM, Barikani M, Entezami AA (2005) Preparation, and properties of an aqueous polyurethane dispersion. *Iran Polym J* 14:163–168. <https://doi.org/10.1002/app.26138>
93. Nabid MR, Omrani I (2016) Facile preparation of pH-responsive polyurethane nanocarrier for oral delivery. *Mater Sci Eng C* 69:532–537. <https://doi.org/10.1016/j.msec.2016.07.017>
94. Nair LS, Laurencin CT (2007) Biodegradable polymers as biomaterials. *Prog Polym Sci* 32(8–9):762–798. <https://doi.org/10.1016/j.progpolymsci.2007.05.017>
95. Nakajima-Kambe T, Shigeno-Akutsu Y, Nomura N, Onuma F, Nakahara T (1999) Microbial degradation of polyurethane, polyester polyurethanes and polyether polyurethanes. *Appl Microbiol Biotechnol* 51(2):134–140. <https://doi.org/10.1007/s002530051373>
96. Noble KL (1997) Waterborne polyurethanes. *Prog Org Coat* 32(1–4):131–136. [https://doi.org/10.1016/S0300-9440\(97\)00071-4](https://doi.org/10.1016/S0300-9440(97)00071-4)
97. Omrani I, Babanejad N, Shendi HK, Nabid MR (2017a) Fully glutathione degradable waterborne polyurethane nanocarriers: preparation, redox-sensitivity, and triggered intracellular drug release. *Mater Sci Eng C* 70:607–616. <https://doi.org/10.1016/j.msec.2016.09.036>
98. Omrani I, Babanejad N, Shendi HK, Nabid MR (2017b) Preparation and evaluation of a novel sunflower oil-based waterborne polyurethane nanoparticles for sustained delivery of hydrophobic drug. *Eur J Lipid Sci Technol* 119(8):1600283. <https://doi.org/10.1002/ejlt.201600283>
99. Panda SS, Panda BP, Mohanty S, Nayak SK (2017) Synthesis and properties of castor oil-based waterborne polyurethane cloisite 30B nanocomposite coatings. *J Coat Technol Res* 14(12):377–394. <https://doi.org/10.1007/s11998-016-9855-8>
100. Park S, Healy KE (2003) Nanoparticulate DNA packaging using terpolymers of poly (lysine-g-(lactide-b-ethylene glycol)). *Bioconjug Chem* 14(2):311–319. <https://doi.org/10.1021/bc025623b>
101. Park SH, Oh KW, Kim SH (2013) Reinforcement effect of cellulose nanowhisker on bio-based polyurethane. *Compos Sci Technol* 86:82–88. <https://doi.org/10.1016/j.compscitech.2013.07.006>
102. Qian L, Guan Y, He B et al (2008) Modified guanidine polymers: synthesis and antimicrobial mechanism revealed by AFM. *Polymer* 49(10):2471–2475. <https://doi.org/10.1016/j.polymer.2008.03.042>
103. Rahman MM, Kim EY, Yun Kwon J, Yoo HJ, Kim HD (2008) Cross-linking reaction of waterborne polyurethane adhesives containing different amount of ionic groups with hexamethoxymethyl melamine. *Int J Adhes Adhes* 28(1–2):47–54. <https://doi.org/10.1016/j.ijadhadh.2007.03.004>
104. Rashvand M, Ranjbar Z, Rastegar S (2011) Nano zinc oxide as a UV-stabilizer for aromatic polyurethane coatings. *Prog Org Coat* 71(4):362–368. <https://doi.org/10.1016/j.porgcoat.2011.04.006>
105. Rosthauser JW, Nachtkamp K (1987) Waterborne polyurethanes. In: Frisch KC, Klempner D (eds) *Advances in Urethane Science and Technology*, vol 10. Technomic, Lancaster, GB, pp 121–162
106. Rother S, Salbach-Hirsch J, Moeller S, Seemann T, Schnabelrauch M, Hofbauer LC, Hintze V, Scharnweber D (2015) Bioinspired collagen/glycosaminoglycan-based cellular microenvironments for tuning osteoclastogenesis. *ACS Appl Mater Interfaces* 7(42):23787–23797. <https://doi.org/10.1021/acsami.5b08419>
107. Ruan H, Fan C, Zheng X et al (2009) In vitro antibacterial and osteogenic properties of plasma sprayed silver-containing hydroxyapatite coating. *Chin Sci Bull* 54(23):4438–4445. <https://doi.org/10.1007/s11434-009-0175-6>
108. Ruggeri V, Francolini I, Donelli G et al (2007) Synthesis, characterization, and in vitro activity of antibiotic releasing polyurethanes to prevent bacterial resistance. *J Biomed Mater Res A* 81(2):287–298. <https://doi.org/10.1002/jbm.a.30984>
109. Saalah S, Abdullah LC, Aung MM, Salleh MZ, Biaka DRA, Basri M, Jusoh ER (2015) Waterborne polyurethane dispersions synthesized from jatropha oil. *Ind Crop Prod* 64:194–200. <https://doi.org/10.1016/j.indcrop.2014.10.046>
110. Saha S, Kocaefe D, Krause C, Larouche T (2011) Effect of titania and zinc oxide particles on acrylic polyurethane coating performance. *Prog Org Coat* 70(4):170–177. <https://doi.org/10.1016/j.porgcoat.2010.09.021>
111. Santamari A, Echart UL, Arbelaiz A, Barreiro F, Corcuera MA, Eceiza A (2017) Modulating the microstructure of waterborne polyurethanes for preparation of environmentally friendly nanocomposites by incorporating cellulose nanocrystals. *Cellulose* 24(2):823–834. <https://doi.org/10.1007/s10570-016-1158-9>
112. Sartori S, Chiono V, Tonda-Turo C, Mattu C, Gianluca C (2014) Biomimetic polyurethanes in nano and regenerative medicine. *J Mater Chem B* 2(32):5128–5144. <https://doi.org/10.1039/C4TB00525B>
113. Seo JW, Kim BK (2005) Preparations and properties of waterborne polyurethane/nanosilica composites: a diol as extender with triethoxysilane group. *J Appl Polym Sci* 131(15). <https://doi.org/10.1002/app.40526>

114. Shah SR, Kasper FK, Mikos AG (2013) Perspectives on the prevention and treatment of infection for orthopedic tissue engineering applications. *Chin Sci Bull* 58(35):4342–4348. <https://doi.org/10.1007/s11434-013-5780-8>
115. Shau MD, Tseng SJ, Yang TF, Cherng JY, Chin WK (2006) *J Biomed Mater Res A* 77A(4):736–746. <https://doi.org/10.1002/jbm.a.30605>
116. Smith AW (2005) Biofilms and antibiotic therapy: is there a role for combating bacterial resistance by the use of novel drug delivery systems. *Adv Drug Deliv Rev* 57(10):1539–1550. <https://doi.org/10.1016/j.addr.2005.04.007>
117. Storey RF, Wiggins JS, Puckett AD (1994) Hydrolysable poly(ester urethane) networks from Llysine diisocyanate and D,L- lactide/e-caprolactone homo and copolyester triols. *J Polym Sci A-Polym Chem* 32(12):2342–2345. <https://doi.org/10.1002/pola.1994.080321216>
118. Sukhawipat N, Saetung N, Saetung A (2016) Synthesis of novel cationic waterborne polyurethane from natural rubber and its properties testing. *Key Eng Mater VI* 705:19–23. <https://doi.org/10.4028/www.scientific.net/KEM.705.19>
119. Tanaka H, Kunimura M (2002) Mechanical properties of thermoplastic polyurethanes containing aliphatic polycarbonate soft segments with different chemical structures. *Polym Eng Sci* 42(6):1333–1349. <https://doi.org/10.1002/pen.11035>
120. Tao Y, Hasan A, Deeb G, Hu C, Han H (2016) Rheological and mechanical behavior of silk fibroin reinforced waterborne polyurethane. *Polymers* 8(3):94. <https://doi.org/10.3390/polym8030094>
121. Tatai L, Moore TG, Adhikari R, Malherbe F, Jayasekara R, Griffiths I, Gunatillake A (2007) Thermoplastic biodegradable polyurethanes: the effect of chain extender structure on properties and in-vitro degradation. *Biomaterials* 28(36):5407–5417. <https://doi.org/10.1016/j.biomaterials.2007.08.035>
122. Thallinger B, Prasetyo EN, Nyanhongo GS, Guebitz GM (2013) Antimicrobialenzymes: an emerging strategy to fight microbes and microbial biofilms. *Biotechnol J* 8(1):97–109. <https://doi.org/10.1002/biot.201200313>
123. Tiller J, Sprich C, Hartmann L (2005) Amphiphilic conetworks as regenerative controlled releasing antimicrobial coatings. *J Control Release* 103(2):355–367. <https://doi.org/10.1016/j.jconrel.2004.12.002>
124. Tillet G, Boutevin B, Ameduri B (2011) Chemical reactions of polymer crosslinking and post-crosslinking at room and medium temperature. *Prog Polym Sci* 36(2):191–217. <https://doi.org/10.1016/j.progpolymsci.2010.08.003>
125. Tsai Y, Li S, Hu SG, Chang WC, Jeng US, Hsu SH (2015) Synthesis of thermoresponsive amphiphilic polyurethane gel as a new cell printing material near body temperature. *ACS Appl Mater Interfaces* 7:27613–27623
126. Tseng SJ, Tang SC, Shau MD, Zeng YF, Cherng JY, Shih MF (2005) Structural characterization and buffering capacity in relation to the transfection efficiency of biodegradable polyurethane. *Bioconjug Chem* 16(6):1375–1381. <https://doi.org/10.1021/bc050005r>
127. Ulrich H (2001) Polyurethanes. In: *Encyclopedia of Polymer Science and Technology*, vol 4. Wiley, New York. <https://doi.org/10.1002/0471440264.pst295>
128. Valerio A, Conti D, Araujo PH, Sayer C, Rocha SP (2015) Synthesis of PEG-PCL-based polyurethane nanoparticles by miniemulsion polymerization. *Colloid Surf B* 135:35–41. <https://doi.org/10.1016/j.colsurfb.2015.07.044>
129. Vroman I, Tighzert L (2009) Biodegradable Polymers. *Materials* 2(2):307–344. <https://doi.org/10.3390/ma2020307>
130. Wang, He K, Zhang W (2013) Optimizing the fabrication processes for manufacturing a hybrid hierarchical polyurethane-cell/hydrogel construct. *J Bioact Compat Polym* 28(4):303–319. <https://doi.org/10.1177/0883911513491359>
131. Wang JZ, Zhu YX, Ma HC, Chen SN, Chao JY, Ruan WD, Wang D, Du FG, Meng YZ (2016) Developing multi-cellular tumor spheroid model (MCTS) in the chitosan/collagen/alginate (CCA) fibrous scaffold for anticancer drug screening. *Mater Sci Eng C* 62:215–225. <https://doi.org/10.1016/j.msec.2016.01.045>
132. Wattanodorn Y (2014) Material performance: antibacterial anionic waterborne polyurethanes/Ag nanocomposites with enhanced mechanical properties. *Polym Test* 40:163–169. <https://doi.org/10.1016/j.polymertesting.2014.09.004>
133. Wijffels RH, Tramper J (1995) Nitrification by immobilized cells. *Enzyme Microb Technol* 17(6):482–492. [https://doi.org/10.1016/0141-0229\(94\)00099-D](https://doi.org/10.1016/0141-0229(94)00099-D)
134. Wu GH (2016) Synthesis of water-based cationic polyurethane for antibacterial and gene delivery applications. *Colloid Surf B* 146:825–832. <https://doi.org/10.1016/j.colsurfb.2016.07.011>
135. Wu GH, Hsu SH (2016) Synthesis of water-based cationic polyurethane for antibacterial and gene delivery applications. *Colloid Surf B* 146:825–832. <https://doi.org/10.1016/j.colsurfb.2016.07.011>
136. Wu CI, Huang JW, Wen YL, Wen SB, Shen YH, Yeh MY (2009) Preparation of antibacterial waterborne polyurethane/silver nanocomposite. *J Chin Chem Soc* 56(6):1231–1235. <https://doi.org/10.1002/jccs.200900177>
137. Wu Y, Lin W, Hao H, Li J, Luo F, Tan H (2017) Nanofibrous scaffold from electrospinning biodegradable waterborne polyurethane/poly(vinyl alcohol) for tissue engineering application. *J Biomater Sci Polym Ed* 28(7):648–663. <https://doi.org/10.1080/09205063.2017.1294041>
138. Xia Y, Larock RC (2010) Vegetable oil-based polymeric materials: synthesis, properties, and applications. *Green Chem* 12(11):1893–1909. <https://doi.org/10.1039/C0CG00264J>

139. Xu D, Meng Z, Han M, Xi K, Jia X, Yu X, Chen Q (2008) Novel blood-compatible waterborne polyurethane using chitosan as an extender. *J Appl Polym Sci* 109(1):240–246. <https://doi.org/10.1002/app.27479>
140. Xu J, Rong X, Chi T, Wang M, Wang Y, Yang D, Qiu F (2013) Preparation, characterization of UV-curable waterborne polyurethane-acrylate and the application in metal iron surface protection. *J Appl Polym Sci* 130(5):3142–3152. <https://doi.org/10.1002/app.39539>
141. Yameen B, Vilos C, Choi WI, Whyte A, Huang J, Pollit L, Farokhzad OC (2015) Drug delivery nanocarriers from a fully degradable PEG-conjugated polyester with a reduction-responsive backbone. *Chem Eur J* 21(32):11325–11329. <https://doi.org/10.1002/chem.201502233>
142. Yang TF, Chin WK, Cherng JY, Shau MD (2004) Synthesis of novel biodegradable cationic polymer: N,N-Diethylethylenediamine polyurethane as a gene carrier. *Biomacromolecules* 5(5):1926–1932. <https://doi.org/10.1021/bm049763v>
143. Yang X, Ren B, Ren Z, Jiang L, Liu W, Zhu C (2015) Synthesis and properties of novel non-ionic polyurethane dispersion based on hydroxylated tung oil and alicyclic isocyanates. *J Mater Sci Chem Eng* 3(1):88–94. <https://doi.org/10.4236/msce.2015.31013>
144. Yen HJ, Hsu SH, Tseng CS, Huang JP, Tsai CL (2009) Fabrication of precision scaffolds using liquid-frozen deposition manufacturing for cartilage tissue engineering. *Tissue Eng Part A* 15(5):965–975. <https://doi.org/10.1089/ten.tea.2008.0090>
145. Yeong WY, Chua CK, Leong KF, Chandrasekaran M (2004) Rapid prototyping in tissue engineering: challenges and potential. *Trends Biotechnol* 22(12):643–652. <https://doi.org/10.1016/j.tibtech.2004.10.004>
146. Yoo HJ, Kim HD (2007) Characteristics of waterborne polyurethane/poly (N-vinyl pyrrolidone) composite films for wound-healing dressings. *J Appl Polym Sci* 107(1):331–338. <https://doi.org/10.1002/app.26970>
147. Yoo HJ, Kim HD (2008) Synthesis and properties of waterborne polyurethane hydrogels for wound healing dressings. *J Biomed Mater Res B Appl Biomater* 85(2):326–333. <https://doi.org/10.1002/jbm.b.30950>
148. Zhang JY, Beckman EJ, Piesco NP, Agrawal S (2000) A new peptide-based urethane polymer: synthesis, biodegradation and potential to support cell growth in-vitro. *Biomaterials* 21(12):1247–1258. [https://doi.org/10.1016/S0142-9612\(00\)00005-3](https://doi.org/10.1016/S0142-9612(00)00005-3)
149. Zhang L, Zhang H, Guo J (2012) Synthesis and properties of UV-curable polyester-based waterborne polyurethane/functionalized silica composites and morphology of their nanostructured films. *Ind Eng Chem Res* 51(25):8434–8441. <https://doi.org/10.1021/ie3000248>
150. Zhang M, Xie X, Tang M et al (2013a) Magnetically ultrasensitive nanoscavengers for next-generation water purification systems. *Nat Commun* 4:1866. <https://doi.org/10.1038/ncomms2892>
151. Zhang S, Yu A, Song X, Liu X (2013b) Synthesis and characterization of waterborne UV-curable polyurethane nanocomposites based on the macromonomer surface modification of colloidal silica. *Prog Org Coat* 76(7–8):1032. <https://doi.org/10.1016/j.porgcoat.2013.02.019>
152. Zhang K, Xu J, Duan X, Lu L, Hu D, Zhang L, Nie T, Brown KB (2014) Controllable synthesis of multi-walled carbon nanotubes/poly(3,4-ethylenedioxythiophene) core-shell nanofibers with enhanced electrocatalytic activity. *Electrochim Acta* 137:518–525. <https://doi.org/10.1016/j.electacta.2014.06.053>
153. Zhang Y, Li Y, Li J, Gao Y, Tan H, Wang K, Li J, Fu Q (2015) Synthesis and antibacterial characterization of waterborne polyurethanes with gemini quaternary ammonium salt. *Sci Bull* 60(12):1114–1121. <https://doi.org/10.1007/s11434-015-0811-2>
154. Zhang YI, He X, Ding M, He W, Li J, Li J, Tan H (2018) Antibacterial and biocompatible cross-linked waterborne polyurethanes containing gemini quaternary ammonium salts. *Biomacromolecules* 19(2):279–287. <https://doi.org/10.1021/acs.biomac.7b01016>
155. Zhou L, Yu L, Ding M, Li J, Tan H, Wang Z, Fu Q (2011) Synthesis and characterization of pH-sensitive biodegradable polyurethane for potential drug delivery applications. *Macromolecules* 44(4):857–864. <https://doi.org/10.1021/ma102346a>
156. Zhou X, Li Y, Fang C, Li S, Cheng Y, Lei W, Meng X (2015) Recent advances in synthesis of waterborne polyurethane and their application in water-based ink: a review. *J Mater Sci Technol* 31(7):708–722. <https://doi.org/10.1016/j.jmst.2015.03.002>
157. Zhou R, Li O, Fan Z, Du D, Ouyang J (2017) Stretchable heaters with composites of an intrinsically conductive polymer, reduced graphene oxide and an elastomer for wearable thermotherapy. *J Mater Chem* 5:1544–1551. <https://doi.org/10.1039/C6TC04849H>



# Medical Applications of Collagen and Hyaluronan in Regenerative Medicine

Lynn L. H. Huang, Ying-Hui Amy Chen, Zheng-Ying Zhuo, Ya-Ting Hsieh, Chia-Ling Yang, Wei-Ting Chen, Jih-Ying Lin, You-Xin Lin, Jian-Ting Jiang, Chao-Hsung Zhuang, Yi-Ching Wang, Hanhhiu Nguyendac, Kai-Wei Lin, and Wen-Lung Liu

## Abstract

In order to develop and commercialize for the regenerative medicinal products, smart biomaterials with biocompatibility must be needed. In this chapter, we introduce collagen and hyaluronic acid (HA) as extracellular matrix as well as deal with the molecular mechanism as

microenvironment, mechanistic effects, and gene expression. Application of collagen and HA have been reviewed in the area of orthopedics, orthopedics, ophthalmology, dermatology and plastic surgery. Finally, the ongoing and commercial products of collagen and HA for regenerative medicine have been introduced.

L. L. H. Huang (✉)

Department of Biotechnology and Bioindustry Sciences, College of Bioscience and Biotechnology, National Cheng Kung University, Tainan, Taiwan

Institute of Clinical Medicine, College of Medicine, National Cheng Kung University, Tainan, Taiwan

Research Center of Excellence in Regenerative Medicine, National Cheng Kung University, Tainan, Taiwan

International Research Center for Wound Repair and Regeneration, Tainan, Taiwan  
e-mail: [lynn@mail.ncku.edu.tw](mailto:lynn@mail.ncku.edu.tw)

Y.-H. A. Chen · Z.-Y. Zhuo · J.-Y. Lin · Y.-X. Lin · J.-T. Jiang · C.-H. Zhuang · Y.-C. Wang · H. Nguyendac

Department of Biotechnology and Bioindustry Sciences, College of Bioscience and Biotechnology, National Cheng Kung University, Tainan, Taiwan

Y.-T. Hsieh · C.-L. Yang · W.-T. Chen · K.-W. Lin · W.-L. Liu

Research Center of Excellence in Regenerative Medicine, National Cheng Kung University, Tainan, Taiwan

## Keywords

Collagen · Hyaluronic acid · Biomaterial

## 15.1 Biomaterials Research for Regenerative Medicine

### 15.1.1 Hyaluronic Acid (HA) and Collagen as Extracellular Matrix (ECM)

To mammalian, such as human, they are composed of different organs, tissues, and cells. To maintain the cell activity and function, the extracellular matrix (ECM) is important. Hyaluronan, which is also called hyaluronic acid (HA) or hyaluronate, is a polysaccharide found in most tissues and body fluids of vertebrates [25]. It is a major component of ECM of the skin, joints, and many other tissues and organs [70]. Besides hyaluronan,



another important ECM is called collagen, which is a large group of families. In human, there are now 28 known collagens, for each type plays an important role to different tissues.

### 15.1.2 The HA and Collagen Cellular Receptors

In mammals, the situation of the tissues is dependent on its cells. However, to cells, how would they execute some specific functions? The answer is about the signaling transduction. In common signaling transductions, there are many molecules that can active the signaling which is called 'ligand', such as some growth factors (GF). Besides GF, hyaluronan and collagen can also be the ligands, to active the signaling to active some functions. For hyaluronan, there are eight known receptors: CD44, RHAMM, ICAM-1, LYVE-1, Stablin-1, HARE, TLR-4 and layilin. Despite there are eight receptors, the most common used receptors for hyaluronan are CD44 and RHAMM, as these two receptors whose biological functions in human and tumor cells have been investigated comprehensively [63]. However, to collagens, there are at least eight human collagen receptors belonging to four different classes: integrins, discoidin domain receptors, immunoglobulin-like receptors and mannose receptors [52]. To humans, integrins function as the major cell receptor for collagen.

#### 15.1.2.1 The Influence of HA and Collagen to the Cell Cytoskeleton and the Organelles

When a receptor binds to a ligand, a signaling transduction will begin and influence the downstream cellular function. In some researches, it had shown that the activation of some signaling by HA and collagens will cause the change of the cell behavior or cell's organelles. For examples, in hyaluronan, it had been shown that in tumor cells, the HA-CD44-ankyrin interaction will causes the cytoskeleton activation and results in cell adhesion, proliferation and migration, and thus, cause the tumor cell progression [9]. Besides, another research had shown that when HA binding to CD44<sub>v3</sub> isoform, it will stimulate

Tiam1-specific GDP/GTP exchange for Rho-like GTPases such as Rac1 and thus promotes cytoskeleton-mediated tumor cell migration [10].

By contrast, there are also some research studying the activation by collagen which cause the changing of cell behavior. A research had shown that the type VIII collagen active the signaling through beta-1 integrin receptors to suppress RhoA—a small GTPase protein in the Rho family, to make optimal configuration of the cytoskeleton and make the stimulation of MMP-2-dependent cell migration [2].

#### 15.1.2.2 The HA and Collagen to the Intracellular Signaling Pathways

Besides the cytoskeleton and the cell behavior, the HA and collagen will also be the ligand and activate the downstream signaling transduction. Now, there have had lots of researches that studying the signaling transduction. In the results, for HA, the researchers have found that hyaluronan will activate the downstream Ras/Raf/MEK/ERK and Ras/PI3K/PTEN/Akt/mTOR signaling pathways [87]. Besides, HA will also activate the NF-κB pathway, as recently NF-κB activation has been shown to have oncogenic effects important in the control of apoptosis, cell cycle, differentiation and cell migration. By contrast, the collagen will also activate the FAK/PI3K/Akt pathway through its integrin receptor [95].

### 15.1.3 Mechanism Effect on Physiological Functions

When the cells are activated by HA or collagen, there are some physiological functions be activated, of course. In a research, it has been shown that HA suppressed the UVB-induced decrease in cell viability and had significant protective effects for HaCaT cells against UVB irradiation [95]. Moreover, another research has shown that in the heart HA is involved in physiological functions, such as cardiac development during embryogenesis, and in pathological conditions including atherosclerosis and myocardial infarction [8]. For collagen, in 2001, a research shows that collagen XVIII is expressed in the epithelium of the

developing mouse lung and kidney, and antibody treatment directed against it can interfere with the development of lung epithelial tips or ureter bud tissue cultured within lung mesenchyme *ex vivo* [53]. Besides, in cardiac tissue, another research shows that collagen XVIII is localized not only in various basement membranes but is also highly expressed throughout the connective tissue core of the endocardial cushions and forming AV valve leaflets [13]. These results show that both HA and collagen are important for the cells to change or maintain some physiological functions.

### 15.1.4 Gene Expression

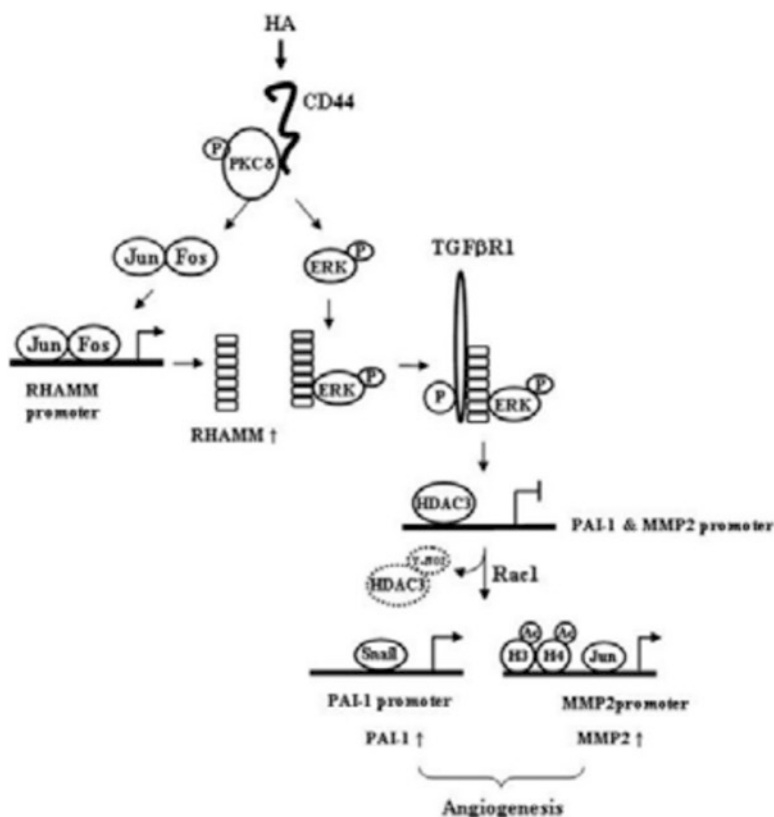
In previous, we have talked about that HA and collagen will activate downstream signaling, as this will influence the gene expression of the cells. Take a research for example, this paper shows that HA induces an interaction between CD44 and PKC $\delta$  and between RHAMM and ERK, as the activation of PKC $\delta$  leads to the induction of RHAMM *via* AP-1. Meanwhile, PKC $\delta$  is also

necessary for the activation of ERK. When HA transactivates TGF $\beta$ R1 *via* PKC $\delta$  and ERK, the activation of TGF $\beta$ R1 by HA is associated with degradation of HDAC3, which results from tyrosine nitration induced by rac1. The decreased HDAC3 expression is responsible for the induction of PAI-1 and MMP-2. In consequence, the upregulated of PAI-1 and MMP-2 will promote angiogenesis (Fig. 15.1) [68]. The research gives a prove that HA-induced gene expression changes are important for angiogenesis. In addition, HA treatment downregulated collagen I expression and upregulated several genes relating to chondrocyte phenotype [59], including collagen II, collagen XI and chondroadherin [76].

### 15.1.5 Collagen and Hyaluronan Effects on Nuclear Cluster Genes

In the activation of the downstream signal by HA and collagen, the signal would also transduct to the nucleus. Interaction of HA with CD44 and

**Fig. 15.1** The mechanism of the HA activation to the downstream PKC $\delta$ /ERK/PAI-1 and MMP-2, which promote the angiogenesis

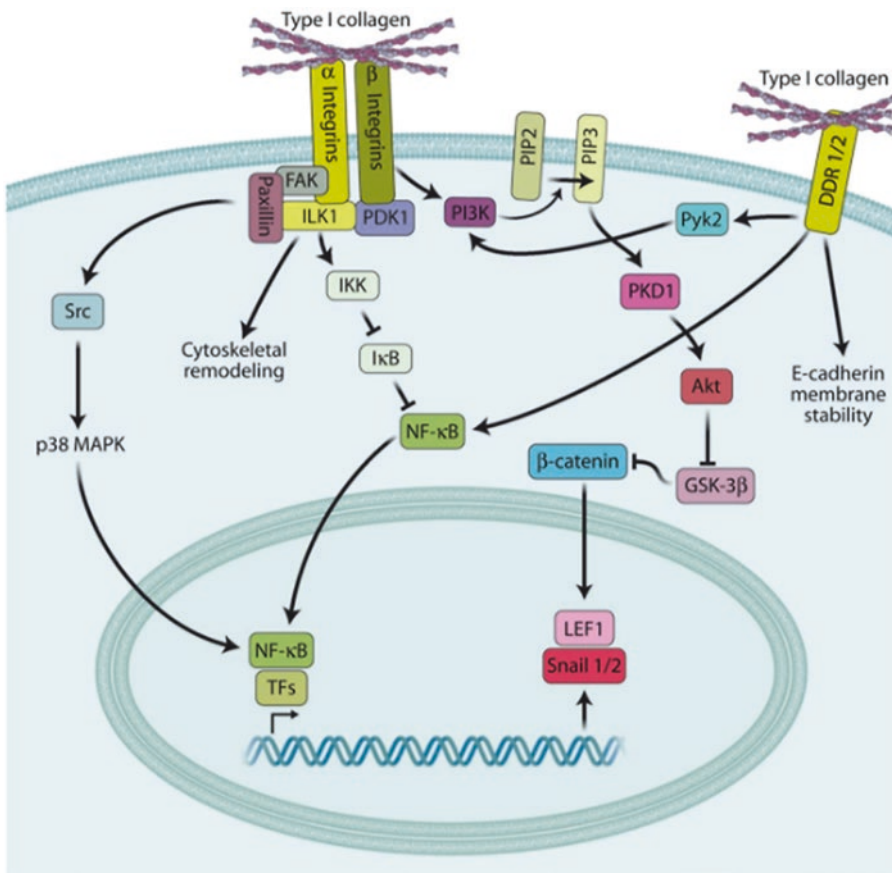


RHAMM induces CD44 receptor clustering and intracellular RHAMM-regulated MAPK activation, which results in ERK phosphorylation and downstream activation of the transcription effectors AP-1 and NF- $\kappa$ B. Active transcription of AP-1 and NF- $\kappa$ B target genes ultimately result in the induction of directed cell migration and release of inflammatory cytokines [83]. For collagen, type I collagen induces EMT through integrin or DDR1/2 signaling. Both receptors activate NF- $\kappa$ B and other transcription factors (TFs) that promote expression of *SNAIL1/2* and *LEF1*. Other pathways are activated by type I collagen through integrins and DDRs, which promote the stabilization and activity of the EMT-associated transcription factors Snail1/2 and LEF-1. DDR1 is also known to form complexes with E-cadherin at the cell surface, which are disrupted upon binding to type I collagen (Fig. 15.2) [31].

## 15.2 Collagen Research in Regenerative Medicine

### 15.2.1 Collagen in Human Physiology

Collagen is a structurally highly conservative biopolymer that is the main component of mammalian connective tissue ECM, consisted of one-third of protein amount [15]. One collagen protein is composed of three peptide chains, at least one of these three contained the repeated amino acid sequence, for example, Gly-X-Y formed Right-handed triple helix in type I collagen [86]. To be defined as a collagen, the protein is characterized by the Gly-X-Y peptide, and is contained at least one collagenous domain (COL domain) and one non-collagenous domain (NC domain) [70]). Collagen type is determined by



**Fig. 15.2** The mechanism of the collagen activation to the downstream NF $\kappa$ B signaling

the number and structure of COL and NC domains. Within the vertebrate genome, there existed at least 45 genes encoding 28 collagen types. The collagen proteins were grouped according to their suprastructure into the categories summarized in Fig. 15.3 [62].

Type I collagen is the most abundant collagen protein in vertebrate connective tissues such as tendon, ligament, bone, skin, and cornea. It is composed of two  $\alpha 1(I)$  and one  $\alpha 2(I)$  peptide chain, each contained more than 1000 amino acid residues, all together formed three spiral short rod-shaped molecule of 1.5 nm diameter and 300 nm length. Collagen functioned as a frame structure for cells and other ECM components. The collagen  $\alpha 1(I)$  CB3 peptide (GFOGER) region is also easy for platelet attachment via  $\alpha 2\beta 1$  integrin interaction, hence

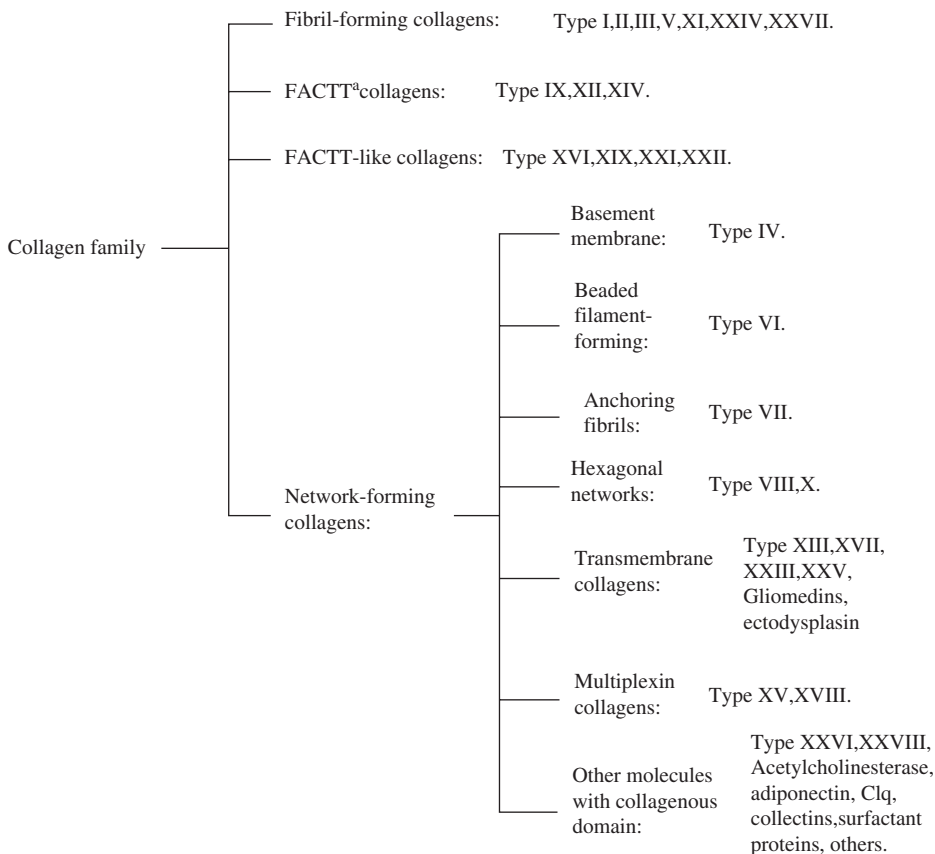
in case of blood cell wall injury and expose of collagen to blood flow, platelets immediately attached and activated by collagen DGEA tetrapeptide, resulted in fast formation of coagulation aggregate and stop of bleeding [22, 36] (Fig. 15.4).

## 15.2.2 Collagen Biomaterial as a Tool in Tissue Engineering

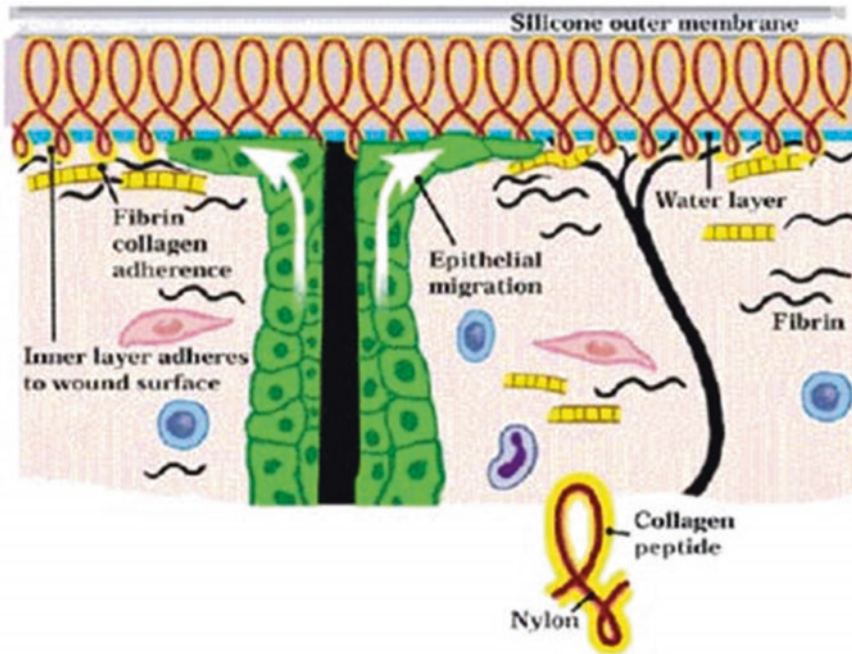
### 15.2.2.1 Application in Hard Tissue Regeneration

#### In Orthopedics

Previous studies were focused on the potential of 3-D structure of collagen as a drug delivery system, regarding its advantages in high biocompatibility,



**Fig. 15.3** General classifications of collagen types



**Fig. 15.4** The structure of BIOBRANE. Silicone outer membrane with Nylon mesh that coated collagen and peptide. This 3-D structure allow epithelial migration and

fibrin collagen adherence. (<http://www.smith-nephew.com/belgique/produits-old/biobrane-/biobrane--technology/>)

degradability, and cell attachment, promotion of angiogenesis. Collagen type I can exhibit all these characteristics, be capable to bind integrin through RGD domain, and activate/enhance cell migration, proliferation, and cell attachment [4, 35, 38, 71, 89]. Type I collagen scaffold is applicable for bone tissue repair after BMP or BSP coating [60, 91]. In 2015, Jo laboratory treated calvarial defect using heparinized collagen membrane; first BMP7 was combined/bound with collagen membrane and covered the bone defect, followed by BMP2 treatment to enhance bone regeneration [42]. During 2014, Missana laboratory discovered that synthesized human rhPTH can effectively increase the bone quality of osteoporosis patient, and combined treatment of rhPTH and atelocollagen can enhance healing and regeneration of skull bone defect [64].

### In Dentistry

Human teeth are structured as a hard tissue fully covered the soft pulp tissue, recent studies in regenerative medicine discovered that chitosan can be applied in the dental field [96, 97]; however, the chitosan may induce early inflammation reaction [47]. Nagai group's research found that degraded atelocollagen can effectively affect 3T3 cell proliferation, and human periodontal ligament fibroblasts can proliferative excellent and highly differentiate when cultured in collagen gel [65]. Based on these knowledges/results, Kawase's group cultured human periosteal sheets in a porous poly(L-lactic acid) (pPLLA) membrane scaffold to generate a 3D skeleton and applied as a grafting biomaterial for stimulation of in vitro mineralization and bone formulation of osteogenic induced cells [45]. The polypeptide

chain of collagen can also promote post-translational modification in osteoblast [98]. During 2016, Salamanca laboratory discovered that the PTFE membrane traditionally utilized in surgery is not bioresorbable, hence required additional second surgery for removal of this membrane, to solve this issue, they developed a bioresorbable membrane, for inducing tissue regeneration. A freeze-dried collagen membrane placed at the boundary of alveolus and bone, not only maintain a normal physiological space, but also achieve regeneration of alveolus bone, reduction of alveolar atrophy and promotion of allograft bone formation induction [77].

### 15.2.2.2 Application in Soft Tissue Regeneration

#### In Ophthalmology

Recent researches established that biomaterials consisted of type I collagen exhibited a novel self-organizing behavior, hence widely utilized as a construct in tissue engineering [33]. During 2014, Chae's group used chondroitin sulfate-polyethylene glycol (CS-PEG) adhesive and collagen-based membrane (collagen vitrigel, abbreviated CV) to treat penetrating ocular injuries, which are applicable to retired militants injured on the battlefields. The vancomycin released by CS-PEG and the CV resembling the corneal shape, combined together, effectively promote the healing of the ocular injuries at corneal and corneoscleral regions. CS-PEG adhesive alone is sufficient for healing of 5-mm to 6-mm length wounds in a porcine cadaver eye model. However, wounds of larger size and similar to those resulted from battlefield injuries required the presence of both CS-PEG and CV for efficient treatment [14].

#### In Dermatology

Due to the incessant increase of chronic or complicated wound prevalences, autologous skin graft or novel material wound dressing only provide modest wound healing function and exterior improvement [72]. Wehrhan's laboratory studied the effect of porcine type I/III collagen membrane on blood vessel vascularization and

epithelialization, and found no significant difference in comparison to treatment by split-thickness skin graft, thus concluded that collagen membrane is a suitable substitute of full-thickness dermal dressing in the future application, caused by its advantages in positively enhanced vascularization and proliferation of epithelial cells at wound site treated [92]. In 2016, Petersen's group developed a novel collagen-gelatin fleece for treatment of deep skin wound on minipig model; comparison with the commercial Matriderm® dressing concluded that, multiple treatment using collagen-gelatin fleece of 150 g/m<sup>2</sup> thickness achieved the best results.

The chronic diabetic wound is a major problem in cases of diabetic patients post-surgery and/or post-trauma; it often leads to severe complications yet no effective treatment method. The causes of difficult skin wound healing are various, ranging from poor angiogenesis to low bioactivity of growth factors and/or cytokines. Skin-derived precursors (SKPs) have been demonstrated to successfully differentiate into vascular cell or neural cell, both playing an important role during skin healing process, but the previous problem of utilization of skin progenitor cells for cell therapy was due to its low cell survival rate. Ke's group co-transplanted a collagen sponge with the SKPs and found that diabetic wound healing was accelerated and local capillary regeneration was accelerated within 14 days, and this facilitation of wound healing was accredited to SKPs in vivo transdifferentiation and paracrine signaling [46].

### 15.2.3 Drug Delivery and Nanomedicine

Starting in the year 1982, scientists started to study regarding how to make collagen into nanoparticle as a tool for drug delivery and drug release [32]. Natural products such as elastin, collagen, and hyaluronic acid, are developed for their potential as a drug carrier [44]. During the purification process, collagen may be degraded due to its fragile chemical structure, cross-linking is often applied to reducing this negative effect

and enhancing the mechanical stability. In exchange, chemical cross-linking agents, for example, formaldehyde or glutaraldehyde, usually comes with toxicity and therefore resulted in reduced biocompatibility [34].

To solve the problem of easy collagen nanoparticle degradation without applying toxic chemical cross-linking agents, Pham's group incorporated D-Glucose for stabilization of collagen nanoparticles [50]. On the other hand, Grant's laboratory cross-linked collagen using gold nanoparticles (AuNPs) and successfully strengthened the mechanical stability of collagen nanoparticles, rendered some resistance against collagen degradation, and maintained natural molecular structure and biocompatibility [34]. Attempt using other metal such as silver also reduced antimicrobial activity and no cell toxicity; for instance, Cardoso's groups stabilized collagen using silver in a 1:6 molar ratio and generated a silver nanoparticles stabilized with type I collagen (AgNPcol) [11]. Also in 2014, Nagarajan's laboratory generated collagen nanofibers by electrospray deposition of under ambient pressure and temperature [66]. Increase of solution conductivity can obtain solid nanoparticles, which exhibited promising potential as a drug carrier as demonstrated by the theophylline incorporation and controlled theophylline release by the cross-linking collagen molecules, and this is applicable as a nasal stent or oral drug [66]. In 2014, Cheng's group developed a collagen-nanoparticle fiber consisted of aligned collagen, which regulates bioactivity of adipose-derived stem cells (ADSCs) through controlled release of platelet-derived growth factor (PDGF) [19]. They found that the ADSCs not only significantly proliferated along the aligned collagen fibrils but also induced toward tenogenic differentiation [19].

Pastorino's group had discovered that oriented collagen can promote cell proliferation and alignment, Langmuir-Blodgett technique allows the formation of a stable collagen film at the air-water interface; this collagen film is then dispositioned by Langmuir-Schaefer technique and later served as a planar surface for 3T3 cell attachment

and proliferation. Collagen film not only enhanced cell attachment, but also oriented cells cultured on it to follow a parallel orientation direction [69].

---

## 15.3 HA Research in Regenerative Medicine

### 15.3.1 HA in Human Physiology

Hyaluronan (HA) is a linear unbranched polysaccharide macromolecule, consist of disaccharide repeats of glucuronic acid and N-acetyl glucosamine, largely present in vertebrate tissue ECM, especially found but no limit to synovial fluid, cartilage, and skin. HA biogenesis was carried out by hyaluronan synthase (HAS) enzymes at plasma membrane [84]. Depending on which hyaluronan synthase generated the HA molecule, the molecular weight could vary from 0.1 million to more than 2 million Daltons (Da). HA macromolecule binds water molecule in the ECM and serves as a structural support scaffold. HA is also characterized to be able to preserve activity of multiple growth factors and cytokines in the ECM. Though traditionally the main functions of HA are categorized as joint lubrication, tissue homeostasis, and as a scaffold for holding tissues together [20], HA also participates in regulation of multiple biological functions such as promotion of cell proliferation and migration, inhibition of wound contraction and scar formation, and effecting angiogenesis and embryonic developing phenotype, embryonic development, lymphocyte migration, tissue regeneration, and cancer cells invasion and transfer/transformation [54, 84, 85, 94].

### 15.3.2 HA Biomaterial as a Tool in Tissue Engineering

HA contributes significantly to cell proliferation and migration, yet it may also be involved in the progression of some malignant tumors.

### 15.3.3 Limitations and Managements of Hyaluronan Scaffolds

Even with the advantages of hyaluronic acid as a scaffold material, implantation of HA-scaffolds induced some foreign reactions. HA-scaffold surface may absorb various body proteins and induce the following ranges of responses and ultimately lead to denaturation. When random proteins and other cells stick to HA-scaffold through this absorption, resident cells near the HA-scaffold target site may release cytokines and other pre-inflammatory mediators; this induction of HA-scaffold inflammation cannot be cleared by microphage phagocytosis due to the large molecular size of HA [75]. Ultimately the cell scaffold-linked inflammation lead to activated hyaluronidases and MMPs causing degradation of the ECM. Both HA-scaffold inflammation and ECM degradation events can cause physical and chemical changes to the HA-scaffold surface, which may be undesirable. The HA-scaffold-derived end products and cellular bioactive molecular on resident/target cell/tissue not only caused autocrine and paracrine effects, can also induce oxidative effect due to the increase in the free radical release. One resolution for solving this limitation is to treat the HA-scaffold biomaterial with bioactive agents, often hyaluronidase inhibitors, such as clinically accepted antioxidant N-acetyl cysteine (NAC) and glutathione [88]. The NAC treatment is advantageous in that it not only quenches the free radical but also protects HA-scaffold from inflammation and denaturation.

---

## 15.4 Biomaterials with Collagen and Hyaluronan for Regenerative Medicine

### 15.4.1 Collagen and Hyaluronan Biomaterials as a Tool in Tissue Engineering

Since 2003, Kuroyanagi laboratory conducted a series of experiments regarding wound dressing materials, exhibiting a double-layered spongy

matrix consisted of one layer of hyaluronan and the other layer contained collagen and its derived peptides [48]. These two layers of the sponge covalently bonded to form a culture dermal substitute (CDS) and applied as a wound dressing. This material was assessed at the cellular level, followed by studies on animal models and eventually clinical studies on human patients. In 2003, Kuroyanagi et al. tested skin defect S-D rats and proved that autologous CDS can provide efficient healing, HA, and collagen incorporated in the double-layered sponge which provides a suitable environment for wound healing, enhanced granulation tissue formation, and compensated for the insufficiency in cases applying to only a single layer of HA and collagen [48]. Even more, collagen is slightly more expensive than HA, hence, this double layer of collagen and HA is cost-down in comparison to double layer of collagen. Later in 2005, Kuroyanagi's group discovered that fibroblasts in CDS produced/secreted various bioactive factors, including cell growth factors and extracellular matrix components that are important for wound healing, this can improve wound condition, enabled the wound site to adapt to later skin autologous transplantation and shortened time duration for full-thickness skin wound healing. This clinical study was conducted on human patients (n = 3) [37]. In 2014, Kuroyanagi et al. discovered that incorporation of EGF (epidermal growth factor) and vitamin C in CDS are potential for enhancing ex vivo/in vitro biogenesis of VEGF (vascular epithelial growth factor) and HGF (hepatocyte growth factor). Induced granulation tissue formation and promoted blood vessel biogenesis were conducted in vivo using diabetes mellitus type 2 mice [49].

### 15.4.2 Collagen and HA in Drug Delivery and Nanomedicine

Collagen type I is the main organic component in the bone extracellular matrix, providing physical structure for glycosaminoglycans binding sites and enhanced cell adhesion through the varied amino acid sequence. GAGs included hyaluronic acid (HA) and chondroitin sulfate (CS). Hofbauer



[28] laboratory in 2012 launched a study regarding the basic mechanism of how these GAGs regulate osteoclast, evaluating/assessing how high degree sulfation of HA and CS may be helpful for improvement of bone fracture and bone defect healing. Experimental model was based on human peripheral blood monocytic cells and osteoclast isolated from mice, Hofbauer's group analyzed the effect of GAGs on osteoclast adhesion, viability, differentiation, morphology, resorption, and proteomic regulation [78]. During 2014, Hofbauer's group published their results regarding sulfation of GAG enhanced osteoclast differentiation and inhibition of osteoblast [79]. Follow-up animal study was conducted in 2016, the research group proved that scaffolds coated with collagen/SHA3 effectively enhance bone mineralization and reduced the amount of demineralized bone matrix, ultimately improve the bone fracture syndrome in diabetic patients, and is a very promising biochemical material for enhancing bone regeneration [73].

### 15.4.3 Limitations and Managements of Collagen and HA-Based Scaffolds

Decrease of collagen, elastin, and HA density resulted in dermis a trophy and skin aging, but local application of collagen cannot significantly improve skin quality, because relatively large molecular size of collagen (130–300 kDa) makes it unable to pass through the epidermis [27]. Collagen and HA are widely applied on wound dressing and scaffolds, even rare but still exists side effects [90]. For example, hyaluronidase and collagenase degraded the scaffold to produce side products which induced inflammation and affected wound healing process [29].

During 2017, Gokce's group discovered by in vivo experiments that collagen-laminin based dermal matrix impregnated with RSV loaded HA-DPPC microparticles exhibited excellent wound healing potential due to its antioxidant activity, and this is useful for application on treatment of chronic diabetic wound. Impregnation of MP-RSV in DM had extended the collagenase deg-

radation time to 2 h, and RSV possess excellent anti-collagenase activity in addition to enhancement of skin fibroblast proliferation. Gokce's research indicated that addition of RSV is not only contributive to wound healing, the anti-collagenase activity is helpful to maintain matrix integrity [29].

## 15.5 Ongoing and Commercial Products for Regenerative Medicine

### 15.5.1 Collagen Products (Summarized in Table 15.1)

Collagen related therapeutic products are widely developed for clinical applications, including wound healing, osteochondral lesions, surgical hemostatic, and aesthetic surgery. Here we briefly described some examples in the following paragraphs and listed in Table 15.1.

#### 15.5.1.1 Collagen for Wound Healing

Most of the previous collagen product is derived from nature, such as bovine and pig. However, the use of collagen supplement in humans these days always raises safety issues. Recently, many companies tend to develop and combine new material. These products usually provide the framework or microenvironment to accelerate wound healing. For example, Helicoll™ is a component of pure Type-I collagen to form an acellular skin that provides a framework. It promotes the regeneration of blood vessels and supports biologic cell migration due to the resorbable properties of Helicoll™. Besides, Helicoll™ also accelerates tissue remodeling significantly compared to other dressings and basically reduces post-treatment care requirements. INTEGRA™ Matrix is composed of collagen-GAG matrix which is made of a 3-D porous matrix of cross-linking bovine tendon collagen and glycosaminoglycan. This tissue provides a scaffold for cellular invasion and capillary growth. BIOBRANE is created from a silicone film with a nylon fabric partially imbedded into the film which presents the sophisticated 3-D structure of tri-filament and collagen has been used chemically bound (Fig. 15.4). Blood/sera clot in the

**Table 15.1** Collagen commercial products

Product name	Type	Compositions	Indication	Reference
<b>Collagen in wound healing</b>				
BIOBRANE	A thin layer	A silicone membrane bonded to a nylon mesh to which peptides from a porcine dermal collagen source have been bonded to the nylon membrane	Superficial and partial-thickness wounds.	<a href="http://www.smith-nephew.com/key-products/advanced-wound-management/other-wound-care-products/biobrane/">http://www.smith-nephew.com/key-products/advanced-wound-management/other-wound-care-products/biobrane/</a>
COLLGEL®	Gel	Fish collagen and its peptides (FCP – fish collagen peptides) extracted from the skin of fish like silver carp, salmon and various marine fish.	Oral wounds	<a href="http://collgel.pl/o-produkcie/">http://collgel.pl/o-produkcie/</a>
Helicoll™	A layer	Bovine high purity Type-I collagen (>97% pure) forming an acellular skin	Ulcers, Abrasions, full-thickness or partial-thickness wounds.	<a href="http://www.woundsource.com/product/helicoll">http://www.woundsource.com/product/helicoll</a>
BICOL®	Sponge	Collagen Sponge	Neurological procedures requiring prolonged retraction and exposure of the brain in surgery.	<a href="http://implant-line.ru/ru/product/bioteck/factory-rosta-osteoplantr-angiostad-bioteck-biotek">http://implant-line.ru/ru/product/bioteck/factory-rosta-osteoplantr-angiostad-bioteck-biotek</a>
PROMOGRANT™	A layer	Sterile, freeze dried composite of 45% oxidized regenerated cellulose (ORC) and 55% collagen	Ulcers, Abrasions, full-thickness or partial-thickness wounds.	<a href="http://www.acelity.com/products/promogran-dressing">http://www.acelity.com/products/promogran-dressing</a>
OASIS®	A thin layer	Porcine small intestinal submucosa (SIS) and freeze-dried sponge prepared from bovine collagen and ORC. Does not contain proteoglycans or glycosaminoglycans (GAGs)	Wounds, ulcers, and Second-degree burns	<a href="http://www.oasiswoundmatrix.com/aboutowm">http://www.oasiswoundmatrix.com/aboutowm</a>
INTEGRA™ Matrix	A thin layer	Collagen-GAG matrix made of a 3-D porous matrix of cross-linked bovine tendon collagen and glycosaminoglycan.	Partial and full thickness wounds, ulcers, second-degree burns	<a href="http://www.ilstraining.com/imwd/imwd/imwd_it_03.html">http://www.ilstraining.com/imwd/imwd/imwd_it_03.html</a>
<b>Collagen in osteochondral lesions</b>				
OSTEOPLANT®	Gel	Bone collagen and special growth factor, this is the type I collagen from antigen purified.	Bone repair or replacement particles for contacting the bone.	<a href="http://implant-line.ru/ru/product/bioteck/factory-rosta-osteoplantr-angiostad-bioteck-biotek">http://implant-line.ru/ru/product/bioteck/factory-rosta-osteoplantr-angiostad-bioteck-biotek</a>
Bio-gen® putty	Cylinder of lyophilized paste	Mixture of cancellous bone granules and collagen extracted from the Achille's tendon.	As osteoconductive materials to be used in bone regeneration surgery.	<a href="http://www.bioteck.com/index.php?option=com_content&amp;view=article&amp;id=66&amp;Itemid=205&amp;lang=en">http://www.bioteck.com/index.php?option=com_content&amp;view=article&amp;id=66&amp;Itemid=205&amp;lang=en</a>

(continued)

**Table 15.1** (continued)

Product name	Type	Compositions	Indication	Reference
Collagen in surgery hemostatic				
ANTEMA®	Tampon	Class III medical device based on resorbable type I collagen extracted from equine Achilles tendon.	Used in acute and chronic ulcerative cutaneous lesions of a vascular, traumatic and as a hemostatic device in surgery.	<a href="http://www.opocrin.it/medical-devices/antemar/">http://www.opocrin.it/medical-devices/antemar/</a>
Hemocollagene	Sponge	Native, non-denaturated, freeze-dried collagen of bovine origin.	Local hemostasis after dental surgical procedures.	<a href="http://www.septodont.co.uk/sites/uk/files/2016-08/Hemocollagene%20-%20Package%20insert.pdf">http://www.septodont.co.uk/sites/uk/files/2016-08/Hemocollagene%20-%20Package%20insert.pdf</a>
Jason® fleece	Tampon	Porcine dermis-derived natural porous collagen.	Arterial and diffuse seeping bleedings especially in situations in which the application of conventional hemorrhage agents are challenging and time-consuming.	<a href="https://botiss-dental.com/products/jason-fleece/">https://botiss-dental.com/products/jason-fleece/</a>

nylon matrix, thereby firmly adhering the dressing to the wound until epithelialization occurs.

OASIS® uses porcine small intestinal submucosa (SIS), freeze-dried sponge prepared from bovine collagen and oxidized regenerated cellulose (ORC) as a framework to provide the optimal environment to restore tissue structure and function. PROMOGRAN™ is a freeze-dried product and it is composed of 45% ORC and 55% collagen. This product maintains a physiologically moist microenvironment at the wound surface and conducive to granulation tissue formation, epithelialization and rapid wound healing. BICOL® is a kind of collagen sponge, which also provides the moist microenvironment to protect the brain from excessive friction when using blade slides over the brain. Another gradient is rarely to be used, such as fish, it also has a lot of collagen. For example, COLLGEL® that is used to reduce the healing time of soft tissues mouth.

### 15.5.1.2 Collagen for Osteochondral Lesions

Most of this collagen product is designed to be gradually resorbed by the osteoclast and replaced by new bone formed through osteoblastic activ-

ity. OSTEOPLANT® is composed of bone collagen and special growth factors that activate vascular endothelial growth factor and promote the angiogenesis. Bio-gen® is a variety of formulas (e.g., sponges, membranes or gels) for each surgical procedures needed. Bio-gen® putty is a mixture of cancellous bone granules and collagen extracted from the horse Achilles's tendon. The tissue which eliminates the antigenic component is reconstructed by osteoclasts and is remodeled by the patient's bone. In this case, collagen stanch the blood to help better adhere the bone and accelerate regeneration processes.

### 15.5.1.3 Collagen in Surgery Hemostatic

When you are bleeding, your body processes complicate procedures to stop bleeding by directly activate platelets that have a good effect on rapid hemostasis. There are several products which are especially used in surgery, such as ANTEMA® and Jason® fleece. ANTEMA® which is made from equine Achilles tendon and Jason® fleece accelerate the thrombocytes which are cross-linked by fibrinogen to make white thrombus that initially stabilizes the wound. Moreover, Jason® fleece can

also be used in diffusing seeping bleedings. Besides, hemocollagene usually is used in local hemostasis after dental surgical procedures.

#### 15.5.1.4 Collagen in Aesthetic Surgery

Recent years, collagen has been become more important in aesthetic and reconstructive surgery, especially in the face. It commonly injects dermal fillers with collagen to wrinkles result in restoration of dermal volume. However, it still have a lot of problem, such as allergic responses and high possibility of developing palpable textural change at the injected site. Zyderm® is extracted from cow skins and the bovine dermal collagen plus 0.3% lignocaine to form a dermal filler. It is used to treat pronounced scars, lines, and furrows. Artecoll is composed 75% bovine collagen, and 25% microspheres of polymethylmethacrylate (PMMA), respectively. PMMA has been used extensively in dental and orthopedic surgical settings, largely as a biocompatible cement [1, 74]. The ultimate goal in treating deep skin creases is to expand dermal layer volume and simultaneously replace dermal collagen [56]. In Artecoll, bovine collagen functions as a transient

carrier of PMMA microspheres, and facilitates their deposition in tissue. The goal of depositing PMMA microspheres in tissue is to elicit a fibrotic process resulting in the formation of microcapsules around each PMMA microsphere. The viscosity of the collagen carrier molecule enables the even distribution of the microspheres in the tissue, thereby promoting tissue ingrowth between the microspheres. As such, a more permanent tissue filling or augmentation is achieved and it is indicated for the correction of contour deformities of the dermis [58].

#### 15.5.2 HA Products

HA is widely applied to therapeutic products for clinical purpose, ranging from osteoarthritis, ophthalmology, cystic fibrosis, papilla regeneration, dermatology, and plastic surgery. Related HA products had entered the market, and many kinds of literature were published regarding the clinical effects of these products. Here we briefly summarized some examples in the following paragraphs and listed in Table 15.2.

**Table 15.2** HA commercial products for osteoarthritis treatment

Product Name	Type	Company	Compositions	Indication	References
SYNVISCO®	Solution	Genzyme Corporation	1. Hylan polymers: 48 mg 2. Sodium chloride: 51 mg 3. Disodium hydrogen phosphate: 0.96 mg 4. Sodium dihydrogen phosphate monohydrate: 0.24 mg	Pain in osteoarthritis (OA) of the knee	1. Clin Rheumatol. <b>2005</b> , 24, 285–289. 2. U. S. food and drug administration, <a href="https://www.accessdata.fda.gov/cdrh_docs/pdf/p940015s012b.pdf">https://www.accessdata.fda.gov/cdrh_docs/pdf/p940015s012b.pdf</a>
Synocrom	Solution	Croma Pharma	Sodium hyaluronate, concentration of 10 mg/ml	Osteoarthritis (OA) of the knee	1. acta medica transilvania <b>2013</b> , 2, 260–263 2. <a href="https://www.fda.gov.tw/MLMS/H0001D.aspx?Type=Lic&amp;LicId=56026198">https://www.fda.gov.tw/MLMS/H0001D.aspx?Type=Lic&amp;LicId=56026198</a>
Suplasyn	Solution	Mylan Institutional	Sodium Hyaluronate solution 10 mg/ml	Pain in osteoarthritis (OA) of the knee	1. Przegl Lek. <b>2011</b> , 68, 307–310. 2. <a href="https://www.suplasyn.com/">https://www.suplasyn.com/</a>

### 15.5.2.1 Hyaluronan for Ophthalmology

HA commercial products are widely developed in the field of ophthalmology due to the great need. Major commercial products such as Healon GV<sup>®</sup>, Viscoat<sup>®</sup>, Biotrue multipurpose solution (MPS), Provisc<sup>®</sup>, Healonid, and Viscorneal(R), are mainly composed of sodium hyaluronate with some modifications due to their individual targeted symptoms.

#### Healon GV<sup>®</sup>

A highly purified non-pyrogenic solution of high molecular weight (~5000 kDa) sodium hyaluronate dissolved in physiological buffer. The solution is highly viscous and helpful in expansion and maintenance of anterior chamber. Applications in eye surgery included and not limited to: cataract, glaucoma filtering, and corneal transplantation. For instances, at early stage of cataract, sufficient amount of Healon GV<sup>®</sup> was slowly injected into front chamber to avoid tissue trauma.

#### Viscoat<sup>®</sup>

A transparent solution with high fluidity that is mainly composed of sodium chondroitin sulfate and sodium hyaluronate. Usage of Viscoat<sup>®</sup> is limited to eye, and the main purposes of this product are maintenance of deep cavity, strengthening of visualization, and protection of corneal endothelium. Additionally, viscoelasticity of this solution can keep vitreous on correct position to prevent forming postoperative cavity. The solution residue will be removed at the end of surgery by perfusion and extraction of balanced salt buffer.

#### Provisc<sup>®</sup>

PROVISC<sup>®</sup> is a sterile, non-pyrogenic, high molecular weight, non-inflammatory highly purified fraction of sodium hyaluronate, and dissolved in physiological sodium chloride phosphate buffer. The viscoelastic properties of Provisc<sup>®</sup> help to push back the vitreous face and prevent the formation of a flat chamber postoperatively. Provisc<sup>®</sup> is indicated for using as an ophthalmic surgical aid in the anterior segment during cataract extraction and intraocular lens

(IOL) implantation. Because it can maintain a deep anterior chamber during anterior segment surgery allowing reduced trauma to the corneal endothelium and surrounding ocular tissues.

#### Healonid

It is the injectable solution composed of Sodium hyaluronate. Depending on the chemical environment, Healonid can exist in the acid, sodium salt or Healonid anion. It can help to heal degenerative joint disease, however, the actual mechanism is not clear. Healonid has two major functions: one is to be the regulation of normal cellular constituents, and the other is to exert an anti-inflammatory action by inhibiting the movement of granulocytes and macrophages.

#### Viscorneal(R)

Viscorneal(R) is the sterile and pyrogen-free solution consisting of hyaluronate sodium, sodium chloride and so on. Sodium hyaluronate is biocompatible and has interesting physical and rheological properties for ophthalmic surgery. Viscoelastic solution of highly purified sodium hyaluronate dissolved in a buffer solution (pH 7 to 7.5). Viscorneal(R) is administered with a graduated disposable syringe, previously filled. Its important functions and usages form a thin protective layer on cells and ocular tissues, allow the lubrication of the intraocular lens before implantation. It is also a coadjuvant in anterior chamber surgery and especially during cataract surgery with or without IOL implantation, and in glaucoma surgery.

### Summary on HA Products for Ophthalmology

Here we compare the functions of HA products above. The comparing result shows that there are the same functions in these five ophthalmology HA products during ophthalmic surgery. Mostly, they can protect ocular tissues from trauma and maintain a deep anterior chamber during anterior segment surgery, and especially users can even take Healonid to facilitate anti-inflammatory action by inhibiting the movement of granulocytes and macrophages.

### 15.5.2.2 HA for Papilla Regeneration.

HA is still the major product for papilla regeneration. No matter it is in any physical state of Hyaluronan, there is still the same function and effect by gel or solution. It is a fact that most of HA products for papilla regeneration are original hyaluronan, this subchapter will choose one product which includes the additional materials to illustrate.

**Corgel™:** Corgel™ is composed of two alginates and three hyaluronic-based biocompatible and injectable hydrogel. Corgel™ can be a cartilage repairing biomaterial, which has the functions like tissue bulking agents or cell delivery matrix because the hydrogel can be formed under physiologic conditions in situ.

### 15.5.2.3 HA for Dermatology and Plastic Surgery

The development of injectable dermal fillers in plastic surgery has become one of the most popular aesthetic medical procedures available to patients who desire facial rejuvenation. The dermal fillers are mainly used for the filling of wrinkles and skin folds caused by disease or age [26]. An ideal material for dermal filler include biocompatibility, reasonable clinical appearance and duration, ease of use and minimal tendency to migrate to distant sites. Currently, the most common procedure is now the injection of hyaluronic acid (HA) fillers. HA-based temporary dermal fillers are being employed with increasing frequency for the treatment of facial skin lines in the aesthetic medical procedures [12]. The characteristics of HA include non-surgical and injectable cosmetic procedure [30]. Until now, many of HA fillers have been developed and available to aesthetic plastic surgery. The main differentiators of HA fillers for aesthetic plastic surgery include the source of HA, the properties of HA fillers, the concentration of HA in each injection being utilized, the particulate size of the HA, the type of cross-linking agent used in the HA, and whether the HA is monophasic or biphasic.

### AdvaCoat™

AdvaCoat™ or AdvaCoat Sinus Gel and Stent is produced from a non-animal, nonpathogenic source using a highly purified HA. It is a biore-sorbable material composed of cross-linked polymers of a derivatized HA. The gel of AdvaCoat™ is placed in using a syringe and the stent is formed in the sinus cavity. The sinus cavity was completely filled with gel (2007). These devices are used for preventing tissues adhesions in the nasal cavity and minimizing edema and bleeding in patients undergoing nasal/sinus surgery (2007).

### Belotero® Balance

The Belotero® range of products exhibit different densities of HA (concentration ranging from 18 to 26 mg/mL) for different purposes of non-surgical and monophasic procedures of rejuvenation [74]. The similar product Belotero® Balance utilizes 22.5 mg/mL HA in a patented matrix technology. The matrix HA of Belotero® Balance is cross-linked with a binding agent (1,4-butanediol diglycidyl ether, BDDE) in two consecutively executed reactions and reconstituted in a physiologic buffer at pH 7 [74]. The pivotal studies indicated of the patients maintained optimal correction at 6 months on the Belotero-treated side of the face. The open-label study of dermal fillers persisted in the majority of subjects without repeated treatment [56].

### Hylaform®

Hylaform® is a sterile, colorless gel implant material, cross-linked with divinyl sulfone, and isolated from an avian (bird) source. The degree of cross-linking is 20%. The concentration of HA in Hylaform® is 4.5–6.0 mg/mL. The gel particle size (500 um) is suitable to severe facial wrinkles and folds [30]. The study of skin testing indicated lip enhancement or augmentation were not recommended. Side effects may occur as a result of the injection with Hylaform® gel. Most of the symptoms of side effects were mild and went away [58].

### Juvederm™ 30 HV

Six different formulations of Juvederm™ HA fillers have been developed, with differing concentrations of HA in each formulation, ranging from 18 to 30 mg/g. Juvederm™ 30 HV (also Juvederm™ Ultra Plus) contain 30 mg/g of HA. The HA of Juvederm™ 30 HV is cross-linked by BDDE to form a 3-dimensional HA gel and kept in phosphate buffered to 6.5–7.3 pH. The HA fillers in Juvederm™ 30 HV exhibit higher concentration of HA and more cross-link than other HA fillers, so it may persist longer than other HA fillers and have a more smooth injection flow [61]. The results of the clinical trial showed significantly greater efficacy than the bovine collagen product [6]. The nasolabial folds treated with product had shown clinically significant correction at 24 weeks after the last treatment [57].

### Restylane Silk

Restylane Silk is a non-animal stabilized HA and purified from a fermentation of equine streptococci. The cross-linking degree in BDDE-modified HA is 1%. The HA concentration is 20 mg/mL with 0.3% lidocaine and its gel particle size is 400 μm. The lidocaine in Restylane Silk has been added to reduce the discomfort associated with the treatment [30, 51]. The clinical study was conducted with Restylane Silk exhibited that 98% of subjects reported improvement in their lip fullness 14 days after injection and 76% of the subjects still had lip improvement 6 months after their injection (FDA).

### Revanesse

The HA of Revanesse cross-linked dissolvable dextranomer beads and is thought to give the products greater longevity and filling power [7]. The clinical study indicated that the improving effect for facial tissue, such as nasolabial folds. The patients in the main study were offered retreatment with Revanesse if they had returned to their previous wrinkle severity or needed optimal correction at 6 months post-treatment [7].

### Other Commercial HA Products

The Captique is non-animal stabilized HA technology. This averted the potential immunological

problems associated with the previous avian source for the HA fillers [30]. The HA of Perlane is *Streptococcus* species of bacteria, chemically cross-linking with BDDE, stabilized and suspended in phosphate buffered saline at pH = 7 and concentration of 20 mg/mL (FDA).

### 15.5.3 Regenerative Products with Collagen and HA

In the past two decades, several regenerative products containing hyaluronan and collagen or gelatin have been developed into the market. These products are bringing great benefits to human life, such as the bioresorbable dressing for postoperative wound healing to eliminate the need for painful packing removal, cell-compatible scaffold for tissue engineering to enhance the efficacy of regenerative medicine, and highly absorbable dietary ingredient for the promotion of skin, joint, connective tissue, tendon and ligament health. Table 15.3 shows a list of regenerative products with hyaluronan and collagen or gelatin.

MeroPack® is an absorbable hyaluronic acid packing material containing 80% esterified HA and 20% collagen (<http://www.medtronic.com/us-en/healthcare-professionals/products/ear-nose-throat/bio-packing/bio-nasal-packing/meropack.html>). It is indicated for use in patients undergoing nasal/sinus surgery as a space-occupying stent in the nasal cavity ([https://www.accessdata.fda.gov/cdrh\\_docs/pdf4/k041381.pdf](https://www.accessdata.fda.gov/cdrh_docs/pdf4/k041381.pdf)). Upon hydration, MeroPack can transform into a biocompatible, mucoadhesive gel and be slowly resorbed by the body within 2 weeks. It could be removed by suctioning if desired. In 2010, Huang [40] reported that MeroPack has lower pain score during packing removal as a nasal dressing after endoscopic sinus surgery in comparison with an unabsorbable cross-linking polyvinyl alcohol packing material (Merocel). MeroPack effectively prevented postoperative hemorrhage for nasal trauma patients, although it does not show distinct advantages on prevention of synechiae formation [39, 40]. MeroPack was suggested reserving for children who are predis-

**Table 15.3** A list of regenerative products with hyaluronan and collagen or gelatin

Product Name	Type	Company	Contains	Indication	References
MeroPack®	Solid	Medtronic plc	80% esterified hyaluronan and 20% collagen	Nasal packing and sinus stent	Hu et al. (2008) and Huang and Huang (2010)
HyStem®-C	Hydrogel	BioTime, Inc			
HyStem®-HP	Hydrogel				
HyStem®-VF	Hydrogel				
BioCell Collagen®	Fine powder for use in capsules and soft gels	Biocell Technology LLC	60% hydrolyzed collagen type II, 10% low-molecular-weight hyaluronic acid, 20% chondroitin sulfate, and 10% uncharacterized components of chicken sternal cartilage		Schauss (2007), Schauss (2012) and Schwartz and Park (2012)

posed to develop postoperative hemorrhages or adhesions, such as resection of the concha bullosa, traumatic surgery with the creation of large raw surfaces on the middle turbinate, and revision surgery with preexisting adhesions.

HyStem® products (HyStem®-C, -HP, and -VF), developed by BioTime, Inc., are low salt hyaluronan-gelatin hydrogels with minor difference in its ingredients or applications (as shown in Table 15.3). These products have applications in cell culture [3, 16, 17], stem cell growth [3, 18, 21, 43, 55], tissue engineering, and animal models of cell-based therapies [5, 21, 67, 99]. Basically, they are a family of research products to mimic a living cell's natural environment (ECM). Liu et al. [55] demonstrated HyStem®-C can support the prolonged maintenance of mouse embryonic stem cells in standard growth medium and human induced pluripotent stem cells (hiPSCs) in MEF-conditioned medium. It has also been proven that frozen mouse embryonic fibroblast cells (NIH 3T3 cells) survival rate can still be maintained at 85–88% after 48 h in HyStem®-C by Chen and Thibeault in 2013 [16]. They [17] also studied the complex interactions among bone marrow-derived mesenchymal stromal cells (BM-MSCs), co-culture assay of normal or scarred human vocal fold fibroblasts in HyStem®-VF 3D hydrogel. Their findings support the hypothesis that fibroblasts and hydrogel-

embedded BM-MSCs are capable of modulating cellular behavior via cytokines and growth factor production, providing an in vitro regenerative milieu for vocal fold scarring.

HyStem®-HP is a hyaluronan–heparin–collagen hydrogel, can be mixed with stem cells to form a stem-cell-hydrogel complex. In 2010, Zhong et al. [99] transplanted neuronal stem cells within a pro-survival HyStem-HP hydrogel into the infarct cavity after stroke in mice models. Their result indicates that HyStem-HP enhances the survival of stem cell transplantation and diminishes cell stress. Espandar et al. [21] proved the human adipose-derived stem cells can also be successfully grown on HyStem®-HP hydrogel in the corneal stroma of rabbits and can express human cornea-specific proteins. Renevia® is one of the HyStem® hydrogel formulations as well ([http://www.biotimeinc.com/wp-content/uploads/2015/](http://www.biotimeinc.com/wp-content/uploads/2015/06/2_HyStem_Technology_clean_v.2.pdf)

06/2\_HyStem\_Technology\_clean\_v.2.pdf; [93]). It is designed as an implantable matrix for the delivery of autologous adipose tissue-derived cells to treat the facial lipoatrophy associated with HIV. Note that, Renevia® is not cleared for marketing in the United States due to the clinical trial has not been submitted to the US FDA for review (<http://www.biotimeinc.com/products-pipeline/renevia/>).



BioCell Collagen<sup>®</sup>, derived from the chicken sternal articular cartilage, is a multifaceted healthy aging dietary ingredient produced by BioCell Technology LLC. Acute and subchronic oral toxicity studies [80] have been conducted in rats at a single dose of 500 mg per kg of body weight and the maximum 1000 mg per kg of body weight for over 90 days. All animals survived and showed no significant changes in their body weights and histopathology throughout the study. In the multiple human clinical trials, BioCell Collagen<sup>®</sup> as a daily supplement could promote joint and skin health [82] and improve osteoarthritis-related symptoms [81]. In the report of Schauss et al. [81], daily supplementation with BioCell Collagen<sup>®</sup> provided significant symptom reduction in patients suffering from osteoarthritic pain and disability. It is believed that BioCell Collagen<sup>®</sup> can stimulate chondrocytes in the cartilage and dermal fibroblasts in skin dermis that synthesize collagen and glycosaminoglycans, providing a potential regenerative mechanism.

## References

1. (2007) Premarket notification 510(k) summary. U S food and drug administration K070496
2. Adiguzel E, Hou G, Sabatini PB, Bendek M (2013) Type viii collagen signals via  $\beta 1$  integrin and rhoa to regulate mmp-2 expression and smooth muscle cell migration. *Matrix Biol* 32(6):332–341. <https://doi.org/10.1016/j.matbio.2013.03.004>
3. Aleksander-Konert E, Padiuszyński P, Zajdel A, Dzierżewicz Z, Wilczok A (2016) In vitro chondrogenesis of Wharton's jelly mesenchymal stem cells in hyaluronic acid-based hydrogels. *Cell Mol Biol Lett* 21:11. <https://doi.org/10.1186/s11658-016-0016-y>. eCollection2016
4. Bard JB, Hay ED (1975) The behavior of fibroblasts from the developing avian cornea. Morphology and movement in situ and in vitro. *J Cell Biol* 67(2PT.1):400–418
5. Bartlett RS, Guille JT, Chen X, Christensen MB, Wang SF, Thibeault SL (2016) Mesenchymal stromal cell injection promotes vocal fold scar repair without long-term engraftment. *Cytotherapy* 18(10):1284–1296. <https://doi.org/10.1016/j.jcyt.2016.07.005>
6. Baumann LS, Shamban AT, Lupo MP, Monheit GD, Thomas JA, Murphy DK, Walker PS, Group. JvZNFs (2007) Comparison of smooth-gel hyaluronic acid dermal fillers with cross-linked bovine collagen: a multicenter, double-masked, randomized, within-subject study. *Dermatol Surg* 33(Suppl 2):S128–S135
7. Beasley KL, Weiss MA, Weiss RA (2009) Hyaluronic acid fillers: a comprehensive review. *Facial Plast Surg* 25:86–94
8. Bonafé F, Govoni M, Giordano E, Caldarera CM, Guarnieri C, Muscari C (2014) Hyaluronan and cardiac regeneration. *J Biomed Sci* 21:100. <https://doi.org/10.1186/s12929-014-0100-4>
9. Bourguignon LYW (2008) Hyaluronan-mediated cd44 activation of rho gtpase signaling and cytoskeleton function promotes tumor progression. *Seinars in Cancer Biol* 18(4):251–259. <https://doi.org/10.1016/j.semcancer.2008.03.007>
10. Bourguignon LYW, Zhu H, Shao L, Chen YW (2000) Cd44 interaction with tiam1 promotes rac1 signaling and hyaluronic acid-mediated breast tumor cell migration. *J Biol Chem* 275(3):1829–1838. <https://doi.org/10.1074/jbc.275.3.1829>
11. Cardoso V, Quelemes P, Amorin A, Primo F, Gobo G, Tedesco A, Mafud A, Mascarenhas Y, Corrêa J, Kuckelhaus S, Eiras C, Leite J, Silva D, dos Santos Júnior J (2014) Collagen-based silver nanoparticles for biological applications: synthesis and characterization. *J Nanobiotechnol* 12(36):1–9. <https://doi.org/10.1186/s12951-014-0036-6>
12. Carruthers J, Carruthers A (2003) A prospective, randomized, parallel group study analyzing the effect of btx-a (botox) and nonanimal sourced hyaluronic acid (nasha, restylane) in combination compared with nasha (restylane) alone in severe glabellar rhytides in adult female subjects: treatment of severe glabellar rhytides with a hyaluronic acid derivative compared with the derivate and btx-a. *Dermatol Surg* 29:802–809
13. Carvalhaes L, Gervásio O, Guatimosim C, Heljasvaara R, Sormunen R, Pihlajaniemi T, Kitten G (2006) Collagen xviii/endostatin is associated with the epithelial-mesenchymal transformation in the atrioventricular valves during cardiac development. *Dev Dyn* 235(1):132–142. <https://doi.org/10.1002/dvdy.20556>
14. Chae JJ, Mulreany DG, Guo Q, Lu Q, Choi JS, Strehin I, Espinoza FA, Schein O, Trexler MM, Bower KS, Elisseff JH (2014) Application of a collagen-based membrane and chondroitin sulfate-based hydrogel adhesive for the potential repair of severe ocular surface injuries. *Mil Med* 179(6):686–694. <https://doi.org/10.7205/MILMED-D-13-00360>
15. Cheema U, Ananta M, Mudera V (2011) Collagen: applications of a natural polymer in regenerative medicine. In: Eberli D (ed) *Regenerative medicine and tissue engineering – cells and biomaterials*. InTech, Rijeka
16. Chen X, Thibeault S (2013) Effect of DMSO concentration, cell density and needle gauge on the viability of cryopreserved cells in three dimensional hyaluronan hydrogel. *Conf Proc IEEE Eng Med*

- Biol Soc 2013;6228–6231. <https://doi.org/10.1109/EMBC.2013.6610976>
17. Chen X, Thibeault SL (2016) Cell-cell interaction between vocal fold fibroblasts and bone marrow mesenchymal stromal cells in three-dimensional hyaluronan hydrogel. *J Tissue Eng Regen Med* 10(5):437–446. <https://doi.org/10.1002/term.1757>. Epub 2013 May 8
  18. Chen D, Qu Y, Hua , Zhang L, Liu Z, Pflugfelder SC, Li DQ (2017) A hyaluronan hydrogel scaffold-based xeno-free culture system for ex vivo expansion of human corneal epithelial stem cells. *Eye (Lond)* 31(6):962–971. <https://doi.org/10.1038/eye.2017.8>. Epub 2017 Feb 17
  19. Cheng X, Tsao C, Sylvia V, Cornet D, Nicoletta D, Bredbenner T, Christy R (2014) Platelet-derived growth-factor-releasing aligned collagen-nanoparticle fibers promote the proliferation and tenogenic differentiation of adipose-derived stem cells. *Acta Biomater* 10(3):1360–1369. <https://doi.org/10.1016/j.actbio.2013.11.017>
  20. Dicker K, Gurski L, Pradhan-Bhatt S, Witt R, Farach-Carson M, Jia X (2014) Hyaluronan: a simple polysaccharide with diverse biological functions. *Acta Biomater* 10(4):1558–1580. <https://doi.org/10.1016/j.actbio>
  21. Espandar L, Bunnell B, Wang GY, Gregory P, McBride C, Moshirfar M (2012) Adipose-derived stem cells on hyaluronan acid-derived scaffold: a new horizon in bioengineered cornea. *Arch Ophthalmol* 130(2):202–208. <https://doi.org/10.1001/archophthalmol.2011.1398>
  22. Farndale RW, Sixma JJ, Barnes MJ, de Groot PG (2004) The role of collagen in thrombosis and hemostasis. *J Thromb Haemost* 2(4):561–573
  23. FDA U Microsoft word – restylane silk patient brochure update 13 june 14.Docx. Administration USfad
  24. FDA U [www.accessdata.fda.gov/cdrh\\_docs/pdf4/p040024s006c.pdf](http://www.accessdata.fda.gov/cdrh_docs/pdf4/p040024s006c.pdf)
  25. Fraser JR, Laurent TC, Laurent BG (1997) Hyaluronan: its nature, distribution, functions and turnover. *J Intern Med* 242(1):27–33
  26. Funt D, Pavicic T (2013) Dermal fillers in aesthetics: an overview of adverse events and treatment approaches. *Clin Cosmet Investig Dermatol* 6:295–316
  27. Genovese L, Corbo A, Sibilla S (2017) An insight into the changes in skin texture and properties following dietary intervention with a nutriscosmeceutical containing a blend of collagen bioactive peptides and antioxidants. *Skin Pharmacol Physiol* 30(3):146–158. <https://doi.org/10.1159/000464470>. Epub 2017 May 20
  28. Goettsch C, Kliemt S, Sinnigen K, von Bergen M, Hofbauer LC, Kalkhof S (2012) Quantitative proteomics reveals novel functions of osteoclast-associated receptor in STAT signaling and cell adhesion in human endothelial cells. *J Mol Cell Cardiol* 53(6):829–837. <https://doi.org/10.1016/j.yjmcc.2012.09.003>. Epub 2012 Sep 15
  29. Gokce EH, Tuncay Tanrıverdi S, Eroglu I, Tsapis N, Gokce G, Tekmen I, Fattal E, Ozer O (2017) Wound healing effects of collagen-laminin dermal matrix impregnated with resveratrol loaded hyaluronan acid-DPPC microparticles in diabetic rats. *Eur J Pharm Biopharm* 119:17–27. <https://doi.org/10.1016/j.ejpb.2017.04.027>. Epub 2017 Apr 28
  30. Gold MH (2007) Use of hyaluronan acid fillers for the treatment of the aging face. *Clin Interv Aging* 3:369–376
  31. Gonzalez D, Medici D (2014) Signaling mechanisms of the epithelial-mesenchymal transition. *Sci Signal* 7(344):re8. <https://doi.org/10.1126/scisignal.2005189>
  32. Gorshkov B, Gorshkova I, Makarieva T, Stonik V (1982) Inhibiting effect of cytotoxic bromine-containing compounds from sponges (aplysiniidae) on  $na^+ - k^+ - atpase$  activity. *Toxicol* 20(6):1092–1094
  33. Gourdie RG, Myers TA, McFadden A, Li YX, Potts JD (2012) Self-organizing tissue-engineered constructs in collagen hydrogels. *Microsc Microanal* 18(1):99–106. <https://doi.org/10.1017/S1431927611012372>. Epub 2012 Jan 4
  34. Grant S, Spradling C, Grant D, Fox D, Jimenez L, Grant DRone R (2014) Assessment of the biocompatibility and stability of a gold nanoparticle collagen bioscaffold. *J Biomed Mater Res A* 102(2):332–339. <https://doi.org/10.1002/jbm.a.34698>
  35. Gullberg D, Gehlsen KR, Turner DC, Ahlén K, Zijenah LS, Barnes MJ, Rubin K (1992) Analysis of alpha 1 beta 1, alpha 2 beta 1 and alpha 3 beta 1 integrins in cell–collagen interactions: identification of conformation dependent alpha 1 beta 1 binding sites in collagen type I. *EMBO J* 11(11):3865–3873
  36. Hamaia S, Farndale RW (2014) Integrin recognition motifs in the human collagens. *Adv Exp Med Biol* 819:127–142. [https://doi.org/10.1007/978-94-017-9153-3\\_9](https://doi.org/10.1007/978-94-017-9153-3_9)
  37. Hasegawa T, Suga Y, Mizoguchi M, Muramatsu S, Mizuno Y, Ogawa H, Kubo K, Kuroyanagi Y (2005) An allogeneic cultured dermal substitute suitable for treating intractable skin ulcers and large skin defects prior to autologous skin grafting: three case reports. *J Dermatol* 32(9):715–720
  38. Heino J (2007) The collagen family members as cell adhesion proteins. *Bioessays* 29(10):1001–1010
  39. Hu KH, Lin KN, Li WT, Huang HM (2008) Effects of Meropack in the middle meatus after functional endoscopic sinus surgery in children with chronic sinusitis. *Int J Pediatr Otorhinolaryngol* 72(10):1535–1540. <https://doi.org/10.1016/j.ijporl.2008.07.006>. Epub 2008 Aug 26
  40. Huang L-I, Huang H-M (2010) Comparison of the effects of meropack and merocel in the middle meatus after functional endoscopic sinus surgery. *J Taiwan Otolaryngol-Head Neck Surg* 45(2):40–45. <https://doi.org/10.6286/2010.45.2.40>. Epub 2008 Aug 26
  41. Hunter GK, Goldberg HA (2005) Identification of the type I collagen-binding domain of bone sialoprotein and characterization of the mechanism of interaction.

- Tye CE1. *J Biol Chem* 280(14):13487–13492. Epub 2005 Feb 8
42. Jo JY, Jeong SI, Shin YM, Kang SS, Kim SE, Jeong CM, Huh JB4 (2015) Sequential delivery of BMP-2 and BMP-7 for bone regeneration using a heparinized collagen membrane. *Int J Oral Maxillofac Surg* 44(7):921–928. <https://doi.org/10.1016/j.ijom.2015.02.015>. Epub 2015 Mar 11
  43. Jones TD, Kefi A, Sun S, Cho M, Alapati SB (2016) An optimized injectable hydrogel scaffold supports human dental pulp stem cell viability and spreading. *Adv Med* 2016:7363579. <https://doi.org/10.1155/2016/7363579>. Epub 2016 May 16
  44. Kaczmarek B, Sionkowska A (2017) Drug release from porous matrixes based on natural polymers. *Curr Pharm Biotechnol* 18(9):721–729. <https://doi.org/10.2174/1389201018666171103141347>
  45. Kawase T, Yamanaka K, Suda Y, Kaneko T, Okuda K, Kogami H, Nakayama H, Nagata M, Wolff LF, Yoshie H (2010) Collagen-coated poly(L-lactide-co-ε-caprolactone) film: a promising scaffold for cultured periosteal sheets. *J Periodontol* 81(11):1653–1662. <https://doi.org/10.1902/jop.2010.100194>. Epub 2010 Jul 14
  46. Ke T, Yang M, Mao D, Zhu M, Che Y, Kong D, Li C (2015) Co-transplantation of skin-derived precursors and collagen sponge facilitates diabetic wound healing by promoting local vascular regeneration. *Cell Physiol Biochem* 37(5):1725–1737. <https://doi.org/10.1159/000438537>. Epub 2015 Nov 9
  47. Kosaka T, Kaneko Y, Nakada Y, Matsuura M, Tanaka S (1996) Effect of chitosan implantatin on activation of canine macrophages and pllymorphonuclear cells after surgical stress. *J Vet Med Sci* 58(10):963–967
  48. Kuroyanagi Y, Kubo K, Matsui H, Kim HJ, Numari S, Mabuchi Y, Kagawa S (2004) Establishment of banking system for allogeneic cultured dermal substitute. *Artif Organs* 28(1):13–21
  49. Kuroyanagi M, Yamamoto A, Shimizu N, Ishihara E, Ohno H, Takeda A, Kuroyanagi Y (2014) Development of cultured dermal substitute composed of hyaluronic acid and collagen spongy sheet containing fibroblasts and epidermal growth factor. *J Biomater Sci Polym Ed* 25(11):1133–1143. <https://doi.org/10.1080/09205063.2014.920171>. Epub 2014 Jun 3
  50. Lam P, Kok S, Bian Z, Lam K, Tang J, Lee K, Gambari R, Chui C (2014) D-glucose as a modifying agent in gelatin/collagen matrix and reservoir nanoparticles for calendula officinalis delivery. *Colloids Surf B: Biointerfaces* 117:277–283. <https://doi.org/10.1016/j.colsurfb.2014.02.041>
  51. Lee JC, Lorenc ZP (2016) Synthetic fillers for racial rejuvenation. *Clin Plast Surg* 43:497–503
  52. Leitinger B, Hohenester E (2007) Mammalian collagen receptors. *Matrix Biol* 3:146–155. <https://doi.org/10.1016/j.matbio.2006.10.007>
  53. Lin Y, Zhang S, Rehn M, Itäranta P, Tuukkanen J, Heljäsvaara R, Peltoketo H, Pihlajaniemi T, Vainio S (2001) Induced repatterning of type xviii collagen expression in ureter bud from kidney to lung type: association with sonic hedgehog and ectopic surfactant protein c. *Dev Dent* 128(9):1573–1585
  54. Liu C-M, Chang C-H, Yu C-H, Hsu C-C, Huang LLH (2009) Hyaluronan substratum induces multidrug resistance in human mesenchymal stem cells via cd44 signaling. *Cell Tissue Res* 336(338):465–475. <https://doi.org/10.1007/s00441-009-0780-3>
  55. Liu Y, Charles LF, Zarembinski TI, Johnson KI, Atzet SK, Wesselschmidt RL, Wight ME, Kuhn LT (2012) Modified hyaluronan hydrogels support the maintenance of mouse embryonic stem cells and human induced pluripotent stem cells. *Macromol Biosci* 12(8):1034–1042. <https://doi.org/10.1002/mabi.201200043>. Epub 2012 Jun 25
  56. Lorenc ZP, Fagien S, Flynn TC, Waldorf HA (2013) Review of key belotero balance safety and efficacy trials. *Plast Reconstr Surg* 132:33S–40S
  57. Lupo MP, Smith SR, Thomas JA, Murphy DK (2008) Effectiveness of juvederm ultra plus dermal filler in the treatment of severe nasoabial folds. *Plast Reconstr Surg* 121:289–297
  58. Manna F, Dentini M, Desideri P, De Pità O, Mortilla E, Maras B (1999) Comparative chemical evaluation of two commercially available derivatives of hyaluronic acid (hylaform from rooster combs and restylane from streptococcus) used for soft tissue augmentation. *J Eur Acad Dermatol Venereol* 3:193–192
  59. Mansson B, Wenglén C, Mörgelin M, Saxne T, Heinegård D (2001) Association of chondroadherin with collagen type ii. *J Biol Chem* 276(35):32883–32888. <https://doi.org/10.1074/jbc.M101680200>
  60. Masi L, Brandi ML, Robey PG, Crescioli C, Calvo JC, Bernabei P, Kerr JM, Yanagishita M (1995) Biosynthesis of bone sialoprotein by a human osteoclast-like cell line (FLG 29.1). *J Bone Miner Res* 10(2):187–196
  61. Medical Insight I (2006) Global market for dermal fillers 2005–2011
  62. Mienaltowski MJ, Birk DD (2014) Structure, physiology, and biochemistry of collagens. *Adv Exp Med Biol* 802:5–29. [https://doi.org/10.1007/978-94-007-7893-1\\_2](https://doi.org/10.1007/978-94-007-7893-1_2)
  63. Misra S, Hascall VC, Markwalk RR, Ghatak S (2015) Interactions between hyaluronan and its receptors (cd44, rhamn) regulate the activities of inflammation and cancer. *Front Immunol* 6. <https://doi.org/10.3389/fimmu.2015.00201>
  64. Missana LR, Jammal MV (2014) Critical size defect regeneration by rhPTH-collagen membrane as a new tissue engineering tool. *J Biomed Mater Res A* 102(12):4358–4364. <https://doi.org/10.1002/jbm.a.35114>. Epub 2014 Feb 24
  65. Nagai N, Mori K, Satoh Y, Takahashi N, Yunoki S, Tajima K, Munekata M (2007) In vitro growth and differentiated activities of human periodontalligament fibroblasts cultured on salmon collagen gel. *J Biomed Mater Res A* 82(2):395–402
  66. Nagarajan U, Kawakami K, Zhang S, Chandrasekaran B, Unni Nair B (2014) Fabrication of solid collagen

- nanoparticles using electrospray deposition. *Chem Pharm Bull (Tokyo)* 62(5):422–428. <https://doi.org/10.1248/cpb.c13-01004>
67. Ogasawara T, Okano S, Ichimura H, Kadota S, Tanaka Y, Minami I, Uesugi M, Wada Y, Saito N, Okada K, Kuwahara K, Shiba Y (2017) Impact of extracellular matrix on engraftment and maturation of pluripotent stem cell-derived cardiomyocytes in a rat myocardial infarct model. *Sci Rep* 7(1):8630. <https://doi.org/10.1038/s41598-017-09217-x>
68. Park D, Kim Y, Kim H, Kim K, Lee Y, Choe J, Hahn J, Lee H, Jeon J, Choi C, Kim Y, Jeoung D (2012) Hyaluronic acid promotes angiogenesis by inducing rhamm-tgfb $\beta$  receptor interaction via cd44-pkc $\delta$ . *Mol Cells* 33(6):563–574. <https://doi.org/10.1007/s10059-012-2294-1>
69. Pastorino L, Dellacasa E, Scaglione S, Giulianelli M, Sbrana F, Vassalli M, Ruggiero C (2014) Oriented collagen nanocoatings for tissue engineering. *Colloids Surf B: Biointerfaces* 114:372–378. <https://doi.org/10.1016/j.colsurfb.2013.10.026>
70. Pawelec K, Best S, Cameron R (2016) Collage: a network for regenerative medicine. *J Mater Chem B* 4(40):6484–6496. <https://doi.org/10.1039/c6tb00807k>
71. Pedchenko V, Zent R, Hudson BG (2004) Alpha(v)beta3 and alpha(v)beta5 integrins bind both the proximal RGD site and non-RGD motifs within noncollagenous (NC1) domain of the alpha3 chain of type IV collagen: implication for the mechanism of endothelial cell adhesion. *J Biol Chem* 279(4):2772–2780. Epub 2003 Nov 10
72. Petersen W, Rahmanian-Schwarz A, Werner JO, Schiefer J, Rothenberger J, Hübner G, Schaller HE, Held M (2016) The use of collagen-based matrices in the treatment of full-thickness wounds. *Burns* 42(6):1257–1264. <https://doi.org/10.1016/j.burns.2016.03.017>. Epub 2016 Jun 11
73. Picke AK, Salbach-Hirsch J, Hintze V, Rother S, Rauner M, Kascholke C, Möller S, Bernhardt R, Rammelt S, Pisabarro MT, Ruiz-Gómez G, Schnabelrauch M, Schulz-Siegmund M, Hacker MC, Scharnweber D, Hofbauer C, Hofbauer LC (2016) Sulfated hyaluronan improves bone regeneration of diabetic rats by binding sclerostin and enhancing osteoblast function. *Biomaterials* 96:11–23. <https://doi.org/10.1016/j.biomaterials.2016.04.013>. Epub 2016 Apr 21
74. Prasetyo AD, Prager W, Rubin MG, Moretti EA, Nikolis A (2016) Hyaluronic acid fillers with cohesive polydensified matrix for soft-tissue augmentation and rejuvenation: a literature review. *Clin Cosmet Investig Dermatol* 9:257–280
75. Ratner BD1, Bryant SJ (2004) Biomaterials: where we have been and where we are going. *Annu Rev Biomed Eng* 6:41–75
76. Responde D, Natoli R, Athanasiou K (2012) Identification of potential biophysical and molecular signalling mechanisms underlying hyaluronic acid enhancement of cartilage formation. *J R Soc Interface* 9(77):3564–3573. <https://doi.org/10.1098/rsif.2012.0399>
77. Salamanca E, Tsai CY, Pan YH, Lin YT, Huang HM, Teng NC, Lin CT, Feng SW, Chang WJ (2016) In vitro and in vivo study of a novel porcine collagen membrane for guided bone regeneration. *Materials (Basel)* 9(11). pii: E949. <https://doi.org/10.3390/ma9110949>
78. Salbach J, Klient S, Rauner M, Rachner TD, Goettsch C, Kalkhof S, von Bergen M, Möller S, Schnabelrauch M, Hintze V, Scharnweber D, Hofbauer LC (2012) The effect of the degree of sulfation of glycosaminoglycans on osteoclast function and signaling pathways. *Biomaterials* 33(33):8418–8429. <https://doi.org/10.1016/j.biomaterials.2012.08.028>. Epub 2012 Sep 4
79. Salbach-Hirsch J, Ziegler N, Thiele S, Moeller S, Schnabelrauch M, Hintze V, Scharnweber D, Rauner M, Hofbauer LC (2014) Sulfated glycosaminoglycans support osteoblast functions and concurrently suppress osteoclasts. *J Cell Biochem* 115(6):1101–1111. <https://doi.org/10.1002/jcb.24750>
80. Schauss AG, Merkel DJ, Glaza SM, Sorenson SR (2007) Acute and subchronic oral toxicity studies in rats of a hydrolyzed chicken sternal cartilage preparation. *Food Chem Toxicol* 45(2):315–321. Epub 2006 Aug 30
81. Schauss AG, Stenehjem J, Park J, Endres JR, Clewell A (2012) Effect of the novel low molecular weight hydrolyzed chicken sternal cartilage extract, BioCell collagen, on improving osteoarthritis-related symptoms: a randomized, double-blind, placebo-controlled trial. *J Agric Food Chem* 60(16):4096–101. <https://doi.org/10.1021/jf205295u>. Epub 2012 Apr 16.
82. Schwartz SR, Park J (2012) Ingestion of BioCell collagen(®), a novel hydrolyzed chicken sternal cartilage extract; enhanced blood microcirculation and reduced facial aging signs. *Clin Interv Aging* 7:267–273. <https://doi.org/10.2147/CIA.S32836>. Epub 2012 Jul 27
83. Schwertfeger K, Cowman M, Telmer P, Turley E, McCarthy J (2015) Hyaluronan, inflammation, and breast cancer progression. *Front Immunol* 6:236. <https://doi.org/10.3389/fimmu.2015.00236>
84. Shukla S, Nair R, Rolle MW, Braun KR, Chan CK, Johnson PY, Wight TN, McDevitt TC (2010) Synthesis and organization of hyaluronan and versican by embryonic stem cells undergoing embryoid body differentiation. *J Histochem Cytochem* 58:345–358. <https://doi.org/10.1369/jhc.2009.954826>
85. Singleton PA, Bourguignon LYW (2004) Cd44 interaction with ankyrin and ip3 receptor in lipid rafts promotes hyaluronan-mediated ca<sup>2+</sup> signaling leading to nitric oxide production and endothelial cell adhesion and proliferation. *Exp Cell Res* 295:102–118
86. Slatter DA, Farndale RW (2015) Structural constraints on the evolution of the collagen fibril: convergence on a 1014-residue col domain. *Open Biol* 5(5):1–7. <https://doi.org/10.1098/rsob.140220>
87. Steelman L, Chappell W, Abrams S, Kempf R, Long J, Laidler P, Mijatovic S, Maksimovic-Ivanic D, Stivala F, Mazzarino M, Donia M, Fagone P,

- Malaponte G, Nicoletti F, Libra M, Milella M, Tafuri A, Bonati A, Bäsecke J, Cocco L, Evangelisti C, Martelli A, Montalto G, Cervello M, McCubrey J (2011) Roles of the raf/mek/erk and pi3k/pten/akt/mTOR pathways in controlling growth and sensitivity to therapy-implications for cancer and aging. *Aging* (Albany NY) 3(3):192–222. <https://doi.org/10.18632/aging.100296>
88. Sunitha K, Suresh P, Santhosh M, Hemshekhar M, Thushara R, Marathe G, Thirunavukkarasu C, Kemparaju K, Kumar M, Girish K (2013) Inhibition of hyaluronidase by n-acetyl cysteine and glutathione: role of thiol group in hyaluronan protection. *Int J Biol Macromol* 55:39–46. <https://doi.org/10.1016/j.ijbiomac.2012.12.047>
89. Taubenberger AV, Woodruff MA, Bai H, Muller DJ, Huttmacher DW (2010) The effect of unlocking RGD-motifs in collagen I on pre-osteoblast adhesion and differentiation. *Biomaterials* 31(10):2827–2835. <https://doi.org/10.1016/j.biomaterials.2009.12.051>. Epub 2010 Jan 6
90. Tutrone WD, Cohen JL (2009) Dissolving collagen fillers: enzymatic degradation of some problematic filler circumstances may now include collagens. *J Drugs Dermatol* 8(12):1140–1141
91. Tye CE, Hunter GK, Goldberg HA (2005) Identification of the type I collagen-binding domain of bone sialoprotein and characterization of the mechanism of interaction. *J Biol Chem* 280(14):13487–13492. Epub 2005 Feb 8
92. Wehrhan F, Nkenke E, Melnychenko I, Amann K, Schlegel KA, Goerlach C, Zimmermann WH, Schultze-Mosgau S (2010) Skin repair using a porcine collagen I/III membrane-vascularization and epithelialization properties. *Dermatol Surg* 36(6):919–930. <https://doi.org/10.1111/j.1524-4725.2010.01569.x>
93. Wirosko B, Mann BK, Williams DL, Prestwich GD (2014) Ophthalmic uses of a thiol-modified hyaluronan-based hydrogel. *Adv Wound Care* (New Rochelle) 3(11):708–716
94. Wu S-C, Chang J-K, Wang C-K, Wang G-J, Ho M-L (2010) Enhancement of chondrogenesis of human adipose derived stem cells in a hyaluronan-enriched microenvironment. *Biomaterials* 31:631–640
95. Xia H, Nho R, Kahm J, Kleidon J, Henke C (2004) Focal adhesion kinase is upstream of phosphatidylinositol 3-kinase/akt in regulating fibroblast survival in response to contraction of type I collagen matrices via a beta 1 integrin viability signaling pathway. *J Biol Chem* 279(31):33024–33034. <https://doi.org/10.1074/jbc.M313265200>
96. Yamada S, Ohara N, Hayashi Y (2003) Mineralization of matrix vesicles isolated from a human osteosarcoma cell line in culture with water-soluble chitosan-containing medium. *J Biomed Mater Res A* 66(3):500–506
97. Yamada S, Ganno T, Ohara N, Hayashi Y (2007) Chitosan monomer accelerates alkaline phosphatase activity on human osteoblastic cells under hypofunctional conditions. *J Biomed Mater Res A* 83(2):290–295
98. Yoshizaki K, Yamada Y (2013) Gene evolution and functions of extracellular matrix proteins in teeth. *Orthod Waves* (English ed) 72(1):1–10. <https://doi.org/10.1016/j.odw.2013.01.040>
99. Zhong J, Chan A, Morad L, Kornblum HI, Fan G, Carmichael ST (2010) Hydrogel matrix to support stem cell survival after brain transplantation in stroke. *Neurorehabil Neural Repair* 24(7):636–644. <https://doi.org/10.1177/1545968310361958>. Epub 2010 Apr 27

---

**Part IV**

**Inorganic Biomaterials for Regenerative  
Medicine**



# Bioceramics for Clinical Application in Regenerative Dentistry

# 16

Ika Dewi Ana, Gumilang Almas Pratama Satria, Anne Handrini Dewi, and Retno Ardhani

## Abstract

Bioceramics represent functional ceramics with significant interest in regenerative medicine area. In orthopedics as well as in oral and maxillofacial surgery, bioceramics have been widely used as bone reconstructive materials. The most common one is hydroxyapatite which have been in the market and clinical applications since the mid of 1970s. Nowadays, a lot of works have been being in the pipeline to develop bioceramics for various clinical applications in regenerative medicine area, including dentistry. Bioceramics have been used and considered promising candidate for periodontal treatment, prevention of relapse, nerve regeneration, vaccine adjuvant, drug delivery technology, even for esthetic medicine and cosmetics. In this chapter, the advantages of bioceramics for regenerative therapy especially in dentistry is discussed. The overview of bioceramics classification is also explained. The future perspective and challenges on the use of bioceramics for next generation regenerative therapy is also discussed.

## Keywords

Bioceramics · Regenerative therapy · Classification · Orthopedic · Maxillofacial surgery

## 16.1 Novel Bioceramics for Regenerative Medicine

Bioceramics is a terminology which refers to ceramics engineered to interact with biological system and applied for biomedical uses, either for therapeutics uses such as body implants, repairs, augmentations, drug delivery vehicles, vaccine adjuvants, or diagnosis. What is ceramics then? According to some previous references, ceramics are highly crystalline structures formed by heating non-metallic mineral salts under high temperature process known as sintering. For example, to fabricate bioactive glasses which also considered as ceramics, some amounts of  $\text{SiO}_2$ ,  $\text{NaO}_2$ ,  $\text{CaO}$ , and  $\text{P}_2\text{O}_5$  are processed at the temperature which gradually raises from  $350^\circ$  to the melting point of the glasses at around  $1400^\circ\text{C}$  [20]. However, due to various purposes and indications on the use of bioceramics inside the body, low or poor crystalline ceramics are also being considered and the fabrication methods also vary not only by high temperature sintering. For example, fabrication method of amorphous calcium phosphate ceramics by wet precipitation

I. D. Ana (✉) · A. H. Dewi · R. Ardhani  
Department of Dental Biomedical Sciences, Faculty of Dentistry, Universitas Gadjah Mada, Yogyakarta, Indonesia  
e-mail: ikadewiana@ugm.ac.id

G. A. P. Satria  
PT Swayasa Prakarsa, UGM Incubation and Start Up, Universitas Gadjah Mada, Yogyakarta, Indonesia

method needs lower temperature [27]. This is because the temperature at which porous ceramics are sintered can affect biological response due to alteration of chemical and topographical surfaces of the materials [18].

Moreover, it is also known from previous researches that crystallinity also influences cell and tissue response. Frank et al. [17] observed that crystallinity affected adsorption of serum components to the surface and the ability of cells to attach, proliferate and differentiate. While according to Oonishi et al. [33] morphological characteristics of the ceramics and size of the granule can also affect bone ingrowth. In view of these phenomena, a lot of researches have been being done to modify ceramics morphology, crystallinity, chemical, and topographical surfaces of the ceramics in order to improve tissue responses shown by enhancement of cell attachment by fibronectin or laminin treatment of ceramics surface, cell proliferation, cell differentiation, including osteogenic capacity of different ceramics.

Beside being considered among the oldest materials used by man, bioceramics also represent functional ceramics. It is because many ceramics are known and has been developed to achieve biocompatible properties to be widely used in orthopedics as bone reconstruction materials. Because of its functionality, ceramics are also used as coating of implants, drug delivery technology, vaccine technology as adjuvant, and cancer therapy including hyperthermia of cancer wherein the body is exposed to high temperature to kill cancer cells. Ceramics are also extensively studied in the area of tissue engineering to construct scaffolds and provide proper microenvironment for tissue to regenerate. Among various ceramics which have been developed and fabricated, hydroxyapatite pays a lot of attention because its similarity to bone apatite as the major component of inorganic phase of bone. Simultaneous but independent works have been done extensively by the group of Jarcho and co-workers in USA, de Groot and team in Europe, as well as Aoki and co-workers in Japan [42] to provide hydroxyapatite for clinical applications and commercialization. Nowadays, a lot more have been in the pipeline for various clinical applications.

It has been reported in the recent literatures, especially by the group of Ishikawa and team [23], that synthetic carbonate apatite revealed the biological activity better than synthetic hydroxyapatite because the incorporation of carbonate into hydroxyapatite caused an increase in solubility, a decrease in crystallinity, a change in crystal morphology, and an enhancement of chemical reactivity owing to the weak bonding resulted [5, 36, 37]. In this context, carbonate apatite will be more soluble *in vivo* compared to hydroxyapatite. The solubility of carbonate apatite will increase the local concentration of calcium and phosphate ions that are necessary for new bone formation. Existence of carbonate in the complex also increases identical properties of the materials with the human apatite or bone apatite [30].

The most important aspect on the clinical application of bioceramics is its bioactivity which leads to biocompatibility of ceramics. The biocompatibility of an implant material, for example, elicits the formation of normal tissue to its surface. Ducheyne [14] observed that once the formation of normal tissue is developed, it allows establishment of an interface capable of supporting the loads normally occur at the site of implantation. During the wound healing process associated with the implantation of bioceramics, angiogenesis takes place and enables the development of capillary blood supply. The possible mechanism is that dissolution of the calcium ions and precipitation reaction on the surface of bioceramics will provide interface for fibroblasts to attach and form an appositional fibrous matrix. The process will also lead to the occurrence of vascular penetration, differentiation of mesenchymal stem cells into osteoblast or other designated cells, based on the composition, structure, topography, crystallinity, and function of the bioceramics. A study done by El-ghannam and co-workers [16] also shows that initial reaction of some bioactive glasses (one of the member of bioceramics) cause a local increase in pH. The local increases in pH will cause alkalization. The alkalization is beneficial when bioceramics are combined with degradable polymers which usually produce acidity when they undergo biodegradable process.



## 16.2 Classification of Bioceramics

According to Tanaka and Yamashita [39], ceramics are generally classified from their chemical compositions into two groups: calcium phosphate (CP) and others, including yttria ( $Y_2O_3$ ) – stabilized tetragonal zirconia ( $ZrO_2$ ) (YTZP), alumina ( $Al_2O_3$ ) and some silicate and phosphate

families of glasses and crystallized glasses (glass ceramics), as depicted in Table 16.1. Among the families of orthophosphate molecules, hydroxyapatite is one of and considered as the most biologically compatible substances used as bone graft substitute material. The hydroxyapatite stoichiometric chemical formula is  $Ca_{10}(PO_4)_6(OH)_2$  and share similarities with the

**Table 16.1** Composition and shapes of the various bioceramics [39]

Category	Materials and compositions	Shapes
Calcium phosphate (CP) group	<b>Hydroxyapatite</b> (HAp or HA)	Sintered body (dense and porous)
	$Ca_5(PO_4)_3OH$	Powder
		Coating
		Composite
		Fiber
	<b><math>\beta</math>-Tricalcium phosphate</b> ( $\beta$ -TCP)	Sintered body (dense and porous)
	$Ca_3(PO_4)_2$	Powder
	<b>Dicalcium phosphate anhydrite</b> (monetite, DCP or DCPA)	Powder
	$CaHPO_4$	
	<b>Dicalcium phosphate dihydrate</b> (brushite, DCP2 or DCPD)	Powder
	$CaHPO_4 \cdot 2H_2O$	
	<b>Calcium pyrophosphate</b> (CPP)	Powder
	$Ca_2P_2O_7$	
	<b><math>\alpha</math>-Tricalcium phosphate</b> ( $\alpha$ -TCP)	Powder
	$Ca_3(PO_4)_2$	
	<b>Tetracalcium phosphate</b> (TeCP)	Powder
	$Ca_4(PO_4)_2O$	
<b>Octacalcium phosphate</b> (OCP)	Powder	
$Ca_8H_2(PO_4)_6 \cdot 5H_2O$		
<b>Amorphous calcium phosphate</b> (ACP)	Powder	
$Ca_3(PO_4)_2 \cdot nH_2O$		
Others	<b>Yttria-stabilized tetragonal zirconia</b> (Y-TZP)	Sintered body (dense)
	$Y_2O_3$ - $ZrO_2$	
	<b>Aluminum oksida</b> (Alumina)	Sintered body (dense)
	$Al_2O_3$	
	<b>Titanium oksida</b> (Titania)	Sintered body (dense)
	$TiO_2$	
	<b>Silicon nitride</b>	Sintered body (dense)
	$Si_3N_4$	
	<b>Silicon carbide</b>	Sintered body (dense)
	$SiC$	
	<b>Carbon</b>	Fiber
	$C$	
	<b>Bioactive glasses system</b>	Bulk
	$SiO_2$ - $P_2O_5$ - $Na_2O$ - $CaO$	Bulk
	$SiO_2$ - $P_2O_5$ - $Na_2O$ - $K_2O$ - $CaO$ - $MgO$	Bulk
$SiO_2$ - $P_2O_5$ - $CaO$ - $Al_2O_3$		
<b>Bioactive glasses ceramics system</b>	Bulk	
$SiO_2$ - $P_2O_5$ - $CaO$ - $MgO$ (A-W)	Fiber	
$SiO_2$ - $P_2O_5$ - $Na_2O$ - $K_2O$ - $CaO$ - $MgO$ (Ceravital)		

mineral phase of bone. Hydroxyapatite have been used in particulate or granule forms and porous blocks. Nowadays, there have been a shifting in the use of hydroxyapatite because it is not identical with human apatite. The difference is because of high crystallinity of hydroxyapatite as the result of high temperature process, which makes hydroxyapatite is difficult to be resorbed during the remodeling process of bone. Thus, carbonate apatite is used as an alternative and better candidate for bone substitution purposes compared to hydroxyapatite [23].

Based on the biological perspective that Mg ion is typically contained in high concentration in cartilage and natural bone tissues during the initial phases of osteogenesis which then it tends to disappear when bone is mature, some researchers also developed Mg substituted carbonate hydroxy apatite [32]. Tampieri and team have been working intensively on Mg substituted carbonate hydroxy apatite. Meanwhile, Daculsi and team also proposed and developed biphasic calcium phosphate (BCP), a group of bioceramics which has identical chemical composition with bone minerals [19]. Either carbonate apatite, some compositions of calcium orthophosphates, and BCP have been already translated into clinical applications.

Another group in the calcium phosphate families is TCP (tri- calcium phosphate). When mixed with water, dissolution of TCP to supply  $\text{Ca}^{2+}$  and  $\text{PO}_4^{3-}$  and precipitation into CDHA will lead to the formation of needle- like crystals of apatite which interlock each other to form a set mass [41]. It is reported that in general TCP is less crystalline than hydroxyapatite, and therefore, more soluble. Bone graft that contains TCP are biocompatible and osteoconductive, but because of its relative solubility it is used in the situation where structural support is less important. Unfortunately, setting time of  $\alpha$ -TCP is too long if free from additives. This long setting time prevents its clinical use. Therefore, a chelating agent such as succinic acid or citric acid is employed to shorten the initial setting reaction, but it prevents compositional transformation to apatite.

The works of Dorozhkin [15] shows that calcium orthophosphate is an important part in the

area of bioceramics, because it represents the inorganic part of major normal and pathological calcified tissues in mammals. Bones, teeth, and antlers are considered as calcium orthophosphate. In a pathological condition, the blockage in blood vessel in atherosclerosis is caused by a solid composite of cholesterol with calcium orthophosphates. As mentioned by the group of Dorozhkin [15], all calcium orthophosphates consist of three major chemical elements, calcium (oxidation state +2), phosphorus (oxidation state +5), and oxygen (reduction state -2), as a part of orthophosphate anions.

Some literatures also indicate the use of coral, which is also considered as bioceramics [4]. For example, coralline derived from marine coral which contains aragonite type of  $\text{CaCO}_3$  is also considered bioceramics. It has been used in its natural mineral form of calcium carbonate for bone substitution purposes, but to some extent it is also converted and used as a starting material to fabricate into calcium hydroxyapatite. Coralline derived from marine coral as natural mineral is already used for bone grafting since 1970 because of its good osteoconduction, bioresorbability, biocompatibility, and biodegradation [7, 8]. Coral shows a good tissue response and is completely resorbed in the body. Moreover, coral (aragonite or calcite forms of calcium carbonate or  $\text{CaCO}_3$ ) is one of the limited number of materials that can form a chemical bond with bone and soft tissues in vivo.

Another group of bioceramics is calcium sulfate hemihydrate ( $\text{CaSO}_4 \cdot 1/2\text{H}_2\text{O}$ ) which is very famous in dentistry and may be considered as the oldest bioceramics used as bone grafting material in the history. In fact, calcium sulfate cement is one of the oldest and sturdiest building materials on earth which is also considered as bioceramics. It is a gypsum product that has been used for at least 5000 years. It is safe, rapidly resorbing material that has been used for bone filling applications for more than 100 years. The use of calcium sulfate or gypsum or POP (Plaster of Paris) is based on its advantages, which include the ability to self-setting and a well-tolerated biological response without eliciting a severe inflammatory response. When calcium sulfate hemihydrate ( $\text{CaSO}_4 \cdot 1/2\text{H}_2\text{O}$ ) is mixed with water, calcium

sulfate dihydrate ( $\text{CaSO}_4 \cdot 2\text{H}_2\text{O}$ ) is formed. This property makes it possible for POP to set in situ when it is applied into a bone defect. Dewi and co-workers [10–12, 34, 40] have been doing efforts to enhance bone formation in POP implantation to overcome problems related to fast degradability of POP by combining it with calcite as well as calcite hydrogel, or the use of cinnamaldehyde as crosslinking agent [13].

The discovery of bioactive glass by Larry Hench and colleagues in 1969 at the University of Florida has been the fundamental insight on the use of bioactive glass, then initiated the field of bioactive ceramics and Bioglass® to be translated into clinical use since 1985. Bioactive glasses are amorphous silicate-based materials which are compatible with human body, bond to bone and stimulate new bone growth while dissolving over time [20]. Bioactive glass can stimulate the body's own regenerative mechanism to restore damaged bone to its original state and function.

When in contact with body fluid, carbonated hydroxyapatite (HCA) layer will be formed on the surface of the glass. The layer will be an interface for the glass to bond to bone. The rapid exchange of  $\text{Na}^+$  and  $\text{Ca}^{2+}$  with  $\text{H}^+$  or  $\text{H}_3\text{O}^+$  from solution will cause hydrolysis of the silica groups which creates Si-OH (silanols). This makes the pH increases as the results of the replacement of  $\text{H}^+$  ions by cations. The increasing hydroxyl concentration leads to the attack of silica glass network. Condensation and repolymerisation of the silanols will leave silica rich layer. The existence of silica-rich layer initiates migration of  $\text{Ca}^{2+}$  and  $\text{PO}_4^{3-}$  on the surface through silica-rich and from the surrounding fluid to form CaO- $\text{P}_2\text{O}_5$ -rich film on the top of silica-rich layer. The CaO- $\text{P}_2\text{O}_5$ -rich film crystallites as it incorporates  $\text{OH}^-$  and  $\text{CO}_3^{2-}$  anions from solution to form a mixed HCA [25].

---

### 16.3 Bioceramics Clinical Products and Applications

The first documented use of synthetic bone graft was reported in 1892 by Van Meekeran, who treated a large bone defect with calcium sulfate

[6]. Since then, materials which are categorized as ceramics have been extensively used as bone graft substitutes in human, known as bioceramics. The most widely used bioceramics materials for bone grafting in human is hydroxyapatite (HA), considering it as major mineral constituent of natural bone matrix [38]. Hydroxyapatite has chemically similar composition and crystalline structure with bone and hard tissue.

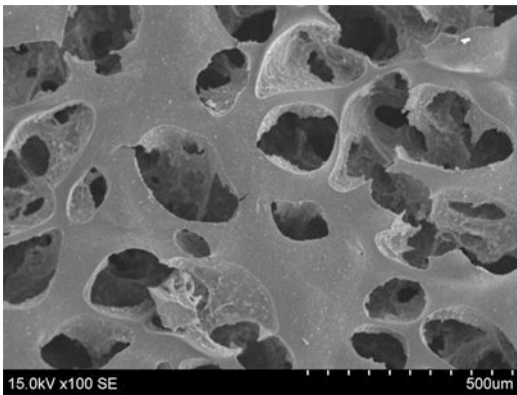
Hydroxyapatite and, to some extent, other calcium based ceramic materials can be regarded as bioactive materials that will support bone ingrowth and osseointegration when used in orthopedic, dental, and maxillofacial application.

The calcium phosphate ceramic that consists hydroxyapatite (HA) and/or beta tri-calcium phosphate ( $\beta$ -TCP) and calcium phosphate-silicate glass are called osteoconductive materials since it allows the apposition of osteoblasts at the material surface. It has also been reported that HA has been developed in variety of forms (powders, porous blocks, or beads) to fill bone defects or voids when large sections of bone have had to be removed (e.g. bone cancer) or when bone augmentations are required (e.g. maxillofacial reconstructions or dental application). It is known that HA is able to directly bond to bones and teeth *in vivo*. In Indonesia, since 2014, dentist and oral and maxillofacial surgeons have been applying carbonate apatite composite, named Gama-CHA, as depicted in Fig. 16.1 and Fig. 16.2. The modified formula is also used to develop bioceramics-based haemostatic sponge wherein a small amount of calcium ions from carbonate apatite will function as better haemostatic agent. The reason for using grafting materials in oral treatment is that the materials can facilitate formation of an alveolar bone regeneration, periodontal ligament and root cementum through the specific mechanisms, those are osteogenesis, osteoconduction and osteoinduction, and the findings have been performed in some studies.

Meanwhile, the use of corals from Goniopora, Porites, Favites, etc. has been long investigated. The coral specimens consist of 99% calcium carbonate in the form of aragonite and 1% of organic material. In the body fluid, coral can be transformed in apatite. Combes and co-workers [9]



**Fig. 16.1** The first Indonesian bone graft, carbonate apatite based bone graft



**Fig. 16.2** Porosity of carbonate apatite ceramics as bone substitute

incorporated into the apatite structure of the surrounding bone tissue. The released calcium ions inhibit the activity of osteoclasts and shift the bone balance toward formation [26]. Meanwhile, the carbonate ions released from  $\text{CaCO}_3$  can substitute phosphates and or hydroxide ions in the structure of bone apatite.

In case of calcium sulfate (CS), also known as Plaster of Paris (POP), it has been used in clinic for many years to treat skeletal defects, either alone or in combination with other bone graft materials [22, 24, 31, 34]. It is safe, rapidly resorbing material that has been used for bone filling applications for more than 100 years. The use of POP is based on its advantages, which include the ability to self-setting and a well-toler-

ated biological response without eliciting a severe inflammatory response. When hemihydrate is mixed with water, dihydrate is formed. This property makes it possible for POP to set in situ when it is applied into a bone defect.

The use of bioactive glass in clinics is based on the process that the surface of the glass will be dissolved and release mineral ions. This leads to the formation of a biologically active, carbonated apatite layer that provides the bonding interface with tissues, as described previously. This adherent interface with tissues resist substantial mechanical forces. In many cases, the interfacial strength of adhesion is equivalent to or greater than the cohesive strength of the implant material or the tissue bonded to the bioactive implant. The clinical applications of bioactive glass require several different forms of material. The use of Bioglass®45S5 implants in the middle of ear surgery to replace ossicles damaged by chronic infection is also successful, and the results are encouraging. Bioglass®45S5 implants have also been used successfully to maintain a nearly 90% retention rate of alveolar ridge for denture wearers [21].

Nowadays there are a lot of efforts have been being done to translate the use of bioceramics as periodontal strip and drug delivery [3], for nerve regeneration scaffold [35], injectable gel to prevent relapse after orthodontics treatment [1, 2], including scaffold for stem cell delivery by using synthetic coral [28, 29].

## 16.4 Future Perspective

It has been a critical issue and a key challenge in the regenerative area on how to ideally replace lost tissue. The conductive strategy will interfere the regenerative process, while enabling the desired host cells to populate the regeneration site. Bioceramics is also recognized to provide local environment for cells to promote proliferation and differentiation and function as instructive extracellular microenvironments for morphogenesis. Thus, bioactivity of ceramics is considered very promising strategy in rehabilitative area. Hydroxyapatite, carbonate apatite,

some calcium orthophosphates including biphasic calcium phosphate, and bioactive glasses are example of products which have been already in clinical applications.

The future challenges of bioceramics are related to acidic condition caused by infections which have been problems in regenerative procedures. Hospital-acquired bone infection, including in the maxillofacial area (even more specifically in tropical settings with high temperature/humidity), will be a costly and critical health issue, and the great difficulty to eradicate. Thus, it is as an absolute necessity and has led clinicians to consider the prevention of infection. Calcium phosphate apatites are best candidates for preparing biomaterials for bone repair. However, calcium phosphate compounds could act as propitious substrates for microbial proliferation. Since the use of antibiotics is often problematic (bacterial resistance), other strategies have to be found, compared and developed. In view of this, the development of bioceramics such with inner antimicrobial properties is considered very strategic and important to overcome the problems in the near future.

## References

- Alhasyimi AA, Pudyani PS, Asmara W, Ana ID (2017) Locally inhibition of orthodontic relapse by injection of carbonated hydroxy apatite-advanced platelet rich fibrin in a rabbit model. *KEM* 758:255–263
- Alhasyimi AA, Pudyani PS, Asmara W, ID A (2018) Enhancement of post-orthodontic tooth stability by carbonated hydroxyapatite-incorporated advanced-platelet rich fibrin in rabbits. *Orthod Craniofac Res* 21:112–118
- Ardhani R, Hafiyah OA, Setyaningsih, Ana ID (2016) Preparation of carbonate apatite membrane as metronidazole delivery for periodontal application. *KEM* 696:250–258
- Ben-Nissan B (2003) Natural bioceramics: from coral to bone and beyond. *Curr Opin Solid State Mater Sci* 7:283–288
- Braig AA, Fox J, Su Z, Wang M, Otsuka W, Higuchi I, Legeros RZ (1996) Effect of carbonate content and crystallinity on the metastable equilibrium solubility behavior of carbonate apatite. *J Colloid Interface Sci* 179:608–617
- Carson JS, Bostrom MPG (2007) Synthetic bone scaffolds and fracture repair. *Inj Int J Care Injured* 3851:533–537
- Chun Wu Y, Min Lee T, Hsun Chiu K, Yu Shaw S, Yu Yang C (2009) A comparative study of the physical and mechanical properties of three natural corals based on the criteria for bone-tissue engineering scaffolds. *J Mater Sci Mater Med* 20:1273–1280
- Cirotteau Y (2001) Behavior of natural coral in a human osteoporotic bone. *Eur J Orthop Surg Traumatol* 11:149–160
- Combes C, Miao B, Bareille R, Rey C (2006) Preparation, physical-chemical characterization and cytocompatibility of calcium carbonate cements. *Biomaterials* 27:1945–1954
- Dewi AH, Ana ID, Wolke JGC, Jansen JA (2013) Behavior of plaster of Paris-calcium carbonate composite as bone substitute. A study in rats. *J Biomed Mater Res A* 101(8):2143–2150
- Dewi AH, Ana ID, Wolke JGC, Jansen JA (2015) Behavior of POP-calcium carbonate hydrogel as bone substitute with controlled release capability: a study in rat. *J Biomed Mater Res A* 103:3273–3283
- Dewi AH, Ana ID, Jansen JA (2016) Calcium carbonate hydrogel construct with cinnamaldehyde incorporated to control inflammation during surgical procedure. *J Biomed Mater Res Part A* 104:768–774
- Dewi AH, Ana ID, Jansen JA (2017) Preparation of a calcium carbonate-based bone substitute with cinnamaldehyde crosslinking agent with potential anti-inflammatory properties. *J Biomed Mater Res A* 105(4):1055–1062
- Ducheyne P (1987) Bioceramics: material characteristics versus in vivo behavior. *J Biomed Mater Res B* 21:219–236
- Dorozhkin SV (2011) Calcium orthophosphates: occurrence, properties, biomineralization, pathological calcification and biomimetic applications. *Biomater* 1:121–164 Taylor and Francis
- El-ghannam A, Ducheyne P, Saphiro IM (1997) Formation of surface reaction products of bioactive glass and their effects on the expression of the osteoblastic phenotype and the deposition of mineralized extracellular matrix. *Biomaterials* 18:295–303
- Frank RM, Klewansky P, Hemmerle J, Tenenbaum H (1991) Ultrastructure demonstration of the importance of crystal size of bioceramic powders implanted into human periodontal lesions. *J Clin Periodontol* 18:669–680
- Frayssinet P, Rouquet N, Fages J, Durant M, Vidalain PO, Bonel G (1997) The influence of sintering temperature on the proliferation of fibroblastic cells in contact with HA bioceramics. *J Biomed Mater Res* 35:337–347
- Gauthier O, Muller R, Von Stechow D, Lamy B, Weiss P, Boulter JM, Aguado E, Daculsi G (2005) In vivo bone regeneration with injectable calcium phosphate biomaterial: a three-dimensional micro-computed tomographic, biomechanical and SEM study. *Biomaterials* 26(27):5444–5453

20. Hench LL et al (1971) Bonding mechanisms at the interface of ceramic prosthetic materials. *J Biomed Mater Res A* 5(6):117–141
21. Hench LL, Wilson J (1993) An introduction to bioceramics. *Advanced series in ceramics*, vol 1, pp 1–24
22. Iezzi G, Fiera E, Scarano A, Pecora G, Piatelli A (2007) Histologic evaluation of provisional implant retrieved from man 7 months after placement in a sinus augmented with calcium sulfate: a case report. *J Oral Implantol* 33(2):89–95
23. Ishikawa K (2015) Carbonate apatite bone replacement. In: Antoniac I (ed) *Handbook of bioceramics and biocomposites*. Springer, Cham
24. Jamali A, Hilpert A, Debes J, Afshar P, Rahban S, Holmes R (2002) Hydroxyapatite/calcium carbonate (HA/CC) vs. Plaster of Paris: a histomorphometric and radiographic study in a rabbit tibial defect model. *Calcif Tissue Int* 1:172–178
25. Jones JR (2008) Bioactive glass. In: Kokubo T (ed) *Bioceramics and their clinical applications*. Woodhead Publishing, Cambridge
26. Kameda T, Mano H, Yamada Y, Takai H, Amizuka N, Kobori M, Izumi N, Kawashima H, Ozawa H, Ikeda K, Kameda A, Hakeda Y, Kumegawa M (1998) Calcium-sensing receptor in mature osteoclasts, which are bone-resorbing cells. *Biochem Biophys Res Commun* 245:419–422
27. Leeuwenburgh SCG, Ana ID, Jansen JA (2010) Sodium citrate as an effective dispersant for the synthesis of inorganic-organic composites with a nano-dispersed mineral phase. *Acta Biomater* 6(3):836–844
28. Mahanani ES, Bachtiar I, Ana ID (2016a) Human mesenchymal stem cells behavior on synthetic coral scaffold. *KEM* 696:205–211
29. Mahanani ES, Herningtyas EH, Bachtiar I, ID A (2016b) Degradation profile and fibroblast proliferation on synthetic coral scaffold for bone regeneration. *AIP Conf Proc* 1755:160007
30. Matsuya S, Lin X, Udoh K, Nakagawa M, Shimogoroy R, Terada Y, Ishikawa K (2007) Fabrication of porous low crystalline calcite block by carbonation of calcium hydroxide compact. *J Mater Sci Mater Med* 18:1361–1367
31. Mazor Z, Mamidwar S, Ricci JL, Tovar NM (2011) Bone repair in periodontal defect using a composite of allograft and calcium sulfate (dentogen) and a calciumsulfate barrier. *J Oral Implantol* 37:287–292
32. Landi E, Tampieri A, Belmonte MM, Celotti G, Sandri M, Gigante A, Grazie PF, Biagini I (2006) Biomimetic Mg- and Mg<sub>2</sub>CO<sub>3</sub>-substituted hydroxyapatites: synthesis characterization and in vitro behavior. *J Eur Ceram Soc* 26(13):2593–2601
33. Oonishi H, Hench LL, Wilson J, Sugihara F, Tsuji E, Kushitani S, Iwaki H (1999) Comparative bone growth behavior in granules of bioceramic materials of various sizes. *J Biomed Mater Res* 44:31–43
34. Orsini G, Ricci J, Scarano A, Pecora G, Petrone G, Iezzi G, Piatelli A (2004) Bone-defect healing with calcium-sulfate particles and cement: an experimental study in rabbit. *Int J Oral Maxillofac Implant* 24:901–909
35. Patriati A, Ardhani R, Pranowo HD, ID A (2016) Effect of freeze-thaw treatment to the properties of gelatincarbonated hydroxy apatite membrane for nerve regeneration scaffold. *KEM* 696:129–144
36. Redey SA, Nardin M, Assolant DB, Rey C, Dellanoy P, Sedel L, Marie PJ (2000) Behavior of human osteoblastic cells on stoichiometric hydroxyapatite and type-a carbonated apatite. *J Biomed Mater Res* 50(3):353–364
37. Suchanek W, Shuk P, Byrappa K, Riman RE, Tenhuisen KS, Janas VF (2002) Mechanochemical-hydrothermal synthesis of carbonated apatite powders at room temperature. *Biomaterials* 23:669–710
38. Supova M (2009) Problem of hydroxyapatite dispersion in polymer matrices: a review. *J Mater Sci Mater Med* 20:1201–1213
39. Tanaka Y, Yamashita K (2008) Fabrication processes of bioceramics. In: Kokubo T (ed) *Bioceramics and their clinical applications*. Woodhead Publishing, Cambridge
40. Thomas MV, Puleo DA (2008) Calcium sulfate: properties and clinical application. *J Biomed Mater Res B* 88:597
41. Tsuru K, Ruslin R, Maruta M, Matsuya S, Ishikawa K (2015) Effects of the method of apatite seed crystals addition on setting reaction of  $\beta$ -tricalcium phosphate based apatite cement. *J Mater Sci Mater Med* 26(10):244–249
42. Wang C, Duan W, Markovic B, Barbara J, Howlett CR, Zhang X, Zreiqat H (2004) Proliferation and bonerelated gene expression of osteoblasts grown on hydroxyapatite ceramics sintered at different temperature. *Biomaterials* 25:2949–2956



# Stem Cell and Advanced Nano Bioceramic Interactions

# 17

Sevil Köse, Berna Kankilic, Merve Gizer,  
Eda Ciftci Dede, Erdal Bayramli, Petek Korkusuz,  
and Feza Korkusuz

## Abstract

Bioceramics are type of biomaterials generally used for orthopaedic applications due to their similar structure with bone. Especially regarding to their osteoinductivity and osteoconductivity, they are used as biodegradable scaffolds for bone regeneration along with mesenchymal stem cells. Since chemical properties of bioceramics are important for regeneration of tissue, physical properties are also important for cell proliferation. In this respect, several different manufacturing methods are used for manufacturing nano scale

bioceramics. These nano scale bioceramics are used for regeneration of bone and cartilage both alone or with other types of biomaterials. They can also act as carrier for the delivery of drugs in musculoskeletal infections without causing any systemic toxicity.

## Keywords

Mesenchymal stem cells · bioceramics · hydroxyapatite · tricalcium phosphate · biphasic calcium phosphate · nanotechnology · osteogenic differentiation · regeneration · osteomyelitis

S. Köse (✉)

Faculty of Health Sciences, Department of Nutrition and Dietetics, Atilim University, Ankara, Turkey

B. Kankilic

Head of Certification, Directorate of Directives, Turkish Standards Institution, Ankara, Turkey

M. Gizer · E. Ciftci Dede

Department of Bioengineering, Hacettepe University, Ankara, Turkey

E. Bayramli

Department of Chemistry, Middle East Technical University, Ankara, Turkey  
e-mail: bayramli@metu.edu.tr

P. Korkusuz

Department of Histology and Embryology, Faculty of Medicine, Hacettepe University, Ankara, Turkey  
e-mail: petek@hacettepe.edu.tr

F. Korkusuz

Department of Sports Medicine, Faculty of Medicine, Hacettepe University, Ankara, Turkey

## 17.1 Introduction

Bioceramics are frequently used to replace or regenerate bone tissue in medicine. They are also used to coat biomedical implants for better osteo-integration [7, 8] and they are an integral part of bone and joint tissue engineering [59]. Calcium sulfate, calcium phosphate, hydroxyapatite (HA) and bio-glasses are the most common synthetic forms of bioceramics [56]. Nano forms of HA in powder, particle, fiber, tube and film increase surface area and may improve biocompatibility [60]. Such bioceramics can be named as advanced biomedical materials and they are considered as medical devices. Nano-bioceramics are practically lighter and stronger than micro forms. They

can also be used for drug and gene delivery. Faster and better tissue regeneration by nano-HA may improve recovery and improve quality of life of patients. Nano-bioceramics are natural components of the bone structure. From the material perspective, bone is a composite consisting of nano-HA rods embedded into a type 1-collagen matrix [58]. Nano-HA can also be used to print bioceramic medical materials, which may decrease the need of autografts and replace allografts [58]. Combining mesenchymal stem cells (MSC) with nano-HA is a new area for research and questions need to be answered on MSC-nano-HA interactions. In this chapter, we focused on MSCs, advanced nano-bioceramics and their potential use on control and treatment of bone infections.

---

## 17.2 Stem Cells for the Regeneration of the Musculoskeletal System

Bone regeneration or repair using advanced metal, polymer or ceramic materials is very common in orthopedic and trauma, maxillofacial and neurosurgery. Current treatment options such as bone grafts and protein-based therapies do not provide satisfactory solutions for large bone defects specifically after infection and tumor cases [2]. Stem cell-based therapies for the repair of massive bone loss or non-unions have emerged as an alternative to existing solutions in recent years. Mesenchymal stem cells (MSC) alone or in combination with advanced nano-bioceramics from various sources are recently studied as treatment options. Tissue-specific adult MSCs are also used in complex injuries such as loss of an extremity for musculoskeletal tissue regeneration [60].

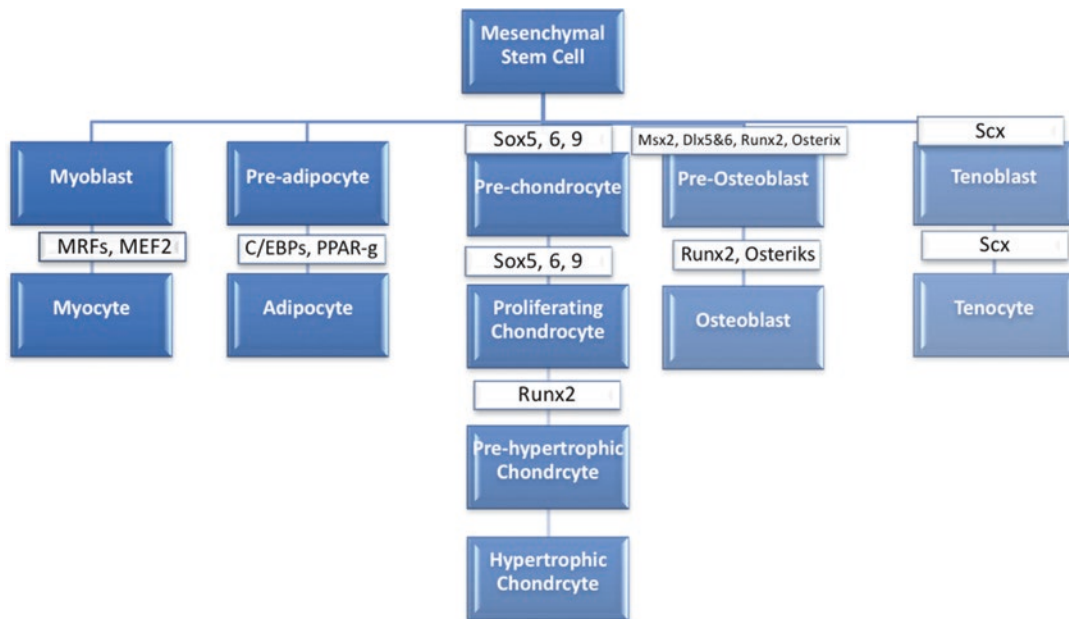
Mesenchymal stem cells migrate to damaged areas, to support and enhance angiogenesis, while preventing fibrosis. They have anti-inflammatory properties and contain regenerative cytokines. They secrete chemokines and may differentiate into connective tissue cells including bone, joint cartilage, ligament, tendon and skeletal muscle cells, which makes them inevitable for

tissue regeneration (Fig. 17.1). These MSCs, which are also known as multipotent cells, can be isolated from many locations, such as bone marrow, adipose and muscle tissue, periosteum, umbilical cord and placenta. They need to be identified and replicated *in vitro* due to their low number and sparse distribution in tissues. They may be used directly or in differentiated forms. In some cases, mesenchymal stem cells can be injected or applied to the injury site directly while they can also be introduced through the circulatory system. In the latter case, most of the MSCs are destroyed in the lungs; therefore, new technology focuses on directing them to the regeneration site [124]. These cells can be combined with natural and synthetic tissue scaffolds with or without any signaling molecules that affect the biological properties of the carrier system in the form of combination therapy. Bone and cartilage regeneration can further be enhanced by efficient transcription of genes *in vivo* by engineering practice to ensure rapid tissue regeneration if possible. Thus, obtained MSCs with autocrine and paracrine effects on damaged host cells may aid multidimensional regeneration. Developing tissue-engineering applications enhanced MSC therapy recently. Mesenchymal stem cells combined with nano-HA especially to keep the administered cells in the damaged area and prevent inflammation and scar tissue formation.

### 17.2.1 What Are Mesenchymal Stem Cells?

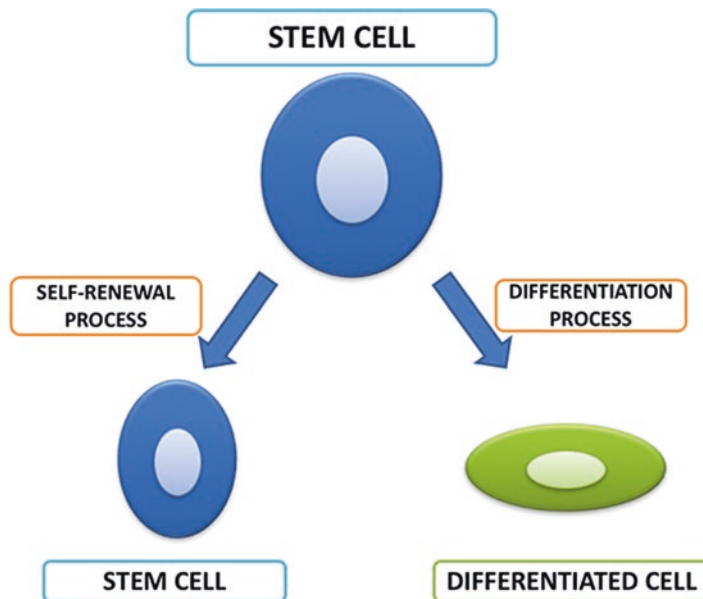
Mesenchymal stem cells both renew themselves and they are capable of differentiate into specific cells (Fig. 17.2). They have typical capacities according to the tissue they are harvesting from and their potential. Totipotent stem cells can differentiate into embryonic and non-embryonic cells (16 cell embryo), pluripotent stem cells, can differentiate into all cell types found in tissues belonging to the three germ layers (e.g. inner cell mass derived from embryonic stem cells); multipotent stem cells, can differentiate into all cell types which belongs to the origin of their germ (e.g. MSCs can differ mesoderm-derived cells





**Fig. 17.1** Proliferation profile of mesenchymal stem cell

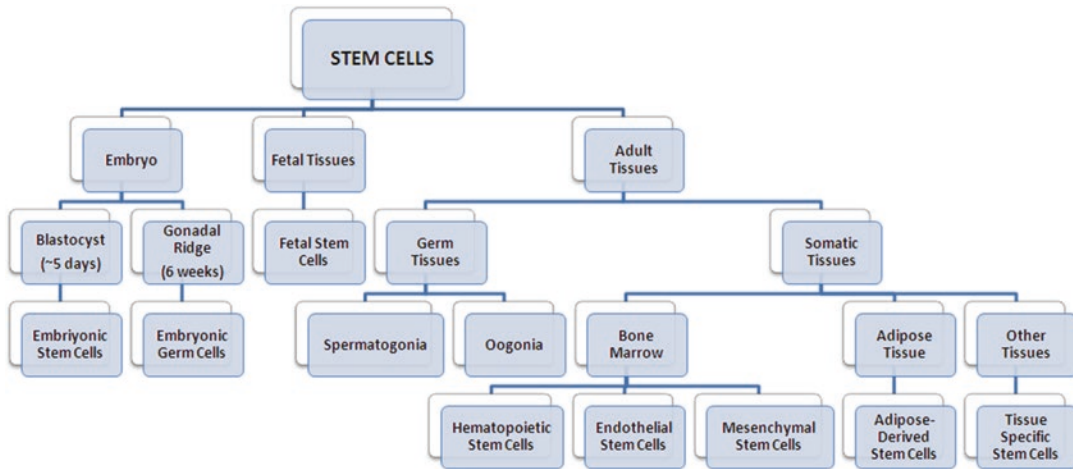
**Fig. 17.2** Signature characteristics of the stem cell



(bone, cartilage, fat)); unipotent (nullipotent) stem cells; can form only a single cell type (eg. Oogonia is generated oocyte cells). (Fig. 17.3).

Another feature of MSCs, which remains as a silent feature (quiescence); they prevent the depletion of adult stem cells in tissues. In case of damage, stem cells in their quiet state are acti-

vated through symmetric or asymmetric division and differentiated into tissue specific cells and regeneration is achieved. Isolated and cultured stem cells have the tendency to create clones (clonogenicity). A single cell clone that includes undifferentiated stem cells has self-renewal property. Mesenchymal stem cells migrate to the



**Fig. 17.3** Stem cells according to their sources

injury site to regenerate the tissue. The microenvironment that MSCs migrate determines the self-renewal and differentiation features [119].

### Stem Cells According to Their Sources and Potentials

**Embryonic stem cells (ESCs);** each cell on day 5 blastocysts (inner cell mass) formed after formation of the zygote is called ESCs. These cells are pluripotent and differentiate into all cells of the body, also they provide advantage with their ability to expand and differentiate *in vitro* and can do genetic modifications. In clinical use however; ESCs are not appropriate as they contain high risk of developing cancer even after differentiation. The use of human ESCs furthermore has ethical and legal problems [108]. Tumor forming risk and immunological responses makes ESCs unavailable to use in humans.

**Fetal Stem Cells** are obtained from 5 to 9 weeks of abortion. These cells are pluripotent/multipotent and have self-renewal features. They are alternatives to ESCs, however their clinical use is again limited due to the risk of tumor formation. Fetal stem cells also have ethical problems [82].

### Induced Pluripotent Stem Cells-iPSc

These cells, which have lost their pluripotency ability gain pluripotency characteristic after various methods/factors. Shinya Yamanaka of Kyoto

University has introduced the term iPSc to the literature in 2006. Yamanaka and his co-workers obtained ESCs like cells with retroviral transfection of 4 pluripotency stimulating genes (Oct4, Sox2, KLF-4, c-Myc) from skin fibroblast cells. Yamanaka and John Gurdon who laid the foundation of cloning, have shown terminally differentiated cells can gain pluripotency and have been awarded with the Nobel Prize for Medicine in 2012 [105].

In the following years, studies with iPSc gained popularity. Improvements such as increasing efficiency of forming cells, using tissue-specific multipotent stem cells rather than terminally differentiated cells, using more convenient method for the clinic use instead of viral transfer, are aimed to increase the chances of clinical use of these cells. The biggest advantages of these cells are; the use of cells obtained from the patient with the lack of immunological incompatibility problems, genetic corrections derived from pluripotent stem cells can be performed and can be differentiated into desired cells. Although it has many advantages compared to embryonic cells, there are important issues before they can be clinically applied. First, iPSc efficiency should be increased using non-viral methods. In addition, these methods must not create any susceptibility to tumor formation. Xenogenic factors should not be used to avoid immunological reactions [122].

iPSc used in maxillofacial surgery, plastic and reconstructive surgery and orthopedic surgery and traumatology generally differentiate into bone and cartilage cells. For this purpose, iPSc are expanded on tissue scaffolds and differentiated into osteogenic/chondrogenic cells. Prefabricated cell containing tissue scaffolds are injected to immune suppressed mice and then bone/cartilage tissue formation is monitored. In addition to direct differentiation, iPSc can be differentiate into MSCs before bone and cartilage cell differentiation. Thus, it is argued that a more controlled protocol should be followed [17].

### Adult Stem Cells (ASCs)

MSCs, especially those of the bone, cartilage, fat, tendon and stroma, differentiate into many different tissue cells (heart, liver, pancreas, nervous system cells) using soluble factors that contribute to tissue and organ regeneration. MSCs are expanded in vitro by protecting its stem cell properties, support hematopoiesis, and when they are transplanted they are not rejected by immunosuppressive properties. Thus, these cells have potential applications in many clinical areas [10].

MSCs are main cells of the connective tissue. They were identified by the first time in 1976. Friedenstein showed cell colonies, which are adhesive and morphologically resembling fibroblasts in bone marrow culture by using fetal calf serum. Also, their differentiation into bone, fat and cartilage cells was demonstrated. Previously, these cells called CFU-F (Colony forming unit-fibroblast) and 'bone marrow stromal fibroblasts', but then they were called as mesenchymal stem/stromal cells [40].

Bone marrow is one of the richest sources of MSCs that host hematopoietic endothelial and mesenchymal stem/progenitor cells originating from the mesoderm [4]. MSCs can be also isolated from other tissues than bone marrow. Mechanical and enzymatic methods are used for the isolation of MSCs in solid tissues. MSCs can be isolated and expanded from bone/periosteum, muscle tissue, dental pulp and maxillofacial tissues, liver, lipoaspiration materials, umbilical cord blood, cord stroma, placenta, amniotic fluid,

synovial fluid, and even stimulation through the peripheral blood. They have many properties like adherence to plastic tissue culture dishes, showing fibroblastoid morphology, differentiation and surface markers and these features are independent from their harvesting tissues. These properties are substantially similar; but the differentiation capacity and functional characteristics may show some changes according to origin of tissue type [86].

In cultures initiated with heterogeneous cell population, MSCs distinguish from other cells with their cell surface molecules, which are different from of hematopoietic stem cells (HSC) and/or tissue specific antigens. In contrast, involved in adhesion, cell-cell, cell-extracellular matrix interactions and stroma-specific antigens are known to be expressed high. However, defining a specific antigen has not been described for MSCs [32]. MSCs which is found in various tissues as support cells, are synthesized a large number of bioactive molecules, cytokines, chemokines, enzymes and the extracellular matrix proteins in relation to these features. MSCs release some growth factors required for hematopoietic cells in bone marrow such as macrophage colony stimulating factor (M-CSF), Flt-ligand, and stem cell factor (stem cell factor/SCF). Furthermore, as well as interleukin-6 (IL-6), IL-7, IL-8, IL-11, IL-12, IL-14, IL-15 cytokines, MSCs are synthesized chemokines including SDF1-alpha (Stromal Derived Factor-1alpha/CXCL12), monocyte chemo attractant protein (monocyte chemo attractant protein-1/MCP-1) [39]. Transplanted MSCs into the injured area of the spinal cord appeared to reduce apoptosis in neuronal cells [45]. In other studies, neurotrophins like BDNF (Brain-derived neurotrophic factor) and NGF- $\beta$  (Nerve growth factor- $\beta$ ) released by the MSCs increases the life of the neuronal cells [5, 25, 63]. Also in vitro co-culture obtained from 25 different bone marrow MSCs and neuronal stem cells obtained from the cerebral cortex of mice showed increased survival and migration properties for neuronal cells [6].

MSCs in vivo are anti-inflammatory and non-immunogenic. They also prevent alloreactive T cell activation and further reactions, inhibit acti-

vated B-lymphocytes and stimulate regulatory T cells. Thus, immunosuppressive effect was through inhibiting lymphocyte proliferation in animals and humans. Besides, a dose-dependent stimulating effect probability is shown on the immune system in some circumstances [80]. As well as the immunomodulatory effect of MSCs, anti-apoptotic factors, angiogenic and antifibrotic properties are also available. These features are explained through their role in wound healing. Mesenchymal stem cells are antifibrotic when they are used after spinal cord injury and they prevent scar tissue formation that may prevent axon regeneration inhibition [51].

### Differentiation Potential of MSCs

The most interesting feature of MSCs, especially for applications in regenerative medicine, is their potential to differentiate into a variety of cell types in appropriate microenvironments including connective tissue. Several researchers stimulated osteogenic, adipogenic, chondrogenic, and myogenic *in vitro* differentiation with appropriate signals and generated hematopoietic stroma formation. Mesenchymal stem cells also present plasticity. They may differentiate to other essential cells in the regeneration area [86]. Myoblast [12], hepatic [75], cardiac [49], renal [3] and neural cell [101] differentiation of bone marrow derived MSCs were published.

MSCs migrate to sites of inflammation and differentiated to requested cells during wound healing. The same property is realized for transplanted MSCs in the damaged area. Rat bone marrow stromal cells transplanted to spinal cord injury differentiated to neurons [26] and astrocytes [128] and functional improvement was documented based on BBB behavioral ratings scoring (Basso, Beattie, Bresnahan Locomotor rating scale) [48, 61, 97].

### Contribution of MSCs to Repair Damaged Tissue

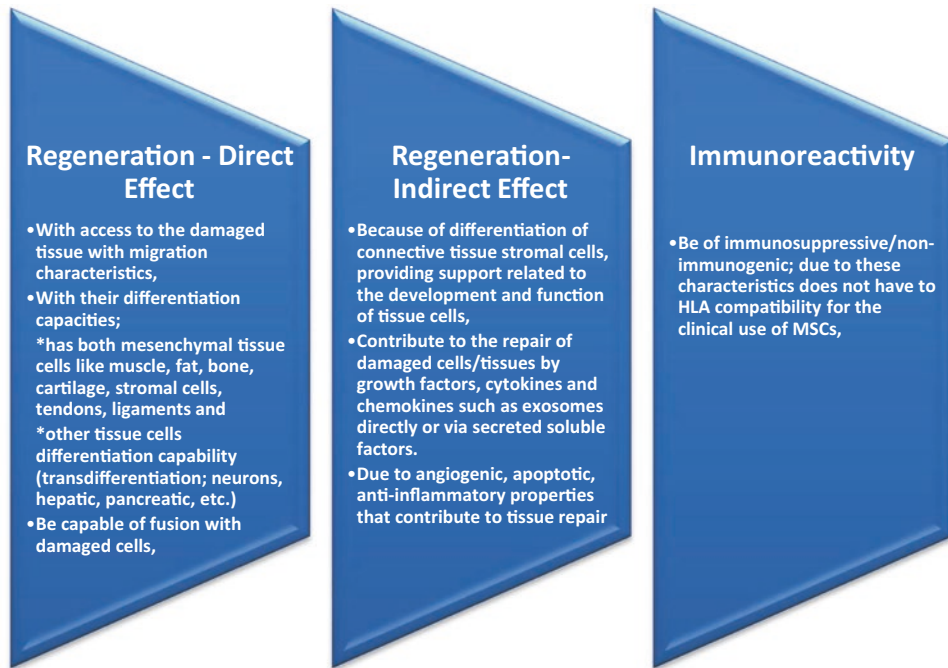
As effective mechanisms of MSCs in damaged tissue repair; differentiation to mature functional cells, cell function recovering after damaged cell-MSC fusion, cell-cell and cell-extracellular matrix relationship with MSCs, releasing of the soluble factors (growth factors, cytokines, che-

mokines, etc.), paracrine factors, enzyme or immunomodulatory, anti-inflammatory, anti-apoptotic, and angiogenic effects can be considered. The most important mechanisms are thought as soluble factors releasing and cell-matrix adhesive relationship [102].

Migration is required for the movement of MSCs from their niche into the damaged tissues. Signal for migration of cells has been shown to come from the damaged tissue microenvironments. Soluble factors like SDF-1 (Stromal Derived Factor-1/CXCL12), MCP-1 (Macrophage Chemoattractant Protein-1) and complement C3 fraction released in the damaged area have important roles in migration [120]. Advantages of MSCs in clinical practice are as follows (Fig. 17.4).

Musculoskeletal diseases (MSDs) are a group of disorders that result from trauma or degeneration in either a single event or repetitive episodes. With the potential to differentiate along mesenchymal lineages, MSCs have been widely used in cell-based therapy for the treatment of MSDs. Lot of studies using MSCs for cell-based therapy in MSDs have shown promising results [33, 37, 41].

Many studies have also investigated the usage of *ex vivo* expanded MSCs in bone regeneration. Three patients with segmental bone defects were successfully treated with autologous MSCs delivered in hydroxyapatite scaffolds [90]. There are several investigations that integrated MSCs into biomaterials like hydroxyapatite and calcium phosphate and showed promising features, including their ease of availabilities, osteoconductivities, and absence of immune responses [11, 95, 114]. A clinical study also reported that full-thickness articular cartilage defects in the patella-femoral joint transplanted with collagen gels containing autologous MSC showed significant and lasting restoration of cartilage after follow-ups at 17 and 27 months [116]. When comparing autologous MSC transplantation with autologous chondrocyte implantation (ACI) for cartilage repair, the MSC transplantation was shown to be more economical, minimize donor-site morbidity, require less surgery, and still as effective as its ACI counterpart in a 2-years follow-up [81].



**Fig. 17.4** Advantages in terms of clinical use of MSCs

Treatment of osteoarthritis (OA) is much more difficult, since the defect is larger and is characterized by an inflammation environment. MSCs embedded in collagen gels have been transplanted to treat patients with knee OA who underwent a high tibial osteotomy, and the effects were compared with the patients who underwent only osteotomy. Although the clinical improvement in each group was not significantly different, the cell-transplanted group achieved better arthroscopic and histological results than the cell-free control group [115]. Another clinical trial involved patients of OA who received intra-articular injections of culture-expanded, bone marrow-derived MSCs, and 63.2% of patients showed improvement at an average follow-up of 11.3 months [24].

For degenerative lumbar conditions, MSCs have been applied for spinal fusion as a component of Osteocel Plus, an alternative allograft cellular bone matrix, to treat patients who underwent a minimally invasive transforaminal lumbar interbody fusion [1]. MSCs with  $\beta$ -tricalcium phosphate ( $\beta$ -TCP) utilized for lumbar spinal fusion

resulted in a successful fusion rate of 93.3%, by autologous iliac crest bone grafts [123].

Consequently, the studies currently available suggest that expanded MSCs have multiple therapeutic effects on MSDs. Based on these significant benefits; MSCs or accumulating MSC-related osteo-biologic products are in development. However, there is still a lack of a gold standard procedure to expand MSCs. Recently, improvement of culture conditions like using a hypoxic culture has been shown to enhance short-term proliferation, long-term expansion efficiency, differentiation potential, stemness, expression of chemokine receptors, migration and engraftment ability.

### 17.3 Advanced Nanobioceramics

Ceramics are nonmetallic inorganic solid materials composed of calcium, silica, phosphorous, sodium, magnesium and potassium, which are found in amorphous (non-crystalline) and crystalline forms [46, 53, 57]. Their presence in amorphous or crystalline form depends on the

arrangement of the ionic bonds [106]. Degradation of ceramics is more durable and harder than most metals generally, but they are also more fragile. Since they have similar chemical properties to the natural structure of bone, they can be used in orthopedic and dental implant applications [106]. Although autologous bone or autografts are still an effective treatment for bone regeneration, the morbidity in the donor zone limits the effectiveness of this procedure. While beneficial results such as osteoconduction, osteoinduction and non-emergent immuno-response from graft applications can be obtained through bioceramics [66]; the problem of the morbidity of the donor region can also be avoided.

Biomaterials have followed an evolutionary process in the direction of usage capacities; first-generation biomaterials have a feature that would only replace the damaged area, but second-generation biomaterials repair the damaged tissue zone. Bioceramics, which are third-generation biomaterials, are used for tissue regeneration due to their surface properties and carrier features [112]. For the purpose of their use, bioceramics are divided into three main classes (Table 17.1); non-resorbable (inert), bioactive or surface-active (semi-inert) and biodegradable (non-inert) [36, 57].

Regeneration of the replacement tissue also is affected by the size and chemical properties of bioceramics. If the cell size in the replacement

tissue zone is between 10  $\mu\text{m}$  and 100  $\mu\text{m}$ , adaptation to the host site makes it important that the bioceramics are in micro dimension while; the presence of protein and molecule sizes in the range of 1 nm to 10 nm induces cytokines that activate cellular pathways required for tissue regeneration nano-size stands out in bioceramics [55, 112].

Because of their similar mineral content and natural biocompatibility; hydroxyapatite (HA), tricalcium phosphate (TCP) and glass ceramics are the most widely used bioceramics [55].

### 17.3.1 Nano-hydroxyapatite Bioceramics

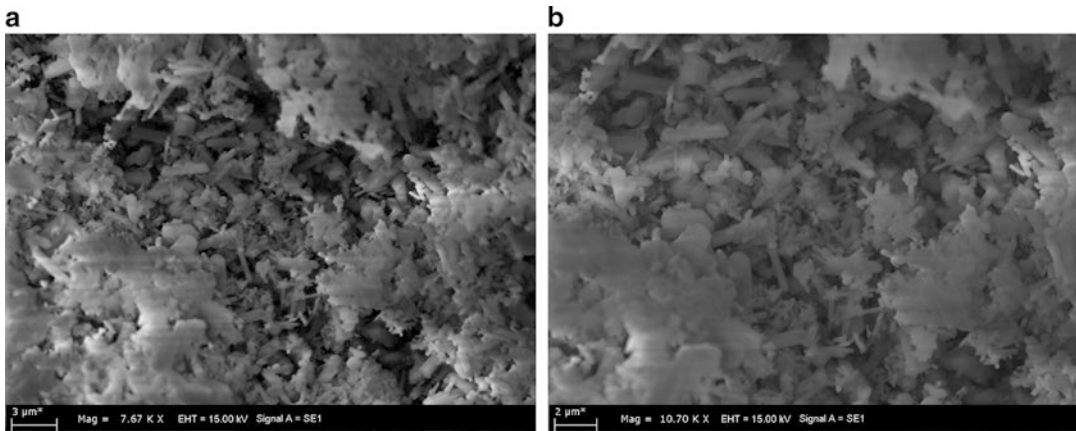
Nano-hydroxyapatite (nHA) is the main inorganic component of bone with  $\text{Ca}_{10}(\text{PO}_4)_6(\text{OH})_2$  molecular formula. It is one of the widely used bioceramics because of its biocompatibility and osteoinduction in bone treatment applications [55, 112, 113].

nHA production is carried out in four different ways; wet chemical synthesis, dry chemical synthesis, high temperature reactions, and biological sources. With these production methods, nHA can be produced from 3 nm to 2000  $\mu\text{m}$  (Fig. 17.5). Wet chemical synthesis is widely used as it is the simplest and most effective method and also final product's Ca:P ratio is approximately 1.67 [36, 76, 112].

In a study poly-(lactic-co-glycolic acid) (PLGA)-collagen bioactive scaffolds containing nHA were investigated for proliferation and bone regeneration in human MSCs, and found that proliferation in nHA-containing scaffolds decreased when compared to other scaffolds but significant increase in alkaline phosphatase (ALP) activation was observed as a sign of osteoblastic differentiation [15]. In another study where scaffolds produced by freeze-drying method containing zein (ZN), chitosan (CS) and nHA at different weight ratios were used with human osteosarcoma cell line MG-63 cells for bone regeneration and the fabricated biomaterial was characterized by X-ray Diffraction (XRD), Fourier Transform Infrared Spectroscopy (FTIR)

**Table 17.1** Bioceramic classes

Bioceramics		
Biodegradable (non-inert)	Bioactive (semi-inert)	Nonresorbable (inert)
Calcium phosphates	Hydroxyapatites	Alumina
Tricalcium phosphates	Silica calcium phosphates	Zirconia
Aluminum calcium phosphates	A/W glass-ceramics	Carbon
Coralline	Oxide- and hydroxide- based bioactive ceramics vd.	Silicone nitride
Zinc calcium phosphorous oxides vd.		Calcium aluminate vd.



**Fig. 17.5** SEM images for nHA at different temperatures (a) 300 °C, (b) 1000 °C

and scanning electron microscope (SEM) methods. Comparisons of the mechanical properties after the characterization studies showed that scaffolds containing nHA at the highest weight ratio were more stable. When scaffolds were examined for cell attachment, biomineralization and cytotoxicity, MTT (3-(4,5 dimethylthiazol-2-yl)-2,5-diphenyltetrazolium bromide) analysis showed that the proliferation of cells decreased as nHA ratio increases. Scaffolds containing nHA at the highest level appear to increase biomineralization [100]. In another study, nHAs were obtained by wet chemistry method at 800 °C, 900 °C and 1000 °C temperatures and after their structural properties was confirmed by XRD and transmission electron microscopy (TEM) analysis; these nHAs were evaluated for their cytotoxic effects on murine fibroblast cell line L929 with MTT test and none of the groups showed any cytotoxic effect [104]. In Dan et al.'s study, nHA was added to improve the physico-chemical and biological properties of the chitosan-gelatin scaffolds and the properties of these scaffolds in bone tissue engineering were examined. According to the results, nHA containing scaffolds showed higher cell viability and cell proliferation than blank scaffolds with MC3T3-E1 cells [29] (Tables 17.2 and 17.3).

### 17.3.2 Nano-tricalcium Phosphate Bioceramics

Tricalcium phosphate (TCP) is also an osteoconductive bioceramic like nHA but has different bioactivity with the chemical formula  $\text{Ca}_3(\text{PO}_4)_2$  and two forms  $\alpha$  and  $\beta$  [14, 68, 93].

Compared to HA, the resorption rate of TCP was higher in the physiological media, while HA was higher in the osteoconductivity. These bioactive properties and degradation levels depend on the ratio of calcium and phosphate ions contained in the bioceramics; as mentioned above while this ratio is 1.67 for HA and 1.5 for both forms of TCP [34, 44, 84]. Due to their composition differences, dissolution rates of  $\alpha$ -TCP and  $\beta$ -TCP are different and  $\alpha$ -TCP dissolves more rapidly than  $\beta$ -TCP [34].

Cao et al. investigated the availability of polylactic acid (PLA) cages in the cervical region for spine surgery by improving their osteoconductivity with nano  $\beta$ -TCP. In this study, with creating an anterior spine fusion model in goats, the effects of autologous bone graft, polyether ether ketone (PEEK) cage and PLA/n $\beta$ -TCP cage were investigated with disc space height measurements and histological evaluation at week 12 along with radiography. As a result, it has been shown that

**Table 17.2** *In vitro* studies with nHA

Material	Produced methods	Characterization methods	Cell Type	Effect	References
PHBV/ PAA-nHA	Electrospinning	FTIR, FE-SEM	Human Fetal Osteoblast (hFOB)	In the group containing nHA, cell proliferation and ALP expression increased by 36.40% and 40.14%, respectively.	[124–126]
PCL/Fibroin/ nHA Scaffold	Supercritical Foaming	SEM	Murine Osteoblastic Cell Line MC3T3-E1	Increase in scaffolds containing nHA of ALP activation	[31]
				Increase in Calcium levels in scaffolds containing nHA and Fibroin according to PCL scaffold	
				Cellular attachment was highest in the PCL/Fibroin/nHA scaffold	
PCL + Fibronectin + nHA Scaffold	Electrospinning	FTIR, SEM	Mouse Mesenchymal Stem Cells (mMSCs)	Increase in Calcium Concentration	[74]
				Increase in ALP activation	
				Increase in OCN, OPN and Runx2 gene expressions	
nHA + Folic Acid	Hydrothermal	TEM, FTIR, UV-Vis Spectroscopy	Human Bone Marrow Mesenchymal Stem Cells (hMSC-bm)	No effect on proliferation and survival	[98]
				Increase in expression of Runx2	
nHA+PCL Composite Films	Solvent and Mechanical Blending Process	EDX, SEM, micro-CT, XRD, FTIR	Human Tenocytes	Increase in cell adhesion	[109]
				Parallel organization of cells was observed	
				Increase in proliferation	

the PLA cages developed with nano  $\beta$ -TCP have better biomechanical stability, and overall intervertebral bone and interbody fusion volume ratio when compared to autologous bone graft and PEEK cages [44].

In an *in vivo* study in the field of endodontic application, nano  $\beta$ -TCP particles were fabricated together with Chitosan/Glycerophosphate/Glyoxal hydrogels to gain thermo-sensitive properties. Physicochemical characterization of the produced bio-molecule was carried out using XRD, FTIR, TEM and SEM. Cytotoxicity studies were performed in normal Wish cells, hepato-

cellular carcinoma cell line HEPG2 cells and breast cancer cell line MCF7 cells via MTT. *In vitro* cytotoxicity assays have shown that the application of composites is safe and *in vivo* studies have been made in the premolar teeth of mongrel dogs. The fabricated composite and Klipdent-PL<sup>®</sup>, a commercial product, has been compared for their histological and inflammatory reactions regarding to bone tissue regeneration. Consequently, fabricated composite was more bioactive than the commercial product and had a positive effect on bone tissue formation by showing osteoconductive properties [84] (Table 17.4).



**Table 17.3** *In vivo* studies with nHA

Material	Produced methods	Characterization methods	Animal and model	Analysis	Effect	References
Injectable nHA-Chitosan-Gelatin Micro-Scaffolds	Cryogelation of gelatin with micro-stencil array chip	SEM	Rabbit; Subchondral Bone Lesion Model	Micro-CT, HE, Masson's Trichrome Staining, Full-body roentgenogram	Fibrosis and thrombosis were not seen Better tibia joint flatness Increase in microarchitecture Normal subchondral bone-like tissue formation	[117, 118]
PCL/nHA/PPF Scaffold	3D Printing – FDM Technique	SEM, EDS, WCA (Water contact angles)	New Zealand albino rabbits, Sprague Dawley rats, New Zealand white rabbits; Intracutaneous Irritation, Subcutaneous Implantation, Orthotopically Implantation	Micro-CT, HE, Masson's Trichrome staining	Irritation was insignificant Inflammatory response was not seen Increase in BMD New bone formation was observed	[22]
Grafted nano HA/PLGA with MSCs and BMP-2 (Tissue engineered g-nano HA/PLGA scaffold)	Solvent casting and Particulate-leaching method	SEM, Energy dispersive X-ray spectroscopy (EDX)	Rabbit; Intramuscular implantation for biodegradation and mineralization analyses and critical radius defect for bone healing investigation	X-ray imaging, H&E and Masson's trichrome staining, Semi-quantitative RT-PCR	Biodegradation and mineralization analyses showed that tissue engineered g-nano HA/PLGA scaffold had good histocompatibility after 8 weeks post-surgery. In bone healing analyses; at 4 weeks post-surgery, enhanced mineralization was observed and at 8 weeks post-surgery newly bone formed and interacted with neighboring bones. The new bone formation was guided by the tissue-engineered scaffold.	[124–126]

**Table 17.4** *In vitro* and *in vivo* studies with nano  $\beta$ -TCP

Material	Characterization method	Study type	Cytocompatibility test and cell type	Animal and model	Analysis	Effect	References
3D Collagen Scaffold + nano $\beta$ -TCP	XRD, SEM, EDS	<i>in vitro</i> and <i>in vivo</i>	CCK-8; mouse osteoblastic MC3T3-E1 cells	Wistar rats; implanted into subcutaneous tissue and implanted on cranial bone with decortication	HE, Masson's Trichrome Staining, ALP	<i>in vitro</i> cell proliferation was increased but the high concentration of $\beta$ -TCP decreased proliferation. <i>in vivo</i> cell and blood vessel ingrowth is increased but high concentration of $\beta$ -TCP (>10.4mg) exhibited low tissue affinity in rats.	[78]
Type I Collagen Scaffold + FGF-2 + nano $\beta$ -TCP	SEM	<i>in vitro</i> and <i>in vivo</i>	CCK-8; Mouse osteoblastic MC3T3-E1 cells	Wistar Rat and Beagle Dog; Implanted into subcutaneous tissue of the back and One-wall intra bony defect model	HE, Masson's Trichrome Staining	Cell attachment and proliferation were higher on the nano- $\beta$ -TCP scaffold compared to collagen scaffold <i>in vitro</i> . In nano- $\beta$ -TCP scaffold group, in growth of fibroblastic cells and blood vessel was observed in rats. Because of dispersed and attached nano- $\beta$ -TCP particles on collagen scaffold, mechanical strength and cell proliferation was increasing.	[83]
PLGA/nano- $\alpha$ -TCP Composite and PLGA/micro- $\alpha$ -TCP Composite	SEM, Thermogravimetric Analysis (TGA)	<i>in vivo</i>	-	Ovine; Sub-critical defect in the distal femoral condyle	Toluidine blue staining, X-ray imaging	Nano size composites degraded more slowly than micro size composites. The area of the newly formed bone was not different between two groups. Osteoclast activation for bone resorbing was observed all composites only for 6 weeks.	[13]
Nano $\beta$ -TCP granules	FTIR, XRD, SEM, Micro-CT, Bruauer-Emmet-Teller(BET)	<i>in vivo</i>	-	Covance Beagle; Mandibular defect	H&E	No toxicologically changes The zone of the newly bone (expect for callus) was larger compared to untreated group	[64]

### 17.3.3 Nano- Biphasic Calcium Phosphate Bioceramics

Nano-biphasic calcium phosphate (nBCP) is an osteoconductive and osteoinductive bioceramic consisting of two calcium phosphate phases, nHA and nTCP. The ratios of nHA and nTCP phases alter the physicochemical properties of nBCP ceramics and resulting in different biological responses [20, 30]. By using TCP in this composite bioceramics, the low dissolution rate of HA is avoided while the similarity to the mineral phase of the bone and mechanical properties increased by the HA content. The advantage of BCP is the possibility to design the ratio of HA [42]. nBCP bioceramics can be produced by sintering, solid-state reaction, flame spray pyrolysis, liquid-microwave sintering and sol-gel techniques. Among these methods, sintering technique with a non-stoichiometric CaP and temperature higher than 750 °C is used more often since it is more simple and economic. Hiep et al. investigated *in vitro* and *in vivo* effects of Polycaprolactone/Poly (lactic-co-glycolic acid)-BCP (PCL/ PLGA) scaffolds produced by solvent evaporation method on osteogenic differentiation. SEM, Energy Dispersive X-Ray Spectrometry (EDS), micro-CT indicated distribution of BCP in the polymer scaffold and the XRD peaks within the characterization study were shown in the expected regions. Following the production stage of the material, proliferation studies were carried out with MTT in hBMSCs (human bone marrow MSCs). In the proliferation experiment, the contribution of BCP to proliferation was investigated by forming control, PCL/PLGA and PCL/PLGA+BCP groups. As a result of the comparison of groups at weeks 1, 2 and 3, there was only a statistically significant difference in the group containing BCP compared to the group containing PCL/PLGA at all three time points. Compared to the control group, only proliferation increase was detected in the group containing BCP at week 3. As a result of fluorescence and Hematoxylin & Eosin (H&E) staining, both scaffold groups seem to support cell migration. When osteopontin (OPN), collagen type 1 (COL1), bone morphogenetic protein-2 (BMP-2)

and osteocalcin (OCN) expression levels were examined, quantitative RT-PCR analysis showed a significant increase in OCN and OPN with BCP. Later, BCP containing scaffolds implanted into rabbits femoral defects and new bone formation was assessed with micro-CT [107].

A clinical study with 48 volunteers by Uzeda et al. evaluated two BCP bioceramics with different nHA/n $\beta$ -TCP ratios and compared them with a commercially available bone ceramic histologically and histomorphometrically. nHA and n $\beta$ -TCP contents of these applied composites were; Biomaterial 1 (60.3% / 29.7%), Biomaterial 2 (78.2% / 21.8%) and Bone Ceramic (61% / 39%), respectively. Volunteers were followed for 6 months and no infection, pain or swelling was observed in any of them when subjected to examination with H&E staining. At the end of 6 months, new bone formation was observed in the biomaterial 1 BCP bioceramics, which had the highest  $\beta$ -TCP ratio [111].

#### 17.3.3.1 Electrospinning and Nano- Bioceramics

As mentioned above, there are many methods in the production of nano-bioceramics however electrospinning is generally preferred due to its ease and cheapness to produce biomaterials in various shapes and sizes (10  $\mu$ m to 10 nm) [21, 47]. Even though polymer materials are produced mostly by electrospinning method, nano-bioceramics can be also used to create an extracellular matrix (ECM) -like structure.

In this method, polymer solution as a viscoelastic fluid or melt is loaded into a syringe-like structure area with electric force and then this fluid is sent to the Taylor cone region, which is in a conical form. An electrostatic force-generating melt or polymer solution that can exceed the surface tension is collected in a non-woven platen or rotary pick-up, or oriented through the spinneret [35, 121].

In a study by Kumar et al., PCL/HA scaffolds containing 100 nm nHA were prepared by electrospinning and characterized by SEM, FTIR and differential scanning calorimetry (DSC). After material characterization, *in vitro* biocompatibility of these scaffolds containing different ratios

of nHA was investigated. Cell proliferation assay was performed with MTT, while apoptosis was performed with Acridine Orange and Propidium Iodide staining and found that proliferation of hMSCs was increased with increasing HA content of scaffolds, and no apoptotic cells were found at fluorescent microscope after staining [62]. In another study scaffolds produced by electrospinning using PCL- Polyvinyl acetate (PVA) and HA were investigated for vascularized craniofacial bone regeneration. *In vitro* studies with DPSCs (Dental pulp stem cells) and hMSCs were similar to those of Kumar et al. It has been shown that the ectopic bone formation studies in mice following *in vitro* experiments supported vascularization and bone formation ability of the produced PCL-PVA + HA scaffolds [88].

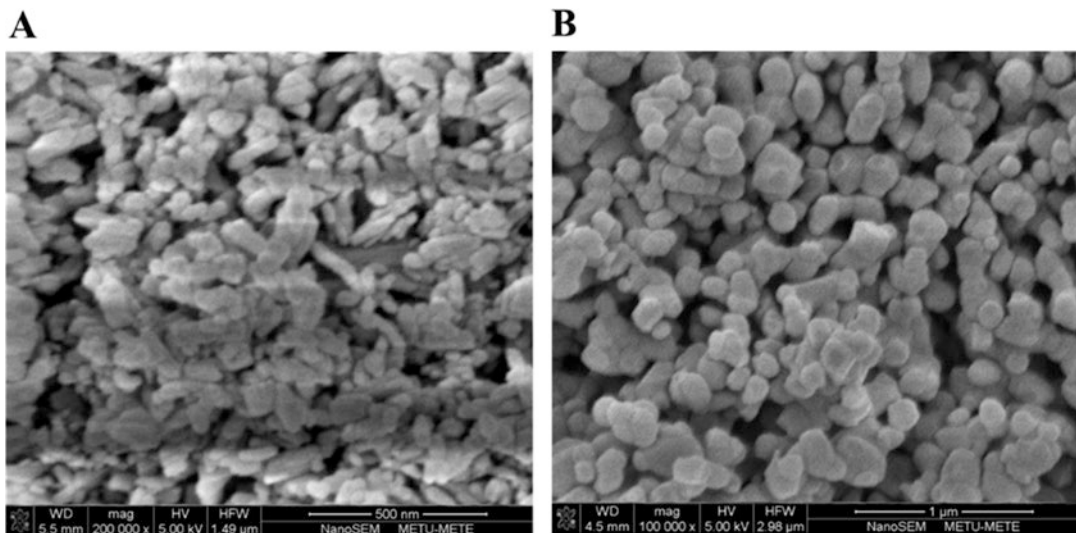
### 17.3.3.2 Enhancing Nano-Bioceramics with Trace Elements

Nano-bioceramics resemble the natural mineral content of bone, and integration of trace elements in the structure of the bone by incorporating the produced ceramic structures is one of the research topics of today. In this route, especially in the field of tissue engineering, it is aimed to develop new bioceramics with higher bioactivity and bio-

mechanical properties by adding Zinc ( $Zn^{+2}$ ), Magnesium ( $Mg^{+2}$ ), Strontium ( $Sr^{+2}$ ) and Boron (B), which are naturally found in biological structures. These elements are participated by interactions with calcium ( $Ca^{+2}$ ) ions in ceramic structures (Fig. 17.6).

In a unit cell of the apatite structure, there are four  $Ca^{+2}$  ions surrounded by nine oxygen (O) atoms, which are called  $Ca^{+2}$  (I) and six  $Ca^{+2}$  ions in each unit cell are  $Ca^{+2}$  (II) and it is allowing the movement of anions due to its large size. For each P atom, it forms the structure with 6  $PO_4^{3-}$  anions coordinated with four O atoms [103]. The  $Ca^{+2}$  (II) region is larger than the  $Ca^{+2}$  (I) region by volume. Different interactions with the two regions have different consequences for this reason. The  $Ca^{+2}$  (I) and  $Ca^{+2}$  (II) regions are important for the crystallinity of the apatite structure and for the incorporation capacities of trace elements.

Magnesium and Strontium are important trace elements in human physiology and cell metabolism. While Mg is found to be 0.72, 1.23 and 0.44% by weight in bone, dentin and enamel, respectively; Sr is also present in the mineral content of the bone and contributes to bone mineralization. These two elements contribute to bone tissue formation at different stages. Studies show



**Fig. 17.6** SEM images for Sr doped nHA at different temperatures (a) 300 °C, (b) 1000 °C

that Sr increases osteoblast activity and inhibits osteoclast activity [16, 94]. Mg plays an important role in bone metabolism by stimulating osteoblast proliferation in the early stages of osteogenesis [91, 103]. Mg interacts with the  $\text{Ca}^{+2}$  (I) region of the apatite structure; the Sr interferes with  $\text{Ca}$  (II)  $^{+2}$  region and prevents crystallization. These interactions also impair the stabilization of the structure and the thermal transformation of the apatite structure supports the transition to  $\beta$ -TCP [92, 103]. These two elements disrupt the stability of apatite structure that causes increased ion release from the material and stimulates cell responses. For bone tissue engineering applications, different concentrations of Sr were doped with nHA and nanohybrid scaffolds' Ca: Sr ratios were 10: 0, 9: 1, 5: 5 and 0:10, respectively. They were represented as HAP, Sr1HAP, Sr5HAP and Sr10HAP, respectively. Nanohybrid scaffolds were evaluated for proliferation and osteogenic differentiation in hBMSCs. In all four nanohybrid scaffolds, cell proliferation and morphology appeared normal in SEM images, and cell numbers increased with the day. The CCK-8 test showed same level of proliferation for all four groups on day 1 and an increase on day 7. SrHA/CS scaffolds show an increase in proliferation on days 3 and 7 compared to HA/CS scaffolds. On days 7 and 14, ALP activation, ALP protein expression, and COL1 protein expression levels were highest in the Sr5HA/CS group compared to other groups. Alizarin Red S staining was done on day 14, to evaluate the ECM mineralization and the highest mineralization was also observed in Sr5HA/CS nanohybrid scaffolds. According to these results, the Sr5HA/CS nanohybrid scaffold had the highest osteoinductivity when compared to other nanohybrid scaffolds and since the Ca: Sr ratio was 5: 5 in this group; it was thought that the combined effect of two ions contributes to this situation [65].

In Geng's study, nHA bioceramics were produced using egg shells as a  $\text{Ca}^{+2}$  source and  $\text{Sr}^{+2}$  bioactivity was investigated in osteoblast-like MG-63 cells by loading  $\text{Sr}^{+2}$  into the produced Egg Shell-nHA (ES-nHA). The fabricated ES-nHA was analyzed by XRD, FTIR, SEM,

TEM and ICP (Inductively Coupled Plasma) methods to show the similarity to nHA structure and the effect of ES-SrnHA on cell proliferation and osteogenic differentiation were also investigated. On both day 3 and 7, the proliferation rate of cells was higher in the ES-SrnHA group. ES-SrnHA bioceramics also had the highest ALP activation level on day 4. Osteogenic differentiation was also analyzed by RT-PCR and same results were obtained due to higher Runx2 (Runt-related transcription factor 2), ALP and OCN mRNA expressions levels [43].

Zinc (Zn) is a trace element that stimulates the synthesis of many proteins and is a cofactor for many enzymes, as well as in the structure of the bone, its effects resemble Sr. Zn also inhibits osteoclastogenesis while stimulating osteoblast activity, such as Sr [103]. Zn interacts with the Ca (II) region of the apatite form and reduces the crystallinity of the apatite form such as Mg and Sr [92]. Predoi and colleagues showed by XRD and FTIR analysis, that the increment of Zn concentration in the composite decreased the crystallinity of HA while increased the fluid lattice. Physico-chemical studies showed that the  $\text{Zn}^{+2}$  ions were displaced by  $\text{Ca}^{+2}$  ions and responsible for this behavior. In the morphological analysis of Zn-nHA bioceramics by SEM, as the Zn concentration increased in the nHA, the particle size decreased. However, there was no difference in the particle size affected by different Zn concentrations. Effect on cell-viability of Zn-loaded nHA bioceramics for 65.5, 125, 250 and 500  $\mu\text{g}/\text{ml}$  doses on HepG2 cells were investigated. Massive cell death was observed as a result of high dose sedimentation. However, bioceramics with the highest Zn concentration showed less toxicity at concentrations of 250 and 500  $\mu\text{g}/\text{ml}$ . According to this result, researchers suggested that nHA bioceramics containing different concentrations of Zn could make a difference in the release of  $\text{Zn}^{+2}$  ions or solubility [89].

In Forero's study, they added nHA and nano-Copper-Zinc alloy (nCuZn) to Chitosan/Gelatin (G/C) scaffold for the improvement of scaffold's biological and mechanical properties. They investigated composites' effects to proliferation, attachment and ALP activations with mouse

embryonic fibroblast cells *in vitro*. *In vivo* studies, they implanted composites to rabbits subcutaneously and they evaluated the results by histological methods. In *in vitro* studies, nCuZn alloy- nHA doped scaffolds increased cell adhesion at 24 h and ALP activation up to day 21 compared to nHA doped scaffolds. The effect of nZnCu/nHa/Ch/G scaffolds on cell proliferation was demonstrated by H&E staining; the cells were adherent to the nZnCu/nHA/Ch/G scaffold surface on day 7 and they were started to be seen on the nZnCu/nHA/Ch/G scaffold pores on day 14. For *in vivo* biocompatibility measurements, H&E staining was carried out at the end of 4th week and it was shown that cell migration was triggered in the nZnCu/nHA/Ch/G scaffold than better the CH/G scaffold [38].

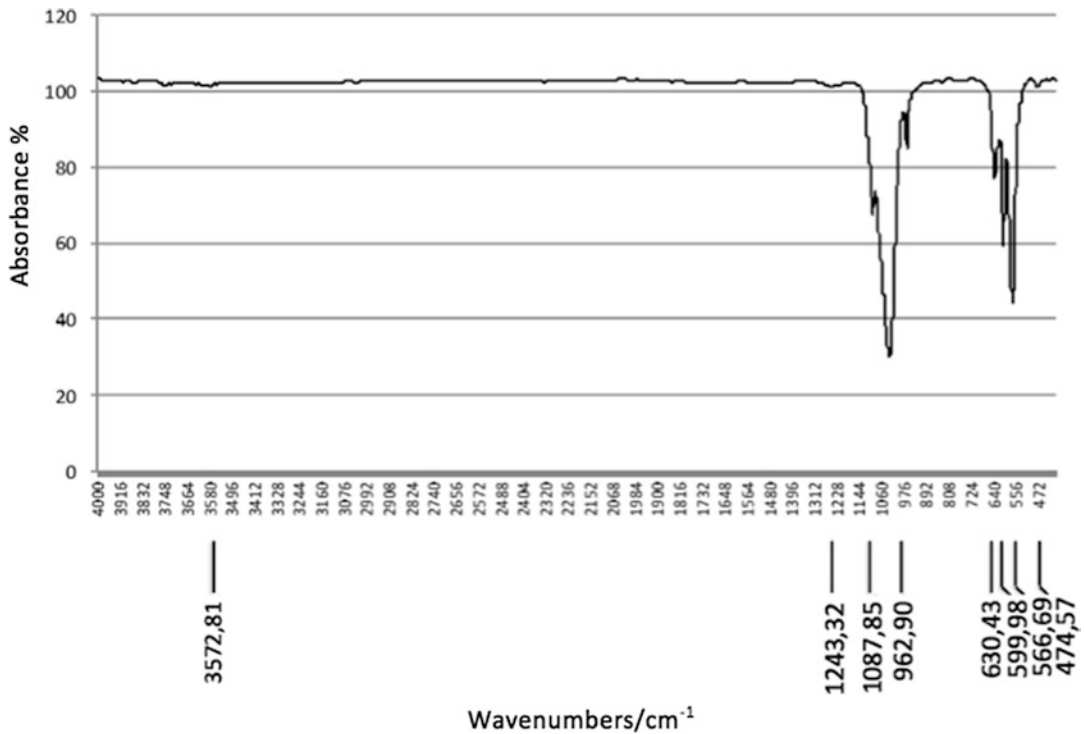
Chou et al. investigated the effect of Zn on  $\beta$ -TCP for proliferation and osteogenic differentiation of mesenchymal stem cells. ICP-MS results showed that the amount of  $Zn^{+2}$  released by  $\beta$ -TCP does not have any side effects. Zn-loaded  $\beta$ -TCP bioceramics increased the proliferation of MSCs and ALP activity up to day 14. On day 14, the amount of calcium, which is a sign of late osteogenic differentiation, was increased in Zn-doped  $\beta$ -TCP according to control and  $\beta$ -TCP and supported by Alizarin red S staining [27].

Boron (B) is another element that is intended to be added to ceramic materials to improve the structural properties of the material and to stimulate biological responses. B has direct and indirect effects on bone structure [87]. In Tuncay's work, nHA and B-nHA, known for their osteoinductive properties, were used to improve the mechanical properties and bioactivity of chitosan scaffolds prepared by microwave irradiation and they were used with osteoblastic MC3T3-E1 cells for investigating the effects of cell attach-

ment characteristics, proliferation effect, early and late osteoblastic differentiation markers. Morphology of composites was investigated with SEM and TEM. XRD, FTIR and RAMAN analyses showed that B loading did not affect the HA structure. XRD diffraction peaks showed that B doped nHA had higher crystallinity than nHA. The proliferation and attachment properties of MC3T3-E1 osteoblastic cells showed better results with B-nHA composites. For the evaluation of B-nHA bioceramic's effect to bone regeneration capacity, early and late osteoblast differentiation markers COL1, RunX2, OCN and OPN gene expressions were investigated and it was shown that COL1, OCN and OPN gene expression significantly increased. But, RunX2 gene expression was similarly increased in both groups with B-nHA and nHA. Authors stated that the mineralization was higher in the chitosan scaffolds with B-nHA [110].

Ciftci's study showed that the proliferation and osteogenic differentiation potential of bone marrow mesenchymal stem cells were similar in HA composite treated and untreated cells but application of B-nHA to cells increased the proliferation. When the amount of calcium was measured, the contribution of the B-nHA composite to the osteogenic differentiation was higher than blank nHA composite (Fig. 17.7) [28].

Another study examining the *in vitro* cytotoxic effects of B by modifying the bioactive glass with two different amounts of B showed that, the cell viability of mouse early osteocyte MLO-A5 cells was reduced in stable environment with bioactive glass containing 35.33% more B, but in a dynamic environment similar to body fluid the viability of the cells increased [73]. The other studies on Mg, Zn, Sr and B are summarized in Table 17.5.



**Fig. 17.7** FTIR spectra of B doped nHA. All of peaks in this diagram belong to PO<sub>4</sub> and OH radicals. The (BO<sub>3</sub>)<sup>-3</sup> characteristic peaks are shown at 1243 cm<sup>-1</sup> and 783–743 cm<sup>-1</sup> vibration band

**Table 17.5** Various trace element loaded nano-bioceramic studies

Trace element	Bioceramic material	Study type	Effects	References
Mg and Zn	Mg-3Zn-HA	<i>In vitro</i>	Increased degradation	[50]
			Increased cell viability	
Mg	Calcium magnesium phosphates	<i>In vitro</i>	Increased degradation	[19]
			Increase in the number of differentiated osteoclasts	
Sr	Sr-nHA	<i>In vitro</i> and <i>in vivo</i>	Enhancing of cell adhesion, proliferation and osteogenic differentiation	[67]
			Increasing of new bone area	
			Increasing of degradation	
Sr	Sr-BCP bone cement	<i>In vitro</i>	Increasing of degradation	[127]
			Good cytocompatibility	

## 17.4 Control and Treatment of Bone Infection with Bioceramics

Osteomyelitis is a musculoskeletal infection caused by many microorganisms, like bacteria, fungi, yeast and viruses. The infection is generally arisen secondary from a contiguous focus of

infection such as trauma, surgery or vascular insufficiency and hematogenous spread. Osteomyelitis can be classified as acute or chronic osteomyelitis; acute osteomyelitis lasts for days and weeks while chronic osteomyelitis lasts for months or years. In the mechanism of infection, microorganisms adhere to host bone tissue with their adhesins specific for host pro-

teins like collagen, fibronectin and bone sialoprotein. Macrophages attack to the pathogen, release proteolytic enzymes and leads to tissue lysate. In the manner of adaptive immunity, pus spreads to vascular channels in the bone and deteriorate blood flow. As the infection progresses to chronic state, necrotic bone is fragmented and sequestrum is formed [18]. Methicillin resistant *Staphylococcus aureus* (MRSA) is the most common pathogen isolated from the infection site but other pathogens like *Staphylococcus epidermidis*, coagulase-negative staphylococci, *Enterobacter* species, *Pseudomonas aeruginosa* and *Mycobacterium* species are also responsible for osteomyelitis. *Staphylococcus aureus* is a gram positive, facultative anaerobe having a spherical shape with 0.5–1.5  $\mu\text{m}$  diameter and forms bead like clusters when colonized. It attaches to the surface with its adhesins and exotoxins and many of its strains are capable of forming biofilm [71].

Biofilm is a three dimensional extracellular polymeric matrix formed by the irreversible attachment of the *Staphylococcus aureus* to a surface. Once *Staphylococcus aureus* attach to a surface, it begins to produce multi-layered biofilms under glycocalyx, or slime layer. Biofilm protects the bacteria from outer environmental conditions like antibiotic agents, phagocytosis, oxygen radical and protease defenses. As biofilm decreases the permeability of antimicrobial agents by acting as a diffusion barrier, in order to eradicate the bacteria within the biofilm, higher concentrations of antimicrobial agents are needed. Also under the protection of a biofilm, mature bacteria colonies can detach from the biofilm and they can migrate and form new biofilms in uninfected areas [77].

Conventionally, infection is treated with surgical debridement and 4–6 week lasting parenteral antibiotic therapy [72]. Actually regarding to the pathophysiology of the osteomyelitis, infection deteriorates the blood circulation and systemically delivered drugs cannot reach to infection area. Drug delivery systems gain attention, since the infection in the body cannot be eradicated by systemic or parenteral drug delivery. Beside the delivery of the drug to the infection area, these

systems also have advantages like improving the efficacy of the drug and diminishing its toxic effects [79]. For drug delivery, there must be a carrier for the drug and drug is released either by diffusion, chemical reaction or solvent activation and transport. Drug release systems have many different types of carrier materials like polymers, ceramics and composites that can be used in their fabrication [96].

In this section novel ceramics and composites used as carrier material for the control and treatment of the osteomyelitis is summarized.

In a study conducted by Kankilic et al., poly-L-lactic acid (PLLA)/ $\beta$ -TCP composites with vancomycin were developed to control implant related osteomyelitis (IRO) in rat model. Rat tibias were inoculated with MRSA and titanium particles to establish the model. After 3 weeks, the presence of the infection was verified by radiology. After the implantation of composites, radiological and histological scores were quantified along with microbiological findings on weeks 1 and 6 and found that, IRO was resolved [54].

Marques et al. robocasted biphasic calcium phosphate scaffolds both un-doped and doped with strontium (Sr) and silver (Ag). The scaffolds were characterized by scanning electron microscopy and its cytotoxicity and proliferation were checked by resazurin colorimetric assay using human osteosarcoma derived MG-63 cell line. The antimicrobial activity of the scaffolds was determined by Mueller-Hinton agar diffusion method using *E.coli* and *S. aureus* strains. The scaffolds doped with Sr and Ag had antibacterial effect against both *E.coli* and *S. aureus* strains with 1 mm and 1.5 mm inhibition zones, respectively [70].

Bakhsheshi-Rad et al. developed novel scaffolds with baghdadite and vancomycin by space holder method. Vancomycin concentrations in the scaffolds were 1, 3 and 5 wt.%, respectively. *In vitro* release of vancomycin was determined by UV spectrophotometer at 280 nm and found that vancomycin bursted from the scaffold in the first 6 h and then released sustainably. After 36 h, approximately 45–75% of the vancomycin trapped in the scaffolds was released and its anti-



microbial activity was confirmed by Kirby-Bauer disc diffusion method for *S. aureus* strain [9].

In 2017, Cao et al. fabricated 8% wt. vancomycin-loaded bone-like hydroxyapatite/poly amino acid (V-BHA/PAA) scaffold for the treatment of chronic osteomyelitis and compared it with 8% wt. vancomycin containing polymethyl methacrylate cement (V-PMMA) against both *in vitro* drug release and antimicrobial properties. Vancomycin *in vitro* released from V-BHA/PAA for 38 days while it was only released for 18 days for V-PMMA. Antimicrobial properties of both materials were determined by agar diffusion method for both *S. aureus* and MRSA strains. The inhibition zones diameters were much larger for V-BHA/PAA than V-PMMA for both strains and bacteriostatic effect of V-BHA/PAA lasted for more than 28 days while it was only last for 14 days for V-PMMA [23].

Seyfoori et al. developed cloxacillin loaded biphasic calcium phosphate scaffold made up of both hydroxyapatite and tricalcium phosphate

with different cloxacillin concentrations of 20, 50, 100 and 200 mg mL<sup>-1</sup>, respectively. The scaffolds were characterized according to scanning electron microscopy, x-ray diffraction spectroscopy and Fourier transform infrared spectroscopy. Cloxacillin is an antibacterial agent against methicillin sensitive *S. aureus* (MSSA). Cloxacillin was released into phosphate buffered saline and the released amount of antibiotic was determined by UV spectrophotometer at 232 nm. For antimicrobial activity, agar well diffusion method was used and zone of inhibitions were determined with inoculation of 0.5 McFarland MSSA suspension. According to results, as the concentration of cloxacillin in the scaffold increased, the diameter of zone of inhibition increased and all the concentrations of cloxacillin loaded to scaffolds are susceptible for the treatment of osteomyelitis [99].

Other studies using bioceramics as carrier material were summarized in Table 17.6.

**Table 17.6** Summary of studies using bioceramics as carrier material

References	Material	Aim	Methods	Results
[52]	Vancomycin-loaded nano-hydroxyapatite (nHA) pellets	To treat chronic osteomyelitis and bone defects caused by MRSA	Powdered nHA were mixed with vancomycin at a concentration of 160 mg vancomycin/g nHA and molded. Pellets without any antibiotic were also prepared as control. Antibacterial activity was determined by agar dilution technique using strains of <i>S. aureus</i> , <i>Escherichia coli</i> ( <i>E. coli</i> ) and MRSA. Later, the pellets were implanted into tibias of New Zealand rabbits with osteomyelitis model. In vivo drug release was determined with high performance liquid chromatography (HPLC). X-ray and histopathological analysis were performed.	Vancomycin released from pellets were effective for both <i>S. aureus</i> and MRSA for 25 days, while it was only effective for <i>E. coli</i> for 7 days. According to in vivo vancomycin release, drug concentration was greater than minimum inhibitory concentration for 12 weeks. Within 3 months, for all animals implanted with vancomycin loaded pellets osteomyelitis was controlled and treated while in control group, none of the animals were treated.

(continued)

**Table 17.6** (continued)

References	Material	Aim	Methods	Results
[117, 118]	Levofloxacin loaded mesoporous silica microspheres/ nano-hydroxyapatite/ polyurethane composite scaffolds (Lev-MSNs/n-HA/ PU)	To treat osteomyelitis in an animal model while comparing with bulk PMMA.	Scaffolds were manufactured by using 1 mg or 5 mg of levofloxacin and characterized with scanning electron microscopy. On the other hand, PMMA was prepared again by using 1 mg or 5 mg of levofloxacin. Osteomyelitis model was established in New Zealand white rabbits with the inoculation of $3 \times 10^7$ CFU/ml <i>S. aureus</i> (ATCC 25923). Rabbits were treated with either debridement only, 1 mg levofloxacin-PMMA, 5 mg levofloxacin-PMMA, 1 mg levofloxacin- Lev-MSNs/n-HA/PU composite scaffolds or 5 mg levofloxacin- Lev-MSNs/n-HA/PU composite scaffolds. At predetermined time points (1, 3, 6 and 12 weeks) x-ray and microCT evaluations were conducted along with immunohistochemical staining.	Radiographically, at 1 week, soft tissue swelling was observed in all treatment groups. At 3, 6 and 12 weeks, the symptoms of chronic osteomyelitis were only observed for debridement group. At 1 week and 3 weeks after implantation, the new bone formation of 5 mg lev-PMMA and 5 mg lev-MSNs/n-HA/PU were significantly different from other groups. But, at 6 weeks and 12 weeks, 5 mg lev-MSNs/n-HA/PU group had the most new bone formation.
[69]	Porous nano-hydroxyapatite/ polyamide 66 (nHP66)-based nanoscaffold materials containing varied concentrations of silver ions ( $\text{Ag}^+$ ) (TA-nHAPA66) and oxidized titanium ( $\text{TiO}_2$ )	To investigate the <i>in vivo</i> antimicrobial and therapeutic effects of TA-nHP66 biomaterials and their <i>in vivo</i> silver release	TA-nHP66 scaffolds were prepared by using either 0.22 wt% Ag + or 0.64 wt% Ag+. As control same scaffolds without any $\text{TiO}_2$ were prepared. Antimicrobial activity was determined by using agar disc diffusion method for both <i>E. coli</i> and <i>S. aureus</i> strains. Osteomyelitis model was established in New Zealand white rabbits with the inoculation of $3 \times 10^7$ CFU/ml <i>S. aureus</i> (ATCC 25923). Infected rabbits were treated with three groups: first group was treated with debridement only, second group was treated with debridement and blank nano-HA/polyamide 66 scaffold implantation, and third group was treated with debridement and 0.64 wt% ag + TA-nHP66 scaffold implantation.	All scaffolds showed antimicrobial activity against both <i>E. coli</i> and <i>S. aureus</i> strains but 0.64 wt% Ag + TA-nHP66 scaffold group had the longest antimicrobial activity. Also Ag + TA-nHP66 scaffold group had potent antibacterial/anti-inflammation effects <i>in vivo</i> and promoted bone formation at the lesion site of osteomyelitis

(continued)

**Table 17.6** (continued)

References	Material	Aim	Methods	Results
[85]	Vancomycin loaded microporous hydroxyapatite scaffolds	To determine the antibacterial effects of vancomycin loaded HA scaffolds	10 mg/mL, 20 mg/mL or 50 mg/mL vancomycin loaded microporous hydroxyapatite scaffolds were fabricated and characterized with x-ray diffraction, FTIR and scanning electron microscopy. In vitro vancomycin release was determined in 280 nm with UV spectrophotometer. Antibacterial activity of the scaffolds were tested with solid diffusion assay against <i>S. aureus</i> strain ATCC 6538 P.	All loaded vancomycin was released from 10 mg/m Land 20 mg/mL vancomycin loaded microporous HA scaffolds in a day while it lasted for 5 days for 50 mg/mL vancomycin loaded microporous hydroxyapatite scaffolds. For all vancomycin loaded scaffolds dose dependent inhibition zones were observed .

## References

- Ammerman JM, Libricz J, Ammerman MD (2013) The role of Osteocel plus as a fusion substrate in minimally invasive instrumented transforaminal lumbar interbody fusion. *Clin Neurol Neurosurg* 115(7):991–994
- Arealis G, Nikolaou VS (2015) Bone printing: new frontiers in the treatment of bone defects. *Injury* 46(Suppl 8):S20–S22
- Asanuma H, Meldrum DR, Meldrum KK (2010) Therapeutic applications of mesenchymal stem cells to repair kidney injury. *J Urol* Jul 184(1):26–33
- Aubin JE (1998) Bone stem cells. *J Cell Biochem Suppl* 30–31:73
- Auffray I, Chevalier S, Froger J, Izac B, Vainchenker W, Gascan H, Coulombel L (1996) Nerve growth factor is involved in the supportive effect by bone marrow-derived stromal cells of the factor-dependent human cell line UT-7. *Blood* 88:1608–1618
- Bai L, Caplan A, Lennon D, Miller RH (2007) Mesenchymal stem cell signals regulate neural stem cell fate. *Neurochem Res* 32:353–362
- Baino F, Tallia F, Novajra G, Minguella J, Montealegre MA, Korkusuz F, Vitale-Brovvarone C (2015) Novel bone-like porous glass coatings on Al<sub>2</sub>O<sub>3</sub> prosthetic substrates. In: *Key engineering materials*, vol 631. Trans Tech Publications, Pfäffikon, pp 236–240
- Baino F, Minguella J, Kirk N, Montealegre MA, Fiaschi C, Korkusuz F, Orlygsson G, Vitale-Brovvarone C (2016) Novel full-ceramic monoblock acetabular cup with a bioactive trabecular coating: design, fabrication and characterization. *Ceram Int* 42(6):6833–6845
- Bakhsheshi-Rad HR, Hamzah E, Ismail AF, Aziz M, Hadisi Z, Kashefian M, Najafinezhad A (2017) Novel nanostructured baghdadite-vancomycin scaffolds: in-vitro drug release, antibacterial activity and biocompatibility. *Mater Lett* 209:369–372
- Barry FP, Murphy JM (2004) Mesenchymal stem cells: clinical applications and biological characterization. *Int. J. Biochem Cell Biol* 36:568–584
- Behnia H, Khojasteh A, Kiani MT, Khoshzaban A, Mashhadi Abbas F, Bashtar M, Dashti SG (2013) Bone regeneration with a combination of nanocrystalline hydroxyapatite silica gel, platelet-rich growth factor, and mesenchymal stem cells: a histologic study in rabbit calvaria. *Oral Surg Oral Med Oral Pathol Oral Radiol* 115(2):7–15
- Beier JP, Bitto FF, Lange C, Klumpp D, Arkudas A, Bleiziffer O, Boos A, Horch RE, Kneser U (2010) Myogenic differentiation of mesenchymal stem cells co-cultured with primary myoblasts. *Cell Biol Int* 35(4):397–406
- Bennett SM, Arumugam M, Wilberforce S, Enea D, Rushton N, Zhang XC, Best SM, Cameron RE, Brooks RA (2016) The effect of particle size on the in vivo degradation of poly (d, l-lactide-co-glycolide)/ $\alpha$ -tricalcium phosphate micro- and nanocomposites. *Acta Biomater* 45:340–348
- Best SM, Porter AE, Thian ES, Huang J (2008) Bioceramics: past, present and for the future. *J Eur Ceram Soc* 28(7):1319–1327
- Bhuiyan DB, Middleton JC, Tannenbaum R, Wick TM (2017) Bone regeneration from human mesenchymal stem cells on porous hydroxyapatite-PLGA-collagen bioactive polymer scaffolds. *Biomed Mater Eng* 28(6):671–685
- Bigi A, Boanini E, Capuccini C, Gazzano M (2007) Strontium-substituted hydroxyapatite nanocrystals. *Inorg Chim Acta* 360(3):1009–1016
- Bilousova G, Jun du H, King KB, De Langhe S, Chick WS, Torchia EC, Chow KS, Klemm DJ, Roop DR, Majka SM (2011) Osteoblasts derived

- from induced pluripotent stem cells form calcified structures in scaffolds both in vitro and in vivo. *Stem Cells*;29(2):206–216
18. Birt MC, Anderson DW, Toby EB, Wang J (2017) Osteomyelitis: recent advances in pathophysiology and therapeutic strategies. *J Orthop* 14(1):45–52
  19. Blum C, Brückner T, Ewald A, Ignatius A, Gbureck U (2017) Mg: Ca ratio as regulating factor for osteoclastic in vitro resorption of struvite bioelements. *Mater Sci Eng C* 73:111–119
  20. Bouler JM, Pilet P, Gauthier O, Verron E (2017) Biphasic calcium phosphate ceramics for bone reconstruction: a review of biological response. *Acta Biomater* 53:1–12
  21. Boyd NR, Boyd RL, Simo GP, Nisbet DR (2011) Synthetic multi-level matrices for bone regeneration. In: *Tissue engineering in regenerative medicine*. Humana Press, New York, pp 99–122
  22. Buyuksungur S, Tanir TE, Buyuksungur A, Bektas EI, Kose GT, Yucel D, Beyzadeoglu T, Cetinkaya E, Yenigun C, Tonuk E, Hasirci V, Hasirci N (2017) 3D printed poly ( $\epsilon$ -caprolactone) scaffolds modified with hydroxyapatite and poly (propylene fumarate) and their effects on the healing of rabbit femur defects. *Biomater Sci* 5(10):2144–2158
  23. Cao Z, Jiang D, Yan L, Wu J (2017) In vitro and in vivo drug release and antibacterial properties of the novel vancomycin-loaded bone-like hydroxyapatite/poly amino acid scaffold. *Int J Nanomedicine* 12:1841–1851
  24. Centeno CJ, Schultz JR, Cheever M, Freeman M, Faulkner S, Robinson B, Hanson R (2011) Safety and complications reporting update on the reimplantation of culture-expanded mesenchymal stem cells using autologous platelet lysate technique. *Curr Stem Cell Res Ther* 6(4):368–378
  25. Chen X, Li Y, Wang L, Katakowski M, Zhang L, Chen J, Xu Y, Gautam SC, Chopp M (2002) Ischemic rat brain extracts induce human marrow stromal cell growth factor production. *Neuropathology* 22:275–279
  26. Chopp M, Zhang XH, Li Y, Wang L, Chen J, Lu D (2000) Spinal cord injury in rat: treatment with bone marrow stromal cell transplantation. *Neuroreport* 11(13):3001–3005
  27. Chou J, Hao J, Hatoyama H, Ben-Nissan B, Milthorpe B, Otsuka M (2015) Effect of biomimetic zinc-containing tricalcium phosphate (Zn-TCP) on the growth and osteogenic differentiation of mesenchymal stem cells. *J Tissue Eng Regen Med* 9(7):852–858
  28. Ciftci E, Köse S, Korkusuz P, Timucin M, Korkusuz F (2014) Boron containing Nano hydroxyapatites (Bn-HAp) stimulate mesenchymal stem cell adhesion, proliferation and differentiation. *Key engineering materials* (p 631)
  29. Dan Y, Liu O, Liu Y, Zhang YY, Li S, Feng XB, Shao XW, Yang C, Yang SH, Hong JB (2016) Development of novel biocomposite scaffold of chitosan-gelatin/Nanohydroxyapatite for potential bone tissue engineering applications. *Nanoscale Res Lett* 11(1):487
  30. Dard M, Larjava H (2017, December 20) Hydroxyapatite/beta-tricalcium phosphate biphasic ceramics as regenerative material for the repair of complex bone defects. *J Biomed Mater Res Part B Appl Biomater*. <https://doi.org/10.1002/jbm.b.34049>
  31. Diaz-Gomez L, García-González CA, Wang J, Yang F, Aznar-Cervantes S, Cenís JL, Reyes R, Degado A, Evora C, Concherio A, Alvarez-Lorenzo C (2017) Biodegradable PCL/fibroin/hydroxyapatite porous scaffolds prepared by supercritical foaming for bone regeneration. *Int J Pharm* 527(1–2):115–125
  32. Docheva D, Popov C, Mutschler W, Schieker M (2007) Human mesenchymal stem cells in contact with their environment: surface characteristics and the integrin system. *J Cell Mol Med* 11(1):21–38
  33. Dong Y, Chen X, Hong Y (2013) Tissue-engineered bone formation in vivo for artificial laminae of the vertebral arch using beta-tricalcium phosphate bioceramics seeded with mesenchymal stem cells. *Spine* 38(21):1300–1306
  34. Dziadek M, Stodolak-Zych E, Cholewa-Kowalska K (2017) Biodegradable ceramic-polymer composites for biomedical applications: a review. *Mater Sci Eng C* 71:1175–1191
  35. Esfahani H, Jose R, Ramakrishna S (2017) Electrospun ceramic nanofiber Mats today: synthesis, properties, and applications. *Materials* 10(11):1238
  36. Farokhi M, Mottaghitalab F, Samani S, Shokrgozar MA, Kundu SC, Reis RL, Fatahi Y, Kaplan DL (2017) Silk fibroin/hydroxyapatite composites for bone tissue engineering. *Biotechnol Adv*
  37. Fehrer C, Brunauer R, Laschober G, Unterluggauer H, Reitingner S, Kloss F, Gully C, Gassner R, Lepperding G (2007) Reduced oxygen tension attenuates differentiation capacity of human mesenchymal stem cells and prolongs their lifespan. *Aging Cell* 6(6):745–757
  38. Forero JC, Roa E, Reyes JG, Acevedo C, Osses N (2017) Development of useful biomaterial for bone tissue engineering by incorporating Nanocopper-zinc alloy (nCuZn) in chitosan/gelatin/Nanohydroxyapatite (Ch/G/nHAp) scaffold. *Materials* 10(10):1177
  39. Fox JM, Chamberlain G, Ashton BA, Middleton J (2007) Recent advances into the understanding of mesenchymal stem cell trafficking. *Br J Haematol* 137(6):491–502
  40. Friedenstien AJ (1980) Stromal mechanisms of bone marrow: cloning in vitro and retransplantation in vivo. *Immunology of bone marrow transplantation*. Springer, Berlin/Heidelberg, pp 19–20

41. Gao J, Caplan AI (2003) Mesenchymal stem cells and tissue engineering for orthopaedic surgery. *Chir Organi Mov* 88(3):305–316
42. Garrido CA, Lobo SE, Turibio FM, LeGeros RZ (2011) Biphasic calcium phosphate bioceramics for orthopaedic reconstructions: clinical outcomes. *Int J Biomater* 2011:1–9
43. Geng Z, Cheng Y, Ma L, Li Z, Cui Z, Zhu S, Yanqin L, Liu Y, Bao H, Li X, Yang X (2017) Nanosized strontium substituted hydroxyapatite prepared from egg shell for enhanced biological properties. *J Biomater Appl* 32(7):896–905
44. Hashemibeni B, Dehghani L, Sadeghi F, Esfandiari E, Gorbani M, Akhavan A, Tahani ST, Bahramian H, Goharian V (2016) Bone repair with differentiated osteoblasts from adipose-derived stem cells in hydroxyapatite/tricalcium phosphate in vivo. *Int J Prevent Med* 7:62
45. Haynesworth SE, Baber MA, Caplan AI (1996) Cytokine expression by human marrow-derived mesenchymal progenitor cells in vitro: effects of dexamethasone and IL-1 alpha. *J Cell Physiol* 166(3):585–592
46. Hench LL (2013) An introduction to bioceramics. World Scientific Publishing Co Inc., Singapore
47. Homaieghor S, Davoudpour Y, Habibi Y, Elbahri M (2017) The electrospun ceramic hollow nanofibers. *Nanomaterials* 7(11):383
48. Horwitz EM, Prockop DJ, Fitzpatrick LA (1999) Transplantability and therapeutic effects of bone marrow-derived mesenchymal cells in children with osteogenesis imperfecta. *Nature Med* 5:309–313
49. Huang Y, Jia X, Bai K, Gong X, Fan Y (2010) Effect of fluid shear stress on cardiomyogenic differentiation of rat bone marrow mesenchymal stem cells. *Arch Med Res* 41(7):497–505
50. Jaiswal S, Kumar RM, Gupta P, Kumaraswamy M, Roy P, Lahiri D (2018) Mechanical, corrosion and biocompatibility behaviour of mg-3Zn-HA biodegradable composites for orthopaedic fixture accessories. *J Mech Behav Biomed Mater* 78:442–454
51. Jaquet K, Krause KT, Denschel J, Faessler P, Nauerz M, Geidel S, Boczor S, Lange C, Stute N, Zander A, Kuck KH (2005) Reduction of myocardial scar size after implantation of mesenchymal stem cells in rats: what is the mechanism? *Stem Cells Dev* 14(3):299–309
52. Jiang JL, Li YF, Fang TL, Zhou J, Li XL, Wang YC, Dong J (2012) Vancomycin-loaded nano-hydroxyapatite pellets to treat MRSA-induced chronic osteomyelitis with bone defect in rabbits. *Inflamm Res* 61(3):207–215
53. Jones JR, Ehrenfried LM, Hench LL (2006) Optimising bioactive glass scaffolds for bone tissue engineering. *Biomaterials* 27(7):964–973
54. Kankilic B, Bilgic E, Korkusuz P, Korkusuz F (2014) Vancomycin containing PLLA/ $\beta$ -TCP controls experimental osteomyelitis in vivo. *J Orthopaedic Surg Res* 9(1):114
55. Kankilic B, Köse S, Korkusuz P, Timucin M, Korkusuz F (2016) Mesenchymal stem cells and nano-bioceramics for bone regeneration. *Curr Stem Cell Res Ther* 11(6):487–493
56. Kankilic B, Ciftci Dede E, Korkusuz P, Timucin M, Korkusuz F (2017) Apatites for orthopedic applications. In: Kaur G (ed) Clinical applications of biomaterials. Springer, Cham, pp 65–90
57. Khang G, Kim SH, Kim MS, Lee HB (2008) Hybrid, composite, and complex biomaterials for scaffolds. In: Principles of regenerative medicine. Elsevier – Academic Press, Amsterdam, pp 636–655
58. Korkusuz F (2013) Editorial comment: Nanoscience in musculoskeletal medicine. *Clin Orthop Relat Res* 471:2530–2531
59. Korkusuz P, Korkusuz F (2004) Hard tissue-biomaterial interactions. In: Yaszemski MJ, Trantolo DJ, Lewandrowski KU, Hasirci V, Altobelli DE, Wise DL (eds) Biomaterials in orthopedics. Marcel Dekker, New York, pp 1–40
60. Korkusuz F, Timucin M, Korkusuz P (2014) Nanocrystalline apatite-based biomaterials and stem cells in orthopaedics. In: Ben-Nissan B (ed) Advances in calcium phosphate biomaterials, Springer series in biomaterials science and engineering. Springer, Heidelberg, pp 373–390
61. Kose S, Aerts Kaya F, Denkbaz EB, Korkusuz P, Cetinkaya FD (2016) Evaluation of biocompatibility of random or aligned electrospun polyhydroxybutyrate scaffolds combined with human mesenchymal stem cells. *Turk J Biol* 40:410–419
62. Kumar S, Stokes JA III, Dean D, Rogers C, Nyairo E, Thomas V, Mishra MK (2017) Biphasic organo-bioceramic fibrous composite as a biomimetic extracellular matrix for bone tissue regeneration. *Front Biosci (Elite Ed)* 9:92
63. Labouyrie E, Dubus P, Groppi A, Mahon FX, Ferrer J, Parrens M, Reiffers J, De Mascarel A, Merlio JP (1999) Expression of neurotrophins and their receptors in human bone marrow. *Am J Pathol* 154:405–415
64. Lee DS, Pai Y, Chang S, Kim DH (2016) Microstructure, physical properties, and bone regeneration effect of the nano-sized  $\beta$ -tricalcium phosphate granules. *Mater Sci Eng C* 58:971–976
65. Lei Y, Xu Z, Ke Q, Yin W, Chen Y, Zhang C, Guo Y (2017) Strontium hydroxyapatite/chitosan nano-hybrid scaffolds with enhanced osteoinductivity for bone tissue engineering. *Mater Sci Eng C* 72:134–142
66. Levengood SKL, Zhang M (2014) Chitosan-based scaffolds for bone tissue engineering. *J Mater Chem B* 2(21):3161–3184
67. Li J, Yang L, Guo X, Cui W, Yang S, Wang J, Yanzen Q, Shao Z, Xu S. (2017) Osteogenesis

- effects of strontium-substituted hydroxyapatite coatings on true bone ceramic surfaces in vitro and in vivo. *Biomedical materials*;13(1):015018
68. Liu B, Lun DX (2012) Current application of  $\beta$ -tricalcium phosphate composites in Orthopaedics. *Orthop Surg* 4(3):139–144
  69. Lu M, Liao J, Dong J, Wu J, Qiu H, Zhou X, Li J, Jiang D, He TC, Quan Z (2016) An effective treatment of experimental osteomyelitis using the antimicrobial titanium/silver-containing nHP66 (nano-hydroxyapatite/polyamide-66) nanoscaffold biomaterials. *Sci Rep* 6:39174
  70. Marques CF, Perera FH, Marote A, Ferreira S, Vieira SI, Olhero S, Miranda P, Ferreira JM (2017) Biphasic calcium phosphate scaffolds fabricated by direct write assembly: mechanical, anti-microbial and osteoblastic properties. *J Eur Ceram Soc* 37(1):359–368
  71. Melicherick P, Cerovsky V, Nesuta O, Jahoda D, Landor I, Ballay R, Fulin P (2018) Testing the efficacy of antimicrobial peptides in the topical treatment of induced osteomyelitis in rats. *Folia Microbiol* 63(1):97–104
  72. Mistry S, Roy S, Maitra NJ, Kundu B, Chanda A, Datta S, Joy M (2016) A novel, multi-barrier, drug eluting calcium sulfate/biphasic calcium phosphate biodegradable composite bone cement for treatment of experimental MRSA osteomyelitis in rabbit model. *J Control Release* 239:169–181
  73. Modglin VC, Brown RF, Jung SB, Day DE (2013) Cytotoxicity assessment of modified bioactive glasses with MLO-A5 osteogenic cells in vitro. *J Mater Sci Mater Med* 24(5):1191–1199
  74. Mohamadyar-Toupanlou F, Vasheghani-Farahani E, Hanaee-Ahvaz H, Soleimani M, Dodel M, Havasi P, Abdolreza A, Taherzadeh ES (2017) Osteogenic differentiation of MSCs on fibronectin-coated and nHA-modified scaffolds. *ASAIO J* 63(5):684–691
  75. Mohsin S, Shams S, Ali Nasir G, Khan M, Javaid Awan S, Khan SN, Riazuddin S (2011) Enhanced hepatic differentiation of mesenchymal stem cells after pretreatment with injured liver tissue. *Differentiation* 81(1):42–48
  76. Mondal S, Dorozhkin SV, Pal U. (2017) Recent progress on fabrication and drug delivery applications of nanostructured hydroxyapatite. *Wiley Interdisciplinary Reviews: Nanomedicine and Nanobiotechnology*. e1504
  77. Moormeier DE, Bayles KW (2017) *Staphylococcus aureus* biofilm: a complex developmental organism. *Mol Microbiol* 104(3):365–376
  78. Murakami S, Miyaji H, Nishida E, Kawamoto K, Miyata S, Takita H, Akasaka T, Fugetsu B, Iwanaga T, Hongo H, Amizuka N (2017) Dose effects of beta-tricalcium phosphate nanoparticles on biocompatibility and bone conductive ability of three-dimensional collagen scaffolds. *Dent Mater* J 36(5):573–583
  79. Nandi SK, Bandyopadhyay S, Da P, Samanta I, Mukherjee P, Roy S, Kundu B (2016) Understanding osteomyelitis and its treatment through local drug delivery system. *Biotechnol Adv* 34(8):1305–1317
  80. Nauta AJ, Kruiselsbrink AB, Lurvink E, Willemze R, Fibbe WE (2006) Mesenchymal stem cells inhibit generation and function of both CD34+–derived and monocyte-derived dendritic cells. *J Immunol* 177(4):2080–2087
  81. Nejadnik H, Hui JH, Feng Choong EP, Tai BC, Lee EH (2010) Autologous bone marrow-derived mesenchymal stem cells versus autologous chondrocyte implantation: an observational cohort study. *Am J Sports Med* 38(6):1110–1116
  82. O'Donoghue K, Fisk NM (2004) Fetal stem cells. *Best Pract Res Clin Obstet Gynaecol* 18(6):853–857
  83. Ogawa K, Miyaji H, Kato A, Kosen Y, Momose T, Yoshida T, Fugetsu B (2016) Periodontal tissue engineering by nano beta-tricalcium phosphate scaffold and fibroblast growth factor-2 in one-wall infrabony defects of dogs. *J Periodontol Res* 51(6):758–767
  84. Pan HB, Zhao XL, Zhang X, Zhang KB, Li LC, Li ZY, Lin KL (2009) Strontium borate glass: potential biomaterial for bone regeneration. *J R Soc Interface*
  85. Parent M, Magnaudeix A, Delebassée S, Sarre E, Champion E, Viana Trecant M, Damia C (2016) Hydroxyapatite microporous bioceramics as vancomycin reservoir: antibacterial efficiency and biocompatibility investigation. *J Biomater Appl* 31(4):488–498
  86. Pittenger MF, Mackay AM, Beck SC (1999) Multilineage potential of adult human mesenchymal stem cells. *Science* 284:143–147
  87. Pizzorno L (2015) Nothing boring about boron. *Integr Med Clin J* 14(4):35
  88. Prabha RD, Kraft DCE, Harkness L, Melsen B, Varma H, Nair PD, Kassem M (2017) Bioactive Nano-fibrous scaffold for vascularized craniofacial bone regeneration. *J Tissue Eng Regen Med* 12(3):1537–1548
  89. Predoi D, Iconaru SL, Deniaud A, Chevallet M, Michaud-Soret I, Buton N, Prodan AM (2017) Textural, structural and biological evaluation of hydroxyapatite doped with zinc at low concentrations. *Materials* 10(3):229
  90. Quarto R, Mastrogiacom M, Cancedda R, Kutepov SM, Mukhachev V, Lavroukov A, Kon E, Marcacci M (2001) Repair of large bone defects with the use of autologous bone marrow stromal cells. *N Engl J Med* 344(5):385–386
  91. Rabiee SM, Nazparvar N, Azizian M, Vashae D, Tayebi L (2015) Effect of ion substitution on properties of bioactive glasses: a review. *Ceram Int* 41(6):7241–7251
  92. Ratnayake JT, Mucalo M, Dias GJ (2017) Substituted hydroxyapatites for bone regeneration: a review of current trends. *J Biomed Mater Res B Appl Biomater* 105(5):1285–1299

93. Ravaglioli A, Krajewski A (2012) *Bioceramics: materials properties applications*. Springer, Cham
94. Ravi ND, Balu R, Sampath Kumar TS (2012) Strontium-substituted calcium deficient hydroxyapatite nanoparticles: synthesis, characterization, and antibacterial properties. *J Am Ceram Soc* 95(9):2700–2708
95. Reddy S, Wasnik S, Guha A, Kumar JM, Sinha A, Singh S (2013) Evaluation of nano-biphasic calcium phosphate ceramics for bone tissue engineering applications: in vitro and preliminary in vivo studies. *J Biomater Appl* 27(5):565–575
96. Saidykhan L, Baka MZBA, Rukayadi Y, Kura AU, Latifah SY (2016) Development of nanoantibiotic delivery system using cockle shell-derived aragonite nanoparticles for treatment of osteomyelitis. *Int J Nanomedicine* 11:661
97. Sakar M, Korkusuz P, Demirbilek M, Cetinkaya DU, Arslan S, Denkbaz EB, Temucin CM, Bilgic E, Hazer DB, Bozkurt G (2014) The effect of poly(3-hydroxybutyrate-co-3-hydroxyhexanoate) (PHBHHx) and human mesenchymal stem cell (hMSC) on axonal regeneration in experimental sciatic nerve damage. *Int J Neurosci* 124(9):685–696
98. Santos C, Gomes P, Duarte JA, Almeida MM, Costa ME, Fernandes MH (2017) Development of hydroxyapatite nanoparticles loaded with folic acid to induce osteoblastic differentiation. *Int J Pharm* 516(1):185–195
99. Seyfoori A, Imani Fooladi AA, Mahmoodzadeh HH (2017) Calcium phosphate-based nanocomposite carriers for local antibiotic delivery against an osteomyelitis agent. *Adv Appl Ceram* 116(6):316–324
100. Shahbazarab Z, Teimouri A, Chermahini AN, Azadi M (2017) Fabrication and characterization of nano-biocomposite scaffold of zein/chitosan/nanohydroxyapatite prepared by freeze-drying method for bone tissue engineering. *Int J Biol Macromol*
101. Song S, Song S, Zhang H, Cuevas J, Sanchez-Ramos J (2007) Comparison of neuron-like cells derived from bone marrow stem cells to those differentiated from adult brain neural stem cells. *Stem Cells Dev* 16(5):747–756
102. Stappenbeck TS, Miyoshi H (2009) The role of stromal stem cells in tissue regeneration and wound repair. *Science* 324(5935):1666–1669
103. Supova M (2015) Substituted hydroxyapatites for biomedical applications: a review. *Ceram Int* 41(8):9203–9231
104. Szymonowicz M, Korczynski M, Dobrzynski M, Zawisza K, Mikulewicz M, Karuga-Kuzniewska E, Wiglusz RJ (2017) Cytotoxicity evaluation of high-temperature annealed nanohydroxyapatite in contact with fibroblast cells. *Materials* 10(6):590
105. Takahashi K, Yamanaka S (2006) Induction of pluripotent stem cells from mouse embryonic and adult fibroblast cultures by defined factors. *Cell* 126(4):663–676
106. Temenoff JS, Mikos AG (2008) *Biomaterials: the intersection of biology and materials science*. Pearson/Prentice Hall, Upper Saddle River
107. Thi Hiep N, Chan Khon H, Dai Hai N, Byong-Taek L, Van Toi V, Thanh HL (2017) Biocompatibility of PCL/PLGA-BCP porous scaffold for bone tissue engineering applications. *J Biomater Sci Poly* 28(9):864–878
108. Thomson JA, Itskovitz-Eldor J, Shapiro SS (1998) Embryonic stem cell lines derived from human blastocysts. *Science* 282:1145–1147
109. Tong SY, Wang Z, Lim PN, Wang W, San TE (2017) Uniformly-dispersed nanohydroxyapatite-reinforced poly( $\epsilon$ -caprolactone) composite films for tendon tissue engineering application. *Mater Sci Eng C* 70:1149–1155
110. Tuncay EO, Demirtas TT, Gumusderelioglu M (2017) Microwave-induced production of boron-doped HAp (B-HAp) and B-HAp coated composite scaffolds. *J Trace Elem Med Biol* 40:72–81
111. Uzeda MJ, de Brito Resende RF, Sartoretto SC, Alves ATNN, Granjeiro JM, Calasans-Maia MD (2017) Randomized clinical trial for the biological evaluation of two nanostructured biphasic calcium phosphate biomaterials as a bone substitute. *Clin Implant Dent Relat Res* 19(5):802–811
112. Vallet-Regi M (2001) Ceramics for medical applications. *J Chem Soc Dalton Trans* 2:97–108
113. Venkatesan J, Kim SK (2014) Nano-hydroxyapatite composite biomaterials for bone tissue engineering—a review. *J Biomed Nanotechnol* 10(10):3124–3140
114. Viateau V, Manassero M, Sensebe L, Langonne A, Marchat D, Logeart-Avrarmoglou D, Petite H, Bensedhoum M (2013) Comparative study of the osteogenic ability of four different ceramic constructs in an ectopic large animal model. *J Tissue Eng Regen Med* 10(3):177–187
115. Wakitani S, Imoto K, Yamamoto T, Saito M, Murata N, Yoneda M (2002) Human autologous culture expanded bone marrow mesenchymal cell transplantation for repair of cartilage defects in osteoarthritic knees. *Osteoarthr Cartil* 10(3):199–206
116. Wakitani S, Nawata M, Tensho K, Okabe T, Machida H, Ohgushi H (2007) Repair of articular cartilage defects in the patello-femoral joint with autologous bone marrow mesenchymal cell transplantation: three case reports involving nine defects in five knees. *J Tissue Eng Regen Med* 1(1):74–79
117. Wang B, Liu W, Xing D, Li R, Lv C, Li Y, Lin J (2017a) Injectable nanohydroxyapatite-chitosan-gelatin micro-scaffolds induce regeneration of knee subchondral bone lesions. *Sci Rep* 7(1):16709
118. Wang Q, Chen C, Liu W, He X, Zhou N, Zhang D, Huang W (2017b) Levofloxacin loaded mesoporous silica microspheres/nano-hydroxyapatite/polyurethane composite scaffold for the treatment of chronic osteomyelitis with bone defects. *Sci Rep* 7:41808

119. Weissman IL (2007) Stem cells: units of development, units of regeneration, and units in evolution. *Cell* 100(1):157–168
120. Xu F, Shi J, Yu B, Ni W, Wu X, Gu Z (2010) Chemokines mediate mesenchymal stem cell migration toward gliomas in vitro. *Oncol Rep* 23(6):1561–1567
121. Xue J, Xie J, Liu W, Xia Y (2017) Electrospun nanofibers: new concepts, materials, and applications. *Acc Chem Res* 50(8):1976–1987
122. Yamanaka S (2012) Induced pluripotent stem cells: past, present, and future. *Cell Stem Cell* 10(6):678–684
123. Zhang P, Gan YK, Tang J, Hao YQ, Wang Y, Sun YH, Zhu ZA, Dai KR (2008) Clinical study of lumbar fusion by hybrid construct of stem cells technique and bio-degradable material. *Zhonghua Wai Ke Za Zhi (Chinese J Surg)* 46(7):493–496
124. Zhang B, Zhang PB, Wang ZL, Lyu ZW, Wu H (2017a) Tissue-engineered composite scaffold of poly (lactide-co-glycolide) and hydroxyapatite nanoparticles seeded with autologous mesenchymal stem cells for bone regeneration. *J Zhejiang Univ Sci B* 18(11):963–976
125. Zhang CL, Huang T, Wu BL, He WX, Liu D (2017b) Stem cells in cancer therapy: opportunities and challenges. *Oncotarget* 8(43):75756–75766
126. Zhang S, Jiang G, Prabhakaran MP, Qin X, Ramakrishna S (2017c) Evaluation of electrospun biomimetic substrate surface-decorated with nanohydroxyapatite precipitation for osteoblasts behavior. *Mater Sci Eng C* 79:687–696
127. Zhu H, Guo D, Qi W, Xu K (2017) Development of Sr-incorporated biphasic calcium phosphate bone cement. *Biomed Mater* 12(1):015016
128. Zurita M, Vaquero J (2006) Bone marrow stromal cells can achieve cure of chronic paraplegic rats: functional and morphological outcome one year after transplantation. *Neurosci Lett* 402(1–2):51–56





# Recent Trends in Hydroxyapatite (HA) Synthesis and the Synthesis Report of Nanostructure HA by Hydrothermal Reaction

Pham Trung Kien, Huynh Dai Phu,  
Nguyen Vu Viet Linh, Tran Ngoc Quyen,  
and Nguyen Thai Hoa

## Abstract

This research summary the trend in synthesis of Hydroxyapatite (HA) using different route such as dry method and wet method (co-precipitation method; emulsion method, hydrolysis method, sol-gel method, hydrothermal method). In addition, the research group also report the technique to synthesis nano-structure HA by hydrothermal reaction using  $\text{Ca}(\text{OH})_2$  and  $\text{H}_3\text{PO}_4$  with the Ca/P molar ratio of 1.67. The mixture after homogenized for 2 h, follow by hydrothermal reaction at different hydrothermal temperature time (100 °C, 150 °C, and 180 °C) and different hydrothermal reaction time (0 h, 12 h and 24 h). The 180 °C-hydrothermal treated-HA has needle-like shape with the diameter of 10 ~ 20 nm and length of below 100 nm, which is similar with human bone. For the hydrothermal reaction, temperature is the key to form nanostructure HA.

## Keywords

Nano structured hydroxyapatite ·  
Hydrothermal reaction · Bone substitute ·  
Calcium phosphate · Biomaterials

## 18.1 Introduction

Biomaterials are the emerging fields that are growing rapidly to fulfill the demand in medicine and dentistry. Over the past few decades, new biomaterials for bone replacement, total hip prosthesis and dental implants have been synthesized and commercialized for various needs. Currently, thousands of these materials can be found easily in the market. The industry market for orthopedic biomaterials over the world is worth over US\$25 billion in 2006 and with a growth rate of more than 5% a year (refer Table 18.1). The market for

P. T. Kien (✉)

Faculty of Materials Technology, Ho Chi Minh City  
University of Technology (HCMUT), Vietnam  
National University (VNU-HCM),  
Ho Chi Minh City, Vietnam  
e-mail: [phamtrungkien@hcmut.edu.vn](mailto:phamtrungkien@hcmut.edu.vn)

H. D. Phu · N. V. V. Linh  
Faculty of Materials Technology, Ho Chi Minh City  
University of Technology (HCMUT), Vietnam  
National University (VNU-HCM),  
Ho Chi Minh City, Vietnam

National Key Lab for Polymer and Composite  
Materials, HCMUT, Ho Chi Minh City, Vietnam

T. N. Quyen

Graduate School of Science and Technology, Department  
of Pharmacy and Medicine, Vietnam Academy of  
Science and Technology, Ho Chi Minh City, Vietnam

N. T. Hoa

Key Lab for Materials Technology, Ho Chi Minh City  
University of Technology,  
Ho Chi Minh City, Vietnam

**Table 18.1** Market share of orthopedic biomaterials over the world in 5 years from 2007 to 2011 [1]

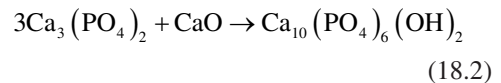
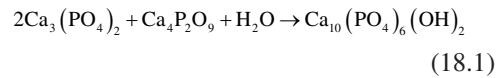
Year	Worldwide sales (US\$ Billions)	Growth (%)
2006	25.764	
2007	27.122	5.3
2008	28.562	5.3
2009	30.989	8.5
2010	31.708	2.5
2011	33.425	5.4
<b>Average growth rate (%)</b>		<b>5.4</b>

orthopedic biomaterials is expected to increase each year due to the need for better solution for injuries, diseases and ageing population all over the world.

The bone substitute biomaterials market consists primarily of bone graft substitutes, bone growth factors, degradable tissue fixation and tissue technologies for cartilage regeneration. Generally, orthopedic prostheses should offer a functional life of at least 20 years to match the life span of most patients. Among these bone graft substitute, Hydroxyapatite or HA [ $\text{Ca}_{10}(\text{PO}_4)_6(\text{OH})_2$ ] is the most attractive bone graft materials due to its excellent bone bonding to host surrounding implantation. Synthetic HA is a very important bone graft materials with the applicable in wide shape such as: bulk ceramic, a ceramic coating, or as one of the component of bone cement. HA is also used as a catalyst for the dehydration and dehydrogenation of primary alcohol due to its strong absorbent in water. Indeed, HA is a material of varying properties depend on its mode of preparation. The special structure of calcium and phosphate group in HA enables the possibility to use HA in divert application. For example, due to HA's similarity in chemical composition to the mineral phase of bone tissue, it is known for its applications in medicine as synthetic bone substitute [2]. In addition to its biological important, HA is researched for various applications such as fluorescent lamps [3], materials for fuel cell [4], or an absorption of waste and harmful materials [5]. For these applications, it has been noticed that a non-stoichio-

metric material is more efficient either in promoting the precipitation of biological apatite on its surface [6, 7] or increasing the reaction rate of water absorbent [8, 9]. The extend of the non-stoichiometry can be evaluated through various technique and expressed by value of x in the formula  $\text{Ca}_{10-x}(\text{HPO}_4)_x(\text{PO}_4)_{3-x}(\text{OH})$ .

Many methods have been used to synthesis HA such as dry methods [10, 11] by heat treatment of finely ground mixed precursor. For example, the mixture of Tricalcium phosphate [TCP:  $\text{Ca}_3(\text{PO}_4)_2$  or  $3\text{CaO} \cdot \text{P}_2\text{O}_5$ ] and Tetracalcium phosphate [TTCP:  $\text{Ca}_4(\text{PO}_4)_2\text{O}$  or  $4\text{CaO} \cdot \text{P}_2\text{O}_5$ ] follow by proper calcination can be used to form HA as shown in Eqs. (18.1) and (18.2)



In general, the solid state reaction result in yield well-crystallized product. However, the disadvantage of this method is the employee of high temperature to produce HA.

Another method use to synthesis HA is wet method. This method comprising co-precipitation method [12–14], emulsion method [15–17], hydrolysis method [18–23], sol-gel method [24–30], hydrothermal method [31–39] due to its advantage in simplicity of the procedure. These methods allow to control the structure, crystallinity, morphology of HA. The wet method can be done in water or in organic solvent. These methods can be performed at room temperature or elevated temperature, under the normal pressure or high pressure using hydrothermal technique. The major disadvantage of wet method is that they sometimes give impurity to the structure of HA or other phase of phosphate present together with HA. In addition, various ions can be incorporated into the structure of HA, leading to the trace impurity. The classification and over view of wet method to synthesis HA are listed as below:

### 18.1.1 Co-precipitation Method

This method is the common method for the preparation of HA. The chemical process consists of a chemical reaction source of Ca, and P in the presence of other additives with the acidic or basic environment. The conditions of the co-precipitation method are variable, but in general, this process is usually carried out at pH values vary from 3 to 12 and at temperatures vary from ambient to the elevated temperature of water. In some way, this method is sometimes performed in the presence of templates.

### 18.1.2 Emulsion Method

The emulsion method is used to synthesize HA which is more efficient, simple and suitable for producing nanostructure HA powder. The advantage of the emulsion method is the precise control of the morphology and distribution of HA's grain size. This technique was originally used to create porous materials as well as to overcome the issue of particle agglomeration. Several sources of Ca and P have been used, but the most popular used are calcium nitrate and phosphoric acid due to its economic and easy to find on the market. Among the surfactants used to prepare the emulsion, some chemicals include: dioctyl sodium sulfosuccinate salt, dodecyl phosphate, polyoxyethylene, nonpolyphenol ether, polyoxyethylene ether, cetyltrimethyl ammonium bromide and sodium dodecyl sulfate. The key factor to study is the type of surfactant, ratio of aqueous and organic phase, pH, temperature condition, concentration of Ca and P source etc.

### 18.1.3 Sol-Gel Method

The sol-gel process is a method of mineralization from a precursor in a solution, preferably organometallic compounds or other suitable precursors. This useful method can be used for the synthesis of porous, dense, bulk, xerogel film coating ceramic as well as aerogel HA. The procedure of the sol-gel method is given in Fig. 18.1.

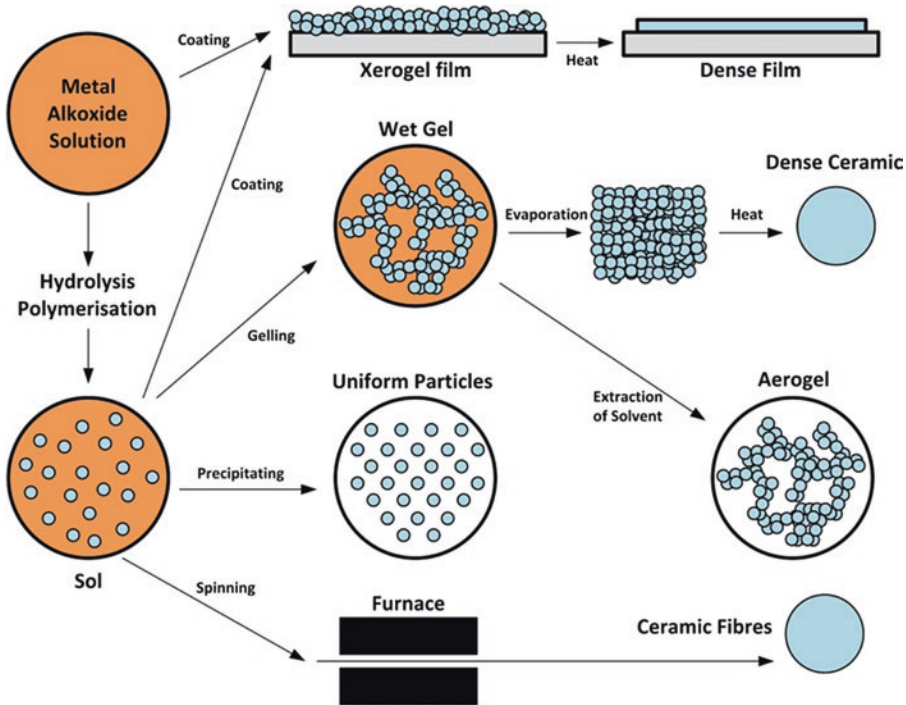
During the gelation, sol particles harden and form the gel network as shown in Fig. 18.2. The sol-gel process has limitations that hinder its scale up to industry scale production. The main disadvantages are: (a) the high cost and scarcity of often used alkoxide-based precursors and (b) the delicate process control culminating in usually time-consuming processes. This process involves hydrolysis of the precursors and the formation of micelles around templates in either an aqueous or an organic phase followed by the gelation of these sols. The key factors to control the gelation depend on: (a) the nature and what kind of solvent used; (b) the temperature and pH used and (c) the chemical nature of the reagent used. In addition, lack of control of certain parameters during the growth of HA may cause the appearance of secondary phases such as CaO,  $\text{Ca}_2\text{P}_2\text{O}_7$ ,  $\text{Ca}_3(\text{PO}_4)_2$  and/or  $\text{CaCO}_3$ .

### 18.1.4 Hydrolysis Method

The aqueous hydrolysis of calcium phosphate to form HA usually follows 2 stages: (a) dissolution and precipitation depending on the source of Ca and P. In the aqueous solution, the Ca and P sources are dissolved with respect to the surrounding environment then its concentration becomes supersaturated with respect to HA, leading to the precipitate of HA. The hydrolysis process applicable to these precursors depends strongly on pH and temperature of environment. The addition of other calcium and phosphate sources are sometimes required to control the stoichiometry of HA.

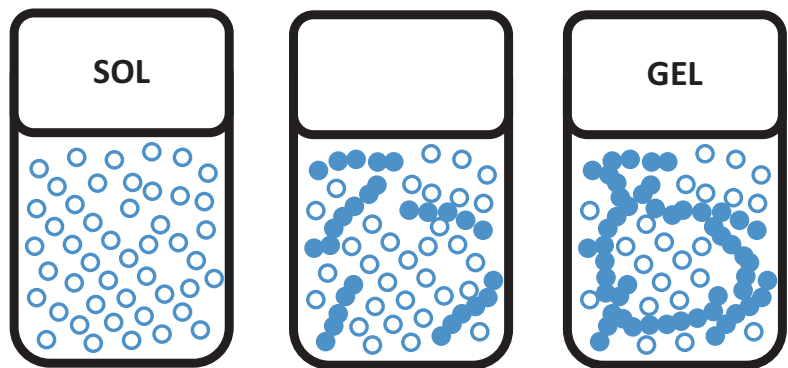
### 18.1.5 Hydrothermal Method

The hydrothermal process is a technique for the growth of crystalline HA with nanoscale. This process is the generic term used to describe a reaction between the calcium source and phosphate precursors in the presence of the following conditions: (a) water or organic solvent; (b) a mixture of water/organic solvent. In case of the water used, it is called the term hydrothermal



**Fig. 18.1** Principle procedure of sol-gel method. (Courtesy: [https://commons.wikimedia.org/wiki/File:Sol-Gel\\_Technology\\_Scheme.png](https://commons.wikimedia.org/wiki/File:Sol-Gel_Technology_Scheme.png))

**Fig. 18.2** The transformation of sol to gel. (Source: [http://www.uk-finishing.org.uk/N-COAT70/sol\\_gel.htm](http://www.uk-finishing.org.uk/N-COAT70/sol_gel.htm))



while organic solvent used is called the term solvothermal; and in case of water/organic solvent system, it is called solvo-hydrothermal. The process happens in the close environment with a high temperature and pressure greater than autogenously ambient pressure, for example inside an autoclave or a pressure vessel. The illustration of autoclave is shown in Fig. 18.3. During the hydrothermal reaction, the medium could be subcritical or supercritical, depending on the pressure and

temperature. Through the effect of medium evaporation and condensation, the pressure increase of reactivity and support for the chemical reaction between chemical reactant. It should be noted that the high pressure permits the formatting of HA in the form of micro or nano crystal size HA, with controlled morphology and porosity through the control of temperature and pressure.

The hydrothermal method can be used to control the interaction between solid/solvent,

**Fig. 18.3** The autoclave system used to synthesis HA. (Courtesy at Department of Ceramic Materials, Faculty of Materials Technology, Ho Chi Minh City University of Technology)



**Fig. 18.4** The ball milling system use for grinding starting materials. (Courtesy at Department of Ceramic Materials, Faculty of Materials Technology, HCMUT)



especially in terms of solubility and also function as a mean to control the nucleation and growth processes. In addition, this technique is often combined with conventional method such as co-precipitation or sol-gel routes.

### 18.1.6 Grinding-Assisted Method

In order to increase the chemical reactivity of Ca and P starting materials, the grinding method is

used is the first step. This method is also termed as mechano-chemical process, which often used the ball milling equipment as shown in Fig. 18.4. The advantage of this method is simplicity, reproducibility and large-scale production of HA. The control of growth HA by this technique focus on the types of chemical agent used, the grinding medium, the diameter and milling medium, the ratio of milling medium, the duration of milling steps and interval pauses, the powder-to-ball mass ratio and the rotation speed.

### 18.1.7 The Microwave (MW)-Assisted Method

In order to active the chemical reaction of Ca and P starting materials, the output energy supplied equipment used common is microwave oven. The MW-assisted preparation of HA produces an increase yield of perfectly crystalline powder. In addition, the obtained HA by MW-assisted method gains particularly homogenous in term of size, porosity and morphology. The activation results from two key factors: (a) purely thermal origin, resulting in molecular agitation that is caused by the inversion of dipole with the extremely rapid heating by the alternation of electric moment field and (b) an electrostatic origin, involving interactions like dipole-dipole between polar molecules and the electric field. The MW-assisted method cause direct effect on the kinetics of activation energy.

### 18.1.8 Ultrasonic-Energy-Assisted Method

The ultrasonic-energy-assisted method or sono-chemical approach can be used to synthesis nanostructure of HA. This method results in nanosized products and perfect to control the morphology, porosity and size of HA. In addition, this ultrasonic-assisted method enhance stimulation of the reaction between the calcium and phosphate precursors to accelerate the rate of reaction in a remarkable manner.

Based on consideration of these references to synthesis HA above, my research group at Department of Ceramic Materials aim to synthesize nanoprecipitated HA by hydrothermal reaction method. The research group succeeded to fabricate HA and Tricalcium phosphate (TCP) [40–47], with the aim to be used as bone substitute. In order to focus on the side effect of nanostructured HA, we aim to use hydrothermal reaction between  $\text{Ca}(\text{OH})_2$  and  $\text{H}_3\text{PO}_4$  used as precursor. This research report the technique to prepare nanostructure HA by coprecipitation method follow by hydrothermal reaction.

## 18.2 Materials and Method

### 18.2.1 Experimental Preparation

All the chemical was purchased from company without purification. The  $\text{Ca}(\text{OH})_2$  and  $\text{H}_3\text{PO}_4$  were supplied by Guangdong Chemical Co (China). In brief, 0.3 mol  $\text{H}_3\text{PO}_4$  was dropped into 0.5 mol  $\text{Ca}(\text{OH})_2$  suspension, so that the Ca/P molar ratio of the mixture was 1.67, according to the stoichiometric of HA. The CaP mixture was homogeneous by stirring at 400 rpm (IKA stirring) for 2 h at room temperature, follow by hydrothermal reaction at different hydrothermal reaction (100 °C, 150 °C and 180 °C) for different duration time (0 h, 12 h and 24 h). The samples after hydrothermal reaction were filtered and washed with double distilled water (DDW) for at least 3 times then follow by the characterization. In comparison with synthesis HA, the human teeth were used for characterization. In brief, the human teeth was supplied by Ho Chi Minh University of Pharmacy by collecting from dental clinic, follow by immersion in phosphate buffer solution (PBS).

### 18.2.2 Material Characterizations

#### 18.2.2.1 X-Ray Diffraction Analysis

The composition of sample before and after hydrothermal reaction were determined using X-Ray diffraction (XRD; D2 Bruker), operated at 40 kV and 40 mA.

#### 18.2.2.2 Scanning Electron Microscopic Observation

The morphology changes of sample before and after hydrothermal reaction were observed using a scanning electron microscope (SEM, S-3400N, JEOL) with an acceleration voltage of 15 kV, after the deposition of gold-palladium coating (Magnetron Sputtering Machine, MSP-1S).

#### 18.2.2.3 Transmission Electron Microscopic Observation

The morphology of sample before and after hydrothermal reaction was observed at nano-scale

using transmission electron microscope (TEM, Hitachi-7000) with an acceleration voltage of 10 kV. The samples were dispersed into ethanol with ultrasonic cleaning, then drop into copper grid for TEM observation.

#### 18.2.2.4 Fourier Transform Infrared Spectroscopy

The chemical bonding of samples was identified by Fourier transform infrared spectroscopy (FTIR, Bruker 400D) in the range of 400–4000  $\text{cm}^{-1}$  using KBr pellet technique.

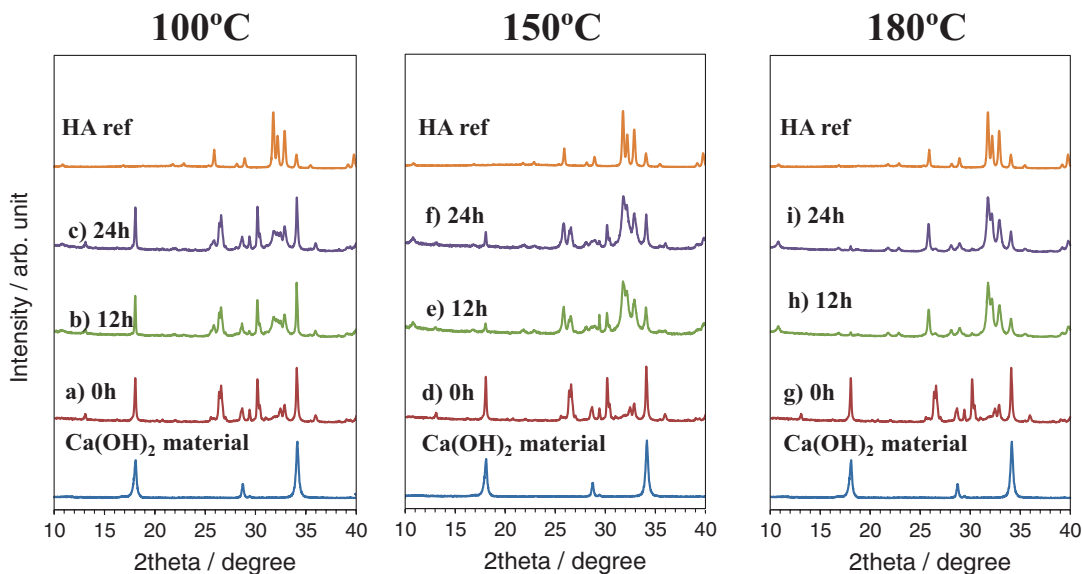
### 18.2.3 Statistical Analysis

For statistical analysis, a one-way factorial ANOVA and Fisher's LSD method, as a post-hoc test, were performed using KaleidaGraph 4.0. Values are expressed as mean  $\pm$  SD. A *p*-Value of  $<0.05$  was considered to be statistically significant.

## 18.3 Results and Discussion

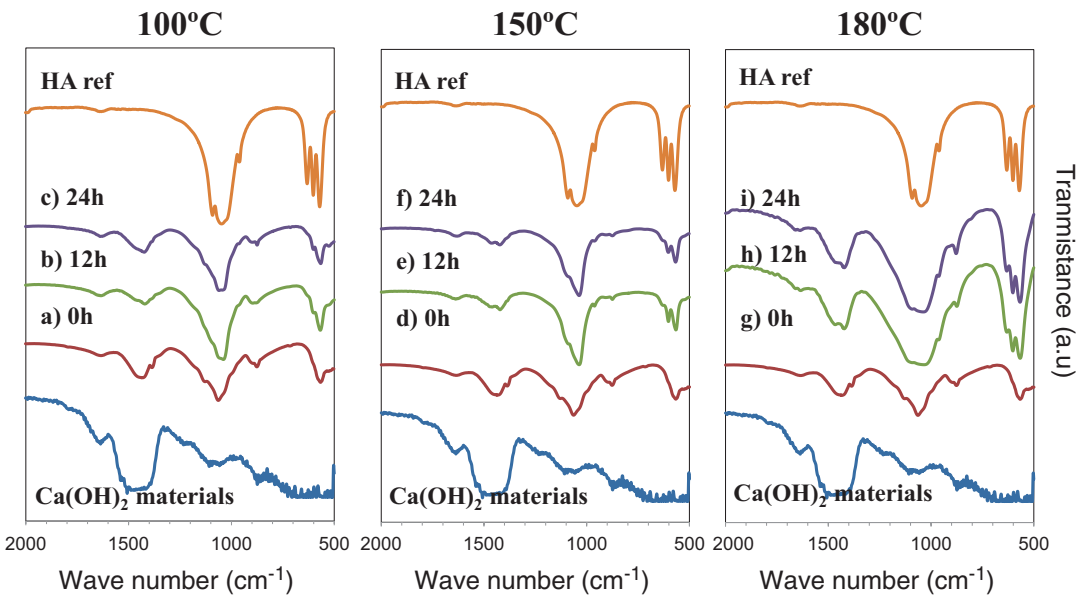
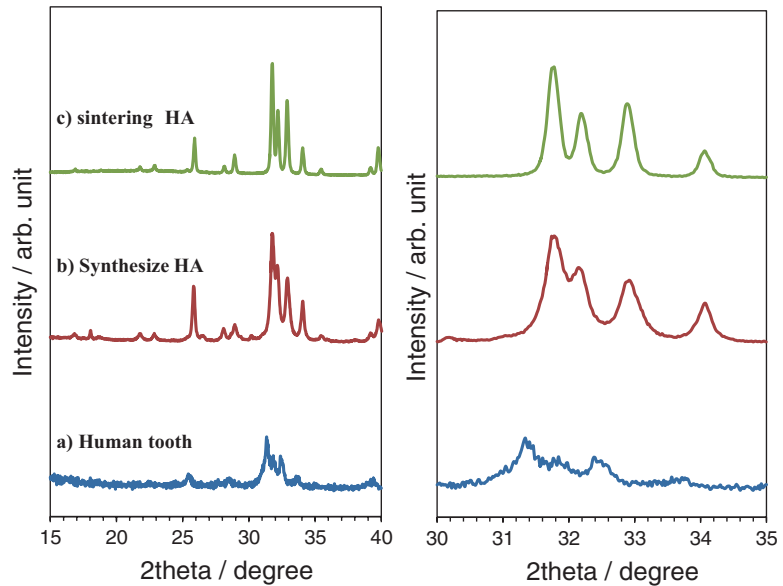
Figure 18.5 shows the typical XRD pattern of samples before and after hydrothermal treatment at different hydrothermal temperature (100 °C, 150 °C and 180 °C) and different hydrothermal time (0 h, 12 h and 24 h). The XRD of  $\text{Ca(OH)}_2$  starting materials and HA standard are shown as reference. Basically, at 100 and 150 °C, the  $\text{Ca(OH)}_2$  is still remained up to 24 h reaction (Fig. 18.5a–f). However, when elevate the hydrothermal temperature up to 180 °C, HA single crystal phase can be obtain after 12 and 24 h, respectively (Fig. 18.5h–i). The synthesis condition of hydrothermal reaction at 180 °C for 24 h is selected to synthesis HA for the next experiment.

Figure 18.6 shows the typical XRD image of human tooth; synthesize HA by hydrothermal condition at 180 °C for 24 h and sintering HA at 900 °C. Basically, the synthesize HA by hydrothermal condition has the crystal structure



**Fig. 18.5** XRD pattern of samples before and after hydrothermal treatment at different hydrothermal temperature (100 °C, 150 °C and 180 °C) and different hydrothermal time (0 h, 12 h and 24 h)

**Fig. 18.6** XRD pattern of (a) human tooth, (b) synthesize HA by hydrothermal condition at 180 °C for 24 h and (c) sintering HA at 900 °C

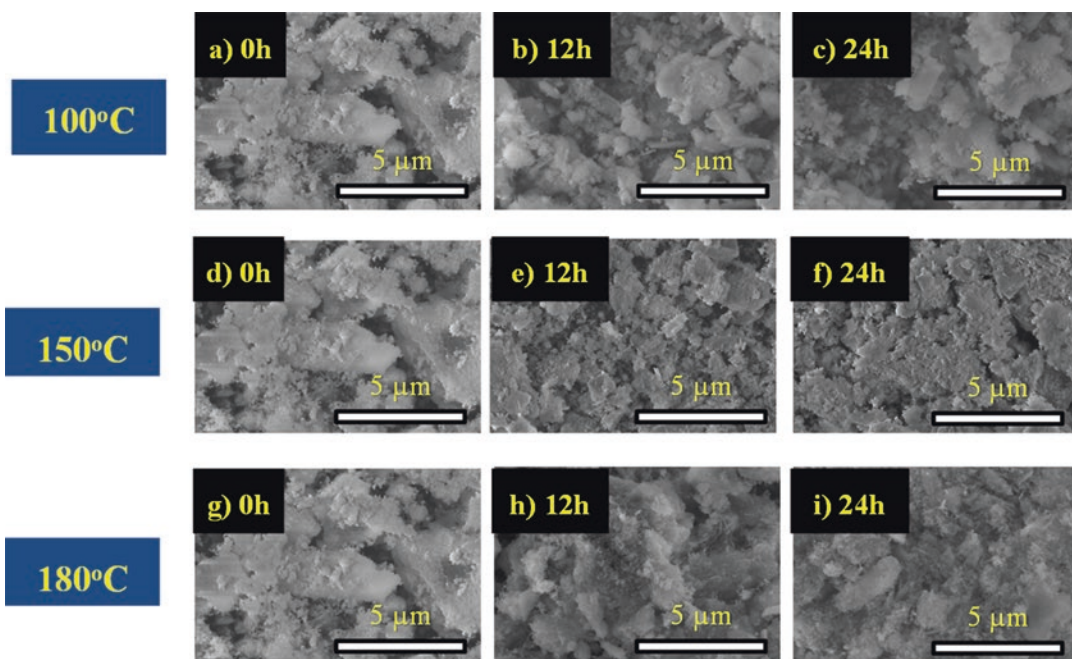


**Fig. 18.7** FTIR patterns of samples before and after hydrothermal treatment at different hydrothermal temperature (100 °C, 150 °C and 180 °C) and different hydrothermal time (0 h, 12 h and 24 h)

similar with that of human teeth. However, the peak shifting at 31.8° can be observed at synthesis HA and sintering HA. It can be explain that in human tooth, there is the minor trace of another element like Zn, Mg, Si co-exist, and substitute to the network of human tooth.

Figure 18.7 shows the FTIR patterns of samples before and after hydrothermal treatment at different hydrothermal temperature (100 °C, 150 °C and 180 °C) and different hydrothermal time (0 h, 12 h and 24 h). The FTIR of Ca(OH)<sub>2</sub> starting materials and HA





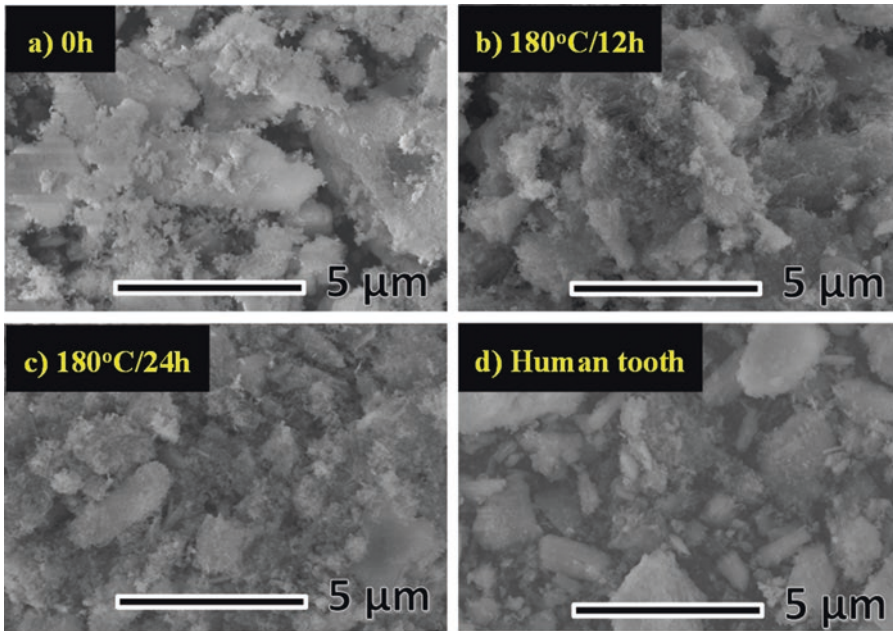
**Fig. 18.8** Typical morphology of samples at magnification of 10,000X before and after hydrothermal treatment at different hydrothermal temperature (100 °C, 150 °C and 180 °C) and different hydrothermal time (0 h, 12 h and 24 h)

standard are shown as reference. Basically, the chemical bonding of  $\text{PO}_4^{3-}$  can be observed at  $1100\text{ cm}^{-1}$  while the present of  $\text{HPO}_4^{2-}$  can be found at  $560$  and  $605\text{ cm}^{-1}$ . In addition, we can observe the CO bonding at  $1458\text{ cm}^{-1}$ . These CO bonding might be derived from  $\text{CO}_2$  in atmosphere, due to the highly absorption of  $\text{CO}_2$  from  $\text{Ca}(\text{OH})_2$  starting materials. There is no different in chemical bonding at  $150\text{ °C}$  and  $180\text{ °C}$ . these data are support for XRD data shown in Figs. 18.5 and 18.6.

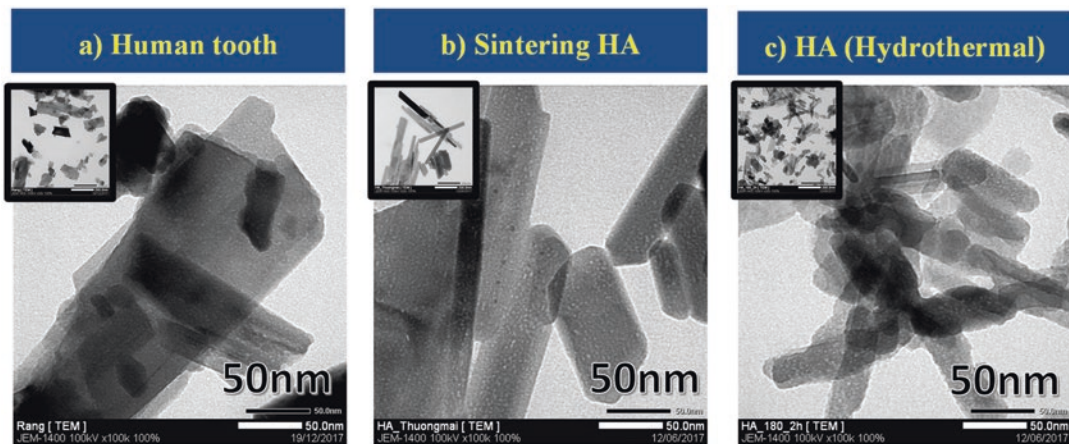
Figure 18.8 shows typical morphology of samples at magnification of 10,000X before and after hydrothermal treatment at different hydrothermal temperature ( $100\text{ °C}$ ,  $150\text{ °C}$  and  $180\text{ °C}$ ) and different hydrothermal time (0 h, 12 h and 24 h). After hydrothermal reaction, the sample contain many needle-like shape crystal and interlock together. The size of needle-like shape crystal increase with the increasing of hydrothermal temperature.

Figure 18.9 shows typical morphology of sample before and after hydrothermal reaction at  $180\text{ °C}$  for 12 and 24 h. In addition, the morphology of human tooth also show as reference. The morphology of  $180\text{ °C}$ -hydrothermal treated-HA is similar with that of human tooth, indicate that  $180\text{ °C}$ -hydrothermal treated-HA can be used as excellent candidate for bone substitute.

Figure 18.10 shows the typical TEM images of human tooth, synthesize HA by hydrothermal condition at  $180\text{ °C}$  for 24 h and sintering HA at  $900\text{ °C}$  at 100,000X. The upper-left photo show the same condition with the magnification of 30,000X. The  $180\text{ °C}$ -hydrothermal treated-HA has needle-like shape structure with the average diameter of  $10\text{ ~ }20\text{ nm}$  and length of below  $100\text{ nm}$ . These nano structure of  $180\text{ °C}$ -hydrothermal treated-HA is very similar with that of human tooth, indicate that  $180\text{ °C}$ -hydrothermal treated-HA can be used as bone substitute materials.



**Fig. 18.9** Typical morphology of (a) sample before hydrothermal reaction; (b) hydrothermal reaction at 180 °C for 12 h; (c) hydrothermal reaction at 180 °C for 24 h and (d) human tooth



**Fig. 18.10** Typical TEM images of (a) human tooth; (b) sintering HA at 900 °C and (c) synthesize HA by hydrothermal condition at 180 °C for 24 h at 100,000X. The upper-left images show the TEM at 30,000X

## 18.4 Conclusions

In this report, the author reviewed the trend of HA synthesis as well as report the process to fabricate nanostructure HA by co-precipitation

method of  $\text{Ca}(\text{OH})_2$  and  $\text{H}_3\text{PO}_4$  follow by hydrothermal reaction method. The hydrothermal treated-HA has needle-like shape with the diameter of 10 ~ 20 nm and length of below 100 nm, which is similar with human bone. For the hydro-

thermal reaction, temperature is the key to form nanostructure HA. These data will be useful for researcher who are looking for different forms of nanostructure HA to suit their intended application.

**Acknowledgement** This research is funded by Vietnam National University Ho Chi Minh City (VNU-HCM) under grant number B2015-20a-01. Some of the material characterization facility is supported by National key lab for Polymer and Composite Materials-HCMUT, VAST and HUFU.

## References

- Driscoll P (2006) Advanced medical technology [Online]. [Accessed 2 Mar 2012]. Available from World Wide Web: <http://mediligence.com/blog/?cat=5>
- Zhao B, Hu H, Mandal SK, Haddon RC (2005) A bone mimic based on the self-assembly of hydroxyapatite on chemically functionalized single-walled carbon nanotubes. *Chem Mater* 17:3235–3241. <http://sci-hub.tw/10.1021/cm0500399>
- Wagner DE, Eisenmann KM, Nestor-Kalinowski AL, Bhaduri SB (2013) A microwave-assisted solution combustion synthesis to produce europium-doped calcium phosphate nanowhiskers for bioimaging applications. *Acta Biomaterialia* 9:8422–8432. <http://sci-hub.tw/10.1016/j.actbio.2013.05.033>
- Wei X, Yates MZ (2012) Yttrium-doped hydroxyapatite membranes with high proton conductivity. *Chem Mater* 24:1738–1743. <http://sci-hub.tw/10.1021/cm203355h>
- Watanabe Y, Ikoma T, Suetsugu Y, Yamada H, Tamura K, Komatsu Y, Tanaka J, Moriyoshi Y (2006) The densification of zeolite/apatite composites using a pulse electric current sintering method: a long-term assurance material for the disposal of radioactive waste. *J Eur Ceram Soc* 26:481–486 <http://sci-hub.tw/10.1016/j.jeurceramsoc.2005.07.032>
- Power AS (1969) Crystal chemistry of bone minerals. *Phys Rev* 49:760–792. <http://sci-hub.tw/10.1152/physrev.1969.49.4.760>
- Radin SR, Ducheyne P (1993) The effect of calcium phosphate ceramic composition and structure on in-vitro behavior. *J Biomed Mater Res* 27:35. <http://sci-hub.tw/10.1002/jbm.820270105>
- Bett JAS, Christener LG, Hall WK (1967) Hydrogen held by solids XII. Hydroxyapatite catalysts. *J Am Chem* 89:5535. <http://sci-hub.tw/10.1021/ja00998a003>
- Joris SJ, Amberg CH et al (1971) *J Phys Chem* 75:3167. <http://sci-hub.tw/10.1021/j100689a024>
- Korber F, Trömel GZ (1932) The formation of HA through a solid-state reaction between tri- and tetra-calcium phosphates. *Electrochem Soc* 38:578–580
- Trömel GZ (1932) Untersuchungen über die Bildung eines halogenfreien Apatits aus basischen Calciumphosphaten. *Physik Chem* 158:422–432. <http://sci-hub.tw/10.1515/zpch-1932-15832>
- Ikoma T, Yamazaki A, Nakamura S, Akao M (1999) Preparation and structure refinement of monoclinic hydroxyapatite. *J Solid State Chem* 144:272–276. <http://sci-hub.tw/10.1006/jssc.1998.8120>
- Tao J, Jiang W, Pan H, Xu X, Tang R (2007) Preparation of large-sized hydroxyapatite single crystals using homogeneous releasing controls. *J Cryst Growth* 308:151–158. <http://sci-hub.tw/10.1016/j.jcrysgro.2007.08.009>
- Zhang Y, Lu J (2008) A mild and efficient biomimetic synthesis of rodlike hydroxyapatite particles with a high aspect ratio using polyvinylpyrrolidone as capping agent. *Cryst Growth Des* 8:2101–2107. <http://sci-hub.tw/10.1021/cg060880e>
- Shum HC, Bandyopadhyay A, Bose S, Weitz DA (2009) Double emulsion droplets as microreactors for synthesis of mesoporous hydroxyapatite. *Chem Mater* 21:5548–5555. <http://sci-hub.tw/10.1021/cm9028935>
- Zhou W, Wang M, Cheung W, Guo B, Jia D (2008) Synthesis of carbonated hydroxyapatite nanospheres through nanoemulsion. *J Mater Sci Mater Med* 19:103–110. <http://sci-hub.tw/10.1007/s10856-007-3156-9>
- Ethirajan A, Ziener U, Chuvilin A, Kaiser U, Cölfen H, Landfester K (2008) Biomimetic hydroxyapatite crystallization in gelatin nanoparticles synthesized using a miniemulsion process. *Adv Funct Mater* 18:2221–2227. <http://sci-hub.tw/10.1002/adfm.200800048>
- Sturgeon JL, Brown PW (2009) Effects of carbonate on hydroxyapatite formed from CaHPO<sub>4</sub> and Ca<sub>4</sub>(PO<sub>4</sub>)<sub>2</sub>O. *J Mater Sci Mater Med* 20:1787–1794. <http://sci-hub.tw/10.1007/s10856-009-3752-y>
- Park H, Baek D, Park Y, Yoon S, Stevens R (2004) Thermal stability of hydroxyapatite whiskers derived from the hydrolysis of  $\alpha$ -TCP. *J Mater Sci* 39:2531–2534
- Sakamoto K, Yamaguchi S, Nakahira A, Kaneno M, Okazaki M, Ichihara J, Tsunawaki Y, Elliott JC (2002) Shape-controlled synthesis of hydroxyapatite from  $\alpha$ -tricalcium bis(orthophosphate) in organic-aqueous binary systems. *J Mater Sci* 37:1033–1041
- Durucan C, Brown PA (2000)  $\alpha$ -Tricalcium phosphate hydrolysis to hydroxyapatite at and near physiological temperature. *J Mater Sci Mater Med* 11:365–371
- Graham S, Brown PW (1996) Reactions of octacalcium phosphate to form hydroxyapatite. *J Cryst Growth* 165:106–115. [http://sci-hub.tw/10.1016/0022-0248\(95\)00994-9](http://sci-hub.tw/10.1016/0022-0248(95)00994-9)
- De Maeyer EAP, Verbeeck RMH, Pieters IY (1996) Effect of K<sup>+</sup> on the stoichiometry of carbonated hydroxyapatite obtained by the hydrolysis of monetite. *Inorg Chem* 35:857–863. <http://sci-hub.tw/10.1021/ic950916k>
- Kim I, Kumta PN (2004) Sol-gel synthesis and characterization of nanostructured hydroxyapatite

- powder. *Mater Sci Eng B* 111:232–236. <http://sci-hub.tw/10.1016/j.mseb.2004.04.011>
25. Feng W, Mu-Sen L, Yu-Peng L, Yong-Xin Q (2005) A simple sol–gel technique for preparing hydroxyapatite nanopowders. *Mater Lett* 59:916–919. <http://sci-hub.tw/10.1016/j.matlet.2004.08.041>
  26. Rajabi-Zamani AH, Behnamghader A, Kazemzadeh A (2008) Synthesis of nanocrystalline carbonated hydroxyapatite powder via nonalkoxide sol–gel method. *Mater Sci Eng C* 28:1326–1329. <http://sci-hub.tw/10.1016/j.msec.2008.02.001>
  27. Hsieh MF, Perng LH, Chin TS, Perng HG (2001) Phase purity of sol–gel-derived hydroxyapatite ceramic. *Biomaterials* 22:2601–2607. [http://sci-hub.tw/10.1016/S0142-9612\(00\)00448-8](http://sci-hub.tw/10.1016/S0142-9612(00)00448-8)
  28. Eshtiagh-Hosseini H, Housaindokht MR, Chahkandi M (2007) Effects of parameters of sol–gel process on the phase evolution of sol–gel-derived hydroxyapatite. *Mater Chem Phys* 106:310–316. <http://sci-hub.tw/10.1016/j.matchemphys.2007.06.002>
  29. Chen J, Wang Y, Chen X, Ren L, Lai C, He W, Zhang Q (2011) A simple sol–gel technique for synthesis of nanostructured hydroxyapatite, tricalcium phosphate and biphasic powders. *Mater Lett* 65:1923–1926. <http://sci-hub.tw/10.1016/j.matlet.2011.03.076>
  30. Velu G, Gopal B (2009) Preparation of nanohydroxyapatite by a sol–gel method using alginate acid as a complexing agent. *J Am Ceram Soc* 92:2207–2211. <http://sci-hub.tw/10.1111/j.1551-2916.2009.03221.x>
  31. Zhang H, Zhang M (2011) Phase and thermal stability of hydroxyapatite whiskers precipitated using amine additives. *Ceram Int* 37:279–286. <http://sci-hub.tw/10.1016/j.ceramint.2010.08.038>
  32. Guo X, Xiao P, Liu J, Shen Z (2005) Fabrication of nanostructured hydroxyapatite via hydrothermal synthesis and spark plasma sintering. *J Am Ceram Soc* 88:1026–1029. <http://sci-hub.tw/10.1111/j.1551-2916.2005.00198.x>
  33. Tsiourvas D, Tsetsekou A, Kammenou MI, Boukos N (2011) Controlling the formation of hydroxyapatite nanorods with dendrimers. *J Am Ceram Soc* 94:2023–2029. <http://sci-hub.tw/10.1111/j.1551-2916.2010.04342.x>
  34. Zhang H, Darvell BW (2011) *Biomaterials* 7:2960–2968
  35. Lin K, Liu X, Chang J, Zhu Y (2011) Facile synthesis of hydroxyapatite nanoparticles, nanowires and hollow nano-structured microspheres using similar structured hard-precursors. *Nanoscale* 3:3052–3055. <http://sci-hub.tw/10.1039/c1nr10334b>
  36. Lee DK, Park JY, Kim MR, Jang DJ (2011) Facile hydrothermal fabrication of hollow hexagonal hydroxyapatite prisms. *CrystEngComm* 13:5455–5459. <http://sci-hub.tw/10.1039/C1CE05511A>
  37. Zhu K, Yanagisawa K, Onda A, Kajiyoshi K, Qiu J (2009) Morphology variation of cadmium hydroxyapatite synthesized by high temperature mixing method under hydrothermal conditions. *Mater Chem Phys* 113:239–243. <http://sci-hub.tw/10.1016/j.matchemphys.2008.07.049>
  38. Cao H, Zhang L, Zheng H, Wang Z (2010) Hydroxyapatite nanocrystals for biomedical applications. *J Phys Chem C* 114:18352–18357. <http://sci-hub.tw/10.1021/jp106078b>
  39. Zhang G, Chen J, Yang S, Yu Q, Wang Z, Zhang Q (2011) Preparation of amino-acid-regulated hydroxyapatite particles by hydrothermal method. *Mater Lett* 65:572–574. <http://sci-hub.tw/10.1016/j.matlet.2010.10.078>
  40. Pham Trung Kien, Tsuru Kanji, Kunio Ishikawa (2015) Development and characterization of porous calcium phosphate cement using  $\alpha$ -tricalcium phosphate bead. In: Vo Van Toi, Tran Ha Lien Phuong (eds) 5th international conference on biomedical engineering in Vietnam. IFMBE proceedings, pp 507–510. [http://sci-hub.tw/10.1007/978-3-319-11776-8\\_125](http://sci-hub.tw/10.1007/978-3-319-11776-8_125)
  41. Nguyen Viet Long, Masayuki Nogami, Yong Yang, Michitaka Ohtaki, Pham TrungKien, Cao Minh Thi (2014) Magnetic metal and oxide based nanoparticles and biomaterials for bioimaging probes for magnetic resonance imaging, Chapter 6. In: Govil JN (ed) *Nanotechnology, Volume 12: bioimaging*. Studium Press LLC, pp 205–221
  42. Pham Trung Kien, Vang Nguyen Hoang Van, Tran Pham Quang Nguyen, Pham Thi Lan Thanh (2018) Evaluation effect of stirring mode on synthesize Hydroxyapatite crystallite used as bone substitute. In: The 6th international conference on biomedical engineering in Vietnam, Ho Chi Minh City, Vietnam, pp 331–334
  43. Pham Trung Kien, Tsuru Kanji, Kunio Ishikawa (2015) Setting reaction of  $\alpha$ -TCP spheres and an acidic calcium phosphate solution for the fabrication of fully interconnected macroporous calcium phosphate. *Ceram Int* 41:13525–13531. <http://sci-hub.tw/10.1016/j.ceramint.2015.07.146>
  44. Kien Pham Trung, Minh Do Quang, Thanh Pham ThiLan (2014) Iron-free hydroxyapatite powder from synthetic Ca(OH)<sub>2</sub> and commercialized Ca(OH)<sub>2</sub>. *Adv Mater Res* 858:103–110
  45. Kunio Ishikawa, Kanji Tsuru, Trung Kien Pham, Michito Maruta, Shigeki Matsuya (2012) Fully-interconnected pore forming calcium phosphate cement. *Key Eng Mater* 493–494:832–835
  46. Pham Trung Kien, Michito Maruta, Kanji Tsuru, Shigeki Matsuya, Kunio Ishikawa (2010) Effect of phosphate solution on setting reaction of  $\alpha$ -TCP spheres. *J Aust Ceram Soc* 46(2):63–67
  47. Radzali Othman, Ahmad Fauzi, Pham Trung Kien, Kunio Ishikawa, Do Quang Minh (2007) Preparation and characterization of  $\beta$ -tricalcium phosphate. *Malaysia J Microsc* 3:193–198



# Modification of Titanium Implant and Titanium Dioxide for Bone Tissue Engineering

Tae-Keun Ahn, Dong Hyeon Lee, Tae-sup Kim, Gyu chol Jang, SeongJu Choi, Jong Beum Oh, Geunhee Ye, and Soonchul Lee

## Abstract

Bone tissue engineering using titanium (Ti) implant and titanium dioxide (TiO<sub>2</sub>) with their modification is gaining increasing attention. Ti has been adopted as an implant material in dental and orthopedic fields due to its superior properties. However, it still requires modification in order to achieve robust osteointegration between the Ti implant and surrounding bone. To modify the Ti implant, numerous methods have been introduced to fabricate porous implant surfaces with a variety of coating materials. Among these, plasma spraying of hydroxyapatite (HA) has been the most commonly used with commercial success. Meanwhile, TiO<sub>2</sub> nanotubes have been actively studied as the coating material for implants, and promising results have been reported about improving osteogenic activity around implants recently. Also porous three-dimensional constructs based on TiO<sub>2</sub> have

been proposed as scaffolding material with high biocompatibility and osteoconductivity in large bone defects. However, the use of the TiO<sub>2</sub> scaffolds in load-bearing environment is somewhat limited. In order to optimize the TiO<sub>2</sub> scaffolds, studies have tried to combine various materials with TiO<sub>2</sub> scaffolds including drug, mesenchymal stem cells, Al<sub>2</sub>O<sub>3</sub>-SiO<sub>2</sub> solid and HA. This article will shortly introduce the properties of Ti and Ti-based implants with their modification, and review the progress of bone tissue engineering using the TiO<sub>2</sub> nanotubes and scaffolds.

## Keywords

Titanium · Implant · Titanium dioxide · Nanotube · Scaffold · Bone

Authors Tae-Keun Ahn and Dong Hyeon Lee have been equally contributed to this chapter.

T.-K. Ahn · T.-s. Kim · G. c. Jang · S. Choi · J. B. Oh  
G. Ye · S. Lee (✉)

Department of Orthopaedic Surgery, CHA Bundang Medical Center, CHA University School of Medicine, Gyeonggi-do, South Korea  
e-mail: [lsceline78@gmail.com](mailto:lsceline78@gmail.com)

D. H. Lee  
Department of Physiology, CHA University School of Medicine, Gyeonggi-do, South Korea

## 19.1 Bone Tissue Engineering

Skeletal injuries account for 25–30% of all musculoskeletal pathologies, and as life expectancy continues to increase in developed country, the incidence is rising gradually [90]. Orthopedic or dental implants, such as plate with screws or joint prostheses, are commonly used as the initial treatment for bone disorders including fracture, osteoarthritis and bone defect after tumor resection etc. Titanium (Ti) is presently the most popular material for these implants with good

biocompatibility [1]. Although recent advances of Ti implant provide the early rigid fixation and bone has the regeneration capacity by itself, certain conditions such as major trauma, chronic infection, large musculoskeletal tumor resection and previous implant failure can still lead to impaired bone healing or major bone defects.

The autologous bone graft from iliac crest is considered the gold standard for enhancing bone healing in bone defect [37]. However, the procedure has drawbacks, including requiring another surgical incision, sometimes not being sufficient for treatment, and having several complications such as pain, neurologic injury, infection and hematoma [16]. Overall, additional strategies and investigations are necessary for bone tissue engineering. A variety of approaches including allograft, implant surface modification, synthetic implant fabrication, and cell-based therapies are being studied in tissue engineering [55].

In recent years, there has been appreciable interest in bone tissue engineering strategies, which utilizes modified Ti implants and titanium dioxide (TiO<sub>2</sub>). Notably, TiO<sub>2</sub> nanotube and scaffold technologies are currently under study for novel bone tissue engineering with their osteoconductive and osteoinductive capabilities. This article will briefly introduce the properties of Ti and modified Ti-based implants, and review the research progress of bone tissue engineering, using TiO<sub>2</sub> nanotube and scaffold in detail.

---

## 19.2 Ti

### 19.2.1 Ti Implant

Biocompatibility without causing inflammatory response and mechanical durability is important attribute in both temporary and permanent implants [54]. Originally used in aeronautics, Ti and its alloys have been of large interest in biomedical applications because of their special properties such as bioinertness, excellent biocompatibility, high fatigue and tensile strengths, low allergenicity and light in weight [1]. In addition, Ti is one of the most abundant elements on the Earth and is distributed in natural mineral

deposits, principally rutile and ilmenite, making it more accessible. On top of that, Ti biomaterials are osteoconductive as they induce new bone formation and form tight bonds with newly formed bones. As a result, the usage of Ti has been successful in orthopedic and dental applications, especially in implantation.

Among the various Ti biomaterials, commercially pure Ti, ASTM F67 and Ti6Al4V are widely used in orthopedic and dental fields. Generally, commercially pure Ti with a single phase alpha microstructure is often used in dental implants, while Ti6Al4V with a two-phase alpha-beta microstructure is most commonly used in orthopedics. Other various types of Ti alloys are summarized in supplemental Table 19.1 [46]. However, still Ti-based implant has the disadvantages including difficulty in achieving a sufficient chemical bond with surrounding bone, particularly during the early stage of implantation due to Ti-based implant being bioinert by nature [23]. Another limitation of Ti-based implant is the substantial mismatch between Young's modulus of Ti ( $E \frac{1}{4}$  100–110 GPa) and that of cortical bone ( $E \frac{1}{4}$  5–27 GPa), which generates a stress-shielding effect at the bone/implant interface [76]. Therefore, it is necessary to modify Ti-based implants in order to properly promote osteogenesis, osteoconduction and osteointegration.

### 19.2.2 Modification of Ti or Ti Alloy Implant Surface

Implants have been developed over three generations. The first generation implants were pure metal that were accidentally discovered. Second generation implants focused on becoming a tissue replacement by matching their physical properties with high biocompatibility and bioinertness. Surface treatments were used to improve the bioactive nature of these implants, especially metals such as Ti alloys that change the physicochemical, mechanical, and electrical properties of their surfaces. The third-generation biomaterials are new materials which can stimulate specific cellular responses at the molecular level. To this

**Supplemental Table 19.1** Various type of Ti alloys and their properties

Material	Tensile strength (MPa)	Yield strength (MPa)	Type
Commercially pure Ti-1 (grade 1–4)	241–552	172–483	$\alpha$
Commercially pure porous Ti	—	—	$\alpha$
Ti-3Al-2.5 V	690	586	$\alpha/\beta$
Ti-5Al-2.5Fe	—	—	$\alpha/\beta$
Ti-5Al-3Mo-4Zr	—	—	$\alpha/\beta$
Ti-6Al-4 V	931	862	$\alpha/\beta$
Ti-6Al-4 V ELI	862	793	$\alpha/\beta$
Ti-6Al-7Nb	862	793	$\alpha/\beta$
Ti-20Cr-0.2Si	874	669	—
Ti-13Cu-4.5Ni	703	—	—
Ti-15Mo	793	655	$\beta$
Ti-15Mo-6Zr-2Fe	1000	965	$\beta$
Ti-12Mo-5Zr-5Sn	—	—	$\beta$
Ti-15Mo-5Zr-3Al	—	—	$\beta$
Ti-15Mo-2.8Nb-0.2Si-0.26O	793	655	$\beta$
Ti-45Nb	483	448	$\beta$
Ti-13Nb-13Zr	860	725	$\beta$
Ti-16Nb-10Hf	486	276	$\beta$
Ti-29Nb-13Ta-4.6Zr	—	—	$\beta$
Ti-35Nb-7Zr-5Ta	827	793	$\beta$
Ti-55.8Ni	1034	345	Intermetallic
Ti-30Ta	—	—	$\beta$
Ti-40Ta	—	—	$\beta$
Ti-50Ta	—	—	$\beta$
Ti-35Zr-10Nb	897	621	$\beta$
Ti-15Zr-4Nb-2Ta-0.2Pd	—	—	$\alpha/\beta$
Ti-15Sn-4Nb-2Ta-0.2Pd	—	—	$\alpha/\beta$
Ti-20Pd-5Cr	880	659	—

end, the bioactivity and biodegradability concepts are combined, as bioabsorbable materials become bioactive and vice versa [32].

Based on these concepts, various methods for modifying Ti or Ti alloy implants have been developed so far in order to obtain high strength and biocompatibility with excellent cellular response at the same time (Table 19.1). Currently, research on the fabrication of porous or rough implant surface with or without material or chemical coating is the most studied [42].

### 19.2.2.1 Porous or Rough Implant Surface

Porous or coarse implant surfaces are well known to improve bone formation by increasing the surface area of implants, cell migration, and attachment to implants. However, there is still

**Table 19.1** Techniques to fabricate porous implant surface

Subtractive techniques	Additive techniques
Blasting	Plasma spraying
Acid etching	Electron-discharge compaction
Anodization	Microwave method
Electro/mechanical polishing	Powder metallurgy (sintering or thermal decomposition)
	Removal of space holder with metal powder particles
	Rapid prototyping
	Biomimetic coating

controversy for the ideal pore size. A pore size of more than 100  $\mu\text{m}$  and a porosity of up to 85% are considered to be optimal for rapid bone ingrowth [92]. However, Wen et al. reported that porous Ti with pore size ranging from 200–

500  $\mu\text{m}$  was good enough for satisfactory bone formation and fluid transport [88]. Otsuki et al. stated that the ideal pore size for bone tissue ingrowth for both levels of porosity was between 500–1500  $\mu\text{m}$  whereas Murphy et al. reported that the optimal pore size for bone ingrowth was approximately 325  $\mu\text{m}$  [56].

Porous implant surface can be constructed by subtractive procedures or additive techniques. The implant subtraction procedure can be implemented through physical, chemical or electrical methods. Typical subtractive techniques include large-grit sands or particle blasting, acid etching and anodization [42]. Blasting is a technique that forces the flow of abrasive material ( $\text{TiO}_2$  or calcium phosphate) to the surface under high pressure to smoothen the rough surface or roughen a smooth surface [28]. Acid etching, which treat acids to form pits on the surface of Ti implant, can be combined with other methods, such as blasting [39]. Anodization is a technique that expands the thickness of the natural oxide layer on the surface of metal components. In any case, the anodically oxidized surfaces have a positive effect on osteoblast behavior and osteointegration.

Next, extensive research was conducted on preparing porous or rough implant surfaces with additive techniques including (1) Thermal spray with different powder particles, (2) Electron-discharge compaction, (3) Biomimetic deposition, etc. [24, 48, 84].

Thermal spraying is the most commonly used method that sprays diverse powdered material to roughen the implant surface. Thermal spraying involves four main process groups: (1) Spray combustion processes, (2) Electric arc spray process, (3) Cold spray, (4) Plasma spray process. A major advantage of thermal spraying is the exceedingly wide array of materials that can be used to produce coatings [24]. Recently, biomimetic coating has emerged as a promising technique as it enables bone formation by immersing substrates in a simulated body fluid solution maintained at 37 °C *in vitro*, a solution that has a very similar ion concentration to that of human body plasma. The technique defines the ability to form a bone-like, carbonated hydroxyapatite (HA) layer [74]. Biomimetic coating method has

been reported to have several advantages which include providing increased control over the chemical composition of the coating, generating a homogeneous film, creating a structure close to bone apatite, decreasing densification temperature, and being sufficient for coating on complex-shaped porous implants [84]. Owing to biomimetic coating technology, cytokine-based engineering, poly(dopamine)-assisted immobilization of Arg-Gly-Asp peptides, hydroxyapatite, or cyclic Arg-Gly-Asp with heparin binding peptide is gaining more attention at the moment [12, 50, 63]. Studies also have shown that the co-deposition of bone morphogenic protein (BMP) with biomimetic calcium phosphate coating can promote the proliferation and differentiation capability of Ti surfaces [95]. The clustering integrin-specific ligands promoted functional integration of the coated Ti implant *in vivo* study [66].

### 19.2.2.2 Various Coating Materials to Enhance Local Cellular Response

Many reports demonstrated that coated Ti surfaces have a significant effect on early events of cellular response, such as the protein absorption, blood clot formation, and cell behaviors occurring upon implantation. Coating materials can be broadly classified into (1) HA based bioceramics, (2) Metal ion incorporated coatings, (3) Extracellular matrix components and/or Growth factors, (4) Drugs, (5)  $\text{TiO}_2$  nanotubes (Table 19.2) [93].

**Table 19.2** Various coating materials

Category	Materials
Calcium phosphate	Hydroxyapatite, tri-calcium phosphate (TCP), bi-phasic phosphate
Metal ions	Calcium, magnesium, fluoride, phosphorous
Growth factor	BMP2, FGF2, IGF-1, IGF-2, TGF- $\beta$ 1, TGF- $\beta$ 2, PDGF
Extracellular matrix	Collagen 1, chondroitin sulfate, RGD peptide, DLTIDDSYWYRI peptide, GFOGER peptide
Drug	Bisphosphonates, strontium, dopamine
$\text{TiO}_2$	Various diameter (15 – 100 nm)



HA is one of the most popular materials for the implant coating with commercial success to date [8, 21]. Traditionally, HA was coated by plasma spraying and have been thought to be osteoconductive. However, HA biomaterials with specific three-dimensional geometries have been shown to bind to endogenous BMPs and osteoblasts directly formed osteoid on HA surface coating, implying that the bone-implant interface is bonded both chemically and biologically to the HA [26]. Thus, some researchers have labeled the material with osteoinductive features [44]. HA is a relatively insoluble calcium ceramic compared to tri-calcium phosphate (TCP). Coatings consisting of a combination of HA and TCP are known as bi-phasic calcium phosphates. The TCP easily dissolves in the body, releasing more ions and increasing the amount of carbonated HA formed on the surface [15, 89]. Furthermore, adding calcium, phosphorus, magnesium and fluoride (F) ions to Ti implants improves osteointegration through apatite deposition [11]. This osteointegrative activity is reported to be mediated by increased osteogenic differentiation of mesenchymal stem cells (MSCs) through integrins  $\alpha 1$ ,  $\alpha 2$ ,  $\alpha 5$ , and  $\beta 1$ , and upregulated BMP-2 secretion by osteoblasts ([14, 59]; J. W. [65, 96]).

Bone stimulants of the transforming growth factor superfamily, particularly BMP, transforming growth factor- $\beta 1$ , platelet-derived growth factor and insulin-like growth factor can be coated to improve the bone healing process locally. BMP-2, which promotes the osteoblastic differentiation of MSCs, is the most commonly used growth factor to achieve osteointegration of implants [41]. Sustained release technique is also being used to coat BMP-2 on implants due to the recently reported risk of ectopic bone formation or tumorigenesis by bolus delivery of BMP-2 [9]. A study led by Bae et al. suggested that the combined coating of BMP-2 and calcium phosphate with biodegradable polymers and extracellular matrix for Ti implants prolonged BMP-2 release and had the improved osteogenesis [5, 31, 40]. In addition,

recent attempts have been made to introduce BMP-2 DNA plasmids using cell transfections that promote sustained BMP-2 secretion [11, 36, 70].

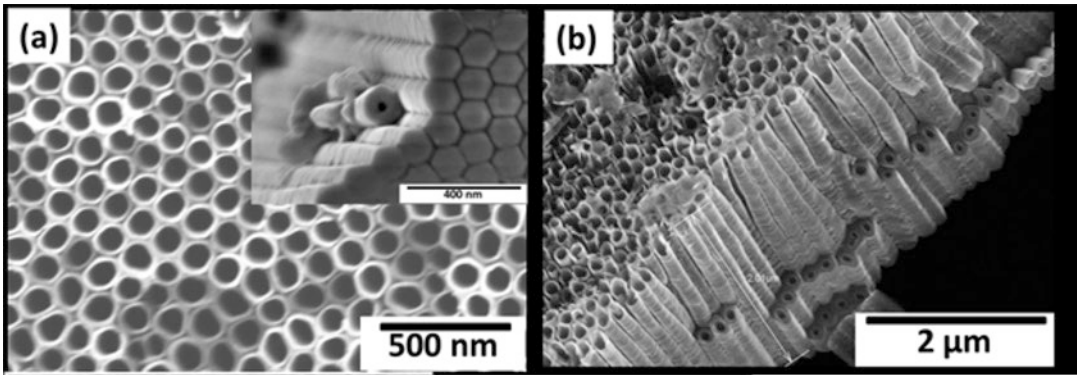
Incorporation of bisphosphonate, such as pamidronate or zoledronate, may be relevant for clinical cases lacking bone support. Bisphosphonate inhibits osteoclast-induced bone resorption and promotes net bone regeneration and osteointegration of osteoporotic healthy bone [22]. Incorporation of strontium, another effective anti-osteoporosis drug, also improved bone formation *in vivo* [3]. Dopamine may be one of the widely used materials for the modification of implant [35, 87, 91].

At last, given the differentiating effects of nanophase structures on osteoblasts, some researchers have proposed TiO<sub>2</sub> nanotube as a means of developing nano-textured implant coatings. This will be discussed in more detail in the following TiO<sub>2</sub> nanotube section.

---

### 19.3 TiO<sub>2</sub>

TiO<sub>2</sub> has been shown to have excellent biocompatibility, the ability of osteoconduction especially when in contact with bone tissue. In the living human body, TiO<sub>2</sub> layer is naturally formed when Ti is exposed to atmospheric or other oxygen-containing environments. However, the spontaneously formed TiO<sub>2</sub> layer on the Ti implant surface, composed of soft and dense TiO<sub>2</sub>, can form a fibrous tissue which prevents osteoblastic cells from strongly adhering onto the surface, leading to the loosening of implant and inflammation [58]. Therefore, numerous studies have reported cases in which the osteogenic effect increased when TiO<sub>2</sub> scaffold and nanotube were combined with other materials [49]. Moreover, porous three-dimensional TiO<sub>2</sub> scaffold has been proposed as a promising material for inducing bone formation from the surrounding tissue in the restoration of critical bone defects [30, 78].



**Fig. 19.1** Scanning electron microscope view of  $\text{TiO}_2$  nanotube arrays (a) Top view (b) Overview. (Reprinted from [75])

### 19.3.1 $\text{TiO}_2$ Nanotube

A major challenge in orthopedic biomaterials is the design of material surfaces which provide optimal osteointegration and at the same time promote durability of the implant. If the surface properties of the biomaterial cannot ensure a stable fixation between the implant surface and surrounding tissue, leading to a fibrous layer undermining load transmission at the bone/implant interface, micro movements would be favored and result in implant failure [53].

Studies have been conducted to select the optimal surface topography for bio applications, and a considerable amount have shown that nanomodifications of the implant surface can affect cellular physiology. Such modifications can allow the implant to mimic the natural extracellular matrix at the nanoscale level [13]. In addition, there was a correlation between nano-level surface structure and cellular functionalities, including improved osteointegration and increased osteogenic differentiation of MSCs [17, 20].

Among the numerous nanostructures available,  $\text{TiO}_2$  nanotube has been widely studied [60, 80].  $\text{TiO}_2$  nanotube was first described by Zwillig et al. in 1991 as “Columnar porous  $\text{TiO}_2$  layers formed electrochemically in fluorinated electrolyte.” [97].  $\text{TiO}_2$  nanotubes coated Ti implant showed superior corrosion resistance and biocompatibility than pure Ti; moreover, the modulus of elasticity was much closer to that of native bone than that of pure Ti [58].

#### 19.3.1.1 Fabrication of $\text{TiO}_2$ Nanotube

Methods for the preparation of  $\text{TiO}_2$  nanotubes include assisted-template method, the sol-gel process, electrochemical anodic oxidation, and hydrothermal treatment. Among the above-mentioned fabrication approaches, the sol-gel, template-assisted, and hydrothermal treatment methods are broadly used in applications such as photocatalysis and solar cells, while those manufactured by electrochemical anodization are more commonly used for biological applications [58]. The electrochemical cell is composed of an anode, which can be any of the following; Ti or Ti alloy and cathode, platinum and electrolyte solution, typically containing HF or  $\text{NH}_4\text{F}$ . Three steps occur in the electrochemical anodization of Ti in F-based electrolyte. First, the oxidation of Ti to  $\text{TiO}_2$  occurs to form a dense oxide film on the surface of Ti. Next, the fluoride anion adsorbed on the Ti surface reacts with the oxide layer to form a porous thin film. Lastly, the produced soluble Ti-F complex  $[(\text{TiF}_6)^{-2}]$  steadily dissolves into the body of the solution on the titanium surface, resulting in a porous  $\text{TiO}_2$  nanotube structure (Fig. 19.1) [4].

#### 19.3.1.2 Effects of $\text{TiO}_2$ Nanotube Diameter

Different diameters of the  $\text{TiO}_2$  nanotubes exhibited clearly different effects on the cellular response. Up to 20 nm diameter is known to be optimal for improved cell adhesion and proliferation [64]. According to Mark et al., a diameter of about 15 nm greatly increased the adhesion, proliferation

and differentiation of MSCs, whereas a diameter of approximately 100 nm was associated with apoptosis [80]. TiO<sub>2</sub> and zirconium dioxide (ZrO<sub>2</sub>) in different crystallization states were used to determine the size impact of the nanotubes and the different fluoride contents in the tubes [6]. The effect of different diameter size was also confirmed in various kinds of living cells including MSCs, hematopoietic stem cells, endothelial cells, osteoblasts and osteoclasts. The size effect is a result of tailored nanotube morphology in that the integrin clustering of the cell membrane leads to a focal adhesion complex with a diameter of approximately 10 nm, hence being an ideal fit for nanotubes with a diameter of 15 nm [64].

### 19.3.1.3 *In Vivo* Studies Using TiO<sub>2</sub> Nanotube

Several *in vivo* studies on the application of TiO<sub>2</sub> nanotube have reported varying results on bone formation. The biocompatibility of TiO<sub>2</sub> nanotube was confirmed by subcutaneous injection of TiO<sub>2</sub> nanotube into rats, and as a result TiO<sub>2</sub> nanotube did not cause chronic inflammation or fibrosis [68]. One study examined the effects of TiO<sub>2</sub> nanotubes on bone formation around the implants and compared the results to those of untreated pure Ti surfaces placed in pig skulls. As a result, the expression of collagen type I in the nanostructured implants was considerably higher than the control group. Regardless, there was no difference observed in osteocalcin expression at any point of time on the implant surface. In addition, the amount of osteogenesis on both implant surfaces was almost the same without any statistical difference [81]. In contrast to these results, Wang et al. reported a notable increase in bone implant contact and gene expression levels in the bone attached to TiO<sub>2</sub> nanotubes by analyzing the histological features and fluorochrome labeling changes after implantation [85].

Similar to this study, von Willmowski et al. reported that osteocalcin expression was increased the most in TiO<sub>2</sub> nanotubes with a diameter of 70 nm when different diameters (15–100 nm) were implanted in pig skull [82]. Using a rabbit tibia model, Ti implants with TiO<sub>2</sub> nanotubes (diameter: 100 nm) have been proven to

have greater pull-out force and bone-to-implant contact area than conventional Ti surfaces [7].

### 19.3.2 TiO<sub>2</sub> Scaffold

As an alternative to bone, one of the most promising biocompatible materials has been proven to be a bioactive ceramic TiO<sub>2</sub> [38, 61, 62]. In previous studies, TiO<sub>2</sub> porous scaffolds have shown to promote good cell adhesion and growth of mouse osteoblasts into TiO<sub>2</sub> structures [72]. Moreover, TiO<sub>2</sub> porous scaffolds provide a better substrate for the proliferation and survival of human MSCs compared to other commercially available bone graft substitutes [73].

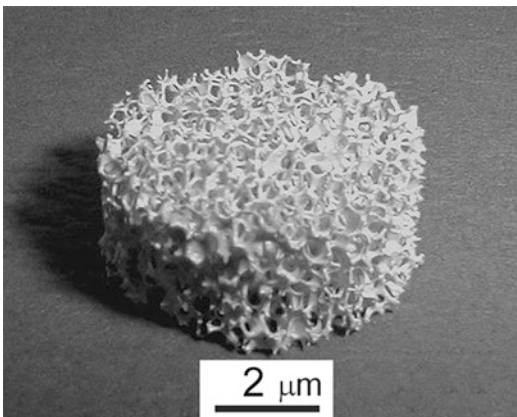
Highly porous TiO<sub>2</sub> scaffold provides a large surface area-to-volume ratio that assists cell adhesion and is required to gain a high cell density within the scaffold. Additionally, a large interconnected pore volume is necessary to permit bone cells to migrate into and subsequently proliferate within the scaffold [33, 51]. Assembly of a highly porous TiO<sub>2</sub> scaffold with the ability to promote fibroblast and osteoblast cell adhesion onto the entire scaffold surface has previously been reported, and preferable pore size ranges from 300 μm to 400 μm (more than 100 μm at least), otherwise vascular tissue cannot grow into the scaffold [19].

Although porous scaffold provides better osteogenic environment, it should be noted that excessively increased porosity and pore size have a detrimental effect on the mechanical strength and therefore cut down the mechanical integrity of the scaffold structure. However, Ceramic TiO<sub>2</sub> is known to have inherently higher compressive strength compared to other common osteoconductive scaffold materials, thus providing better mechanical strength to the scaffold structure. In the case of ceramic TiO<sub>2</sub> scaffolds with a total porosity of less than 85%, high compressive strength values of about 2.5 MPa were reported [77]. This strength was maintained even after implantation on account of the non-resorbable property of TiO<sub>2</sub>. The reported compressive strength values for calcium phosphate ceramic and calcium phosphate ceramic / polymer com-

posite scaffolds with similar porosity are typically much lower than 2 MPa [83]. On the other hand, the compressive strengths of trabecular bone and cortical bone is generally ranged 2–12 MPa and 100–230 MPa, respectively [10].

### 19.3.2.1 Fabrication of TiO<sub>2</sub> Scaffold

The most widely used technique for manufacturing TiO<sub>2</sub> scaffolds is the polymer sponge method where reticulated open-pore ceramics are fabricated through the replication of polymeric porous structures. This is the standard method for producing alumina, zirconium, silicon carbide and other ceramic foams. The foams are produced by coating a ceramic slurry on a polyurethane foam. The polymer, having already the desired macrostructure, serves merely as a sacrificial scaffold for the ceramic coating. The slurry then infiltrates the structure and attaches to the surface of the polymer. Excess slurry is extracted, leaving a ceramic coating on the foam struts. After drying, the polymer is slowly burned away as to minimize damage to the porous coating. Once the polymer is removed, the ceramic is sintered to the desired density. This process reproduces the macrostructure of the polymer and creates a unique microstructure within the struts (Fig. 19.2) [52].



**Fig. 19.2** Macrostructure of TiO<sub>2</sub> scaffold. (Reprinted from [29])

“Reprinted from J Eur Ceram Soc, 24(4), Haugen, H., Will, J., Köhler, A., Hopfner, U., Aigner, J., & Wintermantel, E., Ceramic TiO<sub>2</sub>-foams: characterisation of a potential scaffold, 661-668, Copyright (2004), with permission from Elsevier.”

### 19.3.2.2 *In Vivo* Studies of TiO<sub>2</sub> Scaffold

As with TiO<sub>2</sub> nanotube, several *in vivo* studies have been reported on the application of TiO<sub>2</sub> scaffolds for bone defects. In particular, Tianien et al. investigated the bone formation in TiO<sub>2</sub> scaffolds in extraction sockets of pigs' jaw. After implantation of TiO<sub>2</sub> scaffolds to the bone socket, evidence of angiogenesis and a great quantity of viable mineralized bone tissue was observed, proving that the highly interconnected pore structure of TiO<sub>2</sub> scaffolds had superb osteoconductive capacity and arranged a supportive environment for bone ingrowth [78].

Another study analyzed the *in vivo* performance of the porous TiO<sub>2</sub> scaffolds in a peri-implant cortical defect in the rabbit model. After 8 weeks of implantation of TiO<sub>2</sub> scaffolds to the cortical defect of rabbit's tibia, the defects treated with TiO<sub>2</sub> scaffolds had significantly higher bone volume, bone surface and bone surface-to-volume ratio without any side effects, both in the cortical and bone marrow compartment. Histologic observations verified osteogenesis in the cortical sections of the defects and the existence of freshly developed bone in close proximity to the scaffold surface [30].

### 19.3.2.3 Improving TiO<sub>2</sub> Scaffold Bioactivity by Combination with Other Materials

Since TiO<sub>2</sub> scaffolds themselves are not rigid enough for use as an implant, researchers have tried combining TiO<sub>2</sub> scaffold with other materials to improve its rigidity. For example, Tiainen et al. examined the effect of ZrO<sub>2</sub> addition on the mechanical properties of TiO<sub>2</sub> scaffolds [67]. Up to 40 weight % of the TiO<sub>2</sub> raw material were substituted with ZrO<sub>2</sub> by polymer sponge replication in order to fabricate ultra-porous TiO<sub>2</sub> scaffolds. The addition of ZrO<sub>2</sub> increased the average compressive strength without altering the pore structural parameters of TiO<sub>2</sub> scaffolds. Further ZrO<sub>2</sub> additions led to reduction in the compressive strength as compared to the absence of ZrO<sub>2</sub> [34]. They proposed that combining the exceptional mechanical properties of ZrO<sub>2</sub> with the osteogenic properties of TiO<sub>2</sub> might allow the

production of a profoundly osteoconductive scaffold with great mechanical strength for load-bearing environment, all the while preserving the highly reticulated pore structure necessary for bone regeneration.

In addition, numerous studies have reported cases in which the osteogenic effect increased when TiO<sub>2</sub> scaffold was combined with other materials. For instance, based on the pluripotency of MSCs and osteogenic effects of simvastatin, Pullisaar et al. explored the osteogenic differentiation of adipose tissue-derived MSCs on TiO<sub>2</sub> scaffolds coated with alginate hydrogels with differing concentrations of simvastatin [69, 94]. The study concluded that the TiO<sub>2</sub> scaffolds coated with alginate hydrogel containing simvastatin promotes osteogenic differentiation of stem cells and were proved valid for adipose tissue-derived MSCs based bone tissue engineering.

### 19.3.3 TiO<sub>2</sub> Composite

Copious studies have examined bone tissue-engineering methods by developing composite of osteoinductive biomaterials and three-dimensional cell aggregates based on TiO<sub>2</sub> scaffolds or particles. A research team led by Ferreria et al. created a novel cell aggregate-loaded macroporous scaffolds combining the osteoinductive properties of TiO<sub>2</sub> with hydroxyapatite–gelatin nanocomposites for regeneration of craniofacial defects [18]. In their *in vivo* study, hydroxyapatite–gelatin nanocomposites with enriched macroporous TiO<sub>2</sub> scaffolds were applied to the rats, and the results showed that the scaffolds had a greater strength and osteointegration than the natural calvarial bone at 8 and 12 weeks after implantation [18].

A different team added TiO<sub>2</sub> to the Al<sub>2</sub>O<sub>3</sub>-SiO<sub>2</sub> mixture to increase the bioactivity of the produced scaffold. The scaffold was assembled by rapid fluid infiltration of Al<sub>2</sub>O<sub>3</sub>-SiO<sub>2</sub> solid into a polyethylene non-woven fabric template structure [45, 71]. Both *in vitro* and *in vivo* tests showed potent bone formation with improved mechanical properties in the mixture of Al<sub>2</sub>O<sub>3</sub>-SiO<sub>2</sub> solid with TiO<sub>2</sub> scaffold [57].

Furthermore, a few studies have established procedures for bone tissue engineering by combining TiO<sub>2</sub> nanoparticle components with different materials [25, 48]. In their researches, TiO<sub>2</sub> nanoparticles were introduced to the polymeric matrices composed of collagen and chitosan hydrogels to enhance strength, mechanical properties as well as their bioactivity [2, 47]. Collagen and chitosan were selected as hydrogel components being that they are biopolymers, exist in the extracellular matrix, and have structural similarity with glycosaminoglycan. Additionally it has been reported that modified TiO<sub>2</sub> by pyridoxal 5'-phosphate, an active form of vitamin B<sub>6</sub>, dramatically increases the hemophilic property at the implant-blood interface and inactivated platelet for sufficient supply of growth cytokines and migration of osteoblasts [43].

---

## 19.4 Other Functions of TiO<sub>2</sub>

### 19.4.1 Drug Delivery

A variety of drugs have been loaded into TiO<sub>2</sub> nanotube to test whether the implant can deliver a drug directly to the implant site [27]. The most common drugs loaded to TiO<sub>2</sub> nanotubes are antibiotics such as gentamicin, vancomycin and levofloxacin. Other drugs such as non-steroidal anti-inflammatory drug (indomethacin), anti-lipidemic drug (simvastatin) and certain growth factors are also available for loading [79]. Recently, several advanced approaches have been proposed to achieve a TiO<sub>2</sub> nanotube platform for sustainable drug delivery, including methods triggered by pH, temperature, light, radiofrequency, magnetics and ultrasonic stimulation [86].

### 19.4.2 Cosmetic and Skin Applications

TiO<sub>2</sub> is also widely used in the field of cosmetics considering that it's an effective emulsifier in powder form and is used as a pigment to impart whiteness and opacity to products such as cosmetics, food, pharmaceuticals and most

toothpastes. Especially in cosmetics and skin care products, TiO<sub>2</sub> is used as a pigment, sunscreen, thickener, and tattoo pigment. Indeed, TiO<sub>2</sub> is produced in a wide range of particle sizes, oils and water dispersions, and certain grades in the cosmetics industry.

## 19.5 Conclusion and Future Direction

Ti-based implants are the first choice in the field of orthopedic and dental surgery because of their high biocompatibility. That being the case, certain modifications are necessary in order to obtain a strong osteointegration between the Ti implant and the bone. Various techniques to form a porous implant surface were introduced, including using a coating material or nano-modification by TiO<sub>2</sub> nanotubes. Recently, promising results were reported using TiO<sub>2</sub> nanotubes as the surface modifiers. One of the most emerging methods to obtain TiO<sub>2</sub> nanotubes is electrochemical anodizing with controlled diameters. The advantage of a porous TiO<sub>2</sub> scaffold compared to the other ceramics is that it is biocompatible with relatively superior mechanical properties. However, there have been only a small number of *in vivo* articles on the bone forming ability using TiO<sub>2</sub> nanotubes or scaffolds. Further studies using various animal model under different conditions is needed to optimize and commercialize the TiO<sub>2</sub> nanotubes or scaffolds for clinical applications in orthopedic or dental field. Finally, techniques using TiO<sub>2</sub> nanotube or scaffold has the potential as a novel therapeutic strategy for osteogenesis.

**Acknowledgement** This work was supported by Korea Health Technology R&D Project through the Korea Health Industry Development Institute, funded by the Ministry of Health & Welfare, South Korea (grant number HI16C1559) and by Basic Science Research Program through the National Research Foundation of Korea (NRF) funded by the Ministry of Education (grant number NRF-2016R1D1A1A02937040).

## References

1. Adell R, Eriksson B, Lekholm U, Branemark PI, Jemt T (1990) Long-term follow-up study of osseointegrated implants in the treatment of totally edentulous jaws. *Int J Oral Maxillofac Implants* 5(4):347–359
2. Amini AA, Nair LS (2012) Injectable hydrogels for bone and cartilage repair. *Biomed Mater* 7(2):024105. <https://doi.org/10.1088/1748-6041/7/2/024105>
3. Andersen OZ, Offermanns V, Sillassen M, Almtoft KP, Andersen IH, Sorensen S, Foss M (2013) Accelerated bone ingrowth by local delivery of strontium from surface functionalized titanium implants. *Biomaterials* 34(24):5883–5890. <https://doi.org/10.1016/j.biomaterials.2013.04.031>
4. Awad NK, Edwards SL, Morsi YS (2017) A review of TiO<sub>2</sub> NTs on Ti metal: electrochemical synthesis, functionalization and potential use as bone implants. *Mater Sci Eng C Mater Biol Appl* 76:1401–1412. <https://doi.org/10.1016/j.msec.2017.02.150>
5. Bae SE, Choi J, Joung YK, Park K, Han DK (2012) Controlled release of bone morphogenetic protein (BMP)-2 from nanocomplex incorporated on hydroxyapatite-formed titanium surface. *J Control Release* 160(3):676–684. <https://doi.org/10.1016/j.jconrel.2012.04.021>
6. Bauer S, Park J, Faltenbacher J, Berger S, von der Mark K, Schmuki P (2009) Size selective behavior of mesenchymal stem cells on ZrO(2) and TiO(2) nanotube arrays. *Integr Biol (Camb)* 1(8–9):525–532. <https://doi.org/10.1039/b908196h>
7. Bjursten LM, Rasmusson L, Oh S, Smith GC, Brammer KS, Jin S (2010) Titanium dioxide nanotubes enhance bone bonding in vivo. *J Biomed Mater Res A* 92(3):1218–1224. <https://doi.org/10.1002/jbm.a.32463>
8. Capello WN, D'Antonio JA, Manley MT, Feinberg JR (1998) Hydroxyapatite in total hip arthroplasty. Clinical results and critical issues. *Clin Orthop Relat Res* 355:200–211
9. Carragee EJ, Hurwitz EL, Weiner BK (2011) A critical review of recombinant human bone morphogenetic protein-2 trials in spinal surgery: emerging safety concerns and lessons learned. *Spine J* 11(6):471–491. <https://doi.org/10.1016/j.spinee.2011.04.023>
10. Carter DR, Hayes WC (1976) Bone compressive strength: the influence of density and strain rate. *Science* 194(4270):1174–1176
11. Chen XB, Li YC, Du Plessis J, Hodgson PD, Wen C (2009) Influence of calcium ion deposition on apatite-inducing ability of porous titanium for biomedical applications. *Acta Biomater* 5(5):1808–1820. <https://doi.org/10.1016/j.actbio.2009.01.015>
12. Chien CY, Tsai WB (2013) Poly(dopamine)-assisted immobilization of Arg-Gly-Asp peptides, hydroxyap-

- atite, and bone morphogenic protein-2 on titanium to improve the osteogenesis of bone marrow stem cells. *ACS Appl Mater Interfaces* 5(15):6975–6983. <https://doi.org/10.1021/am401071f>
13. Choi BH, Choi YS, Kang DG, Kim BJ, Song YH, Cha HJ (2010) Cell behavior on extracellular matrix mimic materials based on mussel adhesive protein fused with functional peptides. *Biomaterials* 31(34):8980–8988. <https://doi.org/10.1016/j.biomaterials.2010.08.027>
  14. Cooper LF, Zhou Y, Takebe J, Guo J, Abron A, Holmen A, Ellingsen JE (2006) Fluoride modification effects on osteoblast behavior and bone formation at TiO<sub>2</sub> grit-blasted c.p. titanium endosseous implants. *Biomaterials* 27(6):926–936. <https://doi.org/10.1016/j.biomaterials.2005.07.009>
  15. Daculsi G, Legeros RZ, Nery E, Lynch K, Kerebel B (1989) Transformation of biphasic calcium phosphate ceramics in vivo: ultrastructural and physicochemical characterization. *J Biomed Mater Res* 23(8):883–894. <https://doi.org/10.1002/jbm.820230806>
  16. Dimitriou R, Mataliotakis GI, Angoules AG, Kanakaris NK, Giannoudis PV (2011) Complications following autologous bone graft harvesting from the iliac crest and using the RIA: a systematic review. *Injury* 42(Suppl 2):S3–S15. <https://doi.org/10.1016/j.injury.2011.06.015>
  17. Elizabeth E, Baranwal G, Krishnan AG, Menon D, Nair M (2014) ZnO nanoparticle incorporated nanostructured metallic titanium for increased mesenchymal stem cell response and antibacterial activity. *Nanotechnology* 25(11):115101. <https://doi.org/10.1088/0957-4484/25/11/115101>
  18. Ferreira JR, Hirsch ML, Zhang L, Park Y, Samulski RJ, Hu WS, Ko CC (2013) Three-dimensional multipotent progenitor cell aggregates for expansion, osteogenic differentiation and ‘in vivo’ tracing with AAV vector serotype 6. *Gene Ther* 20(2):158–168. <https://doi.org/10.1038/gt.2012.16>
  19. Fostad G, Hafell B, Førde A, Dittmann R, Sabetrasekh R, Will J, Ellingsen JE, Lyngstadaas SP, Haugen HJ (2009) Loadable TiO<sub>2</sub> scaffolds—a correlation study between processing parameters, micro CT analysis and mechanical strength. *J Eur Ceram Soc* 29(13):2773–2781. <https://doi.org/10.1016/j.jeurceramsoc.2009.03.017>
  20. Frandsen CJ, Brammer KS, Jin S (2013) Variations to the nanotube surface for bone regeneration. *Int J Biomater* 2013:513680. <https://doi.org/10.1155/2013/513680>
  21. Frayssinet P, Hardy D, Rouquet N, Giammara B, Guilhem A, Hanker J (1992) New observations on middle term hydroxyapatite-coated titanium alloy hip prostheses. *Biomaterials* 13(10):668–674
  22. Gao Y, Zou S, Liu X, Bao C, Hu J (2009) The effect of surface immobilized bisphosphonates on the fixation of hydroxyapatite-coated titanium implants in ovariectomized rats. *Biomaterials* 30(9):1790–1796. <https://doi.org/10.1016/j.biomaterials.2008.12.025>
  23. Garcia-Alonso MC, Saldana L, Valles G, Gonzalez-Carrasco JL, Gonzalez-Cabrero J, Martinez ME, Gil-Garay E, Munuera L (2003) In vitro corrosion behaviour and osteoblast response of thermally oxidised Ti6Al4V alloy. *Biomaterials* 24(1):19–26
  24. Gavidia L, Salcido JP, Guda T, Ong JL (2014) Current trends in dental implants. *J Korean Assoc Oral Maxillofac Surg* 40(2):50–60. <https://doi.org/10.5125/jkaoms.2014.40.2.50>
  25. Gerhardt LC, Jell GM, Boccaccini AR (2007) Titanium dioxide (TiO<sub>2</sub>) nanoparticles filled poly(D,L lactid acid) (PDLLA) matrix composites for bone tissue engineering. *J Mater Sci Mater Med* 18(7):1287–1298. <https://doi.org/10.1007/s10856-006-0062-5>
  26. Goodman SB, Yao Z, Keeney M, Yang F (2013) The future of biologic coatings for orthopaedic implants. *Biomaterials* 34(13):3174–3183. <https://doi.org/10.1016/j.biomaterials.2013.01.074>
  27. Gultepe E, Nagesha D, Sridhar S, Amiji M (2010) Nanoporous inorganic membranes or coatings for sustained drug delivery in implantable devices. *Adv Drug Deliv Rev* 62(3):305–315. <https://doi.org/10.1016/j.addr.2009.11.003>
  28. Guo CY, Hong Tang AT, Hon Tsoi JK, Matinlinna JP (2014) Effects of different blasting materials on charge generation and decay on titanium surface after sandblasting. *J Mech Behav Biomed Mater* 32:145–154. <https://doi.org/10.1016/j.jmbbm.2013.12.026>
  29. Haugen H, Will J, Köhler A, Hopfner U, Aigner J, Wintermantel E (2004) Ceramic TiO<sub>2</sub>-foams: characterisation of a potential scaffold. *J Eur Ceram Soc* 24(4):661–668. [https://doi.org/10.1016/S0955-2219\(03\)00255-3](https://doi.org/10.1016/S0955-2219(03)00255-3)
  30. Haugen HJ, Monjo M, Rubert M, Verket A, Lyngstadaas SP, Ellingsen JE, Rønold HJ, Wohlfahrt JC (2013) Porous ceramic titanium dioxide scaffolds promote bone formation in rabbit peri-implant cortical defect model. *Acta Biomater* 9(2):5390–5399. <https://doi.org/10.1016/j.actbio.2012.09.009>
  31. He J, Huang T, Gan L, Zhou Z, Jiang B, Wu Y, Wu F, Gu Z (2012) Collagen-infiltrated porous hydroxyapatite coating and its osteogenic properties: in vitro and in vivo study. *J Biomed Mater Res A* 100(7):1706–1715. <https://doi.org/10.1002/jbm.a.34121>
  32. Hench LL, Polak JM (2002) Third-generation biomedical materials. *Science* 295(5557):1014–1017. <https://doi.org/10.1126/science.1067404>
  33. Hing KA, Annaz B, Saeed S, Revell PA, Buckland T (2005) Microporosity enhances bioactivity of synthetic bone graft substitutes. *J Mater Sci Mater Med* 16(5):467–475. <https://doi.org/10.1007/s10856-005-6988-1>
  34. Holbig E, Dubrovinsky L, Miyajima N, Swamy V, Wirth R, Prakapenka V, Kuznetsov A (2008) Stiffening of nanoscale anatase TiO<sub>2</sub>. 9ZrO<sub>2</sub> upon multiple compression cycles. *J Phys Chem Solids* 69(9):2230–2233. <https://doi.org/10.1016/j.jpccs.2008.04.022>
  35. Hong S, Yang K, Kang B, Lee C, Song IT, Byun E, Park KI, Cho S, Lee H (2013) Hyaluronic acid catechol: a biopolymer exhibiting a pH-dependent adhesive or cohesive property for human neural stem cell

- engineering. *Adv Funct Mater* 23:1774–1780. <https://doi.org/10.1002/adfm.201202365>
36. Hu Y, Cai K, Luo Z, Zhang R, Yang L, Deng L, Jandt KD (2009) Surface mediated in situ differentiation of mesenchymal stem cells on gene-functionalized titanium films fabricated by layer-by-layer technique. *Biomaterials* 30(21):3626–3635. <https://doi.org/10.1016/j.biomaterials.2009.03.037>
  37. Jain A, Kumar S, Aggarwal AN, Jajodia N (2015) Augmentation of bone healing in delayed and atrophic nonunion of fractures of long bones by partially decalcified bone allograft (decal bone). *Indian J Orthop* 49(6):637–642. <https://doi.org/10.4103/0019-5413.168764>
  38. Jokinen M, Patsi M, Rahiala H, Peltola T, Ritala M, Rosenholm JB (1998) Influence of sol and surface properties on in vitro bioactivity of sol-gel-derived TiO<sub>2</sub> and TiO<sub>2</sub>-SiO<sub>2</sub> films deposited by dip-coating method. *J Biomed Mater Res* 42(2):295–302
  39. Kaluderovic MR, Schreckenbach JP, Graf HL (2016) Titanium dental implant surfaces obtained by anodic spark deposition – from the past to the future. *Mater Sci Eng C Mater Biol Appl* 69:1429–1441. <https://doi.org/10.1016/j.msec.2016.07.068>
  40. Kim SS, Gwak SJ, Kim BS (2008) Orthotopic bone formation by implantation of apatite-coated poly(lactide-co-glycolide)/hydroxyapatite composite particulates and bone morphogenetic protein-2. *J Biomed Mater Res A* 87(1):245–253. <https://doi.org/10.1002/jbm.a.31782>
  41. Kimura Y, Miyazaki N, Hayashi N, Otsuru S, Tamai K, Kaneda Y, Tabata Y (2010) Controlled release of bone morphogenetic protein-2 enhances recruitment of osteogenic progenitor cells for de novo generation of bone tissue. *Tissue Eng Part A* 16(4):1263–1270. <https://doi.org/10.1089/ten.TEA.2009.0322>
  42. Le Guehennec L, Soueidan A, Layrolle P, Amouriq Y (2007) Surface treatments of titanium dental implants for rapid osseointegration. *Dent Mater* 23(7):844–854. <https://doi.org/10.1016/j.dental.2006.06.025>
  43. Lee JS, Kim K, Park JP, Cho SW, Lee H (2017) Role of pyridoxal 5'-phosphate at the titanium implant Interface in vivo: increased Hemophilicity, inactive platelet adhesion, and osseointegration. *Adv Healthc Mater* 6(5). <https://doi.org/10.1002/adhm.201600962>
  44. LeGeros RZ (2002) Properties of osteoconductive biomaterials: calcium phosphates. *Clin Orthop Relat Res* 395:81–98
  45. Leivo J, Meretoja V, Vippola M, Levanen E, Vallittu P, Mantyla TA (2006) Sol-gel derived aluminosilicate coatings on alumina as substrate for osteoblasts. *Acta Biomater* 2(6):659–668. <https://doi.org/10.1016/j.actbio.2006.06.001>
  46. Lewallen EA, Riester SM, Bonin CA, Kremers HM, Dudakovic A, Kakar S, Cohen RC, Westendorf JJ, Lewallen DG, van Wijnen AJ (2015) Biological strategies for improved osseointegration and osteoinduction of porous metal orthopedic implants. *Tissue Eng Part B Rev* 21(2):218–230. <https://doi.org/10.1089/ten.TEB.2014.0333>
  47. Lewandowska-Lancucka J, Fiejdasz S, Rodzik L, Koziel M, Nowakowska M (2015) Bioactive hydrogel-nanosilica hybrid materials: a potential injectable scaffold for bone tissue engineering. *Biomed Mater* 10(1):015020. <https://doi.org/10.1088/1748-6041/10/1/015020>
  48. Lifland MI, Kim DK, Okazaki K (1993) Mechanical properties of a Ti-6Al-4V dental implant produced by electro-discharge compaction. *Clin Mater* 14(1):13–19
  49. Lin L, Wang H, Ni M, Rui Y, Cheng T, Cheng C, Pan X, Li G, Lin C (2014) Enhanced osteointegration of medical titanium implant with surface modifications in micro/nanoscale structures. *J Orthop Translat* 2(1):35–42. <https://doi.org/10.1016/j.jot.2013.08.001>
  50. Liu Y, Wu G, de Groot K (2010) Biomimetic coatings for bone tissue engineering of critical-sized defects. *J R Soc Interface* 7(Suppl 5):S631–S647. <https://doi.org/10.1098/rsif.2010.0115.focus>
  51. Lu JX, Flautre B, Anselme K, Hardouin P, Gallur A, Descamps M, Thierry B (1999) Role of interconnections in porous bioceramics on bone recolonization in vitro and in vivo. *J Mater Sci Mater Med* 10(2):111–120
  52. Maquet V, Jerome R (1997) Design of macroporous biodegradable polymer scaffolds for cell transplantation. *Mater Sci Forum* 250:15–42. <https://doi.org/10.4028/www.scientific.net/MSF.250.15>
  53. Mas-Moruno C, Espanol M, Montufar EB, Mestres G, Aparicio C, Javier GF, Ginebra M (2013) Bioactive ceramic and metallic surfaces for bone engineering. *Biomater Surf Sci* 12:337–374. <https://doi.org/10.1002/9783527649600.ch12>
  54. Mavrogenis AF, Dimitriou R, Parvizi J, Babis GC (2009) Biology of implant osseointegration. *J Musculoskelet Neuronal Interact* 9(2):61–71
  55. Miyazaki M, Tsumura H, Wang JC, Alanay A (2009) An update on bone substitutes for spinal fusion. *Eur Spine J* 18(6):783–799. <https://doi.org/10.1007/s00586-009-0924-x>
  56. Murphy CM, Haugh MG, O'Brien FJ (2010) The effect of mean pore size on cell attachment, proliferation and migration in collagen-glycosaminoglycan scaffolds for bone tissue engineering. *Biomaterials* 31(3):461–466. <https://doi.org/10.1016/j.biomaterials.2009.09.063>
  57. Naga SM, El-Kady AM, El-Maghraby HF, Awaad M, Detsch R, Boccaccini AR (2014) Novel porous Al<sub>2</sub>O<sub>3</sub>-SiO<sub>2</sub>-TiO<sub>2</sub> bone grafting materials: formation and characterization. *J Biomater Appl* 28(6):813–824. <https://doi.org/10.1177/0885328213483634>
  58. Nair M, Elizabeth E (2015) Applications of Titania nanotubes in bone biology. *J Nanosci Nanotechnol* 15(2):939–955
  59. Nayab SN, Jones FH, Olsen I (2005) Effects of calcium ion implantation on human bone cell interac-



- tion with titanium. *Biomaterials* 26(23):4717–4727. <https://doi.org/10.1016/j.biomaterials.2004.11.044>
60. Nishiguchi S, Kato H, Neo M, Oka M, Kim HM, Kokubo T, Nakamura T (2001) Alkali- and heat-treated porous titanium for orthopedic implants. *J Biomed Mater Res* 54(2):198–208
  61. Nygren H, Eriksson C, Lausmaa J (1997a) Adhesion and activation of platelets and polymorphonuclear granulocyte cells at TiO<sub>2</sub> surfaces. *J Lab Clin Med* 129(1):35–46
  62. Nygren H, Tengvall P, Lundstrom I (1997b) The initial reactions of TiO<sub>2</sub> with blood. *J Biomed Mater Res* 34(4):487–492
  63. Pagel M, Hassert R, John T, Braun K, Wießler M, Abel B, Beck-Sickingler AG (2016) Multifunctional coating improves cell adhesion on titanium by using cooperatively acting peptides. *Angew Chem Int Ed Engl* 55(15):4826–4830. <https://doi.org/10.1002/anie.201511781>
  64. Park J, Bauer S, von der Mark K, Schmuki P (2007) Nanosize and vitality: TiO<sub>2</sub> nanotube diameter directs cell fate. *Nano Lett* 7(6):1686–1691. <https://doi.org/10.1021/nl070678d>
  65. Park JW, Kim YJ, Jang JH, Song H (2010) Osteoblast response to magnesium ion-incorporated nanoporous titanium oxide surfaces. *Clin Oral Implants Res* 21(11):1278–1287. <https://doi.org/10.1111/j.1600-0501.2010.01944.x>
  66. Petrie TA, Raynor JE, Dumbauld DW, Lee TT, Jagtap S, Templeman KL, Collard DM, García AJ (2010) Multivalent integrin-specific ligands enhance tissue healing and biomaterial integration. *Sci Transl Med* 2(45):45ra60. <https://doi.org/10.1126/scitranslmed.3001002>
  67. Piconi C, Maccauro G (1999) Zirconia as a ceramic biomaterial. *Biomaterials* 20(1):1–25
  68. Popat KC, Leoni L, Grimes CA, Desai TA (2007) Influence of engineered Titania nanotubular surfaces on bone cells. *Biomaterials* 28(21):3188–3197. <https://doi.org/10.1016/j.biomaterials.2007.03.020>
  69. Pullisaar H, Reseland JE, Haugen HJ, Brinchmann JE, Ostrup E (2014) Simvastatin coating of TiO<sub>2</sub> scaffold induces osteogenic differentiation of human adipose tissue-derived mesenchymal stem cells. *Biochem Biophys Res Commun* 447(1):139–144. <https://doi.org/10.1016/j.bbrc.2014.03.133>
  70. Qiao C, Zhang K, Jin H, Miao L, Shi C, Liu X, Yuan A, Liu J, Li D, Zheng C, Zhang G, Li X, Yang B, Sun H (2013) Using poly(lactic-co-glycolic acid) microspheres to encapsulate plasmid of bone morphogenetic protein 2/polyethylenimine nanoparticles to promote bone formation in vitro and in vivo. *Int J Nanomedicine* 8:2985–2995. <https://doi.org/10.2147/ijn.s45184>
  71. Richardson WC Jr, Klawitter JJ, Sauer BW, Pruitt JR, Hulbert SF (1975) Soft tissue response to four dense ceramic materials and two clinically used biomaterials. *J Biomed Mater Res* 9(4):73–80. <https://doi.org/10.1002/jbm.820090411>
  72. Sabetrsekh R, Tiainen H, Reseland JE, Will J, Ellingsen JE, Lyngstadaas SP, Haugen HJ (2010) Impact of trace elements on biocompatibility of titanium scaffolds. *Biomed Mater* 5(1):15003. <https://doi.org/10.1088/1748-6041/5/1/015003>
  73. Sabetrsekh R, Tiainen H, Lyngstadaas SP, Reseland J, Haugen H (2011) A novel ultra-porous titanium dioxide ceramic with excellent biocompatibility. *J Biomater Appl* 25(6):559–580. <https://doi.org/10.1177/0885328209354925>
  74. Saleh MM, Touny AH, Al-Omair MA, Saleh MM (2016) Biodegradable/biocompatible coated metal implants for orthopedic applications. *Biomed Mater Eng* 27(1):87–99. <https://doi.org/10.3233/bme-161568>
  75. Smith YR, Ray RS, Carlson K, Sarma B, Misra M (2013) Self-ordered titanium dioxide nanotube arrays: anodic synthesis and their photo/electro-catalytic applications. *Materials (Basel)* 6(7):2892–2957. <https://doi.org/10.3390/ma6072892>
  76. Thieme M, Wieters KP, Bergner F, Scharnweber D, Worch H, Ndop J, Kim TJ, Grill W (2001) Titanium powder sintering for preparation of a porous functionally graded material destined for orthopaedic implants. *J Mater Sci Mater Med* 12(3):225–231
  77. Tiainen H, Lyngstadaas SP, Ellingsen JE, Haugen HJ (2010) Ultra-porous titanium oxide scaffold with high compressive strength. *J Mater Sci Mater Med* 21(10):2783–2792. <https://doi.org/10.1007/s10856-010-4142-1>
  78. Tiainen H, Wohlfahrt JC, Verket A, Lyngstadaas SP, Haugen HJ (2012) Bone formation in TiO<sub>2</sub> bone scaffolds in extraction sockets of minipigs. *Acta Biomater* 8(6):2384–2391. <https://doi.org/10.1016/j.actbio.2012.02.020>
  79. Vasilev K, Simovic S, Losic D, Griesser HJ, Griesser S, Anselme K, Ploux L (2010) Platforms for controlled release of antibacterial agents facilitated by plasma polymerization. *Conf Proc IEEE Eng Med Biol Soc* 2010:811–814. <https://doi.org/10.1109/iembs.2010.5626566>
  80. von der Mark K, Park J, Bauer S, Schmuki P (2010) Nanoscale engineering of biomimetic surfaces: cues from the extracellular matrix. *Cell Tissue Res* 339(1):131–153. <https://doi.org/10.1007/s00441-009-0896-5>
  81. von Wilmsowsky C, Bauer S, Lutz R, Meisel M, Neukam FW, Toyoshima T, Schmuki P, Nkenke E, Schlegel KA (2009) In vivo evaluation of anodic TiO<sub>2</sub> nanotubes: an experimental study in the pig. *J Biomed Mater Res B Appl Biomater* 89(1):165–171. <https://doi.org/10.1002/jbm.b.31201>
  82. von Wilmsowsky C, Bauer S, Roedel S, Neukam FW, Schmuki P, Schlegel KA (2012) The diameter of anodic TiO<sub>2</sub> nanotubes affects bone formation and correlates with the bone morphogenetic protein-2 expression in vivo. *Clin Oral Implants Res* 23(3):359–366. <https://doi.org/10.1111/j.1600-0501.2010.02139.x>
  83. Wagoner Johnson AJ, Herschler BA (2011) A review of the mechanical behavior of CaP and CaP/poly-

- mer composites for applications in bone replacement and repair. *Acta Biomater* 7(1):16–30. <https://doi.org/10.1016/j.actbio.2010.07.012>
84. Wang X, Li Y, Hodgson PD, Wen C (2010) Biomimetic modification of porous TiNbZr alloy scaffold for bone tissue engineering. *Tissue Eng Part A* 16(1):309–316. <https://doi.org/10.1089/ten.TEA.2009.0074>
85. Wang N, Li H, Lu W, Li J, Wang J, Zhang Z, Liu Y (2011) Effects of TiO<sub>2</sub> nanotubes with different diameters on gene expression and osseointegration of implants in minipigs. *Biomaterials* 32(29):6900–6911. <https://doi.org/10.1016/j.biomaterials.2011.06.023>
86. Wang Q, Huang JY, Li HQ, Chen Z, Zhao AZ, Wang Y, Zhang KQ, Sun HT, Al-Deyab SS, Lai YK (2016) TiO<sub>2</sub> nanotube platforms for smart drug delivery: a review. *Int J Nanomedicine* 11:4819–4834. <https://doi.org/10.2147/ijn.s108847>
87. Wei Q, Zhang F, Li J, Li B, Zhao C (2010) Oxidant-induced dopamine polymerization for multifunctional coatings. *Polym Chem* 1:1430–1433. <https://doi.org/10.1039/C0PY00215A>
88. Wen CE, Mabuchi M, Yamada Y, Shimojima K, Chino Y, Asahina T (2001) Processing of biocompatible porous Ti and mg. *Scr Mater* 45(10):1147–1153. [https://doi.org/10.1016/S1359-6462\(01\)01132-0](https://doi.org/10.1016/S1359-6462(01)01132-0)
89. Wongwitwichot P, Kaewsrirachan J, Chua KH, Ruszymah BH (2010) Comparison of TCP and TCP/HA hybrid scaffolds for osteoconductive activity. *Open Biomed Eng J* 4:279–285. <https://doi.org/10.2174/1874120701004010279>
90. Yelin E, Weinstein S, King T (2016) The burden of musculoskeletal diseases in the United States. *Semin Arthritis Rheum* 46(3):259–260. <https://doi.org/10.1016/j.semarthrit.2016.07.013>
91. Yu J, Wei W, Menyo MS, Masic A, Waite JH, Israelachvili JN (2013) Adhesion of muscel foot protein-3 to TiO<sub>2</sub> surfaces: the effect of pH. *Biomacromolecules* 14(4):1072–1077. <https://doi.org/10.1021/bm301908y>
92. Zena JW, van Williams G, Frederik C, Russell G, Gwendolen CR (2015) Porous titanium for dental implant application. *Metals* 5(4):1902–1920. <https://doi.org/10.3390/met5041902>
93. Zhang BG, Myers DE, Wallace GG, Brandt M, Choong PF (2014) Bioactive coatings for orthopaedic implants-recent trends in development of implant coatings. *Int J Mol Sci* 15(7):11878–11921. <https://doi.org/10.3390/ijms150711878>
94. Zhou Y, Ni Y, Liu Y, Zeng B, Xu Y, Ge W (2010) The role of simvastatin in the osteogenesis of injectable tissue-engineered bone based on human adipose-derived stromal cells and platelet-rich plasma. *Biomaterials* 31(20):5325–5335. <https://doi.org/10.1016/j.biomaterials.2010.03.037>
95. Zhu X, Zhang H, Zhang X, Ning C, Wang Y (2017) In vitro study on the osteogenesis enhancement effect of BMP-2 incorporated biomimetic apatite coating on titanium surfaces. *Dent Mater J* 36(5):677–685. <https://doi.org/10.4012/dmj.2016-189>
96. Zreiqat H, Howlett CR, Zannettino A, Evans P, Schulze-Tanzil G, Knabe C, Shakibaei M (2002) Mechanisms of magnesium-stimulated adhesion of osteoblastic cells to commonly used orthopaedic implants. *J Biomed Mater Res* 62(2):175–184. <https://doi.org/10.1002/jbm.10270>
97. Zwilling V, Aucoeur M, Darque-Ceretti E (1999) Anodic oxidation of titanium and TA6V alloy in chromic media. An electrochemical approach. *Electrochim Acta* 45(6):921–929. [https://doi.org/10.1016/S0013-4686\(99\)00283-2](https://doi.org/10.1016/S0013-4686(99)00283-2)

---

**Part V**

**Smart Natural Biomaterials for  
Regenerative Medicine**



# Silk Fibroin-Based Scaffold for Bone Tissue Engineering

# 20

Joo Hee Choi, Do Kyung Kim, Jeong Eun Song, Joaquim Miguel Oliveira, Rui Luis Reis, and Gilson Khang

## Abstract

Regeneration of diseased or damaged skeletal tissues is one of the challenge that needs to be solved. Although there have been many bone tissue engineering developed, scaffold-based tissue engineering complement the conventional treatment for large bone by completing biological and functional environment. Among many materials, silk fibroin (SF) is one of the favorable material for applications in bone tissue engineering scaffolding. SF is a fibrous protein mainly extracted from *Bombyx mori*. and spiders. SF has been used as a biomaterial for bone graft by its unique mechanical properties, controllable biodegradation rate and high biocompatibility. Moreover, SF

can be processed using conventional and advanced biofabrication methods to form various scaffold types such as sponges, mats, hydrogels and films. This review discusses about recent application and advancement of SF as a biomaterial.

## Keywords

Silk fibroin · Biomaterial · Bone tissue engineering · Bone regeneration · Tissue engineering · Scaffold

## Abbreviations

ALP	Alkaline phosphatase
ASCs	Adipose-derived stem cells
BK	Broussonetia kazinoki
BMSCs	Bone marrow derived mesenchymal stem cells
BMP-2	Bone morphogenic protein-2
DBM	Demineralized bone matrix
3D	3 dimensional
ECM	Extracellular matrix
FDA	Food and Drug Administration
HFIP	Hexafluoro-2-propanol
hMSCs	Human mesenchymal stem cells
HAp	Hydroxyapatite
MSCs	Mesenchymal stem cells
micro-CT	Micro computed tomography
PLGA	Poly(lactide-co-glycolide)

J. H. Choi · D. K. Kim · J. E. Song · G. Khang (✉)  
Department of BIN Convergence Technology,  
Chonbuk National University, Jeonju-si,  
Jeollabuk-do, South Korea  
e-mail: [gskhang@jbnu.ac.kr](mailto:gskhang@jbnu.ac.kr)

J. M. Oliveira · R. L. Reis  
Department of PolymerNano Science & Technology  
and Polymer Fusion Research Center, Chonbuk  
National University, Jeonju-si, Jeollabuk-do,  
South Korea

ICVS/3B's – PT Government Associated Laboratory,  
Braga/Guimarães, Portugal

The Discoveries Centre for Regenerative and  
Precision Medicine, Headquarters at University  
of Minho, Avepark, Guimarães, Portugal

PCL	Polycaprolactam
PGA	Polyglycolide
PEG	Polyethylene glycole
PLA	Poly lactide
SF	Silk fibroin
TCP	Tricalcium phosphate
TE	Tissue Engineering
VEGF	Vascular endothelial growth factor

## 20.1 Introduction

Millions of people worldwide suffer from severe pain by trauma or disease of skeletal tissues. Major clinical challenges are represented to revive a damaged bone. Bone tissue engineering (TE) has been significantly developed over the past two decades and many advances have been made in the establishment in biomaterial scaffolds [53]. Bone TE promotes construction of new bone by using alternative bone grafts. TE construct allows to investigate tissue regeneration, helps to analyze the cellular activity and acts as a microenvironment template for tissue regeneration [22, 28]. One of the main goal is to design a scaffold which mimics the bone hierarchical and complex structure. Polymers such as natural and synthetic polymers, ceramic and metals are used as a material for TE scaffolds [26]. The main challenge to design a scaffold is to choose an appropriate biomaterial. Biocompatibility is one of the most important factor that needs to be considered for any biomaterials. Specific physical, mechanical and degradation properties are needed for different types of tissues [101]. SF is known as a commonly available biomaterial and many attempts have been made to enhance its properties. SF has been used in bone tissue engineering field because of its easy and various processing methods, high mechanical strength, excellent elasticity, biocompatibility, and controllable biodegradability [8]. The number of papers and citations are still increasing in SF application of bone TE. This review will discuss about characteristics and different processing methods of SF as an alternative bone graft in bone tissue engineering.

## 20.2 Bone

A bone is a crucial and structural part of a human body. Bones protect the organs in the body, support movement, regulate the storage of mineral and blood pH and participate in maintaining homeostasis. It is important to understand the knowledge of bone tissue, structure, composition and mechanic to regenerate bone [67]. Bone tissue is a hard tissue which compose of 35% of organic part such as collagen which occupy almost 95% of the organic extracellular matrix (ECM), osteocalcin, osteonectin, hyaluronan and proteoglycans. The rest of the 65% of bone tissue is an inorganic matrix which is consist of hydroxyapatite (HAp), carbonate and inorganic salts [46]. The organic ECM contribute to regulating the stem cell fate and immobilizing cytokines and growth factors. Inorganic part helps to strengthen architecture of bone. Bone tissue has two types of mineralized tissue, cortical bone which is compact and sponge-like cancellous bone. Bone marrow, endosteum, nerves, blood vessels, cartilage and periosteum are also found in the bone tissue [4].

Bone tissue engineering is a strategy to regenerate bones and guide cells into osteogenesis. Alternative bone grafts not only use as grafts but also mimic bone tissue structures which help to accelerate bone regeneration and analyze at cellular level. The goal of bone tissue engineering is to provide a 3 dimensional (3D) bone mimicking structure by means of combining cells, growth factors and scaffolds [96]. The main challenge is to choose an appropriate biomaterial which possesses high biocompatibility and low toxicity. Moreover, mechanical properties of bone graft are crucial for handling surgical implantation and tissue integration [64].

### 20.2.1 Bone Extracellular Matrix (ECM)

The physiology and biomechanical structure of bone tissue must be completely understood in order to design a scaffold that can satisfy the needs of making a functional tissue. Bone has a

very complex microenvironment that embed different cell types such as osteocytes, osteoblasts and osteoclasts and regulate the cell adhesion, proliferation and differentiation [79]. This complex environment named as ECM supply structural and biological properties to the bone tissue. The organic nanocomposite of ECM mainly collagen type I serves a template for inorganic nanocomposite such as HAp which helps bone formation and reconstruction by providing a nucleation center for calcium and phosphate ions. The fibrous network ECM also plays a role in regulating the growth factor activity by controlling the release kinetics [67].

Many studies have demonstrated the bone-mimetic environment scaffolds for bone regeneration. The growth factor combined scaffolds has been extensively and reports show that these scaffolds were more efficient in localized delivery and provided ectopic bone formation [79]. Also challenges have been made for poor vascularization in large bone TE scaffolds by using angiogenic factors. Other studies have shown that angiogenic molecules improved bone healing *in vitro* and *in vivo*. However, these studies do not simulate the bone structure perfectly and more investigations are needed to regulate growth factors in the desired region [33].

### 20.2.2 Scaffolds for Bone Regeneration

Designing an ideal scaffold for bone regeneration require biodegradability, biocompatibility, large surface-area-to-volume-ratio, high mechanical strength, and controlled release of growth factors [79]. A porosity is also an important factor because it facilitates delivery of nutrients, diffuses of waste products, provides a microenvironment for cell adhesion, proliferation and differentiation to shape bone tissue [1, 2]. To enhance the scaffold and tissue interaction, surface chemistry and topographical features should also be considered for a required scaffold. Promoting vascularization is another crucial issue in bone TE scaffold and this is satisfied by incorporating angiogenic growth factors such as

platelet-derived growth factor (PDGF), vascular endothelial growth factor (VEGF), insulin-like growth factor (IGF), or fibrous growth factor (FGF-2) in the scaffolds [118]. Producing the scaffold that fulfill the properties mentioned above require different materials and processing methods. The materials for bone TE are nature origin polymers such as collagen I duck feet's collagen, SF, polysaccharides, elastin and fibrinogen [11, 12, 48, 49, 91, 93]. There are also synthetic polymers for bone scaffold material such as poly(lactide-co-glycolide) (PLGA), polycaprolactam (PCL), polyglycolide (PGA), polyethylene glycole (PEG), or polylactide (PLA) ([1, 20, 49]). Processing methods of bone TE are electrospinning, 3D printing freeze-drying and so on.

---

## 20.3 Silk Fibroin As a Biomaterial

Musculoskeletal defects have been treated using bioactive molecules, scaffolding materials or only cells [79]. Recently, silk which is a bioactive polymer gained its focus on regeneration of orthopedic tissue architecture. Silk is a native-derived protein biopolymer made from silkworms, spiders, mites and flies. Silk from varied sources may differ in properties but the component is chiefly proteins and minor amounts of lipids and polysaccharides [30]. The biomaterial and surface topography of scaffolds where cells adhere influence cell migration, proliferation, phenotype and differentiation [3, 19, 23, 24, 27, 57, 61, 102, 110]. The SF scaffolds have shown the advantage of SF as a biomaterial on mesenchymal stem cells (MSCs) to differentiate with ECM secretion and mineralization [43, 45]. The mechanical properties are also important in bone TE. SF has shown excellent mechanical properties such as tensile strength, toughness and young's modulus in several studies. Biocompatibility, biodegradability and low immunogenicity that are also a crucial factors to consider in TE scaffolding have shown outstanding results [17]. Following paragraphs will discuss about characteristics of SF as a biomaterial.

### 20.3.1 Characteristics of Silk Fibroin (SF)

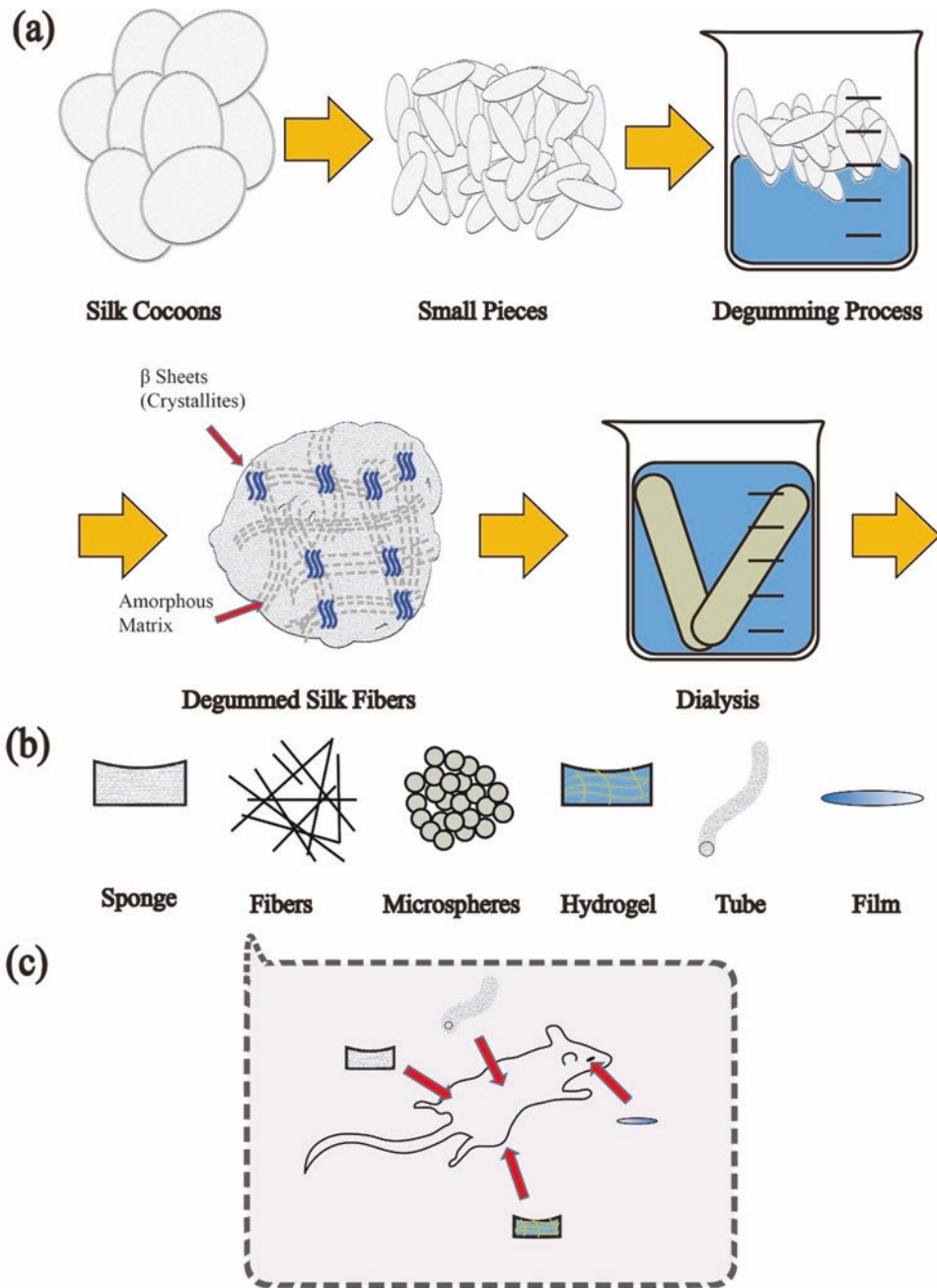
Silk is composed of two different major protein called SF that is made of the fibrous part of the filament and sericin which is a glue-like protein and water soluble. Silk is extracted from different insects such as spiders, *Bombyx mori*, and beetles using different methods. Different silks provide different functions and mechanical properties [95]. The most famous silk is SF from *Bombyx mori*, due to its ease handling, good mechanical properties and high biocompatibility. SF has been used as textiles over thousands of years due to its mass production. Moreover, there are number of studies on SF used in biomedical application. Removal of the sericin component in SF is one of the first step in fabrication of SF scaffold. The sericin, the outer part of silk was known to show allergenic reaction for clinical use. However, it was found that composite of sericin and fibroin caused the adverse reaction and sericin has been found as a biocompatible material in last few years [6, 15, 32, 92, 109, 117]. Degumming process is a thermochemical treatment of the cocoons to remove the glue-like protein sericin (Fig. 20.1). Degummed SF has a crystalline  $\beta$ -sheet which is a main structure of SF. Potassium phosphate or methanol treatment can induce extremely stable  $\beta$ -sheet nanocrystals by increasing glycine content in the SF amino acids sequence. This high glycine constituent allows SF to pack tightly [30, 42, 43, 45, 51, 69, 75, 88, 89]. The crystalline  $\beta$ -sheets are mainly interacted by hydrogen bonds. Although, hydrogen bonds are reported to have weak interactions, hydrogen bonds of SF help to assemble and heal up itself when reforming. The sericin, the outer part of SF is removed in laboratories before use. Degumming process exposes SF to an extreme environment. This not only changes the structure of the silk but also changes the mechanical properties. While degummed SF showed similar Young's modulus, the tensile strength and elongation rate showed difference [25, 55, 64, 107, 113]. These tunable mechanical strengths of SF may attract many researchers to process SF in different forms.

### 20.3.2 Biocompatibility

SF extracted from silk worm is a well-studied biomaterial with a great biocompatibility and low immunity due to its unique structure and chemical composition [10]. The first approach on SF as a biomaterial was attempted in 1995 using fibroblast cells (Minoura et al. 1995). The result showed great cell attachment and proliferation on the surface of *Bombyx mori* SF. After 1 year, SF has been reported to show biocompatibility on blood [63, 82]. SF has been approved by US Food and Drug Administration (FDA) in 1993 and used as a suture. More studies of the immunogenicity and antigenicity of SF were done *in vitro and in vivo* [5, 103]. *In vitro* studies showed that the water absorption ability which is related body fluid and nutrient loss during transplantation was remarkable in SF sponges. Biocompatibility was studied more *in vivo* in SD rat skin. The result showed no sign of infection for up to 4 weeks [88] (Fig. 20.2). Bioengineered composite such as curcumin,  $\beta$ -tricalcium phosphate and *Broussonetia kazinoki* (BK) SF scaffolds were also tested *in vivo* and these studies showed that composites increased the biocompatibility of the SF scaffolds [42, 43, 51]. Properly degummed and sterilized SF is widely accepted for biocompatibility in overall studies. Although SF has been known as a successful biocompatible material for a long time, SF is like any other biomaterials a foreign substances in human body [103]. Further detailed investigations are needed in an adverse immunological response. It is still a challenge to answer a question about long term safety of SF. The immune reaction of SF degraded products is also a concern. With more studies in this regard, it is expected that SF scaffolds will have more potentials in TE.

### 20.3.3 Degradation

Degradation of biomaterial is tested by mass loss and morphology changes assessment. Animal models are used by implantation and examination of histologic and fluorescent studies. SF biodeg-

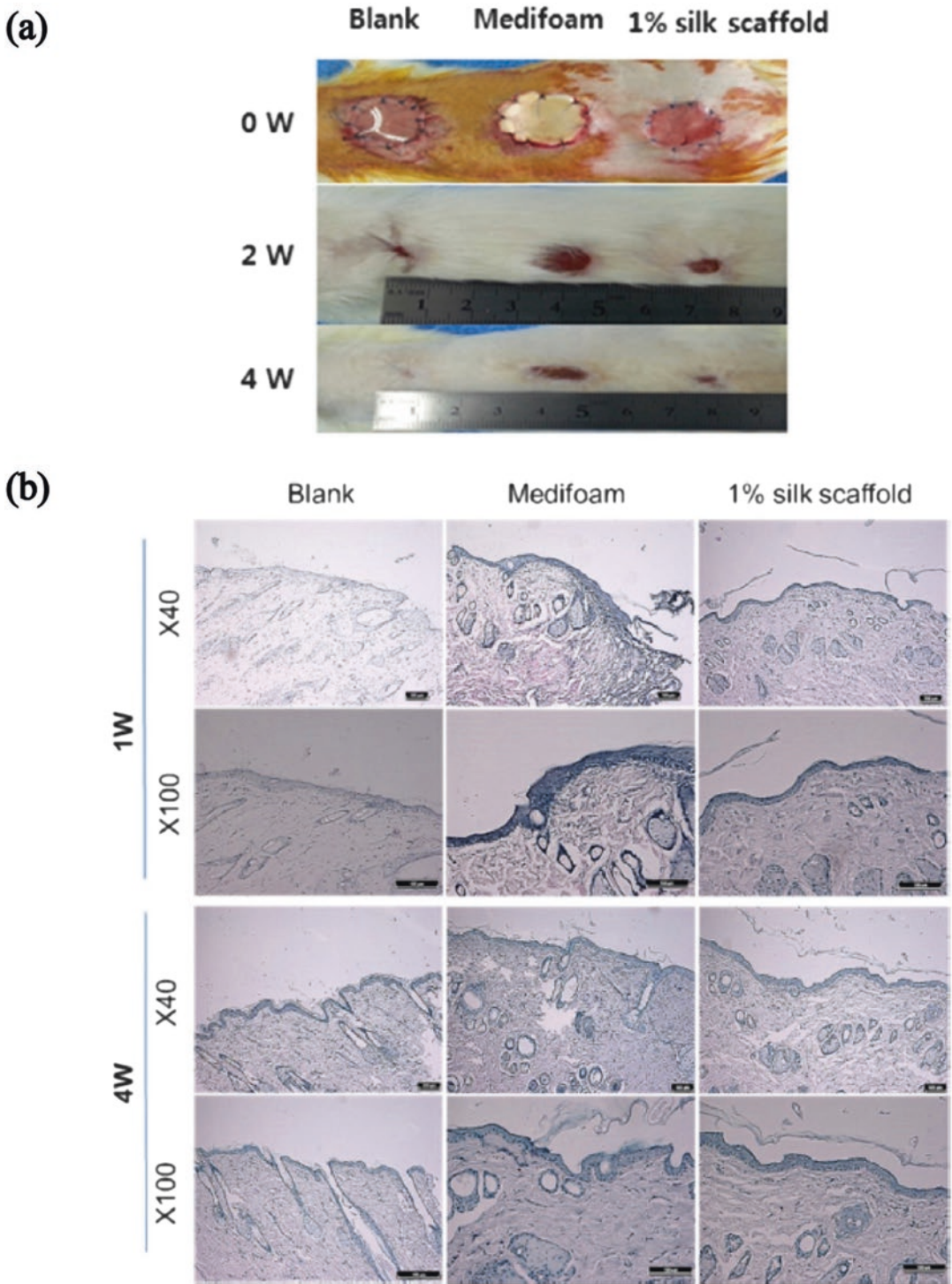


**Fig. 20.1** Illustration of processing SF (a). Schematic representation of different types of SF scaffolds (b). *In vivo* test of SF scaffolds on animal model (c)

radation have been tested in many studies. Combination of biomaterials allow SF degradation rate to increase [10]. Degradation of scaffold in different tissue should possess controllable degradation rate. The understanding of structure

of different tissue and characteristic is crucial for designing a controllable scaffold. The main challenge of SF is the degradation of  $\beta$ -sheet in SF because amyloid of  $\beta$ -fibrils has been reported to have its association with Alzheimer. However, SF





**Fig. 20.2** Gross observation of wounds treated by medifoam and 1% silk sponge (a). Skin stained with H&E for histological observation (b). [88]

has been reported to have non-toxicity on neural cells in *in vitro* studies [43, 45, 70, 71]. The degradation of SF is affected by the content of two type of SF. The insoluble silk I and soluble silk II in water. The methanol treatment increases the  $\beta$ -sheet formation during cross-linking process, resulting an increase in silk II. The fast degradation can be performed with water soluble SF film fabricated without cross-linking process [37, 59]. The lowest rate of  $\beta$ -sheet had shown when the drying time of the scaffold was longer [59]. There are few studies comparing the degradation of different species of SF. The manipulation of degradation time and rate of SF is still challenges for new possibilities in application of tissue engineering and drug release.

### 20.3.4 Mechanical Properties of Silk Fibroin

High mechanical properties are necessary in bone TE scaffolds. The scaffolds should have mechanical compatibility with native bone and transfer load properly. It is known that compressive strength should be 2-12 MPa and 50-500 MPa for modulus to match the mechanical properties of cancellous bone. SF is studied to have high strength, tensile strength and toughness. This polymer is appropriate for bone construct because of its ultimate tensile strength 300-740 MPa, elastic modulus of 10-15 GPa and elasticity of up to 20 % strain-to-failure [26, 40, 43, 50, 53]. The crystalline  $\beta$ -sheets of SF contribute to its mechanical properties. The changes in temperature, pH, mechanical stresses, or exposure to higher salt concentrations or methanol form the crystalline  $\beta$ -sheet [13, 47, 103, 104]. Cells also deposit matrix among the SF which contribute to the bioengineered scaffolds. Studies have shown that the cells incorporated in the composite SF increase the compressive modulus [86, 97]. The curcumin/SF composite have shown that the cells incorporated composite SF has the higher compressive modulus [42]. Also the composite of hydroxyapatite and  $\beta$ -tricalcium phosphate

(TCP) reinforced SF showed that the compressive strength of SF scaffolds increased as the hydroxyapatite  $\beta$ -TCP content increased [51]. The degumming process expose SF to a harsh condition which change SF structure and mechanical properties slightly. This process makes varied mechanical properties such as different  $\beta$ -sheet content, matrix stiffness and composition of SF. Although there are some problems to overcome, SF still surpass other natural derived polymers and some synthetic polymers [73].

### 20.3.5 Porous Structure

Porosity and pore interconnectivity are important features that dictate the final scaffold properties and biological performance. The scaffolds with porous structures are ideal because it closely mimic the physiological microenvironment of a tissue [35, 54]. There are many processing techniques to make the porous structures such as freeze-drying, porogen leaching (e.g. salt), gas-foaming, and electrospinning. The freezing temperature, solution pH and organic solvents amount can control the pore size of the freeze dried sponges [29, 50, 69, 98]. The freeze-drying method makes porosity by the sublimation of ice-crystals. The methanol, glutaraldehyde, or genipin-crosslinking treatments can stabilize the dried 3D scaffold. Also the phosphate or calcium chloride solution can increase compressive strength of the dried silk scaffold which reinforce the osteogenic differentiation [17, 64, 89]. The freeze-thaw process can increase the pore sizes. Salt as a particle for the porous SF scaffolds can produce controlled porosity and pore sizes. It is studied that when compared with salt and sugar, salt leaching results in harder scaffold structure [60]. The average pore sizes and porosity of SF scaffold differ depending on the treatment method. The 3D SF scaffold treated with hexafluoro-2-propanol (HFIP) is known to have higher porosity and average pore size than the methanol treated scaffold. Also the aqueous derived SF

scaffold showed increase in the pore size than the freeze dried SF hydrogel. Selecting a suitable fabrication method can lead to an appropriate scaffold for the target tissue [8].

---

## 20.4 Processing Methods of Silk Fibroin

Selecting an appropriate biomaterial that mimic the micro- and nano-structure of the tissue aimed at regenerate is very important. Above that, suitable architecture is needed for the functionality of the tissue [116]. The choice of material and design of scaffold for bone tissue engineering is decisive factors. The scaffold should support cell proliferation, differentiation, migration and deposition of ECM. Also the scaffold for the bone tissue must have sufficient toughness and matrix deposition considering the fact that the bone is a connective tissue that has major components of collagen type I and hydroxyapatite [79]. The biocompatibility, biodegradability and delivery of growth factors and osteoprogenitor cells delivery capacity is another crucial characteristics that is necessary for a suitable material [94]. The scaffold with porous 3D structure is considered as the most important factors of the bone scaffolds design because it offers proper mechanical properties, controllable porosity and pore sizes and high interconnectivity. The SF is a reasonable selection for the bone TE for its tunable mechanical properties and bio-compatibility. Moreover, the structure of SF scaffolds can support transportation of essential nutrients, oxygen and cell debris. The SF scaffolds can be processed into different structures by different fabrication methods [34, 39, 43, 68, 120]. SF scaffolds can be processed into hydrogels, porous sponges, fibrous mats, microspheres and fibers. In this section, various processing methods to fabricate different types of scaffolds will be discussed.

### 20.4.1 Hydrogels

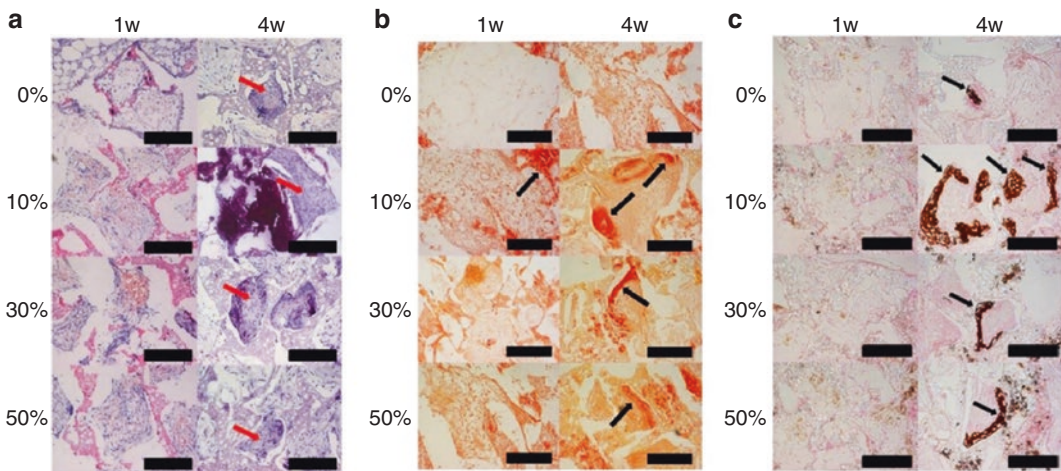
Hydrogels are 3D structure scaffolds which keep high amount of water molecules. In recent days, hydrogels have attracted many researchers as it provide high cell interactions and delivery of cytokines in tissue engineering field. Hydrogels can be used as an injectable medicine to deliver drugs and cells. The hydrogelation of SF can be processed by vortexing, sonication, lowering the PH level, increasing the temperature and ionic strength, freezing and electromagnetic treatment [7, 9, 105, 114, 115]. Gelation process will change the structure of aqueous SF solution from disordered state to  $\beta$ -sheet formation. The sonication process imparts movement of SF molecules and can convert gel in to aqueous solution by taking disulfide bonds apart [58, 81]. Consequently, a hydrogel is formed after sonication. The SF hydrogel fabricated by freezing method provides unique mechanical properties. The frozen SF solution immersed in solvent and kept below frozen temperature. In the previous study, hydrogel fabricated by sonication method reported to increased human mesenchymal stem cells (hMSCs) proliferation and enhanced cellular activities. hMSCs were well encapsulated in the SF based hydrogels. The hMSCs showed osteogenic differentiation in SF hydrogels without adding promoters for osteogenic differentiation. Moreover, SF hydrogel incorporated with VEGF and bone morphogenic protein-2 (BMP-2) has been reported to enhance angiogenesis and bone regeneration. SF hydrogels have the ability to carry different cytokines and growth factors with a minimal incision during surgery which will shorten the recovery time after post-implantation [7, 105, 106, 119]. More recently, Yan et al. proposed a new class of enzymatically crosslinked hydrogels for TE, cancer research and drug delivery applications [111, 112]

### 20.4.2 Sponges

SF sponges with high porosity have been used in bone tissue engineering for bone regeneration. 3D structure of sponge scaffolds support ECM secretion, cell proliferation, cell differentiation and attachment [69, 98]. Sponge scaffolds allow to exchange essential nutrients and oxygen [43]. The pore size and porosity can be controlled in different sizes using various methods such as salt leaching, freeze-drying, or gas foaming. The SF sponges with bioactive ceramics increase the controllability of a porosity and pore sizes.  $\beta$ -TCP incorporated SF sponges showed that as the  $\beta$ -TCP increased, porosity increased and the pore sizes increased which enabled cell attachment and invasions for bone tissues [51]. Another study showed that the SF sponges with hydroxyapatite porosity was controlled similar as the  $\beta$ -TCP/SF. The study showed that the more hydroxyapatite in the SF sponges allowed more cells adhesion and active interaction along the

cells [89] (Fig. 20.3). SF sponges with BK bio-material showed smaller pore sizes than the SF but higher ECM was shown [43, 45].

The degradation of SF based sponge scaffolds can be differ by using different solvent. The use of HFIP on SF scaffolds may take more than 2 years to degrade. However, scaffolds made with aqueous SF solution may take 2–6 months. The advantage of HFIP based SF scaffold on bone tissue engineering using adipose-derived stem cells (ASCs) has been reported. The HFIP based SF scaffold enhanced alkaline phosphatase (ALP) activity, calcium deposition. Apart from the above, the scaffolds fabricated with freeze-drying method with bone lamellar structure showed different result. The scaffolds were treated with methanol which induced  $\beta$ -sheet formation. Moreover, the other group has reported enhancement of osteogenic differentiation of hMSCs cultured on SF aqueous based scaffold compared to HFIP based scaffold. They implanted two different scaffolds into cortical defect area of the



**Fig. 20.3** Histochemistry staining in aqueous-derived silk fibroin scaffolds loaded with various ratios of HAP with rBMSCs after 1 and 4 weeks of implantation *in vivo*:

H&E (a). Alizarin red S (b). Von Kossa (c) (magnification with  $\times 200$ , scale bar = 200  $\mu\text{m}$ ) (red arrows: osteocyte in lacuna, black arrows: mineral). [89]

lambs. After 4 weeks of post-implantation, SF aqueous based scaffold group showed new bone formation while HFIP based scaffold showed necrotic cells without new bone formation [17, 72, 101, 105, 106]. In recent studies, porous SF sponge scaffolds can be monitored in 3D images using micro-CT process without destroying. The main concern of using micro computed tomography (micro-CT) method on SF scaffold is invisible sight of bottom part because SF is not radio opaque material. Due to invisible sight of SF using micro-CT, it is not proper to monitoring the degradation process of SF scaffolds using micro-CT [31, 64].

### 20.4.3 Fibrous Mats

Electrospinning method which is flexible and versatile produces fibrous polymer with different size and diameter. The diameter of electrospun fibers differs from nano to micro size that can allow mimicking the fibrous ECM structure. The control of atmospheric temperature and humidity, voltage, distance between the needle and collector, nozzle configuration, type of collector, and use of different solvent that differ in viscosity, polarity, concentration, volatility and conductivity can manipulate the diameter of porosity of electrospun fibrous mats [43, 45, 66, 67]. By handling these parameters, diameter of the fibers which control the adhesion and proliferation of bone marrow derived mesenchymal stem cells (BMSCs) is controlled. Besides the tunable processing properties, electrospinning is economical and relatively fast in fabrication of scaffolds [21, 56, 76, 77, 79]. In the previous study, BMSCs have been reported to show higher cell proliferation and ECM secretion which is cultured on electrospun SF fibrous mats. ECM structure mimic in tissue engineering application is important to support cell proliferation, migration and attachment [41, 108]. Selecting an appropriate solvent and concentration of SF is important during electrospinning. HFIP is used to fabricate

nanometer-diameter SF fibers. The silk concentration is known to be the most important consideration in producing uniform fibers with a diameter less than 100 nm. Methanol treatment convert SF fibers  $\alpha$ -helix to crystalline  $\beta$ -sheet. Blending with synthetic polymers with SF produce improved properties in hydrophilicity, strength, elongation and osteoconductivity. When electrospinning is combined with freeze-drying, growth factors delivery is facilitated. The growth factors increase the mimic of microenvironment of bone tissue which enhances osteogenic differentiation. Although the electrospinning is easy to use and robust, there are some limits. It is challenging to make a sufficient amount of production, distribute cells uniformly and control the mean pore sizes. Combining other fabrication methods with electrospinning or increasing the time span dramatically can compensate the defect of the electrospinning method [8, 30, 50, 87].

### 20.4.4 Silk Fibroin Composite Scaffold

The incorporation of SF and other biomaterials has been reported to show advantages on bone tissue engineering. The incorporation of calcium phosphate, collagen and different nature derived biomaterials showed bone regeneration in both *in vitro* and *in vivo*. Recently, composite SF scaffolds lead to higher osteoconductivity, osteogenic differentiation and new bone formation rate compared to unmodified scaffolds. The incorporation of HAp with SF due to its great osteoconductivity and enhancement of mechanical properties has been used in electrospinning process. Moreover, incorporation of BMP-2, HAp and SF has been reported to support hMSCs proliferation, osteogenic differentiation and showed high calcium composition [44, 52, 65, 74].

Incorporation with nature derived materials such as aloe vera, chitosan, BK has been proved to enhance osteoconductivity and osteoinductivity [38, 43, 45]. The demineralized bone matrix

(DBM) is widely used material which contains large amount of collagen and BMP-2. The incorporation of DBM powder or DBM particles with SF not only promoted osteogenesis of rat ASCs but also allowed to handle DBM easily. The composition of DBM and SF increased surface roughness and mechanical properties which are important for cell attachment and migration [100].

Recently, SF has been combined with ionic-doped calcium phosphates that can modulate stem cells proliferation and osteogenic potential [78].

The proper compressive strength of scaffold for bone tissue engineering can be achieved by adding new biomaterial or reinforcement of SF itself. In the previous study, SF microfibers and microspheres have been used to enhance mechanical properties. The incorporation of SF particles increase rigidity, roughness of the scaffolds and osteogenic differentiation of cells.

#### 20.4.5 3D Printing

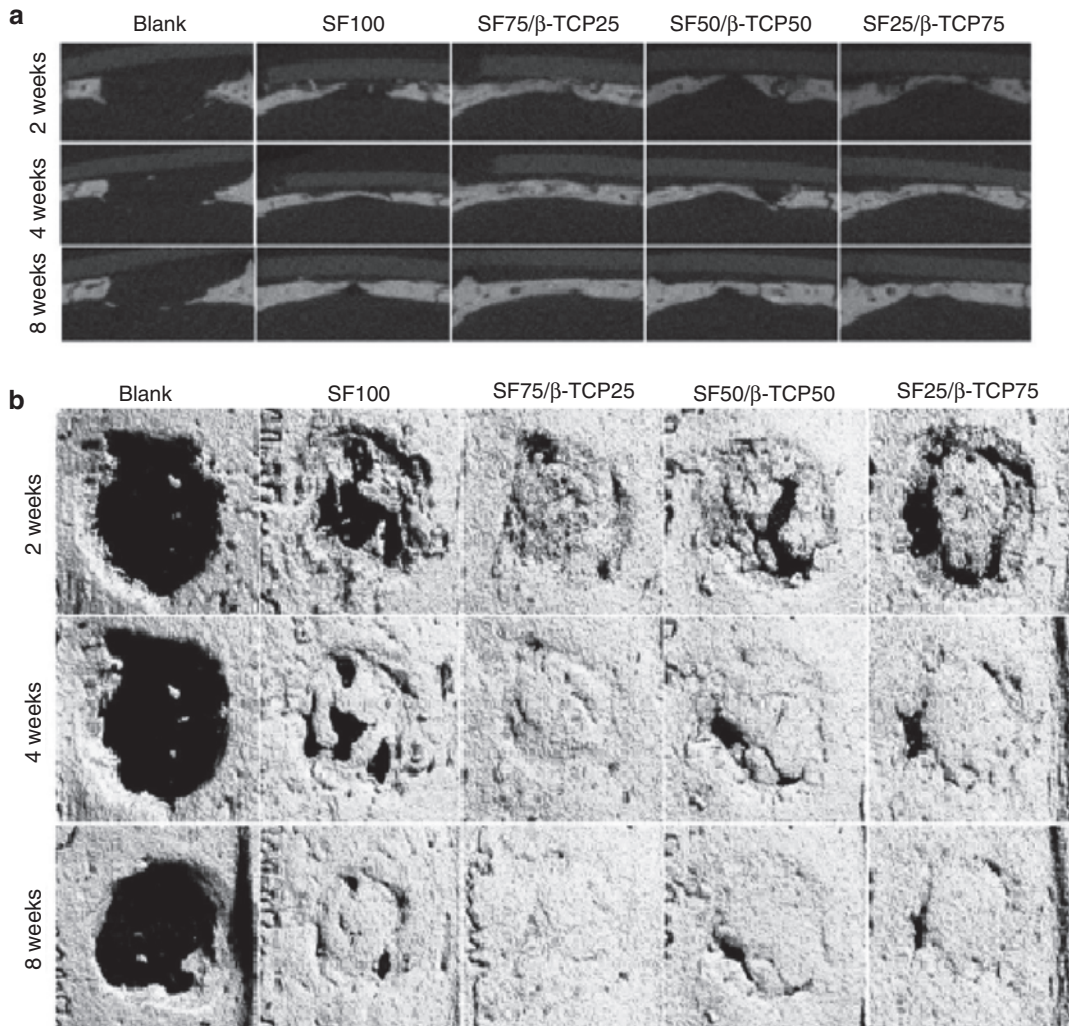
3D printing controls the internal geometry and porosity which influence the cellular behavior. Current scaffold processing methods are unsuccessful in controlling the material properties. The conventional strategies such as freeze drying, porogen leaching, electrospinning, or gas foaming produce random porous scaffolds. The 3D printing combines biomaterials with cells and supporting components with pre-defined internal architecture scaffolds which overcome the conventional methods drawbacks [14, 99]. Also the 3D printing allows cells to encapsulate in biocompatible hydrogels that mechanically and biochemically supportive environment. There are few studies using SF for 3D printing. The  $\beta$ -sheet content modification regulates the stiffness and degradation of the SF scaffolds in 3D printing [14, 16, 80, 83, 90]. Recently, Costa et al. reported on a fast setting SF bioinks which open ups possibilities in the biofabrication of memory-shape

implants for personalized TE [18]. More studies are needed but the 3D printing is regarded as the potential future technique in bone TE.

### 20.5 Bone Regeneration Using Silk Fibroin *In Vivo*

To investigate the regeneration ability of a scaffold, it is difficult to process only with *in vitro* evaluation. Therefore, to evaluate and analyze the new bone formation ability and osteogenesis, *in vivo* evaluation should be performed. SF has been evaluated as sponges, electrospun fibrous mat and hydrogels in different animal models on different locations mainly on calvarial, mandibular and femoral area. The pristine SF scaffold with and without osteogenic cell seeded scaffolds were compared in previous studies. The results demonstrated that there were no significant new bone formation in non-cell seeded group compared to cell seeded group in mice. The similar result was revealed when pre-differentiated hMSCs were used. The mandibular defects of rats and canines were filled with new bone tissue in mineralized or apatite coated SF scaffolds [36, 62, 121]. Although osteogenic cell seeded on SF scaffolds showed advantages on osteoconductivity and osteoinductivity in *in vivo* studies, use of pre-cell cultured scaffolds may not be appropriate in a clinical purpose for human due to isolation process, long duration time and immune rejection problem. To overcome these problems, rather than seeding the cells on the scaffolds, incorporation of bioactive resources such as nature-derived biomaterials and bioactive glasses with SF were attempted. Interestingly, incorporated scaffolds induced new bone formation and mineralization compared to pristine SF scaffolds [43, 45, 84, 85].

The *in vivo* study of  $\beta$ -TCP and SF composite showed that the rate of bone formation was slower in the blank group and increased in the BMSCs seeded scaffolds. The bone regeneration was significantly active in the SF/ $\beta$ -TCP compos-

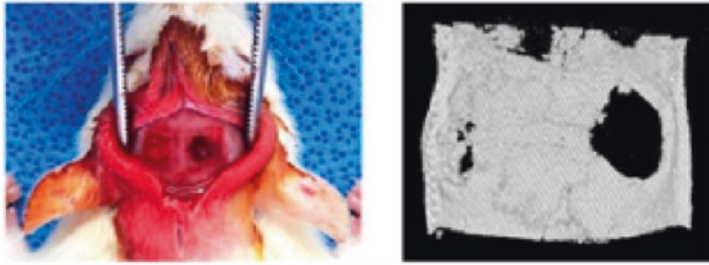
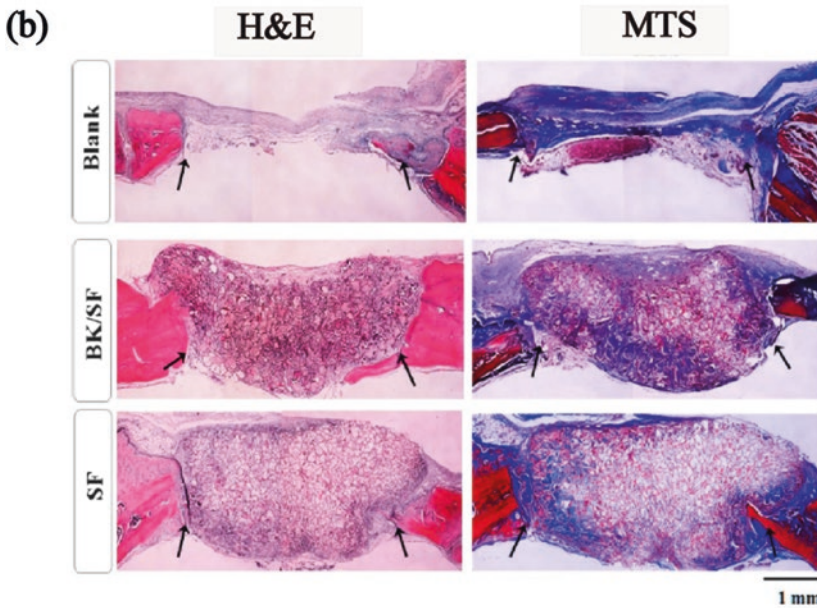


**Fig. 20.4** Micro-CT analysis of SF/  $\beta$ -TCP scaffolds in calvarial defects. Cross-sectional images of calvarial defects (a). 3D images of calvarial defects (b). [51]

ite scaffolds. The histological staining in the defect model implanted with SF/ $\beta$ -TCP showed developed bone tissue and extent of collagen formation was investigated after 8 weeks of scaffold implantation in the defect area [51] (Fig. 20.4). Combination of a SF and biomaterial instead of growth factors and cytokines was also studied. BK powdery extract was applied to make SF scaffold. The BK/SF scaffold implanted area was filled with mineralized bone tissue at 8 weeks but the SF scaffold in the defect area showed almost undetectable newly formed tissue [43, 45] (Fig. 20.5).

## 20.6 Conclusion

SF is a nature-derived biomaterial with tunable mechanical properties and biocompatibility which is favorable for a variety of purpose in TE. SF can be incorporated with different biomaterials to form hybrid composite scaffolds which induce new bone formation and mineralization. These hybrid composite can provide a natural bone environment and expand osteogenic potential. SF can be fabricated to different types of scaffolds such as hydrogels which are injectable or printable, sponges that are porous and fibrous mats in 2D or

**(a) Implantation of scaffold into calvarial defect of SD rats****In vivo evaluation**

**Fig. 20.5** rBMSC-laid scaffolds were implanted into the calvaria defects of female SD rats (a). Histological sections stained with H&E and MTS for calvaria defect treated models. Histological sections stained with H&E

and MTS for calvaria defect treated with SF, BK/SF scaffold, and nontreated (control) at 8 weeks postsurgery (scale bar = 1 mm) (b). [43, 45]

3D constructs by using different processing methods. Improved SF scaffolds can be expected with novel processing techniques and lead to new possibilities on bone tissue engineering. *In vitro* studies using SF scaffolds can contribute to understanding more about bone tissue ECM mineralization, bone resorption occurrence and vascularization as well as bone diseases and therapeutic drugs. *In vivo* studies have been performed on small animals such as rats and rabbits. These results do not suggest that SF can be applied to humans. Further studies such as requirements in clinical trials and suitable commercialized

structures for silk-based scaffolds in bone regeneration are needed. The future of SF in clinical use for bone regeneration is promising and will lead to better life styles and rapid healing for patients with various bone diseases and defects.

**Acknowledgements** This research was supported by Basic Science Research Program through the National Research Foundation of Korea (NRF) funded by the Ministry of Science, ICT & Future Planning (NRF-2017R1A2B3010270) and Korea Health Technology R&D Project through the Korea Health Industry Development Institute (KHIDI), funded by the Ministry of Health & Welfare, South Korea (HI15C2996).



## References

- Adachi T, Osako T, Tanaka M, Hojo M, Hollister SJ (2006) Framework for optimal design of porous scaffold microstructure by computational simulation of bone regeneration. *Biomaterials* 27(21):3964–3972
- Aiba SI, Higuchi M, Gotoh Y, Tsukada M, Imai Y (1995) Attachment and growth of fibroblast cells on silk fibroin. *Biochem Biophys Res Commun* 208(2):511–516
- Amin YS, Van DSJ, Chai YC, Wauthle R, Tahmasebi BZ, Habibovic P, Mulier M, Schrooten J, Weinans H, Zadpoor AA (2014) Bone regeneration performance of surface-treated porous titanium. *Biomaterials* 35(24):6172–6181
- Amini AR, Cato TL, Syam PN (2012) Bone tissue engineering: recent advances and challenges. *Critical reviews™ in biomedical engineering* 40(5):363–408
- Altman GH, Diaz F, Jakuba C, Calabro T, Horan RL, Chen J, Lu H, Richmond J, Kaplan DL (2003) Silk-based biomaterials. *Biomaterials* 24(3):401–416
- Aramwit P, Sorada K, Wanchai DE, Teerapol S (2009) Monitoring of inflammatory mediators induced by Silk sericin. *J Biosci Bioeng* 107(5):556–561
- Bhardwaj N, Sagar C, Subhas CK (2011) Freeze-gelled silk fibroin protein scaffolds for potential applications in soft tissue engineering. *Int J Biol Macromol* 49(3):260–267
- Bhattacharjee P, Kundu B, Naskar D, Kim HW, Maiti TK, Bhattacharya D, Kundu SC (2017) Silk scaffolds in bone tissue engineering: an overview. *Acta Biomater* 63:1–17
- Calderón-Colón X, Xia Z, Breidenich JL, Mulreany DG, Guo Q, Uy OM, Tiffany JE, Freund DE, McCally RL, Schein OD, Elisseeff JH, Trexler MM (2012) Structure and properties of collagen vitrigel membranes for ocular repair and regeneration applications. *Biomaterials* 33(33):8286–8295
- Cao Y, Wang B (2009) Biodegradation of silk biomaterials. *Int J Mol Sci* 10(4):1514–1524
- Cha JG, Cha SR, Lee DH, Shin JH, Song JE, Suh DS, Park CH, Khang G (2016) mEvaluation of osteogenesis on duck's feet derived collagen and demineralized bone particles sponges. *Polymer (Korea)* 40(6):858–864
- Cha SR, Jang NK, Kuk H, Kim EY, Song JE, Park CH, Khang G (2014) Inflammatory response effect of duck S feet derived collagen scaffolds for bone tissue engineering. *Orig Artic* 5(3):84–89
- Chen F, David P, Fritz V (2012) Silk cocoon (*Bombyx Mori*): multi-layer structure and mechanical properties. *Acta Biomater* 8(7):2620–2627
- Chia HN, Benjamin MW (2015) Recent advances in 3D printing of biomaterials. *J Biol Eng* 9(1):1–14
- Chirila TV, Shuko S, Laura JB, Nigel LB, Damien GH (2013) Evaluation of silk sericin as a biomaterial: *in vitro* growth of human corneal limbal epithelial cells on bombyx mori sericin membranes. *Prog Biomater* 2(1):14
- Compan AM, Kyle C, Yong H (2017) Inkjet bioprinting of 3D silk fibroin cellular constructs using sacrificial alginate. *ACS Biomater Sci Eng* 3(8):1519–1526
- Correia C, Bhumiratana S, Yan L, Oliveira AL, Gimble JM, Rockwood D, Kaplan DL, Sousa RA, Reis RL, Vunjak-Novakovic G (2012) Development of silk-based scaffolds for tissue engineering of bone from human adipose-derived stem cells. *Acta Biomater* 8(7):2483–2492
- Costa JB, Silva CJ, Oliveira JM, Reis RL (2017) Fast setting silk fibroin bioink for bioprinting of patient-specific memory-shape implants. *Adv Healthc Mater* 6(22)
- Dalby MJM, Gadegaard N, Tare R, Andar A, Riehle MO, Herzyk P, Wilkinson CD, Oreffo ROC (2007) The control of human mesenchymal cell differentiation using nanoscale symmetry and disorder. *Nat Mater* 6(5):407–413
- Dalton PD, Tim W (2008) Polymeric scaffolds for bone tissue engineering. *Bone* 32(3):2004–2005
- Dimitriou R, Elena J, Dennis M, Peter VG (2011) Bone regeneration: current concepts and future directions. *BMC Med* 9:66
- Elliott NT, Fan Y (2011) A review of three-dimensional *in vitro* tissue models for drug discovery and transport studies. *J Pharm Sci* 100(1):59–74
- Engler AJ, Shamik S, Sweeney HL, Dennis ED (2006) Matrix elasticity directs stem cell Lineage specification. *Cell* 126(4):677–689
- Eun JJ, Kim HM, Kim H, Jeon DY, Park CH (2014) Inflammatory responses to hydroxyapatite/poly(lactic-co-glycolic acid) scaffolds with variation of compositions. *Polymer Korea* 38(2):156–163
- Fan H, Haifeng L, Yue W, Siew LT, James CHG (2008) Development of a silk cable-reinforced gelatin/silk fibroin hybrid scaffold for ligament tissue engineering. *Cell Transplant* 17(12):1389–1401
- Farokhi M, Mottaghtalab F, Samani S, Shokrgozar MA, Kundu SC, Reis RL Fatahi Y, Kaplan DL (2017) Silk fibroin/hydroxyapatite composites for bone tissue engineering. *Biotechnol adv* 36(1):68–91
- Ghibaudo M, Saez A, Trichet L, Xayaphoummine A, Browaeys J, Silberzan P, Buguin A, Ladoux B (2008) Traction forces and rigidity sensing regulate cell functions. *Soft Matter* 4(9):1836
- Griffith LG, Melody AS (2006) Capturing complex 3D tissue physiology *in vitro*. *Nat Rev Mol Cell Biol* 7(3):211–224
- Han KS, Song JE, Tripathy N, Kim H, Moon BM, Park CH, Khang G (2015) Effect of pore sizes of silk scaffolds for cartilage tissue engineering. *Macromol Res* 23(12):1091–1097
- Hardy JG, Thomas RS (2010) Composite materials based on silk proteins. *Prog Polym Sci (Oxford)* 35(9):1093–1115
- Hofmann S, Hilbe M, Fajardo RJ, Hagenmüller H, Nuss K, Arras M, Müller R, Von RB, Kaplan DL, Merkle HP, Meinel L (2013) Remodeling of tissue-

- engineered bone structures *in vivo*. *Eur J Pharm Biopharm* 85(1):119–129
32. Hollander DH (1994) Interstitial cystitis and silk allergy. *Med Hypotheses* 43(3):155–156
  33. Huang YC, Darnell K, Kevin GR, Paul HK, David JM (2005) Combined angiogenic and osteogenic factor delivery enhances bone marrow stromal cell-driven bone regeneration. *J Bone Min Res* 20(5):848–857
  34. Huttmacher DW (2000) Scaffolds in tissue engineering bone and cartilage. *Biomaterials* 21(24):2529–2543
  35. Ikeda R, Fujioka H, Nagura I, Kokubu T, Toyokawa N, Inui A, Makino T, Kaneko H, Doita M, Kurosaka M (2009) The effect of porosity and mechanical property of a Synthetic polymer scaffold on repair of osteochondral defects. *Int Orthop* 33(3):821–828
  36. Jiang X, Zhao J, Wang S, Sun X, Zhang X, Chen J, Kaplan DL Zhang Z (2009) Mandibular repair in rats with premineralized silk scaffolds and BMP-2-Modified bMSCs. *Biomaterials* 30(27):4522–4532
  37. Jin HJ, Park J, Karageorgiou V, Kim JJ, Valluzzi R, Cebe P, Kaplan DL (2005) Water- stable silk films with reduced  $\beta$ -Sheet content. *Adv Funct Mater* 15(8):1241–1247
  38. Jithendra P, Abraham MR, Thambiran K, Asit BM, Chellan R (2013) Preparation and characterization of aloe vera blended collagen-chitosan composite scaffold for tissue engineering applications. *ACS Appl Mater Interfaces* 5(15):7291–7298
  39. Joly P, Duda GN, Schöne M, Welzel PB, Freudenberg U, Werner C, Petersen A (2013) Geometry-driven cell organization determines tissue growths in scaffold pores: consequences for fibronectin organization. *PLoS One* 8(9):e73545
  40. Kapoor S, Subhas CK (2016) Silk protein-based hydrogels: promising advanced materials for biomedical applications. *Acta Biomater* 31:17–32
  41. Ki CS, Park SY, Kim HJ, Jung HM, Woo KM, Lee JW, Park YH (2008) Development of 3-D nanofibrous fibroin scaffold with high porosity by electrospinning: implications for bone regeneration. *Biotechnol Lett* 30(3):405–410
  42. Kim DK, Kim JI, Sim BR, Khang G (2017) Bioengineered porous composite curcumin/silk scaffolds for cartilage regeneration. *Mater Sci Eng C* 78:571–578
  43. Kim DK, Kim JI, Hwang TI, Sim BR, Khang G (2016) Bioengineered osteoinductive broussonetia kazinoki/ silk fibroin composite scaffolds for bone tissue regeneration. *ACS Appl Mater Interfaces Acsami* 9(2):1384–1394
  44. Kim H, Che L, Ha Y, Ryu W (2014) Mechanically-reinforced electrospun composite silk fibroin nanofibers containing hydroxyapatite nanoparticles. *Mater Sci Eng C* 40:324–335
  45. Kim JI, Hwang TI, Ludwig EA, Park CH, Kim CS (2016) A controlled design of aligned and random nanofibers for 3D bi-functionalized Nerve conduits fabricated via a novel electrospinning set-up. *Sci Rep* 6:23761
  46. Kneser U, Schaefer DJ, Polykandriotis E, Horch RE (2006) Tissue engineering of bone: the reconstructive surgeon's point of view. *J Cell Mol Med* 10(1):7–19
  47. Koh LD, Cheng Y, Teng CP, Khin YW, Loh XJ, Tee SY, Low M, Ye E, Yu HD, Zhang YW, Han MY (2015) Structures, mechanical properties and applications of silk fibroin materials. *Prog Polym Sci* 46:86–110
  48. Kook YJ, Lee DH, Song JE, Tripathy N, Jeon YS, Jeon HY, Oliveira JM, Reis RL, Khang G (2017) Osteogenesis evaluation of duck's feet derived collagen/hydroxyapatite sponges immersed in dexamethasone. *Biomater Res* 21(1):1–7
  49. Kuk H, Kim HM, Kim SM, Kim EY, Song JE, Kwon SY, Suh DS, Park CH, Khang G (2015) Osteogenic effect of hybrid scaffolds composed of duck feet collagen and PLGA. *Polymer (Korea)* 39(6):846–851
  50. Kundu B, Rangam R, Subhas CK, Xungai W (2013) Silk fibroin biomaterials for tissue regenerations. *Adv Drug Deliv Rev* 65(4):457–470
  51. Lee DH, Tripathy N, Shin JH, Song JE, Cha JG, Min KD, Park CH, Khang G (2017) Enhanced osteogenesis of  $\beta$ -tricalcium phosphate reinforced silk fibroin scaffold for bone tissue biofabrication. *Int J Biol Macromol* 95:14–23
  52. Li C, vepari C, Jin H-J, Kim HJ, Kaplan DL (2006) Electrospun silk-BMP-2 scaffolds for bone tissue engineering. *Biomaterials* 27(16):3115–3124
  53. Li C, Vepari C, Jin HJ, Kim HJ, Kaplan DL (2014) Scaffold-based regeneration of skeletal tissues to meet clinical challenges. *J Mater Chem B* 2(42):7272–7306
  54. Lin CY, Noboru K, Scott JH (2004) A novel method for biomaterial scaffold internal architecture design to match bone elastic properties with desired porosity. *J Biomech* 37(5):623–636
  55. Liu H, Fan H, Wong EJW, Toh SL, Goh JCH (2008) Silk-based scaffold for ligament tissue engineering. *IFMBE Proc* 20:34–37 IFMBE
  56. Liu J, David GK (2014) Mechanism of guided bone regeneration : a review. *Open Dent J* 8:56–65
  57. Liu L, Ratner BD, Sage EH, Jiang S (2007) Endothelial cell migration on surface- density gradients of fibronectin, VEGF, or both proteins. *Langmuir* 23(22):11168–11173
  58. Lu Q, Huang Y, Li M, Zuo B, Lu S, Wang J, Zhu H, Kaplan DL (2011) Silk fibroin electrogelation mechanisms. *Acta Biomater* 7(6):2394–2400
  59. Lu Q, Hu X, Wang X, Klug JA, Lu S, Cebe P, Kaplan DL (2010) Water-insoluble silk films with silk I structure. *Acta Biomater* 6(4):1380–1387
  60. Makaya K, Terada S, Ohgo K, Asakura T (2009) Comparative study of silk fibroin porous scaffolds derived from salt/water and sucrose/hexafluoroisopropanol in cartilage formation. *J Biosci Bioeng* 108(1):68–75
  61. McMurray RJ, Wann AKT, Thompson CL, Connelly JT, Knight MM (2013) Surface topography regulates

- wnt signaling through control of primary cilia structure in mesenchymal stem cells. *Sci Rep* 3:3545
62. Meinel L, Betz O, Fajardo R, Hofmann S, Nazarian A, Cory E, Hilbe M, McCool J, Langer R, Vunjak-Novakovic G, Merkle HP, Rechenberg B, Kaplan DL, Kirker-Head C (2006) Silk based biomaterials to heal critical sized femur defects. *Bone* 39(4):922–931
  63. Meinel L, Hofmann S, Karageorgiou V, Kirker-Head C, McCool J, Gronowicz G, Zichner L, Langer R, Vunjak-Novakovic G, Kaplan DL (2005) The inflammatory responses to silk films *in vitro* and *in vivo*. *Biomaterials* 26(2):147–155
  64. Melke J, Swati M, Sourabh G, Keita I, Sandra H (2016) Silk fibroin as biomaterial for bone tissue engineering. *Acta Biomater* 31:1–16
  65. Meng W, Kim SY, Yuan J, Kim JC, Kwon OH, Kawazoe N, Chen G, Ito Y, Kang IK (2007) Electrospun PHBV/collagen composite nanofibrous scaffolds for tissue engineering. *J Biomater Sci Polym Ed* 18(1):81–94
  66. Min BM, Lee G, Kim SH, Nam YS, Lee TS, Park WH (2004) Electrospinning of silk fibroin nanofibers and its effect on the adhesion and spreading of normal human keratinocytes and fibroblasts *in vitro*. *Biomaterials* 25:1289–1297
  67. Minoura N, Mohammadi M, Shaegh SA, Alibolandi M, Ebrahimzadeh MH, Tamayol A, Jafari MR, Ramezani M (2018) Micro and Nanotechnologies for Bone Regeneration: recent advances and emerging designs. *J Control* 274(January):35–55
  68. Murphy CM, Matthew GH (2010) The effect of mean pore size on cell attachment, proliferation and migration in collagen glycosaminoglycan scaffolds for tissue engineering. *Biomaterials* 31(3):461–466
  69. Nazarov R, Jin HJ, David LK (2004) Porous 3-D scaffolds from regenerated silk fibroin. *Biomacromolecules* 5(3):718–726
  70. Numata K, Cebe P, Kaplan DL (2010) Mechanism of enzymatic degradation of beta-sheet crystals. *Biomaterials* 31(10):2926–2933
  71. Oh SH, Park IK, Kim JM, Lee JH (2007) *In vitro* and *in vivo* characteristics of PCL scaffolds with pore size gradient fabricated by a centrifugation method. *Biomaterials* 28(9):1664–1671
  72. Oliveira AL, Sun L, Kim HJ, Hu X, Rice W, Kluge J, Reis RL, Kaplan DL (2012) Aligned silk-based 3-D architectures for contact guidance in tissue engineering. *Acta Biomater* 8(4):1530–1542
  73. Padol AR, Jayakumar K, Mohan K, Manochaya S (2012) Natural biomaterial silk and silk proteins : applications in tissue repair. *Int J Mater Biomater Appl* 2(4):19–24
  74. Panda N, Bissoyi A, Pramanik K (2014) Directing osteogenesis of stem cells with hydroxyapatite precipitated electrospun eri-tasar silk fibroin nanofibrous scaffold. *J Biomater Sci Polym Ed* 25(13):1440–1457
  75. Pérez RJ, Elices M, Llorca J, Viney C (2002) Effect of degumming on the tensile properties of silkworm (*bombyx mori*) silk fiber. *J Appl Polym Sci* 84(7):1431–1437
  76. Pérez S, María J, Elena R, Miguel L, José LC, Cristina P (2010) Biomaterials for bone regeneration. *Medicina Oral, Patología Oral Y Cirugía Bucal* 15(3):e517
  77. Petite H, Viateau V, Bensaïd W, Meunier A, De PC, Bourguignon M, Oudina K, Sedel L, Guillemin G (2000) Tissue-engineered bone regeneration. *Nat Biotechnol* 18(9):959–963
  78. Pina S, Canadas RF, Jiménez G, Perán M, Marchal JA, Reis RL, Oliveira JM (2017) Biofunctional ionic-doped calcium phosphates: silk fibroin composites for bone tissue engineering scaffolding. *Cells Tissues Organs* 205(3-4):150–163
  79. Polo CL, Magda LE, Jaime EV (2014) Scaffold design for bone regeneration. *J Nanosci Nanotechnol* 14(1):15–56
  80. Rodriguez MJ, Brown J, Giordano J, Lin SJ, Omenetto FG, Kaplan DL (2017) Silk based bioinks for soft tissue reconstruction using 3-dimensional (3D) printing with *in vitro* and *in vivo* assessments. *Biomaterials* 117:105–115
  81. Samal SK, David LK, Emo C (2013) Ultrasound sonication effects on silk fibroin protein. *Macromol Mater Eng* 298(11):1201–1208
  82. Santin M, Antonella M, Giuliano F, Mario C (1999) *In vitro* evaluation of the inflammatory potential of the silk fibroin. *J Biomed Mater Res* 46(3):382–389
  83. Schacht K, Jüngst T, Schweinin M, Ewald A, Groll J, Scheibel T (2015) Biofabrication of cell-loaded 3D spider silk constructs. *Angew Chem Int Ed* 54(9):2816–2820
  84. Serra E, Eva D, Isabel D, Rosa MB (2010) A comparative study of periodic mesoporous organosilica and different hydrophobic mesoporous silicas for lipase immobilization. *Microporous Mesoporous Mater* 132(3):487–493
  85. Shanmugavel S, Reddy VJ, Ramakrishna S, Lakshmi BS, Dev VG (2014) Aloe vera/silk fibroin/hydroxyapatite incorporated electrospun nanofibrous scaffold for enhanced osteogenesis. *J Biomater Tissue Eng* 4(1):9–19
  86. She Z, Jin C, Huang Z, Zhang B, Feng Q, Xu Y (2008) Silk fibroin/chitosan scaffold: preparation, characterization, and culture with HepG2 cell. *J Mater Sci: Mater Med* 19(12):3545–3553
  87. Shen W, Chen X, Hu Y, Yin Z, Zhu T, Hu J, Chen J, Zheng Z, Zhang W, Ran J, Heng BC, Ji J, Chen W, Ouyang HW (2014) Long-term effects of knitted silk-collagen sponge scaffold on anterior cruciate ligament reconstruction and osteoarthritis prevention. *Biomaterials* 35(28):8154–8163
  88. Shin JH, Lee DH, Song JE, Cho SJ, Park CH, Khang G (2017) Effect of silk sponge concentrations on skin regeneration. *Polymer (Korea)* 41(1):1–6
  89. Sim BR, Kim HM, Kim SM, Kim DK, Song JE, Park H, Khang G (2016) Osteogenesis differentiation of rabbit bone marrow-mesenchymal stem cells in silk scaffold loaded with various ratios of hydroxyapatite. *Polymer (Korea)* 40(6):915–924
  90. Sommer MR, Manuel S, Davide C, André RS (2016) 3D printing of hierarchical silk fibroin structures. *ACS Appl Mater Interfaces* 8(50):34677–34685

91. Song JE, Tripathy N, Shin JH, Lee DH, Cha JG, Park CH, Suh DS, Khang G (2017) In vivo bone regeneration evaluation of duck's feet collagen/PLGA scaffolds in rat calvarial defect. *Macromol Res* 25(10):994–999
92. Soong HK, Kenneth RK (1984) Adverse reactions to virgin silk sutures in cataract surgery. *Ophthalmology* 91(5):479–483
93. Stevens B, Yanzhe Y, Arunesh M, Brent S, Kytai TN (2008) A review of materials, fabrication methods, and strategies used to enhance bone regeneration in engineered bone tissues. *J Biomed Mater Res – Part B Appl Biomater* 85(2):573–582
94. Stevens MM (2008) Biomaterials for bone tissue engineering. *Mater Today* 11(5):18–25
95. Sutherland TD, James HY, Sarah W, Cheryl YH, David JM (2010) Insect silk: one name, many materials. *Ann Rev Entomol* 55(1):171–188
96. Taichman RS (2005) Blood and bone: two tissues whose fates are intertwined to create the hematopoietic stem-cell niche. *Blood* 105(7):2631–2639
97. Talukdar S, Nguyen QT, Chen AC, Sah RL (2011) Effect of initial cell seeding density on 3D-engineered silk fibroin scaffolds for articular cartilage tissue engineering. *Biomaterials* 32(34):8927–8937
98. Tamada Y (2005) New process to form a silk fibroin porous 3-D structure. *Biomacromolecules* 6(6):3100–3106
99. Tan Y, Richards DJ, Trusk TC, Visconti RP, Yost MJ, Kindy MS, Drake CJ, Argraves WS, Markwald RR, Mei Y (2014) 3D printing facilitated scaffold-free tissue unit fabrication. *Biofabrication* 6(2):024111
100. Tian M, Yang Z, Kuwahara K, Nimni ME, Wan C, Han B (2012) Delivery of demineralized bone matrix powder using a thermogelling chitosan carrier. *Acta Biomater* 8(2):753–762
101. Uebersax L, Apfel T, Nuss KMR, Vogt R, Kim HY, Meinel L, Kaplan DL, Auer JA, Merkle HP, Von RB (2013) Biocompatibility and osteoconduction of macroporous silk fibroin implants in cortical defects in sheep. *Eur J Pharm Biopharm* 85(1):107–118
102. Unadkat HV, Hulsman M, Cornelissen K, Papenburg BJ, Truckenmuller RK, Carpenter AE, Wessling M, Post GF, Uetz M, Reinders MJT, Stamatialis D, Van Blitterswijk CA, De Boer J (2011) An algorithm-based topographical biomaterials library to instruct cell fate. *Proc Natl Acad Sci* 108(40):16565–16570
103. Vepari C, David LK (2007) Silk as a biomaterial. *Prog Polym Sci (Oxford)* 32(8–9):991–1007
104. Wang M, Jin HJ, David LK, Gregory CR (2004) Mechanical properties of electrospun silk fibers. *Macromolecules* 37(18):6856–6864
105. Wang X, Jonathan AK, Gary GL, David LK (2008) Sonication-induced gelation of silk fibroin for cell encapsulation. *Biomaterials* 29(8):1054–1064
106. Wang Y, Rudym DD, Walsh A, Abrahamsen L, Kim HJ, Kim HS, Kirker HC, Kaplan DL (2008) *In vivo* degradation of three-dimensional silk fibroin scaffolds. *Biomaterials* 29(24–25):3415–3428
107. Wang Y, Kim HJ, Gordana VN, David LK (2006) Stem cell-based tissue engineering with silk biomaterials. *Biomaterials* 27(36):6064–6082
108. Weir MD, Xu HK (2010) Human bone marrow stem cell-encapsulating calcium phosphate scaffolds for bone repair. *Acta Biomater* 6(10):4118–4126
109. Wen CM, Ye ST, Zhou LX, Yu Y (1990) Silk-induced asthma in children: a report of 64 cases. *Ann Allergy* 65(5):375–378
110. Won YW, Amit NP, David AB (2014) Cell surface engineering to enhance mesenchymal stem cell migration toward an SDF-1 gradient. *Biomaterials* 35(21):5627–5635
111. Yan LP, Silva CJ, Ribeiro VP, Miranda GV, Correia C, Da SMA, Sousa RA, Reis RM, Oliveira AL, Oliveira JM, Reis RL (2016) Tumor growth suppression induced by biomimetic silk fibroin hydrogels. *Sci Rep* 6:31037
112. Yan LP, Oliveira JM, Oliveira AL, Reis RL (2017) Core-shell silk hydrogels with spatially tuned conformations as drug-delivery system. *J tissue eng regen med* 11(11):3168–3177
113. Yao D, Sen D, Lu Q, Hu X, Kaplan DL, Zhang B, Zhu H (2012) Salt-leached silk scaffolds with tunable mechanical properties. *Biomacromolecules* 13(11):3723–3729
114. Yucel T, Peggy C, David LK (2009) Vortex-induced injectable silk fibroin hydrogels. *Biophys J* 97(7):2044–2050
115. Yucel T, Nikola K, Gary GL, Tim JL, David LK (2010) Non-equilibrium silk fibroin adhesives. *J Struct Biol* 170(2):406–412
116. Zadpoor AA (2015) Bone Tissue Regeneration: the role of scaffold geometry. *Biomater Sci* 3(2):231–245
117. Zaoming W, Rosa C, Enrique FC, Richard FL (1996) Partial characterization of the silk allergens in mulberry silk extract. *J Investig Allergol Clin Immunol* 6(4):237–241
118. Zhang W, Chen J, Tao J, Hu C, Chen L, Zhao H, Xu G, Heng BC, Ouyang HW (2013) The promotion of osteochondral repair by combined intra-articular injection of parathyroid hormone-related protein and implantation of a bi-layer collagen-silk scaffold. *Biomaterials* 34(25):6046–6057
119. Zhang W, Wang X, Wang S, Zhao J, Xu L, Zhu C, Zeng D, Chen J, Zhang Z, Kaplan DL, Jiang X (2011) The use of injectable sonication-induced silk hydrogel for VEGF165 and BMP-2 delivery for elevation of the maxillary sinus floor. *Biomaterials* 32(35):9415–9424
120. Zhang Y, Fan W, Ma Z, Wu C, Fang W, Liu G, Xiao Y (2010) The effects of pore architecture in silk fibroin scaffolds on the growth and differentiation of mesenchymal stem cells expressing BMP7. *Acta Biomater* 6(8):3021–3028
121. Zhao J, Zhang Z, Wang S, Sun X, Zhang X, Chen J, Kaplan DL, Jiang X (2009) Apatite-coated silk fibroin scaffolds to healing mandibular border defects in canines. *Bone* 45(3):517–527



# Collagen Type I: A Versatile Biomaterial

# 21

Shiplu Roy Chowdhury, Mohd Fauzi Mh Busra,  
Yogeswaran Lokanathan, Min Hwei Ng,  
Jia Xian Law, Ude Chinedu Cletus,  
and Ruszymah Binti Haji Idrus

## Abstract

Collagen type I is the most abundant matrix protein in the human body and is highly demanded in tissue engineering, regenerative medicine, and pharmaceutical applications. To meet the uprising demand in biomedical applications, collagen type I has been isolated from mammals (bovine, porcine, goat and rat) and non-mammals (fish, amphibian, and sea plant) source using various extraction techniques. Recent advancement enables fabrication of collagen scaffolds in multiple forms such as film, sponge, and hydrogel, with or without other biomaterials. The scaffolds are extensively used to develop tissue substi-

tutes in regenerating or repairing diseased or damaged tissues. The 3D scaffolds are also used to develop *in vitro* model and as a vehicle for delivering drugs or active compounds.

## Keywords

Collagen type I · Biomaterial · Fabrication · Tissue engineering · Tissue substitutes · In vitro model · Drug delivery system

S. R. Chowdhury · M. F. Mh Busra · Y. Lokanathan  
M. H. Ng · J. X. Law  
Tissue Engineering Centre, Faculty of Medicine,  
University Kebangsaan Malaysia,  
Kuala Lumpur, Malaysia  
e-mail: [shiplu@ppukm.ukm.edu.my](mailto:shiplu@ppukm.ukm.edu.my);  
[lyoges@ppukm.ukm.edu.my](mailto:lyoges@ppukm.ukm.edu.my);  
[angela@ppukm.ukm.edu.my](mailto:angela@ppukm.ukm.edu.my);  
[lawjx@ppukm.ukm.edu.my](mailto:lawjx@ppukm.ukm.edu.my)

U. C. Cletus  
Bioartificial Organ and Regenerative Medicine Unit,  
National Defence University of Malaysia,  
Kuala Lumpur, Malaysia

R. Binti Haji Idrus (✉)  
Department of Physiology, Faculty of Medicine,  
University Kebangsaan Malaysia,  
Kuala Lumpur, Malaysia  
e-mail: [ruszyidrus@gmail.com](mailto:ruszyidrus@gmail.com)

## 21.1 Collagen Type I

Collagen is one of the major extracellular matrix (ECM) proteins in animals. It has fibrillary structure, which is essential for tissue scaffold networking to perform its standard functions [39]. The presence of collagen in ECM governs the structural integrity, biochemical properties, and physiological functions of body tissues. It involves regulation of cellular functions that include cell attachment, migration, proliferation, differentiation and gene expression through specific cell receptors and cell binding sites [97]. Collagen also facilitates cellular function by providing growth factors to the cells [129]. So far, 29 types of collagen have been identified and characterised [117], among them, collagen type I is the most abundant, which is present in connective tissues such as skin, tendon, bone, ligament, and cornea [1]. Considering the availability and importance

of collagen type I in maintaining tissue structure and functions, research is extensively conducted to demonstrate its applications in regenerative medicine, tissue engineering, drug discovery and drug delivery. Scaffolds are the integral component of tissue engineering that works by either mimicking the native microenvironment or acting as a delivery vehicle. Collagen type I can be fabricated into different scaffolds and the scaffold properties can be modulated to meet the desired biomedical applications. Taking into account the potential of collagen type I in biomedical applications, in this chapter, the discussion topics revolve around various sources of collagen type I and their characteristics, scaffolding techniques, and applications of collagen type I scaffolds.

### 21.1.1 Source of Collagen Type I

Collagen type I is one of the most abundant proteins in the animal kingdom, and it is extensively used in biomedical applications. It is extracted from various sources, which include mammals, amphibians, fishes, marines, and avians [148]. Since the early 1950s, collagen type I is extracted from mammals such as bovine and porcine skins and bones. However, the outbreak of diseases transmitted from animal to humans such as bovine spongiform encephalopathy, spongiform encephalopathy, and foot-and-mouth disease, besides the religious constraint in using porcine products, alternative sources of collagen type I production are scrutinised. Recently, collagen type I extracted from the tendon of rat tail becomes popular and is used in biological research [161]. Nonmammalian sources such as fish, marines, amphibian, and avians are also used to extract collagen type I [166, 173] to meet the demand. In addition, synthetic collagen and recombinant collagen are a potential source of collagen type I [48]. However, they lack natural microstructure and spatial complexity [1], thus affecting their biological performance [9]. The source and extraction methods of collagen type I are summarised in Table 21.1.

In general, collagen type I is extracted via salt-precipitation, acid-based digestion, and enzymatic isolation using neutral saline solu-

tion, an acidic solution such as acetic acid, hydrochloric acid, as well as an acid-enzyme mixture such as pepsin with acetic acid. The selection of extraction method depends on the material solubility. Both acid and alkaline-based treatments are cost-effective, but the yield of collagen type I is little, besides involving tedious extraction process. In contrast, enzymatic treatment is able to produce collagen type I with high purity and requires less production time, but this method is expensive [137].

Acid-based hydrolysis used to extract collagen type I encompasses either organic acids such as acetic acid or inorganic acid such as hydrochloric acid. It cleaves the crosslink in collagen and solubilises the unbound collagen [91]. The use of low concentration of acetic acid is favourable in extracting collagen type I from mammals, avians, marines and fish [9, 84, 175]. Meanwhile, salt solution such as sodium chloride (NaCl) is used to precipitate collagen from acidic solution prior to dialysis [47]. The neutral saline of sodium chloride is used for specific tissues for solubility, but it is less effective due to the presence of crosslinked structure in collagen [137].

Enzymes such as pepsin, trypsin, pronase, collagenase, and papain are used to extract collagen type I [137]. In general, the enzyme is premixed with an acid solution, and the target material is incubated to extract collagen type I by breaking the intertwined collagen structure. Later, collagen is collected using a low concentration of the acidic solution. This two-step extraction method results in high yield of collagen type I.

### 21.1.2 Characteristics of Collagen Type I

There are 29 types of collagen which are identified in vertebrates so far. They consist of at least 46 polypeptide chains. The structural characteristic of collagen family is the right-handed triple helix of three polypeptide chains. Based on the supramolecular structure, collagens are categorised into fibril-forming, anchoring, network-forming, transmembrane and fibril-associated group [126, 162]. The predominant one in

**Table 21.1** The sources and extraction methods of collagen type I

Animal class	Source & tissue type	Extraction method	References
Mammalian	Bovine skin, bone, pericardium	Acid-based (hydrochloric acid)	[132]
	Porcine skin, bone	Salting out method, Alkaline-based method, Acid-based method, Enzymatic method, Hybrid method	[176]
	Rat tail	Acid-based (Acetic acid)	[161]
	Caprine tendon	Acid-based (Acetic acid)	[9]
	Ovine tendon	Acid-based (Acetic acid)	[47]
Fish	Freshwater fish, marine fish	Acid-based (Acetic acid), Enzymatic method	[118, 131, 166]
Marine	Jellyfish tissues, Jumbo squid mantle	Acid-based (Acetic acid)	[2, 173]
Amphibian	Skin	Acid-based (Acetic acid) + Enzymatic method (pepsin)	[181]
Avian	Skin, skin-dermis	Acid-based (Acetic acid), Enzymatic method (pepsin)	[84, 175]
Human recombinant	Transgenic tobacco plant	Genetic engineering technology	[145, 146]

collagen type I is the fibril-forming group, which is present in all fibrous tissues except cartilage. It consists of two alpha-1 chains, an alpha-2 chain and a regular collagen secondary structure (beta-sheet) [54, 75]. The collagen contains a domain with repetition of the Gly-X-Y motif to form the trimeric collagen triple helix [105]. Glycin (Gly) is found at every third position of polypeptide chains, and the X and Y represent any amino acids, predominantly proline and hydroxyproline. Collagen type I isolated from different species and tissues has different proline and hydroxyproline content. Lower content of these amino acids results in lower denaturation temperature (Td) of collagen type I [118].

The collagen type I monomers self-assemble to form macromolecular fibre via fibrillogenesis. Fibril formation stabilises the collagen molecules at body temperature. Simulation study by [18] revealed that collagen type I fibrils are robust and demonstrate favourable mechanical properties at its usual triple helix length (about 300 nm). The Young Modulus of collagen monomer is estimated to be 6–7 GPa, whereas the atomic force microscope (AFM) measurement of dehydrated fibril of collagen type I is 5 GPa in bovine achilles tendon and 11 GPa in rat tail tendon. The fracture strength of collagen monomer and fibril is estimated to be 11 GPa and 0.5 GPa, respectively. Collagen monomer has higher fracture strength

because it has higher structural order as compared to collagen fibrils [18].

There is no difference of collagen type I chemical characteristics across species. Collagen type I has functional groups that encompass amide I, II and III. The amide groups are detected at peak intensity between  $1450\text{ cm}^{-1}$  and  $1235\text{ cm}^{-1}$  in Fourier transform infrared (FTIR), and the amides indicate collagen helical structure [47, 134]. Via X-ray diffraction (XRD), collagen type I from mammals, avians, marines, fish demonstrate near to amorphous rather than crystalline form [47]. The XRD of collagen in general consists of 2 prominent peaks, where the first peak is sharper than the second [81]. This explains that collagen has an organised structure and majority of them are in amorphous phase [180].

## 21.2 Collagen Scaffolding

Three-dimensional (3D) scaffold is crucial in developing tissue substitutes for clinical applications, as well as *in vitro* model. Moreover, 3D scaffold functions as a delivery vehicle for drug and/or functional factors. A 3D scaffold is essential to provide a microenvironment that mimics the native ECM environment, for cell attachment, proliferation and tissue regeneration [50, 94]. The issues that arise in the fabrication of scaffold are the biocompatibility, immunocompatibility,

macrolevel size and shape, microlevel tissue architecture, nanoscale substrate arrangement, exchange site for gases, nutrients and metabolites, biodegradation rate, cell attachment site, pore size and distribution, exposed surface area, porosity, mechanical properties, biodegradation rate and other properties that mimic the native tissue structure [20, 112].

Collagen type I is used in 3D scaffold fabrication as it is the major component of ECM in various tissues. It is developed as a coating material for existing implants, as a hydrogel or being freeze-dried to form 3D porous scaffolds or thin films in a single or composite form. It is biocompatible, as well as having low immunogenicity and suitable wettability (hydrophilicity) for cell attachment [99]. However, the collagen type I extracted and purified from natural sources lacks the desired mechanical strength [6, 37, 184].

The crosslinking of collagen type I interconnect collagen fibrils to increase the mechanical strength and preserve the scaffold ultrastructure for an extended period by reducing enzymatic degradation *in vivo* [117, 124]. However, crosslinking decreases number of available functional groups, modifies the rheology and potentially causes cytotoxicity [124]. The crosslinking of collagen is categorised into physical, chemical, and enzymatic.

Physical crosslinking includes ultraviolet (UV) irradiation and dehydrothermal (DHT) treatment. UV irradiation is a rapid and controllable technique to increase the mechanical strength of collagen scaffold by inducing chemical and physical changes in collagen. DHT treatment involves exposing collagen to temperature above 90°C in vacuum, which eliminates water from the collagen molecules, so crosslinking occurs through condensation [64]. Physical methods do not employ cytotoxic reagents for crosslinking, and since both UV and DHT treatments sterilise the resulting scaffold, additional disinfection of the produced scaffold is not required.

The conventional chemical crosslinkers are aldehydes such as glutaraldehyde (GTA) [124]. It is widely used because it is cheap, highly reactive

with protein functional groups and highly soluble in aqueous solution [163]. 1-ethyl-3-(3-dimethyl aminopropyl) (EDC) is another chemical crosslinker and known as a zero-length crosslinking agent as EDC does not incorporate new chemical entity into the polymer [56]. An alternative to the crosslinking chemical is genipin, which was isolated from Gardenia fruit [49]. Genipin is more biocompatible and less cytotoxic as a crosslinking agent.

These crosslinkers result in covalent bond crosslinking in collagen. Nevertheless, polycationic molecules such as chitosan produce ionic bonds between amine and carboxyl group in collagen, which are sufficiently tough in increasing the collagen scaffold mechanical strength [29]. Moreover, chitosan is a suitable biomaterial for tissue engineering, widely studied as an injectable solution that forms stable hydrogel inside the body and has antimicrobial properties [29]. In addition, enzymes such as transglutaminase is used as a crosslinking agent to improve mechanical strength and enzymatic degradation of collagen scaffold [27, 150]. The advantage of enzymatic crosslinking is that there is no chemical residue introduced into the collagen scaffold, thus avoiding the risk of cytotoxicity.

### 21.2.1 Decellularization

The tissue microenvironment is a complex structure, in which the effort to mimic the structure is a challenge yet to overcome. The biological scaffold consists of natural ECM such as collagen type I, which can be utilised to reconstruct many human tissues. Decellularization of native tissues preserves the scaffold micro- and macro-architecture and circumvents the need to recreate a suitable tissue-specific scaffold for the development of tissue-engineered organs [117]. Many decellularization methods are utilised to preserve the scaffold structure, ECM content and mechanical properties of the decellularized tissue or organ. One of the methods used is repeated freezing/thawing that lyses the cells and reduces chemical usage for cell lysis [7]. Another



decellularization method is immersion in solutions containing enzymes (trypsin, exonuclease and endonucleases), chemicals (acid to alkaline), chelating agents (EDTA, ionic or non-ionic detergents, zwitterionic detergents) and hyper or hypotonic solutions [7, 117]. Often, immersion is coupled with mechanical agitation to ensure complete perfusion of the solution throughout organ, thus facilitating cell lysis and removal of cell remnants from the organ scaffold [7].

### 21.2.2 Freeze Drying

Freeze drying is used to produce porous structure, often sponge-like structure. This process is based on sublimation, where biomaterial is dissolved in a solvent, frozen, and the solvent is then removed via lyophilisation under high vacuum condition. This method enables control over the mechanical strength, pore size and distribution, porosity, and pore interconnectivity by modifying polymer concentration and freeze-drying parameters [20, 112, 138]. Previous study showed that the collagen type I scaffold produced by freezing at  $-30\text{ }^{\circ}\text{C}$  had higher pore size than that of frozen at  $-80\text{ }^{\circ}\text{C}$  [46].

### 21.2.3 Electrospinning

Electrospinning is a new technique for nanofibrous scaffold fabrication. Thus, the scaffold has a high area-to-volume ratio. The produced scaffold is to mimic the native tissue nanostructure. This technique involves the use of high voltage power supply to generate high electric field between the spinneret (such as needle) and collector (metallic plate or rotating mandrel), that act as two electrodes of opposite polarity [154]. The resulting fibre alignment, thickness, roughness and density is controlled by modifying parameters such as solution properties, voltage, needle to collector distance, collector rotating speed, temperature, and humidity. It is common for collagen type I to be blended with other polymers to increase the mechanical

strength of the resulting electrospun nanofibre mesh [114, 168].

### 21.2.4 Adsorption

Adsorption or coating is the simplest method to obtain a 3D-collagen-combined scaffold. Using this technique, the scaffold frame that is made of other biomaterials and collagen type I is used to coat the 3D scaffold so that the produced scaffold will have the required macro- and micro-architecture, mechanical strength and biological properties suitable for cell attachment, proliferation and maturation. As collagen type I enhances cell growth, the coating of synthetic polymers with inert or less favourable cell growth surface makes the surface suitable for cell growth [8, 122, 156, 178, 185].

### 21.2.5 Solvent Casting and Particulate Leaching

Scaffold fabrication by solvent casting is easy, inexpensive, and versatile in producing thin scaffold layers such as films. The method involves dipping the mould into polymer solution or addition of polymer solution into a cast, and then the solvent is evaporated to create the film. An advantage of using this technique is the ability to control the thickness uniformity of the scaffold. Furthermore, the unidirectional rocking of collagen type I solution during evaporation process is found to orientate the collagen fibrils in an aligned manner, which also enhances the attachment and proliferation of human fibroblast cells on the collagen thin film [47].

Solvent casting is often combined with particulate leaching to fabricate a scaffold that with higher number of pores and/or pore size, and uniform pore morphology. Particulate leaching is also combined with other fabrication techniques such as electrospinning where porosity is adjusted by the polymer to porogen ratio while pore size is determined by the porogen size. The most common porogens are sodium chloride, ammonium bicarbonate, and glucose.

### 21.2.6 Rapid Prototyping (RP)

Rapid prototyping, which is known as solid free-form technique (SFF), refers to computer-aided design (CAD) in designing and fabricating the scaffold. It produces 3D scaffolds via additive layer manufacturing technology, where each scaffold cross-section is layered one by one [154]. Although there are many RP techniques, most of them fall into three categories; fused deposition modelling (FDM), selective laser sintering (SLS), and stereolithography. RP technique can control the matrix design such as shape, size, interconnectivity, orientation and geometry. Furthermore, RP produces scaffolds with reproducible architecture and composition [154]. Thus, the mechanical, chemical and biological properties are adjustable and can be maintained over time. This advanced technology can be integrated with the existing imaging techniques for scaffold customisation, according to the need of each patient.

## 21.3 Type I Collagen-Based Tissue Substitutes

Collagen type I makes up the ECM of most tissues in the human body it provides the microenvironment and surface for cell growth, cell attachment and proliferation. The literature revealed reports on its application as adhesive, tissue void fillers, carriers for cell or structural scaffold in tissue engineering. The following sections discussed the application of collagen type I in tissue-specific engineering and regeneration in the clinic.

### 21.3.1 Skin Substitutes

Collagen is a predominant component in skin ECM as it constitutes 75% of the skin dry weight [147]. Most of the collagen found in the skin are collagen type I, followed by collagen type III. Skin cells, including keratinocytes on the epidermal layer and fibroblast on the dermal layer able to grow on the collagen type I matrix. Often,

collagen type I is used in skin tissue engineering research as it is the most important and abundant ECM of human skin. To date, some type I collagen-based skin substitutes have been clinically tested in randomised control trial to treat different wounds, such as partial and full-thickness burns, split-thickness skin graft (STSG) donor sites, diabetic foot ulcers and venous leg ulcers (Table 21.2). Some of the skin substitutes are solely made of collagen type I (OrCel® and Apligraf®), while others contain additional biomaterials (Integra®, Matriderm®, Biobrane® and TransCyte®). In general, the clinical trials showed that application of these collagen-based skin substitutes, with or without cells, is beneficial in wound healing.

#### 21.3.1.1 Integra®

Integra® Dermal Regeneration Template consists of crosslinked collagen type I and chondroitin-6-sulfate dermal replacement layer with a temporary silicon epidermal cover to reduce fluid loss and prevent infection [67]. About 2–3 weeks after implantation, the dermal regeneration template is revascularized and form the neodermis. After neodermis formation, the silicon cover is removed, for wound closure with split-thickness skin graft (STSG) or engineered epidermis such as cultured epidermal autograft [30, 115]. Integra® is used for skin loss treatment due to trauma, burn, chronic ulcers and resurfacing of chronic scarring [32, 67, 95, 171]. Integra® is useful when an autograft is insufficient. Integra® is readily available and allows time for neodermis formation to improve the subsequent STSG success rate. Nonetheless, Integra® is expensive and requires two-step procedure for permanent wound closure.

#### 21.3.1.2 Matriderm®

Matriderm® is a highly porous matrix made of bovine collagen type I, III and V and elastin. The collagen comes from bovine dermis and elastin is taken from bovine nuchal ligament via hydrolysis [104, 130]. Matriderm® is used as a one-step procedure to promote wound healing in combination with STSG [130, 165]. Even though the application of Matriderm® increases the distance

**Table 21.2** Randomised clinical trials using tissue-engineered skin substitutes made of type I collagen

Skin substitutes	Biomaterials	Cells	Indications	Sample size	Key findings	References
Integra®	Bovine type I collagen and shark glycosaminoglycan (chondroitin-6-sulfate)	–	Diabetic foot ulcers	307 patients	↑ rate of wound closure ↓ time for complete wound closure	[32]
Matriderm®	Bovine type I, III and V collagens and elastin hydrolysate	–	Partial- and full-thickness burns	10 patients	↑ elasticity of regenerated skin	[130]
Biobrane®	Silicone membrane embedded in nylon mesh with porcine dermal type I collagen	–	STSG donor sites	28 patients	↓ inflammation and exudation	[141]
TransCyte®	Silicone membrane bonded nylon mesh coated with porcine dermal collagen	Neonatal fibroblast	Partial-thickness burns	33 patients	↑ rate of re-epithelialisation	[74]
OrCel®	Bovine type I collagen sponge	Neonatal keratinocytes and fibroblasts	STSG donor sites	82 patients	↑ wound closure ↓ scarring	[153]
Apligraf®	Bovine type I collagen matrix	Neonatal keratinocytes and fibroblasts	Venour leg ulcers	293 patients	↑ wound closure ↑ number of patient with complete wound closure	[43]
			Diabetic foot ulcers	208 patients	↑ wound closure ↑ number of patient with complete wound closure	[167]

between skin graft and vasculature, this does not adversely affect the skin graft survival. Matriderm® is used in the treatment of burns, skin graft donor sites, reconstructive wound, trauma wound and diabetic foot ulcers. The use of Matriderm® improves wound elasticity and scar quality [62, 104, 130]. An advantage of using Matriderm® is that wound treatment can be performed in one step, hence no additional surgery required.

### 21.3.1.3 Biobrane®

Biobrane® is a composite scaffold, with type I collagen-coated nylon membrane attached to a silicone membrane [149]. Biobrane® is to treat superficial and partial-thickness wound as well as skin graft donor sites. Upon application, Biobrane® adheres to the wound bed and gets detached as re-epithelialisation is underway. Also, Biobrane® is used to hold autograft and cell suspension [45, 57, 128]. The product contains pores, that drains exudates. Biobrane® is proven to enhance the rate of healing and reepithelialisation while reducing pain and length of hospital stay [51, 76, 82].

### 21.3.1.4 TransCyte® (Dermagraft-TC)

TransCyte®, formerly known as Dermagraft-TC, is a tissue-engineered skin substitute consists of a silicone membrane attached with collagen-coated nylon mesh and seeded with neonatal fibroblasts [74]. Fibroblasts are cultured on the nylon mesh for 4–6 weeks, to allow the formation of a dense matrix enriched in ECM and growth factors [143]. TransCyte® is used to treat partial-thickness burns. The engineered skin is left on the wound until it sloughs off normally, this usually takes 3 weeks. The use of TransCyte® expedites wound re-epithelialisation and reduces the length of hospital stay [4, 74, 98, 111].

### 21.3.1.5 OrCel®

OrCel® is a bilayered tissue-engineered skin consists of collagen type I sponge, seeded with allogeneic neonatal keratinocyte layer and fibroblast layer, that mimics normal skin. The engineered skin has living keratinocytes and fibroblasts that secrete growth factors and cytokines to support

wound healing [153]. It is indicated for the treatment of partial-thickness wounds. As the skin substitute contains living cells, it is more expensive than the acellular skin substitutes [153].

### 21.3.1.6 Apligraf®

Apligraf® is a bilayered living skin equivalent consists of allogeneic neonatal keratinocytes and fibroblasts with bovine collagen type I as supporting matrix. It is a composite skin substitute containing both stratified epidermal and dermal layers [34]. It is the first tissue-engineered skin substitute that was approved by the Food and Drug Administration (FDA) to treat chronic ulcers. Apligraf® is also approved for the treatment of diabetic foot ulcers and venous ulcers [179]. It shows potential in treating epidermolysis bullosa wounds [42]. In addition, Apligraf® is used in the treatment of burns and surgical wounds, including those caused by excisional surgery and biopsy collection [55, 65, 108]. Even though Apligraf® is prepared from allogeneic keratinocytes and fibroblasts, it is immunologically tolerated by recipients [36, 43, 167]. Nonetheless, it is short-lived upon transplantation (less than 4 weeks), depending on the application. Apligraf® promotes wound healing via the secretion of growth factors and cytokines [179].

## 21.3.2 Corneal Substitutes

Cornea is a transparent dome-shaped eye tissue that is responsible for the image focusing on the eye. Cornea contributes to two-thirds of the eye's optical power [172]. The tissue is divided into epithelium, stroma and endothelium layers and it is the outermost part of the eye that covers the iris and pupil [68]. Therefore, cornea serves as a barrier that prevents foreign particles such as germ and dust from going into the eye. Cornea is highly innervated, avascular and immunologically privileged [28]. Collagen type I is the most abundant collagen in the eye tissue, constituting about 75% of total collagen. Besides, cornea also contains collagen types VI and V as well as glycosaminoglycans such as dermatan sulphate, keratin sulphate and heparin sulphate [103].

The development of tissue-engineered cornea is rapidly growing to overcome the shortage of donor cornea, which leaves many people blinded. Nonetheless, most of the studies are still *in vitro* and preclinical stages. Due to its excellent biocompatibility, low immunogenicity and suitable mechanical properties, collagen biomaterial is extensively studied for corneal tissue engineering. Collagen supports the survival of corneal epithelial cells, corneal stromal cells and corneal fibroblast cells, that are used to support new tissue formation [52]. Merrett et al. conducted a study in porcine to compare cross-linking with EDC and N-hydroxysuccinimide (NHS) between collagen types I and III as corneal substitute and it was found that both showed equivalent performance in terms of optical clarity, even when the collagen type III scaffold has superior optical clarity [102]. A clinical study with 10 patients using only EDC-NHS cross-linked collagen type III scaffold found that the best spectacle-corrected visual acuity improved in 4 patients, remained the same in 4 while other the 2 got worse, after 6 months implantation [40]. After 4 years, the corneal substitute promotes endogenous regeneration of corneal tissue and nerves. No rejection happened in any patient, even when no immunosuppressant is given while the best-corrected visual acuity of the transplanted eye had improved [41]. Thus far, none of the type I collagen-based corneal substitutes developed in the laboratory is clinically tested.

### 21.3.3 Vasculature Substitutes

Vascular or circulatory system is made up of vessels that carry blood throughout the body, carry oxygen, nutrients and hormones to the cells, and transport metabolic waste such as carbon dioxide, urea and excessive minerals from the cells to excretory organs to be excreted from the body. Vascular diseases such as atherosclerosis result in narrowing of blood vessels that obstruct blood flow to the cells. In severe cases, blood vessel substitute is needed to replace the obstructed vessel to prevent fatal complication such as myocardial infarction and stroke, that is due to

insufficient blood flow to the targeted tissues [85]. Bypass surgery is performed worldwide to replace the damaged blood vessels. Currently, autologous vascular substitute and synthetic vascular graft made of expanded polytetrafluoroethylene (ePTFE), polyethylene terephthalate (Dacron®) and polyurethane are used for this purpose [123].

Tissue engineering approach is used to prepare vascular substitutes. For vascular tissue engineering, it is important for the graft to be biocompatible, noninflammatory, non-thrombogenic and has mechanical strength that matches the native vessel. Endothelialisation of the vascular substitute luminal surface is critical to ensure long-term patency. Collagen type I is the main component of the vascular wall and is widely used in vascular tissue engineering. Often, collagen type I in vascular tissue engineering is fortified with biomaterials (e.g. silk fibroin, elastin and PCL) because it has weak mechanical strength [13, 33, 101, 183]. Currently, the focus of research shift to vascular substitutes development with multilayer structure that imitates natural vessel. For example, Wu et al. developed a complex trilayer vascular substitute consisting of PLCL/collagen nanofibre as the inner layer, PLGA/silk as the middle layer and PLCL/collagen nanofibre as the outer layer. The trilayer vascular substitute demonstrates suitable mechanical property and supports the growth and organisation of endothelial cells at the inner layer and smooth muscle cells at the middle layer [174]. Several type I collagen-based vascular grafts made of decellularised xenogeneic tissues are clinically tested. Bovine carotid artery graft (Artegraft®) is a natural decellularised collagen vascular graft that shows encouraging clinical results for permanent haemodialysis vascular access and lower extremity bypass [71, 90]. The graft is to enhance long-term patency and provides a pliable conduit with excellent biocompatibility. Apart from Artegraft®, Solcograaft® and ProCol® are other commercially available vascular grafts based on decellularized bovine blood vessels [135, 139]. A decellularized bovine ureter graft (SynerGraft model 100) was tested against polytetrafluoroethylene (ePTFE) for

arteriovenous access in dialysis patients, and it was found that both are comparable in terms of patency and complications [22].

### 21.3.4 Cartilage Substitutes

Purified isolated collagen type I from tissues is utilised in many defected cartilage restorative applications [23]. Studies show that articular cartilage implantation (ACI) is helpful in focal cartilage lesions, but is not recommended for osteoarthritis [17]. The procedure involves the use of periosteal flap fixed to the surrounding cartilage rim, to create a reservoir for culture-expanded chondrocytes [100]. However, this has risk of complications such as periosteal hypertrophy, delamination of transplant, arthrofibrosis and transplant failure [17, 100].

Collagen type I alone or in combination with other biomaterials are used to obtain second generation ACI, where cells are combined with resorbable biomaterials, in matrix-associated autologous chondrocyte implantation or transplantation (MACI/MACT) [164]. Further development resulted in third-generation ACI that delivers autologous cultured chondrocytes using collagen cell carrier scaffolds [17]. Some products associated with clinically available collagen cartilage implants include; MACI, MACT, Atelocollagen, Bioseed C, Neocart, Novocart, Gel MACI, Chondro-Gide, Chondron™ etc., [73].

Clinical studies have shown the effectiveness of MACI-related procedures to regenerate articular cartilage. In a level IV prospective study that used sequential objective patient evaluation to determine MACI results at 6, 18, and 36 months after surgery. The International Cartilage Repair Society (ICRS) and modified Cincinnati score showed significant improvement between preoperative and treatment groups at all times [73, 152]. Furthermore, a randomised, controlled trial comparing Chondro-Gide®, a collagen type I/III matrix to microfracture in a follow-up study at two centres demonstrated good clinical outcome throughout 2 years after operations in small- to medium-sized cartilage defects were conducted [5]. Zhang et al. [182] conducted a 2-year study

aimed to evaluate MACI safety and efficacy as cartilage repair treatment. The primary outcomes were the Knee Injury and Osteoarthritis Outcome Score (KOOS), domains and magnetic resonance imaging results. It was concluded that there is no postoperative complication and adverse event related to MACI [182].

Gille et al. [53] conducted the longest prospective clinical investigation to see the effect of MACI on long-term improvement, where 38 patients treated with MACI were evaluated for up to 16 years after the intervention. Three different scores namely Lysholm-Gilquist score, ICRS score and Tegner score were taken for the evaluation. These three scores significantly improved, which suggests that MACI is a suitable treatment for focal cartilage defects [53].

Recently, Ebert et al. [35] and Schuette et al. [140] conducted 5-year clinical investigation on MACI and MACT. Ebert performed a prospective clinical and radiological evaluation of 31 patients, who underwent MACI via arthroscopy for symptomatic tibiofemoral chondral lesions. Meanwhile, Schuette investigated the patellofemoral and tibiofemoral joints. It was concluded that the procedures demonstrate good clinical and radiological outcome up to 5 years, with high patient satisfaction level [35, 140].

Besides, Devitt et al. [31] performed a systematic 10-year review of randomised controlled trials, which also involved four MACI procedures. It was found that micro-fracture has higher failure than MACI. Larger lesions, of greater than 4.5 cm<sup>2</sup> treated with MACI had better outcome than those with microfracture [31].

### 21.3.5 Ligaments and Tendon Substitutes

Ligament rupture, tendon tear and meniscus loss cause abnormal wear on joints, thus promotes cartilage degeneration and osteoarthritis. Owing to the limited vascularity, injuries sustained by these tissues cannot heal properly [157]. Allograft transplantation is proposed to address these problems. Evidence found suggest that allograft transplantation improves the condition in short and

intermediate term, depending on pain and level of function for daily activities. However, there are limitations such as limited donor tissues, graft selection, preservation, sizing, sterilisation and short shelf life [77, 79]. Hence, there is a need for a readily available approach to restoring functionality of the skeletal structures upon injury. Therefore, Irvine, CA-Pegasus Biologics, Inc. developed OrthADAPT™, a bioimplant for soft tissue repair. OrthADAPT™ is a highly organised collagen Type I scaffold that is used to repair, reconstruct, augment, and reinforce soft tissues in tendons and ligaments. Clinical results demonstrate that OrthADAPT™ does not cause any significant inflammatory response and provides strength throughout the healing process with a rapid, controlled remodelling at the implantation site. It is used to repair rotator cuff injuries and reconstruct anterior shoulder. In both cases, patients had recovered well.

Furthermore, collagen I-based biomaterials are applied in tissue engineering cell therapeutics for the whole menisci [23]. Meniscus provides physical protection to knee cartilage by transmitting load through the joint, by distributing high peak stress on the underlying surface to absorb shock. Due to the orientation of fibre bundle arrangement, the meniscus depicts anisotropic property [157]. To tackle the limitations of allograft transplantation, Regen Biologics Inc. developed a collagen meniscal implant known as Menaflex. Menaflex is a bioimplant derived from bovine collagen to relieve symptoms and prevent joint degeneration for acute or chronic advanced meniscal loss or damage. Menaflex has been developed by applying pressure heat moulding approach to shape a bovine Achilles tendon into a collagen meniscal implant (CMI) [109].

The collagen meniscus implant (CMI) is the first tissue-engineered device that is effective in supporting new meniscus-like tissue at clinics. It is used in thousands of patients, including sportspeople. This provides significant benefit to people who have lost part of their knee meniscus, and those who suffer irreparable acute meniscus injury [127]. Results showed that after CMI implantation, about 75% of the missing meniscal tissue grow back, and the presence of

fibrocartilaginous tissues like normal meniscal tissue is observed [157]. In a 10-year follow-up clinical evaluation, data revealed pain relief and functional improvement of knee joints. It was observed that meniscal allografts shrink and undergo collagen remodelling upon transplantation, which restores mechanical strength. However, the efficacy of the implant on knee osteoarthritis prevention is not yet proven [61].

Actifit® scaffold is another collagen-based bioimplant that provides partial meniscal substitute with histological, radiological, and clinical evaluations comparable to Menaflex. Both have received the European Conformity (CE) approval, whereas the US Food and Drug Administration (FDA) believed that additional data is required to verify their efficacy on chondral degradation and prevention of osteoarthritis [116].

### 21.3.6 Bone Substitutes

A mature bone matrix has organic component (30%) with mainly collagen (90–95%), and inorganic bone mineral made up of salts (70%) [59]. In bone, collagen is laid down by osteoblasts, which are distinguished from mesenchymal stem cells (MSC) [120], as long and thin fibrils of triple helical structure that crosslink to one another in the space around cells. The crosslinks form strong; mature collagen type I fibre that provides bone with tensile strength [119]. Osteoblasts then produce hydroxyapatite that is deposited, in an organised manner into the organic matrix, forming a strong and dense mineralised matrix, which provides compressive strength. Thus, the natural composite of collagen and mineral imparts mechanical property to bone, for it to function as a skeletal structure and provides load-bearing capacity [59].

Autografts remain the standard for filling bone void. However, bone substitutes arise due to morbidity at the donor site and limited availability of autografts. Many products that mimic the bone mineralised matrix are developed as bone substitutes. For instance, collagen type I is coated or incorporated into deproteinised natural bone or 3D synthetic ceramic scaffold. Besides, bone

particulates or ceramic powder are added to collagen slurry and then freeze-dried to form a 3D scaffold. Another method is by adding hydrogel to collagen and bone particulate or ceramic mixture, to form malleable putty. As a coating, collagen matrix provides a favorable topography for cell attachment and proliferation on the mineral scaffold. Such configuration is stable and can be used in load-bearing bone defect site. On the other hand, when only collagen is used as a scaffold, it is extremely porous (> 90%) and absorptive. As collagen scaffold lacks mechanical strength and possesses osteoconductivity, it is coupled with osteoinductive factors such as BMP or osteogenic components such as osteoprogenitor cells or MSC. It is used along with bone marrow aspirate, MSC or osteoprogenitor cells, platelet-rich plasma or growth factors, to improve its osteogenicity. It is applied to repair non-weight-bearing bones such as the alveolar ridge and collarbone, or along with stable bone fixator. An example of commercial collagen scaffold used as fillers at non-load bearing site is CelGro<sup>®</sup> from OrthoCell, Australia. This includes collagen matrices by Zimmer, USA for alveolar ridge augmentation, i.e. BioMend<sup>®</sup>, CurVTM, Zimmer Collagen Capsule, Zimmer Collagen Wedge and Foundation Bone Filling Augmentation Material by J Morita, USA. Most of the collagens used are from bovine.

A more complex configuration is explored where the collagen scaffolds are infused with recombinant human bone morphogenetic protein type-2 (BMP-2), along with cylindrical interbody cage (infused bone is from Medtronic, USA), to be applied on posterior lumbar interbody fusion, which is shown to be promising [58]. However, now there are reports of adverse effects of this product in clinics [38].

In case of bone defect that involves load bearing, collagen scaffolds provide no initial mechanical support, and they must be used with a scaffold or fixation to function as bone substitute. Collagen needs to be mineralised, by coupling it with calcium phosphate-based material. There are many types of mineral/ceramic-collagen composites. Some of the products are listed in Table 21.3. Many are still in clinical trial, and on

long-term follow-ups, so far there is no report on adverse effect. The bone substitutes are convenient and become off-the-shelf solutions to the growing need of bones in orthopaedic and dental fields.

In the dental field, collagen membrane is used over bone graft to guide bone regeneration in alveolar ridge augmentation. The principle of Guided Tissue Regeneration (GTR) is used for decades to treat periodontal lesion using barrier membrane to exclude fast-growing soft tissues such as epithelial cells and fibroblasts from invading the regenerated new bones made of slower-growing alveolar bone [80]. Non-resorbable materials that were used in developing the membranes are replaced with biodegradable collagen membranes. For examples, there are OSSIX<sup>®</sup> PLUS (Datum Dental, USA), BioMend<sup>®</sup> (Zimmer, USA) and Hypro-Sorb F (Bioimplon GmbH, Germany).

### 21.3.7 Neural Substitutes

In the peripheral nervous system, collagens are present as interstitial fibrils (collagen type I) and non-fibrillar component (collagen type IV) in the endoneurium, of the basal lamina surrounding the Schwann cells. The focus of neural tissue engineering is to restore damaged peripheral nerve or central nervous tissue in the spinal cord and brain. The treatment of severed peripheral nerve involves direct reconnection via end-to-end anastomosis or guidance of the existing nerve via graft or conduit (Fig. 21.1) [136]. Many nerve conduits made of either natural or synthetic material are now available. Among them, collagen type I nerve conduit is the most popular. Table 21.4 shows a list of nerve conduits in the market.

The commercial collagen matrices are in the form of conduit or wrap. They serve as a guide for axon regeneration across the nerve gap and help to align the regenerating axons [86, 170]. Also, they function as a barrier to prevent scar formation, while allowing nutrient exchange and neurotrophic factors across the matrix. As they resorb over time (6–12 months) through



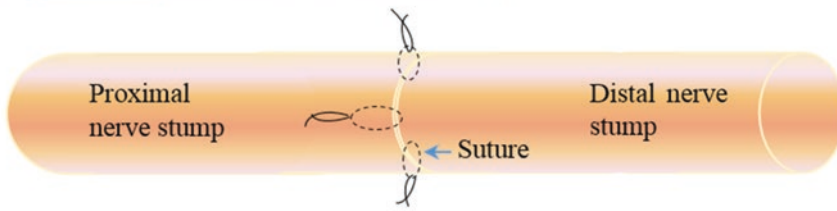
**Table 21.3** Commercial collagen-hydroxyapatite composite

Product	Description	Percentage and type of collagen	Percentage & type of Ceramic	Company	Recommended use
Creos xenogain collagen	Deproteinized bovine bone mineral matrix with collagen	10% porcine collagen type I	90% deproteinized bovine bone mineral	Nobel Biocare, Switzerland	Dental extraction sockets
Bonegold™ Mineralized Collagen Composite	HA embedded within type I collagen woven network of fibres	5% Collagen type I	55% nanosized synthetic HA	Allgens Medical Science & Technology, China	Bone void filler
Bio-Oss Collagen®	Cancellous bone granules with collagen	10% Porcine collagen	90% bovine cancellous bone granules	Geistlich Pharma North America, Switzerland	Filling of periodontal defects, alveolar ridge reconstruction
Healos®	Collagen fibres coated with hydroxyapatite	Type I collagen	Synthetic nanosized HA coating	DePuy Orthopaedics, Inc, US	Bone void filler, spinal surgery
NuOss™	Cancellous granules mixed with bovine collagen	5% of bovine collagen	95% anorganic bovine cancellous granules	ACE surgical supply, US	Ridge Augmentation, filling of intrabody periodontal & peri-implant defects and extraction sockets, elevating the maxillary sinus floor
RegenOss®		Type I collagen fibres	Magnesium-enriched HA nano-crystals	JRI Orthopaedics	Long bone fractures, revision hip arthroplasty to fill acetabular defects and spinal fusion
OssiMend® Block	Carbonate apatite anorganic bone mineral dispersed in type I collagen fibres	20% bovine collagen	80% bovine bone mineral	Collagen Matrix, US	Bone void filler
OssiMend® Putty	Carbonate apatite anorganic bone mineral dispersed in collagen type I fibres	45% bovine collagen	55% bovine bone mineral	Collagen Matrix, US	Bone void filler not intrinsic to the stability of the bony structure
Osteon™ II Collagen or Osteon™ III Collagen	Ceramic added with collagen	Collagen type I	Synthetic HA: β-TCP (30:70 or 60: 40)	Dentium, Korea	Ridge augmentation, extraction site & osteotomy, cystic cavities, sinus lift, periodontal defect
Vitoss® (or) Vitoss® Bioactive	Collagen added with ceramic	20% collagen	80% β-TCP (or) 70% β-TCP/10% BioglassG	Stryker, US	Bone void filler for the skeletal system (i.e., the extremities, pelvis, and posterolateral spine), spinal and trauma surgery, may be used with saline, autogenous blood, and/or bone marrow
EZ Cure™ Plug	Synthetic Bone graft suspended in collagen carrier	COLLAGEN (Type I)	Synthetic ceramic (60% HA: 40% B-TCP)	Biomatlante, Biologics solution, US	Dental extraction sockets

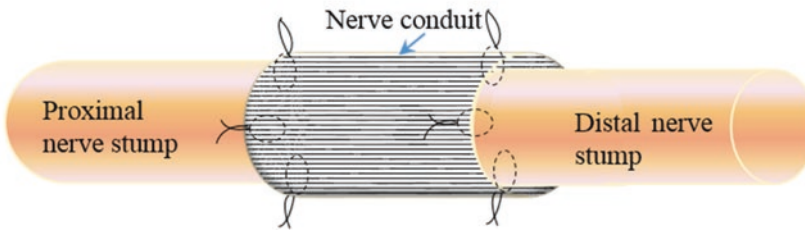
(continued)

**Table 21.3** (continued)

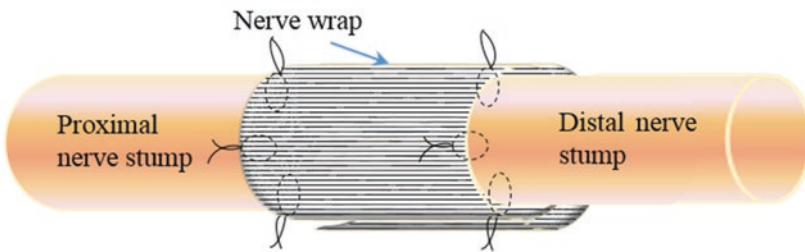
Product	Description	Percentage and type of collagen	Percentage & type of Ceramic	Company	Recommended use
Hypro-Oss	Bovine bone substitution material incorporated with atelocollagen	30% bovine atelocollagen	70% bovine hydroxyapatite	Medical Systems and Devices International Ltd, Israel	Dental
Collapat II®	Direct freeze-dried	Type I (calfskin) collagen	HA	BioMet Inc., US	Aseptic enclosed metaphyseal bone defects
Integra Mozaik™		20% type I collagen	80% TCP	Integra OrthoBiologics, US	Bone void filler
FormaGraft®		Type I collagen	HA, TCP	Maxigen Biotech Inc., US	Bone void filler
CopiOs®		Type I (bovine) collagen	Calcium phosphate, dibasic calcium phosphate	Zimmer	Bone void filler
Cerasorb®		Collagen	β-TCP	Curasan regenerative medicine	Filling, bridging, reconstruction and bone fusion
NanOss® Bioactive 3D		Collagen	Nano-HA	Pioneer surgical	Bone void filler

A) End-to end anastomosis for short nerve gap

## B) Reconnection via a conduit for longer nerve gap



## C) Protection via a wrap for partial nerve defect



**Fig. 21.1** Types of nerve defect repair. (a) Transected nerve with short nerve gap is repaired by direct end-to-end anastomosis. (b) Transected nerve with nerve gap ranging from 0.5 cm to 6 cm is repaired using autograft or nerve conduit (c) Partial defect or crushed nerve is protected by a nerve wrap to facilitate nerve regeneration

**Table 21.4** Commercially available FDA-approved nerve conduits

Product	Material	Structure	Company	Recommended use by the supplier
NeuraGen <sup>R</sup>	Collagen type I	Semipermeable tubular conduit	Integra LifeSciences Co, USA	Repair of peripheral nerve discontinuities where gap closure can be achieved by exion of the extremity
NeuroWrap <sup>TM</sup>	Collagen type I porous	Porous, tubular structure that opens as a wrap	Integra LifeSciences Co, USA	A nerve protector for cases with no substantial loss of nerve tissue, non-constricting encasement for injured peripheral nerves for protection of the neural environment, create an interface between the nerve and the surrounding tissue
NeuroFlex	Collagen type I conduit	Flexible, semipermeable tubular conduit with corrugated walls	Collagen Matrix Inc, USA	Treatment of symptomatic or painful neuromas, interface between the nerve and the surrounding tissue
NeuroMatrix <sup>TM</sup>	Collagen type I	Semipermeable tubular conduit	Collagen Matrix Inc, USA	Tensionless repair or when direct suturing is not possible
NeuroMend <sup>TM</sup>	Collagen type I	Semipermeable tubular structure that opens as a wrap, self-curling membrane with overlap	Collagen Matrix Inc, USA	Design to better match the dimensions of the defect, ability to wrap nerves from 2.0 mm to 12.0 mm in diameter

metabolic pathways, they will be replaced by the regenerating axons and host cells from the proximal nerve stump [88].

The commercial collagen conduits are in the market for decades, and so far, there is no adverse reaction has been reported. The only drawback is that these conduits inefficiently repair nerve gap longer than 3 cm and nerve of large diameter (>2.3 mm) [107]. Nerve autografting which is the standard of transected nerve repair is still the only option available.

Recent improvement of the conduits include the addition of; (a) electrospun collagen nanofibres [77, 79, 92, 93], muscle fibres [63], or PLGA nanofibres coated with collagen [156] into the lumen to guide regeneration of longer nerve gap, (b) collagen binding neurotrophic factors [21, 96] to promote axonal migration, (c) neutralising proteins [87] to antagonise myelin inhibitors, (d) Schwann cells to promote myelination of sensory or motor neurons [15] and (e) MSC to reduce scar formation and improve axonal regeneration [84, 175].

Application of collagen matrix either alone or combined with neurotrophic factors to repair spinal cord in preclinical models have been attempted. However, the feasibility of such innovation is still far-fetched due to the complexity [16, 25, 44, 60].

---

## 21.4 Tissue Substitutes as the *In Vitro* Model

Engineered tissue substitutes do not only contribute to the regeneration and repair of damaged tissues, but it is also an essential tool in studying tissue development and evaluating safety and efficacy of drugs at the earliest stage of development. *In vitro* 3D tissue substitutes provide the opportunity to predict a more accurate cellular response than the 2D testing model, given that the 3D tissue model resembles the native tissues in respect to anatomy, physiology and functionality.

3D skin model is one of the most developed tissue models and used to test the safety and efficacy of cosmetic, pharmaceutical and medi-

cal device products. The demand for skin tissue model increases after the restriction of animal testing for cosmetics (Regulation (EC) No 1223/2009 of the European Parliament and of the Council of 30 November 2009 on cosmetic products. (2009) OJ L 342, pp. 59–209), and the search for a suitable tissue model is still ongoing. Many 3D skin models that resemble the structural, functional and compositional features of the native skin are developed. Skin models are developed for partial thickness, which contains either epidermal or dermal layer, whereas full-thickness has both layers, depending on the test requirement. Since collagen type I is the main ECM of skin, the scaffold made of collagen type I such as decellularized matrix [125], collagen hydrogel [10], collagen-glycosaminoglycan (CG) [14], and chitosan cross-linked CG [142], becomes the ultimate choice to develop partial and full-thickness skin models. In general, epidermal skin model is developed by culturing keratinocytes on decellularized dermal matrix or collagen-based scaffolds. Tissue maturation is performed by exposing keratinocyte cells to air-liquid interface, which induces keratinocyte differentiation and formation of multilayer epidermis layer. Other epidermal cells such as Langerhans cells and monocytes are used to develop epidermal model, depending on the functional requirement. Dermal skin models are developed by culturing dermal fibroblasts with native collagen hydrogel. Culturing keratinocytes on top of the dermal-equivalent leads to the formation of full-thickness skin model. Attempt is made to develop tri-layer full-thickness skin model by incorporating hypodermis layer underneath of dermis layer, using collagen type I and silk scaffolds [11].

In addition to the testing tool, skin model helps to understand the skin cellular behaviour and function. It contributes to the study of skin biology in different ethnic groups, skin aging, drug or cosmetic penetration and their effect on skin cells, and protection against microbes and environmental pollution. The research is now more focused in developing disease-specific skin model, which includes diabetic foot ulcer,

melanoma, psoriasis, vitiligo, squamous cell carcinoma, and genodermatoses [3, 121].

The study of tumorigenic mechanisms in respect to angiogenesis, invasion, and metastasis used to rely on 2D *in vitro* model and small animal models, which is proven inadequate in the discovery of definite treatment for cancer termination and prevention. Recent advancement of scaffold fabrication techniques in interdisciplinary research enables the development of *in vitro* models to deepen the knowledge about tumour biology and discover new treatment strategy. Effort is given to develop *in vitro* model by culturing cancer cells with collagen type I hydrogel to study tumour development [159]. However, to understand the tumorigenic mechanism, focus is shifted to microfluidic-based system, that mimics cancer cell migration across endothelial monolayer into a hydrogel, resembling the extracellular space, and consequently metastasis to other tissues or organs [12, 69, 133]. Similar approach is developed to study the angiogenesis potential using endothelial cells treated with drugs or growth factors [110].

Neural system is one of the most complex systems in human body. To further understand the neural system, tissue engineering approach is employed in tissue reconstruction. Chwalek et al. [26] developed brain-like model resembling white and grey matter of cortex using porous silk sponge immersed in soft collagen matrix [26]. This compartmental architecture mimics the native neural tissue, thus enables the formation of polarised neuronal outgrowth and neuronal network, which can use as a model of the neural system. In another attempt, Li et al. [83] developed a blood-brain barrier model using endothelial cell line monoculture, coculture of endothelial cell line and primary rat astrocytes, with or without collagen type I and IV mixture and Matrigel for drug delivery studies. The developed model generated data equivalent to animal models, and it is then recommended to study the transport of large solutes across the blood-brain barrier. Besides, the formation of other normal and diseased models are also investigated, which include kidney, gastrointestinal tract, using collagen type I as the biomaterial [155, 158].

## 21.5 Collagen Type I Scaffold as Drug Delivery Vehicle

Recent fabrication technology enables the development of controlled delivery systems for drug or bioactive compounds, to improve the therapeutic efficacy by releasing those factors at controlled rate for a longer period. In general, collagen-based scaffolds provide the 3D architecture to promote tissue regeneration. Besides, extensive research is done to encapsulate drug or bioactive compounds on collagen scaffolds to enhance the scaffold functionality. Drug or bioactive compounds from the scaffolds are released simultaneously via diffusion and degradation of the scaffolds. However, natural collagen-based scaffolds degrade faster, unless modification is made via crosslinking or fabricating composite scaffolds. Drugs or bioactive factors such as antibiotics, anticancer, growth factors are encapsulated in the collagen-based scaffolds for delivery.

Delivery of angiogenic factor such as vascular endothelial growth factor (VEGF) is studied extensively to promote the formation of vascular network in the implanted engineered tissue substitutes. Lack of vascularization on the engineered tissue of clinically relevant size causes necrosis in the core of the construct due to insufficient oxygenation and nutrient supply, thus impedes tissue regeneration. Controlled release and physical immobilisation of VEGF were reported to enhance the *in vivo* angiogenesis [78, 151, 160]. However, in tissue substitute, covalent immobilisation is preferable, so that vascularisation takes place in the tissue substitutes rather than the surrounding tissues. Attempts were made to immobilise VEGF on porous collagen scaffolds via crosslinking using EDC [24, 106, 113, 144] or Traut's reagent and sulfo-SMCC [66]. This results in VEGF conjugation and reduces the collagen scaffold degradation rate. VEGF immobilisation on collagen scaffold significantly enhances the infiltration and proliferation of endothelial cells *in vitro*, as compared to the soluble VEGF [113, 144]. In addition, it was demonstrated that gradient distribution of VEGF increases infiltration, not proliferation, of endothelial cells to the centre of

collagen scaffold than the uniformly distributed VEGF, even when the overall concentration of VEGF was the same [113]. Similar observation was reported by He et al. [66] in *in vivo* implantation of conjugated VEGF on collagen scaffold. However, infiltration of endothelial cells on the scaffold is not sufficient to form mature vascular network. Hence, Chiu et al. [24] co-immobilised VEGF and angiopoietin-1 on 3D porous collagen scaffolds, and the formation of capillary-like structure both *in vitro* and *in vivo* was observed. The success of *in vitro* and *in vivo* studies leads to the testing of covalently immobilised VEGF in tissue regeneration. The study conducted by Miyagi et al. [106] developed cardiac patch using porous collagen scaffold with covalently immobilised VEGF and mesenchymal stem cells (MSC), and the tissue construct was implanted on the right ventricle of rat heart. Significant improvement in the proliferation of MSC and endothelial cells was demonstrated *in vitro*. In addition, the increase of blood vessel density was evident in cardiac patch, suggesting the improvement of cell survival and tissue formation.

Delivery of other growth factors is also tested to evaluate their effect on tissue-specific regeneration. In a study by Caliarì et al. [19], it was demonstrated that the incorporation of platelet-derived growth factors (PDGF)-BB and insulin-like growth factor 1 (IGF-1) to aligned collagen-glycosaminoglycan (CG) scaffolds enhances tendon cell motility, viability, and metabolic activity in a dose-dependent manner. Besides, delivery of growth factors PDGF-BB was done using heparinised collagen I suture to repair flexor tendon laceration using *in vitro* model [177]. This study found that the conjugated suture ensures a prolonged release of the PDGF-BB, through increased cell proliferation, without affecting the suture tensile strength. Furthermore, encapsulation of rhTGF- $\beta$ 3 in P(LLA-CL)/collagen nanofibres is proven to be a sustainable delivery system for tracheal cartilage regeneration [169]. Meanwhile, significant bone generation was observed in a murine critical size bone defect model, via the release of

BMP-2 and SDF-1a from heparinised MCM scaffolds [186]. A clinical trial on bovine collagen carrier for recombinant human BMP-7 in the treatment of tibial non-union was proven successful [89]. A comparative study on one diabetic Wistar rat found that chitosan nanoparticle with curcumin in collagen scaffold has potential in diabetic wound healing, thus addressing multiple pathological pathways of the disease [70]. Collagen and chitosan are proven to be wound healing modulator, and curcumin is an anti-inflammatory, antioxidant element. The delivery method is also tested to develop prodrug system for chemotherapy. Diffusion of the prodrug from collagen gel affects cancer metastasis, where it enhances the tumour growth suppression rate and metastasis attenuation [72].

---

## 21.6 Conclusion

So far, collagen-based scaffold prepared using collagen type I is proven to be versatile and efficient in biomedical applications due to its excellent biocompatibility, immunocompatibility, and flexibility towards modification. Although the natural collagen type I lacks mechanical strength, cross-disciplinary innovation enables the discovery of new methods to enhance the mechanical properties, thus extending the application of type I collagen-based scaffolds. In this chapter, the focus is on the application of type I collagen-based scaffold in the formation of tissue substitutes to repair and regenerate damaged tissues, development of *in vitro* tissue models to understand normal and disease tissue biology and drug discovery, and the use of the scaffolds as a vehicle for cells, drug and bioactive compounds. Despite their potential, more effort should be given to developing state-of-the-art collagen-based scaffolds, from bench to bedside. Integration of newly developed techniques and understanding of the complex tissue microenvironment will unlock the path in the development of structurally and functionally tissue-equivalent scaffold.

## References

1. Abou Neel EA, Bozec L, Knowles JC et al (2013) Collagen – emerging collagen based therapies hit the patient. *Adv Drug Deliv Rev* 65:429–456. <https://doi.org/10.1016/j.addr.2012.08.010>
2. Addad S, Exposito JY, Faye C et al (2011) Isolation, characterization and biological evaluation of jellyfish collagen for use in biomedical applications. *Mar Drugs* 9:967–983. <https://doi.org/10.3390/md9060967>
3. Alexandra PM, Rui LR, Rogério PP, Mariana C (2017) Skin tissue models. Academic, London
4. Amani H, Dougherty WR, Blome-Eberwein S (2006) Use of Transcyte and dermabrasion to treat burns reduces length of stay in burns of all size and etiology. *Burns* 32(7):828–832. <https://doi.org/10.1016/j.burns.2006.04.003>
5. Anders S, Volz M, Frick H, Gellissen J (2013) A randomized, controlled trial comparing Autologous Matrix-Induced Chondrogenesis (AMIC®) to microfracture: analysis of 1- and 2-year follow-up data of 2 centers. *Open Orthop J* 3(7):133–143. <https://doi.org/10.2174/1874325001307010133>
6. Awang MA, Firdaus MA, Busra MB, Chowdhury SR, Fadilah NR, Wan Hamirul WK, Reusmaazran MY, Aminuddin MY, Ruzzymah BH (2014) Cytotoxic evaluation of biomechanically improved crosslinked ovine collagen on human dermal fibroblasts. *Biomed Mater Eng* 24:1715–1724. <https://doi.org/10.3233/BME-140983>
7. Badylak SF, Taylor D, Uygun K (2011) Whole-organ tissue engineering: decellularization and recellularization of three-dimensional matrix scaffolds. *Annu Rev Biomed Eng* 13:27–53. <https://doi.org/10.1146/annurev-bioeng-071910-124743>
8. Baek J-Y, Xing Z-C, Kwak G, Yoon K-B, Park S-Y, Park LS, Kang I-K (2012) Fabrication and characterization of collagen-immobilized porous PHBV/HA nanocomposite scaffolds for bone tissue engineering. *J Nanomater* 2012:171804. <https://doi.org/10.1155/2012/171804>
9. Banerjee I, Mishra D, Das T et al (2012) Caprine (Goat) collagen: a potential biomaterial for skin tissue engineering. *J Biomater Sci Polym Ed* 23:355–373. <https://doi.org/10.1163/092050610X551943>
10. Bell E, Ehrlich HP, Sher S, Merrill C, Sarber R, Hull B, Nakatsuji T, Church D, Buttle DJ (1981) Development and use of a living skin equivalent. *Plast Reconstr Surg* 67(3):386–392
11. Bellas E, Seiberg M, Garlick J, Kaplan DL (2012) In vitro 3D full-thickness skin-equivalent tissue model using silk and collagen biomaterials. *Macromol Biosci* 12(12):1627–1636. <https://doi.org/10.1002/mabi.201200262>
12. Bersini S, Jeon JS, Dubini G, Arrigoni C, Chung S, Charest JL, Moretti M, Kamm RD (2014) A microfluidic 3D in vitro model for specificity of breast cancer metastasis to bone. *Biomaterials* 35(8):2454–2461. <https://doi.org/10.1016/j.biomaterials.2013.11.050>
13. Bertram U, Steiner D, Poppitz B, Dippold D, Kohn K, Beier JP, Detsch R, Boccaccini AR, Schubert DW, Horch RE, Arkudas A (2017) Vascular tissue engineering: effects of integrating collagen into a PCL based nanofiber material. *Biomed Res Int* 2017:9616939. <https://doi.org/10.1155/2017/9616939>
14. Black AF, Bouez C, Perrier E, Schlotmann K, Chapuis F, Damour O (2005) Optimization and characterization of an engineered human skin equivalent. *Tissue Eng* 11(5–6):723–733. <https://doi.org/10.1089/ten.2005.11.723>
15. Blais M, Grenier M, Berthod F (2009) Improvement of nerve regeneration in tissue-engineered skin enriched with schwann cells. *J Invest Dermatol* 129(12):2895–2900. <https://doi.org/10.1038/jid.2009.159>
16. Breen BA, Kraskiewicz H, Ronan R, Kshiragar A, Patar A, Sargeant T, Pandit A, McMahon SS (2017) Therapeutic effect of neurotrophin-3 treatment in an injectable collagen scaffold following rat spinal cord hemisection injury. *ACS Biomater Sci Eng* 3(7):1287–1295. <https://doi.org/10.1021/acsbomaterials.6b00167>
17. Brittberg M (2010) Cell carriers as the next generation of cell therapy for cartilage repair: a review of the matrix-induced autologous chondrocyte implantation procedure. *Am J Sports Med* 38(6):1259–1271. <https://doi.org/10.1177/0363546509346395>
18. Buehler MJ (2006) Nature designs tough collagen: explaining the nanostructure of collagen fibrils. *Proc Natl Acad Sci U S A* 103(33):12285–12290. <https://doi.org/10.1073/pnas.0603216103>
19. Caliarì SR, Harley BA (2011) The effect of anisotropic collagen-GAG scaffolds and growth factor supplementation on tendon cell recruitment, alignment, and metabolic activity. *Biomaterials* 32(23):5330–5340. <https://doi.org/10.1016/j.biomaterials.2011.04.021>
20. Carletti E, Motta A, Migliaresi C (2011) Scaffolds for tissue engineering and 3D cell culture. *Methods Mol Biol* 695:17–39. [https://doi.org/10.1007/978-1-60761-984-0\\_2](https://doi.org/10.1007/978-1-60761-984-0_2)
21. Catrina S, Gander B, Madduri S (2013) Nerve conduit scaffolds for discrete delivery of two neurotrophic factors. *Eur J Pharm Biopharm* 85(1):139–142. <https://doi.org/10.1016/j.ejpb.2013.03.030>
22. Chemla ES, Morsy M (2009) Randomized clinical trial comparing decellularized bovine ureter with expanded polytetrafluoroethylene for vascular access. *Br J Surg* 96(1):34–39. <https://doi.org/10.1002/bjs.6434>
23. Chen FM, Liu X (2016) Advancing biomaterials of human origin for tissue engineering. *Prog Polym Sci* 53:86–168. <https://doi.org/10.1016/j.progpolymsci.2015.02.004>
24. Chiu LL, Radisic M (2010) Scaffolds with covalently immobilized VEGF and Angiopoietin-1 for vascularization of engineered tissues. *Biomaterials* 31(2):226–241. <https://doi.org/10.1016/j.biomaterials.2009.09.039>

25. Cholas RH, Hsu HP, Spector M (2012) The reparative response to cross-linked collagen-based scaffolds in a rat spinal cord gap model. *Biomaterials* 33(7):2050–2059. <https://doi.org/10.1016/j.biomaterials.2011.11.028>
26. Chwalek K, Sood D, Cantley WL, White JD, Tang-Schomer M, Kaplan DL (2015) Engineered 3D silk-collagen-based model of polarized neural tissue. *J Vis Exp* 105:e52970. <https://doi.org/10.3791/52970>
27. Ciardelli G, Gentile P, Chiono V, Mattioli-Belmonte M, Vozzi G, Barbani N, Giusti P (2010) Enzymatically crosslinked porous composite matrices for bone tissue regeneration. *J Biomed Mater Res A* 92(1):137–151. <https://doi.org/10.1002/jbm.a.32344>
28. Connon CJ (2015) Approaches to corneal tissue engineering: top-down or bottom-up? *Procedia Eng* 110:15–20. <https://doi.org/10.1016/j.proeng.2015.07.004>
29. Croisier F, Jérôme C (2013) Chitosan-based biomaterials for tissue engineering. *Eur Polym J* 49(4):780–792. <https://doi.org/10.1016/j.eurpolymj.2012.12.009>
30. Dantzer E, Queruel P, Salinier L, Palmier B, Quinot JF (2003) Dermal regeneration template for deep hand burns: clinical utility for both early grafting and reconstructive surgery. *Br J Plast Surg* 56(8):764–774
31. Devitt BM, Bell SW, Webster KE, Feller JA, Whitehead TS (2017) Surgical treatments of cartilage defects of the knee: systematic review of randomised controlled trials. *Knee* 24(3):508–517. <https://doi.org/10.1016/j.knee.2016.12.002>
32. Driver VR, Lavery LA, Reyzelman AM, Dutra TG, Dove CR, Kotsis SV, Kim HM, Chung KC (2015) A clinical trial of integra template for diabetic foot ulcer treatment. *Wound Repair Regen* 23(6):891–900. <https://doi.org/10.1111/wrr.12357>
33. Duan N, Geng X, Ye L, Zhang A, Feng Z, Guo L, Gu Y (2016) A vascular tissue engineering scaffold with core-shell structured nano-fibers formed by coaxial electrospinning and its biocompatibility evaluation. *Biomed Mater* 11(3):035007. <https://doi.org/10.1088/1748-6041/11/3/035007>
34. Eaglstein WH, Falanga V (1997) Tissue engineering and the development of Apligraf®, a human skin equivalent. *Clin Ther* 19(5):894–905. [https://doi.org/10.1016/S0149-2918\(97\)80043-4](https://doi.org/10.1016/S0149-2918(97)80043-4)
35. Ebert JR, Fallon M, Wood DJ, Janes GC (2017) A prospective clinical and radiological evaluation at 5 years after arthroscopic matrix-induced autologous chondrocyte implantation. *Am J Sports Med* 45(1):59–69. <https://doi.org/10.1177/0363546516663493>
36. Edmonds M, European and Australian Apligraf Diabetic Foot Ulcer Study Group (2009) Apligraf in the treatment of neuropathic diabetic foot ulcers. *Int J Low Extrem Wounds* 8(1):11–18. <https://doi.org/10.1177/1534734609331597>
37. El-Sherbiny I, Yacoub M (2013) Hydrogel scaffolds for tissue engineering: progress and challenges. *Glob Cardiol Sci Pract* 2013(3):316–342. <https://doi.org/10.5339/gcsp.2013.38>
38. Epstein NE (2013) Complications due to the use of BMP/INFUSE in spine surgery: the evidence continues to mount. *Surg Neurol Int* 4(Suppl 5):S343–S352. <https://doi.org/10.4103/2152-7806>
39. Exposito JY, Valcourt U, Cluzel C, Lethias C (2010) The fibrillar collagen family. *Int J Mol Sci* 11(2):407–426. <https://doi.org/10.3390/ijms11020407>
40. Fagerholm P, Lagali NS, Carlsson DJ, Merrett K, Griffith M (2009) Corneal regeneration following implantation of a biomimetic tissue-engineered substitute. *Clin Transl Sci* 2(2):162–164. <https://doi.org/10.1111/j.1752-8062.2008.00083.x>
41. Fagerholm P, Lagali NS, Ong JA, Merrett K, Jackson WB, Polarek JW, Suuronen EJ, Liu Y, Brunette I, Griffith M (2014) Stable corneal regeneration four years after implantation of a cell-free recombinant human collagen scaffold. *Biomaterials* 35(8):2420–2427. <https://doi.org/10.1016/j.biomaterials.2013.11.079>
42. Falabella AF, Valencia IC, Eaglstein WH, Schachner LA (2000) Tissue-engineered skin (Apligraf) in the healing of patients with epidermolysis bullosa wounds. *Arch Dermatol* 136(10):1225–1230
43. Falanga V, Margolis D, Alvarez O, Auletta M, Maggiacomo F, Altman M, Jensen J, Sabolinski M, Hardin-Young J (1998) Rapid healing of venous ulcers and lack of clinical rejection with an allogeneic cultured human skin equivalent. *Arch Dermatol* 134(3):293–300
44. Fan J, Xiao Z, Zhang H, Chen B, Tang G, Hou X, Ding W, Wang B, Zhang P, Dai J, Xu R (2010) Linear ordered collagen scaffolds loaded with collagen-binding neurotrophin-3 promote axonal regeneration and partial functional recovery after complete spinal cord transection. *J Neurotrauma* 27(9):1671–1683. <https://doi.org/10.1089/neu.2010.1281>
45. Farroha A, Frew Q, El-Muttardi N, Philp B, Dziewulski P (2013) The use of Biobrane® to dress split-thickness skin graft in paediatric burns. *Ann Burns Fire Disasters* 26(2):94–97
46. Fauzi MB, Chowdhury SR, Aminuddin BS, Ruszymah BHI (2014) Fabrication of collagen type I scaffold for skin tissue engineering. *Regenerative Res* 3(2):59–60
47. Fauzi MB, Lokanathan Y, Aminuddin BS, Ruszymah BH, Chowdhury SR (2016) Ovine tendon collagen: extraction, characterisation and fabrication of thin films for tissue engineering applications. *Mater Sci Eng C* 68:163–171. <https://doi.org/10.1016/j.msec.2016.05.109>
48. Fertala A, Shah MD, Hoffman RA, Arnold VW (2016) Designing recombinant collagens for biomedical applications. *Current Tissue Eng* 5(2):73–84. <https://doi.org/10.2174/2211542005666160616124053>



49. Fujikawa S, Nakamura S, Koga K (1988) Genipin, a new type of protein crosslinking reagent from gardenia fruits. *Agric Biol Chem* 52(3):869–870. <https://doi.org/10.1080/00021369.1988.10868755>
50. Gentleman MM, Gentleman E (2014) The role of surface free energy in osteoblast–biomaterial interactions. *Int Mater Rev* 59:417–429. <https://doi.org/10.1179/1743280414Y.0000000038>
51. Gerding RL, Imbombo AL, Fratianna RB (1988) Biosynthetic skin substitute vs 1% silver sulfadiazine for treatment of inpatient partial-thickness thermal burns. *J Trauma* 28(8):1265–1269
52. Ghezzi CE, Rnjak-Kovacina J, Kaplan DL (2015) Corneal tissue engineering: recent advances and future perspectives. *Tissue Eng Part B Rev* 21(3):278–287. <https://doi.org/10.1089/ten.TEB.2014.0397>
53. Gille J, Behrens P, Schulz AP, Oheim R, Kienast B (2016) Matrix-associated autologous chondrocyte implantation: a clinical follow-up at 15 years. *Cartilage* 7(4):309–315. <https://doi.org/10.1177/1947603516638901>
54. Gistelink C, Gioia R, Gagliardi A, Tonelli F, Marchese L, Bianchi L, Landi C, Bini L, Huysseune A, Witten PE, Staes A, Gevaert K, De Rocker N, Menten B, Malfait F, Leikin S, Carra S, Tenni R, Rossi A, De Paepe A, Coucke P, Willaert A, Forlino A (2016) Zebrafish collagen type I: molecular and biochemical characterization of the major structural protein in bone and skin. *Sci Rep* 6:21540. <https://doi.org/10.1038/srep21540>
55. Gohari S, Gambra C, Healey M, Spaulding G, Gordon KB, Swan J, Cook B, West DP, Lapiere JC (2002) Evaluation of tissue-engineered skin (human skin substitute) and secondary intention healing in the treatment of full thickness wounds after Mohs micrographic or excisional surgery. *Dermatol Surg* 28(12):1107–1114
56. Grabarek Z, Gergely J (1990) Zero-length cross-linking procedure with the use of active esters. *Anal Biochem* 185(1):131–135
57. Greenwood JE, Clausen J, Kavanagh S (2009) Experience with biobrane: uses and caveats for success. *Eplasty* 9:e25
58. Haid RW Jr, Branch CL Jr, Alexander JT, Burkus JK (2004) Posterior lumbar interbody fusion using recombinant human bone morphogenetic protein type 2 with cylindrical interbody cages. *Spine J* 4(5):527–538. <https://doi.org/10.1016/j.spinee.2004.03.025>
59. Hall AC, Guyton JE (2011) Textbook of medical physiology, 12th edn. Elsevier, Philadelphia, pp 957–960 ISBN 978-08089-2400-5
60. Han S, Wang B, Jin W, Xiao Z, Chen B, Xiao H, Ding W, Cao J, Ma F, Li X, Yuan B, Zhu T, Hou X, Wang J, Kong J, Liang W, Dai J (2014) The collagen scaffold with collagen binding BDNF enhances functional recovery by facilitating peripheral nerve infiltrating and ingrowth in canine complete spinal cord transection. *Spinal Cord* 52(12):867–873. <https://doi.org/10.1038/sc.2014.173>
61. Harston A, Nyland J, Brand E, McGinnis M, Caborn DN (2012) Collagen meniscus implantation: a systematic review including rehabilitation and return to sports activity. *Knee Surg Sports Traumatol Arthrosc* 20(1):135–146. <https://doi.org/10.1007/s00167-011-1579-9>
62. Haslik W, Kamolz LP, Nathschläger G, Andel H, Meissl G, Frey M (2007) First experiences with the collagen-elastin matrix Matriderm® as a dermal substitute in severe burn injuries of the hand. *Burns* 33(3):364–368. <https://doi.org/10.1016/j.burns.2006.07.021>
63. Hassan NH, Sulong AF, Ng MH, Htwe O, Idrus RB, Roohi S, Naicker AS, Abdullah S (2012) Neural-differentiated mesenchymal stem cells incorporated into muscle stuffed vein scaffold forms a stable living nerve conduit. *J Orthop Res* 30(10):1674–1681. <https://doi.org/10.1002/jor.22102>
64. Haugh MG, Jaasma MJ, O'Brien FJ (2009) The effect of dehydrothermal treatment on the mechanical and structural properties of collagen-GAG scaffolds. *J Biomed Mater Res A* 89(2):363–369. <https://doi.org/10.1002/jbm.a.31955>
65. Hayes DW Jr, Webb GE, Mandracchia VJ, John KJ (2001) Full-thickness burn of the foot: successful treatment with Apligraf. A case report. *Clin Podiatr Med Surg* 18(1):179–188
66. He Q, Zhao Y, Chen B, Xiao Z, Zhang J, Chen L, Chen W, Deng F, Dai J (2011) Improved cellularization and angiogenesis using collagen scaffolds chemically conjugated with vascular endothelial growth factor. *Acta Biomater* 7(3):1084–1093. <https://doi.org/10.1016/j.actbio.2010.10.022>
67. Heimbach DM, Warden GD, Luterman A, Jordan MH, Ozobia N, Ryan CM, Voigt DW, Hickerson WL, Saffle JR, DeClement FA, Sheridan RL, Dimick AR (2003) Multicenter postapproval clinical trial of Integra® dermal regeneration template for burn treatment. *J Burn Care Rehabil* 24(1):42–48. <https://doi.org/10.1097/01.BCR.0000045659.08820.00>
68. Jay L, Bourget JM, Goyer B, Singh K, Brunette I, Ozaki T, Proulx S (2015) Characterization of tissue-engineered posterior corneas using second- and third-harmonic generation microscopy. *PLoS One* 10(4):e0125564. <https://doi.org/10.1371/journal.pone.0125564>
69. Jeon JS, Zervantonakis IK, Chung S, Kamm RD, Charest JL (2013) In vitro model of tumor cell extravasation. *PLoS One* 8(2):e56910. <https://doi.org/10.1371/journal.pone.0056910>
70. Karri VV, Kuppusamy G, Talluri SV, Mannemala SS, Kollipara R, Wadhvani AD, Mulukutla S, Raju KR, Malayandi R (2016) Curcumin loaded chitosan nanoparticles impregnated into collagen-alginate scaffolds for diabetic wound healing. *Int J Biol Macromol* 93(Pt B):1519–1529. <https://doi.org/10.1016/j.ijbiomac.2016.05.038>

71. Kennealey PT, Elias N, Hertl M, Ko DS, Saidi RF, Markmann JF, Smoot EE, Schoenfeld DA, Kawai T (2011) A prospective, randomized comparison of bovine carotid artery and expanded polytetrafluoroethylene for permanent hemodialysis vascular access. *J Vasc Surg* 53(6):1640–1648. <https://doi.org/10.1016/j.jvs.2011.02.008>
72. Kojima C, Suehiro T, Watanabe K, Ogawa M, Fukuhara A, Nishisaka E, Harada A, Kono K, Inui T, Magata Y (2013) Doxorubicin-conjugated dendrimer/collagen hybrid gels for metastasis-associated drug delivery systems. *Acta Biomater* 9(3):5673–5680. <https://doi.org/10.1016/j.actbio.2012.11.013>
73. Kon E, Filardo G, Di Matteo B, Perdisa F, Marcacci M (2013) Matrix assisted autologous chondrocyte transplantation for cartilage treatment. *Bone Joint Res* 2(2):18–25. <https://doi.org/10.1302/2046-3758.22.2000092>
74. Kumar RJ1, Kimble RM, Boots R, Pegg SP (2004) Treatment of partial-thickness burns: a prospective, randomized trial using Transcyte™. *ANZ J Surg* 74(8):622–626. <https://doi.org/10.1111/j.1445-1433.2004.03106.x>
75. Kwansa AL, De Vita R, Freeman JW (2016) Tensile mechanical properties of collagen type I and its enzymatic crosslinks. *Biophys Chem* 214–215:1–10. <https://doi.org/10.1016/j.bpc.2016.04.001>
76. Lal S, Barrow RE, Wolf SE, Chinkes DL, Hart DW, Hegggers JP, Herndon DN (2000) Bliobrane® improves wound healing in burned children. *Shock* 14(3):314–318
77. Lee JY, Giusti G, Friedrich PF, Archibald SJ, Kemnitzer JE, Patel J, Desai N, Bishop AT, Shin AY (2012a) The effect of collagen nerve conduits filled with collagen-glycosaminoglycan matrix on peripheral motor nerve regeneration in a rat model. *J Bone Joint Surg Am* 94(22):2084–2091. <https://doi.org/10.2106/JBJS.K.00658>
78. Lee KY, Peters MC, Anderson KW, Mooney DJ (2000) Controlled growth factor release from synthetic extracellular matrices. *Nature* 408(6815):998–1000. <https://doi.org/10.1038/35050141>
79. Lee SR, Kim JG, Nam SW (2012b) The tips and pitfalls of meniscus allograft transplantation. *Knee Surg Relat Res* 24(3):137–145. <https://doi.org/10.5792/ksrr.2012.24.3.137>
80. Lee SW, Kim SG (2014) Membrane for the guided bone regeneration. *Maxillofac Plast Reconstr Surg* 36(6):239–246. <https://doi.org/10.14402/jkampr.2014.36.6.239>
81. León-Mancilla BH, Araiza-Téllez MA, Flores-Flores JO, Piña-Barba MC (2016) Physico-chemical characterization of collagen scaffolds for tissue engineering. *J Appl Res Technol* 14(1):77–85. <https://doi.org/10.1016/J.JART.2016.01.001>
82. Leshner AP, Curry RH, Evans J, Smith VA, Fitzgerald MT, Cina RA, Streck CJ, Hebra AV (2011) Effectiveness of Biobrane for treatment of partial-thickness burns in children. *J Pediatr Surg* 46(9):1759–1763. <https://doi.org/10.1016/j.jpedsurg.2011.03.070>
83. Li G, Simon MJ, Cancel LM, Shi ZD, Ji X, Tarbell JM, Morrison B, Fu BM (2010) Permeability of endothelial and astrocyte cocultures: in vitro blood-brain barrier models for drug delivery studies. *Ann Biomed Eng* 38(8):2499–2511. <https://doi.org/10.1007/s10439-010-0023-5>
84. Li H, Yun HY, Baek KJ, Kwon NS, Choi HR, Park KC, Kim DS (2017a) Avian collagen is useful for the construction of skin equivalents. *Cells Tissues Organs* 204(5-6):261–269. <https://doi.org/10.1159/000480659>
85. Li S, Sengupta D, Chien S (2014) Vascular tissue engineering: from in vitro to in situ. *Wiley Interdiscip Rev Syst Biol Med* 6(1):61–76. <https://doi.org/10.1002/wsbm.1246>
86. Li ST, Archibald SJ, Krarup C, Madison RD (1992) Peripheral nerve repair with collagen conduits. *Clin Mater* 9(3-4):195–200
87. Li X, Han J, Zhao Y, Ding W, Wei J, Li J, Han S, Shang X, Wang B, Chen B, Xiao Z, Dai J (2016) Functionalized collagen scaffold implantation and cAMP administration collectively facilitate spinal cord regeneration. *Acta Biomater* 30:233–245. <https://doi.org/10.1016/j.actbio.2015.11.023>
88. Liang X, Cai H, Hao Y, Sun G, Song Y, Chen W (2014) Sciatic nerve repair using adhesive bonding and a modified conduit. *Neural Regen Res* 9(6):594–601. <https://doi.org/10.4103/1673-5374.130099>
89. Lienemann PS, Lutolf MP, Ehrbar M (2012) Biomimetic hydrogels for controlled biomolecule delivery to augment bone regeneration. *Adv Drug Deliv Rev* 64(12):1078–1089. <https://doi.org/10.1016/j.addr.2012.03.010>
90. Lindsey P, Echeverria A, Cheung M, Kfoury E, Bechara CF, Lin PH (2017) Lower extremity bypass using bovine carotid artery graft (Artegraft): an analysis of 124 cases with long-term results. *World J Surg* 42(1):295–301. <https://doi.org/10.1007/s00268-017-4161-x>
91. Liu D, Wei G, Li T et al (2015) Effects of alkaline pretreatments and acid extraction conditions on the acid-soluble collagen from grass carp (*Ctenopharyngodon idella*) skin. *Food Chem* 172:836–843. <https://doi.org/10.1016/j.foodchem.2014.09.147>
92. Liu T, Houle JD, Xu J, Chan BP, Chew SY (2012a) Nanofibrous collagen nerve conduits for spinal cord repair. *Tissue Eng Part A* 18(9-10):1057–1066. <https://doi.org/10.1089/ten.TEA.2011.0430>
93. Liu Y, Ren L, Yao H, Wang Y (2012b) Collagen films with suitable physical properties and biocompatibility for corneal tissue engineering prepared by ion leaching technique. *Mater Lett* 87:1–4. <https://doi.org/10.1016/j.matlet.2012.07.091>
94. Loh QL, Choong C (2013) Three-dimensional scaffolds for tissue engineering applications: role of porosity and pore size. *Tissue Eng Part B Rev* 19(6):485–502. <https://doi.org/10.1089/ten.teb.2012.0437>

95. Lohana P, Hassan S, Watson SB (2014) Integra™ in burns reconstruction: our experience and report of an unusual immunological reaction. *Ann Burns Fire Disasters* 27(1):17–21
96. Lu C, Meng D, Cao J, Xiao Z, Cui Y, Fan J, Cui X, Chen B, Yao Y, Zhang Z, Ma J, Pan J, Dai J (2015) Collagen scaffolds combined with collagen-binding chondrocyte neurotrophic factor facilitate facial nerve repair in mini-pigs. *J Biomed Mater Res A* 103(5):1669–1676. <https://doi.org/10.1002/jbm.a.35305>
97. Lu P, Takai K, Weaver VM, Werb Z (2011) Extracellular matrix degradation and remodeling in development and disease. *Cold Spring Harb Perspect Biol* 3(12):pii: a005058. <https://doi.org/10.1101/cshperspect.a005058>
98. Lukish JR, Eichelberger MR, Newman KD, Pao M, Nobuhara K, Keating M, Golonka N, Pratsch G, Misra V, Valladares E, Johnson P, Gilbert JC, Powell DM, Hartman GE (2001) The use of a bioactive skin substitute decreases length of stay for pediatric burn patients. *J Pediatr Surg* 36(8):1118–1121. <https://doi.org/10.1053/jpsu.2001.25678>
99. Marín-Pareja N, Cantini M, González-García C, Salvagni E, Salmerón-Sánchez M, Ginebra MP (2015) Different organization of type I collagen immobilized on silanized and nonsilanized titanium surfaces affects fibroblast adhesion and fibronectin secretion. *ACS Appl Mater Interfaces* 7(37):20667–20677. <https://doi.org/10.1021/acsami.5b05420>
100. Marlovits S, Zeller P, Singer P, Resinger C, Vecsei V (2006) Cartilage repair: generations of autologous chondrocyte transplantation. *Eur J Radiol* 57(1):24–31. <https://doi.org/10.1016/j.ejrad.2005.08.009>
101. McClure MJ, Sell SA, Simpson DG, Walpoth BH, Bowlin GL (2010) A three-layered electrospun matrix to mimic native arterial architecture using polycaprolactone, elastin, and collagen: a preliminary study. *Acta Biomater* 6(7):2422–2433. <https://doi.org/10.1016/j.actbio.2009.12.029>
102. Merrett K, Fagerholm P, McLaughlin CR, Dravida S, Lagali N, Shinozaki N, Watsky MA, Munger R, Kato Y, Li F, Marmo CJ, Griffith M (2008) Tissue-engineered recombinant human collagen-based corneal substitutes for implantation: performance of type I versus type III collagen. *Invest Ophthalmol Vis Sci* 49(9):3887–3894. <https://doi.org/10.1167/iovs.07-1348>
103. Michelacci YM (2003) Collagens and proteoglycans of the corneal extracellular matrix. *Braz J Med Biol Res* 36(8):1037–1046
104. Min JH, Yun IS, Lew DH, Roh TS, Lee WJ (2014) The use of matrigel and autologous skin graft in the treatment of full thickness skin defects. *Arch Plast Surg* 41(4):330–336. <https://doi.org/10.5999/aps.2014.41.4.330>
105. Miranda-Nieves D, Chaikof EL (2017) Collagen and elastin biomaterials for the fabrication of engineered living tissues. *ACS Biomater Sci Eng* 3(5):694–711. <https://doi.org/10.1021/acsbomaterials.6b00250>
106. Miyagi Y, Chiu LL, Cimini M, Weisel RD, Radisic M, Li RK (2011) Biodegradable collagen patch with covalently immobilized VEGF for myocardial repair. *Biomaterials* 32(5):1280–1290. <https://doi.org/10.1016/j.biomaterials.2010.10.007>
107. Moore AM, Kasukurthi R, Magill CK, Farhadi HF, Borschel GH, Mackinnon SE (2009) Limitations of conduits in peripheral nerve repairs. *Hand (NY)* 4(2):180–186. <https://doi.org/10.1007/s11552-008-9158-3>
108. Muhart M, McFalls S, Kirsner RS, Elgart GW, Kerdel F, Sabolinski ML, Hardin-Young J, Eaglstein WH (1999) Behavior of tissue-engineered skin: a comparison of a living skin equivalent, autograft, and occlusive dressing in human donor sites. *Arch Dermatol* 135(8):913–918
109. Nelson CG, Bonner KF (2013) Inside-out meniscus repair. *Arthrosc Tech* 2(4):e453–e460. <https://doi.org/10.1016/j.eats.2013.07.006>
110. Nguyen DH, Stapleton SC, Yang MT, Cha SS, Choi CK, Galie PA, Chen CS (2013) Biomimetic model to reconstitute angiogenic sprouting morphogenesis in vitro. *Proc Natl Acad Sci U S A* 110(17):6712–6717. <https://doi.org/10.1073/pnas.1221526110>
111. Noordenbos J, Doré C, Hansbrough JF (1999) Safety and efficacy of TransCyte for the treatment of partial-thickness burns. *J Burn Care Rehabil* 20(4):275–281
112. O'Brien FJ (2011) Biomaterials & scaffolds for tissue engineering. *Mater Today* 14(3):88–95. [https://doi.org/10.1016/S1369-7021\(11\)70058-X](https://doi.org/10.1016/S1369-7021(11)70058-X)
113. Odedra D, Chiu LL, Shoichet M, Radisic M (2011) Endothelial cells guided by immobilized gradients of vascular endothelial growth factor on porous collagen scaffolds. *Acta Biomater* 7(8):3027–3035. <https://doi.org/10.1016/j.actbio.2011.05.002>
114. Ouyang Y, Huang C, Zhu Y, Fan C, Ke Q (2013) Fabrication of seamless electrospun collagen/PLGA conduits whose walls comprise highly longitudinal aligned nanofibers for nerve regeneration. *J Biomed Nanotechnol* 9(6):931–943
115. Palao R, Gómez P, Huguet P (2003) Burned breast reconstructive surgery with Integra dermal regeneration template. *Br J Plast Surg* 56(3):252–259
116. Papalia R, Franceschi F, Balzani LD, D'Adamo S, Maffulli N, Denaro V (2013) Scaffolds for partial meniscal replacement: an updated systematic review. *Br Med Bull* 107:19–40. <https://doi.org/10.1093/bmb/ldt007>
117. Parenteau-Bareil R, Gauvin R, Berthod F (2010) Collagen-based biomaterials for tissue engineering applications. *Materials* 3:1863–1887. <https://doi.org/10.3390/ma3031863>
118. Pati F, Adhikari B, Dhara S (2010) Isolation and characterization of fish scale collagen of higher thermal stability. *Bioresour Technol* 101(10):3737–3742. <https://doi.org/10.1016/j.biortech.2009.12.133>

119. Perumal S, Antipova O, Orgel JP (2008) Collagen fibril architecture, domain organization, and triple-helical conformation govern its proteolysis. *Proc Natl Acad Sci U S A* 105(8):2824–2829. <https://doi.org/10.1073/pnas.0710588105>
120. Pittenger MF, Mackay AM, Beck SC, Jaiswal RK, Douglas R, Mosca JD, Moorman MA, Simonetti DW, Craig S, Marshak DR (1999) Multilineage potential of adult human mesenchymal stem cells. *Science* 284(5411):143–147
121. Price BL, Lovering AM, Bowling FL, Dobson CB (2016) Development of a novel collagen wound model to simulate the activity and distribution of antimicrobials in soft tissue during diabetic foot infection. *Antimicrob Agents Chemother* 60(11):6880–6889. <https://doi.org/10.1128/AAC.01064-16>
122. Rabiatal AR, Lokanathan Y, Rohaina CM, Chowdhury SR, Aminuddin BS, Ruszymah BH (2015) Surface modification of electrospun poly (methyl methacrylate)(PMMA) nanofibers for the development of in vitro respiratory epithelium model. *J Biomater Sci Polym Ed* 26(17):1297–1311. <https://doi.org/10.1080/09205063.2015.1088183>
123. Ravi S, Chaikof EL (2010) Biomaterials for vascular tissue engineering. *Regen Med* 5(1):107–120. <https://doi.org/10.2217/rme.09.77>
124. Reddy N, Reddy R, Jiang Q (2015) Crosslinking biopolymers for biomedical applications. *Trends Biotechnol* 33(6):362–369. <https://doi.org/10.1016/j.tibtech.2015.03.008>
125. Regnier M, Schweizer J, Michel S, Bailly C, Prunieras M (1986) Expression of high molecular weight (67K) keratin in human keratinocytes cultured on dead de-epidermized dermis. *Exp Cell Res* 165(1):63–72
126. Ricard-Blum S (2011) The collagen family. *Cold Spring Harb Perspect Biol* 3(1):a004978. <https://doi.org/10.1101/cshperspect.a004978>
127. Rodkey WG (2010) Menaflex (TM) collagen meniscus implant: basic science. In: *The meniscus*. Springer, Berlin, pp 367–371
128. Rogers AD, Adams S, Rode H (2011) The introduction of a protocol for the use of biobrane for facial burns in children. *Plast Surg Int* 2011:858093. <https://doi.org/10.1155/2011/858093>
129. Rozario T, DeSimone DW (2010) The extracellular matrix in development and morphogenesis: a dynamic view. *Dev Biol* 341(1):126–140. <https://doi.org/10.1016/j.ydbio.2009.10.026>
130. Ryssel H, Gazyakan E, Germann G, Ohlbauer M (2008) The use of MatriDerm® in early excision and simultaneous autologous skin grafting in burns—a pilot study. *Burns* 34(1):93–97. <https://doi.org/10.1016/j.burns.2007.01.018>
131. Safandowska M, Pietrucha K (2013) Effect of fish collagen modification on its thermal and rheological properties. *Int J Biol Macromol* 53:32–37. <https://doi.org/10.1016/j.ijbiomac.2012.10.026>
132. Santos MH, Silva RM, Dumont VC, Neves JS, Mansur HS, Heneine LG (2013) Extraction and characterization of highly purified collagen from bovine pericardium for potential bioengineering applications. *Mater Sci Eng C* 33(2):790–800. <https://doi.org/10.1016/j.msec.2012.11.003>
133. Sasaki N, Bos C, Escoffre JM, Storm G, Moonen C (2015) Development of a tumor tissue-mimicking model with endothelial cell layer and collagen gel for evaluating drug penetration. *Int J Pharm* 482(1-2):118–122. <https://doi.org/10.1016/j.ijpharm.2015.01.039>
134. Sasmal P, Begam H (2014) Extraction of type-I collagen from sea fish and synthesis of hap/collagen composite. *Procedia Mater Sci* 5:1136–1140. <https://doi.org/10.1016/j.mspro.2014.07.408>
135. Schmidli J, Savolainen H, Heller G, Widmer MK, Then-Schlagau U, Baumgartner I, Carrel TP (2004) Bovine mesenteric vein graft (ProCol) in critical limb ischaemia with tissue loss and infection. *Eur J Vasc Endovasc Surg* 27(3):251–253. <https://doi.org/10.1016/j.ejvs.2003.12.001>
136. Schmidt CE, Leach JB (2003) Neural tissue engineering: strategies for repair and regeneration. *Annu Rev Biomed Eng* 5:293–347. <https://doi.org/10.1146/annurev.bioeng.5.011303.120731>
137. Schmidt MM, Dornelles RCP, Mello RO, Kubota EH, Mazutti MA, Kempka AP, Demiate IM (2016) Collagen extraction process. *Int Food Res J* 23(3):913–922
138. Schoof H, Apel J, Heschel I, Rau G (2001) Control of pore structure and size in freeze-dried collagen sponges. *J Biomed Mater Res* 58(4):352–357
139. Schröder A, Imig H, Peiper U, Neidel J, Petereit A (1988) Results of a bovine collagen vascular graft (Solcograft-P) in infra-inguinal positions. *Eur J Vasc Surg* 2(5):315–321
140. Schuette HB, Kraeutler MJ, McCarty EC (2017) Matrix-assisted autologous chondrocyte transplantation in the knee: a systematic review of mid- to long-term clinical outcomes. *Orthop J Sports Med* 5(6):2325967117709250. <https://doi.org/10.1177/2325967117709250>
141. Schulz A, Depner C, Lefering R, Kricheldorf J, Kästner S, Fuchs PC, Demir E (2016) A prospective clinical trial comparing Biobrane® Dressilk® and PolyMem® dressings on partial-thickness skin graft donor sites. *Burns* 42(2):345–355. <https://doi.org/10.1016/j.burns.2014.12.016>
142. Shahabeddin L, Berthod F, Damour O, Collombel C (1990) Characterization of skin reconstructed on a chitosan-cross-linked collagen-glycosaminoglycan matrix. *Skin Pharmacol* 3(2):107–114
143. Shahrokhi S, Arno A, Jeschke MG (2014) The use of dermal substitutes in burn surgery: acute phase. *Wound Repair Regen* 22(1):14–22. <https://doi.org/10.1111/wrr.12119>

144. Shen YH, Shoichet MS, Radisic M (2008) Vascular endothelial growth factor immobilized in collagen scaffold promotes penetration and proliferation of endothelial cells. *Acta Biomater* 4(3):477–489. <https://doi.org/10.1016/j.actbio.2007.12.011>
145. Shilo S, Roth S, Amzel T, Harel-Adar T, Tamir E, Grynspan F, Shoseyov O (2013) Cutaneous wound healing after treatment with plant-derived human recombinant collagen flowable gel. *Tissue Eng Part A* 19(13-14):1519–1526. <https://doi.org/10.1089/ten.TEA.2012.0345>
146. Shoseyov O, Posen Y, Grynspan F (2013) Human recombinant type I collagen produced in plants. *Tissue Eng Part A* 19(13-14):1527–1533. <https://doi.org/10.1089/ten.tea.2012.0347>
147. Shoulders MD, Raines RT (2009) Collagen structure and stability. *Annu Rev Biochem* 78:929–958. <https://doi.org/10.1146/annurev.biochem.77.032207.120833>
148. Silvipriya KS, Krishna Kumar K, Bhat AR, Dinesh Kumar B, John A, Lakshmanan P (2015) Collagen: animal sources and biomedical application. *J Appl Pharm Sci* 5(3):123–127. <https://doi.org/10.7324/JAPS.2015.50322>
149. Solanki NS1, Nowak KM, Mackie IP, Greenwood JE (2010) Using Biobrane: techniques to make life easier. *Eplasty* 10:e70
150. Stachel I, Schwarzenbolz U, Henle T, Meyer M (2010) Cross-linking of type I collagen with microbial transglutaminase: identification of cross-linking sites. *Biomacromolecules* 11(3):698–705. <https://doi.org/10.1021/bm901284x>
151. Steffens GC, Yao C, Prével P, Markowicz M, Schenck P, Noah EM, Pallua N (2004) Modulation of angiogenic potential of collagen matrices by covalent incorporation of heparin and loading with vascular endothelial growth factor. *Tissue Eng* 10(9-10):1502–1509. <https://doi.org/10.1089/ten.2004.10.1502>
152. Steinwachs M, Peter CK (2007) Autologous chondrocyte implantation in chondral defects of the knee with a type I/III collagen membrane: a prospective study with a 3-year follow-up. *Arthroscopy* 23(4):381–387. <https://doi.org/10.1016/j.arthro.2006.12.003>
153. Still J, Glat P, Silverstein P, Griswold J, Mozingo D (2003) The use of a collagen sponge/living cell composite material to treat donor sites in burn patients. *Burns* 29(8):837–841
154. Subia B, Kundu J, Kundu S (2010) Biomaterial scaffold fabrication techniques for potential tissue engineering applications. INTECH Open Access Publisher 141–158. <https://doi.org/10.5772/8581>
155. Subramanian B, Rudym D, Cannizzaro C, Perrone R, Zhou J, Kaplan DL (2010) Tissue-engineered three-dimensional in vitro models for normal and diseased kidney. *Tissue Eng Part A* 16(9):2821–2831. <https://doi.org/10.1089/ten.TEA.2009.0595>
156. Sulong AF, Hassan NH, Hwei NM, Lokanathan Y, Naicker AS, Abdullah S, Yusof MR, Htwe O, Idrus R, Hafiah N (2014) Collagen-coated polylactic-glycolic acid (PLGA) seeded with neural-differentiated human mesenchymal stem cells as a potential nerve conduit. *Adv Clin Exp Med* 23(3):353–362
157. Sun J, Vijayavenkataraman S, Liu H (2017) An overview of scaffold design and fabrication technology for engineered knee meniscus. *Materials* 10(1):E29. <https://doi.org/10.3390/ma10010029>
158. Sung JH, Yu J, Luo D, Shuler ML, March JC (2011) Microscale 3-D hydrogel scaffold for biomimetic gastrointestinal (GI) tract model. *Lab Chip* 11(3):389–392. <https://doi.org/10.1039/c0lc00273a>
159. Szot CS, Buchanan CF, Freeman JW, Rylander MN (2011) 3D in vitro bioengineered tumors based on collagen I hydrogels. *Biomaterials* 32(31):7905–7912. <https://doi.org/10.1016/j.biomaterials.2011.07.001>
160. Tabata Y, Miyao M, Ozeki M, Ikada Y (2000) Controlled release of vascular endothelial growth factor by use of collagen hydrogels. *J Biomater Sci Polym Ed* 11(9):915–930
161. Techatanawat S, Surarit R, Suddhasthira T, Khovidhunkit SOP (2011) Type I collagen extracted from rat-tail and bovine Achilles tendon for dental application: a comparative study. *Asian Biomed* 5:787–798. <https://doi.org/10.5372/1905-7415.0506.111>
162. Theocharis AD, Skandalis SS, Gialeli C, Karamanos NK (2016) Extracellular matrix structure. *Adv Drug Deliv Rev* 97:4–27. <https://doi.org/10.1016/j.addr.2015.11.001>
163. Tian Z, Li C, Duan L, Li G (2014) Physicochemical properties of collagen solutions cross-linked by glutaraldehyde. *Connect Tissue Res* 55(3):239–247. <https://doi.org/10.3109/03008207.2014.898066>
164. Tuan RS (2007) A second-generation autologous chondrocyte implantation approach to the treatment of focal articular cartilage defects. *Arthritis Res Ther* 9(5):109. <https://doi.org/10.1186/ar2310>
165. van Zuijlen PP, van Trier AJ, Vloemans JF, Groenevelt F, Kreis RWR, Middelkoop E (2000) Graft survival and effectiveness of dermal substitution in burns and reconstructive surgery in a one-stage grafting model. *Plast Reconstr Surg* 106(3):615–623
166. Veeruraj A, Arumugam M, Balasubramanian T (2013) Isolation and characterization of thermostable collagen from the marine eel-fish (*Evenchelys macrura*). *Process Biochem* 48:1592–1602. <https://doi.org/10.1016/j.procbio.2013.07.011>
167. Veves A, Falanga V, Armstrong DG, Sabolinski ML (2001) Graftskin, a human skin equivalent, is effective in the management of noninfected neuropathic diabetic foot ulcers. *Diabetes Care* 24:290–295
168. Vigneswari S, Murugaiyah V, Kaur G, Khalil HA, Amirul A (2016) Simultaneous dual syringe electrospinning system using benign solvent to fabricate nanofibrous P (3HB-co-4HB)/collagen peptides construct as potential leave-on wound dressing. *Mater Sci Eng C Mater Biol Appl* 66:147–155. <https://doi.org/10.1016/j.msec.2016.03.102>

169. Wang J, Sun B, Tian L, He X, Gao Q, Wu T, Ramakrishna S, Zheng J, Mo X (2017) Evaluation of the potential of rhTGF- $\beta$ 3 encapsulated P(LLA-CL)/collagen nanofibers for tracheal cartilage regeneration using mesenchymal stem cells derived from Wharton's jelly of human umbilical cord. *Mater Sci Eng C Mater Biol Appl* 70(Pt 1):637–645. <https://doi.org/10.1016/j.msec.2016.09.044>
170. Weber RA, Breidenbach WC, Brown RE, Jabaley ME, Mass DP (2000) A Randomized prospective study of Polyglycolic acid conduits for digital nerve reconstruction in humans. *Plast Reconstr Surg* 106(5):1036–1045
171. Weigert R, Choughri H, Casoli V (2010) Management of severe hand wounds with integra® dermal regeneration template. *J Hand Surg Eur* 36(3):185–193. <https://doi.org/10.1177/1753193410387329>
172. Whitford C, Movchan NV, Studer H, Elsheikh A (2017) A viscoelastic anisotropic hyperelastic constitutive model of the human cornea. *Biomech Model Mechanobiol*. <https://doi.org/10.1007/s10237-017-0942-2>
173. Wichuda J, Sunthorn C, Busarakum P (2016) Comparison of the properties of collagen extracted from dried jellyfish and dried squid. *Afr J Biotechnol* 15(16):642–648. <https://doi.org/10.5897/AJB2016.15210>
174. Wu T, Zhang J, Wang Y, Li D, Sun B, El-Hamshary H, Yin M, Mo X (2018) Fabrication and preliminary study of a biomimetic tri-layer tubular graft based on fibers and fiber yarns for vascular tissue engineering. *Mater Sci Eng C Mater Biol Appl* 82:121–129. <https://doi.org/10.1016/j.msec.2017.08.072>
175. Li X, Tan J, Xiao Z, Zhao Y, Han S, Liu D, Yin W, Li J, Li J, Wanggou S, Chen B, Ren C, Jiang X, Dai J (2017b) Transplantation of hUC-MSCs seeded collagen scaffolds reduces scar formation and promotes functional recovery in canines with chronic spinal cord injury. *Sci Rep* 7:43559. <https://doi.org/10.1038/srep43559>
176. Yang H, Shu Z (2014) The extraction of collagen protein from pigskin. *J Chem Pharm Res* 6(2):683–687
177. Younesi M, Donmez BO, Islam A, Akkus O (2016) Heparinized collagen sutures for sustained delivery of PDGF-BB: delivery profile and effects on tendon-derived cells In-Vitro. *Acta Biomater* 41:100–109. <https://doi.org/10.1016/j.actbio.2016.05.036>
178. Zahari NK, Idrus RBH, Chowdhury SR (2017) Laminin-Coated Poly(Methyl Methacrylate) (PMMA) nanofiber scaffold facilitates the enrichment of skeletal muscle myoblast population. *Int J Mol Sci* 18(11):E2242. <https://doi.org/10.3390/ijms18112242>
179. Zaulyanov L1, Kirsner RS (2007) A review of a bi-layered living cell treatment (Apligraf®) in the treatment of venous leg ulcers and diabetic foot ulcers. *Clin Interv Aging* 2(1):93–98
180. Zhang F, Wang A, Li Z, He S, Shao L (2011) Preparation and characterisation of collagen from freshwater fish scales. *Food Nutr Sci* 2(8):818–823. <https://doi.org/10.4236/fns.2011.28112>
181. Zhang J, Duan R (2017) Characterisation of acid-soluble and pepsin-solubilised collagen from frog (*Rana nigromaculata*) skin. *Int J Biol Macromol* 101:638–642. <https://doi.org/10.1016/j.ijbiomac.2017.03.143>
182. Zhang Z, Zhong X, Ji H, Tang Z, Bai J, Yao M, Hou J, Zheng M, Wood DJ, Sun J, Zhou SF, Liu A (2014) Matrix-induced autologous chondrocyte implantation for the treatment of chondral defects of the knees in Chinese patients. *Drug Des Devel Ther* 5(8):2439–2448. <https://doi.org/10.2147/DDDT.S71356>
183. Zhou J, Cao C, Ma X, Lin J (2010) Electrospinning of silk fibroin and collagen for vascular tissue engineering. *Int J Biol Macromol* 47(4):514–519. <https://doi.org/10.1016/j.ijbiomac.2010.07.010>
184. Zhu J, Marchant RE (2011) Design properties of hydrogel tissue-engineering scaffolds. *Expert Rev Med Devices* 8(5):607–626. <https://doi.org/10.1586/erd.11.27>
185. Zuyderhoff EM, Dupont-Gillain CC (2011) Nano-organized collagen layers obtained by adsorption on phase-separated polymer thin films. *Langmuir* 28(4):2007–2014. <https://doi.org/10.1021/la203842q>
186. Zwingenberger S, Langanke R, Vater C, Lee G, Niederlohm E, Sensenschmidt M, Jacobi A, Bernhardt R, Muders M, Rammelt S, Knaack S, Gelinsky M, Günther KP, Goodman SB, Stiehler M (2016) The effect of SDF-1 $\alpha$  on low dose BMP-2 mediated bone regeneration by release from heparinized mineralized collagen type I matrix scaffolds in a murine critical size bone defect model. *J Biomed Mater Res A* 104(9):2126–2134. <https://doi.org/10.1002/jbm.a.35744>



# Tissue-Inspired Interfacial Coatings for Regenerative Medicine

# 22

Mahmoud A. Elnaggar and Yoon Ki Joung

## Abstract

Biomedical devices have come a long way since they were first introduced as a medically interventional methodology in treating various types of diseases. Different techniques were employed to make the devices more biocompatible and promote tissue repair; such as chemical surface modifications, using novel materials as the bulk of a device, physical topological manipulations and so forth. One of the strategies that recently gained a lot of attention is the use of tissue-inspired biomaterials that are coated on the surface of biomedical devices via different coating techniques, such as the use of extracellular matrix (ECM) coatings, extracted cell membrane coatings, and so on. In this chapter, we will give a general overview of the different types of tissue-inspired coatings along with a summary of recent studies reported in this scientific arena.

M. A. Elnaggar  
Center for Biomaterials, Biomedical Research  
Institute, Korea Institute of Science and Technology,  
Seoul, South Korea

Y. K. Joung (✉)  
Center for Biomaterials, Biomedical Research  
Institute, Korea Institute of Science and Technology,  
Seoul, South Korea

Division of Bio-Medical Science and Technology,  
University of Science and Technology,  
Daejeon, South Korea  
e-mail: [ykjoung@kist.re.kr](mailto:ykjoung@kist.re.kr)

## Keywords

Interfacial coating · Supported lipid bilayer ·  
Extracellular matrix · Cellular membrane ·  
Tissue-mimetics

## 22.1 Extracellular Matrix (ECM) Coatings

### 22.1.1 Brief Introduction of ECM

ECM is a diverse and complex network of glycoproteins, proteoglycans and glycosaminoglycans that are secreted and assembled locally to form an adhering platform for cells [1]. Although the composition of the matrix and the spatial correlation between cells and the matrix differ between tissues, it is a component of the environment of all cell types [2]. Each component of the matrix has unique functions that cumulatively leads to ECM's ability to modulate cellular behaviors [3] cell signaling [4] and to provide structural support for a tissue.

It would be wrong to assume that compositions of the ECM of different tissues are in any way identical. On the contrary, the components are different and tissue-specific. In bones, the ECM is composed of 90% collagen type I with minor amounts of collagen III and V and 5% of other non-collagen based proteins such as osteo-

calcin, osteonectin, fibronectin, hyaluronan and others, [5–6] while cartilage ECM mainly consists of collagen and fibronectin [7]. Vascular cells in a formed vascular tissue are embraced by type I, III, IV, XV and XVII collagen, elastin and laminin, fibronectin and other macromolecules [8–10].

### 22.1.2 Quick Overview of ECM Components' Functions

Copious studies have been done to investigate roles of each component of ECMs *in vivo*. These studies have unveiled that each component of an ECM have tissue-dependent roles because cells in a tissue are different. Elastin in a vascular wall regulates the phenotypic switch and inhibits the proliferation and migration of vascular smooth muscle cells (VSMCs) in the cellular level, [11] whereas, in the tissue level, elastin provides elasticity for a vascular wall to recoil, thus withstanding the high pressure of blood. The ability to recoil is an integral part of the process of blood flow, [10] That is the reason why elastin comprises 50% of the vessel's dry weight [12]. On the other hand, fibrinogen and fibronectin were shown to facilitate the adhesion of endothelial cells (ECs) and the proliferation of both ECs and VSMCs [13–15]. Collagen is very stiff protein that limits the decrease in blood vessel tension. Collagen has 24 subtypes that are expressed by different cell types in different tissues. Thus, the interaction of different cell types is different to each and every subtype of collagen [16]. Interaction of ECs with type I collagen, for example, leads to the higher decrease of nitrite synthesis and endothelial nitric oxide synthase (e-NOS) than the interaction of those with type IV collagen [17]. Fibulin, most notably, exhibits its functions by interacting with other ECM proteins, such as assisting elastin assembly, participating in blood clotting along with fibronectin and so on and so forth [10]. We cannot end this section without mentioning that there are other but less studied, yet equally important ECM components, such as laminin, fibrillin, vitronectin and fibrino-

gen. The role of these components could be found summarized elsewhere [10].

### 22.1.3 Recent Studies Utilizing ECM Inspired Biomaterials on Surfaces

As previously mentioned, numerous studies showed the effectiveness of using ECM coatings for regenerative medicine. Despite their success, however, one of the drawbacks of using collagen coatings, for example, is the difficulty in controlling thickness of the layer, thus affecting surface structure [18]. This led Uchida et al. to pursue a novel scaffold using layer-by-layer (LBL) deposition of fibronectin and gelatin on electrospun fibrous poly(carbonate urethane)urea (PCUU) scaffolds, with the long-term goal of fabricating a urinary bladder tissue consisting of smooth muscle and urothelial cells using their scaffolds [19]. The authors reported enhanced adhesion and proliferation of bladder smooth muscle cells (BSMCs), they also observed the migration and attachment of BSMCs on a culture plate toward the PCUU fibers coated with fibronectin and gelatin, suggesting the high potential of this system in future applications.

On the other hand, Huang et al. also utilized the LBL technique, but they used type 1 collagen and RGD peptide functionalized hyaluronic acid with embedded recombinant human bone morphogenic protein-2 (rhBMP-2) with the substrate, being titanium in this case [20]. They were inspired by certain functional properties of ECM components. Primarily ECM components, such as fibronectin and vitronectin, present RGD motif that mainly mediates initial cell recognition and influences cell adhesion [21]. While growth factors such as BMPs stimulate proliferation and differentiation of osteogenic cells, thus accelerating bone formation [22]. With all that is mentioned, authors prepared a polyelectrolyte membrane (PEM) using collagen as a base layer, then the functionalized hyaluronic acid that contains thiol cross-linkers, and the process was repeated to form several consecutive layers with



the rhBMP-2 embedded between the layers. The system showed sustained release of rhBMP-2 for the prolonged period of 2 weeks through glutathione (GSH) responsive degradation, and *in vitro* and *in vivo* results showed the promotion of pre-osteoblast cell response and increased bone-to-implant binding strength.

In another attempt to optimize ECM coating technologies, a research group studied the effects of ECM components on hepatic differentiation from adipose-derived stem cells (ADSCs) [23]. The main driving force behind this study was to produce hydrogel scaffolds from decellularized liver ECM for treatment of liver diseases. They compared the decellularized ECM with type I collagen, fibronectin and Matrigel in the presence and absence of growth factors. Firstly, their results clearly showed that it is possible to produce a 3D gelling scaffold from a decellularized whole-liver matrix. Secondly, the matrix proved to be a superior bio-mimetic environment for enhanced ADSC differentiation when compared to collagen, fibronectin and Matrigel in the presence and absence of growth factors. But it is worth mentioning that the result on differentiation in the presence of growth factors were better than the result in the absence of those.

Human corneal ECs are a cell type with high metabolic rate as evidenced by the fluent cytoplasmic organelles such as mitochondria, Golgi-apparatus, endoplasmic reticulum (ER) and ribosomes [24]. Despite their high metabolic rate, however, those cells do not proliferate *in vivo*, thus severe damage to them due to ocular surgery [25–27] and inflammatory diseases [28] cause stromal and epithelial edema, leading to loss of corneal clarity and visual acuity. This led Koo et al. to design a system made up of ECM coated polydimethylsiloxane (PDMS) [29]. The authors prepared three different types of ECM coated PDMS, fibronectin-collagen I coated PDMS (FC), FNC coating mix® coated PDMS and laminin-chondroitin sulfate coated PDMS (LC) with each sample having 2 subtypes, patterned and un-patterned. They found out that behavior and appearance of human corneal ECs-B4G12 on patterned FC and LC samples were

superior to cells cultured on FNC, which is due to the cells inability to form a confluent monolayer on FNC samples.

---

## 22.2 Natural Cell Membrane Coatings

### 22.2.1 Brief Introduction of the Cell Membrane

In nature, virtually all cells make use of a membrane to separate and shield its components from the outside environment. The cellular membrane structure is based on a two-ply sheet of lipid molecules that are highly dynamic, ordered and decorated with a wide range of biomolecules in a spatiotemporal controlled fashion. This complex interface is crucial for cell function such as in molecular transport and complex intracellular signaling processes [30–32]. The system was described by Singer and Nicholson in 1972 using the ‘fluid mosaic model’. In the model, the lipid bilayer is considered as a two-dimensional liquid phase in which proteins and lipids can move freely [33]. Currently due to newer analytical technologies available, the model has been updated to include variable patchiness, variable thickness and higher protein occupancy than what was previously considered [34].

The analytical studies also suggest that over 1000 different lipids are present in any eukaryotic cell [35]. Based on their chemical structures, three main categories can be defined, glycerophospholipids, sphingolipids and sterols. Not mentioning the huge array of proteins that are either embedded or anchored to the membrane, with each protein providing a distinct job, such transmembrane transport proteins acting as a controlled gate for various species.

### 22.2.2 Quick Overview of Cell Membrane Functions

To give a detailed account of all components of a cellular membrane, we would need a huge num-

ber of books to be able to describe each component. So, in this section, we will give a quick overview of cellular membrane components that are of interest with regenerative medicine. Regarding with membrane lipid components, it is important to know that the major type of phospholipid head group available on the membrane's outer leaflet of mammalian cells are of the phosphatidylcholine family that is zwitterionic [36]. On the other hand, phospholipids with serine head group (negatively charged), are predominantly on the inner leaflet of the membrane, but its importance is related to apoptosis, as when cells die, the serine based phospholipids flip and become available on the outer leaflet, thus signaling macrophages to seek these cells out and engulf them [37]. Other phospholipids that are also available in the membrane of mammalian cells include phosphatidylglycerol, phosphatidylinositol and phosphatidic acid [36].

On a different note, as mentioned previously, cell membranes have a vast number and types of proteins that are either embedded or anchored to it. These are cell adhesion proteins, protein receptors activating intracellular pathways, transport proteins, and so on. One type of these interesting proteins is adhesion molecules such as intercellular adhesion molecule 1 (ICAM-1), a glycoprotein ligand for integrin found on leukocytes, [38] in which leukocytes bind to ECs and transmigrate into tissues when they are activated [39]. Another important super family of proteins on a cellular membrane are cadherin, which is a type of cell adhesion molecules that are important for cell to cell interaction [40]. An example of such proteins is endothelial cadherin (E-cadherin).

Based on this quick overview, it should be understood by readers that cellular bilayer components are very important to be considered when designing a natural cell (or tissue)-mimetic coating, as each component will add a new property to the coating to improve possibility of success of tissue regeneration.

### 22.2.3 Recent Studies Utilizing Cell Membrane Based Biomaterials on Surfaces

One of approaches to increase the biocompatibility and bio-functionality of biomedical surfaces can be use of a continuous two-dimensional phospholipid bilayer assembled on a solid substrate, which is widely known as 'supported lipid bilayer (SLB)'. SLB membranes have proven useful in a wide variety of applications such as antifouling coatings, biosensors, drug delivery and cell culture-based biomolecular studies [41–43] due to SLB's innate biomimicry, bilayer thickness and 2-D fluidic nature, which resembles mechanical and biological properties of natural cell membranes [44]. Generally, the bilayer is formed spontaneously on substrates such as glass, mica and silicon dioxide [45]. While other surfaces encourage saturated vesicle adsorption instead of bilayer formation, such as titanium oxide [46] and gold [47]. Despite that, currently through various methodologies and conditions, the formation of SLBs became possible on a variety of substrates such as aluminum oxide due to its oxide layer on which it is used to prevent the initial adsorption of lipid vesicles [41]. Most widely used and the simplest methodology is the vesicle adsorption-rupture method, which is controlled by various parameters including lipid composition, vesicle concentration, temperature, osmotic pressure, vesicle size, surface chemistry, buffer composition and pH [48].

With growing potential use of artificial SLB in a wide variety of applications, mimicking the extreme complexity of natural cell membranes is not a simple task to achieve because natural cell membranes are decorated with a large amount of proteins that regulate and mediate various cellular functions, locomotion and many more [49]. This led to a recent study in which extracted natural cell membranes are utilized for the formation of SLB covered nanoparticles to be able to fully mimic cells and be *incognito* while circulating in

*vivo* [50–52]. The basic concept is that covering nanoparticles with natural cell membrane based SLB will provide the nanoparticles with an exterior shell that is almost similar to naturally circulating cells, thus the immune system would not consider them as a foreign body.

Another concept was tested by Chen et al., which the group studied the cell proliferation promoting ability of a polycaprolactone (PCL) based nanofiber material that is covered with extracted cell membrane from pancreatic  $\beta$  cells [53]. After fabricating nanofibers via electrospinning, they incubated the fibers with extracted membrane vesicles, then evaluated their proliferative effect on mouse pancreatic  $\beta$  cell line (MIN6 cells). *In vitro* cell studies revealed that the cell membrane covered fibers promoted proliferation much more than the uncovered fibers due to the presence of adhesion molecules such as E-cadherin on the surface of nanofibers coming from a natural cell membrane. Additionally, insulin release test unveiled that  $\beta$  cells grown on the fibers underwent glucose-dependent insulin release behavior. The use of natural cell membrane coating on a certain surface for regenerative medicine is emerging and promising approach and opens the door to copious studies in the future.

## References

- Hay ED (1981) Extracellular matrix. *J Cell Biol* 91(3 Pt 2):205s–223s
- Adams JC, Watt FM (1993) Regulation of development and differentiation by the extracellular matrix. *Development* (Cambridge, England) 117(4):1183–1198
- Mecham RP (2001) Overview of extracellular matrix. *Curr Protoc Cell Biol* Chapter 10, Unit 10.1
- Juliano RL, Haskill S (1993) Signal transduction from the extracellular matrix. *J Cell Biol* 120(3):577–585
- Anselme K (2000) Osteoblast adhesion on biomaterials. *Biomaterials* 21(7):667–681
- Shekaran A, Garcia AJ (2011) Extracellular matrix-mimetic adhesive biomaterials for bone repair. *J Biomed Mater Res A* 96(1):261–272
- Loeser RF, Sadiev S, Tan L, Goldring MB (2000) Integrin expression by primary and immortalized human chondrocytes: evidence of a differential role for  $\alpha 1\beta 1$  and  $\alpha 2\beta 1$  integrins in mediating chondrocyte adhesion to types II and VI collagen. *Osteoarthr Cartil* 8(2):96–105
- Koyama H, Raines EW, Bornfeldt KE, Roberts JM, Ross R (1996) Fibrillar collagen inhibits arterial smooth muscle proliferation through regulation of Cdk2 inhibitors. *Cell* 87(6):1069–1078
- Stegemann JP, Hong H, Nerem RM (2005) Mechanical, biochemical, and extracellular matrix effects on vascular smooth muscle cell phenotype. *J Appl Physiol* 98(6):2321–2327
- Xu J, Shi GP (2014) Vascular wall extracellular matrix proteins and vascular diseases. *Biochim Biophys Acta* 1842(11):2106–2119
- Tersteeg C, Roest M, Mak-Nienhuis EM, Ligtenberg E, Hoefer IE, de Groot PG, Pasterkamp G (2012) A fibronectin-fibrinogen-tropoelastin coating reduces smooth muscle cell growth but improves endothelial cell function. *J Cell Mol Med* 16(9):2117–2126
- Rosenbloom J, Abrams WR, Mecham R (1993) Extracellular matrix 4: the elastic fiber. *FASEB J* 7(13):1208–1218
- Dejana E, Lampugnani MG, Giorgi M, Gaboli M, Marchisio PC (1990) Fibrinogen induces endothelial cell adhesion and spreading via the release of endogenous matrix proteins and the recruitment of more than one integrin receptor. *Blood* 75(7):1509–1517
- Bramfeldt H, Vermette P (2009) Enhanced smooth muscle cell adhesion and proliferation on protein-modified polycaprolactone-based copolymers. *J Biomed Mater Res A* 88(2):520–530
- Naito M, Hayashi T, Kuzuya M, Funaki C, Asai K, Kuzuya F (1990) Effects of fibrinogen and fibrin on the migration of vascular smooth muscle cells in vitro. *Atherosclerosis* 83(1):9–14
- Myllyharju J, Kivirikko KI (2001) Collagens and collagen-related diseases. *Ann Med* 33(1):7–21
- González-Santiago L, López-Ongil S, Rodríguez-Puyol M, Rodríguez-Puyol D (2002) Decreased Nitric Oxide Synthesis in Human Endothelial Cells Cultured on Type I Collagen. *Circ Res* 90(5):539–545
- Chen G, Ushida T, Tateishi T (2002) Scaffold design for tissue engineering. *Macromol Biosci* 2(2):67–77
- Uchida N, Sivaraman S, Amoroso NJ, Wagner WR, Nishiguchi A, Matsusaki M, Akashi M, Nagatomi J (2016) Nanometer-sized extracellular matrix coating on polymer-based scaffold for tissue engineering applications. *J Biomed Mater Res A* 104(1):94–103
- Huang Y, Luo Q, Zha G, Zhang J, Li X, Zhao S, Li X (2014) Biomimetic ECM coatings for controlled release of rhBMP-2: construction and biological evaluation. *Biomater Sci* 2(7):980–989
- Grzesik WJ, Robey PG (1994) Bone matrix RGD glycoproteins: immunolocalization and interaction with human primary osteoblastic bone cells in vitro. *J Bone Miner Res* 9(4):487–496

22. Liu Y, Huse RO, Groot KD, Buser D, Hunziker EB (2007) Delivery mode and efficacy of BMP-2 in association with implants. *J Dent Res* 86(1):84–89
23. Zhang X, Dong J (2015) Direct comparison of different coating matrix on the hepatic differentiation from adipose-derived stem cells. *Biochem Biophys Res Commun* 456(4):938–944
24. Joyce NC (2003) Proliferative capacity of the corneal endothelium. *Prog Retin Eye Res* 22(3):359–389
25. Bourne WM, Nelson LR, Hodge DO (1994) Continued endothelial cell loss ten years after lens implantation. *Ophthalmology* 101(6):1014–1022 discussion 1022–3
26. Friberg TR, Guibord NM (1999) Corneal endothelial cell loss after multiple vitreoretinal procedures and the use of silicone oil. *Ophthalmic Surg Lasers* 30(7):528–534
27. Yachimori R, Matsuura T, Hayashi K, Hayashi H (2004) Increased intraocular pressure and corneal endothelial cell loss following phacoemulsification surgery. *Ophthalmic Surg Lasers Imaging* 35(6):453–459
28. Sengler U, Spelsberg H, Reinhard T, Sundmacher R, Adams O, Auw-Haedrich C, Witschel H (1999) Herpes simplex virus (HSV-1) infection in a donor cornea. *Br J Ophthalmol* 83(12):1405
29. Koo S, Muhammad R, Peh GSL, Mehta JS, Yim EKF (2014) Micro- and nanotopography with extracellular matrix coating modulate human corneal endothelial cell behavior. *Acta Biomater* 10(5):1975–1984
30. Jacobson K, Sheets ED, Simson R (1995) Revisiting the fluid mosaic model of membranes. *Science (New York, NY)* 268(5216):1441–1442
31. Monks CR, Freiberg BA, Kupfer H, Sciaky N, Kupfer A (1998) Three-dimensional segregation of supramolecular activation clusters in T cells. *Nature* 395(6697):82–86
32. Maxfield FR (2002) Plasma membrane microdomains. *Curr Opin Cell Biol* 14(4):483–487
33. Singer SJ, Nicolson GL (1972) The fluid mosaic model of the structure of cell membranes. *Science (New York, NY)* 175(4023):720–731
34. Engelman DM (2005) Membranes are more mosaic than fluid. *Nature* 438(7068):578–580
35. van Meer G (2005) Cellular lipidomics. *EMBO J* 24(18):3159–3165
36. Coskun U, Simons K (2011) Cell membranes: the lipid perspective. *Structure (London, England: 1993)* 19(11):1543–1548
37. Verhoven B, Schlegel RA, Williamson P (1995) Mechanisms of phosphatidylserine exposure, a phagocyte recognition signal, on apoptotic T lymphocytes. *J Exp Med* 182(5):1597–1601
38. Rothlein R, Dustin ML, Marlin SD, Springer TA (1986) A human intercellular adhesion molecule (ICAM-1) distinct from LFA-1. *J Immunol (Baltimore, MD: 1950)* 137(4):1270–1274
39. Yang L, Froio RM, Sciuto TE, Dvorak AM, Alon R, Lusinskas FW (2005) ICAM-1 regulates neutrophil adhesion and transcellular migration of TNF- $\alpha$ -activated vascular endothelium under flow. *Blood* 106(2):584–592
40. Alimperti S, Andreadis ST (2015) CDH2 and CDH11 act as regulators of stem cell fate decisions. *Stem Cell Res* 14(3):270–282
41. Jackman JA, Tabaei SR, Zhao Z, Yorulmaz S, Cho N-J (2015) Self-assembly formation of lipid bilayer coatings on bare aluminum oxide: overcoming the force of interfacial water. *ACS Appl Mater Interfaces* 7(1):959–968
42. Elnaggar MA, Subbiah R, Han DK, Joung YK (2017) Lipid-based carriers for controlled delivery of nitric oxide. *Expert Opin Drug Deliv*:1–13
43. Elnaggar MA, Seo SH, Gobaa S, Lim KS, Bae I-H, Jeong MH, Han DK, Joung YK (2016) Nitric oxide releasing coronary stent: a new approach using layer-by-layer coating and liposomal encapsulation. *Small* 12(43):6012–6023
44. Vafaei S, Tabaei SR, Biswas KH, Groves JT, Cho NJ (2017) Dynamic Cellular Interactions with Extracellular Matrix Triggered by Biomechanical Tuning of Low-Rigidity, Supported Lipid Membranes. *Adv Healthcare Mater* 6(10)
45. Weng KC, Stålgren JJR, Duval DJ, Risbud SH, Frank CW (2004) Fluid biomembranes supported on nanoporous aerogel/xerogel substrates. *Langmuir ACS J Surf Colloids* 20(17):7232–7239
46. Reviakine I, Rossetti FF, Morozov AN, Textor M (2005) Investigating the properties of supported vesicular layers on titanium dioxide by quartz crystal microbalance with dissipation measurements. *J Chem Phys* 122(20):204711
47. Keller CA, Kasemo B (1998) Surface specific kinetics of lipid vesicle adsorption measured with a quartz crystal microbalance. *Biophys J* 75(3):1397–1402
48. Cho N-J, Jackman JA, Liu M, Frank CW (2011) pH-driven assembly of various supported lipid platforms: a comparative study on silicon oxide and titanium oxide. *Langmuir ACS J Surf Colloids* 27(7):3739–3748
49. van Weerd J, Karperien M, Jonkheijm P (2015) Supported Lipid Bilayers for the Generation of Dynamic Cell–Material Interfaces. *Adv Healthc Mater* 4(18):2743–2779
50. Fang RH, Hu CM, Luk BT, Gao W, Copp JA, Tai Y, O'Connor DE, Zhang L (2014) Cancer cell membrane-coated nanoparticles for anticancer vaccination and drug delivery. *Nano Lett* 14(4):2181–2188
51. Dehaini D, Wei X, Fang RH, Masson S, Angsantikul P, Luk BT, Zhang Y, Ying M, Jiang Y, Kroll AV, Gao W, Zhang L (2017) Erythrocyte–platelet hybrid membrane coating for enhanced nanoparticle functionalization. *Adv Mater* 29(16):1606209–n/a
52. Rao L, Bu L-L, Cai B, Xu J-H, Li A, Zhang W-F, Sun Z-J, Guo S-S, Liu W, Wang T-H, Zhao X-Z (2016) Cancer cell membrane-coated upconversion nanoprobes for highly specific tumor imaging. *Adv Mater* 28(18):3460–3466
53. Chen W, Zhang Q, Luk BT, Fang RH, Liu Y, Gao W, Zhang L (2016) Coating nanofiber scaffolds with beta cell membrane to promote cell proliferation and function. *Nanoscale* 8(19):10364–10370



# Naturally-Derived Biomaterials for Tissue Engineering Applications

# 23

Matthew Brovold, Joana I. Almeida,  
Iris Pla-Palacín, Pilar Sainz-Arnal,  
Natalia Sánchez-Romero, Jesus J. Rivas,  
Helen Almeida, Pablo Royo Dachary,  
Trinidad Serrano-Aulló, Shay Soker,  
and Pedro M. Baptista

## Abstract

Naturally-derived biomaterials have been used for decades in multiple regenerative medicine applications. From the simplest cell microcarriers made of collagen or alginate, to highly complex decellularized whole-organ scaffolds, these biomaterials represent a class of substances that is usually first in choice at the time of electing a functional and useful

biomaterial. Hence, in this chapter we describe the several naturally-derived biomaterials used in tissue engineering applications and their classification, based on composition. We will also describe some of the present uses of the generated tissues like drug discovery, developmental biology, bioprinting and transplantation.

Authors Matthew Brovold, Joana I. Almeida, Iris Pla-Palacín, Pilar Sainz-Arnal and Natalia Sánchez-Romero have been equally contributed to this chapter.

M. Brovold · S. Soker (✉)  
Wake Forest Institute for Regenerative Medicine,  
Winston-Salem, NC, USA  
e-mail: [ssoker@wakehealth.edu](mailto:ssoker@wakehealth.edu)

J. I. Almeida · I. Pla-Palacín · N. Sánchez-Romero ·  
J. J. Rivas · H. Almeida  
Health Research Institute of Aragón (IIS Aragón),  
Zaragoza, Spain

P. Sainz-Arnal  
Health Research Institute of Aragón (IIS Aragón),  
Zaragoza, Spain

Aragon Health Sciences Institute (IACS),  
Zaragoza, Spain

P. R. Dachary · T. Serrano-Aulló  
Instituto de Investigación Sanitaria de Aragón  
(IIS Aragón), Zaragoza, Spain

Liver Transplant Unit, Gastroenterology Department,  
Lozano Blesa University Hospital, Zaragoza, Spain

## Keywords

Naturally-derived materials · Tissue decellularization · Tissue engineering · Protein-based biomaterials · Polysaccharide-based biomaterials · Glycosaminoglycans · Extracellular matrix-derived biomaterials · Solid organ bioengineering · Regulatory landscape for naturally-derived biomaterials

P. M. Baptista (✉)  
Instituto de Investigación Sanitaria de Aragón  
(IIS Aragón), Zaragoza, Spain

Center for Biomedical Research Network Liver and  
Digestive Diseases (CIBERehd), Zaragoza, Spain

Instituto de Investigación Sanitaria de la Fundación  
Jiménez Díaz, Madrid, Spain

Biomedical and Aerospace Engineering Department,  
Universidad Carlos III de Madrid, Madrid, Spain

Fundación ARAID, Zaragoza, Spain  
e-mail: [pmbaptista@iisaragon.es](mailto:pmbaptista@iisaragon.es)

## 23.1 Introduction

The use of new advanced experimental strategies, such as bioengineering techniques, will transform the practice of medicine in the coming years. A clear example of this is the quick advancement in the field of tissue engineering, an interdisciplinary field of research that involves the principles of materials science, engineering, life sciences, and medical research. Tissue engineering aims to replace an entire organ or provide restoration of the specific cellular functions [1, 2]. For this purpose, tissue engineering usually works with three essential tools: scaffolds, cells, and growth factors [3].

In recent years, the search and generation of new and suitable scaffolds for tissue engineering has been greatly accelerated. This is especially true in the study of natural biomaterials as they have been found to mimic the biological and mechanical function of the native ECM found *in vivo* in any tissue of the body. Natural biomaterials can be categorized into the following subtypes: protein-based biomaterials (collagen, gelatin, silk) [4], polysaccharide-based biomaterial (cellulose, chitin/chitosan, glucose) [5], glycosaminoglycan-derived biomaterials and tissue/organ-derived biomaterials (decellularized heart valves, blood vessels, livers) [6]. Depending on the final use, they usually share several prominent features: biocompatibility, biodegradability, and non-toxicity, amongst others [7]. However, when the final goal of tissue engineering is the generation of solid organs with bioengineering techniques, the use of protein-based and polysaccharide-based biomaterials presents some disadvantages: a) Mechanical strength is limited, avoiding the generation of larger constructs and restricting their applications at load bearing regions; b) manufacturing variability; c) Potential impurities from the proteins or polysaccharides before implantation, which can be a source of immunogenicity [8, 9]. Despite these disadvantages, almost every tissue and organ in the body has been bioengineered *in vitro* with success. Within the past 20 years, most of the major achievements in tissue engineering were focused on tissues constructed using thin sheets of cells

for tissue replacement, such as skin, small intestine, esophagus, bladder, bone, carotid arteries, amongst others [10–14].

Construction of thicker tissues has been slow due to the limited diffusion of nutrients and oxygen within the engineered tissue mass [15]. Nonetheless, the tissue engineering sector has grown exponentially with breakthroughs reached in this area in the last years, and right now the ultimate goal of the field is the creation of whole-organs using bioengineering techniques for human transplantation. End-stage organ diseases affect millions of people around the world, and for these patients, organ transplantation is the only definitive cure available. However, every year there is a significant gap between the number of patients on the organ waiting list, the number of donors, and the number of patients died waiting for a transplant due to the persistent organ shortage. In 2016, Europe registered 10,893 organ donors, with 59,168 patients in the waiting list for transplantation, and 3795 deceased people waiting for an organ transplant [16]. Multiple alternatives and solutions have been sought in past decades to solve this problem, and at the moment, whole-organ bioengineering seems promising [17] and it could change the actual paradigm of organ shortage in the near future.

The development of decellularization methods for the generation of whole-organ engineering provides the ideal transplantable natural bioscaffold with all the necessary microarchitecture and extracellular cues for cell attachment, differentiation, vascularization, and function [18]. Numerous attempts to generate whole-organs have been made. The most extensively, are some of the major organs: liver, heart, kidney, and lung [4, 19–22]. Although, progress so far has been quite remarkable, significant challenges still need to be overcome in whole-organ bioengineering to transfer this new technology into the clinic. These include identifying appropriate species to provide decellularized tissues, selecting ideal cell sources, localizing signals for differentiation, achieving robust vascularization, optimizing bioreactor perfusion technology along with scalability, and preventing graft immunological rejection [23–25].

## 23.2 Naturally-Derived Biomaterials

The current research into naturally-derived biomaterials should be considered a renaissance as its original interest started with the beginning of recorded human history.

Some of the earliest biomaterial applications have been dated as far back as 3000 BC to the ancient Egyptians who employed coconut shells to repair injured skulls, or wood and ivory as false teeth. In modern times, more sophisticated applications of natural biomaterials emerged with the first replacement surgery using ivory being reported in Germany, 1891 [26].

By the 1950s and 60s, there were records of clinical trials with blood vessel replacement and the first mechanical human cardiac valve implantation [27].

In the biomedical field, natural biomaterials can be classified into several categories according to their origin. These groups can be distinguished as those derived from proteins (for example, collagen, gelatin, silk, and fibrin); polysaccharides (cellulose, chitin/chitosan, alginate and agarose), or glycosaminoglycans (hyaluronic acid, chondroitin sulfate, dermatan sulfate, heparan sulfate and keratan sulfate). In recent years, more complex biomaterials have emerged as in the case of cell/organs-derived matrices.

Despite their nature, they all shared some unique features (such as biocompatibility, biodegradability and remodeling) which have increased the scientific interest in the development of medical/tissue engineering technologies around these biomaterials. Hence, in this section, we provide a brief summary and applications of the most important naturally-derived biomaterials.

---

## 23.3 Protein-Based Biomaterials

### 23.3.1 Collagen

Collagen is the main structural protein of most tissues in the animal kingdom and plays an important role in maintaining the biological and structural integrity of the extracellular matrix (ECM) while also providing physical support to

cells and tissues. At a cellular level, collagen is secreted mainly by fibroblasts and plays key roles in regulating cellular morphology, adhesion, migration and differentiation.

In the human body, collagen comprises approximately 25–35% of the whole-body protein content where it can be found mostly in **fibrous tissues** (skin, tendons and ligaments) and every other tissue that require strength and flexibility, such as bones, **cartilage**, **blood vessels**, corneas, **gut**, **intervertebral discs** and **dentin** (in teeth) [28].

Currently, there are 29 known isoforms of collagen that have been described. Collagen's important biological role has driven this biomaterial to the center of tissue engineering research. In fact, collagen is easily isolated and can be purified on a large scale. Moreover, it has well-documented structural, physical, chemical and immunological properties. Additionally, collagen is biodegradable, biocompatible and has non-cytotoxic properties.

Collagen can also be processed into a variety of forms including cross-linked films, sheets, beads, meshes, fibers, sponges and others [29] expanding its potential applications. Many researchers have illustrated the use of collagen as scaffolds for cartilage and bone [30–32] as well as in bioprosthetic heart valves, vascular grafts, drug delivery systems, ocular surfaces, and nerve regeneration [33]. Additionally, microcapsules containing collagen matrices have been designed in 3-D scaffolds for soft tissue engineering [34]. Regarding liver tissue bioengineering, collagen-coated silicone scaffolds represent an important tool for the development of viable 3D hepatocyte cultures [35]. More recently, *Wang Y et al.* were able to generate crypt-villus architecture of human small intestinal epithelium using microengineered collagen scaffolds [36]. These are just a few examples of the great potential of using collagen as a biomaterial.

### 23.3.2 Gelatin

Gelatin is a biocompatible, biodegradable and fully absorbable biopolymer derived from the hydrolysis of collagen. Due to its biological

nature, great solubility in aqueous systems and its high commercial availability at low cost, gelatin has been commonly used and showed several advantages compared to its parent protein.

Among its many formulations (mainly derived from porcine, fish, and bovine tissue) the most used ones in biological fields include nanoparticles, microparticles, 3D scaffolds, electrospun nanofibers and *in situ* gels [37].

Another important fact regarding this polymer is that it can be crosslinked and chemically modified which expands even more its applications.

As an example of gelatin versatility, [Tayebi L](#) and co-workers, have recently characterized a biocompatible and bio-resorbable 3D-printed structured gelatin/elastin/sodium hyaluronate membrane with great biostability, mechanical strength and surgical handling characteristics which hold great potential for engineered procedures [38].

Furthermore, several other authors have described other applications of gelatin-derived biomaterials from cardiovascular [39], bone [40], skeletal muscle [41] and hepatic tissue engineering [42] to wound healing and injectable fillers [37].

Another very interesting finding was attributed to [Kilic Bektas C.](#), and [Hasirci V.](#), who recently developed a “corneal stroma system” using keratocyte-loaded photopolymerizable methacrylated gelatin hydrogels which could serve as an important alternative to the current products used to treat corneal blindness [43].

Gelatin as a biomaterial shows a wide range of applications. In stem cell research, modifications in gelatin formulations have been shown to influence stem cell fate in injectable cell-based therapies [44].

Gelatin-based delivery systems have also found to be successful in gene and siRNA delivery, by inducing the expression of therapeutic proteins or trigger gene silencing, respectively.

Overall, with the significant progress that has already been made, along with others that will be achieved in a near future, the safe and effective clinical implementation of gelatin-based products is expected to accelerate and expand shortly.

### 23.3.3 Silk

Silks are biopolymers formed by different fibrous proteins (fibroin and sericin) that are segregated by the glandular epithelium of many insects including silkworms, scorpions, spiders, mites and flies.

Silk fibers, in the form of sutures, have been used for centuries, and new research into different formulations (gels, sponges and films) have been encouraging [45].

In the orthopedics medical field and cartilage tissue engineering, many studies have been pointed out the enormous potential of this biomaterial.

Thus, [Sawatjui N et al.](#)..., found very recently that the microenvironment provided by the porous scaffolds based on silk fibroin (SF) and SF with gelatin/chondroitin sulfate/hyaluronate scaffolds enhanced chondrocyte biosynthesis and matrix accumulation [46].

In this line, another silk derived scaffold (curcumin/silk scaffold) was also described as a good candidate for cartilage repair [47] and for meniscal replacement [48].

Another recent investigation conducted by [Hu Y et al.](#), lead to a silk scaffold with increased stiffness and SDF-1 controlled release capacity for ligament repair [49].

On the other hand, [Bryan S. Sack et al.](#), described that silk fibroin derived scaffolds showed promising repair of urologic defects in pre-clinical trials [50].

Although silk fibers also showed broad applications, the more popular ones seems to be related to cartilage engineering.

### 23.3.4 Fibrin

Fibrin is a non-globular protein, involved in blood coagulation, formed from the thrombin-mediated cleavage of fibrinogen.

Numerous studies have exploited fibrin's function as hemostatic plug and wound healing, which suggests fibrin has potential applications in both the medical field and tissue engineering [6].



Among its applications, three-dimensional fibrin gels have been used as scaffolds for cell proliferation and migration. According to *Ye Q., et al.*, fibrin gels can serve as a useful scaffold for cardiac tissue engineering with controlled degradation, excellent cell seeding effects and good tissue development [51].

More recently, *Seyedi F et al.*, have reported that 3D fibrin scaffolds effectively induced the differentiation of human umbilical cord matrix-derived stem cells into insulin producing cells [52].

Other studies reported that hybrid fibrin/PLGA scaffolds may promote proliferation of chondrocytes as well as cartilaginous tissue restoration and may eventually serve as a potential cell delivery vehicle for articular cartilage tissue-engineering [53].

Additionally, a new biomaterial called fibrin glue or fibrin sealant, has been formulated by combining fibrinogen and thrombin at very high amounts along with calcium and Factor XIII. This material is currently used as an adjunct to hemostasis in patients undergoing different types of surgeries. More specifically, *Azizollah Khodakaram-Tafti, et al.*, suggested that autologous fibrin glue appears to be promising scaffold in regenerative maxillofacial surgery [54], just to name one example.

---

## 23.4 Polysaccharides-Based Biomaterials

### 23.4.1 Cellulose

Cellulose is the most abundant natural polymer on Earth; present in the cell walls of green plants, some forms of algae, and can also be produced by bacteria.

Although cellulose is very abundant and has several readily available renewable natural sources, major difficulties in its refinement make it a poor option for a naturally-derived biomaterial, such is the reason why there are no physiological or pharmaceutical applications [55]. Research is currently focused on the simplifica-

tion of the normally intensive methods for the depolymerization of cellulose and the manufacture of its derivatives so that it may be used as a biomaterial.

Recently, chemists were able to generate useful cellulose derivatives such as carboxymethyl-cellulose, cellulose nitrate, cellulose acetate, and cellulose xanthate which are all gaining some interest in the medical and tissue engineering fields [6]. Cellulose acetate for instance has been used to produce cardiac scaffolds [56], while other forms were used for cartilage tissue engineering [57].

One of the latest and curious application of this biomaterial is to use heparinized bacterial cellulose based scaffold for improving angiogenesis in tissue regeneration [58].

### 23.4.2 Chitin/Chitosan

Chitin is the second most abundant natural polysaccharide next to cellulose. It is mostly found in the exoskeletons of arthropods and many insects. Its derivatives which includes chitosan, carboxymethyl chitin, and glyco-chitin have all generated attractive interests in various fields such as biomedical, pharmaceutical, food and environmental industries [59].

In recent years, considerable attention has been given to chitosan (CS)-based materials and their applications in the field of orthopedic tissue engineering. It has garnered this interest because of its intrinsic anti-bacterial nature, porosity, and the ability to be molded in various geometries which are suitable for cell growth and osteoconduction [60]. Chitosan/alginate hybrid scaffolds have also been developed in this field [61]. Moreover, chitosan was also reported to promote angiogenesis and accelerate wound healing response by promoting migration of inflammatory cells to the wound site and collagen matrix deposition in open skin wounds [62–64]. Thus, chitosan hydrogels have been developed in medical therapeutics for third-degree burns [65].

### 23.4.3 Alginate

Alginate is a naturally occurring anionic polymer typically obtained from brown seaweed. Among its excellent biological properties (biocompatibility, low toxicity, and relative low cost), alginate is a readily processable into three-dimensional scaffolding materials such as microspheres, microcapsules, sponges, foams, fibers and hydrogels.

Alginate hydrogels are one of its most popular formulations. In fact, alginate hydrogels can be prepared by various cross-linking methods and their structural similarities to ECM of living tissues that allows a wide range of applications from wound healing management [66] to more complex drug delivery vehicles [67].

Wang *Y et al.* recently described a three-dimensional (3D) printing technology to fabricate the shape memory hydrogels with internal structure (SMHs) by combining sodium alginate (alginate) and pluronic F127 diacrylate macromer (F127DA), which showed a huge prospect for application in drug carriers and tissue engineering scaffold [68].

Another common application of alginate is for the immobilization of cells [69] allowing for large-scale cellular expansion in different bioreactors. This immobilization application was exhibited by *Anneh Mohammad Gharravi et al.*, which have fabricated a bioreactor system containing alginate scaffolds for cartilage tissue engineering [70]. *Beigi MH et al.* also described very recently that 3D alginate scaffolds with co-administration of PRP and/or chondrogenic supplements had a significant effect on the differentiation of ADSCs into mature cartilage [71].

Besides that, encapsulated cells have been proven useful for cell therapies. According to *Coward SM et al.*, alginate encapsulated HepG2 cells, circulating in the plasma of patients suffering with acute liver disease, maintained their hepatic metabolism, synthetic and detoxification activities, indicating that the system can be scaled-up to form the biological component of a bioartificial liver [72].

In another interesting approach has just been published, *Yajima Y., et al* performed perfusion cultivation of liver cells by assembling cell-laden hydrogel microfibers and packed HepG2 into the core of sandwich-type anisotropic microfibers, which were produced using microfluidic devices to structurally mimic the hepatic lobule *in vivo* [73].

*Pipeleers D., et al.*, also reported that human embryonic stem cell (hESC)-derived beta cells encapsulated in alginate microcapsules were protected from the immune system and corrected insulin deficiencies of type-1 diabetic mice for at least 6 months [74]. These are just few examples of the potential of polysaccharides-based biomaterials.

### 23.4.4 Agarose

Agarose, the main constituent of agar, is another polysaccharide naturally found in red algae and seaweed.

Most of the beneficial features shown by alginate are shared by agarose. In fact, agarose and alginate were two of the first materials used as hydrogels for cartilage tissue, showing natural pro-chondrogenic properties and are easy to prepare [75].

On the other hand, recent findings pointed agarose as an excellent candidate for applications involving neural tissue engineering [76–78].

In this line, *Han S et al.*, reported that an agarose scaffold loaded with matrigel could promote the regeneration of axons and guide the reconnection of functional axons after spinal cord injury in rats [79].

In cardiac bioengineering and stem cell biology, agarose was shown to promote cardiac differentiation of human and murine pluripotent stem cells [80].

In other study, high quality valvular interstitial cell aggregates were generated, in agarose micro-wells, which were able to produce their own ECM, resembling the native valve composition [81].

## 23.5 Glycosaminoglycans

Glycosaminoglycans (GAGs) represent a group of long unbranched **polysaccharides** consisting of repeating **disaccharide** units. There are several types of GAGs components including hyaluronic acid (HA), chondroitin sulfate (CS), dermatan sulfate, heparan sulfate, and keratan sulfate.

Among these GAGs, HA and CS are the two most studied in regenerative medicine and tissue engineering field. Some of its applications are described briefly.

### 23.5.1 Hyaluronic Acid

Hyaluronic acid (HA) is a **molecule** comprised of repeating **disaccharide** units of N-acetyl-d-glucosamine and d-glucuronic acid being widely distributed in the most connectives tissues and some body fluids (such as synovial fluid and the vitreous humor of the eye). Its chemical properties (solubility and the availability of its reactive functional groups) make this molecule an excellent candidate for chemical modifications and a very biocompatible material for use in medicine and tissue regeneration.

Research has found that intra-articular injections of MSCs and HA in rabbits showed statistically significant improvements in osteochondral defect healing [82].

In current orthopedics medical practice, HA has a prominent place. In fact, HA injections have been shown to ameliorate osteoarthritis symptoms and shown the ability to delay prosthetic surgeries [83]. Moreover, HA has also become popular as dermatological fillers for treatment of face aging [84].

In tissue engineering, cartilage biodegradable scaffolds made of HA were engineered [85] and HA-collagen hybrid scaffolds were proven robust and offered freely permeable 3-D matrices that enhance mammary stromal tissue development *in vitro* [86]. In other research field, *Kushchayev SV et al*, described that hydrogel had a neuroprotective effect on the spinal cord of rats by decreasing the magnitude of secondary injury after a lacerating spinal cord injury [87].

To conclude, one of the most attractive advantages of HA is that it can be easily and controllably produced in large scale through microbial fermentation avoiding the potential risks of animal-derived biomaterials [88].

### 23.5.2 Chondroitin Sulfate

Chondroitin sulfate (CS) consists of repeating disaccharide units of d-glucuronic acid and N-acetyl galatosamine, sulfated at either 4- or 6-positions [89] and represents the second most used GAG as biomaterial. CS could be obtained from bovine, porcine, chicken, shark and skate cartilage after various extraction and purification processes.

In biomedical applications, CS has been associated with bone and cartilage metabolism and regulation, presenting both anti-inflammatory effects and accelerated bone mineralization capabilities [90].

In animal studies, CS combined with HA and other GAGs administered after arthroscopy were described as beneficial to equine cartilage health by increasing the number of repair cells and decreasing the number of apoptotic cells [91].

In this line research, other biomaterials combinations have been hypothesized. According to *Liang WH, et al.*, CS-Collagen scaffolds could be used to cartilage and skin applications [92].

Recently, *Zhou F et al.*, designed a silk-CS scaffold and proved that this scaffold exhibited good anti-inflammatory effects both *in vitro* and *in vivo*, promoted the repair of articular cartilage defect in animal model [93]. Thus, CS also constitutes one of the FDA approved skin substitute component [94].

---

## 23.6 Extracellular Matrix-Derived Biomaterials

### 23.6.1 Cell-Derived Matrices

In recent years, the development of decellularized ECM has made the fields of cell biology, regenerative medicine and tissue engineering

advance beyond the use of simple natural derived biomaterials.

Cell-derived matrices (CDMs) consist of an acellular complex of different natural fibrillar proteins, matrix macromolecules and associated growth factors that often recapitulate, at least to some extent, the composition and organization of native ECM microenvironments. As an ECM derived material, CDMs provide mechanical and biological support allowing cellular attachment, migration and proliferation; paracrine factor production and differentiation in a tissue-specific manner [34].

The unique ability to produce CDMs *de novo* based on cell source and culture methods makes them an elegant alternative to conventional allogeneic and xenogeneic tissue-derived matrices that are currently harvested from cadaveric sources, suffer from inherent heterogeneity, and have limited ability for customization [95].

The production of CDMs have undergone several evolutions. There are several ways these matrices can be produced through the use of different decellularization strategies that includes chemical, enzymatic, physical, mechanical, or a combination of methods.

Regarding chemical decellularization protocols, the surfactant sodium dodecyl sulfate (SDS) is the most used reagent, which promotes cellular lysis through phospholipid membrane disruption [56]. However, many authors prefer using acids (peracetic acid) or bases (sodium hydroxide) agents to decellularize the ECMs. To supplement this treatment some enzymes like DNase I can be added to prevent the agglutination of DNA.

Due to the toxicity of this approach, some physical and mechanical methods have therefore been developed. These methodologies include the use of temperature (for example, freeze-thaw cycles) or pressure treatments (such as high hydrostatic pressure or supercritical CO<sub>2</sub> content).

Among all CDMs that have been tested, small intestine submucosa (SIS), bladder submucosa, acellular dermis and engineered heart valves represent the most popular ones and will be described briefly.

### 23.6.2 Small Intestinal Submucosa (SIS) and Bladder Submucosa (BS)

One such CDM being extensively used is the Small Intestinal Submucosa (SIS) or the Bladder Submucosa (BS). These are naturally occurring ECM, derived from the thin and translucent tunica submucosa layer of the porcine small intestine or urinary bladder, which remains intact after removing the mucosal and muscular layers. SIS and BS have been shown to be biologically active and its unique combination of intrinsic growth factors, cytokines, GAGs and structural proteins (mainly collagen fibers, fibronectin, vitronectin, etc) provide strength, structural support, stability and biological signals which allow overall cell ingrowth [96–99].

Once the SIS or BS biomaterial is harvested, it is carefully processed to remove all living cells, disinfected and sterilized, and then able to be used as scaffold or for long-term storage in their lyophilized form [100, 101].

Over the years, many applications have emerged. The first application of SIS was associated to Lantz and colleagues, who first used SIS in animal studies as a vascular patch, reported a great tissue-specific regeneration in both arteries and veins [102, 103].

Within the urology field, SIS and BS are also very popular biomaterials. Thus, Kropp and colleagues subsequently demonstrated that SIS, used as an unseeded graft, could promote bladder regeneration, in both small and large animal models, and it was accompanied by serosal, muscle and mucosal layers regeneration, tissue contractibility and biological functionality [104, 105]. Gabouev *et al.* have used BS to bioengineer porcine urinary bladder tissue that they have seeded with smooth muscle and urothelial cells. The resulting tissue displayed the generation of 2 tissue layers with the putative markers of muscle and urothelial cells [106].

In the management of anterior urethral stricture disease, SIS showed promising results. In one study, more than 50 patients were managed with an SIS graft placed in an inlay fashion and

according to a follow-up of 31 months the success rate was around 80% [107]. A second study reported 85% success when SIS was used as either an inlay or on lay patch graft with a mean follow-up of 21 months. However, when used ventrally, it failed in 6 of 10 adult patients [108].

In different clinical areas, SIS has been described as a functional bioscaffold for the intestinal tract. According to Hoepfner et al., SIS application showed a great potential in colon walls regeneration in domestic pigs [109].

In neurological and orthopedic fields, porcine SIS was used in rat peripheral nerve regeneration [110] and chest reconstruction after tumor removal respectively [111]. Based on scientific findings, many companies have been interested in this CDM with many SIS and BS derivatives being currently commercialized. SIS and BS derived devices are now available for hernia and hiatal hernia grafts; dural graft; ENT repair graft; enter cutaneous Fistula Plug and as nerve connector/protector, etc. [112].

### 23.6.3 Acellular Dermis

The acellular dermis (AD) is another example of a CDM, which consists of a soft tissue substitute derived from donated human skin tissue. As the others CDMs, AD undergoes a multi-step process which includes epidermis removal, disinfection and sterilization minimizing the risk for an antigenic or rejection response.

AD was initially used as a type of graft material for the management of burn wounds [113]. However, in the recent years, AD has been used for various applications in reconstructive surgery including head and neck reconstruction as well as chest and abdominal wall reconstruction [114, 115].

Currently, AD has become an integral part of implant breast reconstruction being one of its most important applications in regenerative medicine field [97].

### 23.6.4 Heart Valves

The origin of decellularized cardiac valves matrices may come from xenotransplants or allotransplants showing different outcomes. Rieder, et, al reported immunological differences depending on whether the valves came from human or porcine, showing that decellularized porcine pulmonary valve does not represent a completely non-immunogenic heart valve scaffold [116].

In other studies, the aim was to develop and optimize decellularization protocols to obtain viable scaffolds for this type of applications. For example, mitral valves can be decellularized to obtain structures that generally preserved their microarchitecture, biochemistry, and biomechanics [117]. These CDMs are currently widely studied and tested being now available many commercial options on the market such as Acellular porcine heart valve leaflets from *Epic*<sup>TM</sup> and *SJM Biocor*<sup>®</sup>; porcine acellular valve from *Prima*<sup>TM</sup> Plus or porcine acellular heart valve tissue from *Hancock*<sup>®</sup> II, *Mosaic*<sup>®</sup>, and *Freestyle*<sup>®</sup> [118].

Another important aspect is to know what type of cells may be a functional option for valve replacement. Fang et, al, reported that human umbilical cord blood-derived endothelial progenitor cells (EPCs) may be a promising option to form a functional endothelial layer on decellularized heart valve scaffolds [119].

---

## 23.7 Bioengineering of Solid Organs

The disciplines of tissue engineering (TE) and regenerative medicine (RM) endeavor to eliminate the need for patient to patient tissue and organ transplantation by constructing analogs *in vitro* that will normalize or improve physiological functions of their respective system. The need for further research is paramount, as currently there are 115,000 patients waiting for organ transplants, however there were only 34,000

transplants performed in 2017 in the USA. Programs to reduce the wait list by increasing donors have been met with limited success. The difference in waitlisted patients and transplant recipients has grown in size over the last 14 years. TE and RM would initially eliminate the gap between the waitlisted and recipients culminating by rendering large donor pools obsolete.

### 23.7.1 Liver

Whole-liver engineering has made incremental advances in the recent past. Researchers have been able to successfully decellularize the liver ECM in a variety of different ways [19, 120–124]. Decellularization is achieved by effectively pumping detergents through the vasculature with the use of peristaltic pumps through the portal vein. There have been several successful attempts at reintroducing cells into the decellularized scaffold, namely Baptista and colleagues [19, 124]. Current roadblocks to generate liver tissue capable of completely assuming the full spectrum of native tissue functions are several-fold: The construction of a fully patent vascular network and generation of required number of cells to acquire a basal level of functionality. Vascular network patency is required for normal blood flow as acellular ECM will induce the formation of blood clots as it is highly thrombogenic. Recent advances in revascularization have greatly improved the efficacy of endothelial cell seeding resulting increased vascular patency. In 2015 Ko et al. were able to greatly improve the reendothelialization of the vasculature by the introduction of anti-CD31 antibodies which were injected into the decellularized arteries and veins of the scaffold after being treated with 1-Ethyl-3-[3-dimethylaminopropyl] carbodiimide hydrochloride (EDC) and N-hydroxysuccinimide esters (NHS) thus effectively conjugating the antibody to the acellular liver scaffold [125]. After conjugation, mouse endothelial cells (MS1) were statically seeded and perfused through the liver construct. This resulted in a vascular network evenly seeded with endothelial cells and

was successfully transplanted into a pig [125]. This method allowed the liver construct to maintain biological blood flow and reduced platelet aggregation for a 24-h period. In 2017 Mao et al. were able to obtain a patent vascular network by using porcine umbilical vein endothelial cells (pUVEC) and its human analog (hUVEC). The use UVEC's also allowed for complete coverage of the vasculature and additionally allowed for vascular patency over a period of 72 h in a porcine model [126]. Other methods such as the refinement of the decellularization technique have also yielded positive results [127]. An average male liver is made up of  $\sim 2 \times 10^{11}$  cells [128]. Even achieving the 30% fraction required for complete organ function still is proving a challenge. The preferred source of cells would be autologous liver stem cells, but alternative cell sources are also being studied such as iPSCs, Mesenchymal SCs, and humanized hepatocytes [129–132]. There have been several studies on the transplant of iPSCs into mice suffering CCl<sub>4</sub> induced liver failure. iPSCs show much promise in that they are autologous and are a potentially limitless source for the material required to repopulate a sufficiently sized scaffold. Currently, research has been oriented into making more functional cells similar to their native counterparts [133–136].

### 23.7.2 Heart

As with the liver, similar complication arises in the bioengineering of the heart in terms of generation of the adequate number of cells, and of appropriate scaffold sources. Decellularized ECM has also been successfully used as a scaffold for the seeding of cardiac cells and been transplanted into animal models with some limited success. Specifically, Ott *et al.* was able to successfully transplant the recellularized scaffold where it was able to pump in blood throughout the vasculature for a short period of time [20]. For clinical applications, porcine ECM tissue has been at the forefront of research [137–140]. Decellularized porcine heart valves have been used clinically, however this has not been plausible for

the entire heart itself [141]. As with any xenotransplant the risk of immunogenicity is of paramount importance. In porcine tissues the alpha [1, 3]-galactose epitope is the general cause for rejection in the human host [142]. There have been attempts to remove the epitope through the use of galactosidase during the decellularization process and additionally to genetically engineered pigs to abolish the possibility of synthesis of this particular epitope [142]. Cardiomyocytes and endothelial cells are the two major cell types that comprise the heart. The generation of several billion cells directly from adult stem cells remains elusive in the cardiac field of research as well. Again here we see that iPSCs and human embryonic stem cells have come to the forefront of the field as a possible solution to the problem of culturing the amount of cells required for recellularization [143].

### 23.7.3 Kidney

The bioengineering of the kidney has proven challenging and the cellular makeup of the organ is highly complex consisting of approximately 26 different cell types that perform a litany of functions for the body including the regulation of blood pressure, blood filtration, and ion exchange [144–146]. There are more than a dozen cell based therapies in current clinical trials for the treatment of renal deficiencies [147]. However, this does not help with patients suffering from end-stage renal disease and are in need of total transplant. Recellularization of whole acellular ECM constructs have been attempted by several research institutes which demonstrated the ability to form some native like structure [148–150]. For most of the native functions that have been mimicked have been in terms of the filtration of plasma into a urine-like substance, but have not been able to control overall vascular blood pressure as a normally functioning kidney would do [151]. This has been through the growth of nephron like structures, which were found after the recellularization using pluripotent stem cells [151]. The nephron stem cells were generated by researchers Tagasaki et al. and Taguchi et al. [152]

using a variation of treatments where the directed differentiation of the iPSCs was achieved through the use of Activin A or CHIR90021, a GSK3 $\beta$  inhibitor.

The field of tissue engineering has not yet provided clinicians with the ability to replace defective organs with wholly engineered ones. Yet, highly important steps have been made to replace some function of the organs themselves, but not all. There have been great strides made in the area of decellularization of a multitude of different types of organs. Vascularization of the decellularized organs has also made great advances allowing for a fully patent vasculature that does not undergo thrombosis under blood flow. Finally, the use of autologous iPSCs have garnered a great deal of interest and could serve as the ultimate source of cells for the future of recellularized organ constructs. Satisfying these three needs could greatly benefit the world of transplantation needs throughout the world.

---

## 23.8 Current and Future Applications

### 23.8.1 Drug Development and Toxicology

The development and launching of a new drug into the market continues to be challenging [153]. The average cost is currently 3–5 billion USD and takes approximately 12–15 years of exhaustive research. After a preliminary screening, the potential drugs (or pharmaceutical candidates) are characterized *in vitro* and *in vivo* for their ADME-Tox (absorption, distribution, metabolism, excretion and toxicity) properties before continuing on to clinical trials. However, about 90% of the candidates fail during the final stages of the clinical trials, where 43% are due to a lack of efficacy, and 33% due to the presence of negative adverse effects [154], predominantly in the liver, phenomenon known as DILI (drug-induced liver injury) [155] or in the heart (cardiotoxicity). The principal problem resides in the use of conventional drug screening models (cell lines or animal cell monolayers), which possess a lack of

predictive value of the human tissue response to the drug candidate. Therefore, it is necessary more physiological systems in order to relieve the burden of high failure rates.

The **liver** is the responsible organ for the metabolism, conversion, and elimination of a variety of substances. The majority of the drugs are transformed, there, into metabolites/active substances which could result in toxicity to the liver and to the rest of the body. The principal cause of failure at the clinical trials in humans is the use of unsuitable and inaccurate *in vitro* and *in vivo* hepatic models. In addition, the liver is target of many prevailing diseases, such as infectious HBV, HCV [156], malaria [157], overnutrition-induced (type 2 diabetes, NAFLD, fibrosis, cirrhosis) [158–160] or tumoral diseases (hepatocellular carcinoma represents the 6th most common cancer worldwide) [161]. Therefore, the improvement of hepatic models would be essential for the development of specific drugs for liver diseases.

To reproduce a **hepatic** environment suitable to study the efficacy and toxicology of different drugs, it is essential to maintain the liver parenchymal function *ex vivo*. Currently, models used for drug screening are simply comprised of a monoculture system that is maintained on a collagen substrate under static conditions. However, under these conditions hepatocytes suffer dedifferentiation into fibroblastic-like cells and lose their liver-specific functions due to limited amount of juxtacrine signalling with neighbouring cells, while the majority are in contact with the substratum or the medium which is unlike the native environment. For this reason, this type of drug screening platform is not an optimal model for drug development, testing and efficacy suboptimal models for drug efficacy and safety testing [162]. The development of 2D culture models, such as sandwich culture, produced an rising of the basal and induced drug-metabolizing enzyme activities [163, 164]. Nevertheless, the absence of non-parenchymal cells and hepatic dedifferentiation continued being inherent disadvantages of these models [165]. The co-culture of hepatocytes with non-parenchymal cells, such as Kupffer cells, hepatic stellate cells, and liver

epithelial or sinusoidal endothelial cells helped overcome some of the previous limitations, recovering cellular functionality/longevity, and generating higher expression of CYP and Phase II isoforms than in monotypic culture [166–169]. However, these co-cultures result only in a random mix of diverse cell types without taking into account their specific anatomical relationships. More recently, in order to recreate much better the microenvironment, 3D cultures have been developed. These 3D cultures generally consist of spheroids [170, 171], 3D scaffold systems [172] or microfluidic *in vitro* systems [172, 173]. Up to the present, many commercial 3D co-culture devices are commercialized for drug screening, such as the “Hepatopac” platform [174], the 3D InSight™ Human Liver Microtissues of Insphero, the HepaChip® *in vitro* microfluidic system [175] or the Hprel® microliver platforms [176]. Although several issues have been resolved with the models mentioned above, others continue to be biologically and technically challenging [163, 177].

**Heart** failure is the major cause of morbidity and mortality worldwide. The statistics by the American Heart Association show a decrease in the rates of cardiovascular diseases, in part because of current available treatments and improved patient supervision, however, the burden of disease continues to be high [178]. Consequently, robust translational models that mimic the environment of the heart failure are needed to address questions during development of new therapeutics related to target validation, pharmacodynamic’s research and pharmacokinetic, and biomarker discovery.

The **cardiotoxicity** is a frequent side effect of many novel drugs. A clear example of is the recent research regarding peroxisome proliferator-activated receptor-gamma modulators employed in the treatment of type 2 diabetes. While this drug presents metabolic benefits in the treatment of type 2 diabetes [179, 180] several studies show that this drug is related to a significantly higher risk of heart failure [181]. Therefore, it is essential to establish a translational model for cardiac safety assessment to increase the limited capacity of preclinical screening assays used



for the detection of cardiotoxicity. Currently, *in vitro* assays measure the toxicity in two different cell lines (CHO and HEK cells), which have been genetically modified to artificially express cardiac channels. However, due to the genetic aberrations accumulated in these cells and the failure of ectopically expressed channels to accurately model the same channels found in human cardiomyocytes [182, 183], it is very easy to obtain false negatives and positives, which can lead to the commercialization of potentially lethal drugs and the discard of valuable drugs [184–187]. As mentioned above, in pharmaceutical industries, the cardiotoxicity test models are based on cell lines, animal cardiomyocytes, and small/large animal models [188, 189]. To improve the precision of toxicity screening, preclinical drug tests should be done on adult human cardiomyocytes. However, it has not been possible due to the difficulty of obtaining these cells from patients, and the inability of expanding them in culture. The discovery and development of the iPSC, and the following derivation into cardiomyocytes have done feasible circumvent these hurdles [190, 191]. Generation of iPSC from patients suffering inherited heart disease and their differentiation into cardiac cells have been predicted to serve as a model to study disease pathogenesis and to discover novel drugs [192]. The employment of patient-specific iPSC-cardiomyocytes provides an exceptional opportunity to renovate drug toxicity screening [193]. However, the maturation of these cells has been compared to 16-week old human fetal cardiomyocytes [194], questioning the validity of these cells as compared to the classical animal models. However, the actual progress in differentiation protocols and the combination of many innovate organ-on-a-chip platforms [195], have opened new avenues for *in vitro* engineering as they recapitulate mechanics and physiological responses of tissues in the 3D manner [196, 197]. Hence, it is vital to develop appropriate models of disease, and identify new biomarkers that are more sensitive predictors of the early on-set and/or progression of heart failure to facilitate drug discovery and development.

**Kidneys** are the main organs of the urinary system consisting of complex organs involved in

the secretion of waste substances through urine and the maintenance of osmolarity of blood plasma, homeostasis of body fluids, the balance of electrolytes and pH of the internal environment. Furthermore, they are involved in the production of different hormones like erythropoietin (contributing to erythropoiesis) and renin (contributing to hypertension regulation).

In developed countries, hypertension, obesity, diabetes, and exposure of environmental contaminants are the main detonators of renal failure. Acute kidney injury (AKI) is the rapid loss of renal function, which can develop chronic kidney disease (CKD), reduction of the glomerular filtration rate (GFR) and terminate with end-stage renal disease (ESRD) and death [198]. Furthermore, non-renal complications can be also developed, like cardiovascular disease (CVD), which seems to be one of CKD complications [199].

Despite this imperative urgency in finding clinical tools to reduce the effects of kidney dysfunction, therapeutic advances have failed until today. The main reasons being the lack of knowledge in renal pathophysiology, its association to CVD, poor characterization of predictive biomarkers involved in essential molecular mechanisms, and a lack of precise selection of clinical validation criteria, among others [199, 200].

The complexity in achieving a successful pharmaceutical drug development for kidney disease resides in the fact that many processes can be activated and the many cell types that are involved. Serum creatinine and blood urea nitrogen have been popular biomarkers for renal disease, but resulted in poor candidates for clinical trials because of their poor diagnostic capabilities. Currently, the most relevant molecular pathways include the deeper study of RAAS (renin-angiotensin-aldosterone system), inflammation, hypoxia, phenotypical modulation processes and extracellular matrix (ECM) remodeling [201]. Furthermore, new candidates as KIM-1 (Kidney injury molecule-1), fibrinogen and small RNA species are considered as emerging biomarkers due to characteristics like their stability, sensitivity and predictive capability in animal models, early expression and less complexity [198].

**Lungs** are the principal organs of the respiratory system, with the critical role of extracting oxygen from the air while removing the gaseous waste from the body. Due to the fact that airway epithelial cells are located at the interface with the external environment, this tissue not only acts as a first barrier against inhaled irritants and allergens, but it is also involved in the immune system.

There are several cell culture models for lung drug delivery [202]. For example, SOPC1 (rat tracheal globet cell line) is used as a model for mucus secreting drug absorption, allowing the evaluation of the effect of mucus layer on drug transport in the tracheal epithelium. Another example is the use of the human cell line Calu-3, utilized in the study of drug transport at the bronchial level.

More realistic models of lung tissue are those made in a 3D configuration. For example, Klein et al. developed a system where four kinds of cells (alveolar type II cell line, differentiated macrophage-like cells, masts cells and endothelial cells) were seeded on a microporous membrane to mimic the alveolar surface, making it able to study of the toxic effects of particles within the lungs [203].

In the last few years, companies like Epithelix Sàrl or CellnTec had introduced *in vitro* cell culture models to the market that mimic airways like trachea and bronchi, with the aim to provide alternative solutions for drug development and toxicity assays. Others, like Charles River, offers services related to drug development such screening assays, *in vivo* pharmacology studies, and biomarker services.

Hug et al. Developed a human-cell based, “breathing,” lung-on-a-chip microdevice, forming an alveolar-capillary barrier on a thin PDMS membrane previously coated with ECM that recreated physiological breathing movements [204]. This represents a novel strategy that closely mimics the microarchitecture of the alveolar-capillary unit, constituting an excellent screening platform for toxicity and drug development studies.

Most of the new treatments approved for respiratory diseases are improvements of existing drugs, due to the difficulty in finding new ones.

Some targets of these drugs are leukotriene receptor antagonists (used in asthma control), several epithelial growth factors receptor inhibitors (used for lung cancers) and endothelin receptor antagonists, phosphodiesterase-5 inhibitors and prostanoids (used for Group 1 pulmonary hypertension treatment) [205].

### 23.8.2 Developmental Biology Research

The **liver** is the largest internal gland in the body. It plays a fundamental role in metabolic homeostasis due to provide many essential metabolic exocrine and endocrine functions such as the detoxification and elimination of many substances, maintenance of blood homeostasis, regulation of glucose levels, and production of numerous products such as lipids, proteins, vitamins, and carbohydrates. In addition, the liver possesses a unique regenerative capacity, being able to regenerate most of its function after losing up to three-quarters of its mass because of a partial hepatectomy or toxic injury.

In the third week of gestation, hepatic development and organization begins continuing into postnatal period. The first morphological characteristic is the formation of the hepatic diverticulum on the ventral surface of the foregut cranial to the yolk sac. The anterior portion of the hepatic diverticulum gives rise to the liver and intrahepatic biliary tree, while the posterior portion forms the gall bladder and extrahepatic bile ducts.

The majority of *in vitro* models employ human embryonic and iPSCs [206, 207]. However, these models do not completely recapitulate the simultaneous differentiation of liver progenitors into hepatocytic and biliary fates. The formation of mature bile ducts is particularly laborious *in vitro* [208, 209] thus needs the presence of a 3D environment for effective and suitable cellular polarization [210, 211]. Wang *et al.* demonstrated that scaffolds made from liver ECM possessed that required environmental cues [212]. In 2011, it was demonstrated as the human fetal liver progenitor cells cultured inside a ferret liver ECM developed into a native liver tissue including

hepatocytic and biliary structures [19] indicating a preservation of cell differentiation signals from the ECM among different species. Recently, Vyas *et al.* showed as human fetal liver progenitor cells self-assembled inside acellular liver extracellular matrix scaffolds to form 3D liver organoids, which mimicked many aspects of hepatobiliary organogenesis and resulted in concomitant formation of progressively more differentiated hepatocytes and bile duct structures [213]. In this study, after 3 weeks in culture, there were clear changes in the phenotype of the human hepatoblasts, suggesting parallel lineage specification into hepatocytes and polarized cholangiocytes. Hence, liver tissue scaffolds contains specific and necessary ECM molecules that surround the diverse hepatic zones and regulate specific cell differentiation, function, expansion, and regeneration [214]. As mentioned above, 3D scaffold systems are an excellent model, not only for human liver development, but also for drug development and toxicity screenings. On the other hand, conventional 2D differentiation from pluripotency fails to recapitulate cell connections happening during organogenesis. Recently, the team headed by Professor Barbara Treutlein have used single-cell RNA sequencing to reconstruct hepatocyte-like lineage progression from pluripotency in 2D culture hepatic cells [215]. Then, they developed 3D liver bud organoids by reconstituting hepatic, stromal, and endothelial interactions, and deconstruct diversity during liver bud development. They found that liver bud hepatoblasts diverge from the 2D lineage, and express epithelial migration signatures characteristic of organ budding. In addition, they compared 3D liver buds to fetal and adult human liver single-cell RNA sequencing data, and that their lab-grown liver buds had molecular and genetic signature profiles very similar to those found during human liver cellular development.

The **heart** is the first functional organ in human body, which begins to beat 3 weeks after gestation pumping blood throughout the body via the circulatory system, supplying oxygen and nutrients to as well as extracting wastes from the rest of the organs. The heart is an organ with a complex hierarchical molecular, electrical, and

mechanical organization thus *in vitro* models take into account.

Despite the effort in studying the anatomy and physiology of the human cardiovascular system, little is known about the normal development of human heart and dysregulation in disease at the molecular and cellular level. Until now, the most of our understanding of the cellular and molecular basis for cardiogenesis is based on studies of murine cardiovascular development. Recently, researchers at UC Berkeley and Gladstone Institutes have demonstrated that induced pluripotent stem cells can differentiate and self-organize into cardiac microchambers when spatially confined [216]. In this study, after 2 weeks in culture the cells, which initiated in a 2D surface environment, started taking on a 3D structure as a pulsating microchamber. Furthermore, the cells had self-organized based upon whether they were located along the perimeter or in the middle of the construct. The cells positioned along the edge experienced greater mechanical tension and stress compared to the center of the cellular mass. On the other hand, the cells in the center developed into cardiac muscle cells. Such spatial establishment was perceived as soon as the differentiation began. Hence, it is the first time that it has been demonstrated the cardiac spatial differentiation *in vitro*.

It is crucial to have an in-depth understanding of **kidney** development and regulatory pathways in order to achieve successful tissue engineering.

Kidney formation consists of two processes: nephrogenesis (where glomerulus and tubules are formed), followed by branching morphogenesis (which involves the formation of collection tubes, calyces, pelvis and ureter) [217]. Kidney development starts with the formation of the metanephric kidney, derived from the metanephric mesenchyme (the source of the epithelial cells constituting the mature nephron) and the ureteric bud (originating the epithelial tissue present in the caudal portion of the Wolffian duct). The fully developed kidney is preceded by transient kidney-like structures which do not contribute to the fully functional organ such as the pro-nephros (which degenerates in mammals) and the mesonephros (which originates male reproductive organs).

The ureteric bud formation starts at week five in human fetal gestation, induced by signals produced by the metanephric mesenchyme. Afterwards, the metanephric mesenchyme is invaded by the ureteric bud and ureteric bud branching follows. Simultaneously, cells that are in contact with the invading ureteric bud differentiate from mesenchymal to epithelial cells, which become new nephrons. This process continues up to 20–22 weeks of gestation, when ureteric branch is completed and peripheral branch segments give rise to the collecting duct development.

From weeks 22 to 44 of gestation, the cortical and medullary areas of the kidney are well defined and become morphologically different. Finally, after birth, many medullary stromal cells suffer apoptosis and are replaced by developing loops of Henle. Additionally, stromal cells from nephron tissue differentiate into fibroblasts, lymphocyte-like cells and pericytes.

Kidney ECM is composed of heparin sulfate proteoglycans, hyaluronic acid, collagens, fibronectins and laminins and ECM binds to growth factors like FGF (fibroblast growth factor), VEGF (vascular endothelial growth factor) and HGF (hepatic growth factor) to regulate their activity to support cell growth and differentiation [218, 219].

Despite the fact that there are several well defined processes of kidney development, there is still much to be understood. These investigations are crucial for having a whole knowledge for kidney origin in order to apply it in scientific studies. For example, Kaminski et al. demonstrate the transformation of human and mouse fibroblasts into induced renal tubular epithelial cells (iRECs) using four transcriptional factors (Emx2, Hnf1b, Hnf4 $\alpha$  and Pax8) [220]. The resultant cells have many morphological, transcriptional and functional characteristics of fully differentiated kidney epithelial cells making them available for nephrotoxic agent screening and for the study of hereditary tubular diseases and drug toxicity.

Abolbashari *et al.* used primary adult renal cells isolated from kidney cortical tissue, with the *in vitro* expression of aquaporines 1, 2, 4, ezrin and podocin, showing the presence of cells from

different renal segments. Most of them expressed aquaporin 1 and ezrin, indicative of proximal tubular cells, and other expressed aquaporin 2 and 4, indicative of collecting duct cells. These cells were then seeded in kidney scaffolds, showing promising results regarding to electrolyte and protein absorption, hydrolase activity and erythropoietin production [221].

Embryonic stem (ES) cells have also been used in kidney recellularization with promising results. Song *et al.*, infused these cells via renal artery and ureter, showing their distribution into tubular and vascular structures, with cell multiplication [222]. Despite the fact that ES cells offer promising results in organ recellularization, their use is limited due to ethical questions and their teratogenic potential. For these reasons, other source of cells is employed, such as bone marrow mesenchymal stem cells (BM-MSCs), adipose tissue or amniotic fluid stem cells.

Taguchi *et al.* used human and mouse pluripotent stem cells (PSCs) to derive metanephric mesenchyme. They demonstrate that these progenitors are able to generate 3D nephric tubules and glomeruli with podocytes [223].

**Lungs** are tree-like structures divided into two anatomical zones, the conducting airways and alveoli.

The conducting airways begin with the trachea, which split into two main bronchi, which further branch into smaller airways, the bronchioles. These conducting airways are covered by three different epithelial cells (ciliated, goblet and basal cells) surrounded by fibroblasts, smooth muscle, cartilage, vasculature and neurons. The alveolar epithelium is composed of two epithelial types I (AETI) and II (AETII) [224].

Lungs and trachea arise from the anterior foregut endoderm, the gut tube which will further originate the gastrointestinal tract and organs like lungs, thyroid, liver and pancreas. Lung development starts arounds week 3 during human gestation, with two forming buds that undergo a highly and regulated branching process to form the typical tree-like network of airways of the organ [225, 226], with an established proximal-distal axis. This is followed by the canalicular and saccular stages, where alveoli are formed, in

preparation for respiration at birth. Finally, around the third trimester, full maturation of the alveolus follows, which persists for up to 3 years postnatally. During the stages of endodermal development, lung mesoderm interacts with lung endoderm, promoting branching and cell differentiation into lung lineages [226].

Despite advances in the understanding of lung development and cellular components of its epithelium the diversity and function of all mesenchymal cell types is still poorly understood. Additionally, researchers recently realize how important the vascular and neuronal networks are during lung development [227].

Most of the current models for lung development and homeostasis are based on rodent models.

ALI (Air-Liquid-Interface) method developed in the 80's supposed a great advancement in the field. This system consists on a cell monolayer of epithelial tissue grown on a porous filter that physically separates lung epithelial tissue from the underlying media, resulting in the achieving of proper apical-basal polarization. These systems are combined today with ROCK inhibitors, allowing long term cell culture.

3D environments are more recently used for primary adult human lung tissue culture. One example is the "bronchospheres", where basal stem cells from human or mouse origin are embedded in a gel, allowing the formation of spherical colonies [228]. With these structures, the self-renewal capacity of stem cells and its capability for giving rise to proximal secretory and ciliated cells is known, and they are also used as screening platforms for the study of epithelial responses against different stimuli.

Ghaedi *et al.* reported an efficient differentiation method to obtain definitive endoderm, anterior foregut endoderm and a homogenous population of alveolar epithelial type I and II cells from human iPSCs, which were then seeded into rat or human lung scaffolds. They demonstrated that iPSCs-derived AETII were able to proliferate and give rise to lung cell types [229].

Similarly, Dye *et al.* seeded hPSC-derived lung spheroids in mice lung scaffolds, obtaining

promising results like the formation of airway structures, the creation of many mesenchymal cell types and ciliated and secretory functional cells [230].

Recently, proximal (airway) and distal (alveolar) models can be studied in vitro. However, full integration of both parts in a unique system is still challenging, due to intrinsic differences in each cell type such as the physical environment or ECM composition where different cell types develop [227].

### 23.8.3 Bioprinting

3D Bioprinting consists in the manufacture of artificial constructs. This process uses small amounts of biomaterials and cells that are precisely placed to the most miniscule detail of the organ [231]. This novel technology can be classified according to the final use in tissue and organ fabrication, or pharmaceutical investigation. Nowadays, several medicinal and therapeutic applications include the creation of personalized implants and prosthetics, drug discovery, drug delivery or dosage forms [232], as well as disease models and regenerative medicine.

The principal issue in organ failure is the large number of people waiting for a transplant, which results in long waiting lists due to the few number of available donors. 3D Bioprinting could resolve this problem using cells from the patient's own organ to create a tissue substitute, decreasing the risk of rejection and eliminating the necessity of taking immunosuppressants for life [233]. Although, the main objective of tissue engineering and regenerative medicine is to alleviate the organ donor shortage, 3D Bioprinting possesses some advantages. For example, bioprinting presents a highly precise cell placing, concentration, and diameter of printed cells [234]. At present, 3D Bioprinting is capable of producing complex organs with a high degree of cell density [235]. However, to achieve a correct vascularization is a big challenge. Currently, none of cardiovascular tissue have been bioprinted with entire functions similar to native tissue.

In the field of the **liver research**, Organovo™ has performed 3D vascularized liver constructs containing stellate, endothelial, and hepatocyte cells with high cell viability and a solid zonation, mimicking the native hepatic lobules. Organovo™ currently offers testing services thanks to ExVive™ 3D Bioprinted Human Liver. This tissue can be used in the assessment of drug exposure for acute and chronic toxicity and metabolism studies for more than 28 days. At the present, Organovo is working on bioprinted organs for therapeutic use in humans with a therapeutic tissue program. In this program, the company is emphasizing on developing clinical solutions for pediatric inborn errors of metabolism, and for acute on-chronic liver failure and it plans to develop and conclude its liver tissue design over the next 18 months. The preclinical studies into diseased animal models have shown good engraftment, vascularization, and functionality 60 days after implantation. The company expects to file an Investigation New Drug application in 2020.

Currently, there are two options for **heart** valve replacement surgery: using a mechanical heart valve or using a biological heart valve [236]. However, using the first option requires the patient to take an anti-coagulant for life and on the other hand, biological heart valve has a shorter lifespan which may require replacement [237]. Thus, the capacity to produce bioprinted native heart valves has a direct clinical impact. Sodian *et al.* have employed them for many surgical procedures to correct everything from congenital heart defect [238] to aortic valve replacement operation [239–242] or patients with rare cardiac tumors [243]. Though the surgical models were non-living, it was a step towards bioprinting heart valves. In fact, Sodian and his colleagues were the first in using 3D printing to manufacture engineered heart valves [244, 245]. Recently, Jonathon Butcher's lab have been using this novel technology to fabricate living alginate/gelatin hydrogel valve conduits [246, 247]. When heart tissue suffers damage, the heart pumps blood inefficiently due to the loss of contractile muscle and the formation of stiff scar tissue [248] which can lead to ischemia [249]. One approach

to repair the heart is to transplant cells at the site of the damaged tissue [250], however, one of the main limitations to survival of the implanted cells is the immediate availability of oxygen [251]. To solve that, Yeong *et al.* used 3D bioprinting to produce porous structures, facilitating and ensuring efficient mass transport through the construction [252]. Others used this technology to create a construct containing human cardiac-derived cardiomyocyte progenitor cells and RGD-modified sodium alginate as the ECM [253]. Another approach is the use of bioinks generated from decellularized ECM. Cho's group encapsulated rat myoblasts cells into the heart-derived bioink and observed an increase in many cardiac-specific genes compared to collagen constructs [254]. Thus, 3D printing is a promising field, however, despite the major limitation is still the source of human cardiac cells.

The structure of a whole heart includes multiple cell types, ECM, and multi-scale structures for pumping blood. Thus, a replication using this new technology involves a great effort. BioLife4D is working in to be the next great medical achievement within heart transplants. It is currently developing bioprinted hearts in combination with unspecialized adult induced pluripotent stem cells, which will convert into cardiac cells.

In the field of **kidney research**, Homan *et al.* reported a bioprinting method that creates 3D human renal proximal tubules [255]. The process starts with the printing of a renal proximal tubule with a thermos degradable ink, which models the convoluted pathway of the proximal tubule. Afterwards, a layer of ECM is deposited on top of the printed structure. Then, the ink is removed, resulting in a proximal tubule mold, with a perfusable inlet and outlet. Finally, live human kidney cells are pumped into the mold and adhere, forming a confluent epithelium. This system is placed on a chip and it is able to persist more than 2 months *in vitro*. They describe a method that combines bioprinting, 3D culture and organ-on-a-chip concept, showing an epithelial morphology and functionality comparable to those observed in the same cells cultured in 2D conditions.

Once more, Organovo had performed a 3D bioprinted kidney tissue (ExVive™ Human

Kidney Tissue), which is a complete human bio-printed tissue consisting on an apical layer of polarized primary renal proximal tubule epithelial cells sustained by a collagen IV-rich interface of renal fibroblasts and endothelial cells. This architecture provides an extraordinary system for phenotypic and nephrotoxicity studies.

In contrast, very few works have been published regarding **lung** 3D bioprinting. Horváth *et al.* reported the biofabrication of a human air-blood tissue barrier analogue to lung tissue. It consists on a two cell-layer model of endothelial cells printed in a matrigel ECM bioprinted layer. They achieved the creation of an automated and reproducible way to obtain thinner and homogeneous cell layers, resembling to the naturally occurred environment of the native tissue, where the epithelial cell layer is separated by a thin basement membrane [256].

---

## 23.9 Regulatory Landscape for Naturally-Derived Biomaterials

### 23.9.1 Regulatory Landscape

Development of a tissue-engineered product for clinical use can be challenging. Because of the novelty, complexity and technical specificity, it is essential to understand the regulations that guarantee the quality and safety of these novel products. For this goal, this section of the chapter will be focused on two regulatory agencies with similar objectives, but different systems of operation: The Food and Drug Administration (F. D. A.) and the European Medicines Agency (EMA).

#### 23.9.1.1 Food and Drug Administration

In the US, the FDA's Center for Biologics Evaluation and Research is responsible for ensuring the safety, purity, potency, and effectiveness of many biologically derived products. The term "tissue engineered medical products," (TEMP) has been defined in a standard document of the American Society for Testing and Materials, and

this terminology has been included in the FDA-recognized consensus standards database [257].

TEMP can consist of a variety of different constituents (cells, scaffolds, device...) or any combination of these and the FDA classifies these products as combination products. Congress recognized the existence of combination products when it enacted the Safe Medical Device Act of 1990, and it was defined in the 21 Code of Federal Regulation 1270/1271 Part C 210/211/820 [258, 259].

A combination product's primary mode of action (PMOA) establishes its regulatory and product development framework and determine which center will be responsible for a particular combination product [260]. The PMOA is such an important concept that the FDA published a docket in August 2005 entitled Definition of Primary Mode of Action of a Combination Product. The PMOA is defined as "the single mode of action of a combination product that provides the most important therapeutic effect of the combination product.

#### 23.9.1.2 European Medicines Agency

In the European Union (EU), an Advanced Therapy Medicinal Products (ATMP) is defined as being a Somatic Cell Therapy Medicinal Product (SCTMP), a Tissue Engineered Product (TEP), a Gene Therapy Medicinal Product (GTMP) or a combined ATMP [261].

The Committee for Advanced Therapies (CAT) is a multidisciplinary committee and it was established by EMA to offer high-level expertise to assess the quality, safety and efficacy of ATMPs, so this committee is the responsible for reviewing applications for marketing authorization for Advanced Therapy Medicinal Products [262]. In 2007, the European Parliament and Council of the European Union (EU) issued an amendment to Directive 2001/83/EC and Regulation No. 776/2004 to include regulatory provisions for ATMPs defined in Regulation EC No 1394/2007.

According to this regulation, when a product contains viable cells or tissues, the pharmacological, immunological or metabolic action of those

cells or tissues shall be considered as the principal mode of action of the product. Therefore, a natural-derived biomaterial could be not the only actor in these fields. However, the biomaterial biocompatibility is still an essential requisite, and the new products should be subjected to the same regulatory rules as the others biomedical devices (Regulation EC No 1394/2007) [263].

In addition to the requirements laid down in Article 6 of Regulation No 726/2004 [264], the application for the authorization of an ATMP containing medical devices, biomaterials, scaffolds or matrices shall include a description of the physical characteristics and performance of the product. It should also include the description of the product design method, by the Annex 1 to Directive 2001/83/EC [265].

### 23.9.2 GMP Production

Control of clinical products manufacturing in both EU and the USA is exerted by the use of Good Manufacturing Practice (GMP) regulations and guidelines, to protect the patient from receiving poor quality, unsafe or products that vary from their specifications. Each regulatory body has the responsibility to apply the GMP requirements. The regulatory bodies are:

- The Food and Drug Administration in the USA
- The European Medicines Agency (EMA) for centrally authorized products in Europe
- The National Regulatory Authorities within the various EU member states

GMP regulation includes Good Practice for Tissue and Cells and Good Engineering Practice (GEP) [266]. GMP facilities follow GMP guidelines promulgated by each regulatory agency, with specialized facility designs and highly trained personnel to produce the first clinical prototype faithfully in a controlled and reproducible fashion.

The EU regulates by the publication of GMP directives and GMP Guidelines which are prepared and published in one volume by the

European Commission under the auspices of Directorate General Enterprise. The US control procedures are comparable to EU's practices, whereby the GMP Regulations are published in the Code of Federal Regulations by various executive departments and agencies of Federal Government [267]. In the last years, FDA and EMA are making significant progress toward mutually recognizing each other's GMP inspections. The result of this attempt is the creation of a joint pilot program, allowing more sites to be monitored and reducing unnecessary duplication through the implementation of the International Council for Harmonization (ICH) and relevant regulatory requirements [268].

**Acknowledgements** This work was supported by Gobierno de Aragón and Fondo Social Europeo through a predoctoral Fellowship DGA C066/2014 (P. S-A), Instituto de Salud Carlos III, through a predoctoral fellowship i-PFIS IFI15/00158 (I. P-P). N. S-R was supported by a POCTEFA/Refbio II research grant and FGJ Gobierno de Aragón. J.I.A was supported by Fundação para a Ciência e a Tecnologia (Portugal), through a predoctoral Fellowship SFRH/BD/116780/2016. PMB was supported with the project PI15/00563 from Instituto de Salud Carlos III, Spain.

### References

1. Langer R, Vacanti JP (1993) Tissue engineering. *Science* 260:920–926
2. Hendow EK, Guhmann P, Wright B, Sofokleous P, Parmar N, Day RM (2016) Biomaterials for hollow organ tissue engineering. *Fibrogenesis Tissue Repair* 9:3
3. Ikada Y (2006) Challenges in tissue engineering. *J R Soc Interface* 3:589–601
4. Mazza G, Rombouts K, Rennie Hall A, Urbani L, Vinh Luong T, Al-Akkad W, Longato L et al (2015) Decellularized human liver as a natural 3D-scaffold for liver bioengineering and transplantation. *Sci Rep* 5:13079
5. Azuma K, Izumi R, Osaki T, Ifuku S, Morimoto M, Saimoto H, Minami S et al (2015) Chitin, chitosan, and its derivatives for wound healing: old and new materials. *J Funct Biomater* 6:104–142
6. Bao Ha TL, Minh T, Nguyen D, Minh D (2013) Naturally derived biomaterials: preparation and application. In: *Regenerative medicine and tissue engineering*. <http://dx.doi.org/10.5772/55668>
7. Gunatillake PA, Adhikari R (2003) Biodegradable synthetic polymers for tissue engineering. *Eur Cell Mater* 5:1–16 discussion 16



8. Willerth SM, Sakiyama-Elbert SE (2008) Combining stem cells and biomaterial scaffolds for constructing tissues and cell delivery. In: Stem book. Harvard Stem Cell Institute, Cambridge, MA
9. Bhat S, Kumar A (2013) Biomaterials and bioengineering tomorrow's healthcare. *Biomatter* 3:e24717
10. Yannas IV, Lee E, Orgill DP, Skrabut EM, Murphy GF (1989) Synthesis and characterization of a model extracellular matrix that induces partial regeneration of adult mammalian skin. *Proc Natl Acad Sci U S A* 86:933–937
11. Atala A, Bauer SB, Soker S, Yoo JJ, Retik AB (2006) Tissue-engineered autologous bladders for patients needing cystoplasty. *Lancet* 367:1241–1246
12. Warnke PH, Springer IN, Wiltfang J, Acil Y, Eufinger H, Wehmoller M, Russo PA et al (2004) Growth and transplantation of a custom vascularised bone graft in a man. *Lancet* 364:766–770
13. Zacchi V, Soranzo C, Cortivo R, Radice M, Brun P, Abatangelo G (1998) In vitro engineering of human skin-like tissue. *J Biomed Mater Res* 40:187–194
14. Kaushal S, Amiel GE, Guleserian KJ, Shapira OM, Perry T, Sutherland FW, Rabkin E et al (2001) Functional small-diameter neovessels created using endothelial progenitor cells expanded ex vivo. *Nat Med* 7:1035–1040
15. Griffith LG, Naughton G (2002) Tissue engineering – current challenges and expanding opportunities. *Science* 295:1009–1014
16. Sivaraman A, Leach JK, Townsend S, Iida T, Hogan BJ, Stolz DB, Fry R et al (2005) A microscale in vitro physiological model of the liver: predictive screens for drug metabolism and enzyme induction. *Curr Drug Metab* 6:569–591
17. Moran EC, Dhal A, Vyas D, Lanis A, Soker S, Baptista PM (2014) Whole-organ bioengineering: current tales of modern alchemy. *Transl Res* 163:259–267
18. Peloso A, Dhal A, Zambon JP, Li P, Orlando G, Atala A, Soker S (2015) Current achievements and future perspectives in whole-organ bioengineering. *Stem Cell Res Ther* 6:107
19. Baptista PM, Siddiqui MM, Lozier G, Rodriguez SR, Atala A, Soker S (2011) The use of whole organ decellularization for the generation of a vascularized liver organoid. *Hepatology* 53:604–617
20. Ott HC, Matthiesen TS, Goh SK, Black LD, Kren SM, Netoff TI, Taylor DA (2008) Perfusion-decellularized matrix: using nature's platform to engineer a bioartificial heart. *Nat Med* 14:213–221
21. Katari R, Peloso A, Zambon JP, Soker S, Stratta RJ, Atala A, Orlando G (2014) Renal bioengineering with scaffolds generated from human kidneys. *Nephron Exp Nephrol* 126:119
22. Wagner DE, Bonvillain RW, Jensen T, Girard ED, Bunnell BA, Finck CM, Hoffman AM et al (2013) Can stem cells be used to generate new lungs? Ex vivo lung bioengineering with decellularized whole lung scaffolds. *Respirology* 18:895–911
23. Baptista PM, Orlando G, Mirmalek-Sani SH, Siddiqui M, Atala A, Soker S (2009) Whole organ decellularization – a tool for bioscaffold fabrication and organ bioengineering. *Conf Proc IEEE Eng Med Biol Soc* 2009:6526–6529
24. Bayrak A, Tyralla M, Ladhoff J, Schleicher M, Stock UA, Volk HD, Seifert M (2010) Human immune responses to porcine xenogeneic matrices and their extracellular matrix constituents in vitro. *Biomaterials* 31:3793–3803
25. Bastian F, Stelzmuller ME, Kratochwill K, Kasimir MT, Simon P, Weigel G (2008) IgG deposition and activation of the classical complement pathway involvement in the activation of human granulocytes by decellularized porcine heart valve tissue. *Biomaterials* 29:1824–1832
26. A Brief History of Biomedical Materials (2009) [PDF] DSM, pp 1–2. Available at: [https://www.dsm.com/content/dam/dsm/cworld/en\\_US/documents/brief-history-biomedical-materials-en.pdf](https://www.dsm.com/content/dam/dsm/cworld/en_US/documents/brief-history-biomedical-materials-en.pdf)
27. Heness G, Ben-Nissan B (2004) Innovative bioceramics. *Mat For* 27:104–114
28. Pachence JM (1996) Collagen-based devices for soft tissue repair. *J Biomed Mater Res* 33:35–40
29. Sinha VR, Trehan A (2003) Biodegradable microspheres for protein delivery. *J Control Release* 90:261–280
30. Niknejad H, Peirovi H, Jorjani M, Ahmadiani A, Ghanavi J, Seifalian AM (2008) Properties of the amniotic membrane for potential use in tissue engineering. *Eur Cell Mater* 15:88–99
31. Loss M, Wedler V, Kunzi W, Meuli-Simmen C, Meyer VE (2000) Artificial skin, split-thickness autograft and cultured autologous keratinocytes combined to treat a severe burn injury of 93% of TBSA. *Burns* 26:644–652
32. Branski LK, Herndon DN, Celis MM, Norbury WB, Masters OE, Jeschke MG (2008) Amnion in the treatment of pediatric partial-thickness facial burns. *Burns* 34:393–399
33. Lee CH, Singla A, Lee Y (2001) Biomedical applications of collagen. *Int J Pharm* 221:1–22
34. Robb K, Shridhar A, Flynn L (2017) Decellularized matrices as cell-instructive scaffolds to guide tissue-specific regeneration. *ACS Biomater Sci Eng*. Article. <https://doi.org/10.1021/acsbiomaterials.7b00619>
35. Stock P, Winkelmann C, Thonig A, Böttcher G, Wenske G, Christ B (2012) Application of collagen coated silicone scaffolds for the three-dimensional cell culture of primary rat hepatocytes. *FASEB J* 26:274.272–274.272
36. Wang Y, Gunasekara DB, Reed MI, DiSalvo M, Bultman SJ, Sims CE, Magness ST et al (2017) A microengineered collagen scaffold for generating a polarized crypt-villus architecture of human small intestinal epithelium. *Biomaterials* 128:44–55
37. Echave MC, Saenz del Burgo L, Pedraz JL, Orive G (2017) Gelatin as biomaterial for tissue engineering. *Curr Pharm Des* 23:3567–3584

38. Tayebi L, Rasouliaboroujeni M, Moharamzadeh K, Almela TKD, Cui Z, Ye H (2018) 3D-printed membrane for guided tissue regeneration. *Mater Sci Eng C Mater Biol Appl* 84:148–158
39. Elamparithi A, Punnoose AM, Paul SFD, Kuruvilla S (2017) Gelatin electrospun nanofibrous matrices for cardiac tissue engineering applications. *Int J Polym Mater Polym Biomater* 66:20–27
40. Gu Y, Bai Y, Zhang D (2018) Osteogenic stimulation of human dental pulp stem cells with a novel gelatin-hydroxyapatite-tricalcium phosphate scaffold. *J Biomed Mater Res A* 106:1851–1861
41. Gattazzo F, De Maria C, Rimessi A, Dona S, Braghetta P, Pinton P, Vozzi G et al (2018) Gelatin-genipin-based biomaterials for skeletal muscle tissue engineering. *J Biomed Mater Res B Appl Biomater* 00B:000–000
42. Lewis PL, Green RM, Shah RN (2018) 3D-printed gelatin scaffolds of differing pore geometry modulate hepatocyte function and gene expression. *Acta Biomater* 69:63–70
43. Kilic Bektas C, Hasirci V (2017) Mimicking corneal stroma using keratocyte-loaded photopolymerizable methacrylated gelatin hydrogels. *J Tissue Eng Regen Med* 12:e1899–e1910
44. Amer MH, Rose F, Shakesheff KM, White LJ (2018) A biomaterials approach to influence stem cell fate in injectable cell-based therapies. *Stem Cell Res Ther* 9:39
45. Vepari C, Kaplan DL (2007) Silk as a biomaterial. *Prog Polym Sci* 32:991–1007
46. Sawatjui N, Limpitboon T, Schrobback K, Klein T (2018) Biomimetic scaffolds and dynamic compression enhance the properties of chondrocyte- and MSC-based tissue-engineered cartilage. *J Tissue Eng Regen Med* 12:1220–1229
47. Kim DK, In Kim J, Sim BR, Khang G (2017) Bioengineered porous composite curcumin/silk scaffolds for cartilage regeneration. *Mater Sci Eng C Mater Biol Appl* 78:571–578
48. Warnecke D, Schild NB, Klose S, Joos H, Brenner RE, Kessler O, Skaer N et al (2017) Friction properties of a new silk fibroin scaffold for meniscal replacement. *Tribol Int* 109:586–592
49. Hu Y, Ran J, Zheng Z, Jin Z, Chen X, Yin Z, Tang C et al (2018) Exogenous stromal derived factor-1 releasing silk scaffold combined with intra-articular injection of progenitor cells promotes bone-ligament-bone regeneration. *Acta Biomater* 71:168–183
50. Sack BS, Mauney JR, Estrada CR Jr (2016) Silk fibroin scaffolds for urologic tissue engineering. *Curr Urol Rep* 17:16
51. Ye Q, Zund G, Benedikt P, Jockenhoevel S, Hoerstrup SP, Sakyama S, Hubbell JA et al (2000) Fibrin gel as a three dimensional matrix in cardiovascular tissue engineering. *Eur J Cardiothorac Surg* 17:587–591
52. Seyedi F, Farsinejad A, Nematollahi-Mahani SN (2017) Fibrin scaffold enhances function of insulin producing cells differentiated from human umbilical cord matrix-derived stem cells. *Tissue Cell* 49:227–232
53. Munirah S, Kim SH, Ruszymah BH, Khang G (2008) The use of fibrin and poly(lactic-co-glycolic acid) hybrid scaffold for articular cartilage tissue engineering: an in vivo analysis. *Eur Cell Mater* 15:41–52
54. Khodakaram-Tafti A, Mehrabani D, Shaterzadeh-Yazdi H (2017) An overview on autologous fibrin glue in bone tissue engineering of maxillofacial surgery. *Dent Res J (Isfahan)* 14:79–86
55. Eo MY, Fan H, Cho YJ, Kim SM, Lee SK (2016) Cellulose membrane as a biomaterial: from hydrolysis to depolymerization with electron beam. *Biomater Res* 20:16
56. Entcheva E, Bien H, Yin L, Chung CY, Farrell M, Kostov Y (2004) Functional cardiac cell constructs on cellulose-based scaffolding. *Biomaterials* 25:5753–5762
57. Svensson A, Nicklasson E, Harrah T, Panilaitis B, Kaplan DL, Brittberg M, Gatenholm P (2005) Bacterial cellulose as a potential scaffold for tissue engineering of cartilage. *Biomaterials* 26:419–431
58. Wang B, Lv X, Chen S, Li Z, Yao J, Peng X, Feng C et al (2018) Use of heparinized bacterial cellulose based scaffold for improving angiogenesis in tissue regeneration. *Carbohydr Polym* 181:948–956
59. Park BK, Kim MM (2010) Applications of chitin and its derivatives in biological medicine. *Int J Mol Sci* 11:5152–5164
60. Venkatesan J, Kim SK (2010) Chitosan composites for bone tissue engineering – an overview. *Mar Drugs* 8:2252–2266
61. Li Z, Ramay HR, Hauch KD, Xiao D, Zhang M (2005) Chitosan-alginate hybrid scaffolds for bone tissue engineering. *Biomaterials* 26:3919–3928
62. Kweon DK, Song SB, Park YY (2003) Preparation of water-soluble chitosan/heparin complex and its application as wound healing accelerator. *Biomaterials* 24:1595–1601
63. Ueno H, Yamada H, Tanaka I, Kaba N, Matsuura M, Okumura M, Kadosawa T et al (1999) Accelerating effects of chitosan for healing at early phase of experimental open wound in dogs. *Biomaterials* 20:1407–1414
64. Yu Y, Chen R, Sun Y, Pan Y, Tang W, Zhang S, Cao L et al (2018) Manipulation of VEGF-induced angiogenesis by 2-N, 6-O-sulfated chitosan. *Acta Biomater* 71:510–521
65. Boucard N, Viton C, Agay D, Mari E, Roger T, Chancerelle Y, Domard A (2007) The use of physical hydrogels of chitosan for skin regeneration following third-degree burns. *Biomaterials* 28:3478–3488
66. Thomas S (2000) Alginate dressings in surgery and wound management – part 1. *J Wound Care* 9:56–60

67. Giri TK, Thakur D, Alexander A, Ajazuddin BH, Tripathi DK (2012) Alginate based hydrogel as a potential biopolymeric carrier for drug delivery and cell delivery systems: present status and applications. *Curr Drug Deliv* 9:539–555
68. Wang Y, Miao Y, Zhang J, Wu JP, Kirk TB, Xu J, Ma D et al (2018) Three-dimensional printing of shape memory hydrogels with internal structure for drug delivery. *Mater Sci Eng C Mater Biol Appl* 84:44–51
69. Smidsrod O, Skjak-Braek G (1990) Alginate as immobilization matrix for cells. *Trends Biotechnol* 8:71–78
70. Gharravi AM, Orazizadeh M, Ansari-Asl K, Banoni S, Izadi S, Hashemitarbar M (2012) Design and fabrication of anatomical bioreactor systems containing alginate scaffolds for cartilage tissue engineering. *Avicenna J Med Biotechnol* 4:65–74
71. Beigi MH, Atefi A, Ghanaei HR, Labbaf S, Ejeian F, Nasr-Esfahani MH (2018) Activated platelet-rich plasma (PRP) improves cartilage regeneration using adipose stem cells encapsulated in a 3D alginate scaffold. *J Tissue Eng Regen Med* 12:1327–1338
72. Coward SM, Legallais C, David B, Thomas M, Foo Y, Mavri-Damelin D, Hodgson HJ et al (2009) Alginate-encapsulated HepG2 cells in a fluidized bed bioreactor maintain function in human liver failure plasma. *Artif Organs* 33:1117–1126
73. Yajima Y, Lee CN, Yamada M, Utoh R, Seki M (2018) Development of a perfusable 3D liver cell cultivation system via bundling-up assembly of cell-laden microfibers. *J Biosci Bioeng* 126:1111–1118
74. Pipeleers D, Keymeulen B (2016) Boost for alginate encapsulation in Beta cell transplantation. *Trends Endocrinol Metab* 27:247–248
75. Awad HA, Wickham MQ, Leddy HA, Gimble JM, Guilak F (2004) Chondrogenic differentiation of adipose-derived adult stem cells in agarose, alginate, and gelatin scaffolds. *Biomaterials* 25:3211–3222
76. Gao M, Lu P, Bednark B, Lynam D, Conner JM, Sakamoto J, Tuszynski MH (2013) Templated agarose scaffolds for the support of motor axon regeneration into sites of complete spinal cord transection. *Biomaterials* 34:1529–1536
77. Lynam DA, Shahriari D, Wolf KJ, Angart PA, Koffler J, Tuszynski MH, Chan C et al (2015) Brain derived neurotrophic factor release from layer-by-layer coated agarose nerve guidance scaffolds. *Acta Biomater* 18:128–131
78. Zarrintaj P, Bakhshandeh B, Rezaeian I, Heshmatian B, Ganjali MR (2017) A novel electroactive agarose-aniline pentamer platform as a potential candidate for neural tissue engineering. *Sci Rep* 7:17187
79. Han S, Lee JY, Heo EY, Kwon IK, Yune TY, Youn I (2018) Implantation of a matrigel-loaded agarose scaffold promotes functional regeneration of axons after spinal cord injury in rat. *Biochem Biophys Res Commun* 496:785–791
80. Dahlmann J, Kensah G, Kempf H, Skvorc D, Gawol A, Elliott DA, Drager G et al (2013) The use of agarose microwells for scalable embryoid body formation and cardiac differentiation of human and murine pluripotent stem cells. *Biomaterials* 34:2463–2471
81. Roosens A, Puype I, Cornelissen R (2017) Scaffold-free high throughput generation of quiescent valvular microtissues. *J Mol Cell Cardiol* 106:45–54
82. Kim SS, Kang MS, Lee KY, Lee MJ, Wang L, Kim HJ (2012) Therapeutic effects of mesenchymal stem cells and hyaluronic acid injection on osteochondral defects in rabbits' knees. *Knee Surg Relat Res* 24:164–172
83. Migliore A, Procopio S (2015) Effectiveness and utility of hyaluronic acid in osteoarthritis. *Clin Cases Miner Bone Metab* 12:31–33
84. Gold MH (2007) Use of hyaluronic acid fillers for the treatment of the aging face. *Clin Interv Aging* 2:369–376
85. Yoo HS, Lee EA, Yoon JJ, Park TG (2005) Hyaluronic acid modified biodegradable scaffolds for cartilage tissue engineering. *Biomaterials* 26:1925–1933
86. Davidenko N, Campbell JJ, Thian ES, Watson CJ, Cameron RE (2010) Collagen-hyaluronic acid scaffolds for adipose tissue engineering. *Acta Biomater* 6:3957–3968
87. Kushchayev SV, Giers MB, Hom Eng D, Martirosyan NL, Eschbacher JM, Mortazavi MM, Theodore N et al (2016) Hyaluronic acid scaffold has a neuroprotective effect in hemisection spinal cord injury. *J Neurosurg Spine* 25:114–124
88. Mano JF, Silva GA, Azevedo HS, Malafaya PB, Sousa RA, Silva SS, Boesel LF et al (2007) Natural origin biodegradable systems in tissue engineering and regenerative medicine: present status and some moving trends. *J R Soc Interface* 4:999–1030
89. Lee C-T, Kung P-H, Lee Y-D (2005) Preparation of poly(vinyl alcohol)-chondroitin sulfate hydrogel as matrices in tissue engineering. *Carbohydr Polym* 61:348–354
90. Bali JP, Cousse H, Neuzil E (2001) Biochemical basis of the pharmacologic action of chondroitin sulfates on the osteoarticular system. *Semin Arthritis Rheum* 31:58–68
91. Henson FM, Getgood AM, Caborn DM, McIlwraith CW, Rushton N (2012) Effect of a solution of hyaluronic acid-chondroitin sulfate-N-acetyl glucosamine on the repair response of cartilage to single-impact load damage. *Am J Vet Res* 73:306–312
92. Liang WH, Kienitz BL, Penick KJ, Welter JF, Zawodzinski TA, Baskaran H (2010) Concentrated collagen-chondroitin sulfate scaffolds for tissue engineering applications. *J Biomed Mater Res A* 94:1050–1060
93. Zhou F, Zhang X, Cai D, Li J, Mu Q, Zhang W, Zhu S et al (2017) Silk fibroin-chondroitin sulfate scaffold with immuno-inhibition property for articular cartilage repair. *Acta Biomater* 63:64–75
94. Phillips TJ (1998) New skin for old: developments in biological skin substitutes. *Arch Dermatol* 134:344–349

95. Macadam SA, Lennox PA (2012) Acellular dermal matrices: use in reconstructive and aesthetic breast surgery. *Can J Plast Surg* 20:75–89
96. Chang J, DeLillo N Jr, Khan M, Nacinovich MR (2013) Review of small intestine submucosa extracellular matrix technology in multiple difficult-to-treat wound types. *Wounds* 25:113–120
97. Badylak SF (2004) Xenogeneic extracellular matrix as a scaffold for tissue reconstruction. *Transpl Immunol* 12:367–377
98. Voytik-Harbin SL, Brightman AO, Kraine MR, Waisner B, Badylak SF (1997) Identification of extractable growth factors from small intestinal submucosa. *J Cell Biochem* 67:478–491
99. Chun SY, Lim GJ, Kwon TG, Kwak EK, Kim BW, Atala A, Yoo JJ (2007) Identification and characterization of bioactive factors in bladder submucosa matrix. *Biomaterials* 28:4251–4256
100. Hodde JP, Record RD, Liang HA, Badylak SF (2001) Vascular endothelial growth factor in porcine-derived extracellular matrix. *Endothelium* 8:11–24
101. Voytik-Harbin S, Brightman AO, Waisner B, Robinson J, Lamar CH (1998) Small intestinal submucosa: a tissue-derived extracellular matrix that promotes tissue-specific growth and differentiation of cells in vitro. *Tissue Eng* 4:157–174
102. Lantz GC, Blevins WE, Badylak SF, Coffey AC, Geddes LA (1990) Small intestinal submucosa as a small-diameter arterial graft in the dog. *J Investig Surg* 3:217–227
103. Lantz GC, Badylak SF, Coffey AC, Geddes LA, Sandusky GE (1992) Small intestinal submucosa as a superior vena cava graft in the dog. *J Surg Res* 53:175–181
104. Kropp BP, Sawyer BD, Shannon HE, Rippy MK, Badylak SF, Adams MC, Keating MA et al (1996) Characterization of small intestinal submucosa regenerated canine detrusor: assessment of reinnervation, in vitro compliance and contractility. *J Urol* 156:599–607
105. Kropp BP, Rippy MK, Badylak SF, Adams MC, Keating MA, Rink RC, Thor KB (1996) Regenerative urinary bladder augmentation using small intestinal submucosa: urodynamic and histopathologic assessment in long-term canine bladder augmentations. *J Urol* 155:2098–2104
106. Gabouev AI, Schultheiss D, Mertsching H, Koppe M, Schlote N, Wefer J, Jonas U et al (2003) In vitro construction of urinary bladder wall using porcine primary cells reseeded on acellularized bladder matrix and small intestinal submucosa. *Int J Artif Organs* 26:935–942
107. Fiala R, Vidlar A, Vrtal R, Belej K, Student V (2007) Porcine small intestinal submucosa graft for repair of anterior urethral strictures. *Eur Urol* 51:1702–1708 discussion 1708
108. Albers P (2007) Tissue engineering and reconstructive surgery in urology. *Eur Urol* 52:1579
109. Hoepfner J, Crnogorac V, Marjanovic G, Juttner E, Karcz W, Weiser HF, Hopt UT (2009) Small intestinal submucosa as a bioscaffold for tissue regeneration in defects of the colonic wall. *J Gastrointest Surg* 13:113–119
110. Yi J-S, Lee H-J, Lee H-J, Lee I-W, Yang J-H (2013) Rat peripheral nerve regeneration using nerve guidance channel by porcine small intestinal submucosa. *J Korean Neurosurg Soc* 53:65–71
111. Murphy F, Corbally MT (2007) The novel use of small intestinal submucosal matrix for chest wall reconstruction following Ewing's tumour resection. *Pediatr Surg Int* 23:353–356
112. Kumar V, Ahlawat R, Gupta AK, Sharma RK, Minz M, Sakhuja V, Jha V (2014) Potential of organ donation from deceased donors: study from a public sector hospital in India. *Transpl Int* 27:1007–1014
113. Wainwright DJ (1995) Use of an acellular allograft dermal matrix (AlloDerm) in the management of full-thickness burns. *Burns* 21:243–248
114. Bozuk MI, Fearing NM, Leggett PL (2006) Use of decellularized human skin to repair esophageal anastomotic leak in humans. *JSLs* 10:83–85
115. Lin LM, Lin CC, Chen CL, Lin CC (2014) Effects of an education program on intensive care unit nurses' attitudes and behavioral intentions to advocate deceased donor organ donation. *Transplant Proc* 46:1036–1040
116. Rieder E, Seebacher G, Kasimir MT, Eichmair E, Winter B, Dekan B, Wolner E et al (2005) Tissue engineering of heart valves: decellularized porcine and human valve scaffolds differ importantly in residual potential to attract monocytic cells. *Circulation* 111:2792–2797
117. Granados M, Morticelli L, Andriopoulou S, Kalozoumis P, Pflaum M, Iablonskii P, Glasmacher B et al (2017) Development and characterization of a porcine mitral valve scaffold for tissue engineering. *J Cardiovasc Transl Res* 10:374–390
118. Rana D, Zreiqat H, Benkirane-Jessel N, Ramakrishna S, Ramalingam M (2017) Development of decellularized scaffolds for stem cell-driven tissue engineering. *J Tissue Eng Regen Med* 11:942–965
119. Fang NT, Xie SZ, Wang SM, Gao HY, Wu CG, Pan LF (2007) Construction of tissue-engineered heart valves by using decellularized scaffolds and endothelial progenitor cells. *Chin Med J* 120:696–702
120. Jaramillo M, Yeh H, Yarmush ML, Uygun BE (2017) Decellularized human liver extracellular matrix (hDLM)-mediated hepatic differentiation of human induced pluripotent stem cells (hiPSCs). *J Tissue Eng Regen Med* 12:e1962–e1973
121. Kakabadze Z, Kakabadze A, Chakhunashvili D, Karalashvili L, Berishvili E, Sharma Y, Gupta S (2017) Decellularized human placenta supports hepatic tissue and allows rescue in acute liver failure. *Hepatology* 67:1956–1969
122. Kang YZ, Wang Y, Gao Y (2009) Decellularization technology application in whole liver reconstruct biological scaffold. *Zhonghua Yi Xue Za Zhi* 89:1135–1138
123. Arenas-Herrera JE, Ko IK, Atala A, Yoo JJ (2013) Decellularization for whole organ bioengineering. *Biomed Mater* 8:014106

124. Baptista PM, Vyas D, Moran E, Wang Z, Soker S (2013) Human liver bioengineering using a whole liver decellularized bioscaffold. *Methods Mol Biol* 1001:289–298
125. Ko IK, Peng L, Peloso A, Smith CJ, Dhal A, Deegan DB, Zimmerman C et al (2015) Bioengineered transplantable porcine livers with re-endothelialized vasculature. *Biomaterials* 40:72–79
126. Mao SAGJ, Elgilani FM, De Lorenzo SB, Deeds MC et al (2017) Sustained in vivo perfusion of a re-endothelialized tissue engineered porcine liver. *Int J nTransplant Res Med* 3:031
127. Gilpin A, Yang Y (2017) Decellularization strategies for regenerative medicine: from processing techniques to applications. *Biomed Res Int* 2017:9831534
128. Sohlenius-Sternbeck AK (2006) Determination of the hepatocellularity number for human, dog, rabbit, rat and mouse livers from protein concentration measurements. *Toxicol In Vitro* 20:1582–1586
129. Agmon G, Christman KL (2016) Controlling stem cell behavior with decellularized extracellular matrix scaffolds. *Curr Opin Solid State Mater Sci* 20:193–201
130. Kadota Y, Yagi H, Inomata K, Matsubara K, Hibi T, Abe Y, Kitago M et al (2014) Mesenchymal stem cells support hepatocyte function in engineered liver grafts. *Organogenesis* 10:268–277
131. Hoshiba T, Chen G, Endo C, Maruyama H, Wakui M, Nemoto E, Kawazoe N et al (2016) Decellularized extracellular matrix as an in vitro model to study the comprehensive roles of the ECM in stem cell differentiation. *Stem Cells Int* 2016:6397820
132. Kim M, Choi B, Joo SY, Lee H, Lee JH, Lee KW, Lee S et al (2014) Generation of humanized liver mouse model by transplant of patient-derived fresh human hepatocytes. *Transplant Proc* 46:1186–1190
133. Lee SY, Kim HJ, Choi D (2015) Cell sources, liver support systems and liver tissue engineering: alternatives to liver transplantation. *Int J Stem Cells* 8:36–47
134. Nicolas C, Wang Y, Luebke-Wheeler J, Nyberg SL (2016) Stem cell therapies for treatment of liver disease. *Biomedicine* 4:E2
135. AlZoubi AM, Khalifeh F (2013) The effectiveness of stem cell therapies on health-related quality of life and life expectancy in comparison with conventional supportive medical treatment in patients suffering from end-stage liver disease. *Stem Cell Res Ther* 4:16
136. Sauer V, Roy-Chowdhury N, Guha C, Roy-Chowdhury J (2014) Induced pluripotent stem cells as a source of hepatocytes. *Curr Pathobiol Rep* 2:11–20
137. Moroni F, Mirabella T (2014) Decellularized matrices for cardiovascular tissue engineering. *Am J Stem Cells* 3:1–20
138. Methe K, Backdahl H, Johansson BR, Nayakawde N, Dellgren G, Sumitran-Holgersson S (2014) An alternative approach to decellularize whole porcine heart. *Biores Open Access* 3:327–338
139. Taylor DA, Sampaio LC, Gobin A (2014) Building new hearts: a review of trends in cardiac tissue engineering. *Am J Transplant* 14:2448–2459
140. Weymann A, Loganathan S, Takahashi H, Schies C, Claus B, Hirschberg K, Soos P et al (2011) Development and evaluation of a perfusion decellularization porcine heart model – generation of 3-dimensional myocardial neoscaffolds. *Circ J* 75:852–860
141. Manji RA, Menkis AH, Ekser B, Cooper DK (2012) Porcine bioprosthetic heart valves: the next generation. *Am Heart J* 164:177–185
142. Taylor DA, Parikh RB, Sampaio LC (2017) Bioengineering hearts: simple yet complex. *Curr Stem Cell Rep* 3:35–44
143. Martins AM, Vunjak-Novakovic G, Reis RL (2014) The current status of iPS cells in cardiac research and their potential for tissue engineering and regenerative medicine. *Stem Cell Rev* 10:177–190
144. Al-Awqati Q, Oliver JA (2002) Stem cells in the kidney. *Kidney Int* 61:387–395
145. Bobulescu IA, Moe OW (2006) Na<sup>+</sup>/H<sup>+</sup> exchangers in renal regulation of acid-base balance. *Semin Nephrol* 26:334–344
146. Romagnani P, Remuzzi G, Glasscock R, Levin A, Jager KJ, Tonelli M, Massy Z et al (2017) Chronic kidney disease. *Nat Rev Dis Primers* 3:17088
147. Peired AJ, Sisti A, Romagnani P (2016) Mesenchymal stem cell-based therapy for kidney disease: a review of clinical evidence. *Stem Cells Int* 2016:4798639
148. McKee RA, Wingert RA (2016) Repopulating decellularized kidney scaffolds: an avenue for ex vivo organ generation. *Materials (Basel)* 9:190
149. Figliuzzi M, Bonandrini B, Remuzzi A (2017) Decellularized kidney matrix as functional material for whole organ tissue engineering. *J Appl Biomater Funct Mater* 15:0
150. Yu YL, Shao YK, Ding YQ, Lin KZ, Chen B, Zhang HZ, Zhao LN et al (2014) Decellularized kidney scaffold-mediated renal regeneration. *Biomaterials* 35:6822–6828
151. Du C, Narayanan K, Leong MF, Ibrahim MS, Chua YP, Khoo VM, Wan AC (2016) Functional kidney bioengineering with pluripotent stem-cell-derived renal progenitor cells and decellularized kidney scaffolds. *Adv Healthc Mater* 5:2080–2091
152. Yamanaka S, Yokoo T (2015) Current bioengineering methods for whole kidney regeneration. *Stem Cells Int* 2015:724047
153. Rawlins MD (2004) Cutting the cost of drug development? *Nat Rev Drug Discov* 3:360–364
154. Kola I, Landis J (2004) Can the pharmaceutical industry reduce attrition rates? *Nat Rev Drug Discov* 3:711–715
155. Kaplowitz N (2005) Idiosyncratic drug hepatotoxicity. *Nat Rev Drug Discov* 4:489–499

156. Rizzetto M, Ciancio A (2012) Epidemiology of hepatitis D. *Semin Liver Dis* 32:211–219
157. World Malaria Report (2015) [PDF] WHO. Available at: [http://apps.who.int/iris/bitstream/handle/10665/200018/9789241565158\\_eng.pdf?sequence=1](http://apps.who.int/iris/bitstream/handle/10665/200018/9789241565158_eng.pdf?sequence=1)
158. Smith BW, Adams LA (2011) Nonalcoholic fatty liver disease and diabetes mellitus: pathogenesis and treatment. *Nat Rev Endocrinol* 7:456–465
159. Cusi K (2009) Nonalcoholic fatty liver disease in type 2 diabetes mellitus. *Curr Opin Endocrinol Diabetes Obes* 16:141–149
160. Koppe SWP (2014) Obesity and the liver: nonalcoholic fatty liver disease. *Transl Res: J Lab Clin Med* 164:312–322
161. McGuire S (2016) World cancer report 2014. Geneva, Switzerland: World Health Organization, International Agency for Research on Cancer, WHO press, 2015. *Adv Nutr (Bethesda, MD)* 7:418–419
162. LeCluyse EL, Witek RP, Andersen ME, Powers MJ (2012) Organotypic liver culture models: meeting current challenges in toxicity testing. *Crit Rev Toxicol* 42:501–548
163. Gómez-Lechón MJ, Tolosa L, Conde I, Donato MT (2014) Competency of different cell models to predict human hepatotoxic drugs. *Expert Opin Drug Metab Toxicol* 10:1553–1568
164. Hewitt NJ, Lechón MJG, Houston JB, Hallifax D, Brown HS, Maurel P, Kenna JG et al (2007) Primary hepatocytes: current understanding of the regulation of metabolic enzymes and transporter proteins, and pharmaceutical practice for the use of hepatocytes in metabolism, enzyme induction, transporter, clearance, and hepatotoxicity studies. *Drug Metab Rev* 39:159–234
165. Rowe C, Goldring CEP, Kitteringham NR, Jenkins RE, Lane BS, Sanderson C, Elliott V et al (2010) Network analysis of primary hepatocyte dedifferentiation using a shotgun proteomics approach. *J Proteome Res* 9:2658–2668
166. Bale SS, Golberg I, Jindal R, McCarty WJ, Luitje M, Hegde M, Bhushan A et al (2015) Long-term coculture strategies for primary hepatocytes and liver sinusoidal endothelial cells. *Tissue Eng Part C Methods* 21:413–422
167. Krause P, Saghatolislam F, Koenig S, Unthan-Fechner K, Probst I (2009) Maintaining hepatocyte differentiation in vitro through co-culture with hepatic stellate cells. *In Vitro Cell Dev Biol Anim* 45:205–212
168. Ohno M, Motojima K, Okano T, Taniguchi A (2008) Up-regulation of drug-metabolizing enzyme genes in layered co-culture of a human liver cell line and endothelial cells. *Tissue Eng Part A* 14:1861–1869
169. Tukov FF, Maddox JF, Amacher DE, Bobrowski WF, Roth RA, Ganey PE (2006) Modeling inflammation-drug interactions in vitro: a rat Kupffer cell-hepatocyte coculture system. *Toxicol In Vitro: An Int J Publ Assoc BIBRA* 20:1488–1499
170. Luebke-Wheeler JL, Nedredal G, Yee L, Amiot BP, Nyberg SL (2009) E-cadherin protects primary hepatocyte spheroids from cell death by a caspase-independent mechanism. *Cell Transpl* 18:1281–1287
171. Sakai Y, Yamagami S, Nakazawa K (2010) Comparative analysis of gene expression in rat liver tissue and monolayer- and spheroid-cultured hepatocytes. *Cells Tissues Organs* 191:281–288
172. Godoy P, Hewitt NJ, Albrecht U, Andersen ME, Ansari N, Bhattacharya S, Bode JG et al (2013) Recent advances in 2D and 3D in vitro systems using primary hepatocytes, alternative hepatocyte sources and non-parenchymal liver cells and their use in investigating mechanisms of hepatotoxicity, cell signaling and ADME. *Arch Toxicol* 87:1315–1530
173. Usta OB, McCarty WJ, Bale S, Hegde M, Jindal R, Bhushan A, Golberg I et al (2015) Microengineered cell and tissue systems for drug screening and toxicology applications: evolution of in-vitro liver technologies. *Technology* 3:1–26
174. Chan TS, Yu H, Moore A, Khetani SR, Kehtani SR, Tweedie D (2013) Meeting the challenge of predicting hepatic clearance of compounds slowly metabolized by cytochrome P450 using a novel hepatocyte model, HepatoPac. *Drug Metab Dispos: The Biol Fate Chem* 41:2024–2032
175. Schütte J, Freudigmann C, Benz K, Böttger J, Gebhardt R, Stelzle M (2010) A method for patterned in situ biofunctionalization in injection-molded microfluidic devices. *Lab Chip* 10:2551–2558
176. Baxter GT (2009) Hurel – an in vivo-surrogate assay platform for cell-based studies. *Altern Lab Anim: ATLA* 37(Suppl 1):11–18
177. Guillouzo A, Guguen-Guillouzo C (2008) Evolving concepts in liver tissue modeling and implications for in vitro toxicology. *Expert Opin Drug Metab Toxicol* 4:1279–1294
178. Writing Group M, Mozaffarian D, Benjamin EJ, Go AS, Arnett DK, Blaha MJ, Cushman M, et al (2016) Heart disease and stroke statistics-2016 update: a report from the American heart association. *Circulation*:133:e38–360
179. Duan SZ, Usher MG, Mortensen RM (2008) Peroxisome proliferator-activated receptor-gamma-mediated effects in the vasculature. *Circ Res* 102:283–294
180. Krentz A (2009) Thiazolidinediones: effects on the development and progression of type 2 diabetes and associated vascular complications. *Diabetes Metab Res Rev* 25:112–126
181. Hernandez AV, Usmani A, Rajamanickam A, Moheet A (2011) Thiazolidinediones and risk of heart failure in patients with or at high risk of type 2 diabetes mellitus: a meta-analysis and meta-regression analysis of placebo-controlled randomized clinical trials. *Am J Cardiovasc Drugs* 11:115–128
182. McNeish J (2004) Embryonic stem cells in drug discovery. *Nat Rev Drug Discov* 3:70–80

183. Lu HR, Vlamincx E, Hermans AN, Rohrbacher J, Van Ammel K, Towart R, Pugsley M et al (2008) Predicting drug-induced changes in QT interval and arrhythmias: QT-shortening drugs point to gaps in the ICHS7B guidelines. *Br J Pharmacol* 154:1427–1438
184. Redfern WS, Carlsson L, Davis AS, Lynch WG, MacKenzie I, Palethorpe S, Siegl PK et al (2003) Relationships between preclinical cardiac electrophysiology, clinical QT interval prolongation and torsade de pointes for a broad range of drugs: evidence for a provisional safety margin in drug development. *Cardiovasc Res* 58:32–45
185. Hoffmann P, Warner B (2006) Are hERG channel inhibition and QT interval prolongation all there is in drug-induced torsadogenesis? A review of emerging trends. *J Pharmacol Toxicol Methods* 53:87–105
186. Lacerda AE, Kuryshv YA, Chen Y, Renganathan M, Eng H, Danthi SJ, Kramer JW et al (2008) Alifuzosin delays cardiac repolarization by a novel mechanism. *J Pharmacol Exp Ther* 324:427–433
187. Rodriguez-Menchaca AA, Navarro-Polanco RA, Ferrer-Villada T, Rupp J, Sachse FB, Tristani-Firouzi M, Sanchez-Chapula JA (2008) The molecular basis of chloroquine block of the inward rectifier Kir2.1 channel. *Proc Natl Acad Sci U S A* 105:1364–1368
188. Pouton CW, Haynes JM (2007) Embryonic stem cells as a source of models for drug discovery. *Nat Rev Drug Discov* 6:605–616
189. Braam SR, Tertoolen L, van de Stolpe A, Meyer T, Passier R, Mummery CL (2010) Prediction of drug-induced cardiotoxicity using human embryonic stem cell-derived cardiomyocytes. *Stem Cell Res* 4:107–116
190. Zwi L, Caspi O, Arbel G, Huber I, Gepstein A, Park IH, Gepstein L (2009) Cardiomyocyte differentiation of human induced pluripotent stem cells. *Circulation* 120:1513–1523
191. Otsuji TG, Minami I, Kurose Y, Yamauchi K, Tada M, Nakatsuji N (2010) Progressive maturation in contracting cardiomyocytes derived from human embryonic stem cells: qualitative effects on electrophysiological responses to drugs. *Stem Cell Res* 4:201–213
192. Yoshida Y, Yamanaka S (2010) Recent stem cell advances: induced pluripotent stem cells for disease modeling and stem cell-based regeneration. *Circulation* 122:80–87
193. Liang P, Lan F, Lee AS, Gong T, Sanchez-Freire V, Wang Y, Diecke S et al (2013) Drug screening using a library of human induced pluripotent stem cell-derived cardiomyocytes reveals disease-specific patterns of cardiotoxicity. *Circulation* 127:1677–1691
194. Chen L, El-Sherif N, Boutjdir M (1999) Unitary current analysis of L-type Ca<sup>2+</sup> channels in human fetal ventricular myocytes. *J Cardiovasc Electrophysiol* 10:692–700
195. Eder A, Vollert I, Hansen A, Eschenhagen T (2016) Human engineered heart tissue as a model system for drug testing. *Adv Drug Deliv Rev* 96:214–224
196. Nunes SS, Miklas JW, Liu J, Aschar-Sobbi R, Xiao Y, Zhang B, Jiang J et al (2013) Biowire: a platform for maturation of human pluripotent stem cell-derived cardiomyocytes. *Nat Methods* 10:781–787
197. Hansen A, Eder A, Bonstrup M, Flato M, Mewe M, Schaaf S, Aksehirlioglu B et al (2010) Development of a drug screening platform based on engineered heart tissue. *Circ Res* 107:35–44
198. Champion S, Aubrecht J, Boekelheide K, Brewster DW, Vaidya VS, Anderson L, Burt D et al (2013) The current status of biomarkers for predicting toxicity. *Expert Opin Drug Metab Toxicol* 9:1391–1408
199. Formentini I, Bobadilla M, Haefliger C, Hartmann G, Loghman-Adham M, Mizrahi J, Pomposiello S et al (2012) Current drug development challenges in chronic kidney disease (CKD) – identification of individualized determinants of renal progression and premature cardiovascular disease (CVD). *Nephrol Dial Transplant* 27(Suppl 3):iii81–iii88
200. Miyata T, Kikuchi K, Kiyomoto H, van Ypersele de Strihou C (2011) New era for drug discovery and development in renal disease. *Nat Rev Nephrol* 7:469–477
201. Prunotto M, Gabbiani G, Pomposiello S, Ghiggeri G, Moll S (2011) The kidney as a target organ in pharmaceutical research. *Drug Discov Today* 16:244–259
202. Steimer A, Haltner E, Lehr CM (2005) Cell culture models of the respiratory tract relevant to pulmonary drug delivery. *J Aerosol Med* 18:137–182
203. Klein SG, Serchi T, Hoffmann L, Blomeke B, Gutleb AC (2013) An improved 3D tetra-culture system mimicking the cellular organisation at the alveolar barrier to study the potential toxic effects of particles on the lung. *Part Fibre Toxicol* 10:31
204. Huh D, Matthews BD, Mammoto A, Montoya-Zavala M, Hsin HY, Ingber DE (2010) Reconstituting organ-level lung functions on a chip. *Science* 328:1662–1668
205. Barnes PJ, Bonini S, Seeger W, Belvisi MG, Ward B, Holmes A (2015) Barriers to new drug development in respiratory disease. *Eur Respir J* 45:1197–1207
206. Lancaster MA, Knoblich JA (2014) Organogenesis in a dish: modeling development and disease using organoid technologies. *Science* 345:1247125
207. Medvinsky A, Livesey FJ (2015) On human development: lessons from stem cell systems. *Development* 142:17–20
208. Si-Tayeb K, Lemaigre FP, Duncan SA (2010) Organogenesis and development of the liver. *Dev Cell* 18:175–189
209. Navarro-Alvarez N, Soto-Gutierrez A, Kobayashi N (2010) Hepatic stem cells and liver development. *Methods Mol Biol* 640:181–236
210. Ader M, Tanaka EM (2014) Modeling human development in 3D culture. *Curr Opin Cell Biol* 31:23–28
211. Chistiakov DA (2012) Liver regenerative medicine: advances and challenges. *Cells Tissues Organs* 196:291–312

212. Wang Y, Cui CB, Yamauchi M, Miguez P, Roach M, Malavarca R, Costello MJ et al (2011) Lineage restriction of human hepatic stem cells to mature fates is made efficient by tissue-specific biomatrix scaffolds. *Hepatology* 53:293–305
213. Vyas D, Baptista PM, Brovold M, Moran E, Gaston B, Booth C, Samuel M et al (2017) Self-assembled liver organoids recapitulate hepatobiliary organogenesis in vitro. *Hepatology* 67:750–761
214. Maher JJ, Bissell DM (1993) Cell-matrix interactions in liver. *Semin Cell Biol* 4:189–201
215. Camp JG, Sekine K, Gerber T, Loeffler-Wirth H, Binder H, Gac M, Kanton S et al (2017) Multilineage communication regulates human liver bud development from pluripotency. *Nature* 546:533–538
216. Ma Z, Wang J, Loskill P, Huebsch N, Koo S, Svedlund FL, Marks NC et al (2015) Self-organizing human cardiac microchambers mediated by geometric confinement. *Nat Commun* 6:7413
217. Rosenblum ND (2008) Developmental biology of the human kidney. *Semin Fetal Neonatal Med* 13:125–132
218. Reint G, Rak-Raszewska A, Vainio SJ (2017) Kidney development and perspectives for organ engineering. *Cell Tissue Res* 369:171–183
219. Destefani AC, Sirtoli GM, Nogueira BV (2017) Advances in the knowledge about kidney decellularization and repopulation. *Front Bioeng Biotechnol* 5:34
220. Kaminski MM, Tosic J, Kresbach C, Engel H, Klockenbusch J, Muller AL, Pichler R et al (2016) Direct reprogramming of fibroblasts into renal tubular epithelial cells by defined transcription factors. *Nat Cell Biol* 18:1269–1280
221. Abolbashari M, Agcaoili SM, Lee MK, Ko IK, Aboushwareb T, Jackson JD, Yoo JJ et al (2016) Repopulation of porcine kidney scaffold using porcine primary renal cells. *Acta Biomater* 29:52–61
222. Song JJ, Guyette JP, Gilpin SE, Gonzalez G, Vacanti JP, Ott HC (2013) Regeneration and experimental orthotopic transplantation of a bioengineered kidney. *Nat Med* 19:646–651
223. Taguchi A, Kaku Y, Ohmori T, Sharmin S, Ogawa M, Sasaki H, Nishinakamura R (2014) Redefining the in vivo origin of metanephric nephron progenitors enables generation of complex kidney structures from pluripotent stem cells. *Cell Stem Cell* 14:53–67
224. Dye BR, Miller AJ, Spence JR (2016) How to grow a lung: applying principles of developmental biology to generate lung lineages from human pluripotent stem cells. *Curr Pathobiol Rep* 4:47–57
225. Metzger RJ, Klein OD, Martin GR, Krasnow MA (2008) The branching programme of mouse lung development. *Nature* 453:745–750
226. Herriges M, Morrissy EE (2014) Lung development: orchestrating the generation and regeneration of a complex organ. *Development* 141:502–513
227. Miller AJ, Spence JR (2017) In vitro models to study human lung development, disease and homeostasis. *Physiology (Bethesda)* 32:246–260
228. Rock JR, Onaitis MW, Rawlins EL, Lu Y, Clark CP, Xue Y, Randell SH et al (2009) Basal cells as stem cells of the mouse trachea and human airway epithelium. *Proc Natl Acad Sci U S A* 106:12771–12775
229. Ghaedi M, Calle EA, Mendez JJ, Gard AL, Balestrini J, Booth A, Bove PF et al (2013) Human iPSC cell-derived alveolar epithelium repopulates lung extracellular matrix. *J Clin Invest* 123:4950–4962
230. Dye BR, Hill DR, Ferguson MA, Tsai YH, Nagy MS, Dyal R, Wells JM et al (2015) In vitro generation of human pluripotent stem cell derived lung organoids. *elife* 4:e05098
231. Murphy SV, Atala A (2014) 3D bioprinting of tissues and organs. *Nat Biotechnol* 32:773–785
232. Klein GT, Lu Y, Wang MY (2013) 3D printing and neurosurgery – ready for prime time? *World Neurosurg* 80:233–235
233. Ozbolat IT, Yu Y (2013) Bioprinting toward organ fabrication: challenges and future trends. *IEEE Trans Biomed Eng* 60:691–699
234. Cui X, Boland T, D’Lima DD, Lotz MK (2012) Thermal inkjet printing in tissue engineering and regenerative medicine. *Recent Pat Drug Deliv Formul* 6:149–155
235. Zhang YS, Yue K, Aleman J, Mollazadeh-Moghaddam K, Bakht SM, Yang J, Jia W et al (2017) 3D bioprinting for tissue and organ fabrication. *Ann Biomed Eng* 45:148–163
236. Jana S, Tefft BJ, Spoon DB, Simari RD (2014) Scaffolds for tissue engineering of cardiac valves. *Acta Biomater* 10:2877–2893
237. Chambers J (2014) Prosthetic heart valves. *Int J Clin Pract* 68:1227–1230
238. Sodian R, Weber S, Markert M, Rassouljan D, Kaczmarek I, Lueth TC, Reichart B et al (2007) Stereolithographic models for surgical planning in congenital heart surgery. *Ann Thorac Surg* 83:1854–1857
239. Sodian R, Schmauss D, Markert M, Weber S, Nikolaou K, Haerberle S, Vogt F et al (2008) Three-dimensional printing creates models for surgical planning of aortic valve replacement after previous coronary bypass grafting. *Ann Thorac Surg* 85:2105–2108
240. Sodian R, Weber S, Markert M, Loeff M, Lueth T, Weis FC, Daebritz S et al (2008) Pediatric cardiac transplantation: three-dimensional printing of anatomic models for surgical planning of heart transplantation in patients with univentricular heart. *J Thorac Cardiovasc Surg* 136:1098–1099
241. Sodian R, Schmauss D, Schmitz C, Bigdeli A, Haerberle S, Schmoekkel M, Markert M et al (2009) 3-dimensional printing of models to create custom-made devices for coil embolization of an anastomotic leak after aortic arch replacement. *Ann Thorac Surg* 88:974–978
242. Schmauss D, Schmitz C, Bigdeli AK, Weber S, Gerber N, Beiras-Fernandez A, Schwarz F et al (2012) Three-dimensional printing of models for preoperative planning and simulation of transcatheter valve replacement. *Ann Thorac Surg* 93:e31–e33



243. Schmauss D, Gerber N, Sodian R (2013) Three-dimensional printing of models for surgical planning in patients with primary cardiac tumors. *J Thorac Cardiovasc Surg* 145:1407–1408
244. Sodian R, Loebe M, Hein A, Martin DP, Hoerstrup SP, Potapov EV, Hausmann H et al (2002) Application of stereolithography for scaffold fabrication for tissue engineered heart valves. *ASAIO J* 48:12–16
245. Schaefermeier PK, Szymanski D, Weiss F, Fu P, Lueth T, Schmitz C, Meiser BM et al (2009) Design and fabrication of three-dimensional scaffolds for tissue engineering of human heart valves. *Eur Surg Res* 42:49–53
246. Duan B, Hockaday LA, Kang KH, Butcher JT (2013) 3D bioprinting of heterogeneous aortic valve conduits with alginate/gelatin hydrogels. *J Biomed Mater Res A* 101:1255–1264
247. Duan B, Kapetanovic E, Hockaday LA, Butcher JT (2014) Three-dimensional printed trileaflet valve conduits using biological hydrogels and human valve interstitial cells. *Acta Biomater* 10:1836–1846
248. Cohen S, Leor J (2004) Rebuilding broken hearts. Biologists and engineers working together in the fledgling field of tissue engineering are within reach of one of their greatest goals: constructing a living human heart patch. *Sci Am* 291:44–51
249. Silvestri A, Boffito M, Sartori S, Ciardelli G (2013) Biomimetic materials and scaffolds for myocardial tissue regeneration. *Macromol Biosci* 13:984–1019
250. Cho GS, Fernandez L, Kwon C (2014) Regenerative medicine for the heart: perspectives on stem-cell therapy. *Antioxid Redox Signal* 21:2018–2031
251. Radisic M, Malda J, Epping E, Geng W, Langer R, Vunjak-Novakovic G (2006) Oxygen gradients correlate with cell density and cell viability in engineered cardiac tissue. *Biotechnol Bioeng* 93:332–343
252. Yeong WY, Sudarmadji N, Yu HY, Chua CK, Leong KF, Venkatraman SS, Boey YC et al (2010) Porous polycaprolactone scaffold for cardiac tissue engineering fabricated by selective laser sintering. *Acta Biomater* 6:2028–2034
253. Gaetani R, Doevendans PA, Metz CH, Alblas J, Messina E, Giacomello A, Sluijter JP (2012) Cardiac tissue engineering using tissue printing technology and human cardiac progenitor cells. *Biomaterials* 33:1782–1790
254. Pati F, Jang J, Ha DH, Won Kim S, Rhee JW, Shim JH, Kim DH et al (2014) Printing three-dimensional tissue analogues with decellularized extracellular matrix bioink. *Nat Commun* 5:3935
255. Homan KA, Kolesky DB, Skylar-Scott MA, Herrmann J, Obuobi H, Moisan A, Lewis JA (2016) Bioprinting of 3D convoluted renal proximal tubules on perfusable chips. *Sci Rep* 6:34845
256. Horvath L, Umehara Y, Jud C, Blank F, Petri-Fink A, Rothen-Rutishauser B (2015) Engineering an in vitro air-blood barrier by 3D bioprinting. *Sci Rep* 5:7974
257. Badawy A, Hamaguchi Y, Satoru S, Kaido T, Okajima H, Uemoto S (2017) Evaluation of safety of concomitant splenectomy in living donor liver transplantation: a retrospective study. *Transpl Int* 30:914–923
258. Athanasiou A, Papalois A, Kontos M, Griniatsos J, Liakopoulos D, Spartalis E, Agrogiannis G et al (2017) The beneficial role of simultaneous splenectomy after extended hepatectomy: experimental study in pigs. *J Surg Res* 208:121–131
259. Troisi RI, Berardi G, Tomassini F, Sainz-Barriga M (2017) Graft inflow modulation in adult-to-adult living donor liver transplantation: a systematic review. *Transplant Rev (Orlando)* 31:127–135
260. Okabe H, Yoshizumi T, Ikegami T, Uchiyama H, Harimoto N, Itoh S, Kimura K et al (2016) Salvage splenic artery embolization for saving falling living donor graft due to portal overflow: a case report. *Transplant Proc* 48:3171–3173
261. Scatton O, Cauchy F, Conti F, Perdigo F, Massault PP, Goumard C, Soubrane O (2016) Two-stage liver transplantation using auxiliary laparoscopically harvested grafts in adults: emphasizing the concept of “hypersmall graft nursing”. *Clin Res Hepatol Gastroenterol* 40:571–574
262. Committee for Advanced Therapies (CAT). [http://www.ema.europa.eu/ema/index.jsp?curl=pages/about\\_us/general/general\\_content\\_000266.jsp&mid=WC0b01ac05800292a4](http://www.ema.europa.eu/ema/index.jsp?curl=pages/about_us/general/general_content_000266.jsp&mid=WC0b01ac05800292a4)
263. Kinaci E, Kayaalp C (2017) Systematic review for small-for-size syndrome after liver transplantation-chamber of secrets: reply. *World J Surg* 41:343–344
264. Salman A, El-Garem N, Sholkamy A, Hosny K, Abdelaziz O (2016) Exploring portal vein hemodynamic velocities as a promising, attractive horizon for small-for-size syndrome prediction after living-donor liver transplantation: an egyptian center study. *Transplant Proc* 48:2135–2139
265. Ikegami T, Yoshizumi T, Sakata K, Uchiyama H, Harimoto N, Harada N, Itoh S et al (2016) Left lobe living donor liver transplantation in adults: what is the safety limit? *Liver Transpl* 22:1666–1675
266. Ito D, Akamatsu N, Togashi J, Kaneko J, Arita J, Hasegawa K, Sakamoto Y et al (2016) Behavior and clinical impact of ascites after living donor liver transplantation: risk factors associated with massive ascites. *J Hepatobiliary Pancreat Sci* 23:688–696
267. Halazun KJ, Przybyszewski EM, Griesemer AD, Cherqui D, Michelassi F, Guarrera JV, Kato T et al (2016) Leaning to the left: increasing the donor pool by using the left lobe, outcomes of the largest single-center north american experience of left lobe adult-to-adult living donor liver transplantation. *Ann Surg* 264:448–456
268. Pomposelli JJ, Goodrich NP, Emond JC, Humar A, Baker TB, Grant DR, Fisher RA et al (2016) Patterns of early allograft dysfunction in adult live donor liver transplantation: the a2all experience. *Transplantation* 100:1490–1499



# Mussel-Inspired Biomaterials for Cell and Tissue Engineering

# 24

Min Lu and Jiashing Yu

## Abstract

In designing biomaterial for regenerative medicine or tissue engineering, there are a variety of issues to consider including biocompatibility, biochemical reactivity, and cellular interaction etc. Mussel-inspired biomaterials have received much attention because of its appealing features including strong adhesiveness on moist surfaces, enhancement of cell adhesion, immobilization of bioactive molecules and its amenability to post-functionalization via catechol chemistry. In this review chapter, we give a brief introduction on the basic principles of mussel-inspired polydopamine coating, catechol conjugation, and discuss how their features play a vital role in biomedical application. Special emphasis is placed on tissue engineering and regenerative applications. We aspire to give readers of this book a comprehensive insight into mussel-inspired biomaterials that can facilitate them make significant contributions in this promising field.

## Keywords

Mussel-inspired · Polydopamine · Catechol conjugation · Tissue engineering · Biomedical application

## 24.1 Introduction

The mussel-inspired adhesive mechanism was first introduced by Waite et al. in the 1980s [59]. Marine mussel is renowned for its capability of adhering to various kinds of substrates chemically and physically under moist condition [28]. The previous study demonstrated that this adhesion was due to *Mytilus edulis* foot protein (Mefp), which have the reactive catechol-containing compound 3,4-dihydroxyphenyl-L-alanine (DOPA) and lysine, distributed at the interface between protein and substrates [54, 74]. The ortho-dihydroxyphenyl group of catechol, is responsible for the superior adhesiveness to a wide range of organic and inorganic surfaces [29, 30].

Inspired by this property, plenty of polydopamine coating methods and modified polymers using chemicals with catechol functional groups were developed [38]. Dopamine can exhibit self-polymerization under alkaline conditions to form polydopamine layer on almost all types of organic and inorganic materials [29]. Examples include PDMS [44], PVA [3], PLGA [75] titanium oxide surface [61] and biomaterial scaffold [40, 57]. Another method is catechol conjugation onto

---

M. Lu (✉) · J. Yu  
Biomedical and Tissue Engineering Laboratory,  
Department of Chemical Engineering, National  
Taiwan University, Taipei, Taiwan  
e-mail: B02504041@nut.edu.tw; jiayu@ntu.edu.tw

polymer backbones [49]. There are many developed materials for such approach, including PEG-catechol [31], PEI-catechol [50], chitosan-catechol [49], alginate-catechol [20, 72] and so on.

Polydopamine coating and catechol conjugation enable materials to attain desirable properties and the potential for secondary reaction. For instance, catechol conjugation is a simple method that enhances hydrophilicity or water solubility [23]. Catechol groups permit metal chelation [64] and metal-mediated crosslinking [54], and zwitterionicity of polydopamine provide more versatile application [69]. Furthermore, catechol groups are partially oxidative, which become o-quinone groups that are able to react with amino and thiol groups, facilitating biomolecular adsorption and immobilizations [29, 58]. These characteristics are significant in biomaterial design especially in tissue engineering, because physiochemical interactions between substrates and cell would have impact on cellular functions such as spreading, migration, proliferation and differentiation [62].

In addition, with biomolecules containing thiol or amine groups and various secondary reactions, polydopamine and catechol conjugated derivatives provide novel alternatives for surface immobilization [13, 29]. Studies have reported versatile immobilization of biomolecules such as protein (H.-W. [10]), growth factor [45], peptide [9] and heparin [68]. This functionalization enables polydopamine coating and catechol conjugated derivatives to be utilized for different biomedical applications, such as tissue adhesive [50], antifouling [14], antibacterial activity [55], blood compatibility [68] and drug delivery [34]. The mussel-inspired chemistry brings a wide range of diversity to biomedical fields and have attracted much attention.

The aim of this review chapter is to outline the results of previous research in mussel-inspired biomaterials. In the first section, we will introduce mussel-inspired adhesive property, coating mechanism and catechol derivatives' reactivity, and the mechanism of better cell adhesion. In the next section, cellular interaction and application in tissue engineering will be emphasized. Finally,

other kind biomedical application designed by novel immobilization of biomolecule will be discussed.

---

## 24.2 Principles and Features of Mussel-Inspired Polydopamine Coating and Catechol Conjugation

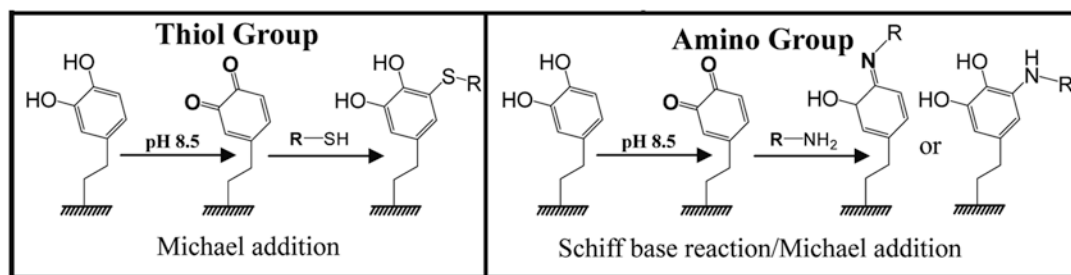
Previous studies have reported that mussel-inspired surface modification or catechol conjugation could improve the functionality of organic and inorganic surfaces and modify unfavorable properties. Here, we list the important features of polydopamine and catechol conjugation that makes mussel-inspired chemistry advantageous in many applications.

### 24.2.1 Attachment Mechanism

Mussel-inspired adhesion is superior due to its moisture-resistant adhesion and its applicability to organic and inorganic surface. In this part, we delve into the chemistry principle behind it, and why this kind of attachment can be multifunctional. There are two major attachment mechanisms: (i) Covalent binding and (ii) noncovalent binding.

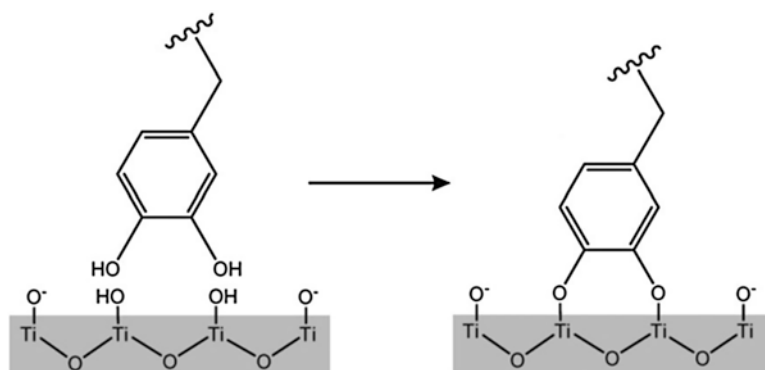
When it comes to mechanisms for adhesion to organic surfaces, the majority relies on the reaction where catechol groups in polydopamine or modified polymers were oxidative and then became o-quinone groups under alkaline condition. This reaction causes covalent binding to organic surfaces that contain amine and/ or thiol groups via aryl-aryl coupling or possibly via Michael-type addition and/or Schiff base reactions (Fig. 24.1) [33, 38, 65].

On the other hand, noncovalent binding interaction such as metal coordination or chelating, hydrogen bonding,  $\pi$ - $\pi$  stacking of the aromatic rings in the dopamine [1, 6, 60, 67] forces polydopamine to form an effective layer over inorganic or metal surfaces. Metal ions like  $\text{Fe}^{3+}$ ,  $\text{Mn}^{2+}$ ,  $\text{Zn}^{2+}$ , and  $\text{Cu}^{2+}$ , etc., can chelate with catechol groups, and metal or metal oxide surfaces



**Fig. 24.1** Typical chemical reactions of catechol groups [65]

**Fig. 24.2** The proposed mechanism of dopamine binding to  $\text{TiO}_2$  surfaces, resulting in the depletion of surface  $\text{Ti-OH}$  groups [15]



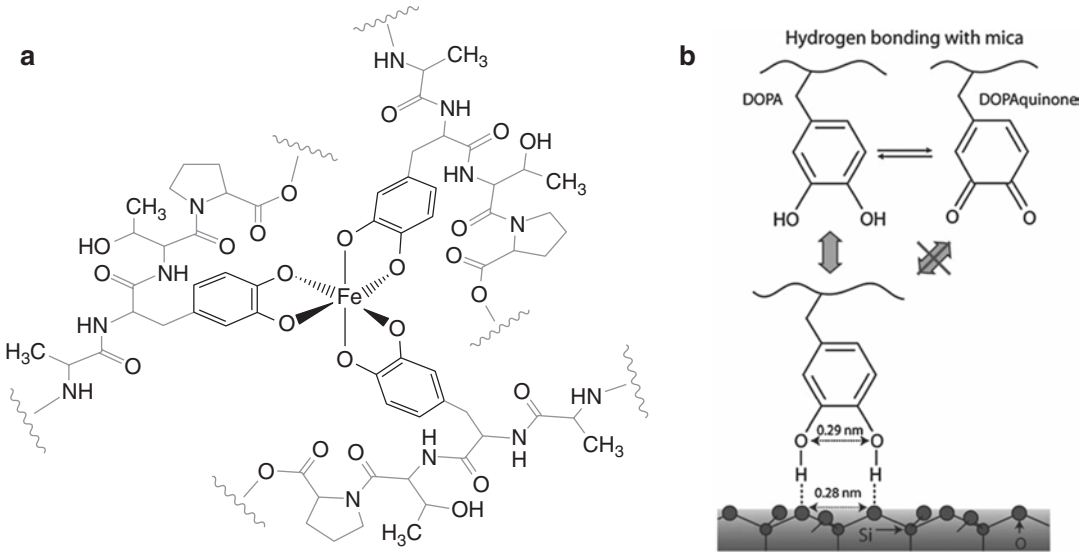
are usually hydroxylated or hydrated under ambient conditions. Coordination and chelate bonding contribute to the adhesion of polydopamine on metal or metal oxide surfaces [67]. Take pervasively used  $\text{TiO}_2$  surface as an example. Messersmith et al. reported that there was the reduction of hydroxyl groups in catechol groups on  $\text{TiO}_2$  surface (Fig. 24.2) [15]. Catechol groups reacted with the surface  $\text{Ti-OH}$ , leading to dehydration and a charge-transfer complex [46, 67]. As a result, some research determined that adhesion increase is roughly proportionally to the increase in dopamine content, however, o-quinone groups exhibit much lower adhesion to metal surfaces than parent catechol groups [53]. This fact also explains the attachment mechanism with metal surfaces. Another example is physical crosslinking vis ferric-ion. Studies demonstrated that the iron center crosslinks with three dopamine residues as shown in Fig. 24.3 [54]. Moreover, hydrogen bonding also contributes another kind of adhesion. The interaction on mica with catechol is the hydrogen bonding of the catecholic OH groups to the oxygen atoms of

the mica surface [42]. Nevertheless, since this has to compete with the surrounding water molecule, it is weaker than previous attachment mechanism.

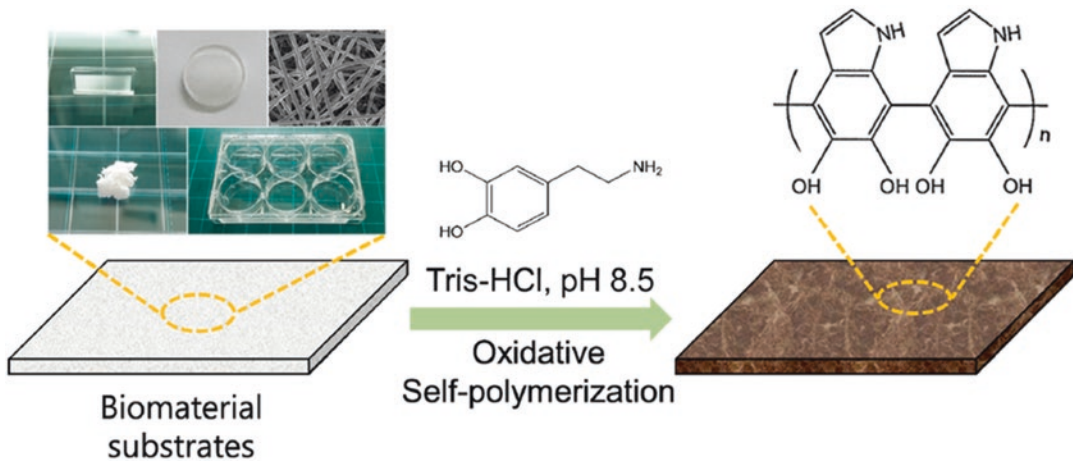
The versatile adhesive properties enable polydopamine and catechol conjugated polymers to serve as tissue adhesive, sealant, surface coating and immobilization of biomolecules. Therefore, with this foundation, we will further discuss the coating mechanisms, ideal features after coated onto material surfaces and how they are related to recent applications.

### 24.2.2 Coating Mechanism

Previous studies have reported that dopamine monomer can undergo self-polymerization under some alkaline condition. The solution oxidative method to produce polydopamine coating on different types of substrates is the most widely investigated. Among all coating methods, the most commonly used is dipping the materials into pH 8.5 Tris-HCl buffer at room temperature



**Fig. 24.3** (a) Proposed mussel adhesive ferric-ion crosslinking and (b) illustration of the proposed binding mechanism of dopamine to mica surfaces [67]



**Fig. 24.4** Polymerization of dopamine at pH = 8.5 [41]

(Fig. 24.4) [29, 32]. Aside from the reaction environment, to successfully fabricate a polydopamine layer onto materials' surface, the concentration of dopamine monomer must be higher than 2 mg/mL [38]. The thickness of the layer can be controlled by tuning the concentration and coating time. However, the maximum thickness of polydopamine layer in a single reaction step is approxi-

mately 50 nm [4]. Higher concentration of the monomer or longer coating time does not increase the thickness of the layer. With the advantages of simple coating mechanism and applicability to wide range of substrates, polydopamine coating play a pivotal role in surface modification of biomaterials such as membrane, scaffold and medical device for biomedical application.

## 24.3 Appealing Characteristics

After the discussion about the fabrication of polydopamine, the reason why this mussel-inspired coating is superior and widely used must be explained. In this section, the hydrophilicity, pH-sensitive charge and useful reactivity for post-functionalization will be discussed, including their principle, application and related researches (Table 24.1).

### 24.3.1 Hydrochemistry

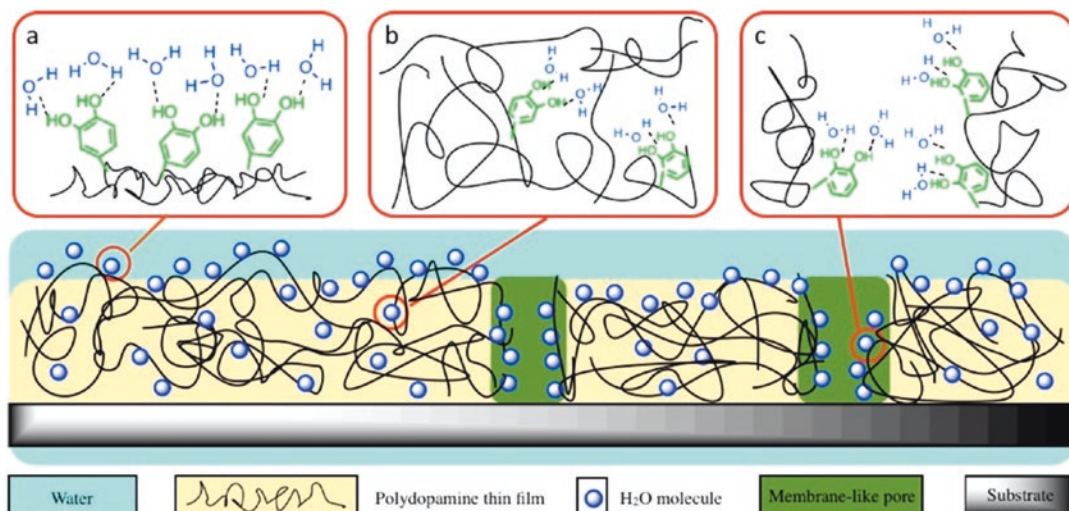
Hydrophilicity is desirable for biomaterials in biomedical application. Hydrophilic surfaces are favored for cell adhesion and this property can be used in tissue engineering compared to hydrophobic substrates [41]. When biomaterials are implanted into human body, it inevitably comes in contact with tissue fluid. The hydrophilicity of surface thus has important influence on cellular response [76]. As a result, to fabricate different kinds of biomaterials with preferred hydrophilicity, many substrates are equipped with polydopamine coating to change their initial hydrophobicity.

There are numerous related researches on the relation between hydrophilicity and the angle of water contact. For instance, Ku et al. reported that by depositing polydopamine on PDMS, PTFE and silicone rubber, their water contact angle decreased by 39°, 49.8° and 35.6° respectively [27]. In another study, Wang et al. showed surfaces coated with polydopamine, the water contact angle increased about 51° than before. The largely decreased contact angle represented that a better hydrophilic surface was obtained, which is beneficial for a biological response [76]. Ku et al. also deposited polydopamine coating on PCL nanofiber scaffold, and observed decreases in the water contact angle for about 76.9°. The polydopamine coating turned the PCL hydrophobicity into hydrophilicity [26].

According to these studies, we conclude that the polydopamine coating can indeed change the hydrochemistry of many types of materials. The hydrochemistry and hydration of polydopamine film has been investigated in a recent research of Zhang et al. where it was pointed out that there might be three types of hydration effects (Fig. 24.5): (i) Hydroxyl groups in polydopamine on the surface would attract water molecules to form hydrogen bonds with water molecules [71].

**Table 24.1** Appealing characteristics of mussel-inspired coating

Appealing characteristics		
	Brief description	Example
Hydrochemistry	Make various substrates more hydrophilic by conjugating catechol groups which can form hydrogen bond in fluid.	1. Reduce water contact angle of various kinds of surface. 2. Improve hydrophilicity of biomaterials to improve cell adhesion and cellular response.
pH-switchable charge	This pH-sensitive charge enables polydopamine to exhibit reversible selectivity for both cations and anions.	1. pH < 4, polydopamine will become positively charged. 2. pH > 4, polydopamine will be negatively charged.
Reactivity of catechol groups	Under alkaline conditions, the catechol groups would be oxidized into the quinone groups, which can react with the nucleophilic amine groups via Schiff base reaction or Michael-type addition. As for thiol-containing molecules, they can react with quinone groups through Michael-type addition.	1. Amenable to design for various applications including immobilization of peptides, growth factors or other biomolecules. 2. Allow biomaterials attach to organic or inorganic surfaces via Schiff base reaction or Michael-type addition, metal coordination or chelating, hydrogen bonding.



**Fig. 24.5** The hydration of polydopamine thin films: (a) surface hydration, (b) bulk hydration, and (c) diffusion of water into the nanopores of polydopamine films [73]

(ii) Some water molecules may be trapped into polydopamine film during the polymerization.  
 (iii) Polydopamine film has a porous structure that the water molecules can penetrate or diffuse [5, 43]. In summary, the hydrophilicity and biocompatibility of polydopamine may serve as an ideal platform for cell adhesion or a water-based lubricant for tissue engineering. For example, the coating can reduce the contact stresses and friction to protect the biomaterials from wear and tear [73].

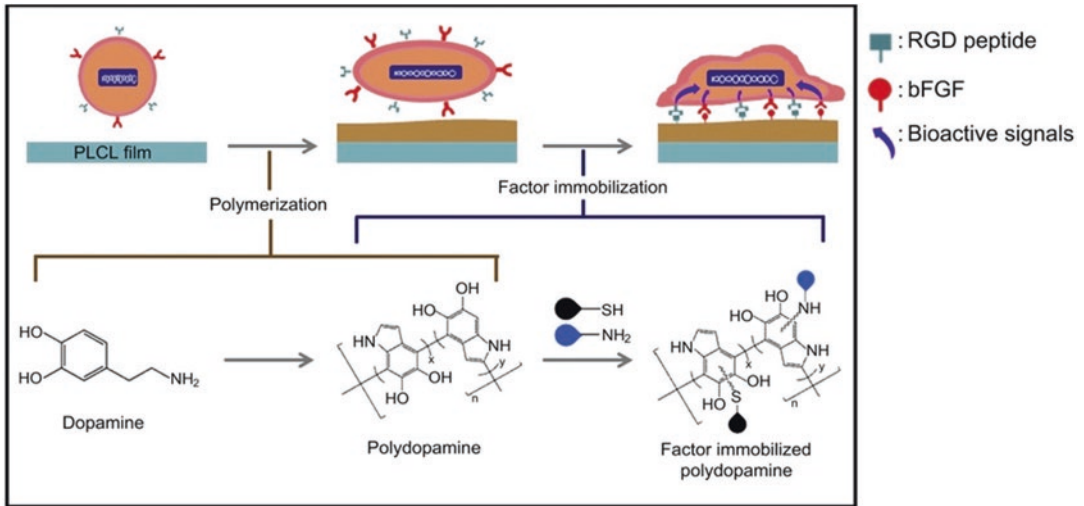
### 24.3.2 pH-Switchable Charge

Polydopamine and its monomer with amino groups and phenolic hydroxyl groups can undergo zwitterionicity. This pH-sensitive charge enables polydopamine to exhibit reversible selectivity for both cations and anions [69]. The isoelectric point is determined to be around pH 4. For pH value lower than 4, the amino groups will be protonated and polydopamine will become positively charged. On the other hand, for pH values higher than 4, polydopamine will be negatively charged due to the deprotonation of the phenolic groups [37].

### 24.3.3 Reactivity and Post-functionalization

The mussel-inspired chemistry mainly relies on the reactivity of catechol groups or quinone groups after oxidation in polydopamine. In this section, we will discuss the chemical reactivity and the secondary reactions after polymerization or catechol conjugation. The post-functionalization is amenable to design for various applications. For instance, biomolecules can be immobilized onto polydopamine-coated substrates or catechol-conjugated polymers. Another example is that catechol-conjugated polymers can adhere to almost all types material surfaces via catechol chemistry. We will briefly introduce the mechanism and some related researches.

First, the most widely investigated reactions are polydopamine that reacts with the amine and/or thiol containing molecules. Under alkaline conditions, the catechol groups would be oxidized into the quinone groups, which can react with the nucleophilic amine groups via Schiff base reaction or Michael-type addition. As for thiol-containing molecules, these nucleophiles are most likely to react with quinone groups through Michael addition reaction [29]. There are



**Fig. 24.6** Schematic diagram of polydopamine-mediated immobilization of bioactive molecules [36]

several researches that utilize this mechanism to immobilize biomolecules. Lee et al. developed a polydopamine-coated poly(lactide-co-caprolactone) substrate to immobilize a cell adhesive peptide, RGD, and an angiogenic growth factor, bFGF (Fig. 24.6). With the immobilization of these biomolecules, better cell adhesion, proliferation and differentiation can be achieved, and these biomaterial may serve as endothelial vascular graft materials [36].

Secondly, catechol conjugated methods also have versatile applications. Lee et al. reported a non-fouling surface fabricated by simply immersing substrates into an aqueous solution of catechol-grafted poly(ethylene) glycol. In contrast to PEG derivatives' limited applicability, this catechol-g-PEG can apply PEGylation on various substrates [31]. Kim et al. developed a catechol-conjugated chitosan to enhance the mucoadhesive property. The catechol groups in hydrocaffeic could be easily conjugated onto chitosan via EDC reaction mechanism, and can form covalent bonding with amines and thiols in mucin [22].

In the following sections, we will discuss how polydopamine or catechol groups interact with cell. Furthermore, we select some influential

mussel-inspired studies, focusing on tissue engineering and other biomedical application.

## 24.4 Cellular Interaction and Application in Tissue Engineering

Many patients suffer from damage or loss of organs/tissue caused by disease or accident. With advanced understanding in cellular biology and development of biomaterials, many researchers have delved into the study of tissue engineering to realize the possibility of replacing damaged human organs with artificial organs and without the concern of immune response [11]. Amongst various biomaterial designs, mussel-inspired biomaterials for tissue engineering and regenerative medicine have attracted much attention due to its advantages such as ideal cell adhesion and immobilization of bioactive molecules. We will discuss tissue engineering researches in bone and vascular tissue regeneration, and some researches about wound healing and cell pattern will also be introduced. Finally, the reason why polydopamine or catechol-conjugated materials have ideal cell adhesion will be explained as followed.



### 24.4.1 Bone Tissue Regeneration and Mineralization

In a world with ever advancing medical technology and healthcare quality, problems associated with aging population have become an important issue. For example, due to injuries there will be more people in need of bone tissue repair [63]. In this part, we discuss researches related to bone regeneration or remineralization, and how mussel-inspired biomaterials are applied in this field.

First, we list some studies that directly utilize properties of polydopamine without immobilization of biomolecules. Rim et al. fabricated poly(L-lactide) electrospun fibers coated with polydopamine. The fibrous structure mimicked the structure of natural bones' extracellular matrix, and the polydopamine coating not only supported the proliferation of human mesenchymal stem cells (hMSCs), but in contrast with the unmodified poly(L-lactide) fibers, also enhanced osteogenic differentiation and calcium mineralization of hMSCs. They concluded that this polydopamine-coated biodegradable fiber is promising for regulating stem cell functions for bone tissue regeneration [47].

Zhou et al. coated polydopamine onto demineralized dentin surface to investigate whether polydopamine can help the latter undergo remineralization. They found that polydopamine could promote remineralization and since catecholamine moieties in polydopamine could bond to  $\text{Ca}^{2+}$ , they facilitate the formation of hydroxyapatite crystals which occupies the surface of dentin's hole. This result demonstrates that coating polydopamine on dentin tissue could be a potentially promising technique for tooth remineralization [78] (Table 24.2).

Zhang et al. prepared dopamine-conjugated alginate beads and fibers to evaluate the influence of polydopamine on cell viability of bone marrow stem cells. The result showed that the  $\text{Ca}^{2+}$  crosslinked dopamine-alginate gel is ideal for cell proliferation and osteogenic differentiation in vitro via PCR and alkaline phosphatase activity assays (Fig. 24.7) [72].

Ma et al. fabricated a 3D-printed bioceramic porous scaffold coated with self-assembled calcium-phosphate/polydopamine layer, which stimulates bone regeneration in vivo. This is a reflection of the characteristics of surface roughness, hydrophilicity, hydroxyl and amino groups provided by polydopamine that enhances cell adhesion and proliferation of rabbit bone mesenchymal stem cells. Furthermore, catechol groups can promote apatite nucleation and mineralization of surfaces, which enhances the differentiation of cells (Fig. 24.8) [40].

Immobilization of bioactive molecules is also a commonly used method in mussel-inspired chemistry. Chien and Tsai designed a one-pot surface modified method that mixed RGD-conjugated poly(ethyleneimine), hydroxyapatite (HA) and bone morphogenic protein-2 (BMP-2) with dopamine solution under alkaline condition. By the facile method, the immobilization of RGD peptides, HA and BMP-2 could be easily achieved. RGD peptides could enhance the adhesion and proliferation of human bone marrow stem cells. HA was able to facilitate osteodifferentiation of cells, and osteoinductive BMP-2 that induces osteogenesis on modified titanium surface with polydopamine (Fig. 24.9). This result demonstrated that this surface modification method has a promising potential for the application of osteointegrative orthopedic and dental implants [9].

Numerous recent researches focus on porous or fibrous scaffold with immobilization of biomolecules via catechol chemistry. Ko et al. fabricated a polydopamine-coated poly(lactic-co-glycolic acid) (PLGA) scaffold with the immobilization of BMP-2. This scaffold promoted the osteogenic differentiation and mineralization of human adipose-derived stem cells (hASCs) in vitro and in vivo. The implantation of scaffold with hASCs enhanced the in vivo bone formation in critical-sized calvarial bone defects (Fig. 24.10) [24]. Zhao et al. developed BMP-2 immobilized PLGA/hydroxyapatite fibrous scaffold via polydopamine coating that enhanced osteogenic differentiation [75].

As another example, Lee et al. fabricated a 3D-printed polycaprolactone (PCL) scaffold immobilizing rhBMP-2 via polydopamine coat-

**Table 24.2** Application in tissue engineering of mussel-inspired biomaterials

Application in tissue engineering				
Field	Research method and feature	Cell type	Result	References
Bone tissue regeneration and mineralization	Coating polydopamine onto the PLA fibers with fibrous structure	hMSC	Supported the proliferation and also enhanced osteogenic differentiation and calcium mineralization of hMSCs in contrast to the unmodified fibers.	[47]
	Coating polydopamine onto demineralized dentin surface to investigate of whether polydopamine can help undergo remineralization	N/A	Polydopamine could promote remineralization since catecholamine moieties in polydopamine could bond to Ca <sup>2+</sup> that facilitate the formation of hydroxyapatite crystals which occupies the surface of dentin's hole.	[78]
	Dopamine-coated alginate beads and fibers	BMSC	The Ca <sup>2+</sup> crosslinked dopamine-alginate gel is ideal for cell proliferation and osteogenic differentiation in vitro.	[72]
	3D-printed bioceramic porous scaffold coated with self-assembled calcium-phosphate/polydopamine layer	rBMSC	The characteristics of surface roughness, hydrophilicity, hydroxyl and amino groups provided by polydopamine that enhances cell adhesion and proliferation of rBMSC. Catechol groups can promote apatite nucleation and mineralization of surfaces, which enhances the differentiation of cells.	[40]
	Immobilizing RGD peptides, HAP and BMP-2 with dopamine solution under alkaline condition via a one-pot surface modified method	hBMSC	RGD peptides could enhance the adhesion and proliferation of hBMSC. HA could facilitate osteodifferentiation of cells, and osteoinductive BMP-2 induces osteogenesis on modified titanium surface with polydopamine.	[9]
	Fabricated a PLGA scaffold with the immobilization of BMP-2 via polydopamine coating	hASC	This scaffold promoted the osteogenic differentiation and mineralization of hASCs in vitro and in vivo and enhanced the in vivo bone formation in critical-sized calvarial bone defects.	[24]
	Developed BMP-2 immobilized PLGA/hydroxyapatite fibrous scaffold via polydopamine coating	MC3T3-E1	BMP-2-immobilized scaffold greatly promoted the attachment and proliferation of MC3T3-E1 cells. Furthermore, the ALP activity, mRNA expression of osteosis-related genes and calcium deposition in MC3T3-E1 cells cultured on BMP-2-immobilized scaffold were significantly increased.	[75]

(continued)

**Table 24.2** (continued)

Application in tissue engineering				
Field	Research method and feature	Cell type	Result	References
	Fabricated a 3D-printed PCL scaffold immobilizing ABMP-2 via polydopamine coating	rMSC	The microporous structure and immobilized ABMP-2 of this 3D scaffold not only promoted cell proliferation but also released ABMP-2 in a controlled and sustained manner.	[35]
Vascular regeneration	Prepared a polydopamine-coated PCL nanofiber scaffold	HUVEC	The coating facilitates cell attachment and viability of HUVECs due to adsorption and immobilization of serum protein on polydopamine layer.	[26]
	Fabricated a polydopamine-coated PLCL film, and then RGD- containing peptide and bFGF were subsequently immobilized by catechol chemistry	HUVEC	Immobilized RGD peptide significantly affected cell migration of HUVEC in wound healing assay model. Moreover, adhesion, proliferation and expression of endothelialization markers were highly stimulated by immobilized bFGF.	[36]
	Applied polydopamine coating on stainless steel (SS) stent	HUVEC/ HUASMC	The polydopamine-coated stent not only enhanced HUVECs attachment, proliferation and migration, but inhibited the proliferation of HUASMCs as well.	[66]
	Polydopamine-coated 316L SS stents were thermally treated at 50, 100 and 150 °C respectively.	EC/SMC	Th150, rich in quinone, was beneficial to immobilize serum protein that enhanced EC adhesion and proliferation. However, Th100 and Th150 had weaker inhibition of SMC proliferation because of less catechol groups.	[39]
Wound healing and skin regeneration	Prepared a bFGF immobilized PLGA fibrous scaffold via polydopamine coating.	HDF	Besides the enhancement of cell adhesion and proliferation due to polydopamine, the bFGF could promote many cell proliferation, such as dermal fibroblasts, keratinocytes, and endothelial cells, and the scaffold accelerated wound healing epithelialization and promotes skin regeneration in vivo.	[57]
	Fabricated a nanofibrous PCL mat blended with mussel adhesive protein (MAP)	Human keratinocyte cell	The materials showed accelerated skin remodeling in a rat wound-healing model because MAP can provide keratinocyte with a biocompatible environment for cell growth and capture inherent growth factors.	[21]

(continued)

**Table 24.2** (continued)

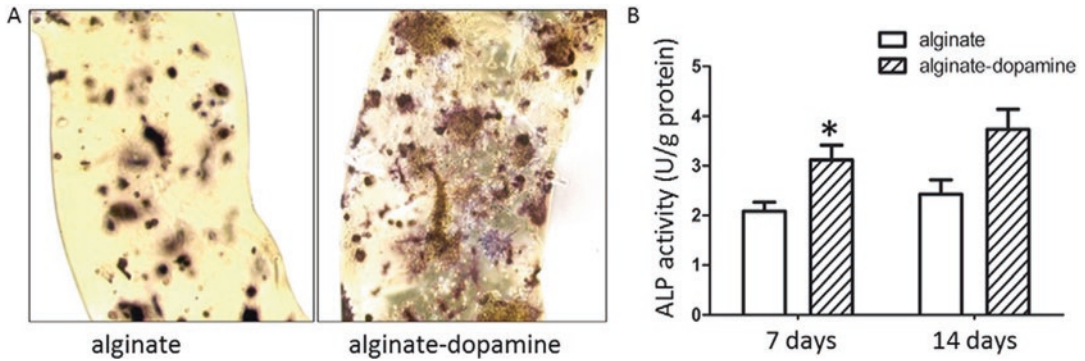
Application in tissue engineering				
Field	Research method and feature	Cell type	Result	References
	A MAP glue containing collagen-binding peptides for regenerative healing and anti-scarring of dermal	NIH3T3	This MAP adhesive hydrogel can accelerate initial wound healing without inducing chronic inflammation by initially providing compatible environments for reepithelialization, neovascularization, and rapid collagen synthesis.	[19]
Cell pattern	Prepared a microchanneled silicon wafer by molding PDMS on surface, and then fabricated polydopamine micropattern	HT1080/ MC3T3-E1/ NIH-3T3	Different mammalian cells successfully adhered to polydopamine-coated pattern and aligned well with the direction.	[25]
	Polydopamine patches are microcontact printed onto PVA	HeLa/ HUVEC	Providing favorable environment for cell growth. Moreover, polydopamine can also be deposited onto PVA in situ during cell culturing.	[3]
	Fabricated a polydopamine-coated superhydrophilic PAMPS brushes	Erythrocyte/ platelet	Polydopamine could facilitate protein adsorption which contributed to cell adhesion and superhydrophilic PAMPS brushes were unfavorable for cell and protein adhesion. Both effects made cell pattern apparently observable.	[17]
	Microcontact printing to coat polydopamine pattern on various substrates for different applications	L929	Polydopamine-coated polystyrene could support L929 cells' adhesion only on polydopamine pattern. PEG-NH <sub>2</sub> and PEG-SH grafted onto polydopamine-coated TCPS successfully restrained cell attachments. Protein immobilization also appeared along with imprinted polydopamine patterns. Polydopamine pattern also exhibited immobilization of gold nanoparticle and the reduction of silver ions on glass slides.	[10]

ing. The microporous structure and immobilized rhBMP-2 of this 3D scaffold not only promoted cell proliferation but also released rhBMP-2 in a controlled and sustained manner that is ideal for a bone-tissue regenerative scaffold (Fig. 24.11) [35].

#### 24.4.2 Vascular Regeneration

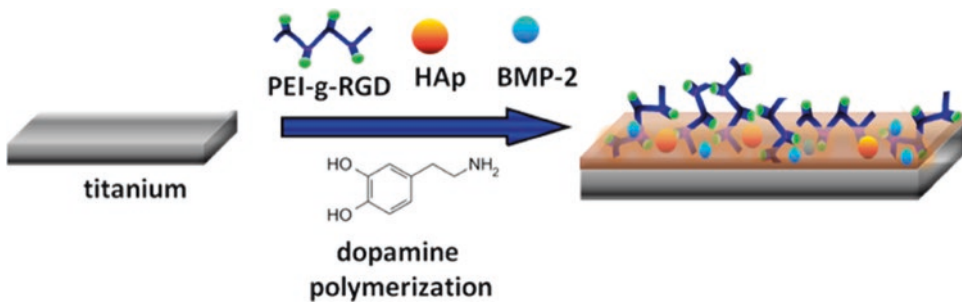
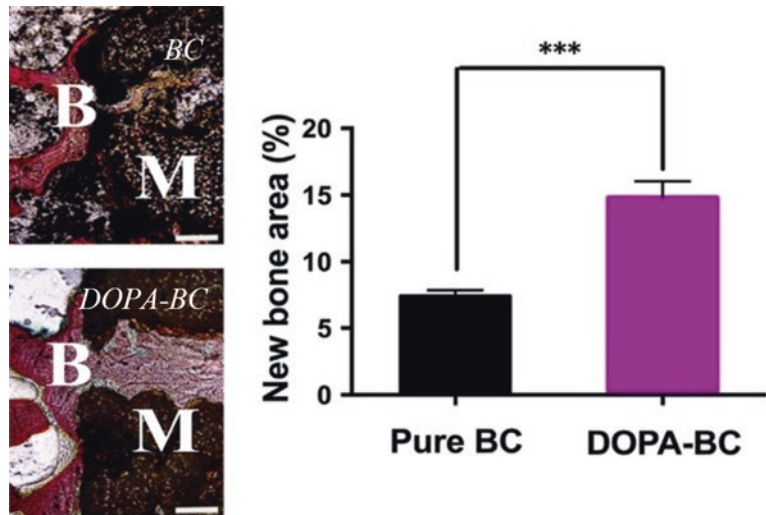
Malfunction in coronary arteries leads to cardiovascular diseases, one of leading causes of death worldwide. The development of vascular graft

materials is one of the important strategies to address this problem. However, endothelialization on vascular grafts is a complex process that involves adhesion, migration, proliferation and differentiation of endothelial cells (EC) [66]. Furthermore, there are complications such as restenosis due to the thrombosis formation and smooth muscle cell (SMC) proliferation [77]. As a result, in this section, we will discuss how previous studies utilized mussel-inspired chemistry to support EC proliferation and inhibit SMC for vascular regeneration.

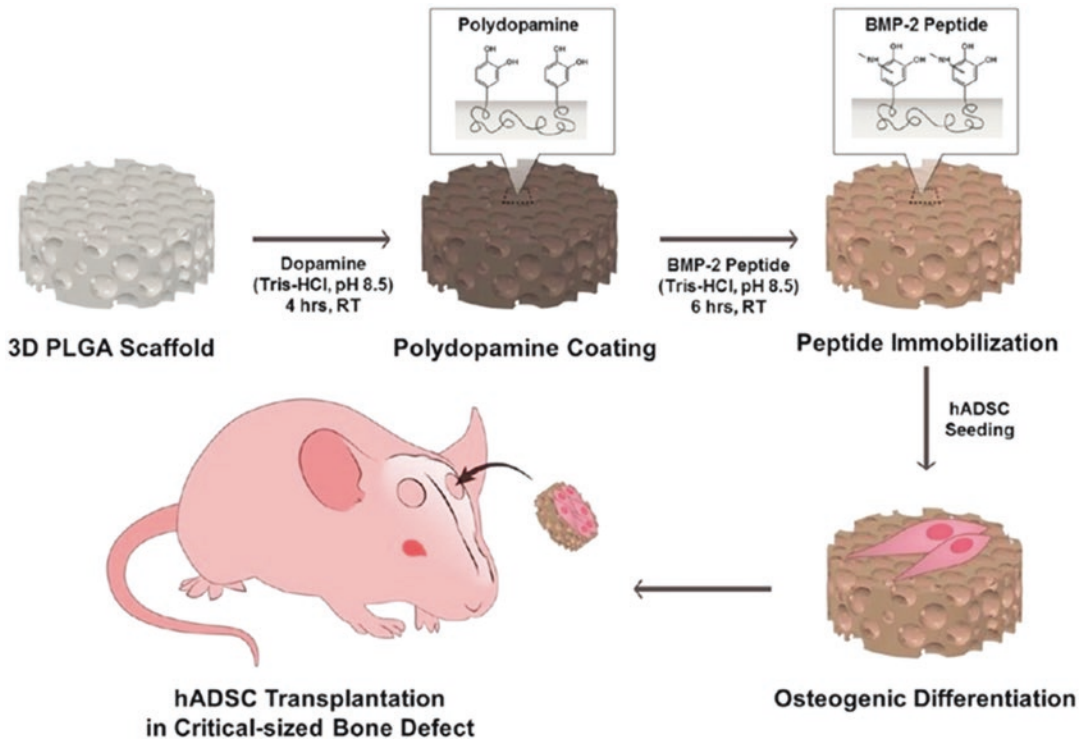


**Fig. 24.7** (a) ALP staining of BMSC grown in alginate and alginate-dopamine fiber after 14 days of osteogenic culture. (b) ALP activity of BMSC grown in alginate and alginate-dopamine fiber at day 7 and 14 of osteogenic culture. (n = 3), \*means  $p < 0.05$

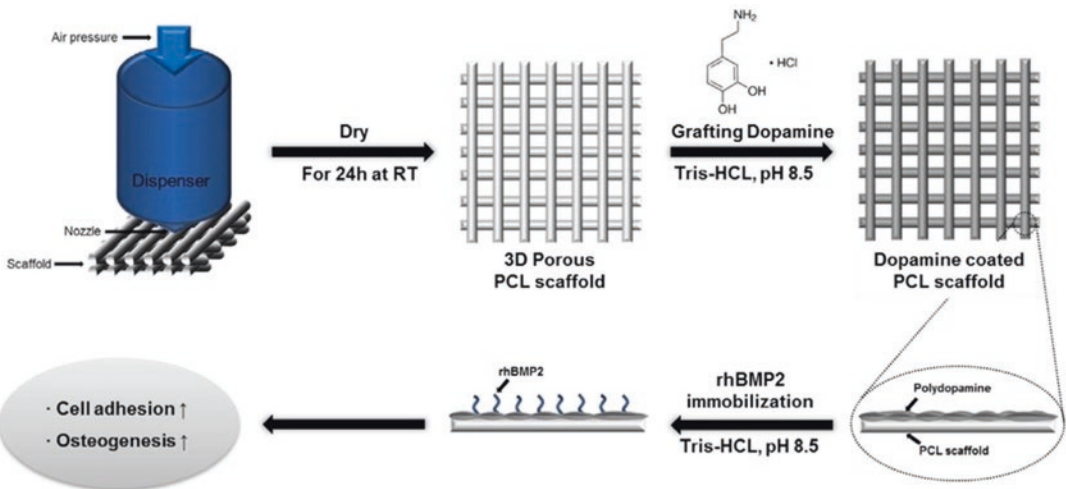
**Fig. 24.8** M represents implanted scaffolds material. B represents newly formed bone. Scaffolds significantly enhanced the *in vivo* new bone formation as compared to pure BC scaffolds due to the formation of mussel-inspired nanostructure. The scale bar is 100 mm (\*\*\*) means  $p < 0.001$ ) [40]



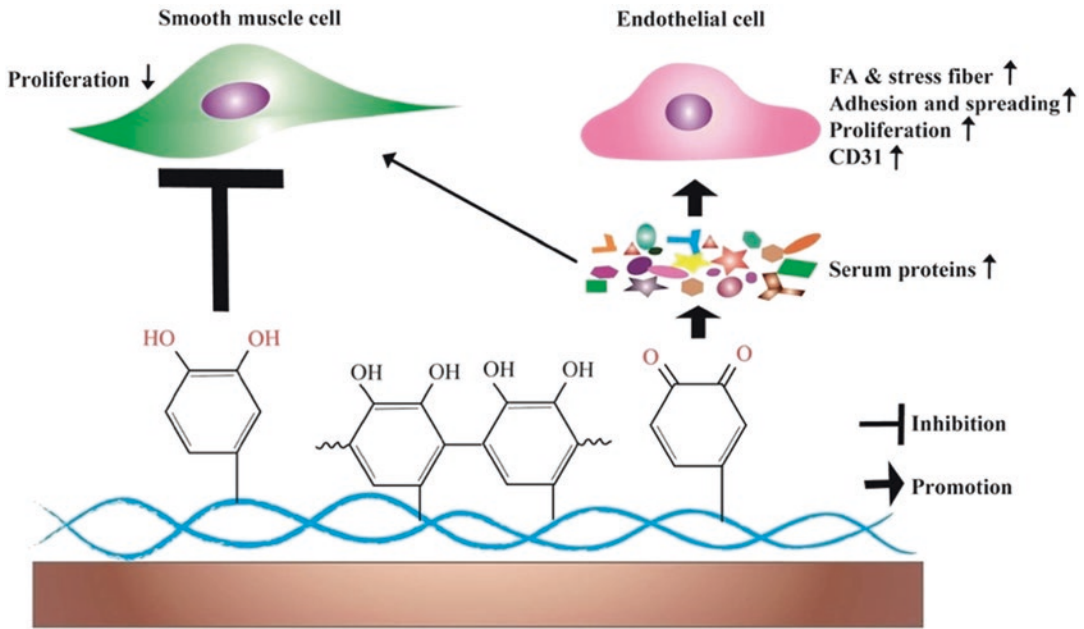
**Fig. 24.9** Illustration of dopamine-assisted immobilization of PEI-g-RGD, hydroxyapatite (HA) nanoparticles, and rhBMP-2 on a titanium substrate [9]



**Fig. 24.10** Schematic illustration of polydopamine-assisted immobilization of BMP-2 peptides on PLGA scaffolds for osteogenic differentiation and bone formation of hADSCs [24]



**Fig. 24.11** Illustration of hybrid 3D porous scaffold [35]



**Fig. 24.12** Schematic illustration of the proposed mechanism of polydopamine selectively modulating endothelial cell and smooth muscle cell behavior [12]

Before we present the studies related to vascular regeneration, we should discuss the reason why SMC needs to be inhibited and how polydopamine can serve that function. Previous studies indicate that by inhibiting the proliferation of SMC in the vessel wall in response to the acute vessel wall injury of angioplasty, one can efficiently reduce the possibility of in-stent restenosis [66]. The antioxidant property of reactive phenolic hydroxyl groups in polydopamine is the reason for its inhibition of SMC. Although the mechanism has not been elucidated, several studies have demonstrated that natural polyphenols, inhibit proliferation and migration of both SMC and EC, and such inhibitory effect on SMC was much stronger than that on EC [12]. The polydopamine coating could promote EC attachment and proliferation, and inhibit SMC growth that undergoes the vascular cell selectivity (Fig. 24.12).

There are some researches of using polydopamine coating or immobilization of bioactive molecules to enhance endothelial cell for vascular tissue engineering. Ku and Park prepared a polydopamine-coated PCL nanofiber scaffold,

showing that the coating can facilitate cell attachment, and due to adsorption and immobilization of serum protein on polydopamine layer, the viability of human umbilical vein endothelial cells (HUVECs) [26]. Lee et al. fabricated a polydopamine-coated poly(lactic acid-co-3-caprolactone) (PLCL) film, and then RGD-containing peptide and basic fibroblast growth factor (bFGF) were subsequently immobilized by catechol chemistry. They found that immobilized RGD peptide significantly affected cell migration of HUVEC compared with bFGF in wound healing assay model. On the other hand, adhesion, proliferation and expression of endothelialization markers were highly stimulated by immobilized bFGF instead of RGD peptide [36].

Mussel-inspired designs for enhancement of EC and inhibition of SMC also have been reported. Yang et al. applied polydopamine coating on stainless steel (SS) stent, and then determined the growth behavior of HUVEC and human umbilical artery smooth muscle cell (HUASMC) cultured on materials. The polydopamine-coated stent not only showed enhancement of HUVEC attachment, prolifera-

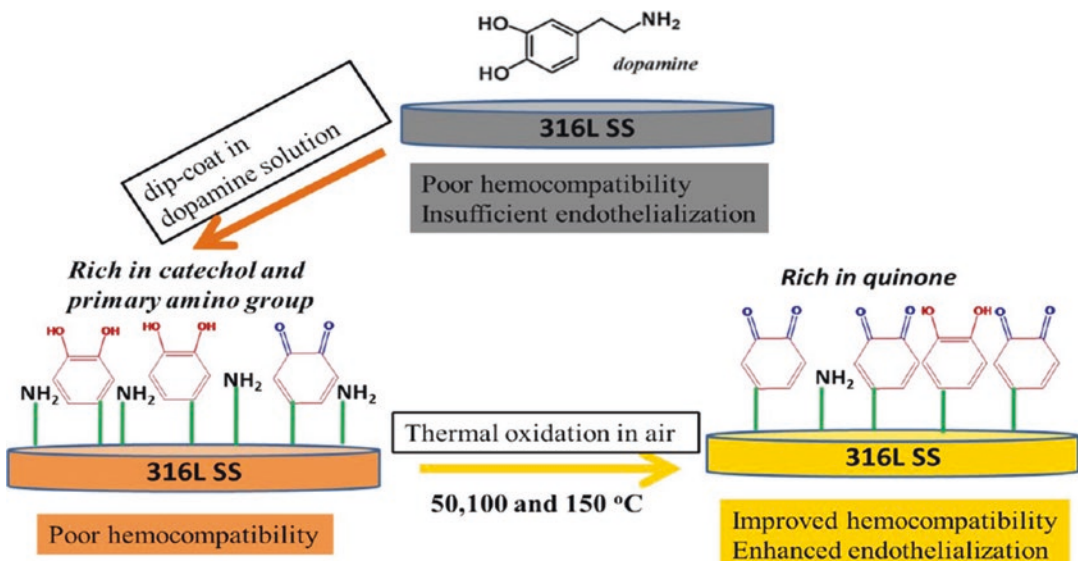
tion and migration, but inhibited the proliferation of HUASMCs as well. The result revealed that polydopamine coating causes 49% and 63% lower attachment on polydopamine-coated stent than on unmodified SS after 1 and 3 days' culture respectively. This advantage of polydopamine coating could address the issues associated with re-endothelialization and restenosis, and improve the viability of the SS stent as vascular devices [66].

Luo et al. presented another interesting study, where polydopamine-coated 316L SS stents were thermally treated at 50, 100 and 150 °C respectively (Fig. 24.13) (Th50, Th100 and Th150). Due to the thermal treatment in the air, the catechol groups in polydopamine would be oxidative and become quinone groups. The result shows that Th150, rich in quinone, was beneficial to adsorb or immobilize serum protein that enhanced EC adhesion and proliferation. Furthermore, being poor in amino, Th150 could maintain the natural conformation of fibrinogen, which thereby inhibited platelet adhesion and activation that provided hemocompatibility. However, the result also revealed that the Th100 and Th150 had weaker inhibition of SMC proliferation than Th50, which could be explained by the reduced

catechol groups. This fact could further prove that the SMCs' behavior might be strongly associated with the surface catechol content. In brief, a simple thermal oxidation of polydopamine modified SS stent demonstrated hemocompatibility and ideal EC proliferation and migration. In addition, a polydopamine surface that could effectively inhibit SMC proliferation depending on the surface catechol content [39].

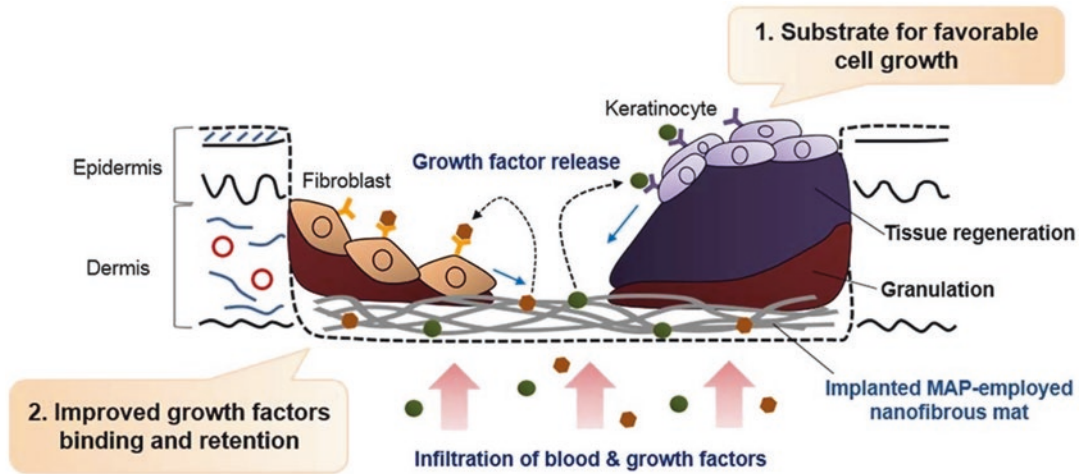
### 24.4.3 Wound Healing and Skin Regeneration

Human body is covered by skin which serves as a protection against outside pathogens. Wound caused by trauma, burn or diabetes should be treated properly to facilitate the healing process and prevent infection or unfavorable scar. Therefore, researches for skin regenerative and wound healing biomaterials have been wide ranging, including mussel-inspired one. Sun et al. prepared a bFGF immobilized PLGA fibrous scaffold via polydopamine coating. The polydopamine could be coated onto various substrates including metal, organic and inorganic ones, and immobilize biomolecules like



**Fig. 24.13** Scheme of 316L SS coated with polydopamine and the different chemical components and possible effect of polydopamine after thermal treatment [39]





**Fig. 24.14** Schematic illustration of suggested mechanisms for enhanced in vivo rat skin regeneration where MAP-blended nanofibrous mats were used [21]

bFGF. Aside from the enhancement of cell adhesion and proliferation of polydopamine, the bFGF could promote many cell proliferation, such as dermal fibroblasts, keratinocytes, and endothelial cells due to its mitogenic and angiogenic characteristics. In vivo results demonstrated that this bFGF-grafted scaffold have faster healing rate, accelerated epithelialization and promotes skin regeneration [57].

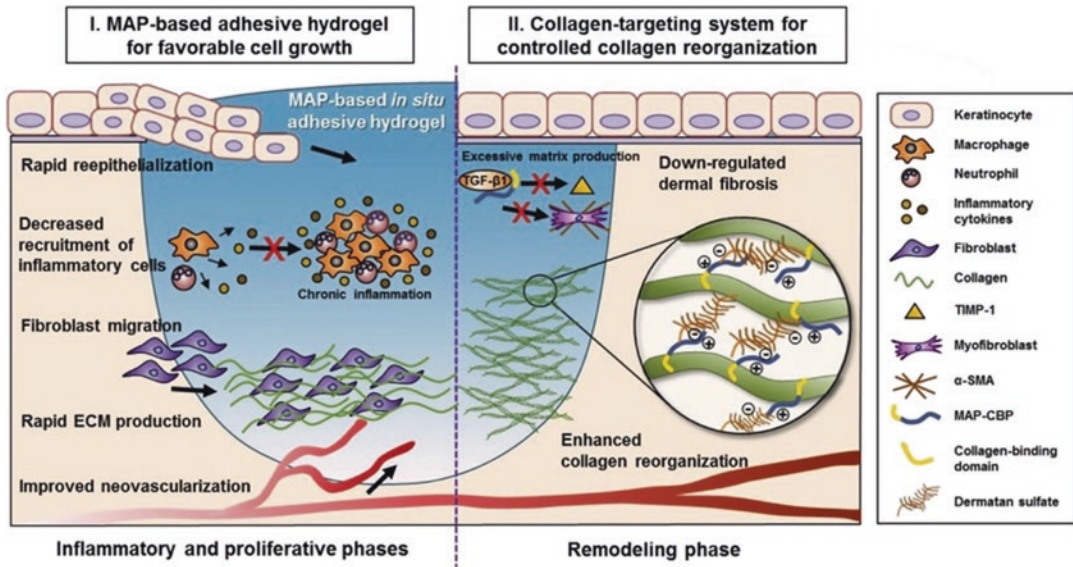
Mussel adhesive protein (MAP) possess desirable characteristics such as strong adhesion under moist condition, low immunogenicity in the human body and biodegradability [28]. Moreover, MAPs can be modified and/or produced via recombinant DNA technology and bacterial expression systems, such that MAPs can have wider applications [7]. Kim et al. fabricated a nanofibrous PCL mat blended with MAP that showed accelerated skin remodeling in a rat wound-healing model (Fig. 24.14). The result might stem from the fact that MAP can provide keratinocyte with a biocompatible environment for cell growth and capture inherent growth factors. The scaffold was expected to be applied in wound healing or other kinds of tissue regeneration [21].

Scar formation is an ongoing topic in clinical research due to its complicated healing mechanism. Jeon et al. developed a MAP glue containing collagen-binding peptides for regenerative

healing and anti-scarring of dermal injury. MAP not only has ideal water-resistant adhesion and biocompatibility but can also stimulate adhesion of type I collagen via hydrogen bonding and electrostatic interactions [18]. This MAP adhesive hydrogel can accelerate initial wound healing without inducing chronic inflammation by initially providing highly compatible environments for re-epithelialization, neovascularization, and rapid collagen synthesis. By fusing collagen-binding peptide, the glue can prevent scar formation by controlling collagen fibril growth, tissue-specific reassembly, and by down-regulating the expression of fibrogenic factors during the remodeling phase. Furthermore, the result in a rat skin excisional model showed that the collagen-targeting glue successfully accelerated initial wound regeneration (Fig. 24.15) [19].

#### 24.4.4 Cell Pattern

Spatial control and organization of living cells on materials, or known as cell patterning, play a vital role in certain applications such as biochips, tissue engineering scaffolds and so on [8]. The basic principle of cell patterning is to fabricate adhesive and nonadhesive regions on substrates to spatially arrange biomolecules [48]. There are many researches utilizing the ideal cell adhesion via

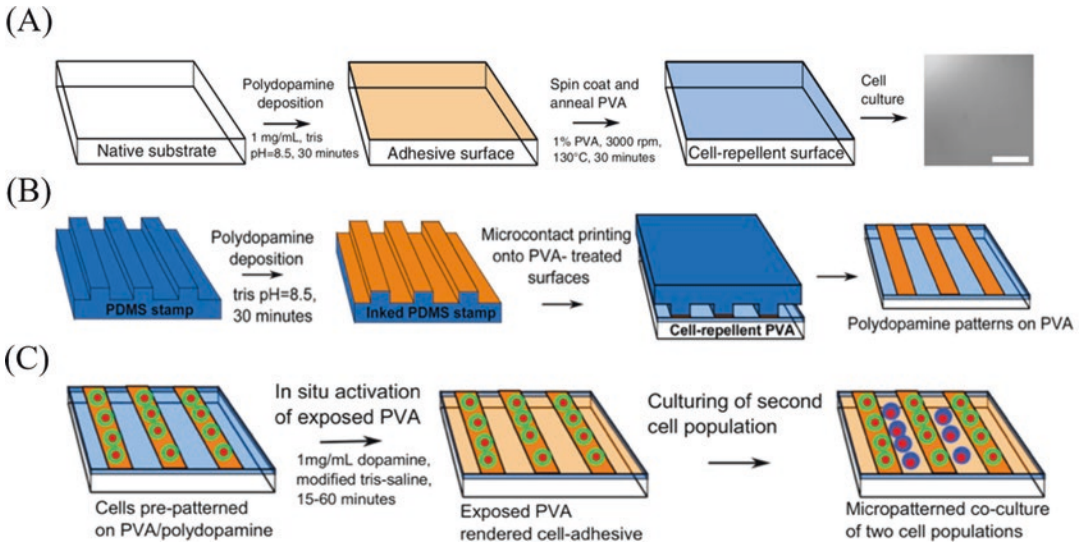


**Fig. 24.15** Schematic illustration of proposed mechanisms for enhanced in vivo scarless skin regeneration where a natural healing-inspired MAP-based collagen-targeting surgical glue was used [19]

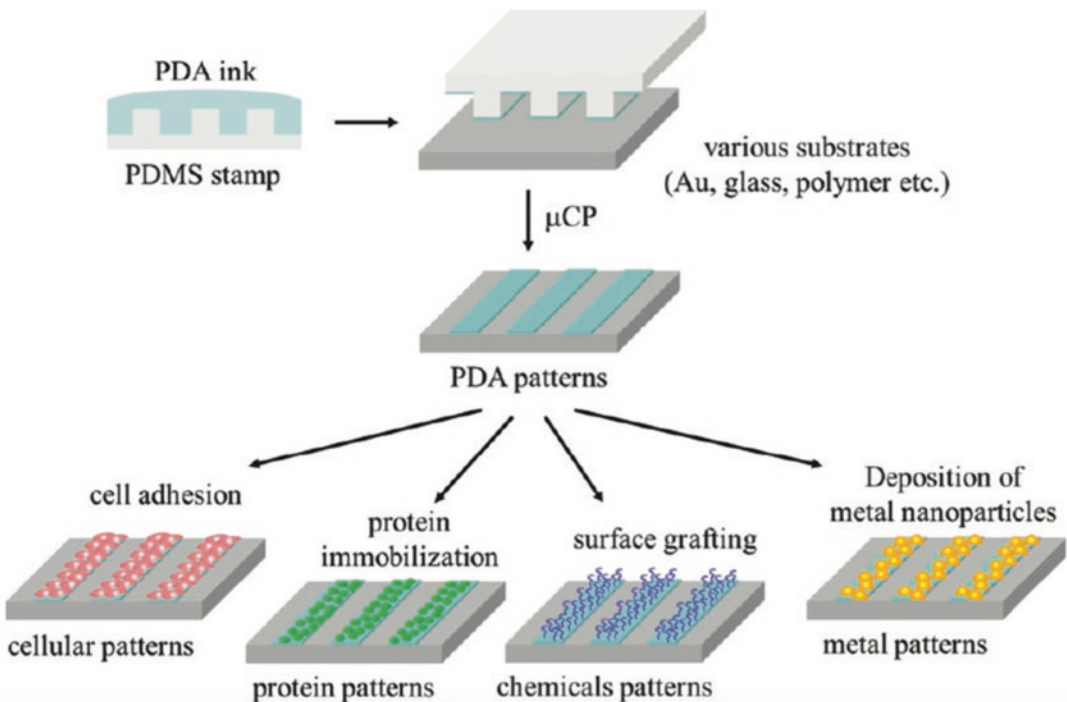
mussel-inspired chemistry. When coating polydopamine, which can enhance cell adhesion on cell-repellent materials, one can achieve living cells array or pattern. For example, Ku et al. first prepared a microchanneled silicon wafer by molding poly-(dimethylsiloxane) (PDMS) on surface, and then fabricated polydopamine micropattern by immersing the materials in dopamine solution. Different mammalian cells, including fibrosarcoma HT1080, mouse preosteoblast MC3T3-E1 and mouse fibroblast NIH-3T3, successfully adhered to polydopamine-coated pattern and aligned well with the direction [25]. Beckwith and Sikorski coated polydopamine onto poly(vinyl alcohol) (PVA) hydrogels to turn cell-repellent property of PVA hydrogel into cell-adhesive one. In their study, polydopamine patches are microcontact printed onto PVA, providing favorable environment for cell growth. Moreover, polydopamine can also be deposited onto PVA in situ during cell culturing. The combination of cell patterning by microcontact printing of polydopamine with in situ polydopamine deposition make patterned cell (similar or dissimilar types) co-cultures successful (Fig. 24.16) [3].

Coating polydopamine onto antifouling polymers has also been investigated. Hou et al. fabri-

cated a polydopamine-coated superhydrophilic antifouling polymers, poly (2-acryl-amido-2-methylpropane sulfonic acid) (PAMPS), brushes. Polydopamine could facilitate protein adsorption which contributed to cell adhesion and superhydrophilic PAMPS brushes were unfavorable for cell and protein adhesion. Both effect made cell pattern apparently observable on polydopamine-coated PAMPS. Besides, polydopamine pattern could also immobilize protein to form protein array [17]. Polydopamine pattern can be utilized in versatile applications such as cell pattern, protein adsorption, surface grafting and metal deposition. Chien et al. utilized microcontact printing to coat polydopamine pattern on various substrates for different applications (Fig. 24.17). Polydopamine-coated polystyrene could support L929 cell adhesion only on polydopamine pattern. PEG-NH<sub>2</sub> and PEG-SH grafted onto polydopamine-coated TCPS via reaction with quinone groups, successfully restrain cell attachments. Protein immobilization also appeared along with imprinted polydopamine patterns on PEG substrates. Polydopamine pattern also exhibited immobilization of gold nanoparticle and the reduction of silver ions on glass slides [10].



**Fig. 24.16** (a) initial cell-repellent PVA surface. (b) polydopamine is deposited in situ on PVA surface that provided new cell adhesive areas for second type of cell [3]. (c) Fabrication of polydopamine patterns on PVA surfaces. (c) The co-culture process starts with patterned cells, then



**Fig. 24.17** Schematic illustration of micropatterned substrates based on polydopamine via microcontact printing and secondary reactions [10]

### 24.4.5 Protein Adsorption and Cell Adhesion

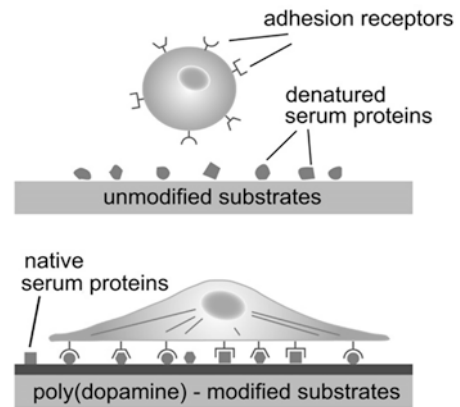
After discussing a variety of dopamine-inspired biomaterials, which have good performance in cell attachment and pattern, we must fully understand and explain the mechanisms that control cell adhesion on biomaterial surfaces. There are two main mechanisms: (i) Functional groups on substrates' surface, via electrostatic interactions or van der Waals force, exhibit weak bonding with glycoproteins and proteoglycans in the cell membrane. (ii) Protein adsorption, which forms a thin layer of cell-adhesive protein domains on substrates' surfaces which binds to transmembrane integrin receptors. The first mechanism is termed nonspecific cell adhesion, and the second one specific cell adhesion [26, 41]).

From previous studies, we know that after oxidation, polydopamine coating with catechol groups and quinone groups can exhibit pH-switchable charge and hydrogen bonding, that may contribute the nonspecific cell adhesion [67, 69]. On the other hand, the reactive o-quinone groups are capable to covalently bond with nucleophile groups such as amino and thiol groups which are largely present in proteins [33]. Therefore, proteins, such as serum protein, can be adsorbed or immobilized onto polydopamine surface that support cell adhesion. This fact lead to the specific cell adhesion mentioned above [26].

Furthermore, there are research indicating that polydopamine can minimize the denaturation of serum proteins by adjusting the surface energy of substrates' surface, which results in better cell adhesion [27]. Equipped with all these mechanisms, polydopamine-coated and catechol-conjugated materials are regarded as ideal biomaterials for cell adhesion (Fig. 24.18.).

## 24.5 Mussel-Inspired Tissue Adhesives

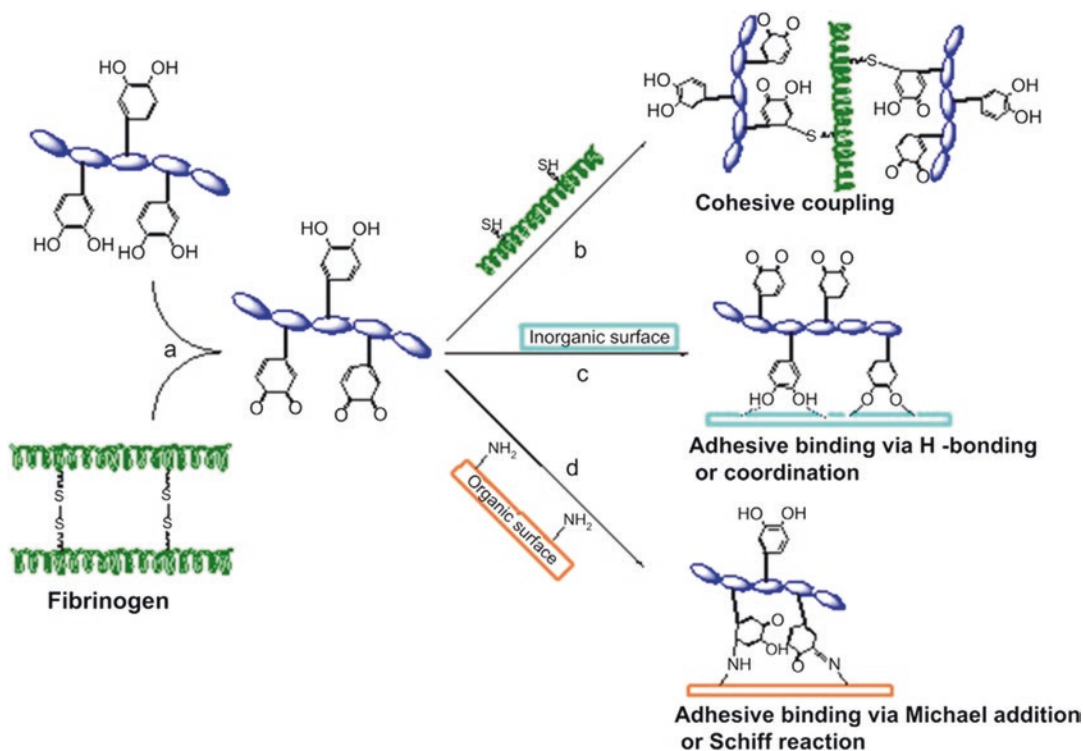
Traditional treatment of wound closure and healing such as sutures has some disadvantageous and is recognized ineffective today. Sutures often cause additional damage and inflammation, and



**Fig. 24.18** Proposed mechanism of serum protein-mediated cell adhesion on polydopamine layer [27]

cannot arrest body fluid of wounds [2, 56]. Tissue adhesives attract much attention nowadays as appealing alternatives to sutures and staples, since they can be applied more quickly, causes less pain and may require less equipment in certain circumstances. On the other hand, two main factors are now affecting the modern practice of surgery. One is cost containment and the other is aging population. Because of aging population and its increase need of medical care and surgery, the accumulated medical cost has become a serious issue. In order to overcome these challenges, the techniques and materials utilized in surgery should be improved. One solution is the effective use of hemostats, sealants, and adhesives. These materials are useful in surgical procedure and are crucial components of the surgical toolbox. The modern-day hemostat, sealant, and adhesive, nevertheless, are still not effective enough. Continued research and development is still required to provide new materials for regenerative medicine [56].

For the purposes of resolving the challenges, new biomaterials and tissue adhesives are necessary. However, the feasibility of tissue adhesive in the moist environment of the human body is a challenge [52]. The wet-resistant adhesive property of mussel protein inspires scientists to developed tissue adhesives which are applicable in wet conditions like MAP glue [19]. There are a wide range of mussel-inspired synthetic biomaterials reported. Ryu et al. fabricated an in-situ cross-



**Fig. 24.19** (a) The oxidation of unabsorbed dopamine to quinone groups by disulfide bond in fibrinogen. (b) Cohesive coupling of reducing thiolates with quinone groups by Michael addition. (c) Adhesive binding with

inorganic surfaces via hydrogen bonding or coordination. (d) Adhesive binding with organic surfaces via Michael addition or Schiff reaction

linkable catechol-conjugated chitosan hydrogel with thiol-terminated Pluronic F-127 via Michael-type addition. The thermosensitive hydrogel is prepared at 4 °C and used at 37 °C such that injection and in-situ gelation possible. It showed robust tissue adhesion and mechanical property in vitro and in vivo, and reducing blood loss from a bleeding rat liver as well [51]. Zhang et al. first synthesized a hyperbranched poly(b-amino ester) polymer termed poly(dopamine-co-acrylate), and then investigated the adhesive strength of various crosslinking methods including NaIO<sub>4</sub>, FeCl<sub>3</sub>, HRP/H<sub>2</sub>O<sub>2</sub> and fibrinogen. This adhesive had an approximately 4-fold increase in wet adhesion strength compared to TISSEEL® and fibrin sealant. The versatile cat-

echol reactivity enabled this tissue adhesive precursor to be crosslinked via different mechanism and apply on a variety of substrates including organic and inorganic ones (Fig. 24.19) [70].

Recent researcher developed a more ideal mussel-inspired tissue adhesive that addresses many ongoing challenges. Inspired by the adhesion mechanism of the mussels that maintain a high concentration of catechol groups in the confined nanospace of their byssal plaque, Han et al. fabricated a polydopamine-clay-polyacrylamide hydrogel. Utilizing the layered structure of clay nanosheets, dopamine was intercalated into the nanospace between the layers. Afterwards, acrylamide monomers were then added and in-situ polymerized to make the hydrogel. Compare

with previous single-use tissue adhesive, the novelty of this hydrogel was that the sufficient free catechol groups in the hydrogel could undergo controllable oxidation process in the confined nanolayers of clay, which leads to repeatable and durable adhesiveness [16].

## 24.6 Conclusion

When working on this review chapter, we found that there were plenty of mussel-inspired researches since it was introduced. Earlier researches focused on the basic wet-resistant adhesive property and functional groups of adhesive protein in mussel byssal plaque, and then its noncovalent and covalent interaction with organic and inorganic surface. Later, ideal features of polydopamine coating such as structure, self-polymerization under alkaline condition, hydrophilicity, surface roughness, pH-sensitive charge, catechol chemistry and secondary reaction via Michael-type addition and/or Schiff base reactions were investigated. Based on further understanding of polydopamine chemistry, many researches, especially tissue engineering, utilized the advantages of biocompatibility, enhancement of cell adhesion and immobilization of bioactive molecules to develop biomaterials like scaffold for regenerative applications. Recently, more versatile biomedical application including surgical tissue adhesives, antifouling surface, antibacterial activity and drug delivery have been invented. Especially, with mussel-inspired wet-resistant adhesive properties, novel tissue adhesives for surgical use play a vital role in regenerative medicine. The mussel-inspired biomaterials have attracted much attention, however, explanations for some mechanisms remains elusive, such as exact polydopamine structure, interactions with different kinds of cells and their adhesion, and long-term in vivo toxicity and applicability. Therefore, based on this review chapter, the future work of mussel-inspired biomaterials is to solve the problem mentioned and then create advanced and innovative mussel-inspired designs for therapeutic in its promising future.

## References

1. Anderson TH, Yu J, Estrada A, Hammer MU, Waite JH, Israelachvili JN (2010) The contribution of DOPA to substrate–peptide adhesion and internal cohesion of mussel-inspired synthetic peptide films. *Adv Funct Mater* 20(23):4196–4205. <https://doi.org/10.1002/adfm.201000932>
2. Annabi N, Yue K, Tamayol A, Khademhosseini A (2015) Elastic sealants for surgical applications. *Eur J Pharm Biopharm* 95(Pt A):27–39. <https://doi.org/10.1016/j.ejpb.2015.05.022>
3. Beckwith KM, Sikorski P (2013) Patterned cell arrays and patterned co-cultures on polydopamine-modified poly(vinyl alcohol) hydrogels. *Biofabrication* 5(4):045009. <https://doi.org/10.1088/1758-5082/5/4/045009>
4. Bernsmann F, Ball V, Addiego F, Ponche A, Michel M, Gracio JJ et al (2011) Dopamine–melanin film deposition depends on the used oxidant and buffer solution. *Langmuir* 27(6):2819–2825. <https://doi.org/10.1021/la104981s>
5. Bridelli MG, Crippa PR (2010) Infrared and water sorption studies of the hydration structure and mechanism in natural and synthetic melanin. *J Phys Chem B* 114(29):9381–9390. <https://doi.org/10.1021/jp101833k>
6. Burzio LA, Waite JH (2000) Cross-linking in adhesive Quinoproteins: studies with model Decapeptides. *Biochemistry* 39(36):11147–11153. <https://doi.org/10.1021/bi0002434>
7. Cha HJ, Hwang DS, Lim S (2008) Development of bioadhesives from marine mussels. *Biotechnol J* 3(5):631–638. <https://doi.org/10.1002/biot.200700258>
8. Chen CS, Mrksich M, Huang S, Whitesides GM, Ingber DE (1997) Geometric control of cell life and death. *Science* 276(5317):1425–1428. <https://doi.org/10.1126/science.276.5317.1425>
9. Chien CY, Tsai WB (2013) Poly(dopamine)-assisted immobilization of Arg–Gly–Asp peptides, hydroxyapatite, and bone morphogenic protein-2 on titanium to improve the osteogenesis of bone marrow stem cells. *ACS Appl Mater Interfaces* 5(15):6975–6983. <https://doi.org/10.1021/am401071f>
10. Chien H-W, Kuo W-H, Wang M-J, Tsai S-W, Tsai W-B (2012) Tunable micropatterned substrates based on poly(dopamine) deposition via microcontact printing. *Langmuir* 28(13):5775–5782. <https://doi.org/10.1021/la300147p>
11. Dalby MJ, Gadegaard N, Tare R, Andar A, Riehle MO, Herzyk P et al (2007) The control of human mesenchymal cell differentiation using nanoscale symmetry and disorder. *Nat Mater* 6:997–1003. <https://doi.org/10.1038/nmat2013>
12. Ding Y, Yang Z, Bi CWC, Yang M, Zhang J, Xu SL et al (2014) Modulation of protein adsorption, vascular cell selectivity and platelet adhesion by mussel-inspired surface functionalization. *J Mater*

- Chem B 2(24):3819–3829. <https://doi.org/10.1039/c4tb00386a>
13. Fan X, Lin L, Dalsin JL, Messersmith PB (2005) Biomimetic anchor for surface-initiated polymerization from metal substrates. *J Am Chem Soc* 127(45):15843–15847. <https://doi.org/10.1021/ja0532638>
  14. Hafner D, Ziegler L, Ichwan M, Zhang T, Schneider M, Schiffmann M et al (2016) Mussel-inspired polymer carpets: direct Photografting of polymer brushes on Polydopamine Nanosheets for controlled cell adhesion. *Adv Mater* 28(7):1489–1494. <https://doi.org/10.1002/adma.201504033>
  15. Hamming LM, Fan XW, Messersmith PB, Brinson LC (2008) Mimicking mussel adhesion to improve interfacial properties in composites. *Compos Sci Technol* 68(9):2042–2048. <https://doi.org/10.1016/j.compscitech.2008.02.036>
  16. Han L, Lu X, Liu K, Wang K, Fang L, Weng L-T et al (2017) Mussel-inspired adhesive and tough hydrogel based on Nanoclay confined dopamine polymerization. *ACS Nano* 11(3):2561–2574. <https://doi.org/10.1021/acsnano.6b05318>
  17. Hou J, Liu T, Chen R, Liu J, Chen J, Zhao C et al (2017) Guided protein/cell patterning on superhydrophilic polymer brushes functionalized with mussel-inspired polydopamine coatings. *Chem Commun* 53(50):6708–6711. <https://doi.org/10.1039/C7CC02460F>
  18. Hwang DS, Sim SB, Cha HJ (2007) Cell adhesion biomaterial based on mussel adhesive protein fused with RGD peptide. *Biomaterials* 28(28):4039–4046. <https://doi.org/10.1016/j.biomaterials.2007.05.028>
  19. Jeon EY, Choi B-H, Jung D, Hwang BH, Cha HJ (2017) Natural healing-inspired collagen-targeting surgical protein glue for accelerated scarless skin regeneration. *Biomaterials* 134(Suppl C):154–165. <https://doi.org/10.1016/j.biomaterials.2017.04.041>
  20. Kastrup CJ, Nahrendorf M, Figueiredo JL, Lee H, Kambhampati S, Lee T et al (2012) Painting blood vessels and atherosclerotic plaques with an adhesive drug depot. *Proc Natl Acad Sci* 109(52):21444–21449. <https://doi.org/10.1073/pnas.1217972110>
  21. Kim BJ, Cheong H, Choi E-S, Yun S-H, Choi B-H, Park K-S et al (2017) Accelerated skin wound healing using electrospun nanofibrous mats blended with mussel adhesive protein and polycaprolactone. *J Biomed Mater Res A* 105(1):218–225. <https://doi.org/10.1002/jbm.a.35903>
  22. Kim, K., Kim, K., Ryu, J. H., & Lee, H. (2015). Chitosan-catechol: a polymer with long-lasting mucoadhesive properties. *Biomaterials* 52(Suppl C):161–170. <https://doi.org/10.1016/j.biomaterials.2015.02.010>
  23. Kim K, Ryu JH, Lee DY, Lee H (2013) Bio-inspired catechol conjugation converts water-insoluble chitosan into a highly water-soluble, adhesive chitosan derivative for hydrogels and LbL assembly. *Biomater Sci* 1(7):783. <https://doi.org/10.1039/c3bm00004d>
  24. Ko E, Yang K, Shin J, Cho S-W (2013) Polydopamine-assisted Osteoinductive peptide immobilization of polymer scaffolds for enhanced bone regeneration by human adipose-derived stem cells. *Biomacromolecules* 14(9):3202–3213. <https://doi.org/10.1021/bm4008343>
  25. Ku SH, Lee JS, Park CB (2010a) Spatial control of cell adhesion and patterning through mussel-inspired surface modification by polydopamine. *Langmuir* 26(19):15104–15108. <https://doi.org/10.1021/la102825p>
  26. Ku SH, Park CB (2010) Human endothelial cell growth on mussel-inspired nanofiber scaffold for vascular tissue engineering. *Biomaterials* 31(36):9431–9437. <https://doi.org/10.1016/j.biomaterials.2010.08.071>
  27. Ku SH, Ryu J, Hong SK, Lee H, Park CB (2010b) General functionalization route for cell adhesion on non-wetting surfaces. *Biomaterials* 31(9):2535–2541. <https://doi.org/10.1016/j.biomaterials.2009.12.020>
  28. Lee BP, Messersmith PB, Israelachvili JN, Waite JH (2011) Mussel-inspired adhesives and coatings. *Annu Rev Mater Res* 41:99–132. <https://doi.org/10.1146/annurev-matsci-062910-100429>
  29. Lee H, Dellatore SM, Miller WM, Messersmith PB (2007a) Mussel-inspired surface chemistry for multifunctional coatings. *Science* 318(5849):426–430. <https://doi.org/10.1126/science.1147241>
  30. Lee H, Lee BP, Messersmith PB (2007b) A reversible wet/dry adhesive inspired by mussels and geckos. *Nature* 448(7151):338–341. <https://doi.org/10.1038/nature05968>
  31. Lee H, Lee KD, Pyo KB, Park SY, Lee H (2010) Catechol-grafted poly(ethylene glycol) for PEGylation on versatile substrates. *Langmuir* 26(6):3790–3793. <https://doi.org/10.1021/la904909h>
  32. Lee H, Rho J, Messersmith PB (2009) Facile conjugation of biomolecules onto surfaces via mussel adhesive protein inspired coatings. *Adv Mater* 21(4):431–434. <https://doi.org/10.1002/adma.200801222>
  33. Lee H, Scherer NF, Messersmith PB (2006) Single-molecule mechanics of mussel adhesion. *Proc Natl Acad Sci U S A* 103(35):12999–13003. <https://doi.org/10.1073/pnas.0605552103>
  34. Lee K, Oh MH, Lee MS, Nam YS, Park TG, Jeong JH (2013) Stabilized calcium phosphate nano-aggregates using a dopa-chitosan conjugate for gene delivery. *Int J Pharm* 445(1):196–202. <https://doi.org/10.1016/j.ijpharm.2013.01.014>
  35. Lee SJ, Lee D, Yoon TR, Kim HK, Jo HH, Park JS et al (2016) Surface modification of 3D-printed porous scaffolds via mussel-inspired polydopamine and effective immobilization of rhBMP-2 to promote osteogenic differentiation for bone tissue engineering. *Acta Biomater* 40:182–191. <https://doi.org/10.1016/j.actbio.2016.02.006>
  36. Lee YB, Shin YM, Lee J-H, Jun I, Kang JK, Park J-C, Shin H (2012) Polydopamine-mediated immobilization of multiple bioactive molecules for the development of functional vascular graft materi-

- als. *Biomaterials* 33(33):8343–8352. <https://doi.org/10.1016/j.biomaterials.2012.08.011>
37. Liu Q, Yu B, Ye W, Zhou F (2011) Highly selective uptake and release of charged molecules by pH-responsive Polydopamine microcapsules. *Macromol Biosci* 11(9):1227–1234. <https://doi.org/10.1002/mabi.201100061>
  38. Liu Y, Ai K, Lu L (2014) Polydopamine and its derivative materials: synthesis and promising applications in energy, environmental, and biomedical fields. *Chem Rev* 114(9):5057–5115. <https://doi.org/10.1021/cr400407a>
  39. Luo R, Tang L, Zhong S, Yang Z, Wang J, Weng Y et al (2013) In vitro investigation of enhanced hemocompatibility and endothelial cell proliferation associated with quinone-rich polydopamine coating. *ACS Appl Mater Interfaces* 5(5):1704–1714. <https://doi.org/10.1021/am3027635>
  40. Ma H, Luo J, Sun Z, Xia L, Shi M, Liu M et al (2016) 3D printing of biomaterials with mussel-inspired nanostructures for tumor therapy and tissue regeneration. *Biomaterials* 111:138–148. <https://doi.org/10.1016/j.biomaterials.2016.10.005>
  41. Madhurakkat Perikamana SK, Lee J, Lee YB, Shin YM, Lee EJ, Mikos AG, Shin H (2015) Materials from mussel-inspired chemistry for cell and tissue engineering applications. *Biomacromolecules* 16(9):2541–2555. <https://doi.org/10.1021/acs.biomac.5b00852>
  42. Malisova B, Tosatti S, Textor M, Gademann K, Zürcher S (2010) Poly(ethylene glycol) Adlayers immobilized to metal oxide substrates through catechol derivatives: influence of assembly conditions on formation and stability. *Langmuir* 26(6):4018–4026. <https://doi.org/10.1021/la903486z>
  43. Meredith P, Sarna T (2006) The physical and chemical properties of eumelanin. *Pigment Cell Res* 19(6):572–594. <https://doi.org/10.1111/j.1600-0749.2006.00345.x>
  44. Perikamana SKM, Shin YM, Lee JK, Lee YB, Heo Y, Ahmad T et al (2017) Graded functionalization of biomaterial surfaces using mussel-inspired adhesive coating of polydopamine. *Colloids Surf B Biointerfaces* 159:546–556. <https://doi.org/10.1016/j.colsurfb.2017.08.022>
  45. Poh CK, Shi Z, Lim TY, Neoh KG, Wang W (2010) The effect of VEGF functionalization of titanium on endothelial cells in vitro. *Biomaterials* 31(7):1578–1585. <https://doi.org/10.1016/j.biomaterials.2009.11.042>
  46. Redfern PC, Zapol P, Curtiss LA, Rajh T, Thurnauer MC (2003) Computational studies of catechol and water interactions with titanium oxide nanoparticles. *J Phys Chem B* 107(41):11419–11427. <https://doi.org/10.1021/jp0303669>
  47. Rim NG, Kim SJ, Shin YM, Jun I, Lim DW, Park JH, Shin H (2012) Mussel-inspired surface modification of poly(L-lactide) electrospun fibers for modulation of osteogenic differentiation of human mesenchymal stem cells. *Colloids Surf B Biointerfaces* 91:189–197. <https://doi.org/10.1016/j.colsurfb.2011.10.057>
  48. Rutz AL, Hyland KE, Jakus AE, Burghardt WR, Shah RN (2015) A multimaterial bioink method for 3D printing tunable, cell-compatible hydrogels. *Adv Mater* 27(9):1607–1614. <https://doi.org/10.1002/adma.201405076>
  49. Ryu JH, Hong S, Lee H (2015) Bio-inspired adhesive catechol-conjugated chitosan for biomedical applications: a mini review. *Acta Biomater* 27:101–115. <https://doi.org/10.1016/j.actbio.2015.08.043>
  50. Ryu JH, Lee Y, Kong WH, Kim TG, Park TG, Lee H (2011b) Catechol-functionalized chitosan/Pluronic hydrogels for tissue adhesives and hemostatic materials. *Biomacromolecules* 12(7):2653–2659. <https://doi.org/10.1021/bm200464x>
  51. Ryu S, Lee Y, Hwang J-W, Hong S, Kim C, Park TG et al (2011a) High-strength carbon nanotube fibers fabricated by infiltration and curing of mussel-inspired catecholamine polymer. *Adv Mater* 23(17):1971–1975. <https://doi.org/10.1002/adma.201004228>
  52. Scognamiglio F, Travan A, Rustighi I, Tarchi P, Palmisano S, Marsich E et al (2016) Adhesive and sealant interfaces for general surgery applications. *J Biomed Mater Res B Appl Biomater* 104(3):626–639. <https://doi.org/10.1002/jbm.b.33409>
  53. Sedó J, Saiz-Poseu J, Busqué F, Ruiz-Molina D (2013) Catechol-based biomimetic functional materials. *Adv Mater* 25(5):653–701. <https://doi.org/10.1002/adma.201202343>
  54. Sever MJ, Weisser JT, Monahan J, Srinivasan S, Wilker JJ (2004) Metal-mediated cross-linking in the generation of a marine-mussel adhesive. *Angew Chem Int Ed Engl* 43(4):448–450. <https://doi.org/10.1002/anie.200352759>
  55. Sileika TS, Kim H-D, Maniak P, Messersmith PB (2011) Antibacterial performance of Polydopamine-modified polymer surfaces containing passive and active components. *ACS Appl Mater Interfaces* 3(12):4602–4610. <https://doi.org/10.1021/am200978h>
  56. Spotnitz WD, Burks S (2008) Hemostats, sealants, and adhesives: components of the surgical toolbox. *Transfusion* 48(7):1502–1516. <https://doi.org/10.1111/j.1537-2995.2008.01703.x>
  57. Sun X, Cheng L, Zhao J, Jin R, Sun B, Shi Y et al (2014) bFGF-grafted electrospun fibrous scaffolds via poly(dopamine) for skin wound healing. *J Mater Chem B* 2(23):3636–3645. <https://doi.org/10.1039/c3tb21814g>
  58. Waite JH, Andersen NH, Jewhurst S, Sun C (2005) Mussel adhesion: finding the tricks worth mimicking. *J Adhes* 81(3–4):297–317. <https://doi.org/10.1080/00218460590944602>
  59. Waite JH, Tanzer ML (1981) Polyphenolic substance of *Mytilus edulis*: novel adhesive containing L-Dopa and Hydroxyproline. *Science* 212(4498):1038–1040. <https://doi.org/10.1126/science.212.4498.1038>
  60. Wang J, Tahir MN, Kappl M, Tremel W, Metz N, Barz M et al (2008) Influence of binding-site density in wet bioadhesion. *Adv Mater* 20(20):3872–3876. <https://doi.org/10.1002/adma.200801140>



61. Weng Y, Song Q, Zhou Y, Zhang L, Wang J, Chen J et al (2011) Immobilization of selenocystamine on TiO<sub>2</sub> surfaces for in situ catalytic generation of nitric oxide and potential application in intravascular stents. *Biomaterials* 32(5):1253–1263. <https://doi.org/10.1016/j.biomaterials.2010.10.039>
62. Williams DF (2008) On the mechanisms of biocompatibility. *Biomaterials* 29(20):2941–2953. <https://doi.org/10.1016/j.biomaterials.2008.04.023>
63. Wu C, Han P, Liu X, Xu M, Tian T, Chang J, Xiao Y (2014) Mussel-inspired bioceramics with self-assembled Ca-P/polydopamine composite nanolayer: preparation, formation mechanism, improved cellular bioactivity and osteogenic differentiation of bone marrow stromal cells. *Acta Biomater* 10(1):428–438. <https://doi.org/10.1016/j.actbio.2013.10.013>
64. Xu C, Xu K, Gu H, Zheng R, Liu H, Zhang X et al (2004) Dopamine as a robust anchor to immobilize functional molecules on the Iron oxide Shell of magnetic nanoparticles. *J Am Chem Soc* 126(32):9938–9939. <https://doi.org/10.1021/ja0464802>
65. Xu LQ, Yang WJ, Neoh K-G, Kang E-T, Fu GD (2010) Dopamine-induced reduction and functionalization of graphene oxide Nanosheets. *Macromolecules* 43(20):8336–8339. <https://doi.org/10.1021/ma101526k>
66. Yang Z, Tu Q, Zhu Y, Luo R, Li X, Xie Y et al (2012) Mussel-inspired coating of polydopamine directs endothelial and smooth muscle cell fate for re-endothelialization of vascular devices. *Adv Healthc Mater* 1(5):548–559. <https://doi.org/10.1002/adhm.201200073>
67. Ye Q, Zhou F, Liu W (2011) Bioinspired catecholic chemistry for surface modification. *Chem Soc Rev* 40(7):4244–4258. <https://doi.org/10.1039/C1CS15026J>
68. You I, Kang SM, Byun Y, Lee H (2011) Enhancement of blood compatibility of poly(urethane) substrates by mussel-inspired adhesive heparin coating. *Bioconj Chem* 22(7):1264–1269. <https://doi.org/10.1021/bc2000534>
69. Yu B, Liu J, Liu S, Zhou F (2010) Pdop layer exhibiting zwitterionicity: a simple electrochemical interface for governing ion permeability. *Chem Commun* 46(32):5900–5902. <https://doi.org/10.1039/C0CC00596G>
70. Zhang H, Bre LP, Zhao T, Zheng Y, Newland B, Wang W (2014) Mussel-inspired hyperbranched poly(amino ester) polymer as strong wet tissue adhesive. *Biomaterials* 35(2):711–719. <https://doi.org/10.1016/j.biomaterials.2013.10.017>
71. Zhang L, Shi J, Jiang Z, Jiang Y, Qiao S, Li J et al (2011) Bioinspired preparation of polydopamine microcapsule for multienzyme system construction. *Green Chem* 13(2):300–306. <https://doi.org/10.1039/C0GC00432D>
72. Zhang S, Xu K, Darabi MA, Yuan Q, Xing M (2016) Mussel-inspired alginate gel promoting the osteogenic differentiation of mesenchymal stem cells and anti-infection. *Mater Sci Eng C Mater Biol Appl* 69:496–504. <https://doi.org/10.1016/j.msec.2016.06.044>
73. Zhang W, Yang FK, Han Y, Gaikwad R, Leonenko Z, Zhao B (2013) Surface and Tribological behaviors of the bioinspired Polydopamine thin films under dry and wet conditions. *Biomacromolecules* 14(2):394–405. <https://doi.org/10.1021/bm3015768>
74. Zhao H, Waite JH (2006) Linking adhesive and structural proteins in the attachment plaque of *Mytilus californianus*. *J Biol Chem* 281(36):26150–26158. <https://doi.org/10.1074/jbc.M604357200>
75. Zhao X, Han Y, Li J, Cai B, Gao H, Feng W, ... Li D (2017) BMP-2 immobilized PLGA/hydroxyapatite fibrous scaffold via polydopamine stimulates osteoblast growth. *Mat Sci Eng C* 78(Suppl C):658–666. <https://doi.org/10.1016/j.msec.2017.03.186>
76. Zhe W, Dong C, Sefei Y, Dawei Z, Kui X, Xiaogang L (2016) Facile incorporation of hydroxyapatite onto an anodized Ti surface via a mussel inspired polydopamine coating. *Appl Surf Sci* 378:496–503. <https://doi.org/10.1016/j.apsusc.2016.03.094>
77. Zhong S, Luo R, Wang X, Tang L, Wu J, Wang J et al (2014) Effects of polydopamine functionalized titanium dioxide nanotubes on endothelial cell and smooth muscle cell. *Colloids Surf B Biointerfaces* 116:553–560. <https://doi.org/10.1016/j.colsurfb.2014.01.030>
78. Zhou Y-Z, Cao Y, Liu W, Chu CH, Li Q-L (2012) Polydopamine-induced tooth remineralization. *ACS Appl Mater Interfaces* 4(12):6901–6910. <https://doi.org/10.1021/am302041b>



Chun-Ho Kim, Sang Jun Park, Dae Hyeok Yang,  
and Heung Jae Chun

## Abstract

Chitosan, a deacetylated chitin, is one of the few natural polymers similar to glycosaminoglycans (GAGs) widely distributed throughout connective tissues. It has been believed that the excellent biocompatibility of chitosan is largely attributed to this structural similarity. Chitosan is also known to possess biodegradability, antimicrobial activity and low toxicity and immunogenicity which are essential for scaffolds. In addition, the existence of free amine groups in its backbone chain enables further chemical modifications to create the additional biomedical functionality. For these reasons, chitosan has found a tremendous variety of biomedical applications in recent years. This chapter introduces the basic contents of chitosan and discusses its applica-

tions to artificial skin, artificial bone, and artificial cartilage in tissue engineering purpose.

## Keywords

Chitosan · Tissue engineering · Scaffold · Regeneration · Skin · Bone · Cartilage

## 25.1 Scaffolds

Tissue engineering is an emerging multidisciplinary approach that incorporates biology, medicine and engineering [7]. As a field of study, the discipline of tissue engineering aims to understand the relationship between structure and function in cell and tissue and to develop biological substitutes that can repair or replace the dead or damaged tissues, organs and/or parts of the human body. The success of tissue engineering may depend on a harmonious interplay of three components; cells for neo-tissue formation; biomaterials to act as scaffolds; biological signaling molecules that instruct cells to form desired tissue type [51]. Among the components, scaffolds play a pivotal role in the field of modern regenerative medicine, because they provide an architectural context in which cells and growth factors can cooperate and represent a wide range of morphological and geometric possibility for suitable clinical application [32]. So far, many biomaterials of natural and synthetic origin have been

C.-H. Kim · S. J. Park

Laboratory of Tissue Engineering, Korea Institute of Radiological and Medical Sciences,  
Seoul, South Korea  
e-mail: [chkim@kcch.re.kr](mailto:chkim@kcch.re.kr); [sjpark@kirams.re.kr](mailto:sjpark@kirams.re.kr)

D. H. Yang

Institute of Cell and Tissue Engineering, College of Medicine, The Catholic University of Korea,  
Seoul, South Korea  
e-mail: [yangdh@catholic.ac.kr](mailto:yangdh@catholic.ac.kr)

H. J. Chun (✉)

Institute of Cell and Tissue Engineering, Department of Biomedical Sciences, College of Medicine, The Catholic University of Korea, Seoul, South Korea  
e-mail: [chunj@catholic.ac.kr](mailto:chunj@ catholic.ac.kr)

adapted for the manufacture of scaffolds with various fabrication techniques to create three-dimensional (3-D) environment mimicking extracellular matrix (ECM) [6, 70], many of which have been the subject of practical development efforts [16, 58]. As natural polymers, collagen and hyaluronic acid can meet the several requirements for scaffold, therefore, have been extensively studied and currently being employed in clinical trials [8, 55]. However, it is crucial that there exists the imbalance between supply and demand in natural polymers because of natural inconsistency in the *in vivo* source; the lot-to-lot variability is always a concern [24]. The additional drawbacks of natural polymers could be the potential impurities that may result in unwanted immune reaction and the difficulties in control mechanical properties [35, 55]. Meanwhile, the main advantage of synthetic polymers over natural polymers is the sufficient availability on demand with constant quality supporting industrial-scale production. Therefore, numerous attempts have been made to use synthetic biodegradable polyesters, such as polylactic acid (PLA), polyglycolic acid (PGA) and their copolymer (PLGA) as the substitute for natural polymeric scaffolds, however, their lack of cell recognition site for cell adhesion, migration and subsequent cellular behaviors often limits applications [32, 65, 69]. Consequently, both natural and synthetic materials have their own merits and demerits have to be complemented.

---

## 25.2 Chitosan

In addition to collagen and hyaluronic acid, a candidate of interest as natural polymeric material for scaffold preparation would be chitin and chitosan. Chitin is the second abundant biopolymer on earth, exceeded only by cellulose [15]. Chitin can be found widely in the exoskeletons of arthropods, shells of crustaceans, and the cuticles of insects [18]. Chitosan, a deacetylated chitin, is

one of the few natural polymers that has free amine groups in its backbone chain, thus has the characteristics of a polymeric hydrogel owing to a high water absorption capacity [34]. It is also known to possess biodegradability, antimicrobial activity and low toxicity and immunogenicity which are essential for scaffolds [29, 67]. For these reasons, chitosan has found a tremendous variety of biomedical applications in recent years.

### 25.2.1 Chemical Structure

Chitosan, produced by deacetylation of chitin, is a linear polysaccharide composed of  $\beta$ -(1 $\rightarrow$ 4)-linked D-glucosamine and N-acetyl-D-glucosamine. The deacetylation process of chitin can not only control degree of deacetylation (DD) but also change the average molecular weight of chitosan. In general, the weight-average molecular weight (Mw) of chitin is in the range from 1.03 to  $2.5 \times 10^6$  g/mole, but the deacetylation process of chitin results in reduced Mw of chitosan to range from 1 to  $5 \times 10^5$  g/mole [62]. Despite the loss in molecular weight of polymer, the main reason for manufacturing chitosan can be the poor solubility of chitin.

In the beginning, because the chemical structure of chitin is very similar to that of cellulose, the studies on solvents for chitin have been carried out together with the development of cellulose. Chitin is a long chain polysaccharide, like cellulose, that shows the degree of polymerization around 7000~15,000 [66]. The inter- and intra-molecular hydrogen bond due to the presence of acetyl amino and hydroxyl bond makes chitin highly aggregated and insoluble in most of organic solvents. The solvents for chitin reported by far include the concentrated salt solutions such as LiCNS, Ca(CNS)<sub>2</sub>, CaI<sub>2</sub>, the strong acids such as HCl, H<sub>2</sub>SO<sub>4</sub> and H<sub>3</sub>PO<sub>4</sub> and other kinds of acids containing carboxylic group such as formic acid, dichloroacetic acid, and trichloroacetic acid, however, in most cases chitin showed very

slow dissolution rate accompanied by severe level of molecular decomposition [64]. Recently, *N,N*-dimethylacetamide, *N*-methyl-2-pyrrolidone and their mixture in the presence of 5% LiCl are known to be a suitable solvent system for cellulose [76]. The main principle is similar to cellulose xanthate, that is  $\text{Li}^+$  ions formed in DMA and NMP solutions bind to the hydroxyl group of cellulose to break the original strong interactions between cellulose chains resulting in dissolution. The same system has been used to solubilize chitin, however, there still exist number of problems awaiting solutions [14, 66]. Chitosan, on the other hand, is easily dissolved in a dilute acid solution in the form of an ammonium salt and has functionality of amino groups, primary and secondary hydroxyl groups for further chemical modifications [5].

### 25.2.2 Nomenclature

Because deacetylated unit (D-glucosamine) and acetylated unit (*N*-acetyl-D-glucosamine) is randomly distributed in chitosan, and because the composition of two residues is entirely dependent upon deacetylation process, nomenclature of chitosan is still controversial. A group of deacetylated chitin whose D-glucosamine residues over 50% (or 60%) is often referred to as chitosan, however, there is no boundary in the nomenclature distinguishing chitin from chitosan [23]. This misunderstanding is probably caused by the fact that the % of DD in commercial chitosan ranges from 60 to 99%. As mentioned above, the important factor in naming 'chitin or chitosan' is the solubility in dilute aqueous acid solutions. That is, regardless of the % of DD, if a deacetylated chitin is insoluble, it cannot be classified into chitosan [64]. In addition to DD, the Mw of chitosan is another important characterization parameter because the application field of chitosan can be widely varied with the distribution of Mw. For biological and functional applications of chitin and chitosan, the international official standard methods to determine DD and Mw of chitin and chitosan, ASTM F2260–03 and

ASTM F2606–13, have been provided to researchers and manufacturers.

### 25.2.3 Distribution of N-Acetyl-D-Glucosamine and D-Glucosamine Units

From chemical point of view, either acids or alkalis can be used to deacetylate chitin, however, alkaline deacetylation is preferred, because glycosidic bonds are very susceptible to acid. As the alkaline deacetylation of chitin, either heterogeneous or homogeneous hydrolysis has been being employed. Heterogeneous hydrolysis employs the severe conditions with hot concentrated NaOH solution within few hours. By this heterogeneous hydrolysis, the deacetylated chitin whose DD up to 80% can be obtained, but they are insoluble. On the contrary, homogeneous hydrolysis using very mild condition at 25 °C of deacetylation temperature produces a soluble chitosan, even though the range of DD is 48–55 [36]. This can be attributed that deacetylation reaction performed under heterogeneous conditions gives an irregular distribution of *N*-acetyl-d-glucosamine and d-glucosamine residues with some block-wise acetyl group distribution along polymeric chains [2]. Thus, solubility and degree of aggregation of chitosan can vary in aqueous solutions leading to changes in their native characteristics. For instance, physico-chemical properties of such chitosans may differ from those of randomly acetylated chitosans obtained under homogeneous conditions.

### 25.2.4 Biocompatible Factors

In addition to good solubility, chitosan has a variety of biocompatible factors compared to chitin. The chemical structure of chitosan is very close to hyaluronic acid, the fourth class and non-sulfated GAG widely distributed throughout connective tissues. It has been believed that the excellent biocompatibility of chitosan is largely attributed to this structural similarity, therefore,

numerous attempts have been made to prepare chitosan based scaffolds for tissue engineering applications [37].

The biodegradability is an essential factor for scaffold preparation because the degradation of scaffold material is a very important process in the tissue remodeling. In the case of chitosan, lysozyme plays a leading role in degradation *in vivo*, and degradation rate is inversely proportional to the degree of crystallinity, which is greatly influenced on DD [73]. Ren et al. reported that each reacylated chitosan matrices with deacetylation degree of 52.6%, 56.1%, and 62.4% has weight half-lives of 9.8 days, 27.3 days, and above 56 days, respectively, with mean molecular weights of 8.4%, 8.8%, and 20.0%, respectively. They also reported that each reacylated chitosan matrices with deacetylation degree of 71.7%, 81.7%, and 93.5% has slow degradation rates, and half-lives of above 84 days both weight and average molecular weight [63].

When chitosan is dissolved, the free amine group of chitosan chain becomes charged as positive, in turn produce the dielectric interactions with negatively charged biologics including the growth factors and the cytokines. The primary amine group can also be utilized as the coupling site for conjugation with biologics in order to build stable interaction. These modifications provide further improvements to chitosan in its biomedical applications [48].

Chitosan is largely known to have a broad antimicrobial activity to which gram-positive, gram-negative and fungi are highly susceptible [61]. Although the precise mechanism for this action has not fully established yet, the most acceptable antimicrobial mechanism includes the presence of positively charged groups in backbone chain and their interactions to negatively charged bacterial wall. This ionic interaction leads the changes in cytoplasmic permeability of bacteria, results in cell death. Chitosan, however, shows its antibacterial activity only in acidic circumstances because of its poor solubility above pH 6.5. In this regards, Kim originally produced the water soluble chitosan derivatives with

ammonium salts and showed their broader spectra of antimicrobial activities [30].

---

### 25.3 Tissue Engineering Applications

For the construction of tissue-engineered organ, three main elements are required; the scaffold, a source of cells and the bio-signaling. 3-D scaffold with various forms takes a role of ECM that function as structural templates for tissue regeneration. For this purpose, the scaffold should have adequate porosity and morphology for transporting of cells, gases, metabolites, nutrients and signal molecules both within the scaffold and between the scaffold and the local environment. In the scaffold with higher porosity and pore size, efficient nutrient supply, diffusion of gas and secretion of metabolites are promoted, however, the interactions between cell-cell become decrease because of low cell attachment. In contrast, lower porosity and pore size results in adverse effects [72]. Therefore, it is necessary to produce scaffolds with appropriate pore size distribution and porosity depending on the cells and tissues.

By virtue of good solubility, chitosan can be manufactured into various forms of scaffolds including fibers, sponges and hydrogels. Madhally prepared chitosan scaffolds of controlled microstructure in several tissue-relevant geometries using freezing and lyophilization technique [48]. Mean pore diameters could be controlled within the range of 1–250  $\mu\text{m}$ . This could be a starting point for design and preparation of chitosan based scaffold materials. Years later, 3-D interconnected open porous chitosan scaffold with controlled pore distribution was prepared [10]. Alcohols were used as non-solvent to induce the liquid-liquid and liquid-solid phase separation via demixing solution. This method enabled to produce the controlled homogeneous micropores and the improved interconnectivity between pores with minimum surface skin layer formation. This interconnectivity of chitosan

scaffold provided the efficient transportation of the substances for cell, therefore, enhanced adhesion as well as proliferation rates of fibroblasts around two folds.

In the meantime, the modifications with ECM components or growth factors to chitosan based scaffolds have been conducted to further increase cell adhesion, proliferation and differentiation through modulation of cellular responses [13, 53]. As the major ECM protein, collagen has been used to enhance cell adhesion to chitosan scaffold in the form of blender of two polymers [49]. Fibronectin as well as laminin have been employed to chitosan for mimicking the biological function of the ECM through immobilization or carbodiimide based crosslinking [12, 27]. Instead of using these macromolecules, there also have been other attempts to make use of small adhesive molecules such as motifs. Many research groups including Ho and Hansson have functionalized chitosan scaffold with arginine-glycine-aspartic acid (RGD) and showed successful cell-scaffold interactions [20, 22].

Proteins and glycoprotein, collagen, laminin and fibronectin, and their amino acid sequence such as RGD, GFOGER and so on are all known to induce cell adhesion and migration through integrin mediated focal adhesion, rather than proliferation and differentiation [21, 38, 68]. There exist, in deed, numerous report that scaffold with ECMs or motifs increases cell proliferation and differentiation, however, the elements that dominate these cellular events are growth factors and cytokines related to receptor tyrosine kinases (RTKs) signaling pathway [41]. A comparative study of cell adhesive peptide and growth factor using chitosan based scaffold also showed the same consequences as mentioned above. Tiğli prepared two kinds of chitosan based scaffolds modified either with RGD or epidermal growth factor (EGF), and found the proliferation trend of ATDC5 murine chondrogenic cells on EGF-chitosan was superior compared to chitosan and RGD-chitosan; although, there was no significant effect on cell attachment [71]. Hence, various types of growth factors including basic fibroblast growth factor (bFGF), transforming growth

factor- $\beta$ 1 (TGF- $\beta$ 1), platelet-derived growth factor-BB (PDGF-BB), and epidermal growth factor (EGF) have been currently introduced to chitosan based tissue engineering scaffold for skin, cartilage and bone [33, 34, 42, 71, 77].

### 25.3.1 Skin

Numerous efforts have been made to develop chitosan based skin substitute because chitosan may play a key role in wound healing phases: blood clotting, inflammation, tissue growth and remodeling. First of all, chitosan has very strong hemostatic activity which is independent on the classical coagulation cascade [60, 78]. Polycations of chitosan bind with host plasmas, cells and tissues inherently charged as negative when come in contact to traumatic wounds. This includes RBCs agglutination, that is, positively charged glucosamine on chitosan strongly attracts negatively charged RBCs to agglutinate; therefore, produce instantaneous clotting together with plasma sorption. The systemic hemostasis activation through platelet adhesion, aggregation and activation follows this fast clot formation. So far, more than 10 chitosan based wound dressing materials including HemCon®, Chitoflex® and Chitoseal® have been commercialized and used as hemostatic dressing [60].

Inflammation is a protective response to eliminate the cause of injury, clear out necrotic cells and tissues through the process of phagocytosis, in turn initiates tissue repair [17]. During proliferation, the factors for tissue regeneration such as, angiogenesis, collagen deposition, granulation and epithelialization occur [52]. Among the cells involved in wound healing process, macrophages may perform indispensable functions in inflammation as well as tissue repair [44, 54]. As a host defender, macrophages recognize and destroy foreign organisms, debride dead and damaged tissue components (classical activation, M1), and produce cytokines, growth factors, and angiogenic factors, which regulate tissue growth and remodeling (alternative activation, M2) [46]. An important point regarding macrophages func-

tion is that chitosan induces both classical and alternative activation in macrophages by the receptor mediated stimulatory effect of chitosan in macrophages, suggesting that chitosan can be one of the functional biomaterials that are responsible for wound healing [26, 74]. Therefore, chitosan scaffolds with various forms that include cross-linked hydrogels, nano-fibrous structures, ion-etched films and so on, fabricated and applied to traumatic or burn wound [1, 28, 47].

In tissue engineering, the focal adhesion is the primary requirement in which cells are communicated. In the case of chitosan, the increase in the content of free amine group increases the attachment of fibroblast but rather decreases the migration and the proliferation [9]. This implies that strong electrostatic interaction between cells and free amine groups in chitosan hinders the cell attachment through the focal adhesion. Kim et al. [31] leveled down this electrostatic property and improved biocompatibility of chitosan through the rigorous dry heat treatment at 110 °C. They had controlled the DD of chitosan based scaffold from 85 to 30% with increase heat treatment time.

The poor focal adhesion capability of chitosan can be enhanced by the addition of ECM components. Ma et al. [45] prepared porous scaffold with the mixture of collagen and chitosan, and found good cytocompatibility to effectively accelerate cell infiltration and proliferation. In addition, much attention has been focused on the use of the growth factor functionalized and/or cell based skin graft. Obara et al. [56] and Alemdaroğlu et al. [3] prepared FGF-2 and EGF incorporated chitosan hydrogel, respectively, and most recently, Yang et al. [74] produced dual growth factors releasing chitosan based hydrogels for accelerated wound healing. Altman et al. [4] had seeded human adipose derived stem cells on chitosan based scaffold and transplanted to wound bed using a murine soft tissue injury model. They found Green Fluorescent Protein (GFP)-positive stem cells on chitosan scaffolds

have differentiated into variety of lineages for soft tissue restoration including fibrovascular, endothelial and epithelial cells up to 4 weeks.

### 25.3.2 Bone

For bone regeneration, hydroxyapatite (HA) and/or tricalcium phosphate (TCP) have been widely employed with polymeric scaffolds because of their unique osseointegrative properties. Lee et al. [40] prepared platelet-derived growth factor (PDGF) loaded chitosan/TCP sponge type scaffold and implanted calvarial defect of rat. The results showed that the addition of PDGF to the scaffold further enhanced bone regeneration. In order to treat large scale bone defect, Ge et al. [19] proposed chitin-HA composite scaffold as a promising candidate to form a structural framework for bone regeneration. They have demonstrated that chitin-HA scaffold provided many requirements for bone tissue regeneration by responding physiological and biological changes and by remodeling the ECM to integrate with surrounding tissue.

Recently, liquid phase chitosan has gained popularity as an injectable scaffold to carry osteoinductive and/or osteoconductive material and to fill out bone defect area for minimally invasive technique. Liu et al. [43] prepared a novel injectable bone substitute material consists of chitosan solution as the liquid phase and TCP powder as the solid phase. The mixture of two components became bone cement upon immersion in SBF, and showed good compressive strength, bioactivity and cytocompatibility enough to have prospect for orthopedic applications. As another approach of injectable scaffold, Park et al. [59] have produced chitosan/alginate based composite that carries recombinant human bone morphogenetic protein-2 (BMP-2) with mesenchymal stem cells and subcutaneously transplanted into the space on the dorsum of nude mice. They have found the trabecular type new

bone formation and concluded that this chitosan/alginate composite could become clinically useful injectable scaffold.

### 25.3.3 Cartilage

In tissue engineering of articular cartilage, the round morphology of chondrocyte represents the maintenance of differentiated chondrocytic phenotype. However, this phenotype is unstable in culture, because chondrocytes may undergo dedifferentiation that involves gradual shift from the synthesis of type II to type I and III collagen, in turn provides the inferior fibrocartilaginous circumstances [75]. This is the major restriction to form hyaline cartilage in cell therapy for repair full thickness destructive cartilage. Therefore, the ideal scaffold that closely mimics the naturally occurring environment in the cartilage matrix is required to stimulate and support chondrogenesis *in vitro* and *in vivo*. GAGs are known to stimulate the chondrogenesis, therefore, use of chitosan as an analog of GAG appears to be ideal for scaffold material of chondrogenesis. In this regard, Lahiji et al. [37] and Iwasaki et al. [25] hypothesized that chitosan based scaffold can support the function and expression of ECM components in chondrocytes, and demonstrated that chitosan leads chondrocytes to have continued expression of collagen II and to maintain their characteristic round morphology. Cui et al. [11] used chitosan to modify poly (L-lactic acid), biodegradable aliphatic polyester, for the purpose of improving cytocompatibility. The bovine articular cartilage chondrocytes cultured on the chitosan modified surface showed beneficial effects on adhesion, proliferation and function. Oliveira et al. [57] have designed and prepared a novel HA/chitosan based bilayered hybrid scaffold using a combination method of sintering and a freeze-drying technique for osteochondral tissue-engineering applications. Both HA and chitosan layer provided an adequate support for osteogenicity and chondrogenicity to seeded MSCs, respectively. Chitosan have been also employed to deliver the growth factors and morphogenetic proteins for further enhanced chondrogenesis in the field of cartilage engineering ([33, 34, 39, 50]).

## 25.4 Future Perspective

With rapid advances and developments of modern sciences and technologies, a new era in tissue engineering and regenerative medicine where scientists with different backgrounds work together to cope with their multidisciplinary has established. For decades, a remarkable achievement has been made to take a major step forward to regenerate skin, cartilage, bone, liver and nervous system. As the second abundant biopolymer on earth, chitosan has also been widely applied to tissue engineering because of its biodegradability, antimicrobial activity and low toxicity and immunogenicity which are essential for scaffolds. However, there still remain problems. Chitosan, similar to the other natural products, has brittleness that limits its practical application; therefore, further efforts are needed to improve mechanical strength. Regarding most of studies using chitosan have been carried out *in vitro*, the additional comprehensive studies using animal models are required to figure out the precise relationship between chitosan and cells or tissues of various organs. Fortunately, HemCon Medical Technologies of the United States commercialized the chitosan based hemostatic bandages for military and emergency use, and hemostatic agents for dentistry. In Canada, Biosyntech developed chitosan based injectable hydrogels, for skin (BST-DermOn), for cartilage (BST-CarGel) and for bone (BST-Ossifil). They are all in clinical trials for FDA approval. These activities truly lead chitosan based scaffolds to a step closer to the practical applications for tissue engineering purpose.

## References

1. Ahmadi F, Oveisi Z, Samani SM, Amoozgar Z (2015) Chitosan based hydrogels: characteristics and pharmaceutical applications. *Res Pharm Sci* 10(1):1–16
2. Aiba S-I (1991) Studies on chitosan: 3. Evidence for the presence of random and block copolymer structures in partially N-acetylated chitosans. *Inter J Biol Macromol* 13(1):40–44. [https://doi.org/10.1016/0141-8130\(91\)90008-I](https://doi.org/10.1016/0141-8130(91)90008-I)
3. Alemdaroğlu C, Değim Z, Celebi N, Zor F, Oztürk S, Erdoğan D (2006) An investigation on burn wound healing in rats with chitosan gel formulation contain-



- ing epidermal growth factor. *Burns* 32(3):319–327. <https://doi.org/10.1016/j.burns.2005.10.015>
4. Altman AM, Yan Y, Matthias N, Bai X, Rios C, Mathur AB, Song YH, Alt EU (2009) IFATS collection: human adipose-derived stem cells seeded on a silk fibroin-chitosan scaffold enhance wound repair in a murine soft tissue injury model. *Stem Cells* 27(1):250–258. <https://doi.org/10.1634/stemcells.2008-0178>
  5. Athanasiou KA, Shah AR, Hernandez RJ, LeBaron RG (2001) Basic science of articular cartilage repair. *Clin Sports Med* 20(2):223–247. [https://doi.org/10.1016/S0278-5919\(05\)70304-5](https://doi.org/10.1016/S0278-5919(05)70304-5)
  6. Barnes CP, Sell SA, Boland ED, Simpson DG, Bowlin GL (2007) Nanofiber technology: designing the next generation of tissue engineering scaffolds. *Adv Drug Deliv Rev* 59(14):1413–1433. <https://doi.org/10.1016/j.addr.2007.04.022>
  7. Bernhard P (2003) *Tissue engineering*. CRC Press, Boca Raton
  8. Bowman S, Awad ME, Hamrick MW, Hunter M, Fulzele S (2018) Recent advances in hyaluronic acid based therapy for osteoarthritis. *Clin Transl Med* 7:6. <https://doi.org/10.1186/s40169-017-0180-3>
  9. Chatelet C, Damour O, Domard A (2001) Influence of the degree of acetylation on some biological properties of chitosan films. *Biomaterials* 22(3):261–268. [https://doi.org/10.1016/S0142-9612\(00\)00183-6](https://doi.org/10.1016/S0142-9612(00)00183-6)
  10. Chun HJ, Kim G-W, Kim C-H (2008) Fabrication of porous chitosan scaffold in order to improve biocompatibility. *J Phys Chem Solids* 69(5–6):1573–1576. <https://doi.org/10.1016/j.jpics.2007.10.104>
  11. Cui YL, Qi AD, Liu WG, Wang XH, Wang H, Ma DM, Yao KD (2003) Biomimetic surface modification of poly(L-lactic acid) with chitosan and its effects on articular chondrocytes in vitro. *Biomaterials* 24(21):3859–3868. [https://doi.org/10.1016/S0142-9612\(03\)00209-6](https://doi.org/10.1016/S0142-9612(03)00209-6)
  12. Custódio CA, Alves CM, Reis RL, Mano JF (2010) Immobilization of fibronectin in chitosan substrates improves cell adhesion and proliferation. *J Tissue Eng Regen Med* 4(4):316–323. <https://doi.org/10.1002/term.248>
  13. Cuy JL, Beckstead BL, Brown CD, Hoffman AS, Giachelli CM (2003) Adhesive protein interactions with chitosan: consequences for valve endothelial cell growth on tissue-engineering materials. *J Biomed Mater Res A* 67(2):538–547. <https://doi.org/10.1002/jbm.a.10095>
  14. de Vasconcelos CL, Bezerril PM, Pereira MR, Ginani MF, Fonseca JL (2011) Viscosity-temperature behavior of chitin solutions using lithium chloride/DMA as solvent. *Carbohydr Res* 346(5):614–618. <https://doi.org/10.1016/j.carres.2010.12.016>
  15. Durkin CA, Mock T, Armbrust EV (2009) Chitin in diatoms and its association with the cell wall. *Eukaryot Cell* 8(7):1038–1050. <https://doi.org/10.1128/EC.00079-09>
  16. Ellis CE, Ellis LK, Korbitt RS, Suuronen EJ, Korbitt GS (2015) Development and characterization of a collagen-based matrix for vascularization and cell delivery. *BioRes Open Access* 491:188–197. <https://doi.org/10.1089/biores.2015.0007>
  17. Ferrero-Miliani L, Nielsen OH, Andersen PS, Girardin SE (2007) Chronic inflammation: importance of NOD2 and NALP3 in interleukin-1 $\beta$  generation. *Clin Exp Immunol* 147(2):227–235. <https://doi.org/10.1111/j.1365-2249.2006.03261.x>
  18. Freier T, Montenegro R, Shan Koh H, Shoichet MS (2005) Chitin-based tubes for tissue engineering in the nervous system. *Biomaterials* 26(22):4624–4632. <https://doi.org/10.1016/j.biomaterials.2004.11.040>
  19. Ge Z, Baguenard S, Lim LY, Wee A, Khor E (2004) Hydroxyapatite-chitin materials as potential tissue engineered bone substitutes. *Biomaterials* 25(6):1049–1058. [https://doi.org/10.1016/S0142-9612\(03\)00612-4](https://doi.org/10.1016/S0142-9612(03)00612-4)
  20. Hansson A, Hashom N, Falson F, Rousselle P, Jordan O, Borchard G (2012) In vitro evaluation of an RGD-functionalized chitosan derivative for enhanced cell adhesion. *Carbohydr Polym* 90(4):1494–1500. <https://doi.org/10.1016/j.carbpol.2012.07.020>
  21. Hersel U, Dahmen C, Kessler H (2003) RGD modified polymers: biomaterials for stimulate cell adhesion and beyond. *Biomaterials* 24(24):4385–4415. [https://doi.org/10.1016/S0142-9612\(03\)00343-0](https://doi.org/10.1016/S0142-9612(03)00343-0)
  22. Ho MH, Wang DM, Hsieh HJ, Liu HC, Hsien TY, Lai JY, Hou LT (2005) Preparation and characterization of RGD-immobilized chitosan scaffolds. *Biomaterials* 26(16):3197–3206. <https://doi.org/10.1016/j.biomaterials.2004.08.032>
  23. Hudson SM, Smith C (1998) Polysaccharide: chitin and chitosan: chemistry and technology of their use as structural materials. In: Kaplan DL (ed) *Biopolymers from renewable resources*. Springer-Verlag, Berlin Heidelberg
  24. Ige OO, Umoru LE, Aribo S (2012) Natural products: a minefield of biomaterials. *ISRN Mater Sci* 2012:983062. <https://doi.org/10.5402/2012/983062>
  25. Iwasaki N, Yamane S-T, Majima T, Kasahara Y, Minami A, Harada K, Nonaka S, Maekawa N, Tamura H, Tokura S, Shiono M, Monde K, Nishimura S-I (2004) Feasibility of polysaccharide hybrid materials for scaffolds in cartilage tissue engineering: evaluation of chondrocyte adhesion to polyion complex fibers prepared from alginate and chitosan. *Biomacromolecules* 5(3):828–833. <https://doi.org/10.1021/bm0400067>
  26. Jeon IH, Mok JY, Park KH, Hwang HM, Song MS, Lee D, Lee MH, Chai KY, Jang SI (2012) Inhibitor effect of dibutylryl chitin ester on nitric oxide and prostaglandin E<sub>2</sub> production in LPS-stimulated RAW 264.7 cells. *Arch Pharm Res* 35(7):1287–1292. <https://doi.org/10.1007/s12272-012-0720-8>
  27. Junka R, Valmikinathan CM, Kalyon DM, Yu X (2013) Laminin functionalized biomimetic nanofibers for nerve tissue engineering. *K=J Biomater Tissue Eng* 3(4):494–502. <https://doi.org/10.1166/jbt.2013.1110>
  28. Kang YO, Yoon IS, Lee SY, Kim DD, Lee SJ, Park WH, Hudson SM (2010) Chitosan-coated poly(vinyl alcohol) nanofibers for wound dressings. *J Biomed*

- Mater Res B Appl Biomater 92(2):568–576. <https://doi.org/10.1002/jbm.b.31554>
29. Khor E, Lm LY (2003) Implantable applications of chitin and chitosan. *Biomaterials* 24(13):2339–2349. [https://doi.org/10.1016/S0142-9612\(03\)00026-7](https://doi.org/10.1016/S0142-9612(03)00026-7)
  30. Kim CH, Choi JW, Chun HJ, Choi KS (1997) Synthesis of chitosan derivatives with quaternary ammonium salt and their antibacterial activity. *Polym Bull* 38(4):387–393. <https://doi.org/10.1007/s002890050064>
  31. Kim CH, Park H-S, Gin YJ, Son Y, Lim S-H, Choi YJ, Park K-S, Park CW (2004) Improvement of the biocompatibility of chitosan dermal scaffold by rigorous dry heat treatment. *Macromol Res* 12(4):367–373. <https://doi.org/10.1007/BF03218413>
  32. Kim MS, Kim JH, Min BH, Chun HJ, Han DK, Lee HB (2011) Polymeric scaffolds for regenerative medicine. *Polym Rev* 51(1):23–52. <https://doi.org/10.1080/15583724.2010.537800>
  33. Kim SE, Park JH, Cho YW, Chung H, Jeong SY, Lee EB, Kwon IC (2003a) Porous chitosan scaffold containing microspheres loaded with transforming growth factor-beta1: implications for cartilage tissue engineering. *J Control Release* 91(3):365–374. [https://doi.org/10.1016/S0168-3659\(03\)00274-8](https://doi.org/10.1016/S0168-3659(03)00274-8)
  34. Kim SJ, Park SJ, Kim SI (2003b) Swelling behavior of interpenetrating polymer network hydrogels composed of poly(vinyl alcohol) and chitosan. *React Funct Polym* 55(1):53–59. [https://doi.org/10.1016/S1381-5148\(02\)00214-6](https://doi.org/10.1016/S1381-5148(02)00214-6)
  35. Ko H-F, Sfeir C, Kumta PN (2010) Novel synthesis strategies for natural polymer and composite biomaterials as potential scaffolds for tissue engineering. *Philos Trans A Math Phys Eng Sci* 368(1917):1981–1997. <https://doi.org/10.1098/rsta.2010.0009>
  36. Kurita K, Sannan T, Iwakura Y (1977) Studies on chitin, 4. Evidence for formation of block and random copolymers of N-acetyl-D-glucosamine and D-glucosamine by hetero- and homogeneous hydrolyses. *Die Makromolekulare Chemie* 178(12):3197–3202. <https://doi.org/10.1002/macp.1977.021781203>
  37. Lahiji A, Sohrabi A, Hungerford DS, Frondoza CG (2000) Chitosan supports the expression of extracellular matrix proteins in human osteoblasts and chondrocytes. *J Biomed Mater Res* 51(4):586–595. [https://doi.org/10.1002/1097-4636\(20000915\)51:4<586::AID-JBM6>3.0.CO;2-S](https://doi.org/10.1002/1097-4636(20000915)51:4<586::AID-JBM6>3.0.CO;2-S)
  38. Lam J, Sequra T (2013) The modulation of MSC integrin expression by RGD presentation. *Biomaterials* 34(16):3938–3947. <https://doi.org/10.1016/j.biomaterials.2013.01.091>
  39. Lee JE, Kim KE, Kwon IC, Ahn HJ, Lee SH, Cho H, Kim HJ, Seong SC, LEE MC (2004) Effect of the controlled-released TGF- beta 1 from chitosan microspheres on chondrocytes cultured in a collagen/chitosan/glycosaminoglycan scaffold. *Biomaterials* 25(18):4163–4173. <https://doi.org/10.1016/j.biomaterials.2003.10.057>
  40. Lee YM, Park YJ, Lee SJ, Ku Y, Han SB, Klokkevold PR, Chung CP (2000) The bone regenerative effect of platelet-derived growth factor-BB delivered with a chitosan/tricalcium phosphate sponge carrier. *J Periodontol* 71(3):418–424. <https://doi.org/10.1902/jop.2000.71.3.418>
  41. Lemmon MA, Schlessinger J (2010) Cell signaling by receptor tyrosine kinases. *Cell* 141(7):1117–1134. <https://doi.org/10.1016/j.cell.2010.06.011>
  42. Liu H, Fan H, Cui Y, Chen Y, Yao K, Goh JC (2007) Effects of the controlled-released basic fibroblast growth factor from chitosan-gelatin microspheres on human fibroblasts cultured on a chitosan-gelatin scaffold. *Biomacromolecules* 8(5):1446–1455. <https://doi.org/10.1021/bm061025e>
  43. Liu H, Li H, Cheng W, Yang Y, Zhu M, Zhou C (2006) Novel injectable calcium phosphate/chitosan composites for bone substitute materials. *Acta Biomater* 2(5):557–565. <https://doi.org/10.1016/j.actbio.2006.03.007>
  44. Liu Y, Stewart KN, Bishop E, Marek CJ, Kluth DC, Rees AJ, Wilson HM (2008) Unique expression of suppressor of cytokine signaling 3 is essential for classical macrophage activation in rodents in vitro and in vivo. *J Immunol* 180(9):6270–6278. <https://doi.org/10.4049/jimmunol.180.9.6270>
  45. Ma L, Gao C, Mao Z, Zhou J, Shen J, Hu X, Han C (2003) Collagen/chitosan porous scaffolds with improved biostability for skin tissue engineering. *Biomaterials* 24(26):4833–4841. [https://doi.org/10.1016/S0142-9612\(03\)00374-0](https://doi.org/10.1016/S0142-9612(03)00374-0)
  46. Macedo L, Pinhal-Enfield G, Alshits V, Elson G, Cronstein BN, Leibovich SJ (2007) Wound healing is impaired in MyD88-deficient mice: a role for MyD88 in the regulation of wound healing by adenosine A2A receptors. *Am J Pathol* 171(6):1774–1788. <https://doi.org/10.2353/ajpath.2007.061048>
  47. Madaghiele M, Demitri C, Sannino A, Ambrosio L (2014) Polymeric hydrogels for burn wound care: advanced skin wound dressings and regenerative templates. *Burns Trauma* 2:20040153. <https://doi.org/10.4103/2321-3868.143616>
  48. Madhally S, Matthew HW (1999) Porous chitosan scaffolds for tissue engineering. *Biomaterials* 20(12):1133–1142. [https://doi.org/10.1016/S0142-9612\(99\)00011-3](https://doi.org/10.1016/S0142-9612(99)00011-3)
  49. Martínez A, Blanco MD, Davidenko N, Cameron RE (2015) Tailoring chitosan/collagen scaffolds for tissue engineering: effect of composition and different crosslinking agents on scaffold properties. *Carbohydr Polym* 132:606–619. <https://doi.org/10.1016/j.carbpol.2015.06.084>
  50. Mattioli-Belmonte M, Gigante A, Muzzarelli RAA, Politano R, De Benedittis A, Specchia N, Buffa A, Biagini G, Greco F (1999) N,N-dicarboxymethyl chitosan as delivery agent for bone morphogenetic protein in the repair of articular cartilage. *Med Biol Eng Comput* 37(1):130–134. <https://doi.org/10.1007/BF02513279>
  51. Mhanna R, Hasan A (2017) 1. Introduction to tissue engineering. In: Hasan A (ed) *Tissue engineering for artificial organs: regenerative medicine, smart diagnostics and personalized medicine*. WILEY-VCH Verlag GmbH & Co. KGaA, Weinheim

52. Midwood KS, Williams LV, Schwarzbauer JE (2004) Tissue repair and the dynamics of the extracellular matrix. *Int J Biochem Cell Biol* 36(6):1031–1037. <https://doi.org/10.1016/j.biocel.2003.12.003>
53. Mochizuki M, Kadoya Y, Wakabayashi Y, Kato K, Okazaki I, Yamada M, Sato T, Sakairi N, Nishi N, Nomizu M (2003) Laminin-1 peptide-conjugated chitosan membranes as a novel approach for cell engineering. *FASEB J* 17(8):875–877. <https://doi.org/10.1096/fj.02-0564fje>
54. Nair MG, Cochrane DW, Allen JE (2003) Macrophages in chronic type 2 inflammation have a novel phenotype characterized by the abundant expression of YM1 and Fizz1 that can be partly replicated in vitro. *Immunol Lett* 85(2):173–180. [https://doi.org/10.1016/S0165-2478\(02\)00225-0](https://doi.org/10.1016/S0165-2478(02)00225-0)
55. O'Brien FJ (2011) Biomaterials & scaffolds for tissue engineering. *Mater Today* 14:88–95. [https://doi.org/10.1016/S1369-7021\(11\)70058-X](https://doi.org/10.1016/S1369-7021(11)70058-X)
56. Obara K, Ishihara M, Ishizuka T, Fujita M, Ozeki Y, Maehara T, Saito Y, Hirofumi Y, Matsui T, Hattori H, Kikuchi M, Kurita A (2003) Photocrosslinkable chitosan hydrogel containing fibroblast growth factor-2 stimulates wound healing in healing-impaired db/db mice. *Biomaterials* 24(20):3437–3444. [https://doi.org/10.1016/S0142-9612\(03\)00220-5](https://doi.org/10.1016/S0142-9612(03)00220-5)
57. Oliveira JM, Rodrigues MT, Silva SS, Malafaya PB, Gomes ME, Viegas CA, Dias IR, Azevedo JT, Mano JF, Reis RL (2006) Novel hydroxyapatite/chitosan bilayered scaffold for osteochondral tissue-engineering applications: scaffold design and its performance when seeded with goat bone marrow stromal cells. *Biomaterials* 27(36):6123–6137. <https://doi.org/10.1016/j.biomaterials.2006.07.034>
58. Ortega-Paz L, Brugaletta S, Sabaté M (2018) Impact of PSP technique on clinical outcomes following bioresorbable scaffolds implantation. *J Clin Med* 7(2):27. <https://doi.org/10.3390/jcm7020027>
59. Park DJ, Choi BH, Zhu SJ, Huh JY, Kim BY, Lee SH (2005) Injectable bone using chitosan-alginate gel/mesenchymal stem cells/BMP-2 composites. *J Craniomaxillofac Surg* 33(1):50–54. <https://doi.org/10.1016/j.jcms.2004.05.011>
60. Pogorielov M, Kalinkevich O, Deineka V, Garbuzova V, Solodovnik A, Kalinkevich A, Kalinichenko T, Gapchenko A, Sklyar A, Danilchenko S (2015) Haemostatic chitosan coated gauze: in vitro interaction with human blood and in-vivo effectiveness. *Biomater Res* 19:22. <https://doi.org/10.1186/s40824-015-0044-0>
61. Rabea EI, Mohamed ETB, Christian VS, Guy S, Walter S (2003) Chitosan as antimicrobial agent: applications and mode of action. *Biomacromolecules* 4(6):1457–1465. <https://doi.org/10.1012/bm034130m>
62. Ravi Kumar MNV (2000) A review of chitin and chitosan applications. *React Funct Polym* 46(1):1–27. [https://doi.org/10.1016/S1381-5148\(00\)00038-9](https://doi.org/10.1016/S1381-5148(00)00038-9)
63. Ren D, Yi H, Wang W, Ma X (2005) The enzymatic degradation and swelling properties of chitosan matrices with different degree of N-acetylation. *Carbohydr Res* 340(15):2403–2410. <https://doi.org/10.1016/j.carres.2005.07.022>
64. Roberts GAF (1992) Derivatives of chitin and chitosan. In: Chitin chemistry. Palgrave, London. [https://doi.org/10.1007/978-1-349-11545-7\\_4](https://doi.org/10.1007/978-1-349-11545-7_4)
65. Roh H, Yang DH, Chun HJ, Khang G (2015) Cellular behavior of hepatocyte-like cells from nude mouse bone marrow-derived mesenchymal stem cells on galactosylated poly(D,L-lactic-co-glycolic acid). *J Tissue Eng Regen Med* 9(7):819–825. <https://doi.org/10.1002/term.1771>
66. Roy JC, Salaün F, Giraud S, Ferri A (2017) Solubility of chitin: solvents, solution behaviors and their related mechanisms. In: Xu Z (ed) Solubility of polysaccharides. InTechOpen. <https://doi.org/10.5772/intechopen.71385>
67. Shahidi F, Abuzaytoun R (2005) Chitin, chitosan, and co-products: chemistry, production, applications, and health effects. *Adv Food Nutr Res* 49:93–135. [https://doi.org/10.1016/S1043-4526\(05\)00000-0](https://doi.org/10.1016/S1043-4526(05)00000-0)
68. Shen B, Delaney MK, Du X (2012) Inside-out, outside-in, and inside-outside-in: G protein signaling in integrin-mediated cell adhesion, spreading, and retraction. *Curr Opin Cell Biol* 24(5):600–606. <https://doi.org/10.1016/j.ceb.2012.08.011>
69. Shin YM, Shin HJ, Yang DH, Koh YJ, Shin H, Chun HJ (2017) Advance capability of radially aligned fibrous scaffolds coated with polydopamine for guiding directional migration of human mesenchymal stem cells. *J Mater Chem B* 5:8725–8737. <https://doi.org/10.1039/C7TB01758H>
70. Tibbitt MW, Anseth KS (2009) Hydrogels as extracellular matrix mimics for 3D cell culture. *Biotechnol Bioeng* 103(4):655–663. <https://doi.org/10.1002/bit.22361>
71. Tıg̈li RS, Gümüřdereliog̈lu M (2008) Evaluation of RGD- or EGF-immobilized chitosan scaffolds for chondrogenic activity. *Int J Biol Macromol* 43(2):121–128. <https://doi.org/10.1016/j.ijbiomac.2008.04.003>
72. van Tienen TG, Heijkants GJC, Buma P, de Groot JH, Pennings AJ, Veth RPH (2002) Tissue ingrowth and degradation of two biodegradable porous polymers with different porosities and pore sizes. *Biomaterials* 23(8):1731–1738. [https://doi.org/10.1016/S0142-9612\(01\)00280-0](https://doi.org/10.1016/S0142-9612(01)00280-0)
73. Vårum KM, Myhr MM, Hjerde RJ, Smidsrød O (1997) In vitro degradation rates of partially N-acetylated chitosans in human serum. *Carbohydr Res* 299(1–2):99–101. [https://doi.org/10.1016/S0008-6215\(96\)00332-1](https://doi.org/10.1016/S0008-6215(96)00332-1)
74. Yang DH, Seo DI, Lee DW, Bhang SH, Park K, Jang G, Kim CH, Chun HJ (2017) Preparation and evaluation of visible-light cured glycol chitosan hydrogel dressing containing dual growth factors for accelerated wound healing. *J Ind Eng Chem* 53:360–370. <https://doi.org/10.1016/j.jiec.2017.05.007>
75. Yoon Y-M, Kim S-J, Oh C-D, Ju J-W, Song WK, Yoo YJ, Hun T-L, Chun J-S (2002) Maintenance of differentiated phenotype of articular chondrocytes by protein kinase C and extracellular signal-regulated protein kinase. *J Biol Chem* 277:8412–8420. <https://doi.org/10.1074/jbc.M110608200>

76. Zhang C, Liu R, Xiang J, Kang H, Liu Z, Huang Y (2014) Dissolution mechanism of cellulose in N,N-dimethylacetamide/lithium chloride: revisiting through molecular interactions. *J Phys Chem B* 118(31):9507–9514. <https://doi.org/10.1021/jp506013c>
77. Zhang Y, Wang Y, Shi B, Cheng X (2007) A platelet-derived growth factor releasing chitosan/coral composite scaffold for periodontal tissue engineering. *Biomaterials* 28(8):1515–1522. <https://doi.org/10.1016/j.biomaterials.2016.11.040>
78. Zhou JC, Zhang JJ, Zhang W, Ke ZY, Zhang B (2017) Efficacy of chitosan dressing on endoscopic sinus surgery: a systematic review and meta-analysis. *Eur Arch Otorhinolaryngol* 274(9):3269–3274. <https://doi.org/10.1007/s00405-017-4584-x>



# Demineralized Dentin Matrix (DDM) As a Carrier for Recombinant Human Bone Morphogenetic Proteins (rhBMP-2)

In Woong Um

## Abstract

A bone graft and bone graft substitute should have at least one of the following properties: it should be (1) osteogenic, (2) osteoinductive and/or (3) osteoconductive. In addition, bone graft substitutes should be biocompatible and bioresorbable as well as easy to use and cost effective. Autologous cancellous bone is the clinical gold standard in bone grafting procedures<sup>1, 4</sup> and it has osteogenic, osteoinductive, and osteoconductive properties. Because of disadvantages associated with harvesting autologous bone graft material, such as requiring an additional operation and possible donor site morbidity, there is a need for an alternative in terms of enhancing the bone healing for the treatment of large bony defects. One possible option is a newly developed biomaterial, the demineralized dentin matrix (DDM). It is based on autogenous tooth dentin and is produced through demineralization. It is osteoconductive and osteoinductive due to the fact that dentin contains extracellular Type I collagen and various growth factors. Based on the demineralization process the factors stay available to the host environment. In 1965, Urist already showed the formation of ectopic bone

after implanting DDM into muscle pouches in rodents. DDM is used for example in dental surgery in the treatment of extraction socket preservation and guided bone regenerations. It functions as a scaffold to support bone regeneration, but can also be used as a carrier for rhBMP-2. When DDM serves as a carrier, it combines the properties of the grafting material with those of the delivered substances. This chapter will present the experimental and clinical studies of DDM for rhBMP-2 carrier as well as alternatives of bone graft substitute.

## Keywords

DDM · Demineralized dentin matrix · rhBMP-2 · Recombinant bone morphogenetic proteins

## 26.1 Scaffold for rhBMP-2 Carrier

### 26.1.1 Carriers for rhBMP-2

Recombinant human bone morphogenetic protein (rhBMP-2) is a water soluble relatively low molecular weight protein that is very difficult to retain in local site for a sufficient period of time due to the body fluids. When administered in a alveolar bone to repair the defect, three dimensional scaffold is necessary not only to maintain the BMP concentration at a local site for a

I. W. Um (✉)  
R&D Institute of Korea Tooth Bank,  
Seoul, South Korea  
e-mail: [h-bmp@hanmail.net](mailto:h-bmp@hanmail.net)

prolonged period of time but also to sustain the form and shape of alveolar bone to be repaired, because the protein will dissipate very easily due to leakage, irrigation and suction around the surgical site [1].

A wide range of BMP carriers of an organic and an inorganic nature have been investigated experimentally and clinically including hydroxyapatite/ $\beta$ -TCP, synthetic, natural polymer and etc. (Table 26.1). The suitable scaffold of rhBMP-2 for alveolar bone regeneration has not been established at this moment.

Other candidates such as hyaluronic acid, fibrin and chitosan have been studied with different success level *in vitro* and *in vivo*. However, the most preferred rhBMP-2 carrier is porous hydroxyapatite and collagen from human bone [2–4] (Table 26.1).

Type I Collagen is the most preferred and commonly used BMP carrier in maxillofacial area and bovine tendon derived Type I collagen has been approved by US FDA in 2007. Since then, composites of rhBMP-2 and absorbable collagen sponges have showed promising results in extraction socket preservation, sinus augmentation procedures. However, the binding capacity of rhBMP-2 to bovine tendon derived collagen is not sufficient compare with bone derived collagen. Therefore the use of rhBMP-2, even though it has been approved by FDA, is restricted due to limitations such as off-label use, squeezing out of collagen and weak mechanical properties [5].

Demineralized bone matrix (DBM) which has intrinsic, limited osteoinductive properties was

also one of the first candidates for BMP carrier [6, 7]. DBM is processed by demineralization of allogenic bone [8]. After removing the major mineral part and the immunogenic components of bone, DBM retains the osteoconductive collagen scaffold and several growth factors including BMP as well as the approximately 2% mineral phase that is different from each demineralization process [3, 9, 10].

DBM functions as a scaffold to support bone regeneration, but can also be used as a carrier for cells or different kinds of pharmaceutical agents (e.g., antibiotic substances) [11]. When DBM serves as a carrier, it combines the properties of the grafting material with those of the delivered substances [12]. However, DBM as a carrier has not gained popularity because of the risk of immunogenicity and the risk of disease transmission.

### 26.1.2 Requirements for rhBMP-2 Carriers

rhBMP-2 requires combination with a suitable carrier to achieve maximal efficacy. Ideal carriers should provide retention of the protein concentration at a local site for a sufficient period of time and degraded gradually according to the biologic environment. Generally accepted characterizations of candidate carrier for rhBMP-2 are adequate porosity to allow cell and blood vessel infiltration, appropriate mechanical stability,

**Table 26.1** Comparison of Dose and release of BMP-2 using four major materials as a carrier system

Categories	Carrier material	BMP-2 Dose	Key results
Inorganic material	HA Granules	10 $\mu$ g	Non-significant
	$\beta$ -TCP Granular implant	1–10 mg	Better fusion rate
Natural origin polymer	Collagen	1 $\mu$ g	Improved bone fusion rates
	Chitosan	5 $\mu$ g	Capable to adopt bone area
Synthetic polymer	PLA	100–800 mg/g	rhBMP-2 depends on the dose
	PLGA	3.5 $\mu$ g, 17.5 $\mu$ g	No synchronization
Composite materials	Collagen- HA	10 $\mu$ g	Anabolic and catabolic agent
	Gelatin/ $\beta$ -TCP	5 $\mu$ g	Bone formation higher in the low p-TCP content

**Table 26.2** Desirable qualities of an ideal rhBMP-2 delivery system

Biocompatibility, low immunogenicity and antigenicity
Biodegradability with biocompatible components, in predictable manner in concert with bone growth
Adequate porosity for cellular invasion and vascularization
Adequate compressive and tensile strength
Enhancement of cellular attachment (but without inducing soft tissue growth at the bone/implant interface)
Amenability to sterilization without loss of properties
Affinity to BMPs and host bone
Enhancement of osteogenic activity of BMP with a restrictive release of BMP at an effective dose during a period coincident with the accumulation and proliferation of target cells
Adaptability to irregular wound site, malleability
Availability to surgeon on short notice

From Brekke et al. [13], Burg et al. [14], Friess [15], and Kirker-Head [3]

biocompatibility, biodegradability, and binding capacity for BMPs [13–15] (Table 26.2).

The main role of the carrier for rhBMP-2 is to retain the factor at the site for a prolonged period of time [4]. Bouxsein reported that collagen sponges soaked with rhBMP-2 in the rabbit ulnar osteotomy model showed retention of rhBMP-2 32% of initial dose at the surgical site 7 days after surgery as compared to only 3% remaining when rhBMP-2 was injected at surgical site [16].

Huber et al. reported that DBM proved *in vitro* to be a suitable carrier for BMP-2, with a documented release over 56 days at concentrations sufficient to stimulate osteogenic differentiation. At the end of the elution experiment, 56 days, bioactive BMP was still captured within the DBM. Using a sheep drill hole defect model, DBM perioperatively mixed with BMP-2 showed strong osteoinductive properties comparable to those of autologous bone and outnumbering the one of DBM alone or empty defects. And with the comparability to the clinical gold standard

autologous bone, DBM mixed with BMP-2 might serve as possible alternative grafting material enabling a controlled osteogenic stimulation [12].

### 26.1.3 rhBMP-2 Combined with Absorbable Collagen Sponge (rhBMP-2/ACS) in Dentistry

Preclinical and clinical research of alveolar bone graft and sinus augmentation for the staged implant placement has demonstrated that rhBMP-2 soaked with absorbable collagen sponge (rhBMP-2/ACS) showed reliable clinical outcomes. Dose dependent clinical studies have determined 1.5 mg/cc as a safe and predictable dose for clinical application.

Boyne et al. [17] reported in a pivotal study the results of bone induction by rhBMP-2/ACS in maxillary sinus floor augmentation as not inferior to those after autogenous bone graft. They found that rhBMP-2 predictably and safely induced adequate loading of endosseous dental implants in patients requiring staged maxillary floor augmentation [18]. The proportion of patients who received dental implants that were functionally loaded and remained functional at 36 months post functional loading was 62% and 76% in the bone graft and 1.5 mg/ml rhBMP-2/ACS treatment groups, respectively.

A randomized prospective study evaluating the use of 1.5 mg/cc rhBMP-2/ACS for extraction socket augmentation showed that rhBMP-2 could predictably form *de novo* bone [19]. Eighty patients requiring local alveolar augmentation for buccal wall defects in the anterior maxilla were evaluated. The adequacy of bone for placement of a dental implant was approximately twice as great in the rhBMP-2/ACS group compare with controls.

In 2007, the FDA approved rhBMP-2 (INFUSE Bone Graft®, Medtronic's, Memphis, TN) soaked with absorbable collagen sponge as an alternative to autogenous bone grafts for sinus augmentations, and for localized alveolar ridge augmentation of defects associated with extraction sockets. However, contraindications for patients with a known hypersensitivity to rhBMP-2 or bovine type I collagen are also specified as well as for the surgical sites related to the vicinity of a resected tumor, active malignancy and infected sites or in pregnant women.

Collagen has a limited capacity for controlled release, and most of the absorbed agent is released during the first day post implantation [5]. The implantation of rhBMP-2 delivered by ACS increases the potential of rhBMP-2 leakage, resulting in ectopic bone formation [20]. The ACS is bovine tendon derived type I collagen. Because of the poor mechanical properties of ACS, the soft tissue walls of the defect can compress it and the use of supraphysiological doses [21] and the insufficient retention of BMP-2 when delivered by a collagen sponge [22] implies operational and biological limitations for the clinical use.

## 26.2 Studies on Demineralized Dentin Matrix (DDM)

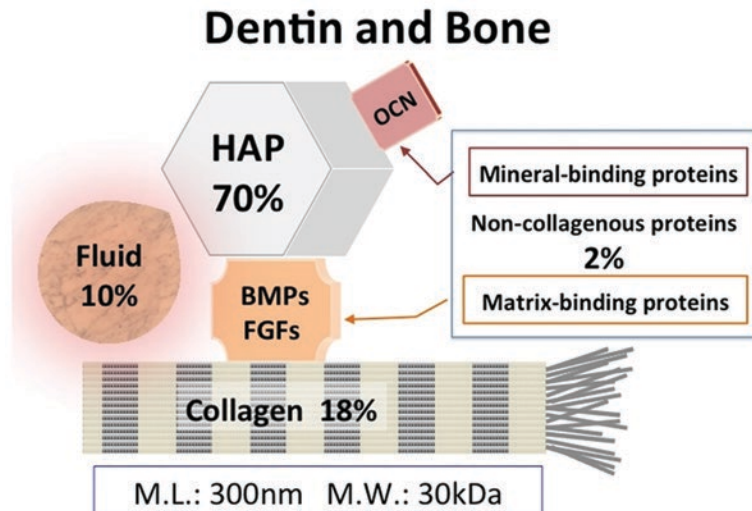
### 26.2.1 Extracellular Matrix (ECM) of Dentin

Bone and dentin has very similar organic and inorganic components; 18% of collagen, 2% of noncollagenous proteins, and 70% of hydroxyapatite in weight volume [23] (Fig. 26.1).

Approximately 90% of the organic material in the dentin consists of type I collagen fibers, primarily type I collagen. The remaining organic components consist of noncollagenous proteins of phosphorylated and non-phosphorylated protein. Diverse growth factors, including bone morphogenetic protein (BMPs), transforming growth factor- $\beta$  (TGF- $\beta$ ), basic fibroblast growth factor (bFGF), and platelet derived growth factors (PDGF), are known to be present in the non-phosphorylated protein fraction (Fig. 26.2).

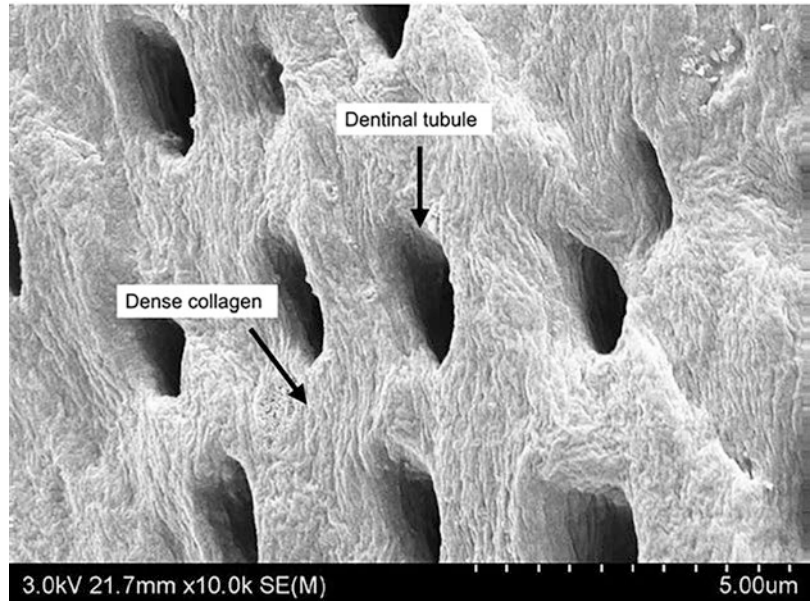
The structural differences [24] between them are the most important points for the release of growth factors and the absorbability of ECM (Fig. 26.2).

**Fig. 26.1** Diagram of common components in dentin and bone. (*HAP* hydroxyapatite, *OCN* osteocalcin, *BMP* bone morphogenetic protein, *FGFs* fibroblast growth factors). (From Murata [23]. J Korean Assoc Oral Maxillofac Surg)

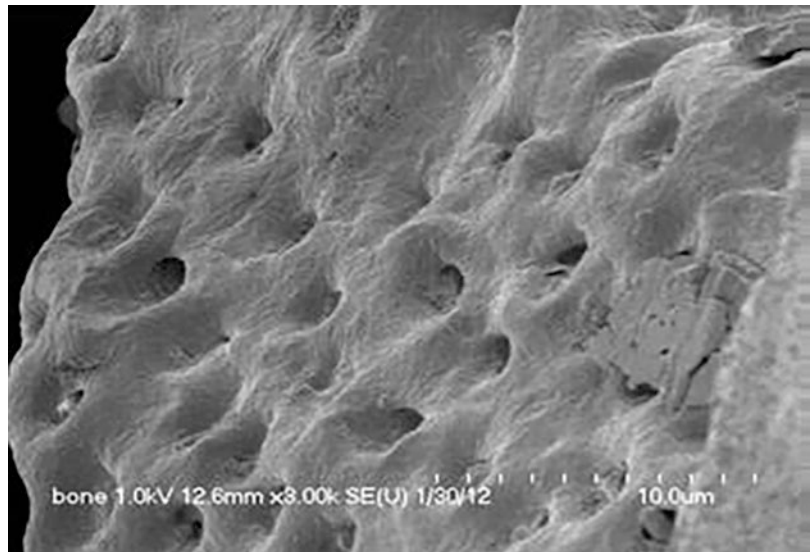




**Fig. 26.2** Scanning electron micrograph of the dentin surface after demineralization ( $\times 10,000$ ). (From Kim et al. [24]. Oral Surg Oral Med Oral Pathol Oral Radiol Endod)



**Fig. 26.3** DDM after rhBMP-2 fixation. (From Um et al. [30]. J Dent App)

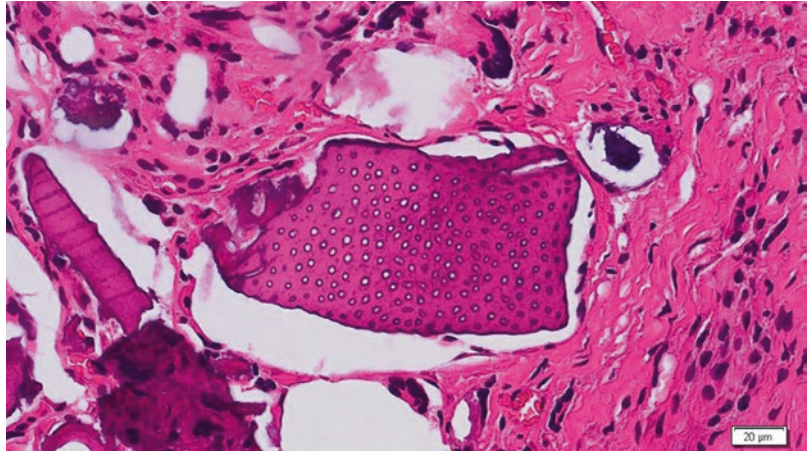


Dentin collagen matrix provides a scaffold for minerals formation and deposition [25, 26] cells adhesion and differentiation [27] and preserving the structural, mechanical and functional integrity of the dentin [28].

The structural differences of dentin from bone are the acellular, avascular, dense collagen matrix with micropore sized dentinal tubules

[24]. Structurally, the dentin matrix consists of dentinal tubules 1–3  $\mu\text{m}$  in diameter [29] that provides micropore spaces of 3.7–5.88% porosity that increase the surface contact area [30] and can accommodate the rhBMP-2 solution, thereby increasing the capacity of dentin to function as an effective scaffold/carrier for rhBMP-2 (Fig. 26.3).

**Fig. 26.4** Histology analyses of a two-week biopsy sample showed the sign of newly deposited osteoid. (H&E,  $\times 200$ ). (From Kim et al. [36]. J Korean Assoc Maxillofac Plast Reconstr Surg)



### 26.2.2 Characterization of DDM (AutoBT®, Korea Tooth Bank, Seoul, Korea)

Human autogenous DDM is one of the most acid insoluble collagenous scaffolds, containing non-collagenous proteins (NCPs) such as bone morphogenetic protein (BMP), in addition to a mineral phase, and is an ideal bone substitute [23, 31–33]. Of clinical importance, DDM based scaffolds are reprocessed, acellular, and microporous Type I collagen [34].

DDM (AutoBT, Korea Tooth Bank, Seoul, Korea), fabricated from patient's own extracted tooth, is mainly processed by dehydration, defatting, and partial demineralization. Dentin demineralization with 0.6 N HCl results in the elimination of the major part of the mineral phase and immunogenic components, while retaining a very low fraction of minerals (5–10 wt.%), the majority of Type I collagen, and NCPs, providing an osteoconductive and osteoinductive scaffold containing several growth factors [35–37] (Fig. 26.4).

Kim et al. analyzed organic components in autogenous tooth bone graft material (AutoBT) and reported that 0.29% (2.89 mg/g), 0.02% (0.029 mg/g), and 1.79% (17.93 mg/g) of proteins were measured by weight (Bradford assay) in root portion, crown and block form of AutoBT respectively [36, 37] (Table 26.3).

**Table 26.3** The highest amounts of proteins were extracted in root form of AutoBT, whereas the lowest amounts were extracted from the crown portion in Bradford assay

Type of AutoBT	Organic component by weight, % (mg/g)
Root portion	0.29 (2.89)
Crown portion	0.02 (0.03)
Block-form	1.79 (17.93)

From Kim et al. [36]. J Korean Assoc Maxillofac Plast Reconstr Surg.

AutoBT autogenous tooth bone graft material

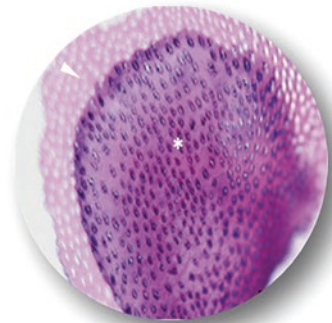
The range of particle size of DDM is from 300  $\mu\text{m}$  to 800  $\mu\text{m}$  in diameter with a median size of 500  $\mu\text{m}$ . Microscopic observations demonstrated that the basic dentin microtexture was preserved after demineralization that starts at the surface and progresses to the interior of dentine particle. Structurally, dentinal tubules are enlarged and dense collagen matrix is loosened [38–41] (Fig. 26.5).

X-ray diffraction (XRD) analysis found that low crystalline structures, domain sizes, and high Ca/P ion dissolution of the DDM were similar to those of autogenous bone with calcium phosphate. These included HA (Ca/P = 1.75), TCP (Ca/P = 1.46), amorphous calcium phosphate (ACP, Ca/P = 1.32), and oc-talcium phosphate (OCP, Ca/P = 1.24) with the plate like crystals [38–42].

**Fig. 26.5** Size and surface demineralization of DDM particle



**Size range: 300-800  $\mu\text{m}$**



**Surface: Demineralization  
Core: Mineralization**

### 26.2.3 Studies on Human Autogenous DDM (AutoBT<sup>®</sup>, Korea Tooth Bank, Seoul, Korea)

Urist first reported that dentin is an osteoinductive material that causes connective tissue to convert to bone by endochondral osteogenesis [8]. After the discovery of bone induction by rabbit demineralized bone matrix in 1965, rabbit demineralized dentin matrix also founded to be osteoinductive in 1967. Demineralized dentin was known to be more inductive than the mineralized dentin that is mainly due to easy release of growth factors in Type I collagen matrix such as BMPs as well as osteocalcin, osteonectin, and dentin phosphoproteins which are known to be involved in bone mineralization [31, 33, 43, 44].

In 1991, Bessho et al. successfully isolated the BMP from human dentin matrix. Although, human dentin derived BMP was different from human bone derived BMP, two types of BMP exhibit the same action in the body. Murata et al. [45] showed that human DDM, including small patches of cementum fabricated from wisdom teeth showed osteoinduction capacity. Kim et al. showed that human DDM (AutoBT, Korea Tooth Bank, Seoul, Korea) grafted into the muscle of nude mice induced cartilage and bone independently, as shown in Fig. 26.4. Newly deposited osteoid on DDM powder indicated osteoinductivity of DDM [35–37].

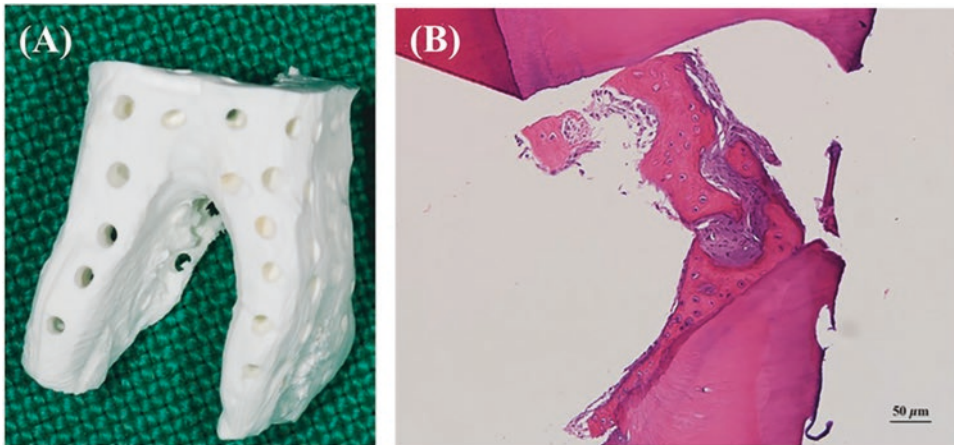
Regarding clinical applications, AutoBT, which was first reported for guided bone regen-

eration in 2010, showed the regeneration of alveolar bone after AutoBT grafts [24]. And the follow up study performed 6 years after the first clinical report showed that the alveolar bone, repaired 3–6 months after AutoBT grafts, had been maintained its volume and shape successfully with minimal marginal bone resorption which had been within the success criteria of implant [46, 47]. Although the number of clinical samples was not enough for the statistical power, the results were consistent with those of other short term follow up studies on AutoBT [38–41].

Pang et al. performed randomized controlled clinical trials of AutoBT (autogenous human DDM, Korea Tooth Bank, Seoul, Korea) to compare with anorganic bovine bone for the extraction sockets augmentation. Both group showed favorable wound healing, reliable implant stability and histological evidence of new bone formation that suggests AutoBT as a viable option for extraction socket preservation [48].

Augmentation of vertical dimension showed that it was as effective as augmentation using anorganic bovine bone both groups showed favorable wound healing, similar amount of implant stability, and histologically confirmed new bone formation. Thus, the results of this study suggest that autogenous tooth graft material is a viable option for alveolar bone augmentation following dental extraction.

Demineralized dentin matrix block (ABTB: Autogenous Tooth Bone Graft Block, Korea Tooth Bank, Seoul, Korea) is 3 Dimensional scaf-



**Fig. 26.6** Fabrication of the ABTB. (a) Macropores (200–300  $\mu\text{m}$ ) that penetrated from the surface to the pulp space provided the space for vascular invasion. (b) Histological findings; A macropore of the ABTB was filled with newly formed osteoid with embedded active

chondrocyte like cells that closely contacted the inner wall of the macropore. Cellular fusion without fibrous tissue invasion was observed on the border between the osteoid and the dentin matrix. (From Kim et al. [49]. Clin Case Rep)

fold that has very similar components and geometry with alveolar bone. Kim et al. reported that ABTB is well incorporated to and remodeled into host alveolar bone (Fig. 26.6) [46].

### 26.3 DDM for rhBMP-2 Carrier (DDM/rhBMP-2)

As many studies on the DDM have investigated the osteoinductive functions and their clinical applications, those on the carriers for rhBMP-2 have also sought to identify the mechanisms and to develop methods to combine with rhBMP-2. Some of most recent approaches that have been employed to study DDM as rhBMP-2 carrier are as follows.

#### 26.3.1 Experimental Studies of DDM for rhBMP-2 Carrier

As a candidate for an rhBMP-2 carrier, Ike et al. reported that xenogenous rhBMP-2 adsorbed into pulverized root and partially DDM proved to be as osteoinductive as an autogenous bone graft [50]. Murata also showed that human DDM particles are insoluble collagenous matrices which

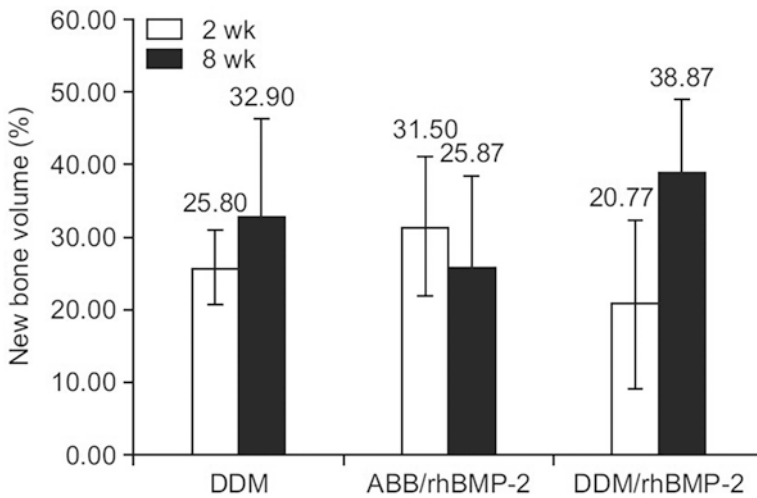
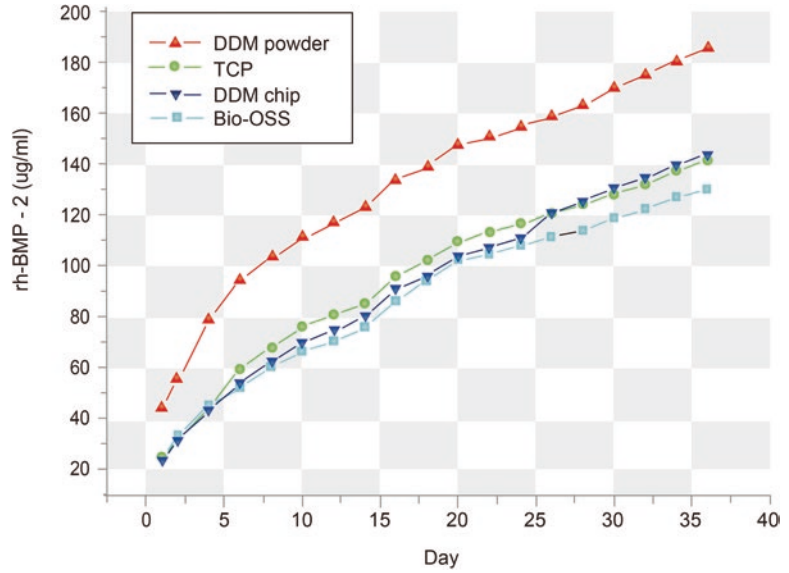
has osteoinductive capacities, and that DDMs might be effective as an rhBMP-2 carrier for alveolar bone repair [51].

The first report of AutoBT (human DDM, Korea Tooth Bank, Seoul, Korea) as a candidate for rhBMP-2 carrier [40] have demonstrated that DDM displays the controlled release kinetics of rhBMP-2 such as release to load ratio and release speed and the osteonectin expression, resulting in augmented mature bone formation compare with tricalcium phosphate (TCP) (Fig. 26.7).

Um et al. examined the bone induction capacity of AutoBT as an rhBMP-2 carrier compare with conventional TCP in the intramuscular pouches of nude mice. AutoBT (human DDM, Korea Tooth Bank, Seoul, Korea) and TCP (CowellMedi, Busan, Korea).

AutoBT (human DDM, Korea Tooth Bank, Seoul, Korea) that were combined with rhBMP-2 (DDM/rhBMP-2) was the experimental group ( $n = 20$ ). rhBMP-2 soaked TCP (TCP/rhBMP-2, CowellMedi, Busan, Korea) was the control group ( $n = 20$ ). Earlier cellular reaction on the DDM surface, more amount of osteoid deposition was seen in early stage compare with TCP groups. Later at 4 weeks, DDM showed compact bone formation while the TCP showed fatty tissue formation [30].

**Fig. 26.7** Comparison of release kinetics over time. Kinetics of rhBMP-2 release from bone graft materials observed *in vitro*. Sustained release of rhBMP-2 was observed for up to 5 weeks. (From Kim et al. [40] J Hard Tissue Biol)



**Fig. 26.8** New bone volume measured by microcomputed tomography. New bone volume increased in DDM (27.5%) and DDM/rhBMP-2 (87.14%) from 2 to 8 weeks compared with the decreased new bone volume in ABB/rhBMP-2 (-17.9%). Values are presented as mean ± stan-

dard deviation. No statistically significant differences were found among the groups. (DDM demineralized dentin matrix, ABB anorganic bovine bone, rhBMP-2 recombinant human bone morphogenetic protein-2). (From Um et al. [34]. J Korean Assoc Oral Maxillofac Surg)

In the rabbit’s calvarial defect, the anorganic bovine bone combined with rhBMP-2 (ABB/rhBMP-2) groups showed osteoconductive bone formation, while the DDM/rhBMP-2 group showed osteoinductive bone formation. And the

amount of new bone formation in DDM/rhBMP-2 was highest among DDM and TCP/rhBMP-2 especially at 8 week of experiment compare to the 2 week of experiment [34] (Fig. 26.8).

### 26.3.2 Clinical Studies of DDM for rhBMP-2 Carrier

To compare the short term outcome of DDM/rhBMP-2 (Bioα, Seongnam, Korea) with hydroxyapatite (HA)/rhBMP-2 (Bioα, Seongnam, Korea), each scaffold was soaked with 0.5 mg/0.5 ml of rhBMP-2 solution for 10 min. Favorable bony healing was obtained in all cases without any severe complications. Successful prosthetic treatment was completed without any osseointegration failure. In this case series study, rhBMP-2 combined with HA or DDM scaffolds can be used for bone graft procedures such as guided bone regeneration [40].

About the effectiveness of allogenic DDM loaded with rhBMP-2 (CowellMedi, Busan, Korea) for alveolar bone repair [46], the clinical findings with respect to the healing process were that there were no remarkable inflammation and immune rejection that impair the healing process and are coincident with those of the previous studies [24, 46–48]. The nanopore structure of dentinal tubules in unique avascular and acellular Type I collagenous dentin matrix seems to make it feasible to carry and release rhBMP-2 effectively on local site based on the previous study.

In the clinical study of histological comparison of autogenous and allogenic DDM loaded with rhBMP-2 (CowellMedi, Busan, Korea) at the site between the implant cover screw and gingiva, as the poor blood supply allows it to simulate a heterotopic condition, three patients undergoing simultaneous implant placement and receiving a different type of graft were included: allogenic DDM loaded with rhBMP-2 (DDM/rhBMP-2), autogenous DDM/rhBMP-2 and autogenous DDM. After 3–6 months of grafts, the antigenicity and immunogenicity of the carrier allogenic DDMs are low enough to maintain both the biocompatibility of the scaffold and the activity of the loaded rhBMP-2 [52, 53].

Jeon et al. reported study to evaluate soft tissue volume change after socket preservation using AutoBT (Korea Tooth Bank, Seoul, Korea), AutoBT combined with rhBMP-2 (CowellMedi, Busan, Korea) (DDM/rhBMP-2) and Bio-Oss collagen (Geistlich, Wolhusen, Switzerland). A

total of 24 participants who were required tooth extraction were randomly divided into three groups according to graft materials. Bio-Oss collagens for the first group, DDM alone for the second, and DDM/rhBMP-2 for the third group were used. According to soft tissue volume changes, each groups showed statistically meaningful volume decreases. Bio-Oss collagen showed 15.4% volume decrease, DDM showed 18.8% and DDM/rhBMP-2 showed 16.1% decrease, respectively. However, there were no significant differences among groups.

Kim et al. reported the healing potential of DDM/rhBMP-2 (CowellMedi, Busan, Korea) in the clinical study of a total of 23 patients with 36 implants. The results showed that favorable osseointegration was obtained in 35 out of 36 implant sites in terms of the implant stability and marginal bone loss [49, 54].

### 26.4 What Is Coming Next in DDM/rhBMP-2 Research?

Lee et al. [55] performed quantitative analysis of proliferation and differentiation of the MG-63 cell line on partially demineralized human dentin matrix (PDDM) by 0.6 N HCl *in vitro* to evaluate the osteogenic potential of DDM and compare it to a mixture of anorganic bovine bone and collagen (Bio-Oss Collagen® Geistlich, Wolhusen, Switzerland).

Cell adhesion and growth on the DDM surface were more abundant, with cells adopting a flat shape and uniform distribution, than on the Bio-Oss Collagen® at all the observation time points. And confocal laser scanning microscopy revealed that the DDM provided better attachment with cytoplasmic propagation than the control. Immunofluorescence assays showed that the fluorescent intensities of osteocalcin and osteonectin as biomarkers of cellular differentiation were higher on the DDM than on Bio-Oss Collagen®.

Until now, research on DDM for rhBMP-2 carrier has been conducted *in vitro* and *in vivo*, as well as clinical trials. The advantages of DDM as BMP carrier compare to the conventional candidate materials are that DDM is osteoconductive

and osteoinductive due to the fact that dentine contains various growth factors. Based on the demineralization process the factors stay available to the host environment. In 1965, Urist already showed the formation of ectopic bone after implanting demineralized dentine into muscle pouches in rodents. DDM is used for example in dental surgery, in the treatment of implant bone graft. It functions as a scaffold to support bone regeneration, but can also be used as a carrier for rhBMP-2. When DDM serves as a carrier, it combines the properties of the grafting material with those of the delivered substances.

Microparticles of dentine are having particle diameter ranging from 300  $\mu\text{m}$  to 800  $\mu\text{m}$ . The nanopores of dentinal tubules (1–3  $\mu\text{m}$ ) provide higher surface to volume ratio that is advantageous to reduced protein diffusion and retains sufficient concentration for recruitment and differentiation of osteoprogenitor cells.

Although all the experimental and clinical researches of DDM/rhBMP-2 reported favorable results and very optimistic futures, we should do more hard work to ensure the clinical safety and efficacy. For example, the suitable concentration and amount of rhBMP-2, the condition of DDM such as particle size, processing method, loading method of rhBMP-2 on DDM and etc. should be confirmed and established by more advanced studies. Furthermore, the possibilities of DDM as stem cell carrier for alveolar bone regeneration would be wide open in dentistry.

## References

1. Seeherman H, Wozney J, Li R (2002) Bone morphogenetic protein delivery systems. *Spine (Phila Pa 1976)* 27(16 Suppl 1):S16–S23
2. Babensee JE, McIntire LV, Mikos AG (2000) Growth factor delivery for tissue engineering. *Pharm Res* 17(5):497–504
3. Kirker-Head CA (2000) Potential applications and delivery strategies for bone morphogenetic proteins. *Adv Drug Deliv Rev* 43(1):65–92
4. Li RH, Wozney JM (2001) Delivering on the promise of bone morphogenetic proteins. *Trends Biotechnol* 19(7):255–265
5. Maeda M, Tani S, Sano A, Fujioka K (1999) Microstructure and release characteristics of the minipellet, a collagen-based drug delivery system for controlled release of protein drugs. *J Control Release* 62(3):313–324
6. Dahners LE, Jacobs RR (1985) Long bone defects treated with demineralized bone. *South Med J* 78(8):933–934
7. Martin GJ Jr, Boden SD, Titus L, Scarborough NL (1999) New formulations of demineralized bone matrix as a more effective graft alternative in experimental posterolateral lumbar spine arthrodesis. *Spine (Phila Pa 1976)* 24(7):637–645
8. Urist MR (1965) Bone: formation by autoinduction. *Science* 150(3698):893–899
9. Dinopoulos HTH, Giannoudis PV (2006) Safety and efficacy of use of demineralised bone matrix in orthopaedic and trauma surgery. *Expert Opin Drug Saf* 5(6):847–866. <https://doi.org/10.1517/14740338.5.6.847>
10. Reddi AH (1998) Role of morphogenetic proteins in skeletal tissue engineering and regeneration. *Nat Biotechnol* 16(3):247–252
11. Bormann N, Schwabe P, Smith MD, Wildemann B (2014) Analysis of parameters influencing the release of antibiotics mixed with bone grafting material using a reliable mixing procedure. *Bone* 59:162–172. <https://doi.org/10.1016/j.bone.2013.11.005>. Epub 2013 Nov 12
12. Elisabeth H, Poblath A-M, Bormann N, Kolarczik N, Schmidt-Bleek K, Schell H, Schwabe P, Duda GN, Wildemann B (2017) Demineralized bone matrix as a carrier for bone morphogenetic Protein-2: burst release combined with long-term binding and Osteoinductive activity evaluated *In Vitro* and *In Vivo*. *Tissue Eng Part A* 23(23–24):1321–1330. <https://doi.org/10.1089/ten.tea.2017.0005>
13. Brekke JH, Toth JM (1998) Principles of tissue engineering applied to programmable osteogenesis. *J Biomed Mater Res* 43(4):380–398
14. Burg KJ, Porter S, Kellam JF (2000) Biomaterial developments for bone tissue engineering. *Biomaterials* 21(23):2347–2359
15. Friess W (2000) Drug delivery systems based on Collagen, *Berichte aus der Pharmazie*. Shaker Verlag, Aachen, pp 94–137
16. Bouxsein ML, Turek TJ, Blake CA, D'Augusta D, Li X, Stevens M, Seeherman HJ, Wozney JM (2001) Recombinant human bone morphogenetic protein-2 accelerates healing in a rabbit ulnar osteotomy model. *J Bone Joint Surg Am* 83-A(8):1219–1230
17. Boyne PJ, Lilly LC, Marx RE, Moy PK, Nevins M, Spagnoli DB, Triplett RG (2005) De novo bone induction by recombinant human bone morphogenetic protein-2 (rhBMP-2) in maxillary sinus floor augmentation. *J Oral Maxillofac Surg* 63(12):1693–1707
18. Itoh K, Udagawa N, Katagiri T, Iemura S, Ueno N, Yasuda H, Higashio K, Quinn JM, Gillespie MT, Martin TJ, Suda T, Takahashi N (2001) Bone morphogenetic protein 2 stimulates osteoclast differentiation and survival supported by receptor activator of nuclear factor-kappaB ligand. *Endocrinology* 142(8):3656–3662

19. Fiorellini JP, Howell TH, Cochran D, Malmquist J, Lilly LC, Spagnoli D, Toljanic J, Jones A, Nevins M (2005) Randomized study evaluating recombinant human bone morphogenetic protein-2 for extraction socket augmentation. *J Periodontol* 76(4):605–613
20. Benglis D, Wang MY, Levi AD (2008) A comprehensive review of the safety profile of bone morphogenetic protein in spine surgery. *Neurosurgery* 62(5 Suppl 2):ONS423–ONS431. <https://doi.org/10.1227/01.neu.0000326030.24220.d8>. discussion ONS431
21. Ripamonti U, Duarte R, Ferretti C (2014) Re-evaluating the induction of bone formation in primates. *Biomaterials* 35(35):9407–9422. <https://doi.org/10.1016/j.biomaterials.2014.07.053>. Epub 2014 Aug 23
22. Seeherman H, Li R, Bouxsein M, Kim H, Li XJ, Smith-Adaline EA, Aiolo M, Wozney JM (2006) rhBMP-2/calcium phosphate matrix accelerates osteotomy-site healing in a nonhuman primate model at multiple treatment times and concentrations. *J Bone Joint Surg Am* 88(1):144–160
23. Murata M (2012) Collagen biology for bone regenerative surgery. *J Korean Assoc Oral Maxillofac Surg* 38:321–325. <https://doi.org/10.5125/jkaoms.2012.38.6.321>
24. Kim YK, Kim SG, Byeon JH, Lee HJ, Um IU, Lim SC, Kim SY (2010) Development of a novel bone grafting material using autogenous teeth. *Oral Surg Oral Med Oral Pathol Oral Radiol Endod* 109(4):496–503. <https://doi.org/10.1016/j.tripleo.2009.10.017>. Epub 2010 Jan 8
25. Tay FR, Pashley DH (2008) Guided tissue remineralisation of partially demineralised human dentine. *Biomaterials* 29(8):1127–1137
26. Tay FR, Pashley DH (2009) Biomimetic remineralization of resin-bonded acid-etched dentin. *J Dent Res* 88(8):719–724. <https://doi.org/10.1177/0022034509341826>
27. Huang GT, Shagranova K, Chan SW (2006) Formation of odontoblast-like cells from cultured human dental pulp cells on dentin *in vitro*. *J Endod* 32(11):1066–1073
28. Marshall GW Jr, Marshall SJ, Kinney JH, Balooch M (1997) The dentin substrate: structure and properties related to bonding. *J Dent* 25(6):441–458
29. Schilke R, Lisson JA, Bauss O, Geurtsen W (2000) Comparison of the number and diameter of dentinal tubules in human and bovine dentine by scanning electron microscopic investigation. *Arch Oral Biol* 45(5):355–361
30. Um IW, Cho WJ, Kim YK (2015) Experimental study on human DemineralizedDentin matrix as rhBMP-2 carrier *In Vivo*. *J Dent App* 2(7):269–273
31. Bang G, Urist MR (1967) Bone induction in excavation chambers in matrix of decalcified dentin. *Arch Surg* 94(6):781–789
32. Butler WT, Mikulski A, Urist MR, Bridges G, Uyeno S (1977) Noncollagenous proteins of a rat dentin matrix possessing bone morphogenetic activity. *J Dent Res* 56(3):228–232
33. Yeomans JD, Urist MR (1967) Bone induction by decalcified dentine implanted into oral, osseous and muscle tissues. *Arch Oral Biol* 12(8):999–1008
34. Um IW, Hwang SH, Kim YK, Kim MY, Jun SH, Ryu JJ, Jang HS (2016) Demineralized dentin matrix combined with recombinant human bone morphogenetic protein-2 in rabbit calvarial defects. *J Korean Assoc Oral Maxillofac Surg* 42(2):90–98. <https://doi.org/10.5125/jkaoms.2016.42.2.90>. Epub 2016 Apr 27
35. Kim KW (2014) Bone induction by demineralized dentin matrix in nude mouse muscles. *Maxillofac Plast Reconstr Surg* 36(2):50–56. <https://doi.org/10.14402/jkampr.2014.36.2.50>. Epub 2014 Mar 30
36. Kim YK, Lee JH, Kim KW, Um IW, Murata M, Ito K (2013) Analysis of organic components and osteoinductivity in autogenous tooth bone graft material. *J Korean Assoc Maxillofac Plast Reconstr Surg* 35(6):353–359
37. Kim YK, Lee JK, Kim KW, Um IW, Murata M (2013) Chapter 16: Advances in biomaterials science and biomedical applications. In: Pignatello R (ed) *Healing mechanism and clinical application of autogenous tooth bone graft material*. InTech, Rijeka, p 405
38. Kim YK, Kim SG, Bae JH, Um IW, Oh JS, Jeong KI (2014) Guided bone regeneration using autogenous tooth bone graft in implant therapy: case series. *Implant Dent* 23(2):138–143. <https://doi.org/10.1097/ID.0000000000000046>
39. Kim YK, Kim SG, Yun PY, Yeo IS, Jin SC, Oh JS, Kim HJ, Yu SK, Lee SY, Kim JS, Um IW, Jeong MA, Kim GW (2014) Autogenous teeth used for bone grafting: a comparison with traditional grafting materials. *Oral Surg Oral Med Oral Pathol Oral Radiol* 117(1):e39–e45. <https://doi.org/10.1016/j.oooo.2012.04.018>. Epub 2012 Aug 30
40. Kim YK, Um IW, An HJ, Kim KW, Hong KS, Murata M (2014) Effects of demineralized dentin matrix used as an rhBMP-2 carrier for bone regeneration. *J Hard Tissue Biol* 23(4):415–422
41. Kim YK, Um IW, Murata M (2014) Tooth bank system for bone regeneration -safety report. *J Hard Tissue Biol* 23:371–376
42. Kim YK, Kim SG, Oh JS, Jin SC, Son JS, Kim SY, Lim SY (2011) Analysis of the inorganic component of autogenous tooth bone graft material. *J Nanosci Nanotechnol* 11(8):7442–7445
43. Huggins CB, Urist MR (1970) Dentin matrix transformation: rapid induction of alkaline phosphatase and cartilage. *Science* 167(3919):896–898
44. Huggins C, Wiseman S, Reddi AH (1970) Transformation of fibroblasts by allogeneic and xenogeneic transplants of demineralized tooth and bone. *J Exp Med* 132(6):1250–1258
45. Murata M, Akazawa T, Takahata M, Ito M, Tazaki J, Hino J, Nakamura K, Iwasaki N, Shibata T, Arisue M (2010) Bone induction of human tooth and bone crushed by newly developed automatic mill. *J Ceram Soc Jpn* 118(6):434
46. Kim YK, Jang HJ, Um IW (2016) A case report of allogenic demineralized dentin matrix loaded with



- recombinant human bone morphogenetic proteins for alveolar bone repair. *J Dent Oral Health* 2(6):45
47. Kim YK, Lee JH, Um IW, Cho WJ (2016) Guided bone regeneration using demineralized dentin matrix: long-term follow-up. *J Oral Maxillofac Surg* 74(3):515.e1–515.e9. <https://doi.org/10.1016/j.joms.2015.10.030>. Epub 2015 Nov 10
  48. Pang KM, Um IW, Kim YK, Woo JM, Kim SM, Lee JH (2017) Autogenous demineralized dentin matrix from extracted tooth for the augmentation of alveolar bone defect: a prospective randomized clinical trial in comparison with anorganic bovine bone. *Clin Oral Implants Res* 28(7):809–815. <https://doi.org/10.1111/clr.12885>. Epub 2016 Jun 8
  49. Kim YK, Pang KM, Yun PY, Leem DH, Um IW (2017) Long-term follow-up of autogenous tooth bone graft blocks with dental implants. *Clin Case Rep* 5(2):108–118. <https://doi.org/10.1002/ccr3.754>. eCollection 2017 Feb
  50. Ike M, Urist MR (1998) Recycled dentin root matrix for a carrier of recombinant human bone morphogenetic protein. *J Oral Implantol* 24(3):124–132
  51. Murata M (2005) Bone engineering using human demineralized dentin matrix and recombinant human BMP-2. *J Hard Tissue Biol* 14(2):80–81
  52. Um IW, Jun SH, Yun PY, Kim YK (2017) Histological comparison of autogenous and allogenic demineralized dentin matrix loaded with recombinant human bone morphogenetic Protein-2 for alveolar bone repair: a preliminary report. *J Hard Tissue Biol* 26(4):417–424
  53. Um IW, Kim YK, Mitsugi M (2017) Demineralized dentin matrix scaffolds for alveolar bone engineering. *J Indian Prosthodont Soc* 17(2):120–127. [https://doi.org/10.4103/jips.jips\\_62\\_17](https://doi.org/10.4103/jips.jips_62_17)
  54. Kim SY, Kim YK, Park YH, Park JC, Ku JK, Um IW, Kim JY (2017) Evaluation of the healing potential of demineralized dentin matrix fixed with recombinant human bone morphogenetic Protein-2 in bone grafts. *Materials (Basel)* 10(9):E1049. <https://doi.org/10.3390/ma10091049>
  55. Lee HJ, Hong JS, Kim YK, Um IW, Lee JI (2017) Osteogenic potential of demineralized dentin matrix as bone graft material. *J Hard Tissue Biol* 26(2):223–230



# Prospects of Natural Polymeric Scaffolds in Peripheral Nerve Tissue-Regeneration

Roqia Ashraf, Hasham S. Sofi, Mushtaq A. Beigh, Shafquat Majeed, Shabana Arjamand, and Faheem A. Sheikh

## Abstract

Tissue-engineering is emerging field and can be considered as a novel therapeutic intervention in nerve tissue-regeneration. The various pitfalls associated with the use of autografts in nerve-regeneration after injuries have inspired researchers to explore the possibilities using various natural polymers. In this context, the present chapter summarizes the advances of the various types of natural polymeric scaffolds such as fibrous scaffolds, porous scaffolds, and hydrogels in nerve-regeneration and repair process. The functionalization of the scaffolds with wide-range of biomolecules and their biocompatibility analysis by employing various cells (e.g., mesenchymal, neural progenitor stem cells) along with the *in vivo* regeneration outcomes achieved upon implantation are discussed here. Besides, the various avenues that have been explored so far in nerve tissue-engineering, the use of the extracellular matrix in enhancing the

functional polymeric scaffolds and their corresponding outcomes of regeneration are mentioned. We conclude with the present challenges and prospects of efficient exploration of natural polymeric scaffolds in the future to overcome the problems of nerve-regeneration associated with various nerve injuries and neurodegenerative disorders.

## Keywords

Nerve tissue-engineering · Natural polymers · Scaffolds · Stem cells · Extracellular matrix

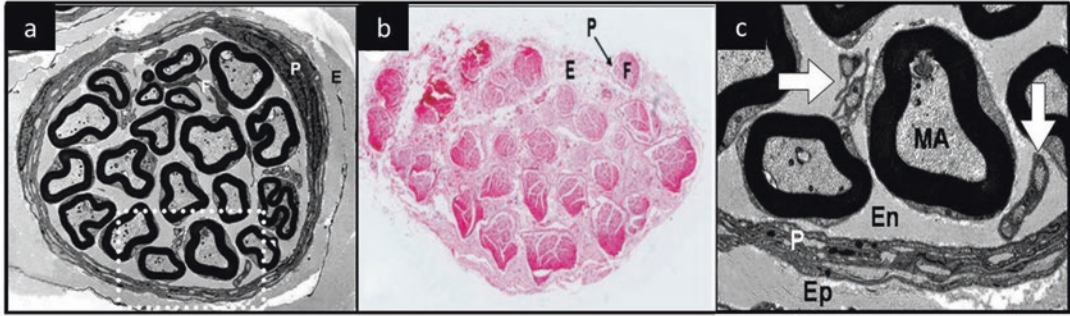
R. Ashraf · H. S. Sofi · M. A. Beigh · S. Majeed  
F. A. Sheikh (✉)  
Department of Nanotechnology, University of  
Kashmir, Srinagar, Jammu and Kashmir, India  
e-mail: [faheemnt@uok.edu.in](mailto:faheemnt@uok.edu.in)

S. Arjamand  
Department of Industrial Fish and Fisheries, Degree  
College Bemina, Cluster University Srinagar,  
Srinagar, Jammu and Kashmir, India

## 27.1 Introduction

### 27.1.1 Micro-Architecture of Nerve Cell

The nervous system is the network of nerves responsible for the control, communication, and coordination in the body. Basically, it is divided into two parts, the peripheral nervous system (PNS) and the central nervous system (CNS). The CNS includes the brain and spinal cord and the PNS constitutes the nerves and ganglia. These acts as a communication link between the whole body and the CNS. Neurons are the functional unit of the nervous system and are electrically excitable and terminally differentiated cells. It comprises of the cell body, neuronal axons, the



**Fig. 27.1** Electron and light microscopy image of the nerve fascicle (F) at (a and b). The (c) highlights the microstructure of nerve showing three layers endoneurium (E/En), perineurium (P), and epineurium (Ep) around

myelinated axons (MA). The white arrows represent the non-myelinated neurons. (Reprinted with permission from Elsevier [88])

cells along with connective tissue stroma and a blood supply [88]. In comparison to CNS, the nerve cells of the PNS have some power of regeneration. The cell bodies of PNS neurons are located within spinal ganglia, their central connections (nerve roots) and axons outstretch through peripheral nerves extending to target organs. PNS contain several types of nerves (e.g., afferent sensory nerves and efferent motor nerves) performing the coordination and functional activities [115]. Each nerve is marked out from the surrounding by a protective layer called epineurium (Fig. 27.1). It consists of loose connective tissue and blood vessels that supply the nerve. Within the epineurium, the nerve fibers are contained and aligned in fascicles. Each fascicle is marked out from the other fascicle by a layer called perineurium. It constitutes of dense perineurial cells and collagen fibers which mark its outer layer. Nerve fibers in the fascicle are supported by a connective tissue in their surrounding called endoneurium. Reticular fibers, fibroblasts, collagen, extracellular matrix (ECM) constitute endoneurium [57]. Besides this, alignment of collagen fibrils around the nerve fibers gives rise to endoneurial tubes. The axons along with Schwann cells (SCs) are enclosed in these tubes. These endoneurial tubules provide the efficacious environment for SCs to proliferate and subsequent regeneration and reinnervation after an injury [124].

### 27.1.2 Importance of Schwann Cells in Nerve-Regeneration

Following injuries, only the nerve cells of the PNS have the power of regeneration and reinnervation. Therefore, permitting some degree of restoration of lost functions, depending upon the graveness of the injury and the quality of the repair in the PNS [4]. Besides, the change at the cellular and molecular levels in Wallerian degeneration, the internal natural ability of the injured neurons to regenerate equally contributes to nerve repair. SCs that are mainly responsible for the myelination of axons play a significant role in the regeneration of nerve cells. Distal SCs at the site of injury switches and dedicate themselves to nerve repair because of their intrinsic flexible different properties that are subdued in oligodendrocytes and neurons of the CNS. SCs at the site of injury proliferate and secrete trophic factors that guide the regeneration process of axotomized neurons [136]. These SCs align themselves along the basal lamina that leads to the formation of the bands of Büngner which offer cues to nerve fiber regeneration. The SCs along with their produced basal lamina (i.e., ECM) and these bands enhance and promote the guided nerve tissue-regeneration by providing the mandatory cellular and molecular factors, including the growth factors [49]. Thus SCs, besides the participation in myelination of axons also participate in guided nerve

tissue-regeneration after an event of nerve injuries. Later on, the recovering neurons will have the ability to reach the distal target organs and subsequent reinnervation restores the lost functions [80]. After peripheral nerve transection, the surgical repair is necessary, to permit the injured axons to grow into the distal degenerating nerve. [42]. This intervention reunites the two nerve stumps proximal and distal. However, this union being difficult, often misguide the axons towards the wrong distal path. Thus, the intervention of autologous grafts is commonly used to overcome this problem [42]. Autografts as the union between the stumps are most commonly used and have remained a gold standard for larger nerve defects that otherwise are difficult to repair. However, their clinical utilization implicates serious drawbacks like lack of donors, donor site morbidity, differences in nerve architecture and SC phenotype mismatch [39, 42].

### 27.1.3 ECM in Nerve Tissue-Regeneration

ECM of the nervous tissue is comprised of various proteins, which include major fibrous proteins collagen, laminin, fibronectin, fibrin [122]. Besides these proteins nidogens, vitronectin, and carbohydrate polymers covalently bound to proteins called proteoglycans are also present. These include heparin, chondroitin, keratin, dermatan and their sulfates [73]. These ECM fibrous components, especially collagen, laminin, fibronectin play an important role in the nerve-regeneration and hence are preferred in nerve tissue-engineering [57]. Nerve fibers in PNS are contained and aligned in the endoneurium as already mentioned above, where SC gets involved in the process of myelination of axons. Besides, their role in myelination of axons they also produce basal lamina in endoneurium. Basal lamina (i.e., ECM) is composed of collagen IV, laminin and fibronectin [16, 25, 113]. These basal lamina layers act as fibrous scaffolds and subsequent proliferation of SCs give existence to bands termed as bands of Büngner. Remembering the role of SCs and basal

lamina contained in the endoneurium especially proteins, various approaches have been explored by tissue-engineering towards the reconstruction of nerve gaps after nerve injuries. Instead, of implantation of grafts nowadays tissue-engineering has achieved new heights in regenerative medicine. Moreover, the nerve tissue-engineering has also been studied greatly and engineered nerve tissue grafts are emerging as an encouraging approach against conventional grafts [61, 174, 175].

### 27.1.4 Tissue-Engineering

Tissue-engineering involves the fabrication of various biocompatible scaffolds for use in *in vivo* transplantation, to replace, repair and/or to regenerate damaged tissue [91]. Tissue-engineering has opened new opportunities and ways towards tissue-regeneration including nerve tissue-regeneration, thus paving a way to overcome the limitations of traditional routes for tissue-engineering like autologous grafts. Polymeric scaffolds of biopolymers are extensively used in the tissue engineering, as fibrous architecture and nanotopographies present in these scaffolds is similar to the ECM present in endoneurium in micro-structural nerve cell anatomy of PNS [9, 31, 128]. Thus, after an event of injury, these scaffolds are capable of guiding the regeneration process across injured lesions.

### 27.1.5 Fabrication and Functionalization of the Scaffolds for Nerve Tissue-Regeneration

Various polymeric scaffolds for nerve tissue-engineering have been fabricated for use in nerve-regeneration. There are a number of approaches that can be utilized for their fabrication like electrospinning [45], phase separation [110], self-assembly [101], templating [154], drawing [79], vapor-phase separation [139], controlled solution synthesis [78], chemical oxidative polymerization

[40], bacterial cellulose synthesis [133] and extraction from plants [98]. Among these methods, electrospinning technique is the widely used strategy because of its simple, governable processing parameters and fiber functionalization. Due to its versatility, this technique is also widely explored for fabrication of polymeric scaffolds in nerve tissue-engineering [17, 18, 38]. Electrospinning involves the fabrication of polymeric nanofibers from a liquid solution under the high electric field in kilovolts supplied by high voltage power supplier. The polymeric droplet when exposed to a high electric field gets a surface positive charge, resulting in a Taylor cone generation. Subsequently, this droplet is driven in the form of a fiber having diameters at nano-scale depositing towards the grounded collector plate [18]. The fabrication of the scaffolds can be modulated by various parameters like viscosity, conductivity, flow-rate, and tip to collector distance [18]. These parameters were simple and easily tunable providing the versatility of this technique. However, the fabrication of fibers with electrospinning mainly produces scaffolds with 2D architecture. The influence on electrospun 2D polymeric scaffolds during *in vitro* experiments with various types of cells has been extensively studied and certain drawbacks like size limitations, low porosity, low thickness and reduced penetration in the scaffolds came forward [22].

Biomaterial-based polymeric scaffolds are frequently exploited in various nerve tissue-regeneration applications. A huge research has been performed and is currently going on towards the fabrication and functionalization of various scaffolds. Blending with proteins and growth factors has made good progress in tissue-engineering, but challenges of technical and ethical issues are of common concern [26] [164]. The role of ECM in nerve repair after injury has been aforementioned keeping this importance in consideration various ECM functionalized scaffolds have gained ample significance in recent years. The use of ECM-based polymeric scaffold in nerve tissue-regeneration has thus reduced the drawbacks associated with cells or growth factor functionalized scaffolds [174].

### 27.1.6 Natural Polymeric Scaffolds in Nerve Tissue-Engineering

Neural scaffolds composed of various biomaterials have been engineered and are providing new hopes to treat various neurodegenerative disorders [122]. Studies have shown that ECM components and biomimetic properties of the scaffolds exert significant influence on the direction and inclination of nerve cells, thus explore the prospects of nerve tissue repair [23, 52]. Natural biopolymers among biomaterials are extensively used for nerve tissue-engineering due to their unique advantages over synthetic polymers [174]. The properties that provide a natural polymers edge over synthetic polymers include biocompatibility, bioactivity, biomimetic properties, mechanical kinetics and controlled degradation [70, 138, 151].

Keeping in view the fact that cells reside in a 3D niche in their physiological habitat, the 3D electrospinning has been introduced to fabricate nanofibers suitable to provide the cells exactly the same 3D niche as they have in their physiological environment [166]. This 3D natural polymeric scaffold promotes better proliferation, cell adhesion, migration, and differentiation [22]. These scaffolds display the almost similar surface topographies like native tissue, thus influence the cells in a positive way than 2D scaffolds. For the best efficiency of the scaffold function, the natural polymers have been used individually and as composites with other polymers [94]. The various forms of natural polymeric scaffolds so far employed in nerve tissue-engineering include fibrous scaffolds, solid porous scaffolds, polymer gels, acellular scaffolds [43, 105]. Natural polymeric scaffolds so far fabricated for nerve tissue-engineering are alginates [97], chitosan [117], collagen [37], silk fibroin [48], fibrin [10], gelatin [54], gellan gum [150] hyaluronic acid [155]. Further improvements in scaffold architecture have to be performed in order to overcome barriers like cell adhesion, proliferation, proper nutrient supply, cell infiltration and mechanical stability [2, 166]. The natural biomaterials manipulated by functionalization in

nerve tissue-engineering so far include collagen, laminin, silk fibroin, gelatin, gellan gum, fibrin and polysaccharides like chitosan, alginates and hyaluronic acid [49, 141]. Studies show that human neural stem cells adhered to various scaffolds like chitin-alginate have been studied for nerve tissue-engineering [108]. Similarly, mesenchymal stem cells derived acellular matrixes have been used to functionalize composite chitosan/silk scaffold nerve reconstruction [62]. Besides these, ECM functionalized scaffolds/hydrogels containing various biomaterial guides or conduits (e.g., chitosan guides) have also been fabricated with the aim to reconstruct peripheral nerve gap [58]. Moreover, various polymeric scaffolds have also been incorporated with different nanoparticles like poly (3, 4-ethylenedioxythiophene) and graphene oxide [168, 180]. These nanoparticles promote scaffold conductivity that in turn contributes towards physiologically relevant electrical stimulation, which is necessary for guided nerve-regeneration [67, 68, 170]. Furthermore, functionalization of scaffolds with various biomolecules (e.g., proteins) is of key importance in tissue-regeneration and it is helpful in achieving the desired experimental results [141]. Thus, remembering the importance of nerve tissue-regeneration post-injury and the different approaches by which various natural polymeric scaffolds can be tailor-manipulated and functionalized. The current chapter focuses on a brief insight towards nerve-regeneration and importance of these techniques in regeneration followed by detailed, recent progress and possibilities of the polymeric scaffolds in nerve tissue-regeneration.

---

## 27.2 Chitosan as Biomaterial

Chitosan (CS) is a polysaccharide derived from the chitin. Chitin is a homo-polysaccharide, found in the exoskeleton of crustaceans, molluscs, and insects, cell walls of green algae, yeasts and mushrooms [36, 137]. CS is obtained from the de-acetylation of the chitin and is composed of monomers D-glucosamine and N-acetyl-

glucosamine joined together by a  $\beta(1-4)$  glycosidic bonds [135, 137]. The three functional groups, one amino group and two hydroxyl groups in the structure of CS contribute to its cationic nature and thus promote the affinity for anionic biomolecules [14, 123]. CS is the only natural polymer to possess this characteristic feature [19]. The content of amino groups and subsequent rate of acetylation/de-acetylation of monomers along with solubility, bioactivity, and biodegradability makes chitosan an amazing polymer in various fields, including tissue-engineering [36, 69].

### 27.2.1 Chitosan Scaffolds in Nerve Tissue-Engineering

CS has been widely explored in nerve tissue-engineering keeping in view its versatility [135, 169]. Guan et al. fabricated a novel composite scaffold with polymers of chitosan/gelatin functionalized with hyaluronic acid and heparin sulfate by freeze-drying technique [63]. Hyaluronic acid and heparin sulfate are glycosaminoglycans, important constituents of ECM. Moreover, the hyaluronic acid has been investigated for playing a considerable role in scaffold designing for tissue-regeneration [81]. It is an anionic biopolymer and has also been investigated for the proliferation of murine neural progenitor cells (NPCs) *in vitro*, together with fibroblast growth factor (FGF-2) [30]. Moreover, hyaluronic acid along with FGF-2 also helps in generation of the neurons from fetal human NPCs at a large scale in the very precise time period [63, 126]. Freeze-drying is the commonly used technique to fabricate porous scaffolds where the freezing rate contributes towards the nucleation and considerable heterogeneity of the scaffold [125]. In the aforementioned study, the three composite scaffolds with varying content of CS/gelatin/hyaluronic acid/heparin sulfate were fabricated. This was followed by analysis of their characteristics in comparison with the pure CS/gelatin scaffold. These scaffolds have been characterized by analysis of their micro-architecture, physiochemical and biological

properties. The pore-size, total porosity and water absorption in composite scaffold showed no significant difference when the CS content was decreased and the content of gelatin with hyaluronic acid and heparin sulfate was increased. However, a significant difference in porosity was observed in comparison with CS/gelatin scaffold. Following the NPCs seeding on these scaffolds and during the subsequent investigation, it was observed that the composite scaffolds of CS/gelatin/hyaluronic acid/heparin sulfate promoted the cell adhesion and cell viability. Moreover, upon proper induction, the neuronal differentiation potentiates considerably compared to CS/gelatin scaffolds [63].

ECM functionalized tissue-engineered nerve grafts are emerging as a primary and potential approach for nerve tissue-regeneration [174]. To overcome the limitations of autografts various artificial conduits or guides of natural polymers have been developed [60]. The nerve gap >15 mm is very difficult to reconstruct [42, 109] hence, various approaches are attempted to overcome this problem [60]. CS has been widely exploited for fabrication of nerve conduits with diverse functionalization. Gonzalez-Perez et al. studied the regeneration power of CS tubes with varying degree of acetylation in the reconstruction of 15 mm sciatic nerve gap in Wistar Hannover rats, compared with silicone tubes and nerve grafts. Compared to the nerve grafts where all rats showed efficient regeneration and reinnervation, about 100%. It was observed 57% in rats with CS guide having (5% acetylation) and with silicone tubes the rats completely failed to regenerate [58]. Considering this generalization, another study fabricated and functionalized the CS conduits with the incorporation of the CS film in the hollow CS conduits. The regeneration outcome was analyzed in the reconstruction of 15 mm long sciatic nerve gap in both healthy and diabetic rats. Results conclude that the regeneration potential of these conduits almost approached the regeneration potential of rats with nerve grafts [116]. Further, exploration of the similar concept by functionalization of CS tubes using collagen enriched with laminin and fibronectin resulting in stabilized and the

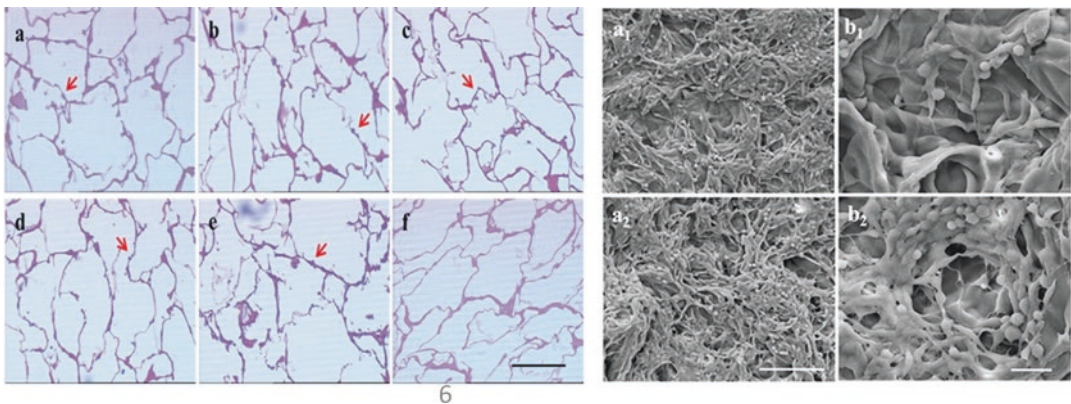
hydrated scaffolds/constructs. The efficiency of these scaffolds enclosed CS tubes were tested in the reconstruction of 15 mm nerve gap in rats. The study demonstrated that the collagen/fibronectin enriched constructs (stabilized scaffold) have revealed increased myelinated fibers, along with increased SC migration and reinnervation compared to the collagen/laminin constructs (stabilized scaffold) and the corresponding hydrated scaffolds [59]. Following the nerve transection, the SCs at the site of injury, possess the ability of proliferation, differentiation and subsequent migration, thereby acting as guidance cues for axon-regeneration [121]. Keeping this in consideration, transplantation of SCs into nerve conduits has recently been explored and the apparent addition of neurotrophic factors demonstrated axonal and functional recovery of nerves [65, 111, 130]. Further, as one more step towards efficient nerve-regeneration by CS, conduits incorporated with the hydrogels containing engineered SCs have been investigated by Meyer et al. Hollow CS nerve conduits with 5% acetylation and functionalization of the conduit lumen by genetically engineered rat SCs and FGF-2 enriched hydrogel scaffold have been used in this study. Overexpression of glial-derived neurotrophic factors (GDNF) and FGF-2 by the SCs demonstrated that release of FGF-2 promoted the efficiency of regeneration by the conduits. Further, the release of FGF-2 by SCs increased the functional recovery up to 57% in bridging the 15 mm sciatic nerve gap, in comparison to the rats where autografts were implanted. On the other hand, GDNF failed to perform these functions [117].

Nerve cells are electrically active cells, generation of electrical impulse and subsequent transfer of stimuli plays an important role in the functioning of the nervous system [159]. Recent research focuses on exploiting this electrical property of the nervous tissue in the fabrication of the electro-active biomaterial for nerve tissue-regeneration [15, 66]. The electrical, physical and chemical properties of these electro-active scaffolds can be manipulated according to experimental requirements related to the particular application [82]. Polymers such as

polypyrrole, polyaniline, poly(3,4-ethylenedioxythiophene) (PEDOT) are known for their conductive nature due to efficient electro-optical properties and thus are contributing significantly in various biomedical applications [41, 68, 171]. Due to the hydrophilicity and poor biodegradability of these conductive polymers, they are often utilized in tissue-engineering as blends of natural polymers [64]. Wang et al. fabricated the conductive polymer with PEDOT nanoparticles enriched CS/gelatin scaffold by *in-situ* interfacial polymerization. In this study, the CS/gelatin hydrogel has been used as a scaffold and subsequent enrichment with varied content of PEDOT nanoparticles promoted its electro-optical properties. The analysis of various characteristics of these scaffolds demonstrated the successful enrichment of 50 nm diameter PEDOT nanoparticles on the scaffolds (Fig.27.2). Further, there was an increase in the electrical conductivity, thermal stability besides improved hydrophilicity and mechanical properties compared to pristine CS/gelatin. Consequently, there was a decrease in biodegradation and water absorption when compared to CS/gelatin scaffolds. Biocompatibility analysis indicated

that upon cell seeding these scaffolds enhanced the cell adhesion and proliferation of neuron-like rat pheochromocytoma (PC12) cells. The gene and subsequent high protein expression analysis concluded that in these cells the neurite growth was enhanced using these scaffolds and thus suggests that it may prove a significant scaffold in nerve-regeneration [168].

The tailoring of the scaffolds towards their ultimate excellence, various functionalization approaches has been explored towards this goal. Tissue-derived ECM, both neural and non-neural has been explored in the functionalization of neural polymeric scaffolds [28, 89]. These scaffolds have been successful in nerve repair, but counter certain limitations like lack of availability of tissue, poor mechanical properties and uncontrollable degradation [11, 100]. To overcome these limitations, new research approaches explore the possibilities of the cell-derived ECM as a substitution to the tissue-derived ECM [102, 162]. Furthermore, Gu and coworkers [62] functionalized the chitosan nerve conduits by silk fibroin (SF) filaments incorporated with ECM-derived from bone marrow mesenchymal stem cell (BMSC) for nerve repair in rats. BMSCs have been exploited



**Fig. 27.2** Histomorphological analysis of H&E staining of scaffold constructs after 3 days of culture; (a) CS/Gelatin; (b) 0.5 PEDOT/CS/Gelatin; (c) 1 PEDOT/CS/Gelatin; (d) 2 PEDOT/CS/Gelatin; (e) 4 PEDOT/CS/Gelatin; (f) CS/Gelatin devoid of cells; scale bar = 200  $\mu$ m and scanning electron microscopy images of scaffold constructs of CS/Gelatin without (a<sub>1</sub> & b<sub>1</sub>) and with

PEDOT(2PEDOT/CS/Gelatin) and cells (a<sub>2</sub> & b<sub>2</sub>); scale bar of (a<sub>1</sub>, a<sub>2</sub>) & (b<sub>1</sub>, b<sub>2</sub>) = 200  $\mu$ m and 50  $\mu$ m, respectively, demonstrating successful enrichment of 50 nm diameter PEDOT nanoparticles on the scaffolds. (Reprinted with copyright permission from Royal Society of Chemistry [168])



extensively in tissue-engineering due to their ability to differentiate into SC-like cells, both *in vitro* and *in vivo* [33, 107]. Scaffolds both CS conduit and SF have been prepared and subsequently cultured with BMSCs in this study. This was followed by the de-cellularization of the BMSCs thus, results in the production of ECM functionalized CS-SF scaffold. Results declared that this scaffold potentiates the regenerative process of implantation in rats to bridge the 10 mm long sciatic nerve lesion compared to pristine CS-SF scaffold [62]. Adding more to this, Xue et al. utilized the dog BMSCs-derived ECM to functionalize the CS-SF scaffold. The de-cellularization of the BMSCs onto these scaffolds was used to reconstruct the 60 mm sciatic gap in dogs. Histological analysis of this scaffold after implantation revealed the promotion of regeneration and reinnervation processes. Further, it was observed that the regeneration output was similar to that of autografts [174].

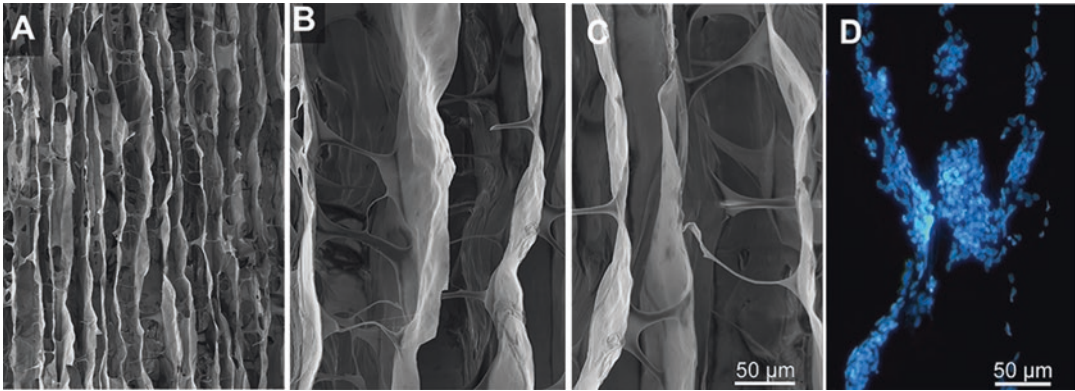
---

## 27.3 Collagen as Biomaterial

Collagen the main structural protein in vertebrates has been extensively investigated for tissue-engineering. Collagen is composed of three polypeptide strands helically wound about each other, forming the triple-stranded  $\alpha$  helical structure [24, 176]. Following synthesis from the endoplasmic reticulum and subsequent delivery to ECM, collagen fibrils assemble in the form of a scaffold-like structure by cross-linking with each other for this enzyme lysyl oxidase plays a significant role [83]. Collagens besides establishing structural unity by making ECM and maintaining functional aspects of the connective tissues present there are also responsible for proper cell adhesion, proliferation, differentiation, migration and cell viability [20, 176]. Collagens being the most abundant constituent in ECM have been widely explored for general tissue-engineering including nerve tissue-engineering.

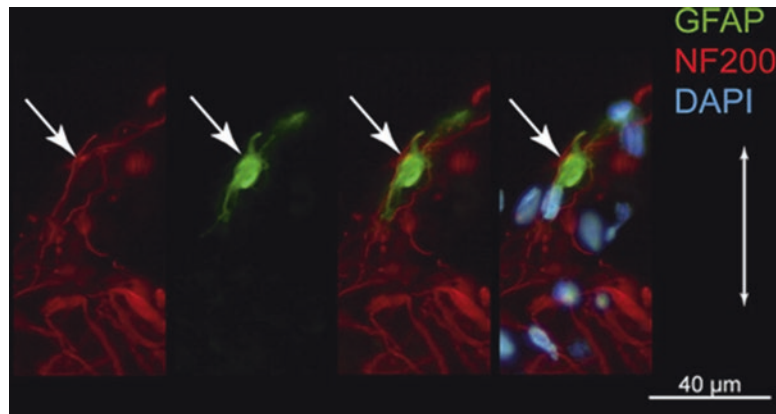
### 27.3.1 Collagen as a Scaffold for Nerve Tissue-Engineering

The investigations for using collagen as a bio-material scaffold for nerve tissue-engineering are increasing in recent years [48]. The properties of the collagen especially its abundance in ECM has made it the most explored polymer in tissue-engineering. Besides the functionalization of scaffolds with various biomolecules, the functionalization with NPCs has also gained importance [131]. The NPCs as cells for functionalization are efficient in regenerating neural tissues as they have the capacity of self-renewal and ability to differentiate into various glial cells [134]. In this context, the regeneration power of the hNPC-derived astrocytes (hNP-AC) adhered on collagen scaffolds were fabricated by a directional freezing process, followed by their interactive studies with the migrating SCs and fibroblasts. Both 2D and 3D cultures used in this study concluded that human neural progenitor cells hNPCs possess strong and effective axon-regeneration power in dorsal root ganglia. Following cell seeding, a homogeneous distribution of the hNP-AC was seen onto the 3D collagen scaffolds (Fig. 27.3) [52]. The axon growth was enhanced by cell seeding when compared to non-seeded scaffolds. Further, interactive studies of SCs and the fibroblasts with the hNP-AC revealed strong intermingling of these cells. Therefore, demonstrates the effective interaction between the hNP-AC, SC, and fibroblasts. These results are contradictory with general properties of SCs/astrocytes and fibroblasts/astrocytes association where they are found in distinct localization [104, 144]. Thus, investigation demonstrated that the 3D collagen scaffold surface morphology substantially excluded the property of CNS and PNS, cells from being distinctive in location and thus this property can be of great significance for implantation and for potentiating the axon-regeneration post-nerve injuries (Fig. 27.4) [52].



**Fig. 27.3** SEM micrographs A (scale bar 200  $\mu\text{m}$ ), B and C (scale bar 50  $\mu\text{m}$ ) of the 3D collagen scaffold representing the micro-architecture of scaffold. Image D represents the DAPI labeled hNP-AC cells. (Reprinted with permission from Elsevier [52])

**Fig. 27.4** Representation of GFAP positive (green) hNP-AC associated with regenerating axon bundles NF200 positive (red). Double headed arrow represent micro-channel orientation reprinted with copyrights permission from Elsevier [52]



Similarly, a 3D scaffold of collagen I for mimicking the nervous tissue was developed and functionalized with the rat NPCs [53]. For the proliferation of these cells, the induction with epidermal growth factor and basic FGF-2 support the neuron growth and promotes the differentiation of the cells into neurons and astrocytes [127]. Recently, the composite scaffold was developed by exploiting the collagen, hyaluronic acid and alginates. The scaffold was prepared by the self-assembly fabrication process with methacrylic anhydride functionalization succeeded by photocrosslinking and grafting with GRGDSP/Ln5-P4. The corresponding characteristics of the scaffolds with varied content revealed that (collagen/methacrylic anhydride, hyaluronic acid/methacrylic anhydride and alginates/methacrylic anhydride) in the ratio (1:2:1) proved to be

optimum concentration. Upon seeding with induced pluripotent stem cells this scaffold stimulated the differentiation of these cells into neurons, thus demonstrated that it can be used as a potential differentiation inducing biomaterial for regeneration [94]. Besides, the uses of collagens as a main polymer in the scaffolds its application has been explored in the development of the 3D microfluidic system for neuronal differentiation. For instance, the 3D collagen hydrogel was fabricated to immobilize the hNSCs and subsequently used to occupy the central channels in the microfluidic device. Further, the aim of this study was to evaluate the differentiation signals coming from the human mesenchymal stem cells hMSCs overexpressing the GDNF that inhabited the channels surrounding the microfluidic device containing hNSCs. The resultant neuronal cells

differentiated under the influence of the hMSCs, exhibited neuron-like features. The *in vivo* results of this study revealed that the 3D microfluidic device can be used as an efficient material for investigation of signals from transplanting stem cells to stimulate endogenous neuronal behavior of the hNSCs [177]. Moreover, collagen I was also utilized for the functionalization of the polycaprolactone (PCL) nano-fibrous scaffold fabricated by electrospinning technique [172]. PCL being the polymer with good mechanical properties [76], and its efficiency to hold neural cells *in vitro* and *in vivo* are well known [165]. MSCs derived from the Wharton's jelly were seeded and then subsequently differentiation by using retinoic acid and sonic hedgehog promoted them into motor neuron-like cells [12]. Furthermore, the incorporation of the collagen as a graft into scaffolds revealed the enhanced differentiation potential. These studies reveal the varied dimensions and prospects of the collagen to be used in nerve tissue-regeneration.

## 27.4 Hyaluronic Acid as Biomaterial

Hyaluronic acid, a heteropolysaccharide is a non-sulfated glycosaminoglycan (GAG) which is composed of repeating disaccharide units of [acidic sugar and amino sugar]. The acidic sugar in the hyaluronic is D-glucuronic acid and amino sugar is N-acetyl-D-glucosamine [84, 142]. Besides, the role of the hyaluronic acid in immobilization of the various drugs, antibodies, growth factors for their controlled release, it has been widely explored for varied applications in wound healing, intra-dermal implants and in nerve tissue-engineering [47, 72].

### 27.4.1 Hyaluronic Acid Scaffolds in Nerve Tissue-Engineering

Hong et al. demonstrated the hyaluronic acid-catechol conjugate can be used in the fabrication of the hydrogel scaffolds [74]. Catechol, present in the proteins of the marine mussels *Mytilus*

*edulis* possesses both adhesive and cohesive properties [163]. The adhesive and cohesive properties play important role in functionalization of the scaffolds [27]. Hong and co-workers developed a novel polymeric conjugate by dopamine coupling with the COOH group of the hyaluronic acid at pH 6 that explored the properties of both hyaluronic acid and catechol. Following characterization, the conjugate showed efficient adhesive and the cohesive properties under acidic (pH less than 2) and alkaline conditions (pH 8–9) respectively. Further, in this study, cross-linking between the catechol moieties in the conjugate solution was induced upon addition of oxidizing agent (i.e., sodium periodate) under alkaline conditions thus, results in the formation of the hydrogel. This lyophilized hydrogel was then used as a scaffold for culturing of the hNSCs. Various synthetic polymers functionalized with this conjugate revealed that hyaluronic acid-catechol conjugate promotes the cell adhesion and differentiation, thus can be considered as a biopolymer for culturing hNSCs for used in nerve tissue-regeneration [74]. The 3D layered hydrogels can also be fabricated by density gradient multilayer polymerization which involves modification of the cell suspension containing polymer by small molecules that act as density influencers [86]. Therefore, in another study, Zhang et al. explored the same approach for their study [179]. The methacrylate functionalized hyaluronic acid was used followed by varied exposures of ultraviolet A to produce hydrogels with different firmness. Based on this, the hydrogels with pore size 10  $\mu\text{m}$  and firmness 100 Pa were used further in this study. The ultimate aim of this study was to investigate the movement of the NPCs towards various glial cells like astrocytes/neurons. Further, investigation of these movements in patients with Rett syndrome (i.e., genetic X-linked syndrome with the mutation in the methyl-CpG binding protein-2 gene) was carried [6]. This gene governs the neuronal development and mutation in this can halt the development process and thus results in neuro-developmental syndrome [32]. So, a comparative investigation based on the migration of the NPCs derived from the induced

pluripotent stem cells (iPSCs) and mutant iPSCs demonstrated that upon induction by either astrocytes or neurons the mutant iPSCs-derived NPCs reveal halted migration. During the harvesting mature neurons confirmed flawed synaptogenesis and neurite outgrowth compared to wild-type NPCs which yield electro-active neurons [179]. This excellent work demonstrated the application of hydrogel scaffolds in monitoring defects associated with various disorders besides their role in regeneration. Therefore, exploring the various dimensions of the polymeric scaffolds to be used in regenerative medicine.

Another step towards finding solutions to various challenges to overcome barriers faced in nerve tissue-regeneration. The development of hyaluronic acid/laminin hydrogel was prepared by using thiol group functionalized hyaluronic acid followed by its cross-linking to poly (ethylene glycol) divinyl sulfone with laminin [1]. This was followed by fabrication using NPCs obtained from the medial and lateral ganglionic eminences of mice. The broad aim of the study was to evaluate the hyaluronic acid/laminin hydrogel scaffold for the retention of the transplant and migratory response to SDF-1 $\alpha$  *in vivo* using mice as animal models. The SDF-1 $\alpha$  also called as CXCL12 is the strong chemokine involved in directing the cells during the developmental process. The interaction of the SDF-1 $\alpha$  with its receptor CXCR4 guides migration of the germ cells besides its role in the immune cell development process [44]. Moreover, the signaling cascade triggered by the binding of SDF-1 $\alpha$  with its receptor CXCR4 is necessary for the preservation of BMSC and NSC niches at post-development stages [153, 160]. It has been reported that SDF-1 $\alpha$  involved in mobilizing the marrow-derived stem cells and NPCs towards injury sites [77]. The transplantation of NPCs within HA/laminin hydrogel potentiates the retention of cells significantly in comparison to bolus transplantation of NPCs on 1st and 3rd days. Moreover, upon exogenous introduction of the SDF-1 $\alpha$  just after the NPCs transplantation,

the scaffold promotes the NPCs migration significantly towards the SDF-1 $\alpha$  [1].

Another study indicated the nerve-regeneration potential of the human periodontal ligament stem cells (PDLSCs) and gingival MSCs after the fabrication of 3D scaffolds [8] PDLSCs being present in the oral cavity and in the tissue wastes of dental clinics, various researchers have confirmed their capacities for multi-lineage differentiation [119, 120]. The hyaluronic acid/alginate hydrogel of varied alginate/hyaluronic acid contents were investigated and the scaffold with alginate: hyaluronic acid content in the ratio of 1:1 showed lowest elastic modulus compared to other hydrogels including the alginate hydrogel alone. The proliferation study of the cells revealed that the high proliferation rate of the gingival MSCs corresponds to the hydrogels with a decrease in elasticity. However, no significant difference in the proliferation of the PDLSCs and hBMSCs was revealed with varying elasticity. This study concludes that alginate/hyaluronic acid scaffolds can prove a potential efficiency to be used in the nerve-regeneration [8]. To promote excellent cell adhesion, proliferation and the differentiation of the neural tissue scaffolds the efficient porosity of the scaffold is mandatory for a bio-mimicking [7]. Recently, as a step to improvise the aforementioned property of the engineered scaffolds, the study evaluated the use of the potassium di-hydrogen phosphate commonly called as urea crystals to induce pores to the hyaluronic acid hydrogels. These urea-templated hydrogels were investigated for bioactivity upon seeding with the NPCs and SCs. The results reveal that NPCs has shown minimal differentiation in templated scaffolds thus preserving their undifferentiated status compared to the non-templated control hydrogels. On the other hand, the SCs cultured on the template-scaffold showed differentiation (though at lower rates) compared to controls [155]. This work suggests that efficient and judicious application of this approach with various biomolecules acting as a sacrificial template can be explored to create scaffolds architecturally similar to neural ECM for better regeneration outcomes.

## 27.5 Silk Fibroin as the Biomaterial

Silk a natural macromolecular polymer is synthesized by various *Lepidopteran larvae* in specialized glands and the following secretion into the lumen of the epithelial cells, it is spun into the fibers. The SF and the sericin are the main proteins present in the silk with SF occupying core position and the sericin marks out its periphery [5, 143, 161]. Mostly the SF-derived from the mulberry silkworm *Bombyx mori* has been commonly used so far in tissue-engineering [87, 145].

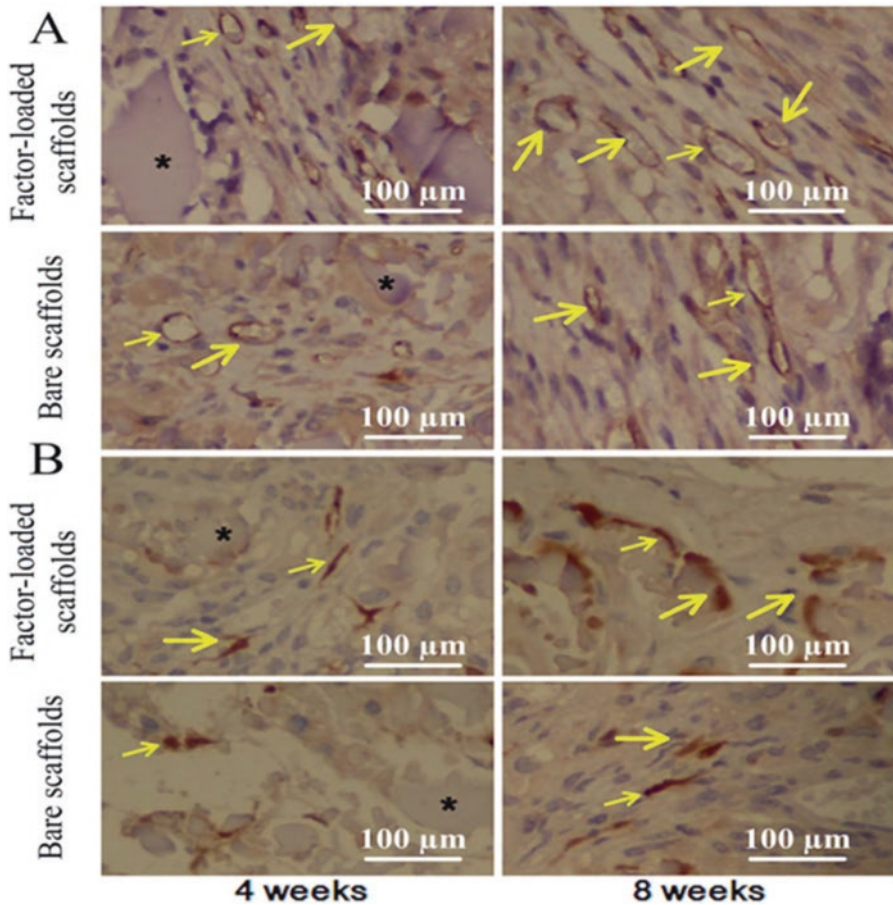
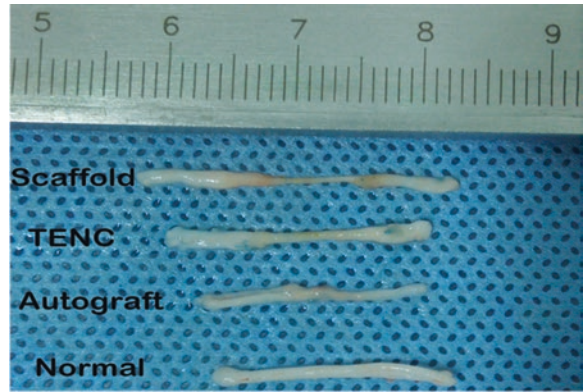
### 27.5.1 Silk Fibroin as a Scaffold for Nerve Tissue-Engineering

However, SF from the non-mulberry silkworms such as *Antheraea mylitta* has also been explored for biomedical and bio-engineering applications. In this context, Subia et al. used the freeze-drying approach of fabrication of scaffolds to evaluate the potential of SF derived from both the sources *Bombyx mori* (mulberry) and *Antheraea mylitta* (non-mulberry) for acting as a scaffold for hNPCs. Following fabrication, the characterization of the scaffolds revealed that the pore size and porosity of the scaffold do not show any significant difference. Hence, both are efficient for cell seeding. Moreover, hNPCs following seeding were investigated for 14 days, comparatively on both the scaffolds and results demonstrate that both have good cell viability and ability to potentiate the proliferation with a substantial increase in the hNPCs marker nestin. Further, there was no significant difference between the results shown by the two scaffolds except for scaffold prepared from the non-mulberry source show a minimal increase in the cell proliferation [152]. Adding more, Xu and coworkers developed the composite scaffold of SF and collagen for sciatic nerve-regeneration in the rats [173]. In this case, the SF and collagen hydrogel was prepared separately following the method elsewhere [140, 146]. Then for the composite scaffold preparation the SF: collagen solution in the ratio of 4:2 was injected into the casting mold and via lyophilization, de-moulding

was achieved. The functionalization of the scaffold was achieved by the SCs isolated from the neonatal rat sciatic nerve and adipose-derived stem cells (ADSCs) obtained from the inguinal region of adipose tissue. After characterization, these functionalized scaffolds were transplanted in the sciatic nerve of rats after a surgical procedure. The electrophysiological examination after implantation revealed no significant variations in compound muscle action potential amplitudes and motor nerve conduction velocity between the rats transplanted with the tissue-engineered scaffold and those bearing autografts. However, these results were significantly lower in rats transplanted with the pure scaffold. Moreover, scaffolds were successfully applied to bridge the 1 cm gap in sciatic nerve of rats (Fig. 27.5) [173].

The SF conduits and simultaneous functionalization of the lumen in the conduit by SF fibers were achieved by the process of the electrospinning by Xue and colleagues [175]. The aim was to test these conduits for the reconstruction of the 10 mm gap in the sciatic nerve in dogs. Post-surgery, the dogs were investigated for 12 months for behavioral and functional recovery and the results demonstrated that SF-based scaffolds revealed almost the same results as revealed by dogs transplanted with autografts. Thus, the study declared that SF-based scaffolds can efficiently be used as a possible alternative for nerve-regeneration. Dual functionalization by the brain-derived neurotrophic factor (BDNF) and vascular endothelial growth factor (VEGF) of SF scaffolds fabricated by electrospinning technique was achieved by Liu et al. [103]. The BDNF is a neurotrophic factor and is responsible for promoting the nerve-regeneration process [3]. On the other hand, VEGF is a strong growth factor involved in the process of vascular permeability and angiogenesis [3]. Moreover, SCs were used in this study for the biocompatibility and bioactivity analysis of scaffolds and factors respectively. Following the implantation in the mouse model, the results revealed the increased revascularization and nerve-regeneration compared to the pristine SF scaffold (i.e., without factors) at 4th and 8th weeks post-transplantation (Fig. 27.6) [103].

**Fig. 27.5** Representation of regenerated nerves after implantation with plain SF/ Collagen scaffold, tissue-engineered nerve conduit (TENC), autograft and, control rats while investigating the reconstruction of 1 cm nerve gap in sciatic nerve. [173]



**Fig. 27.6** Immunohistochemical staining for vessel evaluation at the panel (a) and innervation in SF scaffolds with and without dual factors at 4 and 8 weeks post-implantation at the panel (b). The asterisk sign denotes scaffold frag-

ments and yellow arrows the vessels and neuronal lineages with copyright permission from Royal Society of Chemistry [103]

Recently, another step towards overcoming the problems faced in the regeneration process after an event of injury, Zhao and co-workers fabricated the SF scaffold by electrospinning. Furthermore, the simultaneous incorporation of graphene-oxide was achieved by sonication thus, resulting in the composite graphene-oxide enriched SF scaffolds [180]. Graphene is a carbon-based 2D material with a honeycomb-like lattice configuration, having a single layer of  $sp^2$  hybridized carbon atoms [71]. Besides, exploring various avenues in different fields such as targeted delivery, biosensing, detection and use in various electro-optical and storage devices [181]. The pitfalls like high hydrophobicity, lack of biocompatibility and the low solubility limit its applications in certain fields, including tissue-engineering [178]. Keeping in view, the electro-active property of the graphene and that of nervous tissue (i.e., being electrically-active) Zhao and colleagues explored the incorporation of the graphene in a polymeric scaffold for nerve tissue regeneration. Upon investigating the various characteristics of scaffolds with varied content of graphene, the scaffold with 10% was declared efficient for further use. Moreover, upon seeding of SCs onto this scaffold the cell adhesion, survival and proliferation were carried efficiently. This study thus provides the inspiration to manipulate the scaffolds with electro-active materials for efficient regeneration results [180]. Besides the exploration of various natural polymers in nerve tissue regeneration, the blends of natural/synthetic polymers have also been widely applied in regenerative processes including nerve regeneration [145].

In this context, the poly (lactic acid) (PLA)/SF composite scaffold was fabricated and incorporation of the nerve growth factor (NGF) was achieved by co-axial electrospinning. Moreover, the plasma treatment [178] after the fabrication was given and the scaffold was further studied for the sustained release of the NGF. The differentiation of the PC12 cells was also investigated onto the scaffolds and the results confirmed the ability of the plasma-treated scaffolds as a suitable substrate for regeneration compared to the pure scaffold (i.e., devoid of

plasma treatment) [157]. Similarly, the composite scaffold of SF derived from the *Antheraea pernyi* [178] and poly(L-lactic acid-co-caprolactone) was fabricated by electrospinning. Following the various evaluations, this composite scaffold was declared significantly efficient to support cell survival and proliferation compared to poly(L-lactic acid-co-caprolactone) co-polymer alone upon seeding with SCs [167]. Adding more, the investigations of various characterizations and biocompatibility/bioactivity testing of the laminin functionalized SF/poly(ethylene oxide) scaffolds after seeding of SCs reveal their application in nerve regeneration process [132].

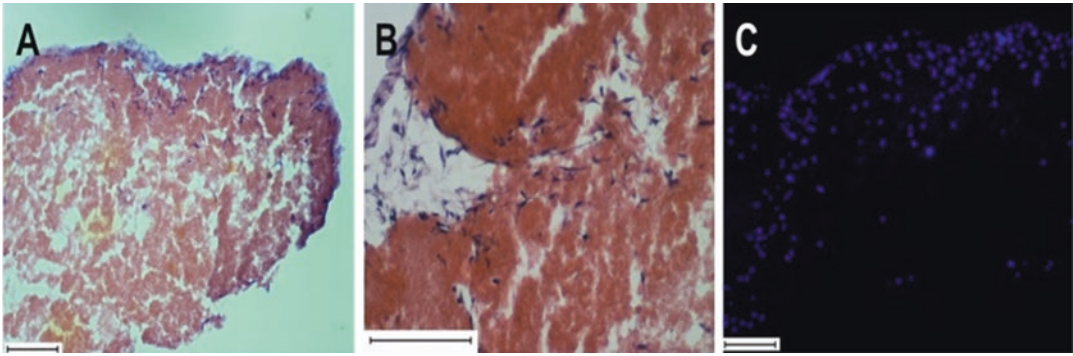
---

## 27.6 Gelatin as Biomaterial

Gelatin is a natural polymer and is obtained by partial hydrolysis from the collagen. It is a soluble fibrous protein and is a constituent of the bones, cartilages, and skins [75]. The abundant sources of gelatin are pig skin, bovine hides, cattle and fish bones with the approximate concentration of 46%, 29.4%, 23.1% and 1.5%, respectively [56, 85]. Besides the biocompatibility and biodegradability, the gelatin is easily available and less expensive commercially, therefore, it has been widely used in bio-engineering field [34, 92].

### 27.6.1 Gelatin as a Scaffold for Nerve Tissue-Engineering

In this regard, gelatin extracted from genipin was successfully electrospun into nanofibers using electrospinning technique. Further, this gelatin was enriched with ECM derived from the de-cellularized brain of rat [13]. The broad aim of their study was to evaluate this ECM enriched scaffold in nerve tissue-engineering. Following the fabrication and succeeded by the cross-linking with gelatin the biocompatibility and bioactivity analysis of these scaffolds was performed by seeding with rat MSCs. The results reveal the cytocompatible property of these scaffolds for MSCs and marrow mononuclear cells. The hematoxylin and eosin staining



**Fig. 27.7** (a) Hematoxylin, (b) Eosin and (c) DAPI staining of decellularized brain-ECM with rat MSCs seeded, scale bar = 25  $\mu\text{m}$  with copyright permission from Elsevier [103]

revealed the expected fibroblast-like extended morphology and DAPI staining reveals the proliferation of both cell types on the ECM enriched mats (Fig. 27.7). This *in vitro* study shows the potential modality to be explored in near future for *in vivo* studies so that it can be regarded as a step in the context of tissue-engineering towards CNS regeneration [13]. Gnavi et al. proposed another step towards the nerve-regeneration process. In this case, gelatin hydrogel scaffolds were encapsulated with VEGF to screen the ability for controlling the release of the cargo and role of enclosed VEGF in nerve tissue-engineering [54]. The agar/gelatin composite in the ratio 20:80 wt.% were prepared and followed by the cross-linking with the genipin [158]. Following this, the incorporation of the VEGF-A165 was initiated [129]. The release of the VEGF from the hydrogel was investigated by ELISA immunoassay and it was confirmed that it is successfully released from the hydrogels. For bioactivity analysis of the VEGF post-release studies, the human umbilical vein endothelial cells (HUVECs) were used. The screening ability of the VEGF to phosphorylate its downstream effectors like VEGFR-2, Erk1/2 and Akt in its signaling cascade successfully revealed its bio-activity. It was also demonstrated that VEGF-A165 released from hydrogel maintains its angiogenic effect upon investigation on HUVECs [21] and potentiates the axon outgrowth as evaluated on the DRG

explants derived from the adult female Wistar rats. Further, investigation of the scaffold enriched with VEGF-A165 was carried by seeding of DRG explants on the hydrogel and results demonstrate that neurite growth was increased. This proves that gelatin-based hydrogels are an efficient source for encapsulation of bioactive molecules for application in regenerative medicine [54].

The encapsulation of various factors in polymeric scaffolds has been implicated further in bio-engineering. For example, the NGF encapsulated with alginate microspheres and subsequently, their integration in nano-fibrous gelatin scaffolds was achieved [110]. This approach utilizes the properties of both the alginates and gelatin in tissue-engineering process. These nano-fibrous scaffolds were prepared by phase separation technique [112], under the influence of paraffin which acts as a porogen. Following the characterization, these scaffolds were evaluated for the regeneration process by seeding of PC12 cells derived from the rat adrenal. The results demonstrate that microsphere loaded scaffold revealed the controlled release of the bioactive NGF, as a result, the neurite growth was observed in PC12 cells. Therefore, suggesting that this scaffold may have potential application in exploring various studies towards nerve-regeneration in CNS [29].



## 27.7 Alginates as Biomaterial

Alginate is a natural anionic polymer, obtained from *Phaeophyceae* (brown algae), including *Laminaria hyperborea*, *Laminaria digitata*, *Laminaria japonica*, *Ascophyllum nodosum* and *Macrocystis Pyrifera* [156]. Moreover, the alginates are also synthesized by some bacterial species, including *Azotobacter* and *Pseudomonas*. Alginates synthesized by these bacterial species furnish the well-defined chemical structure and physical properties compared to alginates derived from brown algae. They have been widely studied due to their potential applications in the bio-engineering field.

### 27.7.1 Alginates as a Scaffold for Nerve Tissue-Engineering

The mild gelation properties of alginates in the presence of divalent cations besides the biocompatibility and low toxicity have made it a suitable candidate to explore its applications in various forms of scaffolds for use in tissue-engineering [95]. These gelling properties have explored many avenues and thus have paved various ways towards the utilization of this property in the fabrication of scaffolds. Li et al. utilized this gelling property of alginates to encapsulate NSCs [97]. In this case, sodium alginate and calcium chloride in varying proportions were prepared and left for gelling to trigger the formation of the beads. After encapsulation of the cells in calcium-alginate, the various parameters like gelling conditions, cell distribution and proliferation were analyzed for the formation and dissociation of the beads. Moreover, the beads with the diameter 2  $\mu\text{m}$  were prepared with 1.5% sodium alginate and 3.5% calcium alginate solution with gelling time for 10 minutes was found efficient for culture. The harvest rate of over 88.5% and the population of the cells encapsulated almost increased two fold during the process. Results demonstrated that these beads can be used as a potential avenue for cell expansion as a 3D scaffold for regeneration [97]. Similarly, alginate micro-beads enriched

with the embryonic stem cells were investigated and upon induction with retinoic acid, the differentiation of the stem cells into neural lineage potentiates [108]. Lu et al. fabricated fibrous scaffold by the interfacial electrostatic interaction of sodium alginate and chitin and simultaneously human pluripotent stem cells were immobilized on them. Following the induction, with the appropriate neural markers noggin/retinoic acid the cells expressed neural progenitor markers thus results in the formation of the mature neurons. Upon implantation in the severe combined immunodeficiency SCID mice, these neurons act efficiently without tumor formation, thus opening new ways of manipulating stem cells for nerve tissue-regeneration [108]. Moving further ahead, the alginates have been applied to immobilize the hNSCs and for investigation of the growth, expansion and differentiation of these cells, the 3D cellular microarray platform was developed. The investigations revealed the expansion of hNPCs and cell survival (though slowly) than conventional 2D scaffolds. Further, differentiation into glial cells was revealed, albeit decrease in neural progenitor markers. Moreover, this approach was utilized to screen the toxicity effects of various molecules on hNSCs [114].

---

## 27.8 Other Polymers in Nerve Tissue-Engineering

There are several other polymers that have been exploited for tissue-engineering, specifically nerve tissue-engineering such as (e.g., gellan gum and fibrin) besides the aforementioned natural polymers. Gellan gum is an anionic polysaccharide produced by bacteria *Sphingomonas elodea* and is approved by the Food and Drug Administration and European Medicines Agency [51]. Gellan molecule upon de-acetylation yields a tetrasaccharide of repeating units of  $\beta$ -D-glucose,  $\beta$ -D-glucuronic acid and  $\alpha$ -L-rhamnose in the ratio of 2:1:1 [118]. It has been also explored for engineering scaffolds for tissue-engineering in recent years [50]. The pitfalls like weak mechanical properties of the traditional

methods [96]. The ionotropic cross-linking and chemical cross-linking for the synthesis of the gellan gum-based hydrogel scaffolds gave existence to an alternative methodology [35, 147]. The cross-linking with biological amines spermidine (SPD) and spermine (SPM) was achieved by the Koivisto and colleagues [93]. These amines are cations in nature and are known to interact with the anionic polymers, for example, gellan gum [106]. Moreover, they serve as cross-linking agents besides their roles as a scavenger in the protection of DNA and in cell proliferation [90]. The reports indicated that at 37 °C these bio-amines act as cross-linking agents after the synthesis of the hydrogels. Further, Koivisto and coworkers achieved the simultaneous functionalization of hydrogels with the laminin. This was succeeded by both encapsulations as well as seeding of the hNPCs and human embryonic stem cells and iPSCs on the hydrogels. After seeding both the SPD and SPM, the cross-linked hydrogels were investigated. Results declare that both hydrogels promotes the cell migration in both the cases and demonstrate that gellan gum hydrogel with 3% SPD concentration stand out from the rest of the hydrogels in the study and thus can prove as a potential candidate for application in regenerative studies [93]. Further, the peptide (GRGDS) functionalized hydrogels of gellan gum has been fabricated for use in tissue-engineering [148]. Gomes and colleagues explored this gellan gum-based hydrogel in the investigation of lumbar spinal cord injury in rats [55]. After synthesis, the bioactivity of gels was tested by encapsulation of the olfactory ensheathing cells derived from neonatal rats and hADSCs [46, 149]. Upon evaluating the *in vitro* studies reveal that co-culturing these cells in hydrogel scaffolds enhanced the neurite growth efficiently. The *in vivo* experiments using the rat as an animal model demonstrate that upon transplantation of gellan gum-GRGDS hydrogel following injury, there was a significant motor recovery in comparison to hydrogel devoid of cells. These results suggest promising gains achieved by gellan gum-GRGDS encapsulated hydrogels [55].

A step towards eliminating the challenges faced by CNS regeneration post-injury, various

biomaterial scaffolds are being exploited and evaluated for overcoming these challenges. In this context, Arulmoli et al. developed a multi-polymeric scaffold for the tissue-engineering purpose [10]. The composite scaffold of fibrin, hyaluronic acid, laminin has been derived from salmon and explored for both neural and vascular tissue-engineering. Fibrin an ECM protein during coagulation cascade is involved in the formation of clots. Besides being biocompatible and non-toxic the fibrin possesses RGD sequence in addition to various adhesion sites. The cleavage of the fibrinogen by thrombin generates fibrin monomers that can be explored for the scaffold designing [99]. The degradation rate of fibrin scaffolds during *in vivo* transplantation is only for a few days so mostly fibrin composite scaffolds are preferred. After the scaffold preparation and characterization, the results revealed that hydrogel scaffold prepared from hyaluronic acid efficiently promoted the axon growth than fibrin alone. Further, the multi-polymeric scaffold support human NPCs viability, proliferation, and differentiation, thus can be used in nerve tissue-regeneration. Moreover, the vascularization potential of the scaffolds was investigated by human cord blood-derived endothelial cells cultured alone with scaffolds and in combination with NPCs, the results concluded that in co-cultures the vascularization improves significantly. It was also revealed that salmon-derived fibrin potentiates the proliferation of the NPCs than the bovine and human fibrin [10].

---

## 27.9 What Is Coming Next?

Tissue-engineering has explored the various ways of fabrication and functionalization of wide-range of scaffolds for nerve tissue-regeneration. However, besides the extensive research carried out in nerve tissue-engineering until now no approved cell-based polymeric tissue implant for application in nerve regeneration are available. Keeping in consideration the impaired sensory and motor ability due to various nerve injuries and the

treatment challenges related to various neurodegenerative disorders, the clinical translation of functionalized polymeric scaffolds is mandatory. In this context, all researchers should further explore their studies towards this goal. Moreover, the extensive research is currently going on towards the realization of this goal and hopefully, we may be able to counter various challenges in nerve tissue-regeneration in the near future.

**Acknowledgments** This work was funded by DST Nano Mission sponsored project (SR/NM/NM-1038/2016) and Science and Engineering Research Board (SERB) research grants (ECR/2016/001429).

## References

1. Addington CP, Dharmawaj S, Heffernan JM, Sirianni RW, Stabenfeldt SE (2017) Hyaluronic acid-laminin hydrogels increase neural stem cell transplant retention and migratory response to SDF-1 $\alpha$ . *Matrix Biol* 60–61:206–216. <https://doi.org/10.1016/j.matbio.2016.09.007>
2. Ajallouei F, Lim ML, Lemon G, Haag JC, Gustafsson Y, Sjöqvist S, Beltrán-Rodríguez A et al (2014) Biomechanical and biocompatibility characteristics of electrospun polymeric tracheal scaffolds. *Biomaterials* 35(20):5307–5315. <https://doi.org/10.1016/j.biomaterials.2014.03.015>
3. Allen SJ, Watson JJ, Shoemark DK, Barua NU, Patel NK (2013) Pharmacology & therapeutics GDNF, NGF and BDNF as therapeutic options for neurodegeneration. *Pharmacol Ther* 138(2):155–175. <https://doi.org/10.1016/j.pharmthera.2013.01.004>
4. Allodi I, Udina E, Navarro X (2012) Specificity of peripheral nerve regeneration: interactions at the axon level. *Prog Neurobiol*. <https://doi.org/10.1016/j.pneurobio.2012.05.005>
5. Altman GH, Diaz F, Jakuba C, Calabro T, Horan RL, Chen J, Lu H, Richmond J, Kaplan DL (2003) Silk-based biomaterials. *Biomaterials* 24:401–416. [https://doi.org/10.1016/S0142-9612\(02\)00353-8](https://doi.org/10.1016/S0142-9612(02)00353-8)
6. Amir RE, Van Den Veyver IB, Wan M, Tran CQ, Francke U, Zoghbi HY (1999) Rett syndrome is caused by mutations in X-linked MECP2, encoding methyl-CpG-binding protein 2. *Nat Genet* 23(2):185–188
7. Annabi N, Nichol JW, Zhong X, Ji C (2010) Controlling the porosity and microarchitecture of hydrogels for tissue engineering. *Tissue Eng Part B Rev* 16(4):371–383. <https://doi.org/10.1089/ten.TEB.2009.0639>
8. Ansari S, Diniz IM, Chen C, Sarrion P, Tamayol A, Wu BM, Moshaverinia A (2017) Human periodontal ligament- and gingiva-derived mesenchymal stem cells promote nerve regeneration when encapsulated in alginate/hyaluronic acid 3D scaffold. *Adv Healthc Mater* 1700670:1700670. <https://doi.org/10.1002/adhm.201700670>
9. Aramwit P, Motta A, Kundu SC (2017) Tissue engineering : from basic sciences to clinical perspectives. *Biomed Res Int* 2017:2–4. <https://doi.org/10.1155/2017/8659036>
10. Arulmoli J, Wright HJ, Phan DTT, Sheth U, Que RA, Botten GA, Keating M et al (2016) Combination scaffolds of Salmon fibrin, hyaluronic acid, and laminin for human neural stem cell and vascular tissue engineering. *Acta Biomater* 43:122–138. <https://doi.org/10.1016/j.actbio.2016.07.043>
11. Badylak SF, Freytes DO, Gilbert TW (2015) Reprint of: extracellular matrix as a biological scaffold material: structure and function. *Acta Biomater* 23:S17–S26. <https://doi.org/10.1016/j.actbio.2015.07.016>
12. Bagher Z, Azami M, Ebrahimi-Barough S, Mirzadeh H, Solouk A, Soleimani M, Ai J, Nourani MR, Joghataei MT (2016) Differentiation of Wharton's jelly-derived mesenchymal stem cells into motor neuron-like cells on three-dimensional collagen-grafted nanofibers. *Mol Neurobiol* 53(4):2397–2408. <https://doi.org/10.1007/s12035-015-9199-x>
13. Baiguera S, Del Gaudio C, Lucatelli E, Kuevda E, Boieri M, Mazzanti B, Bianco A, Macchiarini P (2014) Electrospun gelatin scaffolds incorporating rat Decellularized brain extracellular matrix for neural tissue engineering. *Biomaterials* 35(4):1205–1214. <https://doi.org/10.1016/j.biomaterials.2013.10.060>
14. Baldrick P (2010) The safety of chitosan as a pharmaceutical excipient. *Regul Toxicol Pharmacol* 56(3):290–299. <https://doi.org/10.1016/j.yrtph.2009.09.015>
15. Balint R, Cassidy NJ, Cartmell SH (2014) Conductive polymers: towards a smart biomaterial for tissue engineering. *Acta Biomater* 10(6):2341–2353. <https://doi.org/10.1016/j.actbio.2014.02.015>
16. Bannerman PGC, Mirsky R, Jessen KR, Timpl R, Duance VC (1986) Light microscopic Immunolocalization of laminin, type IV collagen, Nidogen, Heparan Sulphate proteoglycan and fibronectin in the enteric nervous system of rat and Guinea pig. *J Neurocytol* 15(6):733–743. <https://doi.org/10.1007/BF01625191>
17. Bao M, Lou X, Zhou Q, Dong W, Yuan H, Zhang Y (2014) Electrospun biomimetic fibrous scaffold from shape memory polymer of PDLLA-co-TMC for bone tissue engineering. *ACS Appl Mater Interfaces* 6(4):2611–2621. <https://doi.org/10.1021/am405101k>
18. Beachley V, Wen X (2010) Polymer Nanofibrous structures: fabrication, biofunctionalization, and cell interactions. *Prog Polym Sci (Oxford)* 35(7):868–892. <https://doi.org/10.1016/j.progpolymsci.2010.03.003>
19. Bellich B, D'Agostino I, Semeraro S, Gamini A, Cesàro A (2016) 'The good, the bad and the ugly'

- of Chitosans. *Mar Drugs* 14(5):99. <https://doi.org/10.3390/md14050099>
20. Berisio R, Vitagliano L, Mazzarella L, Zagari A (2002) Recent progress on collagen triple Helix structure, stability and assembly. *Protein Pept Lett* 9(2):107–116. <https://doi.org/10.2174/0929866023408922>
  21. di Blasio L, Droetto S, Norman J, Bussolino F, Primo L (2010) Protein kinase D1 regulates VEGF-A-induced  $\alpha\beta 3$  integrin trafficking and endothelial cell migration. *Traffic* 11(8):1107–1118. <https://doi.org/10.1111/j.1600-0854.2010.01077.x>
  22. Bonino CA, Efimenko K, In Jeong S, Krebs MD, Alsberg E, Khan SA (2012) Three-dimensional electrospun alginate nanofiber Mats via tailored charge repulsions. *Small* 8(12):1928–1936. <https://doi.org/10.1002/sml.201101791>
  23. Bozkurt A, Deumens R, Beckmann C, Damink LO, Schügner F, Heschel I, Sellhaus B et al (2009) In vitro cell alignment obtained with a Schwann cell enriched microstructured nerve guide with longitudinal guidance channels. *Biomaterials* 30(2):169–179. <https://doi.org/10.1016/j.biomaterials.2008.09.017>
  24. Brodsky B, Ramshaw JAM (1997) The collagen triple-Helix structure. *Matrix Biol* 15(8–9):545–554. [https://doi.org/10.1016/S0945-053X\(97\)90030-5](https://doi.org/10.1016/S0945-053X(97)90030-5)
  25. Bryan DJ, Robert Litchfield C, Manchio JV, Logvinenko T, Holway AH, Austin J, Summerhayes IC, Rieger-Christ KM (2012) Spatiotemporal expression profiling of proteins in rat sciatic nerve regeneration using reverse phase protein arrays. *Proteome Sci* 10(1):9. <https://doi.org/10.1186/1477-5956-10-9>
  26. Bubela T, Li MD, Hafez M, Bieber M, Atkins H (2012) Is belief larger than fact: expectations, optimism and reality for translational stem cell research. *BMC Med* 10:133. <https://doi.org/10.1186/1741-7015-10-133>
  27. Burdick JA, Prestwich GD (2011) Hyaluronic acid hydrogels for biomedical applications. *Adv Mater* (Deerfield Beach, Fla) 23(12):H41–H56. <https://doi.org/10.1002/adma.201003963>
  28. Burdick JA, Mauck RL, Gorman JH, Gorman RC (2013) Acellular biomaterials: an evolving alternative to cell-based therapies. *Sci Transl Med* 5(176):176ps4. <https://doi.org/10.1126/scitranslmed.3003997>
  29. Büyükköz M, Erdal E, Altinkaya SA (2018) Nanofibrous Gelatine scaffolds integrated with nerve growth factor-loaded alginate microspheres for brain tissue engineering. *J Tissue Eng Regen Med* 12:e707–e719. <https://doi.org/10.1002/term.2353>
  30. Caldwell MA, Svendsen CN (1998) Heparin, but not other proteoglycans potentiates the Mitogenic effects of FGF-2 on mesencephalic precursor cells. *Exp Neurol* 152(1):1–10. <https://doi.org/10.1006/exnr.1998.6815>
  31. Cao H, Liu T, Chew SY (2009) The application of Nanofibrous scaffolds in neural tissue engineering. *Adv Drug Deliv Rev* 61(12):1055–1064. <https://doi.org/10.1016/j.addr.2009.07.009>
  32. Chen WG, Chang Q, Lin Y, Meissner A, West AE, Griffith EC, Jaenisch R, Greenberg ME (2003) Derepression of BDNF transcription involves calcium-dependent phosphorylation of MeCP2. *Science* 302(5646):885–890. <https://doi.org/10.1126/science.1086446>
  33. Chen X, Wang XD, Chen G, Lin WW, Yao J, Gu XS (2006) Study of in vivo differentiation of rat bone marrow stromal cells into Schwann cell-like cells. *Microsurgery* 26(2):111–115. <https://doi.org/10.1002/micr.20184>
  34. Chong EJ, Phan TT, Lim IJ, Zhang YZ, Bay BH, Ramakrishna S, Lim CT (2007) Evaluation of electrospun PCL/gelatin Nanofibrous scaffold for wound healing and layered dermal reconstitution. *Acta Biomater* 3(3 Special Issue):321–330. <https://doi.org/10.1016/j.actbio.2007.01.002>
  35. Coutinho DF, Sant SV, Shin H, Oliveira JT, Gomes ME, Neves NM, Khademhosseini A, Reis RL (2010) Modified Gellan gum hydrogels with tunable physical and mechanical properties. *Biomaterials* 31(29):7494–7502. <https://doi.org/10.1016/j.biomaterials.2010.06.035>
  36. Croisier F, Jérôme C (2013) Chitosan-based biomaterials for tissue engineering. *Eur Polym J* 49(4):780–792. <https://doi.org/10.1016/j.eurpolymj.2012.12.009>
  37. Cruz Gaitán AM, Torres-Ruiz NM, Carri NG (2015) Embryonic neural stem cells in a 3D bioassay for trophic stimulation studies. *Brain Res Bull* 115:37–44. <https://doi.org/10.1016/j.brainresbull.2015.04.006>
  38. Dai Y, Liu W, Formo E, Sun Y, Xia Y (2011) Ceramic nanofibers fabricated by electrospinning and their applications in catalysis, environmental Science, and energy technology. *Polym Adv Technol*. <https://doi.org/10.1002/pat.1839>
  39. Daly W, Yao L, Zeugolis D, Windebank A, Pandit A (2012) A biomaterials approach to peripheral nerve regeneration: bridging the peripheral nerve gap and enhancing functional recovery. *J R Soc Interface* 9(67):202–221. <https://doi.org/10.1098/rsif.2011.0438>
  40. Dan LI, Huang J, Kaner RB (2009) Polyaniline nanofibers: a unique polymer nanostructure for versatile applications. *Acc Chem Res* 42(1):135–145. <https://doi.org/10.1021/ar800080n>
  41. Deng H, Lin L, Ji M, Zhang S, Yang M, Qiang F (2014) Progress on the morphological control of conductive network in conductive polymer composites and the use as electroactive multifunctional materials. *Prog Polym Sci* 39(4):627–655. <https://doi.org/10.1016/j.progpolymsci.2013.07.007>
  42. Deumens R, Bozkurt A, Meek MF, Marcus MAE, Joosten EAJ, Weis J, Brook GA (2010) Repairing injured peripheral nerves: bridging the gap. *Prog Neurobiol* 92(3):245–276. <https://doi.org/10.1016/j.pneurobio.2010.10.002>

43. Dhandayuthapani B, Yoshida Y, Maekawa T, Sakthi Kumar D (2011) Polymeric scaffolds in tissue engineering application: a review. *Int J Polym Sci.* <https://doi.org/10.1155/2011/290602>
44. Doitsidou M, Reichman-fried M, Ko M, Meyer D, Esguerra CV, Leung T, Raz E, Freiburg D (2002) Guidance of primordial germ cell migration by the chemokine SDF-1. *Cell* 111:647–659
45. Doshi J, Reneker DH (1995) Electrospinning process and applications of electrospun fibers. *J Electrost* 35(2–3):151–160. [https://doi.org/10.1016/0304-3886\(95\)00041-8](https://doi.org/10.1016/0304-3886(95)00041-8)
46. Dubois SG, Floyd EZ, Zvonic S, Kilroy G, Wu X, Carling S, Halvorsen YDC, Ravussin E, Gimble JM (2008) Isolation of human adipose-derived stem cells from biopsies and liposuction specimens. *Methods Mol Biol (Clifton, NJ)* 449:69–79. [https://doi.org/10.1007/978-1-60327-169-1\\_5](https://doi.org/10.1007/978-1-60327-169-1_5)
47. Fakhari A, Berkland C (2013) Applications and emerging trends of hyaluronic acid in tissue engineering, as a dermal filler and in osteoarthritis treatment. *Acta Biomater.* <https://doi.org/10.1016/j.actbio.2013.03.005>
48. Farokhi M, Mottaghtalab F, Shokrgozar MA, Kaplan DL, Kim HW, Kundu SC (2017) Prospects of peripheral nerve tissue engineering using nerve guide conduits based on silk fibroin protein and other biopolymers. *Int Mater Rev* 62(7):367–391. <https://doi.org/10.1080/09506608.2016.1252551>
49. Fathi SS, Zaminy A (2017) Stem cell therapy for nerve injury. *World J Stem Cells* 9(9):144–151. <https://doi.org/10.4252/wjsc.v9.i9.144>
50. Ferris CJ, Gilmore KJ, Wallace GG, in het Panhuis M (2013) Modified Gellan gum hydrogels for tissue engineering applications. *Soft Matter* 9(14):3705. <https://doi.org/10.1039/c3sm27389j>
51. Fialho AM, Moreira LM, Granja AT, Popescu AO, Hoffmann K, Sá-Correia I (2008) Occurrence, production, and applications of Gellan: current state and perspectives. *Appl Microbiol Biotechnol.* <https://doi.org/10.1007/s00253-008-1496-0>
52. Führmann T, Hillen LM, Montzka K, Wöltje M, Brook GA (2010) Cell-cell interactions of human neural progenitor-derived astrocytes within a microstructured 3D-scaffold. *Biomaterials* 31(30):7705–7715. <https://doi.org/10.1016/j.biomaterials.2010.06.060>
53. Ge D, Song K, Guan S, Qi Y, Guan B, Li W, Liu J, Ma X, Liu T, Cui Z (2013) Culture and differentiation of rat neural stem/progenitor cells in a three-dimensional collagen scaffold. *Appl Biochem Biotechnol* 170(2):406–419. <https://doi.org/10.1007/s12010-013-0211-5>
54. Gnani S, di Blasio L, Tonda-Turo C, Mancardi A, Primo L, Ciardelli G, Gambarotta G, Geuna S, Perroteau I (2017) Gelatin-based hydrogel for vascular endothelial growth factor release in peripheral nerve tissue engineering. *J Tissue Eng Regen Med* 11(2):459–470. <https://doi.org/10.1002/term.1936>
55. Gomes ED, Mendes SS, Leite-Almeida H, Gimble JM, Tam RY, Shoichet MS, Sousa N, Silva NA, Salgado AJ (2016) Combination of a peptide-modified Gellan gum hydrogel with cell therapy in a lumbar spinal cord injury animal model. *Biomaterials* 105:38–51. <https://doi.org/10.1016/j.biomaterials.2016.07.019>
56. Gómez-Guillén MC, Turnay J, Fernández-Díaz MD, Ulmo N, Lizarbe MA, Montero P (2002) Structural and physical properties of gelatin extracted from different marine species: a comparative study. *Food Hydrocoll* 16(1):25–34. [https://doi.org/10.1016/S0268-005X\(01\)00035-2](https://doi.org/10.1016/S0268-005X(01)00035-2)
57. Gonzalez-Perez F, Udina E, Navarro X (2013) Extracellular matrix components in peripheral nerve regeneration. *Int Rev Neurobiol* 108:257–275. <https://doi.org/10.1016/B978-0-12-410499-0.00010-1>
58. Gonzalez-Perez F, Cobiañchi S, Geuna S, Barwig C, Freier T, Udina E, Navarro X (2015) Tubulization with chitosan guides for the repair of long gap peripheral nerve injury in the rat. *Microsurgery* 35(4):300–308. <https://doi.org/10.1002/micr.22362>
59. Gonzalez-Perez F, Cobiañchi S, Heimann C, Phillips JB, Udina E, Navarro X (2017) Stabilization, rolling, and addition of other extracellular matrix proteins to collagen hydrogels improve regeneration in chitosan guides for long peripheral nerve gaps in rats. *Neurosurgery* 80(3):465–474. <https://doi.org/10.1093/neuros/nyw068>
60. Gu X, Ding F, Yang Y, Liu J (2011) Construction of tissue engineered nerve grafts and their application in peripheral nerve regeneration. *Prog Neurobiol.* <https://doi.org/10.1016/j.pneurobio.2010.11.002>
61. Gu Y, Zhu J, Xue C, Li Z, Ding F, Yang Y, Xiaosong G (2014) Chitosan/silk fibroin-based, Schwann cell-derived extracellular matrix-modified scaffolds for bridging rat sciatic nerve gaps. *Biomaterials* 35(7):2253–2263. <https://doi.org/10.1016/j.biomaterials.2013.11.087>
62. Gu Y, Li Z, Huang J, Wang H, Xiaosong G, Jianhui G (2017) Application of marrow mesenchymal stem cell-derived extracellular matrix in peripheral nerve tissue engineering. *J Tissue Eng Regen Med* 11(8):2250–2260. <https://doi.org/10.1002/term.2123>
63. Guan S, Zhang XL, Lin XM, Liu TQ, Ma XH, Cui ZF (2013) Chitosan/gelatin porous scaffolds containing hyaluronic acid and Heparan sulfate for neural tissue engineering. *J Biomater Sci Polym Ed* 24(8):999–1014. <https://doi.org/10.1080/09205063.2012.731374>
64. Guo B, Ma PX (2014) Synthetic biodegradable functional polymers for tissue engineering: a brief review. *SCIENCE CHINA Chem* 57(4):490–500. <https://doi.org/10.1007/s11426-014-5086-y>
65. Haastert K, Lipkatić E, Fischer M, Timmer M, Grothe C (2006) Differentially promoted peripheral nerve regeneration by grafted Schwann cells overexpressing different FGF-2 isoforms. *Neurobiol Dis* 21(1):138–153. <https://doi.org/10.1016/j.nbd.2005.06.020>
66. Hardy JG, Lee JY, Schmidt CE (2013) Biomimetic conducting polymer-based tissue scaffolds. *Curr*

- Opin Biotechnol 24(5):847–854. <https://doi.org/10.1016/j.copbio.2013.03.011>
67. Hardy J, Cornelison R, Sukhvasi R, Saballos R, Philip V, Kaplan D, Schmidt C (2015a) Electroactive tissue scaffolds with aligned pores as instructive platforms for biomimetic tissue engineering. *Bioengineering* 2(1):15–34. <https://doi.org/10.3390/bioengineering2010015>
68. Hardy JG, Sukhvasi RC, Aguilar D, Villancio-Wolter MK, Mouser DJ, Geissler SA, Nguy L, Chow JK, Kaplan DL, Schmidt CE (2015b) Electrical stimulation of human mesenchymal stem cells on biomaterialized conducting polymers enhances their differentiation towards osteogenic outcomes. *J Mater Chem B* 3(41):8059–8064. <https://doi.org/10.1039/C5TB00714C>
69. Harish Prashanth KV, Tharanathan RN (2007) Chitin/chitosan: modifications and their unlimited application potential-an overview. *Trends Food Sci Technol* 18(3):117–131. <https://doi.org/10.1016/j.tifs.2006.10.022>
70. He Y, Lu F (2016) Development of synthetic and natural materials for tissue engineering applications using adipose stem cells. *Stem Cells Int* 2016:5786257. <https://doi.org/10.1155/2016/5786257>
71. Hess LH, Jansen M, Maybeck V, Hauf MV, Seifert M, Stutzmann M, Sharp ID, Offenhäusser A, Garrido JA (2011) Graphene transistor arrays for recording action potentials from Electrogenic cells:5045–5049. <https://doi.org/10.1002/adma.201102990>
72. Hogan M, Girish K, James R, Balian G, Hurwitz S, Chhabra AB (2011) Growth differentiation Factor-5 regulation of extracellular matrix gene expression in murine tendon fibroblasts. *J Tissue Eng Regen Med* 5(3):191–200. <https://doi.org/10.1002/term.304>
73. Holmberg J, Durbeek M (2013) Laminin-211 in skeletal muscle function. *Cell Adhes Migr* 7(1):111–121. <https://doi.org/10.4161/cam.22618>
74. Hong S, Yang K, Kang B, Lee C, Song IT, Byun E, In Park K, Cho SW, Lee H (2013) Hyaluronic acid catechol: a biopolymer exhibiting a pH-dependent adhesive or cohesive property for human neural stem cell engineering. *Adv Funct Mater* 23(14):1774–1780. <https://doi.org/10.1002/adfm.201202365>
75. Hoque ME, Nuge T, Yeow TK, Nordin N, Prasad RGSV (2014) Gelatin based scaffolds for tissue engineering – a review. *Polym Res J* 9(1):15
76. Horne MK, Nisbet DR, Forsythe JS, Parish CL (2010) Three-dimensional Nanofibrous scaffolds incorporating immobilized BDNF promote proliferation and differentiation of cortical neural stem cells. *Stem Cells Dev* 19(6):843–852. <https://doi.org/10.1089/scd.2009.0158>
77. Imitola J, Raddassi K, In Park K, Mueller F-j, Nieto M, Teng YD, Frenkel D et al (2004) Directed migration of neural stem cells to sites of CNS injury by the stromal cell-derived factor 1 $\alpha$ /CXCL12 chemokine receptor 4 pathway. *Natl Acad Sci* 101(52):18117–18122
78. Jang J, Chang M, Yoon H (2005) Chemical sensors based on highly conductive poly(3,4-Ethylenedioxythiophene) Nanorods. *Adv Mater* 17(13):1616–1620. <https://doi.org/10.1002/adma.200401909>
79. Jeong HE, Lee SH, Kim P, Suh KY (2006) Stretched polymer Nanohairs by Nanodrawing. *Nano Lett* 6(7):1508–1513. <https://doi.org/10.1021/nl061045m>
80. Jessen KR, Mirsky R (2016) The repair Schwann cell and its function in regenerating nerves. *J Physiol* 594(13):3521–3531. <https://doi.org/10.1113/JP270874>
81. Jha AK, Xu X, Duncan RL, Jia X (2011) Controlling the adhesion and differentiation of mesenchymal stem cells using hyaluronic acid-based, doubly cross-linked networks. *Biomaterials* 32(10):2466–2478. <https://doi.org/10.1016/j.biomaterials.2010.12.024>
82. Jin G, Li K (2015) The electrically conductive scaffold as the skeleton of stem cell niche in regenerative medicine. *Mater Sci Eng C* 45:671–681. <https://doi.org/10.1016/j.msec.2014.06.004>
83. Kagan HM, Li W (2003) Lysyl oxidase: properties, specificity, and biological roles inside and outside of the cell. *J Cell Biochem* 88(4):660–672. <https://doi.org/10.1002/jcb.10413>
84. Kakehi K, Kinoshita M, Yasueda SI (2003) Hyaluronic acid: separation and biological implications. *J Chromatogr B Anal Technol Biomed Life Sci* 797(1–2):347–355. [https://doi.org/10.1016/S1570-0232\(03\)00479-3](https://doi.org/10.1016/S1570-0232(03)00479-3)
85. Karim AA, Bhat R (2009) Fish gelatin: properties, challenges, and prospects as an alternative to mammalian gelatins. *Food Hydrocoll*. <https://doi.org/10.1016/j.foodhyd.2008.07.002>
86. Karpiak JV, Ner Y, Almutairi A (2012) Density gradient multilayer polymerization for creating complex tissue. *Adv Mater* 24(11):1466–1470. <https://doi.org/10.1002/adma.201103501>
87. Kasoju N, Bora U (2012) Silk fibroin in tissue engineering:1–20. <https://doi.org/10.1002/adhm.201200097>
88. Kerns JM (2008) The microstructure of peripheral nerves. *Tech Reg Anesth Pain Manag* 12(3):127–133. <https://doi.org/10.1053/j.trap.2008.03.001>
89. Khaing ZZ, Schmidt CE (2012) Advances in natural biomaterials for nerve tissue repair. *Neurosci Lett*. <https://doi.org/10.1016/j.neulet.2012.02.027>
90. Khan AU, Mei YH, Wilson T (1992) A proposed function for Spermine and spermidine: protection of replicating DNA against damage by singlet oxygen. *Proc Natl Acad Sci U S A* 89(23):11426–11427. <https://doi.org/10.1073/pnas.89.23.11426>
91. Khan F, Tanaka M, Ahmad SR (2015) Fabrication of polymeric biomaterials: a strategy for tissue engineering and medical devices. *J Mater Chem B* 3(42):8224–8249. <https://doi.org/10.1039/C5TB01370D>
92. Koh HS, Thomas Y, Chan CK, Ramakrishna S (2008) Enhancement of neurite outgrowth using nano-structured scaffolds coupled with laminin. *Biomaterials*

- 29(26):3574–3582. <https://doi.org/10.1016/j.biomaterials.2008.05.014>
93. Koivisto JT, Joki T, Parraga JE, Paakkönen R, Yla-Ovainen L, Salonen L, Jönkkari I et al (2017) Bioamine-crosslinked Gellan gum hydrogel for neural tissue engineering. *Biomed Mater (Bristol)* 12(2). <https://doi.org/10.1088/1748-605X/aa62b0>
  94. Kuo YC, Hsueh CH (2017) Neuronal production from induced pluripotent stem cells in self-assembled collagen-hyaluronic acid-alginate microgel scaffolds with grafted GRGDSP/Ln5-P4. *Mater Sci Eng C* 76:760–774. <https://doi.org/10.1016/j.msec.2017.03.133>
  95. Lee KY, Mooney DJ (2012) Alginate: properties and biomedical applications. *Prog Polym Sci* 37(1):106–126. <https://doi.org/10.1016/j.progpolymsci.2011.06.003>
  96. Lee C, Shin J, Lee JS, Byun E, Ryu JH, Um SH, Kim DI, Lee H, Cho SW (2013) Bioinspired, calcium-free alginate hydrogels with tunable physical and mechanical properties and improved biocompatibility. *Biomacromolecules* 14(6):2004–2013. <https://doi.org/10.1021/bm400352d>
  97. Li X, Liu T, Song K, Yao L, Ge D, Bao C, Ma X, Cui Z (2006) Culture of neural stem cells in calcium alginate beads. *Biotechnol Prog* 22(6):1683–1689. <https://doi.org/10.1021/bp060185z>
  98. Li H, Wijekoon A, Leipzig ND (2012) 3D differentiation of neural stem cells in macroporous photopolymerizable hydrogel scaffolds. *PLoS One* 7(11). <https://doi.org/10.1371/journal.pone.0048824>
  99. Li Y, Meng H, Liu Y, Lee BP (2015) Fibrin gel as an injectable biodegradable scaffold and cell carrier for tissue engineering. *Sci World J.* <https://doi.org/10.1155/2015/685690>
  100. Liao J, Guo X, Jane Grande-Allen K, Kurtis Kasper F, Mikos AG (2010) Bioactive polymer/extracellular matrix scaffolds fabricated with a flow perfusion bioreactor for cartilage tissue engineering. *Biomaterials* 31(34):8911–8920. <https://doi.org/10.1016/j.biomaterials.2010.07.110>
  101. Liu D, De Feyter S, Cotlet M, Wiesler UM, Weil T, Herrmann A, Müllen K, De Schryver FC (2003) Fluorescent self-assembled polyphenylene dendrimer nanofibers. *Macromolecules* 36(22):8489–8498. <https://doi.org/10.1021/ma0348573>
  102. Liu B-S, Yang Y-C, Shen C-C (2014) Regenerative effect of adipose tissue-derived stem cells transplantation using nerve conduit therapy on sciatic nerve injury in rats. *J Tissue Eng Regen Med* 8(5):337–350. <https://doi.org/10.1002/term.1523>
  103. Liu Q, Huang J, Shao H, Song L, Zhang Y (2016) Dual-factor loaded functional silk fibroin scaffolds for peripheral nerve regeneration with the aid of neovascularization. *RSC Adv* 6(9):7683–7691. <https://doi.org/10.1039/C5RA22054H>
  104. Liuzzi F, Lasek R (1987) Astrocytes block axonal regeneration in mammals by activating the physiological stop pathway. *Science* 237(4815):642–645. <https://doi.org/10.1126/science.3603044>
  105. Lluch, AV, Cruz DMG, Ivirico JLE, Ramos CM, Pradas MM (2014) Polymers as materials for tissue engineering scaffolds. In: *Polymers in regenerative medicine: biomedical applications from nano- to macro-structures*, pp 1–47. <https://doi.org/10.1002/9781118356692.ch1>
  106. López-Cebral R, Paolicelli P, Romero-Caamaño V, Seijo B, Casadei MA, Sanchez A (2013) Spermidine-cross-linked hydrogels as novel potential platforms for pharmaceutical applications. *J Pharm Sci* 102(8):2632–2643. <https://doi.org/10.1002/jps.23631>
  107. Lu, L, Chen X, Zhang CW, Yang WL, Wu YJ, Sun L, Bai LM et al (2008) Morphological and functional characterization of predifferentiation of myelinating glia-like cells from human bone marrow stromal cells through activation of F3/notch signaling in mouse retina. *Stem Cells* 26(2):580–90. <https://doi.org/2007-0106> [pii]r10.1634/stemcells.2007-0106
  108. Lu HF, Lim S-X, Leong MF, Narayanan K, Toh RPK, Gao S, Wan ACA (2012) Efficient neuronal differentiation and maturation of human pluripotent stem cells encapsulated in 3D microfibrillar scaffolds. *Biomaterials* 33(36):9179–9187. <https://doi.org/10.1016/j.biomaterials.2012.09.006>
  109. Lundborg G, Dahlin LB, Danielsen N, Gelberman RH, Longo FM, Powell HC, Varon S (1982) Nerve regeneration in silicone chambers: influence of gap length and of distal stump components. *Exp Neurol* 76(2):361–375. [https://doi.org/10.1016/0014-4886\(82\)90215-1](https://doi.org/10.1016/0014-4886(82)90215-1)
  110. Ma PX, Zhang R (1999) Synthetic nano-scale fibrous extracellular matrix. *J Biomed Mater Res* 46(1):60–72. [https://doi.org/10.1002/\(SICI\)1097-4636\(199907\)46:1<60::AID-JBM7>3.0.CO;2-H](https://doi.org/10.1002/(SICI)1097-4636(199907)46:1<60::AID-JBM7>3.0.CO;2-H)
  111. Madduri S, Gander B (2010) Schwann cell delivery of neurotrophic factors for peripheral nerve regeneration. *J Peripher Nerv Syst* 15(2):93–103. <https://doi.org/10.1111/j.1529-8027.2010.00257.x>
  112. Martin CR (1996) Membrane-based synthesis of nanomaterials. *Chem Mater.* <https://doi.org/10.1021/cm960166s>
  113. McGarvey ML, Baron-Van Evercooren A, Kleinman HK, Dubois-Dalcq M (1984) Synthesis and effects of basement membrane components in cultured rat Schwann cells. *Dev Biol* 105(1):18–28. [https://doi.org/10.1016/0012-1606\(84\)90257-4](https://doi.org/10.1016/0012-1606(84)90257-4)
  114. Meli L, Barbosa HSC, Hickey AM, Gasimli L, Nierode G, Diogo MM, Linhardt RJ, Cabral JMS, Dordick JS (2014) Three dimensional cellular microarray platform for human neural stem cell differentiation and toxicology. *Stem Cell Res* 13(1):36–47. <https://doi.org/10.1016/j.scr.2014.04.004>
  115. Mentis GZ, Alvarez FJ, Shneider NA, Siembab VC, O'Donovan MJ (2010) Mechanisms regulating the specificity and strength of muscle afferent inputs in

- the spinal cord. *Ann N Y Acad Sci* 1198. <https://doi.org/10.1111/j.1749-6632.2010.05538.x>
116. Meyer C, Stenberg L, Gonzalez-Perez F, Wrobel S, Ronchi G, Udina E, Suganuma S et al (2016a) Chitosan-film enhanced chitosan nerve guides for long-distance regeneration of peripheral nerves. *Biomaterials* 76:33–51. <https://doi.org/10.1016/j.biomaterials.2015.10.040>
  117. Meyer C, Wrobel S, Raimondo S, Rochkind S, Heimann C, Shahar A, Ziv-Polat O, Geuna S, Grothe C, Haastert-Talini K (2016b) Peripheral nerve regeneration through hydrogel-enriched chitosan conduits containing engineered Schwann cells for drug delivery. *Cell Transplant* 25(1):159–182. <https://doi.org/10.3727/096368915X688010>
  118. Morris ER, Nishinari K, Rinaudo M (2012) Gelation of Gellan - a review. *Food Hydrocoll.* <https://doi.org/10.1016/j.foodhyd.2012.01.004>
  119. Moshaverinia A, Xu X, Chen C, Akiyama K, Snead ML, Shi S (2013) Acta biomaterialia dental mesenchymal stem cells encapsulated in an alginate hydrogel co-delivery microencapsulation system for cartilage regeneration. *Acta Biomater* 9(12):9343–9350. <https://doi.org/10.1016/j.actbio.2013.07.023>
  120. Moshaverinia A, Chen C, Xu X, Akiyama K, Ansari S, Zadeh HH, Shi S (2014) Bone regeneration potential of stem cells derived from periodontal ligament or gingival tissue sources encapsulated in RGD-modified alginate scaffold. *Tissue Eng A* 20(3–4):611–621. <https://doi.org/10.1089/ten.tea.2013.0229>
  121. Müller HW, Stoll G (1998) Nerve injury and regeneration: basic insights and therapeutic interventions. *Curr Opin Neurol.* <https://doi.org/10.1097/00019052-199810000-00019>
  122. Murphy AR, Laslett A, O'Brien CM, Cameron NR (2017) Scaffolds for 3D in vitro culture of neural lineage cells. *Acta Biomater* 54(February):1–20. <https://doi.org/10.1016/j.actbio.2017.02.046>
  123. Muzzarelli RAA (2009) Chitins and Chitosans for the repair of wounded skin, nerve, cartilage and bone. *Carbohydr Polym.* <https://doi.org/10.1016/j.carbpol.2008.11.002>
  124. Navarro X, Krueger TB, Lago N, Micera S, Stieglitz T, Dario P (2005) A critical review of interfaces with the peripheral nervous system for the control of neuroprostheses and hybrid bionic systems. *J Peripher Nerv Syst* 10(3):229–258. <https://doi.org/10.1111/j.1085-9489.2005.10303.x>
  125. O'Brien FJ, Harley BA, Yannas IV, Gibson L (2004) Influence of freezing rate on pore structure in freeze-dried collagen-GAG scaffolds. *Biomaterials* 25(6):1077–1086. [https://doi.org/10.1016/S0142-9612\(03\)00630-6](https://doi.org/10.1016/S0142-9612(03)00630-6)
  126. Ostenfeld T (2004) Requirement for neurogenesis to proceed through the division of neuronal progenitors following differentiation of epidermal growth factor and fibroblast growth Factor-2-responsive human neural stem cells. *Stem Cells* 22(5):798–811. <https://doi.org/10.1634/stemcells.22-5-798>
  127. Palmer TD, Markakis EA, Willhoite AR, Safar F, Gage FH (1999) Fibroblast growth factor-2 activates a latent neurogenic program in neural stem cells from diverse regions of the adult CNS. *J Neurosci* 19(19):8487–8497. <https://doi.org/10.1523/JNEUROSCI.19-19-08487.1999>
  128. Panzavolta S, Gioffrè M, Letizia M, Gualandi C, Foroni L, Bigi A (2011) Acta biomaterialia electrospun gelatin nanofibers : optimization of genipin cross-linking to preserve fiber morphology after exposure to water. *Acta Biomater* 7(4):1702–1709. <https://doi.org/10.1016/j.actbio.2010.11.021>
  129. Pereira Lopes FR, Lisboa BCG, Frattini F, Almeida FM, Tomaz MA, Matsumoto PK, Langone F et al (2011) Enhancement of sciatic nerve regeneration after vascular endothelial growth factor (VEGF) gene therapy. *Neuropathol Appl Neurobiol* 37(6):600–612. <https://doi.org/10.1111/j.1365-2990.2011.01159.x>
  130. Pfister LA, Papaloizos M, Merkle HP, Gander B (2007) Nerve conduits and growth factor delivery in peripheral nerve repair. *J Peripher Nerv Syst* 12(2):65–82. <https://doi.org/10.1111/j.1529-8027.2007.00125.x>
  131. Potter, W, Kalil RE, Kao WJ (2008) Biomimetic material systems for neural progenitor cell-based therapy. *Front Biosci* 13:806–21. [https://doi.org/2721 \[pii\]](https://doi.org/2721 [pii])
  132. Rajabi M, Firouzi M, Hassannejad Z, Haririan I, Zahedi P (2017) Fabrication and characterization of electrospun laminin-functionalized silk fibroin/poly(ethylene oxide) nanofibrous scaffolds for peripheral nerve regeneration. *J Biomed Mater Res B Appl Biomater*:1–10. <https://doi.org/10.1002/jbm.b.33968>
  133. Rajwade JM, Paknikar KM, Kumbhar JV (2015) Applications of bacterial cellulose and its composites in biomedicine. *Appl Microbiol Biotechnol.* <https://doi.org/10.1007/s00253-015-6426-3>
  134. Reynolds BA, Weiss S (1992) Generation of neurons and astrocytes from isolated cells of the adult mammalian central nervous system. *Science (New York, NY)* 255(5052):1707–1710. <https://doi.org/10.1126/science.1553558>
  135. Ribeiro JCV, Vieira RS, Melo IM, Araújo VMA, Lima V (2017) Versatility of chitosan-based biomaterials and their use as scaffolds for tissue regeneration. *Sci World J* 2017. <https://doi.org/10.1155/2017/8639898>
  136. Ribeiro-Resende VT, Koenig B, Nichterwitz S, Oberhoffner S, Schlosshauer B (2009) Strategies for inducing the formation of bands of Bünger in peripheral nerve regeneration. *Biomaterials* 30(29):5251–5259. <https://doi.org/10.1016/j.biomaterials.2009.07.007>
  137. Rinaudo M (2006) Chitin and chitosan: properties and applications. *Prog Polym Sci (Oxford)* 31(7):603–632. <https://doi.org/10.1016/j.progpolymsci.2006.06.001>
  138. Rodríguez-Vázquez M, Vega-Ruiz B, Ramos-Zúñiga R, Saldaña-Koppel DA, Quiñones-Olvera LF (2015) Chitosan and its potential use as a scaffold for tissue



- engineering in regenerative medicine. *Biomed Res Int* 2015. <https://doi.org/10.1155/2015/821279>
139. Rollings DAE, Tsoi S, Sit JC, Veinot JGC (2007) Formation and aqueous surface wettability of polysiloxane nanofibers prepared via surface initiated, vapor-phase polymerization of organotrichlorosilanes. *Langmuir* 23(10):5275–5278. <https://doi.org/10.1021/la063604a>
  140. Ruan Y, Lin H, Yao J, Chen Z, Shao Z, Lin H, Chen Z (2011) Preparation of 3D fibroin/chitosan blend porous scaffold for tissue engineering via a simplified method. *Macromol Biosci* 11(3):419–426. <https://doi.org/10.1002/mabi.201000392>
  141. Sankar S, Sharma CS, Rath SN, Ramakrishna S (2017) Electrospun fibers for recruitment and differentiation of stem cells in regenerative medicine. *Biotechnol J* 1700263:1–11. <https://doi.org/10.1002/biot.201700263>
  142. Saranraj P, Naidu MA (2013) Hyaluronic acid production and its applications - a review. *Int J Pharm & Biochem Arch* 4(5):853–859 <http://www.ijpba.info/ijpba/index.php/ijpba/article/viewFile/1126/795>
  143. Scheibel TR, Hardy JG, Ro LM (2008) Polymeric materials based on silk proteins. *Polymer* 49:4309–4327. <https://doi.org/10.1016/j.polymer.2008.08.006>
  144. Shearer MC, Niclou SP, Brown D, Asher RA, Holtmaat AJGD, Levine JM, Verhaagen J, Fawcett JW (2003) The astrocyte/meningeal cell interface is a barrier to neurite outgrowth which can be overcome by manipulation of inhibitory molecules or axonal signalling pathways. *Mol Cell Neurosci* 24(4):913–925. <https://doi.org/10.1016/j.mcn.2003.09.004>
  145. Sheikh FA, Ju HW, Moon BM, Lee OJ, Kim J-h, Park HJ, Kim DW et al (2015) Hybrid scaffolds based on PLGA and silk for bone tissue engineering. *J Tissue Eng Regen Med* 10(3):209–221. <https://doi.org/10.1002/term>
  146. Shreiber DI, Barocas VH, Tranquillo RT (2003) Temporal variations in cell migration and traction during fibroblast-mediated gap compaction. *Biophys J* 84(6):4102–4114. [https://doi.org/10.1016/S0006-3495\(03\)75135-2](https://doi.org/10.1016/S0006-3495(03)75135-2)
  147. Silva NA, Salgado AJ, Sousa RA, Oliveira JT, Pedro AJ, Leite-Almeida H, Cerqueira R et al (2010) Development and characterization of a novel hybrid tissue engineering-based scaffold for spinal cord injury repair. *Tissue Eng Part A* 16(1):45–54. <https://doi.org/10.1089/ten.TEA.2008.0559>
  148. Silva NA, Cooke MJ, Tam RY, Sousa N, Salgado AJ, Reis RL, Shoichet MS (2012a) The effects of peptide modified gellan gum and olfactory ensheathing glia cells on neural stem/progenitor cell fate. *Biomaterials* 33(27):6345–6354. <https://doi.org/10.1016/j.biomaterials.2012.05.050>
  149. Silva NA, Sousa RA, Pires AO, Sousa N, Salgado AJ, Reis RL (2012b) Interactions between Schwann and olfactory ensheathing cells with a starch/poly-caprolactone scaffold aimed at spinal cord injury repair. *J Biomed Mater Res A* 100 A(2):470–476. <https://doi.org/10.1002/jbm.a.33289>
  150. Stevens LR, Gilmore KJ, Wallace GG, M. in het Panhuis (2016) Tissue engineering with gellan gum. *Biomater Sci* 4(9):1276–1290. <https://doi.org/10.1039/C6BM00322B>
  151. Stoppel WL, Ghezzi CE, McNamara SL, Black LD III, Kaplan DL (2015) Clinical applications of naturally derived biopolymer-based scaffolds for regenerative medicine. *Ann Biomed Eng* 43(3):657–680. <https://doi.org/10.1007/s10439-014-1206-2>
  152. Subia B, Rao RR, Kundu SC (2015) Silk 3D matrices incorporating human neural progenitor cells for neural tissue engineering applications. *Polym J* 47(12):819–825. <https://doi.org/10.1038/pj.2015.69>
  153. Sugiyama T, Kohara H, Noda M (2006) Maintenance of the hematopoietic stem cell pool by CXCL12-CXCR4 chemokine signaling in bone marrow stromal cell niches. *Immunity* 25(6):977–988. <https://doi.org/10.1016/j.immuni.2006.10.016>
  154. Tao SL, Desai TA (2007) Aligned arrays of biodegradable poly(epsilon-caprolactone) nanowires and nanofibers by template synthesis. *Nano Lett* 7(6):1463–1468. <https://doi.org/10.1021/nl0700346>
  155. Thomas RC, Vu P, Modi SP, Chung PE, Clive Landis R, Khaing ZZ, Hardy JG, Schmidt CE (2017) Sacrificial crystal templated hyaluronic acid hydrogels as biomimetic 3D tissue scaffolds for nerve tissue regeneration. *ACS Biomater Sci Eng* 3(7):1451–1459. <https://doi.org/10.1021/acsbomaterials.7b00002>
  156. Thu B, Smidsrød O, Skjak-Brk G (1996) Alginate gels - some structure-function correlations relevant to their use as immobilization matrix for cells. *Prog Biotechnol* 11(C):19–30. [https://doi.org/10.1016/S0921-0423\(96\)80004-9](https://doi.org/10.1016/S0921-0423(96)80004-9)
  157. Tian L, Prabhakaran MP, Hu J, Chen M, Besenbacher F, Ramakrishna S (2015) Coaxial electrospun poly(lactic acid)/silk fibroin nanofibers incorporated with nerve growth factor support the differentiation of neuronal stem cells. *RSC Adv* 5(62):49838–49848. <https://doi.org/10.1039/C5RA05773F>
  158. Tonda-Turo C, Gnani S, Ruini F, Gambarotta G, Gioffredi E, Chiono V, Perroteau I, Ciardelli G (2017) Development and characterization of novel agar and gelatin injectable hydrogel as filler for peripheral nerve guidance channels. *J Tissue Eng Regen Med* 11(1):197–208. <https://doi.org/10.1002/term.1902>
  159. Tortora GJ, Derrickson B (2014) Principles of Anatomy & Physiology, 14th ed. Wiley, Hoboken. <https://doi.org/10.1017/CBO9781107415324.004>
  160. Van Steenwinckel J, Roste W (2013) Current status of chemokines in the adult CNS. *Prog Neurobiol* 104:67–92. <https://doi.org/10.1016/j.pneurobio.2013.02.001>
  161. Vepari C, Kaplan DL (2009) Silk as a biomaterial. *Prog Polym Sci* 32:991–1007. <https://doi.org/10.1016/j.progpolymsci.2007.05.013>
  162. Volpato FZ, Führmann T, Migliaresi C, Hutmacher DW, Dalton PD (2013) Using extracellular matrix

- for regenerative medicine in the spinal cord. *Biomaterials* 34(21):4945–4955. <https://doi.org/10.1016/j.biomaterials.2013.03.057>
163. Waite JH, Andersen NH, Jewhurst S, Sun C (2005) Mussel adhesion: finding the tricks worth mimicking. *J Adhes* 81(3–4):297–317. <https://doi.org/10.1080/00218460590944602>
164. Walsh S, Midha R (2009) Practical considerations concerning the use of stem cells for peripheral nerve repair. *Neurosurg Focus* 26(2):E2. <https://doi.org/10.3171/FOC.2009.26.2.E2>
165. Wang TY, Forsythe JS, Parish CL, Nisbet DR (2012) Biofunctionalisation of polymeric scaffolds for neural tissue engineering. *J Biomater Appl* 27(4):369–390. <https://doi.org/10.1177/0885328212443297>
166. Wang X, Ding B, Li B (2013) Biomimetic electrospun nanofibrous structures for tissue engineering. *Mater Today* 16(6):229–241. <https://doi.org/10.1016/j.mattod.2013.06.005>
167. Wang J, Sun B, Bhutto MA, Zhu T, Yu K, Bao J, Morsi Y, El-Hamshary H, El-Newehy M, Mo X (2017a) Fabrication and characterization of *Antheraea pernyi* silk fibroin-blended P(LLA-CL) Nanofibrous scaffolds for peripheral nerve tissue engineering. *Front Mater Sci* 11(1):22–32. <https://doi.org/10.1007/s11706-017-0368-x>
168. Wang S, Sun C, Guan S, Li W, Xu J, Ge D, Zhuang M, Liu T, Ma X (2017b) Chitosan/gelatin porous scaffolds assembled with conductive poly(3,4-Ethylenedioxythiophene) nanoparticles for neural tissue engineering. *J Mater Chem B* 5(24):4774–4788. <https://doi.org/10.1039/C7TB00608J>
169. Wani S, Sofi HS, Majeed S, Sheikh FA (2017) Recent trends in chitosan nanofibers : from tissue-engineering to environmental importance: a review. *Mater Sci Res India* 14(2):89–99
170. Willand MP (2015) Electrical stimulation enhances Reinnervation after nerve injury. *Eur J Transl Myol* 25(4):243–248. <https://doi.org/10.4081/ejtm.2015.5243>
171. Wu Y, Feng S, Zan X, Lin Y, Wang Q (2015) Aligned electroactive TMV nanofibers as enabling scaffold for neural tissue engineering. *Biomacromolecules* 16(11):3466–3472. <https://doi.org/10.1021/acs.biomac.5b00884>
172. Xie J, Willerth SM, Li X, Macewan MR, Rader A, Sakiyama-Elbert SE, Xia Y (2009) The differentiation of embryonic stem cells seeded on electrospun nanofibers into neural lineages. *Biomaterials* 30(3):354–362. <https://doi.org/10.1016/j.biomaterials.2008.09.046>
173. Xu Y, Zhang Z, Chen X, Li R, Li D, Feng S (2016) A silk fibroin/collagen nerve scaffold seeded with a co-culture of Schwann cells and adipose-derived stem cells for sciatic nerve regeneration. *PLoS One* 11(1):1–11. <https://doi.org/10.1371/journal.pone.0147184>
174. Xue C, Ren H, Zhu H, Gu X, Guo Q, Zhou Y, Huang J et al (2017a) Bone marrow mesenchymal stem cell-derived acellular matrix-coated chitosan/silk scaffolds for neural tissue regeneration. *J Mater Chem B* 5(6):1246–1257. <https://doi.org/10.1039/C6TB02959K>
175. Xue C, Zhu H, Tan D, Ren H, Gu X, Zhao Y, Zhang P et al (2017b) Electrospun silk fibroin-based neural scaffold for bridging a long sciatic nerve gap in dogs. *J Tissue Eng Regen Med* 12(2):e1143–e1153. <https://doi.org/10.1002/term.2449>
176. Yang C, Hillas PJ, Báez JA, Nokelainen M, Balan J, Tang J, Spiro R, Polarek JW (2004) The application of recombinant human collagen in tissue engineering. *BioDrugs* 18(2):103–119. <https://doi.org/10.2165/00063030-200418020-00004>
177. Yang K, Park H-J, Han S, Lee J, Ko E, Kim J, Lee JS et al (2015) Recapitulation of in vivo-like paracrine signals of human mesenchymal stem cells for functional neuronal differentiation of human neural stem cells in a 3D microfluidic system. *Biomaterials* 63:177–188. <https://doi.org/10.1016/j.biomaterials.2015.06.011>
178. Zhang Y, Ali SF, Dervishi E, Xu Y, Li Z, Casciano D, Biris AS (2010) Cytotoxicity effects of graphene and single-wall carbon nanotubes in neural pheochromocytomaderived Pc12 cells. *ACS Nano* 4(6):3181–3186. <https://doi.org/10.1021/nn1007176>
179. Zhang Z-N, Freitas BC, Qian H, Lux J, Acab A, Trujillo CA, Herai RH et al (2016) Layered hydrogels accelerate iPSC-derived neuronal maturation and reveal migration defects caused by MeCP2 dysfunction. *Proc Natl Acad Sci* 113(12):3185–3190. <https://doi.org/10.1073/pnas.1521255113>
180. Zhao Y, Gong J, Niu C, Wei Z, Shi J, Li G, Yang Y, Wang H (2017) A new electrospun graphene-silk fibroin composite scaffolds for guiding Schwann cells. *J Biomater Sci Polym Ed* 28(18):2171–2185. <https://doi.org/10.1080/09205063.2017.1386835>
181. Zhou K, Thouas GA, Bernard CC, Nisbet DR, Finkelstein DI, Li D, Forsythe JS (2012) Method to impart electro- and biofunctionality to neural ScaffoldOlds using graphene – polyelectrolyte multilayers. *ACS Appl Mater Interfaces* 4(9):4524–4531. <https://doi.org/10.1021/am3007565>



# Chitosan-Based Dressing Materials for Problematic Wound Management

# 28

Ji-Ung Park, Eun-Ho Song, Seol-Ha Jeong, Juha Song, Hyoun-Ee Kim, and Sukwha Kim

## Abstract

Wound healing is a complex mechanism involving a variety of factors and is a representative process of tissue growth and regeneration in our body. Surface-based interactions between the dressing material and the wound may significantly influence the healing phase. Advances in understanding the mechanism of wound healing have led to the development of numerous dressing materials that can accelerate the healing process. However, these materials have a passive role in wound healing. It is therefore necessary to develop novel wound dressing materials, especially effective for clinically problematic wounds. Chitosan-based dressing materials are considered suit-

able for clinically problematic wounds as they exhibit several characteristic features, such as facilitating hemostasis, enhanced wound healing during the inflammatory and proliferative phases, antimicrobial effect, etc. Here, we review the current status of clinically available dressing materials and studies on the biological characteristics of chitosan, and discuss the potential applications of chitosan in multifunctional dressing materials for accelerated wound healing.

## Keywords

Wound healing · Dressing materials · Chitosan

Authors Ji-Ung Park and Eun-Ho Song have been equally contributed to this chapter.

J.-U. Park  
Department of Plastic and Reconstructive Surgery,  
Seoul National University Boramae Hospital,  
Seoul, South Korea

E.-H. Song · S.-H. Jeong  
Department of Materials Science and Engineering,  
Seoul National University, Seoul, South Korea

J. Song  
School of Chemical and Biomedical Engineering,  
Nanyang Technological University,  
Singapore, Singapore

H.-E. Kim (✉)  
Department of Materials Science and Engineering,  
Seoul National University, Seoul, South Korea  
Biomedical Implant Convergence Research Center,  
Advanced Institutes of Convergence Technology,  
Suwon, South Korea  
e-mail: [kimsw@snu.ac.kr](mailto:kimsw@snu.ac.kr)

S. Kim (✉)  
Department of Plastic and Reconstructive Surgery,  
Seoul National University College of Medicine,  
Seoul, South Korea  
e-mail: [kimhe@snu.ac.kr](mailto:kimhe@snu.ac.kr)

## 28.1 Overview of Wound Healing and Dressing Materials

### 28.1.1 Wound Healing Process

Wounds are sites where repair of damaged tissue occurs. It is important to maintain homeostasis at wound sites. Non-healing problematic chronic wounds develop due to local or systemic causes, such as infection, trauma, and aging [33, 62]. The process of wound healing involves a cascade of consecutive biochemical and cellular responses that is generally divided into four phases: hemostasis, inflammatory phase, proliferative phase (including fibroplasia, neovascularization, formation of granulation tissue, and re-epithelialization), and finally, the formation of extracellular matrix and maturation of tissues [6, 55].

The wound healing process is complex, and a wound dressing needs to meet certain requirements to successfully regenerate the tissue. Moreover, nowadays, increase in unfavorable and delayed healing conditions, such as diabetic foot, pressure ulcers, and venous ulcers that alter the normal wound healing process, have led to challenging problems associated with non-healing chronic wounds and increased socioeconomic suffering [44, 51]. The delay in wound healing is a disorganization of coordinated biological responses to tissue injury that results in tissue contraction, epithelialization, and restoration. Under unfavorable conditions, the self-perpetuating inflammatory cascade may result in increased tissue destruction and necrosis rather than healing. Moreover, the longer it takes for spontaneous wound healing, the worse the outcome usually is, with an increasing likelihood of developing not only hypertrophic scarring and unsightly alterations in pigmentation, but also secondary infections and even sepsis [6, 8, 20].

Wound healing begins with the creation of the wound itself, and is mediated by extravasated cytokines and various cells from the injured blood vessels at the wound site. Each phase exhibits dominant biochemical reactions that are associated with specific cells. Moreover, the process of wound healing is a consecutive flow of

overlapping stages in which the effects of several cellular components and cytokines play a role in recovering the normal continuity of and replacement of tissue defect. In particular, during the inflammatory phase, inflammatory cells are actively recruited to the wound site and play important roles in the secretion of growth factors such as transforming growth factor-beta (TGF- $\beta$ ), platelet-derived growth factor (PDGF), and insulin-like growth factor-1 [18, 20]. Moreover, during the proliferative phase, the fibroblast density significantly increases because fibroblasts are recruited to the wound by growth factors released by the inflammatory cells. From this perspective, the type of dressing material used for wound treatment is critical since surface interactions between the dressing material and the wound may significantly influence the healing phase, including cell recruitment and cytokine production [10, 18].

### 28.1.2 Problematic Clinical Wounds and Wound Dressing

With the rapidly growing elderly population, delayed wound healing has significantly increased because chronic diseases such as diabetes, pressure ulcers, and venous ulcers often hinder the normal wound healing processes [4, 22]. Diabetes affects 200 million people worldwide and the number is expected to increase to more than 300 million people in 20 years. More than 15% of diabetics have a diabetic foot, and over a million people undergo leg amputation annually due to unhealed wounds [41]. The incidence of pressure ulcers is steadily increasing due to the increased number of patients with limb paralysis caused by cerebrovascular disease and generalized placebo caused by aging. In Europe, the cost of treating bedsores is >500 million euros annually, and bedsores have been reported to be included in the top four illnesses in terms of cost. In hospitals, the incidence of pressure ulcers is approximately 11% [40, 52]. In the United States, more than 2 million people suffer from burns each year and the cost of treating burns is reportedly >1 billion dollars. The patients with

the most severe burns require long-term inpatient care, and severe burns have led to a high rate of mortality due to secondary infections through the wounds and excessive blood loss [17, 26].

Although definite surgical treatments (which include debridement, skin grafting, or flaps) are often required for treatment of problematic wounds such as severe burns, appropriate wound dressing is a critical part of successful healing that supports complex wound healing processes. Therefore, the development of functional wound dressings for the acceleration of wound healing is necessary to minimize the duration of wound healing and reduce the associated medical cost, in addition to protecting the damaged area against dehydration and infection.

### 28.1.3 Currently Used Wound Dressing Materials

The maintenance of homeostasis is critical for the treatment of various problematic, non-healing clinical wounds. To treat wounds in clinical patients, an ideal wound dressing needs to inhibit exogenous microorganisms and prevent bacterial growth, maintain a controlled moist environment, allow gaseous exchange and promote fluid drainage, and possess a soft and flexible texture with biocompatibility and certain strength.

Recently, commercialized dressing materials composed of synthetic polyurethane foam, embedded hydrogel, or hydrocolloids have been clinically used. However, these materials only satisfy one or few of the required standard characteristics of an ideal wound dressing and play a passive and limited role in wound healing [11, 18].

Various dressing materials have been developed from conventional dressing methods such as the use of gauzes and biological dressing materials such as polyurethane foam, hydrocolloids, hydrofibers, hydrogels, and alginate [10, 28].

The gauze is a simple and inexpensive material to use in a stopgap method, but is often implemented as a dressing. However, there is pain associated with the dressing change, the

wound gets desiccated, and the moist environment is not maintained. Commercially produced polyurethane foam include Medifoam® (Ildong Pharmaceutical, Seoul, Korea), Allevin® (Smith and Nephew, London, UK), Biatain® (Coloplast, Fredensborg, Denmark), and Versiva® (Convatec, Chester, UK) [21]. Polyurethane foam is widely used due to its ability to absorb the exudate, non-adherence to the wound surface, and minimized interference with cellular activity. However, it can aggravate infected wounds and has no special function other than to absorb the exudate [46]. Hydrocolloid agents, including Duoderm® (Convatec) and Comfeel® (Coloplast), exhibit wound protection and necrotic degradation, but also cause cellular damage on the wound surface due to stickiness when removed and are inadequate to use when there is a large amount of exudate. Hydrofiber materials include Aquacell-Ag® (Convatec) and Acticoat® (Smith and Nephew). Silver-containing hydrofibers possess antimicrobial effect to a certain degree, but after use, the debris of the fiber adheres and gets invaginated into the wound and exhibits cytotoxicity against important cell components needed for wound healing, such as keratinocytes and fibroblasts, implying that hydrofibers have limited application in common cases [12, 24, 37]. In addition, various hydrogel components including alginate are used to promote wound healing. Currently, the commercially available hydrogels are Intrasite Gel® (Smith and Nephew), Purilion gel® (Coloplast), and Kaltostat® (Convatec).

### 28.1.4 Development of Chitosan-Based Dressing Material

Currently available dressing materials can be adapted according to the characteristics of the wound to promote wound healing. However, it is necessary to develop a more active and functional dressing material for effective wound healing. The most common approaches for developing new and improved wound dressing materials include synthesizing and modifying biocompatible materials. Studies have attempted to develop

various materials that are effective in wound healing such as hydrocolloids, hydrofibers, alginate, etc. [11, 18, 34]. Among them, chitosan and its composite materials have gained considerable attention because of their biocompatible and non-toxic characteristics, flexibility, and distinctive strength. Across various fields, several studies have been conducted to improve the biological and mechanical properties of chitosan by combining it with other organic or inorganic materials [14, 15, 36, 38, 43]. However, the wound healing capabilities in these studies have not been extensively compared with widely used commercial dressing materials, providing limited information from a practical perspective [19].

---

## 28.2 Chitosan as a Natural Polymer

### 28.2.1 Characteristics of Chitosan

Chitin was first discovered as an insoluble material obtained from mushrooms by Henri Braconot in 1811 [31]. Subsequently, it was also discovered in various organisms, namely in the outer skeleton of crustaceans (crabs, lobsters, shellfish, and shrimp), shell of insects, and even in the cell walls of mycelial fungi [45]. Chitosan, a derivative of chitin, is a natural polysaccharide composed of  $\beta$  (1–4) glycosidic bond-linked D-glucoamine and N-acetyl-D-glucosamine. The degrees of deacetylation (DDA) are key factors that determine the physical property of chitosan. Highly deacetylated chitosan has numerous free amine groups, making it sensitive to pH variation. Amines from chitosan chains are uncharged over pH 6.3 while they are protonized in acidic conditions under pH 6.3, suggesting that chitosan has the potential of being used as an advanced drug delivery system, which can selectively release drugs at certain pH levels [53]. Chitosan is also biodegradable. It is mainly degraded by lysozyme, which is present in human body fluids and tissues. The degradation time is related to the DDA and the copolymer type of chitosan. Higher DDA induces slower degradation rates (chitosan with >90% DDA could not be degraded by lyso-

zyme), and a block-type copolymer exhibits faster degradation mechanics than a random-type copolymer [53].

### 28.2.2 Chitosan-Based Biomaterials

Chitosan has been widely used in versatile biomedical applications, including guided bone regeneration (GBR) membranes carrying drugs, hemostatic agents, and antimicrobial agents. GBR is dominantly applied in dental surgery to support hard tissue growth and integration. It needs to be biocompatible, exclude unwanted cells, and provide the space to allow tissue ingrowth. Chitosan is a biocompatible natural polymer and it can be fabricated into membrane form with interconnected pores where tissues permeate into the membrane, facilitating bone regeneration. Recently, efforts to develop improved chitosan-based GBR were conducted by applying other osteoconductive biomaterials (for e.g., silica, hydroxyapatite, and other natural polymers (for e.g., fibroin) or protein-based growth factors (for e.g., bone morphogenetic protein-2 (BMP-2)) to chitosan membrane. Chitosan/fibroin-hydroxyapatite composite was prepared as a GBR membrane in a rabbit calvarial model for 8 weeks. It was effective in terms of new bone formation and inflammatory response, comparative to commercially available collagen membrane (Bio-Gide) [60]. Similarly, chitosan hybridized with silica xerogel induced mineralization in physiological conditions, enhanced biological properties (such as alkaline phosphatase activity, indices of differentiation and proliferation of ATCC pre-osteoblasts, and promoted bone regeneration significantly *in vivo* [36].

Chitosan is also widely used as a hemostatic agent. Its use as a hemostatic agent or dressing membrane was approved in the USA due to its potential to modulate cell mechanisms and induce rapid blood clotting. The functional  $\text{NH}_3^+$  groups of cationic chitosan enhances platelet aggregation, which results in clot formation. Celox (Medtrade products Ltd., Cheshire, UK) is currently used as a commercial chitosan-based hemostatic agent for severe hemorrhage [42]. It

was already used in emergency situations (such as severe bleeding during cardiothoracic surgery) and military settings. Recently, to enhance thrombosis and hemostasis, composite systems (developed by incorporating zinc ion, cellulose, and kaolin with chitin) have been developed to produce synergistic effects [29, 47, 63]. In addition, based on the applications, various types of composite systems were developed, including porous microspheres for deep and irregular shapes of surgical sites and dressings for covering large areas.

Chitosan exhibits antimicrobial effects against gram-negative bacteria. The primary amines of chitosan disrupt the outer membranes of bacteria, destroying the metabolism effectively. Furthermore, chitosan is a prime polymer to disperse and stabilize inorganic nano-particles, such as silver nano-particles (NPs), which possess anti-microbial effects against sulfur and phosphorous present in the microbial cells. Chitosan is also considered biocidal and has been proposed as a parasitic control agent against *Lernaea cyprinacea*, which is frequently found in gold fish (*Carassius auratus*) aquaria during the spring [2]. Chitosan-silver NPs composite system was also incorporated in electrospun mats in which silver NPs were dispersed homogeneously inside the chitosan fiber and exhibited anti-bacterial effects, especially against *Escherichia coli* [1].

### 28.2.3 Chitosan-Based Composite Biomaterials

Chitosan is extensively used in composite systems with other natural polymers, synthetic polymers, inorganic particles, drugs, or growth factors. For application in the dairy industry, a silica/chitosan composite was developed to immobilize  $\beta$ -galactosidase to increase its stability [54]. Chitosan phosphatic thermosensitive hydrogels—which hold significant potential for minimum injury surgery by regulating the applied heat—were developed using nano-noble Ag@Pd particles [3]. A chitosan/gelatin composite (CG) was developed as a hemostatic agent [32]. CG exhibited excellent liquid absorption and pro-

moted platelet aggregation significantly under *in vitro* conditions. Its hemostatic property was further verified in greater detail using *in vivo* bleeding models (rabbit ear artery injury model and rabbit liver injury model). CG was effective in inducing rapid blot clot formation and swiftly reducing bleeding. In addition, the bony defect healing capability of BMP-2-loaded chitosan/silica hybrid membrane was demonstrated in *in vitro* and *in vivo* studies [35]. Hybrid systems exhibited higher affinity for BMP-2 as a drug carrier to deliver growth factors in a sustained manner. The hybrid system synergetically improved osteoconductivity in GBR, accelerating new bone formation in the regions of defects. Chitosan/silica hybrid also showed great performance as a dressing membrane in wound healing. As nano-scale silica was incorporated in chitosan by sol-gel process, its biological property was enhanced in terms of cellular responses, which accelerated the healing process *in vivo*. Silicon ion released from hybrid systems and the bioactive chitosan-based hybrid membrane itself promoted fibroblast (L929) proliferation *in vitro*. When the hybrid dressing was used in an *in vivo* study, wound closure was accelerated, cellularity level was lowered, TGF- $\beta$  and  $\alpha$ -smooth muscle actin densities increased, and the newly formed collagen matrix was aligned, organized uniformly and dense, as determined from *in vivo* immunohistology assays [50].

---

## 28.3 Chitosan-Based Dressing Materials

### 28.3.1 Functional Benefits of Chitosan as a Dressing Material

Chitosan has been reported to accelerate wound healing in all stages. It prohibits hemorrhage by inducing thrombosis, enhances the function of inflammatory cells (polymorphonuclear leukocytes (PMNs) and macrophages), and activates the fibroblasts to form new collagen matrix in the regions of tissue defects [6]. Furthermore, the chitosan membrane is able to maintain a

physiologically moist microenvironment that promotes healing and formation of granulation tissue and achieves hemostasis. Due to its high potential as an ideal healing agent, chitosan-based products have been commercially fabricated and studied [16, 30, 64]. However, there are concerns regarding its low bioactivity (when it is used *in vivo*) and the unsatisfactory maintenance of the chitosan framework, particularly in the moist condition [27]. Therefore, the development of an efficient chitosan composite system for accelerated wound healing in problematic clinical wounds continues to remain a major challenge.

### 28.3.1.1 Hemostasis

Hemostasis is the first step in the wound healing process. Hemorrhage is controlled by two essential components: platelets and fibrin. Platelets are composed of alpha granules containing crucial signaling proteins, such as PDGF and TGF- $\beta$ , to initiate the wound healing cascade by attracting inflammatory cells to the wound sites [6]. Chitosan helps in the process by inducing an intrinsic pathway of coagulation. Positively charged polymeric chains of chitosan gather negatively charged cell membranes of erythrocytes by electrostatic interactions, leading to agglutination of erythrocytes, formation of a plug at the site of tissue defects and prevention of severe bleeding [13]. Based on the hemostatic property of chitosan, a collagen sponge coated with chitosan/calcium pyrophosphate nanoflowers was developed. The nanoflower-coated collagen sponge promoted hemoglobin adsorption and platelet adhesion *in vitro* and reduced the time required for hemostasis and the extent of bleeding significantly in an *in vivo* hepatic trauma model and a ear artery model as well [67].

### 28.3.1.2 Acceleration of Wound Healing Process

Based on the DDA, chitosan exhibits different cytotoxicities to keratinocytes and human skin fibroblasts. Chitosan with high DDA (89%) stimulated the proliferation of fibroblasts but inhibited human keratinocyte mitogenesis *in vitro*

[25]. In an *in vitro* cell viability study using HaCaT (a cell line of human keratinocyte), it was found that chitosan promoted the release of cytokines from the HaCaT cells to induce apoptic cell death [66]. PMNs, which characteristically react to foreign bodies, were not affected by chitosan when PMNs were isolated in the membrane and reactive oxygen species (ROS) were detected [57]. However, it was reported that chitosan-treated wounds exhibited severe infiltration of PMNs in the early proliferation stage, and granulation was more distinctive at a later stage [64]. Collagen production also increased, as demonstrated by immunohistochemical analysis. Moreover, in open skin wounds, chitosan bandage increased the epithelialization rate and deposition of organized collagen in the dermis, and reduced the number of inflammatory cells significantly *in vivo*.

### 28.3.1.3 Antimicrobial Effect of Chitosan

Chitosan with molecular weight (MW) < 305 kDa exhibited antimicrobial activity against both, gram-negative and gram-positive bacteria [69]. High MW chitosan exhibited an enhanced antimicrobial effect against gram-positive *Staphylococcus aureus*, whereas low MW chitosan showed a high antimicrobial activity against gram-negative *E. coli*. It was suggested that chitosan exhibits antimicrobial effects by two mechanisms in their study: (1) the chitosan polymer chain blocks the nutrients entering through the bacterial membrane, and (2) low MW chitosan enters the bacterial cell wall through pervasion and disrupts the physiological activities of bacteria. The first mechanism is predominantly observed in gram-positive bacteria and the second mechanism is seen in gram-negative bacteria. The antibacterial property of chitosan can be further enhanced by adding other drugs or nano particles. Vancomycin and daptomycin were successfully loaded on chitosan films to alleviate infections after bone fractures, and silver nanoparticles were incorporated in wound dressing material, especially in cases of infected wounds [59, 65].



### 28.3.1.4 Chitosan Composite Dressing Materials

Chitosan-based dressing materials can be enhanced by incorporating antimicrobial or bioactive inorganic particles and grafting biopolymers in the chitosan chain. Chitosan dressing incorporated with zinc oxide and silver nanoparticles exhibited enhanced antibacterial activity that inhibited representative bacteria (such as *S. aureus*, *E. coli*, and *Pseudomonas aeruginosa*), indicating its potential as a dressing material for infected wounds [39]. Chitosan/titanium oxide (TiO<sub>2</sub>) composite improved fibroblast proliferation, induced the expression of fibroblast markers (TGF- $\beta$ , fibroblast growth factor-2, collagen type I, delta like non-canonical notch ligand 1, and proliferating cell nuclear antigen), and showed significant antibacterial effects [7]. Furthermore, the composite could induce an accelerated healing rate by activating the fibroblast signaling pathway during the inherent healing cascade. Sericin extracted from silk fiber was also blended with chitosan as a form of electrospun fiber mats [68]. Sericin provided antioxidant, hydrophilic (to absorb moisture), and antibacterial functions to the chitosan membrane, enhancing the potential of chitosan as a dressing material. An alginate/chitosan-based bi-layer composite could deliver ciprofloxacin hydrochloride continually [23]. The chitosan membrane was present in the exterior of the bi-layer composite to prevent bacterial invasion and control the water vapor transmission ratio, and the inner part of the bi-layer composite consisted of an alginate scaffold, which contained drugs, and drains the exudates from the wounds. Chitosan-silica hybridized membrane coupled with sol-gel technique is also another promising chitosan composite dressing material [49]. It successfully performed wound closure for a full-thickness porcine wound model, accelerated the healing rate, and improved epithelialization, fibroblast proliferation, collagen formation, and inflammatory cell infiltration histologically.

### 28.3.1.5 Scaffold for Drug Delivery

Local-drug delivery systems are beneficial for wound dressing to achieve a high concentration

of drugs at the target sites, while lowering the total amount of serum needed, compared with whole body dosing, which could induce systemic toxicity [11]. Melatonin-loaded chitosan/Pluronic® F127 microspheres were developed as an innovative antimicrobial dressing [56]. Melatonin was entrapped in the microspheres to potentiate chitosan antimicrobial activity against *S. aureus* and five clinical methicillin-resistant *S. aureus* (MRSA) strains, without inducing any deteriorating effects on the composite biocompatibility with skin keratinocytes and fibroblasts. Levofloxacin (Levo, fluoroquinolones, approved in 1996 by the FDA) was successfully delivered through a grafted derivative of chitosan with 2-hydroxyethylacrylate (CS-g-PHEA) to kill methicillin-susceptible *S. aureus*, MRSA, and *P. aeruginosa* [58]. The chitosan/CS-g-PHEA composite shows considerable promise in wound infection management and exhibits tolerability, safety, and antibacterial activity as a potential wound dressing material. Chitosan scaffolds containing growth factors, which can accelerate the healing stage by intervening in the healing cascade directly, were also studied. Chitosan-bFGF scaffold accelerated wound closure in pressure ulcers in an aged mouse model, enhanced angiogenic functions by delivering growth factors, and elevated neutrophil levels, which contributes to the proteolytic conditions of pressure ulcers [48].

### 28.3.2 Clinical Applications of Chitosan-Based Dressing Materials

The wound healing proficiency of chitosan-based dressing was further demonstrated through clinical study in the human body. Azad et al. conducted a clinical study using a mesh-type chitosan membrane (with DDA 75%), incorporated with other protein and mineral contents, and a MW of 1500 kDa [5]. The clinical results obtained post-treatment with the mesh chitosan matrix were in alignment with the results of an *in vivo* animal test, in terms of efficient adherence, hemostasis, healing rate, and re-epithelialization, and the mesh chitosan matrix was found to be significantly

better than Bactigras<sup>®</sup>, a chlorhexidine acetate-impregnated tulle gras, used as the control. It promoted faster healing and re-organized the collagen matrix into healthy and highly acceptable new skin. In another study, clinically treating skin graft donor sites using N-carboxybutyl chitosan showed that vascularization and histoarchitectural order improved and the number of inflammatory cells decreased in the chitosan-treated sites [9]. Stone et al. evaluated the healing effects of a chitosan dressing called Hyphedan (Hainan Kangda Marine Biomedical Corporation, Hong Kong, China) in a clinical study [61]. Twenty patients (11 females and 9 males, mean age: 69 years) were evaluated for 3–6 months for wounds that did not show any indications requiring secondary treatments. The healing rate was accelerated and the nerve and capillary regeneration was enhanced. However, thus far, only a few clinical studies using chitosan-based dressing materials have been conducted, whereas effective wound closure, antimicrobial effects, and histological recovery exhibited by several chitosan-based membranes have been extensively demonstrated using both, *in vitro* and *in vivo* studies.

## 28.4 Conclusion

Current studies demonstrate that chitosan-based dressing materials are considered suitable for clinically problematic wounds. Chitosan can be enhanced in wound healing capability through composite and hybrid systems by incorporating minerals, organic and inorganic components, antimicrobial agents, drugs, and growth factors, according to the characteristics of the wound. Chitosan-based dressing materials show promising clinical applications in problematic and chronic wound treatment as they exhibit efficient adherence, hemostasis, accelerated healing rate, and re-epithelialization in chronic wounds, as demonstrated in several *in vivo* and *in vitro* studies. Our study provides valuable insights into the commercial development of clinically improved wound dressing materials that are not only non-toxic, flexible and durable but also possess supe-

rior biocompatibility and bioactivity, while exhibited accelerated wound healing. In future, it is important to develop standardized prototypes of chitosan-based dressing materials, and to prove their effectiveness in wound healing in humans through clinical trials for various clinical wounds. Chitosan-based dressing materials have significant potential for use as multi-functioning dressing materials, which provide an effective wound healing environment in problematic clinical wounds.

## References

1. Abdelgawad AM, Hudson SM, Rojas OJ (2014) Antimicrobial wound dressing nanofiber mats from multicomponent (chitosan/silver-NPs/polyvinyl alcohol) systems. *Carbohydr Polym* 100:166–178. <https://doi.org/10.1016/j.carbpol.2012.12.043>
2. Abu-Elala NM, Attia MM, Abd-Elsalam RM (2017) Chitosan-silver nanocomposite in goldfish aquaria: new prospective for *Lernaea cyprinacea* control. *Int J Biol Macromol*. <https://doi.org/10.1016/j.ijbiomac.2017.12.133>
3. Ali GW, El-Hotaby W, Hemdan B, Abdel-Fattah WI (2018) Thermosensitive chitosan/phosphate hydrogel-composites fortified with Ag versus Ag@ Pd for biomedical applications. *Life Sci* 194:185–195
4. Augustin M, Mayer G, Wild T (2016) Challenges of aging skin: care and therapy using the example of venous ulcers. *Hautarzt* 67(2):160–168. <https://doi.org/10.1007/s00105-015-3756-0>
5. Azad AK, Sermisintham N, Chandkrachang S, Stevens WF (2004) Chitosan membrane as a wound-healing dressing: characterization and clinical application. *J Biomed Mater Res B Appl Biomater* 69B(2):216–222. <https://doi.org/10.1002/jbm.b.30000>
6. Beanes SR, Dang C, Soo C, Ting K (2004) Skin repair and scar formation: the central role of TGF- $\beta$ . *Expert Rev Mol Med* 5(08). <https://doi.org/10.1017/s1462399403005817>
7. Behera SS, Das U, Kumar A, Bissoyi A, Singh AK (2017) Chitosan/TiO<sub>2</sub> composite membrane improves proliferation and survival of L929 fibroblast cells: application in wound dressing and skin regeneration. *Int J Biol Macromol* 98:329–340. <https://doi.org/10.1016/j.ijbiomac.2017.02.017>
8. Berry DP, Harding KG, Stanton MR, Jasani B, Ehrlich PH (1998) Human wound contraction: collagen organization, fibroblasts, and myofibroblasts. *Plast Reconstr Surg* 102(1):124–131
9. Biagini G, Bertani A, Muzzarelli R, Damadei A, DiBenedetto G, Belligolli A, Riccotti G, Zucchini C, Rizzoli C (1991) Wound management with

- N-carboxybutyl chitosan. *Biomaterials* 12(3):281–286. [https://doi.org/10.1016/0142-9612\(91\)90035-9](https://doi.org/10.1016/0142-9612(91)90035-9)
10. Boateng J, Catanzano O (2015) Advanced therapeutic dressings for effective wound healing—a review. *J Pharm Sci* 104(11):3653–3680. <https://doi.org/10.1002/jps.24610>
  11. Boateng JS, Matthews KH, Stevens HNE, Eccleston GM (2008) Wound healing dressings and drug delivery systems: a review. *J Pharm Sci* 97(8):2892–2923. <https://doi.org/10.1002/jps.21210>
  12. Burd A, Kwok CH, Hung SC, Chan HS, Gu H, Lam WK, Huang L (2007) A comparative study of the cytotoxicity of silver-based dressings in monolayer cell, tissue explant, and animal models. *Wound Repair Regen* 15(1):94–104. <https://doi.org/10.1111/j.1524-475X.2006.00190.x>
  13. Chan LW, Kim CH, Wang X, Pun SH, White NJ, Kim TH (2016) PolySTAT-modified chitosan gauzes for improved hemostasis in external hemorrhage. *Acta Biomater* 31:178–185. <https://doi.org/10.1016/j.actbio.2015.11.017>
  14. Chen J-P, Chang G-Y, Chen J-K (2008) Electrospun collagen/chitosan nanofibrous membrane as wound dressing. *Colloids Surf A Physicochem Eng Asp* 313:183–188. <https://doi.org/10.1016/j.colsurfa.2007.04.129>
  15. Dai M, Zheng X, Xu X, Kong X, Li X, Guo G, Luo F, Zhao X, Wei YQ, Qian Z (2009) Chitosan-alginate sponge: preparation and application in curcumin delivery for dermal wound healing in rat. *Biomed Res Int* 2009:1. <https://doi.org/10.1155/2009/595126>
  16. Dai T, Tanaka M, Huang Y-Y, Hamblin MR (2011) Chitosan preparations for wounds and burns: antimicrobial and wound-healing effects. *Expert Rev Anti-Infect Ther* 9(7):857–879. <https://doi.org/10.1586/eri.11.59>
  17. Dissanaike S, Ha D, Mitchell D, Larumbe E (2017) Socioeconomic status, gender, and burn injury: a retrospective review. *Am J Surg* 214(4):677–681. <https://doi.org/10.1016/j.amjsurg.2017.06.012>
  18. Dreifke MB, Jayasuriya AA, Jayasuriya AC (2015) Current wound healing procedures and potential care. *Mater Sci Eng C* 48:651–662. <https://doi.org/10.1016/j.msec.2014.12.068>
  19. Englehart MS, Cho SD, Tieu BH, Morris MS, Underwood SJ, Karahan A, Muller PJ, Differding JA, Farrell DH, Schreiber MA (2008) A novel highly porous silica and chitosan-based hemostatic dressing is superior to HemCon and gauze sponges. *J Trauma Acute Care Surg* 65(4):884–892. <https://doi.org/10.1097/TA.0b013e318187800b>
  20. Falanga V (2000) Classifications for wound bed preparation and stimulation of chronic wounds. *Wound Repair Regen* 8(5):347–352. <https://doi.org/10.1111/j.1524-475x.2000.00347.x>
  21. Gok NS, Kim HK, Kim SH, Kim WS, Bae TH, Kim MK (2007) Comparative study of Acticoat (R) & Alleyn (R) on infected full-thickness wound of the rat skin. *J Korean Soc Plast Reconstr Surg* 34(2):169–175
  22. Gosain A, DiPietro LA (2004) Aging and wound healing. *World J Surg* 28(3):321–326. <https://doi.org/10.1007/s00268-003-7397-6>
  23. Han F, Dong Y, Song A, Yin R, Li S (2014) Alginate/chitosan based bi-layer composite membrane as potential sustained-release wound dressing containing ciprofloxacin hydrochloride. *Appl Surf Sci* 311:626–634. <https://doi.org/10.1016/j.apsusc.2014.05.125>
  24. Hiro ME, Pierpont YN, Ko F, Wright TE, Robson MC, Payne WG (2012) Comparative evaluation of silver-containing antimicrobial dressings on in vitro and in vivo processes of wound healing. *Eplasty* 12:e48
  25. Howling GI, Dettmar PW, Goddard PA, Hampson FC, Dornish M, Wood EJ (2001) The effect of chitin and chitosan on the proliferation of human skin fibroblasts and keratinocytes in vitro. *Biomaterials* 22(22):2959–2966. [https://doi.org/10.1016/S0142-9612\(01\)00042-4](https://doi.org/10.1016/S0142-9612(01)00042-4)
  26. Hultman CS, van Duin D, Sickbert-Bennett E, DiBiase LM, Jones SW, Cairns BA, Weber DJ (2017) Systems-based practice in burn care. *Clin Plast Surg* 44(4):935–942. <https://doi.org/10.1016/j.cps.2017.06.002>
  27. Jayakumar R, Prabakaran M, Kumar PS, Nair S, Tamura H (2011) Biomaterials based on chitin and chitosan in wound dressing applications. *Biotechnol Adv* 29(3):322–337. <https://doi.org/10.1016/j.biotechadv.2011.01.005>
  28. Kasiewicz LN, Whitehead KA (2017) Recent advances in biomaterials for the treatment of diabetic foot ulcers. *Biomater Sci* 5(10):1962–1975. <https://doi.org/10.1039/C7BM00264E>
  29. Kim GH, Im JN, Kim TH, Lee GD, Youk JH, Doh SJ (2017) Preparation and characterization of calcium carboxymethyl cellulose/chitosan blend non-wovens for hemostatic agents. *Text Res J.* <https://doi.org/10.1177/0040517517712101>
  30. Kojima K, Okamoto Y, Kojima K, Miyatake K, Fujise H, Shigemasa Y, Minami S (2004) Effects of chitin and chitosan on collagen synthesis in wound healing. *J Vet Med Sci* 66(12):1595–1598. <https://doi.org/10.1292/jvms.66.1595>
  31. Labrude P, Becq C (2003) Pharmacist and chemist Henri Braconnot. *Rev Hist Pharm* 51(337):61–78. <https://doi.org/10.3406/pharm.2003.5479>
  32. Lan G, Lu B, Wang T, Wang L, Chen J, Yu K, Liu J, Dai F, Wu D (2015) Chitosan/gelatin composite sponge is an absorbable surgical hemostatic agent. *Colloids Surf B Biointerfaces* 136:1026–1034. <https://doi.org/10.1016/j.colsurfb.2015.10.039>
  33. Lazarus GS, Cooper DM, Knighton DR et al (1994) Definitions and guidelines for assessment of wounds and evaluation of healing. *Arch Dermatol* 130(4):489–493. <https://doi.org/10.1001/archderm.1994.01690040093015>
  34. Lazic T, Falanga V (2011) Bioengineered skin constructs and their use in wound healing. *Plast Reconstr Surg* 127:75S–90S. <https://doi.org/10.1097/PRS.0b013e3182009d9f>

35. Lee EJ, Kim HE (2016) Accelerated bony defect healing by chitosan/silica hybrid membrane with localized bone morphogenetic protein-2 delivery. *Mater Sci Eng C Mater Biol Appl* 59:339–345. <https://doi.org/10.1016/j.msec.2015.10.001>
36. Lee EJ, Shin DS, Kim HE, Kim HW, Koh YH, Jang JH (2009) Membrane of hybrid chitosan-silica xerogel for guided bone regeneration. *Biomaterials* 30(5):743–750. <https://doi.org/10.1016/j.biomaterials.2008.10.025>
37. Lee JH, Chae JD, Kim DG, Hong SH, Lee WM, Ki M (2010) Comparison of the efficacies of silver-containing dressing materials for treating a full-thickness rodent wound infected by methicillin-resistant *Staphylococcus aureus*. *Korean J Lab Med* 30(1):20–27. <https://doi.org/10.3343/kjlm.2010.30.1.20>
38. Li X, Nan K, Li L, Zhang Z, Chen H (2012) In vivo evaluation of curcumin nanoformulation loaded methoxy poly (ethylene glycol)-graft-chitosan composite film for wound healing application. *Carbohydr Polym* 88(1):84–90. <https://doi.org/10.1016/j.carbpol.2011.11.068>
39. Lu Z, Gao J, He Q, Wu J, Liang D, Yang H, Chen R (2017) Enhanced antibacterial and wound healing activities of microporous chitosan-Ag/ZnO composite dressing. *Carbohydr Polym* 156:460–469. <https://doi.org/10.1016/j.carbpol.2016.09.051>
40. Lyder CH (2003) Pressure ulcer prevention and management. *JAMA* 289(2):223–226. <https://doi.org/10.1001/jama.289.2.223>
41. Mauricio D, Jude E, Piaggese A, Frykberg R (2016) Diabetic foot: current status and future prospects. *J Diabetes Res* 2016:2. <https://doi.org/10.1155/2016/5691305>
42. Millner RWJ, Lockhart AS, Bird H, Alexiou C (2009) A new hemostatic agent: initial life-saving experience with Celox (Chitosan) in cardiothoracic surgery. *Ann Thorac Surg* 87(2):e13–e14. <https://doi.org/10.1016/j.athoracsur.2008.09.046>
43. Mohandas A, Anisha B, Chennazhi K, Jayakumar R (2015) Chitosan-hyaluronic acid/VEGF loaded fibrin nanoparticles composite sponges for enhancing angiogenesis in wounds. *Colloids Surf B: Biointerfaces* 127:105–113. <https://doi.org/10.1016/j.colsurfb.2015.01.024>
44. Nussbaum SR, Carter MJ, Fife CE, DaVanzo J, Haught R, Nusgart M, Cartwright D (2018) An economic evaluation of the impact, cost, and medicare policy implications of chronic nonhealing wounds. *Value Health* 21(1):27–32. <https://doi.org/10.1016/j.jval.2017.07.007>
45. Ogura K, Kanamoto T, Itoh M, Miyashiro H, Tanaka K (1980) Dynamic mechanical behavior of chitin and chitosan. *Polym Bull* 2(5):301–304
46. Ozkaynak MU, Atalay-Oral C, Tantekin-Ersolmaz SB (2005) Güner FS polyurethane films for wound dressing applications. In: *Macromolecular symposia*, vol 1. Wiley Online Library, pp 177–184. <https://doi.org/10.1002/masy.200551016>
47. Pan M, Tang Z, Tu J, Wang Z, Chen Q, Xiao R, Liu H (2018) Porous chitosan microspheres containing zinc ion for enhanced thrombosis and hemostasis. *Mater Sci Eng C* 85:27–36. <https://doi.org/10.1016/j.msec.2017.12.015>
48. Park CJ, Clark SG, Lichtensteiger CA, Jamison RD, Johnson AJW (2009) Accelerated wound closure of pressure ulcers in aged mice by chitosan scaffolds with and without bFGF. *Acta Biomater* 5(6):1926–1936. <https://doi.org/10.1016/j.actbio.2009.03.002>
49. Park J-U, Jeong S-H, Song E-H, Song J, Kim H-E, Kim S (2018) Acceleration of the healing process of full-thickness wounds using hydrophilic chitosan-silica hybrid sponge in a porcine model. *J Biomater Appl* 0(0):0885328217751246. <https://doi.org/10.1177/0885328217751246>
50. Park JU, Jung HD, Song EH, Choi TH, Kim HE, Song J, Kim S (2016) The accelerating effect of chitosan-silica hybrid dressing materials on the early phase of wound healing. *J Biomed Mater Res B Appl Biomater* 105:1828. <https://doi.org/10.1002/jbm.b.33711>
51. Raghav A, Khan ZA, Labala RK, Ahmad J, Noor S, Mishra BK (2018) Financial burden of diabetic foot ulcers to world: a progressive topic to discuss always. *Ther Adv Endocrinol Metab* 9(1):29–31. <https://doi.org/10.1177/2042018817744513>
52. Rasero L, Simonetti M, Falciani F, Fabbri C, Collini F, Dal Molin A (2015) Pressure ulcers in older adults: a prevalence study. *Adv Skin Wound Care* 28(10):461–464. <https://doi.org/10.1097/01.ASW.0000470371.77571.5d>
53. Ren D, Yi H, Wang W, Ma X (2005) The enzymatic degradation and swelling properties of chitosan matrices with different degrees of N-acetylation. *Carbohydr Res* 340(15):2403–2410. <https://doi.org/10.1016/j.carres.2005.07.022>
54. Ricardi NC, de Menezes EW, Valmir Benvenuti E, da Natividade Schöffer J, Hackenhaar CR, Hertz PF, Costa TMH (2018) Highly stable novel silica/chitosan support for  $\beta$ -galactosidase immobilization for application in dairy technology. *Food Chem* 246:343–350. <https://doi.org/10.1016/j.foodchem.2017.11.026>
55. Riches DWH (1988) Macrophage involvement in wound repair, remodeling, and fibrosis. In: RAF C (ed) *The molecular and cellular biology of wound repair*. Springer US, Boston, pp 95–141. [https://doi.org/10.1007/978-1-4899-0185-9\\_3](https://doi.org/10.1007/978-1-4899-0185-9_3)
56. Romić MD, Klarić MŠ, Lovrić J, Pepić I, Cetina-Čižmek B, Filipović-Grčić J, Hafner A (2016) Melatonin-loaded chitosan/Pluronic® F127 microspheres as in situ forming hydrogel: an innovative antimicrobial wound dressing. *Eur J Pharm Biopharm* 107:67–79. <https://doi.org/10.1016/j.ejpb.2016.06.013>
57. Santos TC, Marques AP, Silva SS, Oliveira JM, Mano JF, Castro AG, Reis RL (2007) In vitro evaluation of the behaviour of human polymorphonuclear neutrophils in direct contact with chitosan-based membranes. *J Biotechnol* 132(2):218–226. <https://doi.org/10.1016/j.jbiotec.2007.07.497>

58. Siafaka PI, Zisi AP, Exindari MK, Karantas ID, Bikiaris DN (2016) Porous dressings of modified chitosan with poly (2-hydroxyethyl acrylate) for topical wound delivery of levofloxacin. *Carbohydr Polym* 143:90–99. <https://doi.org/10.1016/j.carbpol.2016.02.009>
59. Smith JK, Bumgardner JD, Courtney HS, Smeltzer MS, Haggard WO (2010) Antibiotic-loaded chitosan film for infection prevention: a preliminary in vitro characterization. *J Biomed Mater Res B Appl Biomater* 94B(1):203–211. <https://doi.org/10.1002/jbm.b.31642>
60. Song JM, Shin SH, Kim YD, Lee JY, Baek YJ, Yoon SY, Kim HS (2014) Comparative study of chitosan/fibroin-hydroxyapatite and collagen membranes for guided bone regeneration in rat calvarial defects: micro-computed tomography analysis. *Int J Oral Sci* 6(2):87–93. <https://doi.org/10.1038/ijos.2014.16>
61. Stone CA, Wright H, Devaraj VS, Clarke T, Powell R (2000) Healing at skin graft donor sites dressed with chitosan. *Br J Plast Surg* 53(7):601–606. <https://doi.org/10.1054/bjps.2000.3412>
62. Sullivan TP, Eaglstein WH, Davis SC, Mertz P (2001) The pig as a model for human wound healing. *Wound Repair Regen* 9(2):66–76. <https://doi.org/10.1046/j.1524-475x.2001.00066.x>
63. Sun X, Tang Z, Pan M, Wang Z, Yang H, Liu H (2017) Chitosan/kaolin composite porous microspheres with high hemostatic efficacy. *Carbohydr Polym* 177(Suppl C):135–143. <https://doi.org/10.1016/j.carbpol.2017.08.131>
64. Ueno H, Yamada H, Tanaka I, Kaba N, Matsuura M, Okumura M, Kadosawa T, Fujinaga T (1999) Accelerating effects of chitosan for healing at early phase of experimental open wound in dogs. *Biomaterials* 20(15):1407–1414. [https://doi.org/10.1016/S0142-9612\(99\)00046-0](https://doi.org/10.1016/S0142-9612(99)00046-0)
65. Vimala K, Mohan YM, Sivudu KS, Varaprasad K, Ravindra S, Reddy NN, Padma Y, Sreedhar B, MohanaRaju K (2010) Fabrication of porous chitosan films impregnated with silver nanoparticles: a facile approach for superior antibacterial application. *Colloids Surf B: Biointerfaces* 76(1):248–258. <https://doi.org/10.1016/j.colsurfb.2009.10.044>
66. Wiegand C, Winter D, Hipler UC (2010) Molecular-weight-dependent toxic effects of Chitosans on the human keratinocyte cell line HaCaT. *Skin Pharmacol Physiol* 23(3):164–170
67. Yan T, Cheng F, Wei X, Huang Y, He J (2017) Biodegradable collagen sponge reinforced with chitosan/calcium pyrophosphate nanoflowers for rapid hemostasis. *Carbohydr Polym* 170:271–280. <https://doi.org/10.1016/j.carbpol.2017.04.080>
68. Zhao R, Li X, Sun B, Zhang Y, Zhang D, Tang Z, Chen X, Wang C (2014) Electrospun chitosan/sericin composite nanofibers with antibacterial property as potential wound dressings. *Int J Biol Macromol* 68:92–97. <https://doi.org/10.1016/j.ijbiomac.2014.04.029>
69. Zheng L-Y, Zhu J-F (2003) Study on antimicrobial activity of chitosan with different molecular weights. *Carbohydr Polym* 54(4):527–530. <https://doi.org/10.1016/j.carbpol.2003.07.009>